STUDIES IN APPLIED MECHANICS

1. Mechanics and Strength of Materials (Skalmierski)
2. Nonlinear Differential Equations (Fučik and Kufner)
3. Mathematical Theory of Elastic and Elastico-Plastic Bodies. An Introduction (Nečas and Hlaváček)
4. Variational, Incremental and Energy Methods in Solid Mechanics and Shall Theory (Mason)
5. Mechanics of Structured Media, Parts A and B (Selvadurai, Editor)
6. Mechanics of Material Behavior (Dvorak and Shield, Editors)
7. Mechanics of Granular Materials: New Models and Constitutive Relations (Jenkins and Satake, Editor)
8. Probabilistic Approach to Mechanisms (Sandler)
9. Methods of Functional Analysis for Application in Solid Mechanics (Mason)
10. Boundary Integral Equation Methods in Eigenvalue Problems of Elastodynamics and Thin Plates (Kitahara)
11. Mechanics of Material Interfaces (Selvadurai and Voyiadjis, Editors)
12. Local Effects in the Analysis of Structures (Ladevèze, Editor)
13. Ordinary Differential Equations (Kurzweil)
14. Random Vibration—Status and Recent Developments. The Stephen Harry Crandall Festschrift (Elishakoff and Lyon, Editors)
15. Computational Methods for Predicting Material Processing Defects (Predeleanu, Editor)
16. Developments in Engineering Mechanics (Selvadurai, Editor)
17. The Mechanics of Vibrations of Cylindrical Shells (Markuš)
18. Theory of Plasticity and Limit Design of Plates (Sobotka)
19. Buckling of Structures—Theory and Experiment. The Josef Singer Anniversary Volume (Elishakoff, Babcock, Arbocz and Libai, Editors)
20. Micromechanics of Granular Materials. Proceedings of the US/Japan Seminar on the Micromechanics of Granular Materials, Sendai-Zao, Japan, October 26–30, 1987 (Satake and Jenkins, Editors)
21. Plasticity. Theory and Engineering Applications (Kaliszky)
22. Stability in the Dynamics of Metal Cutting (Chiriacescu)
23. Stress Analysis by Boundary Element Methods (Balaš, Sládek and Sládek)
24. Advances in the Theory of Plates and Shells (Voyiadjis and Karamanlidis, Editors)
25. Convex Models of Uncertainty in Applied Mechanics (Ben-Haim and Elishakoff)
26. Strength of Structural Elements (Życzkowski, Editor)

Strength of Structural Elements

Zbigniew Brzoska *Warsaw University of Technology, Warsaw, Poland*

Zbigniew Kączkowski *Warsaw University of Technology, Warsaw, Poland*

Jerzy Lipka *Warsaw University of Technology, Warsaw, Poland*

Zbigniew Olesiak *Warsaw University, Warsaw, Poland*

Michał Życzkowski *Cracow University of Technology, Cracow, Poland*

Edited by

Michał Życzkowski
Cracow University of Technology, Cracow, Poland

Preface

This volume is devoted primarily to engineering applications of mechanics of deformable solids, mainly in the elastic range. It is concerned basically with unidimensional problems, when just one dimension of a structure is significantly greater than the other two (bars, beams), or when the functions of two or three spatial variables reduce to the function of one variable (circularly-symmetric problems of cylinders, disks and plates).

Problems of this type are of twofold importance. Firstly, many engineering problems can be described with sufficient accuracy just in this way. Secondly, unidimensional problems with known analytical solutions may serve either for testing numerical methods or for the analysis of fundamental concepts and phenomena, whose physical nature in three-dimensional approach might be obscured by the analytical-numerical aspect. The simplicity of unidimensionality is sometimes illusory here: in some cases, even unidimensional problems are regarded as too complicated and the qualitative analysis is made on auxiliary objects which one could define as zerodimensional (Wagner's, Shanley's or Ziegler's models, and the like). The point should also be made that it is impossible for unidimensional problems to be separated out exactly: e.g. when it comes to the problem of elastic torsion of bars of arbitrary cross-section, partial differential equations need to be solved, and three-dimensionality effects occur even more distinctly in problems relating to stress concentration in bars.

Four parts of the present volume are devoted to bars and bar structures, specifically to statics, dynamics and stability of bars of solid cross-section and to statics and stability of thin-walled structures. Part Five is complementary in a way to these problems, it discusses stress concentrations and contact problems. Somewhat different is Part 6, in which circularly-symmetric problems of cylinders, disks and circular plates are the unidimensional problems under investigation. Included here have also been related two-dimensional axially-symmetric problems of cylinders. The authors have confined themselves for the most part to the analysis of elastic behaviour

of structures; however, in Parts 1, 3, 5 and 6, some attention has been paid to respective inelastic problems.

Beside analysis of single bars, also bar structures have been considered, admitting their arbitrary irregularity. A possible regularity of bar structures can greatly simplify calculations; problems of this type have not been examined in greater detail, but the literature on the subject, which is very extensive in Polish, has been cited. The deterministic approach has been followed in all the parts of the book; it can serve as a point of departure for stochastic approaches which are increasingly used in engineering practice.

Michał Życzkowski

1. Introduction

In keeping with the title of this part of the volume, the considerations herein are confined to statics problems. Problems relating to the dynamics and stability of bars are not considered as these are the subject matter of Parts 2 and 3. Therefore, the three parts together contain the foundations of the mechanics of bars of compact cross-section and bar structures, being a part of applied mechanics which in civil engineering is called *structural mechanics*. Structural mechanics, also including the mechanics of thin-walled bars (Part 4) and the mechanics of surface structures (treated separately), is in turn one of the fields of applied mechanics.

Contrary to its name, structural mechanics is not concerned with structures in the strict sense but analyses their static schemata, which represent a certain idealization of actual structures. All structures built of solids take up a specific amount of three-dimensional space, they are essentially three dimensional. In most cases, however, such three-dimensional bodies are replaceable by static schemata composed of bars or of surface elements. Those parts of a structure determined as bars have two transverse dimensions that are markedly smaller than the third one, i.e., the length. For surface elements, one dimension (thickness) is significantly smaller than the other two.

Under loads or other non-static actions (e.g. temperature variation), the structure experiences strains which are accompanied by corresponding states of stress. The question of causality here, in other words, the question of finding the relationships between displacements, strains and stresses, on the one hand, and external causes, on the other, is one of the fundamental problems of structural mechanics. In principle, it can be treated, for example, as a boundary problem of the theory of elasticity or plasticity. However, in practice, considering the rather complex shape of the surface confining the part of space occupied by the structure, the problem cannot possibly be solved on the grounds of strictly mathematical theories. Hence, it is necessary to introduce a number of simplifying assumptions designed to bring theory closer to engineering practice. These assumptions had been the basis of a field

of study which was the predecessor of structural mechanics and which came to be known, though not very logically, as strength of materials. Huber (1951) tried to replace it with the term engineering stereomechanics but was unsuccessful in obtaining support. The departures from exact theories introduced into strength of materials lead to numerous contradictions and inconsistencies which we should well bear in mind. They are discussed in Chapter 2.

Regarding the physical properties of materials, a linearly elastic or rigidly plastic model of a body is accepted as a rule in strength of materials and structural mechanics. The present part will be confined to the assumption that every material conforms to Hooke's linear law. The point of departure for our considerations will therefore be the linear theory of elasticity. This puts definite constraints on the magnitude of external loads; the stresses induced by them cannot be in excess of the limit of proportionality, which is determined experimentally for every material. However, since the moduli of elasticity are very high as a rule, the strains induced by stresses not exceeding the elastic limit must consequently be treated as small quantities. Assuming that the displacements are also much smaller than the dimensions of elements, we can consider equations of equilibrium neglecting both the deformations and displacements of a body. As a result of the linearity of geometric and physical relations, there is the very important and useful principle of superposition, which allows the effects of the sum of different causes to be treated as a sum of effects produced by separate causes.

Naturally, we come across structures which, due either to a high deformability of the material or to a high slenderness ratio (whippiness) of the elements, are subject to displacements or strains that can no longer be treated as small; we shall not deal with them here. Readers interested in the problem can find the relevant information in the specialist textbooks by Kachurin (1965), Perelmuter (1972) or Popov (1948). In Poland, problems relating to high deflections of very slender bars have been the concern chiefly of Waszczyszyn (1962) and Waszczyszyn and Życzkowski (1962).

The aforementioned simplifying assumptions, which are discussed in detail in Chapter 2, when used as a basis of considerations, lead in effect to a situation whereby problems which according to the theory of continuous medium are described by sets of partial differential equations, can be described in terms of bar statics by sets of ordinary differential equations. Departing from the theory of deformable media and superseding it by a deformable bar theory can be regarded as the first stage of discretization of a system; a three-dimensional body is replaced by an unidimensional object—the bar

axis, linked to which are certain global physical characteristics, displacements, loads, strains and generalized internal forces.

As noted above, strength of materials and structural mechanics are founded on mathematically exact theories, yet historically, the foundations of engineering theories had taken shape earlier than the theory of elasticity or plasticity. For example, observations concerning the properties of elastic materials in a uniaxial state of stress and the theoretical foundations of bar bending and torsion, both date to the 17th century and are associated with the names of Hooke and brothers J. and J. Bernoulli (1691, 1742). Later and until the early 19th century, strength of materials was further developed by such distinguished researchers as Young, Poisson (1811), Euler, Lagrange (1788), Navier, de Saint-Venant (1856) and Kirchhoff (1876). As for the beginnings of the general theory of elasticity, we may consider it to be dated to 1822, when Cauchy (1882) generalized Hooke's law to a three-axial state of stress.

Given below is some information and comment concerning other chapters. Chapter 2 deals with the derivation of the differential equations of equilibrium and kinematics and of the relations between static quantities and strains in straight and curved bars. It also contains formulae to determine, knowing the generalized internal forces, the stress distribution in a cross-section of a bar. In the subsequent chapters, which are no longer concerned with strength of materials but with the statics of bars and bar structures, the considerations are confined to determining generalized internal forces.

As we cease to consider single cross-sections, we must first discuss the modes of support of bars and plot diagrams of the links between elements that go into the making of bar structures. These problems are discussed in Chapter 3, in which much attention has been devoted to static determinability and kinematic invariability of bar structures. This question, presented pictorially in Chapter 3, is re-examined later in Chapter 6, wherein the static-kinematic analysis is reduced to examination of the algebraic properties of appropriate matrices.

It may be worthwhile to point out here that the concept of static determinability or indeterminability of structures is specific to bar structures. Any other structures, such as plates, disks or shells (excepting shells in membrane state) are always, regardless of the mode of support, hyperstatic. This is due to the fact that while for bars the number of differential equations of equilibrium (cf. Chapter 2) equals the number of unknown static quantities, i.e., of internal forces, occurring in these equations, in the case of surface structures and three-dimensional bodies, the number of generalized internal

forces acting is larger than the number of differential equations of equilib-
rium. Therefore, if only the boundary conditions permit, all internal forces
in a bar or in a bar structure can be determined on the equilibrium conditions
alone, this being impossible in the case of structures of any other type.

In Chapter 4, we derived the principle of virtual work for deformable
bars, regarding the differential equations of eqilibrium given in Chapter 2
as known and proved. We followed here an argumentation presented, e.g.,
by Nowacki (1952, 1954). A different derivation technique, by which the
calculus of variations is applied to the energy equation, was proposed in the
18th c. by Lagrange (1788). We did not consider other energy theorems
associated with such names as Clapeyron (1857), Menabrea (1858) or
Castigliano (1875). In doing so, we were guided not only by the confines of
the chapter, limited by necessity, but also on the grounds that the universal
character of the principle of virtual work allows also those problems to
be solved, that can be equally well solved on less general energy principles.
We can derive without difficulty Betti's fundamental principle of
reciprocal work (1872), generalized by Maizel (1951), and other particular
reciprocity theorems that follow from it.

In Chapter 5, the reader will find solutions of the sets of equations de-
rived in Chapter 2.. In this way, we are concerned no longer with a single cross-
section but instead we seek functions describing the interesting static and
kinematic quantities over bar length, which depend of course on the bound-
ary conditions. It needs to be made clear that by the general concept of bar
we understand truss members, and equally so straight bars subjected to
bending, called *beams*, and also in-plane curved bars which in the case of
load acting in the plane of the bar axis are called *arches*; but when a load is
acting perpendicularly to that plane, they are called *in–plane curved bars*.
In frameworks, we can also distinguish vertical bars, called *columns*, and
horizontal ones, called *spandrel beams*.

We have related in Chapter 2 the displacements and stresses at an arbitrary
point of the bar's cross-section to the displacements of its axis and to the
generalized internal forces, and correspondingly in Chapter 5, after solving
the ordinary differential equations, the displacements of the axis and the
internal forces to the boundary quantities. In Chapter 6, our concern is to
determine the very same discrete boundary (nodal) quantities using an appro-
priate set of algebraic equations. The sets of these equations are written
in matrix notation which is very convenient for algorithmization of compu-
tations. There is ample literature now on applications of the matrix calculus
to the statics of structures to mention only as examples the monographs
by Asplund (1964, 1966), Livesley (1964), Laursen (1966), Filin (1966),

Przemieniecki (1969), Mitropolski (1969), Maslennikov (1970) and Zurmühl and Falk (1984).

The problem of determining the degree of static indeterminability and kinematic variability of a structure, brought up again here (cf. Chapter 3), involves the investigation of the properties of one of the matrices, this being a routine operation for digital computers. Not considered are other specific techniques of investigating the kinematic invariability of a structure, suited to particular kinds of engineering structures. For example, Frąckiewicz and Legat (1967), Frąckiewicz and Lewiński (1968, 1970), and Frąckiewicz (1970), dealing with surface trusses, found that in specified cases these structures become kinematically variable, or according to the nomenclature used by these investigators, they become "singular". Incidentally, this feature has been noted earlier by Schlink (1907), Prager (1926) and others (cf. Nowacki, 1952).

Static problems concerning bar structures can be solved, generally speaking, by one of two methods: either by the direct flexibility method (force method) or the direct stiffness method (displacement method). For this reason, we have concentrated on discussing the general principles of procedure according to the two methods. All other methods are merely varieties of these two general methods and differ from each other either in notation or in the algorithm used to solve a set of canonical equations, or lastly in the type of structure, to which one of the two methods can be applied. For example, equations with the direct stiffness method can be solved iteratively by the Cross method (Cross, 1930; cf. Dašek, 1951; Błaszkowiak and Kączkowski, 1959, 1966), by the Kani method (Kani, 1954) or by the cracovian method (R. Dowgird and Z. Dowgird, 1952, 1964; Z. Dowgird, 1956). For regular bar structures we frequently use the method of differencee quations, in which usually geometric quantities are the unknowns. The method, dating to the early years of this century (Grüning, 1918; Funk, 1920; Bleich and Melan, 1927), has been revived in connection with the development of computer techniques. In Poland, it was updated by Gutkowski (1965, 1973), Gutkowski *et al.* (1980), and Frąckiewicz (1966). The theory of fibrous media, which relies on the displacement method, can also be the point of departure for static analysis of bar structures (cf. e.g., Peła and Woźniak, 1966; Woźniak, 1969, 1970).

The finite difference method in the matrix approach is used in Chapter 7 to determine the quantities of interest to us in isostatic structures, namely in a multispan hinged beam and in a truss. A number of graphic techniques were devised towards the end of the last century to determine the forces acting in truss members of isostatic trusses. Thus, using Cremona's polygon

of forces (Cremona, 1874, 1879), all members of a plane truss of special design could be determined. Culmann (1866) and Ritter (1888, 1890) developed a technique of determining the forces acting in three truss members present in the cross-section of a truss. The bar-exchange technique devised by Henneberg (1886) served to determine the forces acting in truss members where Cremona's and Ritter's method proved inapplicable. Lastly, the Williot diagram (1877) was used to determine the sideways of plane-truss joints. Graphic methods, applicable not only to static analysis of trusses, have been described in many textbooks, especially those earlier dating, both Polish (e.g., Abakanowicz, 1876; or Thullie, 1917) and others (e.g., Müller-Breslau, 1881, 1892), but also sometimes in recent literature. However, in the computer age the more labourious and less universal graphic techniques of solving static problems are being replaced more and more by analytical methods. For this reason, stopping at the above general information, none of the named (and unnamed) graphic techniques is considered in Chapter 7.

Discussions in Chapter 8 on the applications of the direct flexibility method in the analysis of statically indeterminate structures, focus on the important question of selecting the primary system. Also indicated are the possibilities of diagonalizing the matrix of a set of conditional equations of the direct flexibility method.

Chapter 9 deals wholly with the applications of the direct stiffness method in matrix approach in the static analysis of frames, assuming that the extension of bars, being negligibly small, has no effect on the internal force distribution in the structure. This assumption, which is being adopted as a rule in engineering practice, makes it possible to reduce substantially the number of geometric unknowns; moreover, some frames can be treated as immovable.

Beside problems relating to static analysis of designed structures or of actual structures, engineers may also be interested in the question of synthesis, to be understood as an algorithmized operation with the aim of designing a structure meant to be optimal in a specified sense. This is, however, an engineering problem which is as a rule outside the scope of structural statics. This is because only the minimization of the weight of a structure could be the object of theoretical static investigations. In practice, however, the main point is usually to satisfy various commercial, technological, service, insulating and aesthetic requirements, and the like, which are all unrelated to mechanics. Therefore, by merely mentioning the problem, we call attention to certain questions relating to synthesis, which are considered in Part 3 of this volume, referring the reader at the same time to studies by Wasiutyński (1956) and Wasiutyński and Brandt (1962, 1963).

Throughout the chapter, we have followed the deterministic approach

to loads and physical properties of a structural material and to the size and shape of individual elements. It should however be noted that a good many studies have been published in the past fifty years, in which problems of static analysis and safety of structures are approached in a different way, relying on probability mathematics. The harbinger of this branch of mechanics was Wierzbicki (1961_1, 1961_2). Readers interested in the problem will find a detailed survey of relevant literature as well as information on the foundations of structural mechanics in the probabilistic approach in studies by Bolotin (1968), Eimer (1963) or Murzewski (1976).

2. Bars of Solid Cross-Section

2.1. Tension and Bending of a Straight Bar

Tension and bending of a prismatic bar is sometimes considered under the theory of elasticity (cf. e.g., R. Dowgird and Z. Dowgird, 1964, p. 177), yet with far-reaching assumptions which narrow the application range of the relationships derived under this theory. We, therefore, return to the problem once more, changing at the same time some denotations and adjusting them to the convention used in the statics of structures.

Let us consider a straight bar in a right-handed coordinate system $x_1 = = x$, $x_2 = y$, $x_3 = z$. Let the x-axis coincide with the longitudinal axis passing through the centres of gravity of the cross-sections of the bar and let the y- and z-axis be the principal, central axes of inertia of a cross-section. Shown as an example in Fig. 2.1 is a bar of rectangular cross-section.
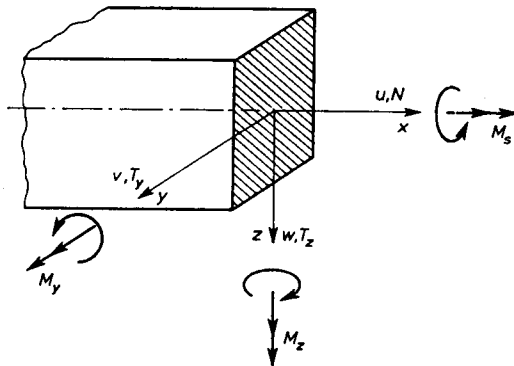

Fig. 2.1. The coordinate system

The first group of equations expresses the equilibrium conditions of an element. We arrive at these conditions based on the following argumentation. Stresses occur in the bar material, their components being the functions

of coordinates x, y, and z. Specifically, the stresses acting in the cross-section are $\sigma_{11} = \sigma_x$, $\sigma_{12} = \tau_{xy}$, $\sigma_{13} = \tau_{xz}$. Their resultants are calculated from the equations

$$N = \int_A \sigma_x \, \mathrm{d}A, \qquad T_y = \int_A \tau_{xy} \, \mathrm{d}A, \qquad T_z = \int_A \tau_{xz} \, \mathrm{d}A, \tag{2.1}$$

$$M_y = \int_A \sigma_x z \, \mathrm{d}A, \qquad M_z = -\int_A \sigma_x y \, \mathrm{d}A, \tag{2.2}$$

where A is the cross-sectional area, N is the longitudinal force, T_y and T_z are the transverse forces and M_y and M_z are the bending moments, whose positive senses are shown in Fig. 2.1. Assume that the torsion moment

$$M_t = \int_A (\tau_{xz} y - \tau_{xy} z) \, \mathrm{d}A \tag{2.3}$$

equals zero.

The resultant external loads acting on the axis of the bar have components as shown in Fig. 2.2. The loads p_x, p_y, p_z are expressed in force units per

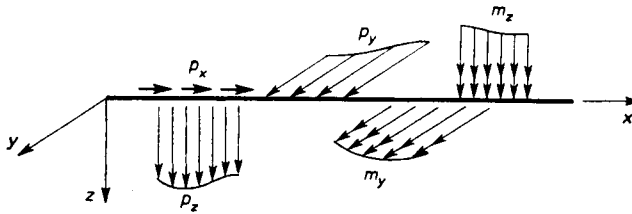

Fig. 2.2. Components of loading of the bar

unit length [N/m] and the loadings, at moments m_y, m_z, in moment units per unit length, i.e., in force units [N]. An element of the considered bar axis of length $\mathrm{d}x$ is under the action of the generalized forces indicated in Fig. 2.3. The equilibrium conditions for all the forces and moments lead to the following static, differential relations:
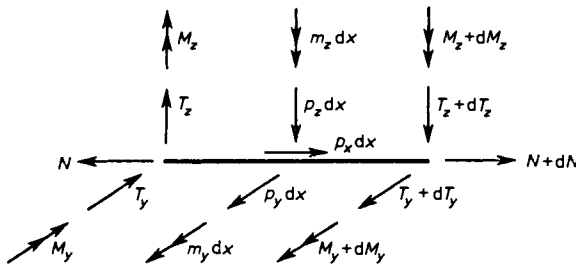

Fig. 2.3. Generalized forces acting on bar element

$$\frac{dN}{dx} + p_x = 0, \qquad \frac{dT_y}{dx} + p_y = 0, \qquad \frac{dT_z}{dx} + p_z = 0, \tag{2.4}$$

$$\frac{dM_y}{dx} - T_z + m_y = 0, \qquad \frac{dM_z}{dx} + T_y + m_z = 0, \tag{2.5}$$

their number being equal to the number of unknowns in (2.1) and (2.2).

The second group of equations is represented by geometric relations between strains and displacements. As for the displacement fields, we preassume that the displacements of individual points of a body can be expressed by three functions of variable x:

$$u(x, y, z) = u(x, 0, 0) - y\frac{dv(x, 0, 0)}{dx} - z\frac{dw(x, 0, 0)}{dx}, \tag{2.6}$$

$$v(x, y, z) = v(x, 0, 0), \qquad w(x, y, z) = w(x, 0, 0). \tag{2.7}$$

Functions dependent only on variable x will be denoted in shorter form omitting the arguments:

$$f(x, 0, 0) = f. \tag{2.8}$$

The assumptions concerning the displacement field, equations (2.6) and (2.7), constitute a mathematical expression of Bernoulli's assumptions, which is fundamental to the theory of bending of bars. According to them, when a bar is under tension or undergoing bending, its cross-sections (a) remain plane, (b) remain perpendicular to the axis of the deformed bar and (c) do not undergo deformation in their plane. Indeed, calculating the strains from the relations given, for example, by Mossakowska *et al.* (1978, p. 23):

$$\varepsilon_x(x, y, z) = \varepsilon_{11}(x, y, z) = \frac{du}{dx} - y\frac{d^2v}{dx^2} - z\frac{d^2w}{dx^2}, \tag{2.9}$$

$$\varepsilon_y(x, y, z) = \varepsilon_z(x, y, z) = 0,$$

$$\gamma_{yz}(x, y, z) = 2\varepsilon_{23}(x, y, z) = 0,$$

$$\gamma_{xy}(x, y, z) = \gamma_{xz}(x, y, z) = 0, \tag{2.10}$$

we find that all Bernoulli's assumptions are satisfied.

Introducing the notations:

$$\varepsilon = \varepsilon_x(x, 0, 0) = \frac{du}{dx}, \qquad \varkappa_y = -\frac{d^2w}{dx^2}, \qquad \varkappa_z = \frac{d^2v}{dx^2}, \tag{2.11}$$

we write equation (2.9) more briefly:

$$\varepsilon_x(x, y, z) = \varepsilon - y\varkappa_z + z\varkappa_y. \tag{2.12}$$

The symbol ε denotes the extension of the bar axis and $\varkappa_y$, $\varkappa_z$—its curvatures or rather their approximate values, calculated from the linearized equations (2.11).

The last group of equations express the relations between static and kinematic quantities. In stress calculations, we use the assumption

$$\sigma_y(x, y, z) = \sigma_z(x, y, z) = 0, \tag{2.13}$$

which is not contradictory to the previously determined state of strain (2.9), (2.10) only for a body with Poisson's ratio ν equalling zero.

Considering the possible occurrence of distortional strains ε^0, $\varkappa_y^0$, $\varkappa_z^0$ due to non-static factors (e.g. temperature increase), we determine the stresses in the bar according to Hoocke's law:

$$\sigma_x(x, y, z) = E[\varepsilon - \varepsilon^0 - y(\varkappa_z - \varkappa_z^0) + z(\varkappa_y - \varkappa_y^0)], \tag{2.14}$$

$$\tau_{yz}(x, y, z) = \tau_{xy}(x, y, z) = \tau_{xz}(x, y, z) = 0, \tag{2.15}$$

where E stands for Young's modulus.

Knowing the stress distribution σ_x in the cross-section of the bar, we can calculate from eqs. (2.1) and (2.2) the values of some of the generalized internal forces:

$$N = EA(\varepsilon - \varepsilon^0),$$
$$M_y = EJ_y(\varkappa_y - \varkappa_y^0), \tag{2.16}$$
$$M_z = EJ_z(\varkappa_z - \varkappa_y^0).$$

The symbols:

$$A = \int_A \mathrm{d}A, \quad J_y = \int_A z^2 \mathrm{d}A, \quad J_z = \int_A y^2 \mathrm{d}A \tag{2.17}$$

introduced here denote the crross-sectional area and the principal, central moments of inertia, respectively.

From the relation (2.16) we can easily find the deformations of the bar axis:

$$\varepsilon = \frac{N}{EA} + \varepsilon^0, \quad \varkappa_y = \frac{M_y}{EJ_y} + \varkappa_y^0, \quad \varkappa_z = \frac{M_z}{EJ_z} + \varkappa_z^0, \tag{2.18}$$

so that after substituting them into eq. (2.14) we arrive at the relationship between the stresses σ_x and the generalized cross-sectional forces:

$$\sigma_x(x, y, z) = \frac{N}{A} + \frac{M_y}{J_y} z - \frac{M_z}{J_z} y. \tag{2.19}$$

The zeroing of the shear stresses (2.15), calculated based on the kinematic assumptions and Hooke's law, might lead to the conclusion that the transverse forces $(2.1)_{2,3}$ equal zero. However, since such a conclusion would involve contradictions in the set of equilibrium equations (2.4), (2.5), we drop the previously accepted Bernoulli's assumptions and disregard satisfying Hooke's

law. But, to find the shear stress distribution in the cross-section, we do use the equilibrium equations, since we consider satisfying them, if only in integral sense, to be a sine qua non.

We, therefore, carry the following argumentation (cf. e.g. Brzoska, 1972, p. 116). An element of the bar bounded by two cross-sections dx apart is again divided into two parts with a cross-section parallel to the x-y plane, located at distance z from this plane (Fig. 2.4a). In order not to complicate
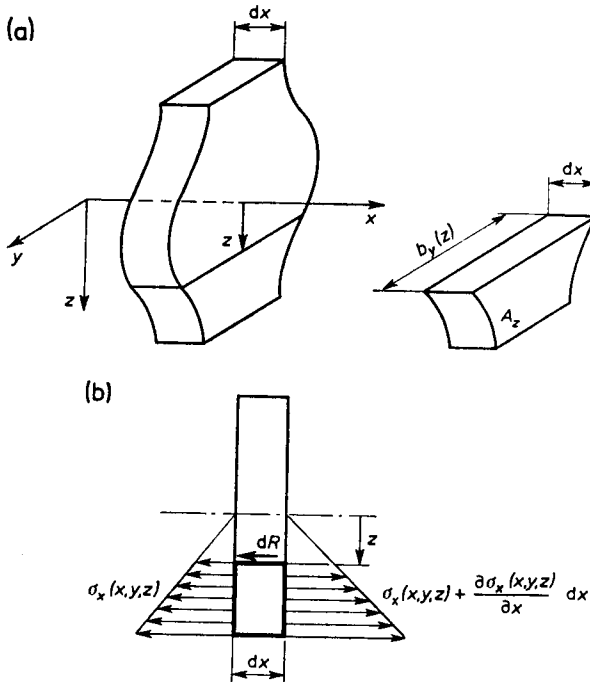

Fig. 2.4. Stress distribution in bar subjected to bending

things, let us assume that in the absence of loads m_y, stresses $\sigma_x(x, y, z)$, derived only from the bending moment M_y, are acting on the element. Their distribution projected onto the x-z plane is shown in Fig. 2.4b.

These stresses give a resultant oriented along the x-axis; the value of that resultant is

$$dR = \int_{A_z} \frac{\partial \sigma_x}{\partial x} \, dx \, dA, \tag{2.20}$$

where A_z stands for the part of the cross-sectional area situated beneath the coordinate z (Fig. 2.4a). Assuming that the shear stresses $\tau_{zx} = \tau_{xz}$,

whose resultant is a force dR, are uniformly distributed on the surface $b_y(z)\,dx$ we obtain

$$\tau_{xz} = \frac{1}{b_y(z)} \int_{A_z} \frac{\partial \sigma_x}{\partial x}\, dA. \tag{2.21}$$

Suffice to use Eqs. (2.19) and (2.5)$_1$ with the aforementioned assumptions to arrive at the following dependence of the shear stresses on the transverse force:

$$\tau_{xz} = \frac{T_z S_y}{J_y b_y}. \tag{2.22}$$

In this equation:

$$S_y = \int_{A_z} z\,dA \tag{2.23}$$

is the static moment of the part of the cross-section denoted by A_z, calculated with respect to the x-y plane, and b_y is the width of the cross-section measured parallel to the y-axis at distance z from the centre of the cross-section.

The analogous equation:

$$\tau_{xy} = \frac{T_y S_z}{J_z b_z} \tag{2.24}$$

requires no additional comment.

Going back to Hooke's law, we can now easily determine the expressions for angular (shear) strains

$$\gamma_{xy} = \frac{T_y S_z}{GJ_z b_z}, \qquad \gamma_{zz} = \frac{T_z S_y}{GJ_y b_y}. \tag{2.25}$$

In these expressions G stands for Kirchhoff's modulus.
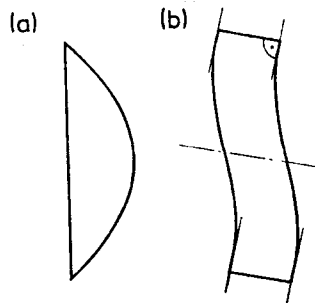

Fig. 2.5. Shear strains of bar element

Here, we run into a successive contradiction with the initial assumptions. From Eqs. (2.22)–(2.25) it follows that the shear stresses and the shear strains which are proportional to them, change at the cross-section level in the manner indicated schematically in Fig. 1.5a. As a result, an element of the bar of volume $A\,dx$ deformed in the way shown in Fig. 2.5b. Maximum shearing strains occur at near half the height of the element, whereas at the extreme fibres they equal zero. As we can see, contrary to Bernoulli's assumptions the cross-section of the bar remains neither plane nor perpendicular to the bar axis. For this reason we present in Section 5.2a beam bending theory involving shear forces, which is based on weaker simplifying assumptions.

The relations derived above, although they refer in principle to a prismatic bar, are also applicable to bars of a slightly variable cross-section. Using the above classical theory of bending of bars, we have to bear in mind that it is an engineering theory. Its assumptions lead to the indicated contradictions and inconsistencies with the mathematical, exact theory of elasticity. The lower the ratio of the transverse dimensions of a bar to its length is, the smaller the errors arising here will be.

2.2. Torsion of a Straight Bar

The classical de Saint-Venant's torsion theory can be taken to be exact only in a very special case, namely in the absence of stresses on the side surface of a prismatic bar and in the presence of such a support of the cross-sections at both ends of the bar that does not restrain their displacements in a direction parallel to the axis of the bar. Knowing the approximate character of this solution, should the named assumptions not be met, we shall use it nevertheless also when the bar is loaded in a more general manner.
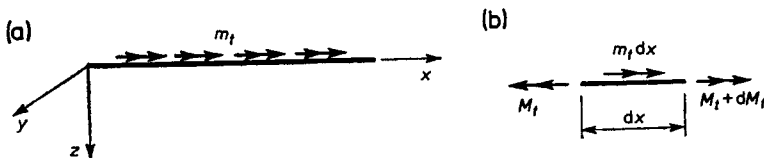

Fig. 2.6. Loadings acting on bar subjected to torsion

Our concern will therefore be a straight bar, not necessarily prismatic, loaded in the manner indicated in Fig. 2.6a. An element of length dx (Fig. 2.6b) will be in equilibrium, if the following equation is satisfied:

$$\frac{dM_t}{dx} + m_t = 0. \tag{2.26}$$

We assume that only shear stresses τ_{xy}, τ_{xz} which together with the twisting moment M_t involved in the relation (2.3), occur under torsion. Consequent upon this assumption is the disappearance of all strains except γ_{xy}, γ_{xz}. Hence, it further follows that a cross-section does not become deformed in its plane and experiences only warping; in other words, it loses its planar shape. Displacements of points of the cross-section in its plane are expressed by linear functions in terms of the coordinates y, z:

$$
\begin{aligned}
v(x, y, z) &= v(x, 0, 0) - z\varphi_t(x), \\
w(x, y, z) &= w(x, 0, 0) + y\varphi_t(x).
\end{aligned}
\tag{2.27}
$$

In these equations, $\varphi_t(x)$ denotes the angle of rotation of the cross-section about the x-axis.

In the absence of stresses σ_x and because body forces X are neglected, the first of the partial equilibrium equations (cf. Huber, 1949, Vol. I, p. 74)

$$
\frac{\partial \sigma_x}{\partial x} + \frac{\partial \tau_{xy}}{\partial y} + \frac{\partial \tau_{xz}}{\partial z} + X = 0
\tag{2.28}
$$

reduces to the form

$$
\frac{\partial \tau_{xy}}{\partial y} + \frac{\partial \tau_{xz}}{\partial z} = 0.
\tag{2.29}
$$

The equation will be satisfied in an identical manner if we express the stresses by derivatives of the stress function ψ:

$$
\tau_{xy} = \frac{\partial \psi}{\partial z}, \qquad \tau_{xz} = -\frac{\partial \psi}{\partial y}.
\tag{2.30}
$$

Hence, the shearing strains γ_{xy}, γ_{xz}, considering Eqs. (2.27), depend on the stress function in the following manner:

$$
\begin{aligned}
\gamma_{xy} &= \frac{\partial u(x, y, z)}{\partial y} + \frac{dv}{dx} - z\varkappa_t = \frac{1}{G} \frac{\partial \psi}{\partial z} + \gamma_{xy}^0, \\
\gamma_{xz} &= \frac{\partial u(x, y, z)}{\partial z} + \frac{dw}{dx} + y\varkappa_t = -\frac{1}{G} \frac{\partial \psi}{\partial y} + \gamma_{xz}^0.
\end{aligned}
\tag{2.31}
$$

The symbol

$$
\varkappa_t = \frac{d\varphi_t}{dx}
\tag{2.32}
$$

denotes unit twist of bar, G is Kirchhoff's modulus and $\gamma_{xy}^0 = -z\varkappa_t^0$, $\gamma_{xz}^0 = y\varkappa_t^0$ are distortional shear strains which we treat as functions of distortional twisting $\varkappa_t^0$, being a kind of twist independent of static loads.

By differentiating the first of the equations of the set (2.31) with respect to z and the second with respect to y, and by subtracting them by sides, we obtain the following differential equation for the stress function:

$$\nabla^2 \psi = -2G(\varkappa_t - \varkappa_t^0),$$ (2.33)

where

$$\nabla^2 = \frac{\partial^2}{\partial y^2} + \frac{\partial^2}{\partial z^2}.$$ (2.34)

In the case of a single-connected cross-section the boundary condition that should be satisfied by the ψ-function on contour of the cross-section is (cf. Mossakowska *et al.*, 1978, p. 183)

$$\psi = 0.$$ (2.35)

We, therefore, have to solve the Poisson's differential equation (2.33) with the boundary condition (2.35). It cannot, however, be solved not knowing the twist of the rod $\varkappa_t$ or the twisting moment M_t which depends on torsion angle in the following manner:

$$M_t = GJ_t(\varkappa_t - \varkappa_t^0).$$ (2.36)

The symbol J_t introduced here is the geometric torsional rigidity of a cross-section and has the dimension of the moment of inertia [m⁴].

We obtain the additional condition required to calculate the missing quantities by proceeding from the definition of the twisting moment (2.3). Substituting into Eq. (2.3) the expression (2.30), we get

$$M_t = -\int_A \left(y\frac{\partial \psi}{\partial y} + z\frac{\partial \psi}{\partial z} \right) dA.$$ (2.37)

It is easily demonstrated that because of the boundary condition (2.35) the expression (2.37) can be transformed into

$$M_t = 2\int_A \psi \, dA.$$ (2.38)

In this way, we have obtained all the necessary elements to determine the twisting moment M_t, the twist $\varkappa_t$ and the stress distribution within the cross-section. It is seen that unlike the previously considered cases, to determine the stresses acting in a torsioned bar, a partial differential equation needs to be solved. This is a single operation which consists of finding a ψ-function corresponding to a given shape of the cross-section.

In the special case of a bar of symmetrical circular cross-section, the geo-

metric torsional rigidity J_t equals the polar moment of inertia of the cross-section, whereas the shear stresses are calculated using the equations:

$$\tau_{xy} = -\frac{M_t}{J_t} z, \qquad \tau_{xz} = \frac{M_t}{J_t} y. \tag{2.39}$$

This is the only case where torsion does not cause warping of the cross-section.

In the more general case of a bar of elliptic cross-section we have

$$J_t = \frac{b^3 c^3}{b^2 + c^2},$$

$$\tau_{xy} = -\frac{M_t}{J_t} \frac{2b^2}{b^2 + c^2} z,$$

$$\tau_{xz} = \frac{M_t}{J_t} \frac{2c^2}{b^2 + c^2} y, \tag{2.40}$$

where b and c stand for the lengths of the semi-axes of the ellipse, running parallel to the y- and z-axis, respectively.

More information on the question of torsion of bars of other cross-sections can be found in studies by Aratyunyan and Abramyan (1963) and Sokolnikoff (1956), and in many textbooks on strength of materials.

2.3. In-Plane Curved Bar

Let us consider a bar with a curved axis lying in the x-y plane. We introduce additional coordinates s, n associated with the bar axis (Fig. 2.7) and assume moreover that the axis n is one of the principal, centroidal axes of inertia
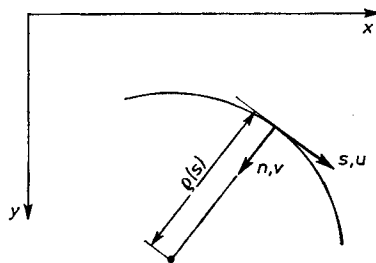

Fig. 2.7. Bar curved in plane xy

of the cross-section. The radius curvature of the bar axis ϱ is a function of the coordinate s.

We shall now consider a bar loaded in its plane and separately a bar under a load perpendicular to its plane. First, let the loads p_s, p_n, m_z, indicated in
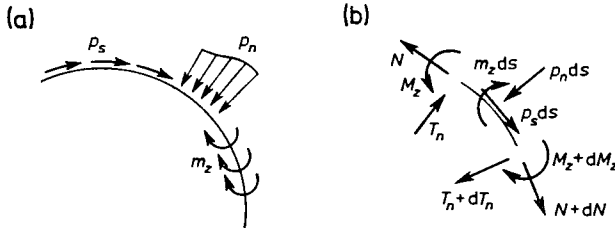
Fig. 2.8. In-plane loadings of bar

Fig. 2.8a, be acting on the bar under consideration. These loads together with the accompanying internal forces (Fig. 2.8b) satisfy the following equations of equilibrium:

$$\frac{dN}{ds} - \frac{T_n}{\varrho} + p_s = 0,$$

$$\frac{dT_n}{ds} + \frac{N}{\varrho} + p_n = 0,$$

$$\frac{dM_z}{ds} + T_n + m_z = 0. \tag{2.41}$$

Wanting to find the dependence of stress on cross-sectional forces, we assume such a displacement field of the rod that would satisfy all Bernoulli's assumptions. Hence, we assume that displacements $u(s, n, z)$ and $v(s, n, z)$
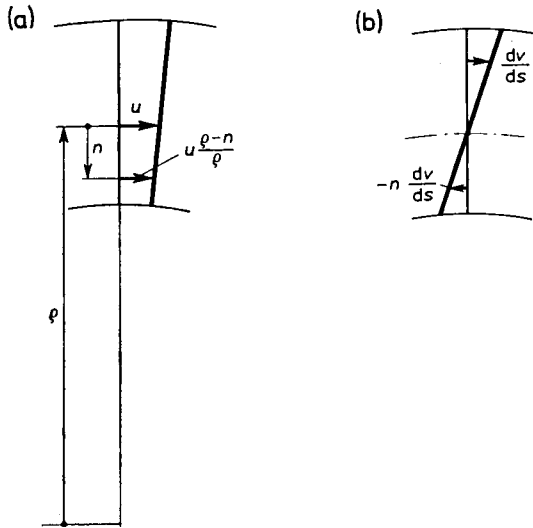

Fig. 2.9. Cross-sectional displacements of curved bar

at an arbitrary point of the bar are described by two functions u and v, which
depend only on the variable s:

$$u(s, n, z) = u\frac{\varrho - n}{\varrho} - \frac{\mathrm{d}v}{\mathrm{d}s}n, \quad v(s, n, z) = v(s). \tag{2.42}$$

The distribution of displacements $u(s, n, z)$ at the cross-section height accom-
panying the axis displacement u is given in Fig. 2.9a, and those induced by
the angle of rotation $\mathrm{d}v/\mathrm{d}s$, are given in Fig. 2.9b. In this particular case,
the axis of the bar does not pass through the centres of gravity of the cross-
sections but is shifted with respect to them by a certain segment η_0, which
we determine below from the static condition.

The displacements (2.42) are accompanied by longitudinal strains, only

$$\varepsilon_s(s, n, z) = \frac{\varrho}{\varrho - n}\left[\left(\frac{\mathrm{d}u}{\mathrm{d}s} - \frac{v}{\varrho}\right) - n\left(\frac{\mathrm{d}^2 v}{\mathrm{d}s^2} + \frac{\mathrm{d}}{\mathrm{d}s}\left(\frac{u}{\varrho}\right)\right)\right]. \tag{2.43}$$

Hence, the stresses $\sigma_s(s, n, z)$ are

$$\sigma_s(s, n, z) = \frac{E\varrho}{\varrho - n}(\varepsilon - n\varkappa_z), \tag{2.44}$$

where

$$\varepsilon = \frac{\mathrm{d}u}{\mathrm{d}s} - \frac{v}{\varrho}, \quad \varkappa_z = \frac{\mathrm{d}^2 v}{\mathrm{d}s^2} + \frac{\mathrm{d}}{\mathrm{d}s}\left(\frac{u}{\varrho}\right) \tag{2.45}$$

express the relative extension and the curvature increment of the bar axis.
The equations (2.45) are a generalization of the relations (2.11) which apply
to strains in a straight bar.

The position of the bar axis is determined from the condition that the longi-
tudinal force N does not depend on the curvature increment $\varkappa_z$. Hence,
it must be

$$\int_A \frac{n}{\varrho - n}\,\mathrm{d}A = 0. \tag{2.46}$$

The following relations occur between the coordinates n measured from the
bar axis and η measured from the centre of gravity, on the one hand, and the
radii ϱ and r stretching to the bar axis and to the centre of gravity, respect-
ively, (Fig. 2.10) on the other:

$$\varrho = r - \eta_0, \quad n = \eta - \eta_0. \tag{2.47}$$

Using these relations, we obtain

$$\int_A \frac{\eta}{r - \eta}\,\mathrm{d}A = \eta_0 \int_A \frac{\mathrm{d}A}{r - \eta} = \psi A. \tag{2.48}$$
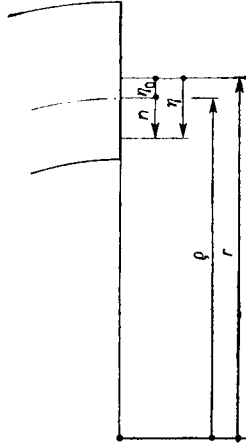
Fig. 2.10. Denotations of geometrical quantities

The parameter

$$\psi = \frac{1}{A} \int_A \frac{\eta}{r-\eta} \, dA \tag{2.49}$$

depends on the shape of the cross-section and on the magnitude of the radius r. For example, for a rectangle of height h, we derive the formula (cf. Huber, 1951, Part III, p. 26)

$$\psi = \frac{r}{h} \ln \frac{r+h/2}{r-h/2} - 1, \tag{2.50}$$

and for a circular cross-section of radius a:

$$\psi = \frac{r - \sqrt{r^2 - a^2}}{r + \sqrt{r^2 - a^2}}. \tag{2.51}$$

Integrating the stresses (2.44) over the entire cross-section, we obtain the value of the longitudinal force:

$$N = EA\varepsilon. \tag{2.52}$$

As for the bending moment M_z, considering the relation (2.46), it is

$$M_z = -\int_A \sigma_s n \, dA = E\varrho \int_A \frac{n^2}{\varrho - n} \, dA \varkappa_z. \tag{2.53}$$

The integral presented here is easily calculated taking into account the relations (2.46) and (2.47)$_2$; finally:

$$M_z = EA\varrho\eta_0 \varkappa_z. \tag{2.54}$$

Having determined the strains ε and $\varkappa_z$ from equations (2.52) and (2.54), we arrive at the following relationship between the stress σ_s and the generalized internal forces:

$$\sigma_s(s, n, z) = \frac{\varrho}{\varrho - n}\left(\frac{N}{A} - \frac{M_z}{A\varrho\eta_0}n\right). \tag{2.55}$$

Plots of the stresses induced by the generalized internal forces N and M_z, brought over to the shifted bar axis, are depicted in Fig. 2.11.
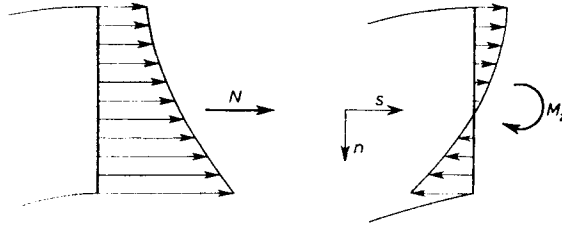

Fig. 2.11. Stress distributions in curved bar

Taking into account the distortional strains ε^0 and $\varkappa_z^0$, Eqs. (2.52) and (2.54) for internal forces can be generalized:

$$N = EA(\varepsilon - \varepsilon^0), \quad M_z = EA\varrho\eta_0(\varkappa_z - \varkappa_z^0). \tag{2.56}$$

We use the equations just derived above only when we deal with a strongly curved bar, i.e., a bar whose cross-section is of a size comparable to the radius of curvature. In the case of slightly curved bars, it is assumed that the coordinate n measured within the cross-section is very small in relation to the radius of curvature ϱ. The obvious corollary is that the line joining the centres of gravity of the cross-sections ($\eta_0 = 0$) can be regarded again as the bar axis. The product $A\varrho\eta_0$ becomes then equal to the moment of inertia:

$$A\varrho\eta_0 = \int_A \frac{\varrho n^2}{\varrho - n}\,\mathrm{d}A \cong \int_A n^2\mathrm{d}A = J_z, \tag{2.57}$$

and the stress distribution σ_s (Fig. 2.11) becomes linear, in keeping with the formula

$$\sigma_s = \frac{N}{A} - \frac{M_z}{J_z}n. \tag{2.58}$$

The shear stress distribution in the cross-section is determined from an equation of type (2.24).

Let us consider in turn a bar loaded from the plane. The forces acting on an element cut out of the bar considered (Fig. 2.12) should satisfy the following conditions of equilibrium:
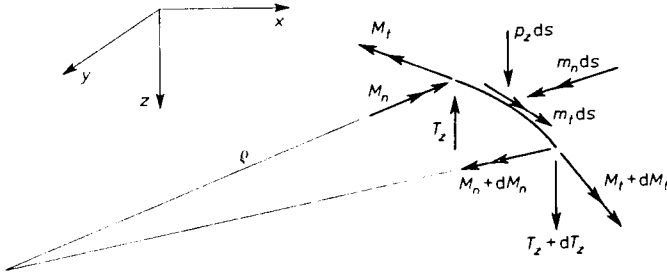

Fig. 2.12. Vertical loadings to bar plane

$$\frac{dT_z}{ds} + p_z = 0,$$

$$\frac{dM_n}{ds} + \frac{M_t}{\varrho} - T_z + m_n = 0, \tag{2.59}$$

$$\frac{dM_t}{ds} - \frac{M_n}{\varrho} + m_t = 0.$$

As for displacements, we assume for the time being that the cross-sections do not suffer warping. As a result, the displacements $u(s, n, z)$, $v(s, n, z)$ and $w(s, n, z)$ of individual points of the rod can be expressed by two functions, w and φ_t, of variable s:

$$u(s, n, z) = -\frac{dw}{ds} z,$$

$$v(s, n, z) = -\varphi_t z, \tag{2.60}$$

$$w(s, n, z) = w + \varphi_t n.$$

These displacements are accompanied by strains:

$$\varepsilon_s(s, n, z) = \frac{z}{\varrho - n}\left(\varphi_t - \varrho \frac{d^2 w}{ds^2}\right),$$

$$\gamma_{sn}(s, n, z) = -\frac{z}{\varrho - n}\left(\frac{dw}{ds} + \varrho \frac{d\varphi_t}{ds}\right), \tag{2.61}$$

$$\gamma_{sz}(s, n, z) = \frac{n}{\varrho - n}\left(\frac{dw}{ds} + \varrho \frac{d\varphi_t}{ds}\right)$$

and stresses:

$$\sigma_s(s, n, z) = \frac{E\varrho z}{\varrho - n} (\varkappa_n - \varkappa_n^0),$$

$$\tau_{sn}(s, n, z) = -\frac{G\varrho z}{\varrho - n} (\varkappa_t - \varkappa_t^0), \tag{2.62}$$

$$\tau_{sz}(s, n, z) = \frac{G\varrho n}{\varrho - n} (\varkappa_t - \varkappa_t^0),$$

where

$$\varkappa_n = -\frac{\mathrm{d}^2 w}{\mathrm{d}s^2} + \frac{\varphi_s}{\varrho}, \qquad \varkappa_t = \frac{\mathrm{d}\varphi_t}{\mathrm{d}s} + \frac{1}{\varrho} \frac{\mathrm{d}w}{\mathrm{d}s}. \tag{2.63}$$

The curvature $\varkappa_n$ and the torsion $\varkappa_t$ are expressed by Eqs. (2.63) which are a generalization of Eqs. (2.11)$_2$ and (2.32). In Eqs. (2.62), we have considered the possibility of distortional strains $\varkappa_n^0$ and $\varkappa_t^0$ occurring.

We confine ourselves in this case to considering a bar of small curvature. Therefore, using the simplifying assumption

$$n \ll \varrho, \tag{2.64}$$

we calculate the bending and twisting moments from the equations

$$M_n = \int_A \sigma_s z \, \mathrm{d}A = E J_n (\varkappa_n - \varkappa_n^0),$$

$$\tag{2.65}$$

$$M_t = \int_A (\tau_{sz} n - \tau_{sn} z) \mathrm{d}A = G J_t (\varkappa_t - \varkappa_t^0).$$

Hence, the stress σ_s can be calculated from the relation

$$\sigma_s(s, n, z) = \frac{M_n}{J_n} \frac{\varrho z}{\varrho - n} \cong \frac{M_n}{J_n} z. \tag{2.66}$$

As far as the shear stresses are concerned, we avail ourselves of the argumentation given in Section 2.2, because the relations (2.62)$_{2,3}$ are applicable only to a rotationally symmetrical section. The shear stresses will be the sum of stresses due to the twisting moment and the transverse force. We calculate the former from Eqs. (2.30), and the latter from (2.22).

3. Fundamental Static-Kinematic Analysis of Bar Structures

3.1. Elements and Their Connections

For the purpose of a fundamental static-kinematic analysis of a skeletal structure, we assume that all its elements are undeformable. In the present chapter, we shall regard as elements of a bar structure single bars, straight or curved, or else such single-branch (Fig. 3.1a) or branched (Fig. 3.1b) bar
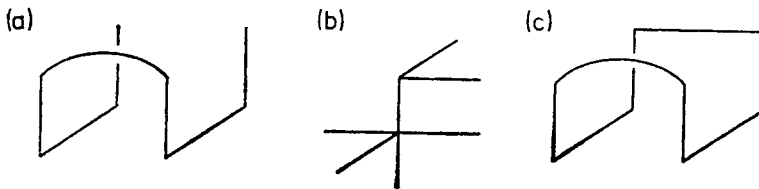
Fig, 3.1. Bar systems: (a) single-branch; (b) branched; (c) closed

systems that contain no hinged joints and make no closed circuits (Fig. 3.1c). In the latter case, only after cutting the circuit do we obtain a bar system which can be treated as an element.

The elements of a bar structure are connected in various ways to the foundation (likewise to be treated as an undeformable body) or to other elements. A joint preventing any relative displacements between two jointed parts of a structure is called a *rigid joint*, and when one of the parts is the foundation, it is called a *fixed support*. A diagram of such a connection is given as two variants in Figs. 3.2a, b. Since a rigid body has six degrees of freedom in space,

Fig. 3.2. Rigid connection

consequently, six connectors are consequently required to immobilize it.
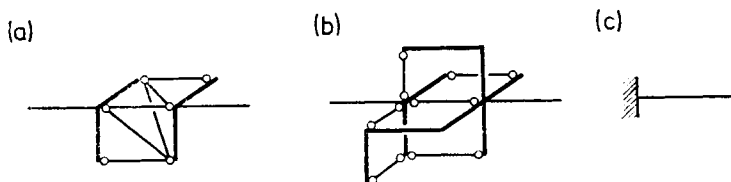Each of the connectors deprives the element of one degree of freedom. For
this reason, six connectors will always be found in every rigid joint. If an
element is fixed to the foundation, this is symbolically indicated as shown
in Fig. 3.2c.
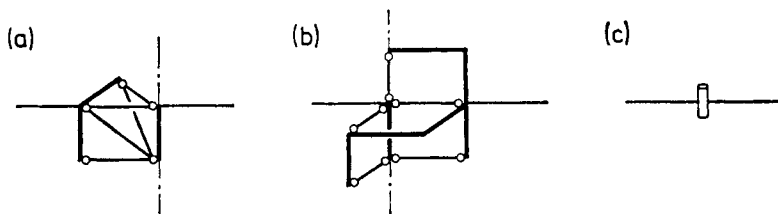
Fig. 3.3. Cylindrical hinge

Figures 3.3a, b show diagrams of a cylindrical hinge whose axis runs
parallel to the z-axis. This particular hinge requires five connectors, thus
leaving the elements with one degree of freedom, i.e., the elements are allowed
to rotate about the axis of the articulated joint. A cylindrical articulation is
denoted symbolically as shown in Fig. 3.3c.
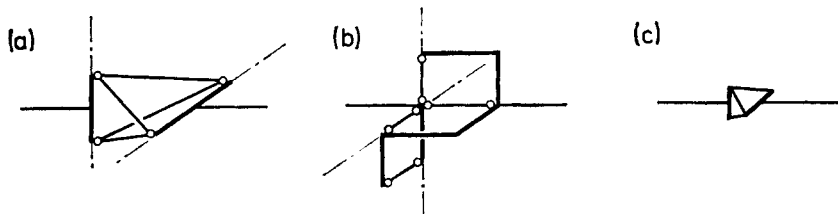
Fig. 3.4. Cardan universal joint

A Cardan joint requires as indicated in Figs. 3.4a, b, four connectors.
This leaves the elements free to rotate against each other about two axes
perpendicular to the bar axis. The symbol for this type of joint is shown
in Fig. 3.4c.
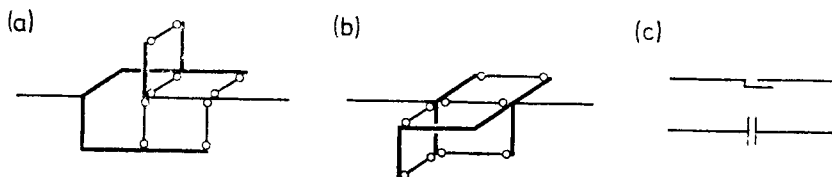
Fig. 3.5. Telescopic joint

Presented in Fig. 3.5 are diagrams and the symbol of the so-called *tele-scopic joint* which does not allow the jonted elements to rotate against each other about the axes of mutual sidesways. Figure 3.6 shows a variation of

(a)   (b)   (c)
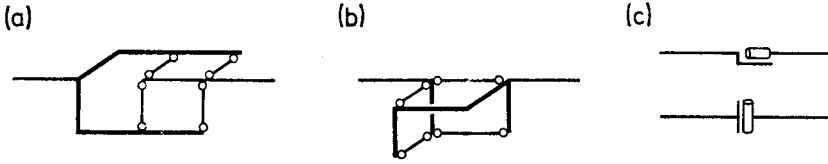
Fig. 3.6. Telescopic-hinged joint

the telescopic joint, in which the rotation of the elements against each other is not constrained in any way.

Lastly, Figs. 3.7a and b show diagrams of a *spherical joint* with three connectors. Such an articulated joint, whose symbols are given in Fig. 3.7c,

(a)   (b)   (c)
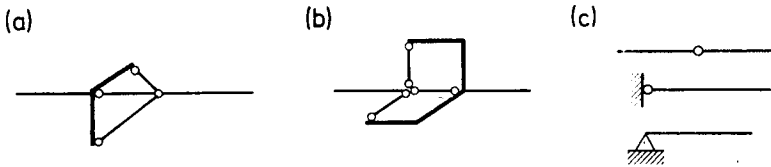
Fig. 3.7. Spherical joint

(a)

(b)

(c)

(d)
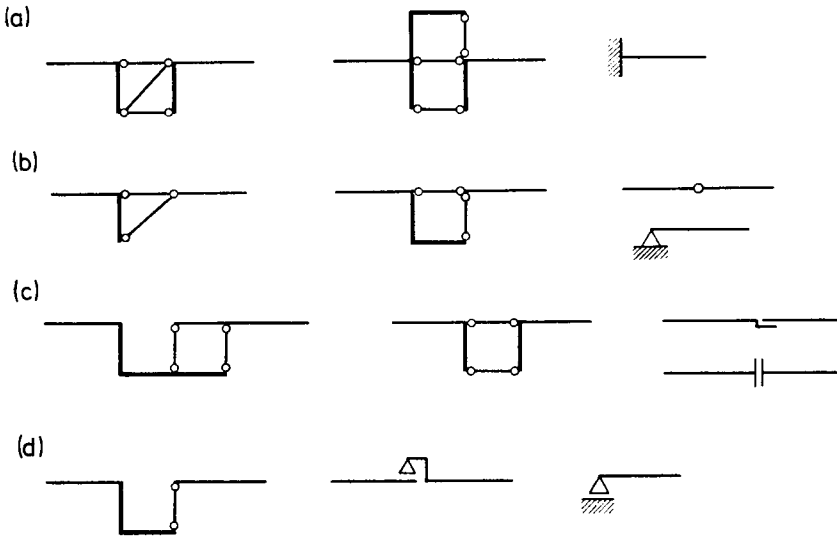
Fig. 3.8. Joints in a plane system: (a) rigid; (b) hinged; (c) telescopic; (d) hinged-slip

allows the two jointed elements to rotate against each other about all three axes.

For the diagrams to be plotted it is necessary to introduce, as seen in the drawings, appropriate branchings at the ends of the jointed elements. This is tantamount to taking into account the transverse dimensions of the jointed bars.

In the case of plane bar structures, each element has only three degrees of freedom in the plane of the structure. Consequently, joints in plane structures are correspondingly simpler. Diagrams and the symbolic connotations of joints of rigid, hinged, telescopic and hinged-slip type, are shown in Fig. 3.8.

A spherical or cylindrical joint can connect more than two elements. If, for example, m elements are involved, we then treat the joint as $(m-1)$-fold. This folllows from the fact that for m elements meeting at a single joint to be

(a)   (b)
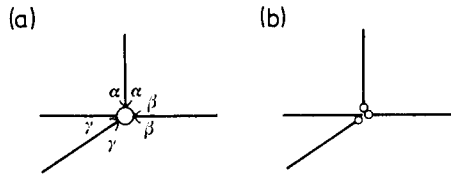
Fig. 3.9. Multiple joint

separated from each other, it is enough to make $m-1$ cross-sections. Figure 3.9a gives as an example an articulated joint connecting four elements and Fig. 3.9b, an equivalent set for three single articulations.

3.2. The Static-Kinematic Discriminant

To analyse a bar structure in static-kinematic terms, we must first divide it into elements in the manner indicated in Figs. 3.1a and b. To this end, we cut the connectors between adjoining elements, and between the bar elements and the foundation, although cross-sectioning in the latter case is not always necessary. For, if we have a bar element build in the foundation, we can treat it as a kind of extension of the rigid foundation.

The overall number of connectors that have to be cut to divide a structure into elements is denoted by t and the number of elements thus set free, by e. Each of the elements now has h degrees of freedom with $h = 6$, when a three-dimensional problem is involved, and $h = 3$, when we deal with a two-dimensional problem. Hence, to immobilize all the bar elements in space or in plane, we need he connectors.

The difference between the number of connectors actually out and the number of connectors necessary to immobilize all the elements we denote by the letter n:

$$n = t - he. \tag{3.1}$$

If the number n is positive, more connectors are then present in the structure than are necessary to immobilize all the elements, consequently the structure or at least part of it is over-rigid. If n is negative, the number of connectors in the structure is then insufficient to immobilize all the elements and at least part of the structure is then kinematically variable. For $n = 0$, we may deal either with a kinematically invariable system or with a system having one part over-rigid and the other kinematically variable.

A structural analysis can also be approached in static terms, instead of kinematic. There is in each of the connectors an unknown axial force involved. The forces acting on each of the separated stiff elements must satisfy h equilibrium conditions. We have, therefore, combined he equilibrium conditions, in which we have t unknown forces acting in the cut connectors. The number n in Eq. (3.1) can thus be treated as the difference between the number of static unknowns and the number of equilibrium equations. Owing to the two interpretations of n, we shall call that number the *static-kinematic discriminant* of a bar structure.

If n is a positive number, then the static conditions will not suffice to calculate the unknown forces. It is therefore certain that at least part of the structure can be regarded as statically indeterminate. It is that same part which we have defined above as over-rigid. When the static-kinematic discriminant is negative, the number of equations is higher than the number of unknowns and at least part of the structure is out of equilibrium. That part is the kinematically variable part. Finally, for $n = 0$, the number of equilibrium equations equals the number of unknowns. In other words, the structure as a whole can be statically determinate and at the same time kinematically invariable, or else a part of it is statically indeterminate, i.e., over-rigid, and the other one, kinematically variable.

3.3. The Degree of Static Indeterminability and the Degree of Kinematic Variability of a Structure

The static-kinematic discriminant can be treated as the difference between the degree of static indeterminability s and the degree of kinematic variability k:

$$n = s - k. \tag{3.2}$$

Positive s connotes the number of static unknowns which cannot be calculated from the equilibrium conditions alone. It also connotes the number of connectors which when cut will not result in an increased number of degrees of freedom of elements, i.e., which will not raise the degree of kinematic variability of a structure. Positive k connotes the number of degrees of freedom of elements of a structure. It also connotes the number of connectors which need to be introduced into a structure to immobilize all its elements.

If the static-kinematic discriminant n is positive, the structure is definitely statically indeterminate, but concomitantly may be kinematically variable. If n is negative, a structure is definitely kinematically variable, but concomitantly may be statically indeterminate. Finally, if $n = 0$, then either the system is statically determinate and kinematically invariable, or statically indeterminate and at the same time kinematically variable.

Let us consider some of the cases noted using examples.
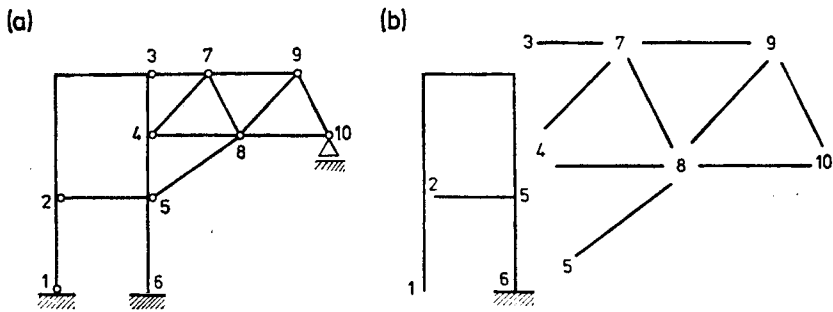
Fig. 3.10. Division of a frame-truss structure into elements

Figure 3.10a shows a plane frame-truss structure which we divide into rigid elements as shown in Fig. 3.10b. Since we have not separated the frame part from the foundation at fixed support 6, the number of free elements equals the number of truss members, $e = 9$. Since we assume that we are dealing with a plane structure loaded in its plane, we let $h = 3$. Calculating the number of cut-off connectors, we take into account the fact that a plane hinge involves two connectors (Fig. 3.8b), and a simple support (Fig. 3.8d) includes one connector. Special care must be taken when multiple hinges are encountered. As far as the considered structure is concerned, we have five single hinges (1, 2, 3, 5, 10), two double (4, 9), one triple (7) and one quadruple (8). Hence, $t = (5+2 \cdot 2+3+4) \cdot 2+1 = 33$ and $n = 33-3 \cdot 9 = 6$. Since the degree of kinematic variability equals zero, the degree of static indeterminability of the structure equals the static-kinematic discriminant and is 6.
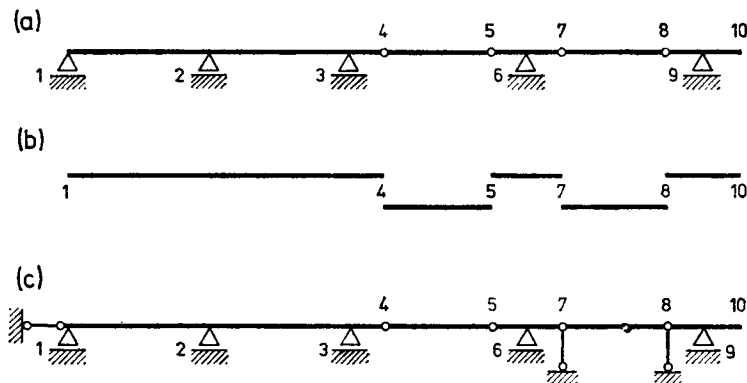
Fig. 3.11. Division of four-span hinged beam into elements

In the case of a four-span hinged beam as shown in Fig. 3.11a, the number of elements (Fig. 3.11b) $e = 5$. In dividing the structure into elements, we have cut $t = 4 \cdot 2 + 5 = 13$ connectors. Since, however, the static-kinematic discriminant, $n = 13 - 3 \cdot 5 = -2$, is negative, the structure must be kinematically variable. The degree of kinematic variability is easiest to determine as the number of additional connectors necessary to immobilize all the elements. We have introduced them at points 1, 7 and 8 (Fig. 3.11c) to find that $k = 3$. Consequently, from Eq. (2.3) we get $s = n + k = -2 + 3 = 1$. The structure is, therefore, once hyperstatic. Indeed, should vertical loads be acting within elements 1–4, i.e., loads parallel to reaction lines 1, 2, 3, these reactions cannot be calculated from the static conditions. One of them, namely zeroing of the sum of projections of the forces on the horizontal axis, will in this case be satisfied in an identical manner, whereas the other two will be insufficient to calculate the three unknowns.
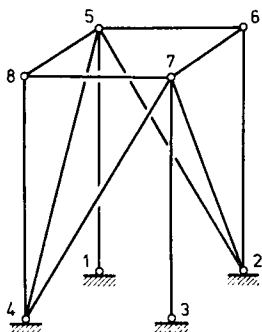
Fig. 3.12. Space truss

In the case of space trusses, in which all the members are connected at both ends to spherical hinges, loadings in the form of moments are precluded, and this applies in particular to moments with vectors parallel to the axes of the truss members. Consequently, the twisting moments zeroing condition for each truss member is satisfied in an identical manner and the number of equilibrium conditions for each member reduces to five. The static-kinematic discriminant can therefore be calculated from Eq. (3.1), letting $h = 5$.

An example of a space truss is shown in Fig. 3.12. The number of elements is equal to the number of truss members, $e = 12$. Of the eight spherical joints, two are single (1, 3), two are double (6, 8), two triple (2, 4) and two quadruple (5,7). Hence, $t = 2 \cdot (1+2+3+4) \cdot 3 = 60$, and the static-kinematic discriminant $n = 60-5 \cdot 12 = 0$. It is readily seen that the considered truss is kinematically invariable and isostatic ($k = s = 0$).

The determination of the degree of kinematic variation of a structure did not present any particular difficulty in the cited example. Where more complicated structures are involved, the determination of the values of k and s may prove to be much more difficult. But, it is of major importance in statics to ascertain whether a structure is not by any chance kinematically variable. For, statics is concerned with structures at rest, not in motion. All mechanisms are by their very nature kinematically variable structures, and these are obviously not of interest to us in this case.

Until recently, kinematic invariability of structures used to be investigated by various graphic methods (cf. Nowacki, 1952, Vol. I, p. 17). In the computer age, these methods are no longer so important. The static-kinematic analysis just described has been now replaced by investigation of the algebraic properties of certain matrices, discussed in Chapter 6.
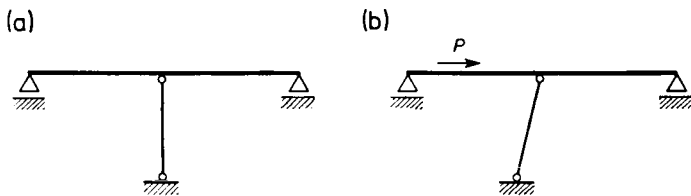
Fig. 3.13. Temporarily kinematically variable structure

To conclude, we may add that in kinematics we distinguish the concepts of unlimited and temporary kinematic variability. For example, the structure shown in Fig. 3.11 is of the unlimited variable type in the sense that the respective displacements are comparable with the dimensions of the elements of the structure. On the other hand, the structure shown in Fig. 3.13a is of the

temporary variable type, because a very small displacement of the beam is accompanied by a slope of the connector (Fig. 3.13b), which prevents further increments of horizontal displacements. In the case of structures required to have a certain stiffness, this being pertinent particularly in building structures, we should be wary of both types of kinematic variability.

4. The Principle of Virtual Work and the Reciprocity Theorems

4.1. The Principle of Virtual Work

The underlying principle of mechanics in general, not only structural mechanics, is the principle of virtual work, from which all further principles and methods of solving static problems may be derived. Although Nowacki (Mossakowska *et al.*, 1978, p. 86) presented in general terms the principle of virtual work and carried through a proof of it, in our opinion, it will be useful in a study devoted to bar structures to recall in brief the argumentation leading to the formulation of this fundamental principle. However, in order not to complicate matters unduly, we shall prove below the principle of virtual work using the example of a straight bar, being one of the elements of a bar structure. The relations derived therefrom will then be broaden without proof to arbitrary bar structures.
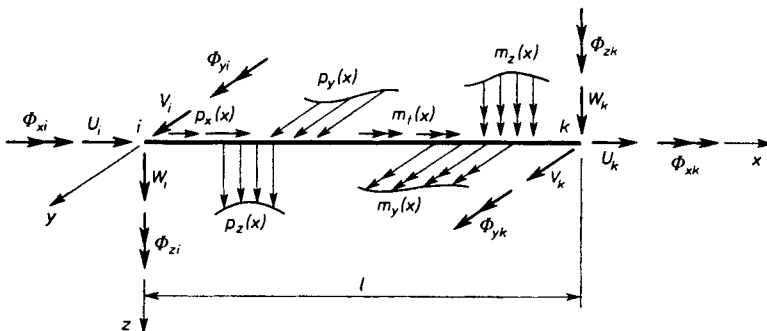
Fig. 4.1. Loadings acting on i-k bar

Let us assume that a bar i-k of length l as shown in Fig. 4.1 is in equilibrium under all the loads indicated in the drawing. Hence, the equilibrium equations (2.4), (2.5) and (2.6) must be satisfied at every point of the bar axis.

After introducing the denotations:*

$$\mathbf{p}_p = \{p_x, p_y, p_z\}, \qquad \mathbf{p}_m = \{m_t, m_y, m_z\}, \tag{4.1}$$

$$\boldsymbol{\sigma}_T = \{N, T_y, T_z\}, \qquad \boldsymbol{\sigma}_M = \{M_t, M_y, M_z\}, \tag{4.2}$$

$$\mathbf{e} = \begin{bmatrix} 0 & 0 & 0 \\ 0 & 0 & -1 \\ 0 & 1 & 0 \end{bmatrix}, \tag{4.3}$$

we write the set of equilibrium equations concisely in matrix form:

$$\frac{d\boldsymbol{\sigma}_T}{dx} + \mathbf{p}_p = \mathbf{0}, \qquad \frac{d\boldsymbol{\sigma}_M}{dx} + \mathbf{e}\boldsymbol{\sigma}_T + \mathbf{p}_m = \mathbf{0}. \tag{4.4}$$

In the above equations, $\mathbf{0}$ denotes the vectors with all zero entries. Introducing in turn the denotations:

$$\mathbf{p} = \{\mathbf{p}_p, \mathbf{p}_m\}, \qquad \boldsymbol{\sigma} = \{\boldsymbol{\sigma}_T, \boldsymbol{\sigma}_M\}, \qquad \mathbf{d} = \begin{bmatrix} \mathbf{I}\dfrac{d}{dx} & \mathbf{0} \\[2mm] \mathbf{e} & \mathbf{I}\dfrac{d}{dx} \end{bmatrix}, \tag{4.5}$$

in which the unitary matrix $\mathbf{I}$ and the zero matrix $\mathbf{0}$ are 3×3 in size, we write the set of equations (4.4) in the form of a single matrix equation:

$$\mathbf{d}\boldsymbol{\sigma} + \mathbf{p} = \mathbf{0}. \tag{4.6}$$

The symbol $\boldsymbol{\sigma}$ used to denote the full set of generalized internal forces has been applied by analogy to the denotation of stresses in a three-dimensional body.

Fig. 4.2. Cross-sectional rotations: (a) in plane xz; (b) in plane xy

* The braces { } signify that the quantities therein make a single column matrix. The matrices are given in bold-face print.

Points lying on the axis of the bar experience displacements u, v, w, and the cross-sections assigned to those points experience rotations φ_s, φ_y, φ_z. To generalize, we assume this time that the cross-sectional 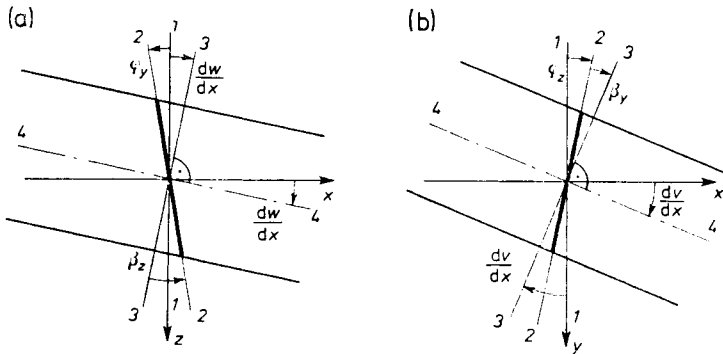rotations φ_y, φ_z are independent of the angles that the deformed axis of the bar makes with the x-axis. Figure 4.2a shows a cross-section of the bar in projection on xz plane, and Fig. 4.2b, on xy plane. The line 1–1 represents the cross-section of the bar in the initial position, and the line 2–2 corresponds to the same cross-section after rotation. The line 3–3 indicates the position in which the cross-section would find itself, had it remained perpendicular to the deformed axis of the bar, 4–4. It is seen that we have dropped here one of Bernoulli's assumptions, that a cross-section remains perpendicular to the deformed axis of a bar.

Hence, the strain equations $(2.11)_{2,3}$ take a more general form:

$$\varkappa_y = \frac{d\varphi_y}{dx}, \qquad \varkappa_z = \frac{d\varphi_z}{dx}, \tag{4.7}$$

and, moreover, additional strains appear:

$$\beta_y = \frac{dv}{dx} - \varphi_z, \qquad \beta_z = \frac{dw}{dx} + \varphi_y, \tag{4.8}$$

which are averaged shear strain angles (cf. Fig. 4.2).

Thus, together with Eqs. $(2.11)_1$ and (2.32) we have six relations which using the following denotations:

$$\mathbf{q}_u = \{u, v, w\}, \qquad \mathbf{q}_\varphi = \{\varphi_s, \varphi_y, \varphi_z\}, \tag{4.9}$$

$$\boldsymbol{\epsilon}_\beta = \{\varepsilon, \beta_y, \beta_z\}, \qquad \boldsymbol{\epsilon}_\varkappa = \{\varkappa_s, \varkappa_y, \varkappa_z\} \tag{4.10}$$

we write in matrix form:

$$\boldsymbol{\epsilon}_\beta = \frac{d\mathbf{q}_u}{dx} + e\mathbf{q}_\varphi, \qquad \boldsymbol{\epsilon}_\varkappa = \frac{d\mathbf{q}_\varphi}{dx}. \tag{4.11}$$

Attention should be directed to the duality of the sets of equations (4.4) and (4.11). Putting into the set of equations (4.4) in place of $\boldsymbol{\sigma}_T$, $\boldsymbol{\sigma}_M$, $\mathbf{p}_p$ and $\mathbf{p}_m$, the quantities $\boldsymbol{\sigma}_\varphi$, $\boldsymbol{\sigma}_u$, $-\boldsymbol{\epsilon}_\varkappa$ and $-\boldsymbol{\epsilon}_\beta$, respectively, we get the set (4.11).

Equations (4.11) can be written even more concisely in the form:

$$\boldsymbol{\epsilon} = \mathbf{d}_\varepsilon \mathbf{q}, \tag{4.12}$$

using the denotations:

$$\mathbf{q} = \{\mathbf{q}_u, \mathbf{q}_\varphi\}, \qquad \boldsymbol{\epsilon} = \{\boldsymbol{\epsilon}_\beta, \boldsymbol{\epsilon}_\varkappa\}, \qquad \mathbf{d}_\varepsilon = \begin{bmatrix} \mathbf{I}\dfrac{d}{dx} & e \\ \mathbf{0} & \mathbf{I}\dfrac{d}{dx} \end{bmatrix}. \tag{4.13}$$

Assume that displacements $\mathbf{q}$ experience now virtual increments $\delta\mathbf{q}$, which are accompanied by virtual increments of strains $\delta\boldsymbol{\epsilon}$ related to the displacements according to a relation of type (4.12).

Regarding virtual displacements, we assume that they are:

(a) very small compared to the bar size (we have made a similar assumption discussing real displacements of the bar).

(b) arbitrary, in the sense that they are independent of real loads acting on the bar,

(c) possible, i.e., consistent with the conditions limiting bar motion (if such constraints actually exist),

(d) time independent,

(e) expressed by class C1 functions.

Each of the six equilibrium equations that enter the matrix equation (4.6) is multiplied by one of the vector-forming functions $\delta\mathbf{q}$, added by sides and integrated in the limits of 0 to l. The operation in matrix notation takes the form*

$$\int_0^l \delta\mathbf{q}^T(\mathbf{d\sigma}+\mathbf{p})\,\mathrm{d}x = 0. \tag{4.14}$$

Expanding the integrand in accordance with Eqs. (4.5) and (4.13)$_1$, we obtain:

$$\int_0^l \left(\delta\mathbf{q}_u^T \frac{\mathrm{d}\boldsymbol{\sigma}_T}{\mathrm{d}x} + \delta\mathbf{q}_u^T\,\mathbf{p}_p + \delta\mathbf{q}_\varphi^T\mathbf{e}\boldsymbol{\sigma}_T + \delta\mathbf{q}_\varphi^T \frac{\mathrm{d}\boldsymbol{\sigma}_M}{\mathrm{d}x} + \delta\mathbf{q}_\varphi^T\mathbf{p}_m \right) \mathrm{d}x = 0. \tag{4.15}$$

The expressions in which derivatives of the cross-sectional forces are present we integrate by parts, getting:

$$[\delta\mathbf{q}^T\boldsymbol{\sigma}]_0^l + \int_0^l \delta\mathbf{q}^T\mathbf{p}\,\mathrm{d}x -$$

$$- \int_0^l \left[\left(\frac{\mathrm{d}\delta\mathbf{q}_u^T}{\mathrm{d}x} - \delta\mathbf{q}_\varphi^T\mathbf{e} \right) \boldsymbol{\sigma}_T + \frac{\mathrm{d}\delta\mathbf{q}_\varphi^T}{\mathrm{d}x}\,\boldsymbol{\sigma}_M \right] \mathrm{d}x = 0. \tag{4.16}$$

Note that the expression by the forces $\boldsymbol{\sigma}_T$ is transformable as follows:

$$\frac{\mathrm{d}\delta\mathbf{q}_u^T}{\mathrm{d}x} - \delta\mathbf{q}_\varphi^T\mathbf{e} = \left(\frac{\mathrm{d}\delta\mathbf{q}_u}{\mathrm{d}x} - \mathbf{e}^T\delta\mathbf{q}_\varphi \right)^T = \left(\frac{\mathrm{d}\delta\mathbf{q}_u}{\mathrm{d}x} + \mathbf{e}\delta\mathbf{q}_\varphi \right)^T = \delta\boldsymbol{\epsilon}_\beta^T. \tag{4.17}$$

---

* The superscript T by a matrix signifies its transposition.

We have made use here of Eq. (4.11)$_1$ and the fact that the matrix $-\mathbf{e}$ is a transposition of the matrix $\mathbf{e}$ given by Eq. (4.3). Substituting (4.17) into (4.16) and transferring the negative expression to the right-hand side of equality sign, and also using the relations (4.11)$_2$, (4.13)$_2$ and (4.5)$_2$, we get

$$[\delta \mathbf{q}^T \boldsymbol{\sigma}]_0^l + \int_0^l \delta \mathbf{q}^T \mathbf{p}\,dx = \int_0^l \delta \boldsymbol{\epsilon}^T \boldsymbol{\sigma}\,dx. \tag{4.18}$$

We now expand the first term of the expression in Eq. (4.18):

$$[\delta \mathbf{q}^T \boldsymbol{\sigma}]_0^l = \delta \mathbf{q}^T(l)\boldsymbol{\sigma}(l) - \delta \mathbf{q}^T(0)\boldsymbol{\sigma}(0). \tag{4.19}$$

The functions $\delta \mathbf{q}$ and $\boldsymbol{\sigma}$ satisfy the following boundary conditions:

$$\delta \mathbf{q}(l) = \delta \mathbf{q}_k, \quad \delta \mathbf{q}(0) = \delta \mathbf{q}_i, \quad \boldsymbol{\sigma}(l) = \mathbf{Q}_k, \quad \boldsymbol{\sigma}(0) = -\mathbf{Q}_i, \tag{4.20}$$

where:

$$\begin{aligned}
\delta \mathbf{q}_j &= \delta \{u, v, w, \varphi_s, \varphi_y, \varphi_z\}_j, \\
\mathbf{Q}_j &= \{U, V, W, \Phi_s, \Phi_y, \Phi_z\}_j,
\end{aligned} \quad j = i, k, \tag{4.21}$$

are respectively the virtual displacements of bar ends and the generalized boundary forces indicated in Fig. 4.1.

Hence, the left side of the equality (4.18) expresses the work of all loads (the boundary forces included) done on the virtual displacements. That work denoted by δL_{ext} can be expressed in the following form:

$$\delta L_{\text{ext}} = \delta \mathbf{q}_i^T \mathbf{Q}_i + \delta \mathbf{q}_k^T \mathbf{Q}_k + \int_0^l \delta \mathbf{q}^T \mathbf{p}\,dx. \tag{4.22}$$

The right side of the equality (4.18) expresses the work of the internal forces done on the virtual displacements. That work, denoted by δL_{int} can also be presented in an expanded form:

$$\begin{aligned}
\delta L_{\text{int}} = \int_0^l \delta \boldsymbol{\epsilon}^T \boldsymbol{\sigma}\,dx &= \int_0^l (\delta \varepsilon N + \delta \beta_y T_y + \delta \beta_z T_z + \\
&+ \delta \varkappa_s M_s + \delta \varkappa_y M_y + \delta \varkappa_z M_z)\,dx.
\end{aligned} \tag{4.23}$$

The principle of virtual work (4.18) can therefore be formulated most simply as follows:

$$\delta L_{\text{ext}} = \delta L_{\text{int}}. \tag{4.24}$$

We have derived it using the example of a single straight bar, but it also holds in the general case of a structure made up of straight and curved bars. Treating all the concentrated forces and moments acting on a structure as func-

tional load distribution $\mathbf{p}$, we can write the expressions for the virtual work of external loads and the virtual work of internal forces in a general form:

$$\delta L_{ext} = \int_s \delta \mathbf{q}^T(s) \mathbf{p}(s) \, ds = \int_s \mathbf{p}^T(s) \, \delta \mathbf{q}(s) \, ds, \qquad (4.25)$$

$$\delta L_{int} = \int_s \delta \boldsymbol{\epsilon}^T(s) \boldsymbol{\sigma}(s) \, ds = \int_s \boldsymbol{\sigma}^T(s) \, \delta \boldsymbol{\epsilon}(s) \, ds. \qquad (4.26)$$

Integration is now applied to all members of the structure. We only have to take care that local coordinates, orthogonal at every point to the bar axis, be used here, so that the generalized internal forces $\boldsymbol{\sigma}$ and the virtual strains $\delta \boldsymbol{\epsilon}$ retain the same physical meaning which we have given them in the case of straight bar.

To conclude, it may be worth noting that in introducing the principle of virtual work, we have made no assumptions concerning the physical laws governing the deformability of material. The virtual work principle expressed by the equality (4.24) holds therefore irrespective of whether the structure material is elastic or not.

4.2. The Principle of Complementary Virtual Work

Consider now a structure on which a certain load $\bar{\mathbf{p}}$, accompanied by internal forces $\bar{\boldsymbol{\sigma}}$, has been acting even before it experienced actual displacements and strains. We assume that this virtual load together with the respective virtual internal forces satisfies at every point of the bar axis the differential equilibrium equations which in the case of a straight bar take the form (4.6). We deal therefore with the very same conditions which in the preceding paragraph were met by real loads.

Displacements $\mathbf{q}$ and strains $\boldsymbol{\epsilon}$ appear only later under real external loads $\mathbf{p}$ and non-static factors. These displacements, it will be remembered, are very small compared to the dimensions of the bars; they do not depend, of course, on virtual loads $\bar{\mathbf{p}}$, they are compatible with the conditions limiting movements of the structure; they are time-independent (a linear elastic body being considered); and they are continuous together with their first derivatives. As we can see, the real displacements $\mathbf{q}$ satisfy all the conditions which in the preceding section we have laid for virtual displacements $\delta \mathbf{q}$.

Therefore, we can write the principle of complementary virtual work without proof in the following form:

$$\bar{L}_{ext} = \bar{L}_{int}. \qquad (4.27)$$

The work done by virtual external loads is expressed by the formula (cf. (4.25))

$$\bar{L}_{ext} = \int_s \bar{\mathbf{p}}^T(s)\,\mathbf{q}(s)\,ds, \tag{4.28}$$

and the work done by virtual internal forces is expressed by (cf. (4.23))

$$\bar{L}_{int} = \int_s \bar{\sigma}^T(s)\boldsymbol{\epsilon}(s)\,ds$$

$$= \int_s (\bar{N}\varepsilon + \bar{T}_\eta\beta_\eta + \bar{T}_\zeta\beta_\zeta + \bar{M}_s\varkappa_s + \bar{M}_\eta\varkappa_\eta + \bar{M}_\zeta\varkappa_\zeta)\,ds. \tag{4.29}$$

We have denoted by η, ζ the principal, centroidal axes of inertia of cross-section, which—depending on the element involved—may be various oriented in space.

Four of the six strains in Eq. (4.31) can immediately be related to static quantities. It will suffice to transform suitably the relations (2.18) and (2.36):

$$\varepsilon = \frac{N}{EA} + \varepsilon^0, \qquad \varkappa_s = \frac{M_s}{GJ_s} + \varkappa_s^0,$$

$$\varkappa_\eta = \frac{M_\eta}{EJ_\eta} + \varkappa_\eta^0, \qquad \varkappa_\zeta = \frac{M_\zeta}{EJ_\zeta} + \varkappa_\zeta^0. \tag{4.30}$$

On the other hand, in Chapter 2 we proceeded from Bernoulli's assumptions and the relationship between the averaged shear-strain angles β_η, β_ζ and the corresponding transverse forces $\bar{T}_\eta$, $\bar{T}_\zeta$ could not be derived. We determine this relationship expressing the virtual work done by the transverse forces $\bar{T}_\eta$, $\bar{T}_\zeta$ as an integral over the cross-sectional area of the work done by the virtual shear stresses $\bar{\tau}_{s\eta}$, $\bar{\tau}_{s\zeta}$ on the shear-strain angles $\gamma_{s\eta}$, $\gamma_{s\zeta}$. For example, we calculate the product $\bar{T}_\eta\beta_\eta$ as follows (cf. (2.34), (2.25)):

$$\bar{T}_\eta\beta_\eta = \int_A \bar{\tau}_{s\eta}\gamma_{s\eta}\,dA = \int_A \frac{\bar{T}_\eta S_\zeta}{J_\zeta b_\zeta G}\frac{T_\eta S_\zeta}{J_\zeta b_\zeta}\,dA = \frac{\bar{T}_\eta T_\eta}{GA}k_\eta, \tag{4.31}$$

where

$$k_\eta = \frac{A}{J_\zeta^2}\int_A \frac{S_\zeta^2}{b_\zeta^2}\,dA \tag{4.32}$$

is a dimensionless parameter which depends on the shape of the cross-section. The value of this parameter for a rectangular cross-section is $\frac{6}{5}$ and for an I-beam with the web lying on the η-axis is roughly:

$$k_\eta \approx \frac{A_{total}}{A_{web}}. \tag{4.33}$$

It follows from Eq. (4.31) that the relations between averaged shear-strain angles and the transverse forces, considering distortional strains, have the following form:

$$\beta_\eta = \frac{k_\eta T_\eta}{GA} + \beta_\eta^0, \qquad \beta_\zeta = \frac{k_\zeta T_\zeta}{GA} + \beta_\zeta^0, \tag{4.34}$$

where k_ζ is expressed by an equation analogous to (4.33) with an appropriate change of the subscript ζ to η.

Substituting Eqs. (4.30) and (4.34), we transform the expression (4.29) for the work done by virtual internal forces, to the following form:

$$\bar{L}_{int} = \int_s \left(\frac{\bar{N}N}{EA} + k_\eta \frac{\bar{T}_\eta T_\eta}{GA} + k_\zeta \frac{\bar{T}_\zeta T_\zeta}{GA} + \frac{\bar{M}_t M_t}{GJ_t} + \frac{\bar{M}_\eta M_\eta}{EJ_\eta} + \frac{\bar{M}_\zeta M_\zeta}{EJ_\zeta} \right) ds +$$

$$+ \int_s (\bar{N}\varepsilon^0 + \bar{T}_\eta \beta_\eta^0 + \bar{T}_\zeta \beta_\zeta^0 + \bar{M}_t \varkappa_t^0 + \bar{M}_\eta \varkappa_\eta^0 + \bar{M}_\zeta \varkappa_\zeta^0) ds. \tag{4.35}$$

Using matrix notation, we get

$$\bar{L}_{int} = \int_s (\bar{\sigma}^T E^{-1} \sigma + \bar{\sigma}^T \varepsilon^0) ds. \tag{4.36}$$

We introduce here the following denotations*:

$$E = \left[EA, \frac{GA}{k_\eta}, \frac{GA}{k_\zeta}, GJ_t, EJ_\eta, EJ_\zeta \right], \tag{4.37}$$

$$\varepsilon^0 = \{\varepsilon^0, \beta_\eta^0, \beta_\zeta^0, \varkappa_s^0, \varkappa_\eta^0, \varkappa_\zeta^0\}. \tag{4.38}$$
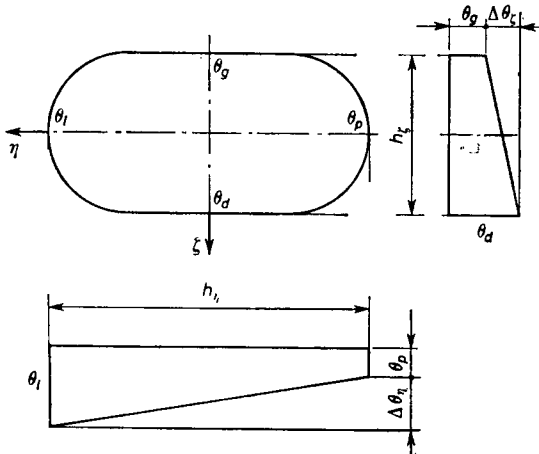

Fig. 4.3. Temperature increments on bar surface

---

* The braces [ ] indicate a diagonal matrix.

Distortional strains can be induced, for example, by a temperature rise $\theta(s, \eta, \zeta)$. We assume that the distribution of that temperature increment is expressed by a linear function of the variables η, ζ:

$$\theta(s, \eta, \zeta) = \theta - \theta_\zeta \eta + \theta_\eta \zeta \tag{4.39}$$

where

$$\theta = \theta(s, 0, 0), \quad \theta_\zeta = -\frac{\partial \theta(s, \eta, \zeta)}{\partial \eta}, \quad \theta_\eta = \frac{\partial \theta(s, \eta, \zeta)}{\partial \zeta}. \tag{4.40}$$

Knowing the temperature increment at the bar surface (Fig. 4.3), we can express the quantities θ_η and θ_ζ as follows:

$$\theta_\eta = \frac{\Delta\theta_\zeta}{h_\zeta}, \quad \theta_\zeta = -\frac{\Delta\theta_\eta}{h_\eta}, \tag{4.41}$$

where the symbols

$$\Delta\theta_\zeta = \theta_d - \theta_g, \quad \Delta\theta_\eta = \theta_l - \theta_p \tag{4.42}$$

stand for the differences of temperature increments occurring in extreme fibres.

The temperature increment (4.41) is accompanied by extension:

$$\varepsilon_s^0(s, \eta, \zeta) = \alpha(\theta - \theta_\zeta \eta + \theta_\eta \zeta). \tag{4.43}$$

The symbol α denotes the coefficient of thermal extension. Comparing Eqs. (4.43) and (2.12), we arrive at the following expressions for distortional strains induced by a temperature increment:

$$\varepsilon^0 = \alpha\theta, \quad \varkappa_\eta^0 = \alpha\theta_\eta, \quad \varkappa_\zeta^0 = \alpha\theta_\zeta. \tag{4.44}$$

The distortional strain matrix (4.38) has, therefore, the following form in this case:

$$\boldsymbol{\epsilon}^0 = \alpha\{\theta, 0, 0, 0, \theta_\eta, \theta_\zeta\}. \tag{4.45}$$

4.3. The Reciprocal Work Theorem

Consider two different static loads independent of each other, $\mathbf{p}_\varrho$ and $\mathbf{p}_\nu$, and acting successively on one and the same elastic structure; and moreover, let various non-static factors produce successively distortional strains $\boldsymbol{\epsilon}_\varrho^0$ and $\boldsymbol{\epsilon}_\nu^0$ in the structure. These causes are accompanied by effects in the form of displacements $\mathbf{q}_\varrho$ and $\mathbf{q}_\nu$, strains $\boldsymbol{\epsilon}_\varrho$ and $\boldsymbol{\epsilon}_\nu$, and internal forces $\boldsymbol{\sigma}_\varrho$ and $\boldsymbol{\sigma}_\nu$.

First, we treat the loads with subscript ϱ as virtual loads and the displacements and strains occurring in state ν as real quantities. Using the principle

of complementary virtual work (4.27) and also Eqs. (4.28) and (4.36), we write

$$\int_s \mathbf{p}_\varrho^T \mathbf{q}_\nu \, ds = \int_s \boldsymbol{\sigma}_\varrho^T \mathbf{E}^{-1} \boldsymbol{\sigma}_\nu \, ds + \int_s \boldsymbol{\sigma}_\varrho^T \boldsymbol{\epsilon}_\nu^0 \, ds. \tag{4.46}$$

Next, changing the order in which the loads are being applied, we treat the loads occurring in state ν as virtual loads, and the respective geometric quantities in state ϱ as real displacements and strains. Equation (4.27) then takes the form

$$\int_s \mathbf{p}_\nu^T \mathbf{q}_\varrho \, ds = \int_s \boldsymbol{\sigma}_\nu^T \mathbf{E}^{-1} \boldsymbol{\sigma}_\varrho \, ds + \int_s \boldsymbol{\sigma}_\nu^T \boldsymbol{\epsilon}_\varrho^0 \, ds. \tag{4.47}$$

Subtracting by sides Eqs. (4.46) and (4.47), and considering the equality

$$\int_s \boldsymbol{\sigma}_\varrho^T \mathbf{E}^{-1} \boldsymbol{\sigma}_\nu \, ds = \int_s \boldsymbol{\sigma}_\nu^T \mathbf{E}^{-1} \boldsymbol{\sigma}_\varrho \, ds, \tag{4.48}$$

we arrive by rearranging the respective terms as the following relation:

$$\int_s \mathbf{p}_\varrho^T \mathbf{q}_\nu \, ds + \int_s \boldsymbol{\sigma}_\nu^T \boldsymbol{\epsilon}_\varrho^0 \, ds = \int_s \mathbf{p}_\nu^T \mathbf{q}_\varrho \, ds + \int_s \boldsymbol{\sigma}_\varrho^T \boldsymbol{\epsilon}_\nu^0 \, ds. \tag{4.49}$$

This is the essence of the general reciprocal work theorem which was proposed by Maizel (1951) taking distortion into account (cf. Mossakowska *et al.*, 1978, p. 247). Omitting the distortion factor, we arrive at the following equation:

$$\int_s \mathbf{p}_\varrho^T \mathbf{q}_\nu \, ds = \int \mathbf{p}_\nu^T \mathbf{q}_\varrho \, ds, \tag{4.50}$$

which is a mathematical expression of the reciprocal work theorem, derived much earlier by Betti.

4.4. The Reciprocal Displacement Theorem

Let us reduce the set of loads $\mathbf{p}_\varrho$ to a single concentrated force or moment of unit value. Similarly, let the load $\mathbf{p}_\nu$ be a single concentrated force or unit moment acting in another place.

Figure 4.4 shows a straight bar, on which two unit forces are acting successively at different points of the bar axis. The loads $\mathbf{p}_\varrho$ and $\mathbf{p}_\nu$ can therefore be expressed with the aid of δ-Dirac's distribution in the following manner:

$$\begin{aligned} \mathbf{p}_\varrho &= \{0, 0, \delta(x - x_\varrho), 0, 0, 0\}, \\ \mathbf{p}_\nu &= \{0, 0, \delta(x - x_\nu), 0, 0, 0\}. \end{aligned} \tag{4.51}$$
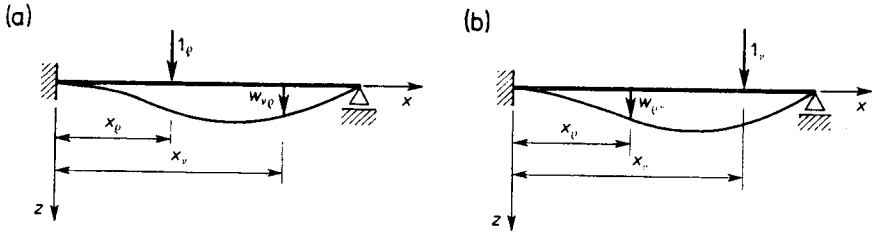
Fig. 4.4. Bar loaded by unit forces

Considering the relation

$$\int_{x_1}^{x_2} f(x)\,\delta(x-x_0)\,dx = f(x_0) \qquad \text{for} \quad x_1 \leqslant x_0 \leqslant x_2, \qquad (4.52)$$

we write

$$\int_0^l \mathbf{p}_\varrho^T \mathbf{q}_\nu\,dx = \int_0^l \delta(x-x_\varrho)\,w_\nu(x)\,dx = w_\nu(x_\varrho) = w_{\varrho\nu},$$

$$\int_0^l \mathbf{p}_\nu^T \mathbf{q}_\varrho\,dx = \int_0^l \delta(x-x_\nu)\,w_\varrho(x)\,dx = w_\varrho(x_\nu) = w_{\nu\varrho}. \qquad (4.53)$$

In $w_{\varrho\nu}$ and $w_{\nu\varrho}$, the first subscript refers to the place at which the displacement occurs, and the second indicates the cause that has induced that displacement. We obtain, therefore, according to Betti's reciprocal theorem (4.50) the relation

$$w_{\varrho\nu} = w_{\nu\varrho} \qquad (4.54)$$

which expresses in this particular case the substance of Maxwell's reciprocal theorem.

Another example is given in Fig. 4.5. In this case:

$$\mathbf{p}_\varrho = \{0, 0, 0, 0, \, \delta(x-x_\varrho), \, 0\},$$

$$\mathbf{p}_\nu = \{0, 0, 0, 0, \, \delta(x-x_\nu), \, 0\}, \qquad (4.55)$$
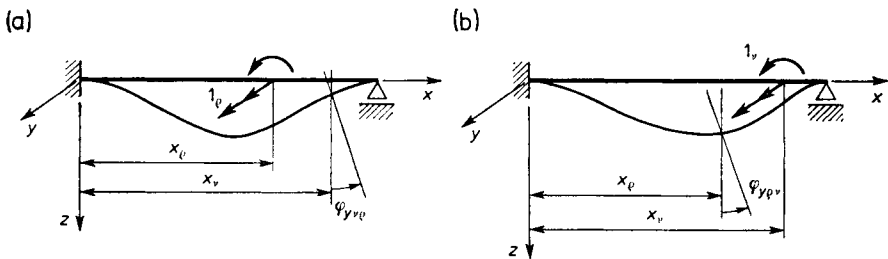

Fig. 4.5. Bar loaded by unit moments

from which the following relations are derived:

$$\int_0^l \mathbf{p}_\varrho^T \mathbf{q}_\nu \, dx = \varphi_{y\nu}(x_\varrho) = \varphi_{y\varrho\nu},$$

(4.56)

$$\int_0^l \mathbf{p}_\nu^T \mathbf{q}_\varrho \, dx = \varphi_{y\nu\varrho}.$$

Consequently, Betti's reciprocal theorem leads in this case to the following form of Maxwell's reciprocal theorem:

$$\varphi_{y\varrho\nu} = \overline{\varphi_{y\nu\varrho}}.$$

(4.57)
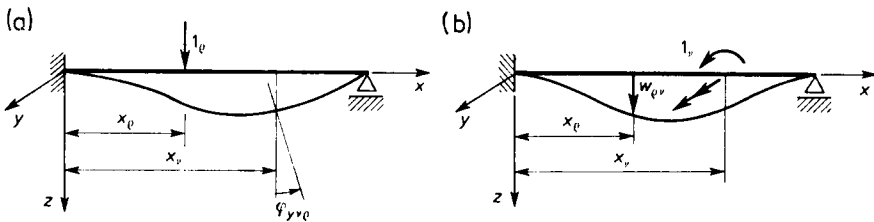
Fig. 4.6. Bar loaded by: (a) unit force; (b) unit moment

Finally, Fig. 4.6 gives the loads $(4.51)_1$ and $(4.55)_2$ which perform the work previously calculated in Eqs. $(4.53)_1$ and $(4.56)_2$. Hence, we have the following equality, which is yet another illustration of Maxwell's reciprocal theorem:

$$w_{\varrho\nu} = \varphi_{y\nu\varrho}.$$

(4.58)

Worth noting here is the seeming incompatibility of the dimensions of the quantities on the left and right side of the equality sign.

The deflection $w_{\varrho\nu}$ was induced by a unit moment. We deal, therefore, with a ratio of a deflection expressed in metres to a structure loading moment, i.e., a quantity expressed in [N · m]. Similarly, using the symbol $\varphi_{y\nu\varrho}$ we have denoted the ratio of an angular quantity expressed in radians to the cause underlying the rotation, i.e., to a force expressed in newtons. The denominations of $w_{\varrho\nu}$ and $\varphi_{y\nu\varrho}$ are therefore identical: $[N^{-1}]$.

Up to the present, we have validated Maxwell's reciprocal theorem for particular examples concerning generalized unit forces and displacements with vectors parallel to the adopted coordinates. We now broaden our considerations to the case of generalized unit forces and displacements with arbitrarily oriented vectors. Let two generalized unit forces be acting on the

considered structure, namely $\mathbf{1}_\varrho$ and $\mathbf{1}_r$, arbitrarily oriented in space and applied in principle to different points of the structure; although in special cases, they may have a common point of application. Where the generalized force $\mathbf{1}_\varrho$ is acting, the other generalized force $\mathbf{1}_r$ induces the displacement $\mathbf{q}_{\varrho r}$; whereas at the point of application of the generalized force $\mathbf{1}_r$ there appears under the load the displacement $\mathbf{q}_{r\varrho}$. If the force in the narrow sense is the load $\mathbf{1}_\varrho$, then the displacement $\mathbf{q}_{\varrho r}$ should be understood as a sidesway vector. If, on the other hand, a unit moment $\mathbf{1}_\varrho$ is acting in the ϱ-system, then the symbol $\mathbf{q}_{\varrho r}$ stands for the angular displacement vector of the cross-section, in which the moment $\mathbf{1}_\varrho$ has been applied. The same interpretation holds for $\mathbf{q}_{r\varrho}$.

The reciprocal work theorem will take in this case the form

$$\mathbf{1}_\varrho \cdot \mathbf{q}_{\varrho r} = \mathbf{1}_r \cdot \mathbf{q}_{r\varrho}. \tag{4.59}$$

Scalar products of two vectors, one of them being unit vector, occur on either side of the equality sign. Let us project the vector $\mathbf{q}_{\varrho r}$ on the direction of $\mathbf{1}_\varrho$ and denote the modulus of this projection by $\delta_{\varrho r}$. This is going to be at the same time the value of the scalar product on the left side of the equality (4.59). Similarly, the projection of $\mathbf{q}_{r\varrho}$ on the direction $\mathbf{1}_r$ has the modulus $\delta_{r\varrho}$ which is at the same time the value of the product on the right side of the equality (4.59). Hence, we can write:

$$\delta_{\varrho r} = \delta_{r\varrho}. \tag{4.60}$$

This is Maxwell's reciprocal theorem written in the most concise form.

4.5. The Reciprocal Reaction Theorem

Consider an arbitrary over-rigid bar structure. Figure 4.7 shows as an example a crooked bar lying in the xz plane, rigidly fixed at both ends. Let us give one of the supports of the structure an arbitrarily oriented unit displacement
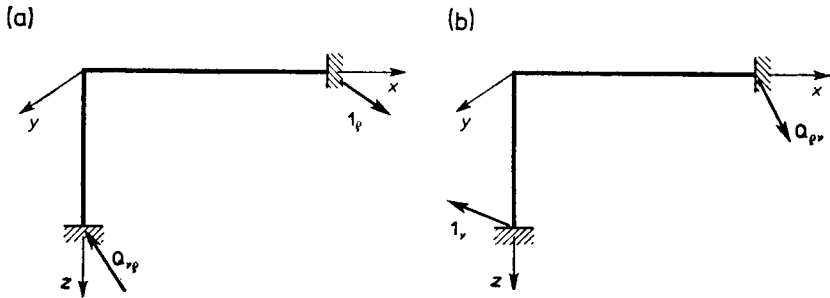
(a)   (b)

Fig. 4.7. Structure with its supports experiencing unit displacements

denoted by 1_ϱ (Fig. 4.7a). Depending on whether we deal with a sidesway or
rotation of the support, the vector 1_ϱ has a length or angle dimension. The
second state of strain of the structure is induced by a unit displacement 1_ν,
imparted to another support (Fig. 4.7b).

Loads of the kinematic type are accompanied by various reactions appear-
ing at the fixing points. Specifically, a reaction in the form of a generalized
force $Q_{\varrho\nu}$ appears at the place of occurrence of 1_ϱ, but it does so under the
influence of 1_ν. If 1_ϱ is a sidesway, then the reaction $Q_{\varrho\nu}$ is a force. But if 1_ϱ
stands for unit rotation, then the reaction $Q_{\varrho\nu}$ is a moment. In the same
way, the $Q_{\nu\varrho}$ type of reaction is related to the 1_ν type of displacement.

It can easily be demonstrated that Betti's reciprocal theorem (4.50) reduces
in this case to an equality of two scalar products:

$$Q_{\varrho\nu} \cdot 1_\varrho = Q_{\nu\varrho} \cdot 1_\nu. \tag{4.61}$$

Projecting $Q_{\varrho\nu}$ on the direction of the unit vector 1_ϱ and denoting the modulus
of this projection by $k_{\varrho\nu}$, we obtain the value of the left side of the equality
(4.61). Similarly, the length of the projection of $Q_{\nu\varrho}$ on the direction 1_ν,
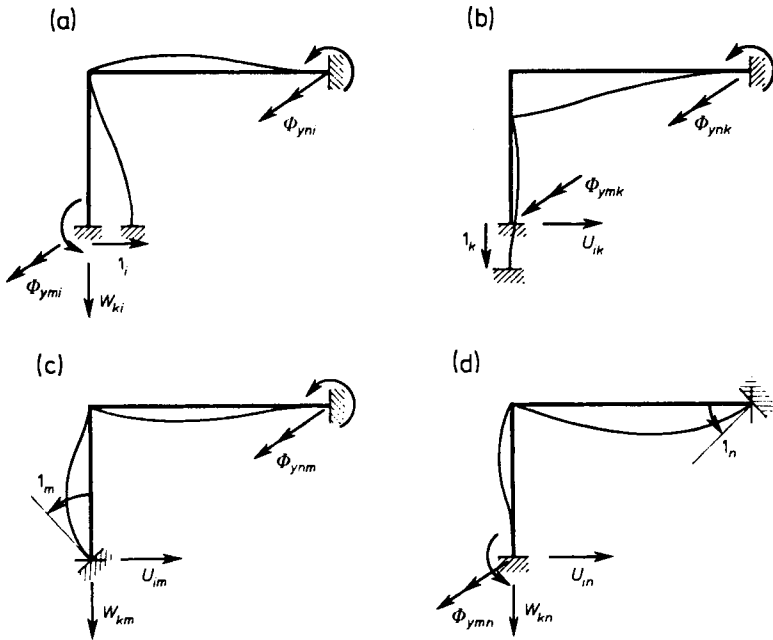

Fig. 4.8. Structure whose support suffered, (a), (b) unit sides way; (c), (d) unit rotations

denoted by $k_{v\varrho}$, is the value of the scalar product on the right-hand side of the equality (4.61). Following therefrom is the relation

$$k_{\varrho v} = k_{v\varrho}, \tag{4.62}$$

which is a mathematical wording of Rayleigh's reciprocal reaction theorem.

Shown as an example in Fig. 4.8 is a structure whose supports have experienced unit sideway (Fig. 4.8a, b) and rotations (Fig. 4.8c, d) in directions parallel to the axes of the adopted coordinate system. The displacements of the supports are accompanied by reactions whose selected components are also indicated in the drawings. The particular relations given below follow from Rayleigh's reciprocal theorem (4.62):

$$U_{lk} = W_{kl}, \qquad \varPhi_{ymn} = \varPhi_{ynm}, \tag{4.63}$$

$$U_{lm} = \varPhi_{yml}, \qquad U_{ln} = \varPhi_{ynl}, \qquad W_{km} = \varPhi_{ymk}, \qquad W_{kn} = \varPhi_{ynk}. \tag{4.64}$$

In so far as we have in Eqs. (4.63) quantities of unquestionably identical dimensions on both sides of the equality sign, one may have doubts as to the correctness of equating forces to moments in Eqs. (4.64). However, if we consider, for example, that the symbol U_{lm} denotes the ratio of the value of a force (reaction) to the cause of that reaction, i.e., to the angular displacement of the support m, and that the symbol $\varPhi_{yml}$ denotes the ratio of the value of a fixing moment to the sidesway of the support i, causing it, it is easily seen that with such interpretation of the denotations, we get both quantities expressed in force units on the left and right side of the equality sign in Eqs. (4.64).

4.6. The Reciprocal Displacement and Reaction Theorem

Let us consider in turn an elastic system which experiences two states of loading independent of each other: static and kinematic. Let a single generalized force $\mathbf{1}_\varrho$ with a modulus equalling one, arbitrarily oriented in space, be acting on a system in state ϱ (Fig. 4.9). In state v, one of the supports experiences a displacement $\mathbf{1}_v$ with an arbitrarily oriented unit vector (Fig.
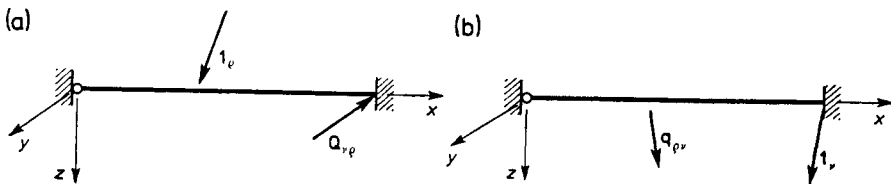

Fig. 4.9. Bar: (a) on which a unit generalized force is acting; (b) whose support experiences unit displacement

4.9b). Let us denote by $Q_{\nu\varrho}$, the reaction to the generalized force 1_ϱ at the place of occurrence of displacemenntt 1_ν, and by $q_{\varrho\nu}$, the displacement where the generalized force 1_ϱ is acting, induced by the displacement of the support 1_ν. If the generallized force 1_ϱ is a force in the narrow sense, then the displacement $q_{\varrho\nu}$ is a deflection. But when 1_ϱ stands for a unit moment, then the quantity $q_{\varrho\nu}$ is an angular displacement of the cross-section. Similarly, in the case of displacement 1_ν, when it is in the nature of a deflection, the reaction $Q_{\nu\varrho}$ is a force. But when 1_ν is an angular displacement of the support, then $Q_{\nu\varrho}$ stands for the fixing moment.

Betti's reciprocal work theorem (4.50) written vectorially takes in this case the form:

$$1_\varrho \cdot q_{\varrho\nu} + Q_{\nu\varrho} \cdot 1_\nu = 0. \tag{4.65}$$

On the right side of the equality sign we have zero, because in state ν the only forces acting on the system are support reactions (Fig. 4.9b) which do not perform any work on the displacements occurring in state ϱ (Fig. 4.9a) because the supports remain immovable.

Let us project the vector $q_{\varrho\nu}$ on the direction of the unit vector 1_ϱ and denote the projection length by $\delta_{\varrho\nu}$. Let us also project $Q_{\nu\varrho}$ on the direction of unit displacement 1_ν and denote the vector of the projection by $k_{\nu\varrho}$. With these denotations, Eq. (4.65) can be written in the form

$$\delta_{\varrho\nu} = -k_{\nu\varrho}. \tag{4.66}$$

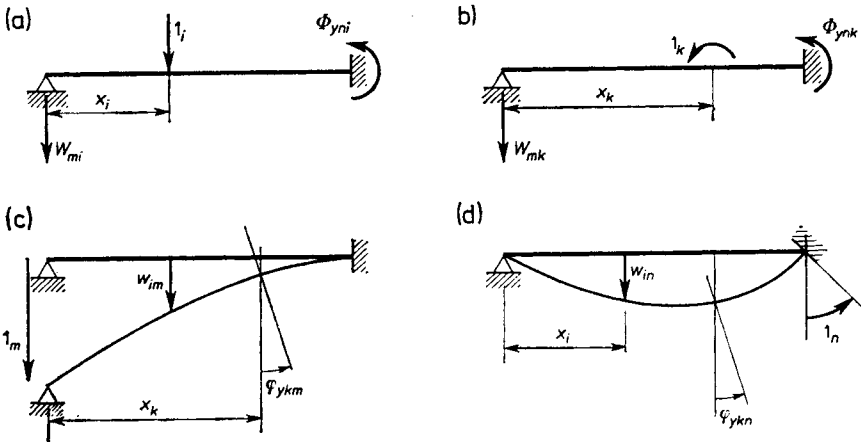This is a mathematical description of the reciprocal displacement and reaction theorem.

Fig. 4.10. Beam under (a), (b) unit generalized forces; (c), (d) experiencing displacements of supports

The theorem takes various forms depending on the character of the generalized force 1_ϱ and displacements 1_r. Figure 4.10 shows a beam loaded in the xz plane by a unit force (Fig. 4.10a), a unit moment (Fig. 4.10b), a unit deflection of the support (4.10c) and a unit rotation of the support (Fig. 4.10d). The relations between the reactions and the corresponding displacements indicated in the drawings are:

$$w_{lm} = -W_{ml}, \qquad \varphi_{ykm} = -W_{mk},$$
$$w_{ln} = -\Phi_{ynl}, \qquad \varphi_{ykn} = -\Phi_{ynk}. \tag{4.67}$$

It is left to the reader to determine the dimensions in which the particular quantities are to be expressed.

4.7. The Reciprocal Displacement and Internal Force Theorem

This time, we shall prove the theorem only for particular examples, without attempting to formulate for the general case. We should explain first of all geometrical meaning of distortional strains distributed in the form of δ-Dirac's distribution. For example, let straight bar lying in the xz plane (Fig. 4.11) experience elongations defined as follows:

$$\varepsilon^0 = \begin{cases} 0 & \text{for} \quad |x-x_0| > e, \\ \dfrac{1}{2e} & \text{for} \quad |x-x_0| \leqslant e. \end{cases}$$

(a)   (b)
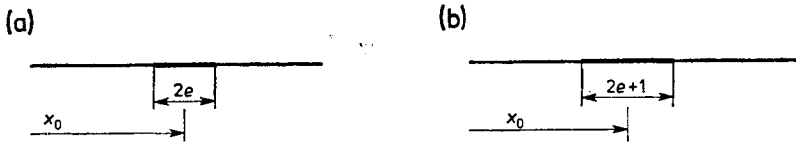
Fig. 4.11. δ-Dirac's distribution of elongation

In this connection, a segment of initial length $2e$ (Fig. 4.11a) will have after deformation the length $2e(1+\varepsilon^0) = 2e+1$ (Fig. 4.11b). As the value of e decreases, the length of the deformed segment approaches one. Hence, the symbol $\varepsilon^0 = 1\delta(x-x_0)$ signifies that an additional bar segment of unit length has appeared in the cross-section $x = x_0$.

Assume in turn that the shear strain angle β_z^0 is expressed:

$$\beta_z^0 = \begin{cases} 0 & \text{for} \quad |x-x_0| > e, \\ \dfrac{1}{2e} & \text{for} \quad |x-x_0| \leqslant e. \end{cases}$$
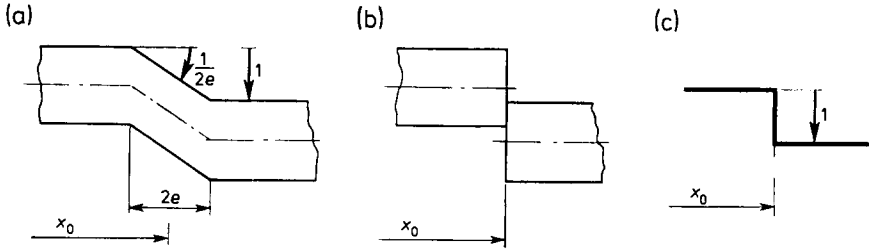
Fig. 4.12. δ-Dirac's distribution of shear strain

It is seen from Fig. 4.12a, which describes the above deformation, that regardless of the length of the segment, $2e$, a transverse jump over a distance equalling a unit segment occurs between the left and right part of the bar. Going over from e to zero in the length of the segment (Fig. 4.12b) is tantamount to the appearance in the cross-section $x = x_0$ of an element of unit length, placed perpendicular to the axis of the bar (Fig. 4.12c). This pattern of distortional, shear strains is described as follows:

$$\beta_z^0 = 1\delta(x-x_0).$$

Finally, let us consider a case of strain in which a fixed curvature of the value $\dfrac{1}{2e}$ occurs over the length $2e$, expressed as follows:

$$\varkappa_y^0 = \begin{cases} 0 & \text{for} \quad |x-x_0| > e, \\ \dfrac{1}{2e} & \text{for} \quad |x-x_0| \leqslant e. \end{cases}$$
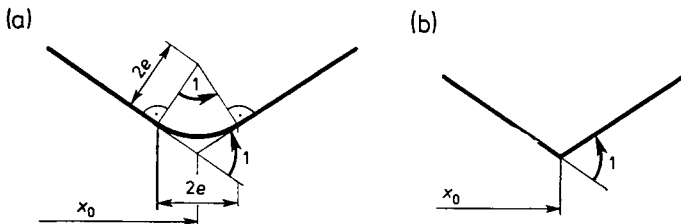
Fig. 4.13. δ-Dirac's distribution of curvature

Figure 4.13a shows the corresponding strain of the bar, and Fig. 4.13b, the same strain on passing with the value of e to zero. Consequently, the strain described by the formula $\varkappa_y^0 = 1\delta(x-x_0)$ is to be understand as a bend of the bar axis by a unit angle in the cross-section $x = x_0$.

A similar reasoning leads us to the conclusion that in describing the distortional strain by the formula $\varkappa_s^0 = 1\delta(x-x_0)$ we mean to say that the right part of the bar has been rotated with respect to the left by unit angle.

Assume now that a distortional strain $\varepsilon_\varrho^0 = 1_\varrho\delta(x-x_\varrho)$ appears in state ϱ. Hence, the matrix (4.40) takes the form

$$\epsilon_\varrho^0 = \{1_\varrho\,\delta(x-x_\varrho), 0, 0, 0, 0, 0\}.$$

Let the generalized internal forces forming the matrix σ_ν constructed as in Eqs. $(4.5)_2$ and (4.2) occur in state ν. The work $L_{\nu\varrho}^0$ performed on strains ϵ_ϱ^0 by those internal forces is

$$L_{\nu\varrho}^0 = \int_0^l \sigma_\nu^T(x)\epsilon_\partial^0(x)\,dx = \int_0^l N_\nu(x)1_\varrho\,\delta(x-x_\varrho)\,dx$$

$$= N_\nu(x_\varrho)1_\varrho = N_{\varrho\nu}1_\varrho. \tag{4.68}$$

If $\beta_{z\varrho}^0(x) = 1_\varrho^*\delta(x-x_\varrho)$ is the strain in state ϱ, then the matrix $\epsilon_\varrho^0(x)$ takes the form

$$\epsilon_\varrho^0(x) = \{0, 0, 1_\varrho\,\delta(x-x_\varrho), 0, 0, 0\},$$

and the value of the work performed by the general internal forces occurring in that ν on the distortional strain in state ϱ is

$$L_{\nu\varrho}^0 = \int_0^l T_{z\nu}(x)1_\varrho\,\delta(x-x_\varrho)\,dx = T_{z\nu}(x_\varrho)1_\varrho = T_{z\varrho\nu}1_\varrho. \tag{4.69}$$

Firstly, in the case of strain $\varkappa_{y\varrho}^0(x) = 1_\varrho\,\delta(x-x_\varrho)$ we have

$$\epsilon_\varrho^0(x) = \{0, 0, 0, 0, 1_\varrho\,\delta(x-x_\varrho), 0\},$$

and the work performed on these strains by the generalized internal forces $\sigma_\nu^s(x)$ is

$$L_{\nu\varrho}^0 = \int_0^l M_{y\nu}(x)1_\varrho\,\delta(x-x_\varrho)\,dx = M_{y\nu}(x_\varrho)1_\varrho = M_{y\varrho\nu}1_\varrho. \tag{4.70}$$

Figure 4.14 shows a bend bar, lying in the xz plane, subjected to independent of each other, unit force 1_i (Fig. 4.14a) and unit moment 1_k (Fig. 4.14b). Moreover, the structure experiences the independent distortional strains $\varepsilon_m^0 = 1_m\delta(x-x_m)$, $\beta_{zn}^0 = 1_n\delta(x-x_n)$ and $\varkappa_{yr}^0 = 1_r\delta(x-x_r)$ as shown in Figs. 4.14c, d, e. The states of loading $j = i, k$ are accompanied by the appearance of generalized internal forces, which in cross-sections $s = m, n, r$ assume the values N_{sj}, T_{zjs}, M_{ysj}. On the other hand, the unit strains induce displacements w_{js}, φ_{yjs} at points of attachment of the generalized forces.
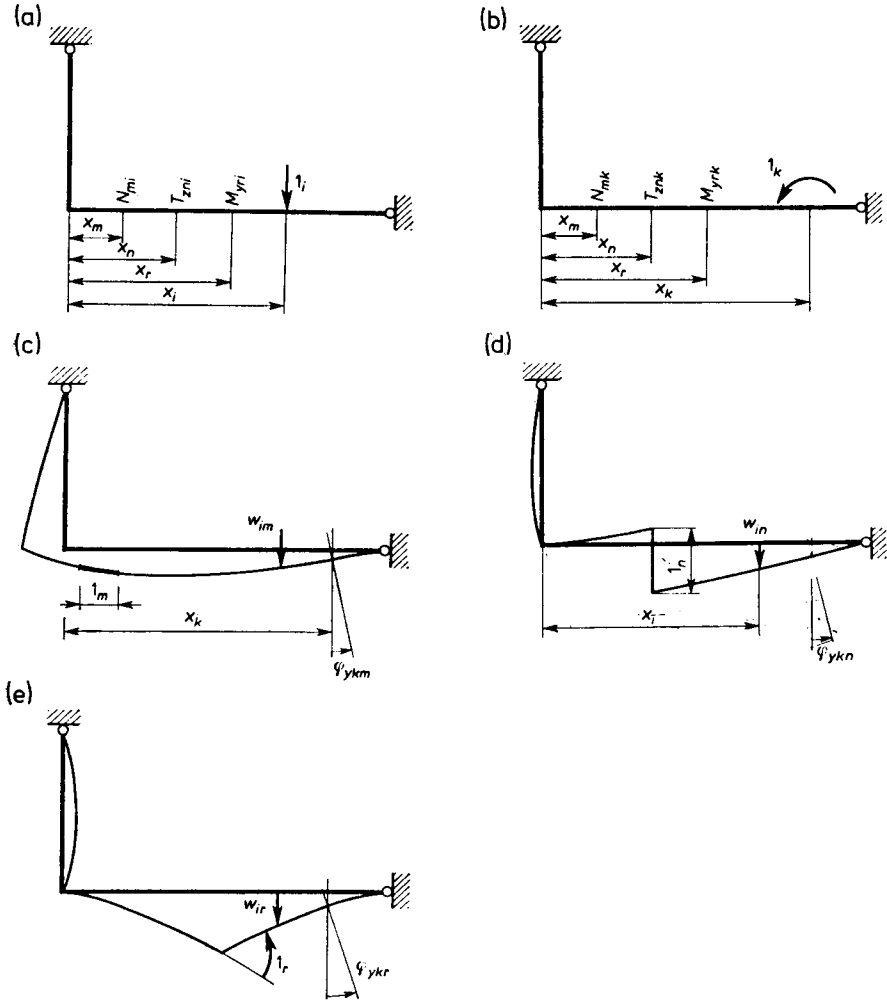
Fig. 4.14. Structure loaded by (a), (b) unit generalized forces; (c)–(e) δ-Dirac's distributions of strains

Using this time a more general form of the reciprocal work theorem (4.49) and considering the relations (4.68)–(4.70), we get:

$$w_{im} = N_{mi}, \qquad w_{in} = T_{zni}, \qquad w_{ir} = M_{yri},$$

$$\varphi_{ykm} = N_{mk}, \qquad \varphi_{ykn} = T_{znk}, \qquad \varphi_{ykr} = M_{yrk}. \tag{4.71}$$

The reciprocal theorems derived in this chapter have numerous applications in the statics of bar structures, especially in the determination of what is known as influence lines, which are discussed later.

5. Internal Forces and Displacements of the Axis of an Element

5.1. The Second Stage of Discretization of a Structure

As we have demonstrated in Chapter 2, all components of the state of stress at an arbitrary point of the cross-section of a bar can be determined knowing the internal forces associated with its axis. Likewise, the displacements within a three-dimensional body and the components of the stage of strain are determinable on geometric quantities referred to the bar axis. As the first stage of discretization of a system, we have treated the replacement of a three-dimensional body by a one-dimensional object in one dimension, which is the static scheme of a bar.

In the next stage of discretization, we switch from bar axes to certain selected points on these axes, these being usually the points of intersection of the axes of several elements. Those points we shall call *joints* of a structure, and the bars joining them we shall call *elements*. In this and the following chapters, we shall regard as elements only single, unfurcated bars containing no discontinuities of shape or cross-section over their length. Therefore, the concept of an element will now be narrower than in Chapter 3. In the sequel the cross-sections adjacent to joints will be called the *characteristic cross-sections*. Putting aside for the time being the methods of determining quantities in characteristic cross-sections, we shall concentrate on the problem of relating the internal forces and the displacements of the axis of an element to boundary values which will be considered as known.

We deal exclusively with elements having the shape of a straight or in-plane curved bar. Bars of more complex shape will not be considered for two reasons. Firstly, they are less commonly used in structures, and secondly, considerable difficulty is encountered in their analysis, since all static and geometric quantities go into a single implicit set of differential equations jointly of 12th order.

5.2. A Straight Element under Tension, Compression or Torsion

Consider a straight bar whose axis runs from point i $(x = 0)$ to point k $(x = l)$. Introducing the dimensionless coordinate

$$\xi = \frac{x}{l}, \quad \xi' = 1 - \xi \tag{5.1}$$

and using denotation

$$f' = \frac{\mathrm{d}f}{\mathrm{d}\xi}, \tag{5.2}$$

we rewrite the set of equations for a bar under tension or compression $(2.4)_1$, $(2.11)_1$ and $(2.16)_1$ in the form

$$N' + p_x l = 0, \quad u' = \varepsilon l, \quad N = EA(\varepsilon - \varepsilon^0). \tag{5.3}$$

These equations have an identical structure to that of the equations for a bar under torsion (2.26), (2.32) and (2.36):

$$M_t' + m_t l = 0, \quad \varphi_t' = \varkappa_t l, \quad M_t = GJ_t(\varkappa_t - \varkappa_t^0). \tag{5.4}$$

Separate analysis of the torsion problem is therefore unnecessary because all considerations concerning a bar under tension — with suitably altered denotations—also apply to a bar under torsion.

Considering the initial conditions $(4.22)_4$ (cf. Fig. 4.1), we first integrate the equation $(5.3)_1$:

$$N(\xi) = -U_i - l \int\limits_{0}^{\xi} p_x \mathrm{d}\xi, \tag{5.5}$$

Using eq. $(5.3)_3$ we then find ε. After substituting this function into Eq. $(5.3)_2$ and after integrating, we obtain the function expressing displacements:

$$u(\xi) = u_i - U_i l \int\limits_{0}^{\xi} \frac{\mathrm{d}\xi}{EA} - l^2 \int\limits_{0}^{\xi} \left(\frac{1}{EA} \int\limits_{0}^{\xi} p_x \mathrm{d}\xi \right) \mathrm{d}\xi + l \int\limits_{0}^{\xi} \varepsilon^0 \mathrm{d}\xi. \tag{5.6}$$

In the special case $EA = \mathrm{const}$, the function (5.7) assumes a simpler form:

$$u(\xi) = u_i - \frac{U_i l}{EA} \xi - \frac{l^2}{EA} \int\limits_{0}^{\xi} p_x(\xi_0) (\xi - \xi_0) \mathrm{d}\xi_0 + l \int\limits_{0}^{\xi} \varepsilon^0 \mathrm{d}\xi. \tag{5.7}$$

We would arrive at the same results by reducing the set of equations (5.1) into a single differential equation of the second order

$$(EAu')' = -p_x l^2 + l(EA\varepsilon^0)', \tag{5.8}$$

and finding its integral by quadratures.

We confine our further considerations to the most common case in practice, $EA = $ const.

The following relations between the boundary values at one end and at the other end of a bar, may be obtained by letting $\xi = 1$ in the functions (5.5) and (5.7):

$$U_k = -U_i - l \int_0^1 p_x \, \mathrm{d}\xi,$$

(5.9)

$$u_k = u_i - \frac{U_i l}{EA} - \frac{l^2}{EA} \int_0^1 p_x \xi' \, \mathrm{d}\xi + l \int_0^1 \varepsilon^0 \, \mathrm{d}\xi.$$

(5.10)

The set of algebraic equations (5.9) and (5.10) must be satisfied irrespective of the boundary conditions that have been imposed on the solution. It cannot therefore be required to satisfy more than two given boundary conditions, and no more than half of them can be in the nature of static conditions.

Consider a particular case, important from an engineering point of view, in which the geometric boundary conditions at both ends are given. We then determine from equation (5.10) the value U_i and after substituting it into the functions (5.5) and (5.8), to obtain the equations for the axial force and for the displacement of cross-sections:

$$N(\xi) = \frac{EA}{l} (u_k - u_i) +$$

$$+ l \int_0^1 p_x(\xi_0) f_1(\xi, \xi_0) \, \mathrm{d}\xi_0 - EA \int_0^1 \varepsilon^0 \, \mathrm{d}\xi,$$

(5.11)

$$u(\xi) = u_i \xi' + u_k \xi + \frac{l^2}{EA} \int_0^1 p_x(\xi_0) f_2(\xi, \xi_0) \, \mathrm{d}\xi_0 +$$

$$+ l \int_0^1 \varepsilon^0(\xi_0) f_1(\xi_0, \xi) \, \mathrm{d}\xi_0.$$

(5.12)

We have introduced here the following denotations:

$$f_1(\xi, \xi_0) = -\xi_0 H(\xi - \xi_0) + \xi_0' H(\xi_0 - \xi),$$

(5.13)

$$f_2(\xi, \xi_0) = \xi_0 \xi' H(\xi - \xi_0) + \xi \xi_0' H(\xi_0 - \xi),$$

(5.14)

in which $H(x)$ denotes Heaviside's function.

The functions f_i are Green's functions of different kind, known in the mechanics of bar (and surface) structures as *influence functions*. Their plots or so-called *influence lines*, have, by virtue of their pictorial character, found

wide uses in static analysis of a particular kind of bar structure, namely that on which loads of fixed direction but of variable position are acting. For this reason, influence lines are usually used in static analysis of bridge structures.

Let the only load acting on a bar be a concentrated force P_x acting at a point with the abscissa $\xi = \xi_P$. We thereby express the load p_x by means of δ-Dirac's distribution:

$$p_x(\xi_0) = \frac{P_x}{l} \delta(\xi_0 - \xi_P). \tag{5.15}$$

Substituting the expression into Eqs. (5.11) and (5.12) we get

$$N(\xi) = P_x f_1(\xi, \xi_P), \quad u(\xi) = \frac{P_x l}{EA} f_2(\xi, \xi_P). \tag{5.16}$$
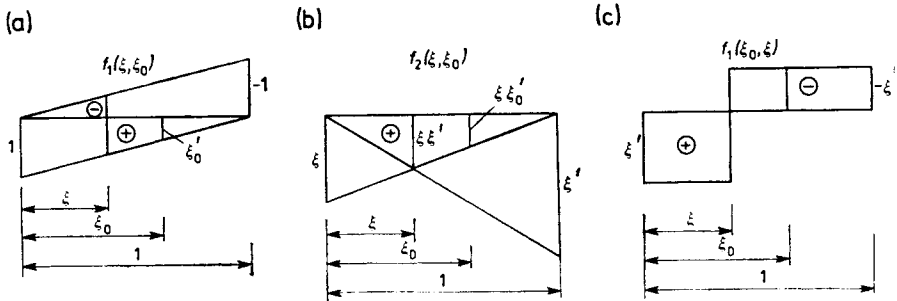
Fig. 5.1. Diagrams of Green's functions

Every ordinate of the influence line shown in Fig. 5.1a can be interpreted as the value of longitudinal force N in cross-section ξ, induced by force $P_x = 1$ acting at the site at which we measure the oridnate of the graph. Similarly, the ordinates of the influence line in Fig. 5.1b multiplied by the parameter l/EA show how the sideway $u(\xi)$ changes as the force $P_x = 1$ moves along the axis of the bar.

The influence function given in Fig. 5.1c expresses the variation of the displacement u in a fixed cross-section ξ under the influence of a unit distortional extension introduced in an arbitrary cross-section ξ_e:

$$l\varepsilon^0(\xi) = \Delta l \delta(\xi - \xi_e), \quad \Delta l = 1. \tag{5.17}$$

We can see that when this additional element is incorporated, for example, at any place to the left of the considered cross-section ($\xi_e < \xi$), the displacement $u(\xi)$ is then positive and equals ξ'.

5.3. Straight Element under Bending

Assume that the bar described in the preceding section is now subjected to bending in the xz-plane. Introducing the dimensionless variable (5.1) and the denotations (5.2), the equations (2.4)$_3$, (2.5)$_1$, (2.16)$_2$, (4.7)$_1$, (4.8)$_2$ and (4.36)$_2$ after suitable rearranging can be given in the form:

$$T_z' + p_z l = 0, \qquad M_y' - T_z l + m_y l = 0, \tag{5.18}$$

$$\varkappa_y = \frac{1}{l}\,\varphi_y', \qquad \beta_z = \frac{1}{l}\,w' + \varphi_y, \tag{5.19}$$

$$M_y = EJ_y(\varkappa_y - \varkappa_y^0), \qquad T_z = \frac{GA}{k_z}\,(\beta_z - \beta_z^0). \tag{5.20}$$

Since the respective relations applying to bending in the xy plane are analogous to Eqs. (5.18)–(5.20), we shall not consider this problem separately. All that has to be remembered is the difference in the signs of the quantities m, φ, M and $\varkappa$.

As in the case of a bar under tension, we find the solution by quadratures:

$$T_z(\xi) = -W_l - l\int_0^\xi p_z\,\mathrm{d}\xi, \tag{5.21}$$

$$M_y(\xi) = -\Phi_{yl} - W_l l\xi - l^2\int_0^\xi p_z(\xi_0)\,(\xi - \xi_0)\,\mathrm{d}\xi_0 - l\int_0^\xi m_y\,\mathrm{d}\xi, \tag{5.22}$$

$$\varphi_y(\xi) = \varphi_{yl} - \Phi_{yl} l\int_0^\xi \frac{\mathrm{d}\xi}{EJ_y} - W_l l^2\int_0^\xi \frac{\xi\,\mathrm{d}\xi}{EJ_y} -$$

$$- l^3\int_0^\xi \left[\frac{1}{EJ_y}\int_0^\xi p_z(\xi_0)\,(\xi - \xi_0)\,\mathrm{d}\xi_0 \right]\mathrm{d}\xi -$$

$$- l^2\int_0^\xi \left(\frac{1}{EJ_y}\int_0^\xi m_y\,\mathrm{d}\xi \right)\mathrm{d}\xi + l\int_0^\xi \varkappa_y^0\,\mathrm{d}\xi, \tag{5.23}$$

$$w(\xi) = w_l - \varphi_{yl} l\xi + \Phi_{yl} l^2\int_0^\xi \frac{\xi - \xi_0}{EJ_y(\xi_0)}\,\mathrm{d}\xi_0 +$$

$$+ W_l l^3\int_0^\xi \frac{\xi - \xi_0}{EJ_y(\xi_0)}\,\xi_0\,\mathrm{d}\xi_0 - W_l l\int_0^\xi \frac{k_z}{GA}\,\mathrm{d}\xi +$$

$$+ l^4 \int_0^\xi \left[\frac{\xi - \xi_1}{EJ_y(\xi_1)} \int_0^{\xi_1} p_z(\xi_0)(\xi_1 - \xi_0) d\xi_0 \right] d\xi_1 -$$

$$- l^2 \int_0^\xi \left(\frac{k_z}{GA} \int_0^\xi p_z d\xi \right) d\xi + l^3 \int_0^\xi \left(\frac{\xi - \xi_0}{EJ_y(\xi_0)} \int_0^\xi m_y d\xi \right) d\xi_0 -$$

$$- l^2 \int_0^\xi \varkappa_y^0(\xi_0)(\xi - \xi_0) d\xi_0 + l \int_0^\xi \beta_z^0 d\xi . \tag{5.24}$$

Since we assume as before that the considered bar is prismatic, we use the simplified form of Eqs. (5.23) and (5.24):

$$\varphi_y(\xi) = \varphi_{yl} - \frac{\Phi_{yl} l}{EJ_y} \xi - \frac{W_l l^2}{EJ_y} \frac{\xi^2}{2} -$$

$$- \frac{l^3}{EJ_y} \int_0^\xi p_z(\xi_0) \frac{(\xi - \xi_0)^2}{2} d\xi_0 -$$

$$- \frac{l^2}{EJ_y} \int_0^\xi m_y(\xi_0)(\xi - \xi_0) d\xi_0 + l \int_0^\xi \varkappa_y^0 d\xi , \tag{5.25}$$

$$w(\xi) = w_l - \varphi_{yl} l\xi + \frac{\Phi_{yl} l^2}{EJ_y} \frac{\xi^2}{2} + \frac{W_l l^3}{EJ_y} \left(\frac{\xi^3}{6} - \gamma_z \xi \right) +$$

$$+ \frac{l^4}{EJ_y} \int_0^\xi p_z(\xi_0) \left[\frac{(\xi - \xi_0)^3}{6} - \gamma_z(\xi - \xi_0) \right] d\xi_0 +$$

$$+ \frac{l^3}{EJ_y} \int_0^\xi m_y(\xi_0) \frac{(\xi - \xi_0)^2}{2} d\xi_0 -$$

$$- l^2 \int_0^\xi \varkappa_y^0(\xi_0)(\xi - \xi_0) d\xi_0 + l \int_0^\xi \beta_z^0 d\xi . \tag{5.26}$$

The dimensionless parameter

$$\gamma_z = \frac{k_z EJ_y}{GAl^2} \tag{5.27}$$

describes the influence of shear strains.

Letting $\xi = 1$ in Eqs. (5.21), (5.22), (5.25) and (5.26), we obtain four relations that must occur between eight boundary values:

$$W_k = -W_l - l \int_0^1 p_z d\xi , \tag{5.28}$$

$$\Phi_{yk} = -\Phi_{yi} - W_i l - l^2 \int_0^1 p_z \xi' \mathrm{d}\xi - l \int_0^1 m_y \mathrm{d}\xi. \tag{5.29}$$

$$\varphi_{yk} = \varphi_{yi} - \frac{\Phi_{yi} l}{EJ_y} - \frac{W_i l^2}{2EJ_y} - \frac{l^3}{2EJ_y} \int_0^1 p_z \xi'^2 \mathrm{d}\xi -$$

$$- \frac{l^2}{EJ_y} \int_0^1 m_y \xi' \mathrm{d}\xi + l \int_0^1 \varkappa_y^0 \mathrm{d}\xi, \tag{5.30}$$

$$w_k = w_i - \varphi_{yi} l + \frac{\Phi_{yi} l^2}{2EJ_y} + \frac{W_i l^3}{6EJ_y} (1 - 6\gamma_z) +$$

$$+ \frac{l^4}{6EJ_y} \int_0^1 p_z(\xi'^3 - 6\gamma_z \xi') \mathrm{d}\xi + \frac{l^3}{2EJ_y} \int_0^1 m_y \xi'^2 \mathrm{d}\xi -$$

$$- l^2 \int_0^1 \varkappa_y^0 \xi' \mathrm{d}\xi + l \int_0^1 \beta_z^0 \mathrm{d}\xi. \tag{5.31}$$

As in the preceding section, we consider a special case here as well, in which at both ends of the bar, only boundary conditions of geometric nature are given. We therefore solve the set of equations (5.30), (5.31) with respect to the unknowns θ_{yi} and W_i, and substitute them into equations (5.21), (5.22), (5.25) and (5.26) to get

$$T_z(\xi) = (1 - \mu_z) \frac{6EJ_y}{l^2} \left(\varphi_{yi} + \varphi_{yk} + 2 \frac{w_k - w_i}{l} \right) +$$

$$+ l \int_0^1 p_z(\xi_0) f_3(\xi, \xi_0) \mathrm{d}\xi_0 + \int_0^1 m_y \theta \mathrm{d}\xi +$$

$$+ 6(1 - \mu_z) \frac{EJ_y}{l} \int_0^1 \varkappa_y^0 (1 - 2\xi) \mathrm{d}\xi - 12(1 - \mu_z) \frac{EJ_y}{l^2} \int_0^1 \beta_z^0 \mathrm{d}\xi, \tag{5.32}$$

$$M_y(\xi) = - \frac{EJ_y}{l} [\varphi_{yi} F(\xi, 0) - \varphi_{yk} F(\xi, 1)] -$$

$$- 6(1 - \mu_z) \frac{EJ_y}{l} \frac{w_k - w_i}{l} (1 - 2\xi) +$$

$$+ l^2 \int_0^1 p_z(\xi_0) f_4(\xi, \xi_0) \mathrm{d}\xi_0 +$$

$$+l\int_0^1 m_y(\xi_0)f_5(\xi,\,\xi_0)\mathrm{d}\xi_0 - EJ_y\int_0^1 \varkappa_y^0(\xi_0)F(\xi,\,\xi_0)\mathrm{d}\xi_0 +$$

$$+6(1-\mu_z)\frac{EJ_y}{l}(1-2\xi)\int_0^1 \beta_z^0\mathrm{d}\xi, \tag{5.33}$$

$$\varphi_y(\xi) = \varphi_{yi}\Psi(\xi)+\varphi_{yk}\Psi(\xi') - \frac{w_k-w_i}{l}\,\theta(\xi)+$$

$$+\frac{3l^3}{2EJ_y}\int_0^1 p_z(\xi_0)f_6(\xi,\,\xi_0)\mathrm{d}\xi_0 + \frac{l^2}{EJ_y}\int_0^1 m_y(\xi_0)f_7(\xi,\,\xi_0)\mathrm{d}\xi_0 +$$

$$+l\int_0^1 \varkappa_y^0(\xi_0)f_5(\xi_0,\,\xi)\mathrm{d}\xi_0 + \int_0^1 \beta_z^0\,\theta(\xi)\mathrm{d}\xi. \tag{5.34}$$

$$w(\xi) = w_i\varGamma(\xi)+w_k\varGamma(\xi') - \varphi_{yi}l\Omega(\xi)+\varphi_{yk}l\Omega(\xi')+$$

$$+\frac{l^4}{6EJ_y}\int_0^1 p_z(\xi_0)f_8(\xi,\,\xi_0)\mathrm{d}\xi_0 + \frac{3l^3}{2EJ_y}\int_0^1 m_y(\xi_0)f_6(\xi_0,\,\xi)\mathrm{d}\xi_0 +$$

$$+l^2\int_0^1 \varkappa_y^0(\xi_0)f_4(\xi_0,\,\xi)\mathrm{d}\xi_0 + l\int_0^1 \beta_z^0(\xi_0)f_3(\xi_0,\,\xi)\mathrm{d}\xi_0. \tag{5.35}$$

New denotations appear here:

$$\mu_z = \frac{12\gamma_z}{1+12\gamma_z}, \tag{5.36}$$

$$f_3(\xi,\,\xi_0) = f_1(\xi,\,\xi_0)+(1-\mu_z)\xi_0\xi'_0(1-2\xi_0), \tag{5.37}$$

$$f_4(\xi,\,\xi_0) = f_2(\xi,\,\xi_0)-\tfrac{1}{2}\xi_0\xi'_0-\frac{1-\mu_z}{2}\,\xi_0\xi'_0(1-2\xi_0)\,(1-2\xi), \tag{5.38}$$

$$f_5(\xi,\,\xi_0) = f_1(\xi,\,\xi_0)-3(1-\mu_z)\xi_0\xi'_0(1-2\xi), \tag{5.39}$$

$$f_6(\xi,\,\xi_0) = (\xi-\xi_0)f_2(\xi,\,\xi_0)-(1-\mu_z)\xi\xi'\xi_0\xi'_0(1-2\xi_0), \tag{5.40}$$

$$f_7(\xi,\,\xi_0) = f_2(\xi,\,\xi_0)-3(1-\mu_z)\xi\xi'\xi_0\xi'_0, \tag{5.41}$$

$$f_8(\xi,\,\xi_0) = [3\xi'^2\Omega(\xi'_0)-(\xi'^3-6\gamma_z\xi')\varGamma(\xi'_0)]\mathrm{H}(\xi-\xi_0)+$$
$$+[3\xi^2\Omega(\xi_0)-(\xi^3-6\gamma_z\xi)\varGamma(\xi_0)]\mathrm{H}(\xi_0-\xi), \tag{5.42}$$

$$F(\xi,\,\xi_0) = 1+3(1-\mu_z)\,(1-2\xi)\,(1-2\xi_0), \tag{5.43}$$

$$\varGamma(\xi) = \varrho(\xi)-\mu_z\chi(\xi), \quad \Omega(\xi) = \omega(\xi)-\tfrac{1}{2}\mu_z\chi(\xi), \tag{5.44}$$

$$\theta(\xi) = 6(1-\mu_z)\xi\xi', \quad \Psi(\xi) = 1-4\xi+3\xi^2+3\mu_z\xi\xi', \tag{5.45}$$

$$\varrho(\xi) = 1 - 3\xi^2 + 2\xi^3,$$
$$\omega(\xi) = \xi - 2\xi^2 + \xi^3, \tag{5.46}$$
$$\chi(\xi) = \xi - 3\xi^2 + 2\xi^3,$$

In deriving the above equations, we have not omitted the influence of transverse forces on strains of the element. In practice, however, we deal mostly with bars with a high slenderness ratio so that the influence of shear on their deformation is negligible. As a result, we can use as a rule simplified equations whereby the general parameters γ_z and μ_z have been neglected.

An alternative solution, leading to the same results, consists of reducing the set of equations (5.18)–(5.20) to a single ordinary differential equation of the fourth order:

$$EJ_y w^{\mathrm{IV}} = l^4(p_z - \gamma_z p_z'') + l^3 m_y' - EJ_y l^2 \varkappa_y^{0''} + EJ_y l\beta_z^{0'''}. \tag{5.47}$$

Finding its integral, we can express the deflection angles φ_y and the internal forces involved by suitable derivatives of the w-function.

The functions (5.37)–(5.46) are influence functions. The diagrams of functions f_3, lf_4, f_5 and θ/l are given in Fig. 5.2. The first one is the influence line

(a)

$l w. T_z^P(\xi_a, \xi)$

(b)

$l.w. M_y^P(\xi_a, \xi)$

(c)

$l.w. M_y^M(\xi_a, \xi)$
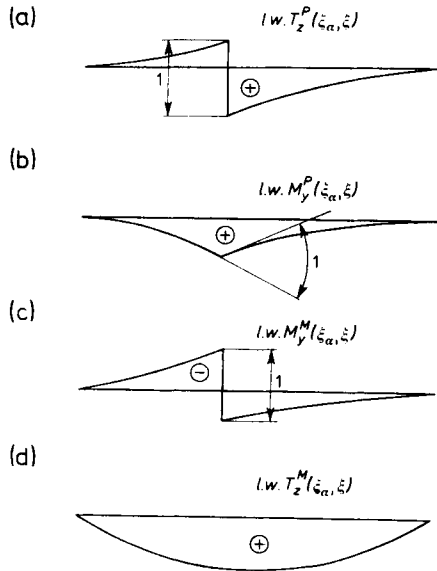
(d)

$l.w. T_z^M(\xi_a, \xi)$

Fig. 5.2. Influence lines for beam fixed at both ends

of the transverse force of section ξ from an unit force moving along a bar fixed at both ends, the second is the influence line of the bending moment from a moving force, the third, the influence line of the bending moment from a moving

unit moment, and lastly, the fourth the influence line of the transverse force from a moving moment. Note that the last line is identical for all cross-sections of the bar; it is independent of the coordinate ξ giving the position of the cross-section. The meaning of the remaining functions in Eqs. (5.32)–(5.35) may be deduced by the reader himself.

In this way, all internal forces and displacements of the axis of an element can be related algebraically to boundary quantities, both static and geometric, and also to the static load and the distortional strains occurring over the length of the element. Thus, a problem requiring in principle that a set of partial differential equations be solved has been reduced as the result of the first stage of discretization to ordinary differential equations which are further reduced to algebraic relations after the second stage.

5.4. Element on an Elastic Foundation

Building structures frequently stand on wall footings which are treated as beams resting on an elastic foundation. That same model is taken also for a bar resting on several, closely spaced elastic support elements. One structure of this type is, for example, a railway rail mounted on sleepers.

Many various models of an elastic foundation have been constructed. The most widely used is the one- or two-parameter model of Winkler (1867). We shall therefore discuss in detail the problem of a bar resting on a Winkler two-parameter foundation. In line with his assumptions, the passive pressure of the foundation is proportional to the displacements of the beam resting on it, acting in opposite sense to that of the displacements. Consequently, if the displacements of a bar subjected to bending are described by two functions, w and φ_y, then these displacements are accompanied by the following reactions of the foundation:

$$p_z^* = -K_w w, \quad m_y^* = -K_\varphi \varphi_y. \tag{5.48}$$

The coefficients of proportionality K_w and K_φ are determined in various ways depending on how the elastic support of the bar is effected. If, for example, soil is to be that support, then we let

$$K_w = \varkappa_w b, \tag{5.49}$$

where b is the width of the beam cross-section, and $\varkappa_w$ [N/m^3], is the foundation modulus which is determined experimentally for different kinds of soil. Considering also the stiffness of soil to horizontal displacements, given by the module $\varkappa_u$, we can express the coefficient of proportionality K_φ (cf. Kączkowski, 1968):

$$K_\varphi = \varkappa_u \frac{bh^2}{4}.$$ (5.50)

The symbol h denotes here the height of the beam cross-section.

If the beam rests on closely spaced cross-beams rigidly fixed at both ends (Fig. 5.3), we can easily arrive at the expression

$$K_w = \frac{24EJ}{a^3c}, \qquad K_\varphi = \frac{2GJ_s}{ac},$$ (5.51)
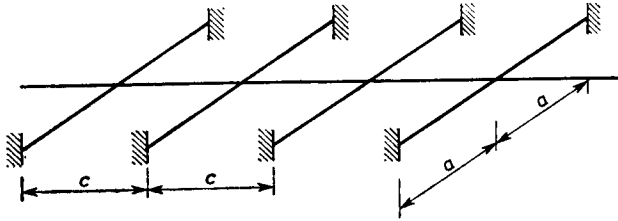

Fig. 5.3. Continuous beam on elastic supports

in which quantities EJ, GJ_s, a, apply to the supporting cross-beams. A similar foundation was studied by Urbanowski (1956).

Additional loads (5.48) need to be considered now in the equilibrium equations

$$T_z' + lp_z - lK_w w = 0,$$
$$M_y' - lT_z + lm_y - lK_\varphi \varphi_y = 0.$$ (5.52)

The set of equations (5.52) differs fundamentally from the set (5.18). Whereas the set of two static equations (5.18) contained only two static unknowns, allowing it to be solved independent of equations involving geometry, the set of two equations (5.52) contains already four unknowns, including two geometric; therefore, it cannot be solved without considering at the same time the relations (5.19) and (5.20). Thus, regardless of boundary conditions, no bar on an elastic foundation can be treated as an isostatic structure, for it is always a structure inherently hyperstatic.

We must therefore reduce the set of equations (5.25), (5.19) and (5.20) to a single differential equation which in the case of a bar of constant cross-section and neglecting distortional strains takes the form

$$w^{IV} - 4tw'' + 4r^2w = f_p.$$ (5.53)

In this equation we have

$$4t = \frac{K_\varphi l^2}{EJ_y} + \beta_w, \qquad 4r^2 = \frac{K_w l^4}{EJ_y}(1+\beta_\varphi),$$ (5.54)

$$\beta_w = \frac{k_z}{GA} K_w l^2, \quad \beta_\varphi = \frac{k_z}{GA} K_\varphi, \tag{5.55}$$

$$f_p = \frac{l^4}{EJ_y}\left[(1+\beta_\varphi)p_z - \gamma_z p_z'' + \frac{m_y}{l}\right]. \tag{5.56}$$

The influence of shear strain is most often neglected in practice and a single-parameter foundation model $(K_\varphi = 0)$ is adopted. Equation (5.53) then takes a simpler form:

$$w^{IV} + 4r^2 w = f_p, \tag{5.57}$$

and in Eqs. (5.54), (5.57), we should let

$$\gamma_z = \beta_w = \beta_\varphi = 0. \tag{5.58}$$

Likewise, using other elastic foundation models, we arrive as a rule at Eq. (5.53). For example, Vlasov and Leontev assume that underlying a beam is an elastic layer of thickness H, Young's modulus E_0 and Poisson's number ν_0. According to their theory, the coefficients (5.54) are calculated from the formulae (Vlasov and Leontev, 1960, p. 74)

$$4t = \frac{E_0}{2(1+\nu_0)} \frac{bHl^2}{EJ_y} \int_0^1 \psi \, d\zeta,$$

$$4r^2 = \frac{E_0}{1-\nu_0^2} \frac{l^4}{EJ_y} \frac{b}{H} \int_0^1 \left(\frac{d\psi}{d\zeta}\right)^2 d\zeta, \quad \zeta = \frac{z}{H}. \tag{5.59}$$

The values of these coefficients depend on how the function $\psi(\zeta)$, which expresses vertical displacements over the elastic layer, is assumed. These authors take it, e.g., to be

$$\psi(\zeta) = 1 - \zeta, \quad \text{or} \quad \psi(\zeta) = \frac{\text{Sh}\,\gamma(1-\zeta)}{\text{Sh}\,\gamma}, \tag{5.60}$$

where γ is a parameter dependent on the elastic properties of the foundation.

Mathematical descriptions of the models proposed by Filonenko-Borodich (1945), Wieghardt (cf. Ylinen and Mikkola, 1967) and others also lead to the differential equation (5.53).

Assuming $r > t$, we express the integral of the differential equation (5.53) by the formula

$$w = A_1 \text{Ch}\,\mu\xi \cos\nu\xi + A_2 \text{Sh}\,\mu\xi \sin\nu\xi + A_3 \text{Ch}\,\mu\xi \sin\nu\xi +$$

$$+ A_4 \text{Sh}\,\mu\xi \cos\nu\xi + \int_0^\xi f_p(\xi_0) w_*(\xi - \xi_0) d\xi_0, \tag{5.61}$$

in which we have the following new denotations:

$$\mu = \sqrt{r+t}, \quad \nu = \sqrt{r-t},$$ (5.62)

$$w_*(\xi) = \frac{\mu \operatorname{Ch}\mu\xi \sin\nu\xi - \nu \operatorname{Sh}\mu\xi \cos\nu\xi}{2\mu\nu(\mu^2+\nu^2)}.$$ (5.63)

We have expressed the particular integral using Cauchy's equation (cf. e.g. Filonenko-Borodich *et al.*, 1949, p. 92), in which the function (5.63) satisfies the homogeneous differential equation (5.53) as well as the following boundary conditions:

$$w_*(0) = w_*'(0) = w_*''(0) = 0, \quad w_*'''(0) = 1.$$ (5.64)

In order to determine from the boundary conditions the integration constants A_i, it is first necessary to find the relationships between the remaining geometric (φ_y) and static (M_y, T_z) quantities and the displacements w. It is readily apparent that these relations have the form

$$\varphi_y = -\frac{(1-\gamma_z\beta_w)w'+\gamma_z w'''}{l(1+\beta_\varphi)} - \frac{k_z}{GA}\frac{lp_z'-m_y}{1+\beta_\varphi},$$ (5.65)

$$M_y = -\frac{EJ_y}{l^2}w'' + \gamma_z K_w l^2 w - \gamma_z l^2 p_z,$$ (5.66)

$$T_z = -\frac{EJ_y}{l^3}\frac{w'''-4tw'}{1+\beta_\varphi} - \frac{\gamma_z lp_z'-m_y}{1+\beta_\varphi}.$$ (5.67)

If the influence of shear strain is to be neglected, the above equations become considerably simplified:

$$\varphi_y = -\frac{w'}{l}, \quad M_y = -\frac{EJ_y}{l^2}w'',$$

$$T_z = -\frac{EJ_y}{l^3}(w'''-4tw') + m_y.$$ (5.68)

The assumption that the foundation is of the one-parameter type ($t = 0$), is accompanied by further simplifications. We then have (cf. (5.62))

$$\mu = \nu = \sqrt{r}.$$ (5.69)

As a result, the functions (5.61) and (5.63) undergo suitable modifications. The latter, for example, takes the form

$$w_*(\xi) = \frac{1}{4\mu^3}(\operatorname{Ch}\mu\xi \sin\mu\xi - \operatorname{Sh}\mu\xi \cos\mu\xi).$$ (5.70)

5.5. Element Subjected to Bending Moment and Large Axial Force

Examining a structure composed of bars loaded by large axial forces, it is necessary to consider their influence on the flexure of elements. Let us first lay out the equilibrium conditions for an infinitely small element dx mentally cut out of the bar. We assume based on the so-called theory of second order that the equilibrated element has already experienced certain displacements (Fig. 5.4). In order to achieve greater generality, we further assume that in
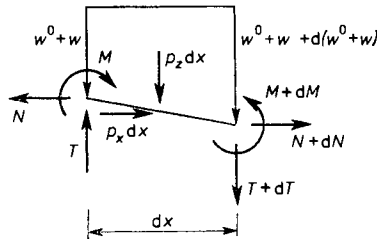

Fig. 5.4. Element of bar subjected to bending and large axial force

addition to deflections w induced by static loadings, the bar has also experienced deflections w^0 accompanying distortional strains.

Acting on element dx are forces N and T, the former being by assumption parallel to the primary axis of the bar and the latter perpendicular to it. Similarly, loadings p_x and p_z have a potential character, i.e., they are acting in fixed directions of a space. Moreover, the bar element is subjected to bending by moment M.

The conditions of equilibrium lead to the following differential relations:

$$\frac{dN}{dx} + p_x = 0, \quad \frac{dT}{dx} + p_z = 0, \quad \frac{dM}{dx} - T + N\frac{d(w+w^0)}{dx} = 0. \quad (5.71)$$

It is seen that four unknowns N, T, M and w are involved in the three differential equations. The problem is therefore statically indeterminate; irrespective of how the bar is supported, it will always be a statically indeterminate structure. The internal forces acting in the bar cannot be determined without introducing additional relationships between the static and geometrical quantities. Incidentally, we have with a similar situation if a bar is resting on an elastic foundation.

Setting out from Bernoulli's assumption, we write

$$M = -EJ\frac{d^2w}{dx^2}. \quad (5.72)$$

In this way we have obtained the missing fourth equation in which no new unknowns are involved.

Equation (5.71) can be solved independent of the other equations of the set whereby the problem is isostatic with respect to axial forces:

$$N = N_0 - \int p_x \, dx. \tag{5.73}$$

We determine the value of N_0 from the boundary condition.

If, however, the boundary conditions are of geometrical nature, not static, the problem becomes significantly more complicated. The set of equations (5.71), (5.72) has to be supplemented then with a fifth, physical equation, namely

$$N = EA \left(\frac{du}{dx} + \frac{1}{2} \frac{d(2w^0 + w)}{dx} \frac{dw}{dx} - \varepsilon^0 \right), \tag{5.74}$$

in which a fifth unknown, u, makes its appearance. In calculating the elongation of element dx, we have considered the influence of deflections w:

$$(1 + \varepsilon^w) \sqrt{dx^2 + (dw^0)^2} = \sqrt{dx^2 + [d(w^0 + w)]^2}; \tag{5.75}$$

hence

$$\varepsilon^w \approx \frac{1}{2} \frac{d(2w^0 + w)}{dx} \frac{dw}{dx}. \tag{5.76}$$

The set of equations becomes non-linear in this case, and considerable difficulty is encountered in solving it.

Since, however, the longitudinal forces in structures used in practice can be calculated with fair accuracy based on the equilibrium conditions, we shall therefore concern ourselves further with the set of equations (5.71), (5.72). After simple transformations it is reducible to the following two differential equations:

$$\frac{dN}{dx} + p_x = 0,$$

$$\frac{d^2}{dx^2} \left(EJ \frac{d^2 w}{dx^2} \right) - \frac{d}{dx} \left(N \frac{dw}{dx} \right) = p_z + \frac{d}{dx} \left(N \frac{dw^0}{dx} \right) \tag{5.77}$$

with two unknowns N and w.

Although this is also non-linear, since Eq. (5.77) contains a product of unknowns, the solution of (5.73) allows the quantity N occurring in this equation to be treated as known.

To narrow down the problem somewhat, let us assume that the members of the structure are prismatic ($EJ = \text{const}$) and that longitudinal force N

is constant over the entire bar length. From an engineering point of view, this assumption should not evoke reservations. For, if the bar has a distinctly variable cross-section or the longitudinal force values vary over a wide range, then nothing stands in the way of dividing the bar into several shorter elements, in which the values EJ and N differ much less from the respective mean values occurring in a given segment.

Hence, by introducing dimensionless variable $\xi = x/l$ and the denotations

$$\lambda^2 = \frac{Nl^2}{EJ}, \quad f(\xi) = \frac{p_z l^4}{EJ} + \lambda^2 w^{0\prime\prime}, \tag{5.78}$$

we give Eq. (5.77)₂ the form

$$w^{IV} - \lambda^2 w'' = f. \tag{5.79}$$

The integral of this equation is the function

$$w = A_1 + A_2 \lambda\xi + A_3 \operatorname{Ch} \lambda\xi + A_4 \operatorname{Sh} \lambda\xi +$$

$$+ \frac{1}{\lambda^3} \int_0^\xi f(\xi_0) \, [\operatorname{Sh} \lambda(\xi - \xi_0) - \lambda(\xi - \xi_0)] \mathrm{d}\xi_0. \tag{5.80}$$

Force T, in keeping with (5.71)₃ is expressed as follows:

$$T = -\frac{EJ}{l^3} [w''' - \lambda^2 (w^0 + w)']. \tag{5.81}$$

All the relations and equations derived above can also be applied to the case of a bar loaded by compressive force S. All that needs to be done is to replace N:

$$N = -S. \tag{5.82}$$

We then have

$$\lambda = l \sqrt{\frac{-S}{EJ}} = i\sigma, \quad \sigma = l \sqrt{\frac{S}{EJ}}. \tag{5.83}$$

Using the known relations

$$\operatorname{Sh} i\sigma\xi = i\sin\sigma\xi, \quad \operatorname{Ch} i\sigma\xi = \cos\sigma\xi, \tag{5.84}$$

we obtain successively

$$w^{IV} + \sigma^2 w'' = f, \quad f = \frac{p_z l^4}{EJ} - \sigma^2 w^{0\prime\prime}, \tag{5.85}$$

$$w = B_1 + B_2\,\sigma\xi + B_3\cos\sigma\xi + B_4\sin\sigma\xi +$$

$$+ \frac{1}{\sigma^3}\int_0^{\xi} f(\xi_0)\,[\sigma(\xi-\xi_0)-\sin\sigma(\xi-\xi_0)]\mathrm{d}\xi_0, \tag{5.86}$$

$$T = -\frac{EJ}{l^3}\,[w''' + \sigma^2(w^0+w)']. \tag{5.87}$$

5.6. Element in the Shape of in-Plane Curved Bar

The sets of differential equations of equilibrium (1.41) and (1.62) can be reduced after simple transformations to the form:

$$T_n = -\frac{\mathrm{d}M_z}{\mathrm{d}s} - m_z, \qquad N = \varrho\,\frac{\mathrm{d}^2M_z}{\mathrm{d}s^2} - \varrho p_n + \varrho\,\frac{\mathrm{d}m_z}{\mathrm{d}s}, \tag{5.88}$$

$$\frac{\mathrm{d}}{\mathrm{d}s}\left(\varrho\,\frac{\mathrm{d}^2M_z}{\mathrm{d}s^2}\right) + \frac{1}{\varrho}\,\frac{\mathrm{d}M_z}{\mathrm{d}s} = -p_s + \frac{\mathrm{d}}{\mathrm{d}s}\,(\varrho p_n) - \frac{\mathrm{d}}{\mathrm{d}s}\left(\varrho\,\frac{\mathrm{d}m_z}{\mathrm{d}s}\right) - \frac{m_z}{\varrho}, \tag{5.89}$$

$$M_n = \varrho\,\frac{\mathrm{d}M_t}{\mathrm{d}s} + \varrho m_t, \tag{5.90}$$

$$T_z = \frac{\mathrm{d}}{\mathrm{d}s}\left(\varrho\,\frac{\mathrm{d}M_t}{\mathrm{d}s}\right) + \frac{M_t}{\varrho} + \frac{\mathrm{d}}{\mathrm{d}s}\,(\varrho m_t) + m_n,$$

$$\frac{\mathrm{d}^2}{\mathrm{d}s^2}\left(\varrho\,\frac{\mathrm{d}M_t}{\mathrm{d}s}\right) + \frac{\mathrm{d}}{\mathrm{d}s}\left(\frac{M_t}{\varrho}\right) = -p_z - \frac{\mathrm{d}^2}{\mathrm{d}s^2}\,(\varrho m_t) - \frac{\mathrm{d}m_n}{\mathrm{d}s}. \tag{5.91}$$

Thus, the problem is to solve two third-order differential equations (5.89), (5.91) and to calculate from Eqs. (5.88) and (5.90) the remaining internal forces.

In the case of a variable radius of curvature ϱ, closed solutions are difficult to obtain altogether impossible. For this reason, we shall consider a special case, though of major practical importance: we assume that the bar axis is in the shape of a circle of radius r. Introducing angular variable ϑ, we write the derivatives with respect to $\mathrm{d}s = r\,\mathrm{d}\vartheta$ in short form:

$$\frac{\mathrm{d}F}{\mathrm{d}s} = \frac{1}{r}\,\frac{\mathrm{d}F}{\mathrm{d}\vartheta} = \frac{F'}{r}. \tag{5.92}$$

Hence Eqs. (5.88)–(5.91) take the form:

$$M_z''' + M_z' = r^2(-p_s+p_n') - r(m_z''+m_z),$$

$$M_t''' + M_t' = -r^2 p_z - r(m_n'+m_t''), \tag{5.93}$$

$$N = \frac{1}{r} M_z'' - rp_n + m_z', \qquad T_n = -\frac{1}{r} M_z' - m_z, \tag{5.94}$$

$$T_z = \frac{1}{r}(M_t'' + M_t) + m_t' + m_n, \qquad M_n = M_t' + rm_t. \tag{5.95}$$

A differential equation of the type

$$M''' + M' = f(\vartheta) \tag{5.96}$$

has the following general integral:

$$M = A + B\cos\vartheta + C\sin\vartheta + \int_0^\vartheta [1 - \cos(\vartheta - \vartheta_0)]f(\vartheta_0)\,d\vartheta_0. \tag{5.97}$$

Hence, the integrals of Eqs. (5.93), with the boundary conditions given only at one end:

$$\begin{aligned}
N(0) &= -U_i, & T_n(0) &= -V_i, & M_z(0) &= -\Phi_{zi}, \\
M_t(0) &= -\Phi_{ti}, & M_n(0) &= -\Phi_{ni}, & T_z(0) &= -W_i
\end{aligned} \tag{5.98}$$

are written as follows:

$$\begin{aligned}
M_z(\vartheta) = &-U_i rf_1 + V_i rf_2 - \Phi_{zi} + \\
&+ \int_0^\vartheta [-rp_s(\vartheta_0)\tilde{f}_1 + rp_n(\vartheta_0)\tilde{f}_2 - m_z(\vartheta_0)]r\,d\vartheta_0,
\end{aligned} \tag{5.99}$$

$$\begin{aligned}
M_t(\vartheta) = &-W_i rf_1 - \Phi_{si}f_3 - \Phi_{ni}f_2 - \\
&- \int_0^\vartheta [rp_z(\vartheta_0)\tilde{f}_1 + m_s(\vartheta_0)\tilde{f}_3 + m_n(\vartheta_0)\tilde{f}_2]r\,d\vartheta_0.
\end{aligned} \tag{5.100}$$

We have introduced the denotations:

$$\begin{aligned}
f_1 &= f_1(\vartheta) = 1 - \cos\vartheta, & f_2 &= f_2(\vartheta) = \sin\vartheta, \\
f_3 &= f_3(\vartheta) = \cos\vartheta, & \tilde{f}_i &= f_i(\vartheta - \vartheta_0), \quad i = 1, 2, 3.
\end{aligned} \tag{5.101}$$

Substituting the function (5.99) into Eqs. (5.94) and the function (5.100) into Eqs. (5.95), we obtain the expressions for the remaining generalized internal forces:

$$N(\vartheta) = -U_i f_3 - V_i f_2 - \int_0^\vartheta [p_s(\vartheta_0)\tilde{f}_3 + p_n(\vartheta_0)\tilde{f}_2]r\,d\vartheta_0,$$

$$T_n(\vartheta) = U_i f_2 - V_i f_3 + \int_0^\vartheta [p_s(\vartheta_0)\tilde{f}_2 - p_n(\vartheta_0)\tilde{f}_3]r\,d\vartheta_0, \tag{5.102}$$

$$T_z(\vartheta) = -W_i - \int_0^{\vartheta} p_z r\,\mathrm{d}\vartheta,$$

$$M_n(\vartheta) = -W_i r\tilde{f}_2 + \varPhi_{st}\tilde{f}_2 - \varPhi_{ni}\tilde{f}_3 + \tag{5.103}$$

$$+ \int_0^{\vartheta} [-p_z(\vartheta_0)r\tilde{f}_2 + m_s(\vartheta_0)\tilde{f}_2 - m_n(\vartheta_0)\tilde{f}_3] r\,\mathrm{d}\vartheta_0.$$

Given in Fig. 5.5 are two groups of loads acting on a curved cantilever bar. The first, containing loads acting in the plane of the bar (Fig. 5.5a),
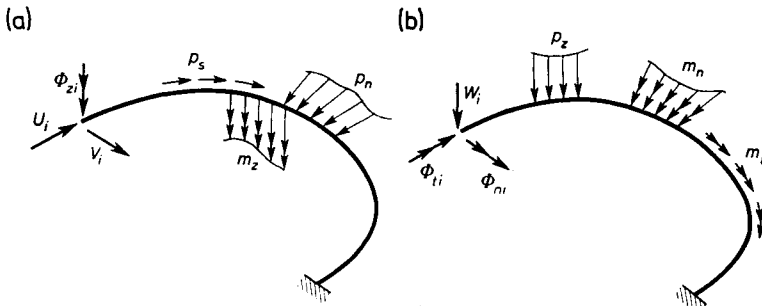

Fig. 5.5. Two loading groups acting on curved bar

induces generalized internal forces N, T_n and M_z, and the other, containing loads acting from the plane (Fig. 5.5b), is accompanied by internal forces T_z, M_t and M_n.

The displacements of the in-plane curved bar can be calculated proceeding from the geometric relations (2.45), (2.63), which, if we consider the shear strains accompanying the transverse forces, take a more general form:

$$\varepsilon = \frac{\mathrm{d}u}{\mathrm{d}s} - \frac{v}{\varrho}, \qquad \varkappa_z = \frac{\mathrm{d}\varphi_z}{\mathrm{d}s}, \qquad \beta_n = \frac{\mathrm{d}v}{\mathrm{d}s} + \frac{u}{\varrho} - \varphi_z, \tag{5.104}$$

$$\varkappa_n = \frac{\mathrm{d}\varphi_n}{\mathrm{d}s} + \frac{\varphi_t}{\varrho}, \qquad \varkappa_t = \frac{\mathrm{d}\varphi_t}{\mathrm{d}s} - \frac{\varphi_n}{\varrho}, \qquad \beta_z = \frac{\mathrm{d}w}{\mathrm{d}s} + \varphi_n. \tag{5.105}$$

The set of these six differential equations can be reduced without difficulty to a set of two third-order differential equations independent of each other:

$$\frac{\mathrm{d}^2}{\mathrm{d}s^2}\left(\varrho\frac{\mathrm{d}u}{\mathrm{d}s}\right) + \frac{\mathrm{d}}{\mathrm{d}s}\left(\frac{u}{\varrho}\right) = \frac{\mathrm{d}^2}{\mathrm{d}s^2}(\varrho\varepsilon) + \frac{\mathrm{d}\beta_n}{\mathrm{d}s} + \varkappa_z,$$

$$\frac{\mathrm{d}}{\mathrm{d}s}\left(\varrho\frac{\mathrm{d}^2w}{\mathrm{d}s^2}\right) + \frac{1}{\varrho}\frac{\mathrm{d}w}{\mathrm{d}s} = \frac{\mathrm{d}}{\mathrm{d}s}\left(\varrho\frac{\mathrm{d}\beta_z}{\mathrm{d}s}\right) + \frac{\beta_z}{\varrho} + \varkappa_t - \frac{\mathrm{d}}{\mathrm{d}s}(\varrho\varkappa_n). \tag{5.106}$$

The remaining generalized displacements depend on the displacements u, w occurring in these equations:

$$v = \varrho \frac{du}{ds} - \varrho\varepsilon,$$

$$\varphi_z = \frac{d}{ds}\left(\varrho \frac{du}{ds}\right) + \frac{u}{\varrho} - \frac{d}{ds}(\varrho\varepsilon) - \beta_n, \qquad (5.107)$$

$$\varphi_t = \varrho \frac{d^2w}{ds^2} - \varrho \frac{d\beta_z}{ds} + \varrho\varkappa_n,$$

$$\varphi_n = -\frac{dw}{ds} + \beta_z. \qquad (5.108)$$

An analogy between the relations (5.104)–(5.108) and (5.88)–(5.91) is readily noticeable here.

Going over to a particular case, namely $\varrho = r = \text{const}$, with the boundary conditions at the initial point of the bar given:

$$u(0) = u_i, \quad v(0) = v_i, \quad w(0) = w_i,$$

$$\varphi_t(0) = \varphi_{ti}, \quad \varphi_n(0) = \varphi_{ni}, \quad \varphi_z(0) = \varphi_{zi}. \qquad (5.109)$$

We obtain relations analogous to the static relations (5.99)–(5.109):

$$u(\vartheta) = u_i f_3 + v_i f_2 + \varphi_{zi} r f_1 +$$
$$+ \int_0^\vartheta [\varepsilon(\vartheta_0)\tilde{f}_3 + \beta_n(\vartheta_0)\tilde{f}_2 + \varkappa_z(\vartheta_0) r\tilde{f}_1] r \, d\vartheta_0,$$

$$v(\vartheta) = -u_i f_2 + v_i f_3 + \varphi_{zi} r f_2 + \qquad (5.110)$$
$$+ \int_0^\vartheta [-\varepsilon(\vartheta_0)\tilde{f}_2 + \beta_n(\vartheta_0)\tilde{f}_3 + \varkappa_z(\vartheta_0) r\tilde{f}_2] r \, d\vartheta_0,$$

$$\varphi_z(\vartheta) = \varphi_{zi} + \int_0^\vartheta \varkappa_z r \, d\vartheta;$$

$$w(\vartheta) = w_i + \varphi_{ti} r f_1 - \varphi_{ni} r f_2 +$$
$$+ \int_0^\vartheta [\beta_z(\vartheta_0) + \varkappa_t(\vartheta_0) r\tilde{f}_1 - \varkappa_n(\vartheta_0) r\tilde{f}_2] r \, d\vartheta_0,$$

$$\varphi_t(\vartheta) = \varphi_{ti} f_3 + \varphi_{ni} f_2 + \int_0^\vartheta [\varkappa_t(\vartheta_0)\tilde{f}_3 + \varkappa_n(\vartheta_0)\tilde{f}_2] r \, d\vartheta_0, \qquad (5.111)$$

$$\varphi_n(\vartheta) = -\varphi_{ti} f_2 + \varphi_{ni} f_3 + \int_0^\vartheta [-\varkappa_t(\vartheta_0)\tilde{f}_2 + \varkappa_n(\vartheta_0)\tilde{f}_3] r \, d\vartheta_0.$$

The practical application of Eqs. (5.110), (5.111) is confined to statically determinate bars.

Aiming to find the displacements and internal forces in a statically indeterminate bar, we should put into the equilibrium equations (2.41) in place of the generalized internal forces, expressions relating them to strains (cf. (2.56), (4.34)) and express the strains by displacements in accordance with Eqs. (5.104) and (5.105). Consequently, we obtain two sets of differential equations, each containing three unknown displacements:

$$
\begin{aligned}
&\alpha_n u'' - u - (1+\alpha_n)v' + r\varphi_z \\
&\qquad = \alpha_n r\varepsilon^{0\prime} - r\beta_n^0 - \frac{r^2 k_n}{GA} p_s, \\
&(1+\alpha_n)u' + v'' - \alpha_n v - r\varphi_z' \\
&\qquad = \alpha_n r\varepsilon^0 + r\beta_n^{0\prime} - \frac{r^2 k_n}{GA} p_n, \\
&u + v' + \gamma_n r\varphi_z'' - r\varphi_z \\
&\qquad = r\beta_n^0 + \gamma_n r^2 \varkappa_z^{0\prime} - \frac{r k_n}{GA} m_z;
\end{aligned}
\tag{5.112}
$$

$$
\begin{aligned}
&w'' + r\varphi_n' = r\beta_z^{0\prime} - \frac{r^2 k_z}{GA} p_z, \\
&-w' + \gamma_z r\varphi_n'' - (1+\gamma_s)r\varphi_n + (\gamma_z+\gamma_s)r\varphi_t' \\
&\qquad = -r\beta_z^0 + \gamma_s r^2 \varkappa_t^0 + \gamma_z r^2 \varkappa_n^{0\prime} - \frac{r k_z}{GA} m_n, \\
&-(\gamma_z+\gamma_s)r\varphi_n' + \gamma_s r\varphi_t'' - \gamma_z r\varphi_t \\
&\qquad = \gamma_s r^2 \varkappa_t^{0\prime} - \gamma_z r^2 \varkappa_n^0 - \frac{r k_z}{GA} m_t.
\end{aligned}
\tag{5.113}
$$

The dimensionless parameters in these equations are:

$$
\alpha_n = \frac{E}{G} k_n, \qquad \gamma_n = \frac{E}{G} \frac{J_z}{Ar^2} k_n,
$$

$$
\gamma_z = \frac{E}{G} \frac{J_n}{Ar^2} k_z, \quad \gamma_t = \frac{J_t}{Ar^2} k_z.
\tag{5.114}
$$

These sets of equations when solved with respect to u and w lead to two identical (with respect to the left-hand side) differential equations of the sixth order:

$$u^{VI} + 2u^{IV} + u'' = r(\varepsilon^{0V} + \varepsilon^{0'''} + \beta_n^{0IV} + \beta_n^{0''}) +$$

$$+ r^2(\varkappa_z^{0'''} + \varkappa_z^{0'}) + \frac{r^3}{EJ_z}(rp_n' - rp_s - m_z'' - m_z) -$$

$$- \frac{r^2}{EA}(p_n''' + p_s^{IV}) - \frac{r^2 k_n}{GA}(p_n''' - p_s''), \tag{5.115}$$

$$w^{VI} + 2w^{IV} + w'' = r(\beta_z^{0V} + 2\beta_z^{0'''} + \beta_z^{0'}) +$$

$$+ r^2(\varkappa_t^{0''} + \varkappa_t^0 - \varkappa_n^{0'''} - \varkappa_n^{0'}) +$$

$$+ \frac{r^3}{EJ_n}(rp_z'' - m_t'' + m_n''') - \frac{r^3}{GJ_t}(rp_z + m_t'' + m_n') -$$

$$- \frac{r^2 k_z}{GA}(p_z^{IV} + 2p_z'' + p_z). \tag{5.116}$$

All the other displacements, and what follows all the internal forces, are a function of displacements u, w. Leaving out the tedious derivations, we present here only the final expressions for generalized displacements, relating them to the static and geometric quantities given by the initial conditions (5.98) and (5.99):

$$u(\vartheta) = u_i f_3 + v_i f_2 + \varphi_{zi} r f_1 +$$

$$+ \int_0^\vartheta [\varepsilon^0(\vartheta_0) \tilde{f}_3 + \beta_n^0(\vartheta_0) \tilde{f}_2 + \varkappa_z^0(\vartheta_0) r f_1] r \, d\vartheta_0 +$$

$$+ \frac{r^2}{EJ_z}(-U_i r g_1 + V_i r g_2 - \Phi_{zi} g_3) +$$

$$+ \frac{r^2}{EJ_z} \int_0^\vartheta [-p_s(\vartheta_0) r \tilde{g}_1 + p_n(\vartheta_0) r \tilde{g}_2 - m_z(\vartheta_0) \tilde{g}_3] r \, d\vartheta_0, \tag{5.117}$$

$$v(\vartheta) = -u_i f_2 + v_i f_3 + \varphi_{zi} r f_2 +$$

$$+ \int_0^\vartheta [-\varepsilon^0(\vartheta_0) \tilde{f}_2 + \beta_n^0(\vartheta_0) \tilde{f}_3 + \varkappa_z^0(\vartheta_0) r \tilde{f}_2] r \, d\vartheta_0 +$$

$$+ \frac{r^2}{EJ_z}(-U_i r g_2 + V_i r g_4 - \Phi_{zi} f_1) +$$

$$+ \frac{r^2}{EJ_z} \int_0^\vartheta [-p_s(\vartheta_0) r \tilde{g}_2 + p_n(\vartheta_0) r \tilde{g}_4 - m_z(\vartheta_0) \tilde{f}_1] r \, d\vartheta_0, \tag{5.118}$$

$$\varphi_z(\vartheta) = \varphi_{zi} + \int_0^\vartheta \varkappa_z^0 r\,d\vartheta + \frac{r}{EJ_z}(-U_i rg_3 + V_i rf_1 - \Phi_{zi}\vartheta) +$$

$$+ \frac{r}{EJ_z} \int_0^\vartheta [-p_s(\vartheta_0)r\tilde{g}_3 + p_n(\vartheta_0)r\tilde{f}_1 - m_z(\vartheta_0)(\vartheta - \vartheta_0)]r\,d\vartheta_0, \quad (5.119)$$

$$w(\vartheta) = w_i + \varphi_{ti} rf_1 - \varphi_{ni} rf_2 +$$

$$+ \int_0^\vartheta [\beta_z^0(\vartheta_0) + \varkappa_t^0(\vartheta_0)r\tilde{f}_1 - \varkappa_n^0(\vartheta_0)r\tilde{f}_2]r\,d\vartheta_0 -$$

$$- \frac{r^2}{EJ_n}(W_i rh_1 + \Phi_{si}h_3 + \Phi_{ni}h_2) -$$

$$- \frac{r^2}{EJ_n} \int_0^\vartheta [p_z(\vartheta_0)r\tilde{h}_1 + m_t(\vartheta_0)\tilde{h}_3 + m_n(\vartheta_0)\tilde{h}_2]r\,d\vartheta_0, \quad (5.120)$$

$$\varphi_t(\vartheta) = \varphi_{ti}f_3 + \varphi_{ni}f_2 +$$

$$+ \int_0^\vartheta [\varkappa_t^0(\vartheta_0)\tilde{f}_3 + \varkappa_n^0(\vartheta_0)\tilde{f}_2]r\,d\vartheta_0 +$$

$$+ \frac{r}{EJ_n}(-W_i rh_3 + \Phi_{ti}h_4 - \Phi_{ni}h_6) +$$

$$+ \frac{r}{EJ_n} \int_0^\vartheta [-p_z(\vartheta_0)r\tilde{h}_3 + m_t(\vartheta_0)\tilde{h}_4 - m_n(\vartheta_0)\tilde{h}_6]r\,d\vartheta_0, \quad (5.121)$$

$$\varphi_n(\vartheta) = -\varphi_{ti}f_2 + \varphi_{ni}f_3 +$$

$$+ \int_0^\vartheta [-\varkappa_t^0(\vartheta_0)\tilde{f}_2 + \varkappa_n^0(\vartheta_0)\tilde{f}_3]r\,d\vartheta_0 +$$

$$+ \frac{r}{EJ_n}(W_i rh_2 + \Phi_{ti}h_6 - \Phi_{ni}h_5) +$$

$$+ \frac{r}{EJ_n} \int_0^\vartheta [p_z(\vartheta_0)r\tilde{h}_2 + m_t(\vartheta_0)\tilde{h}_6 - m_n(\vartheta_0)\tilde{h}_5]r\,d\vartheta_0. \quad (5.122)$$

Besides the function (5.101), we have introduced here a number of new functions:

$$g_1 = g_1(\vartheta) = \vartheta - \frac{3 - \nu + \gamma_n}{2}\sin\vartheta + \frac{1 + \nu + \gamma_n}{2}\vartheta\cos\vartheta,$$

$$g_2 = g_2(\vartheta) = 1 - \cos\vartheta - \frac{1+\nu+\gamma_n}{2}\,\vartheta\sin\vartheta,$$

$$g_3 = g_3(\vartheta) = \vartheta - \sin\vartheta, \qquad\qquad (5.123)$$

$$g_4 = g_4(\vartheta) = \frac{1+\nu-\gamma_n}{2}\sin\vartheta - \frac{1+\nu+\gamma_n}{2}\,\vartheta\cos\vartheta;$$

$$h_1 = h_1(\vartheta) = (\mu_t+\gamma_z)\vartheta - \frac{1+3\mu_t}{2}\sin\vartheta + \frac{1+\mu_t}{2}\,\vartheta\cos\vartheta,$$

$$h_2 = h_2(\vartheta) = \mu_t(1-\cos\vartheta) - \frac{1+\mu_t}{2}\,\vartheta\sin\vartheta,$$

$$h_3 = h_3(\vartheta) = \frac{1+\mu_t}{2}\,(\sin\vartheta - \vartheta\cos\vartheta),$$

$$h_4 = h_4(\vartheta) = \frac{1-\mu_t}{2}\sin\vartheta - \frac{1+\mu_t}{2}\,\vartheta\cos\vartheta, \qquad\qquad (5.124)$$

$$h_5 = h_5(\vartheta) = \frac{1-\mu_t}{2}\sin\vartheta + \frac{1+\mu_t}{2}\,\vartheta\cos\vartheta,$$

$$h_6 = h_6(\vartheta) = \frac{1+\mu_t}{2}\,\vartheta\sin\vartheta,$$

$$\tilde{g}_i = g_i(\vartheta - \vartheta_0) \quad (i = 1, 2, 3, 4),$$

$$\tilde{h}_i = h_i(\vartheta - \vartheta_0) \quad (i = 1, 2, ..., 6)$$

in which we have the denotations (5.114) and:

$$\nu = \frac{J_z}{Ar^2}, \qquad \mu_t = \frac{EJ_n}{GJ_t}. \qquad\qquad (5.125)$$

Obviously, as seen in this case, the boundary quantities at the initial point of the bar could be related to those that correspond to the boundary conditions at the other end of it. Since, however, the general formulae are very complicated, we do not attempt to cite them.

We have derived the equations for displacements of a curved bar considering both the influence of the principal factors, twisting and bending moments in the first place, and the less important ones associated with the longitudinal force and the transverse forces. In practice, those second-ranking factors can as a rule be neglected. This leads to a simplification of Eqs. (5.123) and (5.124), wherein we should led:

$$\nu = \gamma_n = \gamma_z = 0. \qquad\qquad (5.126)$$

The more slender, the bar considered, the smaller the unavoidable errors in calculation will be.

EXAMPLE 5.1

Find the internal forces and the displacements of a circular bar resting on n articulated supports equally spaced apart (Fig. 5.6). The bar is under a uniformly distributed load p_z.
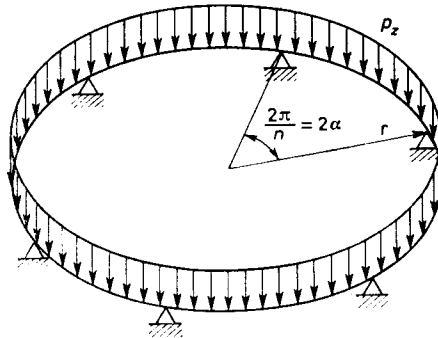

Fig. 5.6. Circular bar resting on n supports

On account of the symmetry of the structure and the loads with respect to n axes of symmetry, we consider only a segment of the bar situated between two neighbouring axes of symmetry, which make an angle $\alpha = \pi/n$ (Fig. 5.7). Because the bar is loaded aut of the plane, all the static and geometric quan-
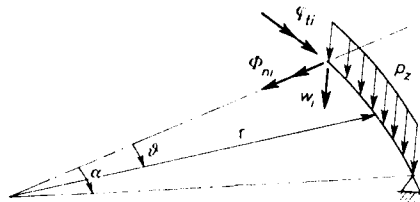

Fig. 5.7. Bar segment between neighbouring axes of symmetry

tities occurring when a load is acting in the plane of the bar, are therefore identically equal to zero. Furthermore, it follows from the symmetry conditions that

$$W_i = \Phi_{ti} = \Phi_{tk} = 0, \qquad \varphi_{ni} = \varphi_{nk} = w_k = 0. \tag{a}$$

On the basis of (5.100) and (5.103) and considering boundary conditions $(a)_1$, we get ultimately the following expression for generalized internal forces:

$$M_t = p_z r^2 \left(\frac{\alpha}{\sin \alpha} \sin \vartheta - \vartheta \right), \quad T_z = -p_z r \vartheta,$$

$$M_n = p_z r^2 \left(\frac{\alpha}{\sin \alpha} \cos \vartheta - 1 \right). \tag{b}$$

The problem is therefore evidently statically determinate; all the internal forces have been determined without having to use geometric relationships. In the second stage, we proceed to calculate the displacements. For this purpose, we first determine from Eqs. (2.56) and (4.34) the strains:

$$\varkappa_t = \frac{p_z r^2}{GJ_t} \left(\frac{\alpha}{\sin \alpha} \sin \vartheta - \vartheta \right), \quad \beta_z = -\frac{p_z r k_z}{GA} \vartheta,$$

$$\varkappa_n = \frac{p_z r^2}{EJ_n} \left(\frac{\alpha}{\sin \alpha} \cos \vartheta - 1 \right). \tag{c}$$

By substituting them into Eqs. (5.111) and performing appropriate integration using the initial geometric conditions, we obtain

$$w = \frac{p_z r^4}{EJ_n} \left[\left(\frac{1+\mu_t}{2} \frac{\alpha^2}{\sin^2 \alpha} \cos \alpha + \frac{1+3\mu_t}{2} \frac{\alpha}{\sin \alpha} \right)(\cos \alpha - \cos \vartheta) + \right.$$

$$\left. + \frac{1+\mu_t}{2} \frac{\alpha}{\sin \alpha} (\alpha \sin \alpha - \vartheta \sin \vartheta) + \frac{\mu_t + \gamma_z}{2} (\alpha^2 - \vartheta^2) \right], \tag{d}$$

$$\varphi_t = \frac{p_z r^3}{EJ_n} \frac{1+\mu_t}{2} \left[\frac{\alpha^2}{\sin^2 \alpha} \cos \alpha \cos \vartheta + \frac{\alpha}{\sin \alpha} (\cos \vartheta + \gamma \sin \vartheta) - 2 \right], \tag{e}$$

$$\varphi_n = \frac{p_z r^3}{EJ_n} \left[\frac{1+\mu_t}{2} \frac{\alpha}{\sin \alpha} \left(\vartheta \cos \vartheta - \frac{\alpha}{\sin \alpha} \cos \alpha \sin \vartheta \right) + \right.$$

$$\left. + \mu_t \left(\vartheta - \frac{\alpha}{\sin \alpha} \sin \vartheta \right) \right]. \tag{f}$$

Note the possibility of performing an interesting pass to the limit. Let us assume that the product $2r\alpha = l$ is a constant quantity independent of α and pass with angle α to zero. As a result of this pass to the limit, the circular bar turns into an infinitely long, straight beam resting on an infinite number of supports of constant, spacing l (Fig. 5.8a). Owing to the multiple symmetry of this statically indeterminate system, we can separate out of that beam an element with clamped both ends (Fig. 5.8b).

Examine the limits to which the functions (b)–(f), expressing the generalized internal forces and displacements of the bar, approach. We consider in detail, for example, the formula for bending moment:
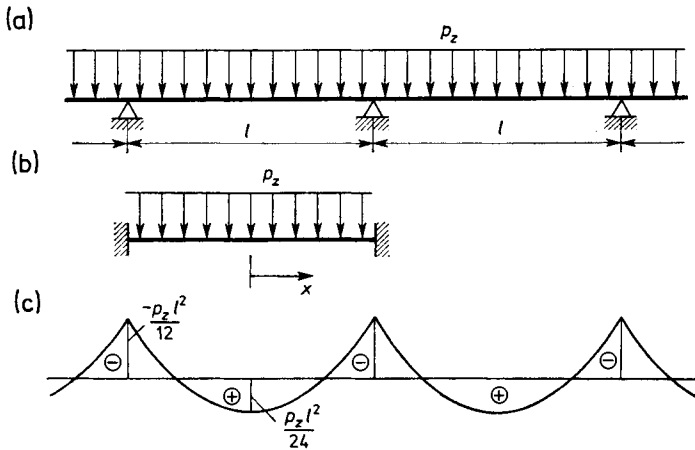
Fig. 5.8. Circular bar after limit transition: (a) continuous beam; (b) beam fixed at both ends — a segment of continuous beam; (c) diagram of moments

$$M_n = \lim_{\alpha \to 0} p_z r^2 \alpha^2 \frac{\alpha \cos \vartheta - \sin \alpha}{\alpha^2 \sin \alpha}$$

$$= \lim_{\alpha \to 0} \frac{p_z l^2}{4} \frac{\alpha \left(1 - \dfrac{\vartheta^2}{2!} + \dfrac{\vartheta^4}{4!} - \cdots \right) - \dfrac{\alpha}{1!} + \dfrac{\alpha^3}{3!} - \dfrac{\alpha^5}{5!} + \cdots}{\alpha^2 \left(\dfrac{\alpha}{1!} - \dfrac{\alpha^3}{3!} + \dfrac{\alpha^5}{5!} - \cdots \right)}$$

$$= \frac{p_z l^2}{24} (1 - 3\xi^2). \tag{g}$$

We hawe used here expansions of trigonometric functions into Maclaurin series and we have introduced the denotation:

$$\xi = \frac{\vartheta}{\alpha} = \frac{2x}{l}. \tag{h}$$

The plot of the function (g) is given in Fig. 5.8c.
In a similar manner, we find:

$$M_t = 0, \quad T_z = -\frac{p_z l}{2} \xi, \tag{i}$$

$$w = \frac{p_z l^4}{384 E J_n} [(1 - \xi^2)^2 + 48 \gamma_z'(1 - \xi^2)],$$

$$\varphi_n = \frac{p_z l^3}{48 E J_n} \xi(1 - \xi^2), \quad \varphi_t = 0, \tag{j}$$

where

$$\gamma_z' = \frac{E}{G} \frac{J_n}{Al^2} k_z.$$ (k)

Therefore, setting out from an isostatic structure in a limit, we have obtained a solution for a hyperstatic structure: a beam fixed at both ends.

EXAMPLE 5.2

Determine the displacements and internal forces in an element that is in the form of a circular arc with articulated supports at both ends and that has a uniformly distributed radial load p_n acting on it (Fig. 5.9a). On account
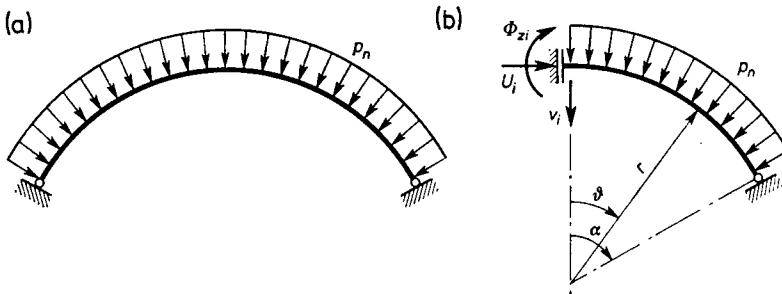

Fig. 5.9. Two-hinged circular arc

of the symmetry of the structure and the loadings involved, we can consider half of the bar provided the support conditions at the ends as shown in Fig. 5.9b are given. Assuming the origin of the coordinate system is on the axis of symmetry and considering the fact that the load is acting only in the plane of the bar, we have the following boundary conditions:

$$V_i = 0, \quad u_i = 0, \quad \varphi_{zi} = 0,$$
$$M_z(\alpha) = 0, \quad u(\alpha) = 0, \quad v(\alpha) = 0.$$ (a)

The unknown initial quantities, U_i, Φ_{zi} and v_i, indicated in Fig. 5.9b are calculated from the given boundary conditions at the other end of the bar; putting them into Eqs. (5.99), (5.102), (5.117)–(5.119), we get:

$$M_z = -p_n r^2 \frac{2\nu \sin \alpha}{\Delta} (\cos \vartheta - \cos \alpha),$$

$$N = -p_n r \left(1 - \frac{2\nu \sin \alpha}{\Delta} \cos \vartheta\right),$$ (b)

$$T_n = -p_n r \frac{2\nu \sin \alpha}{\Delta} \sin \vartheta,$$

$$u = \frac{p_n r^4}{EJ_z} \frac{2\nu}{\varDelta} \left[\frac{1+\nu+\gamma_n}{2} (\vartheta \sin\alpha \cos\vartheta - \alpha \cos\alpha \sin\vartheta) + \right.$$

$$\left. + \cos\alpha(\vartheta \sin\alpha - \alpha \sin\vartheta) \right],$$

$$v = \frac{p_n r^4}{EJ_z} \frac{2\nu}{\varDelta} \left[\frac{1+\nu+\gamma_n}{2} (\alpha - \alpha\cos\alpha\cos\vartheta - \vartheta\sin\alpha\sin\vartheta) - \right. \quad \text{(c)}$$

$$\left. - \left(\alpha\cos\alpha - \frac{1-\nu+\gamma_n}{2} \sin\alpha \right) (\cos\vartheta - \cos\alpha) \right],$$

$$\varphi_z = -\frac{p_n r^3}{EJ_z} \frac{2\nu\sin\alpha}{\varDelta} (\sin\vartheta - \vartheta\cos\alpha),$$

where

$$\varDelta = 2\alpha\cos^2\alpha + (1+\nu+\gamma_n)\alpha - (3-\nu+\gamma_n)\sin\alpha\cos\alpha. \quad \text{(d)}$$

Note that if the influence of longitudinal forces on strains are neglected, i.e., if $\nu = 0$, both the bending moment and the transverse force as well as all the displacements equal zero, and the longitudinal force has a constant value, $N = -p_n r$.

Having at hand the functions (b) and (c), we can pass to the limit in a manner similar to that described in Example 5.1. Fixing the value of the product $2r\alpha = l$ and passing with angle α to zero, we obtain results for a straight
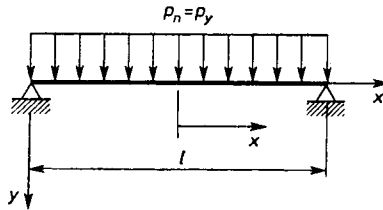
Fig. 5.10. Circular arc after limit transition—simply supported beam

bar with hinged supports at the ends (Fig. 5.10). Performing suitable transformations (cf. (h) from Example 5.1) we arrive at the functions

$$M_z = -\frac{p_n l^2}{8} (1-\xi^2), \quad N = 0, \quad T_n = -\frac{p_n l}{2} \xi, \quad \text{(e)}$$

$$u = 0,$$

$$v = \frac{p_n l^4}{384 EJ_z} [5 - 6\xi^2 + \xi^4 + 48\gamma_n'(1-\xi^2)], \quad \text{(f)}$$

$$\varphi_z = -\frac{p_n l^3}{48 EJ_z} \xi(3-\xi^2),$$

in which besides the symbol (h) from Example (5.1) a new denotation is intro-
duced

$$\gamma'_n = \frac{E}{G} \frac{J_z}{Al^2} k_n. \tag{g}$$

As distinct from the previous example, in which we proceeded from an
isostatic system by pass to the limit to obtain a solution for a hyperstatic
system, in the present example we started out from a hyperstatic structure
and by pass to the limit we obtained a solution of an isostatic problem.

6. Static Equations of Bar Structures and Fundamental Solution Methods

6.1. General Remarks

In Chapter 2, we considered an isolated cross-section of one of the elements of a structure. We demonstrated that it was sufficient to know the generalized internal forces acting in that section, using appropriate simplifying assumptions, to be able to find the stress distribution over the entire cross-section of a bar.

Chapter 5 was devoted to the problem of determining the distributions of displacements and generalized internal forces within a simple element. For this purpose, it was necessary to know the loads acting over the length of the bar and also the geometric and static boundary quantities. Those boundary quantities are the displacements of joints and the generalized forces in characteristic cross-sections.

Thus, all that remained to be done was to calculate the displacements of joints and the generalized forces in characteristic cross-sections, and this problem will be our concern in the present and following chapters. The sought geometric and static quantities make a certain set of discrete unknowns which in order to be calculated require the solution of a set of algebraic equations.

In this way, from problems described in principle by sets of partial differential equations (cf. Chapter 2) through problems in which sets of ordinary differential equations had to be solved, we encounter in this chapter problems which consist in finding solutions of sets of algebraic equations. This means at the same time a switch from considerations of a single cross-section, by way of analysis of an isolated element, to static analysis of a complete bar structure composed of many elements.

The general principles of constructing and solving sets of kinematic equations, equilibrium equations and elasticity equations will be presented using the simple example of a space truss and a plane frame. We shall also discuss

matrices describing the static-kinematic properties of a structure. In the following chapters, we shall present in greater detail the methods used in the statics of bar structures.

6.2. Equations of Kinematics, Equilibrium and Elasticity for a Space Truss

As we have mentioned in Chapter 3, the space truss is a structure composed of straight bars with ends connected to spherical hinges. The structure thus formed should be kinematically invariable in the sense that as long as the bars do not suffer extensions no displacement of the joints can take place. We shall return to this question later.

However, strictly speaking, a space truss has as many degrees of freedom as there are bars with spherical hinges at both ends, since each bar can rotate about its axis. But, this is not very important, since according to the concept of a truss design we understand not only the technique by which it has been constructed but also the character of loading. A truss can be loaded exclusively by forces acting direct on the joint, whereas any loading by moments and any loading within bars is out of question. Due to this limitation of the mode of loading of a truss, each of its members (bars) can be subjected either to tension or compression, and outside the axial force, it does not transmit any other generalized internal forces.

The static scheme of a truss just described departs a long way from the real structure. In engineering practice, the construction of spherical hinges are not even attempted. Stiff joints will be found as a rule at bar linkage points, and hence the question of bars being free to rotate about their axes does not come in all. None the less, on account of the considerable slenderness ratio of truss members, the bending and twisting moments which occur in them due to the stiffness of the joints, are not very great and the accompanying stresses can be viewed as of secondary importance. One of the methods
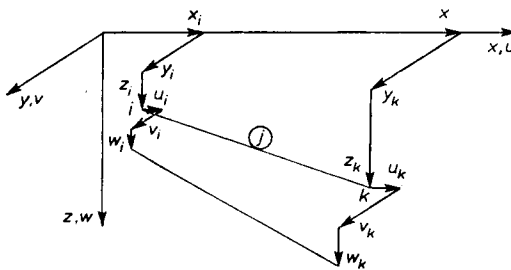

Fig. 6.1. Truss member in primary position and after displacement of joints

to calculate these stresses has been described in the monograph by Błasz-kowiak and Kączkowski (1959, 1966).

Let us number the truss members from 1 to e and allow the quantities applying to the member numbered j (Fig. 6.1), such as length, cross-sectional area, etc., to be denoted by a suitable superscript (l^j, A^j).

We denote the truss joints by numbers 1 to w. In the Cartesian coordinates x, y, z, the original position of the joint numbered i is described by three components, appropriately marked by subscripts: x_i, y_i, z_i.

The original length of the truss member j situated between joints i, k is calculated using the formula

$$l^j = \sqrt{(x_k - x_i)^2 + (y_k - y_i)^2 + (z_k - z_i)^2}. \tag{6.1}$$

Let us treat the bar member as a vector whose origin is at joint i and the final point at joint k, $k > i$. The directional cosines of that bar are

$$\cos(x, j) = \alpha^j = \frac{x_k - x_i}{l^j},$$

$$\cos(y, j) = \beta^j = \frac{y_k - y_i}{l^j}, \tag{6.2}$$

$$\cos(z, j) = \gamma^j = \frac{z_k - z_i}{l^j}.$$

The truss joints i and k experience displacements, their components being u_m, v_m, w_m ($m = i, k$). These are accompanied by an extension of the truss member j, which can easily be determined by projecting the joint displacement differences on the axis of the member:

$$\Delta l^j = (u_k - u_i)\alpha^j + (v_k - v_i)\beta^j + (z_k - z_i)\gamma^j. \tag{6.3}$$

Introducing matrix notation:

$$\mathbf{b}^j = [\alpha, \beta, \gamma]^j, \tag{6.4}$$

$$\mathbf{q}_m = \{u, v, w\}_m, \quad (m = i, k), \quad \mathbf{q}^j = \{\mathbf{q}_i, \mathbf{q}_k\}, \tag{6.5}$$

we express the extension of truss member j in a more concise form:

$$\Delta l^j = [-\mathbf{b}^j, \mathbf{b}^j]\mathbf{q}^j. \tag{6.6}$$

We array the extension of all the truss members in a single column matrix with the number of components e equalling the number of truss members (elements):

$$\boldsymbol{\epsilon} = \{\Delta l^1, \Delta l^2, \dots, \Delta l^e\}. \tag{6.7}$$

Let us also construct a vector containing the displacement components of all the truss joints, numbering w:

$$\tilde{q} = \{q_1, q_2, \ldots, q_w\}. \tag{6.8}$$

In vector $\tilde{q}$, we have considered both the unknowns displacements of free joints and the known (forced) displacements of the supports.

A linear relation occurs between the extensions of truss members and the displacements of joints (cf. Eq. (6.6)), having the following general structure:

$$\epsilon = \tilde{B}\tilde{q}. \tag{6.9}$$

The matrix $\tilde{B}$ is composed of submatrices b^j given by the relation (6.4) and it explains the system of connections between truss joints. To be more specific
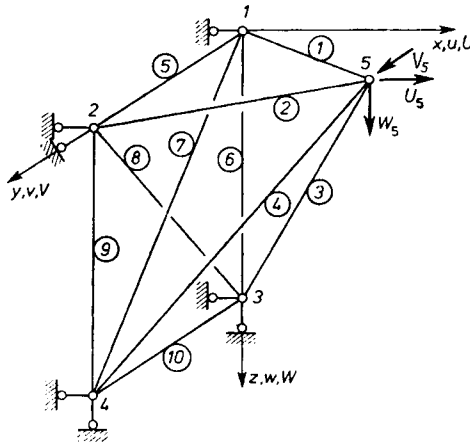
Fig. 6.2. Space truss

in our further considerations, we now consider the truss shown in Fig. 6.2, whose matrix $\tilde{B}$ has the structure:

$$
\tilde{B} =
\begin{array}{c}
 \\
1 \\
2 \\
3 \\
4 \\
5 \\
6 \\
7 \\
8 \\
9 \\
10
\end{array}
\begin{array}{c}
\begin{array}{ccccc}
1 & 2 & 3 & 4 & 5
\end{array} \\
\left[
\begin{array}{ccccc}
-b^1 & & & & b^1 \\
& -b^2 & & & b^2 \\
& & -b^3 & & b^3 \\
& & & -b^4 & b^4 \\
-b^5 & b^5 & & & \\
-b^6 & & b^6 & & \\
-b^7 & & & b^7 & \\
& -b^8 & b^8 & & \\
& -b^9 & & b^9 & \\
& & -b^{10} & b^{10} &
\end{array}
\right]
\end{array}
\tag{6.10}
$$

The numbering of the rows corresponds to the successive numbers of the truss members, whereas the numbers of columns refer to the truss joints. It is seen from the matrix (6.10) that, for example, between joints 1 and 5 there is the truss member 1, and between joints 2 and 5, the member 2, and so forth, and also that, for example, the truss members 2, 5, 8 and 9 meet at joint 2.

It will be useful for practical reasons to regroup the displacements generating the vector $\tilde{\mathbf{q}}$ so that the unknown quantities are located in its top part:

$$\mathbf{q} = \{v_1, w_1, w_2, v_3, v_4, u_5, v_5, w_5\}, \tag{6.11}$$

and the known displacements of supports in its bottom part:

$$\mathbf{r} = \{u_1, u_2, v_2, u_3, w_3, u_4, w_4\}. \tag{6.12}$$

Hence, we have

$$\tilde{\mathbf{q}} = \{\mathbf{q}, \mathbf{r}\}. \tag{6.13}$$

Such a change in the order of components of the vector $\tilde{\mathbf{q}}$ requires a suitable restructuring of the matrix $\tilde{\mathbf{B}}$:

$$\tilde{\mathbf{B}} = [\mathbf{B}, \mathbf{B}_r]. \tag{6.14}$$

The matrix $\mathbf{B}$ should contain those columns of the matrix (6.10), which relate to displacements of the free joints and the matrix $\mathbf{B}_r$, the columns which relate to displacements of the supports. Considering Eq. (6.4), we write:

$$
\mathbf{B} = \begin{array}{c}
\\
1\\2\\3\\4\\5\\6\\7\\8\\ \hline 9\\10
\end{array}
\begin{bmatrix}
-\beta^1 & -\gamma^1 & & & & \alpha^1 & \beta^1 & \gamma^1 \\
& & -\gamma^2 & & & \alpha^2 & \beta^2 & \gamma^2 \\
& & & -\beta^3 & & \alpha^3 & \beta^3 & \gamma^3 \\
& & & & -\beta^4 & \alpha^4 & \beta^4 & \gamma^4 \\
-\beta^5 & -\gamma^5 & \gamma^5 & & & & & \\
-\beta^6 & -\gamma^6 & & \beta^6 & & & & \\
-\beta^7 & -\gamma^7 & & & \beta^7 & & & \\
& & -\gamma^8 & \beta^8 & & & & \\ \hline
& & -\gamma^9 & & \beta^9 & & & \\
& & & -\beta^{10} & \beta^{10} & & &
\end{bmatrix}, \tag{6.15}
$$

$$
\mathbf{B}_r =
\begin{array}{c}
\\
1\\2\\3\\4\\5\\6\\7\\8\\9\\10
\end{array}
\begin{array}{ccccccc}
\underset{u}{1} & \underset{u}{2} & v & \underset{u}{3} & w & \underset{u}{4} & w\\
\left[\begin{array}{c}-\alpha^1\\ \\ \\ \\ -\alpha^5\\ -\alpha^6\\ -\alpha^7\\ \\ \\ \end{array}\right. &
\begin{array}{c} \\ -\alpha^2\\ \\ \\ \alpha^5\\ \\ \\ -\alpha^8\\ -\alpha^9\\ \end{array} &
\begin{array}{c} \\ -\beta^2\\ \\ \\ \beta^5\\ \\ \\ -\beta^8\\ -\beta^9\\ \end{array} &
\begin{array}{c} \\ \\ -\alpha^3\\ \\ \\ \alpha^6\\ \\ \alpha^8\\ \\ -\alpha^{10} \end{array} &
\begin{array}{c} \\ \\ -\gamma^3\\ \\ \\ \gamma^6\\ \\ \gamma^8\\ \\ -\gamma^{10} \end{array} &
\begin{array}{c} \\ \\ \\ -\alpha^4\\ \\ \\ \alpha^7\\ \\ \alpha^9\\ \alpha^{10} \end{array} &
\begin{array}{c} \\ \\ \\ -\gamma^4\\ \\ \\ \gamma^7\\ \\ \gamma^9\\ \gamma^{10} \end{array}\left.\right]
\end{array}.
\qquad (6.16)
$$

We present the relation (6.9) in the following form:

$$\boldsymbol{\epsilon} = \mathbf{B}\mathbf{q} + \mathbf{B}_r\mathbf{r}. \qquad (6.17)$$

When the supports experience no displacements, we leave out the second term of the above formula.

The longitudinal forces in all truss members and the support reactions are unknown static quantities in the truss. These forces together with external loadings should satisfy all the equilibrium conditions. Specifically, the projections on the axes x, y, z of all the forces acting on each truss joint should equal zero. Since the number of truss joints is w, the number of equilibrium equations that can be composed, is then $3w$ for a space truss and $2w$ for a plane truss.

We can construct from the forces acting in the truss members a single column matrix whose number of components equals the number of elements e:

$$\boldsymbol{\sigma} = \{N^1, N^2, \ldots, N^e\}. \qquad (6.18)$$

The external forces acting on joints, including support reactions, are set together into a vector:

$$\tilde{\mathbf{Q}} = \{\mathbf{Q}_1, \mathbf{Q}_2, \ldots, \mathbf{Q}_w\}, \quad \mathbf{Q}_i = \{U, V, W\}_i. \qquad (6.19)$$

Given as an example in Fig. 6.2 are the external forces acting on joint 5.

We derive the equilibrium equations using the principle of virtual work. Let us give all the joints (including support joints) certain virtual increments of displacements which we treat as components of the vector:

$$\delta\tilde{\mathbf{q}} = \{\delta\mathbf{q}_1, \delta\mathbf{q}_2, \ldots, \delta\mathbf{q}_w\}, \quad \delta\mathbf{q}_i = \{\delta u, \delta v, \delta w\}_i. \qquad (6.20)$$

The virtual displacement increments are accompanied by virtual extensions of the bars, forming a single column matrix

$$\delta\boldsymbol{\epsilon} = \{\delta\Delta l^1, \delta\Delta l^2, \ldots, \delta\Delta l^e\}. \qquad (6.21)$$

The relation (6.9) occurs between the virtual strains $d\boldsymbol{\epsilon}$ and the virtual displacements $\delta\tilde{\mathbf{q}}$:

$$\delta\boldsymbol{\epsilon} = \tilde{\mathbf{B}}\delta\tilde{\mathbf{q}}. \tag{6.22}$$

In accordance with the principle of virtual work, the work done by external forces $\tilde{\mathbf{Q}}$ on displacements $\delta\mathbf{q}$ equals the work done by internal forces $\boldsymbol{\sigma}$ on virtual strains $\delta\boldsymbol{\epsilon}$. We write this matrix relation as follows:

$$\delta\tilde{\mathbf{q}}^T\tilde{\mathbf{Q}} = \delta\boldsymbol{\epsilon}^T\boldsymbol{\sigma}. \tag{6.23}$$

Considering the relation (6.22), we express the above formula in a modified form:

$$\delta\tilde{\mathbf{q}}^T\tilde{\mathbf{Q}} = \delta\tilde{\mathbf{q}}^T\tilde{\mathbf{B}}^T\boldsymbol{\sigma}. \tag{6.24}$$

However since, the virtual displacements $\delta\tilde{\mathbf{q}}$ are arbitrary, for the equation of work (6.24) to be satisfied regardless of the displacement values, an entire set of separate equations of equilibrium has to be satisfied:

$$\tilde{\mathbf{Q}} = \tilde{\mathbf{B}}^T\boldsymbol{\sigma}. \tag{6.25}$$

As in the case of displacements $\tilde{\mathbf{q}}$, we divide the vector of joint loadings $\tilde{\mathbf{Q}}$ into two subvectors:

$$\tilde{\mathbf{Q}} = \{\mathbf{Q}, \mathbf{R}\}. \tag{6.26}$$

The first subvector embraces all known external forces and the other, unknown support reactions. For the truss in Fig. 6.2, these subvectors have the structure (cf. (6.11), (6.12)):

$$\begin{aligned} \mathbf{Q} &= \{V_1, W_1, W_2, V_3, V_4, U_5, V_5, W_5\}, \\ \mathbf{R} &= \{U_1, U_2, V_2, U_3, W_3, U_4, W_4\}. \end{aligned} \tag{6.27}$$

The set of equilibrium equations (6.25) can therefore be split into two subsets, using the denotations (6.14)–(6.16):

$$\mathbf{B}^T\boldsymbol{\sigma} = \mathbf{Q}, \quad \mathbf{B}_r^T\boldsymbol{\sigma} = \mathbf{R}. \tag{6.28}$$

The third group of equations covers the relations between geometric quantities $\boldsymbol{\epsilon}$ and static quantities $\boldsymbol{\sigma}$. Considering the distortional strains $\boldsymbol{\epsilon}^0$, we write these relations in the following form:

$$\boldsymbol{\epsilon} = \mathbf{E}^{-1}\boldsymbol{\sigma} + \boldsymbol{\epsilon}^0, \tag{6.29}$$

or inversely:

$$\boldsymbol{\sigma} = \mathbf{E}(\boldsymbol{\epsilon} - \boldsymbol{\epsilon}^0). \tag{6.30}$$

The square symmetric matrix of elasticity $\mathbf{E}$ has in the case of a truss a diagonal structure:

$$\mathbf{E} = [EA^1/l^1, \ldots, EA^j/l^j, \ldots, EA^e/l^e]. \tag{6.31}$$

Introducing the denotation

$$\sigma^0 = -E\epsilon^0, \tag{6.32}$$

we write Eq. (6.30) in a different form:

$$\sigma = E\epsilon + \sigma^0. \tag{6.33}$$

As we can see, the matrix σ^0 can be treated as a specification of the forces acting in the members of a truss which has not experienced strains ($\epsilon = 0$). In other words, in a truss whose joints suffer no displacements, internal forces are liable to appear in those truss members which if set free would undergo change in their length. For example, a uniform temperature increment by t deg would produce in member j of a truss with immobilized joints a longitudinal force of the value

$$N^{j0} = -\frac{EA^j}{l^j}\,\alpha_t tl^j = -EA^j\alpha_t t,$$

because the extension of a free member would be

$$\Delta l^{j0} = \alpha_t tl^j.$$

6.3. Equations of Kinematics, Equilibrium and Elasticity for a Plane Frame

In frames, the influence of longitudinal strains induced by axial forces is many times less than the influence of deflection of bars. Although inextensibility of bars is generally assumed in calculating frames, we shall not neglect, nevertheless, the effect of extensibility in the formulae derived and we shall assume that each of the joints i has three degrees of freedom in the xy plane:

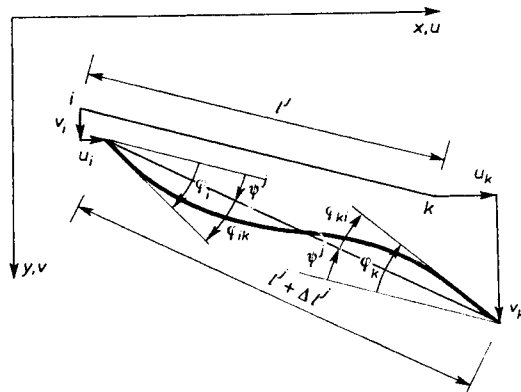$$q_i = \{u, v, \varphi\}_i. \tag{6.34}$$

Fig. 6.3. Framework member before and after displacement of joints

Unlike in the case of trusses whereby just one quantity, extension, described the state of strain of a whole bar, in the case of framework bars, we need to know the generalized strains at both ends of an element. These are the relative angular displacements between the joint and the bar chord, and also the increment in bar length. Figure 6.3 shows bar j situated between joint i and k. Its directional cosines α^j, β^j are expressed by Eqs. (6.1), and the initial length l^j—assuming $z^i = z_k$—by Eq. (6.2). We determine the extension of the bar Δl^j from Eq. (6.3) and the angular displacement of the chord ψ^j from the formula

$$\psi^j = -\frac{u_k - u_i}{l^j} \beta^j + \frac{v_k - v_i}{l^j} \alpha^j. \tag{6.35}$$

The quantities below are the parameters describing strain of the bar:

$$\varphi_{ik} = \varphi_i - \psi^j, \qquad \varphi_{ki} = \varphi_k - \psi^j, \qquad \Delta l^j, \tag{6.36}$$

with which we construct column matrix

$$\epsilon^j = \{\varphi_{ik}, \varphi_{ki}, \Delta l^j\}. \tag{6.37}$$

It is easily seen that for $\varphi_i = \varphi_k = \psi^j$ the element will remain straight.

The strains (6.37) are related to the displacements of joints i, k in the following manner:

$$\epsilon^j = [\mathbf{B}_{ik}, \mathbf{B}_{ki}] \{\mathbf{q}_i, \mathbf{q}_k\}, \tag{6.38}$$

where the matrices $\mathbf{B}_{ik}$, $\mathbf{B}_{ki}$ for $i < k$ have the form

$$\mathbf{B}_{ik} = \begin{bmatrix} -\dfrac{\beta^j}{l^j} & \dfrac{\alpha^j}{l^j} & 1 \\[2mm] -\dfrac{\beta^j}{l^j} & \dfrac{\alpha^j}{l^j} & 0 \\[2mm] -\alpha^j & -\beta^j & 0 \end{bmatrix}, \quad \mathbf{B}_{ki} = \begin{bmatrix} \dfrac{\beta^j}{l^j} & -\dfrac{\alpha^j}{l^j} & 0 \\[2mm] \dfrac{\beta^j}{l^j} & -\dfrac{\alpha^j}{l^j} & 1 \\[2mm] \alpha^j & \beta^j & 0 \end{bmatrix}. \tag{6.39}$$
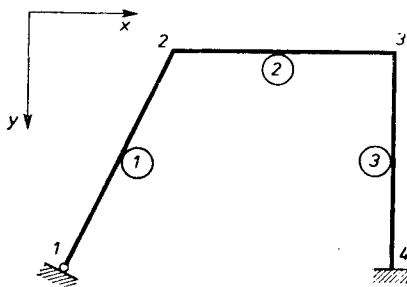

Fig. 6.4. Plane frame

By constructing a common vector of the displacements of all joints (support joints included):

$$\tilde{q} = \{q_1, q_2, \ldots, q_w\}, \tag{6.40}$$

and a common column matrix of the strains of all elements:

$$\epsilon = \{\epsilon^1, \epsilon^2, \ldots, \epsilon^e\}, \tag{6.41}$$

the relationship between them can be expressed by the general formula (6.9). In this case as well, the structure of matrix $\tilde{B}$ will depend on the system of connections between joints. For example, for the frame in Fig. 6.4, the matrix has the form

$$\tilde{B} = \begin{array}{c} \\ 1 \\ 2 \\ 3 \end{array} \begin{bmatrix} \overset{1}{B_{12}} & \overset{2}{B_{21}} & \overset{3}{} & \overset{4}{} \\ & B_{23} & B_{32} & \\ & & B_{34} & B_{43} \end{bmatrix}. \tag{6.42}$$

We regroup the displacements that go into the vector (6.40) in much the same way as for trusses. We place the unknown quantities in the top part of the vector:

$$q = \{\varphi_1, u_2, v_2, \varphi_2, u_3, v_3, \varphi_3\}, \tag{6.43}$$

and the known displacements of supports, in the bottom part:

$$r = \{u_1, v_1, u_4, v_4, \varphi_4\}. \tag{6.44}$$

When the displacement vector $\tilde{q}$ takes the form (6.13), columns of matrix $\tilde{B}$ have to be regrouped according to Eq. (6.14). The submatrices B and B_r for the frame in Fig. 6.4 will have the form

$$
B =
\begin{array}{c}
\\
\\ 1 \\ \\ \\ \\ \\ \\ \\ \\
\end{array}
\begin{array}{c}
\overset{1}{\varphi} \;\; \overset{2}{u v \varphi} \;\; \overset{3}{u v \varphi} \\
\begin{bmatrix}
0 & B_{21} & 0 \\
0 & & \\
\hline
0 & & \\
0 & B_{23} & B_{32} \\
0 & & \\
\hline
0 & & \\
0 & 0 & B_{34} \\
0 & &
\end{bmatrix}
\end{array},
\quad
B_r =
\begin{array}{c}
\overset{1}{u \qquad v} \;\; \overset{4}{u v \varphi} \\
\begin{bmatrix}
-\dfrac{\beta^1}{l^1} & \dfrac{\alpha^1}{l^1} & \\
-\dfrac{\beta^1}{l^1} & \dfrac{\alpha^1}{l^1} & 0 \\
-\alpha^1 & -\beta^1 & \\
\hline
0 & 0 & \\
0 & 0 & 0 \\
0 & 0 & \\
\hline
0 & 0 & \\
0 & 0 & B_{43} \\
0 & 0 &
\end{bmatrix}
\end{array}.
\tag{6.45}
$$

With the above denotations, the set of equations of geometric nature ultimately takes the form (6.17):

The frame is not only loaded by generalized forces acting directly on joints:

$$\tilde{Q} = \{Q_1, Q_2, \ldots, Q_w\}, \qquad Q_i = \{U, V, \Phi\}_i. \tag{6.46}$$

but also by forces acting within individual elements. The loads acting on bar j are shown in Fig. 6.5:

$$p^j = \{p_x(\xi), p_y(\xi), m(\xi)\}^j. \tag{6.47}$$
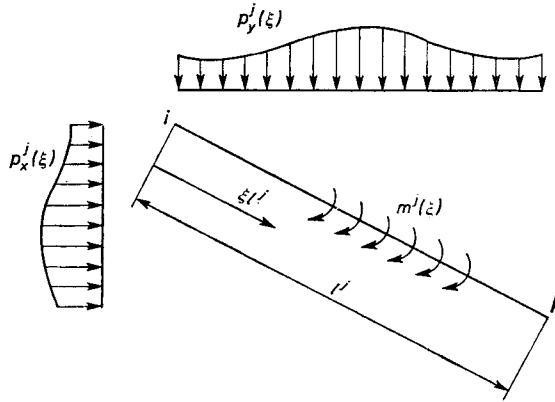
Fig. 6.5. Loadings acting on member of a plane frame

We have assumed that they are functions of the dimensionless variable ξ, measured in each bar from the joint of lower number, varying from 0 to 1. The loadings of all the bars can be arrayed to make a matrix

$$p = \{p^1, p^2, \ldots, p^e\}. \tag{6.48}$$

We take for the basic quantities of generalized internal forces the bending moments in characteristic cross-sections (Fig. 6.6) and the mean axial forces

Fig. 6.6. Moments in characteristic cross-sections of the frame

acting within the bars (cf. trusses). Although the bending moment in cross-section 1–2 placed in an articulated joint equals in principle zero we do not preclude an external moment a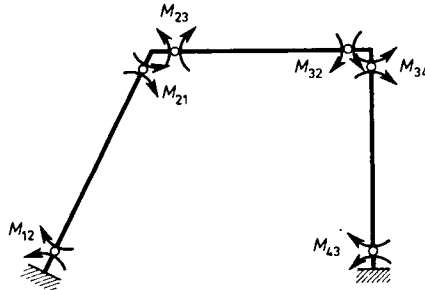cting there. Using those generalized internal forces we form a column matrix, structurally similar to the matrix (6.41):

$$\boldsymbol{\sigma} = \{\sigma^1, \sigma^2, \ldots, \sigma^e\}, \qquad \sigma^j = \{M_{ik}, M_{kl}, N^j\}. \tag{6.49}$$

To obtain the equilibrium equations we use also in this case the principle of virtual work. We therefore give virtual displacements to all the joints of the frame:

$$\delta\tilde{\mathbf{q}} = \{\delta\mathbf{q}_1, \delta\mathbf{q}_2, \ldots, \delta\mathbf{q}_w\}, \qquad \delta\mathbf{q}_i = \{\delta u, \delta v, \delta\varphi\}_i. \tag{6.50}$$

We demand at the same time that the displacements of joints be accompanied by such virtual strains of bars, at which the virtual work done by the internal forces would reduce to the work done by the generalized internal forces laid in the matrix (6.49). The bars must therefore remain straight, and only at their ends can slope discontinuities occur. We obtain this effect introducing a hinge at every bar-joint connection and giving virtual displacements to the
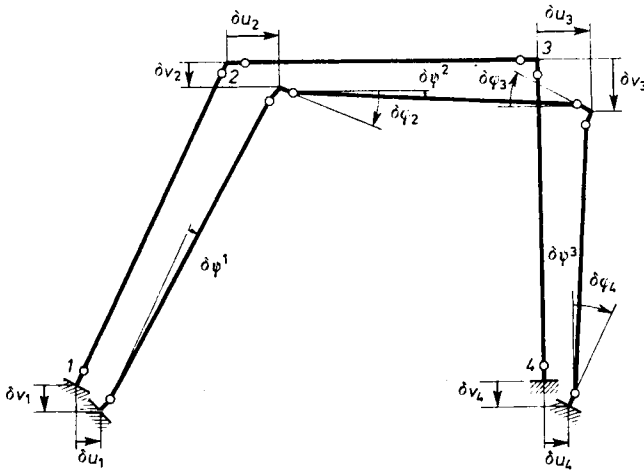
Fig. 6.7. Virtual displacements of frame

joints of the modified structure. Figure 6.7 shows the modified scheme of the frame from Fig. 6.4 together with virtual displacements of the structure.

Hence, the virtual displacements of the bar are (cf. (6.35), (6.36), (6.3)):

$$\delta\psi^j = -\frac{\delta u_k - \delta u_i}{l^j}\,\beta^j + \frac{\delta v_k - \delta v_i}{l^j}\,\alpha^j, \tag{6.51}$$

$$\delta\varphi_{ik} = \delta\varphi_i - \delta\psi^j, \qquad \delta\varphi_{kl} = \delta\varphi_k - \delta\psi^j, \tag{6.52}$$

$$\delta\Delta l^j = (\delta u_k - \delta u_i)\alpha^j + (\delta v_k - \delta v_i)\beta^j. \tag{6.53}$$

We array these strains in a single-column matrix:

$$\delta\boldsymbol{\epsilon} = \{\delta\boldsymbol{\epsilon}^1, \delta\boldsymbol{\epsilon}^2, \ldots, \delta\boldsymbol{\epsilon}^e\},$$
$$\delta\boldsymbol{\epsilon}^j = \{\delta\varphi_{ik}, \delta\varphi_{ki}, \delta\Delta l^j\}. \tag{6.54}$$

It is easily seen that a relationship analogous to (6.9) occurs between the virtual strains (6.54) and the virtual displacements (6.50):

$$\delta\boldsymbol{\epsilon} = \tilde{\mathbf{B}}\delta\tilde{\mathbf{q}}. \tag{6.55}$$

For the frame in Fig. 6.4, the matrix $\tilde{\mathbf{B}}$ is given by Eq. (6.42).

Considering that loadings also occur within bars, we must find the form of virtual displacements between individual joints. Since we have assumed that all the bars remain straight, we express their displacements by linear functions:

$$\delta u^j(\xi) = \delta u_i \xi' + \delta u_k \xi,$$
$$\delta v^j(\xi) = \delta v_i \xi' + \delta v_k \xi,$$
$$\delta\varphi^j(\xi) = \delta\psi^j. \tag{6.56}$$

Taking the above displacements to construct the vector

$$\delta\mathbf{f}^j = \{\delta u(\xi), \delta v(\xi), \delta\psi\}^j \tag{6.57}$$

and using the relation (6.51), we write

$$\delta\mathbf{f}^j = [\mathbf{N}_{ik}, \mathbf{N}_{ki}]\{\delta\mathbf{q}_i, \delta\mathbf{q}_k\}. \tag{6.58}$$

The matrices $\mathbf{N}_{ik}$, $\mathbf{N}_{ki}$ for $i < k$ have the structure

$$\mathbf{N}_{ik} = \begin{bmatrix} \xi' & 0 & 0 \\ 0 & \xi' & 0 \\ \dfrac{\beta^j}{l^j} & -\dfrac{\alpha^j}{l^j} & 0 \end{bmatrix}, \quad \mathbf{N}_{ki} = \begin{bmatrix} \xi & 0 & 0 \\ 0 & \xi & 0 \\ -\dfrac{\beta^j}{l^j} & \dfrac{\alpha^j}{l^j} & 0 \end{bmatrix}. \tag{6.59}$$

We construct from the vectors (6.57) a common vector setting together virtual displacements within all elements of the structure

$$\delta\mathbf{f} = \{\delta\mathbf{f}^1, \delta\mathbf{f}^2, \ldots, \delta\mathbf{f}^e\}. \tag{6.60}$$

The dependence of displacements $\delta\mathbf{f}$ within elements on displacements of joints $\delta\tilde{\mathbf{q}}$ is expressed generally by the formula

$$\delta\mathbf{f} = \tilde{\mathbf{N}}\delta\tilde{\mathbf{q}}, \tag{6.61}$$

in which the matrix $\tilde{\mathbf{N}}$ is constructed in much the same way as the matrix $\tilde{\mathbf{B}}$. For example, for the frame from Fig. 6.4, it is:

$$\tilde{\mathbf{N}} = \begin{bmatrix} \mathbf{N}_{12} & \mathbf{N}_{21} & & \\ & \mathbf{N}_{23} & \mathbf{N}_{32} & \\ & & \mathbf{N}_{34} & \mathbf{N}_{43} \end{bmatrix}. \tag{6.62}$$

After clarifying these points we can now proceed to write the equation for virtual work, i.e., to equate the virtual work done by external loads to the virtual work done by internal forces:

$$\delta \tilde{\mathbf{q}}^T \tilde{\mathbf{Q}} + \int_s \delta \mathbf{f}^T \mathbf{p} \, \mathrm{d}s = \delta \boldsymbol{\epsilon}^T \boldsymbol{\sigma}. \tag{6.63}$$

Putting the relations (6.61) and (6.55) into eq. (6.63), we arrive at the form

$$\delta \tilde{\mathbf{q}}^T \tilde{\mathbf{Q}} + \delta \hat{\mathbf{q}}^T \int_s \tilde{\mathbf{N}}^T \mathbf{p} \, \mathrm{d}s = \delta \hat{\mathbf{q}}^T \tilde{\mathbf{B}}^T \boldsymbol{\sigma}. \tag{6.64}$$

Based on the argumentation followed in discussing the equality (6.24), we arrive at the set of equilibrium equations

$$\tilde{\mathbf{Q}} + \int_s \tilde{\mathbf{N}}^T \mathbf{p} \, \mathrm{d}s = \tilde{\mathbf{B}}^T \boldsymbol{\sigma}. \tag{6.65}$$

Proceeding in like manner as in the case of trusses, we regroup the quantities forming the vector $\tilde{\mathbf{Q}}$ and separate the known quantities forming the vector $\mathbf{Q}$ from the unknown reactions that go into the vector $\mathbf{R}$. For the frame from Fig. 6.4, these vectors have the form

$$\mathbf{Q} = \{\Phi_1, U_2, V_2, \Phi_2, U_3, V_3, \Phi_3\}, \tag{6.66}$$
$$\mathbf{R} = \{U_1, V_1, U_4, V_4, \Phi_4\}. \tag{6.67}$$

The matrices $\tilde{\mathbf{B}}$ (cf. (6.45)) and $\tilde{\mathbf{N}}$ must also be reconstructed along similar lines. In the particular case of the frame in Fig. 6.4, we obtain the matrices $\mathbf{N}$ and $\mathbf{N}_r$ into which the matrix $\tilde{\mathbf{N}}$ should be resolved, using the analogy between these matrices and the matrices (6.45):

$$\mathbf{N} = \begin{bmatrix} 0 & & \\ 0 & \mathbf{N}_{21} & 0 \\ 0 & & \\ \hline 0 & & \\ 0 & \mathbf{N}_{23} & \mathbf{N}_{32} \\ 0 & & \\ \hline 0 & & \\ 0 & 0 & \mathbf{N}_{34} \\ 0 & & \end{bmatrix}, \quad \mathbf{N}_r = \begin{bmatrix} \xi' & 0 & \\ 0 & \xi' & 0 \\ \dfrac{\beta^1}{l^1} & -\dfrac{\alpha^1}{l^1} & \\ \hline 0 & 0 & \\ 0 & 0 & 0 \\ 0 & 0 & \\ \hline 0 & 0 & \\ 0 & 0 & \mathbf{N}_{43} \\ 0 & 0 & \end{bmatrix}. \tag{6.68}$$

Using the above denotations, the set of equilibrium equations (6.65) can be written in the form of two subsets:

$$\mathbf{Q} + \mathbf{Q}^p = \mathbf{B}^T \boldsymbol{\sigma}, \quad \mathbf{R} + \mathbf{R}^p = \mathbf{B}_r^T \boldsymbol{\sigma}, \tag{6.69}$$

in which there is

$$Q^p = \int_s \mathbf{N}^T \mathbf{p} \, ds, \qquad \mathbf{R}^p = \int_s \mathbf{N}_r^T \mathbf{p} \, ds. \tag{6.70}$$

All that remains to be determined are the relations occurring between strains and loads. Let us consider, therefore, one of the frame bars numbered j, placed between joints i and k. Acting on the ends of the bar are moments M_{ik}, M_{ki} inducing angular displacements at joints φ_{ik}^M, φ_{ki}^M, measured from the chord of the bar (Fig. 6.8a). Moreover, the bar is under loads distributed
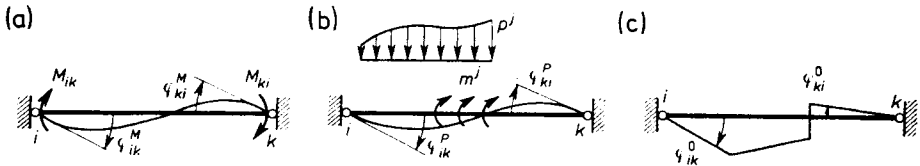

Fig. 6.8. Rotations of characteristic cross-sections under (a) bar-end-moments; (b) static loads; (c) distortional strains

over its length and these are accompanied by rotations at the end cross-sections, φ_{ik}^P, φ_{ki}^P (Fig. 6.8b). In the end, the bar is liable to experience distortional strains which result in additional rotations of the same cross-sections φ_{ik}^0, φ_{ki}^0 (Fig. 6.8c).

The respective relations are determined from the equations derived in Section 5.3. For example, following from Eqs. (5.33) are the relations between the quantities given in Fig. 6.8a:

$$\begin{bmatrix} M_{ik} \\ M_{ki} \end{bmatrix} = \frac{EJ^j}{l^j} \begin{bmatrix} 4-3\mu^j & 2-3\mu^j \\ 2-3\mu^j & 4-3\mu^j \end{bmatrix} \begin{bmatrix} \varphi_{ik}^M \\ \varphi_{ki}^M \end{bmatrix}, \tag{6.71}$$

where in keeping with Eqs. (5.36) and (5.27) we have

$$\mu^j = \frac{12\gamma^j}{1+12\gamma^j}, \qquad \gamma^j = \frac{k^j EJ^j}{GA^j(l^j)^2}. \tag{6.72}$$

It is easy to arrive therefrom at inverse relations

$$\begin{bmatrix} \varphi_{ik} \\ \varphi_{ki} \end{bmatrix} = \frac{l^j}{6EJ^j} \begin{bmatrix} 2+6\gamma^j & -1+6\gamma^j \\ -1+6\gamma^j & 2+6\gamma^j \end{bmatrix} \begin{bmatrix} M_{ik} \\ M_{ki} \end{bmatrix}. \tag{6.73}$$

The determinations of the remaining angles shown in Figs. 6.8b, c should not present any particular difficulty. We either make use of suitable integrals of a differential equation (cf. Section 5.2) or of the principle of virtual work.

Considering not only the angular strains but the extension of a bar as well, using the denotations (6.37), (6.49)$_2$, we get:

$$\epsilon^j = (E^j)^{-1}\sigma^j + \epsilon^{jp} + \epsilon^{j0}, \tag{6.74}$$

where:

$$(E^j)^{-1} = \frac{l^j}{6EJ^j} \begin{bmatrix} 2+6\gamma^j & -1+6\gamma^j & \\ -1+6\gamma^j & 2+6\gamma^j & \\ & & 6\frac{J^j}{A^j} \end{bmatrix}. \tag{6.75}$$

The strains of all the bars of the frame are expressed as

$$\epsilon = E^{-1}\sigma + \epsilon^p + \epsilon^0. \tag{6.76}$$

The symmetric matrix of deformability E^{-1} is a quasidiagonal matrix consisting of the submatrices (6.75):

$$E^{-1} = \begin{bmatrix} (E^1)^{-1} & & & \\ & (E^2)^{-1} & & \\ & & \ddots & \\ & & & (E^e)^{-1} \end{bmatrix}. \tag{6.77}$$

The inverse relation to (6.76) has the form

$$\sigma = E(\epsilon - \epsilon^p - \epsilon^0), \tag{6.78}$$

or by introducing the denotations

$$\sigma^0 = -E(\epsilon^p + \epsilon^0) \tag{6.79}$$

it is expressed by Eq. (6.33). The elasticity matrix

$$E = \begin{bmatrix} E^1 & & & \\ & E^2 & & \\ & & \ddots & \\ & & & E^e \end{bmatrix}, \tag{6.80}$$

consists of the submatrices

$$E^j = \frac{EJ^j}{l^j} \begin{bmatrix} 4-3\mu^j & 2-3\mu^j & \\ 2-3\mu^j & 4-3\mu^j & \\ & & \frac{A^j}{J^j} \end{bmatrix}. \tag{6.81}$$

Among the components of the matrix σ^0 there are the moments M_{ik}^0, M_{ki}^0, which will appear in end cross-sections when the angles φ_{ik}, φ_{ki} are zero. These moments can be induced either by static loads within the bar or by non-static factors (distortions).

6.4. Analysis of a Complete Set of Equations

The equations of kinematics (6.17), equilibrium (6.28), (6.69) and elasticity (6.33) have, regardless of the type of bar structure involved, the following general form:

$$\boldsymbol{\epsilon} = \mathbf{B}\mathbf{q} + \mathbf{B}_r\mathbf{r} \qquad (t), \tag{6.82}$$

$$\mathbf{B}^T\boldsymbol{\sigma} = \mathbf{Q} + \mathbf{Q}^p \quad (g), \qquad \mathbf{B}_r^T\boldsymbol{\sigma} = \mathbf{R} + \mathbf{R}^p \quad (r), \tag{6.83}$$

$$\boldsymbol{\sigma} = \mathbf{E}\boldsymbol{\epsilon} + \boldsymbol{\sigma}_0 \qquad (t). \tag{6.84}$$

Each of the matrix equations consists of a certain number of single equations. We have parenthesized their actual number, expressed by the symbols t, g, r, next to the respective equations of the set (6.82)–(6.84). In trusses, the quantities $\mathbf{Q}^p$, $\mathbf{R}^p$ equal zero in the absence of loads acting within the truss members.

In the set of equations just given, we have the following unknowns: parameters describing the strains in an element, making the matrix $\boldsymbol{\epsilon}$ (t), displacements of free joints set together in the vector $\mathbf{q}$ (g), support reactions making the vector $\mathbf{R}$ (r) and generalized forces in selected cross-sections of bars, going into the matrix $\boldsymbol{\sigma}$ (t). As we can see, the number of unknowns corresponds to the number of equations, which does not however, mean that the set can uniquely be solved for every load.

Of fundamental importance in the further analysis of the set of equations (6.82)–(6.84) is the matrix $\mathbf{B}$ of dimensions $t \times g$. For $t < g$ the number of equilibrium equations is higher than the number of static unknowns, and the structure is kinematically variable. We must therefore exclude this case from further considerations. The set of equations considered, regardless of the kind of load, then has a unique solution and only then if the order* of matrix $\mathbf{B}$ equals the number of its columns g, which we shall call the *degree of geometric indeterminability* of a structure. If the order of matrix $\mathbf{B}$, which we denote by the symbol b, was lower than the degree of geometric indeterminability g, the structure would then kinematically variable. The degree of kinematic variability is calculated from the formula

$$k = g - b. \tag{6.85}$$

It is also applicable to the case where $t < g$.

The difference between the numbers t and g, which give the dimensions of the matrix $\mathbf{B}$, is the static-kinematic discriminant of the structure:

$$n = t - g. \tag{6.86}$$

---

* We shall call the *order* of matrix $\mathbf{B}$ the dimension of its greatest non-singular square matrix which can be separated out of matrix $\mathbf{B}$ by cancelling appropriate rows and columns.

However, since the degree of static indeterminability s equals the sum of numbers n and k in accordance with Eq. (3.2), we thus have

$$s = t - b.$$

As we have previously noted, we ignore kinematically variable structures. Consequently, we shall not deal with such sets of equations (6.82)–(6.84), in which the order of matrix B is lower than the number of its columns. Hence, the degree of static indeterminability of a structure will be equal to the static-kinematic discriminant, expressed by Eq. (6.86). It is self-evident that in the case of a statically determinate structure, the matrix B will be a non-singular square matrix.

It is easily verified that both the truss in Fig. 6.2 and the frame in Fig. 6.4, whose matrices B given by Eqs. (6.15) and (6.86)$_1$ have the dimensions 10×8 and 9×7 respectively, are twofold, statically indeterminate structures. The degree of geometric indeterminability of these structures is 8 and 7, respectively.

As for the frame, it could also be treated as a structure sixfold geometrically indeterminate. For, we need not be interested in the value of angle φ_1 can get rid of this quantity in the set of equations, giving up at the same time the equilibrium condition for the moments in joint 1, incidentally a condition which is identically satisfied. This would involve the necessity of suitably restructuring the elasticity matrix of bar 1; the matrix E^1 would be of the size 2×2. As a result of all these operations, which would disturb the order in which the matrices described in Section 5.3 should be constructed, the matrix B would diminish in size by one row and one column.

6.5. Isostatic Structures

Proceeding in discussing the principal methods of solving the set of equations (6.82)–(6.84), we begin with the special case in which the matrix B is a non-singular square matrix. The structure is then isostatic, and the easiest way to calculate all the unknown quantitites is by finding first of all the internal forces σ from the equilibrium conditions (6.83)$_1$:

$$\sigma = B^{-T}(Q + Q^p). \tag{6.87}$$

Substituting these generalized internal forces into Eqs. (6.83)$_2$ we can calculate the support reactions:

$$R = B_r^T B^{-T}(Q + Q^p) - R^p. \tag{6.88}$$

As for strains $\boldsymbol{\epsilon}$ we determine them not from Eq. (6.84) but from the set of inverse equations (6.76):

$$\boldsymbol{\epsilon} = \mathbf{E}^{-1}\mathbf{B}^{-T}(\mathbf{Q}+\mathbf{Q}^p)+\boldsymbol{\epsilon}^p+\boldsymbol{\epsilon}^0. \tag{6.89}$$

Finally, we determine from the set of equations (6.82) the displacements of the joints:

$$\mathbf{q} = \mathbf{B}^{-1}\mathbf{E}^{-1}\mathbf{B}^{-T}(\mathbf{Q}+\mathbf{Q}^p)+\mathbf{B}^{-1}(\boldsymbol{\epsilon}^p+\boldsymbol{\epsilon}^0)-\mathbf{B}^{-1}\mathbf{B}_r\mathbf{r}. \tag{6.90}$$

Note that the internal forces (6.87) in an isostatic structure depend exclusively on external static loads, but do not depend either on the settlement of supports r or on distortional strains $\boldsymbol{\epsilon}^0$. The matrix $\mathbf{B}^{-1}\mathbf{E}^{-1}\mathbf{B}^{-T} = \mathbf{F}$ relating the displacements $\mathbf{q}$ to the load $\mathbf{Q}$ is, as can be seen, a symmetric matrix. The symmetry of this matrix, called the *flexibility matrix*, substantiates Maxwell's reciprocal theorem previously proved. In a reverse approach, the reciprocity theorems serve to prove that the matrix of a set of equilibrium equations must be a transposition of the matrix of equations of kinematics. This is the essence od Clebsch's theorem (Clebsch, 1862).

6.6. The Direct Stiffness Method (Displacement Method)

In the case of a rectangular matrix $\mathbf{B}$, we can choose between two procedures. The first—natural for matrix calculus—leads through eliminations of static quantities and strains $\boldsymbol{\epsilon}$ to a set of equilibrium equations, in which only displacements $\mathbf{q}$ are the unknowns. On these grounds, the procedure is called the *direct stiffness method (displacement method)*. Attention should be drawn to an analogy between the described procedure to eliminate the unknowns and a method which under the theory of elasticity leads to what is known as displacement equations (Mossakowska *et al.*, 1978, p. 73).

We substitute the strains $\boldsymbol{\epsilon}$ expressed by Eq. (6.82) into eqs. (6.84) and the internal forces $\boldsymbol{\sigma}$ by the displacements $\mathbf{q}$:

$$\boldsymbol{\sigma} = \mathbf{EBq}+\mathbf{EB}_r\mathbf{r}+\boldsymbol{\sigma}^0. \tag{6.91}$$

Next, we substitute the above internal forces into the equilibrium equations $(6.83)_1$:

$$\mathbf{B}^T\mathbf{EBq} = \mathbf{Q}+\mathbf{Q}^p-\mathbf{B}^T\mathbf{EB}_r\mathbf{r}-\mathbf{B}^T\boldsymbol{\sigma}^0. \tag{6.92}$$

In this way, we have obtained a set of g equations in which there are g unknown displacements making the vector $\mathbf{q}$. The matrix

$$\mathbf{B}^T\mathbf{EB} = \mathbf{K}, \tag{6.93}$$

called the *stiffness matrix* is of course symmetric.

Solving the set (6.91), we calculate the internal forces σ which we put in turn into Eqs. (6.83) to calculate the reactions

$$\mathbf{R} = \mathbf{B}_r^T \mathbf{EBq} + \mathbf{B}_r^T \mathbf{EB}_r \mathbf{r} + \mathbf{B}_r^T \sigma^0 - \mathbf{R}^p. \tag{6.94}$$

The symmetry of the matrix $\mathbf{B}_r^T \mathbf{EB}_r$ follows from Rayleigh's reciprocal reaction theorem.

6.7. The Direct Flexibility Method (Force Method)

The other technique of solving the set of equations (6.82)–(6.84), which formally is more complicated, is founded on an analogous argumentation to that which according to the theory of elasticity leads to the Beltrami–Michell stress equations (Mossakowska *et al.*, 1978, p. 85). By eliminations, which will be discussed below, we arrive by this procedure at a set of equations in which the only unknowns are static quantities.

Using this method, we must first suitably split each of the single column matrices ϵ and σ into two submatrices:

$$\epsilon = \{\epsilon_s, \epsilon_x\}, \quad \sigma = \{\sigma_s, \mathbf{X}\}. \tag{6.95}$$

The dimensions of the matrices ϵ_s and σ_s should be equal to the dimension g of the matrix $\mathbf{B}$. Consequently, the dimensions of the other submatrices, ϵ_x, and $\mathbf{X}$, will be n (6.86), i.e., they will be as great as the degree of static indeterminability of the structure.

This approach makes it necessary to suitably split the matrices $\mathbf{B}$, $\mathbf{B}_r$ and $\mathbf{E}^{-1}$:

$$\mathbf{B} = \begin{bmatrix} \mathbf{B}_s \\ \mathbf{B}_x \end{bmatrix}, \quad \mathbf{B}_r = \begin{bmatrix} \mathbf{B}_{rs} \\ \mathbf{B}_{rx} \end{bmatrix}, \quad \mathbf{E}^{-1} = \begin{bmatrix} \mathbf{C}_{ss} & \mathbf{C}_{sx} \\ \mathbf{C}_{xs} & \mathbf{C}_{xx} \end{bmatrix}. \tag{6.96}$$

We demand that the matrix $\mathbf{B}_s$, which is a square matrix of size $g \times g$, be non-singular. It follows that the decomposition of the matrices ϵ and σ into the submatrices (6.95) cannot be arbitrary.

For the truss from Fig. 6.2, in which the number of elements $e = 10$, eight terms occupying the top part of the matrices (6.7) and (6.18) can be assigned to each of the matrices ϵ_s and σ_s, and to each of the matrices ϵ_x and $\mathbf{X}$, two terms numbered 9 and 10. This means that we recognize the forces N_9 and N_{10} to be statically indeterminate quantities, and the truss whose rods 9 and 10 have been cut, as the primary statically determinate system. The dashed horizontal line in Eqs. (6.15), (6.16) separates the matrix $\mathbf{B}_s$ from $\mathbf{B}_x$, and $\mathbf{B}_{rs}$ from $\mathbf{B}_{rx}$.

A similar decomposition of the matrices ϵ and σ into top and bottom part would be wrong for the frame from Fig. 6.4, since the top part of matrix $\mathbf{B}$

given by Eq. (6.45) would be singular. Taking the axial force in bar 3 and the bending moment M_{43} for the unknowns would mean that the frame shown in Fig. 6.9a is the primary system. However, since it is a kinematically variable system, we must abandon such a decomposition of the matrices ϵ and σ.

Fig. 6.9. Primary structure: (a) irregular; (b) regular

On the other hand, if we put the quantities φ_{34} and φ_{43} into the matrix ϵ_x and, correspondingly, M_{34} and M_{43} into the matrix X, then the frame shown in Fig. 6.9b will be the primary system, kinematically invariable. The consequence of such a decomposition of the matrices ϵ and σ will be a suitable restructuring of the matrices (6.45). Their parts (cf. (6.96)) will have the form:

$$
\mathbf{B}_s = \begin{bmatrix} 1 & & & \\ 0 & \mathbf{B}_{21} & & 0 \\ 0 & & & \\ 0 & & & \\ 0 & \mathbf{B}_{23} & & \mathbf{B}_{32} \\ 0 & & & \\ 0 & 0 & 0 & 0 & -\alpha^3 & -\beta^3 & 0 \end{bmatrix}, \quad
\mathbf{B}_{rs} = \begin{bmatrix} -\beta^1/l^1 & \alpha^1/l^1 & \\ -\beta^1/l^1 & \alpha^1/l^1 & 0 \\ -\alpha^1 & -\beta^1 & \\ 0 & 0 & \\ 0 & 0 & 0 \\ 0 & 0 & \\ 0 & 0 & \alpha^3 & \beta^3 & 0 \end{bmatrix},
$$

$$(6.97)$$

$$
\mathbf{B}_x = \begin{bmatrix} 0 & 0 & 0 & 0 & -\beta^3/l^3 & \alpha^3/l^3 & 1 \\ 0 & 0 & 0 & 0 & -\beta^3/l^3 & \alpha^3/l^3 & 0 \end{bmatrix},
$$

$$
\mathbf{B}_{rx} = \begin{bmatrix} 0 & 0 & \beta^3/l^3 & -\alpha^3/l^3 & 0 \\ 0 & 0 & \beta^3/l^3 & -\alpha^3/l^3 & 1 \end{bmatrix}.
$$

$$(6.98)$$

After decomposing the matrices, we give the set of equations (6.82)–(6.84) the form:

$$
\begin{aligned}
\epsilon_s &= \mathbf{B}_s \mathbf{q} + \mathbf{B}_{rs} \mathbf{r}, \\
\epsilon_x &= \mathbf{B}_x \mathbf{q} + \mathbf{B}''_{rx} \mathbf{r},
\end{aligned}
$$

$$(6.99)$$

$$
\begin{aligned}
\mathbf{B}_s^T \sigma_s + \mathbf{B}_x^T \mathbf{X} &= \mathbf{Q} + \mathbf{Q}^p, \\
\mathbf{B}_{rs}^T \sigma_s + \mathbf{B}_{rx}^T \mathbf{X} &= \mathbf{R} + \mathbf{R}^p,
\end{aligned}
$$

$$(6.100)$$

$$\epsilon_s = C_{ss}\sigma_s + C_{sx}X + \epsilon_s^p + \epsilon_s^0,$$
$$\epsilon_x = C_{xs}\sigma_s + C_{xx}X + \epsilon_x^p + \epsilon_x^0. \tag{6.101}$$

We solve the set of equations $(6.99)_1$ with respect to the unknown displacement q:

$$q = B_s^{-1}\epsilon_s - B_s^{-1}B_{rs}r \tag{6.102}$$

and put the displacements thus expressed into the second group of geometric relations $(6.99)_2$:

$$\epsilon_x = B_x B_s^{-1}\epsilon_s - B_x B_s^{-1}B_{rs}r + B_{rx}r. \tag{6.103}$$

In this way, we have obtained a set of n equations, in which only strains ϵ occur as unknowns. Therefore, we deal here with an equivalent of a set of compatibility equations known from the mechanics of continuous media (cf. Mossakowska *et al.*, 1978, p. 28). It follows from the matrix equation (6.103) that strains in the elements of a statically indeterminate structure are not independent of each other; a continuous system satisfying all support conditions cannot possibly be constructed of arbitrarily deformed elements.

Let us treat the internal forces σ_s in the set of equations $(6.100)_1$ as unknowns which we express by other quantities:

$$\sigma_s = B_s^{-T}(Q + Q^p) - B_s^{-T}B_x^T X. \tag{6.104}$$

Substituting the above expression into the remaining group of equations (6.101), we get

$$\epsilon_s = C_{ss}B_s^{-T}(Q + Q^p) - C_{ss}B_s^{-T}B_x^T X + C_{sx}X + \epsilon_s^p + \epsilon_s^0,$$
$$\epsilon_x = C_{xs}B_s^{-T}(Q + Q^p) - C_{xs}B_s^{-T}B_x^T X + C_{xx}X + \epsilon_x^p + \epsilon_x^0. \tag{6.105}$$

The strains thus calculated are substituted into the set of compatibility equations (6.103), which after ordering and introducing the denotations:

$$F = B_x B_s^{-1}C_{ss}B_s^{-T}B_x^T - C_{xs}B_s^{-T}B_x^T - B_x B_s^{-1}C_{sx} + C_{xx}, \tag{6.106}$$

$$F^p = (C_{xs} - B_x B_s^{-1}C_{ss})B_s^{-T}(Q + Q^p) + \epsilon_x^p - B_x B_s^{-1}\epsilon_s^p, \tag{6.107}$$

$$F^r = (B_x B_s^{-1}B_{rs} - B_{rx})r, \qquad F^0 = \epsilon_x^0 - B_x B_s^{-1}\epsilon_s^0, \tag{6.108}$$

takes the form

$$FX + F^p + F^r + F^0 = 0. \tag{6.109}$$

The above set consists of n canonical equations of the force method, in which n numbers of generalized forces X are the unknowns. After solving the set (6.109) and determining the unknowns X, we calculate the other internal forces σ_s. From Eqs. $(6.100)_2$ we determine the support reactions R, from Eqs. (6.101) the strains ϵ, and from (6.102) the displacements of joints q.

6.8. Final Remarks

Comparing the methods presented for solving the set of equations (6.82)–(6.84), we find that the most universal method and simplest in matrix notation, is the displacement method. It is equally applicable to statically indeterminate and determinate systems. It leads to a single set of equations with a symmetric matrix (6.93), $g \times g$ in size. By virtue of the two advantages just named, the method is now the most widely used in engineering practice. Almost all digital computer programmes used for static analysis of bar structures are based on it.

Regarding statically determinate systems, they can also be calculated in the previously described manner (cf. (6.87)–(6.90)). By this technique, we solve first a set of static equations, whose non-symmetric matrix $\mathbf{B}^T$ is likewise $g \times g$ in size. In spite of the asymmetry of the matrix, the set of equations can quite easily be solved in most cases, and the inverse of the matrix $\mathbf{B}^T$ is determined by elementary consideration.

As for the force method, the first thing that needs to be done is to select a primary system that is statically determinate, in other words, to select static quantities which we shall treat as redundant unknowns. This is a very important operation since the right choice of redundant unknowns is determinant of whether the set of canonical equations of the force method will be well- or ill-conditioned. This operation requires intellectual intervention of man, and practically cannot be automated by entrusting it to a digital computer.

The next operation is to invert the asymmetric matrix $\mathbf{B}_s(\mathbf{B}_s^T)$, $g \times g$ in size. Since the primary system is statically determinate, finding the inverse of matrix $\mathbf{B}_s$ is therefore as simple as inverting matrix $\mathbf{B}^T$ for an isostatic system.

As a result of numerous transformations, which have been discussed above, we arrive at a set of canonical equations of the direct flexibility method, whose symmetric matrix (6.106) is $n \times n$ in size.

Although in matrix notation the direct flexibility method may seem unduly complicated, in many cases applying it may prove to be more an advantage than solving the system by the direct stiffness method. This is true in particular when the degree of static indeterminability, $s = n$, is significantly lower than the degree of geometric indeterminability. In both examples of bar structures considered in Sections 6.2 and 6.3, this was precisely the case.

7. Isostatic Systems

Making use of the principles discussed in general terms in Chapter 6, we shall now concern ourselves in greater detail with the static analysis of several iso-static systems most common in practice.

7.1. Multi Span Hinged Beams

Hinged beams, schematically represented in Fig. 7.1a are used chiefly in bridge and industrial structures. The problem, which consists in finding
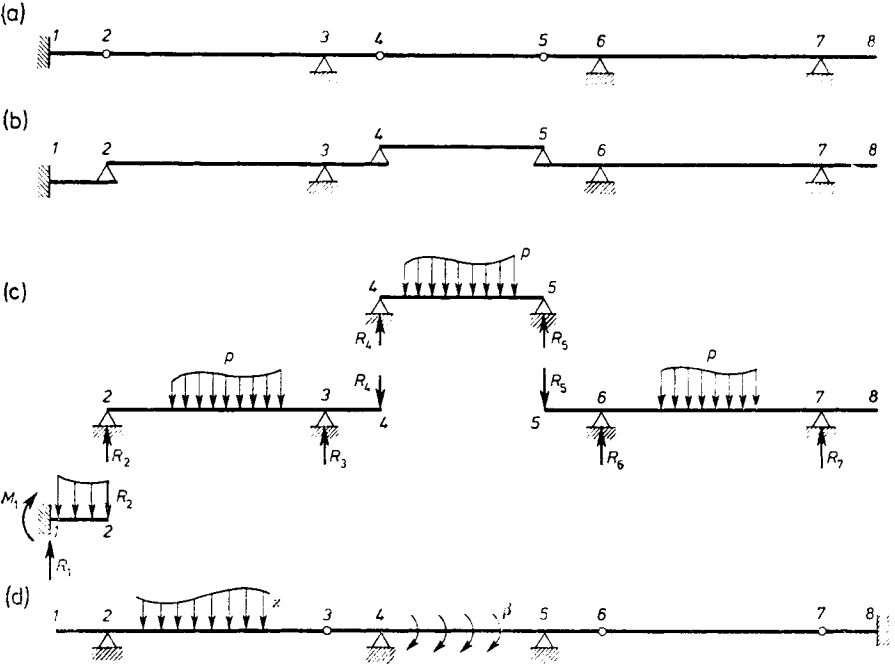

Fig. 7.1. Multispan hinged beam: (a), (b) the schemes of the beam; (c) mode of trans-
mission of loadings; (d) modified scheme

generalized plots of the internal forces in a beam and also in finding the beam's deflection line, can be broken down into several simpler problems wherein single, simply supported or cantilever beams are successively examined. In Fig. 7.1b we have the same beam as in Fig. 7.1a but showing also its structure. We start calculations from the uppermost beam *4–5* and then consider successively beams *5–8*, *2–4* and *1–2* (Fig. 7.1c). After determining the bending moments and the shear forces, this being an elementary problem, we calculate the curvatures $\varkappa$ and the shear strain angles β. We treat these quantities as secondary loads acting on the structure which has been suitably modified as shown in Fig. 7.1d. The moments due to the secondary loads are deflections, and the transverse forces are angular displacements of cross-sections.

The described procedure, although conceptually simple, is nevertheless very tedious; specifically the many successive integrations and other mathematical operations that need to be performed require great care. Although the functions thus derived, which express the distribution of generalized
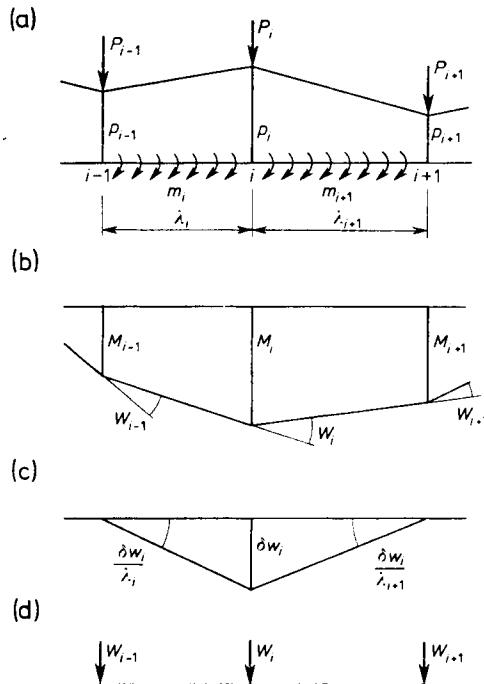
Fig. 7.2. Part of a beam: (a) loading; (b) diagram of moments; (c) virtual displacement; (d) equivalent loadings

internal forces or deflections, allow the sought quantities to be determined in an arbitrary cross-section, these values are practically calculated not at infinitely many points on the axis but in selected cross-sections whose number is obviously finite. For this reason, we shall discuss in more detail the procedure to be followed to determine the generalized internal forces and the displacements in preselected cross-sections of a beam.

First of all, we divide the hinged beam considered into segments in such a way as to get the dividing points to fall on all the discontinuity sites, i.e., beneath supports, at hinges, at places of change in the cross-section or loading, at points of application of concentrated forces, and the like. Apart from that, wherever we find the segments between the discontinuity points too long, we divide them into an arbitrary number of shorter segments as required. The more minute the division we use, the more accurate the results will be. We approximate load p acting on the beam by forces linearly distributed over individual segments, and we also assume that moments m (if any are acting on the beam at all) are constant in each segment (Fig. 7.2a). Moreover, concentrated forces P_i may be acting in joints, their values in support joints being unknown. These loads are accompanied by bending moments whose plot is given segmentally in Fig. 7.2b.

To determine the relationship between the moment values in joints and the external load, we give the beam such a virtual displacement (Fig. 7.2c) that the work done by the generalized internal forces should reduce to the work done by moments M_{i-1}, M_i, M_{i+1}. Hence, we have

$$\delta w_i \left[-M_{i-1}\frac{1}{\lambda_i} + M_i\left(\frac{1}{\lambda_i} + \frac{1}{\lambda_{i+1}}\right) - M_{i+1}\frac{1}{\lambda_{i+1}} \right]$$

$$= \delta w_i P_i + \delta w_i \left[p_{i-1}\frac{\lambda_i}{6} + p_i\left(\frac{\lambda_i}{3} + \frac{\lambda_{i+1}}{3}\right) + p_{i+1}\frac{\lambda_{i+1}}{6} \right] +$$

$$+ \delta w_i (m_i - m_{i+1}). \tag{7.1}$$

The quantities

$$W_i = P_i + p_{i-1}\frac{\lambda_i}{6} + p_i\left(\frac{\lambda_i}{3} + \frac{\lambda_{i+1}}{3}\right) + p_{i+1}\frac{\lambda_{i+1}}{6} + m_i - m_{i+1} \tag{7.2}$$

can be treated as concentrated forces (Fig. 7.2d) which induce bending moments in joints of the beam, of exactly the same value as the loads shown in Fig. 7.2a.

Let us construct the following matrices:

$$\tilde{\mathbf{P}} = \{P_0, P_1, P_2, ..., P_n\}, \tag{7.3}$$

$$\mathbf{p} = \{p_0, p_1, p_2, ..., p_n\}, \tag{7.4}$$

$$\mathbf{m} = \{m_1, m_2, \ldots, m_n\}, \tag{7.5}$$

$$\tilde{\mathbf{W}} = \{W_0, W_1, W_2, \ldots, W_n\}, \tag{7.6}$$

$$\tilde{\mathbf{M}} = \{M_0, M_1, M_2, \ldots, M_n\}, \tag{7.7}$$

$$\tilde{\mathbf{B}} = \begin{array}{c} \\ 0 \\ \\ 1 \\ \\ \\ n \end{array}
\begin{array}{ccccccc}
0 & 1 & 2 & \ldots & n-1 & n \\
\end{array}
\left[\begin{array}{cccccc}
\dfrac{1}{\lambda_1} & -\dfrac{1}{\lambda_1} & & & & \\[2mm]
-\dfrac{1}{\lambda_1} & \dfrac{1}{\lambda_1}+\dfrac{1}{\lambda_2} & -\dfrac{1}{\lambda_2} & & & \\[2mm]
& \ldots & \ldots & \ldots & & \\[2mm]
& & & & -\dfrac{1}{\lambda_n} & \dfrac{1}{\lambda_n}
\end{array}\right], \tag{7.8}$$

$$\tilde{\mathbf{a}} = \frac{1}{6}
\begin{array}{c} \\ \\ \\ \end{array}
\begin{array}{ccccc}
0 & 1 & 2\ldots n-1 & n \\
\end{array}
\left[\begin{array}{cccc}
2\lambda_1 & \lambda_1 & & \\
\lambda_1 & 2\lambda_1+2\lambda_2 & \lambda_2 & \\
& \ldots & \ldots & \ldots \\
& & \lambda_n & 2\lambda_n
\end{array}\right]
\begin{array}{c} 0 \\ 1 \\ \\ n \end{array}, \tag{7.9}$$

$$\tilde{\mathbf{b}} = \begin{array}{c} 0 \\ 1 \\ \\ n-1 \\ n \end{array}
\begin{array}{ccccc}
1 & 2 & \ldots & n-1 & n \\
\end{array}
\left[\begin{array}{ccccc}
-1 & & & & \\
1 & -1 & & & \\
& \ldots & \ldots & & \\
& & & 1 & -1 \\
& & & & 1
\end{array}\right], \tag{7.10}$$

where n denotes the number of segments into which the hinged beam has been divided. Using these denotations, the static relations following from Eqs. (7.1), (7.2) can be written as follows:

$$\tilde{\mathbf{B}}\tilde{\mathbf{M}} = \tilde{\mathbf{W}}, \quad \tilde{\mathbf{W}} = \tilde{\mathbf{P}}+\tilde{\mathbf{a}}\mathbf{p}+\tilde{\mathbf{b}}\mathbf{m}. \tag{7.11}$$

Figure 7.3a, b show as an example a hinged beam together with forces $\tilde{\mathbf{W}}$ acting on it and a plot of the moments.

The set (7.11) consists of $n+1$ equations, and the matrices $\tilde{\mathbf{M}}$, $\tilde{\mathbf{W}}$ contains $n+1$ number of bending moments and joint forces respectively occurring at all points of the division, not excluding the terminal points. Eliminating from the set the known moment values (in the beam from Fig. 7.3, M_2' = M_8 = 0) and ignoring the equations in which unknown force values (W_0, W_6) occur on the right-hand side, we get the set of equations

$$\mathbf{B}^T\mathbf{M} = \mathbf{W}, \quad \mathbf{W} = \mathbf{P}+\mathbf{a}\mathbf{p}+\mathbf{b}\mathbf{m}, \tag{7.12}$$
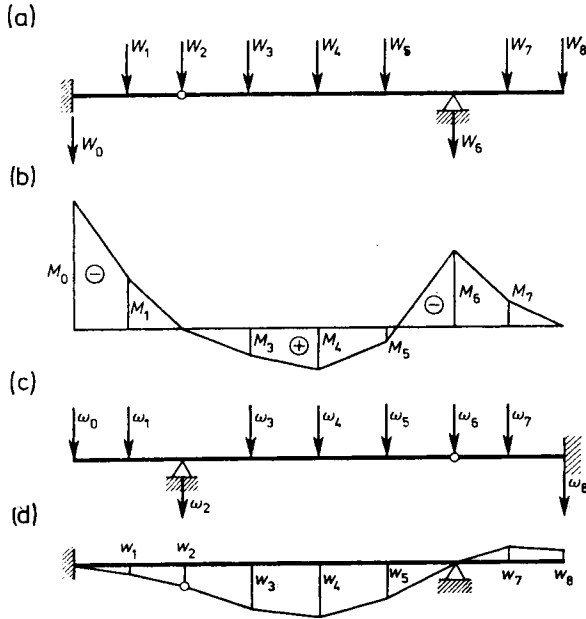
(a)

(b)

(c)

(d)

Fig. 7.3. Hinged beam: (a) equivalent loading; (b) diagram of moments; (c) modified scheme; elastic weights; (d) deflection line

Here, matrix $\mathbf{B}^T$ for the beam from Fig. 7.3 is formed by cancelling columns 2 and 8 and rows 0 and 6 in the matrix

$$
\mathbf{B}^T =
\begin{array}{c}
\\
1\\
2\\
3\\
4\\
5\\
7\\
8
\end{array}
\begin{array}{ccccccc}
0 & 1 & 3 & 4 & 5 & 6 & 7\\
\end{array}
$$

$$
\mathbf{B}^T =
\begin{bmatrix}
-\dfrac{1}{\lambda_1} & \dfrac{1}{\lambda_1}+\dfrac{1}{\lambda_2} & & & & & \\[2mm]
& -\dfrac{1}{\lambda_2} & -\dfrac{1}{\lambda_3} & & & & \\[2mm]
& & \dfrac{1}{\lambda_3}+\dfrac{1}{\lambda_4} & -\dfrac{1}{\lambda_4} & & & \\[2mm]
& & -\dfrac{1}{\lambda_4} & \dfrac{1}{\lambda_4}+\dfrac{1}{\lambda_5} & -\dfrac{1}{\lambda_5} & & \\[2mm]
& & & -\dfrac{1}{\lambda_5} & \dfrac{1}{\lambda_5}+\dfrac{1}{\lambda_6} & -\dfrac{1}{\lambda_6} & \\[2mm]
& & & & & -\dfrac{1}{\lambda_7} & \dfrac{1}{\lambda_7}+\dfrac{1}{\lambda_8} \\[2mm]
& & & & & & -\dfrac{1}{\lambda_8}
\end{bmatrix}.
$$

(7.13)

Similarly, the matrices $\mathbf{P}$, $\mathbf{W}$, $\mathbf{a}$, $\mathbf{b}$ are derived from the matrices (7.3), (7.6), (7.9), (7.10) by cancelling in them the rows with numbers corresponding to those of the supports. For example, for the beam from Fig. 7.3, we have

$$\mathbf{M} = \{M_0, M_1, M_3, M_4, M_5, M_6, M_7\}, \tag{7.14}$$

$$\mathbf{W} = \{W_1, W_2, W_3, W_4, W_5, W_7, W_8\}. \tag{7.15}$$

Just the matrix $\mathbf{B}$ (unlike $\tilde{\mathbf{B}}$) is non-singular, and the set of equations $(7.12)_1$ can be inverted:

$$\mathbf{M} = \mathbf{B}^{-T}\mathbf{W}. \tag{7.16}$$

$\mathbf{B}^{-T}$ is a so-called *influence matrix* of bending moments. Each of its rows, say, row numbered i, contains the values of the bending moment appearing in cross-section i due to a unit force acting at successive joints of the beam. These are therefore the ordinates of the influence line of moment M_i.

On the other hand, each column of $\mathbf{B}^{-T}$, say, that numbered k, contains the values of the bending moments accompanying the setting-up of an elementary force in joint k. These are therefore the ordinate of the plot of moments induced by force $W_k = 1$.

Since the plot of bending moments induced by concentrated forces is a broken line, the transverse forces, constant in each interval, are determined from the relations

$$\mathbf{T} = \lambda^{-1}\tilde{\mathbf{b}}^T\mathbf{M} = \lambda^{-1}\mathbf{c}^T\mathbf{M}, \tag{7.17}$$

$$\lambda = \lceil \lambda_1, \lambda_2, ..., \lambda_n \rfloor, \tag{7.18}$$

and the matrix $\mathbf{c}$ is formed from $\tilde{\mathbf{b}}$ by cancelling in the latter the rows corresponding in number to the joints in which the bending moments are zero.

The bending moments are accompanied by the appearance of curvatures $\varkappa$, and the transverse forces, by shear angles β. Both strains can be treated as secondary loadings. Figures 7.4a, b show a segment of these loadings referring to a beam of piece-wise constant cross-section. The deflection line of the beam has in joints the ordinates indicated in Fig. 7.4c. The virtual load (Fig. 7.4d) induces moments $\overline{M}$ and transverse forces $\overline{T}$, whose plots are given in Figs. 7.4d, e. The principle of virtual work leads to the equality

$$-\frac{w_{i-1}}{\lambda_i} + \left(\frac{1}{\lambda_i} + \frac{1}{\lambda_{i+1}}\right)w_i - \frac{w_{i+1}}{\lambda_{i+1}}$$

$$= \frac{\lambda_i}{6EJ_i}(M_{i-1} + 2M_i) + \frac{\lambda_{i+1}}{6EJ_{i+1}}(2M_i + M_{i+1}) +$$

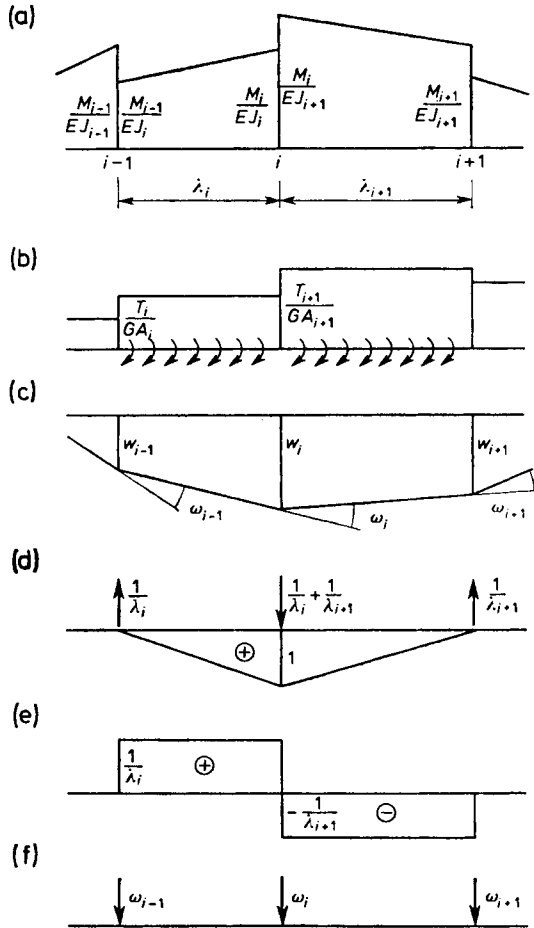$$+ \frac{k_i}{GA_i}T_i - \frac{k_{i+1}}{GA_{i+1}}T_{i+1}. \tag{7.19}$$

Fig. 7.4. Part of a beam: (a), (b) secondary loadings; (c) deflection line; (d), (e) diagrams of moments and transverse forces induced by virtual loading; (f) elastic weights

Considering the relation

$$T_i = \frac{M_i - M_{i-1}}{\lambda_i} ,$$ (7.20)

and introducing the denotation

$$\gamma_i = 3 \frac{EJ_i k_i}{GA_i \lambda_i^2} ,$$ (7.21)

we write the right-hand side of Eq. (7.19) in the form

$$\omega_i = \frac{1-2\gamma_i}{6}\frac{\lambda_i}{EJ_i}M_{i-1}+\left(\frac{1+\gamma_i}{3}\frac{\lambda_i}{EJ_i}+\frac{1+\gamma_{i+1}}{3}\frac{\lambda_{i+1}}{EJ_{i+1}}\right)M_i+$$

$$+\frac{1-2\gamma_{i+1}}{6}\frac{\lambda_{i+1}}{EJ_{i+1}}M_{i+1}. \tag{7.22}$$

Let us introduce the denotations:

$$\tilde{\mathbf{w}} = \{w_0, w_1, w_2, ..., w_n\}, \tag{7.23}$$

$$\tilde{\boldsymbol{\omega}} = \{\omega_0, \omega_1, \omega_2, ..., \omega_n\}, \tag{7.24}$$

$$\mathbf{S} = \frac{1}{E}\begin{bmatrix} \dfrac{1+\gamma_0}{3}\dfrac{\lambda_0}{J_0} & \dfrac{1-2\gamma_0}{6}\dfrac{\lambda_0}{J_0} & \\ \dfrac{1-2\gamma_0}{6}\dfrac{\lambda_0}{J_0} & \dfrac{1+\gamma_0}{3}\dfrac{\lambda_0}{J_0}+\dfrac{1+\gamma_1}{3}\dfrac{\lambda_1}{J_1} & \dfrac{1-2\gamma_1}{6}\dfrac{\lambda_1}{J_1} \\ & \cdots & \cdots & \cdots \end{bmatrix}. \tag{7.25}$$

The geometric relations and the elasticity equations can then be written in the form

$$\tilde{\mathbf{B}}\tilde{\mathbf{w}} = \tilde{\boldsymbol{\omega}}, \quad \tilde{\boldsymbol{\omega}} = \tilde{\mathbf{S}}\tilde{\mathbf{M}}. \tag{7.26}$$

The quantities ω_i can be treated as substitutes, concentrated at the slope discontinuity points of the axis, equivalent to strains continuously distributed in individual intervals of the beam. Those slope discontinuity points of the axis, being secondary loadings, are represented in the form of concentrated forces called *elastic weights* (Nowacki, 1952), that act on a suitably modified system (Fig. 7.3c). The plot of moments inducing secondary loadings is an approximation of the deflection line of the beam considered (Fig. 7.3d).

Proceeding in like manner as in the case of static equations, we remove from the set of equations of geometry (7.26) those equations which contain unknown reactions on the right-hand side, i.e., the slope discontinuity angles of the axes at hinges and the angles of rotation of the end cross-sections of the beam. At the same time, we can neglect in vector w the zero terms, i.e., the displacement values of support joints. Thus, cancelling in $\tilde{\mathbf{B}}$ the columns with numbers relating to support joints and also the rows which bear the numbers of articulated joints, we get the set of equations

$$\mathbf{Bw} = \boldsymbol{\omega}. \tag{7.27}$$

For the beam from Fig. 7.3, the matrix **B** is a transposition of the matrix (7.13), and the matrices **w** and **ω** have the form:

$$\mathbf{w} = \{w_1, w_2, w_3, w_4, w_5, w_7, w_8\}, \tag{7.28}$$

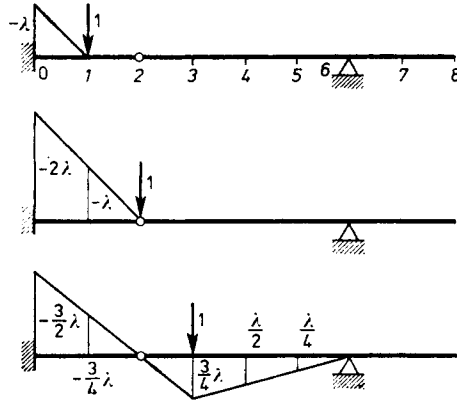$$\boldsymbol{\omega} = \{\omega_0, \omega_1, \omega_3, \omega_4, \omega_5, \omega_6, \omega_7\}. \tag{7.29}$$

In an analogous manner, cancelling in $\tilde{S}$ the columns and rows which bear the numbers of articulated joints, we obtain a symmetric matrix S, relating elastic weights ω to the bending moments M:

$$\omega = SM. \tag{7.30}$$

Hence, using Eqs. (7.27), (7.30) and (7.16) in a successive manner, we get

$$w = B^{-1}\omega = B^{-1}SM = B^{-1}SB^{-T}W. \tag{7.31}$$

The symmetric matrix

$$D = B^{-1}SB^{-T} \tag{7.32}$$

is an influence matrix of displacements w. The row numbered i contains a specification of the ordinates of the influence line of displacement w_i. Incidentally, these ordinates are identical to the values arrayed in column i in which we have the ordinates of the deflection line induced by the unit force set up in joint i.

EXAMPLE 7.1

Determine the matrices and influence lines of the static and geometric quantities for the beam in Fig. 7.3, assuming that all segments λ_i are the same length λ, and that the beam has a constant cross-section described by the quantities $J_i = J$, $\gamma_i = \gamma$. According to these assumptions, the matrix B (cf. (7.13)) takes the form

$$B = \frac{1}{\lambda}
\begin{bmatrix}
-1 & & & & & & \\
2 & -1 & & & & & \\
-1 & 2 & -1 & & & & \\
& -1 & 2 & -1 & & & \\
& & -1 & 2 & & & \\
& & & -1 & -1 & & \\
& & & & 2 & -1
\end{bmatrix}
\begin{matrix}
0 \\ 1 \\ 3 \\ 4 \\ 5 \\ 6 \\ 7
\end{matrix} \tag{a}$$

$$\begin{matrix} 1 & 2 & 3 & 4 & 5 & 7 & 8 \end{matrix}$$

and S (cf. (7.25)) is

$$S = \frac{\lambda}{6EJ}
\begin{bmatrix}
2+2\gamma & 1-2\gamma & & & & & \\
1-2\gamma & 4+4\gamma & & & & & \\
& & 4+4\gamma & 1-2\gamma & & & \\
& & 1-2\gamma & 4+4\gamma & 1-2\gamma & & \\
& & & 1-2\gamma & 4+4\gamma & 1-2\gamma & \\
& & & & 1-2\gamma & 4+4\gamma & 1-2\gamma \\
& & & & & 1-2\gamma & 4+4\gamma
\end{bmatrix}
\begin{matrix}
0 \\ 1 \\ 3 \\ 4 \\ 5 \\ 6 \\ 7
\end{matrix} \tag{b}$$

$$\begin{matrix} 0 & 1 & 3 & 4 & 5 & 6 & 7 \end{matrix}$$

Matrix **B** can be inverted using any of the known matrix inversion algorithms. But, knowing the physical meaning of the factors of matrix $\mathbf{B}^{-1}$, we can also take a different course. Given as examples in Fig. 7.5 are the three non-zero influence lines of the bending moments at the dividing points

Fig. 7.5. Influence lines of bending moments

of the beam. In keeping with the principles discussed in Chapter 5, the influence lines can be treated as plots of moments from secondary unit loadings acting on the modified system, and it is an elementary problem to determine the bending moments from so simple loadings in an isostatic structure. We array the ordinates of these influence lines in columns and put them into the matrix $\mathbf{B}^{-1}$:

$$
\mathbf{B}^{-1} = \frac{\lambda}{4}
\begin{array}{c}
\begin{array}{ccccccc}
0 & 1 & 3 & 4 & 5 & 6 & 7
\end{array} \\
\left[
\begin{array}{ccccccc}
-4 & & & & & & \\
-8 & -4 & & & & & \\
-6 & -3 & 3 & 2 & 1 & & \\
-4 & -2 & 2 & 4 & 2 & & \\
-2 & -1 & 1 & 2 & 3 & & \\
\hline
2 & 1 & -1 & -2 & -3 & -4 & \\
4 & 2 & -2 & -4 & -6 & -8 & -4
\end{array}
\right]
\end{array}
\begin{array}{c}
1 \\ 2 \\ 3 \\ 4 \\ 5 \\ \\ 7 \\ 8
\end{array}
\qquad \text{(c)}
$$

It is easily verified that the rows of matrix (c) contain an array of values of the moments indiced by the unit forces acting at successive joints of the beam considered (Fig. 7.6).

Fig. 7.6. Diagrams of moments induced by the unit forces

We obtain the influence matrix of transverse forces by performing oper-
ations following from the relation (7.17), which we reduce to the form:

$$T = \frac{1}{\lambda} c^T B^{-T} W.$$ (d)

The matrix c^T is constructed from the matrix $\tilde{b}$ (7.10) by cancelling in it
columns 2 and 8:

$$
c^T = \begin{array}{c}
\\
1 \\
2 \\
3 \\
4 \\
5 \\
6 \\
7 \\
8
\end{array}
\begin{array}{cccccccc}
0 & 1 & 3 & 4 & 5 & 6 & 7 \\
\left[\begin{array}{ccccccc}
-1 & 1 & & & & & \\
 & -1 & & & & & \\
 & & 1 & & & & \\
 & & -1 & 1 & & & \\
 & & & -1 & 1 & & \\
 & & & & -1 & 1 & \\
 & & & & & -1 & 1 \\
 & & & & & & -1
\end{array}\right]
\end{array}.
$$ (e)

Hence, after multiplying the matrices according to Eq. (d) we get the influ-
ence matrix of transverse forces:

$$
\frac{1}{\lambda} c^T B^{-T} = \frac{1}{4}
\begin{array}{cccccccc}
1 & 2 & 3 & 4 & 5 & 7 & 8 & \\
\left[\begin{array}{ccccccc}
4 & 4 & 3 & 2 & 1 & -1 & -2 \\
 & 4 & 3 & 2 & 1 & -1 & -2 \\
 & & 3 & 2 & 1 & -1 & -2 \\
 & & -1 & 2 & 1 & -1 & -2 \\
 & & -1 & -2 & 1 & -1 & -2 \\
 & & -1 & -2 & -3 & -1 & -2 \\
 & & & & & 4 & 4 \\
 & & & & & & 4
\end{array}\right]
\begin{array}{c}
1 \\ 2 \\ 3 \\ 4 \\ 5 \\ 6 \\ 7 \\ 8
\end{array}
\end{array}.
$$ (f)

It should be noted that the influence lines of transverse forces (Fig. 7.7a) plotted on matrix (f) apply to a beam loaded indirectly. For only then can transmission of loadings from the platform to selected joints of the beam be guarantee. But, the influence lines of transverse forces in a beam loaded
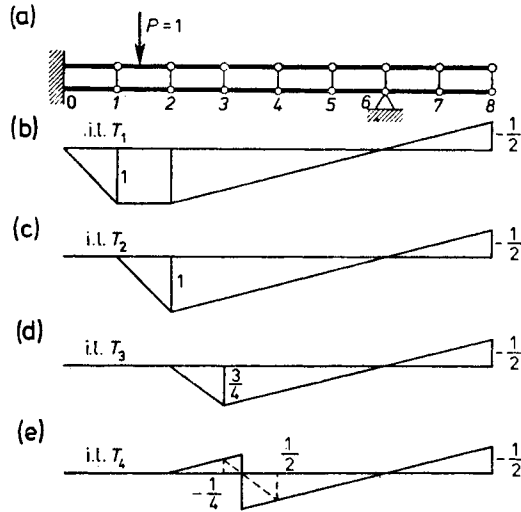
Fig. 7.7. Influence lines of transverse forces in indirectly loaded beam

directly under will easily be obtained extending the right and left branches of the influence line right up to the cross-section considered. For example, Fig. 7.7e shows the influence line of a transverse force in a cross-section placed in interval 4.

Performing the operations prescribed by Eq. (7.32), we can determine influence matrix of displacements:

$$
D = \frac{\lambda^3}{24EJ}
\begin{array}{c}
\begin{array}{ccccccc}
1 & 2 & 3 & 4 & 5 & 7 & 8
\end{array}\\
\left[
\begin{array}{ccccccc}
8+8\gamma & 20+8\gamma & 15+6\gamma & 10+4\gamma & 5+2\gamma & -5-2\gamma & -10-4\gamma \\
 & 64+16\gamma & 48+12\gamma & 32+8\gamma & 16+4\gamma & -16-4\gamma & -32-8\gamma \\
 & & 54+15\gamma & 46+10\gamma & 26+5\gamma & -27-3\gamma & -54-6\gamma \\
 & & & 48+12\gamma & 30+6\gamma & -32-2\gamma & -64-4\gamma \\
 & \text{sym.} & & & 22+7\gamma & -25-\gamma & -50-2\gamma \\
 & & & & & 44+11\gamma & 92+14\gamma \\
 & & & & & & 208+28\gamma
\end{array}
\right]
\begin{array}{c}
1\\2\\3\\4\\5\\7\\8
\end{array}
\end{array}
$$

$$(g)$$

It is already easy to plot on the basis of this matrix the influence lines of joint displacements (Fig. 7.8); these lines are at the same time the deflection lines of the beam induced by the unit forces.
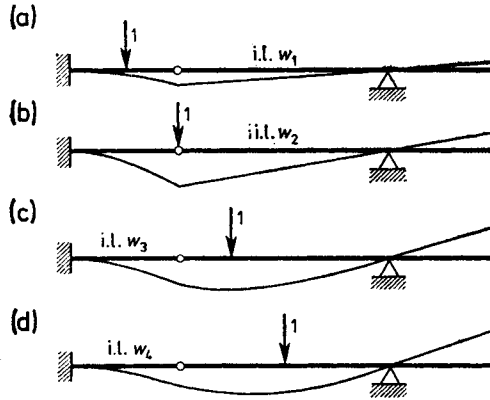
Fig. 7.8. Influence line of displacements of beam joints

The influence matrices thus determined allow the generalized internal forces and the deflection lines from arbitrary loadings to be plotted without difficulty. For example, in the case of a load p uniformly distributed over the entire length of a beam, the vector of equivalent concentrated forces (7.15) has the following components:

$$\mathbf{W} = p\lambda\{1, 1, 1, 1, 1, 1, \tfrac{1}{2}\}. \tag{h}$$
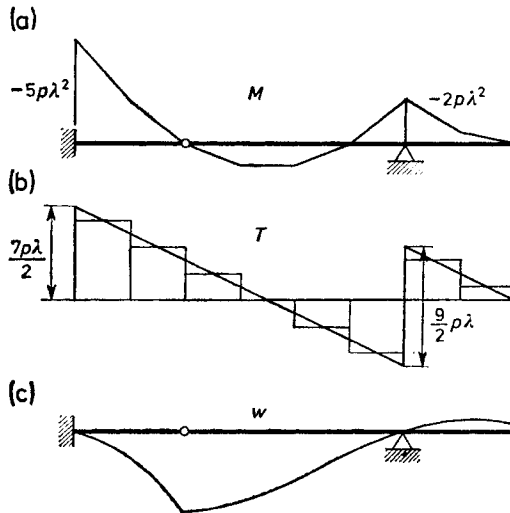
Fig. 7.9. Diagrams: (a) bending moments; (b) transverse forces; (c) deflections

Multiplying the transposed matrix (c) and the matrices (f) and (g) by the vector (h), we obtain the ordinates of plots of the quantities sought:

$$\mathbf{M} = \frac{p\lambda^2}{2}\{-10, -4, 2, 2, 0, -4, -1\}.$$ (i)

$$\mathbf{T} = \frac{p\lambda}{2}\{6, 4, 2, 0, -2, -4, 3, 1\},$$ (j)

$$\mathbf{w} = \frac{p\lambda^4}{24EJ}\{48+24\gamma, 148+40\gamma, 135+42\gamma, 92+36\gamma, 49+22\gamma,$$
$$-15+6\gamma, -14+4\gamma\}.$$ (k)

The plots in question are given in Fig. 7.9. Regarding the plot of transverse forces, the stepped line represents the plot of transverse forces induced by concentrated forces. Connecting with a straight line the points placed in the middle of each sector of the stepped plot, we obtain the plot of transverse forces due to loads acting directly on the beam. We can read from it, e.g., the reaction values in support joints.

7.2. Plane Trusses

A general method for determining the longitudinal forces in bars and the sideways of joints in a space truss was given in Sections 6.2 and 6.4. The same method can of course be applied to plane trusses. However, in many cases, in particular in bridge engineering, trusses generally have the character of a hinged multi-span beam, and vertical forces are their principal loads. In trusses of this type, we are usually not interested in the horizontal components of the joint displacements since vertical displacements are fundamental here, significantly greater than horizontal. The forces in truss members and
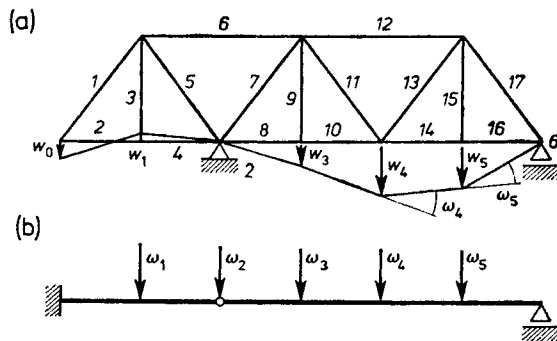
Fig. 7.10. Truss and deflection line of its bottom flange

the vertical displacements of truss joints are determined as a rule using influ-
ence lines (or matrices). However, since every influence line can be treated
as demonstrated before as a certain deflection line, we first present the gen-
eral principles of determining the deflection line of that truss flange along
which the load is moving.

Given as an example in Fig. 7.10a is a truss and the deflection line of its
bottom flange which takes the shape of a broken line. This line can be treated
as a plot of secondary moments due to secondary concentrated loadings.
Consequently, in order to determine the deflection line it is necessary to
determine the slope discontinuity angles ω of the flange and to apply these
secondary loadings to a suitably modified beam system (Fig. 7.10b).

We calculate the slope discontinuity angles using the principle of comple-
mentary virtual work. Therefore, we have to apply virtual loadings capable
of doing the work on slope discontinuity angles of the flange involved (Fig.
7.11). Being self-equilibrating these loadings induce internal forces in only
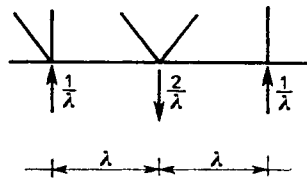
Fig. 7.11. Virtual loading

few truss members. Knowing the real extensions Δl of all truss members,
extensions making the single-column matrix ϵ (cf. Eq. (6.3)), we can calculate
slope discontinuity angles ω of the flange from the formula

$$\omega = \mathbf{Z}\epsilon. \tag{7.33}$$

The symbol ω used here denotes a vector constructed of elastic weights (cf.
(7.29)). The matrix $\mathbf{Z}$ contains a specification of forces acting within the
members of the truss which is being subjected to successive self-equilibrated
virtual loadings (Fig. 7.11).

We apply elastic weights to an hinged beam (Fig. 7.10b). We find from
Eq. (7.31) the unknown deflection line ordinates making the vector $\mathbf{w}$ (cf.
(7.28)). Considering the relation (7.33), we have therefore

$$\mathbf{w} = \mathbf{B}^{-1}\omega = \mathbf{B}^{-1}\mathbf{Z}\epsilon. \tag{7.34}$$

However, the extensions of truss members ϵ, neglecting distortional exten-
sions, are proportional to longitudinal forces N making the matrix σ:

$$\epsilon = \mathbf{E}^{-1}\sigma, \tag{7.35}$$

where the matrix $\mathbf{E}$ is given by Eq. (6.31). If only the vertical forces within the joints of the bottom flange, making the matrix $\mathbf{W}$, are acting on the truss, the relationship between the longitudinal forces making the matrix $\boldsymbol{\sigma}$ and the external loadings $\mathbf{W}$ can be written:

$$\boldsymbol{\sigma} = \mathbf{AW}, \tag{7.36}$$

where $\mathbf{A}$ is the influence matrix of internal forces. Finally, by putting (7.36) into (7.35) and (7.34) we get the relationship between displacements and external forces:

$$\mathbf{w} = \mathbf{B}^{-1}\mathbf{Z}\mathbf{E}^{-1}\mathbf{AW}. \tag{7.37}$$

We know, however, that in view of Maxwell's theorem the matrix $\mathbf{B}^{-1}\mathbf{Z}\mathbf{E}^{-1}\mathbf{A}$ must be symmetric. It follows that the influence matrix of the forces within the truss members is

$$\mathbf{A} = \mathbf{Z}^{T}\mathbf{B}^{-T}. \tag{7.38}$$

Its physical meaning is easy to explain. The influence line of the axial force in truss member k is, it will be recalled, the deflection line of that flange of the truss along which a unit force is moving, the deflection being due to an extension of member k by $\varDelta l_{k} = 1$. We get from Eq. (7.34) the ordinates of this influence line assuming that all components of $\boldsymbol{\epsilon}$ are zero excepting components k which is of unit value. Hence the vector containing the ordinates of the influence line of force N_{k} is obtained from the formula

$$\mathbf{w}_{k} = \mathbf{B}^{-1}\mathbf{Z}_{k}, \tag{7.39}$$

where $\mathbf{Z}_{k}$ is the kth column of $\mathbf{Z}$. The set of ordinates of all the influence lines is obviously expressed by (cf. (7.38))

$$\mathbf{A}^{T} = \mathbf{B}^{-1}\mathbf{Z}. \tag{7.40}$$

EXAMPLE 7.2

Determine the influence matrix of the axial forces for the truss from Fig. 7.10a.

Applying the virtual loadings given in Fig. 7.11, to successive truss joints, we obtain forces in its joints having the values indicated either in Fig. 7.12a (joints *1, 3, 5*) or in Fig. 7.12b (joints *2, 4*). To determine these forces is an elementary problem which can be solved, for example, by way of successive equilibration of joints or using intersections by three truss members. These forces are arrayed in the matrix
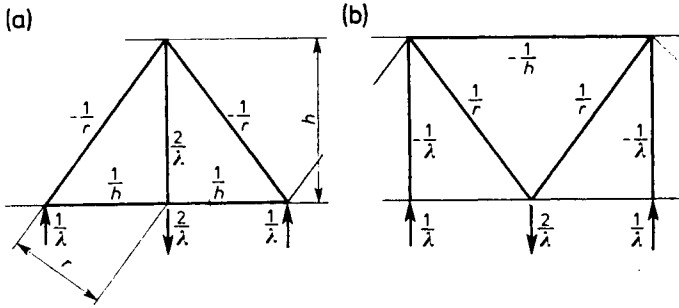
Fig. 7.12. Forces induced in bars by virtual loading

$$
\mathbf{Z} =
\begin{array}{c}
1\\2\\3\\4\\5
\end{array}
\left[
\begin{array}{ccccccccccccccccc}
-\dfrac{1}{r} & \dfrac{1}{h} & \dfrac{2}{\lambda} & \dfrac{1}{h} & & -\dfrac{1}{r} & & & & & & & & & & & \\[2mm]
 & & -\dfrac{1}{\lambda} & 0 & \dfrac{1}{r} & -\dfrac{1}{h} & \dfrac{1}{r} & 0 & -\dfrac{1}{\lambda} & & & & & & & & \\[2mm]
 & & & & & -\dfrac{1}{r} & \dfrac{1}{h} & \dfrac{2}{\lambda} & \dfrac{1}{h} & -\dfrac{1}{r} & & & & & & & \\[2mm]
 & & & & & & & -\dfrac{1}{\lambda} & 0 & \dfrac{1}{r} & -\dfrac{1}{h} & \dfrac{1}{r} & 0 & -\dfrac{1}{\lambda} & & & \\[2mm]
 & & & & & & & & & & -\dfrac{1}{r} & \dfrac{1}{h} & \dfrac{2}{\lambda} & \dfrac{1}{h} & -\dfrac{1}{r} & &
\end{array}
\right] . \quad (a)
$$

(columns numbered 1 2   3 4   5 6   7 8   9 10   11   12 13 14   15 16 17)

We construct the matrix $\mathbf{B}^{-1}$ as described in Section 7.1 (cf. Eq. (c) from Example 7.1). For the beam from Fig. 10b:

$$
\mathbf{B}^{-1} = \frac{\lambda}{4}
\begin{array}{c}
\\0\\1\\3\\4\\5
\end{array}
\begin{array}{ccccc}
1 & 2 & 3 & 4 & 5 \\
\end{array}
\left[
\begin{array}{ccccc}
-4 & -8 & -6 & -4 & -2 \\
 & -4 & -3 & -2 & -1 \\
 & & 3 & 2 & 1 \\
 & & 2 & 4 & 2 \\
 & & 1 & 2 & 3
\end{array}
\right] . \quad (b)
$$

It is easily seen that the influence matrix $\mathbf{A}$ calculated in Eq. (7.38) has the form

	0	1	3	4	5
1	$\dfrac{\lambda}{r}$				
2	$-\dfrac{\lambda}{h}$				
3		1			
4	$-\dfrac{\lambda}{h}$				
5	$-\dfrac{\lambda}{r}$	$-\dfrac{\lambda}{r}$			
6	$\dfrac{2\lambda}{h}$	$\dfrac{\lambda}{h}$			
7	$-\dfrac{\lambda}{2r}$	$-\dfrac{\lambda}{4r}$	$\dfrac{3\lambda}{4r}$	$-\dfrac{\lambda}{2r}$	$-\dfrac{\lambda}{4r}$
8	$-\dfrac{3\lambda}{2h}$	$\dfrac{3\lambda}{4h}$	$\dfrac{3\lambda}{4h}$	$\dfrac{\lambda}{2h}$	$\dfrac{\lambda}{4h}$
9		1			
10	$-\dfrac{3\lambda}{2h}$	$-\dfrac{3\lambda}{4h}$	$\dfrac{3\lambda}{4h}$	$\dfrac{\lambda}{2h}$	$\dfrac{\lambda}{4h}$
11	$\dfrac{\lambda}{2r}$	$\dfrac{\lambda}{4r}$	$-\dfrac{\lambda}{4r}$	$\dfrac{\lambda}{2r}$	$\dfrac{\lambda}{4r}$
12	$\dfrac{\lambda}{h}$	$\dfrac{\lambda}{2h}$	$-\dfrac{\lambda}{2h}$	$-\dfrac{\lambda}{h}$	$\dfrac{\lambda}{2h}$
13	$-\dfrac{\lambda}{2r}$	$-\dfrac{\lambda}{4r}$	$\dfrac{\lambda}{4r}$	$\dfrac{\lambda}{2r}$	$-\dfrac{\lambda}{4r}$
14	$-\dfrac{\lambda}{2h}$	$-\dfrac{\lambda}{4h}$	$\dfrac{\lambda}{4h}$	$\dfrac{\lambda}{2h}$	$\dfrac{3\lambda}{4h}$
15					1
16	$-\dfrac{\lambda}{2h}$	$-\dfrac{\lambda}{4h}$	$\dfrac{\lambda}{4h}$	$\dfrac{\lambda}{2h}$	$\dfrac{3\lambda}{4h}$
17	$\dfrac{\lambda}{2r}$	$\dfrac{\lambda}{4r}$	$\dfrac{\lambda}{4r}$	$-\dfrac{\lambda}{2r}$	$\dfrac{3\lambda}{4r}$

$$A = \qquad\qquad\qquad\qquad\qquad\qquad\qquad\qquad\text{(c)}$$

Figure 7.13 gives the plots of influence lines of the forces in several truss members. These lines can be treated as plots of secondary moments from the loadings specified in matrix (a).
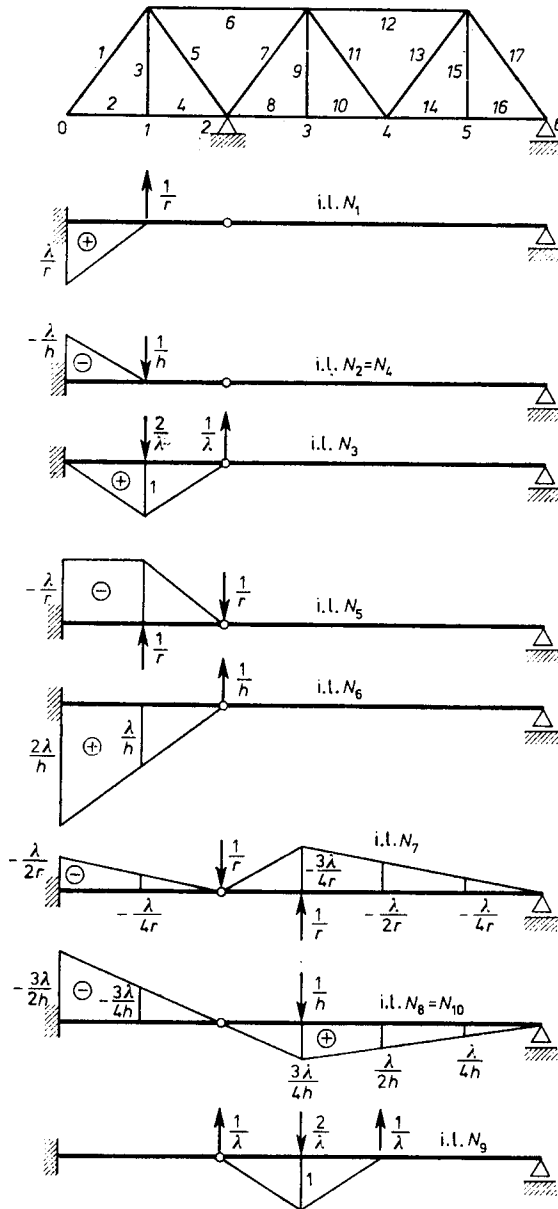
Fig. 7.13. Influence lines of forces in some truss members

8. The Direct Flexibility Method (Force Method)

8.1. The Set of Canonical Equations of the Direct Flexibility Method

Whereas the derivation of the conditional equations of the direct flexibility method by the technique described in Section 6.4 appears to be quite complicated, once we have acquired proficiency in determining the internal forces in isostatic structures, we can obtain the set of equations sought without any particular difficulty, and in effect, solve the considered problem.

As we already know (cf. Section 3.3), a hyperstatic structure is an over-rigid structure; the number of single connectors t, between e elements, is higher than the number of members he necessary to immobilize all elements. After finding the degree of static indeterminability of a structure s we cut off mentally s number of redundant connectors reducing the structure to a system which we call the *primary isostatic system*. But as we eliminate the redundant members, care should be taken that we do not get in effect, a kinematically variable structure, and at the same time, still hyperstatic.

In the hyperstatic structure considered, certain generalized forces occur in the members recognized as redundant. We shall treat these forces as primary static unknowns and call them *redundant quantities* denoted by X_i ($i = 1, 2, \ldots, s$). In an isostatic primary system these forces act in exactly the same way as does external loading.

The known external forces together with the unknown generalized forces X_i give rise to generalized internal forces which in the cross-section generally given by the coordinate s can be arrayed in a single column matrix $\sigma(s)$. Using the principle of superposition, we write

$$\sigma(s) = \sigma_P(s) + \sum_{i=1}^{s} \sigma_i(s) X_i. \tag{8.1}$$

The symbol $\sigma_P(s)$ in the above formula denotes a set of internal forces caused by known external loading, and $\sigma_i(s)$ is a single column matrix containing a specification of the internal forces accompanying load $X_i = 1$.

Constructing a matrix from the columns $\sigma_i(s)$:

$$\sigma_X(s) = [\sigma_1(s), \sigma_2(s), \ldots, \sigma_s(s)], \tag{8.2}$$

and putting together the unknowns X_i into a single column matrix:

$$X = \{X_1, X_2, \ldots, X_s\}, \tag{8.3}$$

we give the relation (8.1) the form

$$\sigma(s) = \sigma_P(s) + \sigma_X(s)X. \tag{8.4}$$

In this way, the internal forces are determined with an accuracy to constants X. With the same accuracy we can determine the strains

$$\begin{aligned}\epsilon(s) &= E^{-1}(s)\sigma(s) + \epsilon^0(s) \\ &= E^{-1}(s)\sigma_X(s)X + E^{-1}(s)\sigma_P(s) + \epsilon^0(s).\end{aligned} \tag{8.5}$$

Distortional strains have also been allowed for in the above formula.

Assume that before the real strains (8.5) appeared, vitrual forces σX were already acting on the isostatic primary system at places where the redundant members had been cut. These forces were accompanied by generalized internal forces

$$\delta\sigma(s) = \sigma_X(s)\,\delta X, \tag{8.6}$$

and also by support reactions

$$\delta R = A_r\,\delta X. \tag{8.7}$$

The matrix A_r relates the reaction values to the causes that generated them.

Virtual forces δX do the work on mutual displacements δ of the cut parts od redundant members, and likewise reactions δR do the work on the displacements of supports r. The work done by these external loadings equals the work done by virtual internal forces on real strains:

$$\delta X^T\delta + \delta R^T r = \int_s \delta\sigma^T(s)\epsilon(s)\,ds, \tag{8.8}$$

or considering the relations (8.6), (8.7):

$$\delta X^T\delta + \delta X^T A_r^T r = \delta X^T \int_s \sigma_X^T(s)\epsilon(s)\,ds. \tag{8.9}$$

Since Eq. (8.9) is to be satisfied regardless of the values of virtual forces δX, therefore, neglecting the matrix δX^T, we obtain from a single equation of work a set of equations geometric in nature. Considering at the same time the fact that the mutual displacements δ of the cut members in a real, hyperstatic structure equal zero, we write the set of these equations as follows:

$$\delta = \int_s \sigma_X^T(s)\epsilon(s)\,ds - A_r^T r = 0. \tag{8.10}$$

Using the relation (8.5) and introducing the denotations

$$\mathbf{D} = \int_s \boldsymbol{\sigma}_X^T(s)\mathbf{E}^{-1}(s)\boldsymbol{\sigma}_X(s)\,\mathrm{d}s,$$

(8.11)

$$\boldsymbol{\delta}_0 = \int_s \boldsymbol{\sigma}_X^T(s)\mathbf{E}^{-1}(s)\boldsymbol{\sigma}_p(s)\,\mathrm{d}s + \int_s \boldsymbol{\sigma}_X^T(s)\boldsymbol{\epsilon}^0(s)\,\mathrm{d}s - \mathbf{A}_r^T\mathbf{r},$$

(8.12)

we get the following set of canonical equations of the force method:

$$\mathbf{D}\mathbf{X} + \boldsymbol{\delta}_0 = \mathbf{0}.$$

(8.13)

We calculate the components of the square symmetric flexibility matrix $\mathbf{D}$ from the relation

$$\delta_{ik} = \int_s \boldsymbol{\sigma}_i^T(s)\mathbf{E}^{-1}(s)\boldsymbol{\sigma}_k(s)\,\mathrm{d}s \quad (i, k = 1, 2, \ldots, s).$$

(8.14)

The symbol δ_{ik} denotes the mutual displacement in the cut member i induced by force $X_k = 1$. The matrix

$$\boldsymbol{\delta}_0 = \{\delta_{10}, \delta_{20}, \ldots, \delta_{s0}\}$$

(8.15)

contains a specification of free terms (independent of $\mathbf{X}$) calculated from the formula

$$\delta_{i0} = \int_s \boldsymbol{\sigma}_i^T(s)\mathbf{E}^{-1}(s)\boldsymbol{\sigma}_P(s)\,\mathrm{d}s + \int_s \boldsymbol{\sigma}_i^T(s)\boldsymbol{\epsilon}^0(s)\,\mathrm{d}s - \mathbf{A}_i^T\mathbf{r}.$$

(8.16)

The above expression connotes the mutual displacement of the cut parts of member i induced by known external loadings, distortional strains and settlement of supports. The symbol $\mathbf{A}_i$ denotes the ith column of $\mathbf{A}_r$.

After solving the set of equations (8.13):

$$\mathbf{X} = -\mathbf{D}^{-1}\boldsymbol{\delta}_0,$$

(8.17)

we can calculate now the internal forces from formula (8.4).

The procedure will be explained using a simple example of a plane frame.

EXAMPLE 8.1

Let us find the internal forces in the frame from Fig. 8.1a induced by: (a) static loading, (b) distortional strains accompanying temperature variation, (c) displacements of supports.

The structure is twice hyperstatic. Suffice therefore to remove two members to obtain a primary isostatic system. Exchanging the stiff connection in joint 1 for an hinged connection, we remove one member and separating the bar at joint C from the support, we remove the other (Fig. 8.1b). In order to show how the redundant X_2 is acting, we had to shift a little the support C.

(a)   (b)
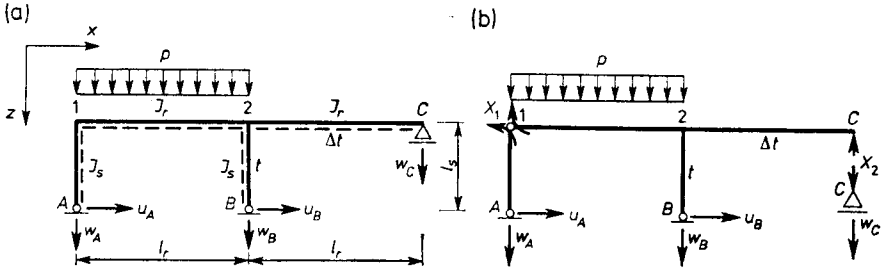
Fig. 8.1. Statically indeterminate frame: (a) considered structure; (b) primary system

In the primary system, the loadings $X_1 = 1$ and $X_2 = 1$ induce general-ized internal forces σ_1 and σ_2, whose plots are given in Fig. 8.2a, b, and loading p induces forces σ_p, the relevant plots are given in Fig. 8.2c. On prac-tical grounds, it is convenient to ascertain at the beginning which side of

(a)

(b)

(c)
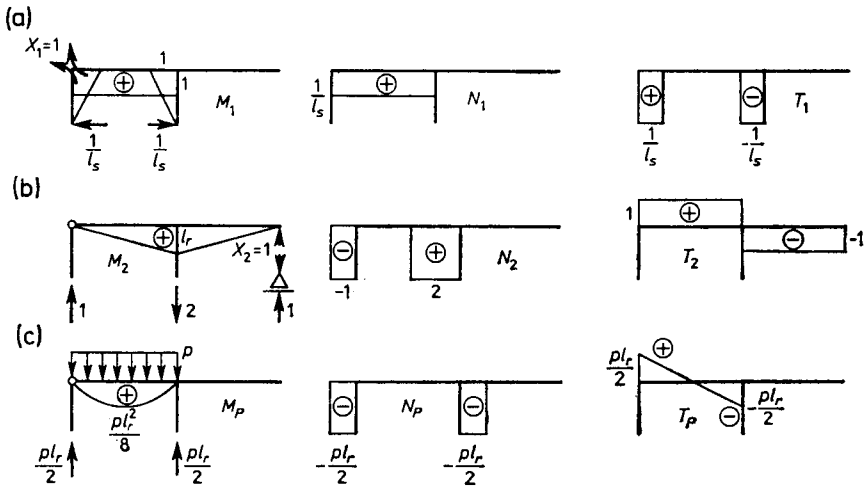
Fig. 8.2. Diagrams of moments, longitudinal forces and transverse forces in basic structure induced by (a), (b) forces $X_i = 1$; (c) external loading

individual bars are bottom. This facilitates the marking of the bending mo-ments. We take it conventionally that the bending moments causing tension on bottom side are positive. The bottom side of bars in the considered frame are indicated in Fig. 8.1a by a dashed line.

In the case of a plane frame, the matrices σ and E^{-1} have the structure

$$\sigma = \{M, N, T\}, \quad E^{-1} = \left[\frac{1}{EJ} \; \frac{1}{EA} \; \frac{k}{GA} \right]. \tag{a}$$

In this connection, Eq. (8.14) takes the form

$$\delta_{ik} = \int_s \left(\frac{M_i M_k}{EJ} + \frac{N_i N_k}{EA} + k \frac{T_i T_k}{GA} \right) ds. \tag{b}$$

Performing appropriate integrations, we get the matrix

$$\mathbf{D} = \frac{l_r^2}{EJ_r} \begin{bmatrix} \frac{1}{l_r}(1 + \frac{2}{3}\varkappa + \nu_1 + 2\gamma_1) & \frac{1}{2} \\ \frac{1}{2} & l_r(\frac{2}{3} + 5\nu_2 + 2\gamma_2) \end{bmatrix}, \tag{c}$$

with the following dimensionless parameters:

$$\varkappa = \frac{l_s}{l_r} \frac{J_r}{J_s}, \qquad \nu_1 = \frac{J_r}{A_r l_s^2}, \qquad \nu_2 = \frac{l_s}{l_r} \frac{J_r}{A_s l_r^2},$$

$$\gamma_1 = \frac{E}{G} \frac{k_s J_r}{A_s l_r l_s}, \qquad \gamma_2 = \frac{E}{G} \frac{k_r J_r}{A_r l_r^2}. \tag{d}$$

To calculate the values δ_{i0} we must first construct the matrix $\mathbf{A}_r$, relating the reactions to redundants $\mathbf{X}$. By arraying the reactions and displacements of the supports in single column matrices

$$\mathbf{R} = \{U_A, W_A, U_B, W_B, W_C\}, \qquad \mathbf{r} = \{u_A, w_A, u_B, w_B, w_C\}, \tag{e}$$

we get (cf. Fig. 8.2a, b):

$$\mathbf{A}_r^T = \begin{bmatrix} -\frac{1}{l_s} & 0 & \frac{1}{l_s} & 0 & 0 \\ 0 & -1 & 0 & 2 & -1 \end{bmatrix}. \tag{f}$$

As for the distortional strain matrix, it has in our example the following components:

$$\boldsymbol{\epsilon}^0 = \left\{ \frac{\alpha_t \Delta t}{h}, \quad \alpha_t t, \quad 0 \right\}. \tag{g}$$

Hence, after performing the operations prescribed by Eq. (8.16) we get

$$\delta_{i0} = \delta_{ip} + \delta_{i\Delta t} + \delta_{it} + \delta_{iu} + \delta_{iw}, \tag{h}$$

where:

$$\delta_{1p} = \frac{pl_r^3}{12EJ_r}, \qquad \delta_{1u} = \frac{1}{l_s}(u_A - u_B),$$

$$\delta_{2p} = \frac{pl_r^4}{24EJ_r}(1 - 24\nu_2), \qquad \delta_{2\Delta t} = \frac{\alpha_t \Delta_t l_{ri}^2}{2h}, \tag{i}$$

$$\delta_{2t} = 2\alpha_t t l_s, \qquad \delta_{2w} = w_A - 2w_B + w_C,$$

$$\delta_{1\Delta t} = \delta_{1t} = \delta_{1w} = \delta_{2u} = 0.$$

The geometric meaning of all these quantities is explained in Fig. 8.3.
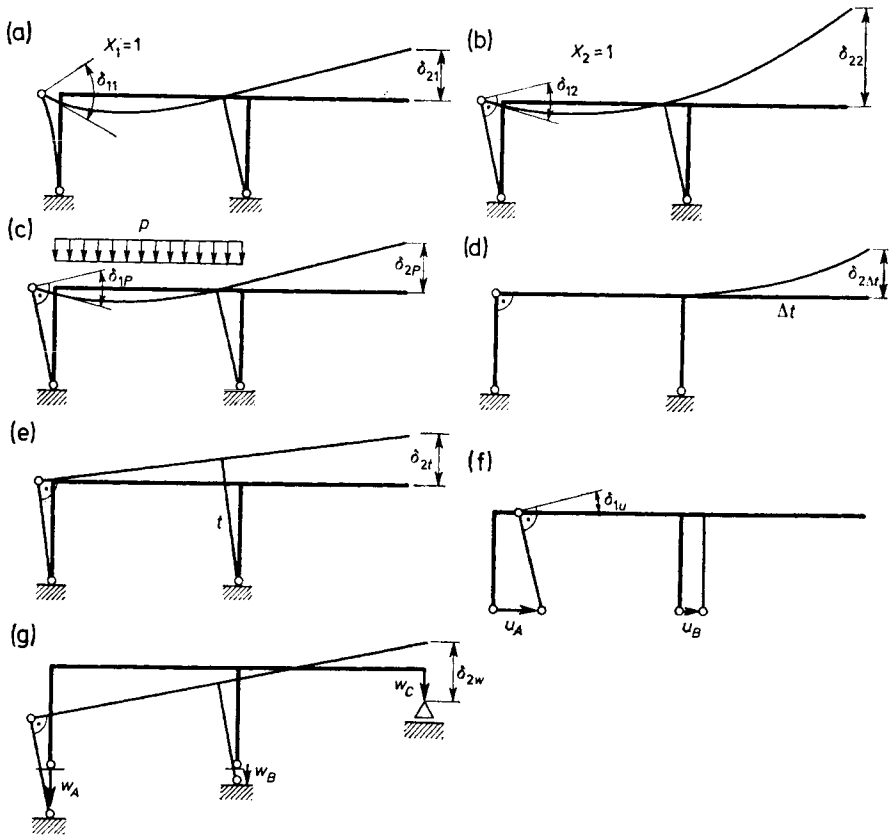
Fig. 8.3. Displacements of primary system induced by (a), (b) forces $X_i = 1$; (c) external
loading; (d), (e) temperature changes; (f), (g) displacements of supports

To give the reader an idea of the order of magnitude of parameters (d),
let us assume for the sake of exemplification that the frame is made up of
bars of rectangular cross-sections, $b \times h_s$ and $b \times h_r$ in size, where h_s/l_s
$= h_r/l_r = 1/10$, $l_s/l_r = 1/2$, $E/G = 5/2$. Based on these assumptions, we
find using formulae (d):

$$\varkappa = 4, \quad v_1 = \frac{1}{300}, \quad v_2 = \frac{1}{1200}, \quad \gamma_1 = \frac{1}{100}, \quad \gamma_2 = \frac{1}{400}. \qquad (j)$$

Evidently, we would not have made any appreciable error neglecting in our
calculations the influences of longitudinal forces (v_i) and shear forces (γ_i)
on deformations of the frame. Therefore, in calculating frameworks composed
of sufficiently slender bars, only the influence of moments (bending and
twisting) on deformations is considered as a rule. The situation changes only

for frames made of very short bars. Assuming, for example, that $h_s/l_s = h_r/l_r = 1/4$, with the previous assumptions still holding, we obtain parameters ν_i and γ_i $\left(\dfrac{10}{4}\right)^2$ times as great:

$$\varkappa = 4, \quad \nu_1 = \frac{1}{48}, \quad \nu_2 = \frac{1}{192}, \quad \gamma_1 = \frac{1}{16}, \quad \gamma_2 = \frac{1}{64}.$$

In further calculations, we neglect the influence of longitudinal and shear forces on the displacement values as this may result only in minor quantitative changes, not in any qualitative changes. Hence, the matrix $\mathbf{D}$ takes the form

$$\mathbf{D} = \frac{1}{6}\frac{l_r^2}{EJ_r}\begin{bmatrix} \dfrac{22}{l_r} & 3 \\ 3 & 4l_r \end{bmatrix}. \tag{k}$$

Its inverse is easy to find

$$\mathbf{D}^{-1} = \frac{6}{79}\frac{EJ_r}{l_r^2}\begin{bmatrix} 4l_r & -3 \\ -3 & \dfrac{22}{l_r} \end{bmatrix}. \tag{l}$$

From Eq. (8.17) we calculate the unknowns:

$$\mathbf{X} = \begin{bmatrix} -5 \\ \dfrac{16}{l_r} \end{bmatrix}a_1 + \begin{bmatrix} 3 \\ \dfrac{22}{l_r} \end{bmatrix}a_2 + \begin{bmatrix} -4 \\ \dfrac{3}{l_r} \end{bmatrix}a_3,$$
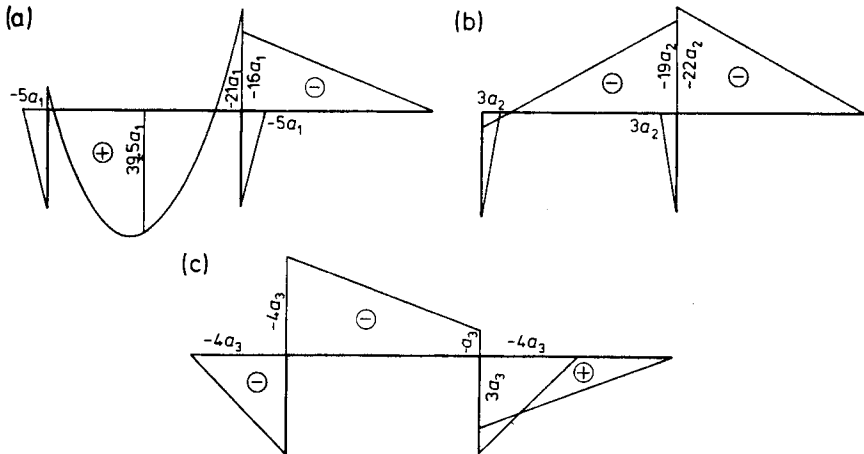
Fig. 8.4. Diagrams of moments induced by (a) statical loading, (b) temperature changes and vertical displacements of supports

$$a_1 = \frac{p l_r^2}{316},$$

$$a_2 = \frac{3}{79} \frac{EJ_r}{l_r} \left(\frac{\alpha_t \Delta t l_r}{h_r} + 2\alpha_t t + 2 \frac{w_A - 2w_B + w_C}{l_r} \right),$$ (m)

$$a_3 = \frac{6}{79} \frac{EJ_r}{l_r} \frac{u_A - u_B}{l_s}.$$

Figure 8.4 gives the plots of moments due to individual external factors. We obtain these moments, in accordance with Eq. (8.4), using the principle of superposition:

$$M = M_p + M_1 X_1 + M_2 X_2.$$ (n)

8.2. Influence Lines

The influence lines of arbitrary quantities from a moving force can be treated, as we know, as deflection lines of the elements of a structure, along which the force is moving. For example, for the frame in Fig. 8.1a, we can expect that only a load acting on the beam *1-2-C* can change its position and value. We are interested in the influence lines of the force moving solely along the beam.

It is convenient to start seeking the influence lines of arbitrary internal force and reactions from finding the influence lines of the redundant quantities. The equation for these influence lines are obtained from Eq. (8.17):

$$X(x) = -D^{-1}\delta_0(x).$$ (8.18)

The coordinate x generally gives the position of the unit force, and the functions whose plots are the influence lines of displacements $\delta_{i0}(x)$ are components of vector $\delta_0(x)$. From Maxwell's theorem it follows that the influence lines of displacements $\delta_{i0}(x)$ are the deflection lines of the respective members of the structure accompanying unit loadings $X_i = 1$. Hence, the deflection lines of the beam shown in Fig. 8.3a, b are the influence lines of the quantity δ_{i0} being sought.

Let us denote the components of matrix $-D^{-1}$ by symbols β_{ik}. The equation for the influence line of the redundant unknown X_i can then be written

$$X_i(x) = \sum_{k=1}^{s} \beta_{ik} \delta_{k0}(x).$$ (8.19)

This means that the influence line of the redundant X_i is the deflection line induced by generalized forces β_{ik} attached at action points of redundants X_k.

(a)   (b)
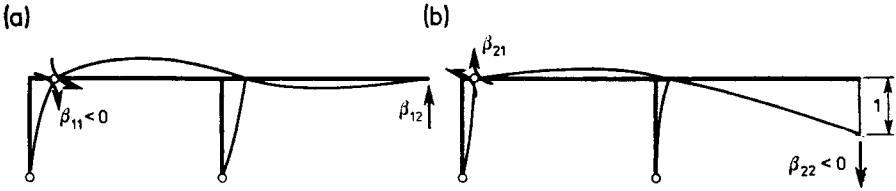
Fig. 8.5. Deformation of primary system under loadings β_{ik}

Figure 8.5 shows the loadings and the accompanying deformations of the
frame, where the deflection lines of the beam are the influence lines of X_i.
Under the influence of the loadings indicated in Fig. 8.5, bending moments
in the frame appear, whose plots relating only to the beam are shown in
Fig. 8.6.

(a)   (b)
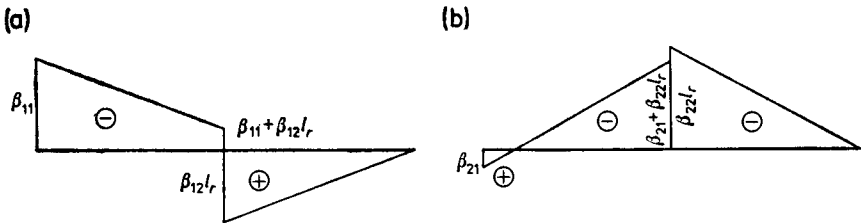
Fig. 8.6. Diagrams of bending moments induced by loadings β_{ik} acting

It will prove useful to solve the following auxiliary problem. Consider
bar $i\text{-}k$ simply supported and loaded at the ends by bending moments M_i,
M_k. The supports of the bar experience displacements w_i, w_k (Fig. 8.7).
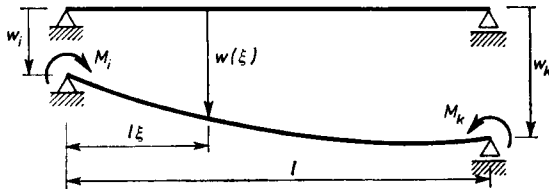
Fig. 8.7. Deflection of simple supported beam induced by end moments and displacements
of supports

Therefore, we have to find the integral of the following differential equa-
tion:

$$w'' = -l^2 x + l\beta',$$ (8.20)

into which we can bring the set of equations (6.19). In Eq. (8.20):

$$\varkappa = \frac{M}{EJ} = \frac{1}{EJ} [M_i(1-\xi) + M_k\xi],$$

$$\beta = \frac{kT}{GA} = \frac{k}{GA} \frac{M_k - M_i}{l}, \qquad w'' = \frac{d^2 w}{d\xi^2}. \qquad (8.21)$$

Substituting the relations (8.21) into Eq. (8.20) and integrating, we get

$$w = w_i\xi' + w_k\xi + \frac{l^2}{3EJ}[M_i\omega_M(\xi) + M_k\omega_M(\xi')]. \qquad (8.22)$$

We have introduced here the following denotations (cf. Fig. 8.8):

$$\omega_M(\xi) = \xi - \tfrac{3}{2}\xi^2 + \tfrac{1}{2}\xi^3, \qquad \xi' = 1 - \xi. \qquad (8.23)$$
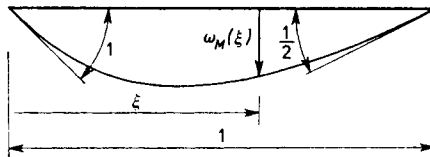
Fig. 8.8. Diagram of function $\omega_M(\xi)$

After finding the influence lines of the redundants, we find the equation for the influence lines of internal forces or reactions using the principle of superposition:

$$Q(x) = Q_P(x) + \sum_{k=1}^{s} Q_k X_k(x). \qquad (8.24)$$

$Q_P(x)$ in the above equation denotes the influence function of the static quantity in an isostatic primary system considered, Q_k is the value of the considered quantity induced by generalized force $X_k = 1$ and $X_k(x)$ is the previously found influence line of the redundant quantity.

The argumentation just presented applies equally to frameworks as to trusses. The influence lines—as deflection lines of the truss—are determined, of course, by the elastic weights method. In between joints, the deflection line of the truss is a straight line (cf. (8.22)).

EXAMPLE 8.2

Let us find the influence lines of redundants, generalized external forces in cross-section α and of reactions U_A, W_A and W_B for the frame in Fig. 8.1a.

Knowing the plots of the moments given in Fig. 8.6 and considering the values given in Eq. (1) from Example 8.1, we can readily write on Eq. (8.18):

$$X_1^{1-2}(\xi) = -\frac{l_r}{79}[8\omega_M(\xi)+2\omega_M(\xi')],$$

$$X_1^{2-c}(\xi) = \frac{l_r}{79}\,6\omega_M(\xi),$$

(a)

and

$$X_2^{1-2}(\xi) = \frac{2}{79}[3\omega_M(\xi)-19\omega_M(\xi')],$$

$$X_2^{2-c}(\xi) = \xi - \frac{44}{79}\,\omega_M(\xi).$$

(b)

The shapes of these lines are shown in Fig. 8.9.
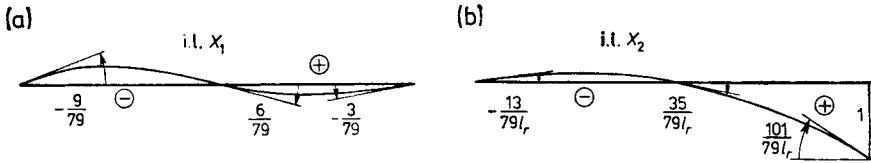
Fig. 8.9. Influence lines of redundants
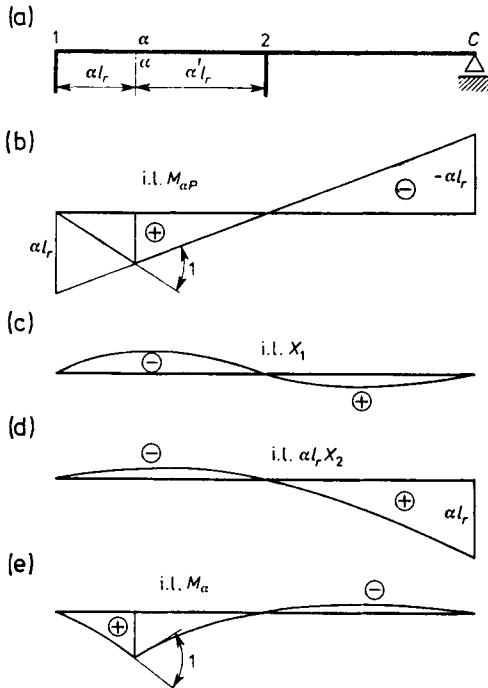
Fig. 8.10. Influence line of bending moment in cross-section α–α

Let us consider in turn the influence line of bending moment M_α in the cross-section located in span 1–2 (Fig. 8.10a), given by the coordinate α ($\alpha' = 1 - \alpha$). In the case of force $P = 1$ moving along the isostatic primary system, the moment M_α varies as illustrated by the plot of influence line $M_{\alpha P}$ (Fig. 8.10b). The moments in cross-section α induced by generalized forces $X_i = 1$ are $M_{\alpha 1} = 1$, $M_{\alpha 2} = \alpha l_r$ (cf. Fig. 8.2a, b). Hence, it is necessary to add to the influence line of $M_{\alpha P}$ the influence lines of X_1 and $\alpha l_r X_2$ (Fig. 8.10c, d). The influence line of M_α is a superposition of all three lines (Fig. 8.10a). In a similar manner we find the influence line of T_α. However, since $T_{\alpha 1} = 0$

(a)   i.l. $T_{\alpha P}$

(b)   i.l. X_2

(c)   i.l. T_α

(d)   i.l. $N_\alpha = -U_A = \frac{1}{l_s} X_1$
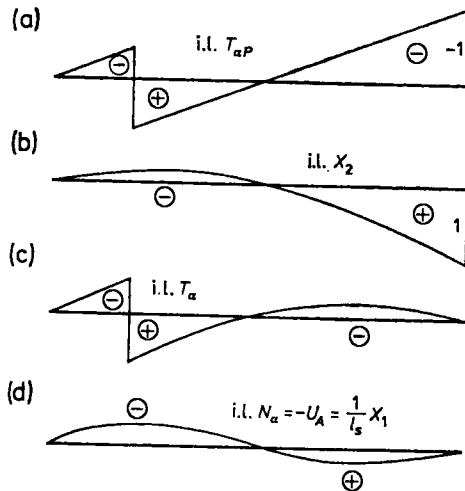
Fig. 8.11. Influence line of shear force in cross-section α–α

(a)   i.l. W_{AP}

(b)   i.l. X_2

(c)   i.l. W_A
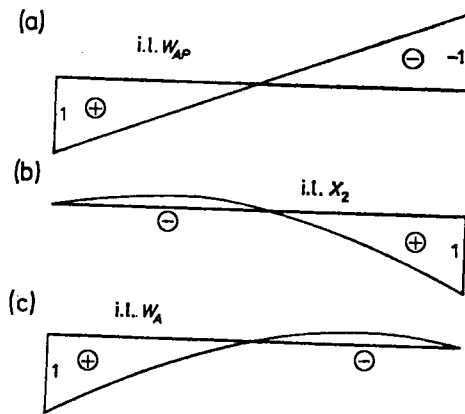
Fig. 8.12. Influence line of reaction W

and $T_{\alpha 2} = 1$ (cf. Fig. 8.2a, b), the influence line of T_α (Fig. 8.11c) is, therefore, a superposition of two influence lines only, $T_{\alpha P}$ and X_2 (Fig. 8.11a, b).

In the primary system, neither force $P = 1$ nor $X_2 = 1$ induces any longitudinal force $(N_{\alpha P} = N_{\alpha 2} = 0)$ in cross-section α. Consequently, the influence line od N_α is the influence line of redundant X_1 multiplied by $N_{\alpha 1} = 1/l_s$ (Fig. 8.11d). It is easily seen that it is at the same time the influence line of $-U_A$, because the positive sense of reaction U_A is opposite to that shown in Fig. 8.2a. The method of finding the influence lines of W_A and W_B (Figs. 8.12, 8.13) requires no further comment.
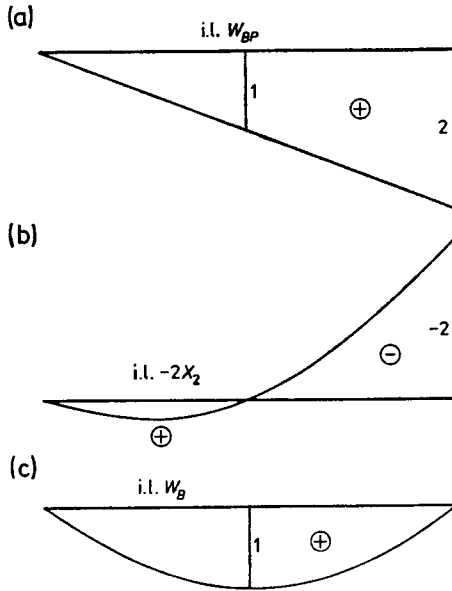
Fig. 8.13. Influence line of reaction W_B

EXAMPLE 8.3

Find the influence lines of redundant X_1 and of the forces in truss members of a onefold hyperstatic truss as shown in Fig. 8.14a. We assume that force $P = 1$ may act on the joints of both the bottom and top flange.

It will therefore be convenient in this case to suspend a weightless and unloaded platform under the truss (Fig. 8.14b), whose joints will experience exactly the same vertical displacements, as do the joints of the top and bottom flanges of the truss. We take as redundant the axial force in truss member 12. Consequently, two trusses simply supported (Fig. 8.14c) will make the isostatic primary system.

(a)

(b)

(c)
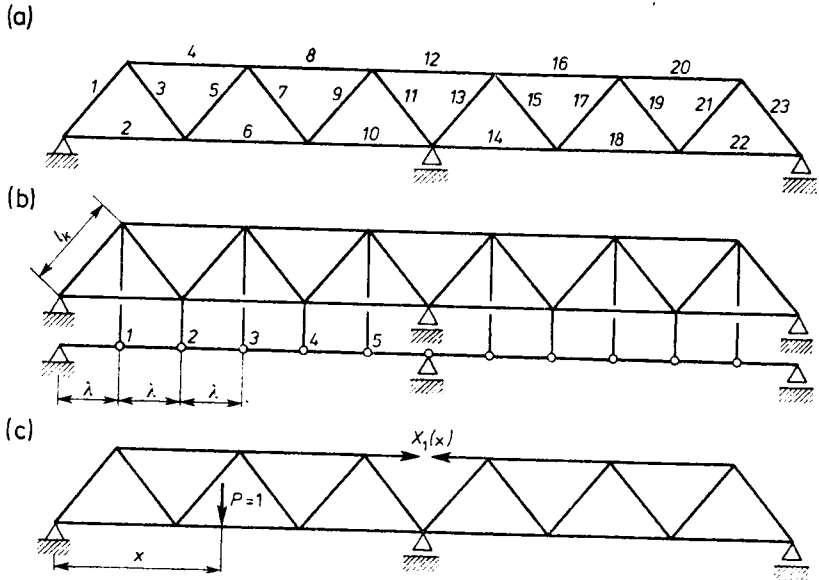
Fig. 8.14. Two-span truss: (a) considered structure; (b) truss with weight less platform; (c) primary system

Using one of the methods described in Section 7.2, we determine the axial forces induced by loading $X_1 = 1$ and array them in a single column matrix:

$$\sigma_1 = \tfrac{1}{6}\{\beta, -1, -\beta, 2, \beta, -3, -\beta, 4, \beta, -5, -\beta, 6\}, \tag{a}$$

where (cf. Fig. 8.14b):

$$\beta = \frac{l_k}{\lambda}. \tag{b}$$

Since a symmetric truss is involved here, we have confined ourselves to putting in matrix (a) only the forces acting in truss members *1–12*.

Denoting the cross-sectional areas of the bottom flange by A_d, those of the top flange by A_g and those of the cross braces by A_k, we express the deformability matrix $\mathbf{E}^{-1}$ as follows:

$$\mathbf{E}^{-1} = \frac{\lambda}{EA_d}\left[\beta\varrho_k, 2\beta\varrho_k, 2\varrho_g, \beta\varrho_k, 2, \beta\varrho_k, 2\varrho_g, \beta\varrho_k, 2, \beta\varrho_k, \varrho_g\right], \tag{c}$$

where:

$$\varrho_k = \frac{A_d}{A_k}, \qquad \varrho_g = \frac{A_d}{A_g}. \tag{d}$$

The product of matrix (c) thus expressed and matrix (a) is an array of extensions of the truss members induced by force $X_1 = 1$:

$$\boldsymbol{\epsilon}_1 = \mathbf{E}^{-1}\boldsymbol{\sigma}_1 = \{\varDelta l^1, \varDelta l^2, \dots, \varDelta l^{12}\}. \tag{e}$$

In this connection, we determine the value δ_{11} this time from the relation

$$\mathbf{D} = \delta_{11} = 2\boldsymbol{\sigma}_1^T \mathbf{E}^{-1}\boldsymbol{\sigma}_1 = \frac{\lambda}{9EA_d}(35 + 38\varrho_g + 3\beta^3\varrho_k). \tag{f}$$

Assuming, for example, the following values:

$$\beta = \frac{3}{2}, \quad \varrho_g = \frac{1}{2}, \quad \varrho_k = 4, \tag{g}$$

we get

$$\mathbf{D} = \delta_{11} = \frac{21}{2}\frac{\lambda}{EA_d}, \quad \mathbf{D}^{-1} = \frac{2}{21}\frac{EA_d}{\lambda}. \tag{h}$$

The influence line of redundant X_1 is the deflection line of the truss under load $X_1 = -1/\delta_{11}$. This force induces extensions of the truss members, which we calculate from the formula

$$\boldsymbol{\epsilon} = \mathbf{E}^{-1}\left(-\frac{1}{\delta_{11}}\right)\boldsymbol{\sigma}_1$$

$$= \frac{1}{63}\{-9, 2, 9, -2, -9, 6, 9, -4, -9, 10, 9, -3\}, \tag{i}$$

in which we have already considered assumptions (g).

We determine from Eq. (7.39) the slope discontinuity angles ω of the deflection line of the platform suspended under the truss (Fig. 8.14b). We obtain the matrix $\mathbf{Z}$ as an array of internal forces induced by the virtual loadings given in Fig. 8.15:
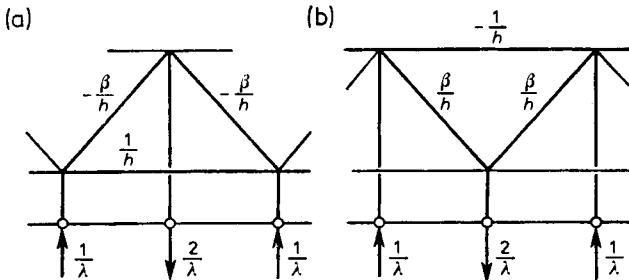
Fig. 8.15. Forces in truss members induced by virtual loadings

$$\mathbf{Z} = \frac{1}{h}\begin{bmatrix} -\beta & 1 & -\beta & & & & & & & & & \\ & & \beta & -1 & & \beta & & & & & & \\ & & & & -\beta & 1 & -\beta & & & & & \\ & & & & & & \beta & -1 & & \beta & & \\ & & & & & & & & -\beta & 1 & -\beta & 0 \end{bmatrix}\begin{matrix}1\\2\\3\\4\\5\end{matrix}$$

(j)

The fact is that the virtual loadings also induce forces in the suspension bars of the platform, but because the load X_1 is not accompanied by extensions of these bars, those forces can be neglected in matrix $\mathbf{Z}$.

Hence, in accordance with (7.39):

$$\boldsymbol{\omega} = \mathbf{Z}\boldsymbol{\epsilon} = \frac{1}{63h}\{2, 2, 6, 4, 10\}. \tag{k}$$

The deflection line of the platform is a plot of secondary moments from secondary loadings $\boldsymbol{\omega}$. Using the method described in Section 7.1, we find successively:

Fig. 8.16. Influence lines of redundant truss member in the case of a force moving (a) along cross braces; (b) over bottom flange; (c) over top flange

$$\mathbf{B} = \frac{1}{\lambda} \begin{bmatrix} 2 & -1 & & & \\ -1 & 2 & -1 & & \\ & -1 & 2 & -1 & \\ & & -1 & 2 & -1 \\ & & & -1 & 2 \end{bmatrix}, \quad \mathbf{B}^{-1} = \frac{\lambda}{6} \begin{bmatrix} 5 & 4 & 3 & 2 & 1 \\ 4 & 8 & 6 & 4 & 2 \\ 3 & 6 & 9 & 6 & 3 \\ 2 & 4 & 6 & 8 & 4 \\ 1 & 2 & 3 & 4 & 5 \end{bmatrix}, \tag{1}$$

and the ordinates of the influence line of X_1 are obtained from the formula

$$X_1 = \mathbf{B}^{-1}\boldsymbol{\omega} = \frac{1}{63}\frac{\lambda}{h}\{9, 16, 21, 20, 15\}. \tag{m}$$
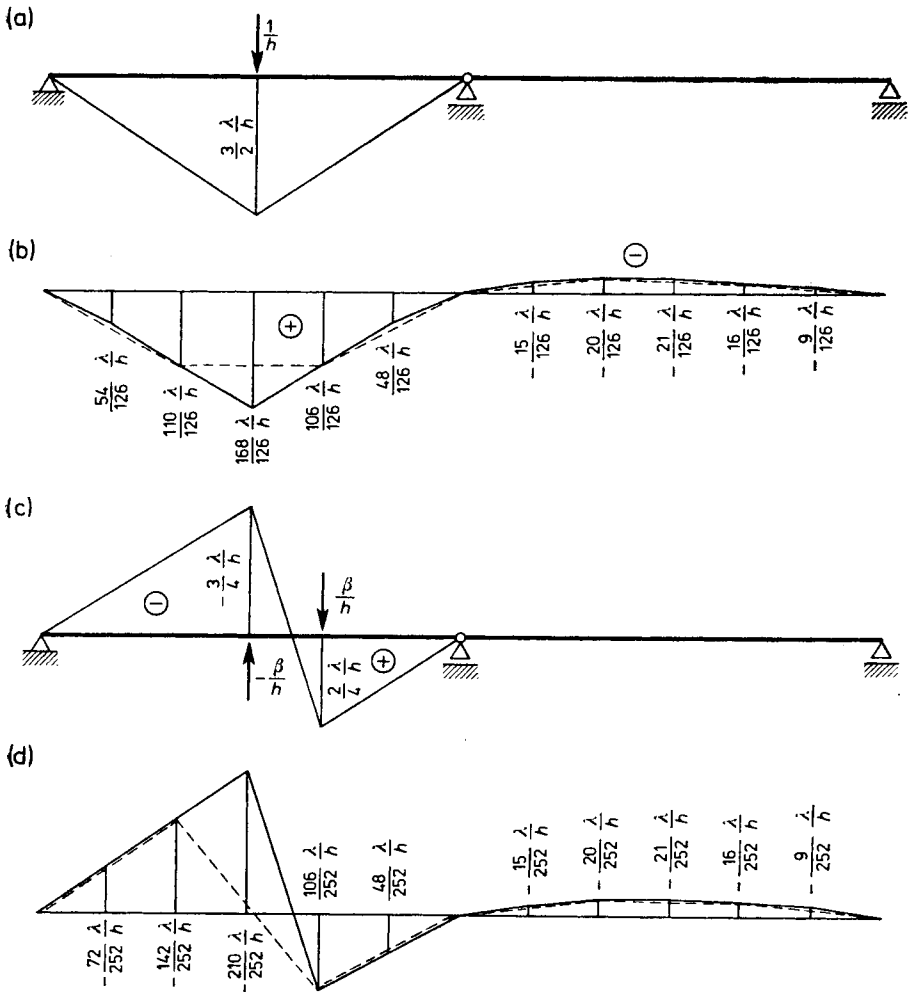
Fig. 8.17. Influence line of forces in truss members 6 and 7

The plot of this influence line is shown in Fig. 8.16a. It expresses the dependence of force $N^{12} = X_1$ on the position of force $P = 1$ moving along the cross braces. But, it will suffice to connect using straight segments the ordinates of this line at even numbered joints to obtain the influence line for the force moving along the bottom flange (Fig. 8.16b). By joining the odd-numbered ordinates we obtain the influence line of the force moving along the top flange (Fig. 8.16c).

The influence line of the force in bar i is determined from the formula

$$N^i = N_P^i + N_1^i X_1 . \tag{n}$$

Specifically, for $i = 6, 7$, we read from Eq. (a)

$$N_1^6 = -\frac{1}{2}, \quad N_1^7 = -\frac{\beta}{6} = -\frac{1}{4} .$$

The plots of influence lines N_P^6, N_P^7 (Fig. 8.17a, c) are plots of secondary moments from the elastic weights arrayed in matrix (j), columns 6, 7. The superposition performed in accordance with Eq. (n) results in the influence lines given in Fig. 8.17b, d. A suitable modification of connections between the ordinates yields influence lines which are valid for a force moving not along cross braces but along one of the flanges. The dashed lines in Fig. 8.17b, d apply to a force travelling along the bottom flange.

8.3. Selection of the Primary System

As we have mentioned above, the force method allows much freedom in selecting the redundant unknowns and the primary system, and it will depend on the actual choice how much work will be required for calculations and how accurate the results will be. The former depends on the degree of filling of flexibility matrix **D**. Therefore, we should work towards getting as many quantities δ_{ik} as possible to equal zero.

That is precisely why, for example, for the continuous beam described in Fig. 8.18a we eliminate by our choice primary systems in the form of a single beam resting on extreme supports (Fig. 8.18b) or in the form of a cantilever (Fig. 8.18c) since we would obtain in either case a complete matrix **D**. It follows that for the system in Fig. 8.18b, the plots of all moments M_i are spread over the entire length of the beam, and in the cantilever case (Fig. 8.18c), each of the plots of m_i has values other than zero at least in the first span of the beam. Therefore, none of the quantities δ_{ik} equals zero. On the other hand, taking a primary scheme as in Fig. 8.18d, in other words, assuming that the bending moments in support cross-sections are the redun-
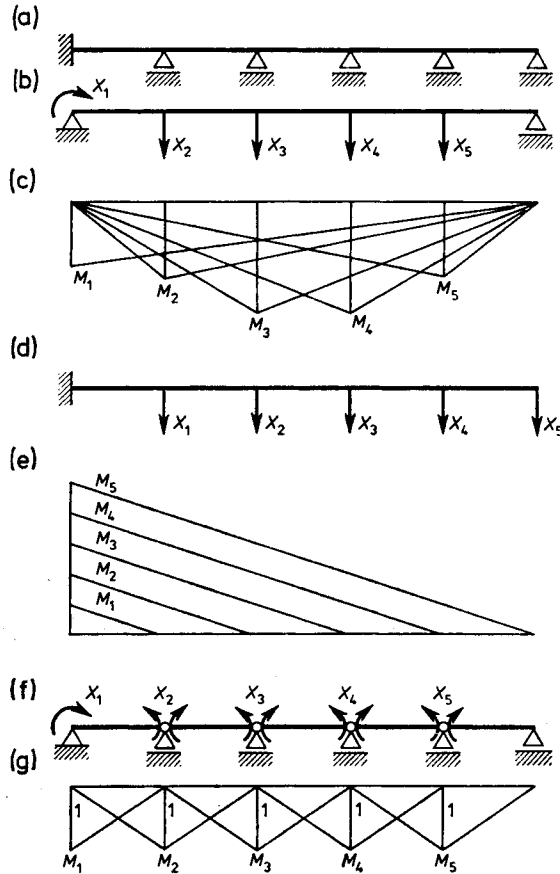
Fig. 8.18. Various possibilities of choosing the primary system for continuous beam

dant unknowns, we arrive at a set of three-term equations with the three-diagonal flexibility matrix

$$\mathbf{D} = \begin{vmatrix} \delta_{11} & \delta_{12} & & & \\ \delta_{21} & \delta_{22} & \delta_{23} & & \\ & \delta_{32} & \delta_{33} & \delta_{34} & \\ & & \cdots & \cdots & \cdots \\ & & & \delta_{n,n-1} & \delta_{nn} \end{vmatrix} . \tag{8.25}$$

As we can see, each of the plots M_i spreads only over to two spans (Fig. 8.18g), due to which:

$$\delta_{ik} = \int_s \frac{M_i M_k}{EJ} \, ds = 0 \quad \text{for} \quad |k-i| \geqslant 2. \tag{8.26}$$

The more spans there are in a continuous beam, the more evident will be
the advantage accruing from the use of such a primary system.

   Similarly, in the case of an over-rigid truss as in Fig. 8.19a, it is better to
assume the forces in cross braces to be unknown (Fig. 8.19c) rather than to

(a)

(b)

(c)
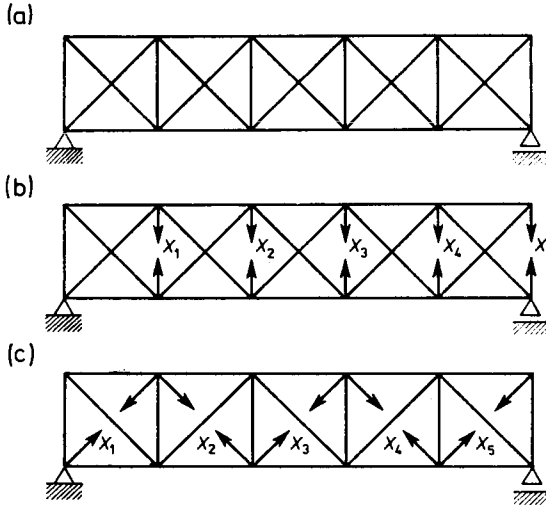
Fig. 8.19. Two methods of choosing the basic structure for plane truss

assume the forces in vertical members to be redundant (Fig. 8.19b). In the
former case, we would deal with a complete flexibility matrix $\mathbf{D}$, and in the
latter, the matrix would have the form given in Eq. (8.25).

(a)   (b)   (c)
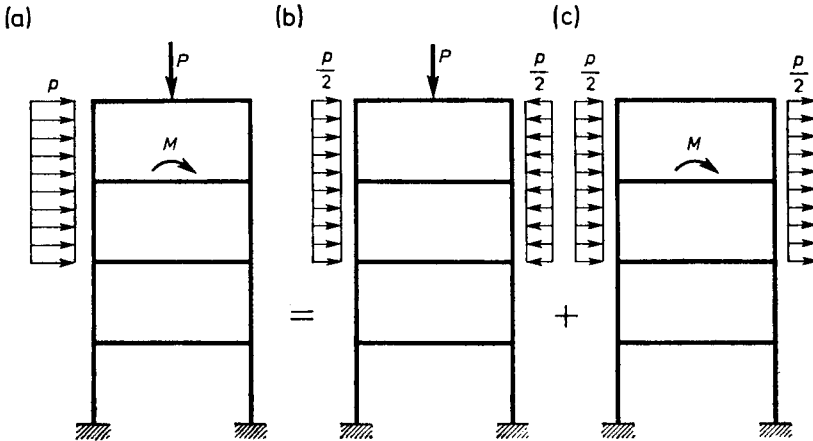
Fig. 8.20. Symmetric frame

For symmetric structures, it pays to split the loading into a symmetric and antisymmetric part and to solve separately each of the component problems. For example, we treat an asymmetric loading of the 12-fold statically indeterminate frame in Fig. 8.20a as the sum of the loadings indicated in Fig. 8.20b, c. For symmetric and antisymmetric loading alike, we consider half of the frame under various support conditions on the axis of symmetry of the structure. A frame symmetrically loaded (Fig. 8.21a) is eightfold hyperstatic and a frame antisymmetrically loaded (Fig. 8.22a) fourfold hyperstatic.
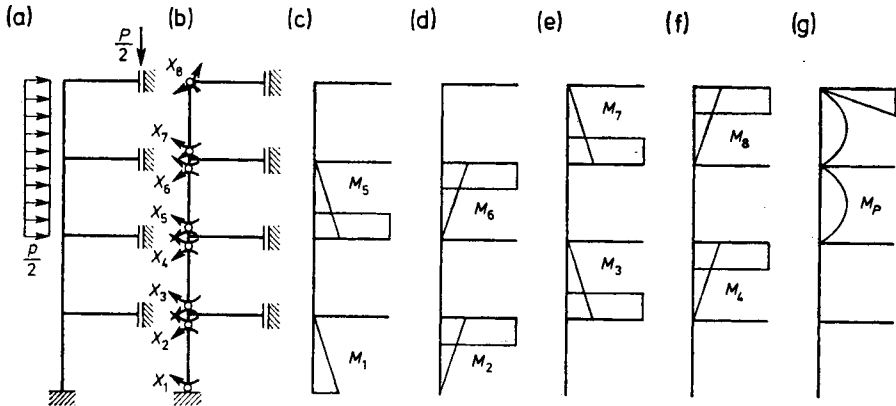
Fig. 8.21. Half-frame symmetrically loaded: (a) considered structure; (b) primary system; (c)–(f) diagrams of moments induced by forces $X_i = 1$; (g) diagram of moments from external loading
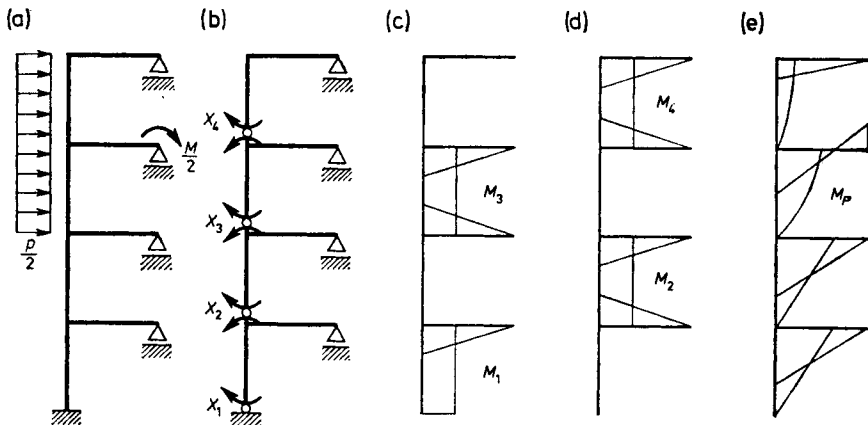
Fig. 8.22. Half-frame antisymmetrically loaded: (a) considered structure; (b) primary system; (c), (d) diagrams of moments induced by forces $X_i = 1$; (e) diagram of moments from external loading

By selecting primary systems in the manner indicated in Figs. 8.21b and 8.22b, we arrive at sets of three-term equations with the three-diagonal flexibility matrix (8.25). The plots of moments M_i given in Figs. 8.21c–g and 8.22c–e indicate that the relation (8.26) applies here.
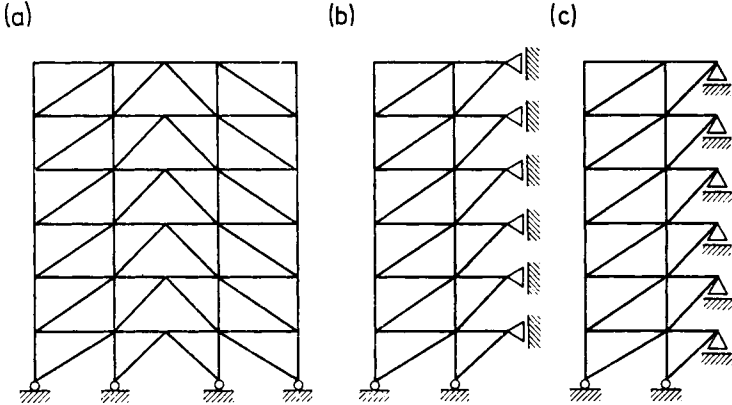
Fig. 8.23. Symmetric truss: (a) considered structure; (b) half-truss symmetrically loaded; (c) half-truss antisymmetrically loaded

The truss from Fig. 8.23a is 12-fold hyperstatic. After resolving the load into symmetric and antisymmetric, we can consider successively the trusses diagrammatically presented in Fig. 8.23b, c. In the case of symmetric load-
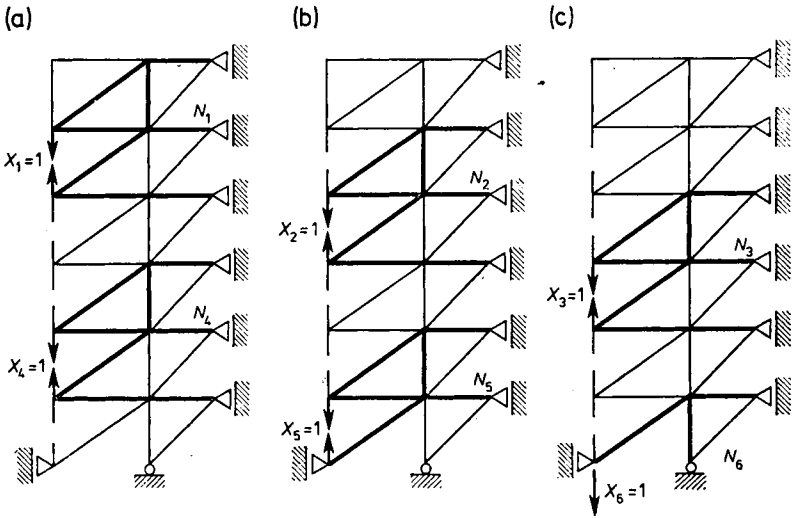
Fig. 8.24. Redundant truss members in the case of symmetrical loading (non-zero forces occur in thickened members)

ing, the joints lying on the axis of symmetry cannot experience horizontal sideways (Fig. 8.23b), whereas antisymmetric loading cannot be accompanied by vertical displacements of these joints (Fig. 8.23c). Both truss systems are sixfold hyperstatic.

It would be wrong to take a primary system in the form of a truss cantilever, since this would lead to the complete matrix of a set of equations. But, by cutting the external vertical truss members and removing the vertical component of reaction in the outer support joint, we obtain primary systems (Figs. 8.24, 9.25), in which the redundant forces induce axial forces only

Fig. 8.25. Redundant truss members in the case of antisymmetrical loading

in a few truss members. Members in which non-zero axial forces occur are indicated in the diagrams by a bold line. In the case of a symmetric system (Fig. 8.24), we arrive at a set of equations with the five-diagonal flexibility matrix:

$$
\mathbf{D} = \begin{bmatrix}
\delta_{11} & \delta_{12} & \delta_{13} & & & \\
\delta_{21} & \delta_{22} & \delta_{23} & \delta_{24} & & \\
\delta_{31} & \delta_{32} & \delta_{33} & \delta_{34} & \delta_{35} & \\
\cdots & \cdots & \cdots & \cdots & \cdots & \\
& & & \delta_{n,n-2} & \delta_{n,n-1} & \delta_{nn}
\end{bmatrix},
\tag{8.27}
$$

wherein with denotations of type (6.18), (6.31), we have

$$
\delta_{ik} = \sigma_i^T \mathbf{E}^{-1} \sigma_k = 0 \quad \text{for} \quad |k-i| \geqslant 3.
\tag{8.28}
$$

With antisymmetric loading (Fig. 8.25), the set of canonical equations has a band matrix of type (8.25).

The kind of primary system selected has a bearing not only on the number of non-zero terms δ_{ik} but on the accuracy of results as well. For example, in the case of two-, three- and four-span continuous beams (Fig. 8.26) uni-

(a)   (b)   (c)
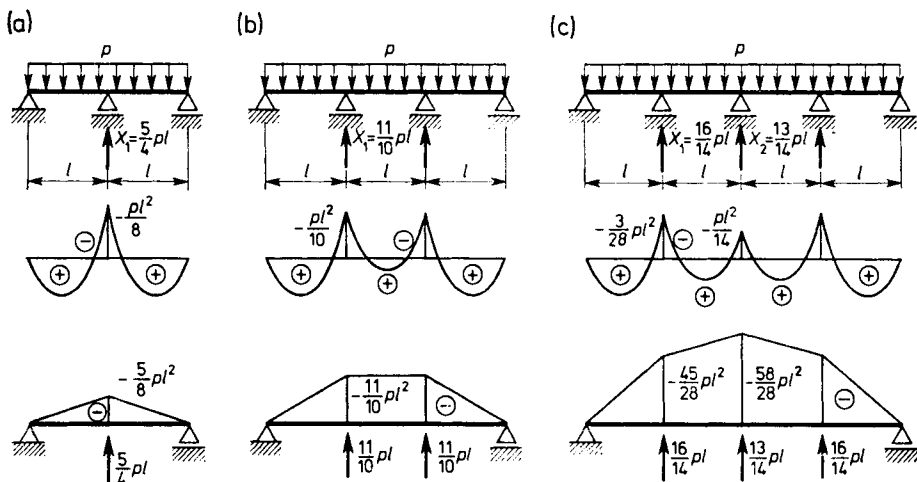
Fig. 8.26. Continuous beams

formly loaded, a beam resting on extreme supports taken for the primary system would involve calculations requiring high accuracy, increasing with the number of spans in the beam. This is due to the fact that the plot of moments induced by redundants alone has increasingly greater ordinates. Consequently, a one percent error made in the determination of the redundants

(a)   (b)   (c)
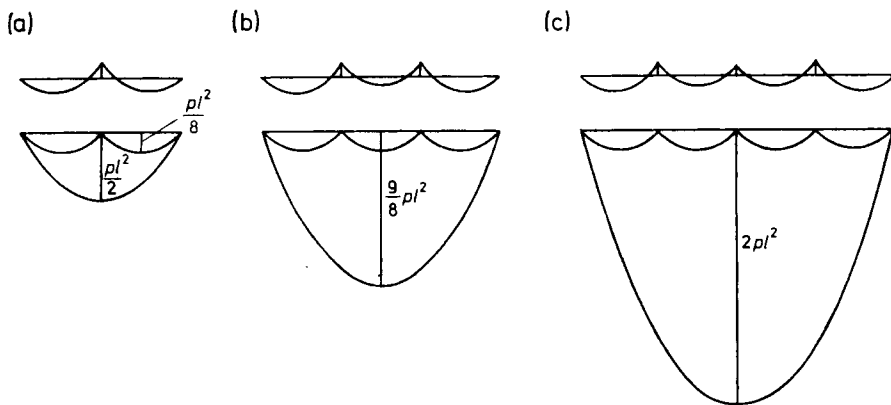
Fig. 8.27. Diagrams of moments from external loading for different primary schemes

gives errors on the order of 5%, 11% and 29% in two-, three- and four-span beams, respectively, for the bending moments actually occurring over the supports.

On the other hand, the influence of the number of unknowns on the accuracy of results cannot be manifested if we take support moments for the redundants. This is due to the fact that the state of strain and stress of the primary system under an external load is far from the real state, more so in the case of an incorrect choice of redundants than in the case of a correct choice of the primary system and redundants. Figure 8.27 shows on the same scale the plots of the ultimate moments and the plots of moments M_P for various primary systems relating to the beams in Fig. 8.26.

It should be noted that an additional difficulty in improving the accuracy of results by means of increasing the number of unknowns comes from the fact that if a wrong primary system has been selected, we then get a set of equations whereby the greater the size of matrix D, the worse it is conditioned

A suitable selection of the primary system may lead in an extreme case, to complete diagonalization of the flexibility matrix D, which obviously greatly facilitates its inversion and further calculations. Getting a diagonalized matrix D is simple particularly for symmetric structures. For example, cutting a three-span beam on the axis of symmetry, tantamount to taking the bending moment and the transverse force in the central cross-section
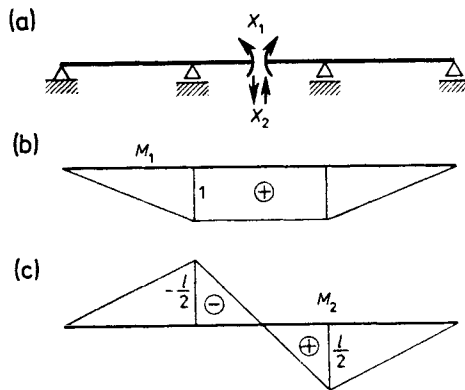
Fig. 8.28. Use of the symmetry of a structure in the choice of primary scheme

(Fig. 8.28a) for the unknown redundants, results in the plots of moments M_i given in Fig. 8.28b, c. Since one plot is symmetric and the other antisymmetric, $\delta_{12} = 0$, and D has the diagonal matrix form: $D = [\delta_{11}, \delta_{22}]$.

The same effect will be obtained in chosing the position of the hinge (Fig. 8.29a) in such way as to get the zeroing conditions for the quantity δ_{12} satisfied:

$$\delta_{12} = \int_s \frac{M_1 M_2}{EJ}\, ds = \frac{l^2(l-5e)}{6EJ(l-e)^2} = 0.$$
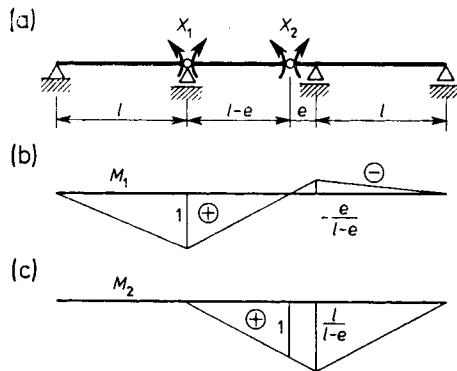
Fig. 8.29. Primary scheme leading to an uncoupled system of equations

It follows that by taking the second hinge to be at distance $e = l/5$, we obtain a diagonal flexibility matrix.

One of the ways of reducing the number of terms δ_{ik} in $\mathbf{D}$ is the use of the group unknowns method which consists of introducing in place of primary unknowns $\mathbf{X}$ appropriate linear combinations of these quantities:

$$\mathbf{X} = \mathbf{G}_{XY}\mathbf{Y}. \tag{8.29}$$

The new unknowns $\mathbf{Y}$ are termed *group unknowns*. The non-singular matrix $\mathbf{G}_{XY}$ is a transformation matrix of one set of unknowns into another.

The primary set of canonical equations of the direct flexibility method (8.13) can be written using slightly modified denotations:

$$\mathbf{D}_X \mathbf{X} + \boldsymbol{\delta}_{0X} = 0. \tag{8.30}$$

Putting into it the relation (8.19) and multiplying the set (8.30) by matrix $\mathbf{G}_{XY}^T$ we get

$$\mathbf{G}_{XY}^T \mathbf{D}_X \mathbf{G}_{XY} \mathbf{Y} + \mathbf{G}_{XY}^T \boldsymbol{\delta}_{0X} = 0. \tag{8.31}$$

With the denotations

$$\mathbf{D}_Y = \mathbf{G}_{XY}^T \mathbf{D}_X \mathbf{G}_{XY}, \qquad \boldsymbol{\delta}_{0Y} = \mathbf{G}_{XY}^T \boldsymbol{\delta}_{0X} \tag{8.32}$$

the set of equations (8.31) takes the form

$$\mathbf{D}_Y \mathbf{Y} + \boldsymbol{\delta}_{0Y} = \mathbf{0}. \tag{8.33}$$

A skilful selection of the coefficients of a matrix G_{XY} results in matrix $\mathbf{D}_Y$ with a smaller number of non-zero terms δ_{ik}.

The operations described can be repeated several times, the end effect being a diagonal matrix. Thus, for example, we pass from group unknowns $\mathbf{Y}$ to subsequent unknowns $\mathbf{Z}$

$$\mathbf{Y} = \mathbf{G}_{YZ}\mathbf{Z}, \tag{8.34}$$

satisfying the set of equations

$$\mathbf{D}_Z \mathbf{Z} + \boldsymbol{\delta}_{0Z} = \mathbf{0}, \tag{8.35}$$

where:

$$\begin{aligned}
\mathbf{D}_Z &= \mathbf{G}_{YZ}^T \mathbf{D}_Y \mathbf{G}_{YZ} = \mathbf{G}_{YZ}^T \mathbf{G}_{XY}^T \mathbf{D}_X \mathbf{G}_{XY} \mathbf{G}_{YZ}, \\
\boldsymbol{\delta}_{0Z} &= \mathbf{G}_{YZ}^T \boldsymbol{\delta}_{0Y} = \mathbf{G}_{YZ}^T \mathbf{G}_{XY}^T \boldsymbol{\delta}_{0X}.
\end{aligned} \tag{8.36}$$

Hence, the transformation matrix of unknowns $\mathbf{X}$ into $\mathbf{Z}$ is

$$\mathbf{G}_{XZ} = \mathbf{G}_{XY}\mathbf{G}_{YZ}. \tag{8.37}$$

The procedure will be explained using the example of a sixfold hyperstatic frame as in Fig. 8.30a. In the first stage of calculations, we select the primary system in the manner indicated in Fig. 8.30b. The plots of moments M_i induced by loadings $X_i = 1$ ($i = 1, 2, ..., 6$) are shown in Fig. 8.30c–h.
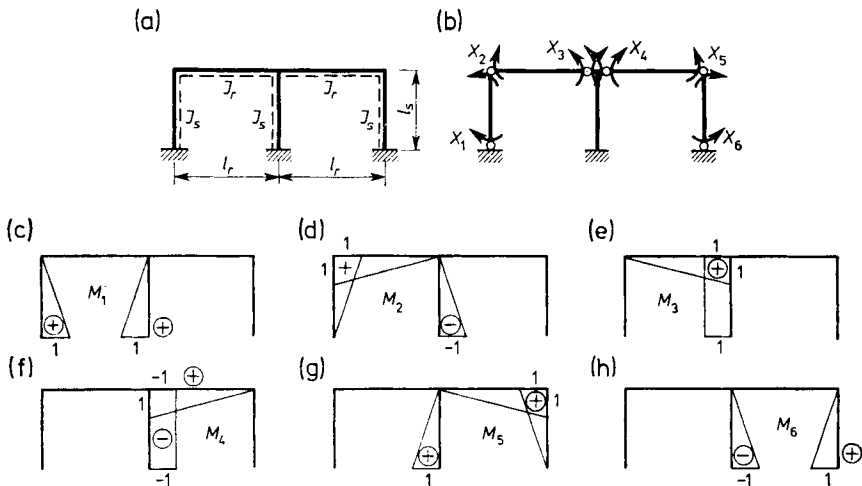
Fig. 8.30. Six-fold statically indeterminate frame: (a) considered structure; (b) primary system; (c)–(h) diagrams of moments induced by forces $X_i = 1$

Matrix $\mathbf{D_X}$ of the respective set of equations is a complete matrix containing no factors δ_{ik} equalling zero. By performing the first transformation of the unknowns, we utilize the symmetry of the system; three group unknowns, Y_a, Y_b, Y_c, result in symmetric plots of the moments (Fig. 8.31a–c) and the
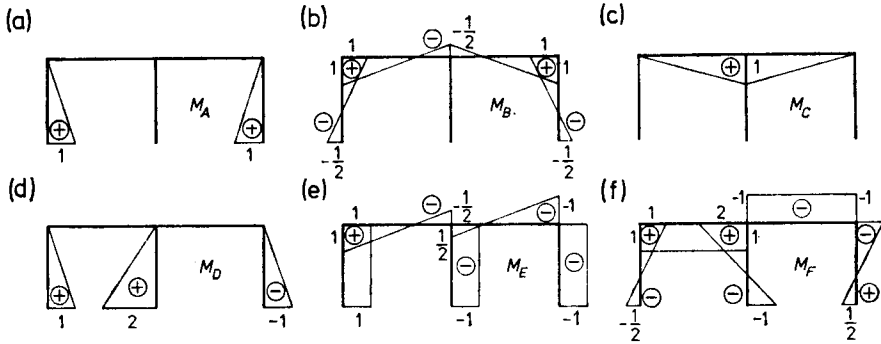
Fig. 8.31. Diagrams of moments induced by group forces $Y_i = 1$

following three, Y_d, Y_e, Y_f result in antisymmetric plots (Fig. 8.31d–f). The transformation matrix $\mathbf{G_{XY}}$ has, therefore, the following structure:

$$
\mathbf{G_{XY}} = \begin{array}{c} \\ 1 \\ 2 \\ 3 \\ 4 \\ 5 \\ 6 \end{array}
\begin{array}{c}
\begin{array}{cccccc} a & b & c & d & e & f \end{array} \\
\left[\begin{array}{cccccc}
1 & & & 1 & & \\
& 1 & & & 1 & \\
& & 1 & & & 1 \\
& & 1 & & & -1 \\
& 1 & & & -1 & \\
1 & & & -1 & &
\end{array}\right]
\end{array}.
\tag{8.38}
$$

The successive columns of this matrix contain arrays of values X_i ($i = 1, 2, \ldots, 6$) which jointly produce the state $Y_r = 1$ ($r = a, b, \ldots, f$). $\mathbf{D_Y}$ has in this case the form

$$
\mathbf{D_Y} = \left[\begin{array}{cccccc}
\delta_{aa} & \delta_{ab} & & & & \\
\delta_{ba} & \delta_{bb} & \delta_{bc} & & & \\
& \delta_{cb} & \delta_{cc} & & & \\
& & & \delta_{dd} & \delta_{de} & \delta_{df} \\
& & & \delta_{ed} & \delta_{ee} & \delta_{ef} \\
& & & \delta_{fd} & \delta_{fe} & \delta_{ff}
\end{array}\right],
\tag{8.39}
$$

and the set of six equations with six unknowns is split into two independent sets, each of them containing three equations with three unknowns.

We select in turn the linear combinations of states Y, so as to get as many coefficients of the new matrix $\mathbf{D}_Z$ as possible to equal zero. The new group unknowns Z_R $(R = A, B, \ldots, F)$ correspond to group unknowns Y, according to the relation (8.34) in which

$$
\mathbf{G}_{YZ} = \begin{array}{c} \\ a \\ b \\ c \\ d \\ e \\ f \end{array}
\begin{array}{cccccc}
A & B & C & D & E & F \\
\end{array}
\left[\begin{array}{cccccc}
1 & -\frac{1}{2} & & & & \\
 & 1 & & & & \\
 & -\frac{1}{2} & 1 & & & \\
 & & & 1 & 1 & -\frac{1}{2} \\
 & & & & 1 & 1 \\
 & & & & -\frac{1}{2} & 1 \\
\end{array}\right].
\tag{8.40}
$$
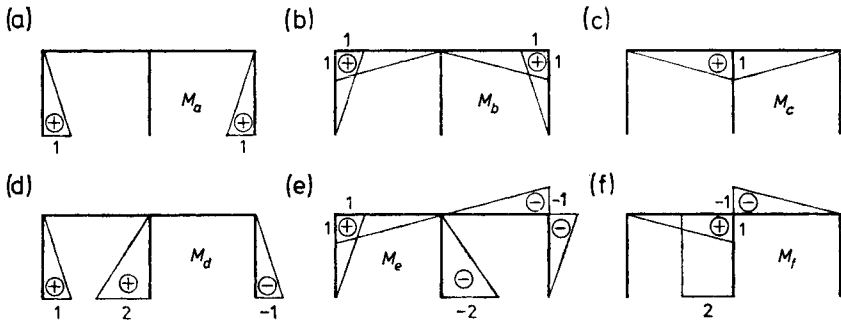
Fig. 8.32. Diagrams of moment induced by group forces $Z_R = 1$

From the plots of moments M_R shown in Fig. 8.32, we can easily determine which of the factors of matrix $\mathbf{D}_Z$ will be zero:

$$
\mathbf{D}_Z = \left[\begin{array}{cccccc}
\delta_{AA} & & & & & \\
 & \delta_{BB} & & & & \\
 & & \delta_{CC} & & & \\
 & & & \delta_{DD} & & \\
 & & & & \delta_{EE} & \delta_{EF} \\
 & & & & \delta_{FE} & \delta_{FF} \\
\end{array}\right].
\tag{8.41}
$$

As we can see, a suitable selection of the group unknowns has made it possible to break down the implicit set of six equations and replace it by four equations each containing one unknown and by a set of two equations with two unknowns.

Knowing the matrices (8.38) and (8.40), we can pass on the basis of Eq. (8.37) directly from the unknowns $\mathbf{X}$ to $\mathbf{Z}$:

$$
\mathbf{G}_{XZ} = \begin{array}{c} \\ 1 \\ 2 \\ 3 \\ 4 \\ 5 \\ 6 \end{array} \begin{array}{c} A \quad B \quad C \quad D \quad E \quad F \\ \left[\begin{array}{cccccc} 1 & -\frac{1}{2} & & 1 & 1 & -\frac{1}{2} \\ & 1 & & & 1 & 1 \\ & -\frac{1}{2} & 1 & & -\frac{1}{2} & 1 \\ & -\frac{1}{2} & 1 & & \frac{1}{2} & -1 \\ & 1 & & & -1 & -1 \\ 1 & -\frac{1}{2} & & -1 & -1 & \frac{1}{2} \end{array} \right] \end{array} .
\tag{8.42}
$$

The respective numbers arrayed in the matrix (8.42) can be found in Fig. 8.32. It is self-evident that instead of having to calculate the factors of matrices $\mathbf{D}_Z$ and $\boldsymbol{\delta}_{0Z}$ in Eqs. (8.36), it is better to make use of direct relations:

$$
\delta_{RS} = \int\limits_{s} \frac{M_R M_S}{EJ}\, \mathrm{d}s, \quad \delta_{R0} = \int\limits_{s} \frac{M_R M_P}{EJ}\, \mathrm{d}s \quad (R, S = A, B, \dots F).
\tag{8.43}
$$

In the special case of a frame or an unhinged arch, the diagonalization effect can also be obtained in $\mathbf{D}$ by the suitable choice of the point of application of the redundants and by their suitable orientation. Consider a bar fixed on both sides, whose curved axis lies in the xy plane. The bar is under the load of forces acting also in this plane (Fig. 8.33a). Neither the internal
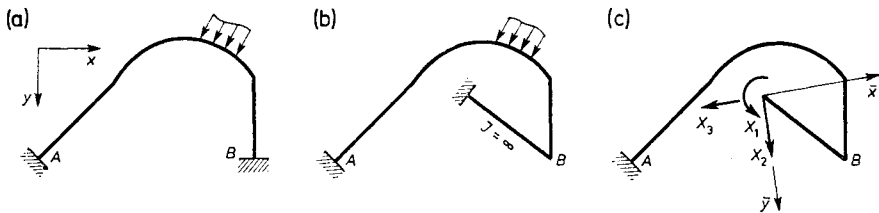
Fig. 8.33. Curved bar: (a) considered structure; (b) transfer of support to elastic pole; (c) primary system

forces nor the deformations of the bar will change, if we transfer the fastening of one of its ends (say, B) to the end of an infinitely rigid arm rigidly connected to a frame at joint B (Fig. 8.33b). We take for the isostatic primary system a cantilever with three unknown redundants acting at the end of it (Fig. 8.33c).

The point of application of the redundants, called the elastic pole, and the directions of the axes $\bar{x}, \bar{y}$ along which the redundants X_2 and X_3 are acting arc selected from the condition under which all terms δ_{ik} disappear, for $i \neq k$. Since

$$
M_1 = 1, \quad M_2 = \bar{x}, \quad M_3 = \bar{y},
\tag{8.44}
$$

we demand that the following conditions be satisfied:

$$\delta_{12} = \int_s \frac{\bar{x}}{EJ} \, \mathrm{d}s = 0,$$

$$\delta_{13} = \int_s \frac{\bar{y}}{EJ} \, \mathrm{d}s = 0, \tag{8.45}$$

$$\delta_{23} = \int_s \frac{\bar{x}\bar{y}}{EJ} \, \mathrm{d}s = 0.$$

Treating the bar as a body with a selfweight:

$$\mu = \frac{1}{EJ}, \tag{8.46}$$

per unit length of the axis, the conditions (8.45) can be interpreted as nulling the static moments and the centrifugal moment of the body considered. This means first that the elastic pole lies in the centre of gravity of a bar of unit weight given by Eq. (8.46), and secondly that the axes $\bar{x}, \bar{y}$, along which the redundants are acting, are the principal axes of inertia of the bar.

Following further this analogy, we find that the coefficients of the diagonal matrix $\mathbf{D}$ express the mass and the principal moments of a bar weighting (8.46):

$$\delta_{11} = \int_s \mu \mathrm{d}s, \qquad \delta_{22} = \int_s \mu \bar{x}^2 \mathrm{d}s, \qquad \delta_{33} = \int_s \mu \bar{y}^2 \mathrm{d}s. \tag{8.47}$$

The elastic pole technique can also be used for an out-of-plane, loaded curved bar, and for a bar making a closed plane circuit. However, the applicability of this technique is rather limited.

To conclude, it should be noted once again that the selection of redundants is of paramount importance for the direct flexibility method. The practical usefulness of the direct flexibility method depends largely on the ingenuity of the engineer who is allowed substantial freedom to use his inventiveness and experience. For this reason, the force method lends itself less to complete algorithmization with the aid of computer technique than does the direct stiffness method. This does not preclude, however, abandoning the use of digital computers for labourious calculations though well prepared beforehand by man's conceptual work.

It must be noted that several techniques of automatic selection of the primary system have been proposed in the literature (cf. Robinson, 1973).

9. The Direct Stiffness Method (Displacement Method)

9.1. Frames with Inextensible Bars

The general principles of procedure for the direct stiffness method have already been discussed in Section 6.4. It can be used, for example, for trusses (Section 6.2), in which the truss members experience estensions, those being the sole strains in these elements. In the case of frames, as we have demonstrated in earlier sections, the influence of longitudinal and transverse forces on strains is slight and can be neglected as a rule. In most cases, therefore the model of a framework is an arrangement of bars which experience bending alone, but are not susceptible to the action of axial forces. Possible extensions of these bars can be caused by non-static agents, e.g., by a rise in temperature.

By assuming bars to be inextensible, it becomes possible to make a distinction between frames with displaceable and non-displaceable joints*. Frames, in which none of the joints can experience sidesways, will be referred to simply as non-displaceable frames, all others, displaceable. To find out which kind of frame is involved, we replace all joints of a frame by hinges and check whether or not the substitute truss thus formed is kinematically variable. The degree of kinematic variability of the substitute truss is the number of geometric parameters describing the sidesways of all joints of the frame. Hence, the degree of geometric indeterminability of a plane frame equals the number of free joints plus the degree of kinematic variability. In calculating the degree of geometric indeterminability of a space frame with inextensible bars, the number of joints should be multiplied by three and the degree of kinematic variability of the substitute truss added to the product.

Whereas the chords of bars in a non-displaceable frame experience no rotations, those in a displaceable frame do rotate at certain angles. Their values (like the sidesway values of joints) can be expressed by geometric

---

* Sidesways of joints are involved here.

parameters, linearly independent of each other, whose number equals the degree of kinematic variability of the substitute truss. The selection of these parameters in the case of frame of an orthogonal grid does not present any appreciable difficulty. For example, the frame in Fig. 9.1a is a 17-fold geo-
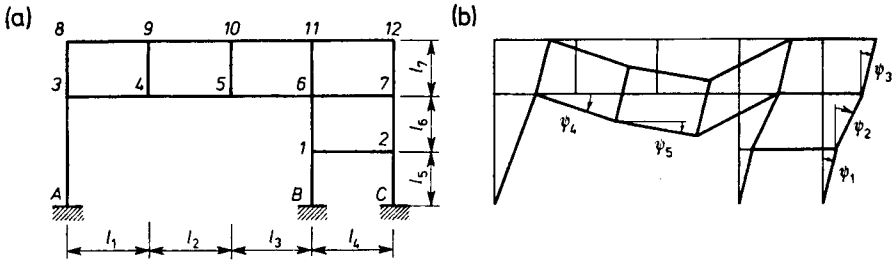
Fig. 9.1. Frame with orthogonal network

metrically indeterminate structure because outside the angular displacements of twelve joints, five unknown sideways occur in addition: three horizontal, bars *1–2*, *3–7* and *8–12*, and two vertical, bars *4–9* and *5–10*.

However, instead of operating with sidesway quantities which differ in denomination from angular displacements of joints, it is better to take for the unknowns the angular displacements of chords ψ_i (Fig. 9.1b). Using these five quantities, we can express the angular displacements of the chords of all bars:

$$\psi_{B1} = \psi_{C2} = \psi_1, \qquad \psi_{16} = \psi_{27} = \psi_2,$$

$$\psi_{38} = \psi_{49} = \psi_{5,10} = \psi_{6,11} = \psi_{7,12} = \psi_3,$$

$$\psi_{34} = \psi_{89} = \psi_4, \qquad \psi_{45} = \psi_{9,10} = \psi_5,$$

$$\psi_{A3} = \frac{\psi_1 l_5 + \psi_2 l_6}{l_5 + l_6},$$

$$\psi_{56} = \psi_{10,11} = -\frac{\psi_4 l_1 + \psi_5 l_2}{l_3}.$$

Somewhat more troublesome is to relate the angular displacements of chords (and joints) to the quantities taken as unknown for frames of non-orthogonal grid.

EXAMPLE 9.1

Let us establish the equations of the direct stiffness method for the frame in Fig. 9.2a.

The structure is sixfold geometrically indeterminate. Outside the rotations of joints, there are two geometric parameters describing the rotations of chords. Figure 9.2b shows the displacements of bars accompanying the rotation of the chord of bar a by angle q_5. Owing to the parallelism of bars
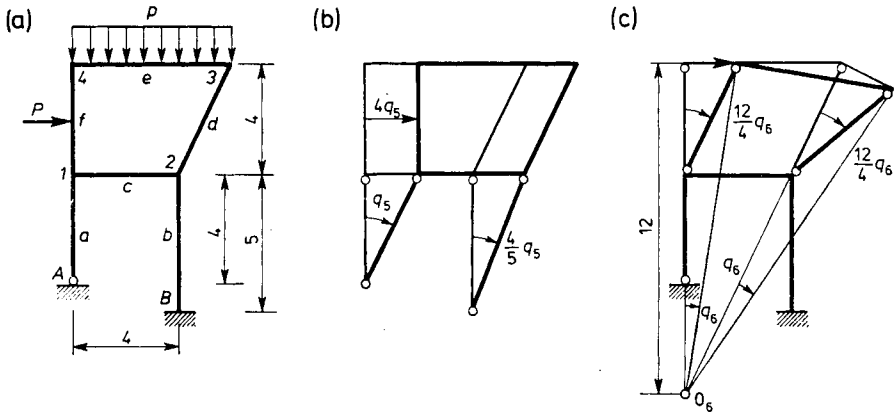
Fig. 9.2. Frame with non-orthogonal network

a and b, the entire top part of the frame shifts horizontally by segment $4\,q_5$, while bar b rotates by angle $\frac{4}{5}q_5$. Figure 9.2c shows the deformation of the frame caused by rotation of bar e by angle q_6 about point O_6 found on the intersection of bars d and f. It is readily apparent that both bars experience identical rotations by angle $\frac{12}{4}\,q_6$.

Hence, we have

$$\varphi_1 = q_1, \quad \varphi_2 = q_2, \quad \varphi_3 = q_3 + q_6, \quad \varphi_4 = q_4 + q_6,$$
$$\psi^a = q_5, \quad \psi^b = 0.8q_5, \quad \psi^c = 0, \quad \psi^d = \psi^f = 3q_6,$$
$$\psi^e = q_6.$$

Neglecting possible displacements of supports, we write the relation (6.82) as follows:

$$\boldsymbol{\epsilon} = \mathbf{Bq}, \tag{a}$$

where

$$\boldsymbol{\epsilon} = \{\varphi_{1A}, \varphi_{B2}, \varphi_{2B}, \varphi_{12}, \varphi_{21}, \varphi_{23}, \varphi_{32}, \varphi_{34}, \varphi_{43}, \varphi_{41}, \varphi_{14}\}, \tag{b}$$

$$
\mathbf{B} =
\begin{array}{c}
 \\
1A \\
B2 \\
2B \\
12 \\
21 \\
23 \\
32 \\
34 \\
43 \\
41 \\
14
\end{array}
\begin{array}{cccccc}
1 & 2 & 3 & 4 & 5 & 6 \\
\end{array}
\left[
\begin{array}{cccccc}
1 & & & & -1 & \\
& & & & -0.8 & \\
& 1 & & & -0.8 & \\
1 & & & & & \\
& 1 & & & & \\
& 1 & & & & -3 \\
& & 1 & & & 1-3 \\
& & 1 & & & \\
& & & 1 & & \\
& & & 1 & & 1-3 \\
1 & & & & & -3
\end{array}
\right],
$$

(c)

$$ \mathbf{q} = \{q_1, q_2, \ldots, q_6\}. \tag{d} $$

By using the principle of virtual work, we derive the equilibrium conditions whose general form is given by Eq. $(6.83)_1$. Regarding the first four equations, their meaning is obvious: the sums of moments acting on successive joints must equal zero. We multiply the first four columns of $\mathbf{B}$ by the single column matrix of the moments in end cross-sections:

$$ \boldsymbol{\sigma} = \{M_{1A}, M_{B2}, M_{2B}, M_{12}, M_{21}, M_{23}, M_{32}, M_{34}, M_{43}, M_{41}, M_{14}\}. \tag{e} $$

With the aim of determining the fifth equation, we subject the frame to virtual displacement δq_5, analogous to that shown in Fig. 9.2b. The work done by external loadings and the moments in end cross-sections on these displacements is:

$$ M_{1A}\delta q_5 + (M_{B2} + M_{2B}) \cdot 0.8\delta q_5 + P \cdot 4\delta q_5 = 0. $$
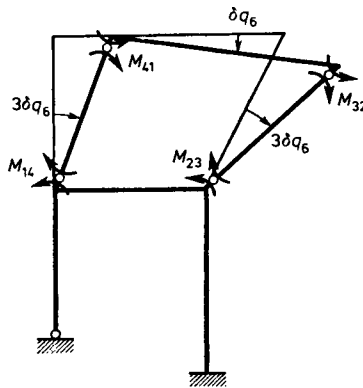
Fig. 9.3. Bar-end-moments doing work on virtual rotations of chords

It is easily seen that the fifth column of $\mathbf{B}$ contains (with opposite signs) the coefficients occurring by the moments in end cross-sections in the equation above. The first non-zero term of vector $\mathbf{Q}^p$ appears here: $Q_5^p = 4P$.

By calculating the virtual work done on displacement δq_6 (cf. Fig. 9.2c), it should be noted that moments M_{32} and M_{41} act not only on bars d and f, but also on joints 3 and 4 rotating along with bar e (Fig. 9.3). Hence, the virtual work in this case:

$$(M_{23}+M_{14})3\delta q_6 + (M_{32}+M_{41})(3-1)\,\delta q_6 + P\cdot 3\delta q_6 \cdot \tfrac{4}{2} + p\cdot 6\delta q_6 \cdot \tfrac{6}{2} = 0.$$

We find the respective coefficients with opposite signs in the sixth column of $\mathbf{B}$. The next term of vector $\mathbf{Q}^P$ is $Q_6^P = 6P + 18p$.

Using Eqs. (6.71) and (6.73) and neglecting the influence of shear forces, we obtain the elasticity matrix

$$\mathbf{E} = \frac{EJ^c}{l^c}
\begin{bmatrix}
3\varkappa^a & & & & & & & & & & \\
 & 4\varkappa^b & 2\varkappa^b & & & & & & & & \\
 & 2\varkappa^b & 4\varkappa^b & & & & & & & & \\
 & & & 4 & 2 & & & & & & \\
 & & & 2 & 4 & & & & & & \\
 & & & & & 4\varkappa^d & 2\varkappa^d & & & & \\
 & & & & & 2\varkappa^d & 4\varkappa^d & & & & \\
 & & & & & & & 4\varkappa^e & 2\varkappa^e & & \\
 & & & & & & & 2\varkappa^e & 4\varkappa^e & & \\
 & & & & & & & & & 4\varkappa^f & 2\varkappa^f \\
 & & & & & & & & & 2\varkappa^f & 4\varkappa^f
\end{bmatrix},
\qquad \text{(f)}$$

where EJ^c/l^c relating to bar c has been taken as a comparative quantity and the denotations

$$\varkappa^i = \frac{J^i}{J^c}\frac{l^c}{l^i} \qquad (i = a, b, d, e, f) \tag{g}$$

have been introduced.

Multiplying the matrix in accordance with Eq. (6.93), we obtain the stiffness matrix:

$$\mathbf{K} = \frac{EJ^c}{l^c} \times$$

$$\times
\begin{bmatrix}
3\varkappa^a+4+4\varkappa^f & 2 & 0 & 2\varkappa^f & -3\varkappa^a & -16\varkappa^f \\
2 & 4\varkappa^b+4+4\varkappa^d & 2\varkappa^d & 0 & -4.8\varkappa^b & -16\varkappa^d \\
0 & 2\varkappa^d & 4\varkappa^d+4\varkappa^e & 2\varkappa^e & 0 & -14\varkappa^d \\
2\varkappa^f & 0 & 2\varkappa^e & 4\varkappa^e+4\varkappa^f & 0 & -14\varkappa^f \\
-3\varkappa^a & -4.8\varkappa^b & 0 & 0 & 3\varkappa^a+7.68\varkappa^b & 0 \\
-16\varkappa^f & -16\varkappa^d & -14\varkappa^d & -14\varkappa^f & 0 & 76\varkappa^d+76\varkappa^f
\end{bmatrix}.$$

$$\text{(h)}$$

The right-hand side of the set of equations (6.92) is—in the present example —the sum of the vector

$$\mathbf{Q}^p = \{0,0,0,0,4P,6P+18p\},\tag{i}$$

and the product—$\mathbf{B}^T\boldsymbol{\sigma}^0$, where

$$\boldsymbol{\sigma}^0 = \{0,0,0,0,0,0,0,3p,-3p,\tfrac{1}{2}P,-\tfrac{1}{2}P\}$$

is an array of moments in end cross-sections induced by an external load acting on a structure with joints experiencing neither angular displacements nor sideswaies. Performing the prescribed operations, we obtain finally the right-hand side of the set of equations:

$$\mathbf{Q}^p-\mathbf{B}^T\boldsymbol{\sigma}^0 = \{\tfrac{1}{2}P,0,-3p,3p-\tfrac{1}{2}P,4P,\tfrac{11}{2}P+18p\}.$$

9.2. Frames on Continuous Foundations

We have discussed in Section 5.4 elements resting on an elastic foundation. These elements may serve as models of continuous foundations, on which frameworks are frequently based. The principles of composing the canonical equations of the direct stiffness method given in Section 6.3 apply also to frames containing elements on an elastic foundation. A fundamental difference appears in the structure of the elasticity matrix $\mathbf{E}$, and what follows, in the transformation equations of the displacement method, which relate static boundary quantities with displacements.

We must therefore begin with our considerations from a bar with no external loads acting over its length and with its ends experiencing forced displacements (Fig. 9.4). Assume that the bar rests on a two-parameter
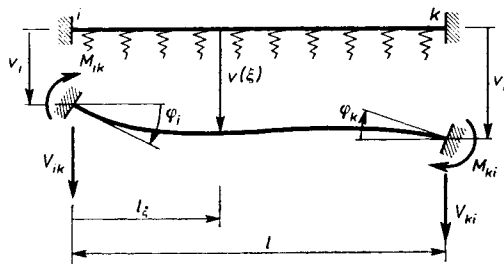
Fig. 9.4. Bar on elastic foundation

Winkler's foundation and that it is sufficiently slender to allow the influence of shear strains on deflection to be neglected. The solution of the problem is described by functions analogous to (5.61) and (5.67), which in the case of a bar subjected to beding in plane xy have the form

$$v = A_1 \operatorname{Ch} \mu\xi \cos\nu\xi + A_2 \operatorname{Sh} \mu\xi \sin\nu\xi + A_3 \operatorname{Ch} \mu\xi \sin\nu\xi + A_4 \operatorname{Sh} \mu\xi \cos\nu\xi,$$

$$\varphi_z = \frac{v'}{l}, \qquad M_z = \frac{EJ_z}{l^2} v'', \qquad T_y = -\frac{EJ_z}{l^3} (v''' - 4tv'). \tag{9.1}$$

We determine the integration constants from the boundary conditions

$$v(0) = v_i, \qquad v(1) = v_k,$$
$$v'(0) = l\varphi_{zi}, \qquad v'(1) = l\varphi_{zk}, \tag{9.2}$$

and then by performing suitable transformations and operations we arrive at the relationships between static and geometric quantities:

$$\begin{bmatrix} M_{zik} \\ M_{zki} \\ lV_{ik} \\ lV_{ki} \end{bmatrix} = \frac{EJ_z}{l} \begin{bmatrix} \alpha & \beta & \vartheta & -\delta \\ \beta & \alpha & \delta & -\vartheta \\ \vartheta & \delta & \gamma & -\varepsilon \\ -\delta & -\vartheta & -\varepsilon & \gamma \end{bmatrix} \begin{bmatrix} \varphi_{zi} \\ \varphi_{zk} \\ v_i/l \\ v_k/l \end{bmatrix}. \tag{9.3}$$

The coefficients of the above matrix of the transformation are expressed as follows:

$$\alpha(\mu, \nu) = 2\mu\nu \frac{\nu CS - \mu cs}{\nu^2 S^2 - \mu^2 s^2},$$

$$\beta(\mu, \nu) = 2\mu\nu \frac{\mu Cs - \nu Sc}{\nu^2 S^2 - \mu^2 s^2},$$

$$\vartheta(\mu, \nu) = (\mu^2 + \nu^2) \frac{\nu^2 S^2 + \mu^2 s^2}{\nu^2 S^2 - \mu^2 s^2},$$

$$\delta(\mu, \nu) = 2\mu\nu(\mu^2 + \nu^2) \frac{Ss}{\nu^2 S^2 - \mu^2 s^2}, \tag{9.4}$$

$$\gamma(\mu, \nu) = 2\mu\nu(\mu^2 + \nu^2) \frac{\nu CS + \mu cs}{\nu^2 S^2 - \mu^2 s^2},$$

$$\varepsilon(\mu, \nu) = 2\mu\nu(\mu^2 + \nu^2) \frac{\mu Cs + \nu Sc}{\nu^2 S^2 - \mu^2 s^2},$$

where:

$$C = \operatorname{Ch}\mu, \qquad S = \operatorname{Sh}\mu, \qquad c = \cos\nu, \qquad s = \sin\nu. \tag{9.5}$$

The above equations apply also to the special case of a beam resting on a one-parameter Winkler's foundation. Considering the relation (5.69), Eqs. (9.4) take as simpler form:

$$\alpha(\mu) = 2\mu \frac{CS - cs}{S^2 - s^2}, \qquad \beta(\mu) = 2\mu \frac{Cs - Sc}{S^2 - s^2},$$

$$\vartheta(\mu) = 2\mu^2 \frac{S^2 + s^2}{S^2 - s^2}, \qquad \delta(\mu) = 4\mu^2 \frac{Ss}{S^2 - s^2}, \tag{9.6}$$

$$\gamma(\mu) = 4\mu^3 \frac{CS + cs}{S^2 - s^2}, \qquad \varepsilon(\mu) = 4\mu^3 \frac{Cs + Sc}{S^2 - s^2}.$$

Equations of type (9.3) and (6.9) applying to other support schemes of bar ends and also appropriate numerical tables can be found, for example, in the monograph by Błaszkowiak and Kączkowski (1966).

Note that in the case of bars resting on an elastic foundation, angular displacements of chords cannot be taken for the geometric unknowns and just displacements of joints. The further procedure is exactly the same as that discussed in Section 6.6.

EXAMPLE 9.2

Compose the canonical equations of the direct stiffness method for the frame shown in Fig. 9.5a.
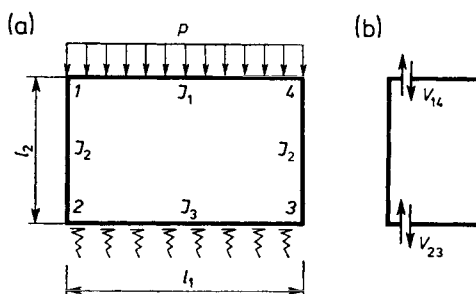
Fig. 9.5. Rectangular frame on continuous footing

Considering the symmetry of the structure and the loadings, the frame should be treated as a three fold geometrically indeterminate structure, in which the unknowns are:

$$\varphi_1 = -\varphi_4 = q_1, \qquad \varphi_2 = -\varphi_3 = q_2,$$
$$v_1 = v_2 = v_3 = v_4 = l_1 q_3.$$

The equilibrium equations for joints *1* and *2* and the equilibrium equation for the vertical forces acting on bar *1–2* (Fig. 9.5b) lead to the set of canonical equations:

$$
\begin{bmatrix}
\dfrac{2EJ_1}{l_1} + \dfrac{4EJ_2}{l_2} & \dfrac{2EJ_2}{l_2} & 0 \\[2mm]
\dfrac{2EJ_2}{l_2} & \dfrac{4EJ_2}{l_2} + (\alpha - \beta)\dfrac{EJ_3}{l_1} & (\vartheta - \delta)\dfrac{EJ_3}{l_1} \\[2mm]
0 & (\vartheta - \delta)\dfrac{EJ_3}{l_1} & (\gamma - \varepsilon)\dfrac{EJ_3}{l_1}
\end{bmatrix}
\begin{bmatrix}
q_1 \\[2mm] q_2 \\[2mm] q_3
\end{bmatrix}
+
\begin{bmatrix}
-\dfrac{pl_1^2}{12} \\[2mm] 0 \\[2mm] -\dfrac{pl_1^2}{2}
\end{bmatrix}
= 0.
$$

9.3. Frames Loaded by Considerable Axial Forces

In many cases, the axial forces occurring in frame bars are so great that their influence on the bending of the bars cannot be neglected. To allow for this influence in our considerations, it is necessary to make appropriate generalizations for the transformation formulae of the direct stiffness method. This is easily achieved setting out from the formulae and equations derived in Section 5.5.
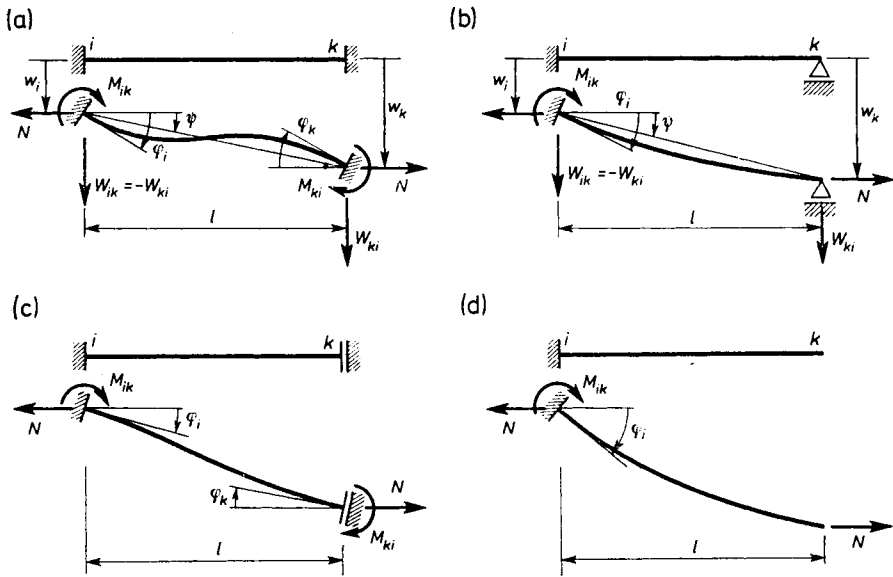
Fig. 9.6. Diagrams of bars by large axial forces

Let us consider successively the schemes of bars shown in Fig. 9.6. Using appropriate conditions of equilibrium, we obtain:
    (a) for a bar elastically clamped at both ends (Fig. 9.6a)

$$\begin{bmatrix} M_{ik} \\ M_{ki} \\ lW_{ki} \end{bmatrix} = \frac{EJ}{l} \begin{bmatrix} \alpha & \beta & -\vartheta \\ \beta & \alpha & -\vartheta \\ -\vartheta & -\vartheta & \delta \end{bmatrix} \begin{bmatrix} \varphi_i \\ \varphi_k \\ \psi \end{bmatrix}, \tag{9.7}$$

whereby using the denotations

$$C = \text{Ch}\,\lambda, \quad S = \text{Sh}\,\lambda, \tag{9.8}$$

we have

$$\alpha(\lambda) = \lambda \frac{\lambda C - S}{\lambda S - 2C + 2}, \qquad \beta(\lambda) = \lambda \frac{S - \lambda}{\lambda S - 2C + 2},$$

$$\vartheta(\lambda) = \lambda^2 \frac{C - 1}{\lambda S - 2C + 2}, \qquad \delta(\lambda) = \lambda^3 \frac{S}{\lambda S - 2C + 2}; \tag{9.9}$$

(b) for a bar clamped at one end and simply supported at the other (Fig. 9.6):

$$\begin{bmatrix} M_{ik} \\ l W_{ki} \end{bmatrix} = \frac{EJ}{l} \begin{bmatrix} \alpha' & -\alpha' \\ -\alpha' & \delta' \end{bmatrix} \begin{bmatrix} \varphi_i \\ \psi \end{bmatrix}, \tag{9.10}$$

where:

$$\alpha'(\lambda) = \lambda^2 \frac{S}{\lambda C - S}, \qquad \delta'(\lambda) = \lambda^2 \frac{C}{\lambda C - S}, \tag{9.11}$$

(c) for a bar clamped at one end and clamped at the other but so that it can slide:

$$\begin{bmatrix} M_{ik} \\ M_{ki} \end{bmatrix} = \frac{EJ}{l} \begin{bmatrix} \alpha'' & \beta'' \\ \beta'' & \alpha'' \end{bmatrix} \begin{bmatrix} \varphi_i \\ \varphi_k \end{bmatrix}, \tag{9.12}$$

where:

$$\alpha''(\lambda) = \lambda \frac{C}{S}, \qquad \beta''(\lambda) = -\frac{\lambda}{S}; \tag{9.13}$$

(d) for a cantilever bar (Fig. 9.6d):

$$M_{ik} = \frac{EJ}{l} \alpha''' \varphi_i, \tag{9.14}$$

where:

$$\alpha'''(\lambda) = \lambda \frac{S}{C}. \tag{9.15}$$

Using the general solution (5.80) with homogeneous boundary conditions, we determine the generalized boundary forces induced by external loading acting transverse to the bar axis or by initial deflection. For the bars presented in Fig. 9.6, they are successively

(a) $w(0) = w'(0) = w(1) = w'(1) = 0,$

(b) $w(0) = w'(0) = w(1) = w''(1) = 0,$

(c) $w(0) = w'(0) = w'(1) = w'''(1) = 0,$ $\qquad (9.16)$

(d) $w(0) = w'(0) = w''(1) = w'''(1) - \lambda^2 w'(1) = 0.$
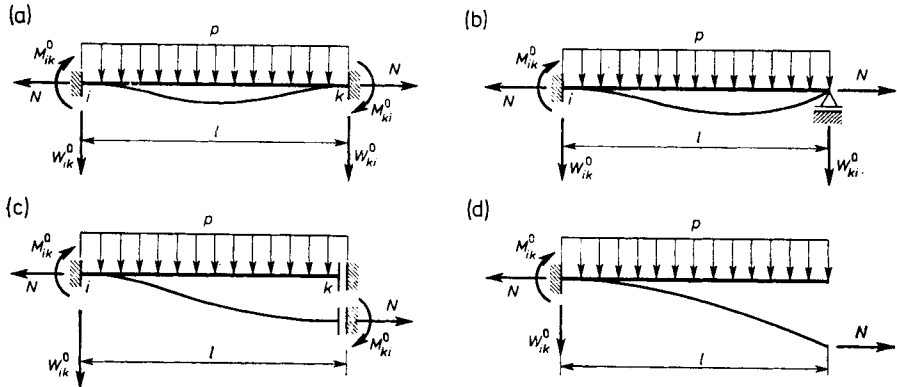
Fig. 9.7. Bars with different support conditions uniformly loaded

For example, uniformly distributed loading p_z (Fig. 9.7) induces support reactions equalling the following values respectively:

(a) $M_{ik}^0 = -M_{ki}^0 = -\dfrac{p_z l^2}{2\vartheta(\lambda)}, \qquad W_{ik}^0 = W_{ki}^0 = -\dfrac{p_z l}{2},$

(b) $M_{ik}^0 = -\dfrac{p_z l^2}{2\alpha(\lambda)}, \qquad W_{ik}^0 = -\dfrac{p_z l}{2}\left(1+\dfrac{1}{\alpha(\lambda)}\right),$

   $\qquad W_{ki}^0 = -\dfrac{p_z l}{2}\left(1-\dfrac{1}{\alpha(\lambda)}\right),$

(9.17)

(c) $M_{ik}^0 = -\dfrac{p_z l^2}{\alpha'(\lambda)}, \qquad M_{ki}^0 = -p_z l^2\,\dfrac{S-\lambda}{\lambda^2 S},$

   $\qquad W_{ik}^0 = -p_z l,$

(d) $M_{ik}^0 = -p_z l^2\,\dfrac{\lambda S - C + 1}{\lambda^2 C}, \qquad W_{ik}^0 = -p_z l.$

In the case of compressed struts, argument λ is an imaginary number (5.83), and functions (9.9), (9.11), (9.13) and (9.15) with the connotations

$\qquad \cos\sigma = c, \qquad \sin\sigma = s$ (9.18)

take the form:

$\qquad \alpha(\sigma) = \sigma\,\dfrac{s-\sigma c}{2-2c-\sigma s}, \qquad \beta(\sigma) = \sigma\,\dfrac{\sigma-s}{2-2c-\sigma s},$

(9.19)

$\qquad \vartheta(\sigma) = \sigma^2\,\dfrac{1-c}{2-2c-\sigma s}, \qquad \delta(\sigma) = \sigma^3\,\dfrac{s}{2-2c-\sigma s},$

$$\alpha'(\sigma) = \sigma^2 \frac{s}{s - \sigma c}, \qquad \delta'(\sigma) = \sigma^3 \frac{c}{s - \sigma c}, \tag{9.20}$$

$$\alpha''(\sigma) = \sigma \frac{c}{s}, \qquad \beta''(\sigma) = -\frac{\sigma}{s}, \qquad \alpha'''(\sigma) = -\sigma \frac{s}{c}. \tag{9.21}$$

The knowledge of transformation formulae in precise form enables more accurate static analysis of frameworks loaded by considerable axial forces. Tables of functions (9.19)–(9.21) can be found, for example, in a paper by Chwalla (1959) and in monographs by Błaszkowiak and Kączkowski (1959, 1966).

Proceeding to establish the conditional equations of the displacement method, it is first necessary to determine the values of the axial forces, since it is precisely these values on which the rigidities of individual bars depend. On the other hand, until the problem is solved, the exact values of the axial forces cannot be known. To break this vicious circle, we must out of necessity confine ourselves to rough estimates of the axial force values.

In the case of frames without sidesway the usual procedure is to substitute the frame by a truss by replacing rigid joints with hinges. The axial forces in the members of such a comparable truss are treated as approximate values of the forces occurring in the frame.

The problem gets somewhat more complicated for frames with sidesway since the equivalent truss would then be geometrically variable. For this reason, one can hardly recommend any particular procedural principle, since the method of estimating the axial force values will depend on the actual pattern of the frame. A multi-story frame is shown as an example in Fig. 9.8a.
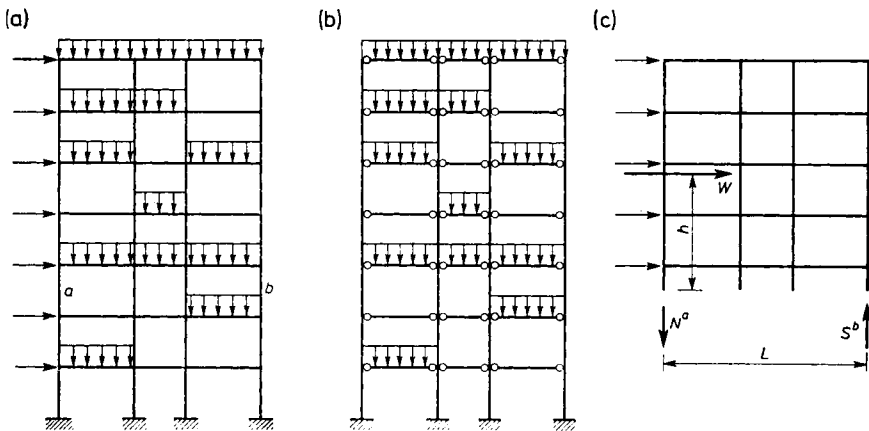
Fig. 9.8. Multi-stage frame: technique of approximate determination of axial forces

The axial forces deriving from vertical loadings can be determined proceeding in much the same way as for a frame without sidesway (Fig. 9.8b). We assume, however, that the horizontal loadings (Fig. 9.8c) are accompanied by the appearance of axial forces only in extreme columns:

$$N^a = S^b = \frac{Wh}{L}.\tag{9.22}$$

The symbol W stands here for the resultant of all horizontal forces located above the cross-section intersecting the story considered at half its height. The meaning of symbols h and L is explained in Fig. 9.8c.

Knowing the approximate values of the axial forces, we can determine the respective parameters σ or λ and put them into the transformation formulae, by means of which we form the elasticity matrix of frame E.

Having obtained the results, we can correct, if necessary, the values of the axial forces and repeat the calculation using the altered elasticity matrix.

It should be strongly emphasized that if axial forces are considered, the use of the principle of superposition is practically precluded. A change in the loading induces as a rule changes of the axial forces, which causes in turn a change in matrices E and K. Consequently, we cannot consider, for example, wind loading and vertical loadings separately and then take their sum. Hence, if the wind is acting on a structure loaded by vertical forces, we have to consider the two loadings jointly.

We shall demonstrate using a simple example the numerical differences obtained based on the theory of first order and of second order.

EXAMPLE 9.3

Determine the internal forces in the frame in Fig. 9.9a, in which all the bars are of identical length l and have identical cross-section with moment of
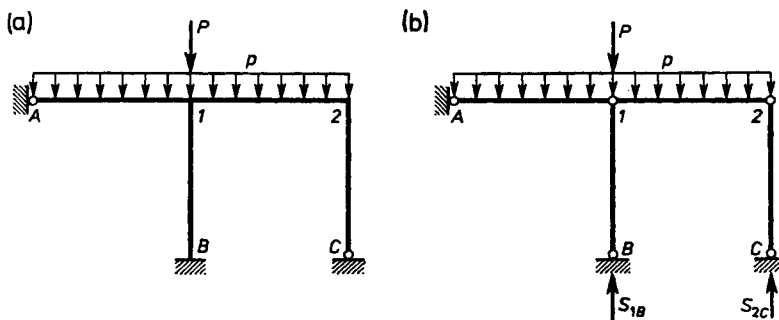
Fig. 9.9. Frame loaded by large axial forces

inertia J. Assume further, that the loadings indicated in the diagram are re-
lated to the parameters describing the rigidity of the columns as follows:

$$P = 2\frac{EJ}{l^2}, \quad p = 2\frac{EJ}{l^3}. \tag{a}$$

The approximate values of the axial forces (cf. Fig. 9.9b) are:

$$S_{1B} = pl+P = 4\frac{EJ}{l^2}, \quad S_{2c} = \frac{pl}{2} = \frac{EJ}{l^2}. \tag{b}$$

According to Eqs. (5.83), (9.19) and (9.20), we calculate successively

$$\sigma_{1B} = 2, \quad \sigma_{2c} = 1,$$
$$\alpha(2) = 3.436, \quad \beta(2) = 2.152, \quad \alpha'(1) = 2.795. \tag{c}$$

The moments at joints in a structure with non-rotable joints are:

$$M^0_{1A} = \frac{pl^2}{8} = \frac{EJ}{4l},$$

$$M^0_{12} = -M^0_{21} = -\frac{pl^2}{12} = -\frac{EJ}{6l}. \tag{d}$$

If we therefore form from all the moments at the joints, the matrix

$$\sigma = \{M_{1A}, M_{1B}, M_{B1}, M_{12}, M_{21}, M_{2c}\}, \tag{e}$$

then matrix σ^0 will have the form

$$\sigma^0 = \frac{EJ}{l}\{\tfrac{1}{4}, 0, 0, -\tfrac{1}{6}, \tfrac{1}{6}, 0\}. \tag{f}$$

We write the equilibrium conditions of joints briefly as:

$$\mathbf{B}^T\sigma = 0, \tag{g}$$

in which

$$\mathbf{B}^T = \begin{bmatrix} 1 & 1 & 0 & 1 & 0 & 0 \\ 0 & 0 & 0 & 0 & 1 & 1 \end{bmatrix}. \tag{h}$$

From equations of the (6.71) type and from Eqs. (9.7) and (9.10), we obtain
the following elasticity matrix of the structure:

$$\mathbf{E} = \frac{EJ}{l}\begin{bmatrix} 3 & & & & & \\ & 3.436 & 2.152 & & & \\ & 2.152 & 3.436 & & & \\ & & & 4 & 2 & \\ & & & 2 & 4 & \\ & & & & & 2.795 \end{bmatrix}, \tag{i}$$

and further the rigidity matrix

$$\mathbf{K} = \mathbf{B}^T \mathbf{E} \mathbf{B} = \frac{EJ}{l} \begin{bmatrix} 10.436 & 2 \\ 2 & 6.795 \end{bmatrix}, \tag{j}$$

and the matrix of free terms

$$-\mathbf{B}^T \boldsymbol{\sigma}^0 = -\frac{EJ}{l} \left\{ \frac{1}{12}, \frac{1}{6} \right\}. \tag{k}$$

Hence, having solved the set of equations

$$\mathbf{K}\mathbf{q} = -\mathbf{B}^T \boldsymbol{\sigma}^0, \tag{l}$$

we obtain

$$\mathbf{q} = \{\varphi_1, \varphi_2\} = \{-0.00348, -0.02350\}. \tag{m}$$

The moments at joints (e) are determined from the relation

$$\boldsymbol{\sigma} = \mathbf{E}\mathbf{B}\mathbf{q} + \boldsymbol{\sigma}^0$$

$$= \frac{EJ}{l} \{0.2396, -0.0120, -0.0075, -0.2276, 0.0657, -0.0657\}. \tag{n}$$

Only now can we obtain more accurate values of the axial forces:

$$S_{1A} = \frac{EJ}{l^2}(0.0657 + 0.0120 + 0.0075) = 0.0852 \frac{EJ}{l^2},$$

$$S_{1B} = \frac{EJ}{l^2}(4 + 0.2396 + 0.2276 - 0.0657) = 4.4015 \frac{EJ}{l^2},$$

$$S_{12} = 0.0657 \frac{EJ}{l^2}, \tag{o}$$

$$S_{2C} = \frac{EJ}{l^2}(1 - 0.2276 + 0.0657) = 0.8381 \frac{EJ}{l^2}.$$

Hence, the respective values of σ are:

$$\begin{aligned} \sigma_{1A} &= 0.292, \quad \sigma_{1B} = 2.098, \\ \sigma_{12} &= 0.256, \quad \sigma_{2C} = 0.915. \end{aligned} \tag{p}$$

Substituting these values into Eqs. (9.19) and (9.20), we find the new elasticity matrix

$$\mathbf{E} = \frac{EJ}{l} \begin{bmatrix} 2.983 & & & & & \\ & 3.375 & 2.170 & & & \\ & 2.170 & 3.375 & & & \\ & & & 3.991 & 2.002 & \\ & & & 2.002 & 3.991 & \\ & & & & & 2.828 \end{bmatrix}, \tag{q}$$

and the corresponding rigidity matrix

$$\mathbf{K} = \frac{EJ}{l} \begin{bmatrix} 10.349 & 2.002 \\ 2.002 & 6,819 \end{bmatrix}.$$ (r)

This time, we calculate the initial moments (cf. (d)) from Eqs. (9.17):

$$M^0_{1A} = \frac{pl^2}{2\alpha(\sigma_{1A})} = 0.2507 \frac{EJ}{l},$$

$$M^0_{12} = -M^0_{21} = -\frac{pl^2}{2\vartheta(\sigma_{12})} = -0.1669 \frac{EJ}{l}.$$

Proceeding further as in the first approximation, we obtain successively:

$$\mathbf{q} = \{-0.00356, \ -0.02343\},$$ (s)

$$\boldsymbol{\sigma} = \frac{EJ}{l} \{0.2400, \ -0.0120, \ -0.0077, \ -0.2280, \ 0.0663, \ -0.0663,$$ (t)

$$S_{1A} = 0.0860 \frac{EJ}{l}, \quad S_{1B} = 4.4017 \frac{EJ}{l},$$

$$S_{12} = 0.0663 \frac{EJ}{l}, \quad S_{2C} = 0.8383 \frac{EJ}{l},$$ (u)

$$\sigma_{1A} = 0.293, \quad \sigma_{1B} = 2.098,$$

$$\sigma_{12} = 0.257, \quad \sigma_{2C} = 0.916.$$ (w)

A comparison of values (w) and (p) shows that the second approximation is—in engineering sense—exact. But if we compare the values of moments at joints (n) obtained in the first approximation and those obtained in the second aproximation (t), we find that already in the first approximation we obtain results charged with an error of barely 0–0.9 per cent. Only in cross-section $B1$, in which the absolute value is more than 30 times less than that of the moment in cross-section $1A$, was the error 2.6 per cent. Therefore, in practice it would be sufficient to stop at the first approximation, and so it is done as a rule.

For the sake of comparison, we may also mention that with the influence of axial forces neglected, we obtain the following moments at joints:

$$\boldsymbol{\sigma} = \frac{EJ}{l} \{0.2397, \ -0.0137, \ -0.0068, \ -0.2260, 0.0685, \ -0.0685\}.$$

In this case, in horizontal bars, in which relatively small axial forces occur, the errors are also not too great, 0.1 to 3.2 percent. On the other hand, the

errors are quite considerable, up to 14.2 per cent, in the bar loaded by the highest axial force.

To conclude, it should be noted that the precise transformation formulae derived in this section, which allow for the influence of axial forces in terms of the theory of second order, enable the stability study of plane and space frames. The stability problems in bars and bar structures are discussed in Part 3 of the present volume.

References to Part 1

Abakanowicz B., 1876, *An Outline of Graphical Statics* (in Polish), Lwów.

Agarev V. A., 1963, *Method of Initial Functions for Two-dimensional Boundary Problems of the Theory of Elasticity* (in Russian), Izd. Akad. Nauk. Ukrain. SSSR, Kiev.

Arutyunyan N. Kh., Abramyan B. L., 1963, *Torsion of Elastic Bodies* (in Russian), Gos. Izd. Fiz.-Mat. Lit., Moskva.

Asplund S. O., 1964, *The Application of Matrix Algebra to Structural Statics* (in Polish), Ossolineum, Wrocław.

Asplund S. O., 1966, *Structural Mechanics. Classical and Matrix Methods*, Prentice Hall.

Bernoulli J. (Jacques), 1691, *Acta eruditorum.*

Bernoulli J. (Jean), 1742, *Opera omnia*, Lausannae–Genevae.

Betti E., 1872, *Il nuovo cimento* 2, 7 and 8.

Bleich F., Melan E., 1927, *Die gewöhnlichen und partiellen Differenzengleichungen der Baustatik*, Berlin.

Błaszkowiak S., Kączkowski Z., 1959, *The Cross Method* (in Polish), PWN, Warszawa.

Błaszkowiak S., Kączkowski Z., 1966, *Iterative Methods in Structural Analysis*, Pergamon Press—PWN, London–Warszawa.

Bolotin V. V., 1961, *Statistical Methods in Structural Mechanics* (in Russian), Gosstroiizdat, Moskva; Polish translation, Arkady, Warszawa 1968.

Borkowski A., 1988, *Analysis of Skeletal Structural Systems in the Elastic and Elastic-Plastic Range*, PWN—Elsevier, Warszawa, Amsterdam, Oxford, New York, Tokyo

Brandt A. M. (ed.), 1977, *Criteria and Methods of Structural Optimization* (in Polish) PWN—Polish Scientific Publishers, Warszawa; English transl.: PWN and Martinus Nijhoff Publishers, Warszawa, The Hague, Boston, Lancaster 1984.

Brzoska Z., 1961, *Statics and Stability of Bar Thin-Walled Structures* (in Polish), Warszawa.

Brzoska Z., 1972, *Strength of Materials* (in Polish), PWN, Warszawa.

Castigliano A., 1875, *Nouva teoria intorno dell'equilibrio dei sistemi elastici*, Atti della Academia delle Scienze, Torino.

Cauchy A. L., 1882, *Oeuvres complètes*, Paris.

Chwalla E., 1959, *Hilfstafeln zur Berechnung von Spannungsproblemen der Theorie zweiter Ordnung und von Knickproblemen*, Stahlbauverlag, Köln.

Clapeyron B. P. E., 1857, *Calcul d'une poutre élastique, repostant librement sur des appuis inégalement espécês*, Paris.

Clebsch A., 1862, *Theorie der Elastizität fester Körper*, Leipzig.

Cremona L., 1874, *Elementi di calculo graphico*, Torino.

Cremona L., 1879, *Le figure reciproche nella statica graphica*, Milano.

Cross H., 1930, *Analysis of continuous frames by distributing fixed-end moments*, Trans. ASCE.

Culmann K., 1866, *Die graphische Statik*, Zürich.

Dašek V., 1951, *Analysis of Frame Structures by Distributing Forces and Moments* (in Czech.), Technicko-vědecke nakladatelstvi, Praha.

Dowgird R., Dowgird Z., 1964, *Calculation of Skeletal Structures with the Use of Cracovians* (in Polish), PWN, Warszawa.

Dowgird Z., 1956, *Cracovians and their Application in Structural Mechanics* (in Polish), PWN, Warszawa.

Dowgird Z., Dowgird R., 1952, *Methods of Calculation of Frame Structures by Means of Cracovians* (in Polish), *Part I. Elementary frames*, PWN, Warszawa.

Dyląg Z., Krzemińska-Niemiec E., Filip F., 1974, *Structural Mechanics* (in Polish), PWN, Warszawa.

Eimer Cz., 1963, "Foundations of safety theory of structures" (in Polish), *Rozpr. Inż.* **11**, 1, 53–135.

Filin A. P., 1966, *Matrices in Statics of Skeletal Structures and Some Elements of Application of Digital Computers* (in Russian), Leningrad—Moskva.

Filonenko-Borodich M. M., 1945, *A Most Simple Model of Elastic Load-Distributing Foundation* (in Russian), Reports of Electrical Engineering Institute of Transport Engineers, No. 63, Transzeldorizdat, Moskva.

Filonenko-Borodich M. M., Izumov S. M., Olisov B. A., Kudryavtsev I. N., Malginov L. L., 1949, *Course of Strength of Materials. Part II* (in Russian), Gostekhizdat, Moskva—Leningrad.

Frąckiewicz H., 1966₁, "Geometry of a discrete set of points", *Arch. Mech. Stos.* **18**, 3, 285–300.

Frąckiewicz H., 1966₂, "Deformation of a discrete set of points", *Arch. Mech. Stos.* **18**, 6, 806–817.

Frąckiewicz H., 1970, *Mechanics of Lattice Media* (in Polish), PWN, Warszawa.

Frąckiewicz H., Legat A., 1967, "On singularity of some non-smooth surface structures" (in Polish), *Rozpr. Inż.* **15**, 2, 323–338.

Frąckiewicz H., Lewiński J., 1968, "Geometrical variability of regular multi-segmental structures. Part I", *Arch. Inż. Ląd.* **14**, 4, 619–629; "Part 2", 1970, *Arch. Inż. Ląd.* **16**, 1, 3–20.

Funk P., 1920, *Die linearen Differenzengleichungen und ihre Anwendung in der Theorie der Baukonstruktionen*, Berlin.

Gierszewski M., 1955, *Frames. Static Analysis* (in Polish), Budownictwo i Architektura, Warszawa.

Gorbunow-Posadov M. I., 1949, *Beams and Plates on Elastic Foundation*, (in Russian), Stroiizdat, Moskva.

Grüning M., 1918, "Anwendung von Differenzengleichungen in der Statik hochgradig statisch unbestimmter Tragwerke", *Eisenbau*, p. 122.

Grüning M., 1925, *Die Statik des ebenen Tragwerkes*, Springer-Verlag, Berlin.

Guldan R., 1949, *Rahmentragwerke und Durchlaufträger,* Springer-Verlag, Wien.

Gutkowski W., 1965, "Two-dimensional grid structures" (in Polish), *Mechanika Teoretyczna i Stosowana*, 3, 3, 79–94.

Gutkowski W., 1973, *Regular Skeletal Structures* (in Polish), PWN, Warszawa.

Gutkowski W., Obrębski J., Bauer J., Gierliński J., Rączka J., Żmijewski K., 1980, *Static Analysis of Space Structures* (in Polish), Arkady, Warszawa.

Henneberg L., 1886, *Statik der starren Systeme*, Darmstadt.

Huber M. T., 1948, *Theory of Elasticity* (in Polish), Vol. I, PAU, Vol. II, 1949, Kraków.

Huber M. T., 1951, *Technical Stereomechanics (Strength of Materials)* (in Polish), PZWS, Warszawa.

Jakubowicz A., Orłoś Z., 1966, *Strength of Materials* (in Polish), WNT, Warszawa.

Jastrzębski P., Mutermilch J., Orlowski W., 1974, *Strength of Materials* (in Polish), Arkady, Warszawa.

Jastrzębski P., Solecki R., Szymkiewicz J., 1970, *Trusses. Structural Analysis* (in Polish), Arkady, Warszawa.

Kachurin W. K., 1965, *Theory of Suspension Structures* (in Polish), Arkady, Warszawa.

Kacner A., 1969, *Bars and Plates of Variable Stiffness* (in Polish), PWN, Warszawa.

Kani G., 1954, *Die Berechnung mehrstöckiger Rahmen*, K. Wittwer, Stuttgart.

Karasiński L., 1930, *Strength of Materials* (in Polish), Student's Aid Organization of Warsaw Technical University, Warszawa.

Kączkowski Z., 1968, *Plates. Static Analysis* (in Polish), Arkady, Warszawa.

Kączkowski Z., 1975, "On the application of grouped loads method to static analysis of space trusses" (in Polish), *Arch. Inż. Ląd.* 21, 1, 113–123.

Kirchhoff G., 1876, *Vorlesungen über mathematische Physik*, Bd. I. *Mechanik*, Leipzig.

Kiselev V. A., 1960, *Structural Mechanics* (in Russian), Gosstroiizdat, Moskva.

Kluger W., 1876, *Lecture on Strength of Materials and Stability of Structures*, Paris.

Krynicki E., Mazurkiewicz Z., 1966, *Frames of Bars of Variable Rigidity* (in Polish), PWN, Warszawa.

Lagrange J. L., 1788, *Mecanique analytique*, Paris.

Laursen H., 1966, *Matrix Analysis of Structures*, New York.

Leśniak Z. K., 1970, *Methods of Optimization of Structures by Means of Digital Computers* (in Polish), Arkady, Warszawa.

Livesley R., 1964, *Matrix Methods of Structural Analysis*, New York.

Maizel V. M., 1951, *Temperature Problems of the Theory of Elasticity* (in Russian), Izd. Akad. Nauk Ukr. SSR, Kiev.

Maslennikov A. M., 1970, *Calculation of Statically Indeterminate Systems in Matrix Form* (in Russian), Leningrad.

Maxwell J. C., 1864, "On the calculation of the equilibrium and stiffness of frames", *Philosophical Magazine*, 4, 27, p. 294.

Menabrea F., 1858, "Nouveau principle sur la distribution des tension dans les systèmes elastiques", Compt. rend. l'Acad. des Sc. Paris, 46, p. 1056.

Mitropolski M. N., 1969, *Application of the Matrix Theory to Solving Problems of Structural Mechanics* (in Russian), Moskva.

Mohr Ch. O., 1906, *Abhandlungen aus dem Gebiete des technischen Mechanik*, Berlin.

Mossakowska Z., Nowacki W., Sokołowski M., Wesołowski Z., 1978, *Engineering Mechanics, Vol. IV, Elasticity* (in Polish), PWN, Warszawa.

Murzewski J., 1976, *Random Limit Analysis of Rod Structures* (in Polish), PWN, Warszawa.

Müller-Breslau H. F. B., 1881, *Elemente der graphischen Statik*, Berlin.

Müller-Breslau H. F. B., 1892, *Die graphische Statik der Baukonstruktionen*, Leipzig.

Nowacki W., 1952, *Structural Mechanics. Part I. Isostatic Systems* (in Polish), PWT, Poznań.

Nowacki W., 1954, *Structural Mechanics. Part 2. Hyperstatic Systems* (in Polish), PWN, Warszawa.

Peła R., Woźniak Cz., 1966, "Introduction to the theory of surface trusses" (in Polish), *Arch. Inż. Ląd.* **12**, 4, 475–490.

Perelmuter A. W., 1972, *Bar-Pull Rod Structures. Principles of Calculations* (in Polish), Arkady, Warszawa.

Poisson S. D., 1811, *Traité de mécanique*, Paris.

Popov E. E., 1948, *Non-linear Problems of Statics of Thin Bars* (in Russian), OGIZ, Leningrad–Moskva.

Prager W., 1926, "Beitrag zur Kinematik des Raumfachwerkes", *Z. angew. Math. Mech.*

Przemieniecki J., 1969, *Theory of Matrix Structural Analysis*, New York.

Rabinovich I. M., 1946, *Structural Mechanics of Skeletal Systems* (in Russian), Stroiizdat, Moskva.

Rakowski G., 1968, *Application of Matrices to the Static and Dynamic Analysis of Straight Bars* (in Polish), Arkady, Warszawa.

Rakowski G., Solecki R., 1965, *Curved Bars. Statical analysis* (in Polish), Arkady, Warszawa.

Ritter W., 1888, *Anwendung der graphischen Statik*, Zürich.

Ritter W., 1890, *Das Fachwerk*, Zürich.

Robinson J., 1973, *Integrated Theory of Finite Element Methods*, Wiley, New York.

de Saint-Venant B., 1856, "La flexion des prismes", *Journal de mathematiques*, Liouville, p. 89.

Schlink W., 1907, "Über Stabilitätsuntersuchung von Raumfachwerke", *Zeitschrift d. Deutschen Mathem. Vereinigung*, **16**.

Sokolnikov I. S., 1956, *Mathematical Theory of Elasticity*, McGraw-Hill, New York.

Thullie M., 1917, *Handbook of Structural Statics* (in Polish), Lwów.

Timoshenko S. P., 1934, *Structural Statics* (in Russian), Gosstroiizdat, Moskva.

Umanskii A. A., 1948, *Space Systems* (in Russian), Stroiizdat, Moskva.

Urbanowski W., 1956, "Some cases of flexure of a round plate connected with an elastic foundation with generalized properties", *Zesz. Nauk. Pol. Warsz. Mech.*, 3, 33–61.

Vlasov V. Z., Leontev H. H., 1960, *Beams, Plates and Shells on Elastic Foundation* (in Russian), Gosizdat. Fiz.-Mat. Literatury, Moskva.

Wasiutyński Z. 1956, "The fundamentals of shape optimization" (in Polish), *Arch. Inż. Ląd.* 2, 1/2, 3–16.

Wasiutyński Z., Brandt A., 1962, "The present state of knowledge in the field of shape optimization of structures (in Polish), *Rozpr. Inż.* 10, 2, 309–332.

Waszczyszyn Z., 1962, "An approximate computation of large elastic deflections of a beam on immovable supports" (in Polish), *Rozpr. Inż.* 10, 1, 97–113.

Waszczyszyn Z., Życzkowski M., 1962. "Finite elastic deflections of a stretchable beam on immovable supports", *Arch. Mech. Stos.*, 14, 1, 61–82.

Wierzbicki W., 1936, "Safety of structures as a probability problem" (in Polish), *Przegląd Techniczny*, Warszawa.

Wierzbicki W., 1961_1, *Objective Methods of Appraisal of Safety of Structures* (in Polish), PWN, Warszawa.

Wierzbicki W., 1961_2, *Structural Mechanics* (in Polish), PWN, Warszawa.

Williot, 1877, *Notations pratiques sur la statique graphique*, Publications scientifiques industrielles.

Winkler E., 1867, *Die Lehre von der Elastizität und Festigkeit*, Prag.

Woźniak Cz., 1969, "On the equations of the theory of lattice structures", *Arch. Mech. Stos.* **21**, 5, 539–555.

Woźniak Cz., 1970, *Lattice Type Plates and Shells* (in Polish), PWN, Warszawa.

Ylinen A., Mikkola M., 1967, "A beam on a Wieghardt-type elastic foundation", *Int. J. Sol. Struct.* **2**.

Zurmühl R., Falk S., 1984, *Matrizen und ihre Anwendungen*, Springer-Verlag, Berlin, Heidelberg, New York, Tokyo.

Zemochkin B. N., 1933, *Calculation of Frames* (in Russian). Gosstroiizdat, Moskva.

Zemochkin B. N., Pashchevskii D. P., 1950, *Structural Statics* (in Russian), Gos. Izd. Arch. i Gradostroitelstva, Moskva.

1. Introduction

In this brief part of the volume in which the subject matter is confined to the dynamics of bars and bar structures, we must take if for granted that the fundamental principles underlying dynamics are known to the reader from analytical mechanics. We refer in particular to Newton's laws (1687) and d'Alembert's principle (1743), as well as Lagrange's equations (1760), based on Euler's variational calculus (1744), and the most general principle of dynamics developed by Hamilton (1824). Those interested are referred to works in the area of theoretical mechanics and vibration theory (e.g. Whittaker, 1944; Ziemba, 1957, 1959; Landau and Lifshits, 1961; Rubinowicz and Królikowski, 1971; Babakov, 1965; Wilde and Wizmur, 1977; Osiński, 1980), and to monographs devoted entirely to the dynamics of solids (Dżygadło *et al.*, 1966; Fung, 1969; Counor, 1973, and others) or to structural dynamics (Timoshenko, 1955; Filippov, 1955, 1965, 1970; Snitko, 1960; Nowacki, 1972; Biggs, 1964; Hurty and Rubinstein, 1964; Panovko, 1971; Sułocki, 1976; Wierzbicki, 1980, and others). Similarly, we assume that the reader is familiar with such concepts as dynamical degrees of freedom or generalized Lagrange's coordinates.

Instead, we shall concentrate on problems strictly related to bar structures and discuss first and foremost the methods of solving dynamic problems, which pertain specifically to these structures. However, it should be made clear that the subject matter even though confined must be handled very concisely, considering that extensive monographs are devoted to the dynamics of bar structures alone (e.g. Chudnovskii, 1952; Koloušek, 1953; Lisowski, 1959; Solecki and Szamkiewicz, 1964).

As we have explained in Part 1, before proceeding to solve problems in the area of structural statics, we must first make a suitable schematization of the real structure considered, namely to replace a three-dimensional body by a system composed of bar or surface elements. A similar schematization is required when we intend to analyse its vibrations.

In dynamic problems, we deal, in addition to time variable external load-

ings, with forces of inertia proportional to mass of the body and accelerations of motion, and also with ,forces induced by the resistance of the medium, which are taken as a rule to be proportional to velocity. Every real body is made of a material with its mass distributed over the entire three-dimensional area occupied by the body. The mass distribution within a body describes therefore the density ϱ of the material that goes into its making measured in kg/m^3. As a result, the forces of inertia occurring in nature are always volume forces of the dimension (N/m^3). In bar structures, in the first, basic state of discretization, the density of the material ϱ is replaced by the mass μ (kg/m) distributed along the bar axis. The general relationship between the mass per unit length of the bar axis and the density of the material is:

$$\mu = \int_A \varrho \, dA, \tag{1.1}$$

in the case of a homogeneous body it takes the form:

$$\mu = \varrho A, \tag{1.2}$$

where A is the cross-sectional area.

In addition, we relate the mass moments of inertia of a cross-section to unit length of the bar axis, defined as follows:

$$I_y = \int_A \varrho z^2 \, dA, \quad I_z = \int_A \varrho y^2 \, dA, \quad I_0 = I_y + I_z. \tag{1.3}$$

In the particular case of a homogeneous body (cf. Part 1, Eq. (2.17)):

$$I_y = \varrho J_y, \quad I_z = \varrho J_z, \quad I_0 = \varrho J_0, \tag{1.4}$$

where J_0 is the polar moment of inertia of a cross-sectional area.

In this part of the book, we shall generalize the assumption concerning the mechanical properties of bodies. Along with linearly elastic bodies, we shall consider also structures of viscoelastic material. For its model we take the so-called *Kelvin–Voigt model*, which is discussed in Chapter 2. It is a body model most commonly used in dynamics, since it enables us to map well the so-called *internal damping effects*, observable during vibrations of a structure. Similarly, the resistance of a viscous medium is accompanied by external damping of vibration of a bar structure. Of course, the material model and types of damping considered do not cover all the problems involved here, to which many authors have devoted monographs and separate dissertations (e.g. Bieniek, 1952; Sorokin, 1962; Nowacki, 1963; Derski and Ziemba, 1968; Pisarenko *et al.*, 1976; Osiński, 1978).

In Chapter 2, our concern is dynamic analysis of single bars with a uniformly distributed mass, i.e., structural elements having infinitely-many

dynamic degrees of freedom. After deriving the differential equations of motion, we consider longitudinal, torsional and flexural (transverse) vibrations of straight and curved bars. In our considerations of transverse vibration of a straight bar, we have taken the model of the so-called *Timoshenko's beam* (1955), i.e., one in which both rotational inertia and strains due to shear forces are taken into account. Omission of these factors leads to solutions applying to vibrations of a slender bar most commonly used in engineering practice. The influence of constant axial forces and of an elastic foundation on transverse vibration of a straight bar has also been considered.

As for methods of solving the equations of motion, they can be classified most generally as analytical or numerical. Of the analytical methods we may cite as examples, the Laplace transform method, consistently used by Nowacki (1963, 1972) and the modal analysis involving the problem of determining the free vibration frequency of a structure. In Chapter 2, we use the latter method. The solutions thus obtained are exact in the sense that all quantities of interest to us can be determined in every cross-section and at every instant with preassumed arbitrary accuracy which depends only on the number of terms considered in the infinite series.

The solutions have been used in Chapter 3 for vibration analysis of bar structures. Two different approaches to the problem have been presented. An argumentation typical of the direct flexibility method leads to Volterra's integral equations. One of the techniques of approximate solving of these equations has been given. Using the direct flexibility method, it is not necessary to determine the frequency and form of free vibrations for the whole of the structure, which is sometimes rather troublesome. It will suffice to know the form of free vibration of individual comprising elements. The other approach, based on the direct stiffness method aims at finding the values and eigenfunctions of the structure as a whole. The application of this technique requires a generalization of the transformation formulae of the direct stiffness method.

Finally, in Chapter 4, we have demonstrated certain approximate methods of numerical analysis of vibration of a structure. They are based on an a priori reduction of the number of degrees of freedom; a structure with infinitely many degrees of freedom has been replaced by one with a finite number. As a result, a problem described by a single partial differential equation changes into one described by a finite number of ordinary differential equations. That reduction of the degrees of freedom can be performed in different ways, but it always leads to the same type of a matrix-differential equation.

Of the many existing techniques for solving this equation, one analogous to that given in Chapter 2 has been chosen and is discussed in greater detail.

It consists in expressing the solution by a sum of eigenvectors multiplied by the respective time functions. There are still many other techniques of matrix-differential integration of equations of motion. Numerous monographs treat these techniques and other problems involved with the use of matrix calculus in dynamics (e.g. Pestel and Leckie, 1963; Rakowski, 1968; Bishop *et al.*, 1972; Legras, 1974; Bathe and Wilson, 1976; Pietrzak *et al.*, 1979; Zurmühl and Falk, 1984). A method developed by Newmark (1959) has come to be widely used, and in Poland, Langer's method (1974) has become very popular. Since these are general methods, applicable not only to bar structures, not much space has been devoted to them in this chapter.

We may also mention the space-time finite elements method whose foundations were laid by Oden (1969) and Argyris and Scharpf (1969), and which was advanced by a different approach by Kączkowski (1975, 1979). It differs essentially from the afore-named methods as it leads directly to a set of algebraic equations, omitting the stage, in which motion is described by a set of ordinary differential equations. For lack of space the method could not be discussed, even cursorily.

As seen from this brief survey of the contents, we have confined ourselves in this part of the book (like in the preceding part) to linear problems of the dynamics of bars and bar structures, presenting at the same time selected methods of solving them. For we proceed from the assumptions that a reader interested in more involved problems, non-linear in particular, will have to fall back on more comprehensive textbooks and monographs devoted exclusively to problems of structural dynamics. The enclosed references may prove of assistance in finding appropriate sources.

2. Bars with Infinitely Many Dynamic Degrees of Freedom

2.1. General Relations

To derive the equations of motion for a bar of continuously distributed mass, we may use the fundamental principles of dynamics. Below, we base our considerations on d'Alembert's principle. In this connection, the loadings occurring in the differential equations of static equilibrium, derived in Part 1, will be complemented with forces of inertia and possibly with external resistance forces. For example, the static equations for a straight bar (cf. Part 1, Eqs. (2.4), (2.5) and (2.26)) convert to the dynamic equilibrium equations:

$$\frac{\partial N}{\partial x} - \mu \ddot{u} - \zeta_u \dot{u} + p_x = 0, \tag{2.1}$$

$$\frac{\partial M_t}{\partial x} - I_0 \ddot{\varphi}_t - \zeta_s \dot{\varphi}_t + m_t = 0, \tag{2.2}$$

$$\frac{\partial T_z}{\partial x} - \mu \ddot{w} - \zeta_w \dot{w} + p_z = 0,$$

$$\tag{2.3}$$

$$\frac{\partial M_y}{\partial x} - T_z - I_y \ddot{\varphi}_y - \zeta_y \dot{\varphi}_y + m_y = 0,$$

$$\frac{\partial T_y}{\partial x} - \mu \ddot{v} - \zeta_v \dot{v} + p_y = 0,$$

$$\tag{2.4}$$

$$\frac{\partial M_z}{\partial x} + T_y - I_z \ddot{\varphi}_z - \zeta_z \dot{\varphi}_z + m_z = 0.$$

Considering the analogies occurring between equations relating to longitudinal vibrations (2.1) and transverse vibrations in the zx plane (2.3), on the one hand, and equations relating to torsional vibrations (2.2) and transverse vibrations in the xy plane (2.4), on the other, we shall consider below only longitudinal vibrations and transverse vibrations in the zx plane. The solutions for torsional vibration will have the same form as the functions describing longitudinal vibration, with the denotations being suitably changed. Likewise,

transverse vibrations in the xy plane are easily described, once the solutions for vibrations of a bar in plane zx are known.

In these equations, we have used denotations given by Eqs. (1.1) and (1.3), which in the special case of a homogeneous bar can be replaced by Eqs. (1.2) and (1.4). The symbols ζ denote coefficients of external resistance which is by assumption proportional to the corresponding velocity of motion.

The main difference between static and dynamic equations is that the number of static equilibrium equations corresponds to the number of unknowns which are the internal forces, whereas in dynamic cases, the number of unknowns, which covers also displacements, is higher than the number of dynamic equilibrium equations. It follows that if only the boundary conditions permit, the set of equations of bar statics can be solved without having to determine the displacements of the structure; the problem of bar statics is said to be *internally* isostatic. Dynamic problems of bar structures on the other hand—regardless of the boundary conditions—are by their very nature internally hyperstatic.

A complete set of equations, whose number corresponds to that of the unknowns therein, must contain both dynamic equilibrium equations of type (3.1)–(3.4) and equations of geometry (cf. Part 1, Eqs. (2.11), (2.32), (4.7) and (4.8)):

$$\varepsilon = \frac{\partial u}{\partial x}, \tag{2.5}$$

$$\varkappa_y = \frac{\partial \varphi_y}{\partial x}, \qquad \beta_z = \frac{\partial w}{\partial x} + \varphi_y, \tag{2.6}$$

and also the relations between strains and internal forces.

The latter relations in the case of a body not dissipating elastic energy can be demonstrated in exactly the same way as in static terms (cf. Part 1, Eqs. (4.32), (4.36)). If, however, the energy dissipation effect within a vibrating body is to be considered, we should take in place of an elastic body model one of the viscoelastic body models,   the Kelvin–Voigt model as a rule.
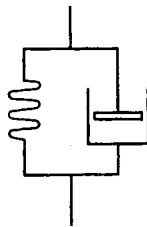
Fig. 2.1. Kelvin–Voigt viscoelastic body model

Various other rheological models, comprehensively discussed, for example, in monographs by Nowacki (1963) or Derski and Ziemba (1968), are applicable to the description of very slow phenomena, such as creep or relaxation, which are observable at least over many hours, but most often over a time measured in years. But, in dynamics we deal with phenomena taking place in seconds.

The Kelvin–Voigt model, presented schematically in Fig. 2.1, leads in uniaxial states of stress to the following stress–strain relations:

$$\sigma = E\varepsilon + \eta_E \dot{\varepsilon} = E(\varepsilon + t_E \dot{\varepsilon}),$$
$$\tau = G\gamma + \eta_G \dot{\gamma} = G(\gamma + t_G \dot{\gamma}). \qquad (2.7)$$

The quantities

$$t_E = \frac{\eta_E}{E}, \qquad t_G = \frac{\eta_G}{G} \qquad (2.8)$$

are so-called *retardation times* of longitudinal and transverse vibrations and these parameters are determined experimentally.

Setting out from the relations (2.7) and the definitions of internal forces (cf. Part 1, Eqs. (2.1)–(2.3)), we obtain the relations between internal forces and strains:

$$N = EA(\varepsilon + t_E \dot{\varepsilon}), \qquad (2.9)$$

$$M_y = EJ_y(\varkappa_y + t_E \dot{\varkappa}_y), \qquad T_z = \frac{GA}{k_z}(\beta_z + t_G \dot{\beta}_z). \qquad (2.10)$$

2.2. Vibration of a Straight Bar

2.2.1. The differential equations of motion

Substituting the relations (2.5) and (2.6) into Eqs. (2.9) and (2.10) and then into the equilibrium equations (2.1)–(2.4), we obtain a set of differential equations of motion for a straight bar:

$$\left(1 + t_E \frac{\partial}{\partial t}\right)\frac{\partial}{\partial x}\left(EA \frac{\partial u}{\partial x}\right) - \mu \frac{\partial^2 u}{\partial t^2} - \zeta_u \frac{\partial u}{\partial t} + p_x = 0, \qquad (2.11)$$

$$\left(1 + t_G \frac{\partial}{\partial t}\right)\frac{\partial}{\partial x}\left[\frac{GA}{k_z}\left(\frac{\partial w}{\partial x} + \varphi_y\right)\right] - \mu \frac{\partial^2 w}{\partial t^2} - \zeta_w \frac{\partial w}{\partial t} + p_z = 0,$$

$$\left(1 + t_E \frac{\partial}{\partial t}\right)\frac{\partial}{\partial x}\left(EJ_y \frac{\partial \varphi_y}{\partial x}\right) - \left(1 + t_G \frac{\partial}{\partial t}\right)\left[\frac{GA}{k_z}\left(\frac{\partial w}{\partial x} + \varphi_y\right)\right] - \qquad (2.12)$$

$$-I_y \frac{\partial^2 \varphi_y}{\partial t^2} - \zeta_y \frac{\partial \varphi_y}{\partial t} + m_y = 0.$$

It is apparent that Eq. (2.11) contains other unknowns than does the set of equation (2.12). It follows that longitudinal vibrations can be considered independent of transverse vibrations. However, the principle of superposition can be used here only when the absolute values of longitudinal forces are small against the critical forces causing buckling of the structure. We return to this problem in Section 2.4.

In order to solve the two vibration problems described by Eqs. (2.11) and (2.12), we use below the method of expanding the quantities sought into a series of eigenfunctions.

2.2.2. Longitudinal (torsional) vibrations of a straight bar

The integral of the differential equation (2.11) consists of the general integral of a homogeneous equation and the particular integral of a non-homogeneous equation. Therefore, we first let $p_x = 0$ and anticipate a solution in the form

$$u(x, t) = a(x)f_1(t) + b(x)f_2(t),$$ (2.13)

where the time functions have the structure

$$f_1 = e^{-\alpha\omega t}\cos\omega't, \quad f_2 = e^{-\alpha\omega t}\sin\omega't.$$ (2.14)

The symbols ω and ω' denote undamped and damped vibration frequency, respectively, and α is the damping coefficient. The derivatives of the function (2.14) are expressed:

$$\dot{f_1} = -\alpha\omega f_1 - \omega'f_2, \quad \ddot{f_1} = -(\omega'^2 - \alpha^2\omega^2)f_1 + 2\alpha\omega\omega'f_2,$$
$$\dot{f_2} = \omega'f_1 - \alpha\omega f_2, \quad \ddot{f_2} = -2\alpha\omega\omega'f_1 - (\omega'^2 - \alpha^2\omega^2)f_2.$$ (2.15)

Substituting the function (2.13) into the differential equation (2.11) and using the relations (2.15), we arrive at the set of ordinary differential equations for the eigenfunctions $a(x)$ and $b(x)$:

$$\frac{d^2a}{dx^2} + \lambda^2 a + \varepsilon\left(\frac{d^2b}{dx^2} + \gamma^2 b\right) = 0,$$

$$-\varepsilon\left(\frac{d^2a}{dx^2} + \gamma^2 a\right) + \frac{d^2b}{dx^2} + \lambda^2 b = 0.$$ (2.16)

In these equations we have used the denotations:

$$\lambda^2 = \frac{\mu(\omega'^2 - \alpha^2\omega^2) + \zeta_u\alpha\omega}{EA(1 - t_E\alpha\omega)},$$

$$\gamma^2 = \frac{2\mu\alpha\omega - \zeta_u}{EAt_E}, \quad \varepsilon = \frac{t_E\omega'}{1 - t_E\alpha\omega}.$$ (2.17)

The set of equations (2.16) can be separated in the case

$$\lambda^2 = \gamma^2. \tag{2.18}$$

Equating the respective terms given by Eqs. (2.17), we arrive at the relation

$$\mu t_E(\omega'^2 + \alpha^2\omega^2) - 2\mu\alpha\omega + \zeta_u = 0. \tag{2.19}$$

In turn, the assumption of the relation between damped and undamped vibrations (ω', ω) and the coefficient of damping α:

$$\omega' = \omega\sqrt{1-\alpha^2}, \tag{2.20}$$

allows the determination of the coefficient of damping according to Eq. (2.19)

$$\alpha = \frac{1}{2}\left(t_E\omega + \frac{\zeta_u}{\mu\omega}\right). \tag{2.21}$$

Substituting Eqs. (2.20) and (2.21) we find that

$$\lambda^2 = \gamma^2 = \frac{\mu\omega^2}{EA}. \tag{2.22}$$

It follows that with the assumptions (2.18) and (2.20) satisfied, the eigenfunctions $a(x)$ relating to damped vibration can be used in the same form as for undamped vibration. These functions should satisfy the differential equation

$$\frac{d^2a}{dx^2} + \lambda^2 a = 0 \tag{2.23}$$

and also given the boundary conditions. The integral of this equation is the function

$$a = A\cos\lambda x + B\sin\lambda x. \tag{2.24}$$

The homogeneous boundary conditions lead to a set of two homogeneous equations on account of the integration constants A, B. Hence, the condition for the existence of non-zero solutions is the vanishing of the principal determinant of the system. We obtain therefore a trigonometric equation having an infinite number of roots λ_k, related by Eq. (2.22) with free vibration frequencies ω_k.

Since the matrix of the set of equations expressing the boundary conditions is singular, we cannot determine uniquely the values of the integration constants, but we can certainly determine their proportions. In order to get rid of that non-uniqueness we have to normalize the eigenfunctions. For this purpose, we fall back on the following argumentation. Each of the eigen-

functions (in a more general case, $EA \neq$ const) satisfies a different differential equation:

$$\frac{\mathrm{d}}{\mathrm{d}x}\left(EA\,\frac{\mathrm{d}a_k}{\mathrm{d}x}\right) + \mu\omega_k^2 a_k = 0,$$

$$\frac{\mathrm{d}}{\mathrm{d}x}\left(EA\,\frac{\mathrm{d}a_j}{\mathrm{d}x}\right) + \mu\omega_j^2 a_j = 0. \tag{2.25}$$

Let us multiply the first of these equations by the eigenfunction a_j and the second by a_k and integrate the difference of the two products over the bar length. The fact to be considered here is that regardless of the boundary conditions that all the eigenfunctions are required to satisfy, the following relation must hold:

$$\int_0^l a_j\,\frac{\mathrm{d}}{\mathrm{d}x}\left(EA\,\frac{\mathrm{d}a_k}{\mathrm{d}x}\right)\mathrm{d}x = -\int_0^l \frac{\mathrm{d}a_j}{\mathrm{d}x}\,EA\,\frac{\mathrm{d}a_k}{\mathrm{d}x}\,\mathrm{d}x. \tag{2.26}$$

In this way, we arrive at the equality

$$(\omega_k^2 - \omega_j^2)\int_0^l a_j\mu a_k\,\mathrm{d}x = 0, \tag{2.27}$$

from which it follows that for $\omega_j \neq \omega_k$

$$\int_0^l a_j\mu a_k\,\mathrm{d}x = 0. \tag{2.28}$$

On the other hand, for $j = k$, we assume that

$$\int_0^l a_k^2\mu\,\mathrm{d}x = m, \tag{2.29}$$

where m denotes the norm expressed in mass units, e.g.,

$$m = \int_0^l \mu\,\mathrm{d}x. \tag{2.30}$$

The relations (2.28) and (2.29) are written in a more concise form:

$$\int_0^l a_j\mu a_k\,\mathrm{d}x = m\delta_{jk}, \tag{2.31}$$

in which we have used the Kronecker symbol δ_{jk}.

From equality (2.28) it follows that the eigenfunctions are mutually orthogonal to the weight of the masses which need not necessarily be uniformly

distributed over the bar. But, sometimes we have multiple roots of the frequency equation, for example, for $j \neq k$, we get $\omega_j = \omega_k$. The equality (2.27) is then also satisfied when the unlike eigenfunctions are orthogonal. But, it is always possible, by a suitable linear combination of non-orthogonal vibration forms, to find forms satisfying the condition (2.28). We return to this question below.

Thus, the general integral of the differential equation (2.11) has the form

$$u(x, t) = \sum_{k=1}^{\infty} a_k(x) q_k(t).$$
(2.32)

The functions $q_k(t)$ in (2.32) are generalized Lagrangian coordinates given by the formula

$$q_k(t) = C_k e^{-\alpha_k \omega_k t} \sin(\omega'_k t + \varphi_k),$$
(2.33)

where C_k and φ_k denote the integration constants dependent on the initial conditions of motion.

We obtain the particular integral of the non-homogeneous differential equation (2.11) by expanding both the load p_x and the displacement u_p into series of eigenfunctions:

$$p_k(x, t) = \sum_{k=1}^{\infty} a_k(x) p_{xk}(t),$$

$$u_p(x, t) = \sum_{k=1}^{\infty} a_k(x) f_k(t),$$
(2.34)

where $f_k(t)$ are the functions sought, and $p_{xk}(t)$ is determined from the formula

$$p_{xk}(t) = \frac{1}{m} \int_0^l p_x(x, t) a_k(x) \mu(x) \, \mathrm{d}x.$$
(2.35)

Substituting the series (2.34) into Eq. (2.11) and considering the relations (2.21)–(2.23) we get

$$\ddot{f}_k + 2\alpha_k \omega_k \dot{f}_k + \omega_k^2 f_k = \frac{p_{xk}}{\mu}, \quad k = 1, 2, \ldots$$
(2.36)

We find the integral of this equation without difficulty using Cauchy's method:

$$f_k(t) = \frac{1}{\mu \omega'_k} \int_0^t p_{xk}(t_0) e^{-\alpha_k \omega_k (t - t_0)} \sin \omega'_k (t - t_0) \, \mathrm{d}t_0.$$
(2.37)

The complete solution of the damped longitudinal vibration problem for a straight bar therefore has the form

$$u(x, t) = \sum_{k=1}^{\infty} a_k(x)[q_k(t) + f_k(t)].$$ (2.38)

We get the undamped vibration by putting $\alpha_k = 0$ in all the above equations.

EXAMPLE 2.1

Find the longitudinal vibrations of a bar fixed in cross-section $x = l$, with its end $x = 0$ loaded from instant $t = 0$ by force $P = $ const. Hence, the external loading is given in the form of function:

$$p(x, t) = P\delta(x)H(t),$$ (a)

where $\delta(x)$ and $H(t)$ are Dirac and Heaviside distributions, respectively.

The boundary conditions which the eigenfunctions (2.24) are required to satisfy

$$EA\frac{da_k}{dx}(0) = 0, \quad a_k(l) = 0,$$ (b)

lead to the relations

$$B_k = 0, \quad \lambda_k = \frac{2k-1}{2}\frac{\pi}{l}.$$ (c)

Using further the condition (2.31) and assuming $m = \mu l/2$, we find the value of the constant $A_k = 1$ and arrive at the following expression for the normalized function:

$$a_k(x) = \cos\left(\frac{2k-1}{2}\frac{\pi x}{l}\right).$$ (d)

According to Eqs. (2.35) and (2.37), substituting (a) and performing a suitable integration, we find the function:

$$f_k = \frac{2P}{\mu l \omega_k^2}\left[1 - e^{-\alpha_k \omega_k t}\left(\cos\omega_k' t + \alpha_k \frac{\omega_k}{\omega_k'}\sin\omega_k' t\right)\right].$$ (e)

However, since at the initial instant, both the displacements of the bar and the displacement velocities equal zero by assumption, the solution of the problem is thus expressed by the function

$$u(x, t) = \frac{2P}{\mu l} \sum_{k=1}^{\infty} \frac{1}{\omega_k^2} \cos\left(\frac{2k-1}{2} \frac{\pi x}{l}\right) \times$$

$$\times \left[1 - e^{-\alpha_k \omega_k t}\left(\cos\omega_k' t + \alpha_k \frac{\omega_k}{\omega_k'}\sin\omega_k' t\right)\right], \tag{f}$$

and in the absence of damping:

$$u(x, t) = \frac{8Pl}{EA\pi^2} \sum_{k=1}^{\infty} \frac{1}{(2k-1)^2} \cos\left(\frac{2k-1}{2}\frac{\pi x}{l}\right)(1-\cos\omega_k t). \tag{g}$$

The last series can be summed. As a result, we obtain a closed expression for displacements of a vibrating bar:

$$u(x, t) = \begin{cases} 0 & \text{for} \quad -x < ct-4jl < x. \\[2mm] \dfrac{Pl}{EA}\dfrac{ct-4jl-x}{l} & \text{for} \quad -(l-x) < ct-(4j+1)l < l-x, \\[2mm] \dfrac{2Pl}{EA}\dfrac{l-x}{l} & \text{for} \quad -x < ct-(4j+2)l < x, \\[2mm] \dfrac{Pl}{EA}\dfrac{4(1-j)l-ct-x}{l} & \text{for} \quad -(l-x) < ct-(4j+3)l < l-x, \end{cases} \tag{h}$$

where

$$c = \sqrt{\frac{EA}{\mu}} = \sqrt{\frac{E}{\varrho}} \tag{j}$$

is the rate of propagation of an undamped longitudinal wave in the bar, and j takes the values 0, 1, 2, ...

2.2.3. Transverse vibrations of a straight bar

We now consider the set of equations (2.12) applying to vibrations of a bar in plane xz. We examine only the case of a bar of constant cross-section.

Proceeding in like manner as for longitudinal vibrations, we seek the solution of homogeneous equations in the form

$$w(x, t) = a(x)f_1(t) + \tilde{a}(x)f_2(t),$$
$$\varphi_y(x, t) = b(x)f_1(t) + \tilde{b}(x)f_2(t), \tag{2.39}$$

where the functions f_i and their derivatives are given by Eqs. (2.14) and (2.15). Putting the functions (2.39) into the differential equations (2.12), we get a set of equations which using the assumptions:

$$t_E = t_G, \qquad \frac{\zeta_w}{\mu} = \frac{\zeta_y}{I_y},$$

$$\alpha = \frac{1}{2}\left(t_G\omega + \frac{\zeta_w}{\mu\omega}\right) = \frac{1}{2}\left(t_E\omega + \frac{\zeta_y}{I_y\omega}\right)$$

(2.40)

is reducible to the form

$$\frac{d^2a}{dx^2} + \lambda_G^2 a + \frac{db}{dx} = 0,$$

$$-\frac{da}{dx} - b + \varkappa^2\left(\frac{d^2b}{dx^2} + \lambda_E^2 b\right) = 0.$$

(2.41)

In these equations:

$$\lambda_G = \frac{\omega}{c_G}, \qquad \lambda_E = \frac{\omega}{c_E},$$

(2.42)

where

$$c_G = \sqrt{\frac{GA}{k_z\mu}} \left(= \sqrt{\frac{G}{k_z\varrho}}\right), \qquad c_E = \sqrt{\frac{EJ_y}{I_y}} \left(= \sqrt{\frac{E}{\varrho}}\right)$$

(2.43)

denote the rates of propagation of shear and bending waves in the bar (the parenthetized formulae apply to a bar of a homogeneous material, for which the relations (1.2) and (1.4) hold). The quantity

$$\varkappa^2 = \frac{EJ_y k_z}{GA}$$

(2.44)

describes the influence of shear strain on vibrations of a beam.

The set of equations (2.41) can be reduced to the relation:

$$b = -\frac{1 + \varkappa^2\lambda_G^2}{1 + \varkappa^2\lambda_E^2}\frac{da}{dx} - \frac{\varkappa^2}{1 + \varkappa^2\lambda_E^2}\frac{d^3a}{dx^3}$$

(2.45)

and to a differential equation of the fourth order for the eigenfunction (a):

$$\left(\frac{d^2}{dx^2} + \lambda_G^2\right)\left(\frac{d^2}{dx^2} + \lambda_E^2\right)a - \frac{\lambda_G^2}{\varkappa^2}a = 0.$$

(2.46)

It is easily seen that with the denotations

$$\psi, \nu = \frac{\sqrt{2}}{2}\sqrt{\sqrt{(\lambda_G^2 - \lambda_E^2)^2 + 4\frac{\lambda_G^2}{\varkappa^2}} \mp (\lambda_G^2 + \lambda_E^2)}$$

(2.47)

the integral of the differential equation (2.46) takes the form

$$a(x) = A\operatorname{Ch}\psi x + B\operatorname{Sh}\psi x + C\cos\nu x + D\sin\nu x.$$

(2.48)

The boundary conditions which the function (2.48) should satisfy, lead to a set of linear equations on account of the integration constants. The determinant of the set equated to zero gives a transcendental equation, from which an infinite number of eigenvalues ω_k can be determined.

In the special case of a beam simply supported at both ends, the functions (2.48), which satisfy all the boundary conditions, are expressed by the formula

$$a_r = D_r \sin \nu_r x, \tag{2.49}$$

where

$$\nu_r = \frac{r\pi}{l} \quad r = 1, 2, \ldots \tag{2.50}$$

But, from the relations (2.42)–(2.45), it follows that the function b_r can be expressed as follows:

$$b_r = \frac{\varkappa^2 \nu_r}{c_E^2 + \varkappa^2 \omega_r^2}\left[c_E^2 \nu_r^2 - \frac{\mu}{I_y}(c_G^2 + \varkappa^2 \omega_r^2)\right]D_r \cos \nu_r x. \tag{2.51}$$

Putting the known quantity ν_r into Eq. (2.47) and using the relations (2.42)–(2.54) we get the biquadratic equation for vibration frequency ω_r:

$$(\omega_r^2 - c_E^2 \nu_r^2)(\omega_r^2 - c_G^2 \nu_r^2) - \frac{\mu}{I_y}c_G^2 \omega_r^2 = 0, \tag{2.52}$$

which has two positive roots:

$$\omega_j, \omega_k$$

$$= \frac{\sqrt{2}}{2}\sqrt{(c_E^2 + c_G^2)\nu_r^2 + \frac{\mu}{I_y}c_G^2 \pm \sqrt{(c_E^2 - c_G^2)^2 \nu_r^4 + 2\frac{\mu}{I_y}(c_E^2 + c_G^2)c_G^2 \nu_r^2 + \frac{\mu^2}{I_y^2}c_G^4}}.$$

$$\tag{2.53}$$

This means that one and the same form of the function a_r, expressing deflections of the beam, is accompanied by two different vibration frequencies, ω_j and ω_k. However, considering the fact that the functions b_j and b_k describing the angular displacements of cross-sections will differ from each other by the value of the coefficient dependent on frequency (cf. (2.51)), we find that the general forms of vibrations corresponding to different frequencies are not identical. Hence, the free vibrations of the beam according to rth sinusoid (2.49) are described by the function

$$w(x, t) = a_r(x)[q_j(t) + q_k(t)], \tag{2.54}$$

in which the time functions are given by Eq. (2.33). The four integration constants, C_j, C_k, φ_j, φ_k in these functions can be selected based on the four

initial conditions of motion, in which initial displacement and angular displacements and initial velocities of these displacements occur.

The Timoshenko's beam model discussed above takes into account both the influence of shear strains and the influence of rotational inertia of the cross-sections of the beam on its vibration. Neglecting these two factors (justifiable in the case of a flexible bar) is tantamount to assuming that the shear stiffness of the beam, GA/k_z, is infinitely great and the mass moment of inertia I_y equals zero. It follows further that the angle of inclination of the cross-section is not a quantity independent of beam deflections but is associated with it according to the relation

$$\varphi_y = -\frac{\partial w}{\partial x}.$$ (2.55)

Finally from Eq. (2.12)$_2$, with damping neglected, it follows that

$$\frac{GA}{k_z}\left(\frac{\partial w}{\partial x}+\varphi_y\right) = EJ_y\frac{\partial^2\varphi_y}{\partial x^2}+m_y = -EJ_y\frac{\partial^3 w}{\partial x^3}+m_y.$$ (2.56)

Substituting this relation into Eq. (3.17)$_1$, we get a single differential equation

$$EJ_y\frac{\partial^4 w}{\partial x^4}+\mu\frac{\partial^2 w}{\partial t^2} = p_z+\frac{\partial m_y}{\partial x},$$ (2.57)

which is most commonly used in practice.

Proceeding in the described manner, we arrive without difficulty at the solution of the problem:

$$w(x,t) = \sum_{k=1}^{\infty} a_k(x)[q_k(t)+f_k(t)].$$ (2.58)

In this equation:

$$a_k(x) = A_k\,\text{Ch}\,\lambda_k x+B_k\,\text{Sh}\,\lambda_k x+C_k\cos\lambda_k x+D_k\sin\lambda_k x,$$ (2.59)

$$q_k(t) = c_k\sin(\omega_k t+\varphi_k),$$ (2.60)

$$f_k(t) = \frac{1}{\mu\omega_k}\int_0^t\int_0^l\left[p_z(x_0,t_0)+\frac{\partial m_y}{\partial x_0}(x_0,t_0)\right]a_k(x_0)\sin\omega_k(t-t_0)\,dx_0\,dt_0,$$ (2.61)

$$\omega_k = \lambda_k^2\sqrt{\frac{EJ_y}{\mu}}.$$ (2.62)

The integration constants in the eigenfunction (2.59) are, of course, not arbitrary but have to be determined from the boundary conditions of the

problem and from normalization of the eigenfunctions. On the other hand, the constants c_k and φ_k in the function (2.60) depend on the initial conditions of motion. If at the initial instant the bar remains at rest, in a state of static equilibrium, the constant c_k then equals zero and the solution (2.58) does not contain the function q_k.

EXAMPLE 2.2

Determine the vibrations of a beam simply supported at both ends, induced by force P travelling along the beam with constant velocity v (Fig. 2.2).
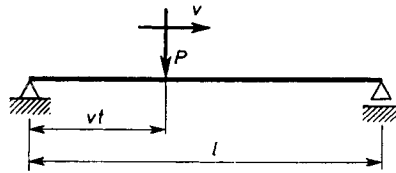
Fig. 2.2. Beam loaded by a moving force

The external load is therefore given in the form of the distribution:

$$p_z(x, t) = P\delta(x - vt). \tag{a}$$

The normalized eigenfunctions, assuming the norm $m = \mu l/2$, have in this case the form

$$a_k(x) = \sin \lambda_k x, \quad \text{where} \quad \lambda_k = \frac{k\pi}{l}. \tag{b}$$

The angular frequency of free vibrations, in accordance with (2.62) is

$$\omega_k = \frac{k^2\pi^2}{l^2}\sqrt{\frac{EJ_y}{\mu}}. \tag{c}$$

Performing successively the operations described by Eq. (2.61), we get

$$f_k = \frac{P}{\mu\omega_k}\int_0^t\int_0^l \delta(x_0 - vt_0)\sin\lambda_k x\sin\omega_k(t - t_0)\,dx_0\,dt_0$$

$$= P\left[\frac{\sin\lambda_k vt}{\lambda_k^2(\lambda_k^2 EJ_y - v^2\mu)} - v\sqrt{\frac{\mu}{EJ_y}}\,\frac{\sin\omega_k t}{\lambda_k^3(\lambda_k^2 EJ_y - v^2\mu)}\right], \tag{d}$$

and introducing the denotations

$$\xi = \frac{x}{l}, \quad \tau = \frac{vt}{l}, \quad \sigma = lv\sqrt{\frac{\mu}{EJ_y}}, \tag{e}$$

we obtain the solution of the problem:

$$w = \frac{2Pl^3}{EJ_y}\left[\sum_{k=1}^{\infty}\frac{\sin k\pi\xi\sin k\pi\tau}{k^2\pi^2(k^2\pi^2-\sigma^2)} - \sigma\sum_{k=1}^{\infty}\frac{\sin k\pi\xi\sin k^2\pi^2\frac{\tau}{\sigma}}{k^3\pi^3(k^2\pi^2-\sigma^2)}\right]. \tag{f}$$

The first of the above series is slower to converge than is the second, but it can be summed and brought to a closed form (cf. Kączkowski, 1963). As a result, the solution of the problem can be given in the form

$$w = \frac{Pl^3}{EJ_y\sigma^2}\left[\left(\frac{\sin\sigma\xi'\sin\sigma\tau}{\sigma\sin\sigma} - \xi'\tau\right)H(\xi-\tau) + \left(\frac{\sin\sigma\xi\sin\sigma\tau'}{\sigma\sin\sigma} - \xi\tau'\right)H(\tau-\xi)\right] - $$

$$-\frac{2Pl^3}{EJ_y}\sigma\sum_{k=1}^{\infty}\frac{\sin k\pi\xi\sin k^2\pi^2\frac{\tau}{\sigma}}{k^3\pi^3(k^2\pi^2-\sigma^2)}, \tag{g}$$

where

$$\xi' = 1-\xi, \quad \tau' = 1-\tau, \tag{h}$$

and H denotes Heaviside's function.

Note that the solutions given in form (f) or (g) relate to the time interval during which force P is present on the beam ($0 < \tau < 1$). But, the beam continues to vibrate after the force has gone, and we obtain the function expressing these vibrations by taking in place of a variable upper integration limit, t, in Eq. (d), a constant value, l/v, equalling the time of travel of the force over the entire length of the beam. Hence, we have: for $\tau > 1$

$$w = \frac{2Pl^3}{EJ_y}\sum_{k=1}^{\infty}\frac{\sigma\sin k\pi\xi}{k^3\pi^3(k^2\pi^2-\sigma^2)}\left[(-1)^k\sin k^2\pi^2\frac{\tau-1}{\sigma} - \sin k^2\pi^2\frac{\tau}{\sigma}\right]. \tag{j}$$

It is worth noting that in the case:

$$\sigma = j\pi, \tag{k}$$

where j is a natural number, the denominators of the respective terms in the series (f), (g) and (j) become equal to zero. The velocity value following from the relations (e) and (k):

$$v_{cr} = \frac{j\pi}{l}\sqrt{\frac{EJ_y}{\mu}} \tag{l}$$

is called a *critical velocity**. But, the fact that the force has reached a critical velocity does not at all mean that the deflections of the beam become infinitely great. A simple pass to the limit enables us to obtain solutions also in case (k). We thus obtain:

$$w = \frac{2Pl^3}{EJ_y\pi^4}\left[\sum_{\substack{k=1 \\ k \neq 1}}^{\infty} \frac{k\sin k\pi\tau - j\sin k^2\pi\frac{\tau}{j}}{k^3(k^2-j^2)}\sin k\pi\xi + \frac{\sin j\pi\tau - j\pi\tau\cos j\pi\tau}{2j^4}\sin j\pi\xi\right],$$

or:

$$w = \frac{Pl^3}{2EJ_yj^4\pi^4}\{7\sin j\pi\xi\sin j\pi\tau - 2j\pi\xi\cos j\pi\xi\sin j\pi\tau - 4j\pi\tau\sin j\pi\xi\cos j\pi\tau -$$

$$- 2j^2\pi^2\xi\tau + 2j\pi[(\cos j\pi\xi\sin j\pi\tau - j\pi\tau)H(\xi-\tau) + (\sin j\pi\xi\cos j\pi\tau -$$

$$- j\pi\xi)H(\tau-\xi)]\} - \frac{2Pl^3}{EJ_y\pi^4}j\sum_{\substack{k=1 \\ k \neq 1}}^{\infty}\frac{\sin k\pi\xi}{k^3(k^2-j^2)}\sin k^2\pi\frac{\tau}{j},$$

for $0 < \tau < 1$, and

$$w = \frac{2Pl^3}{EJ_y\pi^4}\sum_{\substack{k=1 \\ k \neq j}}^{\infty}\frac{j\sin k\pi\xi}{k^3(k^2-j^2)}\left[(-1)^k\sin k^2\pi\frac{\tau-1}{j} - \sin k^2\pi\frac{\tau}{j}\right] -$$

$$- \frac{Pl^3}{EJ_y}\frac{\sin j\pi\xi\cos j\pi\tau}{j^3\pi^3} \tag{m}$$

for $\tau > 1$.

2.3. Vibrations of a Curved Bar

In the present section, we confine our considerations to showing a way by which it is possible to determine undamped vibrations of a bar, with the omission of shear strains and rotational inertia of a cross-section.

---

* Following Kączkowski's (1963) publication, the author received two letters from Timoshenko. In his letter, dated April 8, 1964, he wrote, among others: "Many years ago (Le Genie Civil, 24 December 1921, p. 555) I was interested in vibration of an infinitely long rail supported by a continuous elastic foundation". Noting further the existence of a critical velocity, he wrote: "It would be interesting to investigate the physical meaning of this conclusion".

Our further considerations and formulae are in a way a delayed answer to the question posed by Timoshenko.

2.3.1. In-plane vibrations of a bar

In the case of vibrations in the plane of a bar, the static equilibrium equations given in Part 1, Eq. (2.41) must be supplemented now with forces of inertia, and the ordinary derivatives must be replaced by partial derivatives:

$$\frac{\partial N}{\partial s} - \frac{T_n}{r} + p_s - \mu \ddot{u} = 0,$$

$$\frac{\partial T_n}{\partial s} + \frac{N}{r} + p_n - \mu \ddot{v} = 0, \tag{2.63}$$

$$\frac{\partial M_z}{\partial s} + T_n + m_z = 0.$$

We denote the radius of curvature of the bar by r (instead of ϱ). We get rid of the transverse force in the set of equations (2.63):

$$T_n = -\frac{\partial M_z}{\partial s} - m_z \tag{2.64}$$

and obtain the following set of two differential equations:

$$\frac{\partial N}{\partial s} + \frac{1}{r}\frac{\partial M_z}{\partial s} - \mu \ddot{u} + p_s + \frac{m_z}{r} = 0,$$

$$-\frac{\partial^2 M_z}{\partial s^2} + \frac{N}{r} - \mu \ddot{v} + p_n - \frac{\partial m_z}{\partial s} = 0. \tag{2.65}$$

Proceeding from Eqs. (2.45), (2.59) and (2.60) from Part 1, we express the above equations in terms of displacements:

$$\frac{\partial}{\partial s}\left[EA\left(\frac{\partial u}{\partial s} - \frac{v}{r}\right)\right] + \frac{1}{r}\frac{\partial}{\partial s}\left\{EJ_z\left[\frac{\partial^2 v}{\partial s^2} + \frac{\partial}{\partial s}\left(\frac{u}{r}\right)\right]\right\} - \mu\ddot{u} + p_s + \frac{m_z}{r} = 0,$$

$$-\frac{\partial^2}{\partial s^2}\left\{EJ_z\left[\frac{\partial^2 v}{\partial s^2} + \frac{\partial}{\partial s}\left(\frac{u}{r}\right)\right]\right\} + \frac{1}{r}EA\left(\frac{\partial u}{\partial s} - \frac{v}{r}\right) - \mu\ddot{v} + p_n - \frac{\partial m_z}{\partial s} = 0. \tag{2.66}$$

The set of equations (2.66) can be made explicit assuming that the radius of curvature of the bar and the quantities describing its cross-sections are constant. The coordinate s measured along the axis of the bar can be replaced by the angular variable ϑ:

$$s = r\vartheta. \tag{2.67}$$

Since we have neglected damping, we can therefore anticipate that free vibrations (in the absence of external loadings), will take place according to harmonic time functions:

$$u(\vartheta, t) = \sum_{k=1}^{\infty} u_k(\vartheta) e^{i\omega_k t},$$

$$v(\vartheta, t) = \sum_{k=1}^{\infty} v_k(\vartheta) e^{i\omega_k t}.$$

(2.68)

Finally, denoting

$$\frac{d(\ldots)}{d\vartheta} = (\ldots)', \qquad \frac{EA}{r^2 \mu \omega_k^2} = \varphi, \qquad \frac{EJ_z}{r^4 \mu \omega_k^2} = \psi,$$

(2.69)

and substituting the relation (2.68) into Eqs. (2.66), we get the following set of ordinary homogeneous differential equations:

$$(\varphi + \psi) u_k'' + u_k + \psi v_k''' - \varphi v_k' = 0,$$
$$-\psi u_k''' + \varphi u_k' - \psi v_k^{\mathrm{IV}} + (1 - \varphi) v_k = 0, \qquad \text{for} \quad k = 1, 2, \ldots$$

(2.70)

Performing a few simple operations of this set, we can relate the function v_k to the function u_k:

$$v_k = -\frac{\varphi^2 \psi u_k^{\mathrm{V}} + \varphi \psi (2 + \varphi) u_k''' + (\psi - \varphi^2 \psi - \varphi^3) u_k'}{(1 - \varphi)(\psi - \varphi \psi - \varphi^2)}.$$

(2.71)

The function u_k on its part should satisfy the differential equation of the sixth order:

$$u_k^{\mathrm{VI}} + \left(2 + \frac{1}{\varphi}\right) u_k^{\mathrm{IV}} + \left(1 - \frac{1}{\varphi} - \frac{1}{\psi}\right) u_k'' + \frac{1}{\psi}\left(1 - \frac{1}{\varphi}\right) u_k = 0.$$

(2.72)

The further procedure is similar to that for a straight bar. Seeking the general integral of Eq. (2.72) in the form

$$u_k = e^{\lambda_k \vartheta},$$

(2.73)

we arrive at the following characteristic equation:

$$\lambda_k^6 + \left(2 + \frac{1}{\varphi}\right) \lambda_k^4 + \left(1 - \frac{1}{\varphi} - \frac{1}{\psi}\right) \lambda_k^2 + \frac{1}{\psi}\left(1 - \frac{1}{\varphi}\right) = 0.$$

(2.74)

Its roots depend on parameters φ and ψ, each of them being dependent on its part from the free vibration frequency ω_k. The general integral of Eq. (2.72) will contain six integration constants, which should be determined from the boundary conditions of the problem and from the normalization conditions of eigenfunctions. The equation, from which the free vibration frequencies can be determined theoretically, is a transcedental equation formed by equating the determinant of the sixth degree to zero.

As we can see, the problem does not lend itself practically to an analytical solution; consequently, it has to be solved by numerical methods or by various

approximate techniques. The problem turns out to be somewhat simpler
if we neglect the longitudinal deformations of the bar, in other words, if we
assume that the tensile rigidity, EA, is infinitely great.

2.3.2. Vibrations normal to the plane of a bar

In the case of vibrations normal to the plane of a bar, we modify the static
equilibrium equations given in Part 1, Eq. (2.62):

$$\frac{\partial T_z}{\partial s} - \mu\ddot{w} + p_z = 0, \qquad \frac{\partial M_n}{\partial s} + \frac{M_t}{r} - T_z + m_n = 0,$$

$$\frac{\partial M_t}{\partial s} - \frac{M_n}{r} - I_0\ddot{\varphi}_t + m_t = 0. \tag{2.75}$$

We have neglected here the effects of damping and strains due to shear forces
and the rotational inertia with respect to the n-axis, normal to the axis of the
bar. We eliminate from the set the shear force:

$$T_z = \frac{\partial M_n}{\partial s} + \frac{M_t}{r} + m_n, \tag{2.76}$$

and obtain a set of two equations:

$$\frac{\partial^2 M_n}{\partial s^2} + \frac{\partial}{\partial s}\left(\frac{M_t}{r}\right) - \mu\ddot{w} + p_z + \frac{\partial m_n}{\partial s} = 0,$$

$$\frac{\partial M_t}{\partial s} - \frac{M_n}{r} - I_0\ddot{\varphi}_t + m_t = 0. \tag{2.77}$$

We now use Eqs. (2.66) and (2.68) from Part 1 to arrive at the following set
of two equations with two unknowns:

$$\frac{\partial^2}{\partial s^2}\left[EJ_n\left(-\frac{\partial^2 w}{\partial s^2} + \frac{\varphi_t}{r}\right)\right] + \frac{\partial}{\partial s}\left[\frac{GJ_t}{r}\left(\frac{\partial\varphi_t}{\partial s} + \frac{1}{r}\frac{\partial w}{\partial s}\right)\right] - \mu\ddot{w} + p_z + \frac{\partial m_n}{\partial s} = 0,$$

$$\frac{\partial}{\partial s}\left[GJ_t\left(\frac{\partial\varphi_t}{\partial s} + \frac{1}{r}\frac{\partial w}{\partial s}\right)\right] - \frac{EJ_n}{r}\left(-\frac{\partial^2 w}{\partial s^2} + \frac{\varphi_t}{r}\right) - I_0\ddot{\varphi}_t + m_t = 0. \tag{2.78}$$

Assuming as before a constant cross-section and a constant radius of
curvature r and assuming further that the external loading equals zero and
that the displacements are harmonic time functions:

$$w(\vartheta, t) = \sum_{k=1}^{\infty} w_k(\vartheta)e^{i\omega_k t},$$

$$\varphi_t(\vartheta, t) = \sum_{k=1}^{\infty} \varphi_{tk}(\vartheta)e^{i\omega_k t}, \tag{2.79}$$

we get the following set of ordinary differential equations:

$$-\alpha w_k^{IV} + \beta w_k'' + w_k + (\alpha + \beta) r \varphi_{tk}'' = 0,$$
$$(\alpha + \beta) w_k'' + \beta r \varphi_{tk}'' - (\alpha - \varepsilon) r \varphi_{tk} = 0,$$

(2.80)

in which we have used the denotations:

$$\alpha = \frac{EJ_n}{r^4 \mu \omega_k^2}, \quad \beta = \frac{GJ_t}{r^4 \mu \omega_k^2}, \quad \varepsilon = \frac{I_0}{r^2 \mu}.$$

(2.81)

Eliminating from this set the function φ_{tk}:

$$\varphi_{tk} = \frac{\alpha \beta w_k^{IV} + \alpha(\alpha + 2\beta) w_k'' - \beta w_k}{r(\alpha - \varepsilon)(\alpha + \beta)},$$

(2.82)

we arrive at a single differential equation of the sixth order for the w-function:

$$w_k^{VI} + \left(2 + \frac{\varepsilon}{\beta}\right) w_k^{IV} + \left(1 - \frac{\varepsilon}{\alpha} - \frac{1}{\alpha}\right) w_k'' + \left(\frac{1}{\beta} - \frac{\varepsilon}{\alpha \beta}\right) w_k = 0.$$

(2.83)

The analytical solution of this equation presents similar difficulty to that encountered in the case of in-plane vibration of a curved bar.

More information on vibration of an arch or ring will be found in a study by Federhofer (1950); Dobrzański (1963) describes a procedure for obtaining solutions for vibration of a spatially curved bar.

2.4. The Influence of Axial Forces and Elastic Foundation on Transverse Vibrations of a Bar

In preceding sections we have assumed the deformations of a bar to be so small that their influence on the position of individual forces can be neglected. No appreciable errors result therefrom, provided that the absolute values of axial forces are not very great in the sense that they are at least one order of magnitude less than the values of the critical forces causing instability of the bar. Otherwise, we must consider the eccentricities of axial forces in the equilibrium equations. We should distinguish here two cases. In the first, the axial force is constant, and only the transverse loading is time-dependent, setting the bar into transverse vibrations. Subjected to loading of this type, for example, are factory chimneys or TV towers (cf. Naleszkiewicz and Szaniawski, 1953). Likewise, strings in musical instruments are under constant tension, and they are forced to vibrate by appropriate actions perpendicular to the string axis.

In the second case, bot the axial force and the transverse loading are time functions. We deal then with coupled longitudinal-transverse vibration. This type of vibration occurs in principle in every framework or truss; the

transverse vibration of bars in one direction are transmitted as longitudinal vibration to bars in the other direction. But, in spite of that and considering the great mathematical difficulties that would be encountered in treating the vibration of a structure as a non-linear coupled vibration problem, and also on account of the negligible influence of that coupled action on the final results, only the influence of the constant axial forces on vibration of a structure is considered, if at all, in engineering practice.

In the literature, on the other hand, we come across solutions involving a mixed problem, in which the axial force is treated as a known quantity, constant over the entire bar length and only time-dependent. The differential equation remains then a linear equation, but with time variable factors. This is a problem of so-called *parametric vibration* and of the related dynamic stability. These questions are, however, outside the scope of the present part of the volume.

Along with the influence of constant axial forces we consider in this paragraph the effect of an elastic foundation on undamped transverse vibration of a bar. We take the bar to be sufficiently slender for the influence of rotational inertia and shear strains to be neglected, and we also assume that Winkler's model is the elastic foundation model (cf. Part 1, Section 5.4).
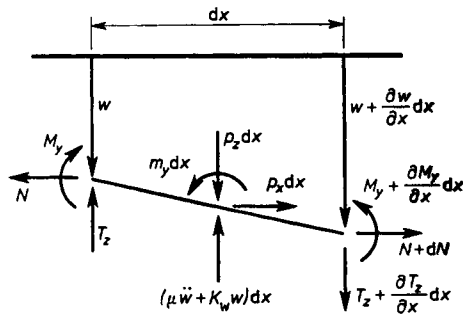
Fig. 2.3. Segment of transversely vibrating bar

With these assumptions, we consider an element of the bar, dx long, together with the loads acting on it (Fig. 2.3). The element has experienced the displacements indicated in the figure.

Thus, we have the following dynamic equations:

$$\frac{\partial T_z}{\partial x} - \mu\ddot{w} - k_z b w + p_z = 0,$$

$$\frac{\partial M_y}{\partial x} - T_z + N\frac{\partial w}{\partial x} + m_y = 0. \tag{2.84}$$

The solution of the static equation:

$$\frac{\mathrm{d}N}{\mathrm{d}x} + p_x = 0 \tag{2.85}$$

we treat as known.

Eliminating from the set (2.85) the transverse force T_z and using the relation

$$M_y = -EJ_y \frac{\partial^2 w}{\partial x^2}, \tag{2.86}$$

we get the differential equation for deflection w:

$$EJ_y \frac{\partial^4 w}{\partial x^4} - \frac{\partial}{\partial x}\left(N\frac{\partial w}{\partial x}\right) + \mu\ddot{w} + k_z bw = p_z + \frac{\partial m_y}{\partial x}. \tag{2.87}$$

We seek the general integral, in the same way as before, in the form

$$w(x, t) = \sum_{k=1}^{\infty} a_k(x) q_k(t), \tag{2.88}$$

where

$$q_k(t) = c_k \sin(\omega_k t + \varphi_k). \tag{2.89}$$

In this way, we reduce the homogeneous, partial differential equation to the following set of ordinary differential equations:

$$EJ_y \frac{\mathrm{d}^4 a_k}{\mathrm{d}x^4} - \frac{\mathrm{d}}{\mathrm{d}x}\left(N\frac{\mathrm{d}a_k}{\mathrm{d}x}\right) - (\mu\omega_k^2 - k_z b)a_k = 0, \quad k = 1, 2, \ldots \tag{2.90}$$

The integral of Eq. (2.90) in closed form can be obtained in the special case $N = \mathrm{const}$ ($p_x = 0$). We will concern ourselves with this particular case henceforth. Therefore, using the denotations

$$\gamma_k = \frac{N}{2EJ_y}, \quad \delta_k^2 = \frac{1}{EJ_y}(\mu\omega_k^2 - k_z b), \tag{2.91}$$

$$\psi_k, \nu_k = \sqrt{\sqrt{\gamma_k^2 + \delta_k^2} \pm \gamma_k}, \tag{2.92}$$

we write the integral of Eq. (2.90) as follows (cf. (2.48)):

$$a_k(x) = A_k \mathrm{Ch}\,\psi_k x + B_k \mathrm{Sh}\,\psi_k x + C_k \cos\nu_k x + D_k \sin\nu_k x. \tag{2.93}$$

Proceeding as in Section 2.2.3 on the basis of the boundary conditions which the functions (2.93) are required to satisfy, we arrive at a set of homogeneous equations with respect to the integration constants. Equating the determinant of this set to zero, we get the equation (usually transcedental) for parameters (2.92) dependent on free vibration frequency.

In a special case of a bar of length l, simply supported at both ends, the function (2.93) will satisfy the boundary conditions, if it is reduced to the form

$$a_k = D_k \sin \nu_k x, \tag{2.94}$$

and the parameter ν_k takes the value

$$\nu_k = \frac{k\pi}{l}. \tag{2.95}$$

Using Eqs. (2.92), (2.93), we find

$$\omega_k = \nu_k^2 \sqrt{\frac{EJ_y}{\mu}} \sqrt{1 + \frac{N}{EJ_y \nu_k^2} + \frac{k_z b}{EJ_y \nu_k^4}}. \tag{2.96}$$

The further procedure has been described in Section 2.2.3. Note that the undamped vibration frequency of the bar expressed by Eq. (2.97) increases with the tensile force N, whereas the compressive force $(N < 0)$ produces a downward trend in the vibration frequency which becomes equal to zero as the axial force assumes the value

$$N_{cr} = -EJ_y \nu_k^2 - \frac{k_z b}{\nu_k^2}. \tag{2.97}$$

We have applied here one of the techniques of determining the critical load causing a buckling of the bar. Structural stability problems are discussed in the next part of the volume.

To conclude, we should note the fact that assuming the bar bending stiffness $EJ_y = 0$ and the foundation module $k_z = 0$, we obtain the values

$$\omega_k = \nu_k \sqrt{\frac{N}{\mu}}, \tag{2.98}$$

applying to a transversely vibrating string pulled by force N.

3. Vibration of Composed Bar Structures

3.1. General Remarks

Modal analysis, previously discussed, is a general method in so far that it can be applied equally well to structures made of straight bars, for which bars the solutions of homogeneous equations given in Section 2.2 are known. However, in the case of skeletal structures the difficulty lies in finding the eigenvalues and the corresponding forms of free vibration. Certain possibilities of surmounting this obstacle are afforded by the displacement method, considered in Section 3.3.

A further difficulty with modal analysis presents in the process of normalizing the eigenforms. They require normalizing when vibrations forced by a moving load or by a load arbitrarily variable in time have to be determined.

In Section 3.2, we present a technique for determining vibrations in a structure composed of straight bars, by which it is no longer necessary to find the global forms of free vibration and the corresponding free vibration frequencies of the whole system. This method is based on an argumentation typical the direct flexibility method discussed in Part 1. However, to obtain results using this method, a suitable equation or a set of Volterra's integral equations needs to be solved.

3.2. The Direct Flexibility Method (Force Method). Volterra's Integral Equations

The procedure specific to the direct flexibility method, it will be recalled, consists in that a real structure is replaced by a so-called *primary system* with a smaller number of external or internal constraints, and in place of the eliminated constraints, general forces are introduced. Along with external loadings, these forces should induce exactly the same strains in the primary system as those developing in the real structure. In dynamics, this condition should be supplemented with the statement that these strains should be ident-

ical at every instant. This is connected, of course, with the fact that the gener-
alized forces introduced at the places of the removed constraints are unknown
time functions.

The procedure will be explained using example of a continuous beam,
a structure rather widely used, especially in civil engineering. Consider two
adjoining spans of the continuous beam shown in Fig. 3.1a. Let an arbitrar-
ily distributed, time-variable load consisting of vertical forces p_r and mo-
ments m_r, be acting on each span. In order not to complicate things unduly,
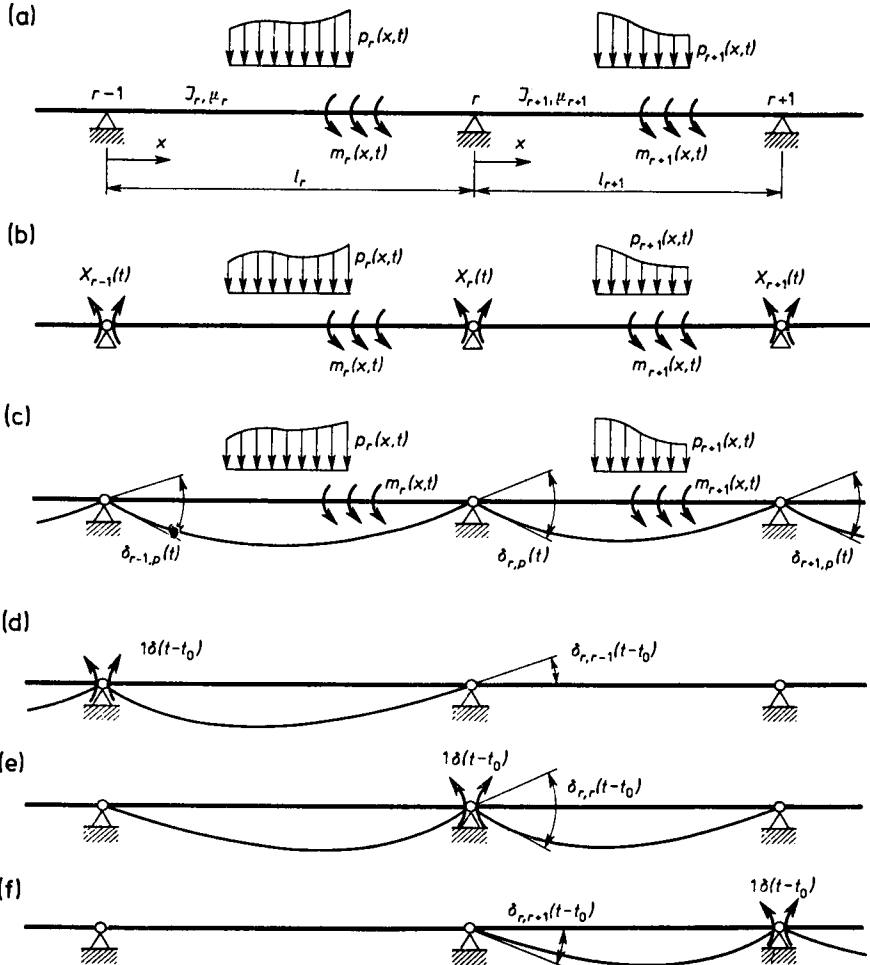
Fig. 3.1. Part of a continuous beam: (a) considered structure; (b) primary scheme;
(c) displacements induced by external loading, (d)–(f) displacements induced by unit
impulses acting in hinges

let us assume that the deflection of each span, w_r, satisfies Eq. (2.57), in which shear strains, rotational inertia and damping are not considered.

Introducing hinges over the supports, we obtain a primary system on which, beside external loads p_r and m_r ($r = 1, 2, ..., n$), support moments X_r ($r = 1, 2, ..., s$) are acting. These are unknown for the time being and are also treated for the present as external loads (Fig. 3.1b). They must be so well matched that under no circumstances should a corner point of the bending line occur over any of the supports. The symbols n and s stand for the number of spans and the number of unknown support moments, respectively. The primary system cannot be said to be isostatic because no such concept exists in dynamics.

Using the principle of superposition, we first consider separately the state of external loadings p_r and m_r at zero values of the support moments. Such a load acting on simply supported beams makes them vibrate (Fig. 3.1c), the vibration exhibiting corner angles $\delta_{r,p}(t)$ over the supports. We can solve this problem using Eqs. (2.58)–(2.62), and also the results from Example 2.2:

$$\delta_{r,p}(t) = \frac{2}{\pi \sqrt{EJ_r \mu_r}} \sum_{k=1}^{\infty} \frac{(-1)^{k+1}}{k} \int_0^t \int_0^{l_r} \left[p_r(x_0, t_0) + \right.$$

$$\left. + \frac{\partial m_r}{\partial x_0}(x_0, t_0) \right] \sin \frac{k\pi x_0}{l_r} \sin k^2 \omega_r^1 (t-t_0) \, dx_0 \, dt_0 +$$

$$+ \frac{2}{\pi \sqrt{EJ_{r+1} \mu_{r+1}}} \sum_{k=1}^{\infty} \frac{1}{k} \int_0^t \int_0^{l_{r+1}} \left[p_{r+1}(x_0, t_0) + \frac{\partial m_{r+1}}{\partial x_0}(x_0, t_0) \right] \times$$

$$\times \sin \frac{k\pi x_0}{l_{r+1}} \sin k^2 \omega_{r+1}^1 (t-t_0) \, dx_0 \, dt_0. \qquad (3.1)$$

In this equation,

$$\omega_r^1 = \frac{\pi^2}{l_r^2} \sqrt{\frac{EJ_r}{\mu_r}}, \qquad r = 1, 2, ..., n, \qquad (3.2)$$

is the first, so-called *fundamental vibration frequency* of beam r, simply supported at both ends.

Next, we have to find the solutions of the auxiliary problems presented graphically in Fig. 3.1d, e, f. Involved here is the determination of functions expressing the corner angle of the beam over the support r due to impulse loadings by moments applied at instant t_0 successively over supports $r-1$, r and $r+1$. As a result, we have in Fig. 3.1d, e, f the symbol $\delta(t-t_0)$ denoting the Dirac delta distribution, whereas the symbols with subscripts (e.g.

$\delta_{r,r-1}(t-t_0)$) denote the corner angles over support r. These angles are functions of $t-t_0$ i.e., the length of time between istant t_0, the instant application of load, and instant t, at which the angle of interest is being determined.

Having solved the auxiliary problems, we can express the global corner angle induced over support r by the unknowns $X_{r-1}(t)$, $X_r(t)$ and $X_{r+1}(t)$ and by the external load:

$$\int_0^t X_{r-1}(t_0)\,\delta_{r,r-1}(t-t_0)\,dt_0 + \int_0^t X_r(t_0)\,\delta_{r,r}(t-t_0)\,dt_0 +$$

$$+ \int_0^t X_{r+1}(t_0)\,\delta_{r,r+1}(t-t_0)\,dt_0 + \delta_{r,p}(t) = 0. \qquad (3.3)$$

Obviously, that angle must be equal to zero at every instant t. The number of equations of type (3.3) corresponds to the number of unknowns $X_r(t)$. In this way, we have obtained a set of Volterra's three-membered integral equations of the 1st kind.

In order to find the functions constituting the kernels of these integral equations, we must first determine the vibration of a simply supported beam, loaded at instant t_m, at a point with coordinate x_m, by a unit impulse moment
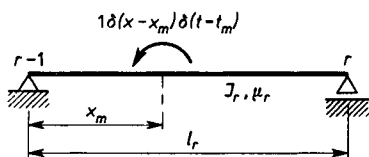
$1\delta(x-x_m)\delta(t-t_m)$

Fig. 3.2. Span of a continuous beam loaded by unit impulse moment

(Fig. 3.2). Therefore, we must perform the integration given by Eq. (2.61), assuming that the load m_r is given by the equation

$$m_r(x, t) = 1\delta(x-x_m)\,\delta(t-t_m). \qquad (3.4)$$

For this purpose, Eq. (2.61)—in the part applying to loading by the moment—has to be expressed in a somewhat different form:

$$f_k(t) = \frac{1}{\mu_r \omega_r^k} \int_0^t \int_0^{l_r} \frac{\partial m_r}{\partial x_0}(x_0, t_0)\,w_{rk}(x_0)\sin\omega_r^k(t-t_0)\,dx_0\,dt_0$$

$$= \frac{1}{\mu_r \omega_r^k} \int_0^t \left\{ [m_r w_{rk}]_0^{l_r} - \int_0^{l_r} m_r(x_0, t_0)\frac{dw_{rk}}{dx_0}(x_0)\,dx_0 \right\}\sin\omega_r^k(t-t_0)\,dt_0.$$

$$(3.5)$$

Since the deflections of the beam r equal zero at both ends, the final form of the integral (3.5) using the relations (2.55) is:

$$f_k(t) = \frac{1}{\mu_r \omega_r^k} \int_0^t \int_0^{l_r} m_r(x_0, t_0) \varphi_{rk}(x_0) \sin \omega_r^k(t - t_0) \, dx_0 \, dt_0. \tag{3.6}$$

Substituting now the relation (3.4) into Eq. (3.6), we get

$$f_k(t) = \frac{1}{\mu_r \omega_r^k} \varphi_{rk}(x_m) \sin \omega_r^k(t - t_m). \tag{3.7}$$

The deflection of the beam loaded in the manner shown in Fig. 3.2 is therefore expressed by the function

$$w_r(x, t) = \frac{1}{\mu_r} \sum_{k=1}^{\infty} \frac{1}{\omega_r^k} w_{rk}(x) \varphi_{rk}(x_m) \sin \omega_r^k(t - t_m). \tag{3.8}$$

However, this time we are interested not so much in the deflection as in the angular displacements of cross-sections of the beam considered:

$$\varphi_r(x, t) = -\frac{\partial w_r}{\partial x} = \frac{1}{\mu_r} \sum_{k-1}^{\infty} \frac{1}{\omega_r^k} \varphi_{rk}(x) \varphi_{rk}(x_m) \sin \omega_r^k(t - t_m). \tag{3.9}$$

Equation (3.9) already enables us to find the appropriate expressions for the kernels of the integral equation (3.3). It suffices to let $x = l_r$, $x_m = 0$, $t_m = t_0$ and to change the sign of the expression (3.9), on account of the difference of the senses of the loadings given in Figs. 3.1d and 3.2, to get

$$\delta_{r,r-1}(t - t_0) = -\frac{1}{\mu_r} \sum_{k=1}^{\infty} \frac{1}{\omega_r^k} \varphi_{rk}(l_r) \varphi_{rk}(0) \sin \omega_r^k(t - t_0). \tag{3.10}$$

In order to find the kernels $\delta_{r,r}(t - t_0)$ we have to take the sum of the two angles occurring by support r; in span r, it is necessary to let $x = x_m = l_r$ and in span $r+1$, $x = x_m = 0$. Hence, we have

$$\delta_{r,r}(t - t_0) = \frac{1}{\mu_r} \sum_{k=1}^{\infty} \frac{1}{\omega_r^k} \varphi_{rk}^2(l_r) \sin \omega_r^k(t - t_0) +$$

$$+ \frac{1}{\mu_{r+1}} \sum_{k=1}^{\infty} \frac{1}{\omega_{r+1}^k} \varphi_{r+1,k}^2(0) \sin \omega_{r+1}^k(t - t_0). \tag{3.11}$$

We obtain the quantity $\delta_{r,r+1}(t - t_0) = \delta_{r+1,r}(t - t_0)$ from Eq. (3.10) by replacing the subscript r by $r+1$.

Using Eqs. (b) and (c) from Example 2.2 and the denotations (3.2), we can present the expressions (3.10) and (3.11) in a more specified form:

$$\delta_{r,r-1}(t-t_0) = \frac{2}{l_r \sqrt{EJ_r \mu_r}} \sum_{k=1}^{\infty} (-1)^{k+1} \sin k^2 \omega_r^1 (t-t_0),\tag{3.12}$$

$$\delta_{r,r}(t-t_0) = \frac{2}{l_r \sqrt{EJ_r \mu_r}} \sum_{k=1}^{\infty} \sin k^2 \omega_r^1 (t-t_0) +$$

$$+ \frac{2}{l_{r+1} \sqrt{EJ_{r+1} \mu_{r+1}}} \sum_{k=1}^{\infty} \sin k^2 \omega_{r+1}^1 (t-t_0).\tag{3.13}$$

Evidently, we have in this way dispensed of the need to determine the frequency and form of free vibration for the structure as a whole, instead we have used solutions for a single simply supported beam, in which the frequencies and forms of free vibration are explicitly determinable. But a new problem has emerged, namely that of solving a set of Volterra's equations. Without attempting to get an exact solution of such a set, one of the numerical techniques should be applied here.

The technique presented below consists of approximating the unknown functions $X_r(t)$ by piece-wise linear functions (Fig. 3.3). As a result, in place
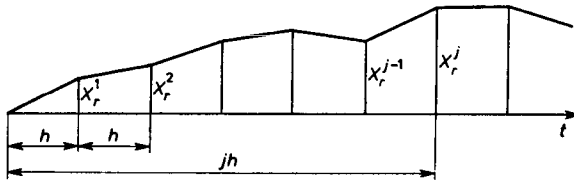
Fig. 3.3. Approximation of function $X_r(t)$

of the functions $X_r(t)$, their ordinates X_r^j at specified instants become the unknowns:

$$t_j = jh, \quad j = 1, 2, \dots\tag{3.14}$$

At the same time, we demand that the continuity conditions (3.3) which should be satisfied, in principle, at any instant t, be now satisfied only in a countable set of instants t_j.

Thus putting

$$X_r(t) = X_r^1 \frac{t}{h}, \quad r = 1, 2, \dots, s, \quad 0 < t < h,\tag{3.15}$$

into the first time interval, we write the conditions (3.3) for instant $t_1 = h$:

$$X_{r-1}^1 \delta_{r,r-1}^{1-1} + X_r^1 \delta_{r,r}^{1-1} + X_{r+1}^1 \delta_{r,r+1}^{1-1} + \delta_{rp}^1 = 0. \tag{3.16}$$

We have used here the denotations:

$$\delta_{r,s}^{1-1} = \delta_{r,s}^0 = \int_0^h \frac{t_0}{h} \delta_{r,s}(h-t_0) dt_0, \qquad s = r-1, r, r+1, \tag{3.17}$$

$$\delta_{rp}^1 = \delta_{rp}(h).$$

In this way, we have obtained a set of three-membered algebraic equations with respect to unknown values X_r^1, which can be solved without difficulty.

In the subsequent intervals, the functions $X_r(t)$ can be expressed by the general formula

$$X_r(t) = X_r^{j-1} \frac{jh-t}{h} + X_r^j \frac{t-(j-1)h}{h}, \qquad (j-1)h < t < jh. \tag{3.18}$$

The condition (3.3) in successive instants t_j can therefore be expressed:

$$X_{r-1}^j \delta_{r,r-1}^{j-j} + X_r^j \delta_{r,r}^{j-j} + X_{r+1}^j \delta_{r,r+1}^{j-j} +$$

$$+ \sum_{m=1}^{j-1} (X_{r-1}^m \delta_{r,r-1}^{j-m} + X_r^m \delta_{r,r}^{j-m} + X_{r+1}^m \delta_{r,r+1}^{j-m}) + \delta_{rp}^j = 0, \tag{3.19}$$

where:

$$\delta_{r,s}^{j-j} = \int_{(j-1)h}^{jh} \frac{t_0-(j-1)h}{h} \delta_{r,s}(jh-t_0) dt_0$$

$$= \int_0^h \frac{t_1}{h} \delta_{r,s}(h-t_1) dt_1 = \delta_{r,s}^0, \tag{3.20}$$

$$\delta_{r,s}^{j-m} = \int_{(m-1)h}^{mh} \frac{t_0-(m-1)h}{h} \delta_{r,s}(jh-t_0) dt_0 +$$

$$+ \int_{mh}^{(m+1)h} \frac{(m+1)h-t_0}{h} \delta_{r,s}(jh-t_0) dt_0$$

$$= \int_0^h \frac{t_1}{h} \{\delta_{r,s}[(j-m)h+h-t_1] + \delta_{r,s}[(j-m)h-h+t_1]\} dt_1, \tag{3.21}$$

$$\delta_{rp}^j = \delta_{rp}(jh). \tag{3.22}$$

All the quantities X_r^m in Eq. (3.19) occurring under the summation sign are already determined from the conditions of type (3.3) at instants $m < j$, where the quantities X_r^j are calculated from the set of equations (3.19) having the same matrix of coefficients $\delta_{r,s}^{j-j} = \delta_{r,s}^{1-1} = \delta_{r,s}^0$, as that in the set (3.16). This means that after a single inversion of the matrix of Eqs. (3.16), the subsequent values can be obtained recurrently.

By substituting the expressions (3.12) and (3.13) into Eqs. (3.20) and (3.21) and performing appropriate integrations, we get:

$$\delta_{r,r-1}^0 = \frac{2l_r}{EJ_r\pi^2} \sum_{k=1}^{\infty} \frac{(-1)^{k+1}}{k^2}\left(1 - \frac{\sin k^2\varepsilon_r}{k^2\varepsilon_r}\right),$$ (3.23)

$$\delta_{r,r}^0 = \frac{2l_r}{EJ_r\pi^2} \sum_{k=1}^{\infty} \frac{1}{k^2}\left(1 - \frac{\sin k^2\varepsilon_r}{k^2\varepsilon_r}\right) +$$

$$+ \frac{2l_{r+1}}{EJ_{r+1}\pi^2} \sum_{k=1}^{\infty} \frac{1}{k^2}\left(1 - \frac{\sin k^2\varepsilon_{r+1}}{k^2\varepsilon_{r+1}}\right),$$ (3.24)

$$\delta_{r,r-1}^{j-m} = \frac{4l_r}{EJ_r\pi^2} \sum_{k=1}^{\infty} (-1)^{k+1} \frac{1-\cos k^2\varepsilon_r}{k^2} \frac{\sin k^2\varepsilon_r(j-m)}{k^2\varepsilon_r},$$ (3.25)

$$\delta_{r,r}^{j-m} = \frac{4l_r}{EJ_r\pi^2} \sum_{k=1}^{\infty} \frac{1-\cos k^2\varepsilon_r}{k^2} \frac{\sin k^2\varepsilon_r(j-m)}{k^2\varepsilon_r} +$$

$$+ \frac{4l_{r+1}}{EJ_{r+1}\pi^2} \sum_{k=1}^{\infty} \frac{1-\cos k^2\varepsilon_{r+1}}{k_2} \frac{\sin k^2\varepsilon_{r+1}(j-m)}{k^2\varepsilon_{r+1}},$$ (3.26)

where

$$\varepsilon_r = \omega_r^1 h.$$ (3.27)

As much as the series in Eqs. (3.12), (3.13) may evoke reservations on account of their divergence, all the series in Eqs. (3.23)–(3.26) are convergent.
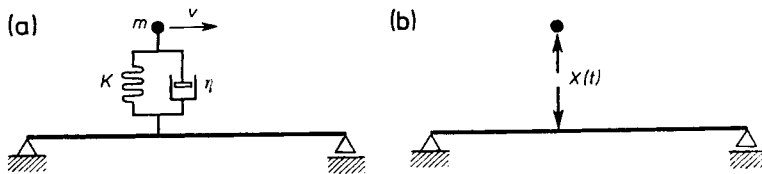
Fig. 3.4. Diagram of a beam loaded by model of vehicle

The presented method of solving dynamic problems can be used, of course, in other cases of bar structures. We arrive at Volterra's integral equations, for example, also in the case of a vehicle of non-negligible mass moving along a bar structure. The simplest model of such a system is shown in Fig. 3.4a. A viscoelastic element, modelling the suspension of the vehicle, has been assumed to be present between mass m and the beam.

Treating the interaction force (Fig. 3.4b) as an unknown, we use the condition

$$X(t) = K(w_m - w_b) + \eta(\dot{w}_m - \dot{w}_b), \tag{3.28}$$

where K and η denote the viscoelastic characteristic of the suspension, and w_m and w_b stand for vertical displacements of the mass and the beam at the place at which the vehicle happens to be at a given instant. This condition leads to Volterra's integral equation of the 2nd kind (cf. Kączkowski, 1965). If no viscoelastic element is present between the mass and the beam, the condition

$$w_m = w_b \tag{3.29}$$

reduces the problem to Volterra's integral equation of the 1st kind. In either case, the method just described can be used.

3.3. The Direct Stiffness Method (Displacement Method)

In the present section we confine our considerations to presenting a method for determining the frequencies and forms of free vibration in frameworks and also for finding solutions involving vibration forced by loads harmonically variable in time. We shall neglect damping, the influence of strains due to shear forces and the influence of rotational inertia under bending.

Both in the case of free and forced vibration, the structure as a whole, consequently each of its elements, will experience harmonic vibration. We must
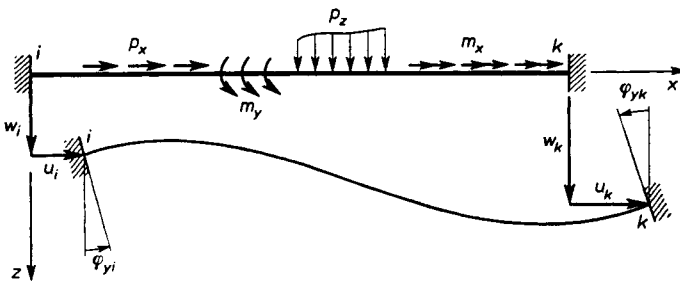
Fig. 3.5. Vibration amplitude of bar ik

therefore consider first of all a single bar, being an element of the bar structure considered. Assume that leads harmonically variable with angular frequency θ are acting on a bar fixed at both ends, whose projection on the xz plane is shown in Fig. 3.5:

$$\bar{p}(x, t) = p(x)e^{i\theta t}. \tag{3.30}$$

At the same time, both supports of the bar experience displacements with the same frequency:

$$\bar{q}_s(t) = q_s e^{i\theta t}, \quad s = i, k. \tag{3.31}$$

The single column matrices occurring in Eqs. (3.30), (3.31) in the general case of spatial vibration, have six components each, which we array:

$$p(x) = \{p_x(x), m_x(x), p_y(x), m_z(x), p_z(x), m_y(x)\}, \tag{3.32}$$

$$q_s = \{u_s, \varphi_{xs}, v_s, \varphi_{zs}, w_s, \varphi_{ys}\}, \quad s = i, k. \tag{3.33}$$

Using the principle of superposition, we consider for the present the case of no external load p acting on the bar. From Eqs. (2.24) and (2.59) after introducing the dimensionless variable $\xi = x/l$, we can express the displacement amplitudes of the bar axis as follows:

$$
\begin{aligned}
u(\xi) &= A\cos\lambda_u\xi + B\sin\lambda_u\xi, \\
\varphi_x(\xi) &= C\cos\lambda_x\xi + D\sin\lambda_x\xi, \\
v(\xi) &= E\,\mathrm{Ch}\,\lambda_v\xi + F\,\mathrm{Sh}\,\lambda_v\xi + G\cos\lambda_v\xi + H\sin\lambda_v\xi, \\
w(\xi) &= J\,\mathrm{Ch}\,\lambda_w\xi + K\,\mathrm{Sh}\,\lambda_w\xi + L\cos\lambda_w\xi + M\sin\lambda_w\xi.
\end{aligned}
\tag{3.34}
$$

The dimensionless parameters occurring here:

$$
\lambda_u = l\theta\sqrt{\frac{\mu}{EA}}, \qquad \lambda_x = l\theta\sqrt{\frac{I_0}{GJ_t}},
$$

$$
\lambda_v = l\sqrt{\theta\sqrt{\frac{\mu}{EJ_z}}}, \qquad \lambda_w = l\sqrt{\theta\sqrt{\frac{\mu}{EJ_y}}}
\tag{3.35}
$$

have been obtained from Eqs. (2.22) and (2.62), taking into account the previously introduced dimensionless variable ξ. Since in this case, the vibration frequency θ is treated as known, the values of parameters (3.35) are defined exactly.

Altogether, twelve integration constants occur in the functions (3.34), and these should be determined from twelve geometric boundary conditions. Using them we obtain:

$$
u(\xi) = u_i\frac{\sin\lambda_u\xi'}{\sin\lambda_u} + u_k\frac{\sin\lambda_u\xi}{\sin\lambda_u}, \tag{3.36}
$$

$$\varphi_x(\xi) = \varphi_{xl} \frac{\sin \lambda_x \xi'}{\sin \lambda_x} + \varphi_{xk} \frac{\sin \lambda_x \xi}{\sin \lambda_x}, \tag{3.37}$$

$$v(\xi) = v_i [A_v f_3(\lambda_v \xi') - B_v f_4(\lambda_v \xi')] +$$

$$+ \frac{l\varphi_{zl}}{\lambda_v} [B_v' f_3(\lambda_v \xi') - A_v f_4(\lambda_v \xi')] + v_k [A_v f_3(\lambda_v \xi) - B_v f_4(\lambda_v \xi)] -$$

$$- \frac{l\varphi_{zk}}{\lambda_v} [B_v' f_3(\lambda_v \xi) - A_v f_4(\lambda_v \xi)], \tag{3.38}$$

$$w(\xi) = w_i [A_w f_3(\lambda_w \xi') - B_w f_4(\lambda_w \xi')] -$$

$$- \frac{l\varphi_{yl}}{\lambda_w} [B_w' f_3(\lambda_w \xi') - A_w f_4(\lambda_w \xi')] +$$

$$+ w_k [A_w f_3(\lambda_w \xi) - B_w f_4(\lambda_w \xi)] +$$

$$+ \frac{l\varphi_{yk}}{\lambda_w} [B_w' f_3(\lambda_w \xi) - A_w f_4(\lambda_w \xi)]. \tag{3.39}$$

Two of four *Krylov* (or *Krylov–Prager*) *functions* occur in the above expressions:

$$f_1(x), f_3(x) = \frac{\mathrm{Ch}\, x \pm \cos x}{2},$$

$$f_2(x), f_4(x) = \frac{\mathrm{Sh}\, x \pm \sin x}{2}. \tag{3.40}$$

The tables of these functions can be found, among others in a textbook by Solecki and Szymkiewicz (1964). We have also introduced the notations:

$$A_r = \frac{\mathrm{Ch}\, \lambda_r - \cos \lambda_r}{1 - \mathrm{Ch}\, \lambda_r \cos \lambda_r},$$

$$B_r, B_r' = \frac{\mathrm{Sh}\, \lambda_r \pm \sin \lambda_r}{1 - \mathrm{Ch}\, \lambda_r \cos \lambda_r}, \qquad r = v, w. \tag{3.41}$$

Knowing the functions describing the displacements of the bar axis, we can determine using the equations given in Part 1 the generalized internal forces,
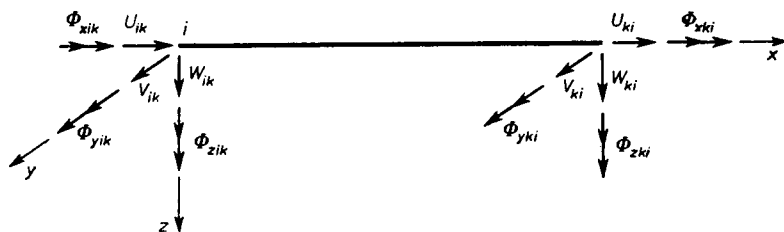
Fig. 3.6. Amplitudes of boundary forces acting on bar *ik*

and specifically their boundary values. Performing appropriate operations, we obtain finally the matrix relationship between boundary forces (Fig. 3.6) and displacements:

$$\begin{bmatrix} Q_{ik} \\ Q_{ki} \end{bmatrix} = \begin{bmatrix} E_{ii} & E_{ik} \\ E_{ki} & E_{kk} \end{bmatrix} \begin{bmatrix} q_i \\ q_k \end{bmatrix}, \tag{3.42}$$

where:

$$Q_s = \{U_s, \Phi_{xs}, V_s, \Phi_{zs}, W_s, \Phi_{ys}\}, \quad s = ik, ki, \tag{3.43}$$

E_{ii}, E_{kk}

$$= \begin{bmatrix} \dfrac{EA}{l}\mu_u & & & & & \\[2ex] & \dfrac{GJ_t}{l}\mu_x & & & & \\[2ex] & & \dfrac{EJ_z}{l^3}\gamma_v & \pm\dfrac{EJ_z}{l^2}\vartheta_v & & \\[2ex] & & \pm\dfrac{EJ_z}{l^2}\vartheta_v & \dfrac{EJ_z}{l}\alpha_v & & \\[2ex] & & & & \dfrac{EJ_y}{l^3}\gamma_w & \mp\dfrac{EJ_y}{l^2}\vartheta_w \\[2ex] & & & & \mp\dfrac{EJ_y}{l^2}\vartheta_w & \dfrac{EJ_y}{l}\alpha_w \end{bmatrix}, \tag{3.44}$$

E_{ik}, E_{ki}

$$= \begin{bmatrix} -\dfrac{EA}{l}\nu_u & & & & & \\[2ex] & -\dfrac{GJ_t}{l}\nu_x & & & & \\[2ex] & & -\dfrac{EJ_z}{l^3}\varepsilon_v & \pm\dfrac{EJ_z}{l^2}\delta_v & & \\[2ex] & & \mp\dfrac{EJ_z}{l^2}\delta_v & \dfrac{EJ_z}{l}\beta_v & & \\[2ex] & & & & -\dfrac{EJ_y}{l^3}\varepsilon_w & \mp\dfrac{EJ_y}{l^2}\delta_w \\[2ex] & & & & \pm\dfrac{EJ_y}{l^2}\delta_w & \dfrac{EJ_y}{l}\beta_w \end{bmatrix}. \tag{3.45}$$

The functions occurring in the matrices (3.44), (3.45):

$$\mu_j = \mu(\lambda_j) = \lambda_j \cot \lambda_j,$$

$$\nu_j = \nu(\lambda_j) = \frac{\lambda_j}{\sin \lambda_j}, \quad j = u, x, \tag{3.46}$$

$$\alpha_r = \alpha(\lambda_r) = \lambda_r \frac{\mathrm{Ch}\,\lambda_r \sin \lambda_r - \mathrm{Sh}\,\lambda_r \cos \lambda_r}{1 - \mathrm{Ch}\,\lambda_r \cos \lambda_r},$$

$$\beta_r = \beta(\lambda_r) = \lambda_r \frac{\mathrm{Sh}\,\lambda_r - \sin \lambda_r}{1 - \mathrm{Ch}\,\lambda_r \cos \lambda_r},$$

$$\vartheta_r = \vartheta(\lambda_r) = \lambda_r^2 \frac{\mathrm{Sh}\,\lambda_r \sin \lambda_r}{1 - \mathrm{Ch}\,\lambda_r \cos \lambda_r},$$

$$\delta_r = \delta(\lambda_r) = \lambda_r^2 \frac{\mathrm{Ch}\,\lambda_r - \cos \lambda_r}{1 - \mathrm{Ch}\,\lambda_r \cos \lambda_r}, \tag{3.47}$$

$$\gamma_r = \gamma(\lambda_r) = \lambda_r^3 \frac{\mathrm{Ch}\,\lambda_r \sin \lambda_r + \mathrm{Sh}\,\lambda_r \cos \lambda_r}{1 - \mathrm{Ch}\,\lambda_r \cos \lambda_r},$$

$$\varepsilon_r = \varepsilon(\lambda_r) = \lambda_r^3 \frac{\mathrm{Sh}\,\lambda_r + \sin \lambda_r}{1 - \mathrm{Ch}\,\lambda_r \cos \lambda_r}, \quad r = v, w,$$

are tabulated, e.g. in the monographs by Koloušek (1953) and Błaszkowiak and Kączkowski (1959, 1966).

The functions (3.47) are easily generalized, taking into account the influence of constant axial forces on transverse vibration. Without citing an appropriate derivation based on the solution (2.93), we present below the derived formulae from a textbook by Nowacki (1967, p. 830):

$$\alpha(\psi_r, \nu_r) = \frac{\psi_r^2 + \nu_r^2}{\Delta_r} (\psi_r \mathrm{Ch}\,\psi_r \sin \nu_r - \nu_r \mathrm{Sh}\,\psi_r \cos \nu_r).$$

$$\beta(\psi_r, \nu_r) = \frac{\psi_r^2 + \nu_r^2}{\Delta_r} (\nu_r \mathrm{Sh}\,\psi_r - \psi_r \sin \nu_r),$$

$$\vartheta(\psi_r, \nu_r) = \frac{\psi_r \nu_r}{\Delta_r} [2\psi_r \nu_r \mathrm{Sh}\,\psi_r \sin \nu_r - (\psi_r^2 - \nu_r^2)(1 - \mathrm{Ch}\,\psi_r \cos \nu_r)],$$

$$\delta(\psi_r, \nu_r) = \frac{\psi_r^2 + \nu_r^2}{\Delta_r} \psi_r \nu_r (\mathrm{Ch}\,\psi_r - \cos \nu_r), \tag{3.48}$$

$$\gamma(\psi_r, \nu_r) = \frac{\psi_r^2 + \nu_r^2}{\Delta_r} \psi_r \nu_r (\psi_r \mathrm{Sh}\,\psi_r + \nu_r \sin \nu_r),$$

$$\varepsilon(\psi_r, \nu_r) = \frac{\psi_r^2 + \nu_r^2}{\Delta_r} \psi_r \nu_r (\psi_r \mathrm{Sh}\,\psi_r \cos \nu_r + \nu_r \mathrm{Ch}\,\psi_r \sin \nu_r).$$

The following denotations are used in them:

$$\varDelta_r = 2\psi_r \nu_r (1 - \mathrm{Ch}\,\psi_r \cos\nu_r) + (\psi_r^2 - \nu_r^2)\,\mathrm{Sh}\,\psi_r \sin\nu_r, \qquad r = v, w, \tag{3.49}$$

$$\psi_v, \nu_v = l\sqrt{\sqrt{\frac{\mu\theta^2}{EJ_z} + \left(\frac{N}{2EJ_z}\right)^2} \pm \frac{N}{2EJ_z}},$$

$$\psi_w, \nu_w = l\sqrt{\sqrt{\frac{\mu\theta^2}{EJ_y} + \left(\frac{N}{2EJ_y}\right)^2} \pm \frac{N}{2EJ_y}}. \tag{3.50}$$

Tables of the functions (3.48) can be found in a paper by Witkowski and Żyszko (1965).

The functions (3.36)–(3.39) may also prove useful when we want to determine the values of generalized boundary forces induced by a load acting within a bar. For, as we know from the reciprocal displacement and reaction theorem, the influence lines are deflection lines induced by unit displacements of the respective supports with opposite senses to the positive senses of the reactions sought. Consequently, we can use the following formulae for reactions to a harmonically variable external load acting on a bar fixed at both ends:

$$U_{ik}^0 = -\int_0^1 \frac{\sin\lambda_u \xi'}{\sin\lambda_u}\, p_x(\xi)\,l\,\mathrm{d}\xi,$$

$$U_{ki}^0 = -\int_0^1 \frac{\sin\lambda_u \xi}{\sin\lambda_u}\, p_x(\xi)\,l\,\mathrm{d}\xi, \tag{3.51}$$

$$V_{ik}^0 = -\int_0^1 [A_v f_3(\lambda_v \xi') - B_v f_4(\lambda_v \xi')]\left[p_y(\xi) - \frac{\mathrm{d}m_z}{l\,\mathrm{d}\xi}(\xi)\right] l\,\mathrm{d}\xi$$

$$= -\int_0^1 [A_v f_3(\lambda_v \xi') - B_v f_4(\lambda_v \xi')] p_y(\xi)\,l\,\mathrm{d}\xi +$$

$$+ \lambda_v \int_0^1 [A_v f_2(\lambda_v \xi') - B_v f_3(\lambda_v \xi')] m_z(\xi)\,\mathrm{d}\xi, \tag{3.52}$$

$$\varPhi_{zik}^0 = -\frac{l^2}{\lambda_v}\int_0^1 [B_v' f_3(\lambda_v \xi') - A_v f_4(\lambda_v \xi')] p_y(\xi)\,\mathrm{d}\xi +$$

$$+ l\int_0^1 [B_v' f_2(\lambda_v \xi') - A_v f_3(\lambda_v \xi')] m_z(\xi)\,\mathrm{d}\xi, \quad \text{etc.} \tag{3.53}$$

For example, in the case of a bar loaded in its mid-length by harmonically variable concentrated force P (Fig. 3.7), we have

$$p_y(\xi) = \frac{P}{l}\,\delta(\xi-\tfrac{1}{2}),\tag{3.54}$$
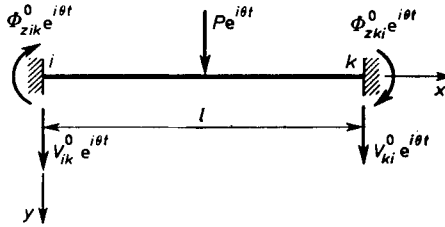
Fig. 3.7. Bar ik loaded by a harmonically variable force

and putting Eqs. (3.52) and (3.53) into this function and considering the relations (3.40), (3.41), we get

$$V_{ik}^0 = -P\left[A_v f_3\left(\frac{\lambda_v}{2}\right) - B_v f_4\left(\frac{\lambda_v}{2}\right)\right]$$

$$= -\frac{P}{2}\,\frac{\mathrm{Sh}\,\lambda_v' + \sin\lambda_v'}{\mathrm{Ch}\,\lambda_v'\sin\lambda_v' + \mathrm{Sh}\,\lambda_v'\cos\lambda_v'}$$

$$= -\frac{P}{2}\,\frac{\varepsilon(\lambda_v')}{\gamma(\lambda_v')},\tag{3.55}$$

$$\Phi_{zik}^0 = -\frac{Pl}{\lambda_v}\left[B_v' f_3\left(\frac{\lambda_v}{2}\right) - A_v f_4\left(\frac{\lambda_v}{2}\right)\right]$$

$$= -\frac{Pl}{4}\,\frac{1}{\lambda_v'}\,\frac{\mathrm{Ch}\,\lambda_v' - \cos\lambda_v'}{\mathrm{Ch}\,\lambda_v'\sin\lambda_v' + \mathrm{Sh}\,\lambda_v'\cos\lambda_v'}$$

$$= -\frac{Pl}{4}\,\frac{\delta(\lambda_v')}{\gamma(\lambda_v')},\tag{3.56}$$

where

$$\lambda_v' = \frac{\lambda_v}{2}.\tag{3.57}$$

Knowing the relationships between the generalized boundary forces and the load acting within the bar, on the one hand, and the displacements of its ends, on the other, we can make use of the analytical procedure typical for the displacement method, described in Part 1, Chapters 6 and 9. The set

of equations (6.82)–(6.84) undergoes, however, certain changes. The point is that this time we have related the boundary forces directly to displacements, giving up the intermediate stage of strain determination.

With such factors of secondary ranking as displacements of supports or distortional strains omitted, we write the set of equations (6.82)–(6.84), Part 1, in the case of harmonic vibrations, as follows:

$$\tilde{\mathbf{q}} = \mathbf{B}\mathbf{q}, \qquad \mathbf{B}^T\boldsymbol{\sigma} = \mathbf{Q} + \mathbf{Q}^p, \qquad \boldsymbol{\sigma} = \mathbf{E}\tilde{\mathbf{q}}. \tag{3.58}$$

The symbol $\tilde{\mathbf{q}}$ (in place of $\boldsymbol{\epsilon}$) denotes here the array of displacements of all bars in local coordinates associated with the axes of these bars.

Ridding the set of equations (3.58) successively of the quantities $\boldsymbol{\sigma}$ and $\tilde{\mathbf{q}}$, we arrive at a set of conditional equations of the displacement method, with displacements $\mathbf{q}$ as the sole unknowns:

$$\mathbf{K}\mathbf{q} = \mathbf{Q} + \mathbf{Q}^p. \tag{3.59}$$

We construct the siffness matrix $\mathbf{K}$ in the familiar manner:

$$\mathbf{K} = \mathbf{B}^T\mathbf{E}\mathbf{B}. \tag{3.60}$$

Having determined displacements $\mathbf{q}$ from Eq. $(3.58)_1$, we calculate displacements $\tilde{\mathbf{q}}$ associated with local coordinates of individual bars, and from Eqs. (3.36)–(3.39) we find the functions expressing the displacements within particular bars; differentiating them, we arrive at the distribution of generalized internal forces, and to be more exact, of their amplitudes, in the structure as a whole.

In the particular case of no external load, we deal with free vibrations, whose frequencies are determined from the condition

$$\det \mathbf{K} = 0. \tag{3.61}$$

This transcendental equation has an infinite number of elements $\theta = \omega_k$. Corresponding to each of these frequencies is a different vibration form which with an accuracy to a constant value can be determined from Eqs. (3.36)–(3.39), finding beforehand the displacements of joints corresponding to that form.

It should, however, be noted that by using the described procedure such forms of free vibration for which the joints experience no displacements may be overlooked. It is necessary, therefore, to check separately whether such forms of vibration are at all possible. Only after they have been considered, can the collection of vibration forms obtained make a complete system of functions with a frequency spectrum containing no gaps.

Given as an example in Fig. 3.8a is a frame consisting of three identical bars; also shown are two forms of free vibration a'_j and a'_k, for which the
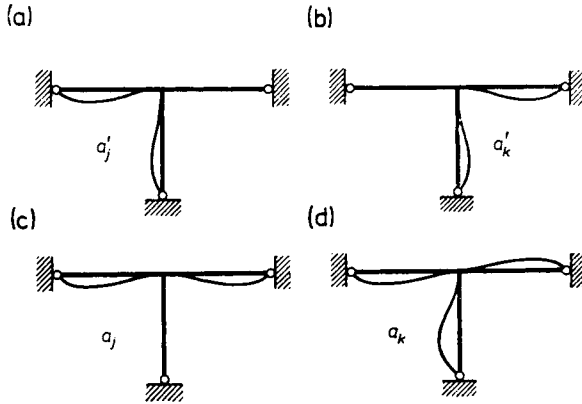
Fig. 3.8. Vibration forms corresponding to one and the same natural vibration frequency

joint of the frame does not experience rotations. These are, moreover, vibration forms corresponding to one and the same frequency $\omega_j = \omega_k$, but failing to satisfy the orthogonality condition. However, using a linear combination of the initial forms, the mutually orthogonal forms $a_j = a'_j + a'_k$, $a_\kappa = a'_j - a'_k$ shown in Fig. 3.8c, d are easily determined.

To normalize the eigenfunctions it is necessary to perform integration over all bars of the system according to the formula

$$\sum_{i=1}^{p} \int_0^{l_p} \mathbf{q}_i^T(x) \mathbf{m}_i \mathbf{q}_i(x) \, dx = m, \tag{3.62}$$

in which we have

$$\mathbf{q}_i(x) = \{u_i(x), v_i(x), w_i(x), \varphi_{si}(x)\}, \tag{3.63}$$

$$m_i = [\mu_i, \mu_i, \mu_i, I_{0i}], \quad i = 1, 2, ..., p. \tag{3.64}$$

How the derived relations are to be used will be demonstrated in the simple example of a plane frame.

EXAMPLE 3.1

Let an external load in the form of a force harmonically variable in time be acting on the frame shown in Fig. 3.9. Determine the vibration amplitudes of the joints and the frequencies and forms of free vibration.
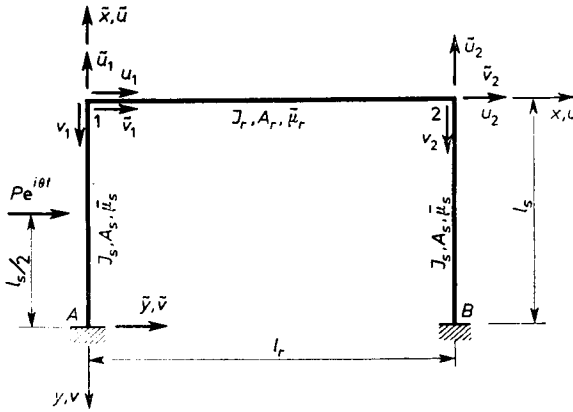
Fig. 3.9. Frame loaded by a harmonically variable force

The displacements of bar ends $A1$, 12 and $2B$ in local coordinates can be arrayed in the vector

$$\tilde{\mathbf{q}} = \{\tilde{u}_1, \tilde{v}_1, \varphi_1; u_1, v_1, \varphi_1, u_2, v_2, \varphi_2; \tilde{u}_2, \tilde{v}_2, \varphi_2\}, \tag{a}$$

which with displacements $\mathbf{q}$ in the global system

$$\mathbf{q} = \{u_1, v_1, \varphi_1, u_2, v_2, \varphi_2\} \tag{b}$$

is connected by means of the matrix

$$\mathbf{B} = \begin{bmatrix} \mathbf{B}_s & 0 \\ \mathbf{I} & 0 \\ 0 & \mathbf{I} \\ 0 & \mathbf{B}_s \end{bmatrix}, \quad \mathbf{B}_s = \begin{bmatrix} 0 & -1 & 0 \\ 1 & 0 & 0 \\ 0 & 0 & 1 \end{bmatrix}. \tag{c}$$

The above submatrices, unitary $\mathbf{I}$ and zero 0 have the dimensions 3×3.

The elasticity matrix of the structure

$$\mathbf{E} = [\mathbf{E}_{A1}, \mathbf{E}_{12}, \mathbf{E}_{2B}] \tag{d}$$

consists of submatrices, which on the basis of Eqs. (3.44), (3.45) can be written:

$$\mathbf{E}_{A1} = \mathbf{E}_{2B} = \begin{vmatrix} \dfrac{EA_s}{l_s}\mu_s & & \\ & \dfrac{EJ_s}{l_s^3}\gamma_s & -\dfrac{EJ_s}{l_s^2}\vartheta_s \\ & -\dfrac{EJ_s}{l_s^2}\vartheta_s & \dfrac{EJ_s}{l_s}\alpha_s \end{vmatrix}, \tag{e}$$

$$E_{12} = \begin{bmatrix} \dfrac{EA_r}{l_r}\mu_r & & & & & \\[2mm] & \dfrac{EJ_r}{l_r^3}\gamma_r & & & \text{symm.} & \\[2mm] & \dfrac{EJ_r}{l_r^2}\vartheta_r & \dfrac{EJ_r}{l_r}\alpha_r & & & \\[2mm] \hline -\dfrac{EA_r}{l_r}\nu_r & & & \dfrac{EA_r}{l_r}\mu_r & & \\[2mm] & -\dfrac{EJ_r}{l_r^3}\varepsilon_r & -\dfrac{EJ_r}{l_r^2}\delta_r & & \dfrac{EJ_r}{l_r^3}\gamma_r & \\[2mm] & \dfrac{EJ_r}{l_r^2}\delta_r & \dfrac{EJ_r}{l_r}\beta_r & & -\dfrac{EJ_r}{l_r^2}\vartheta_r & \dfrac{EJ_r}{l_r}\alpha_r \end{bmatrix}. \quad (f)$$

The above matrices contain functions expressed by Eqs. (3.46), (3.47):

$$\mu_k = \mu(\lambda_{uk}), \quad \nu_k = \nu(\lambda_{vk}), \quad \alpha_k = \alpha(\lambda_{vk}),$$

$$\beta_k = \beta(\lambda_{vk}), \quad \vartheta_k = \vartheta(\lambda_{vk}), \quad \delta_k = \delta(\lambda_{vk}), \quad \quad (g)$$

$$\gamma_k = \gamma(\lambda_{vk}), \quad \varepsilon_k = \varepsilon(\lambda_{vk}), \quad k = r, s,$$

in which in keeping with (3.35):

$$\lambda_{uk} = l_k\theta\sqrt{\dfrac{\bar{\mu}_k}{EA_k}}, \quad \lambda_{vk} = l_k\sqrt[4]{\theta\sqrt{\dfrac{\bar{\mu}_k}{EJ_k}}}. \quad (h)$$

Performing the operations prescribed by Eq. (3.60) we find the stiffness matrix of the system:

$$\mathbf{K} = \begin{bmatrix} \mathbf{K}_{11} & \mathbf{K}_{12} \\ \mathbf{K}_{21} & \mathbf{K}_{22} \end{bmatrix}, \quad (i)$$

$$\mathbf{K}_{11}, \mathbf{K}_{22} = \begin{bmatrix} \dfrac{EJ_s}{l_s^3}\gamma_s + \dfrac{EA_r}{l_r}\mu_r & 0 & -\dfrac{EJ_s}{l_s^2}\vartheta_s \\[3mm] 0 & \dfrac{EA_s}{l_s}\mu_s + \dfrac{EJ_r}{l_r^3}\gamma_r & \pm\dfrac{EJ_r}{l_r^2}\vartheta_r \\[3mm] -\dfrac{EJ_s}{l_s^2}\vartheta_s & \pm\dfrac{EJ_r}{l_r^2}\vartheta_r & \dfrac{EJ_s}{l_s}\alpha_s + \dfrac{EJ_r}{l_r}\alpha_r \end{bmatrix},$$

$$(j)$$

$$\mathbf{K}_{12}, \mathbf{K}_{21} = \begin{bmatrix} -\dfrac{EA_r}{l_r}\nu_r & 0 & 0 \\[3mm] 0 & -\dfrac{EJ_r}{l_r^3}\varepsilon_r & \pm\dfrac{EJ_r}{l_r^2}\delta_r \\[3mm] 0 & \mp\dfrac{EJ_r}{l_r^2}\delta_r & \dfrac{EJ_r}{l_r}\beta_r \end{bmatrix}.$$

Using the formulae (3.58), we determine the vector of the free terms:

$$\mathbf{Q}^p = \left\{ \frac{P}{2} \frac{\varepsilon(\lambda'_{vs})}{\gamma(\lambda'_{vs})}, 0, -\frac{Pl_s}{4} \frac{\delta(\lambda'_{vs})}{\gamma(\lambda'_{vs})} \right\}, 0, 0, 0 \right\},$$

$$\lambda'_{vs} = \frac{\lambda_{vs}}{2}.$$

(k)

It is easily seen that like in statics, the longitudinal deformability of bars has a negligible influence on the vibration of bar structures. We shall, therefore, make on major error, if we presume that $v_1 = v_2 = 0$, $u_1 = u_2$.

The vector of the sought displacements contains, therefore, only three components independent of each other:

$$\mathbf{q} = \{u_1, \varphi_1, \varphi_2\}.$$

(l)

Performing an appropriate limiting procedure, we give the stiffness matrix the form

$$\mathbf{K} = \begin{bmatrix} 2\dfrac{EJ_s}{l_s^3}\gamma_s - \dfrac{EJ_r}{l_r^3}\lambda_{vr}^4 & & & \\[2mm] -\dfrac{EJ_s}{l_s^2}\vartheta_s & \dfrac{EJ_s}{l_s}\alpha_s + \dfrac{EJ_r}{l_r}\alpha_r & \text{symm.} & \\[2mm] -\dfrac{EJ_s}{l_s^2}\vartheta_s & \dfrac{EJ_r}{l_r}\beta_r & \dfrac{EJ_s}{l_s}\alpha_s + \dfrac{EJ_r}{l_r}\alpha_r \end{bmatrix}.$$

(m)

Assume, for example, that

$$l_r = l_s = l, \qquad J_r = J_s = J,$$

$$\bar{\mu}_r = \bar{\mu}_s = \bar{\mu}, \qquad \theta = \frac{1}{l^2}\sqrt{\frac{EJ}{\bar{\mu}}}.$$

(n)

We then have

$$\lambda_{vr} = \lambda_{vs} = \lambda = 1,$$

(o)

and the following set of equations of the displacement method:

$$\begin{bmatrix} 22.256 & -5.948 & -5.948 \\ -5.948 & 7.980 & 2.007 \\ -5.948 & 2.007 & 7.980 \end{bmatrix} \begin{bmatrix} u_1 \\ l\varphi_1 \\ l\varphi_2 \end{bmatrix} = \frac{Pl^3}{EJ} \begin{bmatrix} 0.5014 \\ -0.1253 \\ 0 \end{bmatrix}$$

has the following solution (for comparison, the solution of a corresponding static problem is given in parentheses):

$$\{u, l\varphi_1, l\varphi_2\} = \frac{Pl^3}{EJ}\{0.02812, \ -0.00001, \ 0.02097\}$$

$$\left(= \frac{Pl^3}{EJ}\{0.02530, \ -0.00149, \ 0.01934\}\right).$$

Equating the determinant of matrix (m) to zero leads to the following transcendental equation:

$$[(2\gamma - \lambda^4)(2\alpha + \beta) - 2\vartheta^2](2\alpha - \beta) = 0. \tag{p}$$

For high values of λ, this equation can be substituted by an asymptotic equation:

$$(\cos \lambda - \sin \lambda - \tfrac{1}{2})(\cos \lambda - \sin \lambda + \tfrac{1}{2}) = 0. \tag{q}$$

The approximate roots of this equation have values given by the formulae:

$$\lambda_n = \frac{2n-3}{4}\pi + 1.932 \quad \text{for} \quad n = 5, 9, 13, \ldots,$$

$$\lambda_n = \frac{2n+3}{4}\pi - 1.932 \quad \text{for} \quad n = 6, 10, 14, \ldots,$$

$$\lambda_n = \frac{2n+1}{4}\pi - 1.209 \quad \text{for} \quad n = 7, 11, 15, \ldots,$$

$$\lambda_n = \frac{2n-1}{4}\pi + 1.209 \quad \text{for} \quad n = 8, 12, 16, \ldots$$

Several successive eigenvalues λ and displacements of joints corresponding to free vibration forms (unnormalized) are specified in Table 3.1. Exemplary forms of free vibration are presented diagrammatically in Fig. 3.10.
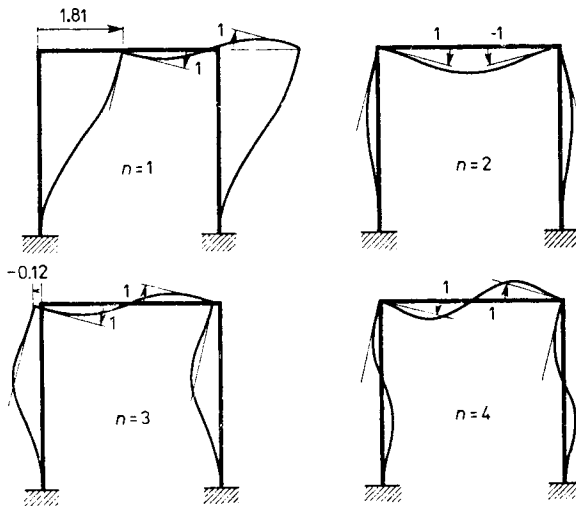
Fig. 3.10. Forms of free vibration of frame

TABLE 3.1

n	1	2	3	4	5	6	7	8	9	10
λ_n	1.79	3.55	4.51	6.71	7.43	9,85	10.51	12.99	13.71	16.13
u_1	1.81	0	-0.12	0	0	0	0	0	0	0
$l\varphi_1$	1	1	1	1	1	1	1	1	1	1
$l\varphi_2$	1	-1	1	1	-1	-1	1	1	-1	-1

4. Structures with a Finite Number of Dynamic Degrees of Freedom

4.1. Some Techniques of Reducing the Number of Degrees of Freedom

4.1.1. General remarks

In many cases it is altogether impossible to find exact, analytical solutions to dynamic problems described by partial differential equations. We also frequently give up seeking analytical solutions, in favour of using computers where every problem has to be worded algebraically. In a successive discretization stage we describe therefore the displacements sought by a finite number of generalized Lagrangian coordinates, in other words, by time functions expressing displacements of specified points of a structure. Correspondingly, the number of dynamic degrees of freedom decreases, since even with a continuous mass distribution along the bars, the position of each elementary body point $\mu \, dx$ depends in a specified manner on the generalized coordinates. This spatial discretization of functions describing the motion of a bar can be achieved by many different methods. Two of them are briefly discussed below.

4.1.2. The finite difference method

The differential equations of motion for a straight or curved bar can be written generally in the form

$$\mathbf{L}_1 \mathbf{f} + \mathbf{L}_2 \dot{\mathbf{f}} + \mathbf{L}_3 \ddot{\mathbf{f}} = \mathbf{p}, \tag{4.1}$$

where the symbols $\mathbf{L}_i$ denote matrices composed of various differential operators with respect to a spatial variable, and by $\mathbf{f}$ we have denoted vectors consisting of the components of the displacements sought. As for the vector $\mathbf{p}$, its components are external loadings. Operator matrices $\mathbf{L}_1$ may contain constant coefficients or coefficients dependent on the spatial variable.

For example, in the case of a curved in-plane loaded bar the set of equa-

tions of motion (2.72) is identical to the matrix equation (4.1) with the substitutions:

$$
\mathbf{L}_1 =
\begin{bmatrix}
\dfrac{\partial}{\partial s}\left(EA\dfrac{\partial}{\partial s}\right)+\dfrac{1}{r}\dfrac{\partial}{\partial s}\left[EJ_z\dfrac{\partial}{\partial s}\left(\dfrac{\cdots}{r}\right)\right] & \dfrac{1}{r}\dfrac{\partial}{\partial s}\left(EJ_z\dfrac{\partial^2}{\partial s^2}\right)-\dfrac{\partial}{\partial s}\left(EA\dfrac{\cdots}{r}\right) \\[3mm]
-\dfrac{\partial^2}{\partial s^2}\left[EJ_z\dfrac{\partial}{\partial s}\left(\dfrac{\cdots}{r}\right)\right]+\dfrac{EA}{r}\dfrac{\partial}{\partial s} & -\dfrac{\partial^2}{\partial s^2}\left(EJ_z\dfrac{\partial^2}{\partial s^2}\right)-\dfrac{EA}{r^2}
\end{bmatrix},
$$

(4.2)

$$
\mathbf{L}_2 = 0, \quad \mathbf{L}_3 = \begin{bmatrix} -\mu & 0 \\ 0 & -\mu \end{bmatrix},
$$

(4.3)

$$
\mathbf{f} = \{u, v\}, \quad \mathbf{p} = \left\{ p_s + \dfrac{m_z}{r}, \quad p_n - \dfrac{\partial m_z}{\partial s} \right\}.
$$

On the other hand, damped vibration of a straight bar, with considerable axial forces taken into account, is described by a single differential equation (cf. (2.72)). It can also be presented as the matrix equation (4.1) but the matrices therein degenerate into single operators or terms:

$$
\mathbf{L}_1 = EJ_y\dfrac{\partial^4}{\partial x^4} - \dfrac{\partial}{\partial x}\left(N\dfrac{\partial}{\partial x}\right) + k_z b = EJ_y\dfrac{\partial^4}{\partial x^4} - N\dfrac{\partial^2}{\partial x^2} + p_x\dfrac{\partial}{\partial x} + k_z b,
$$

$$
\mathbf{L}_2 = EJ_y t_E\dfrac{\partial^4}{\partial x^4} + \zeta_w,
$$

(4.4)

$$
\mathbf{L}_3 = \mu,
$$

$$
\mathbf{f} = w, \quad \mathbf{p} = p_z + \dfrac{\partial m_y}{\partial x}.
$$

(4.5)

Using the finite difference method, we divide the bar under study into segments (usually of identical length), and we treat the ordinates of the functions sought at the dividing points, called nodes, as unknown quantities. They form a vector with n components, where the number of unknowns n depends on the number of dividing points, the number of unknown functions occurring in vector $\mathbf{f}$ and the boundary conditions of the problem.

Let us consider for the sake of example a straight bar whose end $x = 0$ cannot experience displacements. Dividing the bar into identical segments a, we denote the uknown ordinates of the only function w sought at the dividing points, i.e., the generalized coordinates, by the symbols:

$$
q_k(t) = w(ka, t), \quad k = 1, 2, \ldots, n.
$$

(4.6)

If the bar end $x = l$ can experience displacements w, the number n equals the number of segments into which the bar has been divided. Otherwise, the

number of unknowns is reduced by one, i.e., equals the number of internal
dividing points of the bar.

We replace the derivatives in operators L_1 by corresponding difference
quotients, which for the node $x = ka$ (Fig. 4.1) have the form:
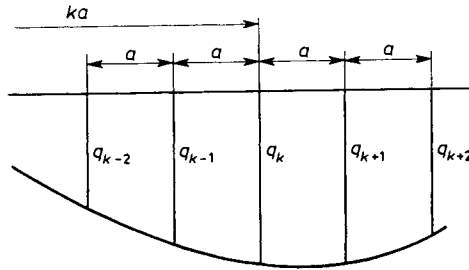
Fig. 4.1. Approximation of displacements of a vibrating bar

$$\frac{\partial w}{\partial x} = \frac{1}{2a}(-q_{k-1}+q_{k+1}),$$

$$\frac{\partial^2 w}{\partial x^2} = \frac{1}{a^2}(q_{k-1}-2q_k+q_{k+1}),$$

$$\frac{\partial^3 w}{\partial x^3} = \frac{1}{2a^3}(-q_{k-2}+2q_{k-1}-2q_{k+1}+q_{k+2}),$$ (4.7)

$$\frac{\partial^4 w}{\partial x^4} = \frac{1}{a^4}(q_{k-2}-4q_{k-1}+6q_k-4q_{k+1}+q_{k+2}), \quad \text{etc.}$$

Hence, the difference equation in the case of operators L_1 given by Eqs. (4.4)
takes the form:

$$\frac{EJ_y}{a^4}(q_{k-2}-4q_{k-1}+6q_k-4q_{k+1}+q_{k+2})-$$

$$-\frac{N_k}{a^2}(q_{k-1}-2q_k+q_{k+1})+\frac{p_{xk}}{2a}(-q_{k-1}+q_{k+1})+$$

$$+(k_z b)_k q_k + \frac{EJ_y}{a^4} t_E(\dot{q}_{k-2}-4\dot{q}_{k-1}+6\dot{q}_k-4\dot{q}_{k+1}+\dot{q}_{k+2})+$$

$$+\zeta_{wk}\dot{q}_k+\mu_k\ddot{q}_k = p_{zk}+\frac{\partial m_y}{\partial x}\bigg|_k.$$ (4.8)

In the vicinity of the bar ends, this equation undergoes certain modifications
which depend on the boundary conditions of the problem. At any rate, we get
as many difference equations of type (4.8) as there are degrees of freedom
allowed to the bar in question.

Most conveniently, the system of these equations can be written in matrix form:

$$\mathbf{Kq} + \mathbf{C\dot{q}} + \mathbf{M\ddot{q}} = \mathbf{Q}. \tag{4.9}$$

The matrices of stiffness $\mathbf{K}$, damping $\mathbf{C}$ and masses $\mathbf{M}$ are square matrices, size $n \times n$, whereas the generalized coordinates q_k and loads Q_k form vectors containing n components each.

4.1.3. The finite element method

Using the finite element method we likewise divide a bar (a structure) into segments and assume that the displacements within each of them depend on those generalized coordinates that express the displacements of the joints bounding a given segment (element). In other words, we assume that an approximate solution of an appropriate set of differential equations has the form:

$$\mathbf{f}(x, t) = \mathbf{N}(x)\mathbf{q}(t), \tag{4.10}$$

where $\mathbf{N}(x)$ is a matrix composed of predetermined shape functions assigned to successive components of the vector of generalized coordinates $\mathbf{q}(t)$. The function $N_i(x)$ has non-zero values only within the elements neighbouring on a joint whose displacement is expressed, e.g., by the generalized coordinate $q_i(t)$.

The point of departure for further considerations can be either one of the energy methods (e.g. Ritz's) or orthogonalization methods (Galerkin's), or the principle of virtual work. We shall make use of the last method. Treating the matrix-differential equation (4.1) as a set of equilibrium conditions for the generalized forces acting on element dx, we multiply this set by virtual increments of displacements $\delta\mathbf{f}$ and integrate the product over all bars of the structure:

$$\int_s \delta\mathbf{f}^T (\mathbf{L}_1\mathbf{f} + \mathbf{L}_2\ddot{\mathbf{f}} + \mathbf{L}_3\mathbf{f} - \mathbf{p})\,ds = 0. \tag{4.11}$$

Using in place of displacements $\mathbf{f}$ their approximation (4.10) and expressing in a similar manner the virtual displacements:

$$\delta\mathbf{f}(x, t) = \mathbf{N}(x)\,\delta\mathbf{q}(t). \tag{4.12}$$

we bring Eq. (4.11) to the form

$$\int_s \delta\mathbf{q}^T\mathbf{N}^T [(\mathbf{L}_1\mathbf{N})\mathbf{q} + (\mathbf{L}_2\mathbf{N})\dot{\mathbf{q}} + (\mathbf{L}_3\mathbf{N})\ddot{\mathbf{q}} - \mathbf{p}]\,ds = 0. \tag{4.13}$$

However, since the virtual increments $\delta\mathbf{q}$ can be arbitrary, the single scalar equation (4.13) can be replaced by a set of n equations for components of

vector q. This set has the form (4.9) but the matrices **K**, **C** and **M** and the vector of free terms **Q** are now calculated using the formulae:

$$\mathbf{K} = \int_s \mathbf{N}^T \mathbf{L}_1 \mathbf{N} ds, \quad \mathbf{C} = \int_s \mathbf{N}^T \mathbf{L}_2 \mathbf{N} ds, \tag{4.14}$$

$$\mathbf{M} = \int_s \mathbf{N}^T \mathbf{L}_3 \mathbf{N} ds,$$

$$\mathbf{Q} = \int_s \mathbf{N}^T \mathbf{p} ds. \tag{4.15}$$

Equations (4.14) require, according to the structure of particular operator matrices $\mathbf{L}_i$, simple transformations whereby several integrations are performed in parts. For example, for operators $\mathbf{L}_i$ given by Eqs. (4.4), we give the matrices (4.14) the form:

$$\mathbf{K} = \int_0^l \frac{d^2 \mathbf{N}^T}{dx^2} EJ_y \frac{d^2 \mathbf{N}}{dx^2} dx + \int_0^l \frac{d\mathbf{N}^T}{dx} \mathbf{N} \frac{d\mathbf{N}}{dx} dx + \int_0^l \mathbf{N}^T k_z b \mathbf{N} dx,$$

$$\mathbf{C} = \int_0^l \frac{d^2 \mathbf{N}^T}{dx^2} EJ_y t_E \frac{d^2 \mathbf{N}}{dx^2} dx + \int_0^l \mathbf{N}^T \zeta_w \mathbf{N} dx, \tag{4.16}$$

$$\mathbf{M} = \int_0^l \mathbf{N}^T \mu \mathbf{N} dx.$$

The finite element method applied do dynamics has been discussed more comprehensively, for example, by Zienkiewicz (1977). A certain variant of that method is the rigid finite element method developed by Kruszewski *et al.* (1975).

4.2. Integration Techniques for Matrix Equations of Motion

4.2.1. *The modal superposition technique*

As in the case of structures with infinitely many degrees of freedom, we have been using a series of eigenfunctions to express vibration, so in the case of vibration described by matrix-differential equations of type (4.9), we can present the solution in the form of a sum of eigenvectors multiplied by the corresponding time functions.

Therefore, we consider first the homogeneous equation

$$\mathbf{Kq} + \mathbf{C\dot{q}} + \mathbf{M\ddot{q}} = 0, \tag{4.17}$$

Let us assume that its solution can be given in the form:

$$\mathbf{q}(t) = \mathbf{a}e^{rt},\tag{4.18}$$

where $\mathbf{a}$ denotes a vector, unknown for the time being and composed of time independent parameters. Substituting the above relation into Eq. (4.17), we get the set of algebraic equations:

$$(\mathbf{K} + \mathbf{C}r + \mathbf{M}r^2)\mathbf{a} = 0,\tag{4.19}$$

which is homogeneous with respect to the components of vector $\mathbf{a}$.

The condition for the existence of a non-zero solution of the set (4.19) is the vanishing of the determinant of the set:

$$\det[\mathbf{K} + \mathbf{C}r + \mathbf{M}r^2] = 0.\tag{4.20}$$

This equation has $2n$ roots which are complex numbers (cf. (2.24)):

$$r_{k1}, r_{k2} = -\alpha_k\omega_k \pm i\omega_k', \quad k = 1, 2, ..., n.\tag{4.21}$$

The symbols ω_k denote vibration frequencies of the structure in the absence of damping, ω_k' are damped vibration frequencies. Substituting the denotations (4.21) into the condition (4.20), we get:

$$\det[\mathbf{K} - \mathbf{C}\alpha_k\omega_k - \mathbf{M}(\omega_k'^2 - \alpha_k^2\omega_k^2) \pm i\omega_k'(\mathbf{C} - 2\mathbf{M}\alpha_k\omega_k)] = 0.\tag{4.22}$$

The condition (4.22) will be satisfied if the two following conditions are simultaneously satisfied:

$$\det[\mathbf{C} - 2\mathbf{M}\alpha_k\omega_k] = 0,\tag{4.23}$$

$$\det[\mathbf{K} - \mathbf{C}\alpha_k\omega_k + \mathbf{M}\alpha_k^2\omega_k^2 - \mathbf{M}\omega_k'^2] = 0.\tag{4.24}$$

From the first condition, we can determine the values for $\alpha_k\omega_k$, and from the second, the damped vibration frequencies.

For vibration of a system with one degree of freedom the following relation (cf. (2.20)) occurs:

$$\omega_k' = \omega_k\sqrt{1 - \alpha_k^2}.\tag{4.25}$$

Assuming that the relation also occurs in the present case, the relation (4.24) can be replaced by the condition, at which we would have arrived for undamped vibration:

$$\det[\mathbf{K} - \mathbf{M}\omega_k^2] = 0.\tag{4.26}$$

Corresponding to each eigenvalue is a different eigenvector

$$\mathbf{a}_k = \{a_{1k}, a_{2k}, ..., a_{nk}\}, \quad k = 1, 2, ..., n,\tag{4.27}$$

whose components should satisfy the set of homogeneous equations:

$$[\mathbf{K} - \mathbf{M}\omega_k^2]\mathbf{a}_k = 0, \quad k = 1, 2, ..., n.\tag{4.28}$$

However, since for each value of ω_k there is a set with a singular matrix (cf. (4.26)), it allows only the proportions between individual components of the eigenvector to be determined. In other words, the set (4.28) consists of only $n-1$ linearly independent equations containing n unknown values a_{ik}. Such a set can therefore be solved with an accuracy to one constant, which may be an arbitrary, non-zero component of vector $\mathbf{a}_k$. Hence, in n sets of type (4.28) we have in all $n(n-1)$ equations containing n^2 unknowns. The missing n equations are obtained from the eigenvector normalization condition.

Let us construct using all the eigenvectors a square matrix called a modal matrix:

$$\mathbf{A} = [\mathbf{a}_1, \mathbf{a}_2, ..., \mathbf{a}_n], \tag{4.29}$$

and correspondingly, using the free vibration frequencies, a diagonal matrix

$$\mathbf{\Omega} = \lceil \omega_1, \omega_2, ..., \omega_n \rfloor. \tag{4.30}$$

We can now replace the set of equations (4.28) consisting of n subsets by a matrix set

$$\mathbf{KA} - \mathbf{MA\Omega}^2 = \mathbf{0}, \tag{4.31}$$

where $\mathbf{0}$ denotes a zero square matrix, $n \times n$. By multiplying Eq. (4.31) by $\mathbf{A}^T$ we get:

$$\mathbf{A}^T\mathbf{KA} = \mathbf{A}^T\mathbf{MA\Omega}^2. \tag{4.32}$$

Based on the symmetry of matrices $\mathbf{K}$ and $\mathbf{M}$, it follows that the products of $\mathbf{A}^T\mathbf{KA}$ and $\mathbf{A}^T\mathbf{MA}$ are also symmetric matrices. But the product of the symmetric matrix $\mathbf{A}^T\mathbf{MA}$ by the non-unitary diagonal 'matrix $\mathbf{\Omega}^2$ can be a symmetric matrix only when $\mathbf{A}^T\mathbf{MA}$ is likewise a diagonal matrix. Consequently, both products of $\mathbf{A}^T\mathbf{KA}$ and $\mathbf{A}^T\mathbf{MA}$ are diagonal matrices. We have proved in this way that the eigenvectors are orthogonal to each other, both with weight factor $\mathbf{K}$ and with weight factor $\mathbf{M}$. But we should recall here the reservation that in the case of multiple roots of Eq. (4.26), the orthogonality of eigenvectors is not so obvious and requires additional operations (described briefly in Section 3.3).

In addition, let us demand that the matrix $\mathbf{A}^T\mathbf{MA}$ be the product of the norm m by the unitary matrix:

$$\mathbf{A}^T\mathbf{MA} = m\mathbf{I}. \tag{4.33}$$

In this way we obtain n additional equations:

$$\mathbf{a}_k^T\mathbf{Ma}_k = m, \quad k = 1, 2, ..., n, \tag{4.34}$$

which together with the set (4.31) allow all the components of the modal matrix (4.29) to be uniquelly determined.

Note that following from the formula (4.33) is the relation

$$A^{-1} = \frac{1}{m} A^T M,$$ (4.35)

and from formula (4.32)

$$A^T K A = m\Omega^2.$$ (4.36)

It should be remembered, however, that the eigenvectors should satisfy at the same time the condition following from the assumption (4.23):

$$[C - 2M\alpha_k\omega_k]a_k = 0.$$ (4.37)

Performing similar operations as before, we arrive at the equation

$$A^T C A = 2A^T M A \alpha \Omega,$$ (4.38)

and because of the equality (4.33), it follows that

$$\alpha = [\alpha_1, \alpha_2, ..., \alpha_n] = \frac{1}{2m} A^T C A \Omega^{-1}.$$ (4.39)

This condition will be satisfied provided that the product of $A^T C A$ is a diagonal matrix. Specifically, this is the case if the damping matrix C can be expressed as the sum of two matrices proportional to the stiffness matrix K and the mass matrix M respectively:

$$C = \tilde{\varkappa}K + \mu M.$$ (4.40)

We then have

$$\alpha = \frac{1}{2}(\tilde{\varkappa}\Omega + \tilde{\mu}\Omega^{-1}).$$ (4.41)

Therefore, we write the general integral of the homogeneous matrix-differential equation (4.17) in the form

$$q(t) = Af(t),$$ (4.42)

where

$$f(t) = \{f_1(t), f_2(t), ..., f_n(t)\},$$ (4.43)

$$f_k(t) = G_k e^{-\alpha_k\omega_k t}\sin(\omega_k' t + \varphi_k), \quad k = 1, 2, ..., n.$$ (4.44)

We determine the integration constants G_k, φ_k from the initial conditions of motion described by generalized coordinates. The number of these conditions, $2n$, corresponds to the number of integration constants sought.

Seeking a particular integral of the non-homogeneous equation (4.9),

we shall follow Cauchy's method used for solving single differential equations. We assume therefore that the solution of Eq. (4.9) has the following structure:

$$q(t) = \int_0^t q^*(t-\tau)M^{-1}Q(\tau)d\tau. \tag{4.45}$$

Taking into account the dimensions of matrices q, M, and Q, we easily find that matrix q^* must be of size $n \times n$. Hence, it is a matrix consisting of n integrals of the homogeneous equation, each of them having a structure of type (4.42):

$$q^*(t) = A[f_1(t), f_2(t), ..., f_n(t)], \tag{4.46}$$

$$f_k = \{f_{1k}(t), f_{2k}(t), ..., f_{nk}(t)\}, \tag{4.47}$$

$$f_{ik} = G_{ik}e^{-\alpha_k\omega_k t}\sin(\omega_k' t + \varphi_{ik}), \quad i, k = 1, 2, ..., n. \tag{4.48}$$

We also demand from the functional matrix $q^*(t)$ that it satisfy the following initial conditions:

$$q^*(0) = 0, \quad \dot{q}^*(0) = I. \tag{4.49}$$

Obviously, the zero matrices 0 and the unitary matrix I all have the size $n \times n$. In this way, we have obtained $2n^2$ conditions from which we can determine n^2 constants G_{ik} and n^2 parameters φ_{ik} occurring in the matrix (4.46).

The first of these conditions (4.49) will be satisfied for

$$\varphi_{ik} = 0 \quad \text{for} \quad i, k = 1, 2, ..., n. \tag{4.50}$$

This enables the matrix (4.46) to be presented as follows:

$$q^*(t) = AF(t)G, \tag{4.51}$$

where $F(t)$ is a diagonal matrix:

$$F(t) = [e^{-\alpha_1\omega_1 t}\sin\omega_1' t, e^{-\alpha_2\omega_2 t}\sin\omega_2' t, ..., e^{-\alpha_n\omega_n t}\sin\omega_n' t], \tag{4.52}$$

and the matrix G is constructed of the coefficients G_{ik}:

$$G = \begin{bmatrix} G_{11} & G_{12} & ... & G_{1n} \\ G_{21} & G_{22} & ... & G_{2n} \\ \cdot & \cdot & \cdot & \cdot \\ G_{n1} & G_{n2} & ... & G_{nn} \end{bmatrix}. \tag{4.53}$$

The second initial condition (4.49) leads to the relation

$$\dot{q}^*(0) = A\Omega'G = I, \tag{4.54}$$

where Ω' denotes a diagonal matrix composed of damped vibration frequencies ω_k'. Considering Eqs. (4.35) and (4.54), we get

$$\Omega'G = A^{-1} = \frac{1}{m}A^T M. \tag{4.55}$$

Hence it follows that

$$\mathbf{G} = \frac{1}{m}\,\mathbf{\Omega}'^{-1}\mathbf{A}^T\mathbf{M}. \tag{4.56}$$

Putting the matrix $\mathbf{G}$ successively into formulae (4.51):

$$\mathbf{q}^*(t) = \frac{1}{m}\,\mathbf{AF}(t)\mathbf{\Omega}'^{-1}\mathbf{A}^T\mathbf{M} \tag{4.57}$$

and (4.45), we arrive at the following particular integral of the set of non-homogeneous differential equations (4.9):

$$\mathbf{q}(t) = \frac{1}{m}\int_0^t \mathbf{AF}(t-\tau)\mathbf{\Omega}'^{-1}\mathbf{A}^T\mathbf{Q}(\tau)\,\mathrm{d}\tau. \tag{4.58}$$

Thus, along with the general integral (4.43) we finally have the complete solution of the damped vibration problem for a structure with a finite number of dynamic degrees of freedom.

The modal superposition technique described is therefore fairly general, leading to exact solutions of a discretized set of equations of type (4.9). However, the use of this technique involves the need to find values and eigenvectors, which in the case of a structure with many dynamic degrees of freedom may prove very troublesome. Furthermore, if damping is to be taken into account, certain assumptions (4.40) concerning the structure of the damping matrix $\mathbf{C}$ need to be made.

4.2.2. Direct integration methods for equations of motion

A different argumentation underlies methods of direct, numerical integration of the sets of equations (4.9). They consist in determining the ordinates of functions $q_k(t)$ in successive instants, giving up at the same time an exact determination of variation of these functions between adjoining instants. We thus come to a successive stage of discretization, and the problem is reduced to a set of algebraic equations; solving it can safely be left to a digital computer.

The numerical integration techniques do not impose any limitations on the form of damping matrix $\mathbf{C}$, and their use, we need no longer cope with the problem of determining the eigenvalues and eigenvectors. They lead, however, to loss accurate results than does the modal superposition technique, because of the requirement of yet one more discretization of the solution.

There are a number of methods of direct integration but for lack of space we have to confine ourselves to sketching the most typical difference diagrams.

The derivatives with respect to time in Eq. (4.9) can be replaced by difference quotients (cf. (4.7)). This leads to the following set of equations at instants $t = sh$, where h is the time interval between successive instants that have elapsed since the beginning of the observations:

$$\mathbf{K}\mathbf{q}^s + \mathbf{C}\frac{\mathbf{q}^{s+1} - \mathbf{q}^{s-1}}{2h} + \mathbf{M}\frac{\mathbf{q}^{s-1} - 2\mathbf{q}^s + \mathbf{q}^{s+1}}{h^2} = \mathbf{Q}^s, \qquad (4.59)$$

$s = 0, 1, 2, \ldots$

Each of the vectors $\mathbf{q}^s$ contains n components.

Following from Eq. (4.59) is the recurrence formula

$$\mathbf{q}^{s+1} = \left[\mathbf{M} + \mathbf{C}\frac{h}{2}\right]^{-1}\left[\mathbf{Q}^s h^2 + (2\mathbf{M} - \mathbf{K}h^2)\mathbf{q}^s - \left(\mathbf{M} - \mathbf{C}\frac{h}{2}\right)\mathbf{q}^{s-1}\right]. \qquad (4.60)$$

Since in dynamic problems the initial conditions of motion are given, we can determine from Eqs. (4.60) the displacements successively at instants $s = 1, 2, \ldots$

More general and more commonly used is the recurrence method developed by Newmark (1959). He set out from the assumption that between displacement, velocity and acceleration vectors the following relations occur:

$$\dot{\mathbf{q}}^{s+1} - \dot{\mathbf{q}}^s = h[(1 - \gamma)\ddot{\mathbf{q}}^s + \gamma\ddot{\mathbf{q}}^{s+1}],$$

$$\mathbf{q}^{s+1} - \mathbf{q}^s = h\dot{\mathbf{q}}^s + h^2\left[\left(\frac{1}{2} - \beta\right)\ddot{\mathbf{q}}^s + \beta\ddot{\mathbf{q}}^{s+1}\right], \qquad (4.61)$$

where the parameters β and γ can take values from the intervals:

$$0 < \beta < \tfrac{1}{2}, \quad 0 < \gamma < 1. \qquad (4.62)$$

Using the relations (4.61), Newmark arrived at the following recurrence formula:

$$\begin{aligned}
\mathbf{q}^{s+1} = {}& (\mathbf{M} + \gamma h\mathbf{C} + \beta h^2\mathbf{K})^{-1}\{\beta h^2\mathbf{Q}^{s+1} + \\
& + (\tfrac{1}{2} + \gamma - 2\beta)h^2\mathbf{Q}^s + (\tfrac{1}{2} - \gamma + \beta)h^2\mathbf{Q}^{s-1} + \\
& + [2\mathbf{M} - (1 - 2\gamma)h\mathbf{C} - (\tfrac{1}{2} + \gamma - 2\beta)h^2\mathbf{K}]\mathbf{q}^s - \\
& - [\mathbf{M} - (1 - \gamma)h\mathbf{C} + (\tfrac{1}{2} - \gamma + \beta)h^2\mathbf{K}]\mathbf{q}^{s-1}\}.
\end{aligned} \qquad (4.63)$$

Following a different argumentation, Zienkiewicz (1977) arrived at an identical formula.

It is easily seen that the difference equation (4.60) is a special type of Eq. (4.63), when we let $\beta = 0$, $\gamma = 1/2$.

The selection of values for parameters β and γ involves the problem of fixing the integration step over time, h. For, depending on the values of these parameters actually selected, the recurrence process may be either uncon-

ditionally or conditionally stable. The recurrence process will be numerically stable, if under arbitrary initial conditions and in the absence of external loadings, all the components of the displacement vector are limited after a large, arbitrary number of recurrences.

In the case of conditional numerical stability, the length of the integration step h cannot be in excess of a specified limited value. For example, if

$$\beta < \tfrac{1}{4}(\tfrac{1}{2}+\gamma)^2, \tag{4.64}$$

then the integration step must satisfy the condition

$$h < \frac{2}{\omega_{\max} \sqrt{(\tfrac{1}{2}+\gamma)^2 - 4\beta}}, \tag{4.65}$$

where $\omega_{\max}$ denotes the root of the highest value in Eq. (4.26). From the above condition we find that the difference scheme (4.60) in particular will be stable, if the inequality below is satisfied:

$$h < \frac{2}{\omega_{\max}}. \tag{4.66}$$

The constraints on parameters β and γ according to Zienkiewicz (1977) are given below which, if satisfied, make the recurrence process unconditionally stable:

$$\beta \geqslant \tfrac{1}{4}(\tfrac{1}{2}+\gamma)^2, \quad \gamma \geqslant \tfrac{1}{2}, \quad \tfrac{1}{2}-\gamma+\beta \geqslant 0. \tag{4.67}$$

The stability and accuracy of various recurrence schemes is considered more comprehensively by Langer (1979) and Kacprzyk and Lewiński (1983).

The briefly described integration techniques for equations of motion involving a structure with a finite number of degrees of freedom are universal insofar that they are applicable not only to bar structures but to structures of any type that can be approximated by a discrete system.

References to Part 2

Argyris J. H., Scharpf D. W., 1969, "Finite elements in time and space", *The Aeron. J. of the Roy. Aeron. Soc.*, **73**.

Babakov I. M., 1965, *Theory of Vibrations* (in Russian), Izd. "Nauka", Moskva.

Bathe K., Wilson E., 1976, *Numerical Methods in Finite Element Analysis*, Prentice-Hall, New Jersey.

Białkowski G., 1975, *Classical Mechanics. Particle and Rigid Body Mechanics* (in Polish), PWN, Warszawa.

Bieniek M., 1952, "Foundations of dynamics of non-elastic bodies" (in Polish), *Arch. Mech. Stos.*, **4**, 1, 43–92.

Biggs, J., 1964, *Introduction to Structure Dynamics*, McGraw-Hill, New York.

Bishop R., Gladwell G., Michaelson S., 1972, *Matrix Vibration Analysis* (in Polish), WNT, Warszawa.

Błaszkowiak S., Kączkowski Z., 1959, *The Cross Method* (in Polish), PWN, Warszawa.

Błaszkowiak S., Kączkowski Z., 1966, *Iterative Methods in Structural Analysis*, Pergamon Press–PWN, London–Warszawa.

Counor R. H., 1973, *Dynamics of Physical Systems* (in Polish), WNT, Warszawa.

Chudnovskii V. G., 1952, *Methods of Computation of Vibrations and Stability of Skeletal Systems* (in Russian), Izd. AN USSR, Kiev.

Derski W., Ziemba S., 1968, *Analysis of Rheological Models* (in Polish), PWN, Warszawa.

Dobrzański L., 1963, "General equations of equilibrium and motion of a spatial curved bar" (in Polish), *Zesz. Nauk. Pol. Warszawskiej*, **75**, *Budownictwo* 20, 117–123.

Dżygadło Z., Kaliski S., Solarz L., Włodarczyk E., 1966, *Vibrations and Waves in Solids* (in Polish), PWN, Warszawa.

Federhofer K., 1950, *Dynamik des Bogenträgers und Kreisringes*, Springer, Wien.

Filippov A. P., 1955, *Vibrations of Elastic Systems* (in Russian), Izd. AN USSR, Kiev,

Filippov A. P., 1965, *Vibrations of Mechanical Systems* (in Russian), Izd. "Naukova dumka", Kiev.

Filippov A. P., 1970, *Vibrations of deforming Systems* (in Russian), Mashinostroenie Moskva.

Frąckiewicz H., 1965, "The dynamics of concentrated masses moving along a beam resting on elastic foundation" (in Polish), *Rozpr. Inż.* **13**, 2, 397–419.

Fung Y. C., 1969, *Foundations of Solid Body Mechanics* (in Polish), PWN, Warszawa.

Hale J. K., 1963, *Oscillations in Nonlinear Systems*, McGraw-Hill, New York–Toronto–London.

Hurty W., Rubinstein M., 1964, *Dynamics of Structures*, Prentice-Hall, New Jersey.

Kacprzyk Z., Lewiński T., 1983, "Comparison of some numerical integration methods

for the equations of motion of systems with a finite number of degrees of freedom",
   Rozpr. Inż., **31**, 2, 213–240.

Kauderer H., 1958, *Nichtlineare Mechanik*, Springer, Berlin.

Kączkowski Z., 1963, "Vibrations of a beam under a moving load", *Proc. of Vibration Problems*, 4, 4, 357–373.

Kączkowski Z., 1965, "Instationäre Schwingungen eines Brückenbalkens unter der Wirkung der verschiebbaren Belastungen", *Wissenschaftliche Zeitschrift der Hochschule f. Arch. u. Bauwesen, Weimar*, **12**, 5/6, 428–433.

Kączkowski Z., 1975, "The method of finite space-time elements in dynamics of structures", *J. of Technical Phys.*, **16**, 1, 69–84.

Kączkowski Z., 1979, "General formulation of the stiffness matrix for the space-time finite elements", *Arch. Inż. Ląd.*, **25**, 3, 351–357.

Koloušek V., 1953, *Baudynamik der Durchlaufträger und Rahmen*, Fachbuchverlag, Leipzig.

Kruszewski J., 1971, "Applications of the rigid finite elements to calculation of natural vibration frequencies of ship structures" (in Polish), *Mech. Teor. i Stos.*, 9, 4, 499–516.

Kruszewski J., Gawroński W., Wittbrodt E., Najbar F., Grabowski S., 1975, *The Rigid Finite Elements Method* (in Polish), Arkady, Warszawa.

Landau L., Lifszic E., 1961, *Mechanics* (in Polish), PWN, Warszawa.

Langer J., 1974, "Dynamic analysis of a bridge span loaded by moving vehicle" (in Polish), *Arch. Inż. Ląd.*, **20**, 4, 591–599.

Langer J., 1979, "Spurious damping in computer-aided solutions of the equations of motion" (in Polish), *Arch. Inż. Ląd.*, **25**, 3, 359–369.

Langer J., 1980, *Structural Dynamics* (in Polish), Wyd. Polit. Wrocławskiej, Wrocław.

Legras J., 1974, *Practical Methods of Numerical Analysis* (in Polish), WNT, Warszawa.

Lisowski A., 1959, *Vibration of Straight Bars and Frames. Selected Problems and Examples* (in Polish), Budown. i Architektura, Warszawa.

Mossakowska Z., Nowacki W., Sokołowski M., Wesołowski Z., 1978, *Technological Mechanics. Vol. IV. Elasticity* (in Polish), PWN, Warszawa.

Naleszkiewicz J., 1953, "Problem of bridge beam dynamics" (in Polish), Arch. Mech. Stos. 5, 4, 517–544; *Bull. Acad. Polon. Sci. Cl. IV*, 1954, **2**, 1, 31–35.

Naleszkiewicz J., Szaniawski A., 1953, "Vibrations and stability of masts and obelisks" (in Polish), *Rozpr. Inż.*

Newmark N., 1959, "A method of computation for structural dynamics", *J. Eng. Mech. Div., ASCE* **85**, EM3, July, 67–94.

Nowacki W., 1963, *Creep Theory* (in Polish), Arkady, Warszawa.

Nowacki W., 1967, *Structural Mechanics* (in Polish), Vol. 2, PWN, Warszawa.

Nowacki W., 1972, *Structural Dynamics* (in Polish), Arkady, Warszawa.

Nowacki W., 1978, *Theory of Elasticity*, In: M. Sokołowski (ed.) *Engineering Mechanics*, Vol. IV, *Elasticity* (in Polish), PWN, Warszawa.

Oden J. T., 1969, "A general theory of finite elements", *Intern. J. of Numerical Methods in Engineering* 1, 205–221, 247–259.

Osiński Z., 1978, *Damping of Mechanical Vibrations* (in Polish), PWN, Warszawa.

Osiński Z., 1980, *Vibration Theory* (in Polish), PWN, Warszawa.

Panovko Ya. G., 1971, *Introduction to the Theory of Mechanical Vibrations* (in Russian), Izd. "Nauka", Moskva.

Pestel E. C., Leckie A. C., 1963, *Matrix Methods in Elastomechanics*, McGraw-Hill, New York.

Pietrzak J., Rakowski G., Wrześniowski K., 1979, *Matrix Structural Analysis* (in Polish), PWN, Warszawa–Poznań.

Pisarenko G. S., Yakovlev A. P., Matveev V. V., 1976, *Vibration Damping Properties of Structural Materials* (in Polish), WNT, Warszawa.

Rakowski G., 1968, *Application of Matrices to the Static and Dynamic Analysis of Straight Bars* (in Polish), Arkady, Warszawa.

Reipert Z., 1969, "Vibration of a beam arbitrarily supported on its edges under a moving load", *Proc. Vibr. Probl.* **10**, 2, 247–260.

Reipert Z., 1970, "Vibration of frames under moving load", *Arch. Inż. Ląd.* **16**, 3, 419–447.

Rubinowicz W., Królikowski W., 1971, *Theoretical Mechanics* (in Polish), PWN, Warszawa.

Schallenkampe A., 1937, "Schwingungen von Trägern bei bewegten Lasten", *Ing.-Archiv*, p. 182.

Snitko N. K., 1960, *Dynamics of Structures* (in Russian), Gosstroiizdat, Leningrad–Moskva.

Sobczyk K., 1973, *Methods of Statistical Dynamics* (in Polish), PWN, Warszawa.

Solecki R., Szymkiewicz J., 1964, *Skeletal and Surface Structures. Dynamic Calculations* (in Polish), Arkady, Warszawa.

Sorokin E. S., 1962, *The Theory of Internal Friction During Vibration of Elastic Systems* (in Russian), Moskva.

Stending H., 1934, "Die Schwingungen von Trägern bei bewegten Lasten", *Ing.-Archiv*, p. 275.

Sułocki J., 1976, *Structural Dynamics—Calculation Methods and Examples* (in Polish), Wyd. Polit. Łódzkiej, Łódź.

Timoshenko S., 1955, *Vibration Problems in Engineering*, D. van Nostrand, Toronto–New York–London.

Whittaker E. T., 1944, *Analytical Dynamics*, Dover Publications, New York.

Wierzbicki T., 1980, *Calculation of Structures Under Dynamic Load* (in Polish), Arkady, Warszawa.

Wilde P., Wizmur M., 1977, *Analytical Mechanics* (in Polish), PWN, Warszawa.

Witkowski M., Żyszko M., 1965, "Flexural vibrations of frame structures composed of bars loaded with large axial forces" (in Polish), *Arch. Inż. Ląd.* **11**, 3, 337–415.

Yu Chen, 1966, *Vibrations: Theoretical Methods*, Addison-Wesley, Reading, Massachusetts.

Ziemba S., 1957, *Vibration Analysis* (in Polish), Vol. I, 1957, Vol. II, 1959, PWN, Warszawa.

Zienkiewicz O. C., 1977, *The Finite Element Method in Engineering Science*, 3rd ed., McGraw-Hill, London.

Zurmühl R., Falk S., 1984, *Matrizen und ihre Anwendungen für angewandte Mathematiker, Physiker und Ingenieure*, Springer, Berlin.

Introduction

In the design of structural elements which can be defined as slender or thin-walled, the analysis of the stability of equilibrium is no less important than the analysis of the equilibrium itself. In fact, an unstable equilibrium stands little chance of being established: it is only possible for certain types of loading controlled by displacements, whereas in the case of control by external forces it cannot practically come about. The stability analysis of equilibrium requires not only departure from the principle of rigidification, consequently, requiring consideration of changes in geometry, but frequently a dynamic approach as well, namely consideration of the stability of motion about the equilibrium point.

Real structures exhibit imperfections in shape and in the mode of application of the load, and they also feature non-homogeneity of the material. As a result, next to the stability analysis of perfect structures, the influence of imperfections on the behaviour of structures must be considered. These are either certain stability problems or problems related to them through significant effects of the changes in geometry; hence, they are discussed in some aspects in the present part.

1. Fundamental Concepts and Stability Criteria

1.1. The Definition of Stability of Equilibrium of an Elastic Body

The *stability of equilibrium* of an elastic body can be defined in most general terms as a particular case of stability of motion of that body. We shall consider first a system with one degree of freedom, described by a generalized coordinate, $q = q(t)$. Lapunov (1907) defined the *stable motion* of such a system as that kind of motion for which minor disturbances of the initial position and initial velocity cause minor disturbances of position and velocity at any instant t. In a special case, we shall call the equilibrium of a system *stable* when giving it a certain small deflection, $q(0)$, and a certain small velocity, $\dot{q}(0)$ (disturbances of the zero state), causes motion with small displacements and velocities at any instant t. In other words, the equilibrium point $q = 0$ is stable when δ_1 and δ_2 can be matched to every pair of arbitrarily small positive numbers $\varepsilon_1, \varepsilon_2$ so that if $|q(0)| < \delta_1$ and $|\dot{q}(0)| < \delta_2$, then $|q(t)| < \varepsilon_1$ and $|\dot{q}(t)| < \varepsilon_2$ for $0 < t < \infty$. Formally, the definition can also be written as a single pair of numbers ε, δ, for example, considering the norm $\sqrt{q^2 + \dot{q}^2}$, but in fact an additional parameter occurs then on reducing q and $\dot{q}$ to dimensionless form which is necessary for a physically correct norm to be introduced. If $\lim_{t \to \infty} q(t) = \lim_{t \to \infty} \dot{q}(t) = 0$, we then speak of *asymptotic stability*. If motion is constrained by ε_1 and ε_2 only for $0 < t < t_1$, then the equilibrium is stable only in a certain finite time interval.

In the case of a deformable system, in particular an elastic system, the kind of equilibrium depends generally on the value of the loading forces. It is usually sufficient to consider only loadings P_i growing proportionally, $P_i = \Lambda P_{i0}$ (simple loading), where Λ is called the *loading parameter* and P_{i0} are certain constants. If at $\Lambda = \Lambda_{\mathrm{cr}}$ the motion about the equilibrium point ceases to be stable, the value of the loading parameter Λ_{cr} is said to be the *critical value*.

Lapunov's definition can be generalized in various ways in the case of continuous deformable systems with an infinite number of degrees of freedom. Koiter (1963, 1965) proposed to replace $|q|$ and $|\dot{q}|$ in this definition with appropriate Gauss' norms (L_2) for the lengths of displacement vectors $\mathbf{u}$ and velocity vectors $\dot{\mathbf{u}}$, namely

$$\|\mathbf{u}\|_2 = \sqrt{\frac{1}{V} \iiint\limits_V u_i u_i \, dV},$$

$$\|\dot{\mathbf{u}}\|_2 = \sqrt{\frac{1}{M} \iiint\limits_V \varrho \dot{u}_i \dot{u}_i \, dV}, \tag{1.1}$$

where V stands for volume of the body, M—its mass, ϱ—density of the material, and $u_i = u_i(x, y, z)$—displacements; moreover, Einstein's summation convention (summation over i) has been applied in Eqs. (1.1). With such a generalization the equilibrium point is stable, if the inequalities $\|u(0)\|_2 < \delta_1$ and $\|\dot{u}(0)\|_2 < \delta_2$ imply that $\|u(t)\|_2 < \varepsilon_1$ and $\|\dot{u}(t)\|_2 < \varepsilon_2$ for $0 < t < \infty$. It is sometimes more convenient to consider the amplitudes instead of the norms (1.1), this corresponding under certain additional assumptions to Chebyshev's norms for displacements and velocities. The dependence of the stability region on the adopted norm was investigated by Shield and Green (1963), Movchan (1963) and Nemat-Nasser and Herrmann (1966).

1.2. The Kinetic Criterion of Stability

A direct application of Lapunov's definition to the study of the stability of equilibrium is called the *kinetic criterion of stability*; in order to avoid terminological misunderstandings we use here the term "kinetic criterion in the broader sense". Its application will be demonstrated using the example of a system with a finite number of degrees of freedom.

Consider motion about the equilibrium point $\mathbf{q} = 0$, where $\mathbf{q}$ denotes a column vector with n generalized coordinates (displacements). We confine ourselves to a linear case, admitting a dependence of the forces (acting on the system when deflected from the equilibrium position) on the displacements and on the velocities. In matrix notation the equations of motion then have the form

$$\mathbf{M\ddot{q}} + \mathbf{C\dot{q}} + \mathbf{Kq} = 0, \tag{1.2}$$

where $\mathbf{M}$ denotes a square matrix of inertia (a symmetric, positively defined mass matrix), whereas the square matrices $\mathbf{C}$ and $\mathbf{K}$ describe the forces acting

on the system while in motion. For classification, we decompose the latter matrices into symmetric and antisymmetric part according to the scheme $C = C_s + C_a$, rewriting (1.2) in the form

$$M\ddot{q} + (C_s + C_a)\dot{q} + (K_s + K_a)q = 0. \tag{1.3}$$

The forces $(-K_s q)$ have the potential

$$U = -\tfrac{1}{2}q^T K_s q, \tag{1.4}$$

where the superscript T denotes a transposed matrix. These forces are said to be *conservative* or *monogenic* (H. H. E. Leipholz)—in most classical stability problems, only forces of this type are involved. All other forces are called *non-conservative* or *polygenic* and as proposed by Ziegler (1953, 1956), they are classified as follows: $(-K_a q)$—circulatory forces, e.g., where follower loadings are involved; $(-C_s\dot{q})$—dissipative forces, e.g., viscous friction forces; $(-C_a\dot{q})$—gyroscopic forces causing no energy dissipation, e.g. in the case of rotating shafts.

Considering the solution of Eq. (1.2) in the typical form for linear equations

$$q = ae^{\lambda t}, \tag{1.5}$$

where λ may be a complex number, we obtain the following equation with an unknown column vector of amplitudes a:

$$(M\lambda^2 + C\lambda + K)a = 0. \tag{1.6}$$

The condition for the existence of non-trivial solutions of this equation

$$\det(M\lambda^2 + C\lambda + K) = 0, \tag{1.7}$$

where det denotes a determinant formed of the square matrix, is an equation of degree $2n$ with respect to λ. It has n pairs of complex, conjugate roots

$$\lambda_j = \gamma_j \pm i\omega_j, \quad j = 1, 2, \ldots n, \tag{1.8}$$

where ω_j are the frequencies of oscillating motion and γ_j—coefficients describing the increase or decrease of the amplitude. The motion about the equilibrium point is stable, and consequently the equilibrium is also stable when all the amplitudes are decreasing time functions (asymptotically stable motion). In this case, loss of stability takes place when the real part of one of the roots γ_j equals zero. If at the same time $\omega_j = 0$, loss od stability is said to take place *by divergence (buckling)*, but if $\omega_j \neq 0$, it then takes place *by flutter* (growth of the amplitude of vibration). The condition $\gamma_j = \omega_j = 0$ signifies the possibility of an equilibrium existing in an adjacent position (neutral equilibrium in the tested position) and it is called the static criterion

of stability, whereas $\gamma_j = 0$ at $\omega_j \neq 0$ is called the *kinetic criterion of sta-bility* (in narrower sense). Thus, the kinetic criterion in the broader sense covers the static criterion and the kinetic criterion in the narrower sense. The case where some γ_j are identically equal to zero should be considered separately. In that case, if all ω_j are different, then the corresponding amplitudes of vibration are constant: the loss of stability by flutter is liable to occur here when two frequencies ω_j become equal, since then a term of the type $t \sin \omega t$ with an infinitely growing amplitude becomes involved.

Equation (1.7) after expanding has the form

$$a_0 \lambda^{2n} + a_1 \lambda^{2n-1} + \ldots + a_{2n-1} \lambda + a_{2n} = 0, \tag{1.9}$$

where the coefficients a_i depend generally on the loading parameter Λ. The non-negativity conditions for the real parts of all the roots of Eq. (1.9) have been formulated by Routh and Hurwitz. They have the form $\Delta_k > 0$, $k = 1$, $2, \ldots, 2n$, where the last determinant has the form

$$\Delta_{2n} = \begin{vmatrix} a_1 & a_0 & 0 & 0 & 0 & \ldots & 0 \\ a_3 & a_2 & a_1 & a_0 & 0 & \ldots & 0 \\ a_5 & a_4 & a_3 & a_2 & a_1 & \ldots & 0 \\ \cdot & \cdot & \cdot & \cdot & \cdot & \cdot & \cdot \\ 0 & 0 & 0 & 0 & 0 & \ldots & a_{2n} \end{vmatrix}, \tag{1.10}$$

and the determinant Δ_k is the principal subdeterminant of the determinant Δ_{2n} (formed by retaining only k of the first rows and columns).

For $n = 2$ (two degrees of freedom, the simplest case in which the matrices can be asymmetric) we obtain four conditions which, assuming $a_0 > 0$, can be reduced to $a_1 > 0$, $a_3 > 0$, $a_4 > 0$ and

$$a_1 a_2 a_3 - a_0 a_3^2 - a_4 a_1^2 > 0 \tag{1.11}$$

(from which it also follows that $a_2 > 0$). The criterion (1.11) is the kinetic criterion in the narrower sense; the static criterion is obviously $a_4 > 0$, since only then does the imaginary part of the root λ_j pass simultaneously through zero.

If $a_1 \equiv a_3 \equiv 0$, then the condition (1.11) will not be satisfied, and equating the left-hand side to zero is an identity and does not constitute a criterion for loss of stability. Thus, the loss of stability by flutter takes place when the roots of the biquadratic equation (1.9) become equal; hence, the kinetic criterion of stability in the narrower sense takes the form

$$a_2^2 - 4a_0 a_4 > 0, \tag{1.12}$$

with $a_0 > 0$, $a_2 > 0$, $a_4 > 0$. For limit transition $a_1 \to 0$, $a_3 \to 0$, the criterion (1.11) does not pass as a rule into (1.12); a transition of this type occurs only in the particular case

$$\lim_{\substack{a_1 \to 0 \\ a_3 \to 0}} \frac{a_3}{a_1} = 2 \frac{a_4}{a_2}. \tag{1.13}$$

The non-vanishing odd coefficients occur primarily as the result of viscous damping; therefore, if (1.13) does not occur, then, in a non-conservative case, even small damping may exert a significant, discontinuous effect on the critical value of the loading parameter Λ.

In the general case of a system with n degrees of freedom, (1.9), the static criterion for loss of stability has the form

$$a_{2n} = 0 \quad \text{it means} \quad \det K = 0. \tag{1.14}$$

An effective form of the criterion (1.14) can of course be formulated by a purely static analysis, without dynamic considerations. In a conservative case where the matrix K is a symmetric matrix, the loss of stability can be defined only by the static criterion (1.14) (flutter cannot take place), so that dynamic analysis is actually unnecessary (Ziegler, 1952; Bolotin, 1961). This applies likewise to the occurrence of gyroscopic forces, defined by the matrix C_a, since buckling then cannot be preceded by flutter (Leipholz et al., 1978). Furthermore, Leipholz (1974) has given certain sufficient conditions justifying the application of the static criterion alone to some non-conservative problems ("conservative systems of the second kind"). In a general non-conservative case, the loss of stability may be determined by either the static criterion or by the kinetic criterion in the narrower sense.

1.3. The Static Criterion of Stability

The static criterion for loss of stability (1.14), which expresses the vanishing of vibration frequency ω, signifies the existence of an equilibrium also in a certain position adjacent to that under investigation. In that case, either a certain new form of equilibrium develops, in other words a bifurcation of the equilibrium form takes place, or else the loading parameter Λ reaches a local maximum, which in a load-controlled process means the appearance of a jump called *snap-through*. (In a particular case, a horizontal inflexion point of the displacement-force curve, reducing the jump to zero, is also possible). In the event of bifurcation, the primary form of equilibrium ceases to be stable in most cases, but the new form of equilibrium may be equally stable as unstable.

For an elastic body with an infinite number of degrees of freedom, the equilibrium can be described by a certain set of differential equations, non-linear in general and of the form

$$N_{1i}[\mathbf{u}]+AN_{2i}[\mathbf{u}] = 0, \quad i = 1, 2, ..., n, \tag{1.15}$$

where N_{1i} and N_{2i} denote respective differential operators, $\mathbf{u}$—displacement vector. To investigate the stability of the equilibrium, we have to consider the effect of geometry changes on the distribution of the internal forces and reactions, i.e., the principle of rigidification has to be neglected. The analysis of stability is closely associated with the study of non-uniqueness of solutions of the set of equations (1.15); in view of the departure from the principle of rigidification, Kirchhoff's theorem of uniqueness of solutions in linear elasticity theory ceases to be valid. The general theory of the static criterion of stability, based on the equations of non-linear elasticity theory, was developed by Biezeno and Hencky (1928), Trefftz (1933), Novozhilov (1948), Ishlinsky (1954) and Bolotin (1956).

If homogeneous boundary conditions are linked to Eqs. (1.15) and if the basic equilibrium position is described by the function $u \equiv 0$ (where u may denote just some characteristic components of the displacement vector, e.g. deflections of a bar), the bifurcation can then also be described by a set of linear differential equations

$$L_{1i}[\mathbf{u}]+AL_{2i}[\mathbf{u}] = 0, \quad i = 1, 2, ..., n, \tag{1.16}$$

where the linear operators L_{1i} and L_{2i} are formed from N_{1i} and N_{2i} by omitting the non-linear expressions (this being, however, not equivalent to returning to the principle of rigidification). The problem (1.16) is a problem of eigenvalues and it enables an exact determination of the critical values of the loading parameter A (Jasiński, 1956), but not the determination of the displacements, i.e., it does not define the postcritical behaviour of the system These displacements, $u = u(x, y, z)$, are determined only with the accuracy to a constant. For a system with an infinite number of degrees of freedom we obtain an infinite sequence of eigenvalues A_j, each of them corresponding to neutral equilibrium, whereas the smallest of them gives the practically important value of the critical loading A. To analyse the loss of stability causing a snap-through, it is necessary as a rule to use equations of non-linear theory of (1.15) type: the loss-of-stability condition requires that the loading parameter A reaches the maximum. In addition, an exact analysis of bifurcation, with non-zero displacements in the fundamental state, $u \neq 0$, calls for the use of non-linear equations; the possibility of linearization has been considered in general terms by Wesołowski (1974).

1.4. The Energy Form of the Static Criterion

We confine ourselves at first to a conservative system with n degrees of freedom, denoting arbitrarily selected generalized coordinates by q_i, $i = 1$, $2, ..., n$. The sum of the potential energy of elastic strain L_e and of the potential U which (with an appropriately chosen arbitrary constant) equals the work done by external forces L_f with opposite sign

$$\Pi = L_e + U = L_e - L_f \tag{1.17}$$

shall be called the *total potential energy*.

A necessary and sufficient condition of equilibrium of a system (for any form of equilibrium) is for Π to be stationary with respect to the generalized coordinates

$$\frac{\partial \Pi(q_j, \Lambda)}{\partial q_i} = 0, \quad i, j = 1, 2, ..., n. \tag{1.18}$$

Denote the coordinates q_i determined by the Eqs. (1.18), i.e., corresponding to the equilibrium point with parameter Λ, by q_i^E and the corresponding value of total potential energy by Π^E. The increment of the coordinates and of the energy in relation to the balance point is denoted by u_i and v, respectively

$$u_i = q_i - q_i^E, \quad v = \Pi - \Pi^E. \tag{1.19}$$

Expanding v into Taylor's series and taking (1.18) into account, we can write

$$v = \frac{1}{2} \frac{\partial^2 \Pi^E}{\partial q_i \partial q_j} u_i u_j + \frac{1}{6} \frac{\partial^3 \Pi^E}{\partial q_i \partial q_j \partial q_k} u_i u_j u_k + ..., \tag{1.20}$$

where the superscript E connotes that the given derivative is calculated at a point corresponding to the equilibrium point, $q_i = q_i^E$, and in addition, Einstein's summation convention is used. The stability of equilibrium depends in the first place on the quadratic form $v_{(2)}$, being the first non-vanishing term of the series (1.20).

By a suitable linear transformation of the generalized coordinates

$$w_i = \alpha_{ij} u_j, \quad i, j = 1, 2, ..., n, \quad \det \alpha_{ij} \neq 0, \tag{1.21}$$

the quadratic form $v_{(2)}$ is reducible to diagonal form

$$v_{(2)} = \frac{1}{2} C_i w_i^2, \tag{1.22}$$

where C_i are certain constants dependent on the loading parameter. The diagonal form (1.22) greatly facilitates the analysis of stability; the coordinates w_i are called the *principal coordinates* and C_i are called the *coefficients*

of stability. If all coefficients C_i are positive, the quadratic form (1.22) then being positive definite, every change of the coordinates u_i or v_i causes an increase in the total potential energy Π, and the equilibrium of the investigated system is stable. The vanishing to the lowest coefficient C_i signifies the critical state and a negative values of just one C_i signifies instability. The number of negative coefficients C_i is called the *degree of instability of the system.* The stability or instability of the critical state, and also the case of semidefiniteness of the quadratic form $v_{(2)}$, irrespective of the value of parameter Λ, require investigation of further terms of the series (1.20) (Thompson and Hunt, 1973; Huseyin, 1975).

For systems with two degrees of freedom, the diagonalization (1.21) corresponds to seeking the principal values of a plane tensor. They are given by the formulae

$$C_{1,2} = \frac{1}{2}\left(\frac{\partial^2 \Pi}{\partial q_1^2} + \frac{\partial^2 \Pi}{\partial q_2^2}\right) \pm \sqrt{\frac{1}{4}\left(\frac{\partial^2 \Pi}{\partial q_1^2} - \frac{\partial^2 \Pi}{\partial q_2^2}\right)^2 + \left(\frac{\partial^2 \Pi}{\partial q_1 \partial q_2}\right)^2}, \qquad (1.23)$$

and the condition of critical state has the form

$$\frac{\partial^2 \Pi}{\partial q_1^2}\frac{\partial^2 \Pi}{\partial q_2^2} - \left(\frac{\partial^2 \Pi}{\partial q_1 \partial q_2}\right)^2 = 0. \qquad (1.24)$$

For a system with n degrees of freedom, the critical-state condition can be written in the following form (Rzhanitzin, 1955; Volmir, 1963):

$$\det\frac{\partial^2 \Pi}{\partial q_i \partial q_j} = 0. \qquad (1.25)$$

In the case of the function Π being analytic, the condition (1.25) is a necessary but not sufficient condition of the critical state.

For systems with an infinite number of degrees of freedom, the positive definiteness of the quadratic form $v_{(2)}$ turns into positive definiteness of the second variation, $\delta^2\Pi > 0$. The vanishing of the second variation

$$\delta^2\Pi = 0 \qquad (1.26)$$

is the criterion of neutral equilibrium, i.e., the criterion of the critical state (a necessary condition). This criterion is very convenient for analysis of snap-through problems. On the other hand, the criterion of bifurcation can be expressed in a simpler way as the condition of equilibrium in the new, adjacent position

$$\delta\Pi_a = 0, \qquad (1.27)$$

where the subscript a means that the total potential energy is calculated not for the fundamental trajectory but for the new forming one. We find, moreover, that the minimum value od Π_a in the adjacent position equals zero, i.e.,

$$\Pi_a = 0 \tag{1.28}$$

is also a criterion of bifurcation. The criterion (1.27) is the basis of Ritz's approximate energy method and (1.28) is the basis of Timoshenko's energy method (Volmir, 1963).

1.5. Stability Versus Buckling

By *buckling* we understand usually the result of loss of stability of the basic form of equilibrium by bifurcation, i.e., the transition of the system to a new equilibrium path. In practice, such an idealized effect is not likely to take place, since in the case of bars under compression, for example, the assumptions of perfect axiality of loading and a perfectly straight axis of bar must hold. It will therefore be useful to broaden the meaning of the term "buckling". As proposed by Wierzbicki (1954) we shall call the phenomenon just described "buckling in the mathematical sense", emphasizing in this way the idealized assumptions of the analysis. On the other hand, by "buckling in the engineering sense" we shall understand all associated phenomena, e.g. eccentric compression of bars with a small initial curvature. Although the analysis of this type of problems is often not a stability analysis in the strict sense, it merits, nevertheless, joint treatment on account of the similar character of the phenomena and the similar approach to the problem (e.g. the necessity of departing from the principle of rigidification), and also owing to the possibility of limit transition from buckling in the engineering sense to buckling in the mathematical sense.

2. Elastic Stability of Axially Compressed Prismatic Bars

2.1. The Euler Problem

We confine ourselves at first to loadings of a spatially fixed direction, i.e., loadings which on loosing stability retain their direction with respect to space, and having a fixed point of application with respect to matter. Such loadings are conservative and the static criterion for stability is sufficient for their critical value to be determined. For a single concentrated force P, the respective critical values for various support modes of a bar were determined in the mid-18th century by L. Euler, considering the equilibrium of the bar in an adjacent position (neutral equilibrium of the straight position).

For statically determinate support modes, we can use directly the basic equation of elastic bending

$$EJw'' = -M, \tag{2.1}$$

where E—Young's modulus, J—axial moment of inertia of cross-section (the least moment of inertia if buckling is possible in any direction), w—deflection, M—bending moment which, taking an appropriate reference system, can be determined by the formula

$$M = Pw. \tag{2.2}$$

Calculation of the critical force is reduced here to the problem of eigenvalues for the differential equation

$$w'' + k^2 w = 0, \quad k = \sqrt{P/EJ}, \tag{2.3}$$

with two homogeneous boundary conditions. In the case of static indeterminability, more boundary conditions are involved; on the other hand, in Eqs. (2.2) and (2.3), we do have unknown reactions. It is more convenient then to use a more general, fourth-order equation of bending

$$w^{IV} + k^2 w'' = 0 \tag{2.4}$$

where the number of boundary conditions always conforms to the order of equation. In formulating the boundary conditions involving the transverse force, notice should be taken of two possible definitions of this force (Timoshenko and Gere, 1961). To distinguish between them we call the force tangent to rotated cross-section—the material transverse force T_m

$$T_m = -EJw''', \tag{2.5}$$

and the force tangent to cross-section of primary orientation—the spatial transverse force T_s

$$T_s = -EJw''' - Pw'. \tag{2.6}$$

Both expressions are appropriate to formulate the boundary conditions, but should be consistent in expressing the respective transverse force by the external loading.

The general integral of Eq. (2.4) has the form

$$w = C_1 \sin kx + C_2 \cos kx + C_3 x + C_4. \tag{2.7}$$
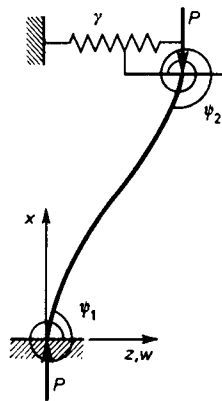
Fig. 2.1. General case of support of bar ends

In the general case of a bar with elastically clamped ends (Fig. 2.1), the system of axes can be fixed with the lower support, to be treated as immovable; one of the boundary conditions then always has the form $w(0) = 0$, whereas the other three conditions can be written in the form

$$w'(0) = \psi_1 l w''(0),$$
$$w'(l) = -\psi_2 l w''(l),$$
$$w(l) = -\gamma l^3 [w'''(l) + k^2 w'(l)], \tag{2.8}$$

where the dimensionless positive constants ψ_1 and ψ_2 describe the rigidity (or rather flexibility) of the clamping (rotation) and γ describes the rigidity

of the sidesway. The values of these constants in typical particular cases of support modes of bar and the corresponding least eigenvalues kl are listed in Table 2.1.

TABLE 2.1. Typical cases of support of bar ends

Case					
$\psi_1 =$	0	∞	0	0	0
$\psi_2 =$	∞	∞	0	∞	0
$\gamma =$	∞	0	∞	0	0
$k_1\,l$	$\dfrac{\pi}{2}$	π	π	4.4934	2π
μ	2	1	1	0.6992	0.5
Degree of re-dundancy	0	0	1	1	2

In a general case, for the boundary conditions (2.8) to be satisfied the determinant

$$
\begin{vmatrix}
0 & 1 & 0 & 1 \\
k & \psi_1 k^2 l & 1 & 0 \\
k\cos kl - \psi_2 k^2 l \sin kl & -k\sin kl - \psi_2 k^2 l \cos kl & 1 & 0 \\
\sin kl & \cos kl & 1+\gamma k^2 l^3 & 1
\end{vmatrix} = 0 \qquad (2.9)
$$

has to vanish, i.e., after expanding, the eigenvalues kl are given by the transcendental equation

$$
2 - [2 + (\psi_1 + \psi_2)(1 + \gamma k^2 l^2)k^2 l^2]\cos kl +
$$
$$
+ [-1 + \psi_1 + \psi_2 + k^2 l^2(\psi_1 \psi_2 - \gamma + \gamma \psi_1 \psi_2 k^2 l^2)]kl\sin kl = 0. \qquad (2.10)
$$

The least critical force P_{cr}, called the *Eulerian force* P_{cr} in the present case, can generally be determined by the formula

$$
P_{cr} = P_E = k^2 EJ = \frac{\pi^2 EJ}{l_r^2}. \qquad (2.11)
$$

In this formula, $l_r = \mu l$ denotes reduced (effective) length; $\mu = \pi/kl$ is a coefficient of support mode, whose values are given by (2.10) and depend on ψ_1, ψ_2 and γ, and for particular case are also listed in Table 2.1.

The critical stress in a bar σ_{cr} (positive under compression) can be determined by the formula

$$\sigma_{cr} = \frac{P_{cr}}{A} = \frac{\pi^2 EJ}{Al_r^2} = \frac{\pi^2 E}{\lambda^2}, \tag{2.12}$$

where A denotes the cross-sectional area of the bar, $\lambda = l_r/i$—slenderness ratio of the bar, $i = \sqrt{J/A}$—radius of gyration of cross-section. The condition of perfectly elastic buckling can be written in the form $\sigma_{cr} \leqslant \sigma_H$, where σ_H denotes the limit of proportionality of material under compression; it follows that

$$\lambda \geqslant \pi \sqrt{\frac{E}{\sigma_H}} \overset{\text{def}}{=} \lambda_{\lim}, \tag{2.13}$$

where the limiting slenderness ratio $\lambda_{\lim}$ is a dimensionless material constant whose value for many structural materials is about 100.

In the case of relatively short bars of a material of high elastic limit, a shortening of the bar before the loss of stability may have a significant effect. That effect can be taken into account by distinguishing the material coordinate X, $0 \leqslant X \leqslant l$, from the space coordinate x and the current length of the arc of the bar axis s. The basic equations of small deflections under longitudinal force $N = -P$, with consistent allowance for the compressibility of the axis have the form

$$EJ\frac{d\varphi}{dX} = -M, \quad \varphi = \frac{dw}{ds}, \quad \frac{ds}{dX} = 1 - \frac{P}{EA}, \tag{2.14}$$

where φ denotes the angle of deflection (slope). It follows therefrom that

$$\frac{d^2w}{dX^2} + \frac{P}{EJ}\left(1 - \frac{P}{EA}\right)w = 0 \tag{2.15}$$

and under boundary conditions of simple support $w(X = 0) = w(X = l) = 0$, we obtain

$$P_{cr} = \frac{\pi^2 EJ}{l^2(1 - P_{cr}/EA)}. \tag{2.16}$$

This is a quadratic equation with respect to the critical force P_{cr}; finally we have

$$P_{cr} = \frac{2P_E}{1 + \sqrt{1 - 4P_E/EA}} = \frac{P_E}{\frac{1}{2} + \frac{1}{2}\sqrt{1 - 4\pi^2/\lambda^2}}, \tag{2.17}$$

where P_E denotes the critical force without the compressibility effect considered. For $\lambda < 2\pi$, elastic buckling of the bar cannot take place at all.

The influence of shear on the value of the critical force can be considered in two ways: either by neglecting or considering in the calculation of the transverse force the additional rotation of the cross-section due to shear (Timoshenko and Gere, 1961). The more accurate of the two is the latter method which leads to the differential equation

$$\frac{\mathrm{d}^2 w}{\mathrm{d}x^2} + \frac{P}{EJ}\left(1 + \frac{nP}{GA}\right)w = 0, \tag{2.18}$$

where G denotes the shear modulus, and n stands for a coefficient dependent on the shape of the cross-section ($n = 1.2$ for rectangular cross-section, $n = 2 \div 6$ for typical thin-walled cross-sections). The respective value of the critical force is

$$P_{cr} = \frac{2P_E}{1 + \sqrt{1 + \frac{4n}{GA}P_E}} \approx \frac{P_E}{1 + \frac{n}{GA}P_E}, \tag{2.19}$$

and it is to be noted that the latter form of this formula, which though approximate is more commonly used in the literature, corresponds to ommission of the additional rotation of the cross-section in calculating the transverse force. The value (2.19) is usually not much smaller than P_E; larger differences are likely to occur in the case of helical springs or built-up columns, latticed or joined by batten plates (Timoshenko and Gere, 1961).

2.2. The Influence of the Behaviour of Loading on the Critical Value

If the bar loading is acting not at the rigid support but at the free end of the bar or between supports, the behaviour of loading in the course of loss of stability then has a significant influence on the critical value. For the sake of example we consider a bar clamped at one end, and loaded at the free end by a concentrated force (Fig. 2.2).

Both the point of application and the direction of the force may change during loss of stability. The shift of the point of application of the force e and the angle of its rotation against the deformed axis of the bar χ may depend on the bending deflection f and the slope α. It turns out that only the linear terms of the respective functions influence the critical value; therefore, the behaviour of loading can be described by four dimensionless parameters, ϱ, ϑ, u, v, as follows:
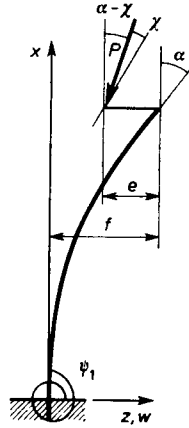
Fig. 2.2. General case of behaviour of loading during buckling

$$e = \varrho L\alpha + \vartheta f,$$

$$\chi = \mu\alpha + \nu \frac{f}{l}. \tag{2.20}$$

Thus, a moment M and a loading component H perpendicular to the undeformed bar ("horizontal") are formed in the course of buckling at the free end

$$M = Pe = Pl\left(\varrho\alpha + \vartheta\frac{f}{l}\right),$$

$$H = P(\alpha - \chi) = P\alpha - P\left(\mu\alpha + \nu\frac{f}{l}\right) = P\left(\eta\alpha - \nu\frac{f}{l}\right), \tag{2.21}$$

where $\eta = 1 - \mu$ is called the "tangency coefficient" describing the rotation of the force with respect to space, which for some applications is more convenient than μ. Before the loss of stability, when $\alpha = f = 0$, obviously $M = H = 0$ as well and the load is acting axially. Exemplary values of parameters ϱ, ϑ, μ and ν are given in Fig. 2.3 for several selected cases of behaviour of loading (Feodosev, 1950; Gajewski and Życzkowski, 1970).

The behaviour of loading (2.21) is non-conservative in general. Since the moment M does elementary work on the angle $(-d\alpha)$, and so does the elementary force H on the displacement $(-df)$, the conservativeness condition, i.e., the condition for the existence of a potential, has the form

$$\frac{\partial M}{\partial f} = \frac{\partial H}{\partial \alpha}, \quad \text{and hence} \quad \vartheta = 1 - \mu = \eta. \tag{2.22}$$
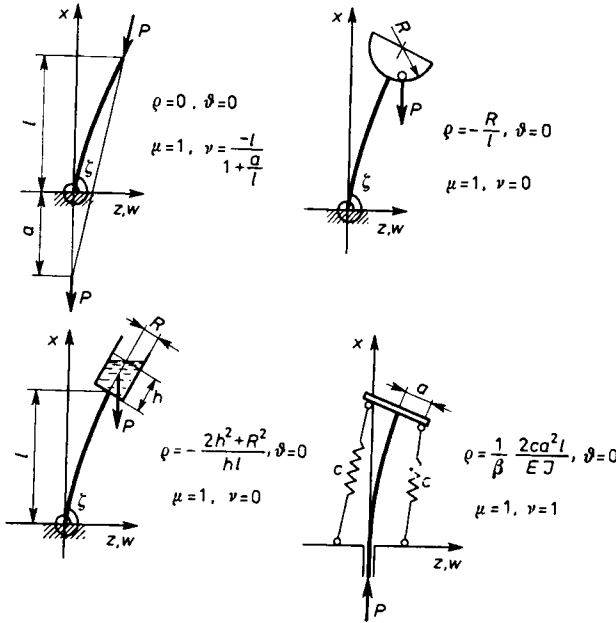
Fig. 2.3. Exemplary behaviour of loading during buckling

All the loadings shown in Fig. 2.3 satisfy the condition (2.22); hence, they are all conservative. The force tangent to the deformed bar axis (a follower force of a materially fixed direction) is described by the values of parameters $\varrho = \vartheta = \mu = \nu = 0$ (i.e., $\eta = 1$); hence, it is non-conservative.

In the case of conservative loadings (2.22), and also in certain non-conservative cases (e.g. in systems defined as "conservative of the second kind" (Leipholz, 1974), the critical load value can be determined by the static criterion. The equilibrium in an adjacent position is described here again by Eq. (2.4) with the general integral (2.7), and the boundary conditions, besides $w(0) = 0$, have the form

$$w'(0) = \psi_1 \, l w''(0),$$

$$w''(l) = -k^2 l \left[\varrho w'(l) + \vartheta \frac{w(l)}{l} \right], \tag{2.23}$$

$$w'''(l) = -k^2 \left[\mu w'(l) + \nu \frac{w(l)}{l} \right].$$

The additional parameter ψ_1 indicates the possibility of elastic clamping of the lower end; for rigid clamping, $\psi_1 = 0$. The conditions (2.23) can be

treated as more general than (2.8), namely (2.22) transform to (2.8) by formal substitution (satisfying the conditio n of conservativeness)

$$\varrho = 1/\psi_2 k^2 l^2, \quad \vartheta = 0, \quad \mu = 1, \quad \nu = 1/\gamma k^2 l^2, \tag{2.24}$$

which, however, exceeds the assumption that the above coefficients are constant and independent of the loading parameter k.

Taking into account the boundary condition (2.23) and equating to zero the respective determinant, we arrive at the following transcendental equation which is more convenient to express by the parameter η instead of μ

$$[2\nu\varrho + 2\eta\vartheta - (\eta + \vartheta)]kl - [2\nu\varrho + \nu + 2\eta\vartheta - (\eta + \vartheta) + 1 +$$
$$+ (\nu\varrho + \varrho + \eta\vartheta)\psi_1 k^2 l^2]kl\cos kl + [\nu - (\nu\varrho + \varrho + \eta\vartheta)k^2 l^2 +$$
$$+ (\nu\varrho + \nu + \eta\vartheta - \eta - \vartheta + 1)\psi_1 k^2 l^2]\sin kl = 0, \tag{2.25}$$

resulting in the critical load within the application range of the static criterion. The limits of this range were studied by Kordas (1963).

Equation (2.25) is symmetrical with respect to parameters ϑ and η, consequently interchange of the values of these parameters causes no change in the critical load. This conclusion turns out to also hold if the more general, kinetic criterion for stability is used. The system which is formed from a given system by interchange of the values of coefficients ϑ and η is called an *adjoint system*. For conservative loadings, $\vartheta = \eta$, (2.22); hence, the adjoint system is identical to the initial one, whereas in the case of non-conservative loadings
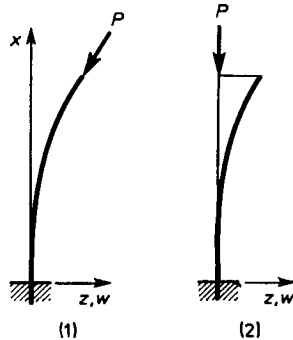
Fig. 2.4. Example of adjoint systems

the critical values calculated for the initial system may be used directly for the adjoint system. Exemplary adjoint systems are given in Fig. 2.4: for the first system (follower force), $\varrho = \vartheta = \mu = \nu = 0$ (i.e., $\eta = 1$) and for the second (a force of a fixed direction of the action line), $\varrho = \eta = \nu = 0$, $\vartheta = 1$.

The basic theorems for adjoint systems have been proved by Nemat-Nasser and Herrmann (1966), Ballio (1967) and Barta (1967).

A general analysis of stability in non-conservative cases $\vartheta \neq \eta$ can be carried out using the kinetic criterion for stability. We shall demonstrate the application of this criterion with the example of a one-parameter problem, using for this purpose the parameter η (the tangency coefficient, Fig. 2.5)
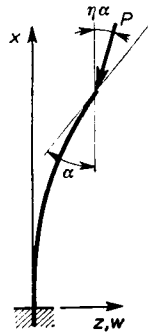
Fig. 2.5. Follower loading with tangency coefficient η

and assuming $\varrho = \vartheta = v = 0$ plus $\psi_1 = 0$ (rigid clamping). Such a load is non-conservative, except in the case where $\eta = 0$ (Eulerian load, of spatially fixed direction and materially fixed point of application). When $\eta < 0$, we call the load *antitangential*; for $0 < \eta < 1$, *subtangential*; for $\eta = 1$, *tangential*; and for $\eta > 1$, *supertangential*. The source of a tangential force can be, for example, a jet engine axially attached to a bar.

The equation of small transverse vibrations about a straight equilibrium position

$$EJw^{\mathrm{IV}} + Pw'' + m\ddot{w} = 0, \tag{2.26}$$

where m denotes the mass of unit length of the bar and the derivatives with respect to time t and marked by dots, can be reduced by substituting $w(x, t) = e^{\mathrm{i}\omega t}f(x)$ into the ordinary differential equation

$$EJf^{\mathrm{IV}} + Pf'' - m\omega^2 f = 0, \tag{2.27}$$

with the general integral

$$f(x) = C_1 \operatorname{sh} k_1 x + C_2 \operatorname{ch} k_1 x + C_3 \sin k_2 x + C_4 \cos k_2 x. \tag{2.28}$$

The coefficients k_1 and k_2 (actually ik_2) are the roots of the respective characteristic equation and equal

$$k_{1,2}^2 = \mp \frac{P}{2EJ} + \sqrt{\frac{P^2}{4E^2J^2} + \frac{m\omega^2}{EJ}}. \tag{2.29}$$

The boundary conditions (2.23) in the present case, $\psi_1 = \varrho = \vartheta = \nu = 0$, $\mu = 1 - \eta$, lead to a transcendental equation of the form

$$\Delta(k_1, k_2, \eta) = F_1(k_1, k_2) + \eta F_2(k_1, k_2) = 0, \tag{2.30}$$

where

$$
\begin{aligned}
F_1 &= 2k_1^2 k_2^2 - k_1 k_2 (k_2^2 - k_1^2)\,\mathrm{sh}\,k_1 l \sin k_2 l + (k_1^4 + k_2^4)\,\mathrm{ch}\,k_1 l \cos k_2 l, \\
F_2 &= (k_2^2 - k_1^2)[(k_2^2 - k_1^2) + 2k_1 k_2\,\mathrm{sh}\,k_1 l \sin k_2 l - \\
&\quad - (k_2^2 - k_1^2)\,\mathrm{ch}\,k_1 l \cos k_2 l].
\end{aligned} \tag{2.31}
$$

Equation (2.30) relates the natural vibration frequency ω to the force P. The static criterion for loss of stability reduces to $\omega = 0$; then also $k_1 = 0$ and $k_2^2 = P/EJ$; the transcendental equation (2.30) becomes a trigonometric equation, and its solution can be written in the form

$$p \overset{\text{def}}{=} \frac{Pl^2}{\pi^2 EJ} = \frac{1}{\pi^2}\left(\arccos \frac{\eta}{\eta - 1}\right)^2. \tag{2.32}$$

Obviously, the same result can be obtained from (2.25).

The static criterion does not lead to any result at $\eta < 0.5$. The critical force is then defined by the kinetic criterion in the narrower sense; in the absence of damping it reduces to the demand that the root ω of Eq. (2.30) be a double root (transition of beat into flutter). This root is double if the following relation holds as well:

$$\frac{\partial \Delta}{\partial \omega} = \left(\frac{\partial F_1}{\partial k_1}\frac{\partial k_1}{\partial \omega} + \frac{\partial F_1}{\partial k_2}\frac{\partial k_2}{\partial \omega}\right) + \eta\left(\frac{\partial F_2}{\partial k_1}\frac{\partial k_1}{\partial \omega} + \frac{\partial F_2}{\partial k_2}\frac{\partial k_2}{\partial \omega}\right) = 0. \tag{2.33}$$

Calculating the derivatives $\partial k_1/\partial \omega$ and $\partial k_2/\partial \omega$ from (2.29), substituting into (2.33) and rearranging, we obtain

$$\left(k_2\frac{\partial F_1}{\partial k_1} + k_1\frac{\partial F_1}{\partial k_2}\right) + \eta\left(k_2\frac{\partial F_2}{\partial k_1} + k_1\frac{\partial F_2}{\partial k_2}\right) = 0. \tag{2.34}$$

The set of equations (2.30) and (2.34) determines the functions $p = p(\eta)$ and $\omega = \omega(\eta)$. The first makes the critical force dependent on the tangency coefficient η and the second gives the corresponding double frequency ω.

The relation $p = p(\eta)$ has been thoroughly investigated by Kordas and Życzkowski (1963). The curve reaches a minimum at point $\eta = 0.5$, being $p = 1.62646$. However, since the kinetic criterion in the narrower sense is valid for $\eta > 0.5$, the function $p = p(\eta)$ increases monotonically in this interval. For $\eta = 1$ (the tangential force), we get $p = 2.03158$, i.e., $P_{\mathrm{cr}} = 20.0509\ EJ/t^2$; Beck (1952) was first to obtain this value. This force is more than eight times as great as the Eulerian value $p = 0.25$ for

$\eta = 0$. Likewise, the stress condition of safety for a bar under a tangential force justifies the assertion that it is significantly less dangerous than a force of fixed direction (Kowalski and Życzkowski, 1967). For $\eta \to \infty$ we obtain an asymptotic value $p \to 4.8405$. That value is nearly 20 times as great as the Eulerian value. The plot of the function $p = p(\eta)$ is given in Fig. 2.6.
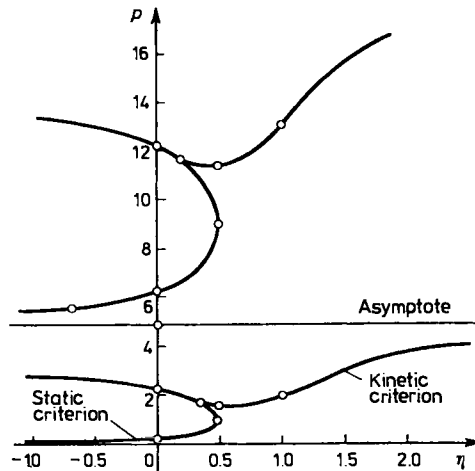
Fig. 2.6. Dependence of the critical force on the tangency coefficient

The influence of the compressibility of the axis on the critical value of loading in the non-conservative case considered here was investigated by Hauger (1975). He demonstrated that when taking compressibility into account there exists a certain boundary value η (dependent on slenderness ratio λ) above which the loss of stability does not take place at all.

In the application range of the kinetic criterion in the narrower sense, the critical force depends on two factors which for the static criterion are insignificant, namely on mass distribution (which may to a certain degree be independent of the rigidity distribution of the bar along the axis) and of the possible damping of vibrations about the equilibrium position.

The influence of the mass distribution has been investigated by Pflüger (1955), Deyneko and Leonov (1955), Kordas and Życzkowski (1963). Pflüger assumed that the mass is in part continuously distributed and in part concentrated at the free end; the other two papers considered two concentrated masses, placed in the centre of the bar and at its free end, but Deyneko and Leonov (1955) confined themselves to $\eta = 1$ and Kordas and Życzkowski (1963) investigated the entire variation range of η. All the authors found a certain most unfavourable mass distribution at which the critical

force is least (less than about 20% of the force calculated for a uniform mass distribution).

The influence of damping of vibrations on the value of the critical force was investigated in the first place on a simple model with two degrees of freedom, proposed by Ziegler (1953), Fig. 2.7. When internal friction (in
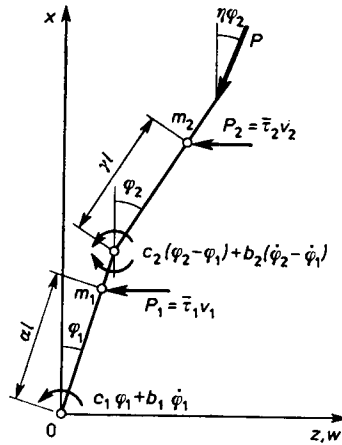
Fig. 2.7. Ziegler's model with two degrees of freedom

hinges) is considered, this causes a reduction of the critical force, i.e., destabilization (Ziegler, 1956; Herrmann and Jong, 1966). On the other hand, the influence of external friction has a stabilizing effect (Gajewski and Życzkowski, 1972; Gajewski, 1972) when the coefficients for the two types of friction tend toward zero, the corresponding critical load depends on the ratio of the coefficients.

For Ziegler's model loaded as in Fig. 2.7, the equation of small vibrations is easiest to derive on the basis of Lagrange's equation of the second kind, generalized to the case of dissipative forces

$$\frac{\mathrm{d}}{\mathrm{d}t}\left(\frac{\partial E_k}{\partial \dot{\varphi}_i}\right) + \frac{\partial L_e}{\partial \varphi_i} + \frac{\partial D}{\partial \varphi_i} = Q_i, \quad i = 1, 2, \tag{2.35}$$

where E_k is the kinetic energy, L_e the elastic strain energy, D the dissipation function, and Q_i the generalized forces, both with and without a potential. (In place of L_e we can also put the total potential energy Π (1.17), and then by Q_i we should understand only the forces having no potential.) In the case considered, allowing both for internal and external damping, the following relations hold:

$$E_k = \frac{l^2}{2}\left[(\alpha^2 m_1 + \tfrac{1}{4}m_2)\dot\varphi_1^2 + \gamma m_2 \dot\varphi_1 \dot\varphi_2 + \gamma^2 m_2 \dot\varphi_2^2\right],$$

$$L_e = \frac{1}{2}\left[(c_1 + c_2)\varphi_1^2 - 2c_2 \varphi_1 \varphi_2 + c_2 \varphi_2^2\right],$$

$$D = \frac{1}{2}\left[(b_1 + b_2)\dot\varphi_1^2 - 2b_2 \dot\varphi_1 \dot\varphi_2 + b_2 \dot\varphi_2^2\right] +$$

$$+ \frac{1}{2}\left[(\alpha^2 \tau_1 + \tfrac{1}{4}\tau_2)\dot\varphi_1^2 + \gamma \tau_2 \dot\varphi_1 \dot\varphi_2 + \gamma^2 \tau_2 \dot\varphi_2^2\right],$$

$$Q_1 = \frac{Pl}{2}(\varphi_1 - \eta\varphi_2),$$

$$Q_2 = \frac{Pl}{2}(1 - \eta)\varphi_2,$$

(2.36)

where l denotes the length of the whole bar model, α and γ describe the position of concentrated masses m_1 and m_2 (Fig. 2.7), c_i denote elastic rigidity of hinges, b_i are the coefficients of internal damping, $\tau_i = l^2\bar\tau_i$ are the coefficients of external damping and η is the tangency coefficient.

Substituting (2.36) into (2.35), we obtain a matrix equation of type (1.2), in which

$$\mathbf{M} = \begin{bmatrix} \alpha^2 m_1 + \tfrac{1}{4}m_2 & \tfrac{1}{2}\gamma m_2 \\ \tfrac{1}{2}\gamma m_2 & \gamma^2 m_2 \end{bmatrix} l^2,$$

$$\mathbf{C} = \begin{bmatrix} b_1 + b_2 + \alpha_1^2 + \tfrac{1}{4}\tau_2 & -b_2 + \tfrac{1}{2}\gamma\tau_2 \\ -b_2 + \tfrac{1}{2}\gamma\tau_2 & b_2 + \gamma^2\tau_2 \end{bmatrix},$$

(2.37)

$$\mathbf{K} = \begin{bmatrix} c_1 + c_2 - \tfrac{1}{2}Pl & -c_2 + \tfrac{1}{2}Pl\eta \\ -c_2 & c_2 + \tfrac{1}{2}Pl(1 - \eta) \end{bmatrix},$$

$$\mathbf{q} = \begin{bmatrix} \varphi_1 \\ \varphi_2 \end{bmatrix}.$$

Matrix $\mathbf{C}$ is symmetric (no gyroscoping forces occurring), and matrix $\mathbf{K}$ is symmetric only for $\eta = 0$, whereas in a general case, the system is non-conservative. Considering the solution in the form (1.5), we arrive at a set of linear homogeneous algebraic equations, and equating to zero the principal determinant of these equations gives the vibration frequency and enables stability analysis.

In the particular case $\alpha = \gamma = \tfrac{1}{4}$ (concentrated masses placed in the centre of the component bars), $m_1 = m_2 = m$ and $c_1 = c_2 = c$, we obtain the following quartic equation:

$$\Omega^4 + (16B_1 + 160B_2 + T_1 + T_2)\Omega^3 +$$
$$+ [(176 - 24(2 - \eta)\beta + 256B_1 B_2 + 16B_1 T_2 + 144B_2 T_2 +$$
$$+ 16B_2 T_1 + T_1 T_2)]\Omega^2 + [128(2 - \beta + \eta\beta)B_1 +$$
$$+ 256(1 + \eta\beta - \beta)B_2 + 8(2 + \eta\beta - \beta)T_1 +$$
$$+ 8(20 + 2\eta\beta - 5\beta)T_2]\Omega + 64[4 - 6(1 - \eta)\beta + (1 - \eta)\beta^2] = 0. \qquad (2.38)$$

In this equation, the following dimensionless quantities were introduced

$$\Omega = l\left(\frac{m}{c}\right)^{1/2}\omega, \quad \beta = \frac{Pl}{c},$$

$$B_i = \frac{b_i}{l\sqrt{mc}}, \quad T_i = \frac{\tau_i}{l\sqrt{mc}}, \quad i = 1, 2. \qquad (2.39)$$

The static criterion $\Omega = 0$ defines the first and second critical force by a simple formula, in which the damping coefficients B_i and T_i do not occur

$$\beta_{1,2} = 3 \mp \sqrt{\frac{5 - 9\eta}{1 - \eta}}. \qquad (2.40)$$

The above formula is not valid in the interval $5/9 < \eta \leqslant 1$, in which the critical force can be determined only by the kinetic criterion in the narrower sense. In the absence of dampings, $B_i = T_i = 0$, Eq. (2.38) is a biquadratic equation and the criterion takes the form (1.12). Hence,

$$\beta_{1,2} = \frac{6(20 - 9\eta) \pm 12\sqrt{-9\eta^2 + 14\eta - 4}}{9\eta^2 - 32\eta + 32}. \qquad (2.41)$$
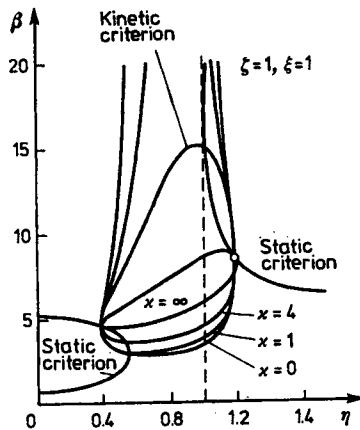
Fig. 2.8. Dependence of critical force on tangency coefficient for Ziegler's model

Even if only one type of damping is considered, Eq. (2.38) is a complete quadratic equation, and the criterion for stability takes the form (1.11). Also following therefrom is a quadratic equation for critical force β, though much more complicated in structure. The respective equations are transformed to (2.41) only in the particular case (1.13) which generally does not occur.

An exemplary plot of $\beta = \beta(\eta)$ is given in Fig. 2.8. Homogeneous damping has been assumed here, $B_1 = B_2 = B$, $T_1 = T_2 = T$, and the critical force is presented in terms of the ratio $T/B = \varkappa$ with $T \to 0$ and $B \to 0$. The external damping causes the critical force to grow, whereas with pure internal damping $\varkappa = 0$, we obtain essential destabilization in relation to the results of Eq. (2.41).

The influence of damping on the stability of real bars was investigated by Bolotin and Zhinzher (1969). They established an essential destabilization due to damping, leading to the disappearance of discontinuity of the function $p = p(\eta)$ at point $\eta = 0.5$, clearly visible in Fig. 2.6 in the case of no damping.

The influence of the behaviour of loading on the loss of stability is very significant in the case of bars in tension. With the Eulerian behaviour of loading (materially fixed point of application, direction fixed in space), the bar cannot lose stability at all (if we disregard the effects of great strains leading to a decrease of the bar cross-section). With a more general behaviour
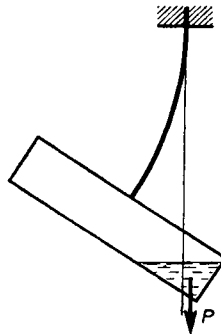
Fig. 2.9. Example of loss of stability of a bar under tension

of loading, loss of stability is possible (e.g. loading of a vessel by a liquid, Fig. 2.9). Problems of this type were investigated by Gajewski and Palej (1974).

2.3. Postcritical Behaviour of Bars under Compression

Linearized equations of the type (2.3) or (2.4) allow the critical force to be determined but do not determine the deflections during buckling, and they do not allow an analysis of the stability of a deflected bar. Such analysis is possible only on the basis of exact non-linear equations, using the exact formula for curvature $\varkappa = -d\varphi/ds$. In the case of a prismatic bar loaded by a concentrated force of fixed direction, instead of (2.3) we can write

$$-EJ\frac{d\varphi}{ds} = Pw, \quad \frac{dw}{ds} = \sin\varphi. \tag{2.42}$$

Hence,

$$EJ\varphi'' + P\sin\varphi = 0, \tag{2.43}$$

where denoted by primes is the differentiation with respect to the variable measured along arc s (the compressibility of the axis has been neglected here; it was considered by Pflüger (1964) and Waszczyszyn and Życzkowski (1962)). Equation (2.43) has a form analogous to the equation of motion of a pendulum (Kirchhoff's analogy). The boundary conditions for a bar clamped at one end, Fig. 2.10, can be written in the form $\varphi'(0) = w(0) = \varphi(l)$
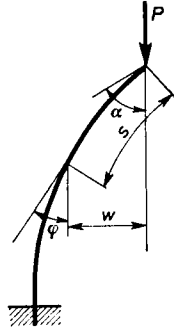
Fig. 2.10. Postcritical behaviour of a bar clamped at one end

$= 0$; moreover, we denote $w(l) = f$, $\varphi(0) = \alpha$. Integrating (2.43), we obtain first

$$EJ\frac{\varphi'^2}{2} = P(\cos\varphi - \cos\alpha), \tag{2.44}$$

and hence,

$$\varphi' = -k\sqrt{2}\sqrt{\cos\varphi - \cos\alpha}. \tag{2.45}$$

Further integration leads to elliptic integrals. In order to reduce them to normal form, the functions of angle φ should be expressed by the functions of $\varphi/2$ and an auxiliary unknown ϑ should be introduced by means of the formula

$$\sin \frac{\varphi}{2} = \sin \frac{\alpha}{2} \sin \vartheta. \tag{2.46}$$

We then obtain

$$F\left(\vartheta, \sin \frac{\alpha}{2}\right) = k(l-s), \tag{2.47}$$

where F denotes an incomplete elliptic integral of the first kind. For $s = 0$ we have $\varphi = \alpha$, i.e., $\vartheta = \pi/2$, and hence the slope at the free end is given by the equation

$$\mathbf{K}\left(\sin \frac{\alpha}{2}\right) = kl, \quad \sin \frac{\alpha}{2} = \mathbf{K}_{-1}(kl), \tag{2.48}$$

where $\mathbf{K}$ denotes complete elliptic integral of the first kind, and $\mathbf{K}_{-1}$ is the inverse function with respect to this integral, The deflection w can be determined by the equations (2.42), (2.45) and (2.46):

$$dw = 2\sin \frac{\varphi}{2} \cos \frac{\varphi}{2} ds = 2\sin \frac{\alpha}{2} \sin \vartheta \sqrt{1 - \sin^2 \frac{\alpha}{2} \sin^2 \vartheta} ds, \tag{2.49}$$

$$dw = -\frac{2}{k} \sin \frac{\alpha}{2} \sin \vartheta d\vartheta, \quad w = \frac{2}{k} \sin \frac{\alpha}{2} \cos \vartheta. \tag{2.50}$$

Letting $s = l$ and $\vartheta = 0$, we calculate the bending deflection

$$f = \frac{2}{k} \sin \frac{\alpha}{2} = \frac{2}{k} \mathbf{K}_{-1}(kl). \tag{2.51}$$

Similarly using the relation $dx = \cos \varphi ds$, we can find the axial displacement of the free end of the bar (approaching of the bar ends) from the formula

$$u = 2l - \frac{2}{k} \mathbf{E}\left(\sin \frac{\alpha}{2}\right), \tag{2.52}$$

where $\mathbf{E}$ denotes the complete elliptic integral of the second kind. The function (2.52) is a compound function because α depends on loading force P according to Eq. (2.48).

More convenient formulae are obtained by denoting the ratio of force P to Eulerian force by m

$$m = \frac{P}{P_E} = \frac{4Pl^2}{\pi^2 EJ} = \frac{4k^2l^2}{\pi^2}, \tag{2.53}$$

namely

$$\sin\frac{\alpha}{2} = K_{-1}\left(\frac{\pi}{2}\sqrt{m}\right),$$

$$\frac{f}{l} = \frac{4}{\pi\sqrt{m}}K_{-1}\left(\frac{\pi}{2}\sqrt{m}\right),$$ (2.54)

$$\frac{u}{l} = 2 - \frac{4}{\pi\sqrt{m}}E\left(\sin\frac{\alpha}{2}\right).$$

Since the minimal value of the integral K is $\pi/2$, the function K_{-1} is determined only for an argument not smaller than $\pi/2$, i.e., $m \geqslant 1$, therefore only in the postcritical region.

The tangent to the free end of the bar will be horizontal if $\alpha = \pi/2$. From Eq. (2.48) it follows that $kl = K(\pi/4) = 1.8541$; hence, $m = 1.3932$, and the corresponding value of approaching of the bar ends is $u/l = 0.5431$. The parameters of maximum bending deflection f are given by the transcendental equation

$$E - 2(1 - k_e^2)K = 0,$$ (2.55)

where k_e denotes the modulus of the elliptic integral. (The traditional denotation k has been replaced here by k_e to distinguish the modulus from the symbol $k = \sqrt{P/EJ}$; in the present case, $k_e = \sin(\alpha/2)$.) Equation (2.55) follows from the differentiation of (2.51) and from the use of the formula for the derivative dK/dk_e. The root of Eq. (2.55) is $k_e = 0.83745$, hence the corresponding angle $\alpha = 113°45'$; from Eq. (2.48), $kl = 2.0773$, hence
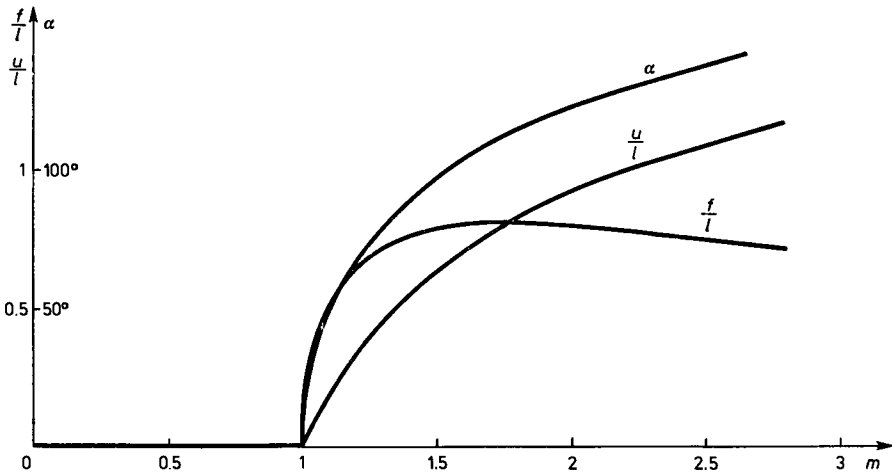
Fig. 2.11. Generalized displacements of free end in terms of loading

$m = 1.7489$ and $(f/l)_{max} = 0.8063$. The free end of the bar will touch the base plane if $u = 1$, i.e. in view of (2.52), $2E = K$. The root of this equation is $k_e = 0.90891$, hence $\alpha = 130°43'$, from Eq. (2.48), $kl = K = 2.3211$, hence $m = 2.1834$; the corresponding deflection value $f/l = 0.7832$. The plots of functions (2.54) are given in Fig. 2.11, and typical deflection lines and trajectory of the free end of the bar, in Fig. 2.12.
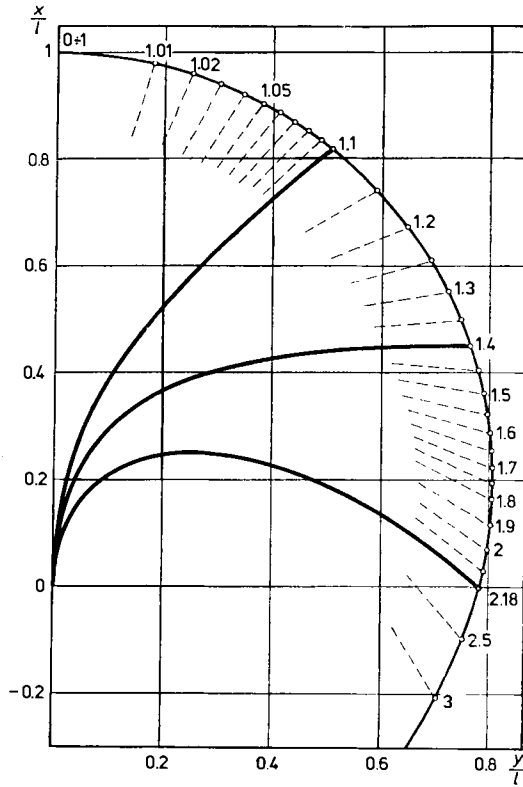
Fig. 2.12. The buckling process: deflection lines in relation to parameter m and locus of the free end positions

Convenient approximate formulae are obtained by expanding the elliptic integrals into power series and by performing suitable operations on the series. Inversion of the series for complete elliptic integral of the first kind

$$K(k_e) = \frac{\pi}{2}\left(1 + \frac{1}{4}k_e^2 + \frac{9}{64}k_e^4 + \frac{25}{256}k_e^6 + \ldots\right) \tag{2.56}$$

is given by (Życzkowski, 1965$_2$)

$$k_c = 2\sqrt{\frac{2}{\pi}\mathbf{K}-1}\left[1-\frac{9}{8}\left(\frac{2}{\pi}\mathbf{K}-1\right)+\frac{167}{128}\left(\frac{2}{\pi}\mathbf{K}-1\right)^2+\ldots\right]. \qquad (2.57)$$

Hence,

$$\sin\frac{\alpha}{2} = 2\sqrt{\sqrt{m}-1}\left[1-\frac{9}{8}(\sqrt{m}-1)+\frac{167}{128}(\sqrt{m}-1)^2+\ldots\right], \qquad (2.58)$$

$$\frac{f}{l} = \frac{8}{\pi}\sqrt{\frac{\sqrt{m}-1}{m}}\left[1-\frac{9}{8}(\sqrt{m}-1)+\frac{167}{128}(\sqrt{m}-1)^2+\ldots\right]. \qquad (2.59)$$

Similarly, by expanding the integral **E** into a series and then substituting (2.57), we find the displacement u from the series

$$\frac{u}{l} = 2-\frac{2}{\sqrt{m}}\left[1-(\sqrt{m}-1)+\frac{3}{2}(\sqrt{m}-1)^2+\ldots\right]. \qquad (2.60)$$

The series (2.60) allows easy determination of the derivative $d(u/l)/dm$ at the point $m = 1$ (at critical force). This derivative equals 2, i.e., $du/dP = 2l/P_E$; the axial flexibility of the bar, equal $du/dP = l/EA$ in the subcritical range, at $P = P_e$ grows stepwise to attain

$$\left.\frac{du}{dP}\right|_{P=P_E} = \frac{l}{EA}+\frac{2l}{P_E} = \frac{l}{EA}\left(1+\frac{2\lambda^2}{\pi^2}\right) \qquad (2.61)$$

(Rzhanitsin, 1955).

Equations (2.48)–(2.61) apply to the equilibrium branch of a deformed bar, which corresponds to bifurcation at the first critical force. The boundary condition $\varphi = \alpha$ for $s = 0$ can also be satisfied letting $\vartheta = 3\pi/2$, $\vartheta = 5\pi/2$, …

Fig. 2.13. Example of a bar whose postcritical behaviour may be unstable

in Eq. (2.46); we then obtain the description of the other branches of equilib-
rium (Malkin, 1926; Frisch-Fay, 1962). The equilibrium of a deflected bar is
stable only along the first branch; the other branches are unstable (Love,
1892; Popov, 1948). With other than Eulerian behaviour of loading, even
the first branch of equilibrium may be unstable; Stern (1979), investigating the
postcritical behaviour of the bar shown in Fig. 2.13, found that with $l_1 < 0.6l$
the deflected equilibrium form is unstable. In the range of small deflections,
this bar does not differ significantly from the bar shown in Fig. 2.3a (force
oriented to a fixed pole), whereas in the case of finite deflections, certain
differences occur due to the motion of the pole along the axis.

2.4. Stability of Bars under Distributed Loadings

In the case of a bar clamped at one end, which is subjected to the action of
a concentrated force and a distributed axial loading of direction fixed in
space and with a materially fixed point of application (e.g. dead weight,
Fig. 2.14), the bending moment is given by the formula

$$M = Pw + \int_0^x q(\xi)[w(x) - w(\xi)]d\xi. \tag{2.62}$$
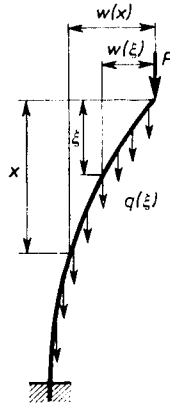
Fig. 2.14. Bar under concentrated force and distributed loading

We confine ourselves to the case $q(\xi) = \text{const}$; after substituting into the
basic equation of bending (2.1) and differentiating to eliminate the integral,
we obtain

$$EJw''' + Pw' + qxw' = 0. \tag{2.63}$$

The general integral of this equation can be expressed by the Bessel function J_n as follows:

$$w' = C_1 \sqrt{P+qx}\, J_{1/3}\left[\frac{2}{3} \sqrt{\frac{(P+qx)^3}{q^2 EJ}}\right] +$$
$$+ C_2 \sqrt{P+qx}\, J_{-1/3}\left[\frac{2}{3} \sqrt{\frac{(P+qx)^3}{q^2 EJ}}\right]. \tag{2.64}$$

Deflections w need not be calculated here, since the two boundary conditions $w'(l) = 0$ and $w''(0) = 0$ already determine the critical state $f(P, q) = 0$. By differentiating and using the formulae for derivatives of the Bessel functions, we obtain the following transcendental equation:

$$J_{1/3}\left[\frac{2}{3} \sqrt{\frac{(P+ql)^3}{q^2 EJ}}\right] J_{2/3}\left(\frac{2}{3} \sqrt{\frac{P^3}{q^2 EJ}}\right) +$$
$$+ J_{-1/3}\left[\frac{2}{3} \sqrt{\frac{(P+ql)^3}{q^2 EJ}}\right] J_{-2/3}\left(\frac{2}{3} \sqrt{\frac{P^3}{q^2 EJ}}\right) = 0. \tag{2.65}$$

Should a distributed loading be acting alone, $P = 0$, the first term approaches zero and we obtain the equation

$$J_{-1/3}\left(\frac{2}{3} \sqrt{\frac{ql^3}{EJ}}\right) = 0. \tag{2.66}$$

The first root of the equation $J_{-1/3}(x) = 0$ equals $x = 1.8663$, following from which is either a distributed critical loading q_{cr} or a critical length l_{cr} if the load (e.g. dead weight) is known

$$q_{cr} = 7.8369 \frac{EJ}{l^3}, \qquad l_{cr} = 1.9863 \sqrt[3]{\frac{EJ}{q}}. \tag{2.67}$$

Greenhill (1881) was first to obtain these values.

Using Eq. (2.63), we can determine the critical state also in the case where the upper end of the bar is clamped with sidesway (horizontal sidesway), since then just a constant clamping moment becomes involved in Eq. (2.62), which disappears with differentiation, and the boundary conditions $w'(0)$ $w'(l) = 0$ do not require $w(x)$ to be calculated. The critical state $f(P, q) = 0$ is given here by the equation

$$J_{1/3}\left[\frac{2}{3} \sqrt{\frac{(P+ql)^3}{q^2 EJ}}\right] J_{-1/3}\left(\frac{2}{3} \sqrt{\frac{P^3}{q^2 EJ}}\right) -$$
$$- J_{-1/3}\left[\frac{2}{3} \sqrt{\frac{(P+ql)^3}{q^2 EJ}}\right] J_{1/3}\left(\frac{2}{3} \sqrt{\frac{P^3}{q^2 EJ}}\right) = 0. \tag{2.68}$$

For $P = 0$, the second term disappears and we get

$$J_{1/3}\left(\frac{2}{3}\sqrt{\frac{ql^3}{EJ}}\right) = 0,$$

$$q_{cr} = 18.9564\,\frac{EJ}{l^3},\qquad(2.69)$$

$$l_{cr} = 2.6664\,\sqrt[3]{\frac{EJ}{q}}.$$

In other cases of support of bar ends, horizontal reactions R occur; in the formula for moment (2.62), terms of Rx type appear, and hence Eq. (2.63) becomes a non-homogeneous equation (the corresponding fourth-order equation would be a homogeneous equation). The general integral of this equation is expressed no longer by a Bessel function but by Lommel functions. The coefficients in the formulae for q_{cr} are (Dinnik, 1913): 18.61 for a simple support at both ends; 29.50 for a simply supported lower end and clamped upper end; 52.31 for simply supported upper end and clamped lower end; 73.56 for clamping at both ends without horizontal sidesway.

In the non-conservative case of distributed tangential loadings (of materially fixed direction) and a concentrated force of Eulerian type, the bending moment is given by the formula

$$M = Pw + \int_0^x q(\xi)[w(x) - w(\xi) - (x - \xi)w'(\xi)]\,d\xi,\qquad(2.70)$$

and after differentiating twice we obtain the equation

$$EJw^{IV} + Pw'' + qxw'' = 0.\qquad(2.71)$$

This equation is also valid for general, non-conservative concentrated loading P, because the second derivative of the moment from horizontal component H disappears. This equation is analogous to (2.63) but with w' replaced by w''. In the case of both ends simply supported, the boundary conditions $w''(0) = w''(l) = 0$ lead to a complete analogy with the aforementioned clamping with sidesway for conservative loading: we obtain Eq. (2.68), and in the case $P = 0$, the critical load q_{cr} is given by (2.69) (Pflüger, 1950). In the adjoint case of a loading of a spatially fixed direction and point of application, the bending moment is

$$M = Pw + qxw.\qquad(2.72)$$

The equation of bending

$$EJw'' + Pw + qxw = 0\qquad(2.73)$$

shows again an analogy to (2.63), and in the case of a simple support at both ends $w(0) = w(l) = 0$, we obtain once more (2.68) and (2.69) in agreement with the general theorem of adjoint systems (Barta, 1967).

In the case of clamping of just one end of the bar, under a distributed tangential loading, the critical value can be determined only by using the kinetic criterion. Leipholz (1962) obtained the approximate value

$$q_{cr} = 40.7 \frac{EJ}{l^3},$$ (2.74)

which is about five times as great as in the conservative case (2.67). Other cases of support of bar ends were considered by Hauger (1966), whereas the case of distributed tangential loading with loading of fixed direction, acting simultaneously, was investigated by Sugiyama and Kawagoe (1975).

Related problems of loss of stability of a bar under a distributed loading are involved in aeroelasticity in analysis of a bar in a parallel fluid flow. By the simplest, "local" hypothesis of the action of such a flow on the bar during loss of stability, it is assumed that the distributed transverse loading p acting on an element of the bar is proportional to the slope (Fig. 2.15):

$$p = 2BbUw',$$ (2.75)
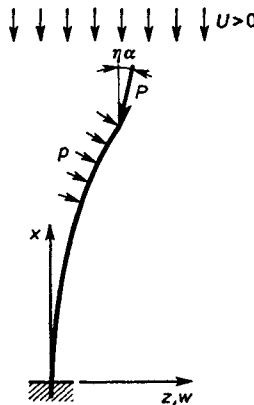
Fig. 2.15. Bar in a parallel fluid flow

where B is a constant describing the properties of the fluid, b is the width of bar of rectangular cross-section (a plate) and U is the stream velocity. The hypothesis (2.75) is sometimes called the *hypothesis* of plane cross-sections (Ilyushin, 1960) or the *piston law* (Ashley and Zartarian) and it finds justification particularly when considering bars in supersonic gas flow.

The case of simultaneous, distributed ("lateral") loading p and concentrated axial force (head resistance) P was considered by Kordas (1965). The loading (2.75) is non-conservative, yet the static criterion made it possible to determine the critical velocity of the stream U as well as a certain part of the interaction curve $f(P, U) = 0$ which divides the PU plane into regions corresponding to stability and instability. The linearized fourth-order equation of bending takes the form

$$EJw^{IV} + Pw'' - 2BbUw' = 0. \tag{2.76}$$

In seeking a solution in the form $w(x) = Ce^{kx}$, we obtain a characteristic equation determining k. It is a quartic equation with one root, $k_1 = 0$, whereas the remaining three are given by Cardano's formulae

$$k_2 = -2\alpha, \quad k_3 = \alpha + i\beta, \quad k_4 = \alpha - i\beta, \tag{2.77}$$

where

$$\alpha = -\frac{1}{2}\left(\sqrt[3]{\frac{BbU}{EJ} + \sqrt{\Delta}} + \sqrt[3]{\frac{BbU}{EJ} - \sqrt{\Delta}}\right),$$

$$\beta = \frac{\sqrt{3}}{2}\left(\sqrt[3]{\frac{BbU}{EJ} + \sqrt{\Delta}} - \sqrt[3]{\frac{BbU}{EJ} - \sqrt{\Delta}}\right), \tag{2.78}$$

$$\Delta = \left(\frac{BbU}{EJ}\right)^2 + \left(\frac{P}{3EJ}\right)^3.$$

The general integral of Eq. (2.76) has, therefore, the form

$$w = C_1 + C_2 e^{-2\alpha x} + C_3 e^{\alpha x}\sin\beta x + C_4 e^{\alpha x}\cos\beta x. \tag{2.79}$$

The boundary conditions are very simple when the head resistance behaves like a tangential force: $w(0) = w'(0) = w''(l) = w'''(l) = 0$. Equating to zero the determinant of the set of linear homogeneous equations leads to a transcendental equation yielding the interaction curve $f(P, U) = 0$:

$$2\alpha e^{-3\alpha l}[(3\alpha^2 - \beta^2)\sin\beta l + 4\alpha\beta\cos\beta l] + \beta(\alpha^2 + \beta^2) = 0. \tag{2.80}$$

In the particular case $P = 0$, it follows from (2.78) that $\beta = -\alpha\sqrt{3}$ and Eq. (2.80) is simplified to the form (Movchan, 1956)

$$2e^{-3\alpha l}\cos(\alpha l\sqrt{3}) + 1 = 0. \tag{2.81}$$

The least root of this equation, in absolute value, equals $\alpha l = -0.92493$; hence,

$$U_{cr} = 3.1651\,\frac{EJ}{Bbl^3}. \tag{2.82}$$

The interaction curve $f(P, U) = 0$ has been investigated in the range of the static criterion and of the kinetic criterion in the narrower sense, for various values of the tangency coefficient η of concentrated force P (Kordas, 1965). The kinetic criterion also determines a certain negative critical value of the stream velocity U at $P = 0$ (despite the fact that the negative value of p in Eq. (2.76) has a stabilizing character and the static criterion cannot be sufficient in this case); this value marks the beginning of flutter on the "tension side" and its absolute value is nearly 20 times as great as (2.82).

2.5. Stability of Bars in an Elastic Medium

In the simplest model of an elastic foundation, proposed by Winkler, the reaction of the foundation q_r is proportional to the deflection of the bar $q_r = cw$ (the local response hypothesis). The basis equation of bending for a bar compressed by axial force P and permanently joined (bilaterally) with a Winklerian foundation, i.e., located in an elastic medium, has the form

$$w^{IV} + k^2 w'' + rw = 0,\tag{2.83}$$

where the following notations have been introduced

$$\frac{P}{EJ} = k^2, \qquad \frac{c}{EJ} = r.\tag{2.84}$$

The roots μ_j of characteristic equation (2.83) can be determined by the formula

$$\mu^2_{1,2,3,4} = -\frac{k^2}{2} \pm \sqrt{\frac{k^4}{4} - r}.\tag{2.85}$$

These roots for a compressive force P and for a positive (stabilizing) foundation coefficient r cannot be real; they can, however, be complex or purely imaginary, depending on the sign of the expression under the root. The sign depends on an unknown value of the critical force which in turn depends on how the bar ends are supported; in the general case, we should consider $k^4 > 4r$ ("strong support of bar ends") and $k^4 = 4r$, as well as $k^4 < 4r$ ("weak support of bar ends").

Under the assumption $k^4 > 4r$, all roots μ_j are imaginary; we express them in the form $\mu_j = im_j$, where

$$m_1 = -m_3 = \sqrt{\frac{k^2}{2} + \sqrt{\frac{k^4}{4} - r}},$$

$$m_2 = -m_4 = \sqrt{\frac{k^2}{2} - \sqrt{\frac{k^4}{4} - r}},\tag{2.86}$$

and the general integral of Eq. (2.83) has the form

$$w = C_1 \sin m_1 x + C_2 \cos m_1 x + C_3 \sin m_2 x + C_4 \cos m_2 x. \tag{2.87}$$

For $k^4 = 4r$, the roots are likewise imaginary, but equal in pairs

$$m_1 = m_2 = -m_3 = -m_4 = k/\sqrt{2} = m, \tag{2.88}$$

and the general integral is

$$w = C_1 \sin mx + C_2 \cos mx + C_3 x \sin mx + C_4 x \cos mx. \tag{2.89}$$

For $k^4 < 4r$, we deal with two pairs of conjugate complex roots $\mu = \pm(\alpha \pm \beta i)$, where

$$\alpha = \tfrac{1}{2}\sqrt{\sqrt{4r} - k^2}, \quad \beta = \tfrac{1}{2}\sqrt{\sqrt{4r} + k^2}, \tag{2.90}$$

and

$$w = C_1 e^{-\alpha x} \sin \beta x + C_2 e^{-\alpha x} \cos \beta x + C_3 e^{\alpha x} \sin \beta x + C_4 e^{\alpha x} \cos \beta x. \tag{2.91}$$

It turns out that the case of a simple support at both ends comes under "strong fixing" (just like clamping at both ends). Assuming $k^4 > 4r$ and using the integral (2.87) with boundary conditions $w(0) = w''(0) = w(l) = w''(l) = 0$ and equating the determinant of the set of linear equations to zero, we arrive at the equation

$$(m_1^2 - m_2^2)^2 \sin m_1 l \sin m_2 l = 0. \tag{2.92}$$

Hence, in view of the assumption $m_1 \neq m_2$ (following from $k^4 > 4r$), we obtain $m_1 l = n\pi$ or $m_2 l = n\pi$, i.e., after using (2.86)

$$k^2 = \frac{P}{EJ} = \frac{n^2 \pi^2}{l^2} + \frac{r l^2}{n^2 \pi^2}. \tag{2.93}$$

The number of half-waves n must be an integer. However, the critical force (2.93) need not necessarily reach a minimum value for $n = 1$; the plots of functions $P = P(r)$ are straight lines for individual n, from which we should select the line yielding the minimum value of P for a given value of r (Fig. 2.16). The adjacent straight lines intersect at points with abscissae $r = n^2(n + 1)^2 \pi^2 / l^2$. But, assuming that n need not be an integer and finding that number from the analytical condition of minimum P, we determine the envelope of the family of straight lines (2.93); in this way we obtain a certain convenient lower estimation of the exact value, namely

$$n = \frac{l}{\pi} \sqrt[4]{r}, \quad P_{cr} = 2EJ\sqrt{r} = 2\sqrt{EJc}. \tag{2.94}$$

This parabola is indicated in Fig. 2.16 by a broken line. It is seen that the parabola (2.94), being the lower estimation, meets the condition $k^4 = 4r$.
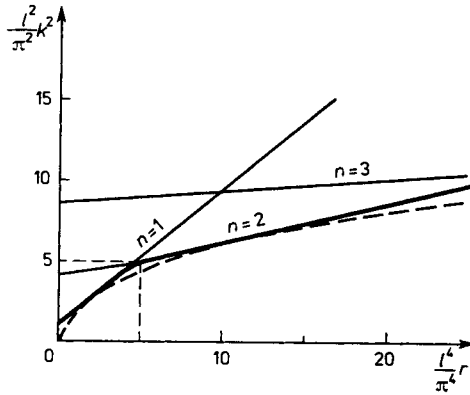
Fig. 2.16. Critical force for a bar in elastic medium

Consequently, the adopted assumption $k^4 > 4r$ was in fact justified. The value (2.94) is an exact value for an inifinitely long bar.

The stability of the postcritical behaviour of a simply supported bar in an elastic medium has been studied by Lekkerkerker (1962), Thompson and Hunt (1973); it turns out that only in two intervals, $0 < rl^4/\pi^4 < 1/3$ and $4 < rl^2/\pi^2 < 16/3$, is the postcritical behaviour stable, whereas in the remaining intervals it is unstable.

As an example of a bar "with weak fixing at the ends" we consider a bar with one end free; the simplest result is obtained taking the other end to extend to infinity, Fig. 2.17. Assume $k^4 < 4r$ in the case considered and use
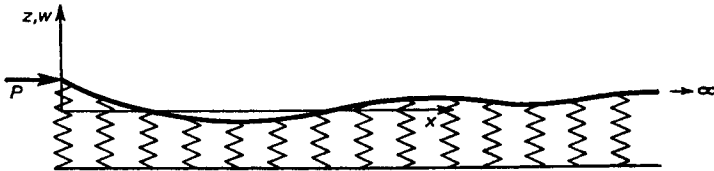
Fig. 2.17. Example of a bar with "weak support of ends"

the integral (2.91). Two boundary conditions in infinity lead to the conclusion $C_3 = C_4 = 0$, whereas the other two have the form $w''(0) = 0$ and $w'''(0) + k^2 w'(0) = 0$. Using these conditions and equating the determinant to zero, we obtain the equation (Rzhanitsin, 1955)

$$\alpha^2 + \beta^2 = k^2, \quad k^2 = \sqrt{\frac{c}{EJ}} = \sqrt{r}. \tag{2.95}$$

Therefore, the critical force equals in this case half the force for an infinitely long simply supported bar. In light of (2.95), the assumption $k^4 < 4r$ is obviously justifiable.

The buckling of bars partially placed in an elastic medium was considered by Granholm (1929) and by Sułocki (1955) who also allowed for non-homogeneity of the foundation, $r = r(x)$.

In many engineering applications, a correct description of the response of a foundation does not admit a local hypothesis of the Winkler type, but is of an integral character (e.g. a foundation of elastic half-plane type or elastic half-space type). The loss of stability is described then by a integro-differential equation; some general considerations and some particular cases have been discussed by Rzhanitsin (1955).

2.6. Multi-Span Bars. Elastic Supports

The calculation of critical forces for multi-span bars, possibly of step-wise variable stiffness, can be based on the general integral (2.7) and does not present any particular difficulty; it may however prove cumbersome, especially in the case of elastic supports and with a considerable number of spans of different length. Many special studies have been devoted to this problem, e.g. by Schleusner (1938), Kornoukhov (1949), Zweiling (1953), Vetter (1960). Equations determining the critical force are derived mostly by the force or displacement method in several variants, e.g. by the generalized equation of three moments.

A convenient matrix approach, useful both in analytical and numerical approaches, was proposed in somewhat differing variants by Rzhanitsin (1955) (initial parameters method), Schnell (1955), and Falk (1956_1, 1956_2) (transfer matrix method). Consider the bar interval $0 < x < l_i$ (in each interval, the variable x can be counted from zero) and denote the deflection, the slope, the bending moment and the transverse force at point $x = 0$ by w_{i-1}, w'_{i-1}, M_{i-1} and T_{i-1}, respectively. The four constants C_{ki} in the integral (2.7) can be expressed by the above quantities; finally we obtain

$$w = \left(\frac{w'_{i-1}}{k} + \frac{T_{i-1}}{k^3 EJ} \right) \sin kx +$$

$$+ \frac{M_{i-1}}{k^2 EJ} \cos kx - \frac{T_{i-1}}{k^2 EJ} x + \left(w_{i-1} - \frac{M_{i-1}}{k^2 EJ} \right). \tag{2.96}$$

The relation (2.96) makes it possible to express the geometric and static quantities at the point $x = l_i$ by the quantities at the point $x = 0$. In matrix notation we obtain

$$W_i^- = A_i W_{i-1}^+, \qquad (2.97)$$

where W_i denotes the column vector of state

$$W_i = \begin{bmatrix} w_i \\ w_i' \\ \dfrac{M_i}{EJ} \\ \dfrac{T_i}{EJ} \end{bmatrix}, \qquad (2.98)$$

and A_i the transfer matrix for span i

$$A_i = \begin{bmatrix} 1 & \dfrac{\sin kl_i}{k} & -\dfrac{1-\cos kl_i}{k^2} & -\dfrac{kl_i - \sin kl_i}{k^3} \\ 0 & \cos kl_i & -\dfrac{\sin kl_i}{k} & -\dfrac{1-\cos kl_i}{k^2} \\ 0 & k\sin kl_i & \cos kl_i & -\dfrac{\sin kl_i}{k} \\ 0 & 0 & 0 & 1 \end{bmatrix}. \qquad (2.99)$$

Owing to the possibility of a discontinuity of the function occurring at the interval boundary (e.g. on the support), the left-side limit of the function has been denoted by W^- and the right-side by W^+. The relationship between these quantities can also be written in matrix form

$$W_i^+ = B_i W_i^-, \qquad (2.100)$$

where B_i denotes the transfer matrix for the node i; for an elastic support of stiffness $\beta_i = R_i/w_i$, where R_i stands for the reaction, this matrix equals

$$B_i = \begin{bmatrix} 1 & 0 & 0 & 0 \\ 0 & 1 & 0 & 0 \\ 0 & 0 & 1 & 0 \\ \dfrac{\beta_i}{EJ} & 0 & 0 & 1 \end{bmatrix}. \qquad (2.101)$$

Performing in this way successive multiplication of the matrices we express W_n^- (where n denotes the number of intervals) by W_0^+

$$W_n^- = A_n B_{n-1} A_{n-1} \cdots A_1 W_0^+. \qquad (2.102)$$

Two components of vector W_0^+ are known by virtue of the boundary conditions and two remain unknown. The vector W_n^- also furnishes two boundary conditions; using (2.102) to express the respective equations by the unknown

components of vector $\mathbf{W}_0^+$ and then equating the determinant of this set to zero, we can determine the critical state. Denoting the resultant product of the transfer matrices by a_{ij}:

$$\mathbf{A}_n \mathbf{B}_{n-1} \mathbf{A}_{n-1} \ldots \mathbf{A}_1 = \begin{bmatrix} a_{11} & a_{12} & a_{13} & a_{14} \\ a_{21} & a_{22} & a_{23} & a_{24} \\ a_{31} & a_{32} & a_{33} & a_{34} \\ a_{41} & a_{42} & a_{43} & a_{44} \end{bmatrix}, \tag{2.103}$$

we obtain for simple support at both ends (the first and third equation being expressed by the second and fourth component of vector $\mathbf{W}_0^+$

$$a_{12} a_{34} - a_{32} a_{14} = 0, \tag{2.104}$$

and for both ends clamped

$$a_{13} a_{24} - a_{23} a_{14} = 0, \tag{2.105}$$

for clamped left-hand end and simply supported right-hand end

$$a_{13} a_{34} - a_{33} a_{14} = 0, \tag{2.106}$$

and so forth. For a rigid intermediate support, $\beta_i \to \infty$, but additional conditions come into play here, $w_i = 0$. There is no major difficulty with generalizing the method to the case of step-wise variable rigidity on supports. Rakowski (1969) proposed a generalization of the matrix method to the case of bars in an elastic medium.

We consider as an example a two-span bar with spans of equal length l, simply supported at the ends and elastically supported at the middle support; we denote the stiffness of this support by β. Multiplying the matrices $\mathbf{A}_2 \mathbf{B}_1 \mathbf{A}_1$ and using the condition (2.104), we obtain (after performing numerous reductions) the equation

$$\sin kl[\beta(kl \cos kl - \sin kl) - 2Pk \cos kl] = 0. \tag{2.107}$$

If $\beta = 0$, we get $kl = \pi/2$ for simply supported bar $2l$ in length. The critical force increases with β, reaching the value $kl = \pi$, i.e.,

$$P_{cr} = \frac{\pi^2 EJ}{l^2} \quad \text{for} \quad \beta = \beta_{lim} = \frac{2P}{l} = \frac{2\pi^2 EJ}{l^3}. \tag{2.108}$$

At this value of β, we deal with double bifurcation of the equilibrium, since then also $\sin kl = 0$: besides the symmetric form of equilibrium in the adjacent position (vanishing of the square bracket), the antisymmetric form is also possible. As β continues to grow, the critical value remains constant; it is given by Eq. (2.108) and corresponds to two antisymmetric half-waves, characteristic for rigid behaviour of the middle support.

3. Approximate Calculation Methods for Critical Loadings

3.1. The Collocation Method

Approximate analytical methods of calculating critical loadings corresponding to bifurcation (eigenvalues) consist in reducing a system with an infinite number of degrees of freedom to one with n degrees of freedom. This is generally accomplished by assuming an approximate equation of deflection line in the form of a sum

$$w(x) = \sum_{i=1}^{n} a_i w_i(x), \tag{3.1}$$

where $w_i(x)$ are functions satisfying all or only some boundary conditions (we shall further omit the summation sign, using the summation convention). The diverse approaches provide an optimal selection of coefficients a_i and of the critical loading parameter Λ. The simplest methods of this type, collocation and iteration methods, are employed either directly or in combination with other methods.

The collocation method (Frazer *et al.*, 1937) demands that the differential equations of general form (1.16) be satisfied at n points (nodes) $x_j, j = 1, 2, \ldots, n$. We obtain the set of equations

$$L_1 [a_i w_i]|_{x=x_j} + \Lambda L_2 [a_i w_i]|_{x=x_j} = 0, \tag{3.2}$$

i.e., in view of the assumed linearity of operators L_1 and L_2, we obtain a set of linear equations with respect to coefficients a_i of the type

$$(\alpha_{ij} + \beta_{ij} \Lambda) a_i = 0, \quad j = 1, 2, \ldots, n. \tag{3.3}$$

Equating the determinant of this set to zero

$$\det(\alpha_{ij} + \beta_{ij} \Lambda) = 0 \tag{3.4}$$

gives n eigenvalues (critical loadings) Λ. Usually, the first critical force, the most important from an engineering point of view, is determined with sufficient accuracy but the higher eigenvalues may even prove to be complex,

and hence charged with a qualitative error (Collatz, 1949). This method permits, however, a considerable uncertainty. In the event of not a very careful choice of function $w(x)$ or not a very careful spacing of nodes x_j, even the value of the first critical force will not be sufficiently accurate, and the error may equally well be from below or from above. In determining the critical force for a simply supported prismatic bar of length $2l$, $-l \leqslant x \leqslant l$ and assuming (3.1) in the form of even polynominals of variable x, taking $n = 3$ leads to an accuracy of 0.0015% for the first critical force and fairly good estimates for the two subsequent forces with the collocation nodes at points $\xi_1 = 1/6$, $\xi_2 = 1/2$, $\xi_3 = 5/6$, where $\xi = x/l$. However, with the nodes spaced at points $\xi_1 = 0$, $\xi_2 = 1/3$, $\xi_3 = 2/3$, the accuracy drops tenfold for the first critical force, and complex values, therefore completely wrong, are obtained for the subsequent critical forces (Collatz, 1949).

3.2. The Iteration Method

The iteration method in analytical version was given by Engesser (1893, 1909) and in graphical version by Vianello (1898). Consider as an example Eq. (2.1) with substituted (2.2), i.e.

$$w'' + \frac{P}{EJ} w = 0. \tag{3.5}$$

Integrating this equation twice we can write

$$w(x) = -\int dx \int \frac{P}{EJ} w(x) dx. \tag{3.6}$$

By substituting on the right-hand side a certain approximate function $w_k(x)$, we obtain, after integrating and taking into account the boundary conditions, the next approximation $w_{k+1}(x)$. Requirement of equality of w_k and w_{k+1} at a certain point $x = x_0$ (collocation for the equation integrated twice) determines an approximate value of critical force P. In the case of a statically indeterminate support, the expression for the bending moment (2.2) contains unknown reactions; however, in integrating (3.6) the boundary conditions we have at hand are in excess, thus allowing the reactions to be calculated. The iterative scheme (3.6) is as a rule very rapidly converging, although exceptional cases exhibiting no convergence are also known (Zweiling, 1953).

By taking the first approximation for a simply supported prismatic bar of length $2l$ to be $w_1 = 1 - \xi^2$ (the possible multiplier in front of the function is irrelevant here), we obtain successively

$$w_2 = \frac{Pl^2}{EJ}\left(\frac{5}{12} - \frac{1}{2}\xi^2 + \frac{1}{12}\xi^4\right),$$

$$w_3 = \frac{P^2 l^4}{E^2 J^2}\left(\frac{61}{360} - \frac{5}{24}\xi^2 + \frac{1}{24}\xi^4 - \frac{1}{360}\xi^6\right).$$

(3.7)

Hence, by assuming the collocation node at point $\xi = 0$ (the centre of simply supported bar), we obtain successively $P = 2.4\ EJ/l^2$, $P = 2.4590\ EJ/l^2$. More accurate results can be obtained taking, for example, the collocation node to be at point $\xi = 1/3$ (since then, in the presence of symmetry, the point $\xi = -1/3$ is also a node), namely successively $P = 2.4545\ EJ/l^2$, $P = 2.4636\ EJ/l^2$ ... instead of the exact value $P = 2.4674\ EJ/l^2$.

3.3. Energy (Variational) Methods

As we have noted in Section 1.4, the static criterion of critical state can also be expressed by the condition of the vanishing of the total potential energy $\Pi = L_e - L_f$ in the adjacent position. In the case of a concentrated load of fixed direction, the work done by external forces, involving an infinitely small deflection $w = w(x)$, can be expressed by the formula

$$L_f = P\left[l - \int_0^l \sqrt{1-(dw/dx)^2}\,dx\right] = \frac{P}{2}\int_0^l w'^2\,dx$$

(3.8)

since by expanding the root into a power series, the higher powers of w' can be omitted. The potential energy of elastic strain with the assumed deflection line $w = w(x)$ is

$$L_e = \tfrac{1}{2}\int_0^l EJw''^2 dx;$$

(3.9)

hence

$$\Pi = \tfrac{1}{2}\int_0^l (EJw''^2 - Pw'^2)\,dx.$$

(3.10)

The Euler–Lagrange equation for this functional has the form

$$(EJw'')'' + Pw'' = 0.$$

(3.11)

This is Eq. (2.4) generalized to the case of variable rigidity EJ; hence, the exact solution realizes the stationary value of the functional (3.10). It is a minimum equalling zero, leading to the formula

$$P = P_{cr} = \frac{\int_0^l EJw''^2 dx}{\int_0^l w'^2 dx}.$$ (3.12)

The Euler–Lagrange equation for the functional (3.12) is also (3.11) (variation of the quotient of functionals is calculated as a differential of the quotient of functions). The exact solution corresponds to the minimum of the functional (3.12); hence, every approximate solution carries an error from above.

The use of Eq. (3.5) or (3.6) in the first term of the integral (3.10), i.e., the substitution of the iterated function into (3.9) without changes (3.8), leads to the formula

$$\Pi^* = \frac{1}{2} \int_0^l \left(\frac{P^2 w^2}{EJ} - Pw'^2 \right) dx.$$ (3.13)

This is the so-called *complementary energy*, equal to the total energy Π in the case of an exact solution, but it is generally different from (3.10). The second-order equation (3.5) is the Euler–Lagrange equation for the functional Π^*; hence, corresponding to the exact solution is the stationary value (3.13). It also equals zero, and we thus have

$$P = P_{cr} = \frac{\int_0^l w'^2 dx}{\int_0^l \frac{w^2}{EJ} dx}.$$ (3.14)

Equation (3.5) is also the Euler–Lagrange equation for the functional (3.14). The exact solution corresponds here again to minimum P_{cr}; hence, the approximate solutions are also charged with an error from above.

Taking $w(x)$ in the form of a sum (3.1), we can determine the most accurate value of P_{cr} from the condition of minimum of this force $\partial P_{cr}/\partial a_i = 0$ (this being equivalent to the diagonalization described in Section 1.4) or from the condition of stationarity of Π or Π^*. The latter approach, leading to simpler calculations, is called the *Ritz method* (Ritz, 1909). For a statically indeterminate support of a bar, the formula for bending energy, expressed by the bending moment, contains also unknown reactions; these can be left in an equation of the type (3.14) and P can be minimized with respect to them as additional parameters.

With a prescribed function $w(x)$ being different from the exact solution, the approximate equation (3.14) always gives more accurate results than does Eq. (3.12) (Lang, 1947). On the other hand, using the iteration (3.6) also in the second term of the integral (3.10), we return to the very same functional Π, yet not for the initial function $w = w_1$ but for the function "corrected by way of iteration", $w = w_2$. The corresponding value of the critical force is now more accurate than the value (2.14) calculated for $w = w_1$. With the Engesser–Vianello iterative process (3.6) being convergent, the approximate values, defined alternately by Eq. (3.12) and (3.14), make a monotone sequence, converging much more rapidly to the exact value of P_{cr} than does the sequence derived from the classical iterative method combined with one-point collocation. We use as an example a sequence of functions (3.7) for approximate calculation of the critical force in a simply supported bar of length $2l$. The results are presented in Table 3.1.

TABLE 3.1. Approximate values of the critical force calculated by the use of the energy method

No.	Formula	Function in numerator	Function in denominator	Approximate value
1	(3.12)	w_1''	w_1'	3
2	(3.14)	w_1'	$w_1 = Cw_2''$	$\dfrac{5}{2} = 2.5$
3	(3.12)	w_2''	w_2'	$\dfrac{42}{17} = 2.4706$
4	(3.14)	w_2'	$w_2 = Cw_3''$	$\dfrac{153}{62} = 2.467742$
5	(3.12)	w_3''	w_3'	$\dfrac{1705}{691} = 2.467439$
	exact value			2.467401

As an example of a bar with statically indeterminate support, we consider a bar clamped at point $x = 0$ and simply supported at point $x = 1$. By using a function satisfying the geometric boundary conditions

$$w = l(\xi^2 - \xi^3), \quad \xi = x/l \qquad (3.15)$$

(the multiplier in front of the function is irrelevant), we can represent the bending moment and the complementary energy by the equations

$$M = Rl(1-\xi)-Pl(\xi^2-\xi^3),$$

$$\Pi^* = \frac{1}{210}\left(\frac{35R^2l^3}{EJ}-\frac{7PRl^3}{EJ}+\frac{P^2l^3}{EJ}-14Pl\right), \qquad (3.16)$$

where R denotes the reaction perpendicular to the x-axis. Minimizing Π^* with respect to R, we obtain $R = P/10$; substitution of this value into Π^* and equating Π^* to zero leads to the following approximate formula:

$$P_{cr} = \frac{280}{13}\frac{EJ}{l^2} = 21.54\frac{EJ}{l^2} \qquad (3.17)$$

instead of the exact value $P_{cr} = 20.19 \; EJ/l^2$. Formula (3.12) does not require the reaction R to the determined, but we then obtain a much less accurate approximation, $P_{cr} = 30 \; EJ/l^2$.

The energy method is used mostly to calculate critical loads for non-prismatic bars or with a longitudinal force variable along the axis $N = N(x)$; in the latter case, Eq. (3.8) requires an appropriate generalization, namely

$$L_f = \frac{1}{2}\int_0^l N(x)w'^2(x)\,dx. \qquad (3.18)$$

For non-conservative loads, the energy method reduces to the Lagrange equations of the second kind (2.35), in which the coefficients a_i in the expression (3.1) apply to the generalized coordinates φ_i (Kordas and Życzkowski, 1963); these equations can also be interpreted as following from Hamilton's variational principle (Levinson, 1966).

3.4. Orthogonalization Methods

By applying the basic transformation of the calculus of variations to the stationarity condition for the functional Π, (3.10), we obtain

$$\int_0^l [(EJw'')''+Pw'']\,\delta w\,dx+EJw''\,\delta w'\Big|_0^l+T_s\,\delta w\Big|_0^l = 0, \qquad (3.19)$$

where T_s denotes the spatial transverse force (2.6). With both geometric and static boundary conditions satisfied by the function w, the last two terms in (3.19) vanish in most cases. Assuming a deflection $w(x)$ in the form (3.1), we obtain $\delta w = \sum w_i(x)\delta a_i$, and since δa_i are arbitrary, (3.19) leads to the conclusion

$$\int_0^l [(EJw'')''+Pw'']w_i(x)\,dx = 0, \quad i = 1, 2, \ldots, n. \qquad (3.20)$$

Equations (3.20) are called *Bubnov–Galerkin equations* (Bubnov, 1913; Galer-kin, 1915) and express orthogonality of the left-hand side of the differential equation (3.11) with the individual approximating functions $w_i(x)$. Applying a similar transformation to the condition of stationarity of the functional Π^*, (3.13), we obtain the equation

$$\int_0^l \left(w'' + \frac{P}{EJ} w \right) w_i(x)\,dx = 0, \quad i = 1, 2, \ldots, n, \tag{3.21}$$

which expresses the orthogonality of w_i with the left-hand side of the differential equation (3.5). In a more general case, if the bending moment is not given by the simple formula $M = Pw$, Eqs. (3.21) take the form

$$\int_0^l \left\{ w'' + \frac{M[w(x), x, \Lambda]}{EJ} \right\} w_i(x)\,dx = 0 \tag{3.22}$$

and they are also called Bubnow–Galerkin equations. The equation (3.20) or (3.22) leads to a set of algebraic linear equations of (3.3) type and they determine an approximate value of the critical force by using the condition (3.4).

The accuracy of results from calculations based on (3.20) and (3.22) corresponds to the accuracy of Eqs. (3.12) and (3.14), provided that the functions $w_i(x)$ satisfy both the geometric and static boundary conditions; otherwise, the accuracy may be less and furthermore the approximation error may no longer necessarily result in overstimation. The integrals (3.20) and (3.22) are usually simpler to calculate than are the integrals in Eqs. (3.12) and (3.14), but an additional complication arises when the more accurate Eq. (3.22) is used in statically indeterminate cases, where unknown reactions appear in the equation of bending moment M. It is necessary then to use iteration of the type (3.6) and before using the orthogonalization method, it is also necessary to determine the reactions from the excessive boundary conditions.

The Bubnov–Galerkin equations in the forms (3.20) and (3.22) which do not account for possible "boundary terms", are not of the invariant type with respect to the adopted reference system (namely, the way of defining deflections w): Actually, if in one system the last term in (3.19) disappears on account of $w = 0$, then as the system is changed, this term generally does not vanish. The selection of a convenient system is very important particularly in the case of a bar with a free end: in order to get the last term to vanish at this point, it is useful to take a system so that $w = 0$, since the alternative

condition $T_s = 0$ at this place introduces through k^2 an unknown value of the critical force into the boundary conditions (2.6).

In the case of non-prismatic bars, the position of the multiplier EJ plays an essential role in equations expressing orthogonalization. In Eq. (3.20), it is placed in the numerator and in Eqs. (3.21) and (3.22), in the denominator. Other formulations of orthogonality equations, e.g.

$$\int_0^l (EJw'' + M) w_i(x) \, dx = 0, \tag{3.23}$$

or

$$\int_0^l \left[w^{\mathrm{IV}} + \left(\frac{M}{EJ} \right)'' \right] w_i(x) \, dx = 0, \tag{3.24}$$

do not follow from the conditions of stationarity of any functional, they do not guarantee approximation errors from above, and the error value itself is generally higher than if Eqs. (3.20) and (3.22) are used, although in special cases the error may be lower.

The Bubnov–Galerkin method has been generalized to non-conservative loadings by Bolotin (1961) and Leipholz (1963, 1967).

3.5. The Trace of the Kernel of Integral Equation Method

The energy and orthogonalization methods lead to estimates of critical loading from above. For estimates from below we can use the trace of the kernel of integral equation method, which has been adapted to bar stability problems by Mazurkiewicz (1961, 1962).

Equation (3.6) can be transformed to the form of Fredholm's integral equation of the second kind

$$w(x) = P \int_0^l \frac{G(x, \xi)}{EJ(\xi)} \, w(\xi) \, d\xi, \tag{3.25}$$

where $G(x, \xi)$ is Green's function adjusted to the boundary conditions of the problem. By introducing a new unknown, $z(x) = w(x)/\sqrt{EJ(x)}$, we obtain the integral equation

$$z(x) = P \int_0^l K(x, \xi) z(\xi) \, d\xi \tag{3.26}$$

with a symmetric kernel

$$K(x, \xi) = \frac{G(x, \xi)}{\sqrt{EJ(x)EJ(\xi)}} \, . \tag{3.27}$$

A lower estimation of the critical force is given by the equation

$$P = \frac{1}{\sqrt{A_2}} = \frac{1}{\sqrt{\int\limits_0^l dx \int\limits_0^l [K(x, \xi)]^2 d\xi}} \, , \tag{3.28}$$

where A_2 is called the *second trace* of the kernel of integral equation. For example, for a simply supported prismatic bar we obtain $P_{cr} = 9.487 \ EJ/l^2$ with a 4% error from below. A further increase in accuracy can be achieved by calculating the higher kernel traces.

3.6. The Method of Assumption of an Exact Solution

The stability analysis of non-prismatic and non-homogeneous bars makes it possible to apply a convenient inverse method. Thus, if we assume a certain equation of deflection line $w = w(x)$, we can find from Eq. (2.1) such a distribution of rigidity $EJ(x)$ of the bar, for which the function $w(x)$ is the exact solution

$$EJ(x) = -\frac{M[w(x), x, P]}{w''(x)} \, . \tag{3.29}$$

By introducing into the assumed equation of deflection line a certain number of free parameters, $w = w(x; a_1, a_2, \ldots, a_n)$, we can subsequently select their value so as to obtain minimum deviations of the resultant rigidity (3.29) from the rigidity of the bar under consideration. The application of this method to elastic-plastic analysis of non-prismatic bars has been discussed by Życzkowski (1954).

3.7. The Finite Difference Method

Dividing a bar into n equal parts of length $h = l/n$ and substituting, for example, in Eq. (3.3), in place of the second derivative a suitable difference scheme, we obtain a set of algebraic equations

$$w_{i+1} + \left(\frac{Ph^2}{EJ_i} - 2\right)w_i + w_{i-1} = 0, \quad i = 1, 2, \ldots, n-1. \tag{3.30}$$

This set contains $n+1$ unknown nodal deflections w_i. The other two equations are obtained from the boundary conditions, e.g., $w_0 = w_n = 0$ in the case

of simple support. The condition for the existence of non-zero solutions of the homogeneous set of linear equations (3.30)

$$
\begin{vmatrix}
\dfrac{Ph^2}{EJ_1}-2 & 0 & 0 & \ldots & 0 & 0 \\[2mm]
1 & \dfrac{Ph^2}{EJ_2}-2 & 1 & \ldots & 0 & 0 \\[2mm]
0 & 1 & \dfrac{Ph^2}{EJ_3}-2 & \ldots & 0 & 0 \\[2mm]
\cdots & \cdots & \cdots & \cdots & \cdots & \cdots \\[2mm]
0 & 0 & 0 & \ldots & 1 & \dfrac{Ph^2}{EJ_{n-1}}-2
\end{vmatrix} = 0
\tag{3.31}
$$

gives an approximate value for the critical force P. The condition (3.31) is of the (3.4) type, but in relation to this general condition, it shows essential simplification resulting from the numerous zero terms in the determinant.

3.8. The Finite Element Method

Consider a bar element $0 < x < h_i$ and assume a certain distribution of deflections in this element due to loss of stability, and depending moreover, on four free parameters $w = w(x; a_1, a_2, a_3, a_4)$. By expressing these parameters by deflections w and slopes φ on the ends of the element, $x_i = 0$ and $x_{i+1} = h$, we can write

$$
w = w(x; w_i, \varphi_i, w_{i+1}, \varphi_{i+1}).
\tag{3.32}
$$

The function (3.32) is called the *shape function*. By treating the bending moments M and the transverse (spatial) forces $T_s = T$ and the axial force N as external loadings for the element, we can determine the virtual work done by these loadings using the formula

$$
\delta L_f = -T_i\,\delta w_i + M_i\,\delta\varphi_i + T_{i+1}\,\delta w_{i+1} - M_{i+1}\,\delta\varphi_{i+1} +
$$
$$
+N\int_0^{h_i} w'\delta w'\,\mathrm{d}x.
\tag{3.33}
$$

Assuming the material to be elastic, the virtual work due to bending is

$$
\delta L_e = \int_0^{h_i} EJw''\delta w''\mathrm{d}x
\tag{3.34}
$$

and after substituting (3.32) it can also be expressed in terms of w_i, φ_i, w_{i+1} and φ_{i+1}. The comparison of (3.33) and (3.34) allows T_i, M_i, T_{i+1}, M_{i+1}

to be expresssed by linear functions of w_i, φ_i, w_{i+1}, φ_{i+1}; in matrix form, we can write

$$\mathbf{F} = \mathbf{K}_i \boldsymbol{\delta}, \tag{3.35}$$

where the square matrix $\mathbf{K}_i$, 4×4, is called the *stiffness matrix* of the element. By "superposing" the stiffness matrices of individual elements, we can construct the global stiffness matrix $\mathbf{K}$, $(2n+2) \times (2n+2)$, for the whole bar. Taking into account the boundary conditions for the bar leads to a set of homogeneous linear equations of type (3.3) and, consequently, to the condition that gives an approximate value of the critical force of type (3.4).

The cubic function $a = \sum\limits_{j=0}^{3} a_j x^j$ is the simplest shape function dependent on four parameters; expressing the coefficients a_j by deflection and slopes at interval boundaries, we obtain

$$a_0 = w_i,$$

$$a_1 = \varphi_i,$$

$$a_2 = \frac{3}{h_i^2}(w_{i+1}-w_i) - \frac{1}{h_i}(\varphi_{i+1}+2\varphi_i),$$

$$a_3 = -\frac{2}{h_i^3}(w_{i+1}-w_i) + \frac{1}{h_i^2}(\varphi_{i+1}+\varphi_i). \tag{3.36}$$

The virtual work done by longitudinal force N and the virtual work due to bending—assuming constant bending rigidity EJ_i in the element considered—are respectively:

$$N \int_0^{h_i} w' \delta w' \mathrm{d}x = Nh_i [a_1 \, \delta a_1 + (a_2 \, \delta a_1 + a_1 \, \delta a_2) h_i +$$

$$+ (a_3 \, \delta a_1 + \tfrac{4}{3} a_2 \, \delta a_2 + a_1 \, \delta a_3) h_i^2 +$$

$$+ \tfrac{3}{2}(a_3 \, \delta a_2 + a_2 \, \delta a_3) h_i^3 + \tfrac{9}{5} a_3 \, \delta a_3 h_i^4], \tag{3.37}$$

$$\delta L_e = EJ_i h_i [4a_2 \, \delta a_2 + 6(a_3 \, \delta a_2 + a_2 \, \delta a_3) h_i + 12 a_3 \, \delta a_3 h_i^2]. \tag{3.38}$$

In the case of variable rigidity $EJ = EJ(x)$, we take either a certain mean value for the element considered or we perform numerical integration of (3.34). Comparing δL_f and δL_e and expressing a_j by w_i, φ_i, w_{i+1} and φ_{i+1} (3.36), we obtain the relationship between generalized forces T and M and generalized displacements w and φ. In matrix form—dividing M by h_i and multiplying φ by h_i so as to equalize the dimensions—we obtain

$$
\begin{bmatrix} T_i \\ \dfrac{M_i}{h_i} \\ T_{i+1} \\ \dfrac{M_{i+1}}{h_i} \end{bmatrix}
$$

$$
= \frac{EJ_i}{h_i^3}
\begin{bmatrix}
12-\frac{6}{5}A & 6-\frac{1}{10}A & -12+\frac{6}{5}A & 6-\frac{1}{10}A \\
6-\frac{1}{10}A & 4-\frac{2}{15}A & -6+\frac{1}{10}A & 2+\frac{1}{30}A \\
-12+\frac{6}{5}A & -6+\frac{1}{10}A & 12-\frac{6}{5}A & -6+\frac{1}{10}A \\
6-\frac{1}{10}A & 2+\frac{1}{30}A & -6+\frac{1}{10}A & 4-\frac{2}{15}A
\end{bmatrix}
\begin{bmatrix} w_i \\ \varphi_i h_i \\ w_{i+1} \\ \varphi_{i+1} h_i \end{bmatrix}, \qquad (3.39)
$$

where

$$
A = \frac{P h_i^2}{E J_i} \tag{3.40}
$$

denotes a dimensionless parameter of loading.

The matrix (3.39) enables direct calculation of the critical forces in the case of approximation of a bar with one finite element. For a simply supported bar, $M_1 = M_2 = w_1 = w_2 = 0$; expressing M_1 and M_2 by non-zero components of the vector of generalized displacements φ_1 and φ_2, we obtain the condition

$$
\begin{vmatrix} 4-\frac{2}{15}A & 2+\frac{1}{30}A \\ 2+\frac{1}{30}A & 4-\frac{2}{15}A \end{vmatrix} = 0, \tag{3.41}
$$

from which $A_1 = 12$, $A_2 = 60$ (instead of π^2 and $4\pi^2$). A better accuracy will be obtained in the case of a bar clamped at one end. Expressing $T_1 = M_1 = 0$ by the non-zero displacements w_1 and φ_1, we obtain the condition

$$
\begin{vmatrix} 12-\frac{6}{5}A & 6-\frac{1}{10}A \\ 6-\frac{1}{10}A & 4-\frac{2}{15}A \end{vmatrix} = 0, \tag{3.42}
$$

from which $A_1 = \frac{4}{3}(13-\sqrt{124}) = 2.4860$ and $A_2 = 32.1807$ (instead of $\pi^2/4$ and $9\pi^2/4$). For a bar clamped at point $x = 0$ and simply supported at point $x = h$, we express the zeroing of M_2 by the only non-zero, generalized displacement φ_2, obtaining $A = 30$ in accordance with the result of the energy formula (3.12) applied to the cubic parabola (3.15).

For a bar clamped at both ends, the approximation with one finite element, taking the shape function in the form of a cubic parabola, is ineffective. Dividing the bar into two elements and superposing two stiffness matrices K_1 and K_2 by the summation of generalized forces T_2 and M_2 from both adjacent intervals, we express the global matrix for the structure as follows (assuming $h_1 = h_2 = h$, $EJ_1 = EJ_2 = EJ$)

$$
\begin{bmatrix} T_1 \\ \dfrac{M_1}{h} \\ \hline T_2 \\ \dfrac{M_2}{h} \\ \hline T_3 \\ \dfrac{M_3}{h} \end{bmatrix} = \dfrac{EJ}{h^3} \times
$$

$$
\times \begin{bmatrix} 12-\frac{6}{5}\varLambda & 6-\frac{1}{10}\varLambda & -12+\frac{6}{5}\varLambda & 6-\frac{1}{10}\varLambda & 0 & 0 \\ & 4-\frac{2}{15}\varLambda & -6+\frac{1}{10}\varLambda & 2+\frac{1}{30}\varLambda & 0 & 0 \\ & & 24-\frac{12}{5}\varLambda & 0 & -12+\frac{6}{5}\varLambda & 6-\frac{1}{10}\varLambda \\ & & & 8-\frac{4}{15}\varLambda & -6+\frac{1}{10}\varLambda & 2+\frac{1}{30}\varLambda \\ \text{(symmetrically)} & & & & 12-\frac{6}{5}\varLambda & -6+\frac{1}{10}\varLambda \\ & & & & & 4-\frac{2}{15}\varLambda \end{bmatrix} \begin{bmatrix} w_1 \\ \varphi_1 h \\ w_2 \\ \varphi_2 h \\ w_3 \\ \varphi_3 h \end{bmatrix}.
$$

$$ \tag{3.43} $$

We construct the global stiffness matrix $(2n+2) \times (2n+2)$ for n elements in a similar way. The generalized forces T_2 and M_2 now have the character of external loadings for the bar; consequently, for the node lying between the supports we have as a rule $T_2 = M_2 = 0$. For a bar clamped at both ends and of length $l = 2h$, we have $w_1 = \varphi_1 = w_3 = \varphi_3 = 0$, and expressing $T_2 = M_2 = 0$ in the function of non-zero displacements w_2 and φ_2, we obtain

$$
\begin{vmatrix} 24-\frac{12}{5}\varLambda & 0 \\ 0 & 8-\frac{4}{15}\varLambda \end{vmatrix} = 0. \tag{3.44}
$$

Hence, $\varLambda_1 = 10$ and $\varLambda_2 = 30$ (instead of the exact values π^2 and 20.19). For a simply supported bar expressing $M_1 = M_2 = T_2 = M_3 = 0$ by non-zero φ_1, w_2, φ_2, φ_3, we obtain the condition

$$
\begin{vmatrix} 4-\frac{2}{15}\varLambda & -6+\frac{1}{10}\varLambda & 2+\frac{1}{30}\varLambda & 0 \\ -6+\frac{1}{10}\varLambda & 24-\frac{12}{5}\varLambda & 0 & 6-\frac{1}{10}\varLambda \\ 2+\frac{1}{30}\varLambda & 0 & 8-\frac{4}{15}\varLambda & 2+\frac{1}{30}\varLambda \\ 0 & 6-\frac{1}{10}\varLambda & 2+\frac{1}{30}\varLambda & 4-\frac{2}{15}\varLambda \end{vmatrix} = 0. \tag{3.45}
$$

Hence, $\varLambda_1 = 2.4860$, $\varLambda_2 = 12$, $\varLambda_3 = 32.1807$ and $\varLambda_4 = 60$. This clearly improves the accuracy compared to (3.41) (for comparison, the $\varLambda$ calculated here should be multiplied by 4).

The finite element method is chiefly being developed for two- and three-dimensional structures; noteworthy contributions concerned with bar sta-

bility include foremost: Hartz (1965), Hicks (1967), Nethercot and Rockey (1971), as well as extensive chapters in the books of Przemieniecki (1968) and Nath (1974).

3.9. Approximate Formulae for Combined Loadings

For purposes of stability analysis of a structure under n independent loadings P_i, $i = 1, 2, ..., n$, the critical state can be described by an equation of the type

$$f(P_1, P_2, ..., P_n) = 0.$$ (3.46)

Equation (3.46) describes a certain hypersurface in a space of loadings P_i. Schaefer (1934) and Papkovich (1934, 1941) proved that in the case of conservative loadings and of neglected geometry changes in the fundamental state, this surface is a convex surface. In that case, the approximate linear equation

$$\sum_{i=1}^{n} \frac{P_i}{P_{i\,cr}} = 1,$$ (3.47)

where $P_{i\,cr}$ denote the critical values of loadings each acting separately, represents in the range of positive P_i a lower estimate of the critical state under combined loadings (Dunkerley's equation). In the case where the sign of one of the loadings, say P_1, does not contribute to the loss of stability (e.g., under torsion), we frequently use approximate formulae of the type

$$\left(\frac{P_1}{P_{1\,cr}}\right)^2 + \frac{P_2}{P_{2\,cr}} = 1$$ (3.48)

(Pflüger, 1964).

For non-conservative loadings, the limit surface may be concave; in that case, (3.47) may no longer give the lower estimate (e.g., concentrated Eulerian force and lateral loading by a fluid flow). If, however, the limit curve consists of two concave segments, just the reverse holds. Namely, the linear equation (3.47) may give an excessively strong lower estimate (e.g., for a concentrated follower force and lateral loading by a fluid flow).

Comprehensive studies on the stability of structures under combined loadings have been carried out by Huseyin (1975).

4. Compressed Elastic Bars with Initial Imperfections

4.1. Classification of Theories

The stability of bars is analysed as a rule assuming axial action of loading and a perfectly straight bar axis before buckling. Real bars, however, depart from these assumptions, it is important, therefore, to evaluate the results obtained for perfect bars from the viewpoint of bars with initial imperfections.

The theory of such bars based on the principle of rigidification (theory of first order) is altogether unsuitable to describe instability and related phenomena. However, if the influence of deflections on the distribution of internal forces and reactions is taken into account in geometrically linear approach (theory of second order), it can be used where subcritical forces are involved, but cannot be used to evaluate deflections under critical force and under supercritical forces. To describe the latter problems, it is necessary to use a geometrically non-linear theory, which Chwalla (1953) referred to as the *theory of third order*. The theory of third order, which we have already used before in Section 2.3 in reference to axially compressed bars, admits finite displacements, assuming at the same time that the strains remain infinitely small; where the theory of finite strains has to be used additionally, one can speak, for the sake of distinction, of the theory of fourth order (Skrzypek, 1979).

4.2. Small Deflections of Eccentrically Compressed Bars

Using the theory of second order for an eccentrically compressed bar clamped at one end, we obtain the equation

$$EJw'' + P(w + e) = 0, \tag{4.1}$$

where e denotes eccentricity which we assume to occur in the principal plane (Fig. 4.1). Taking into account the boundary conditions $w(0) = 0$, with $w'(l) = 0$ leads for a prismatic bar to the equation of deflection line

$$w = e(\tan kl \sin kx + \cos kx - 1),\qquad(4.2)$$
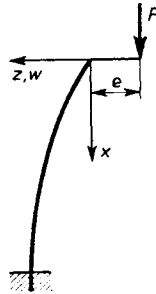
Fig. 4.1. Eccentrically compressed bar

where $k = \sqrt{P/EJ}$, (2.3). The maximum deflection $f = w(l)$ and the maximum bending moment $M_0 = M(l)$ are respectively

$$f = \frac{1 - \cos kl}{\cos kl}\, e, \qquad M_0 = P(e + f) = \frac{Pe}{\cos kl}.\qquad(4.3)$$

As compared with the more accurate theory of third order (Section 4.4), these equations determine f and M_0 with an error from above. With a force approaching the critical force for an axially compressed bar, $kl \to \pi/2$, we obtain $f \to \infty$, $M_0 \to \infty$, which is an absolutely wrong result; a correct result will be obtained only by using the theory of third order. The fact that according to the theory of second order the bending deflection tends to infinity may however serve as a condition specifying critical loadings for perfect bars.

The maximum stress due to bending compression, assuming the material to be elastic, is

$$\sup |\sigma| = \frac{Pe}{W \cos kl} + \frac{P}{A},\qquad(4.4)$$

where W denotes the elastic bending modulus. These stresses depend non-linearly on force P; the non-linearity is associated with the factor $\cos kl$ in the denominator ("secant formula"). For this reason, strength calculations must relate the factor of safety directly to force P, not to stresses.

In the case considered, loss of stability does not actually take place (if possible buckling from xz plane is excluded). But it is liable to occur with

other types of eccentric loading, e.g. in the case of a simply supported bar loaded as in Fig. 4.2 (*Zimmermann's bar*, Zimmermann, 1930). For this bar, the differential equation of bending has the form

$$EJw'' + P\left[w + e\left(1 - \frac{2x}{l}\right)\right] = 0 \tag{4.5}$$
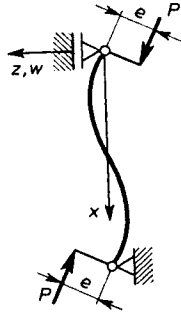
Fig. 4.2. Bar compressed with two eccentricities (Zimmermann's bar)

and after integrating and considering the boundary conditions $w(0) = w(l) = 0$, we obtain

$$w = e\left(-\frac{1 + \cos kl}{\sin kl}\sin kx + \cos kx - 1 + \frac{2x}{l}\right). \tag{4.6}$$

When $kl \to \pi$, the coefficient of the first term in (4.6) becomes indeterminate of 0/0 type; indeed, the boundary conditions are then satisfied at any value of this coefficient, which means bifurcation of the equilibrium form. However, since this bifurcation does not take place at $w = 0$, therefore we cannot claim that the respective value of force $P = \pi^2 EJ/l^2$ is the exact critical value. The exact value can be calculated only when we use the exact expression for curvature, i.e., on the basis of theory of third order. According to Cornelius (1944), the critical force tends to zero, i.e., bifurcation takes place right from the beginning of the loading process.

4.3. Small Deflections of Compressed Bars with Initial Curvature

The equation of bending for weakly curved bars

$$EJ(\varkappa - \varkappa_-) = M, \tag{4.7}$$

where $\varkappa_- = \varkappa_-(x) = -w''(x)$ denotes the initial curvature, prior to the application of the load, in the case $M = Pw$ and according to the theory of second order, takes the form

$$EJw'' + Pw = EJw_-''. \tag{4.8}$$

Equation (4.8) shows an analogy to equations of forced vibrations; the general solution of it for a prismatic bar can be expressed by the Duhamel integral of the form

$$w = C_1 \sin kx + C_2 \cos kx + \frac{1}{k} \int w''_-(\xi) \sin k(x - \xi) \, d\xi. \tag{4.9}$$

For most applications it is more convenient, however, to use Fourier series. In the case of bars clamped at one end $x = l$, and with a free end $x = 0$, we can describe the initial deflection line and the deflection line under loading by the series

$$w_-(x) = \sum_{j=1}^{\infty} a_j \sin \frac{(2j-1)\pi x}{2l},$$

$$w(x) = \sum_{j=1}^{\infty} A_j \sin \frac{(2j-1)\pi x}{2l}, \tag{4.10}$$

where initial amplitudes a_j are treated as known values, whereas amplitudes A_j need to be determined. Substituting (4.10) into (4.8) and comparing the coefficients on both sides of the equation, we obtain

$$A_j = \frac{(2j-1)^2 a_j}{(2j-1)^2 - m}, \quad m = \frac{P}{P_E} = \frac{4Pl^2}{\pi^2 EJ}. \tag{4.11}$$

Also, in this case, the deflections under force $P = P_E$ tend toward infinity (if $a_1 \neq 0$); obviously, this result is wrong, whereas the correct result can be obtained only according to the theory of third order. In the case $a_1 = 0$, the coefficient A_1 for Eulerian force is arbitrary, which means bifurcation; however, also in this case the exact value of the critical force can be determined only based on the theory of finite deflections.

For a simple support we can use in place of (4.10) the series

$$w_-(x) = \sum_{j=1}^{\infty} a_j \sin \frac{j\pi x}{l},$$

$$w(x) = \sum_{j=1}^{\infty} A_j \sin \frac{j\pi x}{l}. \tag{4.12}$$

We then obtain

$$A_j = \frac{j^2 a_j}{j^2 - m}, \quad m = \frac{P}{P_E} = \frac{Pl^2}{\pi^2 EJ}. \tag{4.13}$$

The fastest to grow is the amplitude of the first sinusoid A_1. We denote the increment of this amplitude by δ,

$$\delta = A_1 - a_1 = \frac{m}{1-m} a_1. \tag{4.14}$$

Taking for an imperfect real bar experimental values of two increments of the amplitudes δ_1 and δ_2, corresponding to forces P_1 and P_2, and substituting into (4.14), we obtain as set of two equations. In this set, we can eliminate the initial amplitude, which is difficult to measure, and represent the critical force for a perfect straight bar by the simple equation (Southwell, 1932):

$$P_E = \frac{\delta_2 - \delta_1}{\dfrac{\delta_2}{P_2} - \dfrac{\delta_1}{P_1}}. \tag{4.15}$$

With a larger number of measurements, average values can be used. The different variants of application of Southwell's equation have been discussed by Gregory (1967).

4.4. Finite Deflections of Eccentrically Compressed Bars with Initial Curvature

A more accurate stability analysis of compressed bars with initial imperfections in the Eulerian force range is obtainable based on the theory of third order. We present this problem making use of paper by Życzkowski (1960). Unlike as in Section 2.3, we take here for the dependent variable not angle φ but deflections w. The independent variable s will be measured along the arc, the compressibility of the axis being neglected.

In the s–w system the curvature of the bar axis can be determined by the equation

$$\varkappa = -\frac{d\varphi}{ds} = -\frac{d}{ds} \arcsin \frac{dw}{ds} = -\frac{w''}{\sqrt{1-w'^2}}, \tag{4.16}$$

where the dashes denote differentiation with respect to variable s. The substitution of (4.16) into (4.7) makes an analytical solution possible but only for $\varkappa_- = \text{const}$ (the initial curvature corresponds to a circular arc), and we shall consider only this case here. In the reference system given in Fig. 4.3, Eq. (4.7) takes the form

$$\frac{Pw}{EJ} + \frac{w''}{\sqrt{1-w'^2}} + \varkappa_- = 0. \tag{4.17}$$
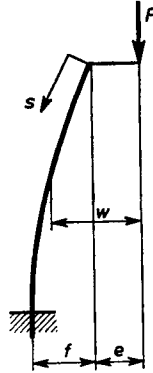
Fig. 4.3. Finite deflections of an eccentrically compressed bar

To simplify the notation of the integrals and elliptic functions obtained later, we introduce dimensionless variables with the multiplier $\pi/2$

$$x = \frac{\pi}{2l} s, \qquad y = \frac{\pi}{2l} w, \tag{4.18}$$

and in addition, we introduce the dimensionless parameters

$$m = \frac{P}{P_E} = \frac{4Pl^2}{\pi^2 EJ}, \qquad \xi = \frac{\pi}{2l} e,$$

$$\vartheta = \frac{\pi}{2l} f, \qquad\qquad \psi = \frac{2l}{\pi} \varkappa_-. \tag{4.19}$$

We now write Eq. (4.17) in the form

$$y'' + (my + \psi)\sqrt{1 - y'^2} = 0, \tag{4.20}$$

where the dashes denote differentiation with respect to the independent variable x. Further, very essential simplifications are obtained by introducing a new dependent variable

$$z = y + \frac{\psi}{m}. \tag{4.21}$$

Equation (4.20) now takes the form

$$z'' + mz\sqrt{1 - z'^2} = 0 \tag{4.22}$$

with the boundary conditions

$$z(0) = \xi + \frac{\psi}{m}, \qquad z\left(\frac{\pi}{2}\right) = \xi + \frac{\psi}{m} + \vartheta, \qquad z'\left(\frac{\pi}{2}\right) = 0. \tag{4.23}$$

These conditions determine two integration constants and unknown bending deflection $\vartheta = \vartheta(m, \psi, \xi)$. The simplification introduced by substituting (4.21) consists essentially in that ξ and ψ now occur only in the form of the sum $\xi + (\psi/m)$; regarding the expression

$$\chi = \psi + m\xi \tag{4.24}$$

as the reduced initial curvature, we reduce the number of parameters to two: m and χ.

Putting $z' = v(z)$ in Eq. (4.22) and integrating, and taking into account two boundary conditions, we write

$$x = \frac{2}{m} \int_{\frac{\chi}{m}}^{z} \frac{d\zeta}{\sqrt{[\zeta^2 - (\vartheta + \chi/m)^2 + 4/m]\,[(\vartheta + \chi/m)^2 - \zeta^2]}} , \tag{4.25}$$

where ζ denotes the integration variable. The elliptic integral (4.25) can be reduced to normal form by introducing a new integration variable β using the formula $\zeta = [\vartheta + (\psi/m)]\cos\beta$; finally

$$x\sqrt{m} = F\left[\arccos\frac{\chi}{\chi + m\vartheta},\ \left(\vartheta + \frac{\chi}{m}\right)\frac{\sqrt{m}}{2}\right] - $$
$$- F\left[\arccos\frac{mz}{\chi + m\vartheta},\ \left(\vartheta + \frac{\chi}{m}\right)\frac{\sqrt{m}}{2}\right], \tag{4.26}$$

where $F(\varphi, k)$ denotes an incomplete elliptic integral of the first kind. The third boundary condition now determines the bending deflection ϑ by an implicit relation of the type $\Phi(\chi, m, \vartheta) = 0$, namely

$$\frac{\pi}{2}\sqrt{m} - F\left[\arccos\frac{\chi}{\chi + m\vartheta},\ \left(\vartheta + \frac{\chi}{m}\right)\frac{\sqrt{m}}{2}\right] = 0. \tag{4.27}$$

In the particular case $\chi = 0$, we obtain, therefore, the second of Eqs. (2.54) for a straight, axially loaded bar.

The implicit function (4.27) enables the calculation of the bending deflection under Eulerian force $m = 1$; it also enables stability analysis in the postcritical region. Substituting $m = 1$ into (4.27), we obtain the equation

$$\frac{\pi}{2} - F\left(\arccos\frac{\chi}{\chi + \vartheta},\ \frac{\vartheta + \chi}{2}\right) = 0. \tag{4.28}$$

By expanding the elliptic integral into a power series of modulus k,

$$F(\varphi, k) = \varphi + \frac{k^2}{4}(\varphi - \sin\varphi\cos\varphi) + $$
$$+ \frac{3k^4}{64}(3\varphi - 3\sin\varphi\cos\varphi - 2\sin^3\varphi\cos\varphi) + \dots \tag{4.29}$$

and by performing appropriate operations on the series (Życzkowski, 1965) we can determine the dimensionless bending deflection ϑ under Eulerian force $m = 1$ by the generalized power series

$$\vartheta = \sqrt[3]{\frac{32}{\pi}}\sqrt[3]{\chi} - \left(1 + \frac{1}{6\pi}\right)\chi + \frac{\pi^2+8}{18\pi^2}\sqrt[3]{\frac{\pi}{32}}\chi^{5/3} + \dots \qquad (4.30)$$

$$= 2.16770\chi^{1/3} - 1.05305\chi + 0.04640\chi^{5/3} + \dots \qquad (4.30a)$$

A simpler approximate formula for the bending deflection of an eccentrically compressed bar has been derived by Życzkowski (1953). The parameter χ in Eq. (4.30) covers both eccentricity and initial curvature, (4.24).

With different signs of eccentricity ξ and initial curvature, the loss of stability of the bar by snap-through is possible. The critical state condition is

$$\frac{\partial m}{\partial \vartheta}\bigg|_{\chi = \text{const}} = 0. \qquad (4.31)$$

Treating (4.27) as an implicit equation, $\Phi(\psi, m, \vartheta) = 0$, which determines the function $m = m(\psi, \vartheta)$, and differentiating it with respect to ϑ at a fixed value of χ, we obtain

$$\frac{\partial \Phi}{\partial \vartheta} + \frac{\vartheta \Phi}{\partial m}\frac{\partial m}{\partial \vartheta} = 0. \qquad (4.32)$$

In view of (4.31), the second term equals zero and the critical state condition takes the form $\partial\Phi/\partial\vartheta = 0$. Since the elliptic integral in (4.27) is a compound function of the variables χ, m and ϑ through argument φ and modulus k, we write this condition as follows:

$$\frac{\partial F}{\partial \varphi}\frac{\partial \varphi}{\partial \vartheta} + \frac{\partial F}{\partial k}\frac{\partial k}{\partial \vartheta} = 0, \qquad (4.33)$$

where

$$\varphi = \arccos\frac{\chi}{\chi + m\vartheta}, \qquad k = \left(\vartheta + \frac{\chi}{m}\right)\frac{\sqrt{m}}{2}. \qquad (4.34)$$

To make use of condition (4.33), we first note that the set of equations (4.27) and (4.34) can be effectively solved with respect to m, ϑ and χ

$$m = \frac{4}{\pi^2}F^2(\varphi, k),$$

$$\vartheta = \frac{k\pi}{F(\varphi, k)}(1 - \cos\varphi),$$

$$\chi = \frac{4}{\pi}kF(\varphi, k)\cos\varphi. \qquad (4.35)$$

Equations (4.35) parametrize the formula for bending deflection (4.27) and are convenient for numerical calculations, especially for checking calculations. But, this time we shall use them in a different way: after calculating the derivatives $\partial \varphi / \partial \vartheta$ and $\partial k / \partial \vartheta$ from Eqs. (4.34), we express these derivatives by virtue of (4.35) again in terms of φ and k, and then substitute into (4.33) obtaining a relatively simple relationship

$$\frac{\partial F}{\partial \varphi} + k \tan \varphi \frac{\partial F}{\partial k} = 0. \tag{4.36}$$

Using the expansion (4.29), we can thereby determine the function $\varphi = \varphi(k)$ using the series

$$\varphi_{cr} = \frac{\pi}{2} + \frac{\pi}{4} k^2 + \frac{13}{32} \pi k^4 + \left(\frac{199}{256} \pi - \frac{1}{192} \pi^3 \right) k^6 + \ldots \tag{4.37}$$

The index cr in Eq. (4.37) and in those that follow denotes parameters of the critical state. Substituting (4.37) into (4.35) and performing operations on the series, we obtain successively

$$m_{cr} = 1 + \frac{3}{2} k^2 + \frac{95}{32} k^4 + \ldots,$$

$$\vartheta_{cr} = 2k + \frac{\pi - 3}{2} k^3 + \frac{7\pi - 34}{16} k^5 + \ldots, \tag{4.38}$$

$$\chi_{cr} = -\frac{\pi}{2} k^3 - \frac{19}{16} \pi k^5 + \ldots$$

By inverting the last of the series, i.e., by expressing k in terms of χ and then substituting into the first one, we can present the critical force and the corresponding bending deflection in terms of the imperfection parameter χ

$$m_{cr} = 1 + \frac{3}{2} \sqrt[3]{\frac{4}{\pi^2}} \chi^{2/3} + \frac{19}{16\pi} \sqrt[3]{\frac{2}{\pi}} \chi^{4/3} + \ldots$$

$$= 1 + 1.11006 \chi^{2/3} + 0.32517 \chi^{4/3} + \ldots,$$

$$\vartheta_{cr} = -2 \sqrt[3]{\frac{2}{\pi}} \chi^{1/3} + \frac{37 - 6\pi}{6\pi} \chi + \ldots$$

$$= -1.72051 \chi^{1/3} + 0.96291 \chi + \ldots \tag{4.39}$$

The critical state occurs therefore with bending deflection ϑ_{cr} having a sign opposite to that of the initial imperfection parameter χ. Such a critical state cannot be attained either with eccentric compression of a straight bar or with axial compression of a bar with initial curvature, since in this situation the bending deflection does not change sign. A critical state leading

to a snap-through is feasible only when eccentricity ξ and primary curvature ψ of opposite sign occur simultaneously; the parameter χ, (4.24), can change sign with increase in the force m, and the bending deflection ϑ can also change sign. It has been demonstrated by Życzkowski (1959) that the critical state occurs only in the interval $\xi_1 < \xi < \xi_2$, where

$$\xi_1 = -\psi,$$

$$\xi_2 = -\psi + \frac{2}{\pi^2}\,\psi^3 - \frac{5}{2\pi^4}\,\psi^5 + \ldots, \tag{4.40}$$

since only then can the straight line $\chi = \chi(m)$ intersect the line $m_{cr} = m_{cr}(\chi)$, (4.39) (Fig. 4.4).

For example, for $\psi = 0.4$ we have $\xi_1 = -0.4$, $\xi_2 = -0.3873$; Figure 4.5 shows the course of deflections for $\xi = -0.5$ (the deflections pass from
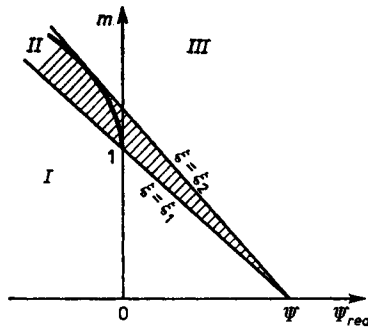
Fig. 4.4. Critical states region of eccentrically compressed bars with initial curvature
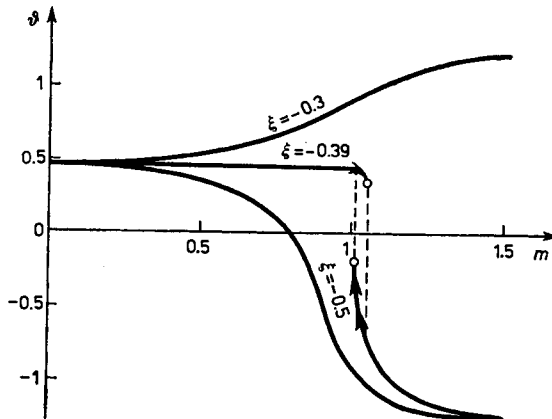
Fig. 4.5. Three types of deflection process in eccentrically compressed bars with initial curvature

positive to negative without jump), $\xi = -0.39$ (loss of stability resulting in a jump) and $\xi = -0.3$ (increasing positive deflections).

The relation $m_{cr} = m_{cr}(\chi)$, (4.39), is a special case in the general theory of the effect of initial imperfections on the critical load value, derived by Koiter (1945). According to this theory, in the symmetrical case considered, with stable postcritical behaviour of a perfect structure, the basic effect is expressed by $\chi^{2/3}$ with a positive coefficient. In other cases, the effect of the imperfection parameter is expressed as follows: in symmetrical case, with unstable postcritical behaviour, by the power 2/3 with a negative coefficient; in asymmetric case, by the power 1/2 with a negative coefficient.

Other cases of finite deflections with eccentric compression of elastic bars have been considered in the papers by Życzkowski (1957) (eccentricity always perpendicular to the deflected bar axis) and by Szuwalski (1970) (a force applied to the deformable part through a rigid element of constant length).

5. Elastic-Plastic Buckling

5.1. Bifurcation of the Equilibrium of Straight Bars

Elastic-plastic behaviour of the material introduces significant differences into stability analysis. The bifurcation of equilibrium forms may be associated with processes plastically active (loading) at every point of the structure or with processes plastically passive (unloading) at every point, or else, in a general case, with the formation of certain active zones and certain passive zones, each governed by different physical equations.

Consider a certain state of equilibrium for a straight axially compressed prismatic bar, described by strain $\varepsilon = $ const and stress $\sigma = f(\varepsilon) = $ const, the latter describing a plastically active process. We superimpose on this
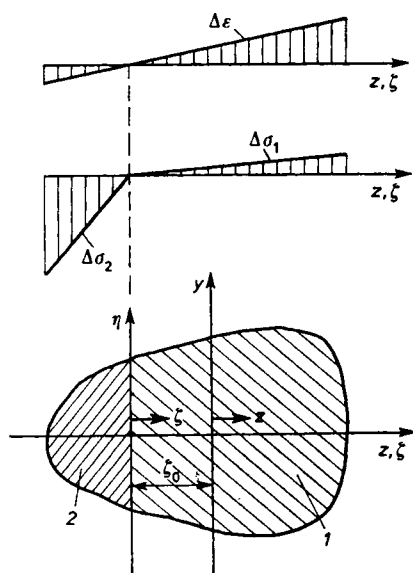
Fig. 5.1. Slastic-plastic buckling of bars with one axis of symmetry of cross-section

state an additional bending strain distribution, $\Delta\varepsilon = \zeta\Delta\varkappa$, where the coordinate ζ is measured from a certain, temporarily undetermined, axis η, parallel to the principal centroidal y-axis termed the *nominal stress axis*; we assume at the same time that the cross-section has at least one axis of symmetry (z-axis, i.e., ζ-axis, Fig. 5.1). If the nominal stress axis passes through the cross-section, it divides this cross-section into region $\zeta > 0$, in which plastically active processes are taking place (region *1*), and region $\zeta < 0$, in which passive processes are taking place (region *2*). Referring to the theory of second order, we assume the strain increments to be small, and we determine the corresponding stress increments using the equations

$$\begin{aligned} \Delta\sigma_1 &= E_t\Delta\varepsilon = E_t\zeta\Delta\varkappa, \quad \zeta > 0, \\ \Delta\sigma_2 &= E\Delta\varepsilon = E\zeta\Delta\varkappa, \quad\ \ \zeta < 0, \end{aligned} \tag{5.1}$$

where $E_t = \mathrm{d}\sigma/\mathrm{d}\varepsilon$ denotes the tangent modulus, whereas the passive processes are governed by the elastic modulus E. The equations of equilibrium in adjacent position have the form

$$\begin{aligned} \Delta\varkappa(E_t S_{1\eta} + E S_{2\eta}) &= \Delta N, \\ \Delta\varkappa[E_t(J_{1\eta} - \zeta_0 S_{1\eta}) + E(J_{2\eta} - \zeta_0 S_{2\eta})] &= \Delta M, \end{aligned} \tag{5.2}$$

where ΔN and ΔM denote increments of the longitudinal force and of the bending moment (reckoned, as usual, with respect to the y-axis), $S_{1\eta}$ and $S_{2\eta}$ denote the static moments, $J_{1\eta}$ and $J_{2\eta}$ are the moments of inertia of the cross-sectional regions *1* and *2* with respect to the nominal stress axis η, and finally, ζ_0 denotes the coordinate ζ of the centre of gravity of the cross-section.

Kármán (1909) assumed that as in the elastic case, bifurcation occurs at $\Delta N = 0$; the nominal stress axis is then given by the equation

$$E_t S_{1\eta} + E S_{2\eta} = 0 \tag{5.3}$$

and the basic equation of bending can be written in the form

$$E_K J\varkappa = M, \tag{5.4}$$

where

$$E_K \overset{\text{def}}{=} \frac{E_t J_{1\eta} + E J_{2\eta}}{J} \tag{5.5}$$

is called *Kármán's reduced modulus*; the symbol J denotes the moment of inertia of the whole cross-section with respect to the centroidal y-axis. The increment symbols Δ have been omitted in Eq. (5.4) because the increments of $\varkappa$ and M are counted from the initial state $\varkappa = M = 0$. The modulus E_K remains in the range $E_t < E_K < E$; the first proposal ever to describe

elastic-plastic buckling by the reduced modulus was presented by A. Considère at an international congress on structures in Paris in 1891, but the effective proposal (5.5) came from Kármán. E_K depends also on the shape of the cross-section; for example, for a rectangular cross-section $b \times h$,

$$\zeta_0 = \frac{\sqrt{E} - \sqrt{E_t}}{2(\sqrt{E} + \sqrt{E_t})} h,$$

$$E_K = \frac{4EE_t}{(\sqrt{E} + \sqrt{E_t})^2},$$

(5.6)

and for a theoretical I-section

$$E_K = \frac{2EE_t}{E + E_t}.$$

(5.7)

Shanley (1946, 1947) observed, however, that in the case of elastic-plastic buckling, Kármán's condition $\Delta N = 0$ is not a necessary condition. Bifurcation is liable to take place also at $\Delta N \neq 0$, namely with an arbitrary position of the nominal stress axis η on the cross-section. The basic equation of bending can then be written in the form

$$E^* J \varkappa = M,$$

(5.8)

where

$$E^* \stackrel{\text{def}}{=} \frac{E_t J_{1\eta} + E J_{2\eta}}{J} - \frac{\zeta_0 \Delta N}{J \varkappa}.$$

(5.9)

Here, we regard the longitudinal force N as positive in compression; corresponding to positive increment ΔN is also positive ζ_0. Hence, the modulus
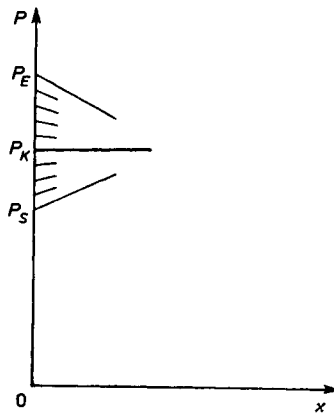
Fig. 5.2. Feasible bifurcations of equilibrium in elastic-plastic range

E^* is a decreasing function of ΔN. We obtain the minimum modulus by using the highest possible value of ζ_0, i.e., with the axis η tangent to the contour of the cross-section on the side of negative z. We then have $A_1 = A$, $A_2 = 0$, and in view of $J_{1\eta} - \zeta_0 S_{1\eta} = J_\eta - \zeta_0^2 A = J$, the second equation (5.2) takes the form

$$E_t J \varkappa = M. \tag{5.10}$$

In the second extreme case, where $A_2 = A$, $A_1 = 0$, the modulus E^* assumes the value E. In a general case, bifurcation may take place at arbitrary value of E^* from the range $E_t \leqslant E^* \leqslant E$, where $E^* < E_k$ for $\Delta N > 0$, and $E^* > E_k$ for $\Delta N < 0$ (Fig. 5.2 where the forces P_K and P_S correspond to moduli E_K and E_t). The negative value of ΔN may occur in a natural way, e.g. in bar structures (Ilyushin, 1960). The theoretical aspects of elastic-plastic buckling are comprehensively discussed in works by Horne (1961) and Sewell (1971), the latter paper containing numerous references.

In the case of an increasing longitudinal force, the least value of critical loading is given by Eq. (5.10). Shanley's theory used a simple model with one degree of freedom, but considerations involving a real bar lead to similar results (Pflüger, 1952). Integrating Eq. (5.9) and taking into account the boundary conditions, we obtain, as in Section 2.1,

$$P_{cr} = P_S = \frac{\pi^2 E_t J}{l_r^2}, \tag{5.11}$$

where the mode of support of the bar is given in terms of reduced (effective) length $l_r = \mu l$; the subscript S stands for Shanley. Eq. (5.11) gives the critical force in an implicit manner, since $E_t = f(\sigma)$ and $\sigma = \sigma_{cr} = P_{cr}/A$. By presenting Eq. (5.11) in the form

$$\sigma_{cr} = \frac{\pi^2 E_t}{\lambda^2}, \tag{5.12}$$

we can determine in any case the inverse function with respect to $\sigma_{cr} = \sigma_{cr}(\lambda)$ using the equation

$$\lambda = \pi \sqrt{\frac{E_t(\sigma_{cr})}{\sigma_{cr}}}. \tag{5.13}$$

In some cases, the critical force or the critical stress may be determined by an explicit equation. Ylinen (1956) proposed to approximate the function $E_t = E_t(\sigma)$ using the equation

$$E_t = \frac{d\sigma}{d\varepsilon} = E \frac{\sigma_0 - \sigma}{\sigma_0 - c\sigma}, \qquad 0 \leqslant \sigma \leqslant \sigma_0, \tag{5.14}$$

where σ_0 denotes the yield point of material and c is a dimensionless constant that is determined experimentally $(c = 0.977$ for most structural steels, $c = 0.875$ for pine wood, $c = 0$ for concrete). The equation

$$\sigma_{\mathrm{cr}} = \frac{\pi^2 E}{\lambda^2} \frac{\sigma_0 - \sigma_{\mathrm{cr}}}{\sigma_0 - c\sigma_{\mathrm{cr}}} \tag{5.15}$$

is a quadratic equation with respect to σ_{cr}; a physical meaning has the root

$$\sigma_{\mathrm{cr}} = \frac{2\sigma_0}{1 + \dfrac{\lambda^2 \sigma_0}{\pi^2 E} + \sqrt{\left(1 + \dfrac{\lambda^2 \sigma_0}{\pi^2 E}\right)^2 - 4c \dfrac{\lambda^2 \sigma_0}{\pi^2 E}}} \,. \tag{5.16}$$

Equation (5.14), treated as a differential equation with respect to the function $\sigma = \sigma(\varepsilon)$, defines the tension-compression stress-strain curve as follows:

$$\varepsilon = \frac{1}{E}\left[c\sigma - (1-c)\sigma_0 \ln\left(1 - \frac{|\sigma|}{\sigma_0}\right)\operatorname{sign}\sigma\right] \tag{5.17}$$

which applies for the entire range $-\sigma_0 < \sigma < \sigma_0$; hence, (5.16) holds for $0 < \lambda < \infty$. The purely elastic range is then reduced to zero but the curve (5.16) approaches Euler's hyperbola asymptotically.

The general equation (5.12) may also be used for the design of bars, i.e., for calculation of the required cross-sectional area of bar A. This unknown quantity occurs both in λ and in σ_{cr}, and also in $E_t(\sigma_{\mathrm{cr}})$. Assuming, however, a certain shape of the cross-section, we can consider the dimensionless shape factor

$$\xi = \frac{A}{i_{\min}^2} \tag{5.18}$$

as known. Multiplying both sides of this equation by the reduced length squared and dividing by the critical force, equal to the product of a given force P and the adopted safety factor with respect to buckling j, we obtain

$$\frac{\xi l_r^2}{Pj} = \frac{\lambda^2}{\sigma_{\mathrm{cr}}} \,. \tag{5.19}$$

Denoting the quantity (*Ylinen's number*) as

$$\frac{\xi l_r^2}{Pj} = \chi \tag{5.20}$$

which is known in the case considered, and substituting (5.12) into (5.19), we obtain

$$\chi = \frac{\pi^2 E_t(\sigma_{\mathrm{cr}})}{\sigma_{\mathrm{cr}}^2} \,. \tag{5.21}$$

It is an inverse function with respect to the one sought, $\sigma_{cr} = \sigma_{cr}(\chi)$, since the knowledge of σ_{cr} helps determine the cross-sectional area by the equation $A = Pj/\sigma_{cr}$. In special cases, Eq. (5.21) can be solved with respect to σ_{cr}; substituting (5.14), we arrive at a cubic equation, for which Ylinen has provided a graphical solution.

A certain original hypothesis of elastic-plastic buckling was proposed by Broszko (1953). He observed that by using formula (2.12) for the critical stress σ_{cr} in the elastic range, the relevant critical strain $\varepsilon_{cr} = \sigma_{cr}/E$ can be expressed by the formula

$$\varepsilon_{cr} = \frac{\pi^2}{\lambda^2} \tag{5.22}$$

which does not contain any material constant. It is, therefore, applicable for every elastic material. Postulating an even further reaching universality of Eq. (5.22), Broszko proposed to use it also in the elastic-plastic range; we then obtain

$$\sigma_{cr} = \frac{\pi^2 E_s}{\lambda^2}, \tag{5.23}$$

where $E_s = \sigma(\varepsilon)/\varepsilon$ denotes the secant modulus. The hypothesis (5.23) finds however no theoretical background, and compared to (5.11) it gives an error from above (to disadvantage of safety).

5.2. Empirical Equations for Critical Stress

By direct experimental studies we can determine the relation $\sigma_{cr} = \sigma_{cr}(\lambda)$ by means of empirical formulae. Combining equations of this type with the basic equation of elastic-plastic buckling theory (5.12), we can determine indirectly the equation of tension-compression stress-strain curve $\sigma = f(\varepsilon)$, corresponding to that empirical equation. We present such an equation in inverse form $\lambda = \lambda(\sigma_{cr})$ and substitute this into (5.12) to obtain

$$E_t(\sigma_{cr}) = \frac{d\sigma}{d\varepsilon} = \frac{1}{\pi^2} \sigma_{cr} \lambda^2(\sigma_{cr}). \tag{5.24}$$

By omitting the subscript of σ_{cr}, no longer necessary now, and by integrating, we can write

$$\varepsilon = \pi^2 \int \frac{d\sigma}{\sigma\lambda^2(\sigma)} + C, \tag{5.25}$$

where the constant C should be determined from the condition $\varepsilon = S/E$ for $\sigma = S$ (the elastic limit).

The simplest equations were formulated by Tetmajer (1890) and Jasiński (1895),

$$\sigma_{or} = A - B\lambda, \tag{5.26}$$

and by Johnson and Ostenfeld (Ostenfeld, 1898)

$$\sigma_{cr} = a - b\lambda^2. \tag{5.27}$$

Equation (5.27) is more convenient and more accurate; we then obtain

$$E_t(\sigma) = \frac{1}{\pi^2 b}(a - \sigma)\sigma, \tag{5.28}$$

$$\varepsilon = \frac{S}{E} + \frac{\pi^2 b}{a}\ln\frac{\sigma(a - S)}{S(a - \sigma)}, \quad S \leqslant \sigma \leqslant a. \tag{5.29}$$

In particular, a very simple relation, $E_t(\sigma)$, is obtained using Rankine's empirical equation

$$\sigma_{cr} = \frac{a}{1 + c\lambda^2}, \tag{5.30}$$

namely

$$E_t = \frac{1}{c}(a - \sigma), \quad 0 \leqslant \sigma \leqslant a. \tag{5.31}$$

It corresponds to Ylinen's equation (5.14) for $c = 0$, recommended, therefore, for concrete. The tension-compression stress-strain curve then departs markedly from Hooke's law.

By introducing Ylinen's number χ, we can also determine the necessary cross-sectional area A. Combining (5.21) and (5.24), we obtain

$$\chi = \frac{\lambda^2(\sigma_{cr})}{\sigma_{cr}}, \tag{5.32}$$

and inversion of this function gives $\sigma_{cr}(\chi)$ and $A = Pj/\sigma_{cr}$. For the Johnson–Ostenfeld equation (5.27), the inversion can be presented effectively as

$$A = \frac{Pj}{a}(1 + b\chi). \tag{5.33}$$

For the Tetmajer–Jasiński equation (5.26), a similar equation was derived, using a somewhat different procedure, by Walczak (1959).

5.3. Small Deflections of Eccentrically Compressed Bars in the Case of Linear Plastic Strain Hardening

By assuming linear strain hardening under eccentric compression, we can easily refer to Shanley's theory, since the tangent modulus $E_t = \text{const}$ above the yield point and it is valid not only for an infinitely small stress increment.

A further simplification of the analysis is obtainable by replacing a real bar with a Ryder–Shanley model consisting of two rigid elements of length L and two deformable bars of length l, which we assume to be short and themselves not subject to buckling. We now load this model with forces P acting
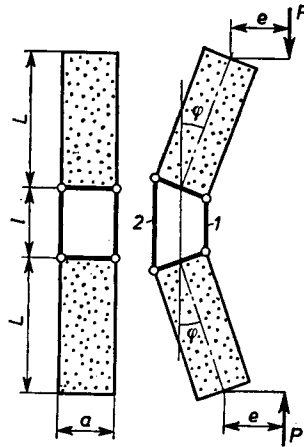
Fig. 5.3. Shanley's model under eccentric compression

on the eccentricity e. We denote the inner bar by the symbol 1 and the outer by 2 (Fig. 5.3); the corresponding longitudinal forces in the bars, N_1 and N_2, we shall consider as positive in compression. The equilibrium equations lead to the relationships

$$N_1 + N_2 = P, \quad (N_1 - N_2)\frac{a}{2} = P(e + L\varphi), \tag{5.34}$$

which are valid in any operating range of the model. With reference to the theory of second order, $\sin\varphi$ has been replaced by the slope φ itself. The equation relating φ to the shortening of the bars is also uniform:

$$2\varphi = \frac{\Delta l_1 - \Delta l_2}{a}, \tag{5.35}$$

whereas the relationships between the shortenings Δl_i and the longitudinal forces N_i depend on the range investigated.

We omit here the analysis of the elastic range, since practically, it does not differ from that discussed in Section 4.2, and we also omit one-sided plastification, but we shall consider two-sided plastification and the change of the plastically active to passive process in the unloaded bar 2. Assuming that a

plastically active process takes place in both bars, which is governed by constant modulus E_t, the geometric equation (5.35) leads to the relationship

$$\varphi = (N_1 - N_2) \frac{l}{2E_t A a}, \tag{5.36}$$

where $A = A_1 = A_2$ denotes the cross-section of each of the bars. The solution of the set of equations (5.34) and (5.36) is

$$N_{1, 2} = \frac{P}{2} \pm \frac{PE_t A a e}{E_t A a^2 - PLl},$$
$$\varphi = \frac{Ple}{E_t A a^2 - PLl}. \tag{5.37}$$

The longitudinal force N_1 increases steadily with the force P, whereas the force N_2 reaches a maximum equalling

$$\tilde{N}_2 = \frac{E_t A a}{2Ll} (\sqrt{a} - \sqrt{2e})^2 \tag{5.38}$$

under the external force

$$\tilde{P} = \frac{E_t A a \sqrt{a}}{Ll} (\sqrt{a} - \sqrt{2e}). \tag{5.39}$$

(We assume here an eccentricity e so small that the value N_2 is not only positive but corresponds to plastification of bar 2.) The corresponding boundary values of N_1 and φ are

$$\tilde{N}_1 = \frac{E_t A a}{2Ll} (a - 2e), \quad \tilde{\varphi} = \frac{1}{L} \sqrt{\frac{e}{2}} (\sqrt{a} - \sqrt{2e}). \tag{5.40}$$

In the case of axial compression $e = 0$, the limit force P tends toward Shanley's critical force for the investigated model

$$P_S = \frac{E_t A a^2}{Ll}. \tag{5.41}$$

In the range $P > \tilde{P}$, the longitudinal force N_2 decreases; hence, the deformation process in bar "2" changes to plastically passive, which is described by the equation

$$\Delta l_2 - \tilde{\Delta l}_2 = (N_2 - \tilde{N}_2) \frac{1}{EA}. \tag{5.42}$$

However, in bar "1" the active process continues to be governed by modulus E_t:

$$\Delta l_1 - \tilde{\Delta l}_1 = (N_1 - \tilde{N}_1) \frac{1}{E_t A}. \tag{5.43}$$

It is convenient here to present the geometric relationship (5.35) in the form

$$\varphi = \tilde{\varphi} + \frac{1}{2a}\left[(N_1 - \tilde{N}_1)\frac{l}{E_t A} - (N_2 - \tilde{N}_2)\frac{l}{EA}\right]. \tag{5.44}$$

Using (5.34) and solving with respect to φ, we obtain

$$\varphi = \frac{1}{1 - \dfrac{PLl}{2Aa^2}\left(\dfrac{1}{E_t} + \dfrac{1}{E}\right)}\left[\tilde{\varphi} + \frac{Pel}{2Aa^2}\left(\frac{1}{E_t} + \frac{1}{E}\right) + \right.$$

$$\left. + \frac{Pl}{4Aa}\left(\frac{1}{E_t} - \frac{1}{E}\right) - \frac{\tilde{N}_1 l}{2E_t Aa} + \frac{\tilde{N}_2 l}{2EAa}\right]. \tag{5.45}$$

The angle φ increases infinitely at

$$P = \frac{2Aa^2 EE_t}{Ll(E + E_t)} = \frac{Aa^2}{Ll}E_K = P_K. \tag{5.46}$$

Therefore, it increases at Kármán's force (5.7), regardless of the eccentricity of force e, Fig. 5.4. We note here a significant difference compared to the elastic
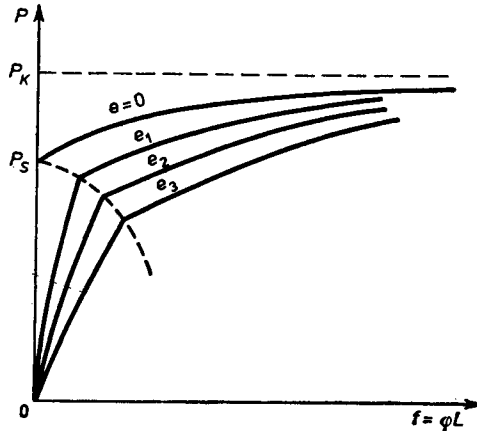
Fig. 5.4. Deflection of Shanley's model under eccentric compression

range: in the elastic range, the very same critical force P_E corresponds to the bifurcation of equilibrium of an axially compressed bar and is an asymptotic value for eccentric compression (according to second-order theory), whereas in the elastic-plastic range with linear strain hardening, bifurcation takes place under Shanley's force P_S, with Kármán's force P_K being an asymptotic value.

In the case of axial compression, $e = 0$, we should substitute $\tilde{\varphi} = 0$, $\tilde{N}_1 = \tilde{N}_2 = P_S/2$ so that Eq. (5.45) simplifies to the form

$$\varphi = \frac{(P-P_S)P_K}{(P_K-P)P_S}\left(\frac{1}{E_t} - \frac{1}{E}\right)\frac{E_t a}{4L}. \tag{5.47}$$

After differentiating, substituting (5.41), (5.46) and $f = \varphi L$ and making simple rearrangements,

$$\left.\frac{dP}{df}\right|_{f=0} = \frac{2E_t Aa}{Ll}. \tag{5.48}$$

Hence, bifurcation of equilibrium of a straight bar is, in fact, connected with a load increment.

It should, however, be made clear that we assume in the above considerations an infinite, plastically passive process in bar "2" as it is being unloaded. For real materials, the process changes to active on the tensile side; this causes a decrease in the force P, and the value P_K is no longer an asymptotic value.

5.4. Perfectly Elastic-Plastic Bars under Eccentric Compression

Strain hardening of real materials is described as a rule by the tangent modulus E_t decreasing as strain increases. In this case, a distinct maximum occurs in the $P = P(f)$ diagram; we call the respective force the *maximal load-carrying capacity* (or *elastic-plastic load capacity*) of a bar. Sometimes, it is also called the *critical force of the second kind*, since it separates the regions of stable and unstable equilibrium of a deformed bar (Leytes, 1954; Pikovskii, 1961).

A certain approximate method of calculating maximal load capacity of eccentrically compressed bars for an arbitrary diagram $\sigma = f(\varepsilon)$ was given by Kármán (1909), and Chwalla (1934). Duberg (see Flügge, 1962) used the collocation method for weakly curved bars under the Ramberg–Osgood plastic strain hardening law. The influence of higher harmonics on load capacity was studied by Malvick and Lee (1965). Much attention has been devoted to eccentrically compressed reinforced concrete columns; we cite here only the study of Gdański (1971), in which he considers the random nature of the process.

The analytical approach is possible first and foremost in the case of a perfectly elastic-plastic material. A detailed analysis of deflections and maximal load-carrying capacity of perfectly elastic-plastic eccentrically compressed bars was presented by Ježek (1937), using the theory of second order (the

linearized equation for curvature). He considered six ranges of bar behaviour: (1) elastic, (2) one-sided plastification on a part of the bar length, (3) partially two-sided and partially one-sided plastification, the remaining part being elastic, (4) one-sided plastification over the entire length, (5) two-sided plastification on one part and one-sided on the remaining part, (6) two-sided plastification over the entire bar length. He introduced a separate relation $f(\sigma_{cr}, \lambda, e) = 0$ for each range, σ_{cr} being mean stress P_{cr}/A, corresponding to maximal load-carrying capacity. In conclusion, Ježek proposed a relatively simple approximate equation covering all ranges. Made explicit with respect to λ, it has the form

$$\lambda^2 = \frac{\pi^2 E}{\sigma_{cr}} \left(1 - \mu_1 \frac{m\sigma_{cr}}{\sigma_0 - \sigma_{cr}}\right)\left(1 - \mu_2 \frac{m\sigma_{cr}}{\sigma_0 - \sigma_{cr}}\right),$$

(5.49)

where the coefficients μ_i depend on the shape of the cross-section (for rectangular cross-section $\mu_1 = \mu_2 = 0.5$), $m = Ae/W$, W denotes the elastic section modulus in bending, and σ_0 is the yield point stress of material. Ježek's theory was further developed by Leytes (1954). In Leytes (1966) he applied third-order theory to the problem of eccentric compression of perfectly elastic-plastic bars integrating numerically the appropriate equation. This theory leads to somewhat higher values for maximal load-carrying capacity, but the differences compared to the use of second-order theory are not so important here as they are in the elastic range.

5.5. Buckling Calculation after Polish Standard

The Polish Standard PN-80/B-03200 (1980) like the corresponding standards in other countries, reduces buckling calculation to compression calculation with a suitable coefficient, called *buckling factor* m_w. This factor, $m_w \geqslant 1$, reduces appropriately the admissible (working) stress R so that the corresponding safety condition takes the form

$$\frac{P}{A} \leqslant \frac{R}{m_w}.$$

(5.50)

On the other hand, force P is to be equal to critical force P_{cr} divided by the degree of safety for buckling j; hence, taking the equality sign in (5.50), we obtain

$$\frac{\sigma_{cr}}{j} = \frac{R}{m_w}.$$

(5.51)

Since critical stress σ_{cr} depends on slenderness ratio λ, tables $m_w = m_w(\lambda)$ for individual materials can be compiled. Following the proposal of Mu-

rzewski (1972), a relative slenderness ratio which makes the value m_w practically independent of material, was introduced into the Standard.

In the elastic range, Euler's equation (2.12) holds; hence, after substituting into (5.51), we obtain

$$\frac{\pi^2 E}{\lambda^2 j} = \frac{R}{m_w}. \tag{5.52}$$

For m_w to be made independent of material, the slenderness ratio λ has been referred to a certain comparative value λ_p, covering the material constants. The comparative slenderness ratio, λ_p, has been defined as a slenderness ratio for which the factor m_w equals 2. For most materials, the buckling of bars with such a slenderness ratio is elastic; hence (5.52) holds here and the following relation as well:

$$\lambda_p = \pi \sqrt{\frac{2E}{Rj}} = \pi \sqrt{\frac{4E}{3R}}, \tag{5.53}$$

with $j = 1.5$, as provided by the Standard (1980), having been substituted in the second form of this equation. In that case, the factor m_w in the elastic range is given by the simple equation

$$m_w = 2 \left(\frac{\lambda}{\lambda_p} \right)^2, \tag{5.54}$$

whereas for $\lambda < \lambda_p$ we deal with elastic-plastic buckling and we use empirically determined factors m_w, staying in the $1 \leqslant m_w \leqslant 2$ range, and being higher than those given by Eq. (5.54). By this approach, a single table $m_w(\lambda/\lambda_p)$ enables sufficiently accurate calculations for a wide class of materials (although, strictly speaking, by this approach the factor m_w in the elastic-plastic range should also depend to a certain degree on the material).

For eccentric compression, Eq. (5.50) takes the form

$$\frac{P m_w}{A} + \frac{M}{W} \leqslant 1.05R, \tag{5.55}$$

where the bending moment M is calculated on the principle of rigidification (on first-order theory).

The calculation technique recommended by the Standard can also be adapted to design work, i.e., to direct selection of the necessary cross-sectional area of an axially compressed bar (Domke, 1938; Życzkowski, 1960₄). Using a transformation similar to (5.19), we can derive the relationship

$$\zeta \stackrel{\text{def}}{=} \frac{Rl_r}{\pi} \sqrt{\frac{\xi j}{2EP}} = \frac{\lambda}{\lambda_p} \sqrt{m_w \left(\frac{\lambda}{\lambda_p} \right)}. \tag{5.56}$$

In this way, the dimensionless coefficient ζ, similar to Ylinen's number, is given by known quantities in the design process, on the one hand; whereas knowing the table of function $m_w = m_w(\lambda/\lambda_p)$ it depends only on λ/λ_p, on the other. Inverting numerically the latter relation we can construct the table of function $m_w = m_w(\zeta)$, and the necessary cross-sectional area is then given by the equation $A = Pm_w/R$. Tables of this type with regard to PN-56/B-03200 are given by Życzkowski (1960[4]); since the Standard does not introduce the relative slenderness ratio, the tables are different for particular materials. However, there is no difficulty in compiling a similar table that would allow for the relative slenderness ratio, and consequently, would be valid for any material.

6. Creep Buckling

6.1. Buckling of Bars with Initial Imperfections Subject to Linear Creep

An evaluation of the stability of a structure of materials subject to creep brings significant differences as compared to elastic or elastic-plastic structures. Creeping is a certain type of motion for a structure, and the stability problems involved here are therefore no longer related to the stability of equilibrium but to that of motion. Assuming small accelerations, a quasistatic analysis of this motion is made as a rule, the force of inertia being neglected. However, such an approach does leads to contradictions when instantaneous deflections (at the instant of load application) are considered, since this amounts to considering infinitely great accelerations. In many cases, the investigated motion is not stable in Lyapunov's sense, but it is admisslble with additional constraints imposed on displacements by determining a certain limited lifetime of the structure t^* for a given load parameter Λ, or else by determining parameter Λ for an assumed time t^*. Conditions of this type can be treated as specific constraints imposed on stiffness rather than on stability. It is also possible to restrict the motion by strength conditions, e.g. conditions preventing brittle creep rupture (Życzkowski and Zaborski, 1974; Boström, 1975). If the motion of a structure under creep conditions is stable in Lapunov's sense for a certain load parameter Λ, then no additional constraints need to be formulated. Nonetheless, even in this case, deflections may grow excessively; therefore, from practical point of view, additional stiffness constraints may prove necessary.

Early studies on creep of compressed bars, examined as a function of time the growth of deflections of bars with initial imperfections under creep described by linear physical laws (Freudenthal, 1946; Ross, 1946; Rzhanitsyn 1946—all dating to 1946). A phenomenon like that should rather be called "creep buckling" which is understood in engineering sense, since, for example, the motion of a bar according to a steady creep law of Maxwell's type is not stable at any value of the compressive force. Rzhanitsyn (1946) also

considered the possibility of change in the creep moduli with time (ageing of material), and also change in the force with time.

Assume that creep of a material in uniaxial stress state can be described by the general linear physical law

$$B_1(t)\,\dot{\varepsilon}+B_2(t)\,\varepsilon = B_3(t)\,\dot{\sigma}+B_4(t)\,\sigma, \tag{6.1}$$

where only three of the $B_i(t)$ functions are independent because the fourth can be eliminated by division. For $B_i(t) = \text{const}$, Eq. (6.1) describes a standard model (the Prager–Hohenemser model) covering Maxwell's and Voigt–Kelvin laws as particular cases. Determining the strain distribution by Bernoulli's hypothesis for slightly curved bars,

$$\varepsilon = \varepsilon_0 + (\varkappa - \varkappa_-)z, \tag{6.2}$$

where $\varkappa_- = \varkappa_-(x)$ denotes the initial curvature, and after substituting into (6.1), multiplying by z and integrating over the cross-sectional area of the bar, we obtain the basic equation of bending and buckling in the following form:

$$B_1(t)J\dot{\varkappa}+B_2(t)J(\varkappa-\varkappa_-) = B_3(t)\dot{M}+B_4(t)M. \tag{6.3}$$

Confining ourselves to small deflections (second-order theory) and to such cases of support of bar ends, in which the bending moment x can be represented by the equation $M = Pw$, where in the general case $P = P(t)$, we obtain

$$B_1(t)J\dot{w}''+B_2(t)J(w''-w_-'')+B_3(t)(P\dot{w}+\dot{P}w)+B_4(t)Pw = 0. \tag{6.4}$$

For axially loaded bars clamped at one end, we can use a Fourier series of the type (4.10); we denote by a_j the amplitudes before applying the load, by A_j the amplitudes after loading (together with instantaneous deflections) and lastly, by $f_j = f_j(t)$ the amplitudes of sinusoids during creep. Substituting the series into (6.4), we arrive at an uncoupled set od linear equations of the type

$$\dot{f}_j+\alpha_j(t)f_j = \beta_j(t), \tag{6.5}$$

where

$$\alpha_j(t) = \frac{B_2(t)-\dfrac{4l^2}{(2j-1)^2\pi^2J}\,[PB_4(t)+\dot{P}B_3(t)]}{B_1(t)-\dfrac{4Pl^2}{(2j-1)^2\pi^2J}\,B_3(t)}, \tag{6.6}$$

$$\beta_j(t) = \frac{B_2(t)a_j}{B_1(t)-\dfrac{4Pl^2}{(2j-1)^2\pi^2J}\,B_3(t)},$$

with the initial condition covering instantaneous elastic strains, $f_j(0) = A_j$. Amplitudes A_j are given by an equation of (4.11) type, namely

$$A_j = \frac{a_j}{1 - \dfrac{4Pl^2}{(2j-1)^2\pi^2 J}\dfrac{B_3(0)}{B_1(0)}} \tag{6.7}$$

since the instantaneous modulus of elasticity equals B_1/B_3.

The integral of Eq. (6.5), taking into account the initial condition (6.7), can be written in the form

$$f_j(t) = \exp[-\gamma_j(t)]\left\{A_j + \int_0^t \beta_j(\tau)\exp[\gamma_j(\tau)]d\tau\right\}, \tag{6.8}$$

where

$$\gamma_j(t) = \int_0^t \alpha_j(\tau)d\tau. \tag{6.9}$$

If force P tends to the limit P_∞ and creep functions (moduli) $B_2(t)$ tend to $B_{2\infty}$ and $B_4(t)$ to $B_{4\infty}$, then

$$\lim_{t\to\infty} f_j(t) = \lim_{t\to\infty} \frac{\beta_j(t)}{\alpha_j(t)} = \frac{a_j}{1 - \dfrac{4P_\infty l^2}{(2j-1)^2\pi^2 J}\dfrac{B_{4\infty}}{B_{2\infty}}}, \tag{6.10}$$

based on the assumption that the denominator is positive for $j = 1$; otherwise, with $a_1 \neq 0$, the deflections of the bar tend to infinity. Therefore, in terms of Lyapunov's criterion, the motion is stable if the denominator in Eq. (6.10) is positive, and also if for every t the denominators in Eqs. (6.6) are positive, since the creep velocity would otherwise increase infinitely. Rzhanitsyn (1965, 1968) considered in detail the case of periodically variable force $P = P(t)$, and also the displacement-controlled process.

For Maxwell's creep law, $B_2 \equiv 0$; hence, the limit (6.10) does not exist and the motion is not stable at any value of force P. In this case as well, $\beta_j(t) \equiv 0$. With $P(t) = $ const, and more exactly $P(t) = PH(t)$, where H stands for Heaviside's function, the motion of the bar is given by the equation

$$f_j(t) = A_j\exp\left[\frac{m}{(2j-1)^2 - m}\frac{E}{\eta}t\right], \tag{6.11}$$

with denotations (4.11). The coefficient in brackets can be called here the *logarithmic velocity of creep buckling*, since

$$\frac{d}{dt} \ln f_j(t) = \frac{m}{(2j-1)^2 - m} \frac{E}{\eta} = \text{const};$$ (6.12)

this quantity affects essentially the course of the phenomenon.

Linear creep buckling under distributed axial loadings was analysed by Życzkowski in a number of papers; in Życzkowski (1960₃) the small parameter method was used to determine the corrected logarithmic velocity of the first harmonic of deflection line, and in Życzkowski (1967) a general solution was obtained, expressed in the form of a Fourier series. Continuous longitudinal non-homegeneity of material was considered in Życzkowski (1958) and discontinuous transverse non-homogeneity (bars composed of various materials), in Życzkowski (1961).

Kowal (1964) studied elastic buckling of a bar in rheological medium (Voigt–Kelvin medium). Buckling of linearly viscoplastic bars was analysed by Madejski (1956). Constitutive linear equations containing time derivatives of higher order were used for creep buckling analysis by Kempner (1952), Lin (1953) (Laplace's transform) and Bunyatyan (1953).

Finite deflections under creep buckling (third-order theory) have been investigated by Życzkowski (1960₂). Transverse displacements (deflections) were found to be limited in size, whereas longitudinal displacements (in the direction of the force) were also large. Although the motion of a bar according to this theory is stable in Lyapunov's sense, on account of the considerable displacements which are inadmissible as a rule in applications, additional stiffness constraints are indispensable.

6.2. Buckling of Bars with Initial Imperfections Subject to Non-Linear Creep

Most structural materials, exhibiting creep, obey non-linear physical laws, differing essentially from (6.1). Non-linear steady creep in a uniaxial state can be described by the general law

$$\dot{\varepsilon} = \varphi(\sigma).$$ (6.13)

Moreover, with change in stress σ, the total strain velocity is the sum of (6.13) and elastic strain velocity $\dot{\sigma}/E$. The simplest function $\varphi(\sigma)$ is the Norton–Bailey power function

$$\dot{\varepsilon} = k\sigma^n = k|\sigma|^n \text{sign } \sigma,$$ (6.14)

where the first, simpler form can be used only for positive σ or for odd integers n, whereas in the general case, the second form of the equation should be used.

Non-linear laws of (6.13) type do not allow the general equation of bend-ing—analogous to (6.3)—to be derived by way of integration over the cross-section. In order to express the longitudinal force and the bending moment by strain, it would be necessary first to invert (6.13), expressing stress by strain, before performing the integration. Such a procedure is very trouble-some with elastic strain allowed for; practically, it can be effected only numerically. On the other hand, an analytical solution is obtainable for a two-point cross-section (theoretical I-section, Fig. 6.1) which guarantees
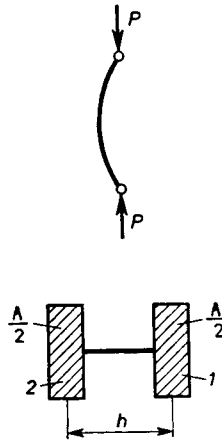
Fig. 6.1. Theoretical I-section

internal static determinacy and replaces stress integration by simple summa-tion.

Assume that force P is applied at instant $t = 0$, $P(t) = PH(t)$. The stresses in flanges 1 and 2 are

$$\sigma_{x1} = \frac{P}{A} + \frac{2M}{Ah}, \quad \sigma_{x2} = \frac{P}{A} - \frac{2M}{Ah}. \tag{6.15}$$

Hence, using the general law (6.13) with elastic strains considered, we determine the strain velocity using the equations

$$\dot{\varepsilon}_{x1} = \varphi \left(\frac{P}{A} + \frac{2M}{Ah} \right) + \frac{2\dot{M}}{EAh},$$

$$\dot{\varepsilon}_{x2} = \varphi \left(\frac{P}{A} - \frac{2M}{Ah} \right) - \frac{2\dot{M}}{EAh}, \tag{6.16}$$

where the expressions in parantheses denote the arguments of the function φ. Bernoulli's hypothesis leads to the relationship $\dot{\varepsilon}_{x1} - \dot{\varepsilon}_{x2} = \dot{\varkappa}h$ (the initial

curvature disappears on differentiating); hence, the basic equation of small deflections (second-order theory) takes the form

$$-\dot{w}''h = \varphi\left(\frac{P}{A} + \frac{2M}{Ah}\right) - \varphi\left(\frac{P}{A} - \frac{2M}{Ah}\right) + \frac{4\dot{M}}{EAh}. \tag{6.17}$$

For a bar simply supported or clamped at one end, we can express the bending moment by the equation $M = Pw$. We then obtain a non-linear third-order partial differential equation (in the case of transverse loadings alone, Eq. (6.17) is a linear equation). To obtain a simple analytical solution in the case of the power function φ, (6.14), Kempner (1952) used a single parameter collocation, and Hoff (1954) used expansion into a Fourier series with only the first term of the series being retained. The simpler approach followed by Kempner is applicable also to an arbitrary function $\varphi(\sigma)$. Taking, for example, a simply supported bar, for which $w(x, t) = f(t) \sin(\pi x/l)$ and demanding that the equation be satisfied at point $x = l/2$, we obtain a non-linear ordinary differential equation

$$\left(\frac{\pi^2 h}{l^2} - \frac{4P}{EAh}\right)\dot{f} = \varphi\left(\frac{P}{A} + \frac{2Pf}{Ah}\right) - \varphi\left(\frac{P}{A} - \frac{2Pf}{Ah}\right). \tag{6.18}$$

By separation of the variables and by formal integration, we get the function inverse with respect to $f = f(t)$

$$t = \frac{\pi^2 h}{l^2}(1 - m)\int_{f_0}^{f}\frac{\mathrm{d}f}{\varphi_1 - \varphi_2}, \tag{6.19}$$

where $m = P/P_E$, $f_0 = a/(1 - m)$, a denotes the initial bending deflection, f_0 is the bending deflection after applying the load, and φ_1 and φ_2 represent the expressions on the right-hand side of Eq. (6.18).

In the case of linear function $\varphi(\sigma)$ (Maxwell's law), we obtain by integration of (5.19) a logarithmic function, i.e., after inverting with respect to f, an exponential function, in agreement with (6.11). The logarithmic function grows to infinity; hence, in a physically linear case, the function $f = f(t)$ is determined for any positive t.

In the case of physical non-linearity, specifically in the case $n > 1$ in the Norton–Bailey law (6.14), a significant qualitative difference should be noted, namely the time cannot increase indefinitely, since the integral (6.19) at $f \to \infty$ turns into a converging improper integral. The time in which bending deflection f tends to infinity has been called by Kempner and Hoff the *critical time*

$$t_{\mathrm{cr}} = \frac{\pi^2 h}{l^2}(1 - m)\int_{f_0}^{\infty}\frac{\mathrm{d}f}{\varphi_1 - \varphi_2}; \tag{6.20}$$

but it would be more justified to call it "life-time of bar". For example, for
the Norton–Bailey law (6.14) with $n = 3$

$$t_{cr} = \frac{\pi^2 h^2 A^3}{24kl^2 P^3} (1-m)\ln\left(1+\frac{3h^2}{4f_0^2}\right).$$
(6.21)

The effect of primary creep on the critical time has been investigated by
Libove (1952), Odqvist (1954) and Hult (1955).

There is an inherent contradiction in the Kempner–Hoff definition of
critical time (6.20); it is the time corresponding to infinitely great deflections
calculated by using the small deflections theory (second-order theory).
That contradiction can be eliminated using third-order theory. Życzkowski
(1960₂), using such a theory, demonstrated that from a theoretical point of
view the Kempner–Hoff definition is incorrect, but from a practical point
of view, the time t_{cr} defines the life-time of bar fairly well, since close to t_{cr}
a violent growth of deflections, strains and stresses takes place (Fig. 6.2).
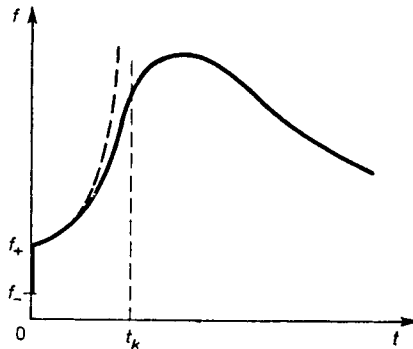
Fig. 6.2. Finite deflections of a bar during creep buckling

However, making a similar analysis for viscoplastic bars, Huang (1976) found
that the plastic effects make it possible to introduce the critical time also
on the basis of third-order theory (defined by the velocity of deflections
tending to infinity).

The critical-time concept can also be connected with other effects. Kopecki
and Zacharzewski (1972) referring to a general conception of Bychawski and
Olszak, took for the critical time criterion a certain value of energy dissipated
during the creep process in a bar.

6.3. Stability of Straight Bars Axially Compressed in Creep Conditions

The theories discussed above analysed only the motion of bars with initial imperfections in creep conditions, i.e., the course of creep buckling in the engineering sense. In the case of axially compressed straight bars, a stability analysis similar to the Eulerian analysis is also possible. But, this involves then not the stability of equilibrium but the stability of motion in axial direction due to compression in creep conditions, on which a small transverse disturbance is superimposed. As the result of "softening" of the material due to creep, the axial motion may cease to be stable. The corresponding time, after which transverse motion with an increasing amplitude is feasible, is also sometimes called the *critical time* t_{cr}, although this definition is completely different from the Kempner–Hoff definition for bars with initial curvature; the latter defines rather the life–time of bar.

The stability of a straight bar in physically linear case was described by Rzhanitsyn in his early paper (1946); the critical state is then defined by the modulus of permanent elasticity and the concept of critical time does not come into play here at all.

The first to analyse stability of a straight bar under non-linear unsteady creep was Shanley (1952) who replaced the modulus E in Euler's equation by the tangent modulus $d\sigma/d\varepsilon$ calculated for an isochronous curve $t = $ const. As an example, we consider the equation of the strain hardening theory

$$\dot{p}\overset{\alpha}{p} = k\sigma^n, \qquad p \overset{\text{def}}{=} \varepsilon - \frac{\sigma}{E}, \tag{6.22}$$

which was studied experimentally by Zhukov *et al.* (1953). This law generalizes the Norton–Bailey steady creep law (6.14), which is obtained when $\alpha = 0$. It describes adequately the behaviour of a large number of materials under stress of fixed sign. However, for reversed loadings it may lead to major errors, since the reduction of non-elastic strain p to zero would imply unlimited increase in creep velocity, which obviously has not been confirmed experimentally. Assuming a constant force $\sigma = $ const, we obtain after integrating and taking into account the initial condition $p(0) = 0$

$$\varepsilon = \frac{\sigma}{E} + [(\alpha+1)k\sigma^n t]^{1/(\alpha+1)}. \tag{6.23}$$

The tangent modulus for an isochronic curve can be determined as the reciprocal of derivative $d\varepsilon/d\sigma$ at $t = $ const. Substituting this modulus into Euler's formula and solving with respect to t, we get

$$t = t_S = \frac{(\alpha+1)^\alpha}{kn^{\alpha+1}\sigma^n}\left(\frac{\pi^2}{\lambda^2} - \frac{\sigma}{E}\right)^{\alpha+1}.$$ (6.24)

For the above critical time, the subscript S refers to the name Shanley.

Gerard (1956) proposed a hypothesis in which the critical state under creep is said to be *determined by the critical strain value*; this hypothesis carries over Broszko's proposal (5.22) to the case of creep buckling. From the comparison of critical (Eulerian) strain with strain due to creep (6.23)

$$\frac{\pi^2}{\lambda^2} = \frac{\sigma}{E} + [(\alpha+1)k\sigma^n t]^{1/(\alpha+1)}$$ (6.25)

we obtain

$$t = t_G = \frac{1}{(\alpha+1)k\sigma^n}\left(\frac{\pi^2}{\lambda^2} - \frac{\sigma}{E}\right)^{\alpha+1}.$$ (6.26)

The theoretical background for the above two hypotheses is unconvincing. A more consistent stability analysis of motion was performed by Rabotnov and Shesterikov (1957). Using the general creep law in the form $\Phi(\sigma, p, \dot{p}) = 0$ (equation of state), they assumed that small disturbances of axial motion are governed by the incremental law

$$\lambda^* \delta\sigma + \mu^* \delta p + \nu^* \delta\dot{p} = 0,$$ (6.27)

where $\lambda = \partial\Phi/\partial\sigma$, $\mu = \partial\Phi/\partial p$, $\nu = \partial\Phi/\partial\dot{p}$, and the asterisks denote the values of these derivatives at yet unknown instant $t = t_{cr}$. Following from Bernoulli's hypothesis is the relationship $\delta p = \delta\varepsilon - \delta\sigma/E = z\delta\varkappa - \delta\sigma/E$, and substituting into (6.27), multiplying by z and integrating over the cross-sectional area, we arrive at the basic equation of small bending superimposed on compression

$$(E\lambda^* - \mu^*)\,\delta M - \nu^*\,\delta\dot{M} + EJ(\mu^*\,\delta\varkappa + \nu^*\,\delta\dot{\varkappa}) = 0.$$ (6.28)

Since increments δM and $\delta\varkappa$ in the considered case of a straight bar are reckoned from the basic state $M = \varkappa = 0$, the symbols δ can be omitted henceforth. Rabotnov and Shesterikov considered on the basis of (6.28) flexural oscillating motion of a bar. However, in the case of Eulerian behaviour of loading constant in time, $P(t) = PH(t)$, the loss of stability is governed by the condition of instantaneous equilibrium in adjacent position, i.e., $\dot{M} = \dot{\varkappa} = 0$ in Eq. (6.28). The corresponding equation of critical state

$$(E\lambda^* - \mu^*)M + EI\mu^*\varkappa = 0$$ (6.29)

leads to the relationship

$$\left(1 - \frac{E\lambda^*}{\mu^*}\right)P - P_E = 0,$$ (6.30)

where P_E denotes Eulerian force.

Equation (6.30) defines the force-time relationship in critical state. In the case of the creep law (6.22), the derivatives λ and μ are

$$\lambda = \frac{\partial \Phi}{\partial \sigma} = -kn\sigma^{n-1}, \qquad \mu = \frac{\partial \Phi}{\partial p} = \alpha \dot{p} p^{\alpha-1}; \tag{6.31}$$

hence, the derivative λ is constant with time, $\lambda^* = \lambda$, but in calculating μ^* we should substitute the integral (6.23) into equation for μ, and in this integral, $t = t_{cr}$

$$\mu^* = \alpha k\sigma^n [(\alpha+1)k\sigma^n t_{cr}]^{-1/(\alpha+1)}. \tag{6.32}$$

Substituting these values into (6.30) and solving with respect to t_{cr}, we obtain

$$t_{cr} = t_{RS} = \frac{\alpha^{\alpha+1}}{(\alpha+1)kn^{\alpha+1}\sigma^n} \left(\frac{\pi^2}{\lambda^2} - \frac{\sigma}{E}\right)^{\alpha+1}, \tag{6.33}$$

where the critical time has been subscripted by RS for the names of Rabotnov and Shesterikov.

By combining Eqs. (6.24) and (6.26), we can determine the ratios of the corresponding times using the formulae

$$t_G : t_S : t_{RS} = 1 : \left(\frac{\alpha+1}{n}\right)^{\alpha+1} : \left(\frac{\alpha}{n}\right)^{\alpha+1}. \tag{6.34}$$

For example, for copper at 270°C, the creep constants are (Zhukov *et al.*, 1953) $\alpha = 7.18$, $n = 19.7$; hence,

$$t_G : t_S : t_{RS} = 1 : 0.0007544 : 0.0002596.$$

The above quantitative differences are considerable, but a significant qualitative difference occurs in the limit case $\alpha \to 0$, when the law (6.22) passes into the Norton–Bailey law describing steady creep. Then, at an arbitrary value of force P, $t_{RS} \to 0$, whereas in the subcritical force range, $t_G \neq 0$, $t_S \neq 0$. From a theoretical point of view, the conclusion $t_{cr} \to 0$ is well understandable, since with steady creep, every deflection of the bar from the straight position will be increasing, which is characteristic for instability of axial motion. However, the real life-time of the bar, especially in cases of small loadings, may be quite long. Therefore, a logically justifiable critical time t_{RS} is rather of theoretical importance, and the life-time of the bar should be determined on an analysis of deflections (Sections 6.1 and 6.2), possibly with additional stress or strain constraints.

A comparison of the Rabotnov–Shesterikov critical time with the Kempner–Hoff critical time (life-time) has been made by Jahsman (1972) (Ryder–Shanley model), Rysz and Życzkowski (1979) (*I*-section bar). The paper by Trojnacki and Życzkowski (1976) is devoted to the determination of t_{RS}

for various loading programs, including some with displacement control. A similarly defined critical time was determined by Zahorski (1965) for the general case of a three-dimensional state of stress; a stability theory for slender bars is obtainable then as a special case.

The Rabotnov–Shesterikov theory may be criticized, since an exact stability analysis of motion calls for examination of the entire range $0 < t < \infty$, whereas the values λ, μ and ν in Eq. (6.28) are taken to be independent of time but equal to the values λ^*, μ^*, ν^* calculated for $t = t_{cr}$. But, Shesterikov (1959) allowed variable values of λ, μ, ν in his analysis and found only minor differences.

A more comprehensive comparison of various creep buckling theories are given in reviews by Hoff (1958), Życzkowski (1960₁), Kempner (see Flügge, 1962), Rzhanitsyn (1965), and Kurshin (1978).

7. Stability and Optimal Design of Compressed Non-Prismatic Bars

7.1. Stability of Elastic Bars

In the case of a variable moment of inertia of cross-section, $J = J(x)$, the critical force is calculated usually by approximate methods (Chapter 3). In some particular cases, exact analytical solutions are also obtainable.

Of the various possibilities of change in dimensions and shape of the cross-section, we should single out, as most common, the proportional change in dimensions of the cross-section in both principal directions (change in dimensions without change in shape, cross-sections geometrically similar to each other, spatial tapering) or change only in one principal direction (affinity of cross-sections to each other, plane tapering). In such cases, if change in a characteristic dimension of the cross-sections is described by the function $a = a_0 f(x)$, then

$$J = [f(x)]^n J_0, \tag{7.1}$$

where $n = 4$ in the case of spatial tapering, $n = 3$ in the case of plane tapering with buckling in the plane of taper, and $n = 1$ in the case of plane tapering with buckling off the plane of tapering. Furthermore, $n = 3$ describes a different, though common case of a thin-walled bar with geometrically similar central lines of the profile and of constant wall thickness (hence, geometrical similarity of cross-sections as a whole does not occur), and $n = 2$ corresponds to spatial tapering of latticed bars of constant cross-sectional area (e.g. four prismatic bars mounted taperwise and joined by batten plates).

For a linear function $a(x)$

$$a = a_0 \left[1 - (1-k)\frac{x}{l} \right], \tag{7.2}$$

where the dimensionless coefficient $k = a_1/a_0$ can be called the *coefficient of tapering* or shortly *tapering of the bar* ($k = 1$ for prismatic bar); the linearized equation of buckling takes the form

$$EJ_0 \left[1 - (1-k)\frac{x}{l} \right]^n w'' + Pw = 0. \tag{7.3}$$

By introducing a dimensionless parameter of critical force ξ and a dimensionless independent variable u

$$\xi = \frac{2l}{(1-k)|n-2|} \sqrt{\frac{P}{EJ_0}}, \quad n \neq 2, \tag{7.4}$$

$$u = 1 - (1-k)\frac{x}{l}, \quad k \leqslant u \leqslant 1, \tag{7.5}$$

we obtain Bessel's equation

$$w'' + \frac{(n-2)^2}{4} \xi^2 u^{-n} w = 0 \tag{7.6}$$

with the general integral (at $n \neq 2$)

$$w = \sqrt{u} \left[C_1 J_{\frac{1}{n-2}} \left(\xi u^{\frac{2-n}{2}} \right) + C_2 Y_{\frac{1}{n-2}} \left(\xi u^{\frac{2-n}{2}} \right) \right], \tag{7.7}$$

where J_n and Y_n denote Bessel functions of the first and second kind, respectively.

In the case of a simply supported bar, $w(k) = w(1) = 0$, we obtain the loss-of-stability condition

$$J_{\frac{1}{n-2}} \left(k^{\frac{2-n}{2}} \xi \right) Y_{\frac{1}{n-2}}(\xi) - J_{\frac{1}{n-2}}(\xi) Y_{\frac{1}{n-2}} \left(k^{\frac{2-n}{2}} \xi \right) = 0, \tag{7.8}$$

whereas in the case of one end clamped $x = 0$, i.e., $u = 1$, and the other end left free, the conditions $w(k) = w'(1) = 0$ with the use of formulae for derivatives of Bessel functions lead to the equation

$$J_{\frac{1}{n-2}} \left(k^{\frac{2-n}{2}} \xi \right) Y_{n-1}(\xi) - J_{n-1}(\xi) Y_{\frac{1}{n-2}} \left(k^{\frac{2-n}{2}} \xi \right) = 0. \tag{7.9}$$

Tables of functions $\xi = \xi(k)$ specifying effectively the critical forces, are given in a paper by Życzkowski (1956₁). Dinnik (1932, 1939) considered bars consisting of a prismatic part and a linearly tapering part (7.2).

In the case $n = 4$ (spatially tapered bars), Bessel functions are functions of 1/2 and 3/2 orders and can be expressed by elementary functions. Equation (7.8) then takes the form

$$\tan \frac{\xi}{k} = \tan \xi, \tag{7.10}$$

and from (7.9) we obtain

$$\xi = -\tan \left(\frac{1-k}{k} \xi \right). \tag{7.11}$$

Equation (7.10) leads to the conclusion

$$\frac{\xi}{k} = \xi + m\pi, \quad m = 1, 2, \ldots \tag{7.12}$$

Hence, the first, least critical force for a simply supported bar is

$$P_{cr} = k^2 \frac{\pi^2 E J_0}{l^2} = \frac{\pi^2 E \sqrt{J_0 J_1}}{l^2}, \tag{7.13}$$

where $J_1 = J(x = 1)$. Equation (7.11) is a transcendental equation; a table of roots of this equation is also given in Życzkowski (1956$_1$). Likewise, in the case $n = 2$, the integral of Eq. (7.3) is expressed by elementary functions (Szelągowski, 1927).

The stability of non-prismatic bars under distributed loadings was considered by Dinnik (1913, 1939), and stability in a fluid flow, by Gajewski (1969).

In the case of non-conservative loadings, especially in the range of the kinetic criterion of stability, considerations must be based on a fourth-order equation of vibrations, which results in essential complications. The small parameter method was used in this case by Gajewski (1966).

If the moment of inertia of cross-sections is variable only step-wise, the deflection line in individual intervals can be described by the general integral (2.7). Difficulty with calculating the critical force is due to the considerable number of boundary conditions that must be satisfied. Tables of the coefficients of critical forces for this case are given by Dinnik (1939). General transcendental equations were derived by Huber (1930) and Falk (1956). Loading with a follower force was considered by Kowalski (1967).

A certain general method for calculating critical forces for non-prismatic bars under loads of fixed direction, with the use of Fourier series, was proposed by Naleszkiewicz (1953). The method was developed by Kacner (1961) and Mazurkiewicz (1965). Ostachowicz (1975) adapted the rigid finite element method to the calculation of critical forces for elastic non-prismatic bars.

7.2. Stability of Bars in Elastic-Plastic Range

With reference to the elastic-plastic buckling theory, proposed by Shanley, the equation for buckling for a non-prismatic bar takes the form (3.10) where this time not only moment of inertia J but also tangent modulus E_t is a compound function of variable x, namely $E_t = E_t[A(x)]$. In typical cases of variability of the bar cross-section

$$A = [f(x)]^m A_0, \tag{7.14}$$

where $m = 2$ for spatially tapered bars, $m = 1$ for plane-tapered bars and for thin-walled bars of constant wall thickness. The linearized equation (5.10) takes the form

$$E_t \{[f(x)]^m A_0\}[f(x)]^n J_0 w'' + Pw = 0, \tag{7.15}$$

where enclosed in braces we have the argument of the function E_t. For example, expressing E_t according to Ylinen's proposal (5.14), we obtain

$$EJ_0 \frac{A_0 \sigma_0 [f(x)]^m - P}{A_0 \sigma_0 [f(x)]^m - cP} [f(x)]^n w'' + Pw = 0. \tag{7.16}$$
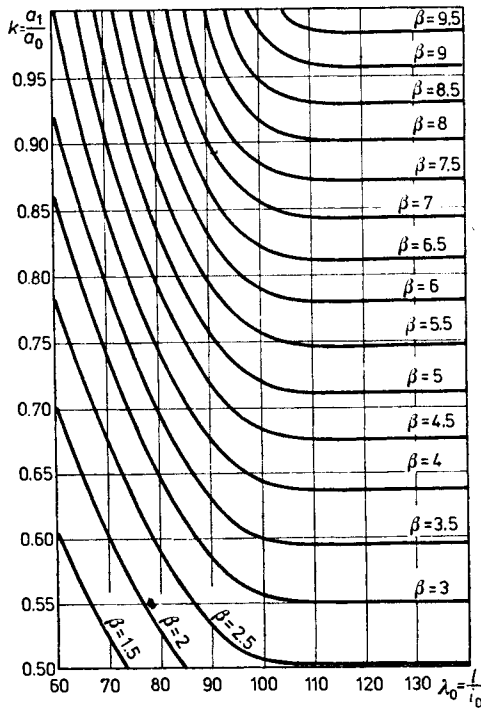
Fig. 7.1. Stability coefficients for non-prismatic bars in elastic-plastic range

Sala (1951) proposed to calculate the eigenvalues of Eq. (7.16) by Nyström's approximate method. Życzkowski (1954) referring to a related equation, in which a somewhat different function, proposed earlier by Ylinen, $E_t = E_t(\sigma)$ is used, applied the method of assumption of an exact solution; he assumed certain functions $w(x)$ and calculated from algebraic equations the corresponding functions $f(x)$ which by an appropriate selection of several parameters could be approximated to the prescribed (linear) functions. For example, if we determine the critical force for spatially linearly tapered simply supported bars (7.2), $m = 2$, $n = 4$, using the equation

$$P_{cr} = \beta \frac{EJ_0}{l^2}, \tag{7.17}$$

then the values of coefficients β, which in the elastic range depend only on $k = a_1/a_0$ and in the elastic-plastic range also on the basic slenderness ratio, $\lambda_0 = l/i_0$, can be read from Fig. 7.1 (for steel St 37).

Elastic-plastic stability of bars of step-wise variable cross-section has been investigated by Wnuk and Życzkowski (1959).

7.3. Optimal Design of Elastic Bars

The problem of optimal design of compressed bars subject to buckling, was formulated by Lagrange but the first effective solutions were given by Clausen (1951), Blasius (1914), Nikolai (1907) (with an additional stress constraint) and Chentsov (1936). They considered Eulerian behaviour of loading (direction fixed in space, point of application materially fixed), treating the dimensions of cross-section as decision variables. Following Gajewski and Życzkowski (1970), we shall cite here a more general solution, involving arbitrary conservative behaviour of loading at the free end of a bar with the other end clamped.

We make use of a fourth-order equation generalizing (2.4) to the case of non-prismatic bars

$$(EJw'')'' + Pw'' = 0, \tag{7.18}$$

or in dimensionless form

$$[g(x)y'']'' + \beta y'' = 0, \tag{7.19}$$

where $y = w/l$, the dimensionless variable x is also referred to the bar length, the coefficient of critical force β is defined by Eq. (7.17), and $J(x) = J_0 g(x)$.

For a four-parameter behaviour of the load acting at the free end of a bar elastically clamped at the other end, (2.20), (2.21), we write the boundary conditions in the form

$$y(0) = 0, \quad y'(0) = \frac{\zeta}{\beta}(gy'')_{x=0},$$

$$(gy'')_{x=1} = -\beta[\varrho y'(1) + \vartheta y(1)],$$ (7.20)

$$[(gy'')]'_{x=1} = -\beta[\mu y'(1) + \nu y(1)],$$

where $\zeta = \psi_1 \beta$ is the coefficient of elastic clamping, and moreover, the conservativeness condition (2.22) is satisfied.

Integrating (7.18) twice and denoting

$$v(x) = y(x) - \frac{B_1}{\beta} - \frac{B_2}{\beta} x,$$ (7.21)

where B_1 and B_2 are the integration constants, we obtain the equation

$$g(x)v'' + \beta v = 0,$$ (7.22)

with boundary conditions following from (7.20), substitution of (7.21) and elimination of B_1 and B_2

$$(1-\vartheta)v(1) - \varrho v'(1) + (\varrho + \vartheta)v'(0) + (\varrho\zeta + \vartheta\zeta + \vartheta)v(0) = 0,$$
$$\nu v(1) + (\mu - 1)v'(1) - (\mu + \nu)v'(0) - (\mu\zeta + \nu\zeta + \nu)v(0) = 0.$$ (7.23)

We now formulate the optimization problem as follows. We seek the minimum of the functional determining the bar volume

$$V = A_0 l \int_0^1 \varphi(x)\,dx,$$ (7.24)

where $\varphi(x) = A(x)/A_0$, with a fixed value of the critical force given by differential equation (7.22) and boundary conditions (7.23). This problem of the calculus of variations of the Lagrange type can be replaced by an ordinary problem of the calculus of variations by eliminating φ directly from Eq. (7.22). For typical variations of the transverse dimensions of the bar we can write

$$\varphi(x) = [g(x)]^\varkappa,$$ (7.25)

where, in view of (7.1) and (7.14), $\varkappa = m/n$ and the value of this coefficient is $1/2$ for spatially tapered bars, $1/3$ or 1 for plane tapered bars, depending on the direction of buckling, and $\varkappa = 1/3$ for thin-walled bars of constant wall thickness. The substitution of (7.25) and (7.22) into (7.24) leads to the problem of minimization of the functional

$$V = A_0 l \int_0^1 \left(-\frac{\beta v}{v''}\right)^\varkappa dx$$ (7.26)

without additional constraints. However, two boundary conditions (7.23) are insufficient to determine the four integration constants of the corresponding Euler–Lagrange equation; therefore, it is necessary for one of the constants to be determined from the transversality condition (the fourth constant remains arbitrary).

A convenient technique of integrating the Euler–Lagrange equation for functional (7.26) was given by Chentsov (1936). If we introduce auxiliary variable t by the equation

$$t = \frac{\partial \tilde{F}}{\partial v''} = A_0 l \varkappa \beta^\varkappa \frac{v^\varkappa}{(-v'')^{\varkappa+1}}, \tag{7.27}$$

where $\tilde{F}$ denotes the function in (7.26), we can write the equation of extremals in the form

$$vt'' - tv'' = 0, \tag{7.28}$$

and after integrating in the form

$$vt' - tv' = C. \tag{7.29}$$

The transversality condition proves that the constant C equals zero for conservative loadings (Gajewski and Życzkowski, 1970). In this case, (7.29) can easily be integrated once more

$$t = C_1 v, \tag{7.30}$$

i.e., after substituting (7.27)

$$v'' v^{\frac{1-\varkappa}{1+\varkappa}} = C_2. \tag{7.31}$$

The further course of integration depends on exponent $\varkappa$. The simplest solution is obtained for $\varkappa = 1$ (plane–tapered bar, buckling out-of-plane of tapering), namely

$$v = A_1 + A_2 x + A_3 x^2. \tag{7.32}$$

One of the constants in the integral (7.32) remains arbitrary, say, $A_1 = 1$ The boundary conditions (7.23) defined the remaining two constants in the general case of loading as follows:

$$A_2 = \frac{\zeta(2\varrho + 2\vartheta - \mu - \nu) - (2\mu + \nu - 2)}{2\mu + \nu - 2\varrho - \vartheta - 1},$$

$$A_3 = \frac{\zeta(\mu + \nu - \varrho - \vartheta) - 1}{2\mu + \nu - 2\varrho - \vartheta - 1}. \tag{7.33}$$

The substitution of (7.32) into (7.22) determines the optimal shape of the bar by the equation

$$g(x) = \frac{\beta}{2A_3}(1+A_2 x+A_3 x^2).$$ (7.34)

Lastly, selecting point $x = x_0$, at which the moment of inertia is J_0, i.e., $g(x_0) = 1$, we find parameter β and the critical force. For example, for a Eulerian behaviour of loading, $\mu = 1$, $\varrho = \vartheta = \nu = 0$, and assuming additionally rigid clamping $\zeta = 0$; then $A_2 = 0$, $A_3 = -1$, $g = \frac{1}{2}\beta(1-x^2)$, and taking $x_0 = 0$, we obtain $\beta = 2$, $P_{cr} = 2EJ_0/l^2$. The volume of the optimal bar is

$$V = A_0 l \int_0^1 g(x)\,\mathrm{d}x = \tfrac{2}{3}A_0 l = \frac{Pl^3}{3E}k,$$ (7.35)

where k is the coefficient of proportionality in the equation $A_0 = kJ_0$. For a prismatic bar,

$$V = Al = \frac{4Pl^3}{\pi^2 E}k;$$ (7.36)

hence, the gain in volume is $(1-\pi^2/12) \cdot 100\% = 17.7\%$.

For a plane-tapered bar with buckling in the plane of tapering where $\varkappa = 1/3$, the general integral of Eq. (7.31) can be written in parametric form

$$v = A_1 \sin^4 z, \quad x = A_2 \cos z(3-\cos^2 z)+A_3.$$ (7.37)

Similarly, for a spatially tapered bar where $\varkappa = 1/2$, we obtain

$$v = A_1 \sin^3 z, \quad x = A_2(z-\tfrac{1}{2}\sin 2z)+A_3.$$ (7.38)

If buckling is feasible in all directions, it is just the latter case that leads to an optimal solution with the two principal moments of inertia of the cross-section being equal. Keller (1960) found that from among all convex solid cross-sections, the optimal shape of the cross-section is an equilateral triangle, and Krzyś (1967) determined the optimal thin-walled cross-section—it is an annulus whose wall thickness is determined from the local stability condition.

Special cases of selection of constants in Eqs. (7.37) and (7.38) are given by Gajewski and Życzkowski (1970). The case of a pole-oriented force was examined in detail in Gajewski and Życzkowski (1969₁) and Gajewski and Palej (1974) optimized bars in tension for various behaviours of loading.

The optimization problem can also be formulated in a purely variational approach, minimizing the functional of total potential energy (3.10) with the isoperimetric condition of constant volume both with respect to $w = w(x)$ and $J = J(x)$. The corresponding functional has the form

$$G(w, J) = \int_0^l [EJw''^2 - Pw'^2 + \Lambda A(J)] \, dx;$$

(7.39)

the equation of extremals with respect to $w(x)$ leads to (3.11) and with respect to $J(x)$ it has the form

$$Ew''^2 + \Lambda \frac{dA}{dJ} = 0,$$

(7.40)

where Λ denotes constant Lagrangian multiplier. The set of equations (3.11) and (7.40) is equivalent to (7.31). This approach was proposed by Taylor (1967); a similar approach for thin-walled bars was employed by Życzkowski (1968). Using a dynamic programming method, Błachut (1977, 1978) optimized compressed bars with large deflections.

The procedure described may lead to false results if deflection lines with an inflection point are involved, e.g., in the case of statically indeterminate support of bar ends. A bar optimally designed for the first critical force, may be found to have a lower value of the second critical force; consequently, the latter is then the decisive one, and the result fails to satisfy the conditions of the problem. For example, a bar clamped at both ends, optimally designed for the symmetric form of buckling, shows a lower value of the critical force for the antisymmetric form. In that case, the bar should be designed simultaneously for both forms of buckling (bimodal optimization, Olhoff and Rasmussen, 1977).

In the case of non-conservative loadings, the critical force may be determined either by the static or kinetic criterion, and the application range of these criteria is not known in advance. Życzkowski and Gajewski (1969) found that the static criterion holds for antitangential forces where $\eta \leqslant 0$. The functional has then also the form (7.26), but constant C in the integral (7.29) is different from zero and is subject to optimization. The range of the kinetic criterion has been investigated by Plaut (1973), Claudon (1975) and Błachut and Gajewski (1980), who all used variational optimization, whereas Kowalski (1967), Bogacz et al. (1980), Bogacz and Mahrenholtz (1980), Mahrenholtz and Bogacz (1981) used parametric optimization and confined themselves to step-wise variable cross-sections.

7.4. Optimal Design in Elastic-Plastic Range

In most cases, optimally designed elastic bars under compression show zero cross-sections; hence, the critical stresses in these cross-sections tend to infinity. With respect to real materials, this involves either the need for an additional stress constraint (Nikolai, 1907), or the need for the elastic-plastic character of buckling to be considered.

Laasonen (1948) was first to formulate the problem of an optimal elastic-plastic column, and he provided a certain approximate solution. Parametric optimization of linearly tapered bars was carried out by Życzkowski (1956₂).

A convenient inverse approach to the problem of optimization of elastic-plastic columns was proposed by Krzyś (1967, 1968), namely by expressing the equation of elastic-plastic buckling (7.15) (for simply supported bars or clamped at one end) in the form

$$E_t(\varphi)J_0\varphi^{1/\varkappa}w'' + Pw = 0,\tag{7.41}$$

where $\varphi(x) = A(x)/A_0$ and E_t depends on φ via the critical stress σ. In a general case, that of an arbitrary material function $E_t(\sigma)$, φ cannot be readily calculated from Eq. (7.41) to be substituted into functional (7.24) in order to obtain the problem of calculus of variations without a subsidiary condition. Krzyś found, however, that by postulating that the function $E_t(\varphi)\varphi^{1/\varkappa}$ is a linear function of variable φ, namely

$$E_t(\varphi)\varphi^{1/\varkappa} = K_1 + K_2\varphi,\tag{7.42}$$
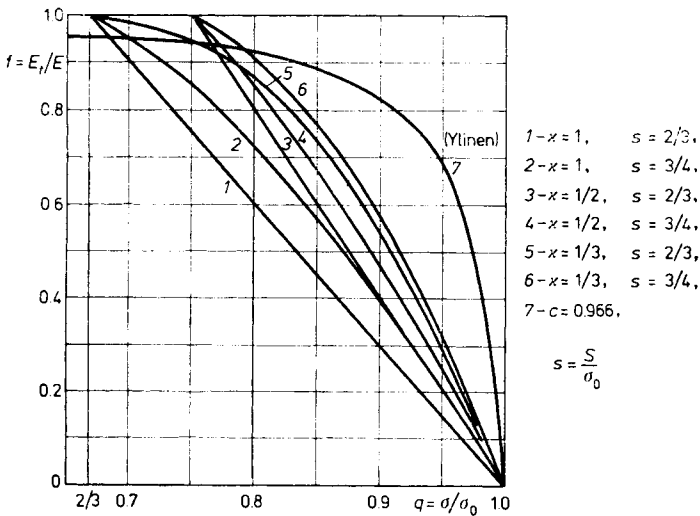
Fig. 7.2. Comparison od Krzyś's law with Ylinen's law

the material can be described equally well as by Ylinen's law (5.14); on the one hand, and, on the other hand, Eq. (7.14) can be made explicit with respect to φ and a simple and effective optimization can be carried out. The physical law corresponding to (7.42) has the form (after satisfying the conditions $E_t(S) = E$ and $E_t(\sigma_0) = 0$)

$$E_t = E \frac{\sigma_0 - \sigma}{\sigma_0 - S} \left(\frac{\sigma}{S} \right)^{\frac{1-\varkappa}{\varkappa}}, \qquad S \leqslant \sigma \leqslant \sigma_0, \tag{7.43}$$

where S denotes the elastic limit of the material. A comparison of (7.43) for various values of S/σ_0 and $\varkappa$ with Ylinen's law (5.14) is given in Fig. 7.2. This law depends on $\varkappa$ (which actually should not be the case), but this relation is not very important. In the case $\varkappa = 1/2$, it coincides with the Johnson–Ostenfeld law (5.27), (5.28).

Expressing $\varphi(x)$ from Eq. (7.41) and substituting (7.42), we obtain

$$\varphi(x) = \frac{\beta}{K_2} \left(-\frac{w}{w''} \right) - \frac{K_1}{K_2}. \tag{7.44}$$

The functional V takes the form

$$V = -\frac{K_1}{K_2} A_0 l + \frac{\beta A_0}{K_2} \int_0^l \left(-\frac{w}{w''} \right) dx. \tag{7.45}$$

Hence, its extremal conforms to the extremal for (7.26) with $\varkappa \doteq 1$; the conformity occurs only for deflections, but the optimal shape following from (7.44) is different from that in the elastic range.
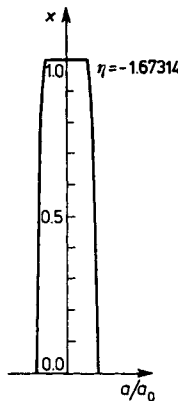
Fig. 7.3. Optimal elastic-plastic bar under an antitangential force

Krzyś determined the optimal shape of thin-walled bars taking into account additionally the wall-stability condition. Gajewski (1971) considered design under general conservative behaviour of loading for solid bars, and Gajewski and Życzkowski (1971), non-conservative loadings in the range of the static criterion of stability. An exemplary optimal shape for antitangential loading with $\eta = -1.673$, $\varkappa = 1/2$, $S/\sigma_0 = 2/3$, is given in Fig. 7.3.

7.5. Optimal Design in Creep Conditions

In Chapter 6, we presented various creep buckling theories. Optimal design of columns in creep conditions depends, therefore, significantly on the theory of buckling actually used, the initial imperfections, the constitutive equations of creep, etc.

The design of columns with initial imperfections, obeying the linear creep law (6.1), is discussed in papers by Wojdanowska (1978) and Wojdanowska and Życzkowski (1980). They demonstrated that for certain particular initial deflection lines, corresponding to the solution of Eq. (7.31) and ensuring a proportional increase in deflections during creep buckling, the optimal shape, furnishing minimal logarithmic velocity of creep (6.12), is consistent with the optimal shape with respect to elastic buckling.

With reference to the Rabotnov–Shesterikov theory of creep buckling for straight bars, the problem of optimal design can be formulated in a different way (Życzkowski and Wojdanowska-Zając, 1970). Equation (6.29), with (6.31), (6.32), and $J = J(x)$, $\sigma = P/A(x)$ substituted into it, takes the form

$$w''(x) + \left\{ \frac{P}{EJ(x)} + \right.$$
$$\left. + \frac{n}{\alpha} [k(\alpha+1)t_{\mathrm{cr}}]^{\frac{1}{(\alpha+1)}} \frac{P^{n/(\alpha+1)}}{J(x)[A(x)]^{(n-\alpha-1)/(\alpha+1)}} \right\} w(x) = 0. \qquad (7.46)$$

We seek functions $w(x)$ and $\varphi(x)$ which realize the minimum of functional (7.24) for a prescribed force P and a prescribed critical time t_{cr}; hence, this is attained with Eq. (7.46) as a subsidiary condition. The two Euler–Lagrange equations have a rather complicated form here, but the Lagrangian multiplier $\lambda(x)$ can be eliminated from them and in combination with (7.46) they can be reduced to a single equation giving the optimal shape of bar. Formally, this equation can be integrated in closed form, but effective here is numerical integration. The optimal shapes for a bar clamped at one end are shown in Fig. 7.4 for $\varkappa = 1$ (plane-tapered bars) for various values of parameter T,
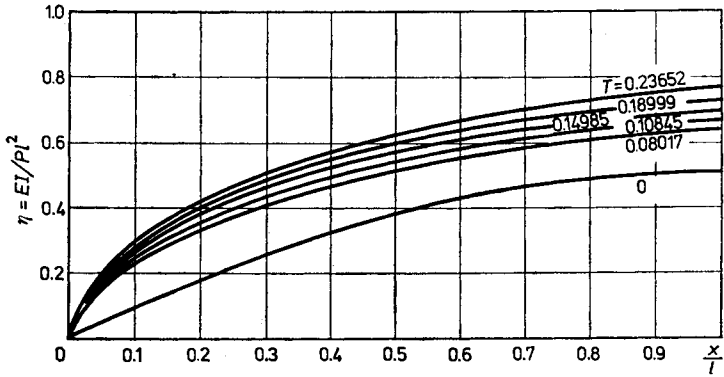
Fig. 7.4. Optimal shapes of bar with respect to creep buckling

proportional to $t_{cr}^{1/(\alpha+1)}$. These values correspond successively to the critical times, be it an hour, a day, a month, a year or ten years. With regard to an optimal elastic bar $(T = 0)$, a marked thickening occurs in the vicinity of the free end of the bar.

8. Spatial Problems of Loss of Stability of Bars

8.1. Fundamental Equations

Let us consider now such cases of stability of straight bars, for which the deflection line after the loss of stability is a spatial curve.

The equilibrium equations for a bar subject to spatial bending by moments M_{b1} and M_{b2} (denoted further as M_1 and M_2, with the subscript corresponding to the direction of the vector of moment) and torsion by moment M_t were derived by Kirchhoff (1859).

$$\frac{dT_1}{ds} + \varkappa_2 N - \vartheta T_2 + q_1 = 0,$$

$$\frac{dT_2}{ds} + \vartheta T_1 - \varkappa_1 N + q_2 = 0,$$

$$\frac{dN}{ds} + \varkappa_1 T_2 - \varkappa_2 T_1 + q_s = 0,$$

$$\frac{dM_1}{ds} + \varkappa_2 M_t - \vartheta M_2 - T_2 + m_1 = 0,$$ (8.1)

$$\frac{dM_2}{ds} + \vartheta M_1 - \varkappa_1 M_t + T_1 + m_2 = 0,$$

$$\frac{dM_t}{ds} + \varkappa_1 M_2 - \varkappa_2 M_1 + m_t = 0.$$

In these equations, T_1 and T_2 denote transverse forces, N is the longitudinal force, q_i are the components of distributed loadings, m_i are the components of continuously distributed moments, and s is the variable measured along the arc. The above equations hold for arbitrary directions 1 and 2, perpendicular to each other in the plane of cross-section; but considering the simplicity of the constitutive equations, we assume them to be the principal directions of cross-section, hence the denotations "1" and "2". Therefore, during the deformation process, "1" and "2" are generally mobile directions,

associated with matter. The principle of rigidification does not hold here; hence, for a bar initially straight, $\varkappa_1$ and $\varkappa_2$ denote the curvatures of the deflected axis and ϑ the unit angle of twist; for a bar initially curved and twisted (Ponomarev et al., 1959)

$$\varkappa_1 = \varkappa_{10} + \frac{d\alpha}{ds} + \varkappa_{20}\varphi - \vartheta_0\beta,$$

$$\varkappa_2 = \varkappa_{20} + \frac{d\beta}{ds} + \vartheta_0\alpha - \varkappa_{10}\varphi, \qquad (8.2)$$

$$\vartheta = \vartheta_0 + \frac{d\varphi}{ds} + \varkappa_{10}\beta - \varkappa_{20}\alpha,$$

where α, β and φ denote the rotation angles of cross-section about the axes "1" and "2" and the axis tangent to the bar axis respectively. $\varkappa_{10}$ and $\varkappa_{20}$ and ϑ_0 denote the initial curvatures and the unit initial angle of twist of the bar.

The moments are related to the geometrical quantities by the constitutive equations. In the linearly elastic range, for the principal directions, we can take (Clebsch, 1862)

$$M_1 = B_1(\varkappa_1 - \varkappa_{10}),$$

$$M_2 = B_2(\varkappa_2 - \varkappa_{20}), \qquad (8.3)$$

$$M_t = C(\vartheta - \vartheta_0),$$

where $B_1 = EJ_1$ and $B_2 = EJ_2$ denote bending rigidities (the latter equations hold only for a straight or slightly curved bar), and C is the rigidity of free torsion. With constrained torsion of a straight bar, the third of Eqs. (8.3) takes the form

$$M_t = C\vartheta - \frac{d}{ds}\left(C_\omega \frac{d\vartheta}{ds}\right), \qquad (8.4)$$

where $C_\omega = EJ_\omega$ denotes the warping rigidity of the cross-section and J_ω is the principal sectorial moment of inertia of the cross-section. Equation (8.4) was applied to the general theory of spatial bending by Vlasov (1940) and Dzhanelidze (1949).

Assuming the axis to be inextensible and rigid in shear, the internal forces T_1, T_2 and N are eliminated so that the set of equations (8.1), (8.2) and (8.3) can be reduced to three equations either with three unknown angles α, β and φ, or with three unknown moments, M_1, M_2 and N_t. These equations give both the fundamental state, before loss of stability, and the critical load as well as the buckling mode. With extensibility of the axis and shear strains

considered, the internal forces T_1, T_2 and N should be related to these strains by appropriate constitutive equations. Subsequently, we will confine ourselves almost exclusively to assuming inextensibility of the axis.

8.2. Stability of Straight Bars under Simultaneous Compression and Torsion

Consider a bar under a compressive force P and a couple M resulting in torsion. In the fundamental state, before loss of stability, only $M_t = M$, $N = -P$ and angle ϑ differ from zero, and all the other quantities in Eqs. (8.1) vanish and the equations are obviously satisfied.

Following the loss of stability, M_1, M_2, T_1, T_2, $\varkappa_1$ and $\varkappa_2$ will appear and we then consider the complete set of equations (8.1). We assume, however, that the above quantities are small, and products of two small quantities can safely be omitted. The distributed loadings equal zero. Using Eqs. (8.3) with $\varkappa_{10} = \varkappa_{20} = \vartheta_0 = 0$, we obtain

$$\frac{dT_1}{ds} - \frac{M_2}{B_2} P - \vartheta T_2 = 0,$$

$$\frac{dT_2}{ds} + \vartheta T_1 + \frac{M_1}{B_1} P = 0,$$

$$\frac{dM_1}{ds} + \left(\frac{C}{B_2} - 1\right)\vartheta M_2 - T_2 = 0,$$

$$\frac{dM_2}{ds} + \left(1 - \frac{C}{B_1}\right)\vartheta M_1 + T_1 = 0,$$

(8.5)

whereas the remaining two equations lead to the conclusion $M_t = \text{const}$, $N = \text{const}$.

After consecutive eliminations, the set of equations (8.5) can be reduced to a single equation with respect to M_1

$$\frac{d^4 M_1}{ds^4} + 2(a+b+c)\frac{d^2 M_1}{ds^2} + 4ab M_1 = 0,$$

(8.6)

where

$$a = \frac{P - (B_1 - C)\vartheta^2}{2B_2},$$

$$b = \frac{P - (B_2 - C)\vartheta^2}{2B_1},$$

(8.7)

$$c = \frac{(B_1 + B_2 - C)^2 \vartheta^2}{2B_1 B_2}.$$

The characteristic equation for (8.5) has four roots

$$t = \pm i \sqrt{(a+b+c) \pm \sqrt{(a+b+c)^2 - 4ab}} \ . \tag{8.8}$$

In the case of equal bending rigidities, $B_1 = B_2 = B$, from which it follows that $a = b$, all the roots (8.8) are imaginary and the solution of Eq. (8.6) is expressed by trigonometric functions. If the boundary conditions of a simple support are satisfied, we arrive at a set of homogeneous equations and consequently at the equation of critical state

$$\frac{P}{B} + \left(\frac{M}{2B}\right)^2 = \left(\frac{\pi}{l}\right)^2, \tag{8.9}$$

where l denotes bar length. Greenhill (1883) was the first to derive this equation.

In the case of different bending rigidities, the roots (8.8) may be—in the compression range ($P > 0$)—either all imaginary or two imaginary and two real, whereas in the tension range they are all complex, conjugated in pairs. This case was studied by Shashkov (1950); his results for different values of parameters $k = B_2/B_1$ and $\lambda = (1/B_1 + 1/B_2)C$ are given in Fig. 8.1.
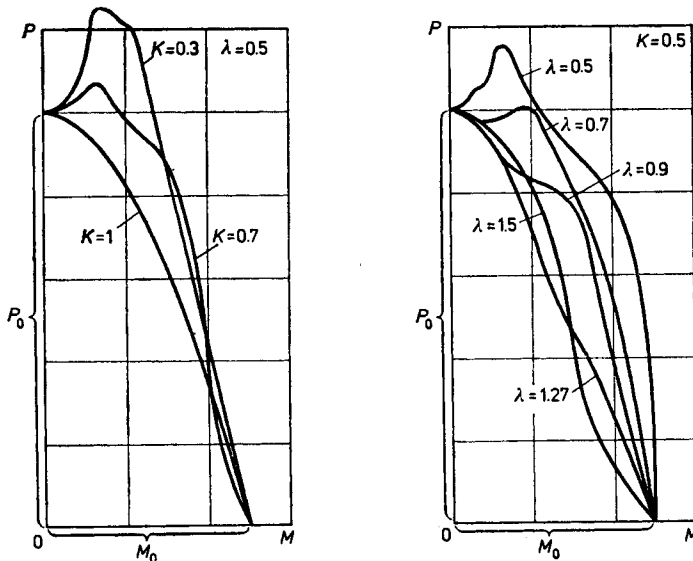
Fig. 8.1. Critical loads of simultaneously compressed and twisted bars with different bending rigidities

In the case of a bar clamped at one end, the behaviour of loading after loss of stability plays an essential role. The study of non-conservative loadings was initiated by Nikolai (1928) and a general conservative case was investigated by Beck (1955).

8.3. Stability of Initially Twisted Bars under Compression

In the case of pure compression of initially twisted bars, in the fundamental state $N = -P$, $\vartheta = \vartheta_0$ (assuming ϑ_0 = const), and the remaining quantities in Eqs. (8.1) vanish. After the loss of stability, Eqs. (8.1) assume a form similar to (8.5), namely after substituting $\vartheta = \vartheta_0$ the first two equations (8.5) hold without change and in the other two the terms with the multipliers C/B_1 and C/B_2 are dropped, being products of two small quantities (since in the primary state, $M_t = 0$). After reduction, we obtain Eq. (8.6), in which a, b and c are given by Eqs. (8.7) omitting the terms containing C and letting $\vartheta = \vartheta_0$.

In what follows, we make such denotations of the axis so that $B_1 \geqslant B_2$. The discussion of the roots (8.8) leads to the conclusion that in the range of small angles of initial twist, $\vartheta_0 < P/B_1$, and in the range of large angles of initial twist, $\vartheta_0 > P/B_2$, all four roots are imaginary whereas in the medium range

$$\frac{P}{B_1} < \vartheta_0 < \frac{P}{B_2} \tag{8.10}$$

we have two imaginary and two real roots (in the case $B_1 = B_2$ which is rather uncommon for initially twisted bars, the range (8.10) vanishes). Tables of critical force values for simply supported, initially twisted bars are given by Ponomarev *et al.* (1959).

In the boundary case $\vartheta_0 \rightarrow \infty$, we obtain the asymptotic equation

$$P_{cr} = \frac{\pi^2}{l^2} \frac{2}{1/B_1 + 1/B_2}, \tag{8.11}$$

so that the equivalent rigidity equals the harmonic mean of rigidities B_1 and B_2.

The first to consider the stability problem of initially twisted bars under compression was Leybenzon (1914) followed by Lurie (1938), Makushin (1952) and Hui (1955). The case of simultaneous compression by a concentrated force and a distributed load was considered by Leipholz (1960) who in addition took into account the influence of torsion (Leipholz, 1961).

8.4. Stability of Helical Springs under Compression

The deflection line of a helical spring after loss of stability is of course a spatial curve, but a sufficiently accurate determination of the critical force will be obtained using the hypothesis of an equivalent bar having rigidities equalling those of the spring and on the basis of analysis of a plane deflection line of that bar.

The first to formulate the equivalent bar hypothesis was Hurlbrink (1910) followed by Grammel (1924). Their studies neglect, however, the influence of shear on the critical force, and in the case of springs, this influence is very significant. The influence of shear was considered by Biezeno and Koch (1925), though only in approximate terms, resulting in significant errors (their theory does not specify the limiting ratio L/D, below which the spring does not undergo buckling). A correct solution based on the equivalent bar hypothesis was given by Haringx (1942); Chernyshev (1946) and Haringx (1948) using the markedly more accurate theory of spatial deflection line obtained almost identical results for small rise angles of spring. Identical results were obtained by Makushin (1950) using the energy method.

Taking into account both the compressibility of the equivalent bar axis and the effect of the transverse force leads to a combination of the effects described by Eqs. (2.15) and (2.18), namely to the equation

$$\frac{d^2 w}{dX^2} + \frac{P}{B_b}\left(1 - \frac{P}{B_c} + \frac{P}{B_s}\right)w = 0, \tag{8.12}$$

where B_b, B_c and B_s denote bending rigidity, compressive rigidity and shearing rigidity, respectively. Integrating Eq. (8.12) and taking into account the boundary conditions, we obtain an equation giving the critical force P_{cr}, which—for arbitrary boundary conditions—can be written in the form

$$P_{cr}\left(1 - \frac{P_{cr}}{B_c} + \frac{P_{cr}}{B_s}\right) = P_E, \tag{8.13}$$

where P_E denotes the critical force calculated neglecting the influence of shearing and shortening (the classical Eulerian force). Equation (8.13), solved with respect to the critical value of spring shortening, leads to the equation

$$\varepsilon_{cr} = \frac{P_{cr}}{B_c} = \frac{1}{2(1 - B_c/B_s)}\left[1 - \sqrt{1 - 4P_E(1/B_c - 1/B_s)}\right], \tag{8.14}$$

or to a more convenient form for applications, namely

$$\varepsilon_{cr} = \frac{P_E}{B_c\left[\frac{1}{2} + \frac{1}{2}\sqrt{1 - 4P_E(1/B_c - 1/B_s)}\right]}. \tag{8.15}$$

Buckling may take place only if

$$P_E \leqslant \frac{1}{4(1/B_c - 1/B_s)};$$ (8.16)

otherwise the shortening of the spring will protect it against buckling. For a real bar, the rigidities B_c and B_s are generally very high and the second term under the root in Eq. (8.15) is negligible, whereas for a bar modelling a spring they are very small, since the compressive rigidity is related here to torsion of the wire, and the shearing rigidity, to bending of the wire. In the case of a spring of a circular wire with diameter d and with mean coil radius R, these rigidities are (Haringx, 1942, 1948; Wahl, 1963)

$$B_c = \frac{Gd^4 l_0}{64nR^3}, \qquad B_s = \frac{Ed^4 l_0}{64nR^3},$$ (8.17)

where n denotes the number of coils and l_0 the length (height) of the spring before deformation. The bending rigidity of the equivalent bar is related to torsion and bending of the wire. It equals

$$B_b = \frac{Ed^4 l_0}{64nR(2+\nu)};$$ (8.18)

hence, for a simple support

$$P_E = \frac{\pi^2 Ed^4}{64nRl_0(2+\nu)},$$ (8.19)

after substituting into (8.14)

$$\varepsilon_{cr} = \frac{1+\nu}{1+2\nu}\left[1 - \sqrt{1 - \frac{1+2\nu}{2+\nu}\left(\frac{2\pi R}{l_0}\right)^2}\right].$$ (8.20)
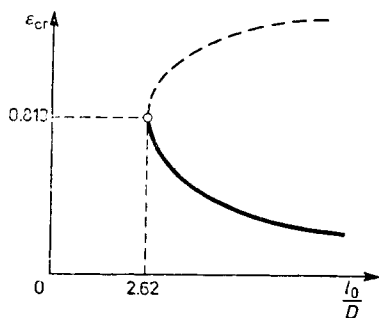
Fig. 8.2. Critical shortening of helical springs

In the case $\nu = 0.3$, we obtain

$$\varepsilon_{cr} = 0.813\left[1 - \sqrt{1 - 6.87\left(\frac{D}{l_0}\right)^2}\right],\tag{8.21}$$

where $D = 2R$; multiplying this value by the compressive rigidity B_c, (8.17), we find the critical force. The plot of function (8.21) is given in Fig. 8.2.

Other shapes of wire cross-section has been considered by Chernyshev (1946) and Makushin (1950). The stability of a spring under torsion has been discussed by Chernyshev (1950), and simultaneous compression and torsion by Maag (1957).

8.5. Lateral Buckling of Beams

In strength aspect, it is advantageous to design the cross-section of a beam in bending as high as possible, but such beams are liable to lose stability of the plane form of bending; i.e., they are liable to sufffer lateral buckling. The early studies devoted to lateral buckling—Prandtl (1899) and Michell (1899)—used equations derived separately for this case, but the analysis of lateral buckling can also be based on the Kirchhoff–Clebsch general equations (8.1), (8.2), (8.3) (Reissner, 1904).

Consider the bending of a straight beam in the principal plane "1", induced by loading q_1. Corresponding to this bending is rigidity B_2; lateral buckling is particularly dangerous when $B_1 \ll B_2$. The fundamental state before the loss of stability in the range of small deflections is given by the equations

$$\frac{\mathrm{d}T_1}{\mathrm{d}s} + q_1 = 0, \qquad \frac{\mathrm{d}M_2}{\mathrm{d}s} + T_1 = 0, \qquad M_2 = B_2\varkappa_2,\tag{8.22}$$

determining functions $T_1(s)$, $M_2(s)$ and $\varkappa_2(s)$, with $N = T_2 = M_1 = M_t = \varkappa_1 = \vartheta = 0$. In the range of large deflections, the third equation comes in, from which it follows that

$$\frac{\mathrm{d}N}{\mathrm{d}s} - \varkappa_2 T_1 = 0\tag{8.23}$$

and then also $N \neq 0$ (N is of the order of $\varkappa_2^2$).

Following the loss of stability of the plane form of bending, a spatial deflection line is formed, which is determined by the remaining three equations (8.1) and the remaining two (8.2). Equations (8.1) we rewrite without any change, underscoring only some terms

$$\frac{dT_2}{ds} + \vartheta T_1 - \underline{\underline{\varkappa_1 N}} + q_2 = 0,$$

$$\frac{dM_1}{ds} + \varkappa_2 M_t - \vartheta M_2 - \underline{T_2} + m_1 = 0, \qquad (8.24)$$

$$\frac{dM_t}{ds} + \varkappa_1 M_2 - \underline{\varkappa_2 M_1} + m_t = 0.$$

The terms underscored once specify the influence of small deflections and the term underscored twice, the additional influence of finite deflections. These influences were investigated on the basis of Eqs. (8.24) by Reissner (1979); they are not very great as a rule and are omitted further, and we replace the variable s by the variable x measured along the undeformed axis.

Functions $T_1(x)$, $M_2(x)$ and $\varkappa_2(x)$ in Eqs. (8.24) may differ from the functions defined by Eqs. (8.22), before the loss of stability, but the differences, treated as small of first order, are multiplied by other small quantities and so in determining the critical state they are neglected. Consequently, Eqs. (8.22) should be substituted into Eqs. (8.24). Using the latter equations and the relationship following from the third of the geometrical equations (8.2) for a straight bar, namely

$$\vartheta = \frac{d\varphi}{ds}, \qquad (8.25)$$

we can write the first two equations of the set (8.24) in the form

$$\frac{d}{dx}(T_2 + \varphi T_1) + (q_2 + \varphi q_1) = 0,$$

$$\frac{d}{dx}(M_1 - \varphi M_2) - (T_2 + \varphi T_1) + m_1 = 0. \qquad (8.26)$$

With "classical" behaviour of loading after the loss of stability (direction fixed in space, point of application materially fixed on the bar axis), the relationships

$$q_2 = -\varphi q_1, \quad m_1 = 0, \quad m_t = 0, \qquad (8.27)$$

are valid and it then follows from (8.26) that

$$T_2 = -\varphi T_1, \quad M_1 = \varphi M_2. \qquad (8.28)$$

These relationships can also derived from purely geometrical considerations. With the load behaving in some other way, the relationships (8.28) generally do not hold, but we shall not consider such cases here.

Substituting (8.25), (8.27) and (8.28) into the third of Eqs. (8.24), and also using the constitutive equations of constrained torsion (8.2.2) and (8.4), we obtain the fourth-order equation

$$(C\varphi')' - (C_\omega \varphi'')'' + \frac{M_2^2(x)}{B_1} \varphi = 0,$$ (8.29)

which for prismatic beams simplifies to the form

$$B_1 C_\omega \varphi^{IV} - B_1 C\varphi'' - M_2^2(x)\varphi = 0.$$ (8.30)

The integration of Eq. (8.30) is very simple in the case $M_2(x) = M_0 = \text{const}$, $T_1 = 0$, i.e., for pure bending before the loss of stability. The general integral has then the form

$$\varphi = A_1 \sin mx + A_2 \cos mx + A_3 \text{Sh} nx + A_4 \text{Ch} nx,$$ (8.31)

where

$$m = \sqrt{-\alpha + \sqrt{\alpha^2 + \beta}}, \quad n = \sqrt{\alpha + \sqrt{\alpha^2 + \beta}},$$
$$\alpha = \frac{C}{2C_\omega}, \quad \beta = \frac{M_0^2}{B_1 C_\omega}.$$ (8.32)

For a simple support of the beam in plane "1", preventing the extreme cross-sections from rotating about the bar axis and simultaneously allowing them to warp, the boundary conditions of Eq. (8.31) can be written in the form $\varphi(0) = \varphi(l) = \varphi''(0) = \varphi''(l) = 0$; hence,

$$\sin ml = 0, \quad m = \frac{\pi}{l},$$
$$M_{0\,cr} = \frac{\pi}{l} \sqrt{B_1 C \left(1 + \frac{C_\omega}{C} \frac{\pi^2}{l^2}\right)}.$$ (8.33)

The second term under the root expresses the influence of constrained torsion; it is negligibly small, especially for beams of appreciable length. The critical moment is therefore proportional to the geometrical mean from the torsional rigidity and the (smaller) bending rigidity of the cross-section.

For a concentrated force P acting at the free end of a cantilever bar, having a direction fixed in space and a materially fixed point of application at the centre of gravity of the cross-section, Eq. (8.30) takes the form

$$B_1 C_\omega \varphi^{IV} - B_1 C\varphi'' - P^2 x^2 \varphi = 0,$$ (8.34)

where variable x is measured from the free end. With a negligible warping rigidity $C_\omega \approx 0$ (e.g. for a cross-section of the shape of a narrow rectangle), the integral of Eq. (8.34) is expressed by Bessel functions

$$\varphi = \sqrt{x}[A_1 J_{1/4}(\beta_1 x^2) + A_2 J_{-1/4}(\beta_1 x^2)],$$ (8.35)

where $\beta_1 = P/2\sqrt{B_1 C}$. The boundary conditions $\varphi(l) = 0$ and $\varphi'(0) = 0$ (vanishing of the torsional moment at the free end) lead to the equation

$$J_{-1/4}(\beta_1 l^2) = 0. \tag{8.36}$$

The least root of the function $J_{-1/4}(x)$ equals 2.0063, hence

$$P_k = \frac{4.013}{l^2}\sqrt{B_1 C}. \tag{8.37}$$

The behaviour of loading after the loss of stability has a very important influence on the critical value of the loading. If the concentrated force is applied not at the centre of gravity of the free cross-section but at a point of coordinate a on the axis in the fundamental bending plane, the critical value will be (Timoshenko and Gere, 1961)

$$P_{cr} = \frac{4.013}{l^2}\sqrt{B_1 C}\left(1 - \frac{a}{l}\sqrt{\frac{B_1}{C}}\right) \tag{8.38}$$

(positive coefficient a corresponds to raising the point of application of the force). The follower type behaviour of loading was studied by Bolotin (1961), Como (1966), Migliacci (1965), Ballio (1967) and Celep (1977). Also the related problem of wing flutter is linked to non-conservative loading (Fung, 1956). A catalogue of critical loads for a considerable number of cases of loading and support of beam ends is given by Nethercot and Rockey (1971).

Fourier series as a method to investigate the general case of loading and cross-sectional variation was used by Piątek (1954). The case of combined loadings was studied in detail by Naleszkiewicz (1954), Brzoska (1965) and Wiśniewski (1964). In beams of monosymmetric section, the shear centre does not coincide with the centre of gravity of cross-section; an appropriate method for calculating critical loads for such beams was given by Weiss (1969).

In engineering applications, lateral buckling of beams is frequently of the elastic-plastic type. The difficulty of analysing this case is involved with the non-homogeneous state of stress before the loss of stability and the multiaxial state after the loss of stability. We can cite here papers by Kachanov (1951), Bentley (1952), Galambos (1964), Yoshida and Imoto (1973) and Lindner and Bamm (1977).

9. Problems of Dynamic Buckling

9.1. Fundamental Equations

In Section 2.2 we have used the kinetic criterion to determine the static stability of bars under a time-constant force. We now consider the case of time-variable forces, acting either in perfect manner (acting axially on straight bars) or in a manner allowing for imperfections. In the latter case, we deal rather with buckling in the engineering sense than with loss of stability.

Longitudinal as well as transverse vibrations may occur in a bar under a compressive force $P(t)$. Taking into account the terms describing geometrical non-linearity up to quadratic included, we describe these vibrations in the elastic range by the equations (Bolotin, 1951, 1953; Piszczek, 1955)

$$\{EA[u' + \tfrac{1}{2}(w')^2]\}' - m\ddot{u} = 0,$$
$$(EJw'')'' - \{EAw'[u' + \tfrac{1}{2}(w')^2]\} + m\ddot{w} = 0, \tag{9.1}$$

where u denotes axial displacements, w are transverse displacements; the dashes denote differentiation with respect to spatial variable x and the dots differentiation with respect to time t. The boundary condition for the end on which compressive force $P(t)$ is acting has the form

$$-EA[u' + \tfrac{1}{2}(w')^2] = P(t); \tag{9.2}$$

if the longitudinal vibrations are negligible (with high longitudinal rigidity in relation to transverse), then (9.2) holds for any point x, and substituting this relationship into the second equation (9.1), we obtain

$$(EJw'')'' + [P(t)w']' + m\ddot{w} = 0. \tag{9.3}$$

This equation was derived (for prismatic bars) by Belaev (1926).

For a simple support, the deflection line can be represented in the form of a Fourier series

$$w(x, t) = \sum_n f_n(t) \sin\frac{n\pi x}{l}; \tag{9.4}$$

the substitution of (9.4) into (9.1) results, for prismatic bars, in a sequence of equations

$$\ddot{f}_n + n^2\omega^2 \left[n^2 - \frac{P(t)}{P_E} \right] f_n = 0,$$ (9.5)

where ω denotes the lowest frequency of transverse natural vibration and P_E is the Eulerian force

$$\omega = \frac{\pi^2}{l^2} \sqrt{\frac{EJ}{m}}, \qquad P_E = \frac{\pi^2 EJ}{l^2}.$$ (9.6)

Fourier series may also be used for other kinds of support.

9.2. Dynamic Stability under Periodic Axial Forces

When function $P(t)$ in Eq. (9.5) is an arbitrary periodic time function, this equation is then called *Hill's equation*.

In a more particular case, if

$$P(t) = P_m + P_a \cos \theta t,$$ (9.7)

where P_m stands for mean value, P_a is the amplitude and θ is the frequency of the exciting force, Eq. (9.5) is called *Mathieu's equation*. We write it in the form

$$\ddot{f}_n + \Omega_n^2 (1 - 2\nu_n \cos \theta t) f_n = 0,$$ (9.8)

where Ω_n denotes nth frequency of transverse vibrations in the presence of compressive force P_m and ν_n is the excitation coefficient, namely

$$\Omega_n^2 = n^2\omega_n^2 \left(n^2 - \frac{P_m}{P_E} \right),$$

$$\nu_n = \frac{P_a}{2(n^2 P_E - P_m)} .$$ (9.9)

To assess the stability limits of the motion described by Eq. (9.8) we assume a solution of periodic form, therefore of constant amplitude. We write it in the form

$$f_n = \sum_k \left(a_{nk} \sin \frac{k\theta t}{2} + b_{nk} \cos \frac{k\theta t}{2} \right)$$ (9.10)

and only in two cases can Eq. (9.8) be satisfied by (9.10), namely when summation covers only odd values of subscript k or when it covers only even k values, zero included. In the case of odd k values, the substitution of (9.10)

into (9.8) and replacement of the products of the trigonometric functions by corresponding sums leads to two infinite sets of equations

$$\left(1+\nu_n-\frac{\theta^2}{4\Omega_n^2}\right)a_{1n}-\nu_n a_{3n}=0,$$

$$\left(1-\frac{k^2\theta^2}{4\Omega_n^2}\right)a_{kn}-\nu_n(a_{k-2,n}-a_{k+2,n})=0, \quad k=3,5,7\ldots; \tag{9.11}$$

$$\left(1-\nu_n-\frac{\theta^2}{4\Omega_n^2}\right)b_{1n}-\nu_n b_{3n}=0,$$

$$\left(1-\frac{k^2\theta^2}{4\Omega_n^2}\right)b_{kn}-\nu_n(b_{k-2,n}-b_{k+2,n})=0, \quad k=3,5,7\ldots \tag{9.12}$$

Equating to zero the determinants of the homogeneous sets of equations (9.11) and (9.12), we obtain, in joint notation

$$\begin{vmatrix} 1\pm\nu_n-\dfrac{\theta^2}{4\Omega_n^2} & -\nu_n & 0 & \cdots \\ -\nu_n & 1-\dfrac{9\theta^2}{4\Omega_n^2} & -\nu_n & \cdots \\ 0 & -\nu_n & 1-\dfrac{25\theta^2}{4\Omega_n^2} & \cdots \\ \cdots & \cdots & \cdots & \cdots \end{vmatrix}=0. \tag{9.13}$$

It can be demonstrated that this determinant is convergent (Bolotin, 1956). Equating to zero only the first term, we obtain

$$1\pm\nu_n-\frac{\theta^2}{4\Omega_n^2}=0. \tag{9.14}$$

Calculating therefrom the ratio θ/Ω and by expanding the root into a power series and leaving only two terms, we obtain Belaev's (1926) approximate formula

$$\frac{\theta}{\Omega_n}=2\pm\nu_n. \tag{9.15}$$

The boundaries of the second instability region can be determined by leaving only even k values in series (9.10). Equating the determinants to zero and leaving in them only two rows and two columns leads to the equations

$$\frac{\theta}{\Omega_n}=\sqrt{1+\tfrac{1}{3}\nu_n^2}, \qquad \frac{\theta}{\Omega_n}=\sqrt{1-2\nu_n^2}. \tag{9.16}$$

The stability regions and the three (shaded) instability regions are shown in Fig. 9.1.
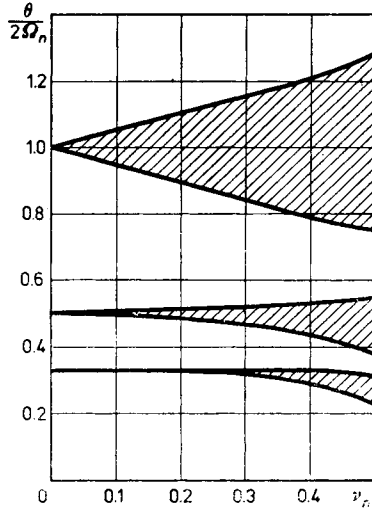
Fig. 9.1. Dynamic stability and instability regions

In the case of viscous damping, described by coefficient ε, the equation for boundaries of the first stability region (9.14) takes the form (Volmir, 1963)

$$\frac{\theta}{2\Omega_n} = \sqrt{1 \pm \sqrt{\nu_n^2 - 4\varepsilon^2/\Omega_n^2}} \,. \tag{9.17}$$
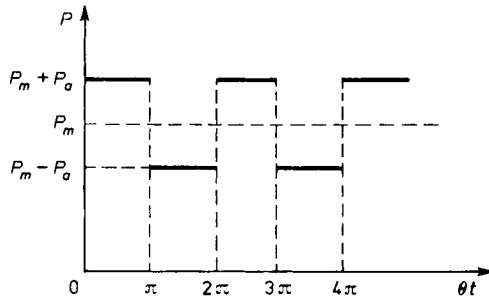
Fig. 9.2. Step-wise variable periodic loading

Another typical periodic loading is step variable loading (Fig. 9.2)

$$P(t) = \begin{cases} P_m + P_a, & 2k\pi < \theta t < (2k+1)\pi, \\ P_m - P_a, & (2k+1)\pi < \theta t < (2k+2)\pi, \end{cases} \quad k = 0, 1, 2, \dots \tag{9.18}$$

Assuming $P_m + P_a < P_E$, the general integrals of Eq. (9.5) after substitution of (9.18) have the form

$$f_n = \begin{cases} C_{1k}\sin p_{1n}t + C_{2k}\cos p_{1n}t, & 2k\pi < \theta t < (2k+1)\pi, \\ C_{3k}\sin p_{2n}t + C_{4k}\cos p_{2n}t, & (2k+1)\pi < \theta t < (2k+2)\pi, \end{cases} \qquad (9.19)$$
$$k = 0, 1, 2, \ldots,$$

where

$$p_{1n} = n\omega \sqrt{n^2 - \frac{P_m + P_a}{P_E}}, \qquad p_{2n} = n\omega \sqrt{n^2 - \frac{P_m - P_a}{P_E}}. \qquad (9.20)$$

Suppose the initial conditions for $t = 0$ have the form $f_n = f_0$ and $\dot{f}_n = v_0$. Let us examine the conditions under which $f_n = s_n f_0$, $\dot{f}_n = s_n v_0$ occurs at instant $t = 2\pi/\theta$, where s_n is a certain multiplier (Den Hartog, 1940). With $|s_n| = 1$ the motion is periodic; hence, it is the stability limit: $|s_n| < 1$ signifies stability, $|s_n| > 1$ signifies instability. By satisfying the continuity conditions for $t = \pi/\theta$, we calculate the values f_n and $\dot{f}_n$ for $t = 2\pi/\theta$; and by demanding that the relationships given above be satisfied, we arrive at a set of linear homogeneous equations with respect to the constants C_{10} and C_{20}. Equating the determinant of these equations to zero leads to a quadratic equation with respect to the multiplier s_n

$$s_n^2 - 2A_n s_n + 1 = 0, \qquad (9.21)$$

where

$$A_n = \cos\frac{\pi p_{1n}}{\theta}\cos\frac{\pi p_{2n}}{\theta} - \frac{1}{2}\left(\frac{p_{1n}}{p_{2n}} + \frac{p_{2n}}{p_{1n}}\right)\sin\frac{\pi p_{1n}}{\theta}\sin\frac{\pi p_{2n}}{\theta}. \qquad (9.22)$$

The solution of Eq. (9.21) is

$$s_n = A_n \pm \sqrt{A_n^2 - 1}; \qquad (9.23)$$

hence, $|s_n| = 1$ with $|A_n| = 1$, and the instability region is given by the inequality

$$\left|\cos\frac{\pi p_{1n}}{\theta}\cos\frac{\pi p_{2n}}{\theta} - \frac{1}{2}\left(\frac{p_{1n}}{p_{2n}} + \frac{p_{2n}}{p_{1n}}\right)\sin\frac{\pi p_{1n}}{\theta}\sin\frac{\pi p_{2n}}{\theta}\right| > 1. \qquad (9.24)$$

The region (9.24) is presented graphically in the paper by Makushin (1947).

The influence of logitudinal vibrations on dynamic stability has been studied on the basis of Eq. (9.1) by Piszczek (1955), who also took into account the physical non-linearity of material. The paper by Bolotin (1953) is devoted to the calculation of transverse vibration amplitudes. A general method, making use of Fourier series, was developed for non-prismatic bars by Piątek (1956).

Dynamic stability of the plane form of bending of beams has been studied by Bolotin (1956), Piszczek (1955) and Wiśniewski (1975). Roliński (1969) has discussed the case of combined action of a constant longitudinal force and a periodically variable torsional moment.

9.3. Buckling under Impact Loadings

In the case of short-term impact loading, we consider either the loss of stability of a straight bar or the deflections of an imperfect bar taking place in time. The latter approach refers to the analysis of buckling in engineering sense.

Here either Eqs. (9.1), with longitudinal vibrations considered, or (9.3) and (9.5) with these vibrations neglected may serve as governing equations. In the case of a bar with initial curvature, w'' in Eq. (9.3) should be replaced by $w'' - w_0''$; and Eq. (9.5) takes the form

$$\ddot{f}_n + n^2\omega^2 \left[n^2 - \frac{P(t)}{P_E} \right] f_n = n^4\omega^2 f_{n0}, \tag{9.25}$$

where f_{n0} denotes the amplitude of nth harmonic of initial deflection.

Consider a sudden application of axial load P at instant $t = 0$ to a bar with initial curvature. If force P is smaller than the Eulerian force, then the solution of Eq. (9.25) is expressed by trigonometric functions and gives the vibrations about the point of equilibrium. If on the other hand, the force is greater that the kth static critical force, then the general integral for $n = 1, 2, \ldots k$ is expressed by hyperbolic functions, namely, with the initial conditions $f_n(0) = f_{n0}$ and $\dot{f}_n(0) = 0$ considered

$$f_n = \left(\frac{\text{Ch}\Omega_n t}{1 - \frac{n^2 P_E}{P}} - \frac{1}{\frac{P}{n^2 P_E} - 1} \right) f_{n0}, \tag{9.26}$$

where Ω_n describes the velocity of deflections of the nth harmonic

$$\Omega_n = n\omega \sqrt{\frac{P}{P_E} - n^2}, \quad n = 1, 2, \ldots, k. \tag{9.27}$$

If Ω_n is treated as a continuous function of variable n, it will reach the maximum at $n = \sqrt{P/2P_E}$; practically speaking, the maximum velocity corresponds to an integer close to $\sqrt{P/2P_E}$. Frequently, if large short-term loadings are involved, then it is much higher than $n = 1$ and several half-waves develop over the bar length, which has been confirmed experimentally (Gerard and Becker, 1952).

For a linearly increasing loading, $P = kt$, by introducing dimensionless "shifted" time

$$\tau = \sqrt[3]{\frac{n^2\omega^2 P_E^2}{k^2}} \left(n^2 - \frac{kt}{P_E} \right). \tag{9.28}$$

Equation (9.5) can be reduced to the form

$$\dot{f}_n + \tau f_n = P_E \sqrt[3]{\frac{\pi^2 n^8}{mk^2 l^2}} f_{n0}. \qquad (9.29)$$

It is a non-homogeneous Bessel equation. Initially, for $t < n^2 P_E/k$, its sol-ution is expressed by functions $J_{1/3}$ and $J_{-1/3}$ and by the particular integral of the non-homogeneous equation, but for higher values of t, it is expressed by modified functions $I_{1/3}$ and $I_{-1/3}$ (Hoff, 1951; Volmir, 1963; Kordecki, 1964).

The effects of coupling of longitudinal and transverse vibrations due to axial impact against an initially curved bar were considered by Gryboś (1970, 1975) who used the small parameter method. Kaliski (1955) made a compre-hensive study of stability of a straight bar under axial impact; he found, however, that the bar failure parameters may be significantly higher than those corresponding to loss of stability. Kaliski also took into account elastic-plastic dynamic strains. A different approach is followed in the paper by Kordecki (1966) concerned with dynamic elastic-plastic buckling of an initially curved bar of I-section: up to the point of first plastification the material is treated as perfectly elastic and once the first plastic hinge is formed, as per-fectly rigid-plastic. Kordecki (1966) explored the possibility of the formation of subsequent hinges of opposite sense.

The problem of stability of structures under impact loads is discussed in detail in the monograph by Gryboś (1980).

10. Stability of Bar Structures

10.1. Stability of Trusses

A truss may lose its stability by bifurcation of the equilibrium form without the occurrence of bending states, by snap-through or by buckling of individual truss members. Bifurcation of the equilibrium of a plane truss may take place in its plane or may cause lateral buckling.

A general stability theory of plane trusses was proposed by Mises (1923), it covers in-plane bifurcation and snap-through but does not cover buckling of bars and lateral buckling.

Suppose that at a joint k of the truss there are members linking this joint to adjacent joints with current subscript i and that a force with components X_k, Y_k is acting at joint k. In this case, the equilibrium equations for joint k take the form

$$\sum_i N_{ik} \cos \alpha_{ik} = X_k,$$
$$k = 1, 2, \ldots, w, \tag{10.1}$$
$$\sum_i N_{ik} \sin \alpha_{ik} = Y_k,$$

where N_{ik} denote the longitudinal forces in the truss members connecting joint k with current adjacent joints i, α_{ik} denote the angles of inclination of truss members to x-axis, and w is the number of joints. In the elastic range, in place of N_{ik} we should substitute

$$N_{ik} = \left(EA \frac{l-l_0}{l_0} \right)_{ik}, \tag{10.2}$$

where l_0 denotes initial length of truss member ik and l is the length after deformation. It does not matter if the strains and displacements involved here are large, provided that they obey Hooke's law. The principle of rigidification does not hold in the analysis of stability; hence, by α_{ik} we should understand the actual angles of inclination of truss members, after deformation.

An elastic system loses stability when small changes in displacements are possible without change in loadings. Equating the variations of Eqs. (10.1) to zero, with substituted (10.2) and $\delta X_k = \delta Y_k = 0$, we obtain a set od $2w-r$ equations, where r denotes the number of reactions,

$$\sum_i \left[-EA \frac{l-l_0}{l_0} \sin \alpha \, \delta\alpha + \frac{EA}{l_0} \cos \alpha \, \delta l \right]_{ik} = 0,$$

$$\sum_i \left[EA \frac{l-l_0}{l_0} \cos \alpha \, \delta\alpha + \frac{EA}{l_0} \sin \alpha \, \delta l \right]_{ik} = 0.$$

(10.3)

In these equations, the changes in angles $\delta\alpha_{ik}$ and changes in lengths δl_{ik} can be expressed by changes in the coordinates of joints x_i, x_k, y_i, y_k as follows:

$$\delta\alpha_{ik} = \frac{1}{l_{ik}} [-\delta(x_k-x_i)\sin\alpha_{ik} + \delta(y_k-y_i)\cos\alpha_{ik}],$$

$$\delta l_{ik} = \delta(x_k-x_i)\cos\alpha_{ik} + \delta(y_k-y_i)\sin\alpha_{ik}.$$

(10.4)

Equations (10.3) after substituting (10.4) contain $2w-r$ unknown virtual displacements δx and δy. Equating the determinant of these homogeneous equations to zero gives the critical state of the truss, and by way of (10.1) they also determine the critical load.

We examine, as an example, the stability of a two-membered truss as in Fig. 10.1, known as the *Mises truss*. The number of joints $w = 3$ and the number of reactions $r = 4$, so that $2w-r = 2$: the coordinates $x_1 = x$ and $y_1 = y$ of joint i (the apex of the truss) are the degrees of freedom. Assume $EA = \text{const}$, so that Eqs. (10.3) can be cancelled by EA. Introducing the notation $l - l_0 = \Delta l$, we obtain

$$-\Delta l_{12} \sin \alpha_{12} \, \delta\alpha_{12} + \cos \alpha_{12} \, \delta l_{12} -$$
$$-\Delta l_{13} \sin \alpha_{13} \, \delta\alpha_{13} + \cos \alpha_{13} \, \delta l_{13} = 0,$$
$$\Delta l_{12} \cos \alpha_{12} \, \delta\alpha_{12} + \sin \alpha_{12} \, \delta l_{12} +$$
$$+ \Delta l_{13} \cos \alpha_{13} \, \delta\alpha_{13} + \sin \alpha_{13} \, \delta l_{13} = 0.$$

(10.5)

Equations (10.4) for truss member 12 take the form

$$\delta\alpha_{12} = \frac{1}{l_{12}} (-\delta x \sin \alpha_{12} + \delta y \cos \alpha_{12}),$$

$$\delta l_{12} = \delta x \cos \alpha_{12} + \delta y \sin \alpha_{12},$$

(10.6)

and a similar form for member 13. Substituting (10.6) into (10.5), we obtain a set of homogeneous equations with δx and δy as unknowns; equating the determinant of this set to zero leads to the determination of the critical state

for arbitrary non-symmetric loading of the truss. This determinant becomes greatly simplified for symmetric loading, namely by force P of vertical direction, since we should then substitute $\alpha_{13} = \pi - \alpha_{12}$. By omitting the subscript "12" and cancelling by 2, we obtain

$$\begin{vmatrix} \cos^2\alpha + \dfrac{\Delta l}{l}\sin^2\alpha & 0 \\[2mm] 0 & \sin^2\alpha + \dfrac{\Delta l}{l}\cos^2\alpha \end{vmatrix} = 0. \tag{10.7}$$

Equation (10.7) defines two critical states. Substituting $\Delta l = l - l_0$ and $l\cos\alpha = c$ (Fig. 10.1), the equations of these critical states take the form

$$\sin^2\alpha\cos\alpha - \frac{c}{l_0} = 0, \tag{10.8}$$

$$\cos^3\alpha - \frac{c}{l_0} = 0. \tag{10.9}$$
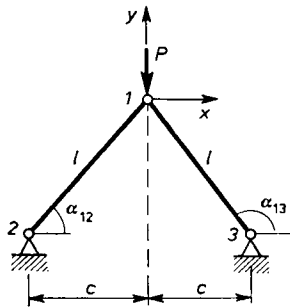
Fig. 10.1. Mises truss system

Equation (10.8) determines the bifurcation of the equilibrium form related to the occurrence of a horizontal displacement, consequently, to the occurrence of asymmetric deformation. Equation (10.9) corresponds to the increment of vertical displacement without change in the force; therefore, it defines a snap-through. The corresponding force P follows from Eqs. (10.1) and (10.2); taking the compressive force to be positive, we obtain

$$P = -2N\sin\alpha = 2EA\left(1 - \frac{1}{l_0}\right)\sin\alpha. \tag{10.10}$$

The length l can be eliminated by the equation $l = c/\cos\alpha$, and the critical angle α is given by Eq. (10.8) or (10.9). In the case of Eq. (10.9) which deter-

mines the snap-through of the truss, the calculation of α presents no difficulty; finally we obtain

$$P_{cr} = 2EA\left[1-\left(\frac{c}{l_0}\right)^{2/3}\right]^{3/2}. \tag{10.11}$$

We shall present here yet another approach to the truss stability problem, relating directly to the matrix approach used in Section 6.2, Part 1. In stability considerations we must admit departures from the principle of rigidification; hence, the finite equation (6.9) in Part 1 does not hold, and only the linear relationship between the generalized strains $\delta\boldsymbol{\varepsilon}$ and the generalized displacements $\delta\mathbf{q}$, (6.22), remains valid here

$$\delta\boldsymbol{\varepsilon} = \mathbf{B}\,\delta\mathbf{q}, \tag{10.12}$$

where $\mathbf{B}$ is a geometric matrix, generally depending on displacements. The relationship between generalized loadings $\mathbf{Q}$ and generalized stresses $\boldsymbol{\sigma}$ follows directly from the virtual work principle, Eq. (6.23) of Part 1:

$$\mathbf{Q} = \mathbf{B}^T\boldsymbol{\sigma}. \tag{10.13}$$

The increment of the loading $\mathbf{Q}$ is

$$\delta\mathbf{Q} = \delta\mathbf{B}^T\boldsymbol{\sigma} + \mathbf{B}^T\delta\boldsymbol{\sigma}. \tag{10.14}$$

The matrix $\delta\mathbf{B}^T$ depends linearly on $\delta\mathbf{q}$; hence, we can write quite formally

$$\delta\mathbf{B}^T\boldsymbol{\sigma} = \mathbf{G}\,\delta\mathbf{q}, \tag{10.15}$$

where the square matrix $\mathbf{G}$ depends linearly on stresses $\boldsymbol{\sigma}$ and non-linearly on displacements $\mathbf{q}$. It is called the *geometric stiffness matrix* (Maier and Drucker, 1973). We transform the second term in the expression (10.14) by introducing the constitutive relationship (6.23) (Part 1, neglecting the initial strains $\boldsymbol{\varepsilon}^0$) and the relationship (10.12). Finally, we have

$$\delta\mathbf{Q} = (\mathbf{G}+\mathbf{B}^T\mathbf{E}\mathbf{B})\,\delta\mathbf{q}. \tag{10.16}$$

The loss of stability takes place when the non-zero increments of displacements $\delta\mathbf{q}$ can correspond to zero increment of loadings $\delta\mathbf{Q}$; hence,

$$\det(\mathbf{G}+\mathbf{B}^T\mathbf{E}\mathbf{B}) = 0. \tag{10.17}$$

The condition (10.17) has a substantially more concise form than has the determinant of the set (10.3) with (10.4) substituted into it; but effective calculations with matrices may prove tedious.

As an example, we apply condition (10.17) to the Mises truss, referring to the previously used denotations. In this case, the column vectors are

$$\mathbf{Q} = \begin{bmatrix} X \\ Y \end{bmatrix}, \quad \boldsymbol{\sigma} = \begin{bmatrix} N_{12} \\ N_{13} \end{bmatrix}, \quad \boldsymbol{\varepsilon} = \begin{bmatrix} \Delta l_{12} \\ \Delta l_{13} \end{bmatrix}, \quad \mathbf{q} = \begin{bmatrix} x \\ y \end{bmatrix}, \tag{10.18}$$

The matrices **B** and **E** are equal (matrix **B** being easier to determine from Eqs. (10.6))

$$\mathbf{B} = \begin{bmatrix} \cos\alpha_{12} & \sin\alpha_{12} \\ \cos\alpha_{13} & \sin\alpha_{13} \end{bmatrix}, \quad \mathbf{E} = \begin{bmatrix} \dfrac{EA}{l} & 0 \\ 0 & \dfrac{EA}{l} \end{bmatrix}. \tag{10.19}$$

To obtain the terms of matrix **G**, we calculate the increments of the terms of matrix $\mathbf{B}^T$ by the formula

$$\delta(\cos\alpha_{12}) = \frac{\partial(\cos\alpha_{12})}{\partial x}\,\delta x + \frac{\partial(\cos\alpha_{12})}{\partial y}\,\delta y \tag{10.20}$$

and multiply the matrix thus formed by the matrix **σ**. After appropriate rearrangement of the terms, we obtain

$$\mathbf{G} = \begin{bmatrix} \dfrac{\partial(\cos\alpha_{12})}{\partial x}N_{12} + \dfrac{\partial(\cos\alpha_{13})}{\partial x}N_{13} & \dfrac{\partial(\cos\alpha_{12})}{\partial y}N_{12} + \dfrac{\partial(\cos\alpha_{13})}{\partial y}N_{13} \\ \dfrac{\partial(\sin\alpha_{12})}{\partial x}N_{12} + \dfrac{\partial(\sin\alpha_{13})}{\partial x}N_{13} & \dfrac{\partial(\sin\alpha_{12})}{\partial y}N_{12} + \dfrac{\partial(\sin\alpha_{13})}{\partial y}N_{13} \end{bmatrix}. \tag{10.21}$$

Using equations of the type

$$\cos\alpha_{12} = \frac{c+x}{\sqrt{(c+x)^2 + \left(\sqrt{l_0^2 - c^2} + y\right)^2}}, \tag{10.22}$$

we calculate the derivatives appearing in (10.21). By introducing the trigonometric functions again, we can write

$$\frac{\partial(\cos\alpha_{12})}{\partial x} = \frac{\sin^2\alpha_{12}}{l_{12}}, \tag{10.23}$$

and finally, using the constitutive equations we obtain

$$\mathbf{G} = \frac{EA}{l} \times$$

$$\times \begin{bmatrix} \dfrac{\Delta l_{12}}{l_{12}}\sin^2\alpha_{12} + \dfrac{\Delta l_{13}}{l_{13}}\sin^2\alpha_{13} & -\dfrac{\Delta l_{12}}{l_{12}}\sin\alpha_{12}\cos\alpha_{12} - \dfrac{\Delta l_{13}}{l_{13}}\sin\alpha_{13}\cos\alpha_{13} \\ -\dfrac{\Delta l_{12}}{l_{12}}\sin\alpha_{12}\cos\alpha_{12} - \dfrac{\Delta l_{13}}{l_{13}}\sin\alpha_{13}\cos\alpha_{13} & \dfrac{\Delta l_{12}}{l_{12}}\cos^2\alpha_{12} + \dfrac{\Delta l_{13}}{l_{13}}\cos^2\alpha_{13} \end{bmatrix}. \tag{10.24}$$

The matrix $\mathbf{B}^T\mathbf{E}\mathbf{B}$ is simpler to calculate

$$\mathbf{B}^T\mathbf{E}\mathbf{B} = \frac{EA}{l}\begin{bmatrix} \cos^2\alpha_{12} + \cos^2\alpha_{13} & \sin\alpha_{12}\cos\alpha_{12} + \sin\alpha_{13}\cos\alpha_{13} \\ \sin\alpha_{12}\cos\alpha_{12} + \sin\alpha_{13}\cos\alpha_{13} & \sin^2\alpha_{12} + \sin^2\alpha_{13} \end{bmatrix}.$$

$$(10.25)$$

After calculating the determinant (10.17), we arrive at an equation determining the critical state. In the case of symmetric loading by vertical force P, after substituting $\alpha_{13} = \pi - \alpha_{12}$, we obtain the determinant (10.7) and the rest of the calculation procedure is as before.

The stability of space trusses has been studied by Ratzersdorfer (1936). This matrix approach also allows a relatively simple approach to elastic-plastic buckling (Maier and Drucker, 1973).

In Polish works on this subject, much attention has been paid to the stability of truss girders (Frąckiewicz, 1971, 1970; Woźniak, 1970; Gutkowski, 1973; Bauer and Gutkowski, 1973; Frąckiewicz and Misiak, 1975; Misiak, 1976). Optimal design of simple lattice systems under stability constraints is discussed in the papers by Wojdanowska-Zając and Życzkowski (1969, 1972) and Wojdanowska (1974), Markiewicz and Życzkowski (1981), and Markiewicz (1980).

10.2. Stability of Frames

The loss of stability of a frame by bifurcation of the equilibrium form is possible in cases where the fundamental state is a momentless state (tension-compression state). With bending occurring, the loss of stability takes place generally by snap-through, and in order to determine the corresponding critical loading, non-linear analysis of deflections is required. The bifurcation may however be then related to the formation of a spatial bending line.

To determine the critical loads corresponding to plane bifurcation, superimposed on the momentless state, a Euler-type analysis is sufficient. The derivation of the corresponding equations of critical state proves very simple, particularly by using the displacement method and with the equations derived in Section 9.3, Part 1. A suitable variant of this method expresses generalized internal forces by generalized displacements, with longitudinal forces occurring in individual bars of the frame. We may recall here that for a prismatic bar elastically clamped at both ends (Fig. 9.6a, Part 1), we obtain

$$\begin{bmatrix} M_{ik} \\ M_{ki} \\ lW_{ki} \end{bmatrix} = \frac{EJ}{l}\begin{bmatrix} \alpha & \beta & -\vartheta \\ \beta & \alpha & -\vartheta \\ -\vartheta & -\vartheta & \delta \end{bmatrix}\begin{bmatrix} \varphi_i \\ \varphi_k \\ \psi \end{bmatrix}$$

$$(10.26)$$

for a bar elastically clamped at one end and simply supported at the other (Fig. 9.6b)

$$\begin{bmatrix} M_{ik} \\ lW_{ki} \end{bmatrix} = \frac{EJ}{l} \begin{bmatrix} \alpha' & -\alpha' \\ -\alpha' & \delta' \end{bmatrix} \begin{bmatrix} \varphi_i \\ \psi \end{bmatrix},$$ (10.27)

for a bar elastically clamped at one end and clamped with sidesway at the other (Fig. 9.6c)

$$\begin{bmatrix} M_{ik} \\ M_{ki} \end{bmatrix} = \frac{EJ}{l} \begin{bmatrix} \alpha'' & \beta'' \\ \beta'' & \alpha'' \end{bmatrix} \begin{bmatrix} \varphi_i \\ \varphi_k \end{bmatrix},$$ (10.28)

and for a cantilever (Fig. 9.6d)

$$M_{ik} = \frac{EJ}{l} \alpha''' \varphi_i.$$ (10.29)

The functions of α, β, ϑ and δ are expressed in the case of tensile force N by hyperbolic functions of argument λ, (9.9), (9.11), (9.13), and (9.15) in Part 1, and in the case of compressive axial force N by trigonometric functions of argument σ, (9.19), (9.20), (9.21), where

$$\lambda = l \sqrt{\frac{N}{EJ}}, \ N > 0; \quad \sigma = l \sqrt{-\frac{N}{EJ}}, \quad N < 0.$$ (10.30)

In the case of loss of stability by bifurcation, the basic equation of displacement method, namely the matrix equation (6.92) in Part 1 takes the form

$$\mathbf{B}^T \mathbf{EB} \delta \mathbf{q} = 0,$$ (10.31)

since a change in the generalized displacements $\delta \mathbf{q}$ is then possible without change in the loadings. The matrices $\mathbf{B}$ and $\mathbf{B}^T$ are present in geometric equations and in equilibrium equations, and the matrix $\mathbf{E}$ follows from (10.26)–(10.29). The condition of existence of non-zero solutions $\delta \mathbf{q}$ of Eq. (10.31)

$$\det(\mathbf{B}^T \mathbf{EB}) = 0$$ (10.32)
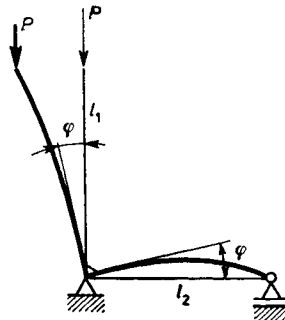
Fig. 10.2. Two-bar frame with a free end

determines the critical state (bifurcation). There is a difference here in comparison to (10.17), namely that matrix $\mathbf{G}$ is not involved in describing here the change of matrix $\mathbf{B}^T$ during the deformation process; in the present problem, this type of effect does not occur.

We consider as an example, a two-bar frame as in Fig. 10.2. It will suffice here to take the angle φ as the generalized displacement q and the moment on the left support M as the generalized internal force. For the vertical bar, it follows from Eq. (10.29) that

$$M = \frac{EJ_1}{l_1}\,\alpha_1'''\varphi, \tag{10.33}$$

and for the horizontal bar, we obtain from Eq. (10.27)

$$M = \frac{EJ_2}{l_2}\,\alpha_2'\varphi, \tag{10.34}$$

where the subscripts by the functions α' and α''' indicate that the values of these functions should be calculated for the corresponding axial forces in the bars: $N_1 = -P$ and $N_2 = 0$. The matrix $\mathbf{B}^T$ has here the form

$$\mathbf{B}^T = [1, 1], \tag{10.35}$$

so that Eq. (10.31) takes the form

$$\frac{EJ_1}{l_1}\,\alpha_1'''\varphi + \frac{EJ_2}{l_2}\,\alpha_2'\varphi = 0, \tag{10.36}$$

and from the condition (10.32) it follows that

$$\frac{J_1}{l_1}\,\alpha_1''' + \frac{J_2}{l_2}\,\alpha_2' = 0. \tag{10.37}$$

The value of the function α_2' for the moment $N_2 = 0$, i.e., $\sigma = 0$, can be calculated by limit transition; $\lim_{\sigma\to 0}\alpha' = 3$, and by substituting α_1''' in accordance with Eq. (9.21) from Part 1, we obtain

$$-\sigma\tan\sigma + 3\,\frac{l_1}{l_2}\,\frac{J_2}{J_1} = 0. \tag{10.38}$$

The transcendental equation (10.38) determines σ, and hence the critical force P, (10.30).

In the case of the right-hand end of the horizontal bar being clamped, in place of the function α' we have the function α. Since $\lim_{\sigma\to 0}\alpha = 4$, equations of (10.38) type have instead of the coefficient 3 the coefficient 4.
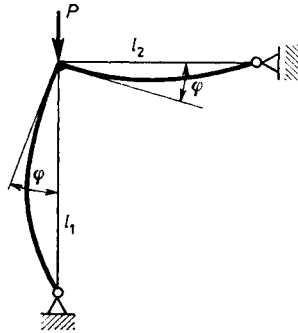
Fig. 10.3. Two-bar frame with simply supported ends

For the two-bar frame shown in Fig. 10.3, we relate moment M in both bars to angle φ using the function α', but for the vertical bar, $\alpha' = \alpha'(\sigma)$, whereas for the horizontal bar, $\alpha' = \alpha'(0)$.

By letting $\alpha'(0) = 3$, we obtain the equation

$$\frac{J_1}{J_2} \frac{l_2}{l_1} \sigma^2 + 3(1 - \sigma \cot \sigma) = 0. \tag{10.39}$$

The stability of such a frame with the load acting non-axially has been investigated by Koiter (1967).

A general linear theory of stability was formulated by Bleich (1919); it is generalized to hold for the case of space frames in the paper of F. Bleich and H. Bleich (1928). The influence of changes in bar length on loss of stability was studied by Mises and Ratzersdorfer (1926). Krynicki nad Mazurkiewicz (1963₁, 1963₂, 1965) and Mazurkiewicz (1966) devoted a series of contributions to the stability of frames consisting of bars of variable rigidities. Nowacki (1956) used integral equations method to solve problems of spatial loss of stability of frames (grids). Wilczyński (1976) is also concerned with spatial (lateral) buckling of frame.

10.3. Stability of Arches

Arches may lose stability either by bifurcation or by snap-through. In snap-through analysis it is important to consider in particular the compressibility of the arch axis. We confine ourselves to bifurcation problems, neglecting axis compressibility; moreover, only in-plane buckling of arch will be considered.

In the case of circular arches, the basic equation follows from (5.115), Part 1, by a suitable adjustment of this equation. We neglect loadings of moment type, distortional terms and terms expressing compressibility and shear

deformations. Instead, we add to normal loadings p_n second-order terms related to the deflection of arch following the loss of stability

$$p_{nt} = -\frac{N_0}{r^2}(v''+v),$$ (10.40)

where N_0 denotes the longitudinal force in the arch (positive under compression), v is the radial displacement (deflection), the dashes denote differentiation with respect to the angular variable ϑ and r is the initial radius of curvature of arch (constant). In this case, the sixth-order equation (5.115) after differentiating and substituting the relationship $u' = v$ [(5.107), of Part 1, putting $\varepsilon = 0$] takes the form

$$v^{\text{VI}}+2v^{\text{IV}}+v''+\frac{r^3}{EJ_z}\left[rp_t'-rp_n''+\frac{N_0}{r}(v^{\text{IV}}+v'')\right]=0.$$ (10.41)

Denote the angle of rotation of cross-section by β and the angle between the initial direction of loading (normal) and the direction of loading after the loss of stability by δ (this angle describes the behaviour of loading after loss of stability). In this case, assuming small deflections and projecting to normal and tangential directions after loss of stability

$$p_n = p, \quad p_t = p(\beta-\delta).$$ (10.42)

Confining ourselves to the case $p = $ const, we obtain

$$EJ_z(v^{\text{VI}}+2v^{\text{IV}}+v'')+r^3\left[pr(\beta'-\delta')+\frac{N_0}{r}(v^{\text{IV}}+v'')\right]=0.$$ (10.43)

We consider first of all the stability of a circular ring under constant load p with three different variants of behaviour of that loading after the loss of stability.

For a spatially fixed direction of loading we should let $\delta = 0$, and substituting $\beta' = (v''+v)/r$ and $N_0 = pr$, we obtain

$$EJ_z(v^{\text{VI}}+2v^{\text{IV}}+v'')+pr^3(v^{\text{IV}}+2v''+v)=0.$$ (10.44)

In seeking the integral of this equation in the form $v = f\sin n\vartheta$, we obtain

$$-EJ_zn^2(n^2-1)^2+pr^3(n^2-1)^2=0.$$ (10.45)

To ensure a cyclic character of deformation, n must be an integer. The least value of critical load is obtained at $n = 2$ (the case $n = 1$ would correspond practically to motion of the ring as a rigid body); hence,

$$p = p_{\text{cr}} = 4\frac{EJ_z}{r^3}.$$ (10.46)

As the second case we consider a materially fixed behaviour of loading (it remains normal to the deflected arch). We then have $\delta = \beta$, and Eq. (10.43) takes the form

$$EJ_z(v^{VI}+2v^{IV}+v'')+pr^3(v^{IV}+v'') = 0.$$ (10.47)

The substitution of the sinusoidal form of deflections with $n = 2$ leads to the equation for critical loading

$$p = p_{cr} = 3\,\frac{EJ_z}{r^3}.$$ (10.48)
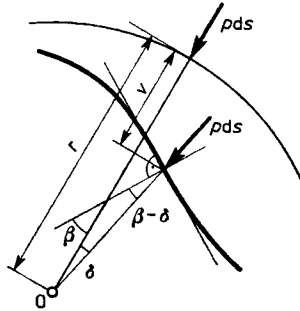
Fig. 10.4. Loading of a circular arch maintaining its direction towards the centre of the circle

The third typical behaviour of loading maintains its direction towards the centre of the cricle. According to Fig. 10.4, we then have $\beta - \delta = v'/r$, and hence Eq. (10.43) takes the form

$$EJ_z(v^{VI}+2v^{IV}+v'')+pr^3(v^{IV}+2v'') = 0$$ (10.49)

from which we have finally, for $n = 2$,

$$p = p_{cr} = 4.5\,\frac{EJ_z}{r^3}.$$ (10.50)

In the case of an arch with the central angle 2α, simply supported at the ends, we can seek a solution of the respective equation in the form

$$v = f\sin\frac{n\pi\vartheta}{\alpha},$$ (10.51)

which satisfies all the boundary conditions. By assuming loading to be normal to the deformed axis of the arch and substituting (10.51) into (10.47), we obtain

$$EJ_z\,\frac{n^2\pi^2}{\alpha^2}\left(\frac{n^2\pi^2}{\alpha^2}-1\right)^{2}+pr^3\,\frac{n^2\pi^2}{\alpha^2}\left(\frac{n^2\pi^2}{\alpha^2}-1\right) = 0.$$ (10.52)

The least loading corresponds to the value $n = 1$, namely

$$p = p_{cr} = \left(\frac{\pi^2}{\alpha^2} - 1\right)\frac{EJ_z}{r^3}.$$ (10.53)

In the case $\alpha = \pi/2$, we obtain the value (10.48), but with $\alpha > \pi/2$ the critical load is lower than for the ring. It corresponds to a deformation close to rigid rotation of the ring, which is not considered in the latter case. To the contrary, as the angle α decreases, the critical load (10.53) tends to grow rapidly. But then, loss of stability connected with the symmetric snap-through of the arch may take place. In the analysis of snap-through, it is necessary to consider compressibility of the arch axis; Timoshenko (1935) and Biezeno (1938) are credited with the first studies in this field, but a more detailed discussion of the problem is given in the monograph by Kornishin and Isanbayeva (1968).

11. Some Recent Results

The present part of the book was written in 1981/82, and so we give here additionally a brief survey of some more recent results. The number of papers published on stability of bars and bar systems may be estimated as 200-300 per annum, and hence we quote and discuss here just some selected, more representative papers.

General approach to stability by using static and kinetic criteria was considered by Koiter (1985), and relevant computational aspects—by Riks (1984). Analytical solutions to thermal buckling of non-uniform columns were given by Gauss and Antman (1984), whereas Banerjee and Williams (1986) elaborated a high-accuracy finite element approach for tapered beam-columns. Elishakoff (1985) discussed random imperfection sensitivity of columns. Non-conservative problems were considered by Kondratev (1985) (non-linear treatment), Leipholz (1986) (energy approach), Elishakoff and Pellegrini (1987) (within the range of static stability criterion).

Much attention was paid to finite deflections described by elastica-type solutions. Panayotounakos (1986), Panayotounakos and Theocaris (1986) discussed continuous column, lying on elastic and on rigid supports, respectively. Physical non-linearity was considered by Haslach (1985), Kounadis and Mallis (1987). Elastica with constrained deflections was analysed by Stein and Wriggers (1984) (finite element solution), Mikhailovski *et al.* (1985) (variational approach, non-linear programming) and by Krikun (1986).

Inelastic buckling of columns was considered by Grabowski (1984) (Bauschinger effect due to preloading by tension), Voronyuk (1984) (physical non-linearity), Sugimoto and Chen (1985) (postbuckling behaviour of tubular members). Inelastic lateral buckling of beams was discussed by Cuk *et al.* (1986), whereas Attard (1986) proposed a finite element approach limited to elastic range.

Optimal design of columns under stability constraints was discussed mainly in multimodal formulation, allowing for various possible simultaneous buckling modes. Gajewski (1985), Plaut *et al.* (1986) considered optimal

column in an elastic medium. Bochenek (1987) determined optimal column subject to buckling in two planes, with different support conditions in these planes; Błachut and Życzkowski (1984) optimized a column under creep conditions. Wang *et al.* (1986) found optimal shape of beams with respect to lateral buckling.

Stability of bar structures was developed mainly in the direction of non-linear treatment. Elastica-type solutions for frames were obtained by Christodoulou and Kounadis (1986), Kahn and Wagner (1987); a simplified approach was suggested by Kounadis (1985). Non-linear analysis of bar members of frames is due to Chen and Lui (1985_2); they discussed also relevant stability criteria in the United States (1985_1). Kondoh *et al.* (1986) derived a non-linear theory of bar members of space frames; Simitses *et al.* (1986) considered sway buckling of multistorey frames. Anderson and Williams (1987) developed a program for buckling and vibration of frames with repetitive geometry. Non-linear theory of stability of trusses was developed by Teixeira de Freitas *et al.* (1985), Karamanlidis and Gesch-Karamanlidis (1986), and of arches— by Botoz and Jameux (1986).

Optimal structural design of arches under stability constraints was considered by Błachut and Gajewski (1981_1, 1981_2) (multimodal optimal design for in-plane buckling, funicular arches and extensible arches, respectively), and by Bochenek and Gajewski (1986) (for in-plane and for out-of-plane buckling). Finally, we mention that many particular solutions may be found in the book by Gajewski and Życzkowski (1988), and in CISM lecture notes edited by Życzkowski (1989).

References to Part 3

Alfutov N. A., 1978, *Principles of Calculations of Stability of Elastic Systems* (in Russian), Mashinostroenie, Moskva.

Ballio G., 1967₁, "Sulla trava alta sollecitata da carichi di tipo non conservativo", *Rend. Ist. Lombardo* A101, 2, 307–330.

Ballio G., 1967₂, "Sistemi aggiunti in problemi non conservativi di stabilità elastica", *Rend. Ist. Lombardo* A101, 2, 331–360.

Barta J., 1967, "Sätze über die Stabilität der Ruhestellung eines elastischen Gebildes", *Acta Techn. Acad. Sci. Hung.* **59**, 1/2, 165–182.

Bauer J., Gutkowski W., 1973, "Stability of regular bar structures" (in Polish), *Arch. Inż. Ląd.* **19**, 1, 37–56.

Beck M., 1952, "Die Knicklast des einsteitig eingespannten tangential gedrückten Stabes", *Z. angew. Math. Physik* **3**, 3, 225–228.

Beck M., 1955, "Knickung gerader Stäbe unted Druck und konservativer Torsion", *Ing.-Archiv* **23**, 231.

Belaev N. M., 1924, *Stability of Prismatic Bars under Variable Longitudinal Loading* (in Russian), Inzhenernye sooruzheniya i stroitel'naya Mekhanika, Put', Leningrad, pp. 149–167; *Works on the theory of elasticity and plasticity* (in Russian), Moskva, 1967, pp. 146–173.

Bentley K., 1952, "Lateral stability of beams", *4th Congress IVBH*, Cambridge, 419.

Bergan P. G., Syvertsen T. G., 1978, *Kneckning av aøyler og rammer*, Tapir, Trondheim.

Biezeno C. B., 1938, "Das Durchschlagen eines schwach gekrümmten Stabes", *Z. Angew. Math. Mechanik* **18**, 21.

Biezeno C. B., Grammel R., 1939, *Technische Dynamik*, Springer, Berlin.

Biezeno C. B., Hencky H., 1928, "On the general theory of elastic stability", *Proc. Acad. Sci. Amsterdam* **31**, 6; **32** (1929), 4.

Biezeno C., Koch J., 1925, "Die Knickung von Schraubenfedern", *Z. Angew. Math. Mechanik* **5**, 279.

Birger I. A., Panovko Ya. G. (Ed.), 1968, *Strength, Stability, Vibrations* (Manuals in Russian), Vol. 3, Mashinostroeniye, Moskva.

Blasius H., 1914, "Träger kleinster Durchbiegung und Stäbe grösster Knickfestigkeit bei gegebenem Materialverbrauch", *Z. Math. Physik* **62**, 182.

Bleich F., 1919, "Die Knickfestigkeit elastischer Stabverbindungen", *Eisenbau* **10**, 27.

Bleich F., Bleich H., 1928, "Die Stabilität räumlicher Stabverbindungen", *Z. Österr. Ing.- und Architektenvereines*, 345.

Bleich F., 1952, Buckling Strength of Metal Structures, McGraw-Hill, New York.

Błachut J., 1977, "Shape optimization of a strut under compression at finite deflections by using dynamic programming method" (in Polish), *Mech. Teor. i Stos.* **15**, 3, 373–385.

Błachut J., 1978, "Shape optimization of a strut with dead weight by using dynamic programming method, *Mech. Teor. i Stos.* **16**, 3, 343–351.

Błachut J., Gajewski A., 1980, "A unified approach to optimal design of columns", *Solid Mech. Arch.* **5**, 4, 363–413.

Bogacz R., Irretier H., Mahrenholtz O., 1980, "Optimal design of structures subjected to follower forces", *Ing.-Archiv* **49**, 1, 63–71.

Bogacz R., Mahrenholtz O., 1980, "Optimally stable structures subjected to follower forces", *IUTAM Symp. "Structural Control", Waterloo 1980*, 139–158.

Bolotin W. V., 1951, "On transverse vibrations of bars caused by periodic longitudinal forces" (in Russian), Academy of Sciences of USSR, *Sbornik Poperechn. Koleban. i krit. skorosti*, **1**, 46–77.

Bolotin V. V., 1953_1, "On a parametric excitation of transverse vibration" (in Russian), *Sbornik Poperechn. Koleban. i krit. skorosti*, **2**, 5–44.

Bolotin V. V., 1953_2, "Determination of amplitudes of transverse vibrations caused by longitudinal forces" (in Russian), *Sbornik Poperechn. Koleban. i krit. skorosti*, **2**, 45–64,

Bolotin V. V., 1956_1, *Dynamic Stability of Elastic Systems* (in Russian), Gostekhizdat, Moskva.

Bolotin V. V., 1956_2, "Problems of a general theory of stability" (in Russian), *Prikl. Mat. i Mekh.* **20**, 5, 561–577.

Bolotin V. V., 1961, *Non-Conservative Problems of the Theory of Elastic Stability* (in Russian), Fizmatgiz, Moskva.

Bolotin V. V., Zhinzher N. I., 1969, "Effects of damping on stability of elastic systems subjected to nonconservative forces", *Int. J. Solids and Struct.* **5**, 965–989.

Boström P. O., 1975, "Creep buckling considering material damage", *Int. J. Solids and Struct.* **11**, 765–775.

Březina V., 1962, *Load Bearing Capacity of Steel Bars and Girders* (in Czech), Czechoslovak Academy of Sciences, Prague.

Britvec S. J., 1973, *The Stability of Elastic Systems*, Pergamon Press, New York.

Broszko M., 1953, "Über die unelastische Knickung prismatischer Stäbe", *Bull. Acad. Pol. Sci., Ser. Sci. Techn.* **1**, 3, 71–74.

Brush D. O., Almroth B. O., 1975, *Buckling of Bars, Plates, and Shells*, McGraw-Hill, New York.

Brzoska Z., 1965, *Statics and Stability of Bar and Thin-Walled Structures* (in Polish), PWN, Warszawa.

Bubnov I. G., 1913, "Remarks on the Work by Prof. S. P. Timoshenko *On Stability of Elastic Systems*" (in Russian), *Sborn. Inst. Inzh. Putei Soobshch.* **31**.

Bunyatyan L. B., 1953, "Stability of a thin-walled bar with consideration of creep of materials" (in Russian), *Izv. Akad. Nauk ASSR, Ser. Fiz.-Mat.-Tekhn. Nauk* **6**, 2.

Bürgermeister G., Steup H., 1957, *Stabilitätstheorie*, Teil 1, Akademie-Verlag, Berlin.

Bürgermeister G., Steup H., Kretzchmar H., 1963, *Stabilitätstheorie*, Teil 2, Akademie-Verlag, Berlin.

Celep Z., 1977, "On the lateral stability and eigencurves of elastic beams subjected to vertical and follower forces", *Acta Mechanica* **25**, 3/4, 257–265.

Chajes A., 1974, *Principles of Structural Stability Theory*, Prentice-Hall, Englewood Cliffs, N. J.

Chen W. F., Atsuta T., 1977, *Theory of Beam-Columns*, Mc Graw-Hill, Vol. 1, New York; Vol. 2, New York, 1978.

Chentsov N. G., 1936, "Minimum weight columns" (in Russian), *Trudy CAGI*, 265.

Chernyshev N. A., 1946, *Stability of Springs in Compression* (in Russian), Sbornik "Novye metody rascheta pruzhin", Mashgiz, Moskva.

Chernyshev N. A., 1950, *Stability of Torsion Springs* (in Russian), Sbornik "Novye metody rascheta pruzhin", Mashgiz, Moskva.

Chwalla E., 1934, "Die Theorie des aussermittig gedrückten Stabes aus Baustahl", *Stahlbau* 7, 161.

Chwalla E., 1953, "Über die Behandlung der Stabilitätsfragen in den deutschen und österreichischen Stahlbaunormen", *Stahlbau* 22, 4, 73.

Claudon J. L., 1975, "Characteristic curves and optimum design of two structures subjected to circulatory loads", *J. Mécanique* 14, 3, 531–543.

Clausen T., 1851, "Über die Form architektonischer Säulen", *Bull. Phys.-Mat. Acad. St. Petersburg* 9, 368; *Mélanges Math. et Astron.* 1 (1849–1953), 279.

Clebsch A., 1862, *Theorie der Elastizität fester Körper*, Leipzig.

Collatz L., 1949, *Eigenwertaufgaben mit technischen Anwendungen*, Geest und Portig, Leipzig.

Como M., 1966, "Lateral buckling of a cantilever subject to a follower transversal force", *Int. J. Solids and Struct.* 2, 3, 515–523.

Como M., 1967, *Teoria della stabilità dell'equilibrio elastico*, Liguori, Napoli.

Cornelius W., 1944, "Der elastisch gebettete Druckstab als Spannungsproblem", *Stahlbau* 17, 91.

Croll J. G., Walker A. C., 1973, *Elements of Structural Stability*, Wiley, New York.

Deineko K. S., Leonov M. Ya., 1955, "A dynamic method of investigation of stability of struts subjected to compressive forces" (in Russian), *Prikl. Mat. i Mekh.* 19, 6, 738–744.

Den Hartog J. P., 1940, *Theory of Vibrations*, McGraw-Hill, New York; 2nd ed., 1956.

Dinnik A. N., 1913, *Application of Bessel Function to the Problems of the Theory of Elasticity. Part I, Statics* (in Russian), Donski Polit. Institut; *Collected Works* (in Russian), Vol. 2, Akad. Nauk USSR, Kiev, 1955.

Dinnik A., 1932, "Design of columns of varying cross-section", *Trans. ASME, Applied Mechanics*, September 1932.

Dinnik A. N., 1939, *Buckling* (in Russian), GTTI, Moskva; Akad. Nauk SSSR, Moskva, 1955.

Dinnik A. N., 1946, *Stability of Arches* (in Russian), Gostekhizdat, Moskva.

Domke O., 1938, "Das Entwerfen von Säulen auf Grund des ω-Verfahren", *Bauingenieur* 19, 661.

Dym C. L., 1974, *Stability Theory and its Applications to Structural Mechanics*, Noordhoff, Leyden.

Dzhanelidze G. Yu., 1949, "Generalized relationships of the theory of thin bars" (in Russian), *Reports of Academy of Sciences of USSR* 66, 4.

Engesser F., 1891, "Die Knickfestigkeit gerader Stäbe", *Z. Bauverwaltung* 11, 483.

Engesser F., 1893, "Über die Berechnung auf Knickfestigkeit beanspruchter Stäbe aus Schweiß- und Gußeisen", *Z. Österr. Ing.- und Arch.-Vereins* 45, 38, 506–508.

Engesser F., 1909, "Über die Knickfestigkeit von Stäben veranderlichen Trägheitsmomentes", *Z. Österr. Ing.- und Arch.-Vereins* 63, 34, 544–548.

Falk S., 1956₁, "Die Knickformeln für den Stab mit n Teilstücken konstanter Biegesteifigkeit", *Ing.-Archiv* **24**, 2, 85–91.

Falk S., 1956₂, "Die Berechnung des beliebig gestützten Durchlaufträgers nach dem Reduktionsverfahren", *Ing.-Archiv* **24**, 3, 216–232.

Feodosyev V. I., 1950, *Collected Exercises and Problems in Strength of Materials* (in Russian), Gostekhizdat, Moskva–Leningrad.

Flügge W. (Ed.), 1962, *Handbook of Engineering Mechanics*, Mc Graw-Hill, New York–Toronto–London 1962; Chapter 44, C. Libove, *Elastic Stability*, Ch. 52, J. E. Duberg, *Inelastic Buckling*; Ch. 54, J. Kempner, *Viscoelastic Buckling*.

Frazer R. A., Jones W. P., Skan Sylvia W., 1937, "Approximation to functions and to the solutions of differential equations", *Rep. and Memoranda 1799, Aero. Res. Comm. 1937*.

Frąckiewicz H., 1970, *Mechanics of Lattice Media* (in Polish), Institute of Fundamental Technological Research, Polish Academy of Sciences, PWN, Warszawa.

Frąckiewicz H., 1971, "Buckling of lattice plates," *Arch. Mech. Stos.* **23**, 4, 495–515.

Frąckiewicz H., Misiak J., 1975, "Stability of a plane form of bending in two-flange lattice girders with a pole-oriented force" (in Polish), *Rozpr. Inż.* **23**, 2, 287–298.

Freudenthal A. M., 1946, "Some time effects in structural analysis", *Rep. 6th Int. Congr. Appl. Mech.*, Paris.

Frisch-Fay R., 1962, *Flexible Bars*, Butterworths, London.

Fung Y. C., 1956, *An Introduction to the Theory of Aeroelasticity*, Wiley, New York.

Gajewski A., 1966, "Stability of certain non-prismatic and non-homogeneous bars compressed by a follower force" (in Polish), *Rozpr. Inż.* **14**, 4, 591–608.

Gajewski A., 1969, "Stability of non-prismatic bars in fluid stream" (in Polish), *Mech. Teor. i Stos.* **7**, 3, 311–321.

Gajewski A., 1971, "Optimum shaping of an elastic-plastic column under general conservative behaviour of loading" (in Polish), *Rozpr. Inż.*, **19**, 1, 65–83.

Gajewski A., 1972, "On the destabilizing effect in a non-conservative system with slight internal and external damping", *Proc. Vibr. Probl.* **13**, 2, 187–198.

Gajewski A., Palej R., 1974, "Stability and shape optimization of an elastically clamped bar under tension (in Polish), *Rozpr. Inż.* **22**, 2, 265–279.

Gajewski A., Życzkowski M., 1969, "Optimum shaping of a bar compressed by a pole-oriented force" (in Polish), *Rozpr. Inż.* **17**, 2, 299–329.

Gajewski A., Życzkowski M., 1970, "Optimum design of elastic columns subjected to a general conservative behaviour of loading", *Z. Angew. Math. Physik* **21**, 5, 806–818.

Gajewski A., Życzkowski M., 1971, "An optimum forming of a bar compressed with subtangential force in elastic-plastic range", *Arch. Mech. Stos.* **23**, 2, 147–165.

Gajewski A., Życzkowski M., 1972, "The influence of a simultaneous internal and external non-homogeneous friction on the stability of non-conservative systems" (in Polish), *Mech. Teor. i Stos.* **10**, 1, 127–142.

Galambos T. V., 1964, "Inelastic lateral buckling of beams", *Trans. ASCE* **129**, 657.

Galerkin B. G., 1915, "Bars and shells" (in Russian), *Vestnik Inzhenerov* **19**, 897–908.

Gdański K., 1971, "The problem of buckling and limit load bearing capacity of slender reinforced concrete columns" (in Polish), *Arch. Inż. Ląd.* **17**, 1, 191–217.

Gerard G., 1956, "A creep buckling hypothesis", *J. Aero. Sci.* **23**, 9, 879–882.

Gerard G., 1962, *Introduction of Structural Stability Theory*, McGraw-Hill, New York–Toronto–London.

Gerard G., Becker H., 1952, "Column behaviour under conditions of impact". *J. Aero. Sci.* **19**, 1, 58–62.

Grammel R., 1923, "Das kritische Drillungsmoment von Wellen", *Z. Angew. Math. Mechanik* **3**, 262–266.

Grammel R., 1924, "Die Knickung von Schraubenfedern", *Z. Angew. Math. Mechanik* **4**, 384.

Granholm H., 1929, "On the Elastic Stability of Piles Surrounded by a Supporting Medium", Stockholm.

Greenhill A. G., 1881, "On height consistent with stability", *Proc. Camb. Phil. Soc.* **4**, 65–75.

Greenhill A. G., 1883, "On the strength of shafting when exposed both to torsion and to end thrust", *Proc. Inst. Mech. Eng.*, 182–209.

Gregory M., 1967, *Elastic Instability*, Spon, London.

Gryboś R., 1970, "Asymptotic solution to the problem of impact buckling of a strut", *Proc. Vibr. Probl.* **11**, 2, 179–196.

Gryboś R., 1975, "Impact stability of a bar", *Int. J. Eng. Sci.* **13**, 463–478.

Gryboś, R., 1980, *Stability of Structures under Impact Load* (in Polish), Applied Mechanics Series of Institute of Fundamental Technological Research of the Polish Academy of Sciences, PWN, Warszawa.

Gutkowski W., 1973, *Regular Bar Structures* (in Polish), Instytut Podst. Probl. Techniki PAN, PWN, Warszawa.

Haringx J. A., 1942, *Proc. Konink. Ned. Akad. Wetenschappen* **45**, 533.

Haringx J. A., 1948, "On highly compressible helical springs and rubber rods and their application for vibration-free mountings", *Philips Res. Rept.* **3**, 401–449; **4** (1949), 49–80.

Hartmann F., 1937, *Knickung, Kippung, Beulung, Deuticke*, Leipzig–Wien.

Hartz B. J., 1965, "Matrix formulation of structural stability problems", *Proc. ASCE, J. J. Struct. Div.* **91**, 141–157.

Hauger W., 1966, "Die Knicklasten elastischer Stäbe unter gleichmäßig verteilten und linear veränderlichen, tangentialen Druckkräften", *Ing.-Archiv* **35**, 4, 221–229.

Hauger W., 1975, "Stability of compressible rod subjected to nonconservative forces", *J. J. Appl. Mech.* **42**, 4, 887–888.

Herrmann G., Jong I. C., 1966, "On nonconservative stability problems of elastic systems with slight damping", *J. Appl. Mech.* **33**, 1, 125–133.

Hicks G. W., 1967, "Finite-element elastic buckling analysis", *Proc. ASCE, J. Struct. Div.*, **93**, 6, 71–86.

Hoff N. J., 1951, "The dynamics of the buckling of elastic columns", *J. Appl. Mech.* **18**, 1, 68–74.

Hoff N. J., 1954, "Buckling and stability", *J. Roy. Aero. Soc.* **58**, 3–52.

Hoff N. J., 1956, *The Analysis of Structures*, Wiley, New York, Chapman and Hall, London.

Hoff N. J., 1958, "A survey of the theories of creep buckling", *Proc. 3rd U.S. Nat. Congr. Appl. Mech.*, Pergamon Press, 29–49.

Hoff N. J., 1964, "Reversed creep: a remark to the creep buckling theory of Rabotnov and Shesterikov", *J, Mech. Phys. Solids* **12**, 2, 113–123.

Horne M. R., 1961, "The stability of elastic-plastic structures", *Progress in Solid Mechanics* **2**, 277–322.

Huang N. C., 1976, "Creep buckling of imperfect columns", *J. Appl. Mech.* **43**, 131–136.

Huber M. T., 1930, "Critical loading for columns with step-wise variable section" (in Polish), IBTL, Warszawa, also *Pisma*, Vol. 2, PWN, Warszawa, 1956, pp. 483–500.

Hui E., 1955, "Knickung verwundener Stäbe unter Druck", *Österr. Ing.-Archiv* 9, 4, 288–319.

Hult J. A. H., 1955, "Critical time in creep buckling", *J. Appl. Mech.* 22, 3, 432.

Hurlbrink E., 1910, "Berechnung zylindrischer Druckfedern auf Sicherheit gegen seitliches Ausknicken", *Z. VDI* 54, 138.

Huseyin K., 1975, *Non-linear Theory of Elastic Stability*, Noordhoff, Leyden.

Ilyushin A. A., 1960, "On elastic-plastic stability of structures with bar members" (in Russian), *Inzh. Sbornik* 27, 87–91.

Ishlinskii A. Yu., 1954, "Analysis of problems of equilibrium of elastic solids from the point of view of the theory of elasticity" (in Russian), *Ukr. Mat. Zhurnal* 6, 2.

Jahsman W. E., 1972, "Creep stability of a column with coupled geometric imperfection and material behaviour effects", *Proc. IUTAM Symp. Creep in Structures II*, Springer, pp. 360–369.

Jasiński F. S., 1895, "Zu den Knickfragen", *Schw. Bauzeiztung* 25, 10, 63–64.

Jasiński F. S., 1894, *On Longitudinal Bending Strength* (in Russian), *St. Petersburg; Studies on the Stiffness of Bent Bars*, ed. by Przegląd Techniczny, Warszawa, 1895 and *Arch. Mech. Stos.* 8, 3, 1956, 319–390.

Johnston B. G. (Ed.), 1960, *Guide to Design Criteria for Metal Compression Members*, Wiley, New York; ed. II, 1966; *Guide to Stability Design Criteria for Metal Structures*, Wiley, New York, 1976.

Ježek K., 1937, *Die Festigkeit von Druckstäben aus Stahl*, Springer, Wien.

Kachanov L. M., 1981, "Stability of a plane bending form beyond the elastic limit" (in Russian), *Prikl. Mat. i Mekh.* 15, 1, 2 and 5.

Kacner A., 1961, "Bending, stability and vibration of bars of a variable cross-section" (in Polish), *Rozpr. Inż.* 9, 3, 425–441.

Kaliski S., 1955, "Impact stability of bars" (in Polish), *Biuletyn WAT* 4, 14, 4–118.

Kármán T., 1909, "Untersuchungen über Knickfestigkeit", *Mitt. u. Forschungsarb. VDI*, 81, Berlin.

Keller J. B., 1960, "The shape of the strongest column", *Arch. Rat. Mech. Analysis* 5, 4, 275–285.

Kempner J., 1952, "Creep bending and buckling of linear viscoelastic columns", *PIBAL Rep.* No. 195, *Brooklyn*; *NACA TN* 3136, Jan. 1954.

Kempner J., 1952_2, "Creep bending and buckling of non-linearly viscoelastic columns", *PIBAL Rep.* No. 200, *Brooklyn*; *NACA TN* 3137, Jan. 1954.

Kirchhoff G. R., 1859, Über das Gleichgewicht und die Bewegung eines unendlich dünnen elastischen Stabes", *J. Reine Angew. Math. Crelle* 56, 285–313.

Knops R. J., Wilkes E. W., 1973, *Theory of Elastic Stability*, Encycl. of Physics, Vol. VIa/3, 125–302, Springer, Berlin.

Koiter W. T., 1945, "On the stability of elastic equilibrium", Delft 1945 (in Dutch), *NASA Techn. Transl.* F10 (1967), 833 (English transl.).

Koiter W. T., 1963, "On the concept of stability of equilibrium for continuous bodies", *Koninkl. Ned. Akad. van Wetensch.* B66, 173—177.

Koiter W. T., 1965, "The energy criterion of stability for continuous elastic bodies", *Koninkl. Ned. Akad. van Wetensch.* B68, 107–113.

Koiter W. T., 1967, "Postbuckling analysis of a simple two–bar frame", *Recent Progress Appl. Mech.* (Odqvist Volume), Stockholm, 337–354.

Kollbrunner C. F., Meister M., 1955, *Knicken*, Springer, Berlin–Göttingen–Heidelberg; 2nd ed., 1961.

Kopecki H., Zacharzewski J., 1972, "Dissipated energy as a criterion of rheological stability of compressed bar". (in Polish), *Arch. Bud. Masz.* 19, 4, 559–564.

Kordas Z., 1963, "Stability of an elastically clamped bar in the general case of loading" (in Polish), *Rozpr. Inż.* 11, 3, 435–448.

Kordas Z., 1965, "Stability of a bar in a parallel fluid stream with head resistance considered" (in Polish), *Rozpr. Inż.* 13, 1, 19–41.

Kordas Z., Życzkowski M., 1963, "On the loss of stability of a rod under a super-tangential force", *Arch. Mech. Stos.* 15, 1, 7–31.

Kordecki Z., 1964, "Buckling of slender bars under short-term loads" (in Polish), *Rozpr. Inż.* 12, 2, 309–322.

Kordecki Z., 1966, "Non-elastic buckling of a bar under short-term load (in Polish), *Rozpr. Inż.* 14, 1, 69–81.

Kornishin M. S., Isanbayeva F. S., 1968, *Flexible Plates and Panels* (in Russian), Nauka, Moskva.

Kornoukhov N. V., 1949, *Strength and Stability of Bar Systems* (in Russian), Stroiizdat, Moskva.

Korotkin Ya. I., Lokshin A. Z., Sivers N. L., 1953, *Bending and Stability of Bars and Ba. Systems* (in Russian), Mashgiz, Moskva–Leningrad.

Kowal Z., 1964, "Stability of an axially compressed elastic bar in a viscoelastic medium" (in Polish), *Arch. Inż. Ląd.* 10, 2, 197–204.

Kowalski A., 1967, "Stability of bars of a piece-wise variable cross-section compressed by a follower force" (in Polish), *Rozpr. Inż.* 15, 2, 197–209.

Kowalski A., Życzkowski M., 1967, "The stress safety condition in the case of non-conservative elastic stability problems" (in Polish), *Mech. Teor. i Stos.* 5, 4, 411–423.

Krynicki E., Mazurkiewicz Z., 1963, *Frames with Bars of Variable Cross-Section* (in Polish), Arkady, Warszawa; 2nd ed., Institute of Fundamental Technolgical Research, PWN, Warszawa, 1966.

Krynicki E., Mazurkiewicz Z., 1963, "Bending and buckling of frameworks of solid bars of variable cross section" (in Polish), *Arch. Inż. Ląd.* 9, 2, 191–211.

Krynicki E., Mazurkiewicz Z., 1965, "Bending and buckling of space frames of bars of variable rigidities" (in Polish), *Rozpr. Inż.*, 13, 2, 361–396.

Krzyś W., 1967, "Shape optimization of compressed thin-valled columns of a closed section in stability aspect" (in Polish), *Zesz. Nauk. Polit. Krak.* 4.

Krzyś W., 1968, "Optimale Formen gedrückter dünnwandiger Stützen im elastisch-plastischen Bereich", *Wiss Z. Techn. Univ. Dresden* 17, 2, 407–410.

Kurshin L. M., 1978, "Stability at creep", *Izv. AN USSR* (Works of the Academy of Sciences, of the Soviet Union Mechanics of Solids) (in Russian), *Mehk. Tv. Tela* 3, 125–160.

Laasonen P., 1948, "Nurjahdustuen edullisimmasta poikkipinnanvalinnasta", *Tekn. Aikakauslehti* 38, 2, 49.

Lang H. A., 1947, *Quart. Appl. Math.* 5, 510.

Lapunov A. M., 1892, *A General Problem of Stability of Motion* (in Russian), Kharkov.

Lavrentev M. A., Ishlinskii A. Yu., 1949, "Dynamic forms of loss of stability in elastic systems" (in Russian), *Doklady AN SSSR* 65, 6.

Leibenzon L. S., 1914, "Strength of twisted columns" (in Russian), *Bulletin of Higher Courses for Women in Tyflis* 1; *Collected Works* 1, 23–38, 1951.

Leipholz H., 1960, "Knickung verwundener Stäbe unter Druck einer konservativen, kontinuierlich und gleichmäßig verteilten Belastung", *Ing.-Archiv* **29**, 4, 262–279.

Leipholz H., 1961, "Der schlanke Stab unter konservativer Belastung als Variationsproblem", *Ing. -Archiv* **30**, 2, 105–116.

Leipholz H., 1962, "Die Knicklast des einseitig eingespannten Stabes mit gleichmässig verteilter, tangentialer Längsbelastung", *Z. Angew. Math. Physik* **13**, 6, 581–589.

Leipholz H., 1963, "Über die Konvergenz des Galerkinschen Verfahrens bei nichtselbstadjungierten und nichtkonservativen Eigenwertproblemen", *Z. Angew. Math. Physik* **14**, 1, 70–79.

Leipholz H., 1963, "Über das statische Kriterium bei nichtkonservativen Stabilitätsproblemen der Elastomechanik", *Ing.-Archiv* **32**, 3, 214–220.

Leipholz H., 1967, "Über die Wahl der Ansatzfunktionen bei der Durchführung des Verfahrens von Galerkin", *Acta Mech.* **3**, 3, 295–317.

Leipholz H., 1970, *Stability Theory*, Academic Press, New York, *Stabilitätstheorie*, Teubner, Stuttgart, 1968.

Leipholz H. H. E., 1974, "On conservative elastic systems of the first and second kind", *Ing-Archiv* **43**, 255–271.

Leipholz H. (Ed.), Huseyin K., Życzkowski M., 1978, *Stability of Elastic Structures*, CISM Courses and Lectures No. 238, Springer, Wien–New York.

Leites S. D., 1954, *Stability of Steel Bars in Compression* (in Russian), Stroiizdat, Moskva.

Leites S. D., 1965, "Studies on finite deformations of elastic-plastic bars subjected to eccentric compressive forces" (in Russian), *Prikl. Mech.* **2**, 4, 72–77.

Lekkerkerker J. G., 1962, "On the stability of an elastically supported beam subjected to its smallest buckling load", *Koninkl. Nederl. Akad. van Wetensch.* **B65**, 190.

Levinson M., 1966, "Application of the Galerkin and Ritz methods to nonconservative problems of elastic stability", *Z. Angew. Math. Physik* **17**, 3, 431–442.

Libove C., 1952, "Creep buckling of columns", *J. Aero. Sci.* **19**, 7, 459.

Lin T. H., 1953, "Stresses in columns with time dependent elasticity", *Proc. 1st Midwestern Conf. Solid Mech.*, Urbana, 196–199.

Lindner J., Bamm D., 1977, "Influence of realistic yield stress distributions on lateral torsional buckling loads", *Prel. Rep. 2nd Int. Colloquium Stability of Steel Structures*, Liège, 213–216.

Love A. E. H., 1892, *A Treatise on the Mathematical Theory of Elasticity*, Cambridge; further editions: 1906, 1920, and 1927.

Lurie A. I., 1938, "Bending and stability of naturally twisted straight bars" (in Russian), *Prikl. Mat. i Mekh.* **2**, 1, 55–58.

Maag H., 1957, "Knickung von Schraubenfedern unter Druck und konservativer Torsion", *Ing.-Archiv* **25**, 2.

Madejski J., 1956, "Buckling of a prismatic bar as a dynamic plasticity theory problem" (in Polish), *Rozpr. Inż.* **4**, 3, 351–366.

Mahrenholtz O., Bogacz R., 1981, "On the shape of characteristic curves for optimal structures under non-conservative loads" *Ing.-Archiv* **50**, 2, 141–148.

Maier G., Drucker D. C., 1973, "Effects of geometry change on essential features of inelastic behaviour", *J. Eng. Mech. Div., Proc. ASCE* **99**, 4, 819–834.

Makushin V. M., 1947, "Dynamic stability of the state of stress of elastic bars" (in Russian), *Trudy Kafedry sopr. mat. MVTU Baumana*, 3.

Makushin V. M., 1950, *Transverse Vibration and Stability of Helical Springs* (in Russian), "Dinamika i prochnost' pruzhin", AN SSSR, Moskva.

Makushin V. M., 1952, "Stability of Straight Bars Subjected to Compressive Forces" (in Russian), *Tr. Mosk. Aviats. Inst.* **17**.

Malkin I., 1926, "Formänderung eines axial gedrückten dünnen Stabes", *Z. Angew. Math. Mech.* **6**, 73.

Malvick A. J., Lee L. H. N., 1965, "Buckling behaviour of an inelastic column", *J. Eng. Mech. Div., Proc. ASCE* **91**, 3, 113–127.

Markiewicz M., 1980, "Forming of simple trusses under elastic-plastic stability conditions by way of determination of the contour of complete non-uniqueness" (in Polish), *Rozpr. Inż.* **28**.

Markiewicz M., Życzkowski M., 1981, "Contour of complete non-uniqueness as a method of structural optimization with stability constraints", *J. Optimiz. Theory Appl.* **4**.

Matevosyan R. R., 1961, *Stability of Complex Bar Systems* (in Russian), Stroiizdat, Moskva.

Mayer R., 1921, *Die Knickfestigkeit*, Springer, Berlin.

Mazurkiewicz Z., 1961, "Application of the method of kernel traces of integral equation in bar stability problems" (in Polish), *Arch. Inż. Ląd.* **7**, 4, 507–531.

Mazurkiewicz Z., 1962, "Approximate determination of the critical force with error evaluation for buckling of a bar of variable cross-section" (in Polish), *Rozpr. Inż.* **10**, 1, 181–190.

Mazurkiewicz Z., 1965, "Buckling of straight bars of variable bending rigidities" (in Polish), *Rozpr. Inż.* **13**, 3, 623–635.

Mazurkiewicz Z., 1966, "Bending, buckling and vibrations of elastic structures composed of nonhomogeneous rectilinear bars with cross-sections varying in an arbitrary manner", *Arch. Mech. Stos.* **18**, 5, 649–695.

Michell A. G. M., 1899, "Elastic stability of long beams under transverse forces", *Phil. Mag.* (5th series) **48**, 298–309.

Migliacci A., 1965, "Instabilità delle travi alte sotto carichi transversali di tipo non conservativo", *Cemento* **62**, 12, 17–27.

Mises R., 1923, "Über die Stabilitätsprobleme der Elastizitätstheorie", *Z. Angew. Math. Mech.* **3**, 406–422; *Selecta*, 1. Providence 1963, 217–244.

Mises R., Ratzersdorfer J., 1926, "Die Knicksicherheit von Rahmentragwerken", *Z. Angew. Math. Mech.* **6**, 181.

Misiak J., 1976, "Stability of lattice girders subjected to the action of pole-oriented forces" (in Polish), *Rozpr. Inż.* **24**, 4, 683–697.

Movchan A. A., 1956, "On the vibration of plates moving in gas" (in Russian), *Prikl. Mat. i Mekh.* **2**, 211–222.

Movchan A. A., 1963, "On the stability of processes of deformation of continuous media" (in Russian), *Arch. Mech. Stos.*, **15**, 5, 659–682.

Murzewski J., 1972, "Calculation of steel bars for buckling by means of a unified table of coefficients" (in Polish), *Inż. i Bud.* **29**, 7, 245–248.

Naleszkiewicz, J., 1953, *Elastic Stability Problems* (in Polish), Wyd. Komunikacyjne, Warszawa; 2nd ed., PWN, Warszawa, 1958.

Naleszkiewicz J., 1954, "Quantification of elastic instability effects" (in Polish), *Arch. Mech. Stos.* **6**, 1, 3–32; 2, 261–290.

Nath B., 1974, *Fundamentals of Finite Elements for Engineers*, The Athlone Press, London.

Nemat-Nasser S., Herrmann G., 1966, "On the stability of equilibrium of continuous systems", *Ing.-Archiv* **35**, 1, 17–24.

Nemat-Nasser S., Herrmann G., 1966, "Adjoint systems in non-conservative problems of elastic stability", *AIAA Journal*, 4 12, 2221–2222.

Nethercot D. A., Rockey K. C., 1971_1, "Finite element solutions for the buckling of columns and beams", *Int. J. Mech. Sci.* 13, 945–949.

Nethercot D. A., Rockey K. C., 1971_2, "A unified approach to the elastic lateral buckling of beams", *Struct. Eng.* 49, 7, 321–330.

Nikolai F. L., 1907, "Lagrange's problem on most convenient shape of columns" (in Russian), *Izv. Petersburg Pol. Inst.* 8; *Trudy po Mekhanike*, Moskva, 1955, pp. 9–44.

Nikolai E. L., 1928, "On stability of a rectilinear form of equilibrium of a bar subjected to compressive and twisting forces" (in Russian), *Izv. Leningr. Pol. Inst.*, 31; *Trudy po Mekhanike*, Moskva, 1955, pp. 357–387.

Novozhilov V. V., 1948, *Principles of Non-linear Theory of Elasticity* (in Russian), Gostekhizdat, Leningrad–Moskva.

Nowacki W., 1956, "On stability problems of straight bars and plane grids" (in Polish), *Arch. Inż. Ląd.*, 2, 4, 359–380.

Odqvist F. K. G., 1954, "Influence of primary creep on column buckling", *J. Appl. Mech.* 21, 3, 295.

Olhoff N., Rasmussen S. H., 1977, "On single and bimodal optimum buckling loads of clamped columns", *Int. J. Solids Struct.* 13, 605–614.

Osgood W. M., 1935, "The double-modulus theory of column action". *Civil Engineering* 5, 3, 173–175.

Ostachowicz W., 1975, "A discrete model for calculating natural vibration and stability of axially loaded bars of arbitrarily variable cross-section" (in Polish), *Mech. Teor. i Stos.* 13, 3, 475–492.

Ostenfeld A., 1898, "Exzentrische und zentrische Knickfestigkeit", *Z. Ver. Deutsch. Ing.* 94, 1462.

Panovko Ya. G., 1965, *On the Modern Concept of Elastic-Plastic Buckling* (in Russian), Probl. ustoich. v stroit. mekh., Moskva, pp. 92–103.

Panovko Ya. G., Gubanova I. I., 1964, *Stability and Vibration of Elastic Systems* (in Russian), Nauka, Moskva; 2nd ed., Moskva, 1967; 3rd ed., Moskva, 1979.

Papkovich P. F., 1937, *Proc. 4th Int. Congr. Appl. Mech., Cambridge 1934*; Trudy Leningr. Korabl. Inst.

Papkovich F. P., 1941, *Structural Mechanics of Ships* (in Russian), 2nd part, Sudpromgiz, Leningrad.

Petre A., 1966, *Theory of Aeroelasticity* (in Romanian), Ed. Academiei RSR, Bucureşti.

Pflüger A., 1950, *Stabilitätsprobleme der Elastostatik*, Springer, Berlin–Göttingen–Heidelberg, further editions: 1964, 1975.

Pflüger A., 1952, "Zur plastischen Knickung gerader Stäbe", *Ing.-Archiv* 20, 5, 291–301.

Pflüger A., 1955, "Zur Stabilität des tangential gedrückten Stabes", *Z. Angew. Math. Mechanik* 35, 5, 191.

Piątek M., 1954, "Elastic lateral buckling of straight bars in a general case" (in Polish), *Arch. Mech. Stos.* 6, 2, 235–260.

Piątek M., 1956, "Dynamic stability of axially loaded bars of an arbitrarily variable cross-section" (in Polish), *Arch. Mech. Stos.* 8, 1, 51–68.

Pikovskii A. A., 1961, *Statics of Bar Systems with Compressed Elements* (in Russian), Fizmatgiz, Moskva.

Piszczek K., 1955, "Longitudinal and transverse vibrations of axially loaded bars of an arbitrarily variable cross-section as a non-linear problem" (in Polish), *Arch. Mech. Stos.* 7, 3, 345–362.

Piszczek K., 1956, "Dynamic stability of the plane form of bending under various boundary conditions" (in Polish), *Rozpr. Inż.* **4**, 2, 175–225.

Plaut R. H., 1971, "On the stability and optimal design of elastic structures", *Stability Study No.* **6**, *Univ. Waterloo, Sol. Mech. Div.* 547–577.

Plaut R. H., 1975, "Optimal design for stability under dissipative, gyroscopic or circulatory loads", *IUTAM Symp. Optimization in Structural Design, Warsaw 1973*, Springer, 168–180.

Polish Standard PN-80/B-03200, Steel Structures, Wyd. Normalizacyjne, Warszawa, 1980.

Ponomariev S. D., Biderman V. L., Likhariev K. K., Makushin V. M., Malinin N. M., Feodosev V. I., 1959, *Strength Calculations in Mechanical Engineering* (in Russian), Vol. 3, Mashgiz, Moskva.

Popov E. P., 1948, *Non-linear Problems of Statics of Thin Bars* (in Russian), Gostekhizdat, Leningrad, Moskva.

Prandtl L., 1899, *Kipperscheinungen*, Diss. Nürnberg–München.

Przemieniecki J. S., 1968, *Theory of Matrix Structural Analysis*, McGraw-Hill, New York–Toronto–London.

Rabotnov Yu. N., Shesterikov S. A., 1957, "Stability of bars and plates in the conditions of creep" (in Russian), *Prikl. Mat. i Mekh.* **21**, 3, 406–412.

Rakowski G., 1969, "Matrix analysis of stability of a straight bar on deformable foundation" (in Polish), *Arch. Inż. Ląd.* **15**, 4, 661–689.

Ratzersdorfer J., 1936, *Die Knickfestigkeit von Stäben und Stabwerken*, Springer, Wien.

Reissner E., 1979, "On lateral buckling of end-loaded cantilever beams", *Z. Angew. Math. Physik* **30**, 1, 31–40.

Reissner H., 1904, "Über die Stabilität der Biegung", *Sitz.-Ber. Berl. Math. Gesellschaft* **3**, 53–56.

Ritz W., 1909, "Über eine neue Methode zur Lösung gewisser Variationsprobleme der mathematischen Physik", *Z. Reine Angew. Math.* **135**, 1–61.

Roliński J., 1969, "Some problems of dynamic stability of shafts loaded by a pulsating torque and a constant axial force", *Zag. Drgań Niel.* **8**, 231–285.

Roorda J., 1972, *Concepts in Elastic Structural Stability*, Mechanics Today 1, Pergamon Press, pp. 322–372.

Ross A. D., 1946, "The effect of creep on instability and indeterminacy investigated by plastic models", *Struct. Eng.* **24**, 413.

Rysz M., Życzkowski M., 1979, "Unsteady creep of a bar compressed by an eccentric force arbitrarily variable in time" (in Polish), *Rozpr. Inż.* **27**, 1, 155–170.

Rzhanitsin A. R., 1946, "Processes of deformation of structures consisting of elastic-viscous elements (in Russian), *Dokl. Akad. Nauk SSSR* **52**, 25, 1.

Rzhanitsin A. R., 1949, *Some Problems of Mechanics of Systems Deforming in Time* (in Russian), Gostekhizdat, Moskva–Leningrad.

Rzhanitsin A. R., 1955, *Stability of Equilibrium of Elastic Systems* (in Russian), Gostekhizdat, Moskva.

Rzhanitsin A. R., 1965, *Stability at Creep* (in Russian), Probl. Ustoich. w Stroit. Mekh., Moskva, pp. 104–118.

Rzhanitsin A. R., 1966, *Theory of Creep* (in Russian), Stroiizdat, Moskva.

Sala, I., 1951, "Über die unelastische Knickung eines verjüngten Stabes", *Suomen Teknillinen Korkeakoulu*, Helsinki, Vol. 3.

Schaefer H., 1934, Diss. Hannover; *Z. Angew. Math. Mech.* **14**, 367.

Schleusner A., 1938, *Die Stabilität des mehrfeldrigen elastisch gestützten Stabes*, Forschungshefte aus dem Gebiete des Stahlbaues 1, Springer, Berlin.

Schnell W., 1955, "Berechnung der Stabilität mehrfeldriger Stäbe mit Hilfe von Matrizen", *Z. Angew. Math. Mech.* **35**, 269.

Sewell M. J., 1971, "A survey of plastic buckling", "Stability", *Study No. 6, University of Waterloo, Sol. Mech. Div.*, 85–197.

Shanley F. R., 1946, "The column paradox", *J. Aero. Sci.* **13**, 12, 678.

Shanley F. R., 1947, "Inelastic column theory", *J. Aero. Sci.* **14**, 5, 261–268.

Shanley F. R., 1952, *Weight-Strength Analysis of Aircraft Structures*, McGraw-Hill, New York.

Shashkov I. Ye., 1950, "On stability of a prismatic bar subjected to compressive and torsional forces with an arbitrary form of cross-section" (in Russian), *Inzh. Sbornik* **7**, 101–122.

Shesterikov S. A., 1959, "On criterion of stability at the presence of creep" (in Russian), *Prikl. Mat. i Mekh.* **23**, 6, 1101–1108.

Shield R. T., Green A. E., 1963, "On certain methods in the stability theory of continuous systems", *Arch. Rat. Mech. Anal.* **12**, 4, 354–360.

Skrzypek J., 1979, "Plastic strains and analysis of the forms of loss of load capacity of geometrically non-linear toroidal shells" (in Polish), *Zesz. Nauk. Pol. Krak.* **2**.

Smirnov A. F., 1958, *Stability and Vibration of Structures* (in Russian), Transzheldorizdat, Moskva.

Snitko N. K., 1956, *Stability of Compressed and Compressed and Bent Bar Systems* (in Russian), Stroiizdat, Leningrad–Moskva.

Snitko N. K., 1968, *Stability of Bar Systems in Elastic-Plastic Range* (in Russian), Stroiizdat, Leningrad.

Southwell R. V., 1932, "On the analysis of experimental observations in problems of elastic stability", *Proc. Roy. Soc.* **A135**, 601.

Southwell R. V., 1936, *An Introduction to the Theory of Elasticity*, Oxford University Press, Oxford.

Stern J., 1979, "Der Gelenkstab bei großen elastischen Verformungen", *Ing.-Archiv* **48**, 3, 173–184.

Streletskii N. S., 1959, *Work of Compressed Columns* (in Russian), Stroiizdat, Moskva.

Sugiyama Y., Kawagoe H., 1975, "Vibration and stability of elastic columns under the combined action of uniformly distributed vertical and tangential forces", *J. Sound and Vibr.* **38**, 3, 341–355.

Sułocki J., 1955, "Buckling of a bar in elastic medium" (in Polish), *Arch. Mech. Stos.* **7**, 4, 561–575.

Supple W. J., (Ed.), 1973, *Structural Instability*, IPC Science and Technology Press, Guildford.

Szelągowski F., 1927, *On the Question of Stability of Bars of Variable Moment of Inertia* (in Polish), ed. by *Przegląd Techniczny*, Warszawa.

Szuwalski K., 1970, "A case of eccentric compression in non-linear approach" (in Polish), *Rozpr. Inż.* **18**, 2, 267–280.

Taylor J. E., 1967, "The strongest column: an energy approach", *J. Appl. Mech.* **34**, 486–487,

Tetmajer L., 1890, *Mitt. Anstalt zur Prüfung von Baumaterialen*, 4, Methoden und Resultate. Zürich 1890; 8, Zürich 1896.

Tetmajer L., 1903, *Die Gesetze der Knickungs- und der zusammengesetzten Druckfestigkeit der technisch wichtigsten Baustoffe*, Deuticke, Leipzig–Wien.

Thompson J. M. T., Hunt G. W., 1973, *A General Theory of Elastic Stability*, Wiley, London–New York.

Timoshenko S. P., 1935, "Buckling of flat curved bars and slightly curved plates", *J. Appl. Mech.* **2**, 1, 17–20.

Timoshenko S. P., 1936, *Theory of Elastic Stability*, McGraw-Hill, New York.

Timoshenko S. P., Gere J. M., 1961, *Theory of Elastic Stability*, McGraw-Hill, New York–Toronto–London.

Trefftz E., 1933, "Zur Theorie der Stabilität des elastischen Gleichgewichts", *Z. Angew. Math. Mechanik* **13**, 2, 160–165.

Trojnacki A., 1975, "The effect of friction in articulated joints on the course of buckling of a strut" (in Polish), *Mech. Teor. i Stos.* **13**, 3, 363–371.

Trojnacki A., Życzkowski M., 1976, "Investigation of the Rabotnov–Shesterikov creep stability under general loading programs", *Rozpr. Inż.* **24**, 2, 253–266.

Vetter H., 1960, *Stabwerkknickung*, VEB Verlag Technik, Berlin.

Vianello L., 1898, "Untersuchung der Knickfestigkeit gerader Stäbe", *Zeitschr. Ver. Deutsch. Ing.* **42**, 1436–1443.

Vlasov V. Z., 1940, *Thin-Walled Elastic Bars* (in Russian), Stroiizdat, Moskva; 2nd ed., Fizmatgiz, Moskva, 1959.

Volmir A. S., 1963, *Stability of Elastic Systems* (in Russian), Fizmatgiz, Moskva; 2nd ed., *Stability of Deformable Systems*, Nauka, Moskva, 1967.

Wahl, A. M., 1963, *Mechanical Springs*, McGraw-Hill, New York–Toronto–London.

Walczak J., 1959, "Adaptation of Tetmajer's formula to strength dimensioning of bars by direct method" (in Polish), *Czas. Techn.* **64**, 6/7, 22–26.

Wang C. T., 1953, *Applied Elasticity*, McGraw-Hill, New York.

Waszczyszyn Z., Życzkowski M., 1962, "Finite elastic deflections of a stretchable beam on immovable supports", *Arch. Mech. Stos.* **14**, 1, 61–82.

Waszczyszyn Z. (Ed.), Życzkowski M., Roorda J., Massonnet Ch., 1981, *Modern Methods of Structural Stability Analysis* (in Polish), Ossolineum, Polish Academy of Sciences, Wrocław.

Weiss S., 1969, "Remarks on stability criteria in the case of flexure of a thin-walled bar" (in Polish), *Arch. Inż. Ląd.* **15**, 3, 623–640.

Weiss S., *Stability of Metal Structures* (in Polish), Arkady, Warszawa (to appear).

Wesołowski Z., 1974, "Stability of non-perfect elastic systems, *Bull. Acad. Pol., Ser. Sci. Techn.* **22**, 4, 171–175.

Wierzbicki W., 1954, "On the formation of buckling in straight bars" (in Polish), *Rozpr. Inż.* **14**, 1, 1–66.

Wilczyński A., 1976, "Stability of the plane form of bending of a beam with a broken axis" (in Polish), *Mech. Teor. i Stos.* **14**, 1, 163–173.

Wiśniewski S., 1964, "Stability of the plane form of a beam axially compressed by forces applied at end-points" (in Polish), *Arch. Bud. Maszyn* **11**, 2, 429–434.

Wiśniewski S., 1975, Dynamic stability of the plane form of a beam axially compressed by periodically variable forces aplied at end-points" (in Polish), *Arch. Bud. Masz.* **22**, 4, 429–436.

Wnuk M., Życzkowski M., 1959, "The influence of weakening of a bar on the critical force in elastic-plastic range" (in Polish), *Rozpr. Inż.* **7**, 3, 311–336.

Wojdanowska R., 1974, "Optimum forming of truss systems under creep conditions with

reference to the Rabotnov–Shesterikov buckling theory" (in Polish), *Mech. Teor. i Stos.* **12**, 3, 245–263.

Wojdanowska R., 1978, "Optimal design of weakly curved compressed bars with Maxwell type creep effects" *Arch. Mech. Stos.* **30**, 6, 845–851.

Wojdanowska R., Życzkowski M., 1972, "Shape optimization of truss systems under creep conditions with reference to the Kempner–Hoff buckling theory" (in Polish), *Arch. Inż. Ląd.* **18**, 4, 511–530.

Wojdanowska R., Życzkowski M., 1980, "On optimal imperfect columns subjected to linear creep buckling", *J, Appl. Mech.* **47**, 2, 438–439.

Wojdanowska-Zając R., Życzkowski M., 1969, "Shape optimization of trusses with consideration of stability conditions" (in Polish), *Rozpr. Inż.* **17**, 347–358.

Woźniak C., 1970, *Surface Netlike Girders*, IPPT PAN-PWN, Warszawa.

Ylinen A., 1956, "A method of determining the buckling stress and required cross-sectional area for centrally loaded straight columns in elastic and inelastic range", *Mem. Ass. Int. Ponts Charp.* **16**, 529–550 (Finnish original in *Tekn. Aikakausl.* **38** (1948), 9).

Yoshida H., Imoto Y., 1973, "Inelastic buckling of restrained beams", *J. Eng. Mech. Div., Proc. ASCE* **99**, 343.

Zahorski S., 1965, "Instability of a non-linearly viscoelastic column under finite compression", *Arch. Mech. Stos.* **17**, 6, 801–821.

Zhukov A. M., Rabotnov Yu. N., Churikov F. S., 1953, Experimental verifications of some theories of creep (in Russian), *Inzh. Sbornik* **17**, 163–170.

Ziegler H., 1952, "Die Stabilitätskriterien der Elastomechanik", *Ing.-Archiv* **20**, 1, 49–56.

Ziegler H., 1953, "Linear elastic stability", *Z. Angew. Math. Physik* **4**, 89–121, 167–185.

Ziegler H., 1956, "On the concept of elastic stability", *Adv. Appl. Mech.* **4**, 351–403.

Ziegler H., 1968, *Principles of Structural Stability*, Blaisdell, Waltham.

Zimmermann H., 1930, *Die Lehre vom Knicken auf neuer Grundlage*, W. Ernst und Sohn, Berlin.

Zweiling K., 1953, *Gleichgewicht und Stabilität*, VEB Verlag Technik, Berlin.

Życzkowski M., 1953, "Deflection of a bar eccentrically compressed under critical force" (in Polish), *Rozpr. Inż.* **1**, 4, 1–12.

Życzkowski M., 1954, "Elastic-plastic buckling of some non-prismatic bars" (in Polish), *Rozpr. Inż.* **2**, 2, 233–289.

Życzkowski M., 1956_1, "Calculation of critical forces for elastic non-prismatic bars by partial interpolation method" (in Polish), *Rozpr. Inż.* **4**, 3, 367–412.

Życzkowski M., 1956_2, "On the choice of optimum shape of axially compressed bars" (in Polish), *Rozpr. Inż.* **4**, 4, 441–456.

Życzkowski M., 1957, "Influence of the decrease of eccentricity on deflections of eccentrically compressed bars" (in Polish), *Rozpr. Inż.* **5**, 3, 399–412.

Życzkowski M., 1959_1, "Some problems of creep buckling of homogeneous and non-homogeneous bars", *IUTAM Symp. Non-Homogen., Warszawa, 1958*, Pergamon Press, pp. 353–363.

Życzkowski M., 1959_2, "Finite deflections of eccentrically compressed bars with initial curvature" (in Polish), *Book in memoriam of W. Wierzbicki*, Warszawa, pp. 479–518.

Życzkowski M., 1960_1, "A survey and classification of studies on creep buckling" (in Polish), *Czas. Techn.* **65**, 1, 1–7.

Życzkowski M., 1960_2, "Geometrically non-linear creep buckling of bars", *Arch. Mech. Stos.* **12**, 3, 379–411.

Życzkowski M., 1960₃, "Influence of a dead weight on creep buckling of bars" (in Polish), *Rozpr. Inż.* **8**, 3, 511–528.

Życzkowski M., 1960₄, "On the question of extension of the Polish Standard PN-56/B-03200 as to include strut dimensioning" (in Polish), *Arch. Inż. Ląd.* **6**, 3, 383–393.

Życzkowski M., 1965₁, "Creep buckling of bars featuring discrete transverse non-homogeneity" (in Polish), *Arch. Bud. Masz.* **8**, 3, 383–393.

Życzkowski M., 1965₂, "Operations on generalized power series", *Z. Angew. Math. Mechanik* **45**, 4, 235–244.

Życzkowski M., 1967, "General solution for the linear creep buckling of heavy bars", *Recent Progr. Appl. Mech.* (Odqvist Volume), Stockholm, pp. 573–586.

Życzkowski M., 1968, "Optimale Formen des dünnwandigen geschlossenen Querschnittes eines Balkens bei Berücksichtigung von Stabilitätsbedingungen", *Z. Angew. Math. Mechanik* **48**, 7, 455–462.

Życzkowski M., Gajewski A., 1971, "Optimal structural design in non-conservative problems of elastic stability", *Symp. IUTAM Instabil. Cont. Systems 1969*, Springer, pp. 295–301.

Życzkowski M., Wojdanowska-Zając R., 1972, "Optimal structural design with respect to creep buckling", *Symp. IUTAM Creep in Struct. II, 1970*, Springer, pp. 371–387.

Życzkowski M., Zaborski A., 1975, "Creep rupture phenomena in creep buckling problems", *Symp. IUTAM Mech. Visco-El. Media 1974*, Springer, pp. 283–290.

Additional references

Anderson M. S., Williams F. W., 1987, "BUNVISRG: exact frame buckling and vibration program, with repetitive geometry and substructuring", *J. Spacecraft and Rockets* **24**, 4, 353–361.

Attard M. M., 1986, "Lateral buckling analysis of beams by the FEM", *Comput. and Struct.* **23**, 2, 217–231.

Banerjee J. R., Williams F. W., 1986, "Exact Bernoulli–Euler static stiffness matrix for a range of tapered beam-columns", *Int. J. Numer. Meth. Eng.* **23**, 9, 1615–1628.

Batoz J. L., Jameux J. P., 1986, "Post-flambement et grand deplacements d'arcs plans", *J. Mec. Theor. et Appl.* **5**, 2, 237–257.

Błachut J., Gajewski A., 1981₁ "On unimodal and bimodal optimal design of funicular arches", *Int. J. Solids and Struct.* **17**, 7, 653–667.

Błachut J., Gajewski A., 1981₂, "Unimodal and bimodal optimal design of extensible arches with respect to buckling and vibration", *Optimal Control Appl. Methods* **2**, 4, 383–402.

Błachut J. Życzkowski M., 1984, "Bimodal optimal design of clamped-clamped columns under creep conditions", *Int. J. Solids and Struct.* **20**, 6, 571–577.

Bochenek B., 1987, "Multimodal optimal design of a compressed column with respect to buckling in two planes", *Int. J. Solids and Struct.* **23**, 5, 599–605.

Bochenek B., Gajewski A., 1986, "Multimodal optimal design of a circular funicular arch with respect to in-plane and out-of-plane buckling", *J. Struct. Mech.* **14**, 3, 257–274.

Chen W. F., Lui E. M., 1985₁, "Stability design criteria for steel members and frames in the United States", *J. Constr. Steel Res.* **5**, 1, 31–74.

Chen W. F., Lui E. M., 1985₂, "Columns with end restraint and bending in load and resistance design factor", *Eng. J. (USA)* **22**, 3, 105–132.

Christodoulou A. A., Kounadis A. N., 1986, "Elastica buckling analysis of a simple frame", *Acta Mech.* **61**, 1–4, 153–163.

Cuk P. E., Bradford M. A., Trahair N. S., 1986, "Inelastic lateral buckling of steel beam-columns", *Can. J. Civ. Eng.* **13**, 6, 693–699.

Elishakoff I., 1985, "Reliability approach to the random imperfection sensitivity of columns", *Acta Mech.* **55**, 1/2, 151–170.

Elishakoff I., Pellegrini F., 1987, "Exact and effective approximate solutions of some divergence-type non-conservative problems", *J. Sound and Vibr.*, **114**, 1, 143–147.

Gajewski A., 1985, "Bimodal optimisation of a column in an elastic medium with respect to buckling or vibration", *Int. J. Mech. Sci.* **27**, 1/2, 45–53.

Gajewski A., Życzkowski M. 1988. *Optimal Structural Design under Stability Constraints*, Kluwer, Dordrecht, pp. 486.

Gauss R. C., Antman S. S., 1984, "Large thermal buckling of nonuniform beams and plates", *Int. J. Solids and Struct.* **20**, 11/12, 979–1000.

Grabowski J., 1984, "Buckling of steel bars subjected to preliminary plastic elongations" (in Polish), *Mech. Teor. Stos.* **22**, 3/4, 621–635.

Haslach H. W., Jr., 1985, "Post-buckling behaviour of columns with non-linear constitutive equations", *Int. J. Non-Linear Mech.* **20**, 1, 53–67.

Kahn R., Wagner W., 1987, "Überkritische Berechnung ebener Stabtragwerke unter Berücksichtigung einer vollständig geometrisch nichtlinearen Theorie", *Z. angew. Math. Mech.* **67**, 4, 197–199.

Karamanlidis D., Gesch-Karamanlidis H., 1986, "Pre-and postbuckling finite element analysis of thin-walled one-dimensional structures (trusses, cables, etc.)", *Ing.-Archiv* **56**, 5, 362–370.

Koiter W. T., 1985, "Elastic stability", *Z. Flugwiss. und Weltraumforsch.* **9**, 4, 205–210.

Kondoh K., Tanaka K., Atluri S. N., 1986, "An explicit expression for the tangent-stiffness of a finitely deformed 3-D beam and its use in the analysis of space frames", *Comput. and Struct.* **24**, 2, 253–271.

Kondratiev V. M., 1985, *Vibrations and Stability of Non-linear Systems under Follower Forces* (in Russian), Fan, Tashkent.

Kounadis A. N., 1985, "An efficient simplified approach for the non–linear buckling analysis of frames", *AIAA Journal* **23**, 8, 1254–1259.

Kounadis A. N., Mallis J. G., 1987, "Elastica type buckling analysis of bars from non-linearly elastic material", *Int. J. Non-Linear Mech.* **22**, 2, 99–107.

Krikun A. N., 1986, "Postbuckling compression of a slender column with constrained deflections" (in Russian), *Izv. AN SSSR, Mekh. Tverd. Tela*, **6**, 165–169.

Leipholz H. H. E., 1986, "On an energylike functional for the calculation of buckling loads of completely supported rods subjected to follower forces", *Mech. Res. Commun.* **13**, 1, 33–37.

Mikhaylovsky E. I., Tarasov V. N., Kholmogorov D. V., 1985, "Postbuckling behaviour of a compressed column with rigid constrains on deflections" (in Russian), *Prikl. Mat. Mekh.* **49**, 1, 156–160.

Panayotounakos D. E., 1986, "Non–linear and buckling analysis of continuous bars lying on elastic supports, based on the theory of elastica", *Ing.-Archiv* **56**, 5, 351–361.

Panayotounakos D. E., Theocaris, P. S., 1986, "Non–linear and buckling analysis of continuous bars lying on rigid supports", *AIAA Jurnal* **24**, 3, 479–484.

Plaut R. H., Johnson L. W., Olhoff N., 1986, "Bimodal optimization of compressed columns on elastic foundations", *J. Appl. Mech.* **53**, 1, 130–134.

Riks E., 1984, "Some computational aspects of the stability analysis of non–linear structures", *Comput. Meth. Appl. Mech. and Eng.* **47**, 3, 219–259.

Simitses J. G., Vlahinos A. S., Simitses G. J., 1986, "Sway buckling of unbraced multistorey frames", *Comput. and Structures* **22**, 6, 1047–1054.

Stein E., Wriggers P., 1984, "Stability of rods with unilateral constraints, a finite element solution", *Comput. and Struct.* **19**, 1/2, 205–211.

Sugimoto H., Chen W. F., 1985, "Inelastic post-buckling behavior of tubular members", *J. Struct. Eng.* **111**, 9, 1965–1978.

Teixeira de Freitas J. A., Moitinho de Almeida J. P. B., Virtuoso F. B. E., 1985, "Non–linear analysis of elastic space trusses", *Meccanica* **20**, 2, 144–150.

Voronyuk I. S., 1984, "Criteria of instability of non–linearly elastic columns" (in Russian), *Probl. Prochn.* **10**, 92–97.

Wang C. M., Thevendran V., Teo K. L., Kitipornchai S., 1986, "Optimal design of tapered beams for maximum buckling strength", *Eng. Struct.* **8**, 4, 276–284.

Życzkowski M. (Ed.), Gajewski A., Olhoff N., Rondal J., Seyranian A. P., 1989, *Structural Optimization Under Stability and Vibration Constraints*, CISM Lecture Notes, Springer, Wien.

1. The Strength Scheme of a Thin-Walled Bar

1.1. The Thin-Walled Bar Structure

A typical prismatic thin-walled bar (Fig. 1.1) consists of a cylindrical skin and ribs which generally run perpendicular to its generatrices. The skin geometry is determined by the central line (contour) of the cross-section perpendicular to the generatrices and by skin thickness h measured perpendicular
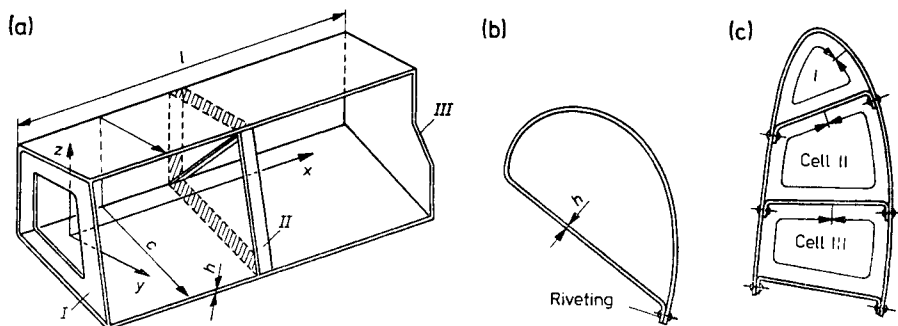
Fig. 1.1. Structure of a thin-walled bar; (a) open thin-walled bar with frame-type rib I, disk-type III and truss-type II. In the last, the shaded part plays a dual role, that of skin and rib element; (b) single cell tube; (c) multicell tube

to the contour. The latter may be a function of coordinate s measured along the contour, i.e. $h(s)$, which is, by assumption, many times smaller than the overall length c of the contour. The contour length c itself is markedly smaller than bar length l. When the skin contour is not a closed line, the bar is open (Fig. 1.1a), but when it is a closed line, the bar is called a *single cell* or *multicell tube* (Fig. 11.1b, c). The ribs are joined to the skin over the entire length c. They may be either in the form of plane thin-walled bulkheads (disks) or frames, or trusses. They are necessary for the skin to maintain its shape and for transverse loads to be correctly* applied, and for this reason, they must

---

* That is, to enable the skin to work in the membrane state of stress (non-flexural), in which the skin is very rigid and material utilization optimal.

be stiff in their planes. If at the same time the number of loadings is small and if their position along the bar is fixed, then statically indispensable ribs* are required only in the loaded cross-section. On the other hand, if the loadings can move along the length of the bar, or are surface forces, e.g. aero-dynamic forces, the spacing of the ribs depends on the bending rigidity of the skin itself and is as a rule of the order of a geometrical mean of the overall dimensions of the contour. Such individual ribs are generally very flexible in the direction perpendicular to their planes and cannot transmit any appreci-able loadings in this direction.

It is seen from the above description that thin-walled bars represent a special case of cylindrical shells with internal constraints due to the existence of ribs. However, analysis of such shells is a difficult problem and the results have very complicated form. For this reason various simplified methods are used. The most common one is the analysis based on the following assump-tions:

    I. The ribs are perfectly rigid in their planes and perfectly flexible in the direction perpendicular to them.

    II. The ribs are so closely spaced that the support provided for the skin by the ribs can be trated as continuous.

    III. In an open bar, the unit elongation of the skin in the direction of the generatrices is determined neglecting its shearing strains.

The engineering theory of thin-walled bars of open cross-section developed by Vlasov (1959), in which the above simplifications are utilized has been widely accepted in research.

1.2. Strains and Stresses in the Bar Skin

Displacements of investigated point K of the skin contour are defined as u_K and η, ξ in local coordinates x_K, s, n bound to point K itself or as u_K, v_K, w_K in a general system** bound to selected pole B (Fig. 1.2). These displacements, by virtue of assumptions I and II (Section 1.1), can be expressed by the dis-placements of the bar cross-section as a whole, i.e. by v_B and w_B of pole B and angle of rotation φ with respect to x_B-axis. Assuming that angle φ is small, we obtain for point K with coordinates y_B and z_B

$$v_K = v_B + \varphi z_B, \qquad w_K = w_B - \varphi y_B, \tag{1.1}$$

---

    * Outside these ribs, called force ribs, there may exist additional ribs whose presence is justified for reasons of.

    ** The x_B-, x_K-axes and the central longitudinal x-axis have the direction of the genera-trices, and it is assumed at the same time that $x_B = x_K = x$. The y_B and z_B-axes are parallel to the central y, z-axes of the bar cross-section.
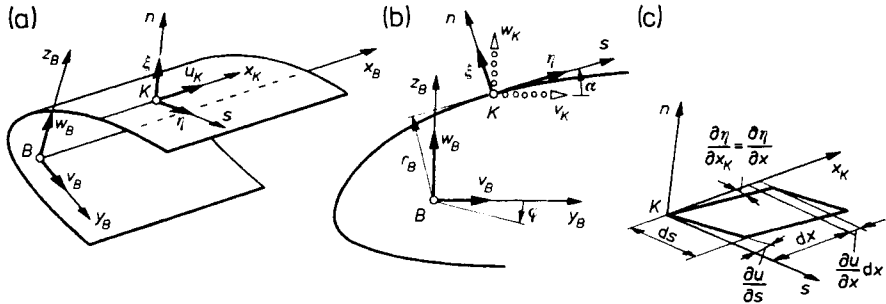
Fig. 1.2. Displacements in the skin: (a) coordinates: general x_B, y_B, z_B, and local x, s, n, and displacements in these coordinates; (b) displacements in the plane of cross-section; (c) deformation of element in x, s plane

and tangential displacements η in local coordinates n, s

$$\eta = v_K \cos \alpha + w_K \sin \alpha = v_B \cos \alpha + w_B \sin \alpha + \varphi r_B, \tag{a}$$

where $r_B = z_B \cos \alpha - y_B \sin \alpha$ is the distance of pole B from the tangent to the contour at point K.

The result (a) along with assumption III (Section 1.1), whereby shearing strain γ is negligible, gives the longitudinal displacement u_K of point K. For, it is apparent from Fig. 1.2c that

$$\gamma = \frac{\partial \eta}{\partial x} + \frac{\partial u_K}{\partial s} = \frac{dv_B}{dx} \cos \alpha + \frac{dw_B}{dx} \sin \alpha + \frac{d\varphi}{dx} r_B + \frac{\partial u_K}{\partial s} = 0, \tag{b}$$

which after integrating with respect to s leads to

$$u_K = u_B - v'_B \int \cos \alpha \, ds - w'_B \int \sin \alpha \, ds - \varphi' \int r_B \, ds, \tag{c}$$

where u_B is an arbitrary function of x, and v'_B, w'_B, φ' are derivatives of v_B, w_B and φ with respect to x. Moreover, Fig. 1.3 shows that*

$$\int \cos \alpha \, ds = y, \quad \int \sin \alpha \, ds = z, \quad \int r_B \, ds = \int d\omega_B = \omega_B, \tag{d}$$

where w_B is the double area of figure $PHKB$, a so-called *sectorial area* with respect to pole B. It will be positive when going from P to K; the rotation of vector BH is clockwise.

---

* By introducing u_B we are allowed to choose freely the lower limits of integrals (c). This allows the values of the first two integrals (d), i.e., the coordinates of point K, to be determined in the central y, z-axes. Similarly, in the third integral, initial point P can be chosen arbitrarily.
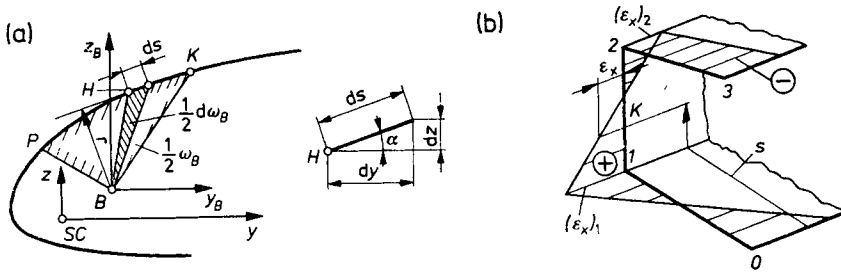
Fig. 1.3. Determination of sectorial area ω_B and distribution of ε_x in a bar with plane walls

A consequence of relations (c) and (d) is the result in which

$$u_K = u_B - y v'_B - z w'_B - \omega_B \varphi'. \tag{1.2}$$

The first three terms describe the displacement of the cross-section as a rigid plane, whereas the term $\omega_B \varphi'$ is the so-called *warping (deplanation)* of the cross-section.

Equation (1.2) enables us in turn to determine longitudinal strain ε_x in the x-direction

$$\varepsilon_x = \partial u_K / \partial x = u'_B - y v''_B - z w''_B - \omega_B \varphi' \tag{1.3}$$

from which it is seen that in a bar with plane walls (Fig. 1.3b), ε_x on individual walls is a linear function of s.

Relations (1.2) and (1.3) follow from pure geometry. In order to determine the stresses, additional assumptions are necessary:

IV. By virtue of the fact that the thickness h of the skin is small and according to the existence of ribs, the most important are only stress components σ_x and τ_{xs} parallel to the central surface of the skin* (Fig. 1.4a).

V. If transverse loads are applied exclusively in the planes of the ribs, the stress distribution σ_x along skin thickness h can then be taken to be uniform.

VI. By virtue of the fact that the skin is a thin-walled structure, we assume a linear distribution of τ_{xs} along thickness h owing to which τ_{xs} is a sum of the membrane coponent $\tau_{mean} = \tau_b$ and the linearly varying component given by the value τ_V (Fig. 1.4b).

---

* The existence of ribs rigid in their planes, and the assumptions such as in the theory of plates eliminate from consideration stresses σ_n, τ_{xn}, τ_{sn}. That same property of ribs would impose, moreover, the condition $\varepsilon_s \equiv 0$ and $\sigma_s = -\nu\sigma_x$. However, due to fact that the number of ribs is finite, the assumption that $\varepsilon_s \approx -\nu\varepsilon_x$ and $\sigma_s \approx 0$ is more justified.
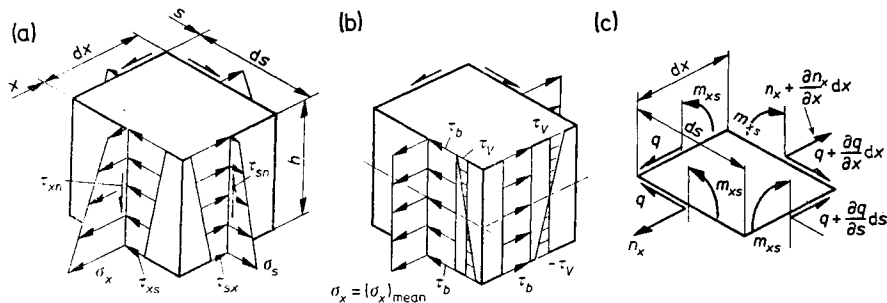
Fig. 1.4. State of stress in skin element: (a) real image; (b) simplified image: stresses resolved into components: membrane component τ_0 and flexural τ_V; (c) n_x, q, m_{xs} flow system in element

As a result of assumptions IV, and V and Hooke's law, we obtain from Eq. (1.3) normal stresses in the cross-section

$$\sigma_x = E\varepsilon_x = E(u'_B - yv''_B - zw''_B - \omega_B \varphi'). \tag{1.4}$$

It is customary in the analysis of thin-walled bars to express membrane stresses σ_x and τ_b by so-called *normal flows* n_x and shear flows q

$$n_x = \sigma_x h, \quad q = \tau_{\mathrm{mean}} h = \tau_b h, \tag{1.5}$$

and stresses σ_V by moment flow m_{xs}

$$m_{xs} = \tau_V h^2/6. \tag{1.6}$$

Flows n_x, q and m_{xs} represent the intensity of the respective quantity per unit length measured on the central surface of the skin. It is apparent from (1.4) that these flows depend on x and s, and that their system acting on an element of the skin is as shown in Fig. 1.4c. It at the same time there are no external loadings on this element, then it follows from the equilibrium equations of force projections on axes s and x that

$$\frac{\partial q}{\partial x} = 0, \quad \frac{\partial n_x}{\partial x} + \frac{\partial q}{\partial s} = 0. \tag{1.7a, b}$$

Therefore, if there are no external loadings on the skin lying between the ribs, flow q depends only on s and by integrating Eq. (1.7b) with repect to s, we obtain

$$q(s) = q_0 - \int_0^c \frac{\partial n_x}{\partial x} \, ds, \tag{1.8}$$

where q_0 is the shear flow on generatrix $s = 0$. If this generatrix is the free edge of the skin, then $q_0 = 0$.

2. Statics of Bars of Open Cross-Section*

2.1. Simple Bending of Bar. The Shear Centre

In the case of a bar, where the angle of rotation $\varphi(x) \equiv 0$, displacements v_K and w_K of all points of the cross-section investigated are independent of pole B actually selected. We introduce in this case the notations

$$u_B = u(x), \quad v_K = v_B = v(x), \quad w_K = w_B = w(x). \tag{a}$$

We then obtain from (1.4) a plane distribution of σ_x^I

$$\sigma_x^I = E(u' - yv'' - zw'') \tag{2.1}$$

yielding three effort components (generalized stresses), namely longitudinal force N and bending moments M_y and M_z with respect to the central y-and z-axis. Their values are determined from the reduction of elementary forces $\sigma_x^I h \, ds$ (Fig. 2.1)

$$N = \int_0^c \sigma_x^I h \, ds, \quad M_y = -\int_0^c \sigma_x^I z h \, ds, \quad M_z = -\int_0^c \sigma_x^I y h \, ds, \tag{2.2}$$
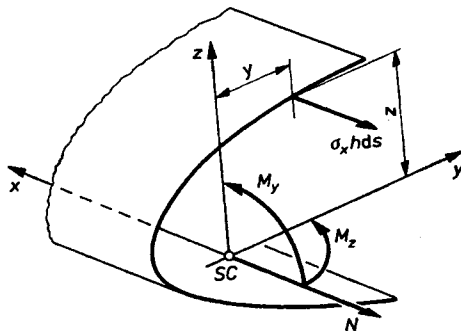
Fig. 2.1. Components of cross-sectional effort dependent on σ_x

* References: Timoshenko (1945), Feodosev (1949), Nowiński (1951), Bornscheuer (1952), Lansing (1953), Arutyunyan and Yulkanyan (1954), Klimov (1957), Pikovski and Derkachev (1959), Heilig (1961), Cywiński (1964), Bažant (1965), Wilde (1968), Hutter (1969).

where the symbol $\int\limits_0^c$ stands for integration over the entire contour, and the positive senses of M_y and M_z have been taken according to Fig. 2.1. Taking σ_x^l based on (2.1), we obtain after integrating

$$N = EAu', \qquad M_y = EJ_y w'' + EJ_{yz} v'', \qquad M_z = EJ_z v'' + EJ_{yz} w'', \qquad (2.3a)$$

where $A = \int\limits_0^c h\,ds$ is the total cross-sectional area, J_y, J_z are the moments of inertia with respect to the centroidal y-and z-axis, J_{yz} is the product of inertia with respect to the same axes, where

$$J_y = \int\limits_0^c z^2 h\,ds = \int\limits_0^c z^2 dA, \qquad J_z = \int\limits_0^c y^2 dA, \qquad J_{yz} = \int\limits_0^c yz\,dA. \qquad (2.4)$$

If y and z are centroidal principal axes, $J_{yz} = 0$, and then it follows from (2.3a) that

$$u' = N/EA, \qquad v'' = M_z/EJ_z, \qquad w'' = M_y/EJ_y, \qquad (2.5a)$$

which after substituting into (2.1) and (1.5) gives flow n_x^l

$$n_x^l = \sigma_x^l h = \left(\frac{N}{A} - \frac{M_y z}{J_y} - \frac{M_z y}{J_z}\right) h. \qquad (2.6a)$$

In some cases, it is more convenient to use the centroidal but not principal system of the y- and z-axes and then from Eqs. (2.3a) we obtain

$$u = N/EA, \qquad v'' = \mathfrak{M}_z/EJ_z, \qquad w'' = \mathfrak{M}_y/EJ_y, \qquad (2.5b)$$

where the auxiliary quantities, $\mathfrak{M}_y$ and $\mathfrak{M}_z$, are

$$\mathfrak{M}_y = \varkappa\left(M_y - M_z \frac{J_{yz}}{J_z}\right), \qquad \mathfrak{M}_z = \varkappa\left(M_z - M_y \frac{J_{yz}}{J_y}\right). \qquad (2.7a)$$

The dimensionless coefficient $\varkappa$

$$\varkappa = 1\Big/\left(1 - \frac{J_{yz}^2}{J_y J_z}\right), \qquad (2.7b)$$

occurring here is always positive. Finally, in place of (2.6a) we have

$$n_x^l = \sigma_x^l h = \left(\frac{N}{A} - \frac{\mathfrak{M}_y z}{J_y} - \frac{\mathfrak{M}_z y}{J_z}\right) h. \qquad (2.6b)$$

The results (2.6) known in strength of materials determine from (1.8) shear flows $q = q^l$. Thus, if the axes y, z are centroidal principal and $N = $ const, then from (2.6)

$$q^{\mathrm{I}} = \frac{1}{J_y} \frac{\mathrm{d}M_y}{\mathrm{d}x} \int_0^s zh\,\mathrm{d}s + \frac{1}{J_z} \frac{\mathrm{d}M_z}{\mathrm{d}x} \int_0^s yh\,\mathrm{d}s, \qquad \text{(b)}$$

with $s = 0$ taken for the free edge of the skin, where $q_0 = 0$.

The integrals occurring in (b) are functions of the upper limit of integration, coinciding with the point K being examined. These are static moments S_y and S_z about the y- and z-axes of the part of the cross-setcion between free edge 0 and point K (Fig. 2.2), i.e.

$$S_y^{0,s} = \int_0^s zh\,\mathrm{d}s = \int_0^s z\,\mathrm{d}A, \qquad S_y^{0,s} = \int_0^s yh\,\mathrm{d}s = \int_0^s y\,\mathrm{d}A. \qquad \text{(2.8)}$$
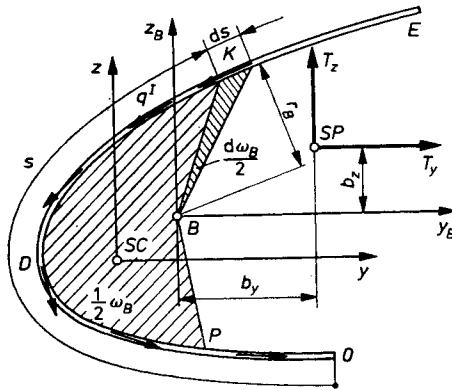
Fig. 2.2. Determination of flow q^{I} and shear centre

As we know from strength of materials, the derivatives $\mathrm{d}M_y/\mathrm{d}x$ and $\mathrm{d}M_z/\mathrm{d}x$ are the respective shearing forces, T_z and T_y,

$$T_z = \mathrm{d}M_y/\mathrm{d}x, \qquad T_y = \mathrm{d}M_z/\mathrm{d}x. \qquad \text{(2.9)}$$

As a result, shear flow q^{I} corresponding to non-torsional bending of the bar is

$$q^{\mathrm{I}} = \frac{T_z}{J_y} S_y^{0,s} + \frac{T_y}{J_z} S_z^{0,s}. \qquad \text{(2.10a)}$$

If the centroidal axes y, z are not principal, then we have in (b), accordintg to (2.6b), the derivatives $\mathrm{d}\mathfrak{M}_y/\mathrm{d}x$ and $\mathrm{d}\mathfrak{M}_z/\mathrm{d}x$, which by virtue of relations (2.7) and (2.8) lead to so-called *equivalent shearing forces*

$$\mathfrak{T}_z = \frac{\mathrm{d}\mathfrak{M}_y}{\mathrm{d}x} = \varkappa\left(T_z - T_y\,\frac{J_{yz}}{J_z}\right),$$

$$\mathfrak{T}_y = \frac{\mathrm{d}\mathfrak{M}_z}{\mathrm{d}x} = \varkappa\left(T_y - T_z\,\frac{J_{yz}}{J_y}\right), \qquad \qquad \text{(2.11)}$$

which after substituting in (2.10a) results in:

$$q^{\mathrm{I}} = \frac{\mathcal{T}_z S_y^{0,s}}{J_y} + \frac{\mathcal{T}_y S_z^{0,s}}{J_z}.$$ (2.10b)

If Eqs. (2.10) yield $q^{\mathrm{I}} > 0$, then the sense of q^{I} is as in Fig. 2.2. It can easily be proved that the result (2.10) gives two identities

$$-\int_0^c q^{\mathrm{I}} ds \cos\alpha = T_y, \qquad -\int_0^c q^{\mathrm{I}} ds \sin\alpha = T_z,$$ (c)

expressing that the sum of projections of flows q^{I} is always equal to shearing forces T_z and T_y. At the same time the result (2.10) must satisfy the third condition, namely that the sum of elementary moments $q^{\mathrm{I}} ds\, r_B = q^{\mathrm{I}} d\omega_B$ with respect to arbitrarily chosen point B must be identically equal to the moment of resultant foces T_y and T_z, i.e.

$$\int_0^c q^{\mathrm{I}} d\omega_B = T_z b_y - T_y b_z,$$ (d)

where b_y, b_z are the arms of forces T_z and T_y with respect to point B in the $y_B z_B$ system of axes. Taking now q^{I} from Eq. (2.10b) and considering that T_y and T_z are independent, two equations

$$b_y = \frac{\varkappa}{J_y} \int_0^c \left(S_y^{0,s} - \frac{J_{yz}}{J_z} S_z^{0,s} \right) d\omega_B,$$

$$b_z = -\frac{\varkappa}{J_z} \int_0^c \left(S_z^{0,s} - \frac{J_{yz}}{J_y} S_y^{0,s} \right) d\omega_B$$ (e)

follow from identity (d). The final* form of relationships (e) is as follows:

$$b_y = -\frac{\varkappa}{J_y} \left(\int_0^c \omega_B zh\, ds - \frac{J_{yz}}{J_z} \int_0^c \omega_B yh\, ds \right),$$ (2.12a)

$$b_z = \frac{\varkappa}{J_z} \left(\int_0^c \omega_B yh\, ds - \frac{J_{yz}}{J_y} \int_0^c \omega_B zh\, ds \right),$$ (2.12b)

---

* Integrating by parts we obtain, for example

$$\int_0^c S_y^{0,s} d\omega_B = |S_y^{0,s} \omega_B|_0^c - \int_0^c \omega_B dS_y^{0,s} = 0 - \int_0^c \omega_B zh\, ds,$$

since $dS_y^{0,s} = zh\, ds$. The second integral is similarly calculated.

where $1/\varkappa = 1 - (J_{yz}^2/J_y J_z)$. If the axes y, z are principal

$$b_y = -\frac{1}{J_y} \int_0^c \omega_B zh \, ds, \qquad b_z = \frac{1}{J_z} \int_0^c \omega_B yh \, ds. \tag{2.13}$$

Point SP given by coordinates b_y and b_z is called the *shear centre* of the cross-section. It represents the point through which resultant shearing force T must pass when the bar is subjected to torsionless bending. The position of this point in the cross-section does not depend on the points B and P actually choosen. In other words, of for a given cross-section we take different points B and B' and P and P' (Fig. 2.3a), then the coordinates b_y, b_z, b_y', b_z' derived from Eqs. (2.12) or (2.13) are bound by the relations

$$b_y' = b_y - \Delta b_y, \qquad b_z' = b_z - \Delta b_z. \tag{f}$$
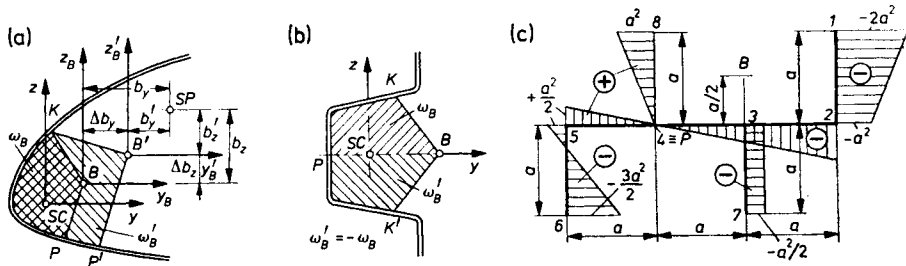
Fig. 2.3. Position study of the shear centre (SP) and determination of sectional area ω_B

If the cross-sections has an axis of symmetry (Fig. 2.3b), then SP lies on this axis, since for symmetrically situated points K and K' the values ω_B are opposite and the integral in the second of Eqs. (2.13) is zero. The position of SP for several typical cross-sections is given in Table 2.1. It is seen here that in cross-sections of the channel type (Fig. 2.3a, b), SP lies outside the
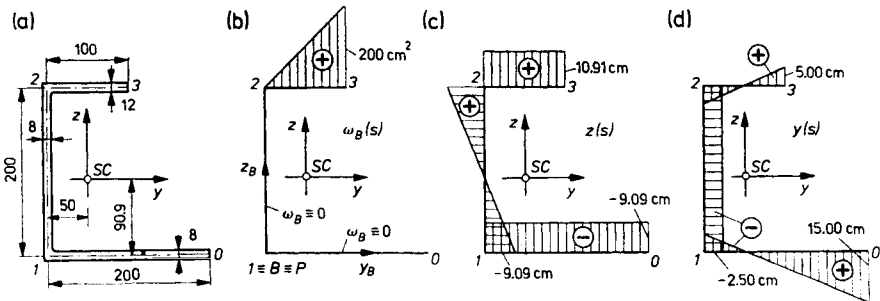
Fig. 2.4. Stages of determination of SP of open cross-section $J_y = 3298$ cm^4, $J_z = 1434$ cm^4, $J_{yz} = -800$ cm^4

cross-section. In the case of point symmetry, SP lies in this centre. Lastly, in star-shaped sections with plane walls, SP lies at the point of intersection C, irrespective of the number and size of the arms.

An illustration of the calculation of b_y and b_z for a "single stream" profile is given for the channel section (Fig. 2.4a). Taking points B and P in corner 1, we determine the area $\omega_B(s)$ (Fig. 2.4b), whose positive values agree with the condition from Section 1.2, and also the plots $z(s)$ and $y(s)$ (Fig. 2.4c, d). Based on these data we find

$$\int_0^c \omega_B zh\,ds = 13092 \text{ cm}^5, \quad \int_0^c \omega_B yh\,ds = 2000 \text{ cm}^5$$

and from (2.12) the coordinates

$$b_y = -4.98 \text{ cm}, \quad b_z = 4.17 \text{ cm},$$
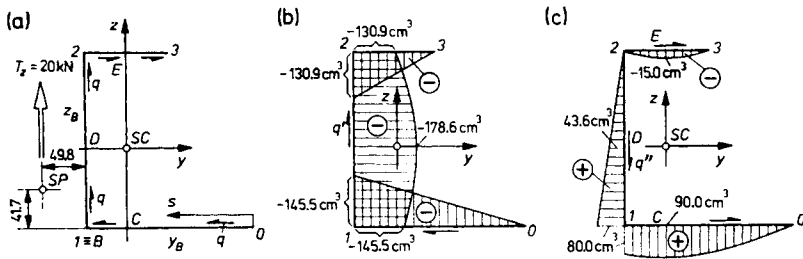
Fig. 2.5. Determination of shear flow in the cross-section from Fig. 2.4.

which fix the position of SP in the image of the cross-section (Fig. 2.5). Force $T_z = 20$ kN applied at this point gives the shear flows

$$q' = \mathfrak{T}_z S_y^{0,s}/J_y, \quad q'' = \mathfrak{T}_z S_z^{0,s}/J_z,$$

whose values are proportional to $S_y^{0,s}$ and $S_z^{0,s}$ (Fig. 2.5b, c), and the total flow

$$q^1 = q'+q''.$$

For a branched "multi-stream" cross-section (Fig. 2.3c), area ω_B is determined in two stages. In the first, we select conventionally the principal stream $1, \dots, 6$ and ω_B is calculated as if branches 4, 8 and 3, 7 were non-existent. In the second stage, ω_B is calculated for each branch separately taking for the starting point the respective ω_B calculated for the principal sequence.

2.2. Torsion of an Open Prismatic Bar

The general case of loading of a bar (Fig. 2.6) can be divided into bending by a force system, as considered in Sectoin 2.1, in which each of the component forces is applied at the shear centre, and torsion by a moment M^* system
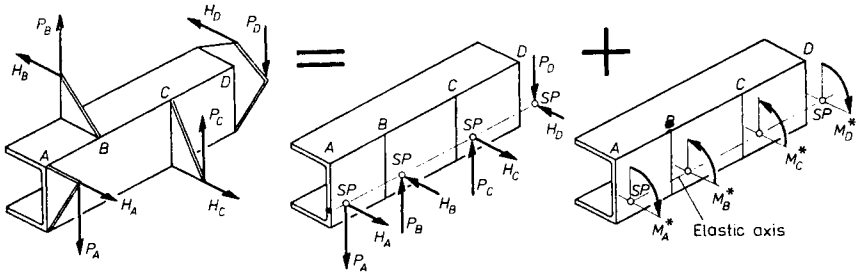
Fig. 2.6. Decomposition transverse loading into flexural and torsional

causing the cross-section to twist by angle $\varphi(x)$ with respect to the as yet unknown longitudinal axis. Generally, function $\varphi(x)$ is non-linear, which results in the occurrence of normal stresses

$$\sigma_x^{II} = -E\omega_B\varphi''. \tag{a}$$

These stresses are proportional to sectorial area ω_B with respect to the centre of rotation B (Fig. 2.7). It is obvious that in the present torsion case the resultant moments of elementary forces $\sigma_x^{II}h\,ds$ with respect to the y- or z-axes and the resultant longitudinal force all equal zero, i.e.

$$\int_0^c \sigma_x^{II}h\,dsz = 0, \quad \int_0^c \sigma_x^{II}h\,dsy = 0, \quad \int_0^c \sigma_x^{II}h\,ds = 0. \tag{b}$$

A confrontation of the first two conditions (b) with Eqs. (2.12) gives, considering (a), $b_y = b_z = 0$, i.e., with torsion involved, centre SP coincides with centre of rotation B of the cross-section, and the axis of twist is identical with the so-called *elastic axis* connecting the shear centres. The third of conditions (b) also distinguishes the so-called *principal sectorial area* $\omega_B = \omega_0$ for which, obeying the postulate $B = SP$,

$$\int_0^c \omega_0 h\,ds = 0. \tag{c}$$

The condition (c) permits the determination of the position of an origin P defining the value ω_0. Figure 2.7b shows that the shift of this origin from
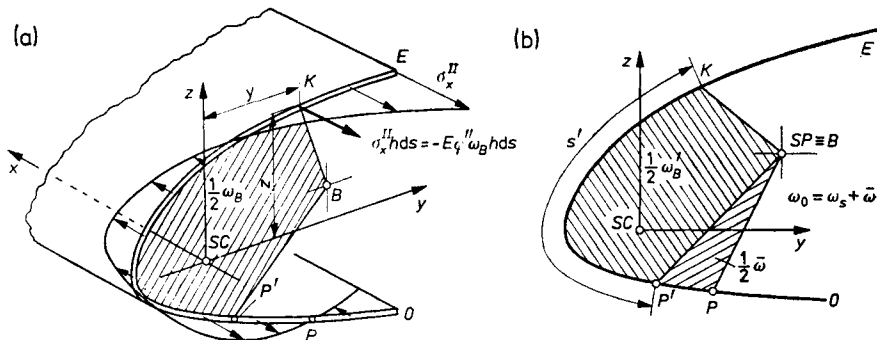
Fig. 2.7. Determination of the characteristics of σ_x^{II} distribution and of the principal sectorial area

P' to P changes the area $\omega_B' = \omega_s$, corresponding to point K by a constant quantity $\bar{\omega}$. If this altered value is to be

$$\omega_0 = \omega_s + \bar{\omega},$$ (2.14a)

then it immediately follows from condition (c) that

$$\bar{\omega} = -\frac{1}{A} \int_0^c \omega_s h \, ds,$$ (2.14b)

where $A = \int_0^c h \, ds$ is the total area of cross-section.

By putting into (a) symbol ω_0 instead of ω_B, we obtain the normal stress σ_x^{II} due to the torsion of the bar

$$\sigma_x^{II} = -E\varphi' \omega_0$$ (2.15a)

and the corresponding stress flow n_x^{II}

$$n_x^{II} = \sigma_b^{II} h = -E\varphi'' \omega_0 h.$$ (2.15b)

The form of Eq. (2.15b) departs from analogous expressions (2.6) in the case of bending. With unification in mind, we introduce a new effort (generalized stress) component in the cross-section, the so-called *bimoment** B, given by

---

* The physical sense of the bimoment, as with concepts N, M_y and M_z, follows from the concept of work. Thus the expressions

$$N = \int_0^c n_x \, ds, \quad M_y = \int_0^c (n_x ds)(-z), \quad M_z = \int_0^c (n_x ds)(-y)$$

give respectively the work done by flow n_x on displacement $u = 1$ or on displacements $(-z)$ or $(-y)$ for slopes $\vartheta_y = w' = 1$ or $\vartheta_z = v' = 1$. By analogy, the bimoment expresses the work done by n_x on displacement $u = -\omega_0 \varphi'$ (cf. Eq. (1.2)), if unit twist $\varphi' = 1$ m^{-1}.

the relation

$$B = \int_0^c n_x(-\omega_0)\,ds = \int_0^c (n_x^I + n_x^{II})(-\omega_0\,ds) \qquad (2.16a)$$

and by substituting (2.6) and (2.15b) and taking (b) into consideration, we have

$$B = \int_0^c n_x^{II}(-\omega_0)\,ds = E\varphi'' \int_0^c \omega_0^2 h\,ds = EJ_\omega \varphi'', \qquad (2.16b)$$

where $J_\omega = \int_0^c \omega_0^2 h\,ds = \int_0^c \omega_0^2\,dA$ is the so-called *principal sectorial moment of inertia* of cross-section (measured in m^6). Apparently, the bimoment depends only on n_x^{II}, and the quantities σ_x^{II} and n_x^{II} expressed by B are

$$\sigma_x^{II} = -\frac{B\omega_0}{J_\omega} \quad \text{or} \quad n_x^{II} = -\frac{B\omega_0}{J_\omega}\,h. \qquad (2.17)$$

A graphical representation of the bimoment must take into account that the n_x^{II} flow system is self-equilibrated by virtue of conditions (b) (Fig. 2.8).
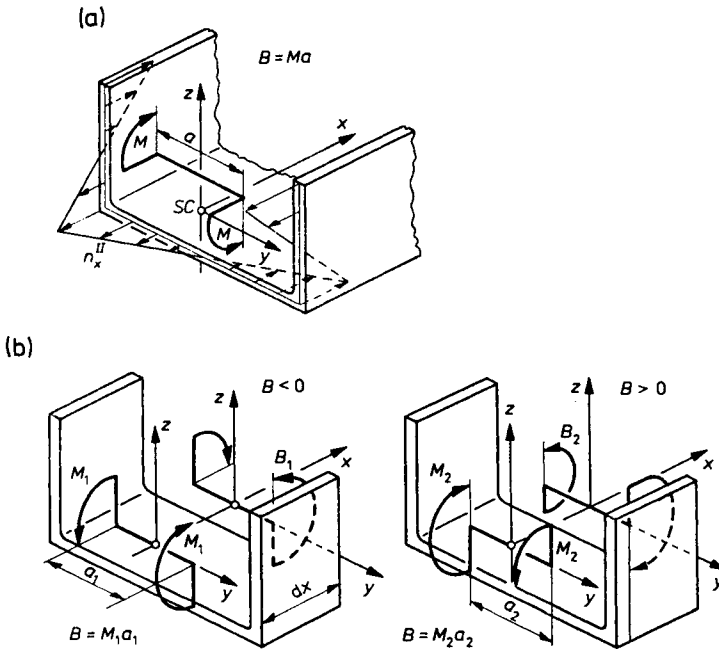
Fig. 2.8. Conventional image of bimoment B and conventional determination of its sign

For this reason, a conventional representation of the bimoment is a set of two moments $+M$ and $-M$ pushed apart so as to obtain $B = Ma$. Likewise, conventionally connoted is the sign of the bimoment.

By putting σ_x^{II} into (1.8), we obtain the shear flow

$$q^{II} = -\int_0^c \frac{\partial n_x^{II}}{\partial x}\, ds = E\varphi'''\int_0^s \omega_0 h\, ds \qquad (d)$$

with $s = 0$ taken at the free edge, where $q_0 = 0$. Defining the static sectorial moment $S_\omega^{0,s}$ of part of cross-section OK (Fig. 2.7) as

$$S_\omega^{0,s} = \int_0^s \omega_0 h\, ds \qquad (2.18a)$$

we obtain the shear flow due to the torsion of the bar

$$q^{II} = ES_\omega^{0,s}\varphi'''. \qquad (2.18b)$$
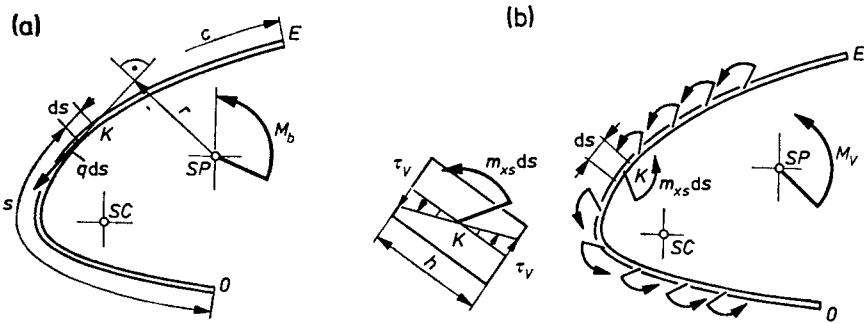
Fig. 2.9. Determination of torsional moment $M_s = M_b + M_v$

It can easily be proved that the resultant of flows q^{II} is only moment M_b (Fig. 2.9a), whose value calculated with respect to SP is

$$M_b = \int_0^c q^{II} r\, ds = \int_0^c q^{II} d\omega_0 = \int_0^c ES_\omega^{0,s}\varphi''' d\omega_0 \qquad (e)$$

and by using (2.18a) and integrating by parts we have

$$M_b = -E\varphi'''\int_0^c \omega_0^2 h\, ds = -EJ_\omega\varphi''', \qquad (2.19)$$

where J_ω is the principal sectorial moment of inertia.

Moment M_b determined from (2.19) is not the total torsional moment. Due to linear variation of τ_{xs} along thickness h (Fig. 1.4), moment M_v

(Fig. 2.9b) occurs as a resultant of moment flows m_{xs}. On account of the similarity of the strains, their value is as in the theory of plates

$$m_{xs} = D(1-v)\varkappa_{1,2} = D(1-v)(d\varphi/dx), \tag{f}$$

where $D = Eh^3/12(1-v^2)$ is the bending rigidity of the skin, $\varkappa_{1,2} = d\varphi/dx$ is the unit twist of skin element independent of s due to nondeformability of the ribs. Substituting result (f) into (1.6), we get

$$\tau_V = 6m_{xs}/h^2 = Eh\varphi'/2(1+v) = Gh\varphi' \tag{g}$$

as an extremal value of the second stress component, τ_{xs} (Fig. 1.4b). This second component is identical to the de Saint Venant torsion known from the theory of elasticity, and the corresponding moment is

$$M_V = G\varphi'\left(\frac{1}{3}\int_0^c h^3 ds\right) = GJ_s\varphi', \tag{2.20}$$

where $J_s = (\int_0^c h^3 ds)/3$ is a purely geometrical quantity (m^4). Using result (2.20), we can determine from (g) the stresses due to pure torsion

$$\tau_V = (M_V/J_s)h(s). \tag{2.21}$$

The sum of M_b and M_V gives total torsional moment M_s

$$M_s = M_b + M_V = GJ_s\varphi' - EJ_\omega\varphi'''. \tag{2.22}$$
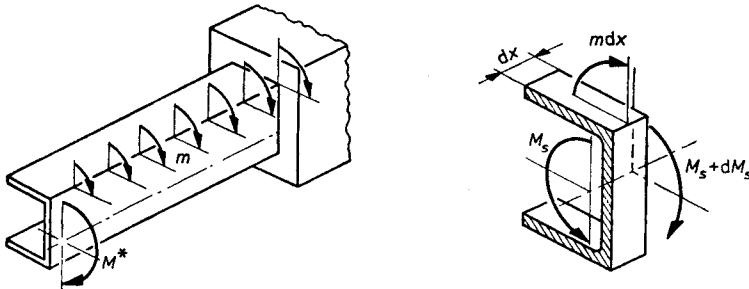
Fig. 2.10. Equilibrium with continuous loading m

This fundamental equation (2.22), is given in a modified form when a load is acting on a bar (Fig. 2.10). Since

$$\frac{dM_s}{dx} = -m, \tag{2.23}$$

equation (2.22) takes the form

$$C\varphi'' - C_\omega\varphi^{IV} = -m, \tag{2.24}$$

where $C = GJ_s$ is the so-called *torsional rigidity* and $C_\omega = EJ_\omega$ is the so-called *restrained warping rigidity*.

The above analysis brings out a specificity of torsion as compared with the simple bending of a bar (Section 2.1), where the generalized stresses (N, M_y, M_z, T_y, T_z) determine uniquely the stresses. In the case of torsion, moment M_s distributes into M_V and M_b, corresponding to two different work mechanisms. Thus, with pure torsion (component M_V) only shear stresses τ_V are involved, whereas with restrained torsion (component M_b) we have both shear stresses $\tau_b^{II} = q^{II}/h$ and normal stresses σ_x^{II}. This distribution depends on rigidities C and C_ω and on the boundary conditions, i.e., on the way in which the bar is supported. In this aspect, the torsion problem for an open bar is internally statically indeterminate in a different sense than in the case of other internal forces.

Using the bimoment concept (2.1b), Eq. (2.24) can be given as a set of two equations

$$B = EJ_\omega \varphi'' = C_\omega \varphi'', \quad B'' - k^2 B = +m, \tag{2.25}$$

where $k^2 = C/C_\omega$.

2.3. Determination of Quantities ω_0, J_ω, $S_\omega^{0,s}$

It is necessary in torsion analysis to calculate the geometric parameters, i.e., the principal sectorial area ω_0, the principal sectorial moment of inertia J_ω and the sectorial static moment $S_\omega^{0,s}$ dependent on coordinate s. To this end,

(a) we must find the position of SP and of initial point P' of the count of area $\omega_B = \omega_s$ with respect to SP as a pole (Fig. 2.7b);

(b) observing the rule (Section 2.1) concerning the sign of area ω, we must determine successively ω_s, correction term $\bar{\omega}$ (2.14b) and ω_0 (2.14a). It is useful to indicate the plot of ω_s and ω_0 on the image of the cross-section.
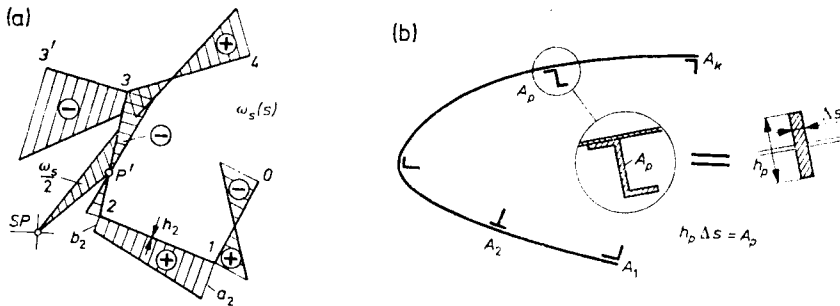
Fig. 2.11. Some details of calculation of geometric charactersitics

TABLE 2.1 Geometrical characteristics of open cross-sections

Cross-section	Position SP	Picture of area ω_0	Picture of moment S_ω	Moment J_ω
(I-section)	$b_y = \dfrac{H}{1+\psi}$ $\psi = \left(\dfrac{B_1}{B_2}\right)^3 \dfrac{h_1}{h_2}$	$\dfrac{B_2(H-b_y)}{2}$ $\dfrac{B_1 b_y}{2}$ SP	$\dfrac{B_2^2(H-b_y)h_2}{8}$ $\dfrac{B_1^2 b_y h_1}{8}$	$J_\omega = \dfrac{B_1^3 H^2 h_1}{12(1+\psi)}$
(channel)	$b_z = \dfrac{B}{2(1+\psi)}$ $\psi = \dfrac{H h_2}{6 B h_1}$	SP $\omega_{03} = \dfrac{Hb_z}{2}$ $\omega_{01} = \dfrac{H(B-b_z)}{2}$	$S_{\omega 2}$ $-\dfrac{1}{2}S_{\omega 3}$ $S_{\omega 3}$ $S_{\omega 3} = \dfrac{(B-b_z)^2 Hh}{4}$, $S_{\omega 2} = \dfrac{B^2 Hh_1 \varphi}{1+\varphi}$	$J_\omega = \dfrac{B^2 H^2(B-3b_z)h_1}{6} + I_z b_z^2$
(Z-section)	SP $\equiv$ SC $\psi = \dfrac{Hh_2}{2Bh_1}$	$\omega_{02} = -\dfrac{BH}{4(1+\varphi)}$ $\omega_{01} = \dfrac{BH(1+2\varphi)}{4(1+\varphi)}$	$S_{\omega 2} = \dfrac{B^2 Hh_1 \varphi}{4(1+\varphi)}$	$J_\omega = \dfrac{B^3 H^2 h_1}{12} \times \left[2 - \dfrac{3\psi}{(1+\psi)^2}\right]$

$$J_\omega = \frac{B^3 H^2 h}{6} \cdot \frac{4+3\psi}{2-(1-\psi)^3}$$

$$J_\omega = 2R^5 n\left[\frac{\beta_0^3}{3} + 2\eta M_1 + \eta^2 M_2 + \psi L_3^2\right],$$

$$M_1 = \beta_0 \cos\beta_0 - \sin\beta_0,$$

$$M_2 = \frac{\beta_0 - \sin\beta_0 \cos\beta_0}{2}$$

$$S_{\omega 2} = \frac{B^2 H h(2+\psi^2)}{4[2-(1-\psi)^3]}$$

$$L_1 = \frac{\beta_0^2 - \beta^2}{2}$$

$$L_2 = \cos\beta - \cos\beta_0$$

$$L_3 = \beta_0 - \eta \sin\beta_0$$

$$S_\omega = R^3 h[L_1 - \eta L_2 + \psi L_3]$$

$$\omega_{01} = BH - \frac{b_y}{\sqrt{2}}(H-B)$$

$$\omega_{0,2} = -\frac{b_y H}{\sqrt{2}}$$

$$\omega_0 = R^2(\beta - \psi \sin\beta)$$

$$b_y = \frac{B}{\sqrt{2}} \cdot \frac{\psi(3-2\psi)}{2-(1-\psi)^3}$$

$$\psi = \frac{B}{H}$$

$$b_y = \eta R, \quad \eta = \frac{K_1}{K_2}$$

$$K_1 = 2\sin\beta_0(1+\psi\beta_0) - 2\beta_0 \cos\beta_0$$

$$K_2 = \beta_0 + 2\psi \sin^2\beta_0 - \sin\beta_0 \cos\beta_0$$

$$\psi = \frac{A_p}{Rh}$$
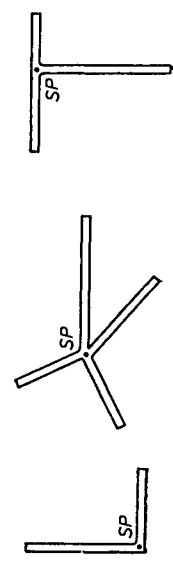
In a cross-section of the number of plane walls intersecting at one point, there is $SP = C$, $\omega_0(s) = 0$, $S_\omega(s) = 0$, $J_\omega = 0$

For a section with plane walls, such plots (Fig. 2.11a) are comprised of a num-
ber of straight sectors. In symmetrical cross-sections, it is recomended to place
the initial point P on the axis of symmetry, since then $\bar{\omega} = 0$;

(c) we must consider the existence of stringers or flanges equivalent to
local wall thickenings h_p (Fig. 2.11b). In a branched cross-section, the
calculation of ω_s proceeds in two stages (Fig. 2.3c);

(d) in calculating $S_\omega^{0,s}$ of a one-stream section, we must always take the
origin $s = 0$ at the free edge. In a section with stringers, $S_\omega^{0,s}$ jumps by $A_p(\omega_0)_p$
at the attachment point of the stringer to the skin, where $(\omega_0)_p$ is the principal
sectorial area corresponding to the attachment point. Jumps of $S_\omega^{0,s}$ also occur
in multisequential sections, namely at the branching place; $S_\omega^{0,s}$ calculated
for the principal sequence has a jump ΔS_ω equal to the sectorial static moment
of the branch concerned, counted from its free edge. It is convenient to repre-
sent the plot of $S_\omega^{0,s}$ on the image of the cross-section in terms of ω_s and ω_0;

(e) if the contour of the section consists of plane walls (Fig. 2.11a) and
thickness h_i of individual walls s_i is constant, then

$$J_\omega = \tfrac{1}{3} \sum_{i=1}^{n} (a_i^2 + a_i b_i + b_i^2) s_i h_i, \qquad (2.26)$$

where s_i, b_i are values of ω_0 at end-points of wall s_i.
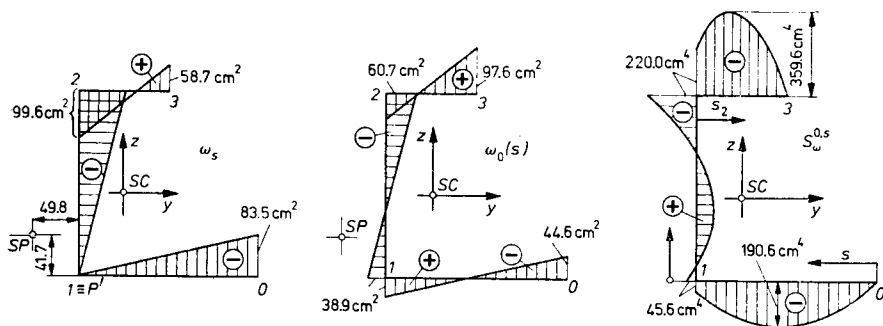
Fig. 2.12. Determination of geometric characteristics for channel bar from Fig. 2.4

An illustration of calculations for a channel section (Fig. 2.4) is given
in Fig. 2.12. Thus, ω_s was determined taking the origin P' in the corner 1,
from which $\bar{\omega}$ was obtained and then $\omega_0(s)$. The sectorial static moment S_ω
was calculated taking origin $s = 0$ at free edge O. Lastly $J_\omega = 53.7 \times 10^3$ cm^6
was determined from (2.26).

The characteristic quantities, $\omega_0(s)$, s_ω and J_ω, for several selected cross-
sections are given in Table 2.1.

2.4. Examples of Torsion of an Open Bar

The analysis begins with the solution of Eq. (2.24)

$$- C_\omega \varphi^{IV} + C\varphi'' = -m.$$

This solution has the form $\varphi = \varphi_m + \varphi_0$, where φ_m is a particular solution and φ_0 the general solution of the homogeneous equation, i.e. with $m(x) \equiv 0$,

$$\varphi_0 = \Phi_1 + \Phi_2 kx + \Phi_3 \sinh kx + \Phi_4 \cosh kx, \tag{2.27}$$

where $\Phi_1, \ldots, \Phi_4$ are the integration constants, and the parameter

$$k = \sqrt{C/C_\omega} = \sqrt{GJ_s/EJ_\omega} \quad (1/\text{m}). \tag{2.28}$$

If $m(x)$ is a continuous function of x over the entire bar length, the constants Φ_i are then determined from the conditions at bar ends (two conditions at each end) relative to the constrains imposed. Typical boundary conditions are specified in Table 2.2.

If a bar is loaded by a number of concentrated moments or if $m(x)$ is a discontinuous function, continuity of the angle of twist and warping must be assured at joining points of consecutive segments i and $i+1$

$$\varphi_i = \varphi_{i+1}, \quad \varphi'_i = \varphi'_{i+1} \tag{2.29a}$$

continuity of stresses σ_x^{II}, i.e.

$$\varphi''_i = \varphi''_{i+1} \tag{2.29b}$$

and lastly, equilibrium of the torsional moments

$$(C\varphi' - C\varphi''')_{i+1} - (C\varphi' - \omega\varphi''')_i = -M_i, \tag{2.29c}$$

where M_i is the concentrated moment at the joining point of segments i and $i+1$.
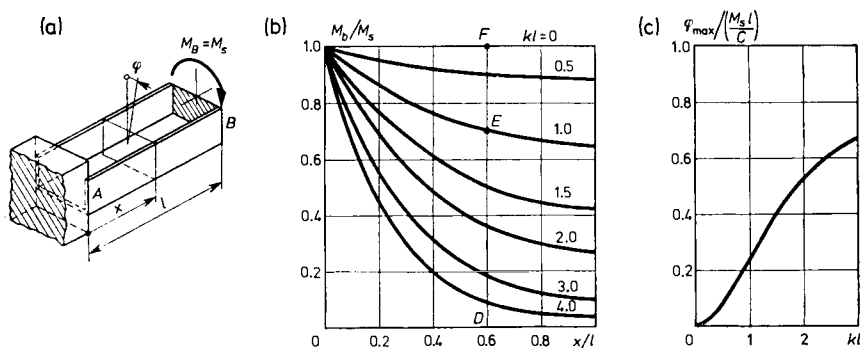
Fig. 2.13. Analysis of the effect of clamping

An illustration of the procedure is the analysis of a prismatic cantilever bar clamped at end A and loaded at free end B by moment M_B (Fig. 2.13a). Since $m \equiv 0$, then $\varphi_m \equiv 0$, $\varphi = \varphi_0$, and constants Φ_i are determined from the conditions

$$(\varphi)_{x=0} = 0; \quad (\varphi')_{x=0} = 0, \quad (\varphi'')_{x=l} = 0; \quad (C\varphi' - C_n\varphi''')_{x=l} = M_B$$

yielding

$$\Phi_1 = -\Phi_4 = -(M_B/kC)\tanh kl, \quad \Phi_2 = -\Phi_3 = M_B/kC,$$

and

$$\varphi = \frac{M_B l}{C}\left[\frac{x}{l} - \frac{\sinh kl - \sinh k(l-x)}{kl\cosh kl}\right]. \tag{2.30}$$

With this result, we determine using (2.19) and (2.20)

$$M_V = C\varphi' = M_B\left[1 - \frac{\cosh k(l-x)}{\cosh kl}\right], \quad M_b = M_B\frac{\cosh k(l-x)}{\cosh kl} \tag{2.31}$$

as parts of moment $M_s = M_B$ corresponding to pure torsion (M_V) and restrained torsion (M_b). The extremal twist angle

$$\varphi_{max} = \varphi_{x=l} = \frac{M_B l}{C}\left(1 - \frac{\tanh kl}{kl}\right). \tag{2.32}$$

The value M_b/M_s is a function of coordinate x and the dimensionless parameter $kl = \sqrt{C/C_\omega}l$ (Fig. 2.13b). This same plot gives the value M_V/M_s as the ordinate EF complementing the ordinate $DE = (M_b/M_s)$ to one. It is apparent that in the vicinity of the clamped cross-section, $M_b \approx M_s$ and decreases with approach to the free end. If $kl < 0.25$, the contribution of pure torsion is negligible and nearly the entire moment is transmitted by restrained
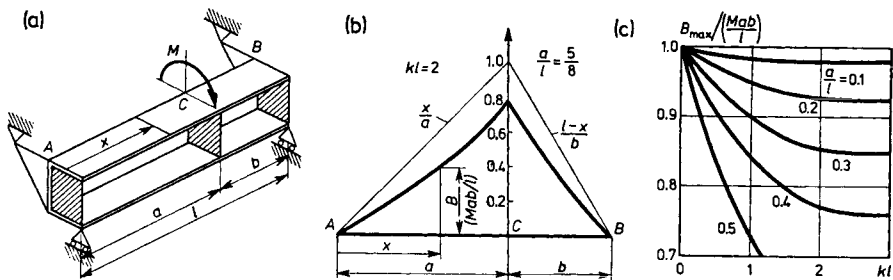
Fig. 2.14. Torsion of a bar supported at both ends: (a) sketch of the bar; (b) typical plot of $B(x)$; (c) value of $B_{max}\left(\frac{a}{l}, kl\right)$

torsion. Clamping also gives a reduction of twist angle φ_{max} compared to the value $(M_s l/C)$ that would be obtained the in absence of clamping (Fig. 2.13c).

A fundamental problem is torsion of abar with ends supported as in variant 2 in Table 2.2 and loaded in cross-section C by moment M (Fig. 2.14a). Because $m \equiv 0$ then $\varphi_m \equiv 0$. The twist angle is obtained from Eq. (2.27), bearing in mind that constants Φ in segments AC and CB are different, because function $M_s(x)$ has a jump in cross-section C. The solution, therefore has, the form of two functions with eight constants Φ and Φ^*

$$\varphi_1 = \Phi_1 + \Phi_2 kx + \Phi_3 \sinh kx + \Phi_4 \cosh kx, \quad 0 \leqslant x \leqslant a,$$

$$\varphi_2 = \Phi_1^* + \Phi_2^* kx + \Phi_3^* \sinh kx + \Phi_4^* \cosh kx, \quad a \leqslant x \leqslant 1.$$

The values of these constants are derived from four support conditions

$$(\varphi_1)_{x=0} = 0, \quad (\varphi_1'')_{x=0} = 0, \quad (\varphi_2)_{x=l} = 0, \quad (\varphi_2'')_{x=l} = 0$$

and four conditions (2.29) for $x = a$, i.e.

$$\varphi_1 = \varphi_2, \quad \varphi_1' = \varphi_2', \quad \varphi_1'' = \varphi_2'', \quad C_n \varphi_1''' - C_n \varphi_2''' = M.$$

After determining therefrom constants Φ and Φ^* we obtain the functions

$$\varphi_1 = \frac{Mb}{C}\left(\frac{x}{1} - \frac{\sinh kb}{kb}\frac{\sinh kx}{\sinh kl}\right),$$

$$\varphi_2 = \frac{Ma}{C}\left[\left(1 - \frac{x}{l}\right) - \frac{\sinh ka}{ka}\frac{\sinh k(1-x)}{\sinh kl}\right],$$

(2.33)

their first derivatives and bimoments $B = C_n \varphi''$

$$\varphi_1' = \frac{M}{C}\left(\frac{b}{l} - \frac{\sinh kb \cosh kx}{\sinh kl}\right),$$

$$\varphi_2' = -\frac{M}{C}\left[\frac{a}{l} - \frac{\sinh ka \cosh k(l-x)}{\sinh kl}\right],$$

(2.34)

$$B_1 = -M\frac{\sinh kb \sinh kx}{k \sinh kl}, \quad B_2 = -M\frac{\sinh ka \sinh k(l-x)}{k \sinh kl}$$

(2.35)

and the value of the bimoment in cross-section $x = a$

$$(B_1)_{x=a} = (B_2)_{x=a} = -\frac{Mab}{l}\left(\frac{\sinh ka}{ka}\frac{\sinh kb}{kb}\frac{kl}{\sinh kl}\right).$$

(2.36)

A typical diagram of the bimoment, therefore of stresses σ_x^{II} (Eq. 2.17) as well, has extremum B_{max} in the loaded cross-section (Fig. 2.14b). This value is always lower than the value Mab/l corresponding to the case $C = 0$

(Fig. 2.14c). Very important are the values $(\varphi_1')_{x=0}$ and $(\varphi_2')_{x=l}$, which according to (1.2) give the warping of the end cross-sections

$$(\varphi_1')_{x=0} = \varphi_A' = \frac{M}{C}\left(\frac{b}{l} - \frac{\sinh kb}{\sinh kl}\right),$$

$$(\varphi_2')_{x=l} = \varphi_B' = -\frac{M}{C}\left(\frac{a}{l} - \frac{\sinh ka}{\sinh kl}\right).$$

(2.37)

It is interesting that the torsional moment in AC and CB is (Mb/l) and $(-Ma/l)$, respectively; therefore, it splits as in the case of pure torsion.

By superposing the above basic solution, more complex problems can be solved, e.g., the action of moments $M_1, \ldots, M_k$ (Fig. 2.15a) or the action of distributed loading m (Fig. 2.15b).
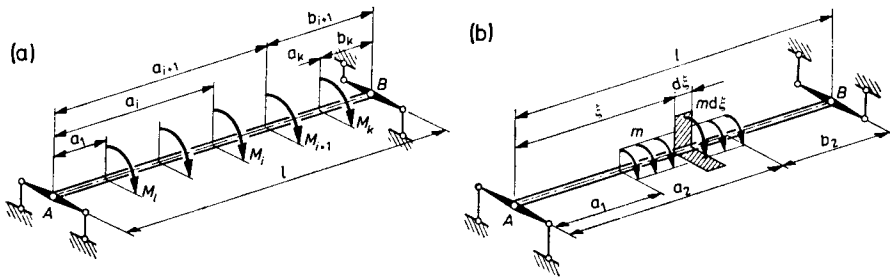
Fig. 2.15. Application of results of the basic solution (Fig. 2.14) for complex problems

The restrained torsion can also be caused by longitudinal loading with a non-zero bimoment (Fig. 2.16a). The analysis of such a problem reduces to solving Eq. (2.24) with conditions (2.29a) the same and (2.29b, c) altered. Thus, at the joining of segments "i" and "$i+1$" loaded by a system of longi-
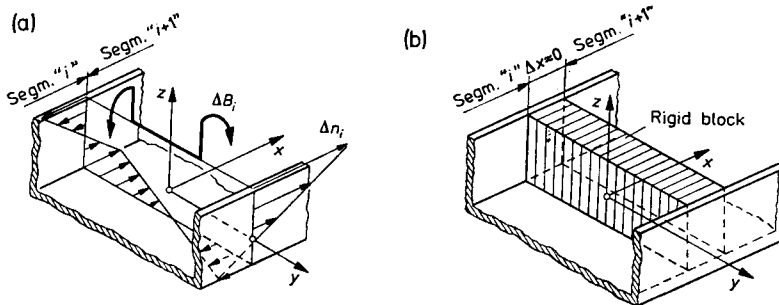
Fig. 2.16. The discontinuity variants of longitudinal flows: (a) external loading by system Δn; (b) elimination of warping

tudinal flow $\Delta n_i(s)$, the stress bimoment experiences a jump, whereas the torsional moment does not change, i.e.

$$(C_\omega\varphi'')_{i+1}-(C_\omega\varphi'')_i = \Delta B_i, \quad (C_\omega\varphi'-C\varphi''')_i = (C\varphi'-C_\omega\varphi''')_{i+1}, \quad (2.38)$$

where in accordance with the definition (2.16a) bimoment ΔB_i equals:

$$\Delta B_i = -\int_0^c \Delta n_i\omega_0\,ds. \quad\quad (2.39)$$

A problem similar to the above (Fig. 2.16b) is when at contact of segments "i" and "$i+1$", the bar has an undeformable block. The continuity conditions at the said contact now have the form

$$\varphi_i = \varphi_{i+1}, \quad \varphi_i' = \varphi_{i+1}' = 0, \quad (C_\omega\varphi'')_i = (C_\omega\varphi'')_{i+1}. \quad\quad (2.40)$$
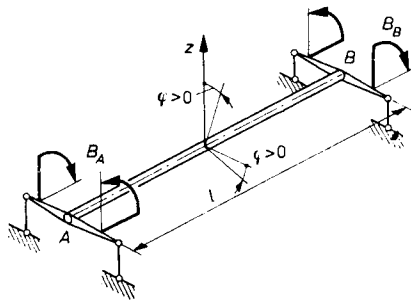
Fig. 2.17. Loading of a bar by boundary bimoments

A very important example is the loading of a bar (Fig. 2.17) supported as shown in Fig. 2.14 by bimoments B_A and B_B. Based on (2.27), with the obvious boundary conditions,

$$(\varphi)_{x=0} = 0, \quad (C_\omega\varphi'')_{x=0} = B_A, \quad (\varphi)_{x=l} = 0, \quad (C_\omega\varphi'')_{x=l} = B_B,$$

we obtain all the quantities of interest, such as

$$\varphi = -\frac{B_A}{C}\left[\left(1-\frac{x}{l}\right)-\frac{\sinh k(l-x)}{\sinh kl}\right]-\frac{B_B}{C}\left(\frac{x}{l}-\frac{\sinh kx}{\sinh kl}\right), \quad\quad (2.41)$$

$$\varphi_A' = (\varphi')_{x=0} = \frac{B_A}{Cl}\left(1-\frac{kl}{\tanh kl}\right)-\frac{B_B}{Cl}\left(1-\frac{kl}{\sinh kl}\right), \quad\quad (2.42)$$

$$\varphi_B' = (\varphi')_{x=l} = \frac{B_A}{Cl}\left(1-\frac{kl}{\sinh kl}\right)-\frac{B_B}{Cl}\left(1-\frac{kl}{\tanh kl}\right), \quad\quad (2.42b)$$

$$B = C_\omega\varphi'' = \frac{B_A\sinh k(l-x)+B_B\sinh kx}{\sinh kl}. \quad\quad (2.42c)$$

These results superposed on the basic solution (Fig. 2.14) or its generalizations (Fig. 2.15) allow the analysis on many cases pertaining to engineering; the latter are cited in monographs, e.g. Kolbrunner and Hajdin (1972), Rutecki (1966), Vlasov (1959).
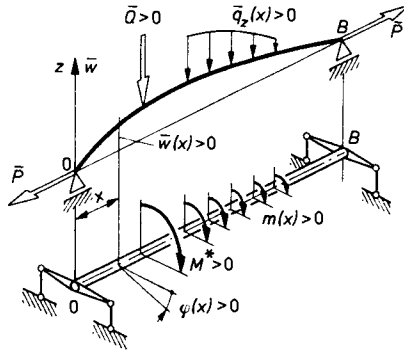
Fig. 2.18. Analogy of the case of bending and torsion

It is interesting that the correctness of the solutions and the physical image of the problem are easily assessed if we use the analogy of Eq. (2.24) and the equation of deflection curve $\bar{w}(x)$ for a beam subjected to bending under load $\bar{q}_z$ and to tension by force $\bar{P}$ (Fig. 2.18). This equation is

$$\overline{EJ}_y \bar{w}^{\mathrm{IV}} - \overline{P}\bar{w}'' = -\bar{q}_z \tag{a}$$

and it is apparent that identity $\bar{w} \equiv \varphi$ holds if

$$\overline{EJ}_y = C_\omega, \quad \overline{P} = C, \quad \bar{q}_z = -m, \quad q = -M^* \tag{b}$$
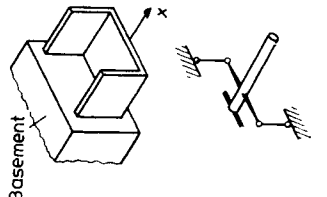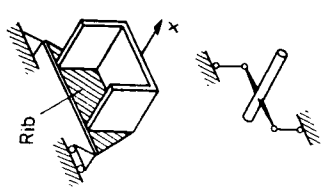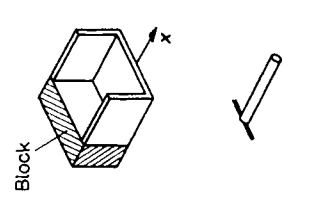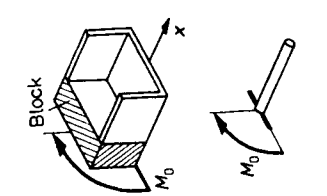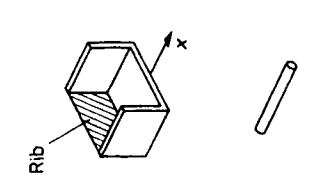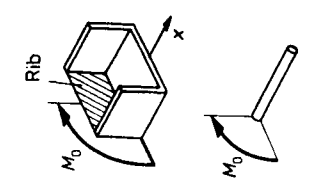
and if the boundary conditions of $\bar{w}$ and φ are identical. Consequent upon this is the identity of the respective static quantities, $\overline{EJ}_y \bar{w}'' = C_\omega \varphi'' = B$, $\overline{EJ}_y \bar{w}'' = C_\omega \varphi''' = -M_b$ and so forth. Their values in a real bar are lower than would be in the case of a bar in which $C = 0$. It follows that the presence of a longitudinal force in a beam subjected to bending always reduces the value of the bending moment and of the shearing force. Thus, in a bar (Fig. 2.14) for which an analogy is a beam with simply supported ends A and B loaded by concentrated force $\overline{Q} = M$, the inaccessable value of bimoment B that cannot be exceeded amounts

$$B = C_\omega \varphi''' < \overline{Q}ab/l = Mab/l,$$
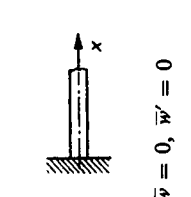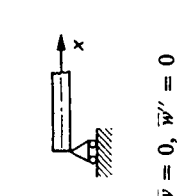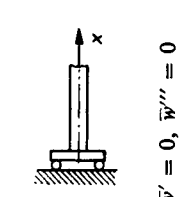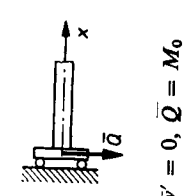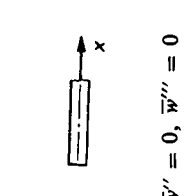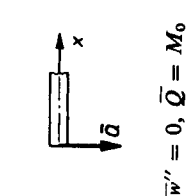
which is clearly illustrated by Fig. 2.14b.

TABLE 2.2. Boundary conditions of a bar subjected to torsion

1. Complete clamping, rotation and warping eliminated	2. No rotation, warping unrestrained	3. Rotation unrestrained, zero warping	4. As in 3, end loaded by moments	5. Free end closed by rib	6. Free end loaded by moment M
Basement	Rib	Block	Block	Rib	Rib
$\varphi = 0, \varphi' = 0$	$\varphi = 0, \varphi'' = 0$	$\varphi' = 0, \varphi''' = 0$	$\varphi' = 0, \varphi''' = -\dfrac{M_0}{C_n}$	$\varphi'' = 0, \varphi''' = k^2\omega$	$\varphi'' = 0$ $\varphi''' - k^2\varphi' = -\dfrac{M_0}{C_\omega}$

Analogy to beam subjected to bending (case $C = 0$)

$\bar{w} = 0, \bar{w}' = 0$	$\bar{w} = 0, \bar{w}'' = 0$	$\bar{w}' = 0, \bar{w}''' = 0$	$\bar{w}' = 0, \bar{Q} = M_0$	$\bar{w}'' = 0, \bar{w}''' = 0$	$\bar{w}'' = 0, \bar{Q} = M_0$

2.5. Simplified Torsion Analysis of a Straight Bar

In many problems important from an engineering point of view, the value $kl = l\sqrt{C/C_n}$ is small, e.g. $kl < (1/3)$. In this case, we can assume that $M_V = 0$, $M_s = M_b = -C\,\varphi_\omega''$; that is, only restrained torsion prevails in the bar, and Eq. (2.24) takes the form

$$C_\omega \varphi^{IV} = -m \tag{2.43a}$$

identical with the equation of deflection curve $\bar{w}(x)$ for a beam

$$\bar{EJ}_y \bar{w}^{IV} = -\bar{q}_z \tag{2.43b}$$

with transverse loading $q_z = -m$, beam rigidity $\bar{EJ}_y = C_\omega$ and boundary conditions according to Table 2.2, in which parameter $k = 0$. The representation of these relationships is given in the lower part of the table so that an analogous beam can be formed and results known from strength of materials
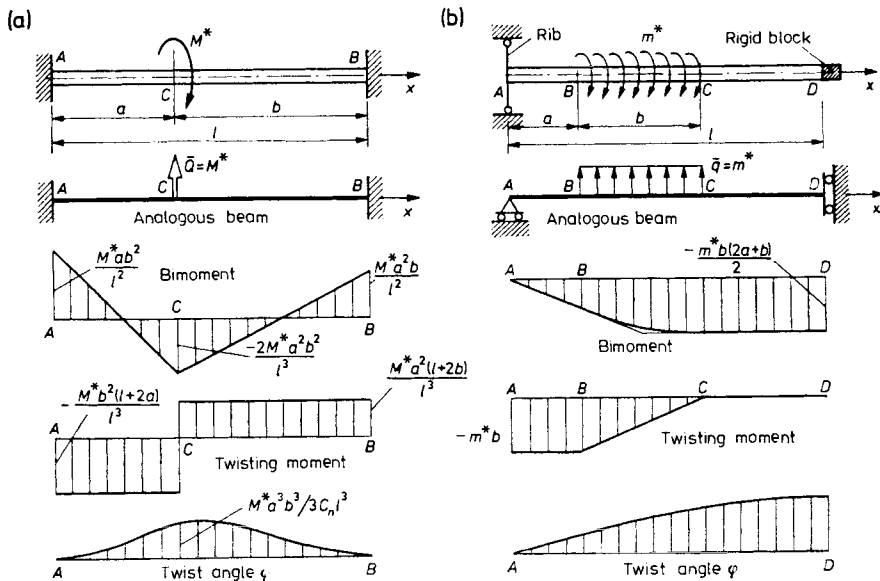
Fig. 2.19. Examples of simplified analysis of restrained torsion: (a) bar clamped at both ends, loaded by concentrated moment; (b) bar supported at left end, with the free end blocked

can be transposed. A few examples of such an application are given in Fig. 2.19, and a certain peculiarity here is the introduction of supports into the analogous beam, which transmit the bending moment but do not transmit the transverse force (Fig. 2.19b).

The analogy considered also serves to check the correctness of a structure which will be satisfactory if the equivalent beam is at least statically determinate. For example, if end D in the bar (Fig. 2.19b) were closed by a rib, not by a block, then according to Table 2.2, the equivalent beam would have at that place the free end and would be a mechanism, not a rigid structure.

2.6. Limitations in Application of Theory

Owing to the simplifying assumptions adopted in Chapter 1, there are unsolvable problems in the theory of thin-walled bars, and these are moreover of two kinds. One is characterized by a very restricted (local) action region many times smaller in size than the cross-section of the bar. Serving as an example here is the shear stress concentration located at a corner at the skin contour (Fig. 2.20a). The real shear stress distribution differs significantly from linear distribution, the most important parameter being radius ϱ of the internal fillet. As follows from the theory of elasticity, real maximum shear stresses τ_i occur on the inner suface (Fig. 2.20b); they are

$$\tau_i = \xi_V \tau_V + \xi_b \tau_b, \tag{2.44a}$$

where the stress-concentration coefficients amount to

$$\xi_V \approx 1 + (h/4\varrho), \quad \xi_b = 1 + (h/2\varrho). \tag{2.44b}$$
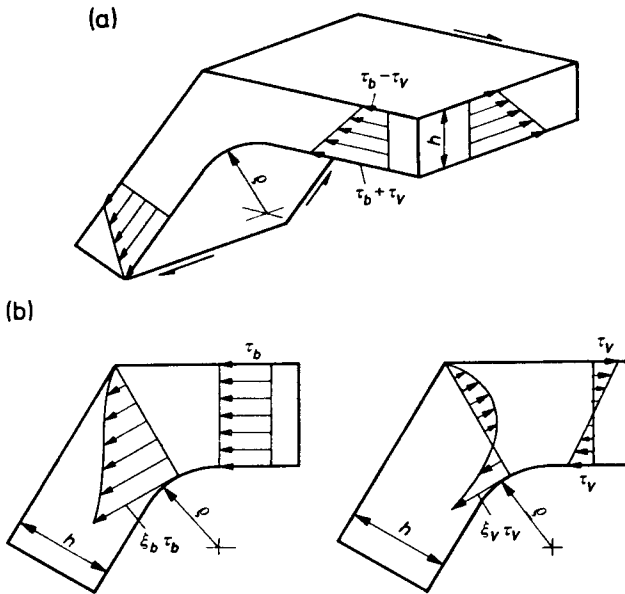
Fig. 2.20. Example of a local problem

This stress concentration, owing to the possibility of the material becoming locally plasticized, has no influence on the strength of the structure, when only the loadings are constant; but it may prove important in the event of fatigue loadings being a potential crack nucleus.

Similar local problems exist in riveted or welded joints of the skin.

Problems of the second kind are result because of the differences between actual load application and the theoretical model. This is exemplified by the
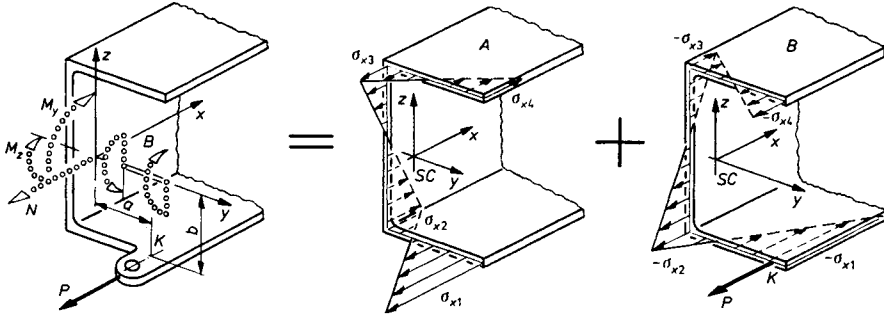
Fig. 2.21.   Distribution of load on statically equivalent primary state (I) and self-equilibrated state (II)

action of longitudinal concentrated force P (Fig. 2.21) producing in the loaded cross-section an effort with components

$$N = P, \quad M_y = Pb, \quad M_z = Pa$$

and with bimoment B determined from the definition (2.26a)

$$B = \int_0^c n_x \omega_0 \, ds = \lim_{\Delta s \to 0} \left(\frac{P}{\Delta s} \right) \omega_{0K} \Delta s = P \omega_{0K}, \tag{2.45}$$

where ω_{0K} is the principal sectorial area for point K. Corresponding to this effort is the σ_x distribution statically equivalent to force P calculated from (2.6) and (2.17), therefore conforming to the theoretical model. If this basic state (A) can be separated out, the residual force system in the loaded cross-section is then a self-equilibrated state (B). According to Saint Venant's principle, state (B) vanishes with distance from the loaded cross-section. However, unlike bars of a solid section, the rate of decay of state (B) depends on the structure of the bar in the vicinity of the loaded cross-section. If there is no rib in the loaded cross-section (Fig. 2.21), the decay of state (B) down to negligible values then depends on the bending rigidity of the skin. In real structures, this proceeds in a segment of the bar, which is equal to length to several mean overall dimensions of the cross-section. By mounting a rib in

the loaded cross-section, this length, l_0, is cut roughly by half (Fig. 2.22a) and the situation is improved in so far as it comes closer to the ideal which is to achieve the basic state (A) over as large a part of the bar as possible. The best solution from an engineering aspect is to mount two ribs and a front wall (Fig. 2.22b), by which a thin-walled body is formed and in which all
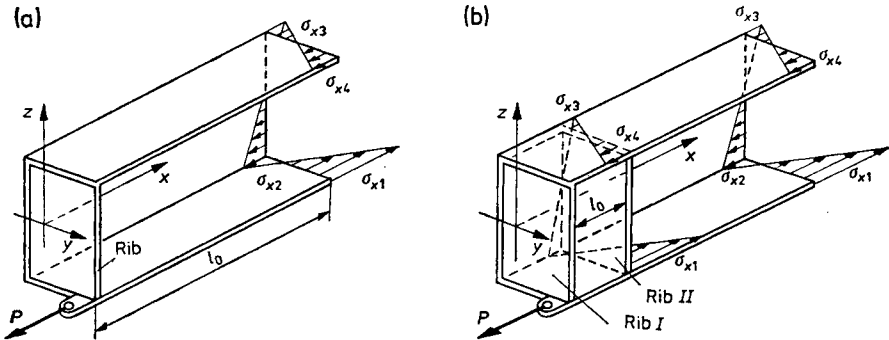
Fig. 2.22. The influence of bar structure on realization of the primary state

overall dimensions are comparable. Such a body is a sufficiently rigid element to transform with engineering accuracy i.e., force P in the cross-section of rib I, into the basic state (A) in the cross-section of rib II. As distinct from the previous variants, the bending rigidity of the skin is not a statically indispensable factor here and is neglected as a rule.

The mounting of such a thin-walled body is necessary from an engineering point of view also if the n_x distribution along the contour is subject to change. A situation like that occurs in the event of a sudden change in the bar cross-section.

3. Statics of Bars of Tubular Cross-Section*

3.1. Pure Torsion of Thin-Walled Tubes

Strength analysis of a tube (Fig. 3.1a) can always be reduced to the analysis of an open bar. This is achieved by cutting the skin along the generatrix (Fig. 3.1b) and introducing shear flows q_0 in the new formed edges $s = 0$ and $s = c$.

One of the loading variants for such a disected tube is a state in which
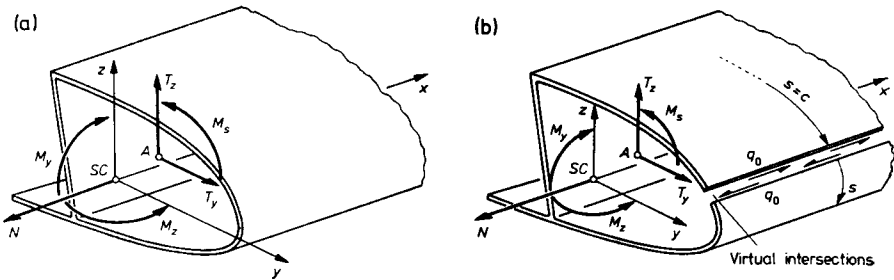
Fig. 3.1. Reduction of tube analysis to the open-bar problem
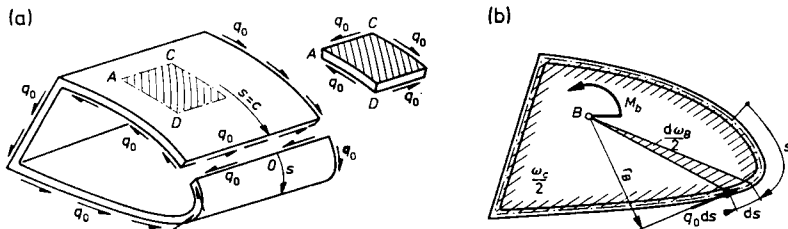
Fig. 3.2. State of stress with pure torsion of single cell tube

* References: Ebner and Köller (1937), Umanskii (1939), Argyris and Dunne (1944, 1947), Adadurov (1948), Benscoter (1954), Urban (1955), Dąbrowski (1958), Novitski (1958), Nowiński (1959), Heiling (1962), Rüdiger (1964).

$n_x \equiv 0$. In keeping with (1.8), sheer flow then exists throughout the skin (Fig. 3.2a)

$$q(s) = q_0 = \text{const.} \tag{a}$$

In the cross-section, the resultant of this flow is zero, whereas the resultant moment of forces $q_0 \, ds$ with respect to pole B (Fig. 3.2b) is

$$M_b = \int_0^c q_0 \, ds r_B = q_0 \oint d\omega_B = q_0 \omega_c, \tag{3.1}$$

where $\oint d\omega_B = \omega_c$ is the double area bounded by the skin contour. Thus, the present case represents so-called *pure torsion* of the tube, with no normal stresses σ_x involved. The deformations occurring here are determined by two quantities, namely by angle $\varphi(x)$ and by longitudinal displacement u_K of points of the skin. Because $\sigma_x \equiv 0$, u_K does not depend on x and represents warping of the cross-section. Its value is calculated as in Section 1.2 but shear strain γ of the skin* should be considered. Thus, taking pole B to be on the axis of rotation we find the displacements $\eta = \varphi r_B$ (Fig. 1.2) and from Eq. (b), Section 1.2

$$\gamma = \frac{q_0}{Gh} = \frac{d\varphi}{dx} r_B + \frac{du_K}{ds}. \tag{3.2}$$

By integrating (3.2) with respect to s, we obtain warping u_K of point K

$$u_K = -\omega_B \varphi' + \frac{q_0}{G} \int_0^s dp, \tag{b}$$

where $dp = ds/h$ is the dimensionless differential of the element of contour, ω_B is the sectorial area corresponding to point K (Fig. 1.3), and we assume also that for edge $s = 0$, displacement $u_0 = 0$. By virtue of continuity, displacement u_K corresponding to $s = c$ equals $u_K = u_0 = 0$, i.e.

$$(u_K)_{s=c} = 0 = \frac{q_0}{G} \oint dp - \omega_c \varphi'. \tag{c}$$

Hence, taking (3.1) into consideration, we obtain the relation

$$M_b = \frac{G\omega_c^2}{p_c} \varphi', \tag{3.3a}$$

---

* Omitting it would mean taking the structure to be infinitely rigid, which is obviously erroneous.

involving moment M_b and unit angle of twist $\varphi' = d\varphi/dx$, and

$$p_c = \oint \frac{ds}{h} \tag{3.3b}$$

is the dimensionless length of the whole contour. Moment M_b corresponds to a uniform distribution of τ_{xs} along thickness h and is complemented by flows m_{xs} (Fig. 1.4) giving according to (2.20) the moment $M_V = GJ_s\varphi'$. Consequently, total moment M_t equals

$$M_t = M_b + M_V = G\left(\frac{\omega_c^2}{p_c} + J_t\right)\varphi' = C\varphi', \tag{3.4a}$$

where C is the pure torsion rigidity of the tube

$$C = G\left(\frac{\omega_c^2}{p_c} + J_t\right). \tag{3.4b}$$

Usually, M_V is neglected and $M_t = M_b$. Equations (3.1) and (3.3) thus simplified are called *Bredt's equations*. Eliminating M_s from them, we determine q_0/G, and after substituting into (b), we obtain the warping of point K as

$$u_K = -\left(\omega_B - \omega_c \frac{p_s}{p_c}\right)\varphi' = -\omega'\varphi', \tag{3.5a}$$

where the dimensionless length of the arc defining point K

$$p_s = \int_0^s ds/h, \tag{3.5b}$$

and $\hat{\omega}$ is the sectorial are of point K of the tube defined as

$$\hat{\omega} = \omega_B - (\omega_c p_s/p_c), \tag{3.5c}$$

which depends on three parameters (the coordinates of the centre of rotation B and the selected origin $s = 0$), as in open cross-sections. It follows from

(a)   (b)
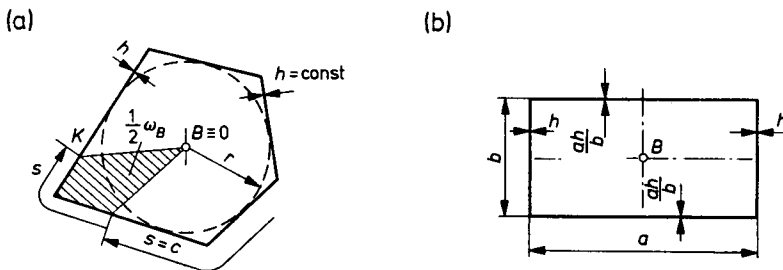
Fig. 3.3. Examples of tubular cross-sections with zero warping

Eq. (3.5c) that tubular cross-sections may exist for which $\hat{\omega}(s) \equiv 0$. One such form is represented by tubes having $h = \text{const}$, with a polygonal contour circumscribed on a circle and with point $B \equiv 0$ (Fig. 3.3a) for which

$$\omega_B = sr, \quad \omega_c = cr, \quad p_s = s/h, \quad p_c = c/h.$$

Hence, it follows that $\hat{\omega} = 0$. Another example are tubes, in which the thickness of plane walls is inversely proportional to their distance from centre of twist B (Fig. 3.3b). Cross-sections for which $\hat{\omega} \equiv 0$ suffer no deplanation in torsion.

Pure torsion of multicell tubes is analysed in similar manner, the only difference being that the change for an open cross-section requires as many longitudinal intersections as there are cells in the tube (Fig. 3.4b). Flows $q_1, q_2, \ldots$
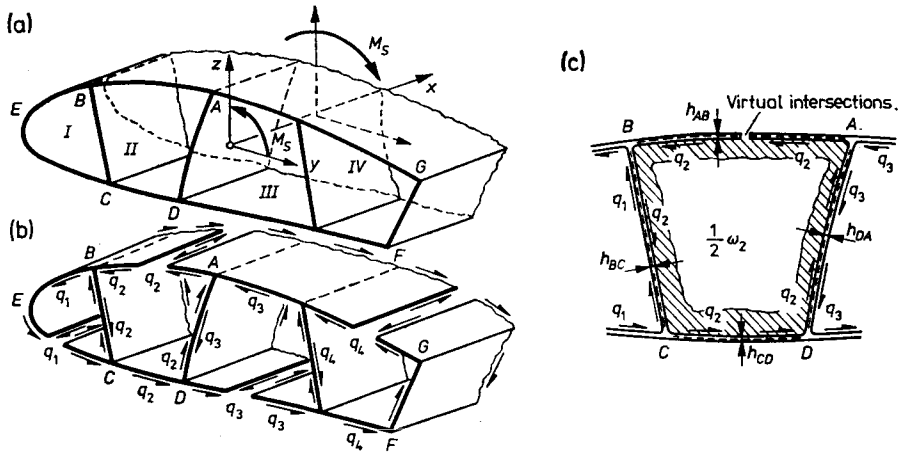
Fig. 3.4. Pure torsion of a multicell tube

which can be manifested here, are acting in walls belonging to a given cell, e.g., q_2 is acting only in the elements of contour $ABCD$. If all flows are acting in the walls common to two cells, say in AD or BC, a resultant flow comes from superposition, i.e., $q_2 - q_1$ in wall BC. These flows produce twist angle φ' in the isolated cell $ABCD$ as in a single cell tube, except that in Eqs. (b) and (c), flow q_0 is not constant over the circumference. As a result, Eq. (c) takes the form

$$\frac{q_1}{G} \int_{AB} \frac{ds}{h} + \frac{(q_2 - q_1)}{G} \int_{BC} \frac{ds}{h} + \frac{q_2}{G} \int_{CD} \frac{ds}{h} + \frac{q_2 - q_3}{G} \int_{DA} \frac{ds}{h} - \varphi' \omega_2 = 0, \quad \text{(d)}$$

where ω_2 is the double area of the investigated cell *ABCD*. Transforming this and denoting cell "2" as cel "*i*" to generalize, we obtain the equation

$$-p_{i,i-1}q_{i-1}+p_{i,i}q_i-p_{i,i+1}q_{i+1} = G\omega_i\varphi' \tag{3.6a}$$

in which the dimensionless lengths of the common walls between the examined cell "*i*" and cells "*i*−1" and "*i*+1" are

$$p_{i,i-1} = \int_{BC} \frac{ds}{h_{BC}}, \quad p_{i,i+1} = \int_{DA} \frac{ds}{h_{DA}} \tag{3.6b}$$

and the dimensionless length of the whole contour of cell "*i*"

$$p_{i,i} = \int_{AB} \frac{ds}{h_{AB}} + \int_{BC} \frac{ds}{h_{BC}} + \int_{CD} \frac{ds}{h_{CD}} + \int_{DA} \frac{ds}{h_{DA}} = \oint \frac{ds}{h}. \tag{3.6c}$$

As a result, we have as many equations as there are cells, i.e., as there are flows q_i. An additional unknown is twist angle φ' which owing to non-deformability of the ribs is identical for all cells. The missing equation follows from the equivalence of resultant moment M_s and the sum of moments $M_{bi} = q_i \cdot \omega_i$ of all K cells, i.e.

$$M_t = \sum_{1}^{k} q_i\omega_i. \tag{3.7}$$

The advantage of a multicell tube lies in the equalization of the shear stress values. If, for example, the outer sheet *ABECD* of the tube (Fig. 3.4) were substantially thickner than the sheet *DFGA* and if there were no inner walls, say, *BC*, *DA*, ... then with torsion of such a single cell tube the shear stresses in sheet *SFGA* would be much higher than in *ABECD*, since q_0 = const. Where inner walls are present, the flows will increase in the stiffer part *ABECDA*, and in the remaining part they will decrease in relation to q_0 so that in effect values $\tau_b = q/h$ become more equalized. If the outer sheet has roughly a constant thickness, the shear flows in those inner walls are not very great and the tube behaves practically like a single cell tube.

3.2. Simple Bending of a Tubular Bar

The case of simple bending of a bar, in which by assumption $\varphi(x) \equiv 0$, becomes similar to that considered in Section 2.1 after longitudinal intersection of the skin (Fig. 3.1b). Thus, retaining the assumptions from Chapter 1, we obtain the very same equations (2.1)–(2.7). The difference is first apparent in determining shear flow q^1 since by virtue of the existence of flow q_0 at the

introduced intersection of $s = 0$, q_0 will occur in Eq. (1.8) and in relations (2.10). In effect we have

$$q^1 = q_0 + \frac{T_z}{J_y} S_y^{0,s} + \frac{T_y}{J_z} S_z^{0,s} \tag{3.7a}$$

if y and z axes are centroidal principal, and

$$q^1 = q^0 + \frac{\mathfrak{X}_z}{J_y} B_y + \frac{\mathfrak{X}_y}{J_z} S_z \tag{3.7b}$$

if they are centroidal but not principal. The definitions of shearing forces, T_z, T_y, and quantities $\mathfrak{X}_z$, $\mathfrak{X}_y$ are as in Section 2.1. Moments $S_y^{0,s}$, and $S_z^{0,s}$ are calculated as if the cross-section are open.

The condition providing the value q_0 is that there is no relative longitudinal displacement between edges $s = 0$ and $s = c$. This displacement may develop as a result of shear strains of the skin as given by Eq. (3.2), in which we now have $\varphi(x) \equiv 0$. In this way, we obtain

$$(u_K)_{s=c} - (u_K)_{s=0} = 0 = \oint \frac{q^1}{Gh} \, ds, \tag{a}$$

hence, after applying (3.7), it follows that

$$q_0 = -\frac{\mathfrak{X}_z}{J_y p_c} \oint S_y^{0,s} dp - \frac{\mathfrak{X}_y}{J_z p_c} \oint S_z^{0,s} dp, \tag{3.8}$$

where symbols dp and p_c are as in Section 3.1. This value of q_0 substituted into (3.7b) yields the total flow

$$q^1 = \frac{\mathfrak{X}_z}{J_y} \left(S_y^{0,s} - \frac{1}{p_c} \oint S_y^{0,s} dp \right) + \frac{\mathfrak{X}_y}{J_z} \left(S_z^{0,s} - \frac{1}{p_c} \oint S_z^{0,s} dp \right), \tag{3.9}$$

whose resultant has components identically equal to the real shearing forces T_y and T_z. Concomitantly, the moment of flow q^1 must be identically equiv-
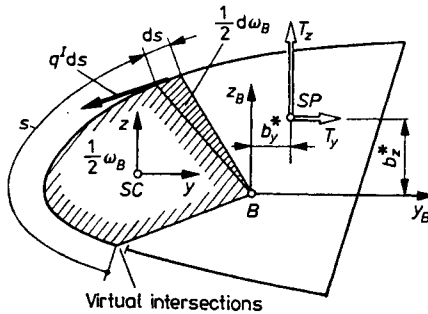
Fig. 3.5. Determination of the shear centre in a tubular cross-section

alent to the moment of resultant forces T_y and T_z with respect to the chosen pole B (Fig. 3.5), i.e.

$$\oint q^1 d\omega_B \equiv T_z b_y^* - T_y b_z^*, \tag{b}$$

where b_y^*, b_z^* are the arms of forces T_z and T_y with respect to point B.

Employing now q^1 from (3.9), we obtain, by virtue of forces T_y and T_z being independent, two coordinates

$$b_y^* = \frac{\varkappa}{J_y} \oint \left(S_y^{0,s} - \frac{J_{yz}}{J_z} S_z^{0,s} \right) d\hat{\omega}_B,$$

$$b_z^* = -\frac{\varkappa}{J_z} \oint \left(S_z^{0,s} - S_y^{0,s} \frac{J_{yz}}{J_y} \right) d\hat{\omega}_B, \tag{c}$$

where $\varkappa$ is given by relation (2.7b), and

$$d\hat{\omega}_B = d\omega_B - \frac{\omega_c}{P_c} dp \tag{d}$$

is the differential of sectorial area $\hat{\omega}$ (Eq. 3.5c). It is evident that equations (c) are similar to Eqs. (e) in Section 2.1 for an open bar, with the difference, however, being that sectorial area ω_B has been replaced by $\hat{\omega}_B$. The transformations of Eqs. (c) are also similar giving in effect

$$b_y^* = \frac{-\varkappa}{J_y} \left[\oint \hat{\omega}_B zh \, ds - \frac{J_{yz}}{J_z} \oint \hat{\omega}_B yh \, ds \right], \tag{3.10a}$$

$$b_z^* = \frac{\varkappa}{J_z} \left[\oint \omega_B yh \, ds - \frac{J_{yz}}{J_y} \oint \hat{\omega}_B zh \, ds \right], \tag{3.10b}$$

as coordinates in the y_B, z_B system of shear centre SP of the tube. This point has exactly the same meaning and properties as for an open cross-section.

$$J_y = 12507 \, cm^4, \quad J_y = 39587 \, cm^4,$$
$$J_{yz} = -2083 \, cm^4$$
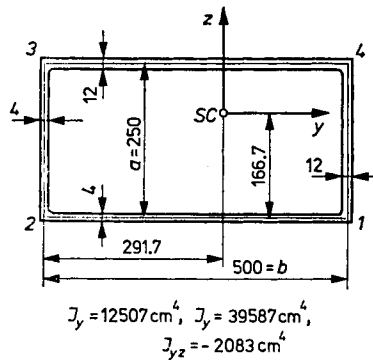
Fig. 3.6. Data for a numerical example

The calculation rules are also similar. Specifically, any point of the cross-section can be taken for pole B. When y and z axes are centroidal principal, we should put in Eqs. (3.10) $J_{yz} = 0$ and $\varkappa = 1$.

The successive stages of calculating b_y^*, b_z^* are presented in the example of a rectangular tube (Fig. 3.6), in which taking pole B to be in corner 2,
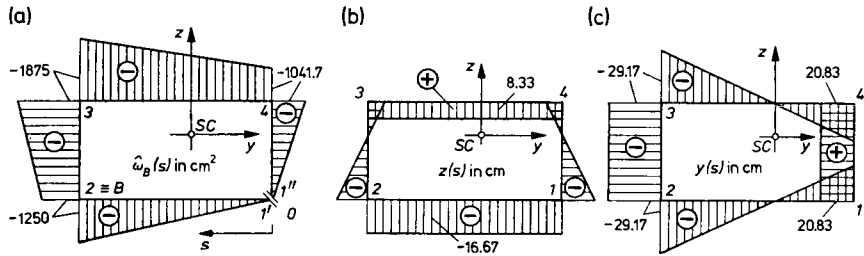
Fig. 3.7. Initial data for position determination of SP

and introducing the apparent intersection in corner 1 (Fig. 3.7a), we determine $\hat{\omega}_B(s)$ and $z(s)$ and $y(s)$ (Fig. 3.7b, c). The elementary integrals

$$\oint \hat{\omega}_B zh\,ds = -458.8 \times 10^3 \text{ cm}^5, \qquad \oint \hat{\omega}_B yh\,ds = 859.4 \times 10^3 \text{ cm}^5$$

yield after substituting into (3.10)

$$b_y^* = 34.16 \text{ cm}, \qquad b_z^* = 19.91 \text{ cm}.$$

Positive values b_y^* and b_z^* should be measured from pole B complying with the positive senses of the central y, z axes.

In a similar manner, we can follow the stages of determining flow q^1 taking, for example, force $T_z = 50$ kN placed at SP. Retaining the intersection of contour in corner 1, we calculate successively $\mathfrak{T}_z S_y^{0,s}/J_y$, $\mathfrak{T}_y S_z^{0,s}/J_z$ and
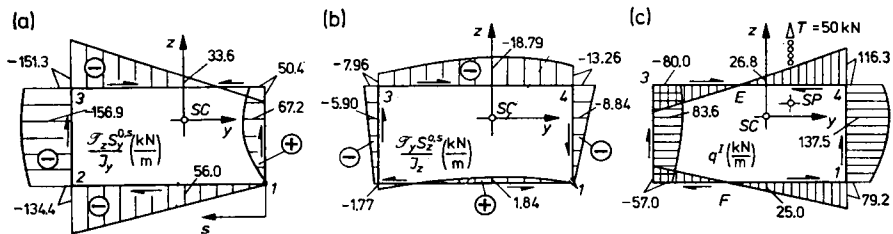
Fig. 3.8. Calculation of q^1 flow distribution with $T_z = 50$ kN

transfer their diagrams onto the illustration of the cross-section in Fig. 3.8. The elementary integrals of Eq. (3.8) yield $q_0 = 79.2$ kN/m > 0, meaning that its direction is opposite to the direction of the positive coordinate s.

Superposing the components (Fig. 3.8a, b) with constant q_0, we obtain the diagram of flow q^1 (Fig. 3.8c). It is seen that with torsionless bending the bar behaves like two-channel sections joined along generatrices E and F. This is a typical feature of all tubular sections.
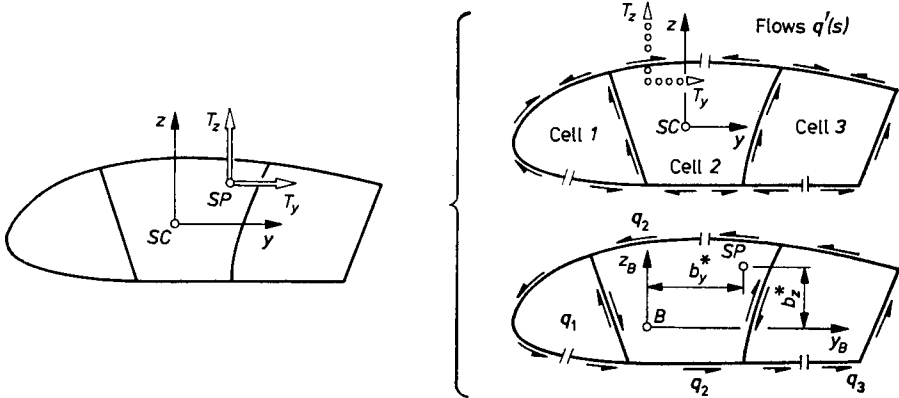
Fig. 3.9. Stages of determining SP of multicell cross-section

A similar procedure is followed for multicell cross-sections (Fig. 3.9). The total flow q^1 is the sum of flows q_i resulting from the introduction of apparent intersections, as in Fig. 3.4b, and the flow

$$q' = (\mathfrak{T}_z S_y^{0,s}/J_y) + (\mathfrak{T}_y S_z^{0,s}/J_z), \tag{3.11}$$

which is calculated as if the apparent intersections were real and the cross-section open. The flows are calculated from the set of equations (3.6) modified by the term $\oint_i (q'\,ds/h)$ representing the relative displacement at the edge of intersection of cell "i" induced by q', i.e.

$$p_{i,i-1}q_{i-1} + p_{i,i}q_i - p_{i,i+1}q_{i+1} + \oint_i q'\,dp = 0, \tag{3.12a}$$

where the quantities p are given by Eqs. (3.6b, c). Having q^1, we can determine from equivalence equation (b) the coordinates b_y^* and b_z^* of the shear centre with respect to chosen pole B. This equation now takes the form

$$\sum_1^k q_i \omega_i + \oint q'\,d\omega_B = T_z b_y^* - T_y b_z^*, \tag{3.12b}$$

where $\sum q_i \omega_i$ is the moment of flows q_i (cf. Eq. (3.7b)), and the second term is the moment of flow q'. It is advisable to carry out the calculations in two independent sequences, the first corresponding to the action of force T_z

alone and the second, to the action of force T_y alone, and it is convenient to map the solution stages in the diagram of the cross-section. Specifically, this applies to true directions of flow q'.

3.3. Restrained Torsion of a Tubular Bar

With the shear centre determined (Sec. 3.2), we can make a division of loading into bending and torsion (Fig. 2.6). The latter has already been partially examined in Section 3.1 for pure torsion, in which M_t = const and the cross-section is free to warp. The warping is described by Eq. (3.5), i.e.

$$u_K = -\hat{\omega}_B \varphi' = -\left(\omega_B - \omega_c \frac{p_s}{p_c}\right)\varphi' \qquad \text{(a)}$$
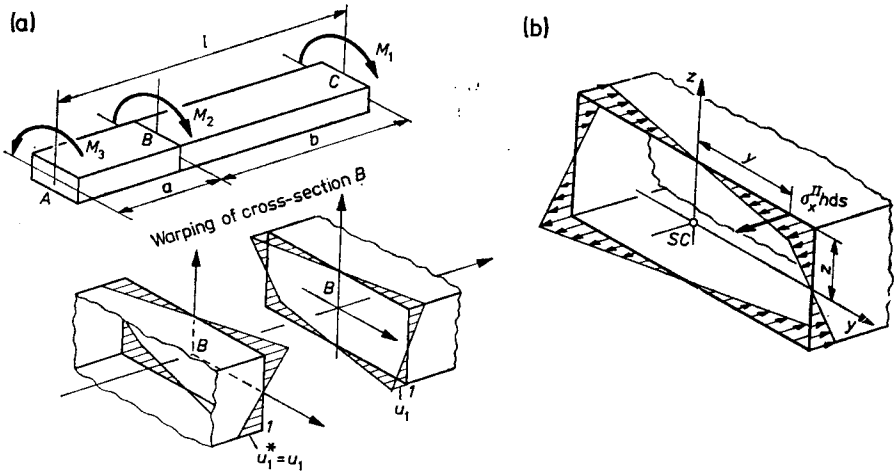
Fig. 3.10. Generation of restrained torsion in a tube

and φ' follows from (3.4). When M_t = const (Fig. 3.10), the use of the pure torsion model would give a discontinuity of displacements u in the cross-section of application of moment M_2. For the discontinuity to be eliminated, the existence of normal stresses σ_x^{II} with resultant N and moments M_y and M_z equalling zero is required, i.e.

$$\oint \sigma_x^{II} h \, ds = 0, \quad \oint \sigma_x^{II} h_z \, ds = 0, \quad \oint \sigma_x^{II} h_y \, ds = 0. \qquad \text{(b)}$$

As with open bars, torsion analysis of a tube, in which the existence of σ_x^{II} is considered, is called *restrained torsion*.

This problem has been analysed by many authors, resulting in effect in a number of approximate solutions, of which Umanski's solution (1939) is

widely accepted. It is founded on the same assumptions as in Section 1.2, outside assumption II concerning neglibility of shear strains since it turns out that with restrained torsion of tubular bars, shear and normal stresses are of the same order. Instead, we assume that warping u in restrained torsion has the same character as in pure torsion, which means that it is proportional to $\hat{\omega}_B$

$$u_K(x, s) = -f(x)\hat{\omega}_B,\tag{3.13}$$

where $f(x)$ is the function controlling the magnitude of warping. The value of normal stresses follows from assumption (3.13)

$$\sigma_x^{II} = E\frac{\partial u}{\partial x} = -E\hat{\omega}_B \cdot \frac{df}{dx}\tag{3.14}$$

satisfying conditions (b), which leads consequently to

$$\oint \hat{\omega}_B h\, ds = 0, \quad \oint \hat{\omega}_B z h\, ds = 0, \quad \oint \hat{\omega}_B y h\, ds = 0.\tag{c}$$

The last two conditions (c) show on confrontation with (3.10) that pole B with respect to which $\hat{\omega}_B$ is calculated must be taken to be at the shear centre (SP). The first condition is as for an open cross-section, amounting to a suitable choice of origin P defining the value of area $\hat{\omega}_B$. By introducing as in Section 2.2, the weighted mean value

$$\bar{\omega} = -\frac{1}{A}\oint \hat{\omega}_B h\, ds,\tag{3.15a}$$

we obtain the principal sectorial area of a tubular cross-section

$$\hat{\omega}_0 = \hat{\omega}_B + \bar{\omega},\tag{3.15b}$$

which plays the same role as ω_0 for an open cross-section (Eq. (2.14)) and is calculated in a similar manner.

   Using u determined from (3.13) we can determine shear stresses τ_b^{II}. Considering that in the case of torsion, pole $B \equiv SP$ has no displacement, we obtain from Eq. (b), Section 1.2

$$\gamma = \frac{\tau_b^{II}}{G} = \frac{d\varphi}{dx}r_B + \frac{\partial u_K}{\partial s} = r_B\varphi' - f(x)\frac{d\hat{\omega}_B}{ds}.\tag{d}$$

Taking Eq. (3.5c) into account, we determine

$$\frac{d\hat{\omega}_B}{ds} = \frac{d\omega_B}{ds} - \frac{\omega_c}{p_c}\frac{1}{h} = r_B - \frac{\omega_c}{p_c}\frac{1}{h},\tag{e}$$

whence finally the membrane shear stresses

$$\tau_b^{II} = G\left[r_B(\varphi' - f) + \frac{\omega_c}{p_c}\frac{f}{h}\right].\tag{f}$$

It is apparent that stresses τ_B^{II} and σ_x^{II} depend on $f(x)$. Owing to the approximate character of the solution, this function is determined from the condition of minimum total potential energy $\Pi = L - U$ of the system, where

$$U = \int_0^l \oint \left[\frac{(\sigma_x^{II})^2}{2E} + \frac{(\tau_b^{II})^2}{2G} \right] h \, ds \, dx, \quad L = \int_0^l m\varphi \, dx \tag{g}$$

are the strain energy of the bar (U) and the work (L) done by loadings $m\,dx$ on displacement φ. By substituting into (g) expressions (3.14) and (f) with the condition that $B = SP$, i.e., $\hat{\omega}_B = \hat{\omega}_0$ and by integrating over the whole contour, we obtain

$$\Pi = \int_0^l \left\{ m\varphi - \left[\frac{E\hat{J}_\omega}{2} (f')^2 + \frac{G(J_r - J_b)}{2} f^2 - \right.\right.$$

$$\left.\left. - G(J_r - J_b)f\varphi' + \frac{GJ_r}{2} (\varphi')^2 \right] \right\} dx. \tag{h}$$

The purely geometric quantities introduced here

$$\hat{J}_\omega = \oint (\hat{\omega}_0)^2 h \, ds, \quad J_r = \oint r_B^2 h \, ds, \quad J_b = \frac{\omega_c^2}{p_c} \tag{3.16}$$

have a definite physical meaning. Thus, by analogy with open bars, $\hat{J}_\omega$ (m^6) is the principal sectorial moment of inertia of the cross-section and J_r (m^4) is the pseudopolar moment of inertia, being a sum of products of the surface $h\,ds$ by square normal length r_B. Lastly, J_b (m^4) is the principal part of pure torsion rigidity $C \approx GJ_b$ of the tube.

The postulate of minimum Π gives two Euler's equations

$$\frac{\partial\bar{\Psi}}{\partial f} - \frac{d}{dx}\left(\frac{\partial\bar{\Psi}}{\partial f'} \right) = 0, \quad \frac{\partial\bar{\Psi}}{\partial\varphi} - \frac{d}{dx}\left(\frac{\partial\bar{\Psi}}{\partial\varphi'} \right) = 0,$$

where $\bar{\Psi}$ is functional (h). Determining the respective derivatives, we obtain a set of two equations
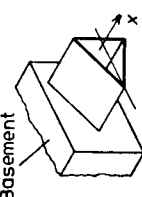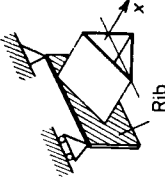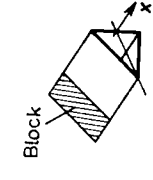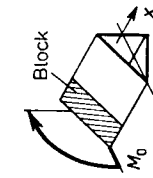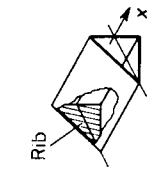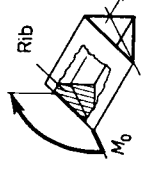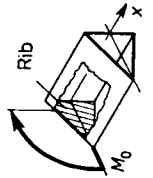
$$E\hat{J}_\omega f'' - G(J_r - J_b)f + G(J_r - J_b)\varphi' = 0, \tag{3.17a}$$

$$GJ_r\varphi'' - G(J_r - J_b)f' = -m. \tag{3.17b}$$

These equations define twist angle φ and function $f(x)$ describing deplanation u of the cross-section as

$$\varphi = \varphi_m + \varphi_0, \quad f = f_m + f_0, \tag{3.18}$$

TABLE 3.1. Boundary conditions of tubular bar subjected to torsion

1. Clamping, warping and rotation eliminated	2. No rotation, free warping	3. Unrestrained rotation, zero warping	4. As in 3, end loading by a moments	5. Free end closed by rib	6. Free end loaded by moment M
$\varphi = 0, f = 0$	$\varphi = 0, f' = 0$	$f = 0, \varphi' = 0$	$f = 0,$ $\varphi' = \dfrac{M_0}{GJ_r}$	$f' = 0,$ $\varphi'\left(-1 - \dfrac{J_b}{J_r}\right)f = 0$	$f' = 0,$ $\varphi' - \left(1 - \dfrac{J_b}{J_r}\right)f = \dfrac{M_0}{GJ_r}$

where $\varphi_m(x)$ and $f_m(x)$ are the particular solutions corresponding to given loading $m(x)$. Functions φ_0 and f_0,

$$\varphi_0 = \Phi_1 + \Phi_2 kx + \Phi_3 \sinh kx + \Phi_4 \cosh kx, \tag{3.19a}$$

$$f_0 = F_1 + F_2 kx + F_3 \sinh kx + F_4 \cosh kx, \tag{3.19b}$$

are solutions of the homogeneous set (3.18), in which Φ_i, F_i are constants of integration, and

$$k = \sqrt{\frac{GJ_b}{E\hat{J}_\omega}\left(1 - \frac{J_b}{J_r}\right)} \quad (1/m). \tag{3.20}$$

Constants F_i and Φ_i are interrelated at the same time by the relations

$$F_1 = \Phi_2 k, \quad F_2 = 0, \quad F_3\left(1 - \frac{J_b}{J_r}\right) = \Phi_4 k, \quad F_4\left(1 - \frac{J_b}{J_r}\right) = \Phi_3 k, \tag{3.21}$$

owing to which only four constants are independent and have to be determined from two boundary conditions in each of the two end cross-sections of the bar. As for the conditions themselves, they follow from (3.13) and (3.14) or from the kinematic constraints for angle φ, or lastly from Eq. (3.17b) giving after integration the relation

$$GJ_r\varphi' - G(J_r - J_b)f = M_t, \tag{3.22}$$

involving torsional moment M_t as a function of φ' and f. The complete illustration of typical conditions is given in Table 3.1.

When $J_r = J_b$, the set of Eq. (3.18) splits into two independent equations

$$E\hat{J}_\omega f'' = 0, \quad GJ_r\varphi'' = GJ_b\varphi'' = -m; \tag{i}$$

the second one coincides with (3.4a) and corresponds to pure torsion of the bar. Such a case is feasible when the cross-section remains plane with torsion, i.e., when $\hat{\omega} \equiv 0$, and consequently $\hat{J}_\omega = 0$ and $\sigma_x^{II} \equiv 0$.

Having function $f(x)$, we can determine σ_x^{II} from (3.14), but to calculate flows $q_b^{II} = \tau_b^{II} h$ it is necessary to remove the contradiction resulting from the approximate character of the solution. The point is that while stresses τ_b^{II} described by relation (f) satisfy the global condition of equivalence of moments

$$\oint \tau_b^{II} r_B \, dsh = M_t, \tag{j}$$

they fail to satisfy the equilibrium equation of element (1.7b). This contradiction can be eliminated assuming that real flow q_b^{II} follows from (1.7b), which by applying (3.14) and (3.15) gives

$$q_b^{II} = q_0 - \int_0^s \frac{\partial n_x}{\partial x} \, ds = q_0 + Ef'' \int_0^s \hat{\omega}_0 h \, ds = q_0 + EF'' S_\omega^{0,s}, \tag{k}$$

where $S_\omega^{0,s} = \int_0^s \hat{\omega}_0 h \, ds$ is the sectorial static moment and q_0 is the flow at point $s = 0$ determined from the equivalence of moment M_t and moment od flows q_b^{II}, i.e.

$$M_t = \oint q_b^{II} r_B \, ds = q_0 \omega_c + Ef'' \oint S_\omega^{0,s} d\omega_B. \tag{m}$$

This value of q_0 substituted into (k) gives finally

$$q_b^{II} = \frac{M_t}{\omega_c} + Ef'' \hat{S}_\omega^{0,s}, \tag{3.23a}$$

where $\hat{S}_\omega^{0,s} = S_\omega^{0,s} + \overline{S}_\omega$ is the principal sectorial static moment, in which the weighted mean value $\overline{S}_\omega$

$$\overline{S}_\omega = -\frac{1}{\omega_c} \oint S_\omega^{0,s} d\omega_B \tag{3.23b}$$

(a)   (b)   (c)
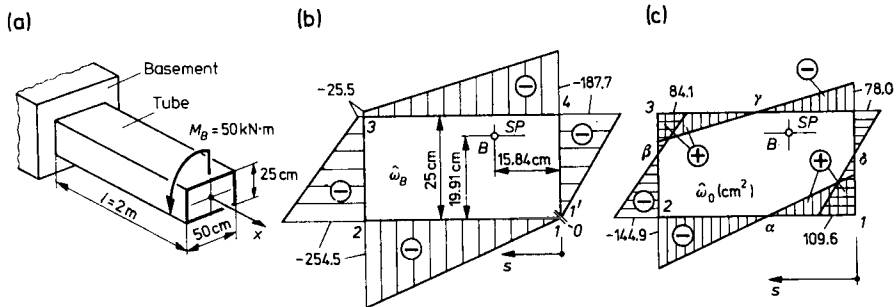
Fig. 3.11. Numerical example: (a) sketch of the structure; (b) sectorial area $\hat{\omega}_B(s)$; principal sectorial area $\hat{\omega}_0$

plays much the same role as quantity $\overline{\omega}$ in calculating $\hat{\omega}$ (Eq. (3.15)). Flow q_b^{II} thus calculated yields no resultant force, whereas the resultant moment of the term $Ef'' \hat{S}_\omega^{0,s}$ equals zero.

An example illustrating the calculating procedure is torsion analysis of an cantilever bar (Fig. 3.11) of a cross-section as in Figs. 3.6 and 3.7. Taking pole B to be at the previously fixed SP and initial point $s = 0$ to be in corner 1, we determine from (3.5) the area $\hat{\omega}_B(s)$ (Fig. 3.11b), using the auxiliary quentities $\omega_c = 2500$ cm^2, $p_c = \oint ds/h = 250$. The plot of $\hat{\omega}_B$ makes it possible to determine from (3.15a) $\overline{\omega} = 109.6$ cm^2, whence we obtain the principal

area $\hat{\omega}_0(s)$ (Fig. 3.11c) and using Eq. (2.26), the value $\hat{J}_\omega = 394.7 \times 10^3$ cm⁶. The final step in calculating the geometric parameters of the cross-section is to determine from (3.16) the values $J_r = 286.8 \times 10^2$ cm⁴ and $J_b = 250 \times \times 10^2$ cm⁴.

In the second stage, i.e., in the determination of $\varphi(x)$ and $(f)x$, the first step is to calculate from (3.20) parameter $k = 5.590 \times 10^{-2}$ cm⁻¹, with $kl = 11.18$, taking $E/G = 2.6$. Since loading $m = 0$, Eqs. (3.19) provide the solution, with conditions as specified in Table 3.1, i.e.

$$(\varphi)_{x=0} = 0, \quad (f)_{x=0} = 0, \quad (f')_{x=l} = 0,$$

$$[GJ_r \varphi' - G(J_r - J_b)f]_{x=l} = M_B.$$

Substituting (3.19) into these conditions, we get the equations

$$\Phi_1 + \Phi_4 = 0, \quad F_1 + F_4 = 0, \quad F_3 \cosh kl + F_4 \sinh kl = 0,$$

$$GJ_b \Phi_2 k = M_B,$$

whence after using (3.21), we obtain finally

$$\varphi(x) = \frac{M_B l}{GJ_b} \left[\frac{x}{l} - \left(1 - \frac{J_b}{J_r}\right) \frac{\sinh kl - \sinh k(l-x)}{kl \cosh kl} \right], \tag{3.24a}$$

$$f(x) = \frac{M_B}{GJ_b} \left[1 - \frac{\cosh k(l-x)}{\cosh kl} \right]. \tag{3.24b}$$

The extremal angle of twist occurs for $x = l$

$$\varphi_{max} = \frac{M_B l}{GJ_b} \left[1 - \left(1 - \frac{J_b}{J_r}\right) \frac{\tanh kl}{kl} \right] = 0.989 \frac{M_B l}{GJ_b}.$$

Since $M_B l/GJ_b$ is the angle of pure torsion of a cantilever bar, it is evident that the influence of clamping on angle φ is negligible.
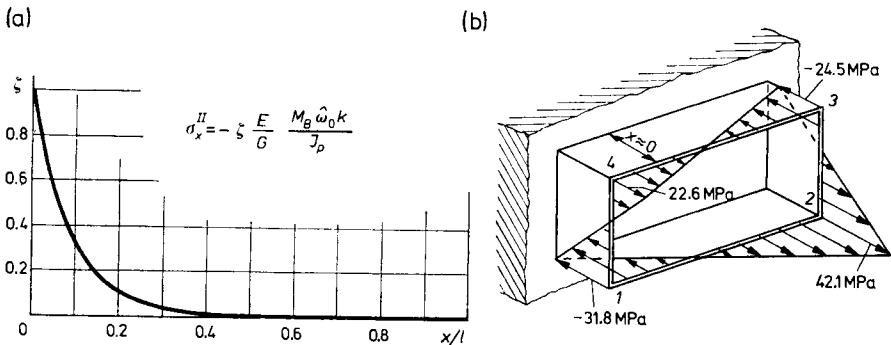
Fig. 3.12. Character of σ_x^{II} stress variation: (a) σ_x^{II} variation in function (x/l); (b) σ_x^{II} distribution in clamped cross-section

The determination of stresses σ_x^{II} and flows q_b^{II} marks the final stage of analysis. From Eqs. (3.14) and (3.24b) we obtain

$$\sigma_x^{II} = -\frac{M_B\hat{\omega}_0}{J_b}\left(\frac{E}{G}k\right)\frac{\sinh k(l-x)}{\cosh kl}$$

as the product of function y and function s associated with $\hat{\omega}_0$ (Fig. 3.11c). The first of these functions (Fig. 3.12a) indicates a prominently local influence of clamping, practically disappearing at a distance equalling the mean size of the cross-section. Only for a clamped cross-section does σ_x^{II} attain values comparable to maximum shear stress value $\tau_{max} = M_B/\omega_c h_{min}$ with pure torsion. The distribution of stresses σ_x^{II} in cross-section $x = 0$ (Fig. 3.12b) is a copy of the plot $\hat{\omega}_0(s)$.

To obtain the value of q_0^{II} we must determine $S_\omega^{0,s} = \int_0^s \hat{\omega} h \, ds$. Taking the origin $s = 0$ to be in corner l and the direction of integration to be $1, 2, 3, \ldots$ (Fig. 3.11c), we obtain a diagram (Fig. 3.13a), from which the mean value
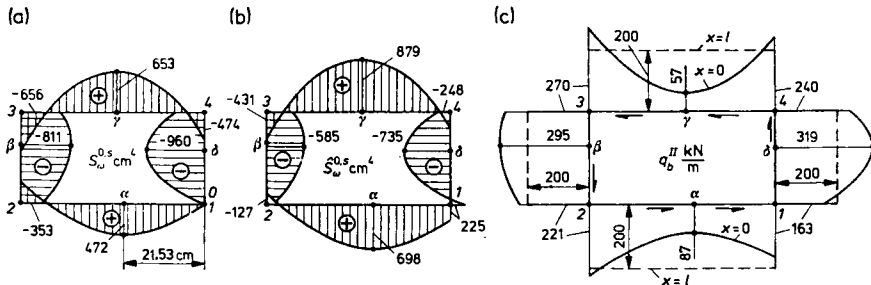
Fig. 3.13. Determination of shear flow q_b^{II}: (a) static sectorial moment $S_{\omega}^{0,s}$; (b) Static principal sectorial moment $\hat{S}_\omega^{0,s}$; (c) distribution of flows q_b^{II} for $x = 0$ and $x = l$

$\bar{S}_\omega = 225.5$ cm^4 is determined according to (3.23b). This term added to $S_\omega^{0,s}$ gives the principal static moment of $\hat{S}_\omega^{0,s}$ (Fig. 3.13b). After using (3.24b) to determine

$$Ef'' = -\frac{EM_B}{GJ_b}\frac{k^2\cosh k(l-x)}{\cosh kl} = -\frac{M_B}{\hat{J}_\omega}\frac{\cosh k(l-x)}{\cosh kl}\left(1-\frac{J_b}{J_r}\right),$$

we calculate q_b^{II} from (3.23a). The result for $x = 0$ (clamped end) and $x = l$ (free end) is given in Fig. 3.13c. It is seen that

$$(q_b^{II})_{x=l} \approx \text{const} = M_B/\omega_c = 200 \text{ kN/m}$$

as with pure torsion. In the clamped cross-section, the distribution of $q_0^{II}(s)$ is more irregular, with the extreme values in points α, β, γ, δ, at which $\hat{\omega}_0 = 0$ (Fig. 3.11c). This irregularity of the distribution is local in nature, similar to the state of σ_x^{II} (Fig. 3.12a).

3.4. Simplified Determination of Flows q in Tubular Bars

Since restrained torsion in tubes is local in nature as seen from the example in Fig. 3.11, the analysis can be simplified by omission of stresses σ_x^{II} and of the member $Ef''S_\omega^{0,s}$ in Eq. (3.32a). As a result, flows n_x determined from (2.6a) or (2.6b) are complete normal flows and flows q determined from (3.7a) or (3.7b), for example

$$q = q_0 + \frac{\mathfrak{T}_z S_y^{0,s}}{J_y} + \frac{\mathfrak{T}_y S_z^{0,s}}{J_z} \tag{3.7b}$$

are complete shear flows in all cases. This allows the determination of q_0 from the equivalence of moments with respect to chosen pole B (Fig. 3.14a), i.e.

$$M_B = \oint q\,d\omega_B = q_0\omega_c + \frac{\mathfrak{T}_z}{J_y} \oint S_y^{0,s}d\omega_B + \frac{\mathfrak{T}_y}{J_z} \oint S_z^{0,s}d\omega_B, \tag{a}$$

where M_B is the twisting moment with respect to pole B. Flow q_0 derived therefrom when substituted into (3.7b) leads to the result

$$q = \frac{M_B - T_z b_y + T_y b_z}{\omega_c} + \frac{\mathfrak{T}_z S_z^{0,s}}{J_y} + \frac{\mathfrak{T}_y S_z^{0,s}}{J_z}, \tag{3.25}$$

where b_y, b_z are the coordinates of shear centre SP of an open cross-section (Eqs. (2.12) or (2.13)) so calculated as if the virtual intersection of the tube actually existed. This result is understandable since the last two terms of Eq. (3.25) are flows in an open cross-section loaded by forces T_y and T_z transmitted to point SP, whereas the first term is the flow of pure torsion by moment $(M_B - T_z b_y + T_y b_z)$ resulting from the transfer of the transverse loading from point B to SP.

The unit angle of twist $\varphi' = d\varphi/dx$ follows from a modification of Eq. (3.2), in which in place of $q_0 = $ const we obtain q from Eq. (3.25) and then in place of Eq. (c), Section 3.1, we have

$$\varphi' = \frac{1}{G\omega_c} \oint q\,dp. \tag{3.26}$$

After some transformations, we obtain

$$\varphi' = \frac{p_c}{G\omega_c^2}(M_B - T_z b_y^* + T_y b_z^*), \qquad (3.27)$$

where b_y^* and b_z^* are coordinates of the shear centre of the tube (Eqs. (3.10)). This result is easy to understand, because the action of loading T_y, T_z and M_B at point B is equivalent to the torsionless action of forces T_y and T_z transmitted to SP and to moment $M_B - T_z b_y^* + T_y b_z^*$ acting at SP.

The simplification introduced here enables us to determine flows q without having to determine SP. This fact can be utilized when the purpose of analysis is stress distribution alone.
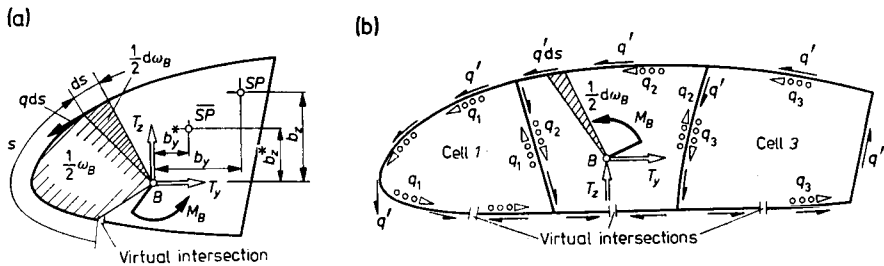
Fig. 3.14. Simplified determination of flows q in tubes: (a) single cell tube, SP — centre of virtually opened cross-section, $\overline{SP}$—shear centre of real tube; (b) multicell tube

A similar simplification can be used for multicell tubes (Fig. 3.14c). By introducing virtual intersections (Fig. 3.10) and by determining flow q' from (3.11), we have an equation of (3.12a) type

$$-p_{i,i-1}q_{i-1} + p_{i,i}q_i - p_{i,i+1}q_{i+1} + \oint_i q'\,dp = G\omega_i\varphi', \qquad (3.28a)$$

in which the right-hand side equals this time a value other than zero but results from the existing rate of twist φ' which is identical for all k of the cells of the cross-section. An additional equation which is required to make the set of equations (3.28a) complete is the condition of equivalence of external moment M_B and shear flow moments, its form being similar to (3.12b), i.e.

$$\sum_1^k q_i\omega_i + \oint q'\,d\omega_B = M_B. \qquad (3.28b)$$

The set (3.28) is usually solved numerically. The result is a complete answer, since determined here are flows q and quantity φ'.

4. Statics of Bars of Deformable Cross-Section*

4.1. The Physical Image of Phenomena. A Partitioning of the Problem

The theory described in Chapters 2 and 3 is founded on the model of a structure with infinitely densely spaced ribs, undeformable in their planes. One of the results of this theory is that a change in transverse loading is accompanied by a change in shear flows q, as seen in the example of con-
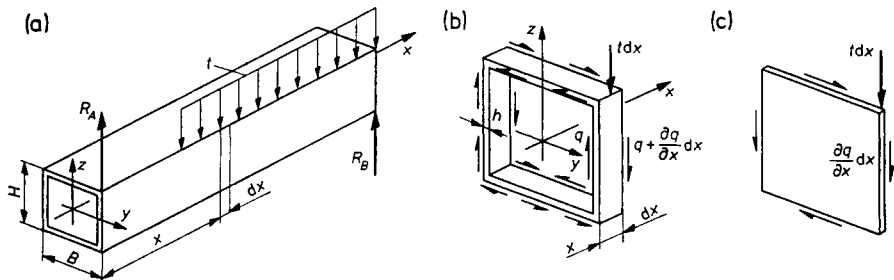
Fig. 4.1. Formation of deformability of cross-section: (a) sketch of the structure and loading system; (b) statics of elementary slice; (c) role of elementary rib

tinuous loading of a bar (Fig. 4.1a). The loading of a cut-out slice (Fig. 4.1b) consists here of force $t\,dx$ and two shear flow systems

$$q(s) \quad \text{and} \quad q(s) + \frac{\partial q(s)}{\partial x}\,dx$$

which represent the reactions of the rest of the structure and are given by Eqs. (3.7) and (3.23) or by the approximate expression (3.25). If a rib were to exist in the examined slice as envisaged by the applied model, then the action of self-equilibrated loading $t\,dx$, $q(s)$ and $q+(\partial q/\partial x)dx$ would be locked

in the rib itself (Fig. 4.1c), and the presented force system would be the correct and final solution.

The described situation undergoes a change, since in fact the number of ribs is finite (Fig. 1.1), and it is the skin itself that must act for the non-existent rib in the slice. This is possible only when the skin walls exhibit bending rigidity. This rigidity is, however, of the order of $Eh^3/12$ and even a small self-equilibrated loading (Fig. 4.1b) may cause a deformation of the cross-section comparable to displacements of the cross-section as a rigid entity. This fact has a bearing on displacements v_K and ω_K of the fibre (Fig. 1.2) and changes thereby the σ_x and τ distribution.

It is evident from the illustration presented that the theory used up to this point calls for a modification when considerable transverse forces are introduced in the segment of the bar between the actually existing ribs. Exact analysis of such a case (Fig. 4.2) presents one of the difficult problems under
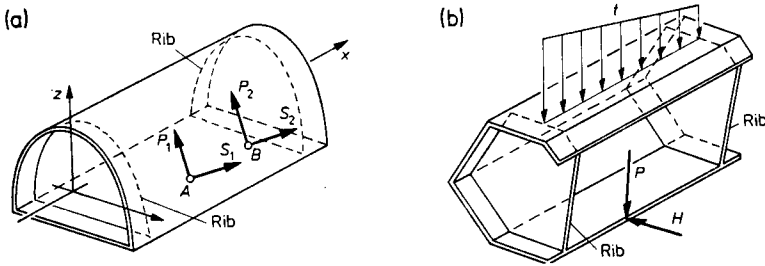
Fig. 4.2. Examples of plate-shell problems in thin-walled bars

the theory of plates and shells and its solution has a very complicated form. For this reason, the deformability problem of cross-section is considered in the theory of thin-walled bars in approximative approach. One of the simplifications introduced here is the division of overall loading (Fig. 4.3a) into local, which is self-equilibrated in between sucecssive ribs (Fig. 4.3b), and global,
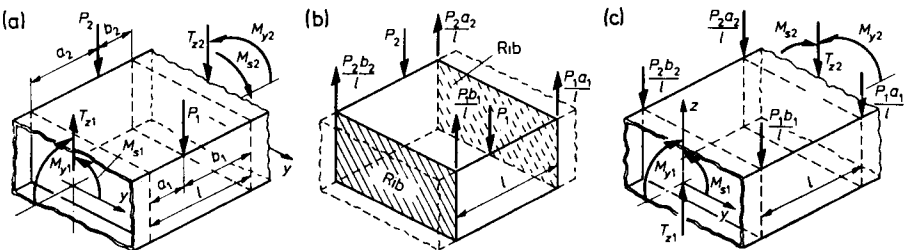
Fig. 4.3. Decomposition of loading into local and global

statically equivalent to real loading but applied only in the planes of the ribs (Fig. 4.3c). It follows from the very nature of local loading that its action decays with distance from the loaded segment. This permits analysis of the local state to be simplified by neglecting the interaction of adjacent segments and it also permits the loaded segment to be considered apart from other segments.

4.2. Analysis of Local Loading in Membrane Approach

The problem of the involvement of local loading can be solved in a relatively simple way for a bar with plane walls. In keeping with the previously introduced simplification, the object of investigation is a segment of a bar (Fig. 4.4a) consisting of two ribs connected by a number of narrow, presumably
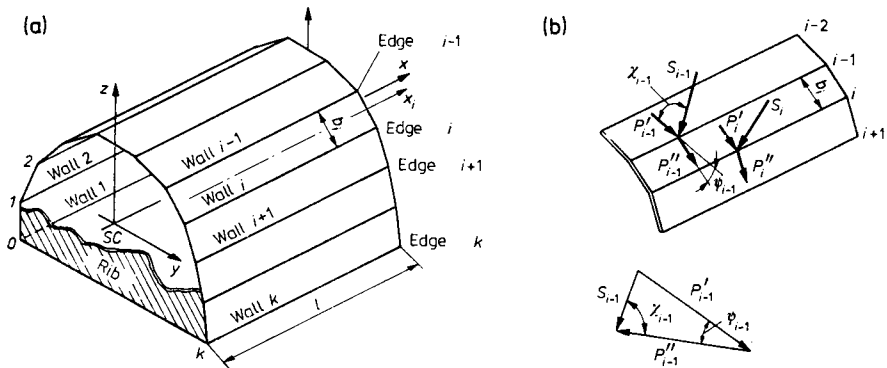
Fig. 4.4. Geometry of bar segment and the wall loading system

rectangular walls. The description of the geometry of the structure, besides the global x, y, z system and coordinate s, relating to the bar as a whole, is complemented by an appropriate numbering of the edges walls and by local coordinates for each wall, whose axis $x_i \| x$ divides the width of wall b_i in half. Regarding distributed loads S (N/m), they are assumed to be perpendicular to the bar axis and applied to wall edges (Fig. 4.4b). Each of such loadings say, S_i, can be resolved into loadings P_i' and P_i'' laying in the planes of adjacent walls and at right angle to edge i. Since the analogous distribution for edge $i-1$ gives loadings P_{i-1}' and P_{i-1}'', the total loading of ith wall is an algebraic sum

$$P_i = P_{i-1}'' + P_i', \text{ (N/m).} \tag{a}$$

These loadings are acting usually on every wall, and it can be assumed that
they are given by the same* function of x with an accuracy to a constant
value.

Switching to the analysis of internal forces, it is useful to map the inter-
actions between the virtually isolated wall i and the rest of the structure,
Due to the bending rigidity of the skin, these interactions consist of a plate
group in the form of flows of bending moment m, torsional moment m_{xt}
and shearing forces t_s, and a disk (membrane) group covering flows n_s and q.
For the sake of simplicity of analysis, it is advised to decompose it into two
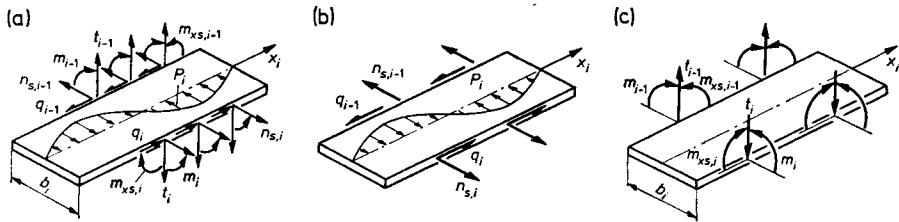
Fig. 4.5. Division of loading of a wall into membrane (b) and flexural (c) states

states, the first, the membrane state, represented by n_s and q (Fig. 4.5b),
and the second, the bending state, represented by the plate group (Fig. 4.5c).
Favouring such a decomposition is the fact that the membrane state usually
satisfies the equilibrium condition for each element and partially also the
displacement continuity conditions. As a result, this part of the solution,
although incomplete, gives an idea of the order of the quantities involved.
The membrane solution proceeds in two stages. In the first, we isolate a wall
and assume that flows $q_{i-1} = q_i = 0$ (Fig. 4.5b); thus, the wall works like
a beam on two supports (ribs) under load P_i (Fig. 4.6a). The effort of the
cross-section consists of bending moment $M_i^{(0)}(x)$ and shearing force $T_x^{(0)}(x)$
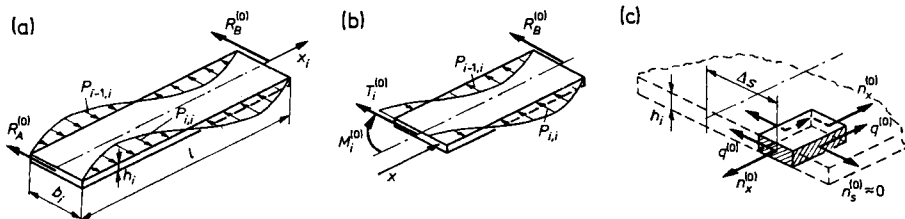
Fig. 4.6. First stage of membrane problem

---

* The case of loadings differing in character being involved, can always be represented
as a superposition.

(Fig. 4.6b). Owing to the identical character of loadings P in all the walls, these effort components can be expressed in the form

$$M_i^{(0)} = B_i F(x), \quad T_i^{(0)} = dM_i^{(0)}/dx = B_i F'(x), \quad (4.1a,b)$$

where $F(x)$ is a function dependent on the character of loading and identical for all walls, B_i is a constant corresponding to wall i being examined. Stress flows* n_x and q developing in this stage (Fig. 4.6c) are determined based on the theory of beam bending

$$n_x^{(0)} = \frac{12 M_i^{(0)} \Delta s}{b_i^3}, \quad q^{(0)} = \frac{3 T_i^{(0)}}{2 b_i} \left[1 - \left(\frac{2 \Delta s}{b_i} \right)^2 \right], \quad (4.2a,b)$$

where Δs is measured from the axis of symmetry of the wall. The longitudinal strain of edge i has here the value

$$\varepsilon_x^{(0)} = \frac{(n_x^{(0)})_s = b_i/2}{E h_i} = \frac{6 M_i^{(0)}}{E b_i^2 h_i}, \quad (b)$$

whereas the strain of that same edge of wall $i+1$ with the coordinate $\Delta s = -b_{i+1}/2$ is

$$\varepsilon_x^{(0)} = \frac{6 M_{i+1}^{(0)}}{E b_{i+1}^2 h_{1+1}}. \quad (c)$$
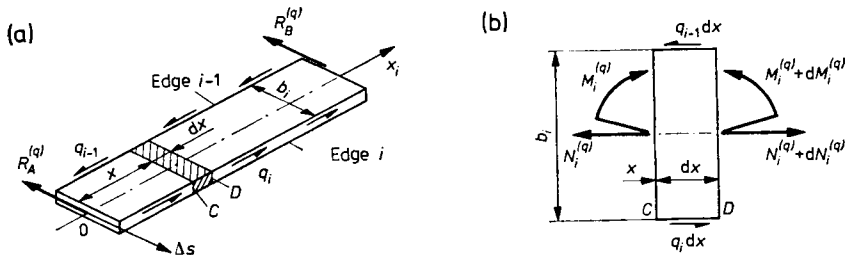
Fig. 4.7. Second stage of membrane problem

As we can see, these strains differ in value and sign. The discontinuity of displacements caused by this is eliminated by shear flows q not considered up to this point (Fig. 4.7a), inducing an effort with components $N_i^{(q)}$ and $M_i^{(q)}$. These components satisfy the equilibrium equation of element (Fig. 4.7b)

$$\frac{dN_i^{(q)}}{dx} = q_{i-1} - q_i, \quad \frac{dM_i^{(q)}}{dx} = -\frac{b_i}{2} (q_{i-1} + q_i). \quad (4.3)$$

---

* Tangential flow n_s is neglected like in Chapters 2 and 3.

Flow $n_x^{(q)}$ corresponding to this effort on the edge $\Delta s = b_i/2$ of wall i

$$n_x^{(q)} = \frac{N_i^{(q)}}{b_i} + \frac{6M_i^{(q)}}{b_i^2} \tag{4.4}$$

gives the tensile strain

$$\varepsilon_x^{(q)} = \frac{n_x^{(q)}}{Eh_i} = \frac{N_i^{(q)}}{Eb_ih_i} + \frac{6M_i^{(q)}}{Eb_i^2h_i}. \tag{d}$$

The total tensile strain of edge i of wall i is the sum of expressions (b) and (d) and must be equal to the tensile strain of edge i of wall $i+1$. A result therefrom is the equation

$$\frac{6M_i^{(0)}}{Eb_i^2h_i} + \frac{N_i^{(q)}}{Eb_ih_i} + \frac{6M_i^{(q)}}{Eb_i^2h_i} = -\frac{6M_{i+1}^{(0)}}{Eb_{i+1}^2h_{i+1}} + \frac{N_{i+1}^{(q)}}{Eb_{i+1}h_{i+1}} - \frac{6M_{i+1}^{(q)}}{Eb_{i+1}^2h_{i+1}}, \tag{4.5}$$

which after differentiating with respect to x and using relationships (4.1) and (4.3) leads to the relation

$$\frac{q_{i-1}}{b_ih_i} + 2\left(\frac{1}{b_ih_i} + \frac{1}{b_{i+1}h_{i+1}}\right)q_i + \frac{q_{i+1}}{b_{i+1}h_{i+1}} = \frac{3T_i^{(0)}}{b_i^2h_i} + \frac{3T_{i+1}^{(0)}}{b_{i+1}^2h_{i+1}}. \tag{4.6}$$

Equations (4.6) make a set yielding the flows q being sought. Owing to the identical character of loadings P, these flows are given by the same function as are shearing forces $T^{(c)}$, i.e.

$$q_{i-1} = Q_{i-1}F'(x), \quad q_i = Q_iF'(x), \dots, \tag{4.7}$$

where Q_{i-1}, Q_i, ... are constant quantities. Consequently, the set of equations (4.6) changes into the set

$$\frac{Q_{i-1}}{b_ih_i} + 2\left(\frac{1}{b_ih_i} + \frac{1}{b_{i+1}h_{i+1}}\right)Q_i + \frac{Q_{i+1}}{b_{i+1}h_{i+1}} = \frac{3B_i}{b_i^2h_i} + \frac{3B_{i+1}}{b_{i+1}^2h_{i+1}}, \tag{4.8}$$

in which all the quantities therein are constant.

Having determined Q_i, we obtain the total effort of the cross-section from superposition of (4.1) and from the integrals of Eqs. (4.3), in which $[N_i^{(q)}]_{x=0} = 0$ and $[M_i^{(q)}]_{x=0} = 0$. The result is

$$M_i = \left[B_i - \frac{(Q_{i-1}+Q_i)b_i}{2}\right]F(x); \quad N_i = (Q_{i-1}-Q_i)F(x), \tag{4.9}$$

$$T_i = B_iF'(x),$$

whence we can calculate flows n_x and q

$$n_x = \left\{\frac{12\Delta s}{b_i^3}\left[B_i - \frac{(Q_{i-1}+Q_i)b_i}{2}\right] + \frac{Q_{i-1}-Q_i}{b_i}\right\}F(x), \tag{4.10a}$$

$$q = \left[\frac{3B_i}{2b_i}\left(1 - \frac{4\Delta s^2}{b_i^2}\right) + \frac{Q_{i-1}}{4}\left(\frac{2\Delta s}{b_i} - 1\right)\left(\frac{6\Delta s}{b_i} + 1\right) + \right.$$

$$\left. + \frac{Q_i}{4}\left(\frac{2\Delta s}{b_i} + 1\right)\left(\frac{6\Delta s}{b_i} - 1\right)\right]F'(x). \tag{4.10b}$$

Note that Eq. (4.10b) is approximate and has an accuracy exactly the same as that of the theory of beam bending.

In many cases, it is convenient to represent loadings P of each wall as Fourier series

$$P_i = \sum_{n=1}^{\infty} P_{i,n} \sin\frac{n\pi x}{l}, \quad 0 \leqslant x \leqslant l, \tag{4.11}$$

where $P_{i,n}$ are the amplitudes of the nth harmonic for wall i. Treating each of the harmonics separately, we obtain in the first stage (Fig. 4.6)

$$M_{i,n}^{(0)} = \frac{P_{i,n}l^2}{n^2\pi^2}\sin\frac{n\pi x}{l}, \quad T_{i,n}^{(0)} = \frac{P_{i,n}l}{n\pi}\cos\frac{n\pi x}{l}. \tag{4.12a,b}$$

Confronting this result with Eqs. (4.1), we get

$$B_{i,n} = \frac{P_{i,n}l}{n\pi}, \quad F(x) = \frac{l}{n\pi}\sin\frac{n\pi x}{l}, \quad F'(x) = \cos\frac{n\pi x}{l}, \tag{4.13}$$

whereby, substituting into (4.7) and (4.8) we have

$$q_{i-1} = Q_{i-1,n}\cos\frac{n\pi x}{l}, \quad q_i = Q_{i,n}\cos\frac{n\pi x}{l}, \dots \tag{4.14}$$

The constant quantities $Q_{i-1,n}$, $Q_{i,n}$ are given by the equations

$$\frac{Q_{i-1,n}}{b_i h_i} + 2\left(\frac{1}{b_{i+1}h_{i+1}} + \frac{1}{b_i h_i}\right)Q_{i,n} + \frac{Q_{i+1,n}}{b_{i+1}h_{i+1}}$$

$$= \frac{3l}{n\pi}\left(\frac{P_{i,n}}{b_i^2 h_i} + \frac{P_{i+1,n}}{b_{i+1}^2 h_{i+1}}\right). \tag{4.15}$$

The subsequent stages of analysis consist in utiliting relations (c), (4.9) and (4.10), respectively. Specifically, the total components of the cross-sectional effort have the form

$$M_i = M_{i,n}\sin\frac{n\pi x}{l}, \quad N_i = N_{i,n}\sin\frac{n\pi x}{l},$$

$$T_i = \frac{P_{i,n}l}{n\pi}\cos\frac{n\pi x}{l}, \tag{4.16}$$

where $M_{i,n}$, $N_{i,n}$ are the respective amplitudes.

The above analysis is illustrated by an example (Fig. 4.8a) of a double-symmetric rectangular tube loaded by force S which is equilibrated by forces $S/2$ in the planes of the end ribs. The first stage of the problem (Fig. 4.6) reduces to analysis of loaded wall 2, for which concentrated force S consti-
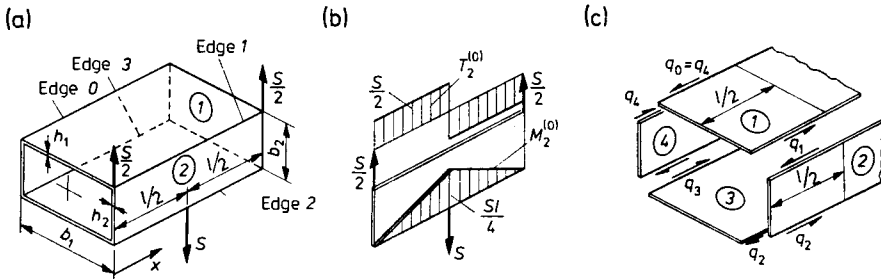
Fig. 4.8. Numerical example

tutes loading P_2 (Fig. 4.8b). The corresponding moment $M_2^{(0)}$ and shearing force $T_2^{(0)}$ are

$$M_2^{(0)} = Sx/2, \qquad T_2^{(0)} = S/2, \qquad 0 \leqslant x < l/2,$$
$$M_2^{(0)} = S(l-x)/2, \qquad T_2^{(0)} = -S/2, \qquad l/2 < x \leqslant l.$$

Since functions $M_2^{(0)}(x)$ and $T_2^{(0)}(x)$ are discontinuous, flows $q_0, q_1, q_2, q_3,$ $q_4 = q_0$ (Fig. 4.8c) should be determined for each interval x separately. Thus, for $x(0, l/2)$ derived from Eqs. (4.1),

$$F(x) = x, \qquad F'(x) = 1, \qquad B_1 = B_3 = B_4 = 0, \qquad B_2 = S/2.$$

This result leads to four equations (4.8). However, owing to the symmetry of the structure and the antisymmetry of loading $q_1 = q_2$, $q_3 = q_4 = q_0$, only a set of two equations for edge $i = 2$ and $i = 3$ remains to be considered

$$\frac{Q_2}{b_2 h_2} + 2 \left(\frac{1}{b_2 h_2} \cdot \frac{1}{b_1 h_1} \right) Q_2 + \frac{Q_3}{b_1 h_1} = \frac{3S}{2 b_2^2 h_2},$$

$$\frac{Q_2}{b_1 h_1} + 2 \left(\frac{1}{b_1 h_1} + \frac{1}{b_2 h_2} \right) Q_3 + \frac{Q_3}{b_2 h_2} = 0.$$

After solving this set, with $b_1 h_1 = 2 b_2 h_2$, we obtain

$$q_2 = q_1 = Q_2 F'(x) = 0.381 \, S/b_2,$$
$$q_3 = q_4 = q_0 = Q_3 F'(x) = -0.048 S/b_2.$$

When we examine interval $l/2 < x < l$ in a similar manner, we obtain values opposite to those given above. Using next Eqs. (4.9) and (4.10), we determine for cross-section $x = (l/2) - 0$ the distribution of stresses σ_x and flows q

(Fig. 4.9). One can see here what an essential correction is introduced in the σ_x distribution by the cooperation of all four walls. For, if we were to stop at the first stage (Fig. 4.8b), then in the investigated cross-section we would have $(\sigma_x)_{max} = 1.500 \ Sl/b_2^2 h_2$, i.e. a value roughly four times as great as the
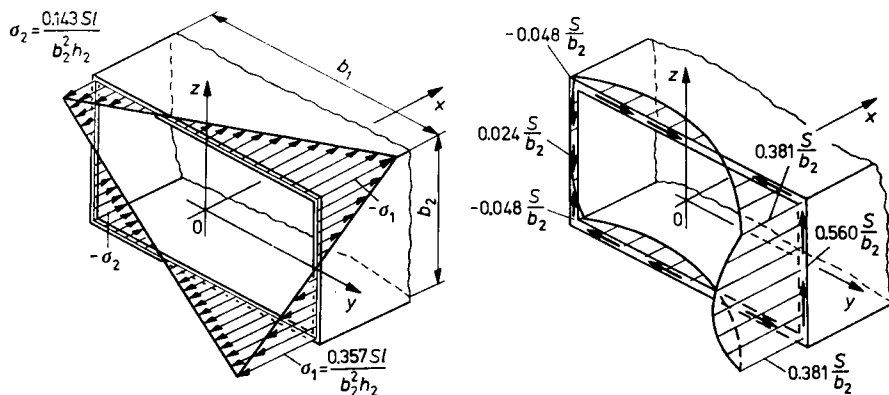
Fig. 4.9. Distributions of stress σ_x and flow q for $x = (l/2) - 0$

final value from Fig. 4.9. Also important is the change in the work done by the investigated structure compared to a bar having a rib in the loaded cross-section. In this latter case, if restrained torsion were neglected, the σ_x distribution in horizontal walls *1* and *2* would be uniform and the value of σ_x determined from (2.6a) would be roughly 3.3 times less than that in Fig. 4.9.

Similarly, flows q (Fig. 4.9) do not compare favourably with the corresponding flows in a bar provided with an appropriate rib, although the differences are smaller here, not exceeding 30%.

As we have indicated previously, the membrane approach must be supplemented by analysis of the bending state. This proves necessary when the membrane state cannot assure equilibrium of an individual wall, e.g. in the structure (Fig. 4.2b) loaded at the free edge by force P perpendicular to the edge wall. Similarly, supplementary analysis is required when a plane-walled skin represents an approximation of a cylindrical shell. Contrary to expectations, a more accurate reproduction of the real contour of the skin achieved by increasing the number of plane walls gives a divergence of the membrane solution consisting in increased irregularities of the σ_x and q distributions. As distinct from these cases, flexural analysis in the case of tubular structures with few walls does not involve essential corrections, and the membrane theory therefore yields reliable results.

Additional bending stresses occur, because loadings are very often pressure distributed over the surface of the skin. With such loadings the skin walls work like plates, and the bending stresses can be then quite considerable. The deformations of across-section occurring here may be comparable to those occurring in the membrane approach.

4.3. Analysis of Local Loading in Bending Approach

The decomposition of the analysis introduced in Section 4.2 (Fig. 4.5) can be compared to a statically indeterminate problem, in which the membrane state is the primary state satisfying the equilibrium conditions but not providing compatibility of displacements, i.e. leading to some discontinuities in deformations. The role of the bending state is to eliminate these discontinuities of the primary state. The determination of these discontinuities is the first stage of analysis of the bending state.

Both the first stage and the whole of this part of the problem are very simple to solve if loadings P_i of each wall are represented by a Fourier series (4.11), since then only one harmonic of the loading need be investigated

$$P_{i,n}\sin\frac{n\pi x}{l} = \bar{P}_i\sin\frac{n\pi x}{l} \qquad (i = 1, ..., k), \tag{4.17}$$

where $\bar{P}_i = P_{i,n}$ is a simplified notation of the amplitude with subscript n omitted. The same notation is used for other quantities.

After solving the membrane problem using (4.12)–(4.16), we obtain the total bending moment of wall i

$$M_i = \bar{M}_i\sin\frac{n\pi x}{l} = \left[\frac{\bar{P}_i l}{n} - \frac{(Q_{i-1}+Q_i)b_i}{2}\right]\frac{l}{n\pi}\sin\frac{n\pi x}{l}. \tag{4.18}$$

The corresponding deflection v_i of wall i in its plane is derived from the solution of the equation

$$(Eb_i^3 h_i/12)(\mathrm{d}^2v_i/\mathrm{d}x^2) = -M_i \tag{a}$$

using boundary conditions $(v)_{x=0} = (v_i)_{x=l} = 0$ and has the form

$$v_i = \bar{v}_i^{(0)}\sin n\pi x/l, \tag{4.19a}$$

where the amplitude $\bar{v}_i^{(0)}$ is

$$\bar{v}_i^{(0)} = \frac{6}{Eb_i^2 h_i}\frac{l^3}{n^3\pi^3}\left[\frac{2l}{b_i n\pi}\bar{P}_i - (\bar{Q}_{i-1}+\bar{Q}_i)\right]. \tag{4.19b}$$

Knowing the deflections (4.19) for each wall, we can find the deformation of the bar cross-section. Since the selected edge i belongs to walls i and $i+1$

with different deflections $\bar{v}_i^{(0)} \sin n\pi x/l$, and $\bar{v}_{i+1}^{(0)} \sin n\pi x/l$, the adjustment of these walls to each other requires additional displacements w_i^* and w_i^{**} perpendicular to these walls (Fig. 4.10). This is feasible, since the walls are thin and long and are thereby practically non-rigid both with respect to bending
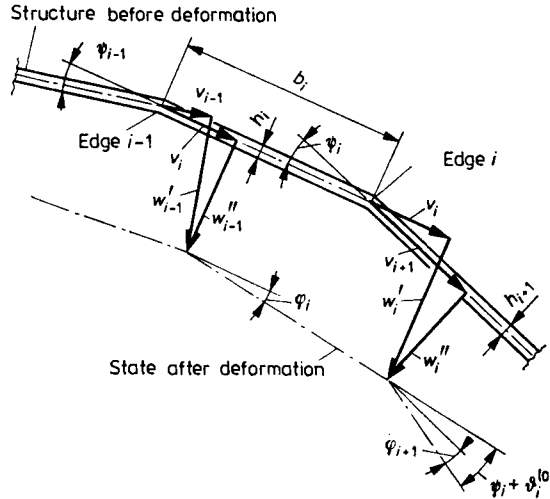
Fig. 4.10. Displacements in primary (membrane) state: v_{i-1}, v_i, v_{i+1}—deflections of walls in their planes; w_i', w_i''—additional displacements at the edge i giving wall adjustment; ψ_i—natural angle between walls en edge i; φ_i, φ_{i+1}—angles of rotation of walls induced by displacements w

in the direction perpendicular to the wall and with respect to torsion. Taking this into account, we can add such w_i^* and w_i^{**} on edge i common to walls i and $i+1$ in order to get identical displacement, whence we obtain relations valid for arbitrary x

$$w_i^* \sin \psi_i = v_{i+1} - v_i \cos \psi_i, \quad w_i^{**} \sin \psi_i = v_{i+1} \cos \psi_i - v_i \tag{4.20}$$

and also for amplitudes $\bar{w}_i^*$ and $\bar{w}_i^{**}$. Knowing w^* and w^{**} for each edge, we can determine the angles of rotation of the adjacent walls, φ_i and φ_{i+1} or their amplitudes $\bar{\varphi}_i^{(0)}$ and $\bar{\varphi}_{i+1}^{(0)}$

$$\bar{\varphi}_i^{(0)} = (\bar{w}_i^* - \bar{w}_{i-1}^{**})/b_i, \quad \bar{\varphi}_{i+1}^{(0)} = (\bar{w}_{i+1}^* - \bar{w}_i^{**})b_{i+1}, \tag{4.21}$$

and the change in amplitude $\bar{\vartheta}_i^{(0)}$ of primary angle $\bar{\psi}_i$

$$\bar{\vartheta}_i^{(0)} = \bar{\varphi}_{i+1}^{(0)} - \bar{\varphi}_i^{(0)} = \frac{w_{i+1}^* - w_i^{**}}{b_{i+1}} - \frac{w_i^* - w_{i-1}^{**}}{b_i}, \tag{4.22}$$

with $\vartheta_i^{(0)} > 0$ corresponding to increase of angle ψ_i. By substituting express-
ions (4.20) into (4.22), we obtain the relation

$$\overline{\vartheta}_i^{(0)} = \mu_{i+2,i}\overline{v}_{i+2}^{(0)} + \mu_{i+1,i}\overline{v}_{i+1}^{(0)} + \mu_{i,i}\overline{v}_i^{(0)} + \mu_{i-1,i}\overline{v}_{i-1}^{(0)} \qquad (4.23\text{a})$$

which connects $\overline{\vartheta}_i^{(0)}$ of the edge i to amplitudes $\overline{v}^{(0)}$ of four successive walls
set up symmetrically to this edge*. Amplitudes $\overline{v}^{(0)}$ determined from (4.19b)
are functions of known loading amplitudes $\overline{P}_i$ and amplitudes $\overline{Q}$ known
from the solution of the set of equations (4.15). Coefficients μ depend only
on the geometry of the cross-section, they are constant for all harmonics,
and their form is

$$\mu_{i+2,i} = \frac{1}{b_{i+1}\sin\psi_{i+1}}, \qquad \mu_{i+1,i} = -\frac{\cot\psi_{i+1}+\cot\psi_i}{b_{i+1}} - \frac{1}{b_i\sin\psi_i},$$

$$(4.23\text{b})$$

$$\mu_{i,i} = \frac{\cot\psi_i + \cot\psi_{i-1}}{b_i} + \frac{1}{b_{i+1}\sin\psi_i}, \qquad \mu_{i-1,i} = \frac{1}{b_i\sin\psi_{i-1}}.$$

The $\overline{\vartheta}_i^{(0)}$ calculated are the displacement discontinuities of the primary
state which must be compensated by the bending state. In the latter, of the
complete flow scheme (Fig. 4.11a), we keep only moment m and shearing
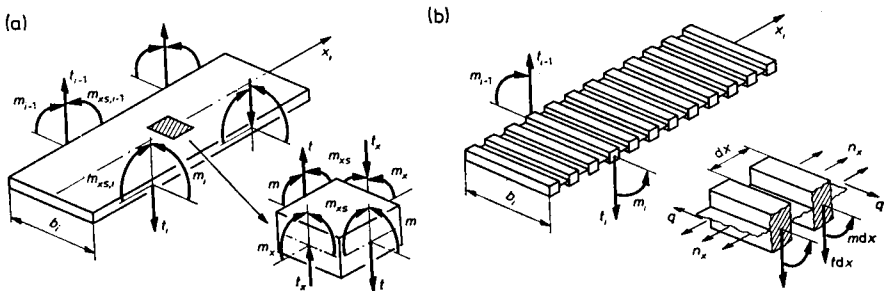
Fig. 4.11. Complete (a) and simplified (b) skin bending model

forces t flows acting in tangential direction. This simplification corresponds
to the replacement of the real wall by a row of narrow beams perpendicular
to the x_i-axis and connected by a flexible membrane transmitting only flows
n and q (Fig. 4.11b). This model developed by Vlasov (1959) is justified by
the high values of ratio l/b_i.

---

* It follows from the above that for an open cross-section (Fig. 4.4a), $\vartheta_i^{(0)}$ exists for
$2 \leqslant i \leqslant k-2$ and the number of amplitudes $\overline{\vartheta}^{(0)}$ is $k-3$. For a tubular structure edge
"0" coincides with edge k and the number of $\overline{\vartheta}^{(0)}$ equals k.

Due to the bending states there are also moment flows acting on the edes. These edge flows are also the nth harmonic of argument $\pi x/l$. At the selected edge j (Fig. 4.12a), they are

$$m_j = \bar{m}_j \sin(n\pi x/l). \tag{4.24}$$
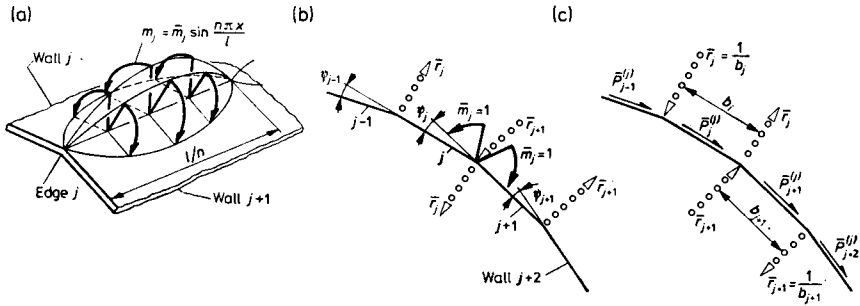
Fig. 4.12. Stages of analysis of the bending state

This action, in which we take for the time being $\bar{m}_j = 1$, can be resolved into two components by introducing zero reaction groups r. The first consisting of m_j flows and one reaction group r (Fig. 4.12b) with values

$$r_j = \bar{r}_j \sin \frac{n\pi x}{l} = \frac{1}{b_j} \sin \frac{n\pi x}{l}, \quad r_{j+1} = \bar{r}_{j+1} \sin \frac{n\pi x}{l} = \frac{1}{b_{j+1}} \sin \frac{n\pi x}{l} \tag{4.25}$$

is self-equilibrated within two walls j and $j+1$ only.

The second component consisting of reactions r_j and r_{j+1} alone (Fig. 4.12c) is the loading determined in Section 4.2. It is particularly these reactions that give in the planes of four successive walls tangential loadings P, whose amplitudes $\bar{P}$ are

$$\bar{P}_{j-1} = -\frac{1}{b_j \sin \psi_{j-1}}, \quad \bar{P}_j = \frac{\cot \psi_{j-1} + \cot \psi_j}{b_j} + \frac{1}{b_{j+1} \sin \psi_j},$$

$$\bar{P}_{j+1} = -\frac{1}{b_j \sin \psi_j} - \frac{\cot \psi_j + \cot \psi_{j+1}}{b_{j+1}}, \quad \bar{P}_{j+2} = \frac{1}{b_{j+1} \sin \psi_{j+1}}. \tag{4.26}$$

Bearing in mind the previously introduced simplified notation, amplitudes $\bar{P}_{j-1} = P_{j-1,n}, \ldots, \bar{P}_{j+2} = P_{j+2,n}$ should be substituted into Eqs. (4.15) in order to determine from their solution the flows $q_{i,j}$ induced by $m_j = 1 \cdot \sin(n\pi x/l)$ on all edges of the structure, i.e., $i = 1, \ldots, k-1$. All these quantities, i.e., $\bar{P}_{j-1}, \ldots, \bar{P}_{j+2}$ and $q_{i,j}$ put into (4.19) give amplitudes $\bar{v}_{i,j}$, which allows in turn the determination of changes $\bar{\vartheta}_{i,j}$ in angles ψ_i from (4.23). We should

follow this procedure repeatedly for each edge j, according to which the existence of loadings m_j is feasible*. As a result we obtain the symmetrical square matrix $[\bar{\vartheta}_{i,j}]$. The complete change in the angle induced by moments m_j and corresponding to the membrane component (Fig. 4.12c) is the sum

$$\sum_{j=i_1}^{i_2} \bar{\vartheta}_{i,j} m_j,$$ (a)

where i_1, i_2 are the numbers of limiting edges described in the footnote.

Outside the change in angle ψ_i given by Eq. (a), a change is induced by a component (Fig. 4.12b) consisting of three moments m_{i-1}, m_i and m_{i+1}. With the assumed wall model (Fig. 4.11b) the change in angle ψ_i corresponding to this system is

$$\frac{b_i}{6D_i}(m_{i-1}+2m_i)+\frac{b_{i+1}}{6D_{i+1}}(2m_i+m_{i+1}),$$ (b)

where $D_i = Eh_i^3/12(1-\nu^2)$ is the plate bending rigidity of wall i. The complete change in angle Ψ_i is the sum of expression (a), (b) and angle $\vartheta_i^{(0)}$ expressed by Eqs. (4.23). By virtue of continuity of displacements it must equal zero. This leads to an equation which interrelates the amplitudes

$$\sum_{j=i_1}^{i_2} \vartheta_{i,j}\bar{m}_j + \frac{b_i}{6D_i}\bar{m}_{i-1} + \frac{1}{3}\left(\frac{b_i}{D_i}+\frac{b_{i+1}}{D_{i+1}}\right)\bar{m}_i + \frac{b_{i+1}}{6D_{i+1}}\bar{m}_{i+1} + \bar{\vartheta}_i^{(0)} = 0.$$

(4.27)

We get as many equations (4.27) as there are unknowns $\bar{m}_i$. By solving them, we can find all the stresses and displacements involved. This result corresponds only to one harmonic of loading (4.17). To obtain the full result, the procedure should be repeated for each of the remaining harmonics and these partial results superposed.

The solution obtained covers cases where the loads are applied at the egdes. But, surface loadings also occur, especially in problems, in the field of civil engineering. The initial solving stage constists in examining each wall treated as a rectangular plate supported at the edges and transmitting the loadings in accordance with the adopted model (Fig. 4.11b). Under these

---

* For a tube, m_j may exist on all edges since edge "0" coincides with edge "k" and in that case $i_1 = 1 \leqslant j \leqslant k = i_2$. If the cross-section is open and if there are no loadings perpendicular to walls 1 and k on edges "0" and "k" (Fig. 4.4a) then on edges "1" and "$k-1$", flows $m_1 = m_{k-1} = 0$, since walls 1 and k adjust themselves freely to the rest of the structure. In that case, $i_1 = 2 \leqslant j \leqslant k-2 = i_2$ and the number of unknown m_j is $k-3$. When loadings perpendicular to walls 1 and k exist on the extreme edges, then the number of unknown m_j continues to be $k-3$ since the values m_1 and m_{k-1} are determined from equilibrium equations.

conditions every element of width dx behaves like a beam of length b_i, and reactions at the ends $t_{i-1}^{(0)}$ and $t_i^{(0)}$ are joined to loadings S (Fig. 4.4b), influencing thereby the loading system P of the membrane state, as well as the free terms $\bar{\vartheta}^{(0)}$ in the set of equations (4.27).

An illustration of the presented solution is the analysis of the bending state in a structure (Fig. 4.8). In view of the symmetry of the structure, it is useful to resolve loading S into two components, symmetric and antisymmetric. In the former, there is no change in angles $\bar{\psi}_i$, meaning that in Eqs. (4.27),
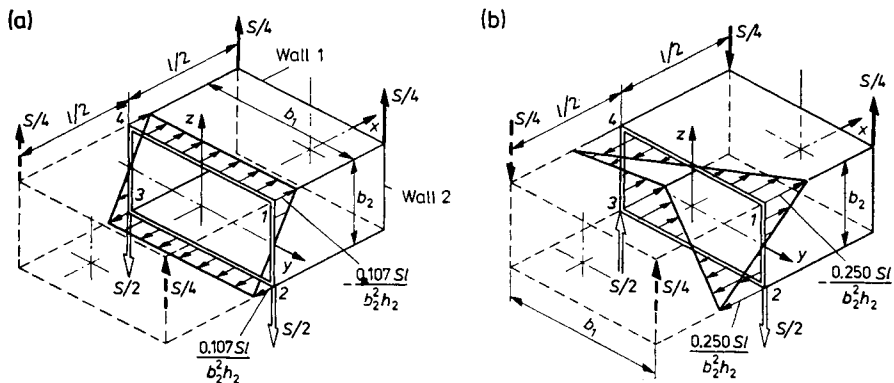
Fig. 4.13. Decomposition of the problem from Fig. 4.8 into symmetrical and antisymmetrical and the corresponding decomposition of σ_x (Fig. 4.9) for $x = l/2$

the terms $\vartheta_i^{(0)} = 0$, from which it follows that also $\bar{m}_i = 0$; consequently, there is no bending of the walls. We deal with a different situation in the antisymmetric state (Fig. 4.13b). Loadings $S/2$, identical to loadings P_2 and P_4 of walls 2 and 4 can be represented by a Fourier series

$$P_2 = P_4 = \sum_{1,3,\dots}^{\infty} (-1)^{(n-1)/2}(S/l)\sin(n\pi x/l).$$

Confronting this result with (4.11), we find from (4.15) amplitudes $Q_{i,n}$, and because of the double symmetry of the cross-section, $Q_{1,n} = Q_{2,n} = Q_{3,n} = Q_{4,n}$. As a result, with $b_1 h_1 = 2b_2 h_2$,

$$Q_{1,n} = Q_{2,n} = Q_{3,n} = Q_{4,n} = \frac{2S(-1)^{(n-1)/2}}{3\pi n b_2}.$$

Substituting into (4.19), we obtain for $i = 1$ and $i = 2$

$$\bar{v}_1^{(0)} = -\frac{4Sl^3(-1)^{(n-1)/2}}{\pi^4 n^4 Eb_1 b_2^2 h_2}, \qquad \bar{v}_2^{(0)} = \frac{4Sl^3(-1)^{(n-1)/2}}{\pi^4 n^4 Eb_2^3 h_2},$$

as the deflection amplitudes of walls 1 and 2, and also for walls 3 and 4, since $\bar{v}_3^{(0)} = \bar{v}_1^{(0)}$ and $\bar{v}_4^{(0)} = \bar{v}_2^{(0)}$. Substituting $\bar{v}_i^{(0)}$ into (4.23), in which $\bar{\psi}_1 = \pi/2$, we determine the change in angles ψ_i, i.e.

$$-\bar{\vartheta}_1^{(0)} = \bar{\vartheta}_2^{(0)} = -\bar{\vartheta}_3^{(0)} = \bar{\vartheta}_4^{(0)} = \frac{16Sl^3(-1)^{(n-1)/2}}{\pi^4 n^4 E b_1 b_2^3 h_2}.$$

As a result, the deformation of a cross-section in the membrane state consists in change of a rectangle for a parallelogram (Fig. 4.14a). Analysis,
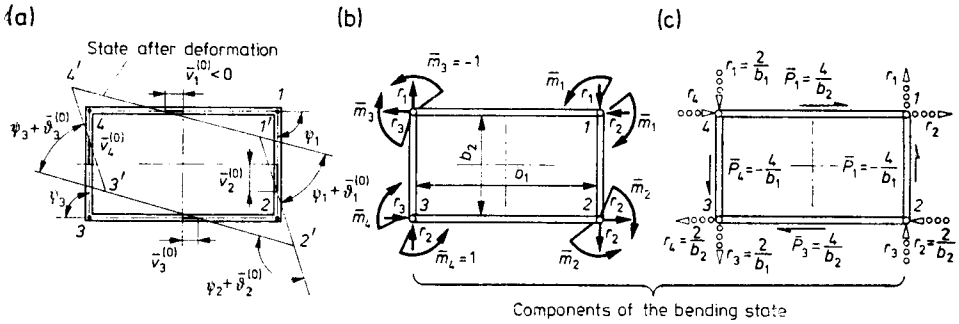
Fig. 4.14. Determination of initial quantities for bending analysis

of the bending state is simplified by the double symmetry of the structure, owing to which amplitudes $\bar{m}_i$ are $\bar{m}_1 = -\bar{m}_2 = \bar{m}_3 = -\bar{m}_4$ (Fig. 4.14b). Thus, introducing zero reaction groups r and performing a decomposition (Fig. 4.14b, c) as in Fig. 4.12b, c we solve first of all the membrane part with amplitudes $\bar{P}_1 = \bar{P}_3 = 4/b_2$ and $\bar{P}_2 = \bar{P}_4 = -4/b_1$. As a results, all amplitudes Q_i are equal and their value determined from Eq. (4.15) with $b_1 h_1 = 2b_2 h_2$ is

$$\bar{Q}_1 = \bar{Q}_2 = \bar{Q}_3 = \bar{Q}_4 = -4l/3\pi n b_1 b_2.$$

Knowing $\bar{P}_i$ and $\bar{Q}_i$ we can determine as previously from (4.19)

$$\bar{v}_1 = \bar{v}_3 = \frac{64l^4}{\pi^4 n^4 E b_1^3 b_2 h_1}, \qquad \bar{v}_2 = \bar{v}_4 = -\frac{32l^4}{\pi^4 n^4 E b_1 b_2^3 h_2}$$

as the deflection amplitudes of walls, and next from (4.23)

$$\bar{\vartheta}_1 = -\bar{\vartheta}_2 = \bar{\vartheta}_3 = -\bar{\vartheta}_4 = \frac{64l^4}{\pi^4 n^4 E b_1^2 b_2^2}\left(\frac{1}{b_2 h_2} + \frac{2}{b_1 h_1}\right)$$

$$= \frac{128l^4}{\pi^4 n^4 E b_1^2 b_2^2} \frac{1}{b_2 h_2}$$

as the amplitude of change in angle ψ due to the action of the group of four moments $\overline{m}$. The corresponding illustration of the deformed cross-section (Fig. 4.15a) gives the whole term expressed by (a).
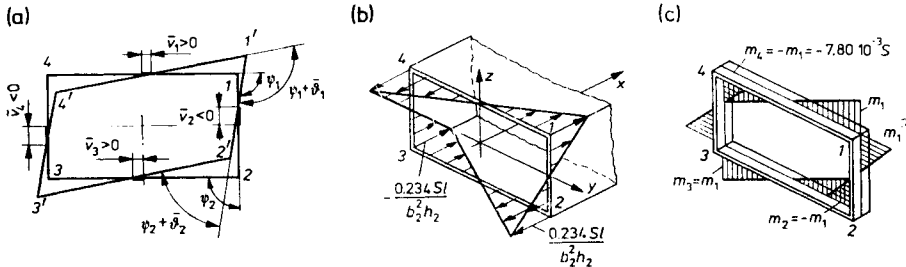
Fig. 4.15. Solution of the bending state in local antisymmetrical loadings: (a) deformations for the component from Fig. 4.14c; (b) final σ_x distribution for antisymmetrical state (Fig. 4.13c); (c) distribution of bending moments in cross-section $x = l/2$.

The determination of component (b) corresponding to the loadings from Fig. 4.14b yields for $i = 1$

$$\frac{\overline{m}_1}{6}\left(\frac{b_1}{D_1} + \frac{b_2}{D_2}\right),$$

owing to which the complete equation (4.27) for $i = 1$ is

$$\frac{128 l^4}{\pi^4 n^4 E b_1^2 b_1^2}\frac{\overline{m}_1}{b_2 h_2} + \frac{\overline{m}_1}{6}\left(\frac{b_1}{D_1} + \frac{b_2}{D_2}\right) - \frac{16 S l^3 (-1)^{(n-1)/2}}{\pi^4 n^4 E b_1 b_2^3 h_2} = 0,$$

and after simple transformations

$$\overline{m}_1\left\{1 + \left[1 + \frac{b_1 h_1}{b_2 h_2}\left(\frac{h_2}{h_1}\right)^4\right]\left[\left(\frac{b_1 b_2^2}{l^2 h_2}\right)^2 \frac{\pi^4 n^4}{64}\right]\right\} = \frac{Sb_1}{8l}(-1)^{(n-1)/2}.$$

Using also the following structural parameters

$$b_2/h_2 = 10, \quad b_1/l = 0.5, \quad h_1 = h_2, \quad b_1 h_1 = 2 b_2 h_2,$$

we obtain for harmonics $n = 1, 3, 5, \ldots$, respectively,

$$\overline{m}_1/S = 7.683 \times 10^{-3}, \quad -0{,}108 \times 0^{-3}, \quad 0{,}014 \times 10^{-3}, \ldots$$

We see that in this particular case, only the first harmonic $m_{i,1} = 7.683 \times 10^{-3}\ S\sin\pi x/l$ is of practical importance. Knowing m_i, we can determine by superposition the stresses in all the elements, for example, in the middle cross-section (Fig. 4.15b, c). Superposing also the result (Fig. 4.13a) and confronting it with the membrane solution (Fig. 4.9), it is seen that the correction introduced by the bending state is negligible. This result can be con-

sidered the rule, when the loads are applied at the edges and if the angles ψ_i at the edges of the walls are appreciable. The situation is different when we deal with surface loadings, or when the angles are small since in that case the bending of the walls may play a significant role.

4.4 Analysis of Global Loadings. A Segmental Model of Bar

The influence of deformability of the cross-section caused by a finite number of ribs occurs also in global loadings (Fig. 4.3). It appears with a change in the distribution of stress $\sigma_x(x)$ and shear flows q as compared to a model with an infinite number of ribs. The nature of these changes is seen in the preceding example of a rectangular tube subjected to torsion (Fig. 3.11), in which the restrained warping in the clamped cross-section gave rise to the formation of stresses σ_x^{II} (Fig. 3.12). In a real three-rib structure identically loaded (Fig. 4.16a), a self-equilibrated σ_x^{II} system (Fig. 4.16b) will also occur in the clamped
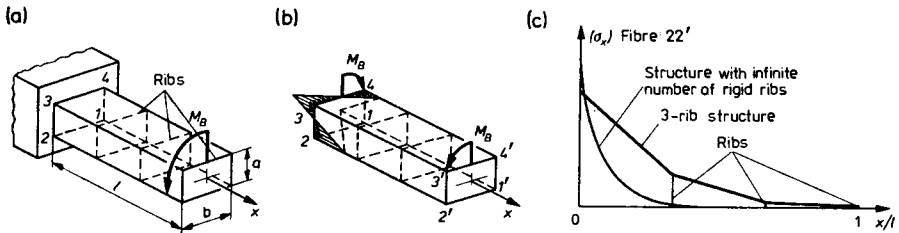
Fig. 4.16. Influence of finite number of ribs with global loading

cross-section, eliminating warping. However, owing to the deformability of the cross-section, in the segments between successive ribs the stresses σ_x^{II} are linear functions of x (Fig. 4.16c). It becomes obvious, if we cut a segment of the into individual walls (Fig. 4.17a, b), then the interactions of the rest of the structure, in keeping with the scheme adopted in Section 4.2, constitute linearly distributed stresses σ_x' and σ_x'' reducing to forces N_i' and N_i'' and
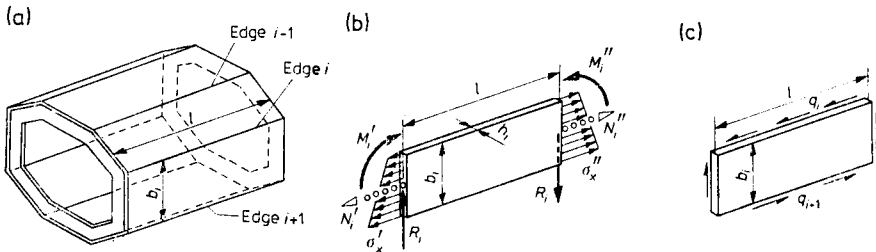
Fig. 4.17. Bar segment and statics of its walls

moments M_i' and M_i''. Wall equilibrium is given by rib reactions R_i, owing to which the shearing force T_i = const. It then follows from Eqs. (4.6) that the interactions between the walls, i.e., shear flows q_i, are also constant. Consequently, we have a linear change in membrane stresses $\sigma_x(x)$. Compared to these, the stresses of the bending state (Section 4.3) are negligible.

The analysis of global loadings in thin-walled bars with a finite number of ribs, or, more generally, in thin-walled structures has a rich literature*. Common to these studies is the substitution of a real structure by a system with a finite number of elements, therefore with a finite number of degrees of freedom. The division of the bar into segments is natural under the circumstances. A further simplification is the idealization of the skin by a so-
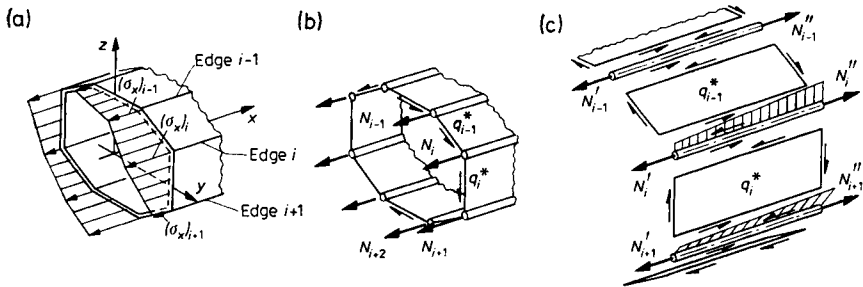
Fig. 4.18. Equivalent semi-monocoque structure

called *semimonocoque structure*, namely, introding fictious longitudinal booms (Fig. 4.18a, b) of rigidity

$$(EA)_i = \tfrac{1}{2}[(Ebh)_i + (Ebh)_{i+1}]. \tag{4.28}$$

The role of the walls is divided in such a way that the booms transmit only longitudinal forces N_i equivalent to real longitudinal forces carried by the walls. As for the walls themselves, they carry only constant flows q_i^* (Fig. 4.18c). We have consequently linear variation $N_i(x)$ and the relation following from the equilibrium of boom i

$$(q_i^* - q_{i-1}^*)l = -(N_i'' - N_i'). \tag{4.29}$$

With such a model of the structure the analysis amounts to the determination of forces N_i in cross-sections of booms corresponding to ribs, i.e., the connecting places of the segments (Fig. 4.19). This is usually a statically indeterminate problem. If the bar is a tube, a statically determinate coupling

---

* The studies of Argyris *et al.* (1944, 1956) are a classical example. Their generalization is the finite elements method: its up-to-date forms was elaborated by Zienkiewicz (1972) and its uses have spread to many fields of science.
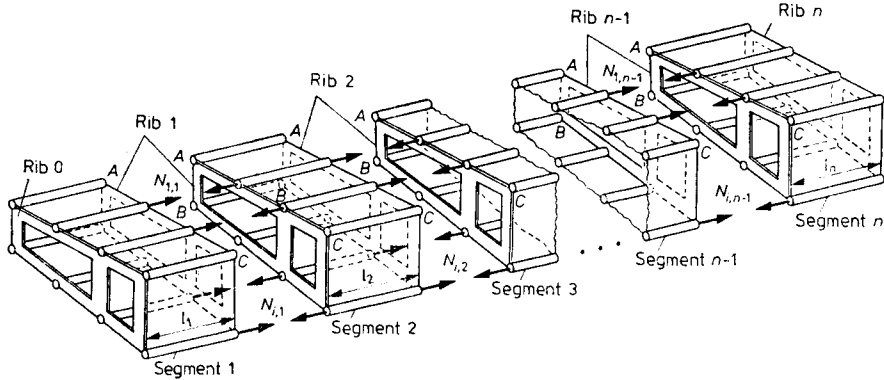
Fig. 4.19. Division of structure into segments and visualization of statically indeterminate forces $N_{i,r}$, $(1 \leqslant i \leqslant k-3)$ $(1 \leqslant r \leqslant n-1)$

of two segments requires that they be joined only at three points of contour A, B, C not lying in a straight line. Thus, in a tube with k booms, the connection of adjacent segments is $(k-3)$-fold statically indeterminate; thus, the degree of static indeterminability in a system with n segments is

$$(n-1)(k-3). \tag{4.30}$$

One of the methods for solving such a problem is the force method. Taking the forces in booms A, B, C to be the reactions of statically determinate
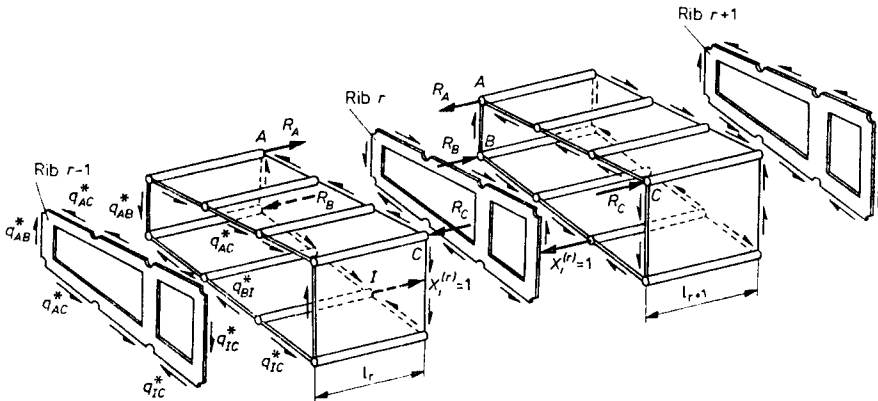
Fig. 4.20. State of unit loading $X_i^{(r)} = 1$. Loading $X_i^{(r)}$ equilibrated within each segment by reactions R_A, R_B, R_C, induces forces $n(x)$ in flanges A, B, C and in flange I, all linearly variable in terms of x. Acting in walls are flows q^*, constant in sheets AB, AC, CI, IB, determined from (4.29) and from the equilibrium of moments of rib $(r-1)$. There are analogous flows in sector $r+1$. Rib r is loaded by the sum of shear flows from segments r and $r+1$

connections, all the other forces $N_{i,r}$ $(1 \leqslant i \leqslant k-3)$ acting in the cross-sections of successive ribs r $(1 \leqslant r \leqslant n-1)$ are the unknowns

$$N_{i,r} = X_i^{(r)},$$

for which we construct successively unit states (i) corresponding to loading $X_i^{(r)}$. The working elements in these states are skin elements of segments r and $r+1$ and ribs $r-1, r, r+1$ (Fig. 4.20). The flexibility matrix $[\mathbf{B}]$ of $n-1$ degrees determined therefrom according to general rules is symmetrical and has a five-member band structure, each of its elements being a symmetrical (block) matrix of $k-3$ degrees. Hence

$$\mathbf{B} = \begin{bmatrix} [\mathbf{B}^{(1,1)}] & [\mathbf{B}^{(1,2)}] & [\mathbf{B}^{(1,3)}] & 0 & 0 & 0 & 0 \dots 0 \\ [\mathbf{B}^{(2,1)}] & [\mathbf{B}^{(2,2)}] & [\mathbf{B}^{(2,3)}] & [\mathbf{B}^{(2,4)}] & 0 & 0 & 0 \dots 0 \\ [\mathbf{B}^{(3,1)}] & [\mathbf{B}^{(3,2)}] & [\mathbf{B}^{(3,3)}[& [\mathbf{B}^{(3,4)}] & [\mathbf{B}^{(3,5)}] & 0 & 0 \dots 0 \\ 0 & [\mathbf{B}^{(4,2)}] & [\mathbf{B}^{(4,3)}] & [\mathbf{B}^{(4,4)}] & [\mathbf{B}^{(4,5)}] & [\mathbf{B}^{(4,6)}] & 0 \dots 0 \\ \cdot \cdot \cdot \cdot \cdot \cdot \cdot \cdot \cdot \cdot \cdot \cdot \cdot \cdot \cdot \cdot \cdot \cdot \cdot \cdot \cdot \cdot \cdot \cdot \cdot \cdot \cdot \\ 0 & \dots & 0 & 0 & [\mathbf{B}^{(n-1,n-3)}] & [\mathbf{B}^{(n-1,n-2)}] & [\mathbf{B}^{(n-1,n-1)}] \end{bmatrix},$$

$$(4.31a)$$

where the superscripts r, t of elements $\mathbf{B}^{(r,t)}$ correspond to the rib numbering. Blocks $[\mathbf{B}^{(r,t)}]$ are usually complete matrices

$$\mathbf{B}^{(r,t)} = \begin{bmatrix} \alpha_{1,1}^{(r,t)} & \alpha_{1,2}^{(r,t)} & \dots & \alpha_{1,k-3}^{(r,t)} \\ \cdot \cdot \cdot \cdot \cdot \cdot \cdot \cdot \cdot \cdot \cdot \cdot \cdot \cdot \cdot \\ \alpha_{k-3,1}^{(r,t)} & \alpha_{k-3,2}^{(r,t)} & \dots & \alpha_{k-3,k-3}^{(r,t)} \end{bmatrix}$$

$$(4.31b)$$

in which the terms $\alpha_{i,j}^{(r,t)}$ allow for the deformability of the booms, walls and ribs. Their value is numerically equal to the work done by state $\binom{r}{i}$ on deformations in state $\binom{t}{j}$. If, for example, the force in boom "m" in states $\binom{r}{i}$ and $\binom{t}{j}$ is $n_m^{(r,i)}$ and $n_m^{(t,j)}$ respectively, then the contribution of this boom to deformability is

$$\int_0^{l_m} \frac{n_m^{(r,i)} n_m^{(t,j)}}{(EA)_m} \, dx, \tag{a}$$

where l_m is the boom's length. Similarly, we calculate the influence of deformability of wall "m", in which the shear flows are $(q^*)_m^{(r,i)}$ and $(q^*)_m^{(t,j)}$ and then

$$\frac{(q^*)_m^{(r,i)} (q^*)_m^{(t,j)} (bl)_m}{(Gh)_m}. \tag{b}$$

Compared to the simple expressions (a) and (b), the influence of rib deformability depends on whether the rib is a truss, a' disk or a frame (Fig. 1.1).

When the rib is a complete disk, this influence is practically negligible. This is also the case when the skin walls are plane and the rib is a truss. Lastly, if all the ribs are undeformable, blocks $\mathbf{B}^{(r,t)}$ in which $t = R+2$, disappear, and matrix $\mathbf{B}$ becomes a three-member band matrix.

If the bar is open, the degree of static indeterminability is subject to change; it is

$$(n-1)(k-4). \tag{4.30b}$$

This is due to the fact that a statically determinate linkage of adjacent open segments requires that they be joined at four points of contour A, B, C, D (Fig. 4.21) since each of the segments by itself has one degree of freedom.
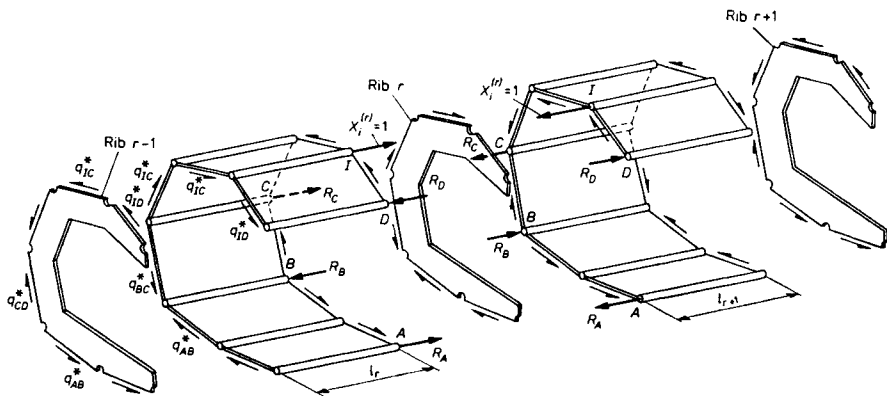
Fig. 4.21. State of unit loading $X_i^{(r)}$ of open cross-section. Reactions R_A, R_B, R_C, R_D equilibring force $X_i^{(r)} = 1$ within each sector induce forces in flanges linearly variable in terms of X, and constant flows q^* determined from (4.29) and from the equilibrium conditions of moments of one of the ribs, say $r-1$. Rib r is loaded by the sum of flows q from both segments
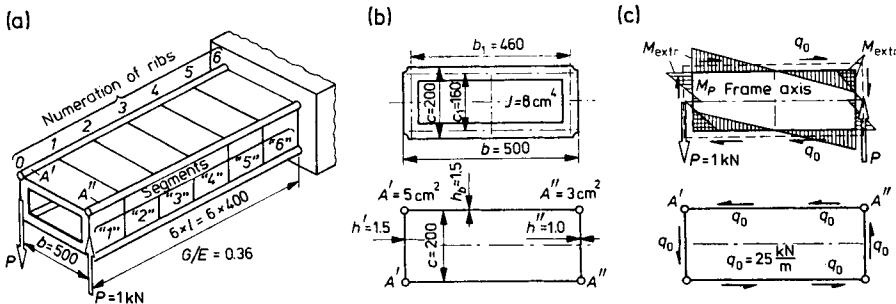
Fig. 4.22. Example of analysis of a 4-flange semi-monocoque structure: (a) sketch of the structure; (b) geometry of frame-type rib and of cross-section of tube; (c) statically determinate state of the structure

We can take for the primary state every statically admissible external force system satisfying the equilibrium conditions. Knowing this state we can determine according to general rules the free terms $Y_i^{(r)}$ and then the unknown $X_i^{(r)}$ from a set of equations which in the matrix notation has the form

$$\mathbf{B}\{X\} + \{Y\} = 0, \tag{4.32}$$

where $\{X\}$ and $\{Y\}$ are column vectors.

An example of the analysis is a two-variant study of a regular 6-segment, 4-flanged semimonocoque structure (Fig. 4.22) with frame-type ribs which in the second variant are replaced by disk-type ribs. The primary state is pure torsion given by Eq. (3.1), from which we obtain $q_0 = \text{const} = Pb/\omega_c = 25$ kN/m throughout the skin and the statics of rib "0" introducing forces P. Under the frame-type rib variant, the rib is subject to bending in its plane (Fig. 4.22c), with $(M)_{\text{extr}} = 500$ Nm in the corners and jump $|M_p| = 125$ Nm in cross-sections of the eccentric application of forces P. Under the disk-type rib variant, the rib "0" is in pure shear, with $q_{\text{rib}} = q_0$.

Since the number of booms (flanges) is $k = 4$ in the examined structure, consequently there is only a single force $X^{(r)}$ in the cross-section of every rib,
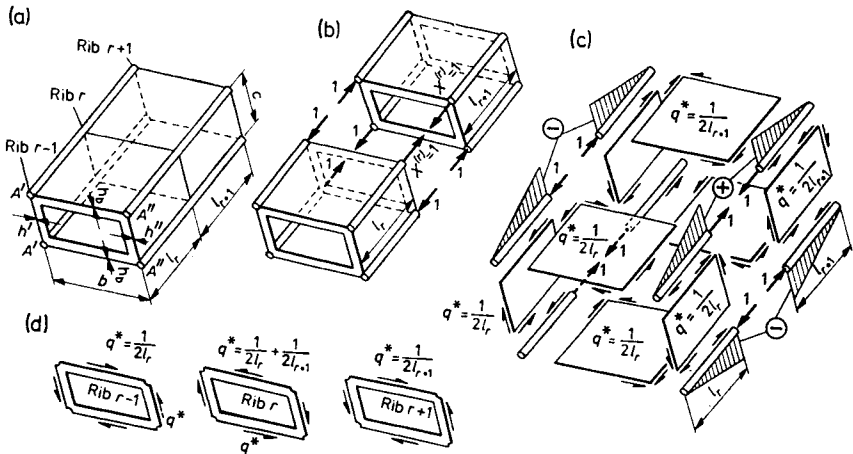
Fig. 4.23. State of unit loading $X^{(r)} = 1$: (a) sketch of the structure; (b) interaction of segment r and $r+1$; (c) internal forces in flanges and walls; (d) rib statics

and matrices $\mathbf{B}^{(r,t)}$ are specified by a single term, $B^{(r,t)} = \alpha_{1,1}^{(r,t)}$. The determination of $\alpha_{1,1}^{(r,t)}$ on the basis of state $X^{(r)} = 1$ (Fig. 4.23) gives

$$B^{(r,r-2)} = \frac{K_{r-1}}{l_r l_{r-1}},$$

$$B^{(r,r-1)} = -\frac{K_{r-1}}{l_r l_{r-1}}\left(1+\frac{l_{r-1}}{l_r}\right) - \frac{K_r}{l_r^2}\left(1+\frac{l_r}{l_{r+1}}\right) - \frac{p_r}{4Gl_r} + \frac{l_r}{3EA_r^*},$$

$$B^{(r,r)} = \left[\frac{K_{r-1}}{l_r^2} + \frac{K_r}{l_r^2}\left(1+\frac{l_r}{l_{r+1}}\right)^2 + \frac{K_{r+1}}{l_{r+1}^2}\right] + \tag{4.33}$$

$$+ \frac{1}{4G}\left(\frac{p_r}{l_r} + \frac{p_{r+1}}{l_{r+1}}\right) + \frac{2}{3E}\left(\frac{l_r}{A_r^*} + \frac{l_{r+1}}{A_{r+1}^*}\right),$$

$$B^{(r,r+1)} = -\frac{K_r}{l_r l_{r+1}}\left(1+\frac{l_r}{l_{r+1}}\right) - \frac{K_{r+1}}{l_{r+1}^2}\left(1+\frac{l_{r+1}}{l_{r+2}}\right) - \frac{p_{r+1}}{4Gk_{r+1}} + \frac{l_{r+1}}{3EA_{r+1}^*},$$

$$B^{(r,r+2)} = \frac{K_{r+1}}{l_{r+1}l_{r+2}},$$

where the dimensionless circumference of segment p_r and the quantity A_r^* are

$$p_r = \left(\frac{2b}{h_b} + \frac{c}{h_c'} + \frac{c}{h_c''}\right)_r, \qquad \frac{1}{A_r^*} = \left(\frac{1}{A'} + \frac{1}{A''}\right)_r. \tag{4.34}$$

The quantity K_r reflects the deformability of rib r. Thus, if the rib is a single-cell frame of constant rigidity EJ_r, then

$$K_r = [(b_1 c_1)^2 (b_1 + c_1)/96EJ]_r, \tag{4.35a}$$

but if it is a solid wall of thickness h_r, then

$$K_r = (bc/4Gh_r)_r. \tag{4.35b}$$

In a regular structure, when all the segments are identical, Eqs. (4.32) take the form

$$B^{(r,r-2)} = B^{(r,r+2)} = \frac{K}{l^2},$$

$$B^{(r,r-1)} = B^{(r,r+1)} = -\frac{4K}{l^2} - \frac{p}{4Gl} + \frac{l}{3EA^*}, \tag{4.36}$$

$$B^{(r,r)} = \frac{6K}{l^2} + \frac{2p}{4Gl} + \frac{4l}{3EA^*}.$$

Equations (4.33)–(4.36) give all the elements of matrix B, and the clamping in the cross-section of undeformable rib 6 is taken into account introducing fictitious segment 7 of zero length. Due to this modification, the elements of matrix $B^{(r,t)}$ for $r \leqslant 4$ are given by the simplified Eqs. (4.36), whereas for $r = 5$ and $r = 6$, it is necessary to use the general Eqs. (4.33). The final step in the preparatory stage is to determine the free terms $Y^{(r)}$, of which only

$Y^{(1)}$ and $Y^{(6)}$ are non-zero. The term $Y^{(1)}$ follows from the deformability of rib "0" and $Y^{(6)}$ is derived from the deformability of the walls of segment 6. Regarding the calculation of forces X from Eqs. (4.32) it is useful to calculate them twice, taking firstly $Y^{(1)} = 0$, $Y^{(6)} \neq 0$ and secondly $Y^{(1)} \neq 0$, $Y^{(6)} = 0$. The results obtained in this way (Fig. 4.24), indicated by dashed
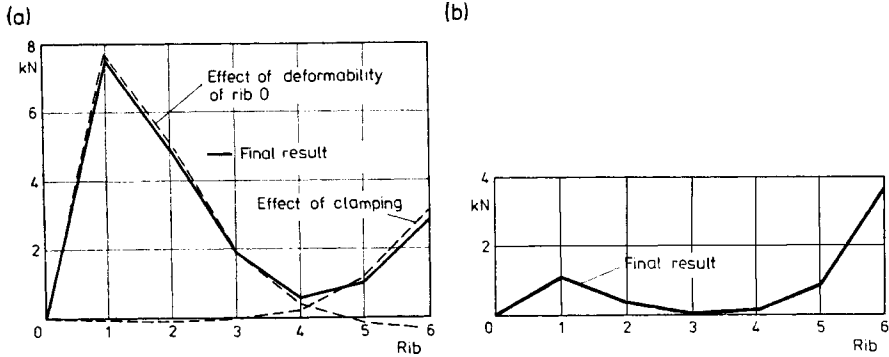
Fig. 4.24. Plot of longitudinal force in flange A in the structure from Fig. 4.22: (a) variant with frame type ribs; (b) variant with solid-wall ribs, 1 mm thick

lines in the diagram, illustrate separately the influence of the clamping of cross-section "6" and separately the influence of deformability of rib "0" introducing the couple of forces P. It is seen that the effect of clamping is very similar in both variants of the construction, and the force values in the booms are much the same. The reason for this the assumed non-deformability of the cross-section at the clamping place, due to which the flexibility of the remaining ribs is of lesser importance. On the other hand, the effect of rib deformability in the two variants is distinctly different. For frame type-ribs, it features forces in the bands seven times as great as that for disk-type ribs and a slower rate of their decrease.

The second solving method is the displacement method, its detailed description will be found in the literature, e.g. Dąbrowski (1960) and Ebner and Köller (1937). In problems featuring a high degree of static indeterminability, this method is simpler with regard to calculation than the force method.

Irrespective of the solving method, problems encountered in practice are divided into three groups according to the correction caused by forces X. In the first group, the correction accounts for a few percent of the value of forces of the primary state. These are as a rule cases where the differences of warping in a structure with disk-type ribs induced by transverse loadings

are the source of forces X. The second group covers problems relating to clamping of a structure with disk-type ribs or relating to transverse loadings introduced into a construction with medium flexible ribs. In this group, the correction introduced by forces X is of the same order of magnitude as the internal forces of the primary state. Lastly, the third group covers problems involving a structure with whippy ribs (frame-type) or a structure with cut-outs. Here, the ultimate image of internal forces may differ by one order of magnitude from the primary state values.

5. Statics of Curved Bars*

Curved thin-walled bars (expansion pipe joints, machine elements, and the like) as used in engineering are usually plane curved, whereas their loadings may equally well be two- or three-dimensional (Fig. 5.1). A characteristic
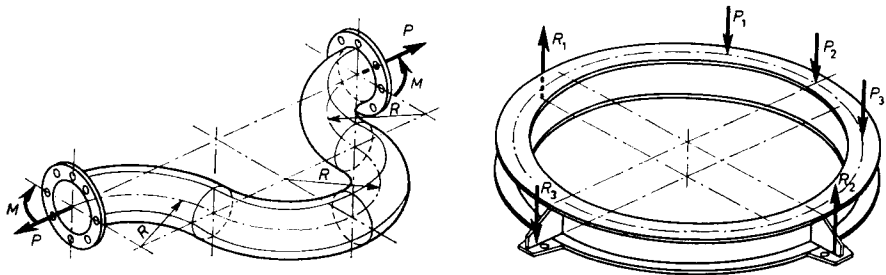
Fig. 5.1. Engineering examples of plane curved thin-walled bars

feature of their structure is wide-spaced ribbing or even no ribs at all. This fact in combination with the natural curvature of a bar changes the character of stress distribution in the bar and is caused by the deformability of the cross-section. This change is much greater than in the case of a straight bar.

5.1. Plane Bending of a Curved Bar. Special Case

The simplest case in the class of problems presently examined is that of pure bending of a ribless bar of constant curvature, whose skin is made up of plane walls and cylindrical shells (Fig. 5.2a). If the stress system in all cross-sections, including the extreme ones, is identical, then by virtue of the axial symmetry of the problem the meridional sections remain plane after deformation. The deformation is the sum of two components, the first consisting in rotation of adjacent cross-sections about each other, with primary angle $d\alpha$ in the

---

* References: Feodosev (1949), Goldenveizer (1949), Grinberg (1949), Wilde (1956), Dąbrowski (1960), Biderman (1977).
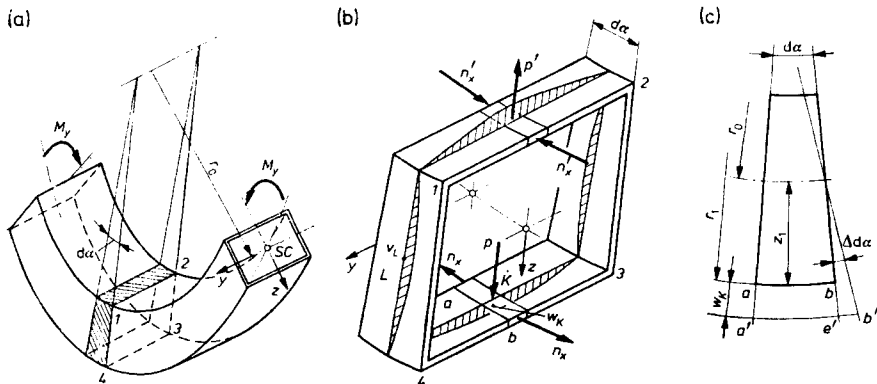
Fig. 5.2. Pure bending of plane curved bar: (a) sketch of the structure; (b) force system and deformation of the cross-section; (c) determination of unit elongations of cylindrical wall of bar

elementary slice changing to $d\alpha + \Delta d\alpha$. The second one follows from the deformation of the cross-section, and the cause of it is that flows n_x induced by moments M_y (Fig. 5.2b) give resultant pressure $p = n_x/r_1$ perpendicular to strip 3, 4 od the skin. Pressure p causes bending of this strip as a beam fixed in plane walls 2, 3 and 1, 4. Strip 1, 2 behaves similarly, the differences, however, being that its loading p' has the opposite sense compared to that of strip 3, 4. As a result, sides 1, 2 and 3, 4 deflect on the outside, and the vertical sides bend towards the centre*. Consequently, unit elongation ε_x of fibre K is

$$\varepsilon_x = (\overline{a'b'} - \overline{ab})/\overline{ab} = [(\overline{a'b'} - \overline{a'e'}) + (\overline{a'e'} - \overline{ab})]/\overline{ab}.$$

Considering (Fig. 5.2c) that $\overline{a'b'} - \overline{a'e'} = (z_1 + w_K)\Delta\, d\alpha \approx z_1 \Delta\, d\alpha$, $\overline{a'e'} - \overline{ab} = w_K d\alpha$, $\overline{ab} = (r_0 + z_1)d\alpha = r_1 d\alpha$, we get

$$\varepsilon_x = \frac{z_1}{r_1}\left(\frac{\Delta\, d\alpha}{d\alpha}\right) + \frac{w_K}{r_1}, \qquad (5.1a)$$

where r_1 and z_1 are the radius of curvature of the wall and its distance from the neutral layer, respectively, and w_K is the radial displacement of fibre K being investigated.

The result (5.1a) together with the presented strain image show a close analogy to the known problem of axially symmetrical bending of a pipe

---

* The described image corresponds to the situation when pressures p and p' have senses as in Fig. 5.2b.
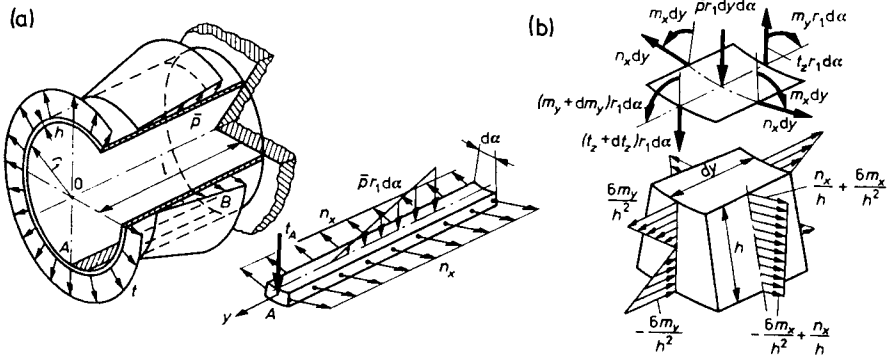
Fig. 5.3. Axially symmetrical bending of shell as an analogy to statics of the cylindrical wall from Fig. 5.2: (a) sketch of the structure; (b) effort components and stress system in the element

(Fig. 5.3), in which using denotations from Fig. 5.2, elongation ε_x and cell flows n_x can be expressed as:

$$\varepsilon_x = w_K/r_1, \qquad n_x = Ehw_K/r_1, \tag{a}$$

and flows of bending moments m_x and m_y and a shearing forces t as:

$$m_x = \nu m_y, \qquad m_y = D\frac{d^2 w_K}{dy^2}, \qquad t_z = \frac{dm_y}{dy} = D\frac{d^3 w_K}{dy^3}, \tag{5.2}$$

where $D = Eh^3/12(1-\nu^2)$ is the plate rigidity of the skin. Moreover, following from the obvious equilibrium equation

$$dt_z/dy = \bar{p} - (n_x/r_1) \tag{b}$$

is the well-known differential equation

$$D\frac{d^4 w_K}{dy^4} + \frac{Eh}{r_1^2}w_K = \bar{p}. \tag{c}$$

The only difference in the present case is in ε_x given this time by Eq. (5.1a), due to which tangential flow n_x is expressed by the relation

$$n_x = Eh\varepsilon_x = \frac{Ehz_1}{r_1}\left(\frac{\Delta d\alpha}{d\alpha}\right) + \frac{Ehw_K}{r_1}, \tag{5.3}$$

differing from the previous relation with respect to the first term. Considering that now external loading $\bar{p} = 0$, we obtain from (b) and (a)

$$D\frac{d^4 w_K}{dy^4} + \frac{Eh}{r_1^2}w_K = -\frac{Ehz_1}{r_1^2}\left(\frac{\Delta d\alpha}{d\alpha}\right), \tag{d}$$

with the value of the right-hand side of the equation being constant because all the quantities, the relative change in angle $d\alpha$, i.e., $(\Delta d\alpha/d\alpha)$, included, are constant.

Taking this into account and introducing the parameter

$$k^4 = \frac{3(1-\nu^2)}{r_1^2 h^2},$$ (5.4a)

we reduce Eq. (d) to the form

$$w_K^{IV} + 4k^4 w_K = -4k^4 z_1 \left(\frac{\Delta d\alpha}{d\alpha}\right).$$ (5.4b)

The solution of Eq. (5.4b) is

$$w_K = -z_1 \left(\frac{\Delta d\alpha}{d\alpha}\right) + A_1 e^{-ky}\sin ky + A_2 e^{-ky}\cos ky +$$
$$+ A_3 e^{-k(l-y)}\sin k(l-y) + A_4 e^{-k(l-y)}\cos k(l-y),$$ (5.5)

where $A_1, \ldots, A_4$ are integration constants and l is the arbitrarily chosen length, say, the length of wall 3, 4 (Fig. 5.2b). In this form, $w_K(y)$ is the sum of the constant term and two "damped vibrations" starting out from boundaries $y = 0$ and $y = l$. When l is sufficiently great, then most important for $y = 0$ are the terms with A_1 and A_2, and for $y = l$, the terms with A_3 and A_4. In a case like that, constants A_1 and A_2 can be determined with engineering accuracy from the conditions at boundary $y = 0$, and constants A_3 and A_4, from the conditions for $y = l$. These are geometric conditions, i.e., conditions giving the boundary values of w_K or dw_K/dy, or else static conditions, i.e., conditions giving the boundary values of m_y and t_y from Eqs. (5.2).

It is sometimes useful to use the function of w_K in the form

$$w_K = -z_1 \left(\frac{\Delta d\alpha}{d\alpha}\right) + B_1 \sinh ky \sin ky + B_2 \cosh ky \cos ky +$$
$$+ B_3 \sinh ky \cos ky + B_4 \cosh ky \sin ky,$$ (5.6)

which is the result of the transformation of relation (5.5). Constants B_1 and B_2 correspond here to a symmetric solution with respect to $y = 0$ and constants B_3 and B_4 to an antisymmetric solution.

The above analysis applies only to cylindrical walls, e.g., 1, 2 and 3, 4 in Fig. 5.2b. For plane walls, e.g., 1, 4 and 2, 3 in Fig. 5.2, the state of deformation is a superposition of a plane problem with rotation of the radial sides by angle $\Delta d\alpha$ (Fig. 5.4a) and a bending induced by the reactions of the cylindrical walls (Fig. 5.4b). The former is identical with the problem of plane
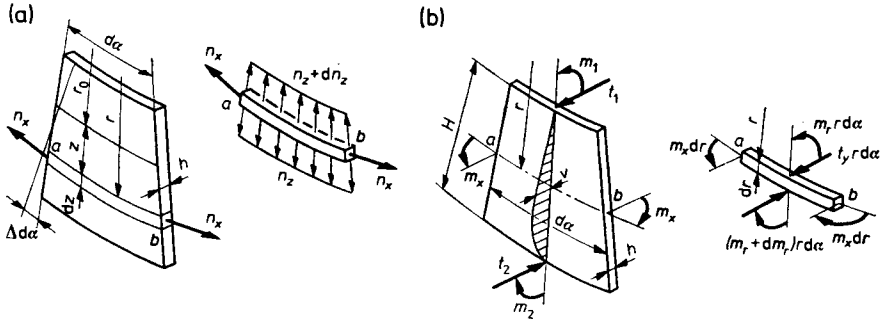
Fig. 5.4. Statics of plane wall of a curved bar subjected to bending

bending of a curved bar of rectangular cross-section $H \times h$, where the longitudinal strain

$$\varepsilon_x = \frac{z}{r}\left(\frac{\Delta\,d\alpha}{d\alpha}\right),\tag{5.7a}$$

and the normal stress flow*

$$n_x = Eh\varepsilon_x = \frac{Ezh}{r}\left(\frac{\Delta\,d\alpha}{d\alpha}\right),\tag{5.7b}$$

where $r = r_0 + z$ is the radius of the fibre being investigated. In many cases when $H \ll r$, we use, with engineering accuracy, $r = \text{const}$, e.g. $r = r_0$.

The other componential problem presents axially symmetrical bending of a circular plate of thickness h, in which by using the denotations from Fig. 5.4b we obtain moment flows m_r and m_x

$$m_r = D\left(\frac{d^2v}{dr^2} + \frac{\nu}{r}\frac{dv}{dr}\right), \quad m_x = D\left(\frac{1}{r}\frac{dv}{dr} + \nu\frac{d^2v}{dr^2}\right).\tag{e}$$

Wall deflection v is given by the equation

$$\frac{d^3v}{dr^3} + \frac{1}{r}\frac{d^2v}{dr^2} - \frac{1}{r^2}\frac{dv}{dr} = \frac{t_y}{D},\tag{f}$$

where t_y is the shearing force flow. In normal applications, $r \gg H$ and we can then neglect in Eqs. (e) and (f) the terms with r in the denominator**. As a result we obtain the simplified relations

$$m_r = D\frac{d^2v}{dr^2}, \quad m_t = \nu D\frac{d^2v}{dr^2}, \quad t_y = D\frac{d^3v}{dr^3},\tag{5.8}$$

---

* Neglected here, as usual, is the influence of flows n_z.

** The error produced by such an approximation is of the order $(H/r)^2$.

which are identical to those for cylindrical bending of a plate. The hitherto
unknown quantities involved in these relations, namely radius r_1 of the neutral
layer and the quantity $(\varDelta d\alpha/d\alpha)$ are determined based on the static conditions

$$\int_A n_x ds = 0, \qquad \int_A n_x z\, ds = M_y. \tag{5.9a,b}$$

The first tells us that in pure bending, longitudinal force $N = 0$ and the second
one expresses the equivalence of the sum of elementary moments $(n_x ds)z$
and resultant moment M_y, and integration of the respective quantities covers
the entire cross-section of the bar. The determination of these two quantities
provides the basis for determining the normal stresses, as indicated in Fig.
5.3b.

As an example of an analysis we take the bending of a slightly curved
thin-walled bar with a box-shaped cross-section (Fig. 5.5a). For slight cur-
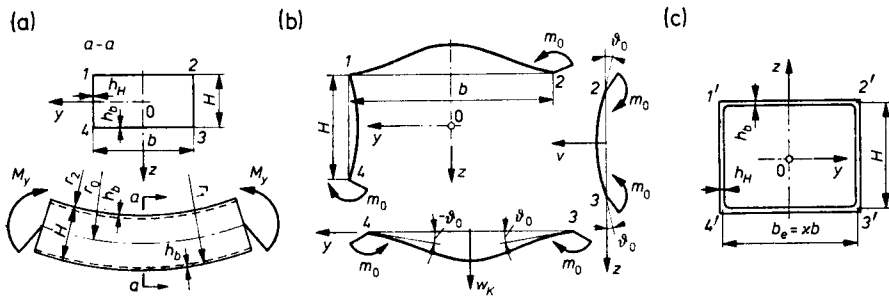
Fig. 5.5. Example of bending analysis of a curved bar of box-shaped cross-section

vature, we can assume that $r_1 \approx r_2 \approx r_0$ and then by virtue of the symmetry
of the cross-section with respect to the centroidal y-axis, the deformations
of cylindrical walls $1, 2$ and $3, 4$ are identical. Moreover, the deflection of
the vertical walls can be described by the simplified Eqs. (5.8). In this situation,
the neutral layer coincides with the y-axis, and flows $n_x(y)$ on walls $1, 2$ and $3, 4$
have identical absolute values. The $n_x(y)$ distribution follows from the solution
of Eq. (5.6), which for isolated wall $3, 4$ (Fig. 5.5b) satisfies the following
conditions:

$$(w'_K)_{y=0} = 0, \quad (w'''_K)_{y=0} = 0, \quad (w_K)_{y=b/2} = 0, \quad (Dw''_K)_{y=b/2} = m_0.$$

The first two conditions follow from the symmetry of deformations and from
the absence of shearing force t_z for $y = 0$. The third condition means that the
deformation of wall $1, 4$ in its plane is practically negligible. Lastly, the
fourth condition describes the elastic clamping of wall $3, 4$ in vertical walls

2, 3 and *4, 1*. Moment m_0 follows from the solution of the elementary problem for wall *2, 3*

$$m_0 = (2D_1/H)(-\vartheta_0),$$

where $D_1 = Eh_H^3/12(1-\nu^2)$. Considering that $\vartheta_0 = (dw_K/dy)_{y=b/2}$, we write the last condition as

$$\left(Dw_K'' + \frac{2D_1}{H}\, w_K'\right)_{y=b/2} = 0.$$

Substituting the first two conditions into the solution of (5.6), we obtain $B_3 = B_4 = 0$, and the remaining ones gives

$$B_1 \sinh \frac{kb}{2} \sin \frac{kb}{2} + B_2 \cosh \frac{kb}{2} \cos \frac{kb}{2} = \frac{H}{2}\left(\frac{\Delta\, d\alpha}{d\alpha}\right),$$

$$B_1\left(\cosh \frac{kb}{2} \sin \frac{kb}{2} + \sinh \frac{kb}{2} \cos \frac{kb}{2} + \psi kb \cosh \frac{kb}{2} \cos \frac{kb}{2}\right) -$$

$$- B_2\left(\cosh \frac{kb}{2} \sin \frac{kb}{2} - \sinh \frac{kb}{2} \cos \frac{kb}{2} + \psi kb \sinh \frac{kb}{2} \sin \frac{kb}{2}\right) = 0,$$

where $\psi = (H/b)(h_b/h_H)^3$ is a dimensionless parameter describing the relative rigidity of the vertical and cylindrical walls. By solving the above set of equations, we obtain constants B_1 and B_2

$$B_1 = H\left(\frac{\Delta\, d\alpha}{d\alpha}\right)\left(\cosh \frac{kb}{2} \sin \frac{kb}{2} - \sinh \frac{kb}{2} \cos \frac{kb}{2} + \right.$$

$$\left. - \psi kb \sinh \frac{kb}{2} \sin \frac{kb}{2}\right) \Big/ \overline{\Psi}(kb),$$

$$B_2 = H\left(\frac{\Delta\, d\alpha}{d\alpha}\right)\left(\cosh \frac{kb}{2} \sin \frac{kb}{2} + \sinh \frac{kb}{2} \cos \frac{kb}{2} + \right.$$

$$\left. - \psi kb \cosh \frac{kb}{2} \cos \frac{kb}{2}\right) \Big/ \overline{\Psi}(kb),$$

where

$$\overline{\Psi}(kb) = \sinh kb + \sin kb + \psi kb(\cosh kb + \cos kb).$$

Knowing B_1 and B_2, we obtain from (5.6) deflection w_K and from (5.3) the value of n_x, with $z_1 = H/2$, $r = r_0$ and $h = h_0$. The result

$$n_x = -\frac{Eh_b}{r_0}(B_1 \sinh ky \sin ky + B_2 \cosh ky \cos ky)$$

depends on $(\varDelta\,d\alpha/d\alpha)$. This quantity can be determined from (5.6) but it is simpler to find the force

$$N_{1,2} = \int_{-b/2}^{b/2} n_x\,dy$$

$$= -\frac{Eh_b}{kr_0}\left[(B_1+B_2)\cosh\frac{kb}{2}\sin\frac{kb}{2} - (B_1-B_2)\sinh\frac{kb}{2}\cos\frac{kb}{2}\right],$$

transmitted by wall *1, 2*. After transformations, we have

$$N_{1,2} = -\frac{EH}{2r_0}\left(\frac{\varDelta\,d\alpha}{d\alpha}\right)bh_b\,\frac{(\cosh kb-\cos kb)+\psi(kb/2)(\sinh kb+\sin kb)}{(kb/2)\varPsi(kb)}.$$

Since the factor $(-EH/2r_0)(\varDelta\,d\alpha/d\alpha)$ is the stress σ_x in the upper fibres of walls *1, 4* and *2, 3*, the remaining term is the effective area of wall *1, 2*

$$A_{\text{effect.}} = bh_b\varkappa,$$

TABLE 5.1. Effective width of flanges under plane bending

Type structure	Effective width
	$\varkappa = \dfrac{2}{kb}\dfrac{\sinh kb+\sin kb}{2+\cosh kb+\cos kb}$ for $kb > 4\varkappa \approx \dfrac{2}{kb}$
	$\varkappa = \dfrac{1}{kb}\dfrac{\sinh kb+\sin kb}{\cosh kb+\cos kb}$ for $kb > 4\varkappa \approx \dfrac{1}{kb}$
	$\varkappa$ $= \dfrac{\sinh 2kb+\sin 2kb+\psi kb(\cosh 2kb+\cos 2kb-2)}{kb[2-\cosh 2kb+\cos 2kb+2\psi kb(\sinh 2kb-\sin 2kb)]}$ $\psi = (H/2b)(h_b/h_H)^3$
$k = \sqrt[4]{3(1-\nu)/R^2h_b^2}$	ν—Poisson's number

where the dimensionless coefficient

$$\varkappa = \frac{2(\cosh kb - \cos kb) + \psi kb(\sinh kb + \sin kb)}{kb[\sinh kb + \sin kb + \psi kb(\cosh kb - \cos kb)]} < 1$$

describes the incomplete utilization of the cylindrical wall caused by deformation of the cross-section. Such an interpretation makes it possible to introduce the concept of substitute undeformable cross-section (Fig. 5.5c), equivalent to the real structure with regard to rigidity and strength. The concept of effective width $b_e = b\varkappa$ introduced above and the concept of equivalent cross-section are used in practice to determine $(\Delta \, d\alpha/d\alpha)$ and the value $(\sigma_x)_{extr}$. If the bar is slightly curved, then

$$\frac{\Delta \, d\alpha}{d\alpha} = \frac{M_y R}{EJ_{ye}}, \quad (\sigma_x)_{extr.1} = \frac{M_y z_1}{J_{ye}}, \quad (\sigma_x)_{extr.2} = \frac{M_y z_2}{J_{yd}},$$

where z_1, z_2 are the distances of the extreme fibres from the neutral layer, and J_{ye} is the moment of inertia of the cross-section with flanges having effective widths. For example, for a box-shaped cross-section, we have

$$J_{ye} = (H^3 h_H/6) + (b_e H^2 h_b/2).$$

Coefficients $\varkappa$ for several typical cross-sections are specified in Table 5.1.

5.2. General Case of Plane Bending of a Bar

A generalization of the problem solved in Section 5.1 is the case of pure bending of a bar with a constant curvature, whose contour is of an arbitrary shape (Fig. 5.6a). If we take, as previously, the stress distribution to be identical in all cross-sections, then the meridional cross-sections remain plane after
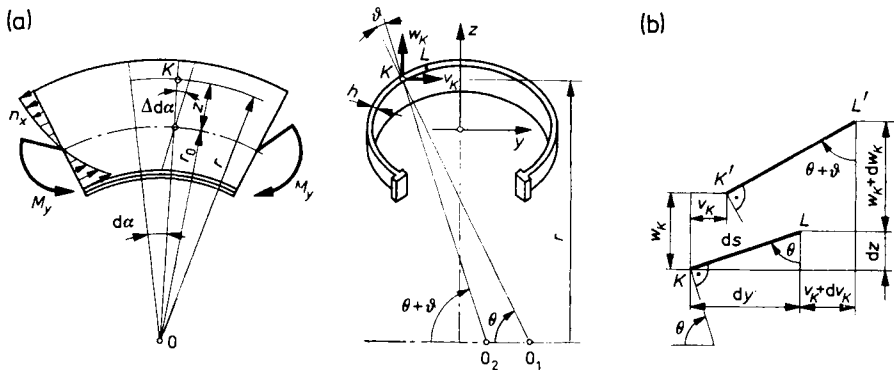
Fig. 5.6. Plane bending of a curved bar of arbitrary contour: (a) geometry of the structure and displacements; (b) displacements in a cross-sectional plane

deformation, the only difference being that now fibre K has a displacement
with two components, $v_K(s)$ and $w_K(s)$, and not with one as in Fig. 5.2. This
fact does not influence elongation ε_x, which continues to be given by Eq.
(5.1a) but instead of constants z_1 and r_1 we use $z(s)$ and $r(s)$ corresponding to
fibre K. As a result

$$\varepsilon_x = \frac{z}{r}\left(\frac{\varDelta\,d\alpha}{d\alpha}\right) + \frac{w_K}{r}. \tag{5.1b}$$

Although by knowing $v_k(s)$ and $w_k(s)$, we obtain the deformation appear-
ance of the cross-section; yet, it is more convenient also to introduce angle
ϑ of rotation of the normal to the contour. Neglecting at the same time the
elongation of the contour in the plane of the cross-section, we obtain from
Fig. 5.6b the equations*

$$dw_K/ds = -\vartheta\sin\theta, \quad dv_K/ds = \vartheta\cos\theta, \tag{a}$$

which allows the deformation of the cross-section to be described by ϑ. This
same angle expresses in an equally simple manner the change in curvature
$\varkappa_t$ in the cross-section, namely,

$$\varkappa_t = d\vartheta/ds. \tag{b}$$

The next stage in the analysis is to describe the internal forces and their rela-
tionships resulting from the equilibrium. By virtue of the axial symmetry,
involved here are normal stress flows n_x and n_t, m_x and m_t moment flows,
and shear flow t (Fig. 5.7a, b). They satisfy the equilibrium of projections
on the radial direction and on the 0-0 axis (Fig. 5.7c)

$$d[r(t\sin\theta - n_t\cos\theta)]/ds + n_x = 0, \quad t\cos\theta + n_t\sin\theta = n_0, \tag{c}$$
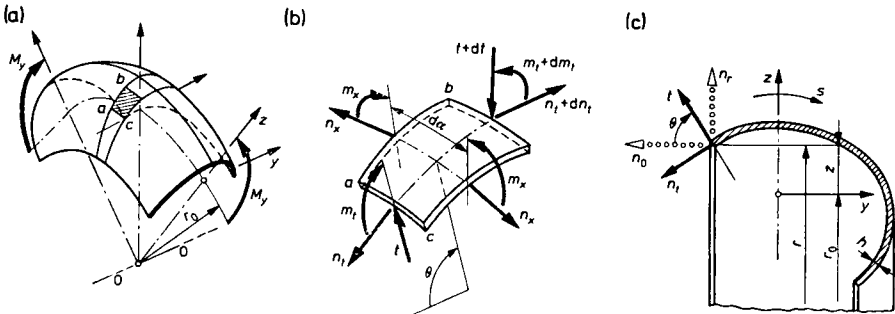
Fig. 5.7. Forces acting in plane bending of a curved bar: (a) sketch of the structure; (b)
statics of an element; (c) equilibrium of the part cut along the parallel

---

* Element KL (Fig. 5.6b), for which $dz = ds\cos\theta$, $dy = ds\sin\theta$, moves to position
$K'L'$. Since by assumption $\overline{KL} = \overline{K'L'}$, we have $dz^* = dz + dw_K = ds\cos(\theta + \vartheta)$, dy^*
$= dy + dv_K = ds\sin(\theta + \vartheta)$; hence, considering that $\cos\vartheta \approx 1$, $\sin\vartheta \approx \vartheta$, we obtain Eqs. (a).

and the equilibrium of moments with respect to the a-c axis

$$d(rm_t)/ds - m_x \cos\theta - tr = 0,\tag{d}$$

where n_0 is the flow in the direction of 0-0 axis. When the cross-section is open, $n_0 = 0$, but when it is a pipe, then $n_0 r$ per unit central angle is constant. Its value is derived from the identity of displacement v_K at the beginning and at the end of the contour.

Considering that the length of the bar is considerably greater than its transverse dimensions, we can simplify the above description of forces and their relationship with strains. Thus, we can neglect n_t wherever it occurs jointly with n_x. The same applies to m_x in confrontation with m_t, as in Eq. (d) for example. Consequently, we can use the simplified relationships

$$n_x = Eh\varepsilon_x, \quad m_t = -D\varkappa_t = -Dd\vartheta/ds.\tag{e}$$

Transforming relations (a)–(e) and Eq. (5.1b), and introducing the radial flow

$$n_r = t\sin\theta - n_t\cos\theta\tag{f}$$

we obtain a set of five 1st order linear equations

$$\frac{d(r\varepsilon_x)}{ds} = -\vartheta\sin\theta + \cos\theta\left(\frac{\Delta\,d\alpha}{d\alpha}\right), \quad \frac{d\vartheta}{ds} = -\frac{m_t}{D},$$

$$\frac{d(n_r r)}{ds} + Eh\,\varepsilon_x = 0, \quad \frac{d(m_t r)}{ds} = (n_r\sin\theta + n_0\cos\theta)r,\tag{5.10}$$

$$\frac{dv_K}{ds} = \vartheta\cos\theta.$$

In these equations, neglecting n_0, we have 5 unknowns, i.e. five quantities, ε_x, ϑ, v_K, n_r, m_t, and two constant parameters: $\Delta\,d\alpha/d\alpha$ and radius r_0. Additional equations are the conditions (5.9) in the form

$$\int_A Eh\varepsilon_x ds = 0, \quad \int_A Eh\varepsilon_x z ds = -M_y,\tag{5.9a,b}$$

with the contribution of m_x flows omitted in the second equation.

It is justifiable to leave the solution in the form of (5.10) and (5.9) since for a cross-section of arbitrary shape, results are obtainable only by using the numerical method and with the use of a digital computer, for which integration of 1st order linear equations is a routine operation. The integration process itself depends on the form of the cross-section. If the cross-section is open, then $n_0 = 0$ and so the last equation (5.10) determining v_K is independent from others. For the remaining four equations, we get the relation

given below, which follow from the condition that edges $s = 0$ and $s = c$ are free*:

$$n_r = 0, \qquad m_t = 0, \tag{g}$$

which are sufficient for the unique determination of ε_x, ϑ, n_r and m_t as a function of parameter $\Delta d\alpha/d\alpha$. Its value is determined from Eq. (5.9b), in which by virtue of relation (5.9a), we can put radius r in place of coordinate z. The deformation of the cross-section itself, i.e., the determination of $v_K(s)$ and $w_K(s)$, is obtained by integration of Eqs. (a), whereby the right-hand sides are already known. The constant of integration for v_K can be taken arbitrarily since its possible change means displacement of the structure as a rigid body, whereas the constant for w_K is taken assuming for the radius of the neutral layer r_0 that $(w_K)_{r=r_0} = 0$. The quantity r_0 thus defined is determined from Eq. (5.9a).

In a tubular cross-section, flow $n_0 \neq 0$, which makes it necessary to solve the full set of equations (5.10). Starting out from an arbitrary point of the contour, e.g. one corresponding to $\theta = 0$, in which there are the initial values $(\varepsilon_x)_0$, $(\vartheta)_0$, $(n_r)_0$, $(m_t)_0$ and an arbitrarily taken value of $(v_K)_0 = 0$, we integrate Eqs. (5.10) also assuming certain initial values of parameters $\Delta d\alpha/d\alpha$ and $n_0 r = \text{const}$. This yields the sought quantities $\varepsilon_x(s)$, $\vartheta(s)$, $n_r(s)$, $m_t(s)$ and $v_K(s)$ as linear functions of the four initial quantities and the two parameters. Finally, making use of five continuity conditions for $\theta = 2\pi$

$$(\varepsilon_x)_0 = (\varepsilon_x)_{\theta=2\pi}, \quad \ldots, \quad (m_t)_0 = (m_t)_{\theta=2\pi}, \quad (v_K)_{\theta=2\pi} = 0, \tag{h}$$

we obtain a set of five algebraic linear equations with one free parameter, $\Delta d\alpha/d\alpha$; its value is determined as before from (5.9b).

The procedure described becomes simplified if the cross-section is symmetrical to the plane of curvature of the bar. The following conditions occur at two points of the axis of symmetry, namely $\theta = -\pi/2$ and $\theta = \pi/2$

$$\vartheta = 0, \qquad n_r = 0, \qquad v_K = 0, \tag{i}$$

and $(\varepsilon_x)_0$ and $(m_t)_0$ remain the unknown initial quantities. Taking the initial point at $\theta = -\pi/2$ and solving the homogeneous set (5.10) for two combinations of initial conditions

$$(\varepsilon_x)_0 = 1, \quad (\vartheta)_0 = 0, \quad (n_r)_0 = 0, \quad (m_t)_0 = 0, \tag{j}$$

$$(\varepsilon_x)_0 = 0, \quad (\vartheta)_0 = 0, \quad (n_r)_0 = 0, \quad (m_t)_0 = 1 \tag{k}$$

---

* If an open cross-section is symmetrical to the plane of the bar, then retaining conditions (g) for $s = 0$, we can make use of the symmetry conditions for $s = c/2$

$$\vartheta = 0, \qquad n_r = 0.$$

and the twice non-homogeneous set (5.10) for the two selected combinations of parameters, the first being $\Delta \, d\alpha/d\alpha = 1, n_0 r = 0$ and the second, $(n_0 r) = 1$, $\Delta d\alpha/d\alpha = 0$, we obtain from superposition of ϑ, n_r and v_K as linear functions $(\varepsilon_x)_0$, $(m_t)_0$, $(n_0 r)$ and $(\Delta d\alpha/d\alpha)$. An example is

$$\vartheta = \vartheta_\varepsilon(\varepsilon_x)_0 + \vartheta_m(m_t)_0 + \vartheta_n(n_0 r) + \vartheta_\alpha(\Delta \, d\alpha/d\alpha),$$

where $\vartheta_\varepsilon(s)$, $\vartheta_m(s)$, $\vartheta_n(s)$, $\vartheta_\alpha(s)$ are influence functions corresponding to consecutive solutions of (j), (k), ...

Finally, taking the particular values of ϑ_ε, ... for $(s)_{\theta = \pi/2}$, we obtain from conditions (i) a set of three equations which after they are solved provide all the quantities dependent only on parameter $\Delta d\alpha/d\alpha$ determined from Eq. (5.9b).

The analysis is further simplified if the bar is slightly curved, i.e., if we can take radius $r = $ const in Eqs. (5.10), e.g. one equal to the radius corresponding to the centroid of the cross-section*. In such a case, flow $n_0 = 0$ not only for open cross-sections but also for tubes with two axes of symmetry.

The numerical method of solving set (5.10), which is the rule, can be replaced in specific cases by the analytical method. One such case is when cross-section consist of plane and cylindrical walls as considered in Section 5.1. Another example is tubular cross-sections of a regular contour (circular, elliptical) for which the sought quantities can be presented by Fourier series over the contour perimeter. In effect, we obtain a set of algebraic linear equations with respect to unknown coefficients of these series. The accuracy of the solution depends here on the number of terms taken for analysis.

Apart from the presented solution, which is approximate by assumption, there are more accurate solutions based on the theory of shells, in which all the components of internal forces (5.7b), i.e., m_t, m_x, n_t, n_x and t are considered. An example of these solutions is described in Bidermann's paper (1977).

The general considerations are illustrated by results (Fig. 5.8) borrowed from Feodosev (1949) for the case of bending of a pipe of elliptical cross-section, which is important from an engineering point of view.

$$\frac{1}{R}\left(\frac{\Delta d\alpha}{d\alpha}\right) = \frac{M_y}{\varkappa E J_y}, \quad \sigma_x = -\frac{M_y z}{J_y}\left(1 - \frac{\xi z^2}{a^2}\right)$$

a/b	1.0	1.5	2.0	3.0	4.0	5.0	
η	0.833	0.662	0.584	0.499	0.459	0.439	$\varkappa = 1 - \dfrac{\eta}{\zeta + (R^2 h^2/a^4)}$
ζ	0.750	0.602	0.530	0.454	0.415	0.392	$\zeta = \dfrac{1}{0.833 + (R^2 h^2/a^4)}$
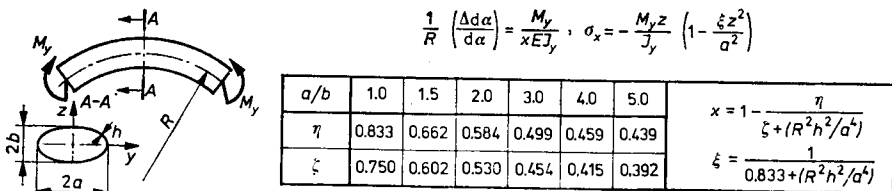
Fig. 5.8. Results of flexure analysis of thin-walled elliptical tube

---

* This simplification must not be put into Eq. (5.9b).

5.3. Three-Dimensional Loading of a Plane Curved Bar

Under analysis is a thin-walled bar, in which one of the principal central axes, e.g. z-axis, lies in the plane of curvature, and the loading is perpendicular to that plane (Fig. 5.9a). The effort of the cross-section consists of shear-
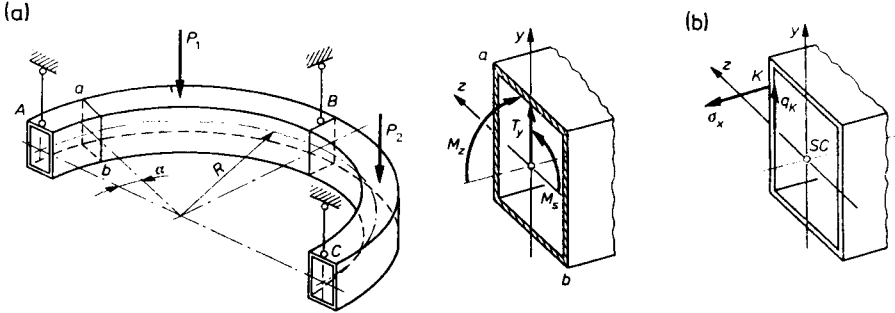
Fig. 5.9. Bending of a curved bar out of its plane of initial curvature

ing force T_y, bending moment M_z and torsional moment M_t. The behaviour of a structure depends upon the deformability of the cross-section. Thus, if the bar is densely ribbed*, it is justified to assume the cross-section to be undeformable, and the course of analysis depends on whether the cross-section of the bar is tubular or open. In the former case, we use, with engineering accuracy, ordinary strength equations neglecting normal stresses due to restrained torsion and also the influence of curvature upon the stress
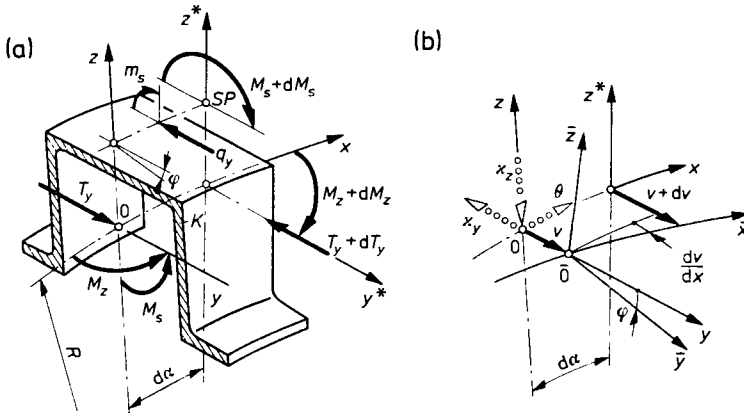
Fig. 5.10. Effort components of cross-section and displacements under out-of-plane loading of curved bar

---

* A *measure of the density* is the ratio of rib spacing l to mean overall dimensions H_{mean} of the cross-section. As a rough measure of dense ribbing we can take $l/H_{mean} \approx 0.5$.

distribution. In other words, stresses σ_x (Fig. 5.9b) are given by Eq. (2.6a), in which $N = 0$ and $M_y = 0$, i.e.

$$\sigma_x = -M_y z / J_y \tag{a}$$

and flows q, by Eq. (3.25). When the cross-section of the bar is open, restrained torsion plays a significant role in the behaviour of the bar, since pure torsion rigidity is small. In this case we begin the analysis with the equilibrium equations of an element (Fig. 5.10a)

$$\frac{dT_y}{dx} + q_y = 0, \quad \frac{dM_z}{dx} + \frac{M_t}{R} - T_y = 0, \quad \frac{dM_t}{dx} - \frac{M_z}{R} + m_t = 0,$$

$$\tag{5.11}$$

in which we have known continuous loads q_y (N/m) and m_t (Nm/m) applied to the elastic axis connecting the shear centres of the cross-sections. The difference between the radius of curvature of R-axis and the radius of the elastic axis is neglected here.

The second step of the analysis is to describe the deformation of the bar. On account of the assumed symmetry of the cross-section and the specific loading, there is no displacement along the z-axis, i.e., $w = 0$. The remaining parameters, namely, displacement v and angle of rotation φ, shift the $Oxyz$ coordinate system to position $\overline{O}\overline{x}\overline{y}\overline{z}$ (Fig. 5.10b). If the Ox-axis of the bar were straight here, then such a shift would affect neither the curvature of the axis in Oxy plane, i.e. $\varkappa_z = d^2v/dx^2$, nor the rate of twist $\theta = d\varphi/dx$. The situation is different when the bar is curved since the existence of a natural curvature in Oxz plane, i.e., $\varkappa_y = 1/R$, produces a significant change in curvature and torsion in the deformed system, whose new values $\bar{\varkappa}_z$ and $\bar{\theta}$ are

$$\bar{\varkappa}_z = \varkappa_z \cos(\bar{z}, z) + \varkappa_y \cos(\bar{z}, y) + \theta \cos(\bar{z}, x),$$

$$\bar{\theta} = \varkappa_z \cos(\bar{x}, z) + \varkappa_y \cos(\bar{x}, y) + \theta \cos(\bar{x}, x), \tag{b}$$

where with sufficient accuracy, the directional cosines between the axes of $Oxyz$ and $\overline{O}\overline{x}\overline{y}\overline{z}$ systems are

$$\cos(\bar{z}, z) = \cos(\bar{x}, x) = 1, \quad \cos(\bar{z}, y) = \varphi,$$

$$\cos(\bar{z}, x) = \cos(\bar{x}, z) = 0, \quad \cos(\bar{x}, y) = v'.$$

Substituting these data into Eqs. (b) we obtain

$$\bar{\varkappa}_z = v'' + (\varphi/R), \quad \bar{\theta} = \varphi' - (v'/R) \tag{5.12}$$

and after using the basic relations from Chapter 2, the bending moment M_y and torsional moment M_t are found to be

$$M_z = EJ_z[v'' + (\varphi/R)],$$
$$M_t = -C_\omega[\varphi''' - (v'''/R)] + C[\varphi' - (v'/R)],$$
(5.13)

where C_ω and C are the warping rigidity and pure torsion rigidity, respectively. Putting these results into Eqs. (5.11), we arrive finally at a set of two differential equations, namely

$$\left(EJ_z + \frac{C_\omega}{R^2}\right)v^{IV} - \frac{C}{R^2}v'' - \frac{C_\omega}{R}\varphi^{IV} + \frac{EJ_z + C}{R}\varphi'' + q_y = 0,$$

$$\frac{C_\omega}{R}v^{IV} - \frac{EJ_z + C}{R}v'' - C_\omega\varphi^{IV} + C\varphi'' - \frac{EJ_z}{R^2}\varphi + m_t = 0.$$
(5.14)

The integrals of these equations, i.e., $v(x)$ and $\varphi(x)$, are the sum of general solutions, when $m_t = 0$ and $q_y = 0$, and particular solutions. The eight constants of integration involved here are determined from four boundary conditions at one end of the bar and four at the other end. These conditions are either static or kinematic. The former, those associated with bending of the bar, specify the values of M_z and shearing force T_y, and those associated with torsion, specify the boundary values of M_t or the self-equilibrated stress σ_x^{II} system given according to (2.16) by bimoment B

$$B = C_\omega\bar{\theta} = EJ_\omega[\varphi'' - (v''/R)].$$
(5.15)

A similar division exists with respect to kinematic conditions which set the boundary conditions of displacement v or angle of deflection dv/dx, or the values of the angle of rotation φ and warping of the cross-section given by the rate of twist $\bar{\theta} = \varphi' - (v'/R)$. For example, if the bar ends are supported and normal stresses σ_x^{II} equal zero, then the set of conditions for each end has the form

$$v = 0, \quad \varphi = 0, \quad v'' + (\varphi/R) = 0, \quad \varphi'' - (v''/R) = 0,$$
(c)

and when the ends are clamped, v, φ, v' and φ' become zero.

The solving method outlined here allows the analysis of a number of problems considered important from an engineering point of view, provided that in keeping with the adopted assumption the curvature of the bar is not too great, e.g. $R/H_{mean} > 10$. As for the stresses, they are determined as for straight bars and, for example, stresses σ_x, according to Eqs. (2.6) and (2.17), are

$$\sigma_x = -\frac{M_z y}{J_z} - \frac{B\omega_0}{J_\omega},$$
(5.16)

where M_z and B are derived from relations (5.13) and (5.15).

(a)   (b)   (c)
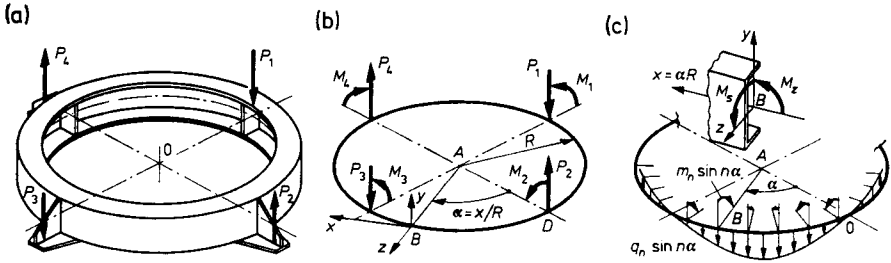
Fig. 5.11. Analysis of circular ring loaded out of its plane

Very important in particular is the problem of a ring loaded perpendicularly to its plane (Fig. 5.11a). By representing the loading using a Fourier series of argument $\alpha = x/R$

$$q_y = \sum_{k=1}^{\infty} q_k \sin k\alpha + \sum_{k=1}^{\infty} \bar{q}_k \cos k\alpha,$$

$$m_t = m_0 + \sum_{k=1}^{\infty} m_k \sin k\alpha + \sum_{k=1}^{\infty} \bar{m}_k \cos k\alpha,$$
(5.17)

and substituting (5.17) into Eqs. (5.14), we obtain for each harmonic a set of two linear equations giving amplitudes V_k (or $\bar{V}_k$) and Φ_k (or $\bar{\Phi}_k$) of the series

$$v(\alpha) = \sum_{k=1}^{\infty} V_k \sin k\alpha + \sum_{k=1}^{\infty} \bar{V}_k \cos k\alpha,$$

$$\varphi(\alpha) = \frac{\Phi_0}{R} + \frac{1}{R} \sum_{k=1}^{\infty} \Phi_k \sin k\alpha + \sum_{k=1}^{\infty} \bar{\Phi}_k \cos k\alpha.$$
(5.18)

These equations for $k \geqslant 1$ are

$$\delta_{v,v} V_k + \delta_{v,\varphi} \Phi_k + (q_k R^3 / EJ_z) = 0,$$

$$\delta_{\varphi,v} V_k + \delta_{\varphi,\varphi} \Phi_k - (m_k R^3 / EJ_z) = 0,$$
(5.19)

where dimensionless coefficients δ are given by the relations

$$\delta_{v,v} = k^4(1+\eta_\omega) + k^2, \quad \delta_{v,\varphi} = \delta_{\varphi,v} = -k^4\eta_\omega - k^2(1+\eta_s),$$

$$\delta_{\varphi,\varphi} = 1 + k^2\eta_s + k^4\eta_\omega,$$

which also involves dimensionless parameters η:

$$\eta_\omega = C_\omega / EJ_z R^2,$$

$$\eta_s = C / EJ_z.$$

Note that for $k \geqslant 2$, amplitudes q_k and m_k of the self-equilibrated loadings are independent of each other, unlike for $k = 1$, whereby due to the ring being in equilibrium, relations do exist between them, namely

$$q_1 R = m_1 \quad \text{or} \quad \bar{q}_1 R = \bar{m}_1. \qquad \qquad '$$

For the zero harmonic, when the only loading is $m_t = m_0$, deflection $v \equiv 0$, and the twist angle

$$\varphi = \Phi_0/R = m_0 R^2/EJ_z. \tag{5.20}$$

The idea of solution (5.18) is also applicable if the bar is not a complete ring all that needs to be done is to use $\alpha = 2\pi x/l$ (l—bar length) in place of $\alpha = x/R$ in the series (5.17). Moreover, the result should be matched to the imposed boundary conditions by including the solution of the homogeneous Eqs. (5.14).

6. Stability of Thin-Walled Bars*

One should recall that open thin-walled bars have pure torsion rigidity C appreciably smaller than flexural rigidity EJ_y or EJ_z. This fact is significant in stability problems of structures involving such bars. Thus, in a typical strut buckling problem, the loss of stability may be flexural, torsional-flexural or local buckling in nature. In the first two cases the initially straight axis of the bar becomes curved (Fig. 6.1a), but the cross-section of the bar keeps
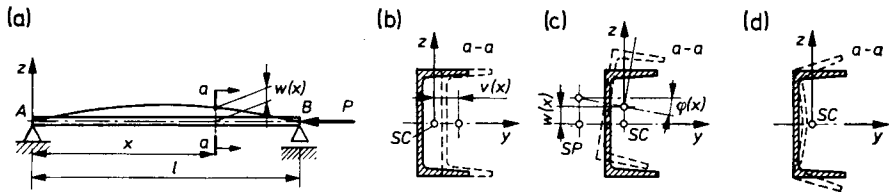
Fig. 6.1. Form of loss of stability of a thin-walled bar: (a) sketch of the bar; (b) flexural buckling; (c) rtosional-flexural buckling; (d) local buckling. The initial position of the cross-section is indicated by a solid line

its shape, undergoing either simple displacement $v(x)$ (flexural buckling) (Fig. 6.1b) or else displacement $w(x)$ and rotation $\varphi(x)$ (flexural-torsional buckling) (Fig. 6.1c). With local buckling, the cross-section is deformed in such a way that its corners do not undergo displacements (Fig. 1.6d). The last problem comes under plate or shell stability and will not be considered here. It turns out that for a thin-walled bar, any of these cases may occur, depending on its slenderness ratio $\lambda_z = l/i_z$. For example, for a channel bar (Fig. 6.2), when $\lambda_z > \lambda_C$ the least critical stress corresponds to flexural buckling in the xy-plane; when $\lambda_E < \lambda_z < \lambda_C$, the most likely to occur is torsional-flexural buckling for which $w(x) \neq 0$ and $\varphi(x) \neq 0$; and lastly

* References: Timoshenko (1945), Ambartsumyan (1953), Bolotin (1953), Kappus (1953), Langhaar (1953), Obraztsov (1953), Kachanov (1956), Broude (1957), Pikovski and Derkachev (1959), Timoshenko (1963).
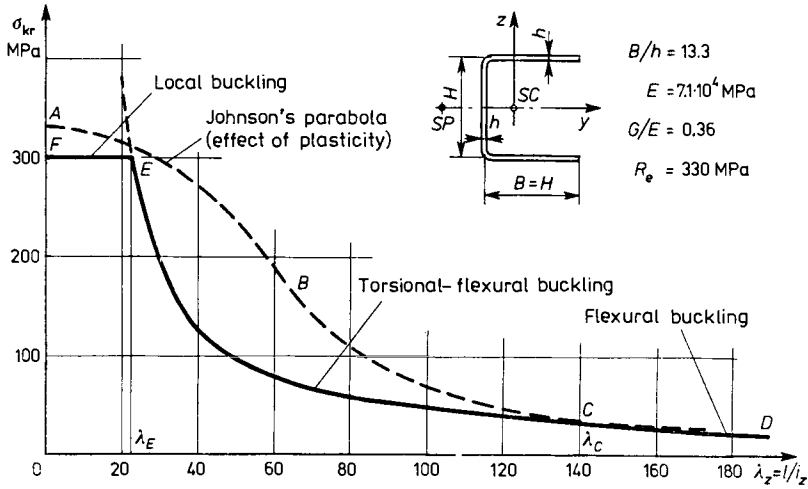
Fig. 6.2. Typical plot of $\sigma_{\text{cr}}(\lambda_z)$ for a bar of symmetrical open cross-section

for very small slenderness ratios, we deal with local buckling. As a result, the relation $\sigma_{\text{cr}}(\lambda_z)$ is described by line *FECD* instead of line *ABCD* corresponding to flexural buckling.

6.1. Torsional-Flexural Buckling of a Centrally Compressed Bar

In confining stability analysis to a static approach, we should examine the conditions for the existence of equilibrium of a bar in a deflected position from the state of primary equilibrium, i.e., simple compression (Fig. 6.3a), characterized by uniformly distributed stresses $\sigma_x = -\sigma_0$ in cross-sections. This deflection, given by displacements of the centre of gravity $v(x)$, $w(x)$
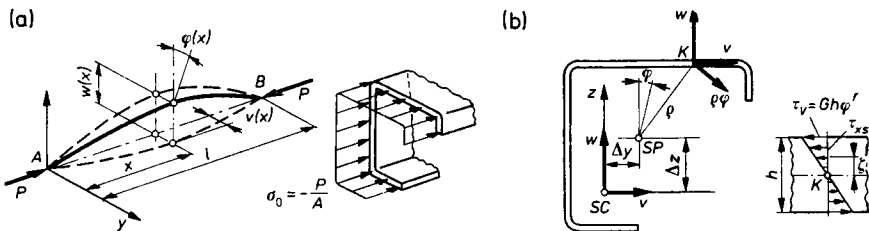
Fig. 6.3. Characteristic quantities for torsional-flexural buckling: (a) deflection of the bar axis; (b) displacements in cross-sectional plane and state of dominant stress τ_{xs}

and by angle of rotation $\varphi(x)$ with respect to shear centre SP, causes a change in stresses σ_x. In accordance with Eqs. (2.1) and (2.15), these new values are

$$\sigma_x = -\sigma_0 - Eyv'' - Ezw'' - E\omega_0\varphi'', \tag{a}$$

where ω_0 is the principal sectorial area of the cross-section and y and z are centroidal coordinates of selected point K. Moreover, shear stresses will appear in the skin, which are linearly variable along the thickness (Fig. 2.9b), whose extremal values according to Eq. (g), Section 2.2, are

$$\tau_V = Gh\varphi'. \tag{b}$$

If the energy criterion is taken for the method of analysis, then knowing the results (a) and (b) we can determine the change in strain energy δL_e caused by the additional deflection. For, in accordance with the assumptions from Section 1.2 we have

$$\delta L_e = \int_V \left(\frac{\sigma_x^2}{2E} + \frac{\tau_{xs}^2}{2G} \right) dV - \frac{\sigma_0^2 Al}{2E}, \tag{c}$$

where integration covers the entire volume V of the bar, and the term $\sigma_0^2 Al/2E$ is the strain energy in the initial state. Using σ_x and $\tau_{xs} \approx \tau_V(2\xi/h)$, we can perform integration over cross-sectional area A. Considering that y and z are centroidal axes, we thus obtain

$$\delta L_e = \frac{1}{2} \int_0^l [EJ_y(w'')^2 + 2EJ_{yz}w''v'' + EJ_z(v'')^2 + C_\omega(\varphi'')^2 + C(\varphi')^2]dx, \tag{6.1}$$

where J_y, J_z, J_{yz} are the moments of inertia and product of inertia with respect to the y and z axes and C_ω and C are restrained warping and pure torsion rigidity, respectively (Section 2.2).

Next to quantity δL_e, the other indispensable component required to formulate the energy criterion of stability is the work done by external forces. Owing to deplanation of the cross-section, the work done by forces $\sigma_0 \, dA$ varies for different fibres. Thus, for fibre K(Fig. 6.3b), whose displacements v_K and w_K in the plane of the cross-section are

$$v_K = v + (z - \Delta z)\varphi, \qquad w_K = w - (y - \Delta y)\varphi, \tag{d}$$

the shortening of this fibre is with an accuracy to small of higher order

$$u_K = \frac{1}{2} \int_0^l [(v_K')^2 + (w_K')^2]dx. \tag{e}$$

As a result, the change in the potential energy of force $\sigma_0\,dA$ compressing fibre K is $(\sigma_0\,dA)\,u_K$, and for the bar

$$\delta L_f = \int_A \sigma_0\,dA\left\{\int_0^l \frac{1}{2}[(v_K')^2+(w_K')^2]dx\right\}. \tag{f}$$

By substituting the derivatives v_K' and w_K' determined from (d) into (f) and by integrations over cross-sectional area A, we arrive at the result

$$\delta L_f = \frac{P}{2}\int_0^l [(w')^2+(v')^2+r_{SP}^2(\varphi')^2-2\Delta z v'\varphi'+2\Delta y w'\varphi']dx, \tag{6.2}$$

where $P = \sigma_0 A$ is the compressive force of the bar and r_{SP} is the polar radius of gyration of the cross-section with respect to SP.

As proved in the detailed study of stability, Part 3, Section 1.4, the total change in potential energy $\delta\Pi = \delta L_e - \delta L_f$ has a stationary value in the critical state. This fact leads in effect to three Euler–Lagrange equations corresponding to consecutive variations of quantities w, v and φ. For a prismatic bar, these equations are

$$EJ_y w^{IV}+EJ_{yz}v^{IV}+P_{cr}w''+P_{cr}\Delta y\varphi'' = 0,$$
$$EJ_z v^{IV}+EJ_{yz}w^{IV}+P_{cr}v''-P_{cr}\Delta z\varphi'' = 0, \tag{6.3}$$
$$C_\omega\varphi^{IV}+(P_{cr}r_{SP}^2-C)\varphi''+P_{cr}\Delta y w''-P_{cr}\Delta z v'' = 0,$$

and the connotation $P = P_{cr}$ is meant to emphasize that the state under study is critical. Along with these equations, we obtain so-called *natural boundary conditions*. For example, it follows from the variation of w for $x = 0$ and $x = l$ that

$$w = 0 \quad \text{or} \quad P_{cr}(w'+\Delta y\varphi')+EJ_y w'''+EJ_{yz}v''' = 0, \tag{g}$$
$$w' = 0 \quad \text{or} \quad EJ_y w''+EJ_{yz}v'' = 0.$$

Of these conditions, two are kinematic in nature ($w = 0$, $w' = 0$), and the remaining ones represent respectively the equilibrium of shearing forces or the zeroing of bending moment $M_y = EJ_y w''+EJ_{yz}v''$. Similarly, based on the variation of v and φ, we obtain two groups of four conditions each; consequently, the set of equations (6.3) can be solved taking for each of the end cross-sections two conditions for each of the quantities w, v and φ.

The general solution of set (6.3) has the form

$$w = \sum_{m=1}^{6} W_m\left(\frac{x}{l}\right)^{m-1} + \sum_{n=1}^{6} W_n e^{\varkappa_n(x/l)},$$

$$v = \sum_{m=1}^{6} V_m \left(\frac{x}{l}\right)^{m-1} + \sum_{n=1}^{6} V_n e^{\varkappa_n(x/l)}, \tag{6.4}$$

$$\varphi = \sum_{m=1}^{6} \Phi_m \left(\frac{x}{l}\right)^{m-1} + \sum_{n=1}^{6} \Phi_n e^{\varkappa_n(x/l)},$$

where W, V and Φ are integration constants and $\varkappa_n$ are the roots of a sextic equation

$$\begin{vmatrix} [\varkappa^2(EJ_y/l^2)+P_{cr}] & (EJ_{yz}/l^2)\varkappa^2 & P_{cr}\Delta y \\ (EJ_{yz}/l^2)\varkappa^2 & [\varkappa^2(EJ_z/l^2)+P_{cr}] & P_{cr}\Delta z \\ P_{cr}\Delta y & -P_{cr}\Delta z & [\varkappa^2(C_\omega/l^2)-C+P_{cr}]r_{SP}^2 \end{vmatrix} = 0, \tag{6.5}$$

which depend on the value of P_{cr}. Treating these roots as given and formulating 12 boundary conditions corresponding to a particular case of bars supporting, we obtain a set of 12 linear equations, homogeneous with respect to constants W, V and Φ and with coefficients dependent on roots $\varkappa$. Only 12 constants are independent in these equations, the others are derived from relation (6.3). The final stage of analysis is to set the characteristic determinant of 12th degree to zero, which leads to an equation, usually transcendental, giving the numerical value of $\varkappa$ and therefore of P_{cr} as well.

The solution outlined is so complicated that effective results are obtainable only numerically. There are, nevertheless, cases where the value of P_{cr} is given by simple relations. The simplest of all is the case where the shear centre SP coincides with the centroid of the cross-section*, i.e., where $\Delta y = \Delta z = 0$ and y and z axes are principal axes. As we can see, set (6.3) changes then into three independent equations. If in addition there is no coupling between quantities w, v and φ under boundary conditions, then loss of stability occurs either in the form of flexural buckling where $w \neq 0$ or $v \neq 0$, respectively, or in the form of torsional buckling, where $\varphi \neq 0$, but $w = v \equiv 0$. The critical values of P corresponding to flexural buckling ($w \neq 0$, $v \neq 0$) are

$$P_{cr1} = P_w = \xi_w \frac{\pi^2 EJ_y}{l^2}, \qquad P_{cr2} = P_v = \xi_v \frac{\pi^2 EJ_z}{l^2}, \tag{6.6}$$

with coefficients ξ_w and ξ_y depending on the modes of support of the bar ends in the xz and xy planes. Torsional buckling is described by the relation

$$\varphi(x) = \Phi_0 + \Phi_1(x/l) + \Phi_2 \sin(\varkappa x/l) + \Phi_3 \cos(\varkappa x/l), \tag{6.7a}$$

---

* Such a situation occurs in cross-sections with two or more axes of symmetry, and also in the case of point symmetry.

where the dimensionless parameter $\varkappa$ equals

$$\varkappa^2 = (P_{cr}r_0^2 - C)l^2/C_\omega. \tag{6.7b}$$

In the latter, $r_0 = \sqrt{J_0/A} = \sqrt{(J_y + J_z)/A}$ is the polar radius of gyration with respect to centroid SC.

The values of constants $\Phi_0, \ldots, \Phi_3$ are determined from the bar support. Thus, if both ends cannot rotate but are free to warp, then

$$(\varphi)_{x=0} = (\varphi)_{x=l} = 0, \quad (\varphi'')_{x=0} = (\varphi'')_{x=l} = 0.$$

Using (6.7a) we obtain the set of equations

$$\Phi_0 = 0, \quad \Phi_3 = 0, \quad \Phi_1 + \Phi_2 \sin\varkappa = 0, \quad \Phi_2(\varkappa_2/l^2)\sin\varkappa = 0.$$

Non-zero solution of this set and equilibrium in twisted form occur when $\varkappa = n\pi$ $(n = 1, 2, \ldots)$; and then

$$\varphi(x) = \Phi_2 \sin(\varkappa x/l),$$

and the corresponding critical force value

$$P_{cr3} = P_\varphi = \frac{1}{r_0^2}\left(\frac{n^2\pi^2 C_\omega}{l^2} + C\right). \tag{6.8a}$$

The value P_{cr} is lowest when $n = 1$, i.e.

$$(P_\varphi)_{min} = \frac{1}{r_0^2}\left(\frac{\pi^2 C_\omega}{l^2} + C\right). \tag{6.8b}$$

It is seen that P_{cr} is a sum of two terms, the first decreasing with the slenderness ratio of the bar, whereas the other has a constant value. It follows that for very slender bars, the lowest of the three critical values P_{cr} corresponds to flexural buckling (Eqs. (6.6)). For medium slenderness ratios, the lowest may prove the value (6.8b). To avoid this type of situation, the simplest course to follow is to increase rigidity C.

The solution (6.8) constitutes an analogy to flexural buckling of a simply supported bar. Under any other support conditions, the critical loading is

$$P_\varphi = \frac{1}{r_0^2}\left(\frac{\xi_\varphi \pi^2 C_\omega}{l^2} + C\right), \tag{6.9}$$

where ξ_φ are the coefficients listed in Table 6.1, identical with similar coefficients ξ_w and ξ_v of flexural buckling.

A fundamental case in engineering is the buckling of a strut simply supported at the ends. The end cross-sections cannot twist with respect to the bar axis, but they can warp unrestrained. The corresponding boundary conditions for $x = 0$ and $x = l$

$$y = w = \varphi = 0, \quad v'' = w'' = \varphi'' = 0 \tag{h}$$

TABLE 6.1. Coefficient ξ_φ of clamping with torsional buckling

Rib

Block

$\xi_c = 1/4$

$\xi_\varphi = 4$

$\xi_\varphi = 2.046$

Rib

P

P

P
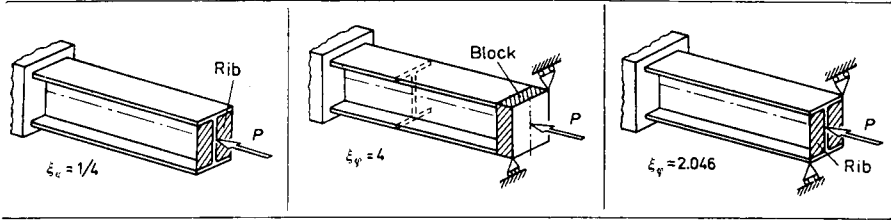
impose a solution of (6.3) in the form

$$w = B_w \sin(\pi x/l), \quad v = B_v \sin(\pi x/l), \quad \varphi = B_\varphi \sin(\pi x/l), \tag{i}$$

where B_w, B_v and B_φ are constant values. Substituting (i) into (6.3), we obtain the set of homogeneous equations

$$(P_w - P_{cr}) B_w + P_{vw} B_v - P_{cr} \Delta y B_\varphi = 0,$$
$$P_{vw} B_w + (P_v - P_{cr}) B_v + P_{cr} \Delta z B_\varphi = 0, \tag{6.10}$$
$$-P_{cr} \Delta y B_w + P_{cr} \Delta z B_v + (P_\varphi - P_{cr}) r_{SP}^2 B_\varphi = 0,$$

linear with respect to B_w, B_v and B_φ. The brief denotations

$$P_w = \frac{\pi^2 E J_y}{l_2}, \quad P_v = \frac{\pi^2 E J_z}{l^2}, \quad P_{vw} = \frac{\pi^2 E J_{yz}}{l^2},$$

$$P_\varphi = \frac{1}{r_{SP}^2} \left(\frac{\pi^2 C_\omega}{l^2} + C \right),$$

except for P_{vw}, have an obvious physical meaning. Thus, P_w and P_v are flexural buckling loadings in the xz and xy planes and P_φ is torsional buckling loadings.

A non-zero solution of set (6.10), determining the buckling of the bar, will be obtained when the characteristic determinant of this set equals zero. This leads to the equation

$$(P_w - P_{cr})(P_v - P_{cr})(P_\varphi - P_{cr}) r_{SP}^2 - P_{cr}^2 [(P_w - P_{cr}) \Delta z^2 + (P_v - P_{cr}) \Delta y^2] -$$
$$- P_{vw}^2 (P_\varphi - P_{cr}) r_{SP}^2 - 2 P_{cr}^2 P_{vw} \Delta y \Delta z = 0, \tag{6.11}$$

giving three values of P_{cr}. A discussion of these values is easiest if y and z are centroidal principal axes, since then $P_{vw} = 0$. Thus, when one of the axes, for example y, is the axis of symmetry, then $\Delta z = 0$ and one of the roots of Eq. (6.11) is

$$(P_{cr})_1 = P_v = \pi^2 E J_z / l^2, \tag{j}$$

and the other two have the values

$$\left.\begin{array}{c}(P_{cr})_2\\(P_{cr})_3\end{array}\right\} = \frac{\psi(P_w+P_\varphi)\pm\sqrt{\psi^2(P_w+P_\varphi)^2-4\psi P_w P_\varphi}}{2}, \tag{6.12}$$

where $\psi = (r_{SP}/r_0)^2$ and with $r_0 = \sqrt{J_0/A}$ as in (6.7b). The smallest value of P_{cr} determines which form of buckling is the most likely to occur.

It is a fact that when the shear centre does not lie on any of the principal central axes, the smallest of the roots of Eq. (6.11) is smaller than the smallest of forces P_v, P_w, P_φ. This means that torsional-flexural buckling is the most likely to occur. The form of deformation of the bar depends on the slenderness ratio. With high ratios, P_v or P_w is the smallest of the initial quantities. If it is P_v, then the form of buckling corresponding to the least force P_{cr} approaches the flexural type, in which amplitude B_v is dominant, and the others, B_w and B_φ, are very small. For low slenderness ratios and for a sufficiently thin skin, P_φ becomes the lowest initial value and consequently, deformation which comes close to being purely torsional, corresponds to the lowest force P_{cr}, with amplitude B_φ playing the dominant role.

Similarly, simple results are obtainable for other types of bar support. Thus, if the ends are clamped, i.e., if for $x = 0$ and $x = l$

$$v = w = \varphi = 0, \quad \text{and} \quad v' = w' = \varphi' = 0,$$

then Eq. (6.11) remains the same, except for the difference that

$$P_w = \frac{4\pi^2 EJ_y}{l^2}, \qquad P_v = \frac{4\pi^2 EJ_z}{l^2},$$

$$P_{vw} = \frac{4\pi^2 EJ_{yz}}{l^2}, \qquad P_\varphi = \frac{1}{r_{SP}^2}\left(\frac{4\pi^2 C_\omega}{l^2}+C\right). \tag{k}$$

Lastly, if one end of the bar is clamped and the other is free, or if one is clamped and the other is simply supported, Eq. (6.11) remains unchanged, but in denotations (k) we should use the coefficients $\pi^2/4$ or 20.19 in place of $4\pi^2$.

6.2. Torsional-Flexural Buckling of a Bar on Elastic Foundation

The problems examined in Section 6.1 can be applied to trusses in which the bar investigated is jointed to all the others only at the ends. In practice, one also encounters cases where a strut is elastically supported over its entire length by rest of the structure so as to prevent free displacement of a certain fibre N with coordinates y_N and z_N (Fig. 6.4). It is assumed that the reactions of these constraints are continuously distributed and their intensities $K_y v_N$ and $K_z w_N$ are proportional to displacements v_N and w_N of fibre N. Expressing
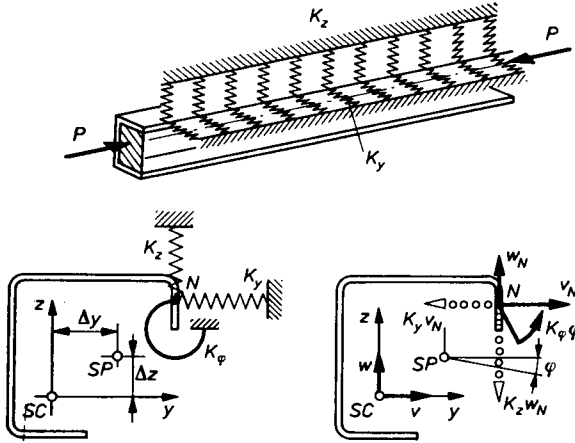
Fig. 6.4. Torsional-flexural buckling of bar on elastic foundation

v_N and w_N by displacements v and w of the centroid of the cross-section and by angle of rotation φ, we obtain

$$K_y v_N = K_y[v+(z_N-\varDelta z)\varphi], \qquad K_z w_N = K_z[w-(y_N-\varDelta y)\varphi], \qquad \text{(a)}$$

where K_y, K_z are constants (N/m²) that represent the reaction per unit length with unit displacement. An additional constraint, besides those already considered, may be elastic clamping preventing rotation of the cross-section, providing the moment of intensity

$$K_\varphi \varphi, \qquad \text{(b)}$$

where K_φ (Nm/m radian) is the respective clamping rigidity.

The easiest method to assess the influence exerted by this type of constraint on the value of P_{cr} in the energy criterion. Compared to Section 6.1, it differs only in the expression of δL_e, in this case increased by the energy

$$\frac{1}{2}\int_0^l \{K_y[v+(z_N-\varDelta z)\varphi]^2+K_z[w-(y_N-\varDelta y)\varphi]^2+K_\varphi\varphi^2\}\,dx, \qquad \text{(6.13)}$$

that is accumulated in the elastic joints; expression (6.2) giving δL_f remains unchanged. Knowing how that in critical state the change $\delta\Pi = \delta L_e - \delta L_f$ has a stationary value, we obtain the following set of three Euler–Lagrange equations:

$$EJ_y w^{IV}_{i} + EJ_{yz} v^{IV} + P_{cr} w'' + P_{cr}\varDelta y\varphi'' + K_z[w-(y_N-\varDelta y)\varphi] = 0,$$

$$EJ_z v^{IV} + EJ_{yz} w^{IV} + P_{cr} v'' - P_{cr}\varDelta z\varphi'' + K_y[v+(z_N-\varDelta z)\varphi] = 0,$$

$$C_\omega \varphi^{IV} + (P_{cr} r_{SP}^2 - C) \varphi'' + P_{cr} \Delta y w'' - P_{cr} \Delta z v'' + K_\varphi \varphi - \tag{6.14}$$
$$- K_z[w - (y_N - \Delta y) \varphi](y_N - \Delta y) + K_y[v + (z_N - \Delta z) \varphi](z_N - \Delta z) = 0.$$

The solution of Eqs. (6.14) and the discussion of the results proceeds in a manner similar to that described in Section 6.1. The most important from an engineering point of view is the case of the bar simply supported at the ends described by conditions (h), Section 6.1, for which the solution of set (6.14) has the form

$$w = B_w \sin \frac{n\pi x}{l}, \quad v = B_v \sin \frac{n\pi x}{l}, \quad \varphi = B_\varphi \sin \frac{n\pi x}{l}, \tag{c}$$

where B_w, B_v, B_φ are constants and n is a natural number. Substituting expression (c) into (6.14) we obtain a cubic equation, analogous to (6.12), resulting in three values of P_{cr} of which only the lowest is of practical importance.

An especially simple case is when the bar axis is an elastically supported fibre and when centroid SC coincides with SP, since then $\Delta y = \Delta z = y_N = z_N = 0$. Moreover if, we take y and z axes as principal, then each of Eqs. (6.14) becomes independent, and for simply supported ends we obtain from the substitution of (c) the following values of P_{cr}:

$$(P_{cr})_1 = P_w = \frac{\pi^2 E J_y}{\Lambda^2} + \frac{K_z \Lambda^2}{\pi^2},$$

$$(P_{cr})_2 = P_v = \frac{\pi^2 E J_z}{\Lambda^2} + \frac{K_y \Lambda^2}{\pi^2}, \tag{6.15}$$

$$(P_{cr})_3 = P_\varphi = \frac{1}{r_{SP}^2} \left(\frac{\pi^2 C_\omega}{\Lambda^2} + C + \frac{K \Lambda^2}{\pi^2} \right),$$

where $\Lambda = l/n$ is the buckling half-wave length and r_{SP} is the polar radius gyration with respect to SP. It is seen that all these forces depend on the number of half-waves n, which should be selected so that the respective force reaches a minimum.

In a similar way, we examine the case where y-axis is the axis of symmetry ($\Delta z = 0$) and elastically supported fibre N coincides with SP ($y_N = \Delta y$, $z_N = 0$). In this situation, the second of Eqs. (6.14) describes flexural buckling in the xy plane of symmetry, with P_{cr} being identical with P_v according to (6.15). The remaining two equations (6.14) are coupled, i.e., the other forms of buckling are torsional-flexural. The respective values of P_{cr} are given by Eq. (6.12) with quantities P_w and P_φ derived from (6.15). The values of n should be selected so that the critical force reaches a minimum.

6.3. Torsional-Flexural Buckling in an Elastic Medium

There are cases in engineering applications where the displacement of a certain fibre N of a strut is wholly or partially eliminated. Thus, a continuous support (Fig. 6.5a) gives the conditions $v_N = w_N = 0$ which results in displacements v and w becoming dependent on angle φ

$$w = (y_N - \Delta y)\varphi, \quad v = -(z_N - \Delta z)\varphi. \tag{a}$$
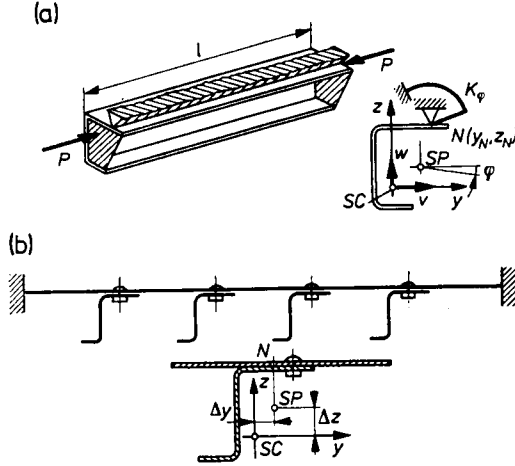
Fig. 6.5. Selected cases of torsional-flexural buckling in an elastic medium

Simultaneously, there may exist an elastic clamping with rigidity K_φ suppressing the freedom of rotation. All these facts account for the change of $\delta\Pi = \delta L_e - \delta L_f$ being expressed by the relation

$$\Delta\Pi = \frac{1}{2}\int_0^l [(C_\omega)_N(\varphi'')^2 + C(\varphi')^2 + K_\varphi\varphi^2]dx - \frac{P}{2}\int_0^l r_N^2(\varphi')^2dx, \tag{b}$$

which follows from substituting Eqs. (a) into (6.1) and (6.2) including the member $K_\varphi\varphi^2/2$ representing the energy of elastic joints. The quantity introduced here

$$(C_\omega)_N = C_\omega + EJ_y(y_N - \Delta y)^2 - 2EJ_{yz}(y_N - \Delta y)(z_N - \Delta z) + EJ_z(z_N - \Delta z)^2 \tag{c}$$

represents the warping rigidity with the centre of rotation placed at point N, and whereby the quantity

$$r_N = \sqrt{r_0^2 + y_N^2 + z_N^2} \tag{d}$$

is the polar radius of gyration with respect to point N.

The condition that $\delta\Pi$ has a stationary values gives in accordance with the calculus of variations the equation

$$(C_\omega)_N \varphi^{IV} + (P_{cr} r_N^2 - C)\varphi'' + K_\varphi \varphi = 0. \tag{6.16}$$

It is very simple to solve this equation and determine critical force P_{cr} if the end cross-section of bar cannot rotate but are free to warp, since then

$$\varphi = B_\varphi \sin(n\pi x/l), \tag{e}$$

and the corresponding force

$$P_{cr} = (P_\varphi)_N = \frac{1}{r_N^2}\left(\frac{\pi^2 (C_\omega)_N}{\Lambda^2} + C + \frac{K_\varphi \Lambda^2}{\pi^2}\right), \tag{6.17}$$

where $\Lambda = l/n$ is the buckling half-wave length chosen so that the value P_{cr} is minimal. This result is analogous to the value $(P_{cr})_3$ obtained (6.15).

Another important case in engineering (Fig. 6.5b) is when a stringer (or a number of stringers) is connected to a thin-walled panel precluding horizontal displacement of the respective flange of the stringer. If the centroidal y and z axes of the stringer are chosen so that the y-axis is parallel to the panel, then the absence of displacement of this flange gives the condition

$$v + (z_N - \Delta z)\varphi = 0, \tag{f}$$

thus interrrelating displacement v and angle φ. Determining v therefrom and substituting it into (6.1) and (6.2) we obtain change $\delta\Pi$ in the potential energy of the system

$$\delta\Pi = \frac{1}{2}\int_0^l [EJ_y(w'')^2 - 2EJ_{yz}(z_N - \Delta z)w''\varphi'' + (C_\omega)_N(\varphi'')^2 + C(\varphi')^2 +$$

$$+ K_z w^2 + K_\varphi \varphi^2]dx - \frac{P}{2}\int_0^l [(w')^2 + r_N^2(\varphi')^2 + 2\Delta yw'\varphi']dx, \tag{g}$$

and the elastic clamping of the bar restraining the free rotation and the displacement in the direction of z-axis is taken into account here. The quantities $(C_n)_N$ and r_N continue to be given by relations (c) and (d), in which $y_N = \Delta y$ (Fig. 6.5b). From the condition of stationary value $\delta\Pi$ we obtain the equations

$$EJ_y w^{IV} + P_{cr} w'' + K_z w - EJ_{yz}(z_N - \Delta z)\varphi^{IV} + P_{cr}\Delta y\varphi'' = 0,$$

$$(C_n)_N \varphi^{IV} + (P_{cr} r_N^2 - C)\varphi'' + K_\varphi \varphi - EJ_{yz}(z_N - \Delta z)w^{IV} + P_{cr}\Delta yw'' = 0. \tag{6.18}$$

The solution and the discussion of the results are very much the same as in the previously analysed cases. Thus, if z-axis is the axis of symmetry, the coupling of Eqs. (6.17) disappear and flexural buckling is independent of

torsional buckling. If at the same time the stringer is simply supported, then the values of critical forces equal respectively P_w according to (6.15) and $(P_\varphi)_N$ according to (6.17), and depend on K_z and K_φ. In real structures, the coefficient of clamping K_z is negligible but K_φ is very important in view of the low pure torsion rigidity C. The values of K_φ depend on whether the
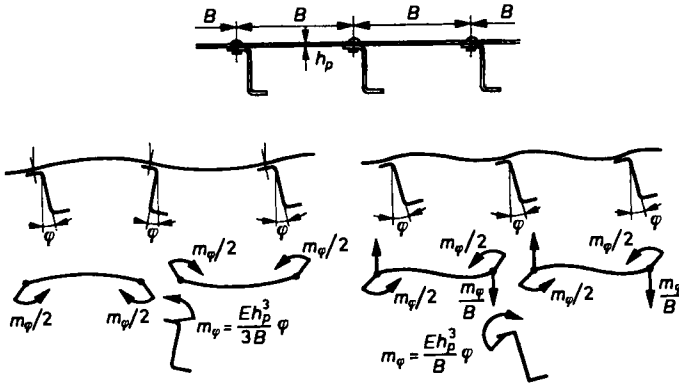
Fig. 6.6. Determination of elastic clamping K_φ in the case of torsional-flexural buckling in an elastic medium

rotation of adjacent cross-sections is opposite or conformable (Fig. 6.6); they are respectively

$$K_\varphi = m_\varphi/\varphi = Eh_p^3/3B, \qquad K_\varphi = Eh_p^3/B. \tag{h}$$

When the cross-section of the bar is arbitrary, buckling has the torsional-flexural form. With simply support ends, the solution of set (6.18) is

$$w = B_w \sin(n\pi x/l), \qquad \varphi = B_\varphi \sin(n\pi x/l),$$

giving in effect a set of two homogeneous equations

$$(P_w - P_{cr})B_w - [P_{vw}(z_N - \Delta z) + P_{cr}\Delta y]B_\varphi = 0,$$
$$- [P_{vw}(z_N - \Delta z) + P_{cr}\Delta y]B_w + (P_{\varphi N} - P_{cr})r_N^2 B_\varphi = 0, \tag{i}$$

where $P_w = \pi^2 EJ_y/\Lambda^2$, $P_{vw} = \pi^2 EJ_{yz}/\Lambda^2$ and $\Lambda = l/n$, whereas $P_{\varphi N}$ continues to be given by (6.17). Setting the determinant of this set to zero we obtain the equation

$$(P_w - P_{cr})(P_{\varphi N} - P_{cr})r_N^2 - [P_{vw}(z_N - \Delta z) + P_{cr}\Delta y]^2 = 0, \tag{6.19}$$

giving two values P_{cr}. The quantities P_w, $P_{\varphi N}$, P_{vw} depend on the number of half-waves n, which should be chosen so as to get the lowest P_{cr}.

The figure shows a cross-section with dimensions $B = 100$, $h_p = 1$, and values:

$z_N = 12.5$ mm
$A = 0.58$ cm^2
$J_y = 0.553$ cm^4
$J_z = 0.138$ cm^4
$J_{yz} = -0.207$ cm^4
$E = 2.7G = 7.1 \cdot 10^4$ MPa
$C = 0.733$ N·m^2
$C_{\omega N} = 4.42 \cdot 10^{-3}$ N·m^4
$K_\varphi = \dfrac{Eh_p^3}{3B} = 237 \dfrac{\text{N·m}}{\text{m·rad}}$
$r_N^2 = 2.79$ cm^2
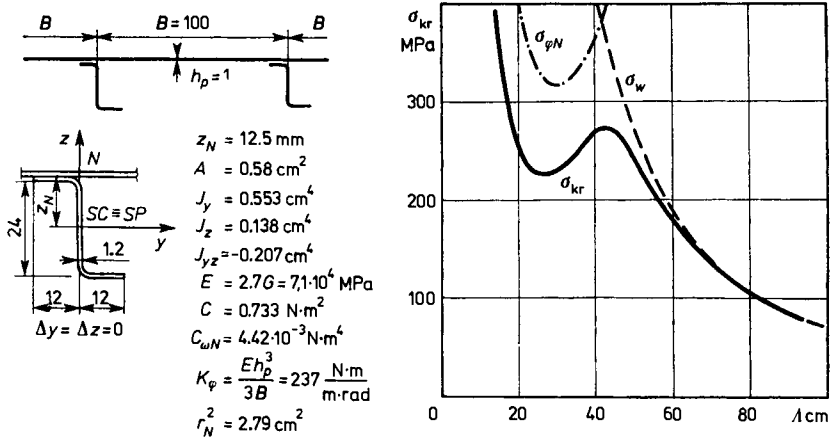
Fig. 6.7. Example of analysis of torsional-flexural buckling in an elastic medium

An illustration of relation (6.19) is given in Fig. 6.7 showing $\sigma_{cr} = P_{cr}/A$ as function of the half-wave length Λ. As we can see, the value σ_{cr} is lowest from both $\sigma_w = P_w/A$ and $\sigma_{\varphi N} = P_{\varphi N}/A$ but for greater Λ, σ_{cr} approaches σ_w. This is an indication that in this case flexural deformations are dominant, whereas the rotation of cross-sections is very small. The minimum in the curve σ_{cr} occurs with Λ correspondingly roughly to the minimum of $\sigma_{\varphi N}$, whereas the maximum σ_{cr} is at Λ corresponding roughly to $\sigma_w = \sigma_{\varphi N}$. The plot of $\sigma_{cr}(\Lambda)$ thus obtained can be used to evaluate minimum σ_{cr} from the set of values corresponding to $\Lambda_1 = l$, $\Lambda_2 = l/2$, $\Lambda_3 = l/3$, ... or from length l that gives an optimum set of values σ_{cr}.

6.4. Lateral Buckling of Beams Subjected to Bending

With bending of a thin-walled beam of open cross-section, a deformation is liable to occur, in which apart from a displacement of cross-sections their rotation with respect to the longitudinal axis occurs, as well. The simplest example of these problems is pure bending by moments $M_y = $ const, $M_z = $ const with compressive force P contributing at the same time (Fig. 6.8a). The solution of the problem follows from condition that the total potential energy Π has a stationary value. Thus, if a given displacement of the cross-section is defined by w, v and φ (Fig. 6.8b), then the elastic energy L_e continues to be expressed by Eq. (6.1).

$$L_e = \frac{1}{2}\int_0^l [EJ_y(w'')^2 + EJ_z(v'')^2 + C_\omega(\varphi'')^2 + C(\varphi')^2]\mathrm{d}x, \qquad (a)$$
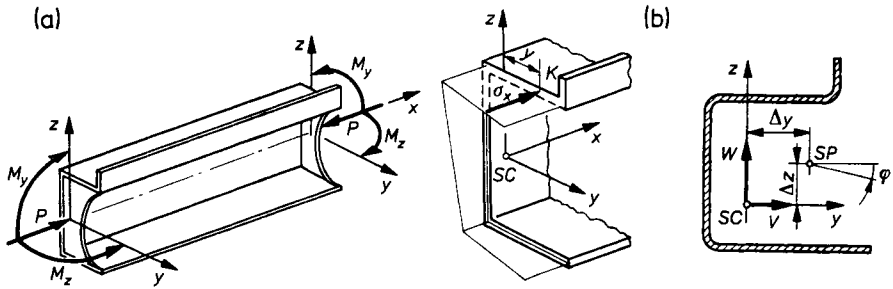
Fig. 6.8. Loading, stress and displacement system in the case of lateral buckling

in which without lessening the generality of the analysis, y and z are centroidal principal axes. On the other hand, the second energy constituent Π, i.e., the work done by loadings L_f, is different from that determined using (6.2), since the stresses σ_x are not constant but are expressed by the equation

$$\sigma_x = -\frac{P}{A} - \frac{M_y z}{J_y} - \frac{M_z y}{J_z}, \tag{b}$$

which following the argumentation from Section 6.1 gives

$$L_f = \frac{1}{2} \int_0^l \int_A \left(\frac{P}{A} + \frac{M_y z}{J_y} + \frac{M_z y}{J_z} \right) [(v_K')^2 + (w_K')^2] \, dA \, dx. \tag{c}$$

Integrating over cross-sectional are A we obtain

$$L_f = \frac{P}{2} \int_0^l [(w')^2 + (v')^2 + r_{SP}^2 (\varphi')^2 + 2\Delta y w' \varphi' - 2\Delta z v' \varphi'] \, dx +$$

$$+ \frac{1}{2} \int_0^l M_y [a_y (\varphi')^2 + 2v' \varphi'] \, dx + \frac{1}{2} \int_0^l M_z [a_z (\varphi')^2 - 2w' \varphi'] \, dx, \tag{6.20}$$

where the quantities a_y and a_z are defined as follows:

$$a_y = \frac{1}{J_y} \int_A (y^2 + z^2) z \, dA - 2\Delta z, \qquad a_z = \frac{1}{J_z} \int_A (y^2 + z^2) y \, dA - 2\Delta y. \tag{6.21}$$

Using expressions (a) and (6.20) to define energy $\Pi = L_e - L_f$, we obtain from the stationarity condition the set of equations

$$EJ_y w^{IV} + P w'' + P\Delta y \varphi'' - M_z \varphi^{IV} = 0,$$
$$EJ_z v^{IV} + P v'' - P\Delta z \varphi'' + M_y \varphi^{IV} = 0,$$

$$C_\omega \varphi^{IV} - (C - P r_{SP}^2 - M_y a_y - M_z a_z) \varphi'' + P\Delta y w'' - \qquad (6.22)$$
$$- P\Delta z v'' - M_z w'' + M_y v'' = 0,$$

and a group of natural boundary conditions. For example, it follows from the variation of w that for $x = 0$ and $x = l$

$$w = 0, \quad \text{or} \quad P(w' + \Delta y \varphi') + M_z \varphi' + EJ_y w'' = 0,$$
$$w' = 0, \quad \text{or} \quad w'' = 0. \qquad (d)$$

The set of equations (6.22) and conditions (d) in the case $M_y = M_z = 0$ become set (6.3) and conditions (g) from Section 6.1 describing torsional-flexural buckling of a bar.

The set of equations (6.22) serves as a basis for many analyses. Thus, in the case $P = 0$, lateral buckling of a beam occurs under pure bending, described by the equations

$$EJ_y w^{IV} - M_z \varphi'' = 0, \quad EJ_z v^{IV} + M_y \varphi'' = 0,$$
$$C_\omega \varphi^{IV} - (C - M_y a_y - M_z a_z) \varphi'' + M_y v'' - M_z w'' = 0. \qquad (6.23)$$

Their solution depends on the boundary conditions. If, for example, the beam is simply supported so as to preclude their rotation with respect to the x-axis, but do not to constrain warping, and moment M_z is not involved, then set (6.23) is satisfied letting*

$$v = B_v \sin(\pi x / l), \quad \varphi = B_\varphi \sin(\pi x / l). \qquad (e)$$

In effect, we get the set of linear equations

$$P_v B_v - M_y B_\varphi = 0, \quad -M_y B_v + (C_z - M_y a_y) B_\varphi = 0, \qquad (f)$$

in which $P_v = \pi^2 EJ_z / l^2$ is the critical force of flexural buckling in the xy-plane, and the equivalent torsion rigidity

$$C_z = C + (\pi^2 C_\omega / l). \qquad (g)$$
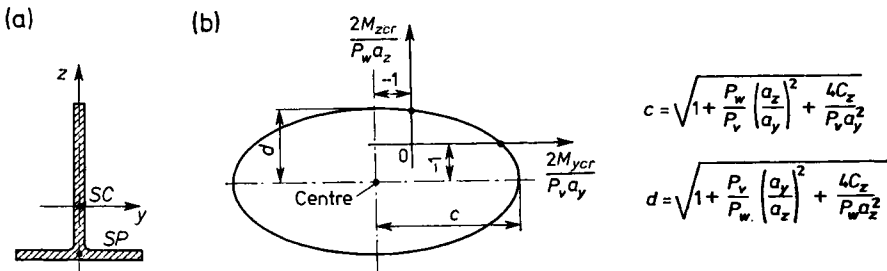
Fig. 6.9. Some elements of lateral buckling study of a beam

---

* Omitted in the analysis is elementary integration of the first equation (6.23) independent of the other two.

The beam in the state of lateral buckling will be in equilibrium when the determinant of Eqs. (f) equals zero; hence, the critical values of moment $(M_y)_{cr1} < 0$ and $(M_y)_{cr2} > 0$ are

$$\left.\begin{array}{c} (M_y)_{cr1} \\ (M_y)_{cr2} \end{array}\right\} = -\frac{P_v a_y}{2} \pm \sqrt{\left(\frac{P_v a_y}{2}\right)^2 + P_v C_z}. \tag{6.24}$$

The important conclusion is that both answers following from (6.24) have an engineering meaning. For example, in a T-section (Fig. 6.9a) the case $M_y = (M_y)_{cr1}$ corresponding to compression of the bottom flange is entirely different from the situation where $M_y = (M_y)_{cr2}$. In a cross-section symmetrical to the y-axis, both moments have an identical absolute value since $a_y = 0$ and then

$$|M_y|_{cr} = \frac{\pi}{l} \sqrt{EJ_z\left(C + C_\omega \frac{\pi^2}{l^2}\right)}. \tag{6.25}$$

Similar analysis for pure bending in the xy-plane, where $M_y = 0$, gives

$$(M_z)_{cr} = -\frac{P_w a_z}{2} \pm \sqrt{\left(\frac{P_w a_z}{2}\right)^2 + P_w C_z}, \tag{6.26}$$

where $P_w = \pi^2 EJ_y/l^2$ is the critical force of flexural buckling in the xz-plane. Lastly, with M_y and M_z acting simultaneously and with the beam simply supported, the solution of set (6.23) gives the relation

$$\frac{M_{y\,cr}^2}{P_v} + \frac{M_{z\,cr}^2}{P_w} + M_{y\,cr} a_y + M_{z\,cr} a_z - C_z = 0, \tag{6.27}$$

interrelating the critical values $(M_y)_{cr}$ and $(M_z)_{cr}$. Its graphic representation in coordinates $(2M_{y\,cr}/P_v a_y)$ and $(2M_{z\,cr}/P_w a_z)$ is an ellipse (Fig. 6.9b) with a centre at coordinates $(-1, -1)$.

Besides the case of pure bending, other problems encountered in engineering involve lateral buckling induced by transverse forces, therefore when moments M_y and M_z are functions of x. The set of equations obtained from the stationarity condition of energy Π, analogous to (6.23) has variable coefficients, with w, v and φ being the unknowns. This fact gives rise to considerable difficulty in solving this set. The difficulty can be avoided by determining the stationarity Π only approximately by one of the known direct methods.

A problem related to lateral buckling is eccentric compression of a bar, being a special case of loading (Fig. 6.8), when $M_y = Pe_z$, $M_z = Pe_y$. The solution of this problem is described by the set of equations (6.22), i.e.

$$EJ_y w^{IV} + Pw'' + P(\Delta y - e_y)\varphi'' = 0,$$
$$EJ_z v^{IV} + Pv'' - P(\Delta z - e_z)\varphi'' = 0,$$

$$C_\omega \varphi^{IV} - [C - P(r_{SP}^2 + a_y e_z + a_z e_y)] \varphi'' + \tag{6.28}$$
$$+ P(\Delta y - e_y) w'' - P(\Delta z - e_z) v'' + 0.$$

As essential difference compared with the stability problems examined up to the present follows from the non-homogeneity of the support conditions. Thus, in the basic case, when the simply supported ends cannot rotate with respect to the x-axis but are free to warp, the set of 12 boundary conditions, for $x = 0$ and $x = l$, has the form

$$EJ_y w'' = Pe_z, \qquad EJ_z v'' = Pe_y, \qquad \varphi'' = 0, \tag{h}$$

$$w = 0, \qquad\qquad v = 0, \qquad\qquad \varphi = 0, \tag{i}$$

with the first two conditions (h) expressing the presence of moments $M_y = Pe_z$ and $M_z = Pe_y$ in the end cross-sections. Integrating set (6.27) twice, we get finally

$$EJ_y w'' + Pw + P(\Delta y - e_y) \varphi = Pe_z,$$

$$EJ_z v'' + Pv - P(\Delta z - e_z) \varphi = Pe_y, \tag{6.29}$$

$$C_\omega \varphi'' - [C - P(r_{SP}^2 + a_y e_z + a_z e_y)] \varphi +$$
$$+ P(\Delta y - e_y) w - P(\Delta z - e_z) v = 0,$$

with six boundary conditions (i), but without conditions (h) which are already incorporated in set (6.29). In turn, the solution of set (6.29) is the sum of the solution in the form of three constants, w_s, v_s, φ_s, determined from the following three equations

$$w_s + (\Delta y - e_y) \varphi_s = e_z, \qquad v_s - (\Delta z - e_z) \varphi_s = e_y,$$
$$(\Delta y - e_y) w_s - (\Delta z - e_z) v_s + (r_{SP}^2 + a_y e_z + a_z e_y) \varphi_s = C/P, \tag{j}$$

and the general solution w_0, v_0, φ_0 of the homogeneous set (6.29). The latter solution has the form

$$w_0 = \sum_{n=1}^{3} W_n \sin \varkappa_n \frac{\pi x}{l} + \sum_{n=1}^{3} W_n^* \cos \varkappa_n \frac{\pi x}{l},$$

$$v_0 = \sum_{n=1}^{3} V_n \sin \varkappa_n \frac{\pi x}{l} + \sum_{n=1}^{3} V_n^* \cos \varkappa_n \frac{\pi x}{l}, \tag{k}$$

$$\varphi_0 = \sum_{n=1}^{3} \Phi_n \sin \varkappa_n \frac{\pi x}{l} + \sum_{n=1}^{3} \Phi_n^* \cos \varkappa_n \frac{\pi x}{l},$$

where W_n, V_n, Φ_n (or W_n^*, V_n^*, Φ_n^*) are constants interrelated by the equations,

$$(P_w \varkappa_n^2 - P) W_n - P(\Delta y - e_y)\Phi_n = 0,$$
$$(P_v \varkappa_n^2 - P) V_n + P(\Delta z - e_z)\Phi_n = 0, \tag{l}$$

which reduce the number of independent constants to six. The quantities $\varkappa_n$ ($n = 1, 2, 3$) are positive (real or imaginary) values of the roots of the equation

$$\begin{vmatrix} P_w \varkappa^2 - P & 0 & -P(\Delta y - e_y) \\ 0 & P_v \varkappa^2 - P & P(\Delta z - e_z) \\ -P(\Delta y - e_y) & P(\Delta z - e_z) & [\pi^2 C_\omega / l^2]\varkappa^2 + C - P(r_{SP}^2 + a_y e_z + a_z e_y)] \end{vmatrix} = 0, \tag{m}$$

where $P_w = \pi^2 E J_y / l^2$, $P_v = \pi^2 E J_z / l^2$ are the critical forces of pure flexural buckling in the xz and xy planes. It is also true that only one root $\varkappa$ can be an imaginary quantity, and the therefore the corresponding sin and cos functions in expression (k) should be replaced by sinh and cosh. The last stage of the solution is to determine the constant $W, ..., \Phi^*$ based on conditions (i). For example, for cross-section $x = 0$ we obtain

$$w_s + \sum_{n=1}^{3} W_n^* = 0, \qquad v_s + \sum_{n=1}^{3} V_n^* = 0, \qquad \varphi_s + \sum_{n=1}^{3} \Phi_n^* = 0. \tag{6.30}$$

In a general case, analysis is easiest to carry out numerically. In a special situation, results are obtainable in a more lucid form. Thus, when force P is applied at SP, i.e., when $e_y = \Delta y$, $e_z = \Delta z$, Eqs. (6.29) become independent. The deflections occurring in the xz and xy planes are

$$w = e_z \left\{ 1 - \cos \left[\varkappa_1 \frac{\pi}{2} \left(1 - \frac{2x}{l} \right) \right] \sec \varkappa_1 \frac{\pi}{2} \right\},$$
$$v = e_y \left\{ 1 - \cos \left[\varkappa_2 \frac{\pi}{2} \left(1 - \frac{2x}{l} \right) \right] \sec \varkappa_2 \frac{\pi}{2} \right\}, \tag{n}$$

where $\varkappa_1 = \sqrt{P/P_w}$, $\varkappa_2 = \sqrt{P/P_v}$. These deflections, hence the stresses as well, increase very quickly as the value of force P approaches the lesser of forces P_v and P_w. Beside these flexural forms of deformation, there is also the possibility of equilibrium of the bar in a torsional form $\varphi = \Phi \sin(\pi x / l)$, where force P reaches the critical value P_φ,

$$P_\varphi = \left(\frac{\pi^2 C_\omega}{l^2} + C \right) \bigg/ (r_{SP}^2 + a_y e_z + a_z e_y). \tag{6.31}$$

The real behaviour of the bar with increasing force depends on the mutual proportions between forces P_w, P_v and P_φ. If, for example, P_φ is markedly

smaller than P_v and P_w, then the bar will fail due to torsion caused by the unavoidable deviations of the bar from perfect shape.

We deal with a similarly simple case where the cross-section of the bar has an axis of symmetry, say, y, and in addition $e_z = 0$. In such a situation, the bar has deflection v described by relation (n) and moreover torsional-flexural displacements $w = W\sin(\pi x/l)$ and $\varphi = \Phi\sin(\pi x/l)$ may develop as force P reaches a critical value P_{cr} determined from the equation

$$(P_w - P_{cr})(P_\varphi - P_{cr})(r_{SP}^2 + a_z e_y) - P_{cr}^2(\Delta y - e_y)^2 = 0, \qquad (6.32)$$

where P_φ is obtained from (6.31) taking into account that in the cross-section symmetrical to y-axis, the quantity $a_y = 0$. It is evident that the value P_{cr} depends on the eccentricity e_y.

The most significant conclusion to be derived from the analysis of eccentric compression is that in this case there is no loss of stability in the classical sense, since deflections w and v, and in a general case, angle φ as well, show an uptrend right from the beginning of loading. For these reasons, the analysis of eccentrically compressed thin-walled bars should be carried for bars of solid cross-section in terms of the stress criterion or in terms of rigidity of the element.

7. Some Recent Results*

The present part of the book was written in 1982/83, and so we give here additionally a brief survey of some more recent results. The number of papers published on thin-walled bars may be estimated as 100–150 per annum, hence we quote and discuss here just some selected, more representative papers.

Though the definition of shear centre is very well known, still some papers discussed effective methods of its evaluation: Rutenberg and Zaslavsky (1984) (non-symmetric open profiles), and Stickforth (1986) (dependence on Poisson's ratio). Computational problems of bending with torsion of open thin-walled beams were considered by Tralli (1986).

Much attention was paid to geometrically non-linear problems. Finite deflections in bending were considered by Møllmann (1986), Wu and Gould (1987); non-linear effects in torsion were discussed by Wekezer (1985$_2$) (variable sections) and by Attard (1986$_1$, 1986$_2$), whereas Moore (1986), Chan and Kitipornchai (1986), Attard and Somervaille (1987) analysed combined bending with torsion. Deformable cross-sections were considered by Boswell and Zhang (1984) (box sections, finite element method) and by Schade (1987). Curved thin-walled beams were discussed by Hikosaka and Takami (1985), Karamanlidis and Jasti (1987).

Stability problems of thin-walled beams and columns received also much attention. Stability in bending was considered by Królak and Kołakowski (1983) (trapezoidal section, bending with axial force), Jetteur et al. (1984) (box section, interaction of shear lag with plate buckling of compression flange), Benson (1985) (open circular section, non-linear analysis), Roberts and Burt (1985) (I-beams), Roberts (1986) (compound monosymmetric beams), Chen and Mang (1986) (I-beams with multilayer flanges). Stability in torsion was discussed by Wekezer (1985$_1$) and Yang (1987) (a general theory for open profiles, extension of Vlasov's assumptions). In the case of thin-walled columns the most important problems are connected with

---

* Chapter written by M. Życzkowski in 1988.

mode interaction, with interaction of local and overall buckling. Such problems were considered by Benito and Sridharan (1984/85) (box section), Rondal and Maquoi (1985) (box section), Sridharan and Ali (1986) (doubly symmetric sections), Toneff *et al.* (1987). Elastic-plastic buckling and effect of self-stresses was discussed by Grądzki and Kowal-Michalska (1985) and by Weiss (1985) (eccentric compression).

Optimal design of thin-walled beams was considered by Szefer and Mikulski (1984) (elastic arches with I-sections, variable width, stress constraints), Matulewicz and Szymczak (1985) (I-beams subject to torsion), Hui (1986) (design of optimal imperfections in box columns), Friedman and Fuchs (1987) (continuous beams), Rysz and Życzkowski (1988) (optimal design of closed cross-section of a beam subject to bending with torsion under creep conditions).

A fairly wide variety of problems of thin-walled bars is discussed in the book by Murray (1985).

References to Part 4

Adadurov R. A., 1948, "Stresses and strains in a cylindrical shell with rigid cross sections" (in Russian), *Dokl. Ak. Nauk* **62**, 2.

Ambartsumian S. A., 1953, "On the problem of solution of stability of thin-walled bars" (in Russian), *Dokl. Ak. Nauk Armyanskoi SSR* **17**, 1.

Argyris J. H., Dunne P. C., 1947, "The general theory of cylindrical and conical tubes under torsion and bending loads", *Journ. Roy. Aer. Soc.* **21**, 23 (1944).

Argyris J. H., Kelsey S., 1956, "The matrix force method of structural analysis and some new applications", *R. and M.* 3034, Feb.

Arutunyan N. H., Gulkanian N. O., 1954, "On the center of bending of some prismatic bars with a polygonal cross-section" (in Russian), *Prikl. Mat. i Mekh.* **18**, 5.

Bažant Z., 1965, "Non-uniform torsion of thin-walled bars of variable section", *Int. Ass. for Bridge and Struct. Eng.*, **25**, Zürich.

Benscoter S. U., 1954, "A theory of torsion-bending for multicell beams", *Journ. of Appl. Mech.*, **21**, 1.

Biderman W. L., 1977, *Mechanics of Thin-Walled Structures* (in Russian), Mashinostroenie.

Bolotin W. W., 1963, "Integral equations of restricted torsion and stability of thin-walled bars" (in Russian), *Prikl. Mat. i Mekh.* **17**, 2.

Bornscheuer F. W., 1952, "Systematische Darstellung des Biege und Verdrehvorganges unter besonderer Berücksichtigung der Wölbkrafttorsion", *Stahlbau* **21**, 1.

Broude B. M., 1957, "On stability of slightly curved end eccentrically loaded flanged beams, (in Russian) in: *Selected solution of space structures*, 4, Gosstroizdat.

Brzoska Z., 1965, *Statics and Stability of Skeletal and Thin-Walled Structures* (in Polish), PWN, Warszawa.

Cywiński Z., 1984, "Torsion des dünnwandigen Stabes mit veränderlichen einfach symmetrischen offenem Querschnitt", *Stahlbau* **10**.

Dąbrowski R., 1958, "Torsion of thin-walled bridge and hydrotechnical structures with open cross-section" (in Polish), *Rozprawy Inż.* **12**.

Dąbrowski R., 1960, "Equations of bending and torsion of a curved thin-walled bar with asymmetric cross-section", *Arch. Mechan. Stosowanej*.

Dąbrowski R., 1968, *Gekrümmte dünnwandige Träger*, Springer, Berlin.

Dzhanelidze G. J., Panevko G., 1958, *Statics of Thin-Walled Elastic Bars* (in Russian), Gostekhizdat, Moskva.

Ebner H., Köller H., 1937, "Zur Berechnung des Kraftverlaufs in versteiften Zylinderschalen", *Luftfahrtforschung* **14**.

Elenewski G. S., 1954, *Structural Mechanics of a Wing with Variable Cross-Section* (in Russian), Oborongiz.

Feodosev V. I., 1949, *Elastic Elements in Fine Mechanics* (in Russian), Oborongiz.

Goldenweizer A. L., 1949, "On the theory of thin-walled bars" (in Russian), *Prikl. Mat. i Mekh.* **13**, 6.

Golubev O. P., 1963, "A generalization of the theory of thin-walled bars" (in Russian), *Trudy Leningrad. Politekh. Instituta* **225**.

Gruber E., 1932, "Berechnung prismatischer Scheibenwerke", *Abhand. Int. Ver. für Brückenbau u. Hochbau.*

Gryunberg N. J., 1949, "Bending and torsion of curvilinear bars" (in Russian), *Works of the Laboratory of Structural Mechanics of Central Research Institute of Industrial Building.*

Heilig R., 1961, "Der Schubverformungseinfluss auf die Wölbkrafttorsion von Stäben mit offenem Profil", *Stahlbau* **30**, 4.

Heilig R., 1961, "Beitrag zur Theorie der Kastenträger beliebiger Querschnittsform", *Stahlbau.* **11**; Addendum, Stahlbau 4, 1962.

Hutter K., 1969, "Eine Analogie zwischen dem querbelastetem Zugstab und dem Stab unter gemischten Torsion", *Int. für Bauwiss. Forsch. Zurich.*

Kachanov L. M., 1956, "Stability of thin-walled bars at elastic-plastic deformations" (in Russian), *Dokl. Akademii Nauk SSSR* **107**, 5.

Kappus R., 1953, "Zentrisches und exentrisches Drehknicken von Stäben mit offenem Profil", *Stahlbau* **1**.

Klimov W. I., 1957, "Calculation of shells of aircraft structures with open cross-section" (in Russian), *Trudy MAI*, No. 89, Oborongiz.

Kollbrunner C. F., Hajdin N., 1972, *Dünnwandige Stabe*, Springer, Berlin.

Lacher G., 1962, "Zur Berechnung des Einflusses der Querschnitsverformung auf die Spannungsverteilung bei durch elastische Querschotte versteiffen Tragwerken mit prismatischen offenem oder geschlossenem biegesteifen Querschnitt unter Querlast", *Stahlbau*, **11**, 12.

Langhaar H. I., 1953, "On torsional flexural buckling of columns", *Journ. of Frankl. Institute*, 2.

Lansing W., 1953, "Thin-walled members in combined torsion and flexure", *Trans. Am. Soc. Civ. Eng.*

Novitski W. W., 1958, "Approximate methods of calculation of strength of cylindrical shells with an invariable closed cross-section" (in Russian), in: *Selected Papers: Calculation of Space Structures*, Vol. 4, Moskva.

Nowiński J., 1959, "Theory of thin-walled bars", *Applied Mechanics Reviews* **12**.

Nowiński J., 1961, "Theory of bars of tapered thin-walled cross-section" (in Polish), *Works of Main Aviation Institute*, Warszawa.

Obraztsov T. E., 1953, "On the calculation of stability of thin-walled bars in bending" (in Russian), *Trudy MAT* **26**, Oborongiz.

Pikovskii A. A., Derkachev A. A., 1959, "On the solution of thin-walled bars under compression-bending", in: *Selected Papers 'Solution of Space Structures'*, No. 5, Moskva.

Przemieniecki J. S., 1958, "Matrix analysis of shell structures with flexible frames", *Aeron. Quarterly*, **9**, 4.

Rutecki J., 1966, *Thin-Walled Load-Bearing Structures* (in Polish), PWN, Warszawa.

Rüdiger D., 1964, "Wölbkrafttorsion dünnwandiger Hohlquerschnitte", *Ing. Archiv.*, **33**, 5.

Schapitz E., 1963, *Festigkeitslehre für den Leichtbau*, VDI-Verlag, Düsseldorf.

Strugatskii J. M., 1964, "Some problems of solution of prismatic complex systems" (in Russian) in *Selected Papers: 'Solution of Space Structures'*, Vol. 11, Moskva.

Szmelter K., Dacko W., Dobrociński S., Wieczorek M., 1979, *Finite Element Method in Structural Analysis* (in Polish), Arkady, Warszawa.

Timoshenko S., 1945, "Theory of bending, torsion and buckling of thin-walled member of open cross-section, *Jour. of Frankl. Inst.* 3.

Timoshenko S., Gere J. M., 1963, *Theory of Elastic Stability* (in Polish), Arkady, Warszawa.

Umanskii A. A., 1939, *Torsion and Bending of Thin-Walled Aircraft Structures* (in Russian), Oborongiz.

Urban T. W., 1955, *Theory of Solution of Thin-Walled Skeletal Structures* (in Russian), Transzheldorizdat.

Vlasov W. Z., 1948, *Thin-Walled Space Systems* (in Russian), Gosstroiizdat.

Vlasov W. Z., 1959, *Thin-Walled Elastic Bars* (in Russian), Gos. Izd. Fiz. Mat. Lit. Moskva.

Wilde P., 1956, "Curvilinear beams with open thin-walled cross section", *Arch. Mech. Stos.* **1**.

Wilde P., 1968, "The torsion of thin-walled bars with variable cross-section", *Arch. Mech. Stos.*, **4**.

Zienkiewicz C. C., 1972, *Finite Element Method* (in Polish), Arkady, Warszawa.

Additional references

Attard M. M., 1986[1], "Non-linear theory of non-uniform torsion of thin-walled open beams", *Thin-Walled Struct.* **4**, 2, 101–134.

Attard M. M., 1986[2], "Non-linear shortening and bending effect under pure torque of thin-walled open beams", *Thin-Walled Struct.* **4**, 3, 165–177.

Attard M. M., Somervaille I. J., 1987, "Non-linear analysis of thin-walled, open beams", *Comput. and Struct.* **25**, 3, 437–443.

Benito R., Sridharan S., 1984/85, "Mode interaction in thin-walled structural members", *J. Struct. Mech.* **12**, 4, 517–542.

Benson R. C., 1985, "Post-buckling analysis for the bending of a long beam with a thin, open, circular cross-section", *J. Appl. Mech.* **52**, 1, 129–132.

Boswell L. F., Zhang S. H., 1984, "The effect of distortion in thin-walled box-spine beams". *Int. J. Solids and Struct.* **20**, 9/10, 845–862.

Chan S. L., Kitipornchai S., 1986, "Geometric non-linear analysis of asymmetric thin-walled members", *Univ. Queensland Dept. Civ. Eng. Res. Rept.* **73**, 1–51.

Chen Z. S., Mang H. A., 1986, "Zum Stabilitätsverlust bei mehrlamelligen Druckgurten von Stahlträgern mit I-förmigem Querschnitt", *Z. angew. Math. Mech.* **66**, 4, 33–35.

Friedman Z., Fuchs M. B., 1987, "Multilevel optimal design of thin-walled continuous beams", *Comput. and Struct.* **25**, 3, 405–414.

Grądzki R., Kowal-Michalska K., 1985, "Elastic and elasto-plastic buckling of thin-walled columns subjected to uniform compression", *Thin-Walled Struct.* **3**, 2, 93–108.

Hikosaka H., Takami K., 1985, "Formulation of distortional behavior of thin-walled curved beam with open cross-section", *Proc. Jap. Soc. Civ. Eng.* **356**, 91–100.

Hui D., 1986, "Design of beneficial geometric imperfections for elastic collapse of thin-walled box columns", *Int. J. Mech. Sci.* **28**, 3, 163–172.

Jetteur P., Maquoi R., Škaloud M., Zörnerova M., 1984, "Interaction of shear lag with plate buckling on longitudinally stiffened compression flanges", *Acta Techn. ČSAV* **29**, 3, 376–397.

Karamanlidis D., Jasti R., 1987, "Curved mixed beam elements for the analysis of thin-walled free-form arches", *Ing.-Archiv* **57**, 5, 361–367.

Królak M., Kołakowski Z., 1983, "Stability of a thin-walled trapeziform girder under normal force and bending moment" (in Polish), *Arch. Bud. Maszyn* **30**, 1/2, 45–57.

Matulewicz Z., Szymczak C., 1985, "Optimal design of thin-walled I-beams undergoing torsion", *Thin-Walled Struct.* **3**, 2, 135–144.

Moore D. B., 1986, "A non-linear theory for the behaviour of thin-walled sections subject to combined bending and torsion", *Thin-Walled Struct.* **4**, 6, 449–466.

Møllmann H., 1986, "Theory of thin-walled elastic beams with finite displacements", *Lect. Notes Eng.* **19**, 195–209.

Murray N. W., 1985, *Introduction to the Theory of Thin-Walled Structures*, Oxford, Clarendon Press, 447 pp.

Roberts T. M., 1986, "Instability of compound monosymmetric beams", *Int. J. Mech. Sci.* **28**, 1, 61–69.

Roberts T. M., Burt C. A., 1985, "Instability of monosymmetric I-beams and cantilevers", *Int. J. Mech. Sci.* **27**, 5, 313–324.

Rondal J., Maquoi R., 1985, "Stub-column strength of thin-walled square and rectangular hollow sections", *Thin-Walled Struct.*, **3**, 1, 15–34.

Rutenberg A., Zaslavsky A., 1984, "On the shear center of nonsymmetric open thin-walled sections", *Isr. J. Technol.* **22**, 4, 263–266.

Rysz M., Życzkowski M., 1988, "Optimal design of a thin-walled cross-section subject to bending with torsion against creep rupture", *Int. J. Mech. Sci.* **30**, 2, 127–136.

Schade D., 1987, "Eine eindimensionale Darstellung der Torsion und Profilverformung von dünnwandigen, prismatischen Stäben", *Ing.-Archiv* **57**, 6, 420–430.

Sridharan S., Ali M. A., 1986, "An improved interactive buckling analysis of thin-walled columns having doubly symmetric sections", *Int. J. Solids and Struct.* **22**, 4, 429–443.

Stickforth J., 1986, "Über den Schubmittelpunkt", *Ing.-Archiv* **56**, 6, 438–452.

Szefer G., Mikulski L., 1984, "Optimal design of elastic I-section arches" (in Polish), *Rozpr. Inż.* **32**, 4, 467–480.

Toneff D. J., Stiemer S. F., Osterrieder P., 1987, "Local and overall buckling in thin-walled beams and columns", *J. Struct. Eng. (USA)* **113**, 4, 769–786.

Tralli A., 1986, "A simple hybrid model for torsion and flexure of thin-walled beams", *Comput. and Struct.* **22**, 4, 649–658.

Weiss S., (1985), "Post-buckling strength of eccentrically compressed steel columns with slender webs" (in Polish), *Arch. Inż. Lqd.* **31**, 1/2, 41–56.

Wekezer J. W., 1985[1], "Instability of thin-walled bars", *J. Eng. Mech.* **111**, 7, 923–935.

Wekezer J. W., 1985[2], "Non-linear torsion of thin-walled bars of variable, open cross-sections", *Int. J. Mech. Sci.* **27**, 10, 631–641.

Wu J., Gould Ph. L., 1987, "Large displacement analysis for pure bending of thin-walled beams"", *J. Eng. Mech.* **113**, 4, 522–528.

Yang Yeong-Bin, 1987, "Stability of thin-walled beams, a general theory", *Lect. Notes Eng.* **26**, 280–289.

1. Introduction

In this short chapter we aim to present the problems of stress concentration
and contact stresses, significant both from the congnitive as well as practical
point of view. Because of limited space let us discuss the most important and
simplest solutions referring to the statical problems only, and certain aspects
of the theory. At the present state of knowledge, it is difficult to consider the
stress concentration problems without at least an elementary presentation
of the fundamental notions of fracture mechanics. From the standpoint of
the stress theory in elastic solids, the cracks constitute the limiting case of stress
concentration in the vicinity of cavities when the value of stresses increases
infinitely at a crack tip. Here we have to explain the meaning of the notions
of the stress concentration factor and the stress intensity factor and to point
out the differences between these notions.

The problems of contact stresses as well as the concepts of fracture mech-
anics are closely connected with those of the theories of strength. The
concepts of the strength theories assume the existence of certain strength
criteria and the determination of the reduced stress while infinitely increasing
stresses are inadmissible. In the case of a solid with cracks, in the formulation
of the fracture mechanics, the occurrence of the infinitely increasing stresses
does not necessarily mean material failure, however the propagation of the
cracks leading to the catastropic fracture cannot be allowed under any cir-
cumstances. Already Huber, the author of the known strength hypothesis,
had believed (Huber, 1948) that "to derive a general strength criterion is
hopeless". He also wrote how Voigt already in 19th century was right
about doubting whether the strength criteria could be formulated by means
of the constants characteristic for a given material as could be done in the
case of elastic effects. Huber appreciated Griffith's concept and reckoned
that the strength phenomena depend not only on the material itself
but also on the dimensions and the shape of a body and the distribution of
stresses in it (Huber, 1948). As examples he cites the high strength of thin
wires and cases of solids in contact over curved surfaces. The most important

features are the type of the material (brittle, ductile), the structure of the internal cracks, the distribution of the applied forces, dynamical effects, the shape and the size of structural components, etc.

The failure of a material or a structural component is not necessarily caused by fracture. If we understand failure to mean that the structure, or its components, changes such that it ceases to meet the specifications for which it was designed, then the failure can be generated by a number of factors. The failure of a structure can result from creep of its components, or due to plastic yield of a certain part of the structure component, or by a number of causes described commonly as ageing of the material. In the case of bending of beams the regions of perfectly plastic yield are called *plastic hinges*, and depending on the type of the structure and the distribution od loading, they may result in collapse of the whole structure. A failure of a structure may be caused also by a loss of stability or by resonance vibrations. On the other hand, the friction and moving contact stresses may exert abrasive wear of the surface, including change in the shape of the structural member. In roller and ball bearings the effects of spalling and chipping are encountered. Fracture can accompany these kinds of failure; for brittle materials however it is, as a rule, the main reason of the failure. The fracture of the material can develop from dynamic as well as static loadings. For about one and a half (Forrest, 1962) century, intensive investigations on fatigue fracture (Kocańda, 1972; Forrest, 1962) have been carried out. A sudden application od loadings and the wave of stress generated in such a way can result in a catastrophic propagation of a crack or cracks which until the passage of the wavefront were not deleterious to the structure (Liebowitz, 1968–1972; Sih, 1973, 1978; Yoffe, 1951). Thousands of papers and a great number of books and monographs have been written on each of these effects. The theory of cracks is closely connected with the theory of dislocations (McClintock and Argon, 1970), and the theory of disclinations (Likhachev and Khairov, 1975; de Wit, 1977). As a rule the development of a crack is accompanied by a zone of plastic deformations in the neighbourhood of the crack tips (Dugdale, 1960; Rice, 1968, 1982; Panasyuk, 1968)

The contact problems constitute a vast class of the problems of the mechanics of a solid body. In the most cases the forces acting between solids are transmitted by a contact of the bounding surfaces of the solids. However, not all the cases where the solids are in contact belong to the class of contact problems from the standpoint of the theory. We exclude the problems for which the distribution of the contact forces are known beforehand. As for contact problems, we consider these when the boundary conditions at the contact region are prescribed in terms of the displacements. Contact problems

have already been considered in the XIX century. The renown paper by Hertz (1881) refers to the contact of elastic spheres and cylinders, problems which have been referred to as "hertzian". In this field many known monographs have been published. Let us note the monographs by Shtayerman (1961) and Galin (1953, 1980), and a recent one by Gladwell (1980), which provides the reader with encycloapeadic state of the knowledge in the field of contact problems within the classical theory of elasticity and cites over 750 references in the field. The problems discussed in recent years have referred to the contact of solids with reinforcements, anisotropic and non-homogeneous media, solids with wavy boundaries (Dundurs *et al.*, 1973; Dundurs, 1975) with bonding or semi-bonding taken into account (Dundurs *et al.*, 1973; Golub and Mossakovskii, 1960; Grigorovich, 1973; Keer *et al.*, 1972; Sneddon *et al.*, 1975; Willis, 1966) or with the forces of adhesion. This does not exhaust the contact problems being considered. We can mention here the problems of contact with an elastic structural component such as a membrane, plate, shell or their systems (Grigorovich, 1973; Updike and Kalnins, 1970). Abramov (1937) was the first to notice that the singularities appearing in the case of contact with friction taken into account have an oscillatory character. In the Soviet literature this is called *Abramov's effect*. These types of singularities occur also in the theory of cracks in the problems of cracks in the surface of bonding of the materials with different material constants. Many authors have dealt with problems of contact with an elastic foundation of the Winkler type, and of the more general type (Hetenyi, 1946, 1964; Golub and Mossakovskii, 1960; Popov, 1982; Sneddon *et al.*, 1975). A new original method based on the contemporary algebraic logic method of cybernetics is presented in a monograph by Rvachev and Protsenko (1977).

Frequently, a contact of two bodies generates permanent deformation; then the solution depends significantly on the region of contact. We do not discuss an important domain of contact problems concerning the methods of photoelasticity and the methods of hardness measurements (Shaw, 1973; Frocht, 1948; Jakubowicz and Orłoś, 1978). The experimental methods of the photoelasticity enable us to determine easily the stress distribution in a solid, particularly in two-dimensional cases. There are methods to deal with the three-dimensional problems as well.

The contact problems with heat sources taken into account have also attracted the interest of investigators. The three-dimensional problems without any symmetry taken into account are difficult to solve analytically. The same remark holds in many dynamic problems. The approximate solutions are being obtained by numerical methods and the use of a computer. The finite

element method and boundary element method have recently become popular. The dynamic problems can be split into two classes, namely the problems of contact of moving bodies with or without friction, and with known velocity, over the surface of a semi-space or a layer, and the wave propagation and vibrations. An example is a hammer hitting a piece of hot metal on an anvil. Still another class of contact problems constitute the problems of thermo-elasticity with the coupling of the field of temperature and that of displacement taken into account.

In recent years the approach in solving the problems of the solids body mechanics (not only) has changed considerably due to rapid development of personal and small computers. It is no longer necessary to devise analytical inventive methods applicable to particular problems, instead the general methods based on the finite element methods (FEM) or boundary element method (BEM) serve the purpose (Du Qinghua (Ed.), 1986; Atluri (Ed.), 1986; Luxmoore et al. (Eds.), 1987). The theoretical research deals rather with the proofs of uniqueness and existence of the solutions and with constructions of the models of new materials.

The development of the fracture mechanics reflects in a number of international and local conferences organized to discuss the progress in this field of research and the application of the numerical methods, first of all FEM and BEM in solving the problems. The Seventh International Conference on Fracture has taken place in Houston, USA in March 1989. Each Congress of IUTAM, also the last one XVIIth Congress in Grenoble, France, August 1988 includes the problems of fracture mechanics in its program. The European Group on Fracture organizes biennially the European Conferences on Fracture. To date the following were organized: ECF1(1976)—Compiégne, France, D. Francois, ECF2(1978)—Darmstadt, ERG, D. Gross, ECF3(1980)–London, UK, J. C. Radon, ECF4 (1982)—Loeben, Austria, K. L. Maurer, ECF5 (1984)—Lisbon, Portugal, L. Faria, ECF6 (1986)—Amsterdam, the Netherlands, H. C. van Elst (see van Elst and Bakker (Eds.), 1986) and ECF7 (1988)—Budapest, Hungary, E. Czoloby. The following areas of the fracture mechanics show rapid progress:

1. Analysis of micromechanism of fracture and adjustments of crack tip models by combining numerical and experimental methods,

2. Unification of test procedures for characterizing both the elastic-plastic material behaviour (J-resistance curves) and the fatique and creep fracture mechanics,

3. Clarification of damage mechanisms and material diagnostics for complex loading situations, taking into account the influence of the environment,

4. Further development of engineering methods for the assessment of fracture safety and their application to engineering structures.

The avalanche of papers devoted to fracture mechanics is being published in a great many journals on solid body mechanics. The oldest specialized journal in this field is *Intern. J. of Fracture* (published since 1956), recently a new journal on the subjects began appearing, namely *Theoretical and Applied Fracture Mechanics*, comprising fracture mechanics technology and mechanics and physics of fracture.

The theoretical and experimental investigations dealing with the fracture mechanics take into account various coupled fields like hygrothermoelasticity (Sih, Michopoulos and Chou (Eds.), 1986) or different materials: ceramics (Shah, 1985), composites (Herrmann, 1986), concrete (Series).

In contact problems the development is observed not only in the application of new computational methods but also in the problems connected with wear and trybology (Galin, 1976; Galin and Goryacheva, 1977; Aleksandrov, 1983), and the problems of heat generated by friction during the motion of contacting bodies (Galin and Goryacheva, 1977; Aleksandrov, 1983).

2. Stresses Around Cavities and Notches

2.1. Stress Concentration, Neuber's Problem

The precise knowledge of the stresses which would take place in the structural components under the acting forces, field of temperature and perhaps some other external influences is an important factor in constructing machines or designing structures. The aim, difficult to achieve for a constructor or designer, is to obtain the state of stress close to a uniform one. This usually means the possibility of designing a construction that is lighter and by all probability cheaper. On the other hand, there are some constructional reasons to design holes, grooves, notches, etc., which perturb and change any uniform stress state. It also happens that certain changes have to be made on an existing structure. We have to be aware of the redistribution of stresses in a structural component exerted by drilling a hole, and we have to realize that the redistribution of stresses may depend on the place. We have to make all efforts to avoid any damage or failure of the structure. Therefore, the investigations in this field of engineering science, both theoretical and experimental, are of great importance for practical design.

   The first theoretical solutions of such problems within the framework of the classical theory of elasticity can be traced even to the 19th century, and are credited to Kirsch (1898) who determined the distribution of stresses around a circular hole in the case of simple tension, bending, and shear. Inglis' solution referring to the state of stresses and strain around an elliptical hole in an infinite plate was published in 1913. This solution is most frequently cited due to the fact that Griffith used the solution in his derivation of the theory of fracture. The earlier solution (1910) by Kolosov can be found in his doctoral thesis. The method of complex variable proved to be very useful in solving such problems. The applications of the method together with the method of conformal mappings initialized by Kolosov was developed by Muskhelishvili and his collaborators. Besides the fundamental monograph by Muskhelishvili (1935) we mention here

important monographs by Kolosov (1935), Savin (1968) and Vainberg (1969).

The monograph by Neuber (1937) has fundamental value, the first edition appeared in 1937; the enlarged edition was published in 1958 (English and Russian translations' of the monograph exist). Neuber obtained solutions of the problems on the theory of elasticity for various solid bodies with notches by a pertinent choice of curvilinear coordinates system in plane as well as in spatial problems. The reader may find in his monograph a number of original solutions referring to the cases of tension, bending, torsion, and shear.

The methods of photo-elasticity proved to be very useful and effective in experimental investigations. Together with the introduction of anisotropic materials, plastics, laminates, composites, etc. to practical applications, the theory and experimental investigations concerning such materials had to be developed, particularly for the problems of stress concentration in structural components made of these new materials. We are not able to discuss in a short chapter many particular solutions. We confine ourselves to the presentation of main theoretical methods used in the theory of isotropic materials for elastic and homogeneous bodies, and elastic-plastic materials. These methods can be easily modified and generalized in the cases of more complicated continua. Then, however, the universality of the classical methods is lost. Also the lack of space does not allow us to consider the nonlinear problems of the theory of elasticity, large deformations, and other more complicated cases.

As far as the strength of materials or of structure components is concerned, the constructor is interested in finding the stress distribution, and first of all in determining the places at which the highest values of the strength effort occur. In the cases where the increase in the stresses results from the existence of stress concentrators in the form of notches, holes, faults, grooves, etc., we introduce the notion of the coefficient of stress concentration.

By the *effective coefficient* of stress concentration, in static case we understand the ratio of the strength without a concentrator to that of the same structural component with a concentrator, for example a notch. In a similar way we define the effective coefficient of stress concentration for cyclic loadings, then we replace the static strength by the fatique strength, and the experimental tests are performed for a symmetric cycle. Another notion which we introduce when considering the stress concentration is the *coefficient of shape*. It is equal to the quotient of the highest value of normal (or shear) stress in the direct neighborhood of the notch, or another concentrator, to the respective value of the nominal stress computed by the methods of the strength of materials, for the same structural component of constant

cross-section diminished by the notch (or the surface replacing another stress concentrator). The stress concentrators can be classified as follows. We shall distinguish stress concentration arising from the existence of notches, holes or cavities, and inclusions of different materials. The notches may differ depending on their geometry. Thus we have the notches: shallow or deep, internal or external, single and multiple, rounded- and sharp-ended. We also distinguish the notches which are plane, axially symmetric, and spatial (for example key slots or blade grooves).
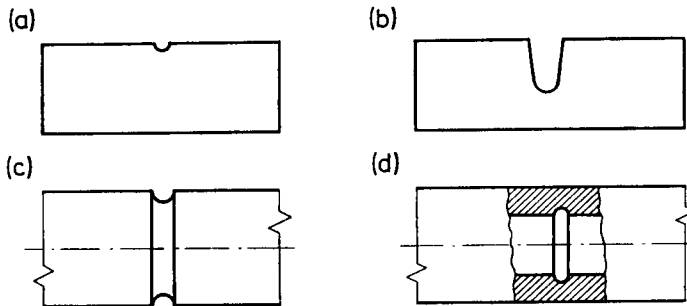
Fig. 2.1. Notch types: (a), (b) in plate; (c), (d) external and internal grooves

The common feature of the stress distribution within the elastic range in the neighborhood of any stress concentrator is its fast decay with distance. In presenting the solutions for the two-dimensional case we shall be using the method of a complex variable while in the axially symmetrical case we shall follow Neuber's approach.

2.2. Stress Concentration in Two-Dimensional Problems

The methods of a complex variable proved to be particularly useful in the solutions of the two-dimensional problems of the theory of elasticity. In the problems of notches and holes, and the cases without body forces taken into account, the equations of equilibrium assume the following form:

$$\sigma_{\alpha\beta,\beta} \equiv \sum_{\beta=1}^{2} \frac{\partial \sigma_{\alpha\beta}}{\partial x_\beta} = 0, \quad \alpha, \beta = 1, 2; x_1 \equiv x, x_2 \equiv y. \tag{2.1}$$

All stress components are denoted here consistently by the symbol σ; in engineering notation σ_{xy} is denoted by τ_{xy}. The equations of compatibility reduce to the single one. It can be expressed in terms of stresses

$$\sum_{\alpha,\beta=1}^{2} \sigma_{\alpha\alpha,\beta\beta} = 0.$$ (2.2)

In the case of the first boundary value problem, i.e. where the boundary conditions are prescribed in terms of the stresses, we have

$$\sum_{\beta=1}^{2} \sigma_{\alpha\beta}\cos(n,\beta) = X_{\alpha}, \qquad \alpha,\beta = 1,2,$$ (2.3)

where X_1, X_2 are the components of the external stress vector acting on the boundary in the directions x_1, and x_2, respectively; n denotes the external normal.

The system of partial differential equations (2.1) and (2.2) can be reduced to a single biharmonic equation

$$\sum_{\alpha,\beta=1}^{2} U_{,\alpha\alpha\beta\beta} = 0,$$ (2.4)

where U is Airy's function. The stress components can be expressed in terms of the Airy function:

$$\sigma_{11} \equiv \sigma_{xx} = \frac{\partial_2 U}{\partial y^2}, \qquad \sigma_{22} \equiv \sigma_{yy} = -\frac{\partial^2 U}{\partial x^2},$$

$$\sigma_{12} = \sigma_{xy} = \tau_{xy} = -\frac{\partial^2 U}{\partial x \partial y}.$$ (2.5)

The Airy function can be represented in the form of two analytical functions of complex variable $z = x + iy$

$$U(x,y) = \text{Re}[\bar{z}\varphi_1(z) + \chi_1(z)],$$ (2.6)

where Re denotes the real part of the expression in brackets, $\varphi_1(z)$ and $\chi_1(z)$ are analytical functions of complex variable, and $\bar{z} = x - iy$. Thus, the problem reduces to determining two analytical functions from the conditions along the contour, which in the case of the first boundary condition (prescribed stresses) takes the form

$$\frac{\partial U}{\partial x} + i\frac{\partial U}{\partial y} = \varphi_1(z) + z\overline{\varphi_1'(z)} + \overline{\psi_1(z)} = i\int_0^s (X_n + iY_n)\,ds$$

$$= f_1 + if_2 + \text{const} \qquad \text{on contour } L,$$ (2.7)

where

$$\psi_1(z) = \chi_1'(z) \equiv \frac{d\chi_1}{dz}.$$

The components of the stress tensor can be determined from the Kolosov–Muskhelishvili formulae

$$\sigma_{xx}+\sigma_{yy} = 2[\varphi_1'(z)+\overline{\varphi_1'(z)}], \tag{2.8}$$

$$\sigma_{yy}-\sigma_{xx}+2i\sigma_{xy} = 2[\bar{z}\varphi_1''(z)+\psi_1(z)]. \tag{2.9}$$

In the case where we are interested in finding the stress distribution around a hole in an infinite region, contour L is single-connected. If we assume the origin of the coordinate system inside the hole, then functions $\varphi_1(z)$ and $\psi_1(z)$ can be written in the form

$$\varphi_1(z) = -\frac{X+iY}{2\pi(1+\varkappa)}\ln z+(B+iC)z+\varphi_1^0(z), \tag{2.10}$$

$$\psi_1(z) = \frac{X-iY}{2\pi(1+\varkappa)}\ln z+(B_1+iC_1)z+\psi_1^0(z), \tag{2.11}$$

where for plane state of stress $\varkappa = (3-\nu)/(1+\nu)$, while for the plane state of strain $\varkappa = 3-4\nu$, and X and Y are the components of the resultant vector of all tractions acting along the hole contour; B, C, B_1 and C_1 are real constants. $\varphi_1^0(z)$ and $\psi_1^0(z)$ can be presented in the form of series

$$\varphi_1^0(z) = \sum_{k=0}^{\infty} a_k' z^{-k},$$

$$\psi_1^0(z) = \sum_{k=0}^{\infty} b_k' z^{-k}. \tag{2.12}$$

If the boundary of the hole is free from stresses, then $X = Y = 0$, and constants $B+iC$, and B_1+iC_1 can be determined from the conditions at infinity. Let us denote $\sigma_{xx}(\infty) = p$, $\sigma_{yy}(\infty) = q$, and $\sigma_{xy}(\infty) = t$; we then obtain

$$4B = p+q, \quad 2B_1 = (q-p)\cos 2\alpha, \quad 2C_1 = (p-q)\sin 2\alpha, \quad C = 0. \tag{2.13}$$

A very popular method for solving these problems consists in the use of the conformal mapping of region S outside the hole on the interior of a unit circle γ. The mapping will be denoted by $z = \omega(\zeta)$, no the circumference of the unit circle γ it takes the values σ.

The boundary condition on the contour of the hole has to be transformed to the boundary condition on the circumference of the circle

$$\varphi(\sigma)+\frac{\omega(\sigma)}{\overline{\omega'(\sigma)}}\overline{\varphi'(\sigma)}+\overline{\psi(\sigma)} = f_1+if_2+\text{const}, \tag{2.14}$$

where

$$\varphi(\sigma) \equiv \varphi_1[\omega(\sigma)], \psi(\sigma) \equiv \psi_1[\omega(\sigma)].$$

Using the new coordinate system, we obtain

$$\sigma_{\varrho\varrho} + \sigma_{\theta\theta} = 2[\Phi(\zeta) + \overline{\Phi(\zeta)}], \qquad (2.15)$$

$$\sigma_{\theta\theta} - \sigma_{\varrho\varrho} + 2i\sigma_{\varrho\theta} = \frac{2\zeta^2}{\varrho^2\overline{\omega'(\zeta)}} [\omega(\zeta)\Phi'(\zeta) + \omega'(\zeta)\Psi(\zeta)], \qquad (2.16)$$

where

$$\Phi(\zeta) = \frac{\varphi'(\zeta)}{\omega'(\zeta)}, \qquad \Psi(\xi) = \frac{\psi'(\zeta)}{\omega'(\zeta)},$$

$\sigma_{\varrho\varrho}$, $\sigma_{\theta\theta}$, and $\sigma_{\varrho\theta}$ are equal to the stress components $\sigma_{x'x'}$, $\sigma_{y'y'}$ and $\sigma_{x'y'}$ in a moving coordinate system x', y', with the origin at the point considered and the Oy axis coinciding with the tangent to curve $\varrho = \text{const}$ at the same point.

Assuming that the mapping function is of the form

$$z = \omega(\zeta) = c\left(\zeta^{-1} + \sum_{k=1}^{n} e_k \zeta^k\right) \qquad (2.17)$$

and substituting into Eqs. (2.10) and (2.11), we obtain

$$\varphi(\zeta) = \frac{X+iY}{2\pi(1+\varkappa)} \ln\zeta + c\frac{B+iC}{\zeta} + \varphi_0(\zeta), \qquad (2.18)$$

$$\psi(\zeta) = -\frac{X-iY}{2\pi(1+\varkappa)} \ln\zeta + c\frac{B_1+iC_1}{\zeta} + \psi_0(\zeta), \qquad (2.19)$$

where

$$\varphi_0(\zeta) = \sum_0^\infty a_k \zeta^k \quad \text{and} \quad \psi_0(\zeta) = \sum_0^\infty b_k \zeta^k$$

are two holomorphic functions of ζ inside the unit circle. Substituting $\varphi_0(\zeta)$ and $\psi_0(\zeta)$ into Eqs. (2.18) and (2.19) and comparing the coefficients at equal powers, we obtain a system of algebraic equations for the coefficients a_k and b_k.

Another method consists in (compare Muskhelishvili, 1935) the application of the Harnack theorem. The boundary conditions can then be represented in the form of the equivalent functional equations:

$$\varphi(\zeta) + \frac{1}{2\pi i} \int_\gamma \frac{\omega(\sigma)}{\overline{\omega'(\sigma)}} \frac{\overline{\varphi_0'(\sigma)}}{\sigma - \zeta} d\sigma + \overline{b}_0 = \frac{1}{2\pi i} \int_\gamma \frac{f_1^0 + if_2^0}{\sigma - \zeta} d\sigma, \qquad (2.20)$$

$$\psi_0(\zeta) + \frac{1}{2\pi i} \int_\gamma \frac{\overline{\omega(\sigma)}}{\omega'(\sigma)} \frac{\varphi_0'(\sigma)}{\sigma - \zeta} d\sigma = \frac{1}{2\pi i} \int_\gamma \frac{f_1^0 - if_2^0}{\sigma - \zeta} d\sigma, \qquad (2.21)$$

where $f_1^0 + i f_2^0$ denote the reduced boundary conditions for functions $\varphi_0(z)$ and $\psi_0(z)$:

$$f_1^0 + i f_2^0 = f_1 + i f_2 - \frac{X + iY}{2\pi} \ln \sigma - \frac{Bc}{\sigma} -$$

$$- \frac{\omega(\sigma)}{\overline{\omega'(\sigma)}} \left[\frac{X - iY}{2\pi(1 + \varkappa)} \sigma - \overline{B} c \sigma^2 \right] - (B_1 - i C_1) \overline{c} \sigma. \tag{2.22}$$

First we consider the problem of an elliptical cavity. This problem has already been solved, by Inglis (1913) using another method. The function conformally mapping the exterior of the ellipse on the interior of the unit circle assumes the form

$$z = \omega(\zeta) = c(\zeta^{-1} + m\zeta), \tag{2.23}$$

where c is a complex constant, $|m| \leqslant 1$ characterizes the eccentricity of the ellipse, for $m = 0$ the ellipse becomes a circle, for a real $c = R$, and $m = +1$ the ellipse degenerates to a straight segment corresponding to a crack. If the semi–axes of the ellipse are given and equal to a and b, we get

$$m = \frac{a - b}{a + b}, \qquad R = \frac{a + b}{2},$$

and function $z = \omega(\zeta)$ reduces to the following form:

$$\omega(\zeta) = \frac{a + b}{2} \zeta^{-1} + \frac{a - b}{2} \zeta. \tag{2.24}$$

After performing corresponding evaluations, we obtain for example in the case where $\sigma_{xx}(\infty) = p$, and the remaining stress components vanish at infinity:

$$\varphi(\zeta) = \frac{pR}{4} [\zeta^{-1} + (2e^{2i\alpha} - m)\zeta], \tag{2.25}$$

$$\psi(\zeta) = -\frac{pR}{2} \left[\zeta^{-1} e^{-2i\alpha} + \frac{\zeta^3 e^{2i\alpha} + (me^{2i\alpha} - m^2 - 1)\zeta}{m\zeta^2 - 1} \right]. \tag{2.26}$$

The hoop stress $\sigma_{\theta\theta}$ along the contour of the ellipse takes the following form:

$$\sigma_{\theta\theta} = p \frac{1 - m^2 + 2m\cos 2\theta - 2\cos 2(\theta + \alpha)}{1 - 2m\cos 2\theta + m^2}, \tag{2.27}$$

where α denotes the angle between x-axis and the direction of loading p. For $\alpha = 0$ we obtain

$$\sigma_{\theta\theta} = p \frac{1 - m^2 + 2m - 2\cos 2\theta}{1 - 2m\cos 2\theta + m^2}. \tag{2.28}$$

The maximum value of the hoop stress along the contour takes place for $\theta = \pm\pi/2$ and amounts to

$$\sigma_{\theta\theta} = p\left(1+2\frac{a}{b}\right). \tag{2.29}$$

The minimum value of the hoop stress appears for $\theta = 0$, and is equal to $\sigma_{\theta\theta} = -p$. In the case of a circular cavity $a = b$, the highest value of hoop stress is three times as much as the uniform stress, without the hole, and the coeffi-
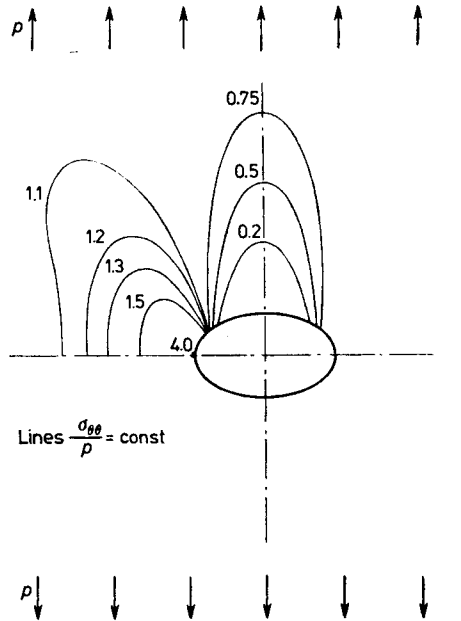
Fig. 2.2. Lines $\sigma_{\theta\theta}/p = $ const about an elliptical hole
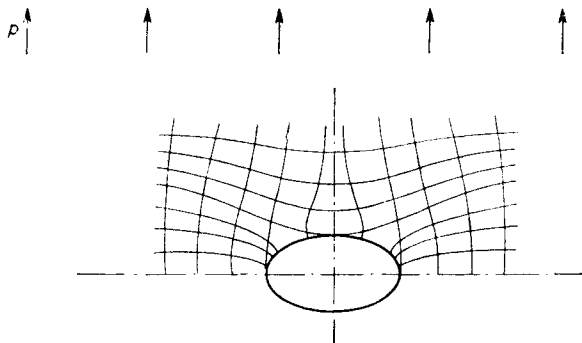
Fig. 2.3. Trajectories of principal stresses

cient of shape is equal to 3. It is evident from (2.29) that the coefficient of shape (i.e. the ratio $\sigma_{\theta\theta}/p$) increases with the ratio of semi-axes a/b. In Fig. 2.2 we show the lines of equal maximal stress, while in Fig. 2.3 the principal stress trajectories for the ellipse with ratio $a/b = 3/2$.

In the second example, we envisage a cavity in the form of a rectangle. To solve the problem we have to determine first the function mapping the exterior of the rectangle on the unit circle. The existence of such a mapping is ensured by Riemann's theorem which can be found in any more advanced book on the functions of a complex variable, or conformal mappings. Riemann's theorem also ensures that a conformal mapping is unique and continuous provided the mapped contour is a smooth curve of continuous tangent. If we round off the vertices of the rectangle we shall be able to use the approximate methods. The mapping function $\omega(\zeta)$ can then be easily obtained from Schwartz–Christoffel integral up to any prescribed accuracy. Without going into theoretical details, in the case of a rectangular cavity, function $z = \omega(\zeta)$ can represented in the form of the following infinite series:

$$z = \omega(\zeta) = c\left\{\zeta^{-1} + \frac{1}{2}(a+\bar{a})\zeta + \frac{1}{24}(a^2 - \bar{a}^2)\zeta^3 + \right.$$

$$+ \frac{1}{80}(a^2 - \bar{a}^2)(a-\bar{a})\zeta^5 + \frac{1}{896}[5(a^4 + \bar{a}^4) - 4(a^2 + \bar{a}^2) - 2]\zeta^7 +$$

$$+ \frac{1}{2304}[7(a^5 + \bar{a}^5) - 5(a^3 + \bar{a}^3) - 2(a+\bar{a})]\zeta^9 + \dots, \tag{2.30}$$

where $a = \exp(2k\pi i)$, $\bar{a} = \exp(-2k\pi i)$, k is a number dependent on the ratio of two sides of the rectangle, e.g. for a square $k = 1/4$, for a rectangle with the ratio of sides $5:1$, $k = 5/36$, and so on. If we take into account a finite number of the terms in the series (2.30), then instead of the rectangle we map a contour with rounded off vertices, and the sides which differ from straight segments. We can assume that the radius of rounding is not greater than a certain r_0, and that the sides of the "rectangle" do not vary from the straight line segment by more than a certain ε. Series (2.30) is rapidly convergent and we are able to find the number of terms of the series such that the above requirements are fulfilled. In the case of the ratio of the rectangle $5:1$ we obtain $a = \exp(\frac{10}{36}\pi i)$ and the mapping function in the form

$$\omega(\zeta) = c(\zeta^{-1} + 0.643\zeta - 0.098\zeta^3 - 0.038\zeta^5 - 0.011\zeta^7 + \dots). \tag{2.31}$$

Constant c can be determined from the condition that a particular point of the rectangle passes into a prescribed point of the unit circle. In a special case where the uniform field of stress is directed along the y-axis and is perpendicu-

lar to the longer side of the rectangle, then taking into account five terms of the expansion into series (2.31) we obtain the following formulae:

$$\varphi(\zeta) = pc(0.25\zeta^{-1} - 0.586\zeta + 0.055\zeta^3 + 0.018\zeta^5 + 0.003\zeta^7),$$

$$\psi(\zeta) = pc\ \frac{0.5 - 1.256\zeta^2 - 0.172\zeta^4 + 0.252\zeta^6 + 0.100\zeta^8}{\zeta - 0.643\zeta^3 + 0.293\zeta^5 + 0.189\zeta^7 + 0.078\zeta^9}\ . \tag{2.32}$$
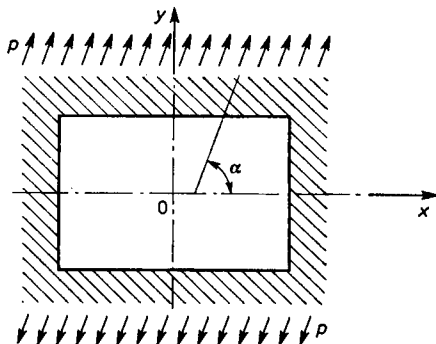
Fig. 2.4. Rectangular hole

The formulae for stress are obtained by substituting formulae (2.32) into (2.15) and (2.16) and the separation of the real and imaginary parts. In Fig. 2.5 we presented the lines of equal principal stresses σ_{max} and σ_{min} for the
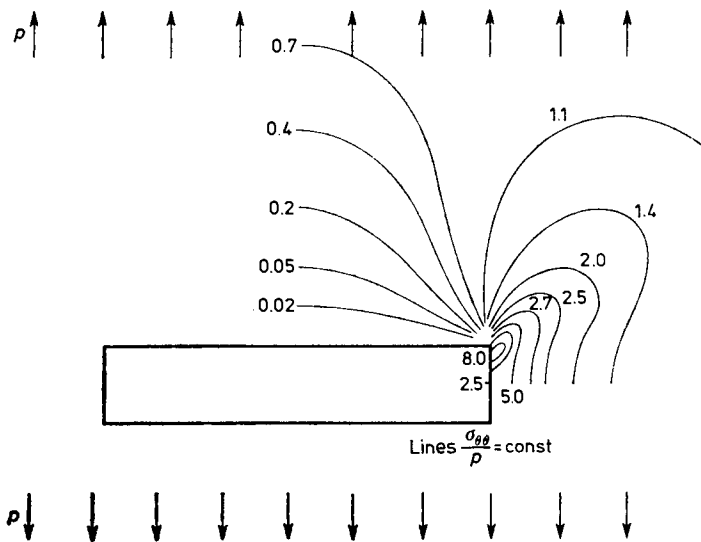
Fig. 2.5. Lines $\sigma_{\theta\theta}/p = $ const about a rectangular hole

rectangle with the ratio of sides 5:1 and the angle at which the loading acts $\alpha = 90°$.

Interesting results are given in Table 2.1, the coefficients of shape $\sigma_{\theta\theta}/p$ for 10 points are given on the circumference of the rectangle with the ratio of sides 5:1 and for four angles α. The results are approximate and have been obtained by means of formulae (2.32).

TABLE 2.1. Coefficients of shape $\sigma_{\theta\theta}/p$ for rectangles $a/b = 5$

$\theta°$	$\alpha = 0$	$\alpha = \pi/6$	$\alpha = \pi/3$	$\alpha = \pi/2$
0	−0.768	+0.033	+1.641	+2.420
20	−0.152	−0.452	+9.070	+8.050
25	+2.692	−2.519	+12.556	+7.030
30	+2.812	−2.264	+5.541	+1.344
40	+1.558	−0.278	+1.214	−0.644
90	+1.192	+0.653	−0.412	−0.940
140	+1.558	+1.877	−1.880	−0.644
150	+2.812	+7.466	−2.078	+1.344
160	−0.152	+5.096	+2.115	+8.050
180	−0.768	+0.033	+1.641	+2.420

The detailed discussion referring to these and similar problems for rectangular and triangular cavities, together with the corresponding diagrams of equal stresses σ_{max} τ_{max}, and σ_{min}, and of the trajectories of the principal stresses can be found in the monograph by Savin (1968).

The third example concerns pure bending of a beam of rectangular cross-section (only in this case do we have simultaneously both, the two-dimensional state of stress and pure bending). In the case of pure bending of a beam without a cavity we have the following state of stress:

$$\sigma_{xx}^0 = -\frac{M}{J}\, y, \quad \sigma_{yy}^0 = 0, \quad \sigma_{xy}^0 = 0, \tag{2.33}$$
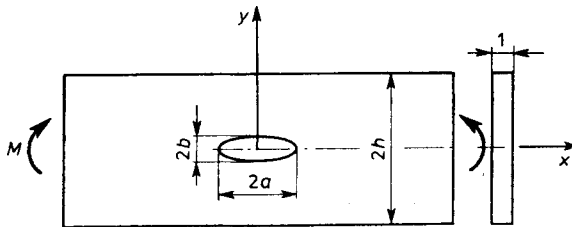
Fig. 2.6. Plate with an elliptic hole

where M denotes the bending moment, J is the moment of inertia of the cross-section of unit width, with respect to the z-axis. Thus the stress function $U^0(x, y)$ has the following form:

$$U^0(x, y) = -\frac{M}{6J} y^3.$$ (2.34)

We then, determine functions $\varphi^0(z)$ and $\psi^0(z)$

$$\varphi^0(z) = -\psi^0(z) = i \frac{Mz^2}{8J}.$$ (2.35)

Let us assume that an elliptical hole has been made in the beam (Fig. 2.6) such that its axis coincides with the neutral axis of the beam. The method considered here refers to the holes of other shapes as well. If the hole is not placed in the beam axis, we then have to superpose to the solution obtained above for the bending, the solution of the layer compressed by the pressure $p = -Md/J$ where d is the distance of the centre (say, of the ellipse) to the neutral axis. For the case where the hole is placed on the neutral axis of the beam, we obtain after the mapping of the contour on the unit circle

$$\varphi(\zeta) = \varphi_1(\zeta) + i \frac{M}{8J} [\omega(\zeta)]^2,$$

$$\psi(\zeta) = \psi_1(\zeta) - i \frac{M}{8J} [\omega(\zeta)]^2.$$ (2.36)

The boundary conditions for the stress-free hole assume the form

$$f_1^0 + if_2^0 = -i \frac{M}{8J} [\omega(\sigma) - \overline{\omega(\sigma)}]^2,$$

$$f_1^0 - if_2^0 = i \frac{M}{8J} [\overline{\omega(\sigma)} - \omega(\sigma)]^2$$ (2.37)

(compare with Eq. (2.22)).

Making use of the derived formula, we obtain

$$\varphi(\zeta) = i \frac{MR^2}{8J} [\zeta^{-2} + (2m-1)\zeta^2],$$

$$\gamma(\zeta) = i \frac{MR^2}{8J} [(1-2m)\zeta^2 + \frac{2(1-m)^2(m+\zeta)^2}{m\zeta^2 - 1} \zeta^2 - \zeta^{-2}].$$ (2.38)

After pertinent evaluations, we obtain the hoop stress

$$\sigma_{\theta\theta} = \frac{MR}{J} \frac{(1+m-2m^2)\sin\theta + (m-1)\sin 3\theta}{1+m^2 - 2m\cos 2\theta}.$$ (2.39)

In the case where $m = \dfrac{a-b}{a+b} = 1/3$, we have

$$\sigma_{\theta\theta} = \frac{MR}{J} \frac{4\sin\theta - 2\sin 3\theta}{5 - 4\cos 2\theta}.$$ (2.40)

The highest values of hoop stress occur for $\theta = \pi/2$:

$$\sigma_{\theta\theta|\max} = \frac{Mb}{J}(1+b/a).$$ (2.41)

For $b \neq 0$, $a = 0$ we obtain the crack along the y axis and the infinite stress concentration. Practically, it means that plastic deformations appear even for small values of moments. For the crack along the x-axis ($b = 0$, $a \neq 0$), there is no stress concentration, the existence of such a crack does not change the stress distribution.

In a similar way we can determine the stresses around the holes in the case of bending of beams of rectangular cross-section with shear forces taken into account.

2.3. Plastic Zone Due to Stress Concentration

It is evident from the above discussion that when we assume elastic deformations, then the cavities in a uniform two-dimensional stress field generate an increase in stresses, frequently multiple. As a rule, such a stress concentration exceeds the yield limit and produces zones of plastic deformations. The exact solution of elastic plastic problems is difficult, first of all due to the fact that the boundary between the elastic and plastic regions is not known beforehand.

Let us assume that we have succeeded in constructing a stress function in the plastic zone. We denote

$$U(x, y) = \begin{cases} U_1(x, y) & \text{in the plastic region,} \\ U_2(x, y) & \text{in the elastic region.} \end{cases}$$

The stress function has to be biharmonic in the elastic region, i.e. it has to satisfy equation (2.4) while in the plastic region it satisfies a yield condition which according to the Huber-Mises strength hypotheses takes for plane strain of an incompressible material the form

$$(\sigma_{yy} - \sigma_{xx})^2 + 4\sigma_{xy}^2 = \left(\frac{\partial^2 U_1}{\partial x^2} - \frac{\partial^2 U_1}{\partial y^2}\right)^2 + 4\left(\frac{\partial^2 U_1}{\partial x \partial y}\right)^2 = \frac{4}{3}\sigma_{\text{red}}^2 = 4k^2.$$

(2.42)

In this case we have the boundary conditions:
on the cavity contour

$$\sigma_{nn} = -q, \qquad \sigma_{n\theta} = \tau,$$

where n is the direction of the normal to the contour; and at infinity

$$\sigma_{xx}(\infty) = p_1, \qquad \sigma_{yy}(\infty) = p_2, \qquad \sigma_{xy}(\infty) = -t. \tag{2.43}$$

On the boundary of the elastic and plastic region we obtain the conditions

$$\frac{\partial^2 U_1}{\partial x^2} = \frac{\partial^2 U_2}{\partial x^2}, \qquad \frac{\partial^2 U_1}{\partial y^2} = \frac{\partial^2 U_2}{\partial y^2}, \qquad \frac{\partial^2 U_1}{\partial x\,\partial y} = \frac{\partial^2 U_2}{\partial x\,\partial y}. \tag{2.44}$$

As an example we shall consider a circular cavity with a qiven pressure, besides at inifity there are constant loadings p_1 and p_2 acting (compare Galin, 1953). The loadings and the region of plastic deformations are shown in
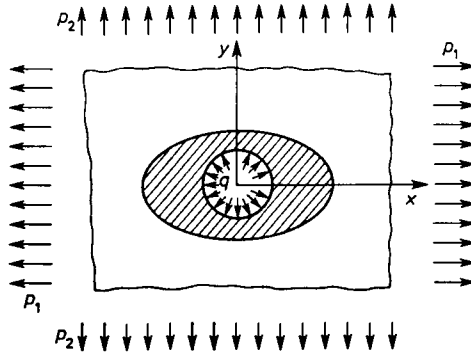
Fig. 2.7. Zone of plastic strains

Fig. 2.7. Let us consider the boundary conditions corresponding to a constant pressure acting on the boundary of the cavity and the loadings at infinity:

$$\sigma_{rr}(r = R) = -q, \qquad \sigma_{r\theta}(R) = 0, \qquad \sigma_{xx}(\infty) = p_1,$$
$$\sigma_{yy}(\infty) = p_2, \qquad \sigma_{xy}(\infty) = 0. \tag{2.45}$$

The solution of Eq. (2.42), with the first two boundary conditions (2.45) taken into account, assumes the following form:

$$U_1(x, y) = k(x^2+y^2)\ln\frac{\sqrt{x^2+y^2}}{R} - \frac{q+k}{2}(x^2+y^2). \tag{2.46}$$

Now we find the formulae for the stresses in the region of the plastic deformations

$$\sigma_{xx} + \sigma_{yy} = 2k - 2q + 4k \ln \frac{\sqrt{x^2+y^2}}{R} = 2(k-q) + 2k \ln \frac{z\bar{z}}{R^2},$$

$$\sigma_{yy} - \sigma_{xx} + 2i\sigma_{xy} = 2k \frac{\bar{z}}{z}.$$

(2.47)

The problem has been reduced to finding function $U_2(x, y)$ and the contour L surrounding the circular cavity of radius R from the conditions

$$\frac{\partial^2 U_2}{\partial x^2} + \frac{\partial^2 U_2}{\partial y^2} = \begin{cases} 2(k-q) + 2k \ln \dfrac{z\bar{z}}{R^2} & \text{on } L, \\ p_1 + p_2 & \text{for } z \to \infty, \end{cases}$$

(2.48)

$$\frac{\partial^2 U_2}{\partial x^2} + \frac{\partial^2 U_2}{\partial y^2} - 2i \frac{\partial_2 U_2}{\partial x \, \partial y} = \begin{cases} 2k \dfrac{\bar{z}}{z} & \text{on } L, \\ p_2 - p_1 & \text{for } z \to \infty. \end{cases}$$

Each biharmonic function exterior to a certain contour L can be represented by means of two holomorphic functions in the same domain

$$\frac{\partial^2 U_2}{\partial x^2} + \frac{\partial^2 U_2}{\partial y^2} = 2[\Phi_2^*(z) + \overline{\Phi_2^*(z)}],$$

$$\frac{\partial^2 U_2}{\partial x^2} - \frac{\partial^2 U_2}{\partial y^2} - 2i \frac{\partial^2 U_2}{\partial x \, \partial y} = 2[\bar{z}\Phi_2^*{}'(z) + \Psi_2^*(z)].$$

(2.49)

After mapping $z - \omega(\zeta)$ of contour L on the exterior of the unit circle γ we obtain

$$2[\Phi_2(\zeta) + \overline{\Phi_2(\zeta)}] = \begin{cases} 2(k-q) + 2k \ln \dfrac{\omega(\zeta)\overline{\omega(\zeta)}}{R^2} & \text{on } \gamma, \\ p_1 + p_2 & \text{for } \zeta \to \infty, \end{cases}$$

$$2 \left[\frac{\overline{\omega(\zeta)}}{\omega'(\zeta)} \Phi_2'(\zeta) + \Psi_2(\zeta) \right] = \begin{cases} 2k \dfrac{\overline{\omega(\zeta)}}{\omega(\zeta)} & \text{on } \gamma, \\ p_2 - p_1 & \text{for } \zeta \to \infty. \end{cases}$$

(2.50)

All the boundary conditions will be satisfied if we assume that the contour separating the elastic and plastic regions is an ellipse while the mapping on the unit circle takes the form

$$z = \omega(\zeta) = c\left(\zeta + \frac{p_2 - p_1}{2k} \zeta^{-1}\right).$$

(2.51)

Omitting the details of the solution, we show that all the boundary conditions will be satisfied provided functions $\Phi_2(\zeta)$ and $\Psi_2(\zeta)$ are represented by the formulae

$$\Phi_2(\zeta) = k\ln c - k\ln R + k\ln\left(\zeta + \frac{\beta}{\zeta}\right) + \frac{k-p}{2} - k\ln\zeta,$$

$$\Psi_2(\zeta) = k\frac{\overline{\omega}(\zeta^{-1})}{\omega'(\zeta)}\,\zeta^{-1}, \qquad \beta = \frac{p_2 - p_1}{2k}.$$

(2.52)

The second of the conditions will be satisfied of constant c takes the value

$$c = R\exp\left[\frac{1}{2k}\left(\frac{p_1 + p_2}{2} + q - k\right)\right].$$

(2.53)

The semi-axes of the ellipse can be determined by constants c and β. We thus obtain

$$a = c(1 + \beta), \qquad b = c(1 - \beta).$$

In two cases the ellipse becomes a circle, namely if the loadings at infinity disappear, and if their absolute value and signs are equal.

The semi-inverse method can be used in determining the contours separating the elastic and plastic regions also in more complicated cases. We can assume that contour L is a known curve and then determine the loadings necessary to produce such a plastic field of deformations. However, usually the solution is not unique. In the general case, the determination of the region of plastic deformations and the solution of the elastic plastic problems encounters substantial difficulties.

2.4. Notches in the Two-Dimensional State of Strain or Stress

The solution of the differential equations of equilibrium, called *Navier's equations* (sometimes also *Lamé's equations*) which in the case of vanishing body forces can be written in the form

$$\sum_{j=1}^{2} u_{i,jj} + \frac{1}{1-2\nu}\,u_{j,ji} = 0,$$

(2.54)

can be expressed in terms of two harmonic functions. This representation takes the form

$$u_i = \varphi_{,i} + (x_j\psi_j)_{,i} - 4(1-\nu)\psi_i,$$

(2.55)

where φ is a scalar function while $\boldsymbol{\psi} = (\psi_1, \psi_2, \psi_3)$ a vector function. This is a known representation used by Papkovitch–Neuber (compare *Technological Mechanics*, 1978). We have used the notation $u_1 = u$, $u_2 = v$, $u_3 = w$, $i = 1, 2, 3$; the subscript after the comma denotes derivative, e.g. $\varphi_{,i} \equiv \delta\varphi/\partial x_i$. The repetition of the same subscript denotes the summation

convention (for example, $x_j \psi_j \equiv \sum\limits_{j=1}^{3} x_j \psi_j$). The functions introduced here have nothing in common with the functions used in the complex variable method and denoted by the same letters. The functions in the Papkovitch-Neuber representation φ and ψ_i are harmonic, i.e. they satisfy Laplace's equation

$$\sum_{j=1}^{2} \varphi,_{jj} = 0, \quad \sum_{j=1}^{2} \psi_{i,jj} = 0. \tag{2.56}$$

Substituting formulae (2.55) into Hooke's law, we obtain

$$\sigma_{ij} = 2\mu[F,_{ij} - 2(1-\nu)(\psi_{i,j} + \psi_{j,i}) - \nu \delta_{ij} F,_{kk}], \tag{2.57}$$

where F denotes the stress function

$$F = \varphi + \sum_{j=1}^{2} X_j \psi_j, \tag{2.58}$$

and δ_{ij} is Kronecker's delta

$$\delta_{ij} = \begin{cases} 0, & i \neq j, \\ 1, & i = j, \end{cases}$$

It turns out that of the four functions φ, and ψ_i one is redundant, even in the most general case of a three-dimensional state of stress in a single-connected body. The discussion referring to the completeness of the solution, and the corresponding proofs can be found in the monographs on the theory of elasticity (e.g. *Technological Mechanics*, 1978) and in the original papers. In the case of the two-dimensional state of strain or stress, two functions $\varphi(x, y)$ and $\psi_1(x, y)$ are sufficient to solve the problems of notches. It results, in fact, from the treatment in the preceding part of this chapter. It is convenient to introduce two new harmonic functions $\Phi_0(x, y)$ and $\Phi_1(x, y)$ and new stress function F_1, related in the following manner with the previous ones:

$$\varphi = 2(1-\nu)\Phi_1 + \Phi_0, \quad \psi_1 = \frac{\partial \Phi_1}{\partial x}, \tag{2.59}$$

$$F = F_1 + 2(1-\nu)\Phi_1.$$

Then substituting formulae (2.57), returning to the typical notation, and taking into account that the solution does not depend on x_3, we obtain

$$\sigma_{xx} = -2\mu \frac{\partial^2 F_1}{\partial y^2}, \quad \sigma_{yy} = -2\mu \frac{\partial^2 F_1}{\partial x^2}, \quad \sigma_{xy} \equiv \tau_{xy} = 2\mu \frac{\partial^2 F_1}{\partial x\, \partial y},$$

$$\sigma_{zz} = -2\mu\nu \left(\frac{\partial^2 F_1}{\partial x^2} + \frac{\partial^2 F_1}{\partial y^2} \right). \tag{2.60}$$

Let us pass to the elliptical system of curvilinear coordinates system ξ, η. The transformation to the Cartesian coordinates system takes the form

$$x = \sinh\xi\cos\eta, \quad y = \cosh\xi\sin\eta. \tag{2.61}$$

The coordinates of the elliptical system are obviously orthogonal; the curves $\xi = $ const are the ellipses while $\eta = $ const are the hyperbolae

$$\left(\frac{y}{\sin\eta}\right)^2 - \left(\frac{x}{\cos\eta}\right)^2 = 1,$$

$$\left(\frac{x}{\sinh\xi}\right)^2 + \left(\frac{y}{\cosh\xi}\right)^2 = 1. \tag{2.62}$$

We omit here quite elementary, though tedious, evaluation leading to the derivation of the formulae for the stress function, non-vanishing components of the stress tensor, displacements and strains in the elliptical coordinate system. Let us confine ourselves to three cases, namely tension, pure bending and shear. The advantage of the introduction of the elliptical coordinates is that the curves $\eta = $ const describe the boundary of a large class of notches which have the properties of the notches encountered in engineering.
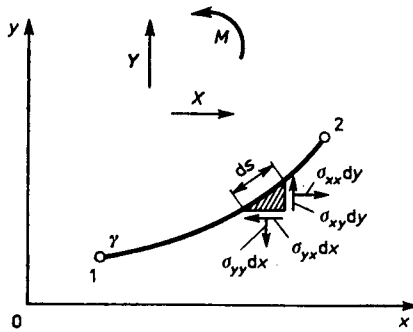
Fig. 2.8. Stress at a notch surface

In Fig. 2.8 curve γ is a part of the profile of the notch. It is easy to see that the infinitesimal force dX acting on the boundary of the arc, in x axis direction is equal to

$$dX = -\sigma_{xx}dy + \sigma_{xy}dx \tag{2.63}$$

and similarly, the infinitesimal force dY,

$$dY = \sigma_{yy}dx - \sigma_{xy}dy. \tag{2.64}$$

We determine the stress components by means of the stress function given by formula (2.60), and we omit the subscript at F_1, obtaining

$$dX = 2\mu d\left(\frac{\partial F}{\partial y}\right), \quad dY = -2\mu d\left(\frac{\partial F}{\partial x}\right). \tag{2.65}$$

Upon integrating with respect to s, we obtain

$$X\Big|_1^2 = \int_1^2 dX = 2\mu \frac{\partial F}{\partial y}\Big|_1^2, \quad Y\Big|_1^2 = \int_1^2 dY = -2\mu \frac{\partial F}{\partial x}\Big|_1^2 \tag{2.66}$$

and in a similar way the bending moment

$$M\Big|_1^2 = \int_1^2 (s\,dY - y\,dX) = 2\mu\left(F - x\frac{\partial F}{\partial x} - y\frac{\partial F}{\partial y}\right). \tag{2.67}$$

2.4.1. Simple tension

In this case, if we assume that the force acts in the direction of the x-axis which is at the same time the axis of symmetry, we can write

$$\Phi_0 = A(y\eta - x\xi) + B\cosh\xi\cos\eta, \quad \Phi_1 = A\xi, \tag{2.68}$$

whence we obtain the stress function

$$F = \cosh\xi(A\eta\sin\eta + B\cos\eta). \tag{2.69}$$

It follows from formula (2.66) that the boundary of the notch is stress-free provided that for $\eta = \pm\eta_0$ the derivatives $\partial F/\partial x$ and $\partial F/\partial y$ are constant. Let us calculate

$$\frac{\partial F}{\partial x} = \frac{\sinh\xi\cosh\xi}{h^2}(B - A\sin^2\eta), \tag{2.70}$$

where $h^2 \equiv \sinh^2\xi + \cos^2\eta$.

From the condition that the boundary is stress-free we obtain $B = A\sin^2\eta_0$, and consequently upon substitution the constant value of $\partial F/\partial y$. If d denotes a constant thickness of the slab and $2a$ is its width between the tips of the notches, than $p = P/2ad$ is the mean value of stress. Upon determining constant A from the condition that the resultant of the normal stress component in the cross-section is equal to the external force, and taking into account the boundary conditions along the notch, we obtain the following formulae for the stress tensor components:

$$\sigma_{\xi\xi} = \frac{p\sin\eta_0}{h^2(\eta_0 + \sin\eta_0\cos\eta_0)}\cosh\xi\cos\eta\left(2 + \frac{\cos^2\eta_0 - \cos\eta}{h^2}\right),$$

$$\sigma_{\eta\eta} = \frac{p\sin\eta_0}{h^4(\eta_0+\sin\eta_0\cos\eta_0)}\cosh\xi\cos\eta(\cos^2\eta-\cos^2\eta_0), \qquad (2.71)$$

$$\sigma_{\xi\eta} = \frac{p\sin\eta_0}{h^4(\eta_0+\sin\eta_0\cos\eta_0)}\sinh\xi\sin\eta(\cos^2\eta_0-\cos^2\eta).$$

Upon determining the radius of curvature at the notch apex, and making use of hyperbola equation $(2.62)_1$, for $\eta=\eta_0$ we obtain the relations

$$\frac{a}{\varrho} = \tan^2\eta_0, \qquad \left(1+\frac{a}{\varrho}\right)^{-1/2} = \cos\eta_0. \qquad (2.72)$$

Now, the ratios of the maximum value for the normal stress component to the mean stress can be expressed in terms of a/ϱ:

$$\frac{\sigma_{max}}{p} = \frac{2(1+a/\varrho)\sqrt{a/\varrho}}{(1+a/\varrho)\tan^{-1}\sqrt{a/\varrho}+\sqrt{a/\varrho}}. \qquad (2.73)$$
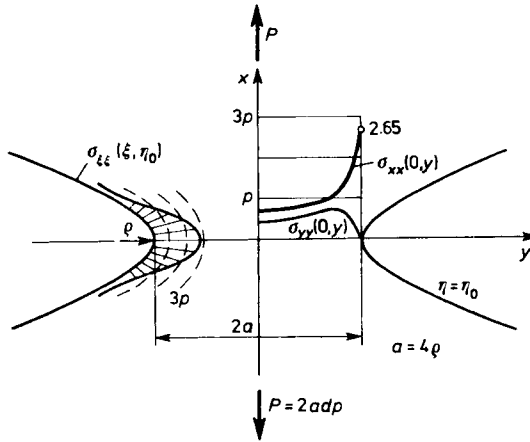
Fig. 2.9. Stress pattern in a surrounding of the notch vertex; tension
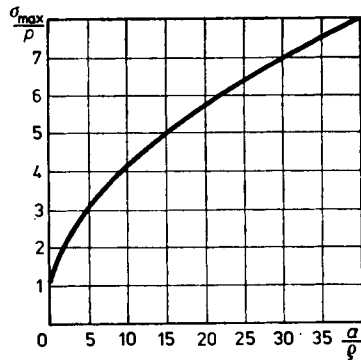
Fig. 2.10. Diagram of function $\sigma_{max} = pf(a/\varrho)$

The diagram of the function described by Eq. (2.73) is shown in Fig. 2.10. The influence of the notch radius at the apex is evident. The redistribution of the normal stress component induced by the existence of the notch is shown in Fig. 2.9.

2.4.2. Pure bending

In this case we take into account the following two harmonic functions

$$\Phi_0 = A\cosh 2\xi \sin(2\eta) + B\eta, \quad \Phi_1 = -4A\sinh \xi \sin\eta, \tag{2.74}$$

and the stress function in the form

$$F = A\sin(2\eta) + B\eta. \tag{2.75}$$

The boundary of the notch is stress-free provided

$$B = -2A\cos(2\eta_0). \tag{2.76}$$

The above condition assures vanishing of both the first derivatives $\partial F/\partial x$, and $\partial F/\partial y$ for $\eta = \pm \eta_0$. The bending moment can be calculated from formula (2.67)

$$M = -2Ad(\sin(2\eta_0) - 2\eta_0\cos(2\eta_0)), \tag{2.77}$$

where, as before, d denotes the slab thickness and $2a$ is its width. This time p denotes the maximum value of the normal bending stress, i.e.

$$p = \sigma_{xx}(0, a) = \frac{Ma}{J} = \frac{3}{2}\frac{M}{da^2},$$

where J is the inertia moment of the cross-section with respect to the z-axis. We then obtain

$$A = -\frac{p}{3}\frac{\sin^2\eta_0}{\sin(2\eta_0) - 2\eta_0\cos(2\eta_0)}. \tag{2.78}$$

In the elliptical coordinate system we obtain the following stress tensor components:

$$h^4\sigma_{\xi\xi} = A\sin(2\eta)(\cos(2\eta) - \cos(2\eta_0) - 4h^2),$$
$$h^4\sigma_{\eta\eta} = A\sin(2\eta)(\cos(2\eta_0) - \cos(2\eta)), \tag{2.79}$$
$$h^4\sigma_{\xi\eta} = A\sinh(2\xi)(\cos(2\eta) - \cos(2\eta_0)).$$

In a similar way as before we introduce the ratios σ_{max}/p, and a/ϱ, where ϱ denotes the radius of curvature at the notch apex:

$$\frac{\sigma_{max}}{p} = \frac{4a/\varrho \sqrt{a/\varrho}}{3\left[\sqrt{a/\varrho} + (a/\varrho - 1)\tan^{-1}\sqrt{a/\varrho}\right]}. \tag{2.80}$$
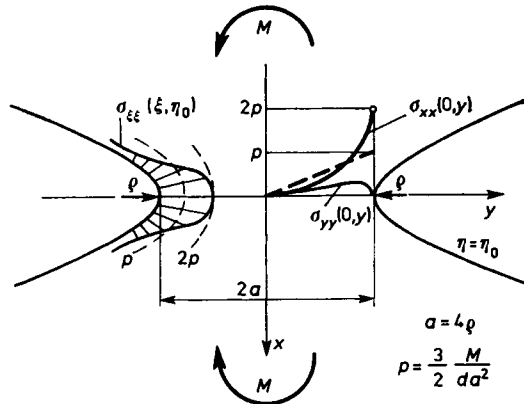
Fig. 2.11. Stress pattern in a surrounding of the notch vertex, bending
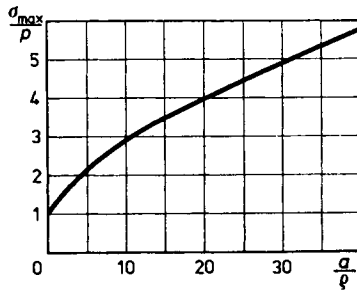
Fig. 2.12. Diagram of function $\sigma_{max} = pf(a/\varrho)$

The distributions of the normal stress components $\sigma_{xx}(0, y)$ and $\sigma_{yy}(0, y)$ are shown in Fig. 2.11 and compared with the linear diagram resulting from the elementary theory of beams. Figure 2.12 illustrates the function expressed by formula (2.80).

2.4.3. Pure shear

The conditions of pure shear are satisfied if we assume the following forms for the harmonic functions Φ_0 and Φ_1, and the stress function F:

$$\Phi_0 = A \sin\xi \sin\eta, \quad \Phi_1 = B\eta,$$
$$F = \sinh\xi(A \sin\eta + B\eta \cos\eta). \tag{2.81}$$

The stresses on the boundary $\eta = \pm\eta_0$ vanish if we assume that

$$A = -B\cos^2\eta_0. \tag{2.82}$$

If condition (2.82) is satisfied, then $\partial F/\partial x$ vanishes while $\partial F/\partial y$ is constant for $\eta = \pm\eta_0$, and consequently, as shown already, the boundary is stress-free. From the condition that the integral of the shear stress component in the cross-section $x = 0$ is equal to the shear force T, we obtain

$$B = -\tau \, \frac{\sin\eta_0}{\eta_0 - \sin\eta_0\cos\eta_0}, \tag{2.83}$$

where

$$\tau = \frac{T}{2ad}.$$

Upon substitution we obtain the stress tensor components:

$$h^4\sigma_{\xi\xi} = B\sinh\xi\sin\eta(\cos^2\eta - \cos^2\eta_0 - 2h^2),$$
$$h^4\sigma_{\eta\eta} = B\sinh\xi\sin\eta(\cos^2\eta_0 - \cos^2\eta), \tag{2.84}$$
$$h^4\sigma_{\xi\eta} = B\cosh\xi\cos\eta(\cos^2\eta_0 - \cos^2\eta).$$
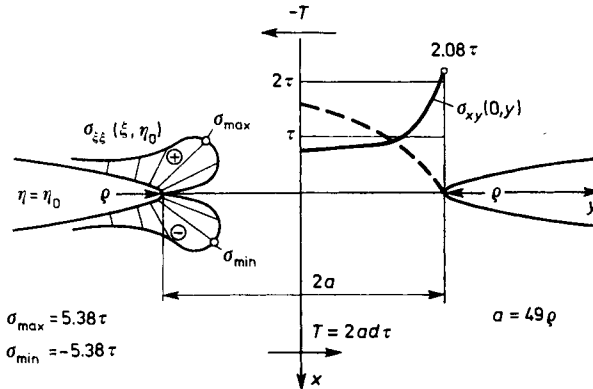
Fig. 2.13. Stress pattern on a surrounding of the notch vertex, shear

The distribution of shear stress $\sigma_{xy}(0, y)$ is given in Fig. 2.13. The character of the distribution of the stress is entirely different from the coorresponding diagram for the beams of the rectangular cross-section without a notch. Besides, normal stresses $\sigma_{\xi\xi}(\eta = \pm\eta_0)$ of considerable value occur in this case.

The conclusions which can be drawn on the basis of the examples considered refer to the deep notches. In the above cases we were assuming that the region on which the forces, corresponding to the three fundamental schemes of loadings, were applied was unbounded. The stresses decrease rapidly with the distance from the apex of the notch, and thus the solutions obtained give very good approximations for the plane structural components with deep notches. It is evident that the existence of the notches induces a considerable

redistribution of stresses dependent on the mode of the loading and on the curvature of the notch at the apex. The maximum value of the stress concentration takes place at the apex of the notch. Similar effects occur with shallow notches, though they are not as profound. In order to obtain numerical results for shallow notches, multiple notches, and the others, the problem has to be solved from the beginning with the corresponding assumptions concerning the shapes of the notches. A number of solutions and the diagrams can be found in the monographs by Neuber, and in relevant books (Savin and Tulchii, 1976; Sih, 1973).

2.5. Stress Concentration in the Vicinity of the Notches for Axially Symmetric Cases

Similarly as in the case of notches in the structural components of rectangular cross-sections leading to the two-dimensional state of stress, the problems of notches in the axially symmetric structural component require solutions of differential equations of the axially symmetric problems of the theory of elasticity. Also in this case, we assume that the notches are deep and that cavities have a shape similar to a disc.

This time we introduce the ellipsoidal system of coordinates:

$$x = \sinh \xi \cos \eta, \quad y = \cosh \xi \sin \eta \cos \zeta,$$
$$z = \cosh \xi \sin \eta \sin \zeta. \tag{2.85}$$

In each of the cases considered it is sufficient to determine three of four harmonic functions φ, ψ_i (2.56), and the stress function F (2.58), and then to determine the stress tensor components (Neuber, 1958). In the case of the problem with a spherical cavity, the ellipsoidal coordinate system reduces obviously to the spherical one. Upon determining functions φ and ψ_i, and the stress function F, we are able to determine the displacement vector $\mathbf{u} = (u_\xi, u_\eta, u_\zeta)$ in the ellipsoidal coordinate system:

$$u_\xi = \frac{1}{h} \left\{ \frac{\partial F}{\partial \xi} - 4(1-\nu)[\Phi_1 \cosh \xi \cos \eta + \sinh \xi \sin \eta (\Phi_2 \cos \zeta + \Phi_3 \sin \zeta)] \right\},$$

$$u_\eta = \frac{1}{h} \left\{ \frac{\partial F}{\partial \eta} + 4(1-\nu)[-\cosh \xi \cos \eta (\Phi_2 \cos \zeta + \Phi_3 \sin \zeta) + \right.$$
$$\left. + \Phi_1 \sinh \xi \sin \eta] \right\}, \tag{2.86}$$

$$u_\zeta = \frac{1}{\cosh \xi \sin \eta} \frac{\partial F}{\partial \zeta} + 4(1-\nu)(\Phi_2 \sin \zeta + \Phi_3 \cos \zeta),$$

where

$$h \equiv \sqrt{\sinh^2 \xi + \cos^2 \eta}.$$

Here the main difficulty is to find potentials φ, and ψ_i such that the boundary conditions are satisfied. Below, we shall discuss two special cases, namely pure bending, and pure torsion. The detailed derivation as well as the solutions referring to the particular cases of tension and shear, and also to all four modes of loadings for cylinders with elongated ellipsoidal cavities can be found in the monograph by Neuber (1958) and in original papers cited therein.

2.5.1. Pure bending

The bending moment in the narrowest cross-section, expressed in the ellipsoidal coordinate system takes the following form of the double integral:

$$M = \int_0^{\eta_0} \int_0^{2\pi} [\sigma_{\xi\xi} \sin\eta \cos\eta \cos\zeta - \sigma_{\xi\eta} \sinh\xi \cosh\xi \cos\zeta +$$

$$+ \sigma_{\xi\zeta} h \sinh\xi \cos\eta \sin\zeta] \cosh\xi \sin\eta \, d\eta \, d\zeta. \tag{2.87}$$

The following potentials satisfy the conditions of the problem, particularly the boundary conditions on the surface of the notch:

$$\varphi = A \frac{\sin\eta \sin\zeta}{\cosh\xi(1+\cos\eta)} + B\left[\cosh\xi(\sinh\xi V - 1) + \right.$$

$$\left. + \frac{1}{3\cosh\xi}\right] \sin\eta \cos\eta \cos\zeta, \tag{2.88}$$

$$\psi_1 = C(\cosh\xi V - \tanh\xi) \sin\eta \cos\zeta,$$

$$\psi_2 = D(\sinh\xi V - 1)\cos\eta, \qquad \psi_3 = 0,$$

where $V = \coth^{-1}(\sinh\xi)$; $A, B, C,$ and D are constants which can be determined from the condition that the constants, in the terms dependent on ξ, in the formulae for stress components $\sigma_{\eta\eta}$, $\sigma_{\xi\eta}$, and $\sigma_{\eta\zeta}$ vanish for $\eta = \eta_0$. In this way we can obtain 8 equations of which only three are independent. The fourth equation can be obtained from Eq. (2.87). We omit here complicated formulae for the components of the stress tensor. The normal stress component at the apex of the notch can be written in the following form:

$$\sigma_{\xi\xi}(0, \eta_0, 0) = \frac{\sigma_n}{N} \frac{3}{4}(\sqrt{a/\varrho+1} + 1)[3a/\varrho - (1-2\nu)\sqrt{a/\varrho+1} + 4 + \nu], \tag{2.89}$$

where

$$\sigma_n = \frac{4M}{\pi a^3}, \qquad N = 3(a/\varrho+1) + (1+4\nu)\sqrt{a/\varrho+1} + \frac{1+\nu}{1+\sqrt{1+a/\partial}}.$$

σ_n denotes the maximum stress in a beam without any cavity, bent by moment M.

It is worth noting that now the stress components depend on Poisson's ratio ν. At the apex of the notch, and in its neighborhood the normal, hoop stress component does not vanish as well

$$\sigma_{\xi\xi}(0, \eta_0, 0) = \frac{3}{4} \cdot \frac{\sigma_n}{N} \frac{a}{\varrho} \left[3\nu \sqrt{1+a/\varrho} + 1 + \nu \right]. \tag{2.90}$$

Now we are able to draw the line of equal values of the normal stress acting on the plane $x = 0$. It turns out that the values of $\sigma_{xx}(0, y, z)$, greater than those calculated from the elementary formula are distributed within the zone resembling the new moon, and not in the shape, for example, of a circle segment, as one could assume erroneously judging from the elementary considerations (see Fig. 2.14).
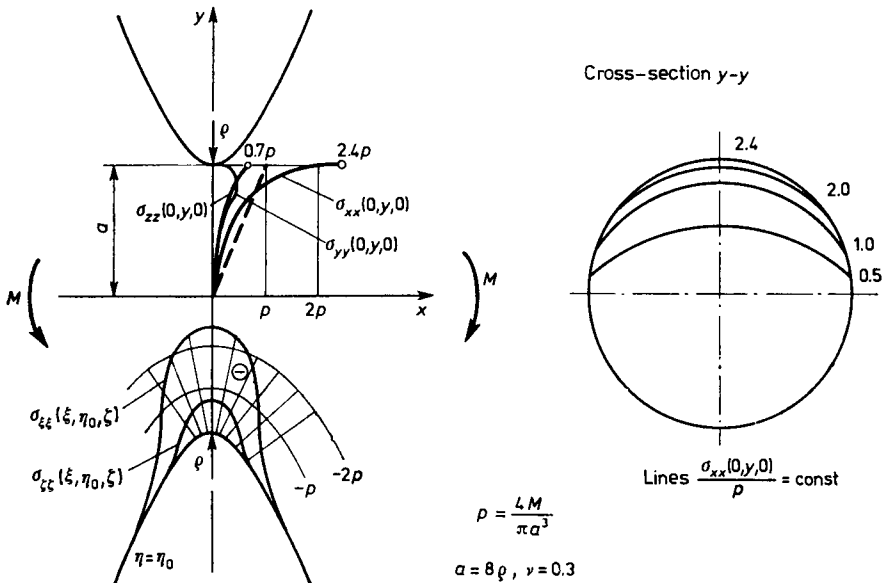
Fig. 2.14. Stress pattern in a surrounding of the notch vertex, bending

2.5.2. Pure torsion

The torque expressed in the elliptical coordinate system assumes the following form:

$$M = 2\pi \int_0^{\eta_0} \sigma_{\xi\zeta} \sqrt{\sinh^2\xi + \cos^2\eta} \, \cosh^2\xi \sin^2\eta \, d\eta. \tag{2.91}$$

The solution of the differential equations of the theory of elasticity, satisfying the boundary conditions on the surface of the notch, can be constructed by means of the following potentials:

$$\varphi = 0, \psi_1 = 0, \psi_2 = -f(\xi, \eta)\sin\zeta, \quad \psi_3 = f(\xi, \eta)\cos\zeta, \quad (2.92)$$

where

$$f(\xi, \eta) = A(\cosh\xi V - \tanh\xi)\sin\eta.$$

The distribution of the shear stress component $\sigma_{\xi\zeta}$ assumes the following form:

$$\sigma_{\xi\zeta} = -4(1-\nu)C\frac{\sin\eta}{h\cosh^2\xi}. \quad (2.93)$$

Substituting into formula (2.92), we obtain

$$M = -\frac{8}{3}\pi(1-\nu)C(2+\cos\eta_0)(1-\cos\eta_0)^2. \quad (2.94)$$

The maximum shear stress, calculated from the elementary formula, in the case of torsion of a cylinder is known to be

$$\tau_n = \frac{2}{\pi}\cdot\frac{M}{a^3}. \quad (2.95)$$

Making use of Eqs. (2.94) and (2.95) and eliminating M and C from Eq. (2.93), and next taking into account the formula for the radius of curvature at the apex of the notch, obtained from the equation of the ellipse $\eta = \eta_0$,
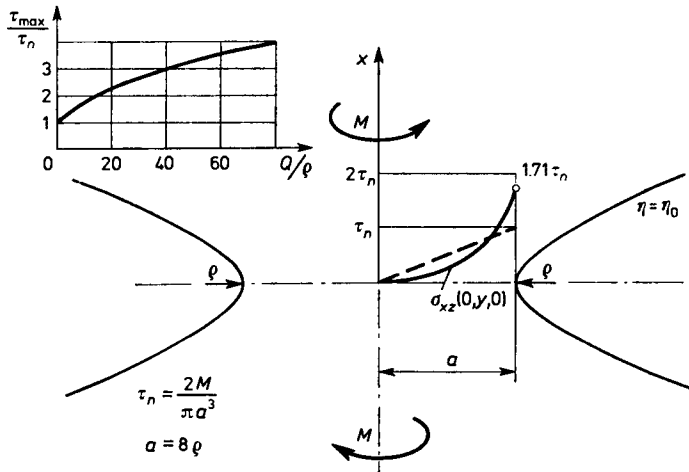
Fig. 2.15. Stress pattern in a surrounding of the notch vertex, torsion

we obtain the value of the maximum shear stress dependent on the ratio a/ϱ (Fig. 2.15)

$$\tau_{max} = \tau_n \frac{3\left(1+\sqrt{1+a/\varrho}\right)^2}{4\left(1+2\sqrt{1+a/\varrho}\right)} \,. \tag{2.96}$$

2.5.3. Bending and torsion of a cylinder with an ellipsoidal cavity

Without the derivation we show the diagrams of the normal stresses $\sigma_{xx}(0, y, 0)$ produced by pure bending, and the shear stresses $\sigma_{\xi\zeta}$ due to torsion of the cylinder with a concentric, axially symmetric, elongated, ellipsoidal cavity. For comparison we present also the stresses computed by the elementary method. The formulae used in the computation and the related method of solution is similar to that considered above in the case of the notches. It is worth noting (Figs. 2.16 and 2.17) that the stresses not only change their

Fig. 2.16. Bending; ellipsoidal void   Fig. 2.17. Torsion; ellipsoidal void

values also there is an essential redistribution of the stresses changing their character. The coefficient of shape, i.e. the influence of the cavity is more pronouncing in the case of bending than in the case of torsion.

3. Stress Concentration in Plates and Shells

3.1. Stress in Plates Around Holes

In the general case of thick plates the problem reduces to the solution of a corresponding problem of the three-dimensional theory of elasticity. There is then no general rule, each case has to be considered separately, and as a rule the solution reduces to the application of the method of finite elements and the use of a computer. In the case of thin plates we can envisage the whole class of problems by means of a unified method, namely the method of a complex variable, and of the conformal mappings. The problem of the bending of thin plates can be reduced to a single differential equation of the fourth order on function $w(x, y)$ of two independent variables, denoting the normal component of the displacement vector of the mid-plane of the plate, i.e. the deflection of the neutral plane of the plate

$$\nabla^4 w(x, y) = -\frac{p(x, y)}{D}, \tag{3.1}$$

where $p(x, y)$ is the loading normal to the plane of the plate, $D = Eh^3/[12(1-\nu^2)]$ denotes the bending plate rigidity, and h is the plate thickness. In order to examine the problems of holes in thin plates and their influence it is sufficient to assume that the bending moments acting along the boundary of the plate are the only loadings. Equation (3.1) then becomes the biharmonic equation.

All the statical quantities, namely bending moments, torques, and shear forces can be expressed in terms of the derivatives of $w(x, y)$. We thus obtain the following formulae:

$$M_x = -D\left(\frac{\partial^2 w}{\partial x^2} + \nu\frac{\partial_2 w}{\partial y^2}\right),$$

$$M_y = -D\left(\frac{\partial^2 w}{\partial y^2} + \nu\frac{\partial^2 w}{\partial x^2}\right),$$

$$M_{xy} = -D(1-\nu)\frac{\partial^2 w}{\partial x \, \partial y}, \tag{3.2}$$

$$T_x = -D\frac{\partial}{\partial x}\left(\frac{\partial^2 w}{\partial x^2} + \frac{\partial^2 w}{\partial y^2}\right),$$

$$T_y = -D\frac{\partial}{\partial y}\left(\frac{\partial^2 w}{\partial x^2} + \frac{\partial^2 w}{\partial y^2}\right).$$

To solve the problem we have to know the boundary conditions. Usually it is assumed that the boundary conditions on the contour of the hole correspond to the free boundary. As an example we consider a simply supported plate of radius a, and next the plate of the same outer radius with the concentric hole of radius b. The comparison of the solutions of the two cases enables us to find the redistribution of bending moments generated by the existence of the hole. Similarly we can compare the solutions for other cases of circular and annular plates loaded by a system of forces and bending moments (Vainberg and Vainberg, 1959).

Let us assume that the plate is loaded by the bending moments M on the supports. Thus we obtain the solution of the partial differential equation (3.1) satisfying the boundary conditions of the simple support for $r = a$ and stress free for $r = b$ (i.e. on the hole). We have:
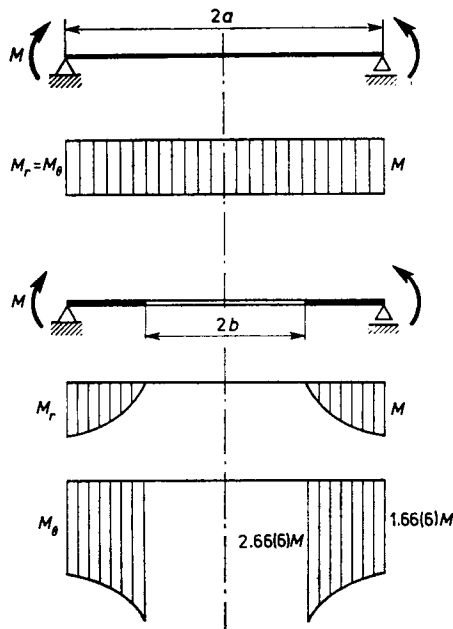
Fig. 3.1. Circular plate with a hole; action of bending moment

(i) the plate without a hole

$$w = \frac{M}{2(1+\nu)D}(a^2 - r^2), \qquad M_r(r) = M_\theta(r) = M, \tag{3.3}$$

(ii) the plate with the hole of diameter $2b$

$$w = \frac{M}{2D}\frac{a^2}{(1+\nu)(a^2-b^2)}\left(a^2 - r^2 - 2\frac{1+\nu}{1-\nu}a^2\ln\frac{r}{a}\right), \tag{3.4}$$

$$M_r = \frac{Ma^2}{(a^2-b^2)r^2}(r^2-b^2), \qquad M_\theta = \frac{Ma^2}{(a^2-b^2)r^2}(r^2+b^2).$$

It is evident from the above formulae that the existence of a very small hole of radius $b \to 0$ results in doubling of the hoop moment M_θ and vanishing, according to the boundary condition at $r = b$, of the radial moment $M_z(b)$. If, for example, $a = 2b$ then on the boundary $r = b$ we obtain $M_\theta = \frac{8}{3}M$.

For the sake of comparison we assume that the plate is subjected to the uniform loading $p(r) = q$. We then obtain the following solutions:
(i) the circular plate ($r \geqslant b$)

$$w = \frac{q}{64(1+\nu)D}\left\{(5+\nu)a^4 - 4(3+\nu)b^2a^2 + 2(1-\nu)b^4 - \right.$$

$$\left. - 2r^2\left[(3+\nu)(a^2 - 2b^2) + (1-\nu)\frac{b^4}{a^2}\right] - 4b^2(b^2 + 2r^2)(1+\nu)\ln\frac{r}{a}\right\},$$

$$M_r = \frac{q}{16}\left[4(1+\nu)b_2\ln\frac{r}{a} + (3+\nu)(a^2 - r^2) + (1+\nu)b^4\left(\frac{1}{a^2} - \frac{1}{r^2}\right)\right], \tag{3.5}$$

$$M_\theta = \frac{q}{16}\left[4(1+\nu)b^2\ln\frac{r}{a} - (1+3\nu)r^2 + (3+ +\nu)a^2 - 4(1-\nu)b^2 + \right.$$

$$\left. + (1-\nu)b^4\left(\frac{1}{a^2} + \frac{1}{r^2}\right)\right],$$

(ii) the annular plate with the hole of diameter $2b$

$$w = \frac{q}{64D}\left\{\frac{2}{1+\nu}[(3+\nu)(a^2 - 2b^2)+k](a^2-b^2) - (a^4-r^4) - \right.$$

$$\left. - \frac{4}{1-\nu}k\ln\frac{r}{a} - 8b^2r^2\ln\frac{r}{a}\right\},$$

where

$$k = b^2\left[3+\nu+4(1+\nu)\frac{b^2}{a^2-b^2}\ln\frac{b}{a}\right],$$

$$M_r = \frac{q}{16}\left[(3+\nu)(a^2-r^2)+k\left(1-\frac{a^2}{r^2}\right)+4(1+\nu)b^2\ln\frac{r}{a}\right], \tag{3.6}$$

$$M_\theta = \frac{q}{16}\left[2(1-\nu)(a^2-2b^2)+(1+3\nu)(a^2-r^2)+\right.$$

$$\left.+k\left(1+\frac{a^2}{r^2}\right)+4(1+\nu)b^2\ln\frac{r}{a}\right].$$
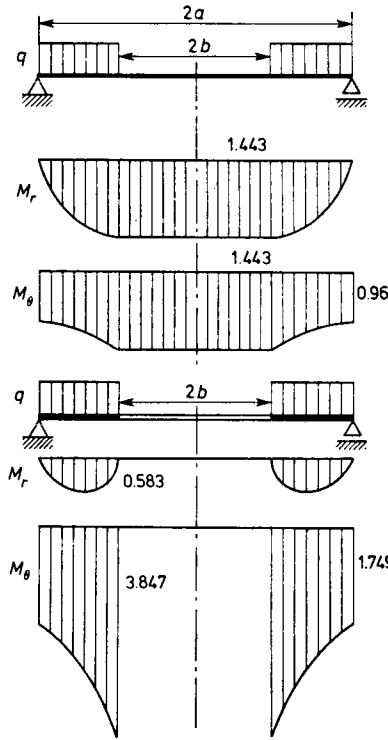
Fig. 3.2. Circular plate with a hole; continuous loading

In Fig. 3.2 we presented the diagrams of the bending moments in the case where the loading is applied on the annular surface $b = 0.5a < r < a$, and for $qa^2 = 16$. The existence of the hole has resulted in the increase of the hoop moment by $3.847/1.443 = 2.6660$ times while in the case of pure bending, and with the same geometry of the plate, we obtain the ratio $8/3 = 2.666(6)$. As we see the difference appears at the fourth place after the decimal point.

As in the case of Airy's function (compare with Eq. (2.6)) the deflection

of the plate can be similarly expressed by two analytical functions of the complex variable $z = x+iy$

$$w(x, y) = \text{Re}[\bar{z}\varphi(z)+\chi(z)]. \tag{3.7}$$

Upon substitution into Eq. (3.2), we obtain the following formulae:

$$\begin{aligned}
M_y - M_x + 2iM_{xy} &= 2D(1-\nu)[\bar{z}\varphi''(z)+\psi'(z)], \\
M_x + M_y &= -2D(1+\nu)[\varphi(z)+\overline{\varphi'(z)}], \\
T_x - iT_y &= -4D\varphi''(z),
\end{aligned} \tag{3.8}$$

where

$$\psi = \frac{d\chi}{dz}.$$

The bending moments, torques, and shear forces have to be uniquely determined. It means that function $\varphi(z)$ has to be determined with an accuracy up to the expression $iCz+\alpha+i\beta$ while $\psi(z)$ up to $\alpha'+i\beta'$ where C, α, β, α', and β' are real constants. If we substitute $\varphi(z) = iCz+\alpha+i\beta$ and $\psi(z) = \alpha' +i\beta'$ into the formula for the displacements $u=iv = -\delta[\varphi(z)+z\overline{\varphi'(z)}+\overline{\psi(z)}]$ where δ denotes the distance from the neutral plane, we find that the components of the displacement correspond to a motion of the plate as a rigid body, without any deformation. In the case of double-connected regions, functions $\varphi(z)$ and $\psi(z)$ assume the following form:

$$\begin{aligned}
\varphi(z) &= Az\ln z+a\ln z+\varphi^*(z), \\
\psi(z) &= a\ln z+\psi^*(z),
\end{aligned} \tag{3.9}$$

where A denotes a real constant, a is a complex constant, $\varphi^*(z)$, and $\psi^*(z)$ are the functions uniquely defined in the plate region. The principal vector of forces and the principal moment along the contour L surrounding the hole can be also expressed by $\varphi(z)$ and $\psi(z)$. We obtain respectively

$$\begin{aligned}
P^* &= 2iD[\varphi'(z)-\overline{\varphi'(z)}]|_L, \\
M_x^* + iM_y^* &= D\{(1-\nu)[\overline{\psi(z)}+z\overline{\varphi'(z)}]-(3+\nu)\varphi(z)-2z[\overline{\varphi'(z)}-\varphi'(z)]\}|_L.
\end{aligned} \tag{3.10}$$

The typical boundary conditions discussed in this method are the following ones:

(i) The first problem. Given bending moments normal to the contour $m(s) = M_n(s)$, and Kirchhoff's forces $p(s) = N_n+\partial M_{nt}/\partial s$, in terms of the boundary arc length.

(ii) The second problem. Prescribed the deflection of the boundary and the value of the derivative in the direction normal to the boundary $\partial w(s)/\partial n$.

(iii) Mixed problem. On the part of the boundary the conditions are prescribed as for the first problem while on the remaining part as for the second problem.

If we introduce the notation

$$f_1 + if_2 = \frac{1}{(1-\nu)D} \int_0^s \left[m(s) + i \int_0^s p(s) \, ds \right] (dx + i \, dy), \tag{3.11}$$

where the integration takes place along the arc of the boundary from a definite point, the boundary conditions can then be written in a simple form (e.g. for the first problem):

$$\varkappa_1 \varphi(z) + z \overline{\varphi'(z)} + \overline{\psi(z)} = f_1 + if_2 + iCz + C_1. \tag{3.12}$$

Here $\varkappa_1 = -(3+\nu)/(1-\nu)$, C denotes a real constant and C_1 a complex constant. In the case of a clamped edge, we make use of the formulae for the derivatives of displacement $w(z)$ in the normal and tangential direction to the contour, and upon relevant evaluations, we obtain the boundary condition in the form

$$\varphi(z) + z \overline{\varphi'(z)} + \overline{\psi(z)} = g_1 + ig_2, \tag{3.13}$$

where

$$g_1 + ig_2 = \left(\frac{\partial w}{\partial n} + \frac{\partial w}{\partial s} \right) \exp(i\alpha),$$

and where α denotes the angle between the normal with respect to the contour and the x-axis. Passing to the new coordinate system $\zeta = \varrho + i\theta$ and introducing the notation $z = \omega(\zeta)$, $\varphi(z) = \varphi[\omega(\zeta)] = \varphi_1(\zeta)$, $\psi(z) = \psi[\omega(\zeta)] = \psi_1(\zeta)$,

$$\varphi[\omega(\zeta)] = \varphi_1(\zeta), \psi(z) = \psi[\omega(\zeta)] = \psi_1(\zeta),$$

$$\Phi(\zeta) = \frac{\varphi_1'(\zeta)}{\omega'(\zeta)}, \qquad \Psi(\zeta) = \frac{\psi_1'(\zeta)}{\omega'(\zeta)},$$

we obtain the formulae

$$M_\varrho + M_\theta = -2D(1-\nu)[\Phi(\zeta) + \overline{\Phi(\zeta)}],$$

$$M_\theta - M_\varrho + 2iM_{\varrho\theta} = \frac{2D(1-\nu)\zeta^2}{\varrho^2 \omega'(\zeta)} [\overline{\Phi'(\zeta)}\overline{\omega(\zeta)} + \Psi(\zeta)\omega'(\zeta)], \tag{3.14}$$

$$T_\varrho - iT_\theta = -\frac{4D\zeta}{\varrho|\omega'(\zeta)|} \Phi'(\zeta).$$

In this new system of coordinates, upon performing the conformal mapping, we obtain the boundary conditions (3.12) and (3.13) on the contour of the circle $\zeta = \sigma$ in the form

$$\varkappa_1 \varphi_1(\sigma) + \frac{\omega(\sigma)}{\overline{\omega'(\sigma)}} \overline{\varphi_1'(\sigma)} + \overline{\psi_1(\sigma)} = f_1 + if_2,$$

$$\varphi_1(\sigma) + \frac{\omega(\sigma)}{\overline{\omega'(\sigma)}} \overline{\varphi_1'(\sigma)} + \overline{\psi_1(\sigma)} = g_1 + ig_2.$$

(3.15)

The solution of the problem of a plate with a hole can be obtained by superposition. Let us assume that the stress state in the plate without the hole is known. We denote this state of stress by M_x^0, M_y^0, M_{xy}^0, T_x^0, T_y^0. The state of stress in the plate with the hole and stress-free contour will be presented as the superposition of two states of stress in the plate without the hole, and a certain additional state denoted by M_x^*, M_y^*, M_{xy}^*, T_x^*, T_y^*. Thus we obtain

$$M_x = M_x^0 + M_x^*, \qquad M_y = M_y^0 + M_y^*, \text{ and so on,}$$

$$\varphi(z) = \varphi^0(z) + \varphi^*(z),$$

(3.16)

$$\psi(z) = \psi^0(z) + \psi^*(z).$$

Passing to the new system of coordinates we obtain, making use of formulae (3.16),

$$\varphi_1(\zeta) = \varphi_1^0(\zeta) + \varphi_1^*(\zeta),$$

$$\psi_1(\zeta) = \psi_1^0(\zeta) + \varphi_1^*(\zeta).$$

(3.17)

Let us substitute formulae (3.17) into the boundary condition (3.12). Since we have assumed that the moments and shear forces vanish on the contour of the hole, the right-hand side of the equation is equal to zero (provided that C and C_1 are also equal to zero, the assumption which has no influence on the value of stresses). Functions $\varphi_1^0(\zeta)$ and $\psi_1^0(\zeta)$, corresponding to the solution of the plate without the hole, are known by assumption. Let us calculate along the contour of the hole γ the following expression:

$$\varkappa_1 \varphi_1^0(\sigma) + \frac{\omega(\sigma)}{\overline{\omega'(\sigma)}} \overline{\varphi_1'^0(\sigma)} + \overline{\psi_1'^0(\sigma)} = -f_1^0 - if_2^0,$$

(3.18)

where σ denotes the points on curve γ. Making use of Eq. (3.12), and next multiplying the conjugated equation by $\dfrac{1}{2\pi i} \cdot \dfrac{d\sigma}{\sigma - \zeta}$ and performing the integration, we obtain the functional equations from which we are able to determine functions $\varphi_1^*(\zeta)$ and $\psi_1^*(\zeta)$, and consequently the additional bending moments and shear forces generated by the existence of the hole:

$$\varkappa_1 \varphi_1^*(\zeta) + \frac{1}{2\pi i} \int_\gamma \frac{\overline{\omega(\sigma)}}{\overline{\omega'(\sigma)}} \overline{\varphi_1^{*\prime}(\sigma)} \frac{d\sigma}{\sigma-\zeta} = \frac{1}{2\pi i} \int_\gamma (f_1^0 + if_2^0) \frac{d\sigma}{\sigma-\zeta},$$

$$\psi_1^*(\zeta) + \frac{1}{2\pi i} \int_\gamma \frac{\overline{\omega(\sigma)}}{\omega'(\sigma)} \overline{\varphi_1^{*\prime}(\sigma)} \frac{d\sigma}{\sigma-\zeta} = \frac{1}{2\pi i} \int_\gamma \overline{f_1^0 + if_2^0} \frac{d\sigma}{\sigma-\zeta}. \tag{3.19}$$

The methods of finding functions $\varphi_1^*(\zeta)$ and $\psi_1^*(\zeta)$ from Eqs. (3.19) are discussed in known monographs (Muskhelishvili, 1935; Savin and Tulchyi, 1971). Now, let us consider some examples.

1. Let us consider the cylindrical bending of a rectangular plate with an elliptical hole. In the case of the plate without a hole, the non-zero bending moments are $M_x^0 = M$, and the solution of the differential equation takes the form

$$w_0(x, y) = -\frac{M}{2D(1-\nu^2)}(x^2 - y^2). \tag{3.20}$$

It is an easy matter to verify that functions $\varphi^0(z)$ and $\psi^0(z)$ are given by the formulae

$$\varphi^0(z) = -\frac{Mz}{4D(1+\nu)}, \quad \chi^0(z) = -\frac{Mz^2}{4D(1-\nu)}. \tag{3.21}$$

If we take into account function $z = \omega(\zeta)$, mapping the exterior of the ellipse on the interior of the unit circle, in the form $z = \frac{a+b}{2}\left(\zeta^{-1} + \frac{a-b}{a+b}\zeta\right)$, we then obtain the following formulae:

$$\varphi_1^0(\zeta) = -\frac{M(a+b)}{4D}\left[\frac{1}{2(1+\nu)}(\zeta^{-1} + m\zeta) + \frac{1-m}{3+\nu}\zeta\right],$$

$$\chi_1^0(\zeta) = -\frac{M(a+b)^2}{8D}\left[\frac{1}{2(1-\nu)}(\zeta^{-1} + m\zeta)^2 - \right.$$

$$\left. -\left(\frac{m}{2}\cdot\frac{m-1}{1-\nu} + \frac{1-m}{2(3+\nu)}\right)\zeta^2 + \left(\frac{m-1}{1-\nu} + \frac{m(m-1)}{3+\nu}\ln\zeta\right)\right], \tag{3.22}$$

where $m = \frac{a-b}{a+b}$, a and b denote the semi-axes of the ellipse. The hoop moment on the contour of the elliptical hole has the form

$$M_\theta = M\left[1 + \frac{2(1+\nu)(1-m)(m-\cos 2\theta)}{(3+\nu)(m^2 - 2m\cos 2\theta + 1)}\right]. \tag{3.23}$$

For example, for $\nu = 0.3$, and $a = 3b$ the maximum value of $M_\theta = 1.263\ M$ occurs at points $\theta = \pm\pi/2$.

2. In order to compare the corresponding formulae in the case of pure bending we take $M_x^0 = M_y^0 = M$. We then obtain

$$\varphi_1^0 = -\frac{M(a+b)}{2D}\left[\frac{1}{2(1+\nu)}(\zeta^{-1}+m\zeta)-\frac{m\zeta}{3+\nu}\right],$$

$$\chi_1^0 = -\frac{M(a+b)^2}{4D}\left[\frac{2m\zeta^2}{(3+\nu)(1-\nu)}-\frac{(m^2+1)\nu-m^2+3}{(3+\nu)(1-\nu)}\ln\zeta\right], \qquad (3.24)$$

$$M_\theta = M\left[2-\frac{4m(1+\nu)(m-\cos 2\theta)}{(3+\nu)(m^2-2m\cos 2\theta+1)}\right].$$

In this case the maximum value of the hoop moment, also for $\nu = 0.3$, and $a = 3b$ amounts to $M_\theta = 3.576\ M$, for $\theta = 0, \pi$ while $M_\theta = 1.475\ M$ for $\theta = \pm\pi/2$.
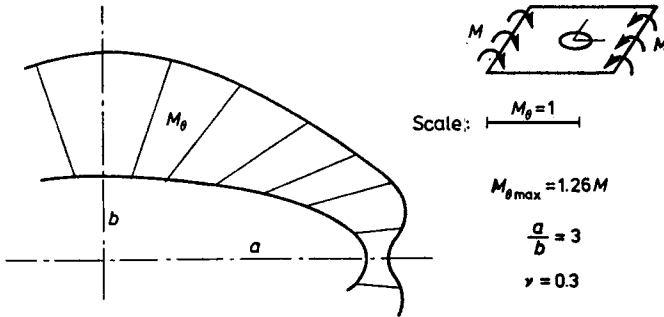
Fig. 3.3. Bending moments along an elliptical hole

In Fig. 3.3 we present the diagram of the hoop moments along the elliptical hole in the case of cylindrical pure bending of a rectangular plate.

3. Let us consider the case of the cylindrical bending of a rectangular plate with the rectangular hole in the plate axis. Let us take function $z = \omega(\zeta)$ mapping the exterior of the rectangular hole on the interior of the unit circle in the approximate form whereby only four terms of the expansion are taken into account

$$z = \omega(\zeta) = R(\zeta^{-1}+0.5\zeta-0.125\zeta^3-0.038\zeta^5), \qquad (3.25)$$

where $R \approx (2/7)(a+b)$ and a and b denote the sides of the rectangular hole. The approximate form of the function (3.25) denotes that the hole is rectangular only approximately, and that the vertices are rounded off with the radius of curvature $\varrho \approx 0.04a$. For the ratio of sides $a/b = 3.24$ we obtain

$$\varphi_1^0(\zeta) = -\frac{MR}{4D(1+\nu)}\left(\zeta^{-1}+\frac{1}{2}\zeta-\frac{1}{8}\zeta^3-\frac{3}{80}\zeta^5\right)-$$

$$-\frac{MR}{2D}(a\zeta_1+a_3\zeta^3+a\zeta^5),$$

$$\chi_1^0(\zeta) = -\frac{MR^2}{4D(1-\nu)}\left(\zeta^{-1}+\frac{1}{2}\zeta-\frac{1}{8}\zeta^3+\frac{3}{80}\zeta^5\right)+$$

$$+\frac{MR^2}{2D}(c\ln\zeta+c_2\zeta^2+c_4\zeta^4+c_6\zeta^6+c_8\zeta^8+c_{10}\zeta^{10}),$$

(3.26)

where for $\nu = 0.3$ we obtain the following values of the constants:

$a_1 = 0.157244$, $\quad a_3 = 0.039130$, $\quad a_5 = 0.011364$, $\quad c = 1.302730$,

$c_2 = 14.437305$, $\quad c_4 = 32.3340006$, $\quad c_6 = 0.038488$, $\quad c_8 = 0.006696$,

$c_{10} = 0.0010004$.

Assuming in accordance with the boundary condition $M_\varrho = 0$, we obtain from Eq. (3.14) the formula for the hoop bending moment

$$M_\theta = M\left[1+\frac{2(1+\nu)(B+C\cos2\theta+D\cos4\theta+E\cos6\theta)}{365-316\cos2\theta+144\cos4\theta+96\cos6\theta}\right],$$

(3.27)

where the constants B, C, D, and E depend on Poisson's ratio, and for $\nu = 0.3$ have the following values: $B = 0.030618$, $C = -6.029029$, $D = -30.326493$, $E = -14.545454$.

4. In order to compare the results, we examine the case of pure bending of a plate with a rectangular hole. Taking into account the same mapping function as before, given by Eq. (3.25), and considering a plate with an identical rectangular hole, we obtain

$$\varphi_1^0(\zeta) = -\frac{MR}{2D(1+\nu)}\left(\zeta^{-1}+\frac{1}{2}\zeta-\frac{1}{8}\zeta^3-\frac{3}{80}\zeta^5\right)-$$

$$-\frac{MR}{D}(a_1\zeta+a_3\zeta^3+a_5\zeta^5),$$

(3.28)

$$\chi_1^0(\zeta) = \frac{MR^2}{2D}(c\ln\zeta+c_2\zeta^2+c_4\zeta^4+c_6\zeta^6),$$

where, for $\nu = 0.3$, we obtain the following values of the constants:

$a_1 = -0.155379$, $\quad a_3 = 0.0366428$, $\quad a_5 = 0.011364$, $\quad c = 1.4318011$,

$c_2 = -0.923463$, $\quad c_4 = 3.316833$, $\quad c_6 = 0.108225$.

Now the bending moment M_θ can be expressed by the following approximate formula:

$$M_\theta = M\left[2 + \frac{2(1+\nu)(B+C\cos 2\theta+D\cos 4+E\cos 6\theta)}{365-316\cos 2\theta+144\cos 4\theta+96\cos 6\theta}\right], \qquad (3.29)$$

where, for $\nu = 0.3$, we obtain $B = -66.337729$, $C = 116,06599$, $D = 55.912486$, $E = -29.090909$.
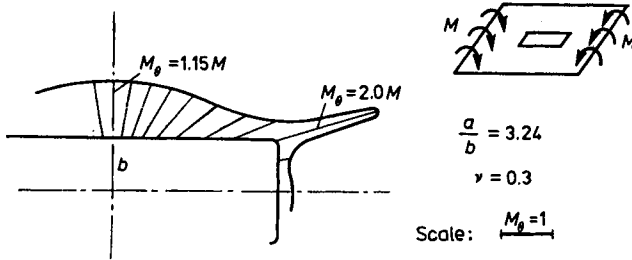
Fig. 3.4. Bending of circular plate having a rectangular hole
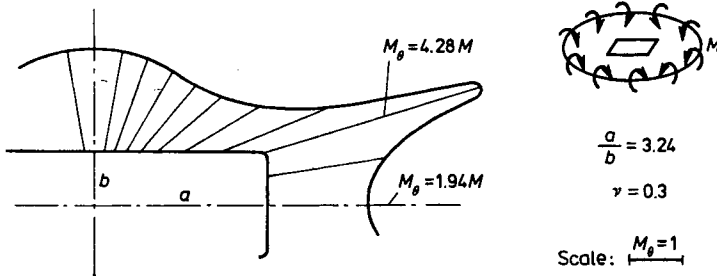
Fig. 3.5 Bending of circular plate having a rectangular hole

In Figs. 3.4 and 3.5 we have shown the distribution of the bending hoop moment along the boundary of the approximately rectangular hole, where four terms in the expansion (3.25) have been taken into account, in the cases of cylindrical and pure bending of the plate. The ordinates of the bending moments M_θ are measured along the radius in the polar coordinate system. In the case of cylindrical bending the maximum bending moment occurs at the "vertices" of the rectangle and amounts to 1.998 M, and at the middle of the longer side of the rectangle (1.149 M). Similarly in the case of pure bending we obtain the values of the bending moment M_θ at the "vertices" $M_\theta = 4.280$ M, and at the midpoint of the shorter side $M_\theta = 1.944$ M.

In both cases the decrease in the value of the radius of curvature at the rounded off vertices entails the increase in the value of the bending moment.

In the exact case of the rectangle, we obtain the singularity in the value of the hoop bending moment, which becomes unbounded within the framework of the theory of elasticity.

3.2. Effect of Reinforcements on the Stress Concentration Around Holes

The notches and holes in the structural components are, as a rule, the neccessities resulting from the working conditions of the structure. From the standpoint of the strength of materials, the notches and holes generate the stress redistribution and the stress concentration dependent on the shapes of the holes or notches, the way of application of forces, mechanical properties of the material, and so on. In many cases we try to avoid or to reduce the stress concentration by corresponding shape design of the structural component, the use of certain reinforcements, thickening the region surrounding the hole. It is difficult to mention all the means used by constructors having in attempt to decrease the stress concentration. Sometimes, it turns out that an additional hole or even a decrease in rigidity serves the purpose.

There is another aspect to deal with such problems. There are many reasons for two or more structural components having to be connected, for example a bent plate and a pipe passing through the hole. The question then arises how such two components affect each other and how the stress concentration changes as a result. The investigation of the influence of the reinforcements on the stresses around the holes is significant in engineering practice. The solutions of particular cases of the bending and tension of the plates with reinforcements around the holes, are given in a catalogue Savin and Tulchyi (1976), and in monographs Savin and Tulchyi (1971) and Vainberg and Vainberg (1959) and in the original papers cited therein.

The simplest case constitutes a circular plate (in fact annular) with a concentric hole and reinforcement in the shape of an annulus, and different material constants. A similar problem involves a circular plate with a hole and step-wise varying thickness. We can pass from the problem of the plate with varying thickness to the problem with reinforcing annulus assuming

$$\frac{D_1}{D_p} = \left(\frac{\delta_1}{\delta_p}\right)^3,$$

where D_1 denotes the bending rigidity of the annular reinforcement, δ_1 the thickness of the inner annulus of the plate of varying thickness, and D_p and δ_p the same quantities for the plate and the outer part of the plate with varying thickness, respectively. In the case where the hole is circular we make use of the polar system of coordinates. We obtain the following formulae:

$$M_\theta - M_r + 2iM_{r\theta} = 2D(1-v)[\bar{z}\varphi''(z)+\psi'(z)]\exp(2i\theta),$$

$$M_\theta + M_r = -4D(1+v)\,\mathrm{Re}\,[\varphi'(z)],\tag{3.30}$$

$$T_r - iT_\theta = -4D\varphi''(z)\exp(i\theta).$$

Let us denote by R_0 and R_1 the inner and outer radii of the reinforcing annulus, respectively. The problem can be generalized to the case of a number of n annuli of different bending rigidity. If functions $\varphi_1(z)$ and $\psi_1(z)$ are the solutions in the region of the annulus, and $\varphi_p(z)$ and $\psi_p(z)$ in the region of the plate, respectively, then the boundary conditions for $r = R_0$ take the form

$$D_1\{(1-v_1)[\bar{z}\varphi_1'(z)+\psi_1(z)]-(3+v_1)\overline{\varphi_1(z)}\} = f_1 - if_2,\tag{3.31}$$

where

$$f_1 - if_2 = -R_0\int_0^\theta\left[im(\theta)+R_0\int_0^\theta p(\theta)\,d\theta\right]\exp(-i\theta)\,d\theta,$$

$m(\theta)$ is the distribution of the bending moments on the unit length of the boundary, $p(\theta)$ of the shear forces, respectively. The boundary condition on the contour L bounding the plate takes the following form:

$$D_p\{(1-v_p)[\bar{z}\varphi_p'(z)+\psi_p(z)]-(3+v_p)\overline{\varphi_p(z)}\} = f_{1p} - if_{2p},\tag{3.32}$$

where in the case where L is the contour of the circle of radius R_2, we obtain

$$f_{1p} - if_{2p} = -R_2\int_0^\theta\left[im(\theta)+R_2\int_0^\theta p(\theta)\,d\theta\right]\exp(-i\theta)\,d\theta.$$

Besides the above boundary conditions we have to satisfy the continuity conditions between the plate and the annulus, for $r = R_p$. The first condition denotes the continuity of Kirchhoff's force, the second one the continuity of the radial bending moments, the third one the continuity of the displace-

ments: $u+iv = -\delta\left(\dfrac{\partial w}{\partial x}+i\,\dfrac{\partial w}{\partial y}\right),$

$$D_1(1-v_1)[\psi_1(z)+\bar{z}\varphi_1'(z)]-(3+v_1)\overline{\varphi_1(z)}\}$$
$$= D_p\{(1-v_p)[\psi_p(z)+\bar{z}\varphi_p'(z)]-(3+v_p)\overline{\varphi_p(z)}\},\tag{3.33}$$

$$\psi_1(z)+\bar{z}\varphi_1'(z)+\varphi_1(z) = \psi_p(z)+\bar{z}\varphi_p'(z)+\overline{\varphi_p(z)},\tag{3.34}$$

$$\mathrm{Re}[\chi_1(z)+\bar{z}\varphi_1(z)] = \mathrm{Re}[\chi_p(z)+\bar{z}\varphi_p(z)].\tag{3.35}$$

The easiest examples of the problems to solve concern pure bending of an infinite plate with the hole of circular cross-section and annular reinforcement and a circular plate with concentric hole and annulus. The value of

stress concentration depends to a large extent on the ratio of the bending rigidity of the plate to that of the annulus. In the limit cases we obtain the plate with the hole without the reinforcing annulus or the rigid clamping along the boundary between the plate and annulus. Let us consider cylindrical bending of the plate strip with a circular hole and concentric annulus. The plate strip is bent by moments $M_x = M$. We then obtain for the plate $(r > R_p)$:

$$\chi(z) = -\frac{MR_p^2}{4D}\left(\frac{1}{1-\nu}z^2R_p^{-2}+\alpha\ln z+\alpha_{-2}R_p^2z^{-2}\right),$$

$$\varphi(z) = -\frac{MR_p}{4D}\left(\frac{1}{1+\nu}zR_p^{-1}+\beta_{-1}R_pz^{-1}\right),$$

(3.36)

and for the annulus $R \leqslant r \leqslant R_p$:

$$\chi_1(z) = -\frac{MR^2}{4D}(a_2z^2R^{-2}+a\ln z+a_0+a_{-2}R^2z^{-2}),$$

$$\varphi_1(z) = -\frac{MR}{4D}(b_3z^3R^{-3}+b_1zR^{-1}+b_{-1}Rz^{-1}),$$

(3.37)

where the coefficients α, α_{-2}, β_{-1}, a_0, a, a_{-2}, a_2, b_{-1}, b_1, and b_3 can be determined from the system of algebraic equations resulting from the boundary conditions and the continuity conditions between the plate and the annulus. We have, for example,

$$\alpha = -\frac{2n^2}{1+\nu}\left\{1-\frac{2[(1+\nu_1)+n^2(1-\nu_1)]}{L}\right\},$$

$$b_1 = \frac{2n^2}{(1+\nu)L}(1-\nu_1),$$

where $n^2 = R_p/R$ denotes the ratio of the annulus radius to that of the hole, ν_1 is the Poisson ratio for the annulus while

$$L = (1-\nu_2^2)(n^2-1)\frac{D_p}{D}+(1-\nu)[(1+\nu_1)+n^2(1-\nu_1)];$$

the remaining coefficients can be expressed by similar formulae. The bending moments, radial and hoop, and the shear forces assume the following form:

$$M_r = \frac{M}{2}\left\{\left(1-\frac{1-\nu}{2}\alpha R_p^2r^{-2}\right)+\right.$$

$$\left.+[1-2\nu\beta_{-1}R_p^2r^{-2}+3(1-\nu)\alpha_{-2}R_p^4r^{-4}]\cos 2\theta\right\},$$

$$M_\theta = \frac{M}{2}\left\{\left(1 + \frac{1-\nu}{2}\alpha R_p^2 r^{-2}\right) - \right.$$ (3.38)

$$\left. - [1 + 2\nu\beta_{-1}R_p^2 r^{-2} + 3(1-\nu)\alpha_{-2}R_p^4 r^{-4}]\cos 2\theta\right\},$$

$$T_r = 2MR^2 r^{-3}\beta_{-1}\cos 2\theta,$$
$$T_\theta = 2MR^2 r^{-3}\beta_{-1}\sin 2\theta.$$

Similar formulae can be written for the reinforcing annulus (Savin, 1968).
The following conclusions can be drawn from the above discussion.
1. It is helpful to apply the reinforcing annuli made of the materials whose bending rigidity is greater than that of the plate.
2. The clamping of the hole results in the stress concentration of σ_{rr}.
3. The diagrams and the nomograms for the determination of the optimum ratio of the bending rigidities dependent on the ratio of the diameters of the hole and that of the annulus can be found in monographs (see Savin and Tulchyi, 1973) or in the original reports. The case of the cylindrical bending of the plate is given in diagram form in Fig. 3.6.
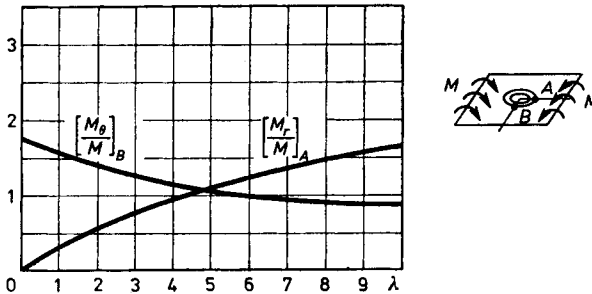
Fig. 3.6. Diagram of bending moments

3.3. Stress Concentration Around the Holes in Thin Shells

The holes in elastic shells generate, as a rule, stress concentrations and redistribution of stresses. The results of usually quite complicated solutions can be found in the original paper on the subject. It is difficult to give a general method or even the directions that would be valid in all cases considered, unless we advise to use the numerical approach and apply, say, the finite element method. The solutions of the stress concentration problems around the holes in shells are more complicated than in the case of the plates or two dimensional problems of the theory of elasticity since here also the radii of the shell curvature play a significant role. The results valid for a spherical

or ellipsiodal shell can be unacceptable in the case of the hyperboloidal shell. The sign of the Gauss curvature plays here an essential role. In the theory of shells in each particular case we consider separately the corresponding boundary value problem.

Here we confine ourselves to the presentation of only certain general remarks referring to characteristic features of the stress concentration around the holes in the theory of elastic shells. As examples, most common in the engineering practice, let us mention here the stress concentration around the holes in spherical domes, in tanks at the places of joints with the manholes, bottom outlets, and instalation holes. Much more complicated problems are encountered with aeronautical, aeroplane, and naval structures. However, in these problems we have to consider the dynamical effects and the dynamical stress concentration (see Sih (Ed.), 1973) which are not discussed here.

In the statical cases the following characteristic factors affect the stress concentration in shells:

(i) The coefficient of shape increases with the decrease in the curvature of the contour; the stress concentration can be unbounded at the points where the tangent to the contour ceases to be continuous.

(ii) The stress concentration depends considerably on the values of the curvature radii of the shell, and on the sign of Gauss' curvature of the shell surface.

(iii) From the standpoint of the strength, it is particularly undesirable to place the holes in the regions of high stress values.

(iv) If the shell without a hole is in a membrane state of stresses, the existence of the hole may change it and generate the bending state of stress.

4. Theory of Fracture of Structural Components

4.1. Traditional Strength Criteria

There are two fundamental assumptions in the classical strength hypotheses: the first is that the material of which a structural component has been manufactured is ideally continuous, and the second is that the pertinent strength criterion, or condition, can be formulated within the framework of the linear theory of elasticity. To this purpose one has to determine the state of stress and strain, and next to find the regions of extremal values of certain representative quantities. The increase in loadings can generate in such regions cracks or permanent, plastic deformations of values considered to be unsafe. We thereby speak of the strength effort of the material, having in mind a certain function the numerical value of which describes the extent that unsafe values of the permanent strain of cracks are attained.

The strength hypotheses have a long history (Timoshenko, 1966). Chronologically, the first one was the maximum tensile stress theory belonging to Galileo. This theory could not be accepted as a universal one since it failed for example in the case of pure compression, leading to an unbounded value of strength. The formulation of the maximum tensile stress theory can be found in the papers by Mariotte (Huber, 1948). This hypothesis became popular and was used for a long period of time mainly in Germany. The next theory worth noting is the hypothesis of the maximum difference of the principal stresses, called the *theory of the maximum shear*. The two theories belong to the group of the hypotheses of a single constant since according to these theories one quantity defines the strength criterion. The newer theories of this type include the energy hypotheses: maximum strain energy theory (Beltrami, 1885), the maximum distortion strain energy theory (Huber, 1904, von Mises, 1913) (though the idea of such a theory was already mentioned in a letter of Maxwell to Thomson), and the modified theory of the maximum distortion strain energy (Huber, 1905; cf. Huber, 1948). The hypothesis of slip with friction can be traced as far back as 1772 in a

paper by Coulomb and belongs to the theories with two constants. Its generalization by Mohr gained much popularity in Europe at the beginning of 20th century, however this concept was fiercely criticized for certain logical errors by Voigt, and by Huber in Poland.

The elastic strain energy accumulated in a unit volume of a body in a three-dimensional state of stress can be expressed by the formula

$$\Phi = \frac{1}{2}\,\varepsilon_{ij}\sigma_{ij}, \quad i,j = 1,2,3. \tag{4.1}$$

If we assume that the uniform compression has no practical influence on the strength effort of the material we shall be able to neglect the voluminal part of the strain energy Φ_v. We then obtain the following expression for the pure distortion strain energy:

$$\Phi_f = \Phi - \Phi_v = \frac{1+\nu}{6E}\,[(\sigma_{xx}-\sigma_{yy})^2 + (\sigma_{yy}-\sigma_{zz})^2 +$$
$$+ (\sigma_{zz}-\sigma_{xx})^2 + 6(\sigma_{xy}^2 + \sigma_{yz}^2 + \sigma_{zx}^2)]. \tag{4.2}$$

In the case of the uni-axial state of stress, i.e. where $\sigma_{xx} = \sigma$, is the only non-vanishing stress component, we obtain

$$\Phi_f = \frac{1+\nu}{6E}\,\sigma^2. \tag{4.3}$$

If we next assume that σ denotes the reduced stress and compare the both formulae, we obtain

$$\sigma_{red}^2 = \sigma_{xx}^2 + \sigma_{yy}^2 + \sigma_{zz}^2 - \sigma_{xx}\sigma_{yy} - \sigma_{yy}\sigma_{zz} - \sigma_{zz}\sigma_{xx} +$$
$$+ 3(\sigma_{xy}^2 + \sigma_{yz}^2 + \sigma_{zx}^2). \tag{4.4}$$

The numerical value of σ_{red} cannot, at any point of the structural member, exceed the value of the admissible stress which we assume as the safe stress found from the tension test or the compression test

$$|\sigma_{red}| \leqslant |\sigma_{adm}|.$$

It turns out that the formula for the distortion strain energy (4.2) can have, up to a multiplicative constant, certain other physical or mathematical interpretations. We get the identical formula when comparing two second invariants of the stress deviators. This postulate belongs to von Mises, and criterion (4.4) is called the *Huber–Mises condition*. We should add that formula (4.2) multiplied by a constant is equal to the octahedral shear stress component squared, and when multiplied by another constant the mean

value of the squares of the principal shear stresses. These hypotheses concern isotropic and homogeneous materials. There are numerous strength theories that take into account the other invariants of the stress tensor, or consider the probability of the occurrence of microcracking or of plastic regions. Here, we can mention Burzyński's theory of invariants which generalizes the concept of von Mises, and the theories in which the appearance of micro-cracks is treated in a different way than the yielding. In this respect we can mention Davidenkov-Fridman theory (compare Krzyś and Życzkowski, 1962). The corresponding theories for anisotropic materials also have been developed (Tsai, 1971). So far, attempts to formulate a universal strength theory have failed, and it seems to us that the construction of such a universal hypothesis is not feasible.

4.2. Theoretical Strength, Calculations Based on the Strength Theories

The numerical value of the admissible stresses is found from an experimental test for ultimate strength, for example from the tension test. The ultimate strength differs considerably from the theoretical strength of an ideal material. The theoretical strength can be obtained by considering the interaction of two layers of atoms. In a rough approximation the forces acting between the layers of atoms can be represented in the form of the diagram 4.1, where r_0
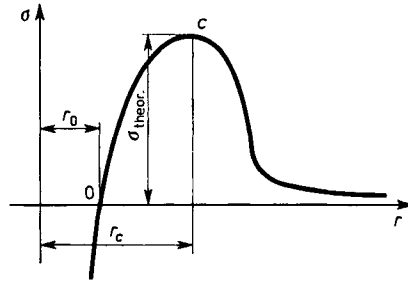
Fig. 4.1. Intermolecular interaction forces

denotes the distance between the two layers. Point O corresponds to the rela-tive equilibrium state between the forces of attraction and repulsion, r_c is the distance for which the maximum value of stress occurs (or in other words the theoretical strength), and the angle of the tangent at point O denotes Young's modulus. Approximating curve OC by the sinusoidal one (Kacha-nov, 1974)

$$\sigma \cong \sigma_{\text{theor}} \sin\left(\frac{\pi}{2} \frac{r_0 \varepsilon}{r_c - r_0}\right), \quad \text{where} \quad \varepsilon = \frac{r - r_0}{r_0},$$

we obtain $E = (d\sigma/d\varepsilon)|_{\varepsilon=0}$, whence we have $\sigma_{\text{theor}} = 10^{-1}\ E$, while the ultimate value of strength, for example for steel amounts to $\sigma_{\text{ult}} \cong 2 \cdot 10^{-3}\ E$. Practically, all the strength theories are based on the assumption of a continuous medium, usually linearly elastic one. However, a series of important aspects is tacitly neglected. For example:

  (i) The effect of scale is neglected. Instead of considering a structural member, we investigate the "material" without taking into account the geometry of the specimen.

 (ii) We do not consider the structure of the material, assuming its continuity. It is not immaterial whether the part of the structure is made of metal or plastic, etc.

(iii) The effect of the boundary, and surface quality are usually neglected.

(iv) The process of failure itself is not considered. In most of the strength theories it is immaterial whether the failure has been caused by fracturing, yielding, or creep.

    Attempts were made to determine why the theoretical strength is so much different from the ultimate strength test. Here, we shall mention only two interesting experiments. Yoffe with his collaborators investigated the tensile strength of monocrystals of white salt under conditions where the surfaces of the salt specimen were moistened. The results of the experiments have proved that the theoretical value of the strength was real, and the tests gave the values of the same order of magnitude as the computed theoretical strength. Similar results can be obtained in the investigations of the metal monocrystals in the form of small diameter strings. Also in these experiments the strength was close to theoretical and the relative elastic elongation was equal to 0.05. The explanation of the discrepancy between the theoretical and ultimate values of strength becomes evident when we take into account the results of metallographic investigations supplying us with the data concerning the structure of the material. As a rule the material is never ideally homogeneous, but frequently of grain structure with cracks between crystals, and with inclusions. It turns out that the state of stresses close to uniform in the case of a homogeneous body is disturbed by the existence of internal and boundary cracks and small inclusions. Metallurgical investigations exhibit the existence of dislocations and cracks of dimensions from interatomic up to macrocracks. We arrive at the following conclusion: the state of stress has to be determined by taking into account the internal structure of the material which, incidently, can be random. The state of stress of a body with cracks can be determined even within the framework of the linear theory of elasticity. However, it then turns out that the stresses increase unboundedly at crack tips and depend on the value and direction of the applied loadings.

The calculations based on any strength theory fail in such cases since even for very small forces the existence of the cracks means that the admissible stress exceeded. A similar effect occurs in the cases of sharp notches. Experimental evidence shows that small loadings are not sufficient for the failure of a specimen or the development of the cracks in the specimen. The state of stress can be determined from the theory of an elastic or elastic-plastic continuum. Thus, we are interested in finding the critical values of the lovdings which cannot be exceeded, otherwise the catastrophic increase of a crack can be expected. The methods of the theory of elasticity do not provide us, without additional postulates, the means to solve such problems. In the problems of the mechanics of fracture we can distinguish a series of problems. By the *mathematical theory of cracks* we understand the theory enabling us to solve the boundary value problems within the framework of the theory of elasticity, or another theory of continuum, statical, quasistatical and dynamical one. This is not the theory of fracture yet. The critical loadings can be determined when we introduce certain additional assumptions. Such a problem was posed and solved for the first time by Griffith in 1920 (Griffith, 1921).

4.3. Griffith's Theory, Fracture of Brittle Materials

Griffith investigating cracking of glass came to the conclusion that a low strength of brittle materials results from the existence of microcracks and the stress concentration around the crack tips. It is known from experiments that if the critical value of loading has to be exceeded, then the crack starts developing creating new surface. Griffith assumed that in the process of a crack developing the energy necessary to create new surface plays an essential role. Let us take a single crack of length $2l$ in an infinite plate and let us compute the elastic strain energy for the plate with the crack $U = U_0 - -\Delta U$ where U_0 denotes the strain energy of the plate without the crack, ΔU denotes the change of the elastic potential due to the existence of the crack, and γ is the surface energy of the unit free surface. U can be found from the solution of the corresponding problem of the theory of elasticity. Griffith had taken into account the solution of Inglis who considered a plate with an elliptical hole. The passage to the limit zero with the shorter semi-axis of the ellipse corresponds to the solution of the crack problem. In the case of the plane stress state, we obtain

$$\Delta U = \pi l^2 p^2 / E, \tag{4.5}$$

while for the plane state of strain

$$\Delta U = \frac{1-\nu^2}{E}\,\pi p^2 l^2. \tag{4.6}$$

The energy consists of the elastic potential and the surface energy

$$\Phi = U + 4\gamma l = U_0 - \Delta U + 4\gamma l. \tag{4.7}$$

The necessary condition for the existence of the extremum of function (4.7) is that the first derivative of the function vanishes. After simple calculations we obtain the value of the critical loading. We obtain for the plane state of stress

$$p_{cr} = \sqrt{\frac{2E\gamma}{\pi l_{cr}}}, \tag{4.8}$$

and similarly for the plane state of strain

$$p_{cr} = \sqrt{\frac{2E\gamma}{\pi l_{cr}(1-\nu^2)}}. \tag{4.9}$$

These formulae refer to the plate of unit width. The diagram of function Φ and its maximum for l_{cr} is shown in Fig. 4.2. The value of the surface
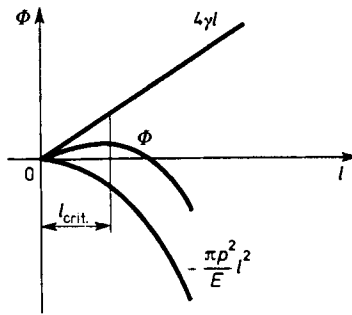
Fig. 4.2. Diagram of the function Φ in Griffith's criterion

energy has to be determined experimentally. Griffith found it by investigating the surface tension of the liquid, or semi-liquid qlass in the temperature range of 750–1100°C, and next, finding that the tension is almost linearly dependent on temperature, he extrapolated it linearly to 15°C. The value of the surface energy at 15°C was used in finding the critical length of the cracks. The experimental results agreed well with the theory for the plane state of stress. On the other hand, when the critical length and load are known, we can compute using this theory the value of the surface energy at room temperature. In spite

of the very simple approach Griffith's theory constitutes a very good point
of departure, and the limiting case of more complicated theories. In this
respect Griffith's fracture mechanics plays a role similar to that of the theory
of elasticity in the mechanics of deformable solids. On the other hand, the
Griffith concept constituted a breakthrough in the approach to the problems
of the strength effort of brittle materials. The main point is that the strength
of brittle materials cannot be determined by the methods ot the theory of
elasticity only, without an introduction of an additional assumption, in this
case the notion of the surface energy. In later theories, the concept of the
surface energy was replaced by taking into account some other quantities,
for example the forces of cohesion in the theory of Khristyanovich–Baren-
blatt. For brittle materials the plastic zone in the vicinity of the crack tips
is negligible, theoretically it is assumed that there is no plastic region at all.
In the case of quasi-brittle materials the plastic region does exist, and the
value of the energy of the plastic dissipation exceeds considerably the numeri-
cal value of surface energy. Moreover, the extrapolation for finding the
value of the surface energy for metals in the manner carried out by Griffith
for glass, may be considered doubtful.

4.4. The Modes of Cracks, Stress Intensity Factors

Theoretically cracks are treated as surfaces or lines of discontinuity of the
displacement vector. In the Cartesian coordinate system, for $\mathbf{u} = \mathbf{i}u+\mathbf{j}v+\mathbf{k}w$,
a crack can mean the discontinuity of all three components of the displace-
ment vector u, v, and w. Departing from this fact, Irwin distinguished in a
two-dimensional case three possible kinematical modes of the mutual
displacement of crack surfaces. In Fig. 4.3 we have shown the three modes
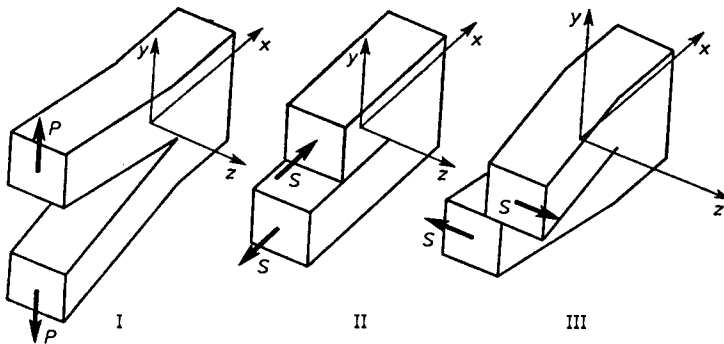
Fig. 4.3. Kinetic modes of cracking

of cracks and the corresponding displacements. Mode I—tensile, the displacements of the crack surfaces are normal to the undeformed crack surface. Mode II—longitudinal shear, the displacements of the crack surfaces are such that they slide each with respect to the other, remaining in the same plane of the plate. Mode III—transversal shear, the crack surfaces slide mutually, however this time in the direction perpendicular to the plate plane. This case is called "anti-plane".

If we use the coordinate system as shown in Fig. 4.3, and solve the corresponding equations of the theory of plasticity, for the loadings corresponding to the three modes of displacements, we shall find that the behaviour of the stress components in the neighborhood of the crack tip, can be written in the following form, respectively for the modes I, II, and III:

$$\sigma_{yy}(x, 0) = \frac{k_{\mathrm{I}}}{\sqrt{2(x-a)}} + O(1), \quad \sigma_{xy}(x, 0) = \frac{k_{\mathrm{II}}}{\sqrt{2(x-a)}} + O(1),$$

$$\sigma_{yz}(x, 0) = \frac{k_{\mathrm{III}}}{\sqrt{2(x-a)}} + O(1). \tag{4.10}$$

The three coefficients k_{I}, k_{II}, and k_{III} are called the *stress intensity factors* for normal and shear stress, respectively. They determine the local behaviour of the stresses, and play an important role in the theory of quasi-brittle materials. The theoretical values of the stress intensity factors, occurring in formulae (4.10) can be found from the solutions of two-dimensional problems of the theory of elasticity, for example in the plane state of strain, or generalized plane state of strain, and they depend on the geometry of the crack, and on the applied loadings (*Technological Mechanics*, 1978). The influence of the plastic zone is neglected here. The stress intensity factor k_{I} can be computed (Cherepanov, 1974), from the formula

$$k_{\mathrm{I}} = \frac{2}{\pi} \int_0^1 \frac{p(u)}{\sqrt{1-u^2}} \, du, \tag{4.11}$$
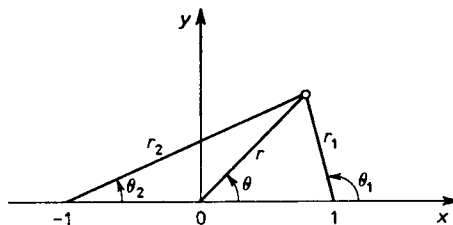
Fig. 4.4. Coordinate system

where $p(x)$ denotes the distribution of pressure on the crack surfaces. We can pass to the coordinate system shown in Fig. 4.4, obtaining very useful formulae:

$$\sigma_{xx} = \frac{rk_{\mathrm{I}}}{\sqrt{ar_1 r_2}} \left[\cos(\theta - \tfrac{1}{2}\theta_1 - \tfrac{1}{2}\theta_2) - \frac{1}{r_1 r_2} \sin\theta \sin\tfrac{3}{2}(\theta_1 + \theta_2) \right],$$

$$\sigma_{yy} = \frac{rk_{\mathrm{I}}}{\sqrt{ar_1 r_2}} \left[\cos(\theta - \tfrac{1}{2}\theta_1, -\tfrac{1}{2}\theta_2) + \frac{1}{r_1 r_2} \sin\theta \sin\tfrac{3}{2}(\theta_1 + \theta_2) \right], \qquad (4.12)$$

$$\sigma_{xy} = \frac{rk_{\mathrm{I}}}{\sqrt{ar_1 r_2}} \cos\tfrac{3}{2}(\theta_1 + \theta_2).$$

For the constant pressure p_0, we obtain $k_{\mathrm{I}} = p_0 \sqrt{a}$. The tables of the stress intensity factors can be found in many books and monographs, for example in Tada et al. (1973, Sih (1973) and Cherepanov (1974). If p is a uniform loading at infinity, normal to the crack surface, $2a$ the length of the crack, we then obtain $k_{\mathrm{I}} = p \sqrt{a}$. Similarly $k_{\mathrm{II}} = \tau \sqrt{a}$, $k_{\mathrm{III}} = \tau \sqrt{a}$ where τ denotes the shear stress directed along the x- and y-axes, respectively. The modes of the two-dimensional problems of cracks have their correspondence in the axially symmetric problems. Mode 1 denotes tension of a cylinder or bar of circular cross-section with a concentric crack perpendicular to the cylinder axis. Mode 2 corresponds to the loading by shear forces while Mode 3 is nothing else but the case of pure torsion (see Fig. 4.5).

Now the stress intensity factors assume the following values: $k_1 = \dfrac{2\sqrt{a}}{\pi}$ p_0 where p_0 is the pressure in a penny-shaped crack in an infinite body. In
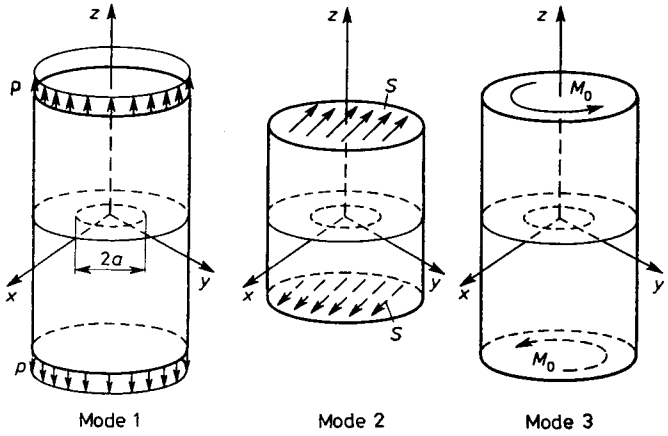
Fig. 4.5. Kinetic modes of cracks; axial symmetry case

the case of a torsion of the cylinder of radius R and torque M_0 the stress intensity factor is equal to $k_3 = \dfrac{a^{3/2}}{\sqrt{\pi R^4}} M_0$. The determination of the stress intensity factor requires, in each case, the solution of the relevant boundary value problem, or a mixed, initial boundary value problem in the dynamical case.
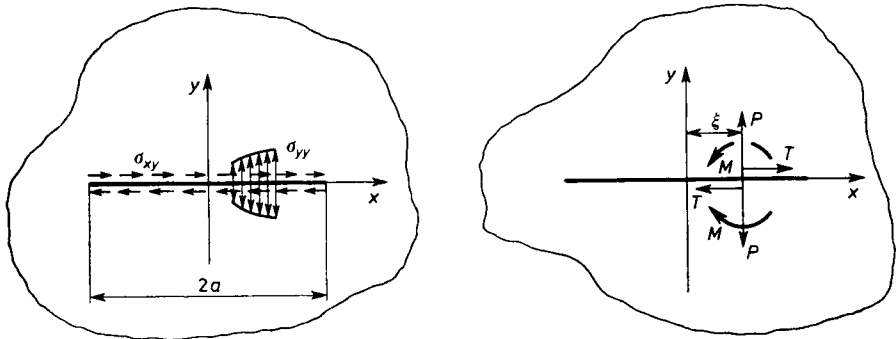
Fig. 4.6. Loading of a crack

Below we list a few examples of the stress intensity factors:

(a) An elastic space with a single crack of length $2a$, two-dimensional problem:

$$k_1 = \frac{1}{\sqrt{\pi a}} \int_{-a}^{a} \sigma_{yy}(x, 0) \sqrt{\frac{a+x}{a-x}} \, dx + a \int_{-a}^{a} \frac{m(x)}{(a-x)\sqrt{a^2 - x^2}} \, dx,$$

$$(4.13)$$

$$k_{\mathrm{II}} = \frac{1}{\sqrt{\pi a}} \int_{-a}^{a} \sigma_{xy}(x, 0) \sqrt{\frac{a+x}{a-x}} \, dx,$$
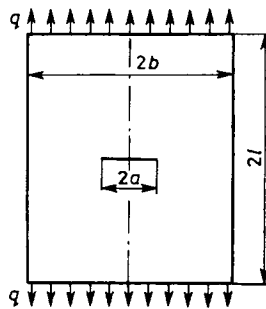
Fig. 4.7. Symmetrical crack

where $m(x) = dM(x)/dx$. For concentrated forces $P(\xi)$ and $T(\xi)$ and a concentrated moment applied at point ξ, we obtain

$$k_{\mathrm{I}} = \frac{1}{\sqrt{\pi a(a^2 - \xi^2)}} \left[P(a+\xi) + \frac{Ma}{a-\xi} \right],$$

$$k_{\mathrm{II}} = \frac{T(a+\xi)}{\sqrt{\pi a(a^2 - \xi^2)}} .$$

(4.14)

(b) Stretched rectangular plate with an internal crack:

$$k_{\mathrm{I}} = q\sqrt{\pi a}\, F(a/b),$$

(4.15)

where function $F(a/b)$ is given below:

a/b	0	0.1	0.2	0.3	0.4	0.5	0.6	0.7	0.8	0.9
$F(a/b)$	1	1.006	1.025	1.058	1.109	1.187	1.303	1.488	1.811	2.470
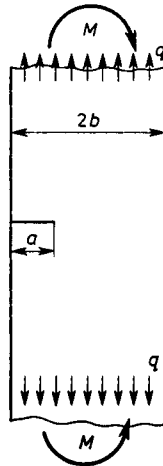
Fig. 4.8. Edge crack

(c) Tension and bending of a layer with a boundary crack:
tension:

$$k_{\mathrm{I}} = q\sqrt{\pi a}\, \frac{1.11 + 5(a/2b)^4}{1 - a/2b},$$

(4.16)

bending by moment M:

$$k_{\mathrm{I}} = 6M(2b-a)^{-3/2}\zeta,$$

(4.17)

where ζ is given in the table below:

$a/2b$	0.05	0.1	0.2	0.3	0.4	0.5	0.8	1.0
ζ	0.36	0.49	0.60	0.66	0.69	0.72	0.73	0.73
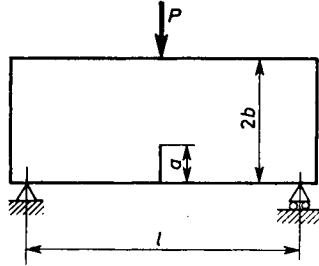
Fig. 4.9. Edge crack; bending

(d) Bending of a free-supported beam with a boundary crack:

$$k_I = \frac{3Pl}{8} F(a/2b),\tag{4.18}$$

where for $l = 8b$ we have:

$$F(a/2b) = 1.090 - 1.735a/2b + 8.20(a/2b)^2 - 14.18(a/2b)^3 + 14.57(a/2b)^4,$$

and for $l = 16b$:

$$F(a/2b) = 1.107 - 2.120\,a/2b + 7.71(a/2b)^2 - 13.55(a/2b)^3 + 14.25(a/2b)^4.$$

(e) Specimen of the double cantilever type:

$$k_I = \frac{P}{b} \sqrt{a}\, F_1,\tag{4.19}$$
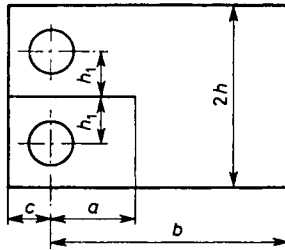
Fig. 4.10. A sample with a crack for strength testing
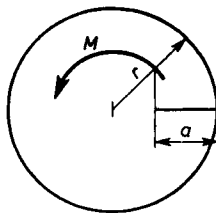
Fig. 4.11. Edge crack; torsion

where

$$F_1(a/b) = 29.6 - 185.5a/b + 655.7(a/b)^2 - 1017.0(a/b)^3 + 638.9(a/b)^4.$$

(f) Circular cylinder with a radial crack under torsion:

$$k_3 = \sqrt{\pi} \, M \, \frac{(1+\alpha)^{3/2}(1-\alpha)^3 [2(1-\alpha) + \sqrt{\alpha}\,(mJ_0 + J_1)]}{\alpha^2 a^{5/2} \{2\pi^2 - [2(1-\alpha)^2 A^2 + \alpha(A+B)^2]\}}, \tag{4.20}$$

where

$$\alpha = 1 - a/r, \quad m = \tfrac{1}{2}(\alpha + 1/\alpha),$$

$$J_0 = 4\tan^{-1}\sqrt{\alpha}, \quad J_1 = -\frac{1-\alpha}{4\alpha}\left[4\sqrt{\alpha} - (1-\alpha)J_0\right],$$

$$A = \frac{1}{\alpha}\left[\frac{(1+\alpha)^2}{\sqrt{\alpha}}\tan^{-1}\sqrt{\alpha} - (1-\alpha)\right], \quad B = \frac{1-\alpha}{\alpha}[2 - \tfrac{3}{4}(1-\alpha)A].$$

There are the monographs devoted to the stress intensity factors (Sih, 1973; Tada *et al.*, 1973). Only in the simplest cases can the state of stresses in solids with cracks be determined exactly; usually we can obtain approximate solutions only, and consequently the stress intensity factors are also approximate. The list of the stress intensity factors is far from being complete. A number of dynamic problems, certain three-dimensional problems, and those with the diffusion effects for the bodies with cracks of more complicated shapes still await solution.

From the practical point of view the stress intensity factors in the solids with cracks under the following loadings are of particular interest:
(1) cyclic loading,
(2) monotonic loading of plates under bending,
(3) monotonic loading of structures with the effect of creep,
(4) long duration loading of structures in the chemically active atmosphere.

4.5. Irwin's Criterion

An important step in the development of fracture mechanics was made in the investigations of Irwin (1958) and Orowan. Griffith's idea was generalized to the case of quasi-brittle materials with a distinct plastic zone surrounding the crack tips. The modification of Griffith's criterion consisted in taking into account, besides the surface energy, the work of plastic strain necessary to generate a unit of new surface of the crack. Thus, instead of formula (4.8), we obtain

$$p_{cr} = \sqrt{\frac{2E(\gamma + \gamma_p)}{\pi l_{cr}}}, \tag{4.21}$$

where γ_p denotes specific work of the plastic strain of the newly generated crack surface. In accordance with Orowan's experiments, for low-carbon steel γ_p is about three times greater than γ; therefore, in rough calculations γ can be neglected with respect to γ_p. In the experiments of Felbeck and Orowan (1955) it was shown that Irwin's theory agrees well with the results of experiments on steel specimens, and that in the process of fracturing of semi-brittle materials the speed of propagation of cracks plays a significant role. By generalizing Griffith's theory and introducing the notion of the stress intensity factor, Irwin formulated the fracture criterion in the following way. He determined experimentally the critical value k_{cr} for a given state of stress. Next, he made a comparison with the value of the computed stress intensity factor. The crack is stable (i.e. it does not start propagating) if, for the first mode and the plane state of stress, the following condition holds:

$$k_I \leqslant k_{Icr}. \tag{4.22}$$

The material constant k_{Icr}, determined experimentally, was referred to by Irwin as the fracture toughness. For ideally brittle materials, and a low value of the work of plastic strain, Irwin's criterion reduces to that of Griffith. Cracks for which condition (4.22) is satisfied are called *cracks in the equilibrium state*. If the condition is not valid the system looses its stability and the crack starts propagating. In Griffith's criterion there occurs the derivative of the internal energy with respect to the crack length, or in other words the work of the decohesion forces on the unit of newly created crack surface. In the case of the boundary conditions in stresses and a two-dimensional problem, we denote

$$2b\mathscr{G} = \frac{\partial U}{\partial l}, \tag{4.23}$$

where b is the width of the plate. There exists the following relationship between the forces of decohesion and the stress intensity factor:

$$E\mathscr{G} = \begin{cases} k_I^2, & \text{for the plane state of stress,} \\ (1-\nu^2)k_I^2, & \text{for the plane state of strain,} \end{cases} \tag{4.24}$$

where E is Young's modulus and ν Poisson's ratio. In this way, material constant k_{Icr} (fracture toughness) can be replaced by constant $\mathscr{G}_{Icr}$, and the condition of the loss of stability of the crack, for the first mode and the plane state of stress, can be written in the form:

$$\mathscr{G}_I \leqslant \mathscr{G}_{Icr}. \tag{4.25}$$

$\mathscr{G}_{Icr}$ is also determined experimentally while $\mathscr{G}_I$ is computed from the solution of the corresponding boundary value problem of the theory of elasticity.

4.6. Other Concepts and Hypotheses

Barenblatt (1959) formulated in the mathematical form and developed a concept of Khristyanovich (in 1955) who observed in rock mechanics that the shape of a crack opened by an internal pressure is not elliptical or ellipsoidal as it follows from the solutions of the boundary value problems of the linear theory of elasticity. In fact, the crack faces at its tips close smoothly in such a way that the derivative to the boundary line of the cross-section is equal to zero at the crack tips. Barenblatt formulates the theory in the form of three hypotheses:

 (i) The width of the end zone at the crack tip is small as compared with the crack dimensions. In this region there are acting forces of interatomic attraction. It means that we do not consider the micro-cracks.

 (ii) The shape of the crack in the vicinity of its tip does not depend on the applied forces, and for a given material and under the same conditions is always the same. If the crack starts propagating, the shape at the crack tip does not change. This is the so-called *hypothesis of autonomicity* of the end region of the crack.

(iii) The crack faces converge smoothly. The angle at the crack tip is zero. The stresses in the vicinity of the crack tip are finite.

In the case of ideally brittle bodies, after introducing the forces of cohesion $G(x)$ which are assumed to act at a very thin region of the crack tip, we obtain the following estimations for the normal stress component $\sigma_{yy}(x, 0)$ and the displacements normal to the crack surfaces $v(x, 0)$ in terms of the distance from the crack tip

$$\sigma_{yy}(x_1) = \frac{k_I}{\sqrt{2x_1}} + G(l) + O\left(\sqrt{x_1}\right),$$

$$v(x_2) = \pm \frac{2(1-\nu^2)}{E} k_I \sqrt{2x_2} + O(x_2^{3/2}).$$

(4.26)
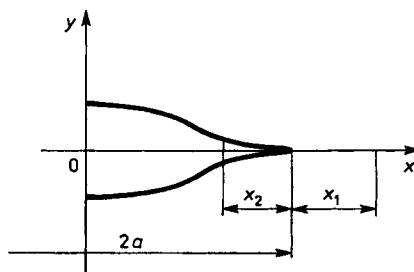
Fig. 4.12. Shape of the crack if cohesion forces are taken into account

In the case where the shape of the crack is as assumed in Hypothesis (iii), we find that the stress intensity factor due to both the pressure on the crack surfaces and the cohesion forces $k_I = k_{Iq} + k_{IG}$ has to vanish. Thus, we get

$$k_{Iq} = \frac{1}{\pi} \int_0^d \frac{G(t)}{\sqrt{t}} \, dt, \tag{4.27}$$

where d is the width of the region of cohesion forces. Barenblatt's theory differs from that of Irwin in the interpretation, while the numerical values for the critical loadings are the same.

Interesting results of the experiments on thin sheets of steel with internal cracks under tension were obtained by Dugdale (1960). It turns out that under the conditions of the plane state of stress the region of plastic deformations in the neighborhood of the crack does not correspond to the previously known theoretical solutions for an elastic-plastic body. The plastic region in such cases reduces to a very thin layer of plastic strain in the plane of the crack. The theoretical solution of the problem can be obtained if we assume that the crack has been extended by the region of plastic strain in which there are the tensile surface forces acting, normal to the extended surface of the crack, and equal to the values of stresses at yield limit. As we see, the problem is mathematically analogous to that with the forces of cohesion. The difference concerns only the width of the regions of the forces of cohesion, and of the plastic strain. The region of plastic strain is much wider than the region of the forces of cohesion, on the other hand, the cohesion forces are considerably higher than the values of the stresses at yield limit. The theoretical solution can be found in a paper by Leonov and Panasyuk (Panasyuk, 1968).

In this short chapter we have discussed the most important criteria of the stability for macro-cracks and the initiation of crack propagation. We departed from the assumption that the continuum outside the cracks was continuous. Within the framework of the same assumption of continuity there exist other criteria. We mention here the crack opening displacement criterion (COD-criterion) corresponding to the strength hypothesis of the maximum strain, abandoned long ago, and now revived in fracture mechanics. In fact, any strength theory can serve in formulating the loss of stability criterion in fracture mechanics.

In this chapter we did not discuss the many important problems such as the dynamics of fracture and the kinematics and dynamics of the cracks at various speeds, higher and lower than the corresponding wave speeds. We did

not consider the problems of crack bifurcation, the aspects of the mechanics of fatigue, not to metion the numerous applications.

Fracture mechanics is developing very rapidly. The results of the theoretical and experimental investigations are being published in many scientific journals of which at least three are devoted exclusively to fracture mechanics. The extensive source of knowledge in this field constitutes the seven-volume monograph edited by Liebowitz (1968–1972) there is also a Russian translation available.

5. Contact Problems

5.1. Attempt of Classification of the Contact Problems

The term contact problems is ambiguous. If by this term we understand that the forces are transmitted by a contact of the bodies, it will be easier to list the problems which are not contact. Let us say that a certain part of the surface bounding a solid is pressed by a sack full of sand and given mass m while in the second case the pressure is exerted by a rigid body of a known shape and the same mass. Only in this second case we can speak of a contact problem. Generally speaking, by a contact problem we mean such that the boundary conditions at a certain part of the bounding surface of the solid are prescribed in the displacements, not in the terms of known tractions. By contact problems we also understand such that solids of comparable Young's moduli meet at a part of the bounding surface, and the contour of the contact will be determined from the solution of the problem. If instead of the sack with sand we imagine a thin shell, for example an inflated baloon meeting with a solid of much higher rigidity we still can speak of a contact problem, however for the shell.

Therefore, we can distinguish the following classification of contact problems. The contact problem can be regarded by the way in which the forces are applied; thus, we have the statical contact problems, quasi-statical, and dynamical ones. Dynamical problems include the problems of collision and impact.

The first contact problems were posed and solved at the end of the last century by Boussinesq and Hertz (Hertz, 1881) and by Dinnik at the beginning of this century (Dinnik, 1909). These investigations found many applications, and resulted in the development of the theoretical papers, namely dealing with the problems of contact with rigid punches, the contact of elastic bodies, and compression of balls and rollers. The punch problems

are important in structural mechanics, and the compression of balls and rollers in all types of bearings: ball, rolling, and needle bearings but also slide and sleeve bearings.

The following problems can be treated as contact ones:

(1) shafts with fixed wheels or disks, the problems of fitting;
(2) slide and thrust bearings. These problems resulted in the development of tribology;
(3) gear transmissions, and worm gears, contact of teeth;
(4) contact of wheel sets with rails, contact of rails with foundation;
(5) air strips, dynamical contact with airplane wheels;
(6) contact of thin, flexible structures with rigid ones;
(7) effect of temperature, creep on the contact stresses;
(8) geometrical and physical nonlinearity in contact problems, plastic regions.

Hardness of materials is closely connected with contact problems. Here, we mention only these tests which lead to the definition of the hardness from the standpoint of solid-body mechanics. The statical pressing into the surface of the tested material of a ball, a cone, or of a pyramid of harder material is known as the hardness test of Brinell, Rockwell, Vickers, Knoop, and others (Shaw, 1973). A nondestructive method of determining hardness consists in rebounding of a ball of known mass, volume, and hardness from the tested surface. The altitude of the reflected ball is the measure of the hardness (Shore's scleroscope).

After World War II, a new revival of interest in this problem was observed, in both theory and experiment. Presumably, the first monograph on contact problems in the theory of elasticity was written by Shtayerman (1961). Since then, many monographs, original papers, and review articles have been pubslished. A part of these solutions is connected with ¡the development of computers and numerical technique. Nevertheless, a number of new analytical methods have been devised, and the domain of investigation has been extended by new problems as well. We can mention here the contact problems of wavy surfaces (Dundurs *et al.*, 1973), stochastic problems, bonded contact, the influence of porosity, filtration, etc. The interesting, theoretical achievement of the recent years is the application, in the contact problems of the theory of elasticity, of the methods of algebraic logic (Rvachev and Protsenko, 1977) known in metha-mathematics and cybernetics. An extensive monograph on contact problems in the classical theory of elasticity was written by Gladwell (1980); the list of references in that book exceeds 750.

5.2. Problems of Punches on Elastic Semi-Space

We search within the framework of the theory of elasticity of an isotropic body, for solutions of the contact boundary value problems of the differential equations of elastostatics, or elastodynamic which in the vector form (*Technological Mechanics*, 1978, Vol. IV, Eq. (2.42)) assume the following form:

$$\mu \nabla^2 \mathbf{u} + (\lambda + \mu) \operatorname{grad} \operatorname{div} \mathbf{u} = 0 \quad (\text{or } \varrho \ddot{\mathbf{u}}). \tag{5.1}$$

We shall discuss several more important solutions of the problems of the two-dimensional state of strains and spatial, first of all axially symmetric. From the standpoint of the theory contact problems belong to the problems with mixed boundary conditions. The methods of solution are numerous. In the two-dimensional cases, usually the method of Kolosov–Muskhelishvili is used. The method of integral transforms has gained popularity, in particular problems, the dual integral equations, and the Wiener–Hopf method. In axially symmetric problems, the Hankel transforms are applied, in plane problems sine and cosine Fourier transforms, while for the wedge problems the Mellin integral transform is used. We shall envisage a few fundamental solutions.

PROBLEM i. Frictionless, undeformable punch of plane base, presented in Fig. 5.1. In this case we have the following boundary conditions:
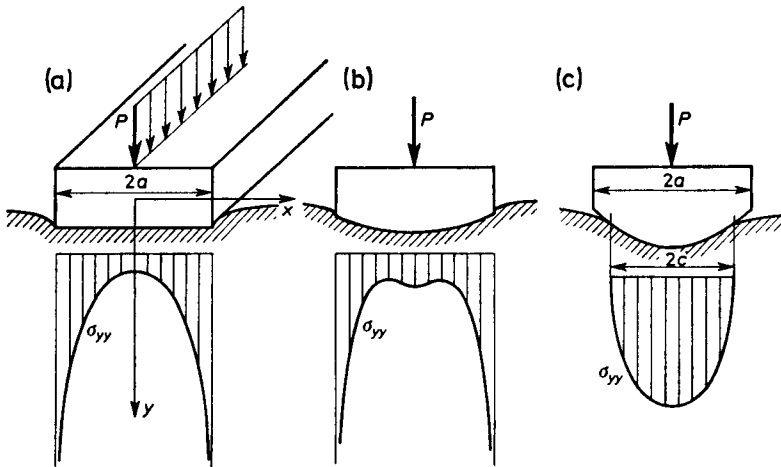
Fig. 5.1. Punches with planar and curved basis

$$v(x, 0) = \delta, \quad x \in (-a, +a),$$

$$\sigma_{yy}(x, 0) = 0, \quad x \in (-\infty, -a) \cup (+a, +\infty), \tag{5.2}$$

$$\sigma_{xy}(x, 0) = 0, \quad x \in (-\infty, +\infty).$$

The contact stress (Sadovski's solution; *Technological Mechanics*, 1978) assumes the form

$$\sigma_{yy}(x, 0) = -\frac{P}{\pi \sqrt{a^2 - x^2}}, \quad x \in (-a, +a). \tag{5.3}$$

There is the relation between the applied force P (on running 1 cm) and the displacement of the base of punch with respect to the undeformed state:

$$E\pi\delta = 2(1 - \nu^2) P \ln 2. \tag{5.4}$$

PROBLEM ii. Undeformable, frictionless punch with a curved, convex base. The boundary conditions (5.2) have to be modified:

$$v(x, 0) = \delta - f(x), \quad x \in (-a, +a),$$

$$\sigma_{yy}(x, 0) = 0, \quad x \in (-\infty, -a) \cup (+a, +\infty), \tag{5.5}$$

$$\sigma_{xy}(x, 0) = 0, \quad x \in (-\infty, +\infty),$$

where $f(x)$ is a continuous convex function. In the case where punch is of the form shown in Fig. 5.1b, there is the singularity in the value of contact stresses for $-x \to -a$, $x \to +a$, and the discontinuity of displacement v at points $x = \pm a$, as in the case in Fig. 5.1a.

PROBLEM iii. This case corresponds to Fig. 5.1c. Here the extent of the contact is not known beforehand and has to be determined from the solution. The boundary conditions assume the following form:

$$v(x, 0) = \delta - f(x), \quad x \in (-c, +c),$$

$$\sigma_{yy}(x, 0) = 0, \quad x \in (-\infty, -c) \cup (+c, +\infty), \tag{5.6}$$

$$\sigma_{xy}(x, 0) = 0, \quad x \in (-\infty, +\infty),$$

where c is unknown, and can be determined from the additional condition that the stresses at points $x = \pm c$ have to be continuous. This results from the assumption that displacements and its derivatives are continuous in the whole range $x \in \langle -a, +a \rangle$.

PROBLEM iv. Punch with a plane base under non-symmetric loading, or symmetric force and a moment in plane xy. In the case of a moment we have the following boundary conditions, corresponding to Fig. 5.2a:
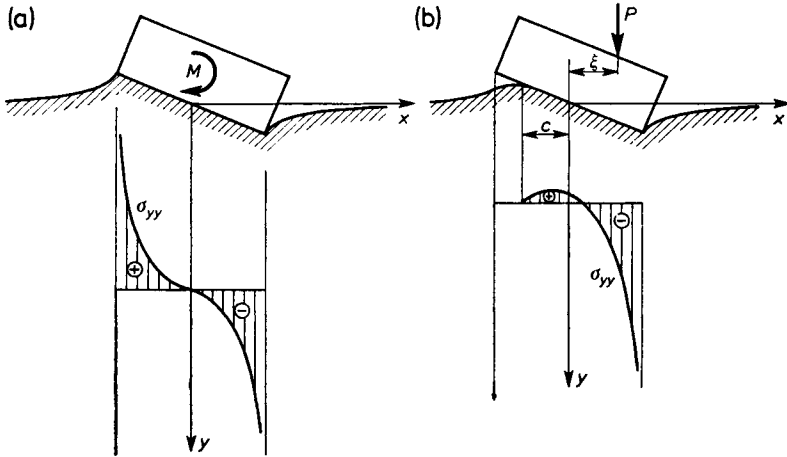
Fig. 5.2. Punch with planar basis

$$v(x, 0) = \varepsilon x, \quad x \in (-a, +a),$$
$$\sigma_{yy}(x, 0) = 0, \quad x \in (-\infty, -a) \cup (+a, \infty), \tag{5.7}$$
$$\sigma_{xy}(x, 0) = 0, \quad x \in (-\infty, +\infty).$$

The stress singularities and discontinuity of the derivative of displacements $v(x, 0)$ occur at the end points of the segment $\langle -a, +a \rangle$. For the negative values of coordinate x the contact stresses are tensile; the base of the punch is bonded over the whole surface to the semi-space below.

In the case shown in Fig. 5.2b we obtain the following boundary conditions:

$$v(x, 0) = \varepsilon_1 x + \delta, \quad x \in (-c, +a),$$
$$\sigma_{yy}(x, 0) = 0, \quad x \in (-\infty, -c) \cup (+a, +\infty), \tag{5.8}$$
$$\sigma_{xy}(x, 0) = 0, \quad x \in (-\infty, +\infty),$$

and the condition of the continuity of the displacement derivative at $x = -c$, or, in other words, the condition of the continuity of contact stress at that point. From the equilibrium condition, we have the following relationships for the resultant force and moment:

$$P = \int_{-c}^{+a} \sigma_{yy}(x, 0) \, dx, \quad M = \int_{-c}^{+a} x \sigma_{yy}(x, 0) \, dx.$$

If the value of force P is so high that there is a separation over the segment $\langle -a, -c \rangle$, then the pressure under the punch (Galin, 1953) can be expressed by the formula

$$\sigma_{yy}(x, 0) = -\frac{P}{\pi \sqrt{a^2 - x^2}} + \frac{E \varepsilon_1 x}{2(1 - \nu^2) \sqrt{a^2 - x^2}}. \tag{5.9}$$

Besides, we can determine the relation between the angle of rotation and the force for the case where foundation begins to tear away from the base:

$$\pi E a \varepsilon_1 = 2(1 - \nu^2) P. \tag{5.10}$$

The moment generating the rotation about angle ε_1 is equal to

$$M = Pa + \int_{-a}^{+a} \sigma_{yy}(x, 0)(a - x) dx = \tfrac{1}{2} Pa. \tag{5.11}$$

Thus the tensile contact forces appear in the case where $\xi > a/2$.

PROBLEM V. Indentation of an undeformable wedge. In this case, the assumption of the continuity of the displacement derivative breaks down at the vertex of the wedge. Consequently, we can expect the contact stress singularity at this point. The two cases presented in Fig. 5.3 a, b differ as follows. In the
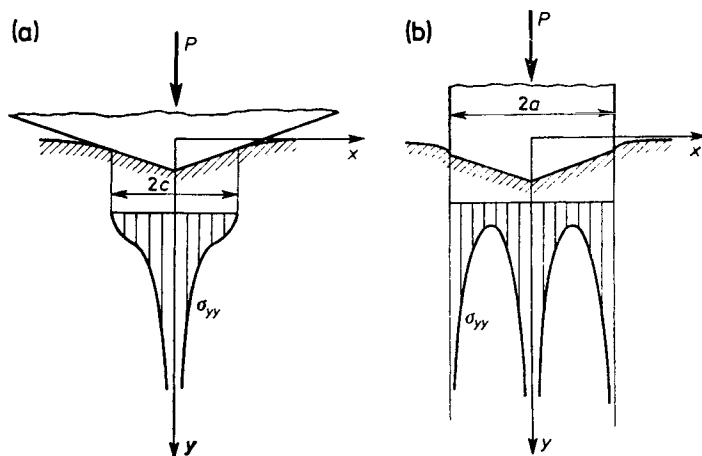
Fig. 5.3. Wedge pushing

case (a) we obtain the logarithmic singularity at the origin of the coordinate system, i.e. at the wedge vertex, while for the remaining segment of contact the stresses are finite. If the axis of the wedge coincides with the y-axis we obtain the boundary condition in the form

$$v(x, 0) = \delta - \frac{x}{c} \delta_1; \tag{5.12}$$

the remaining boundary conditions are as in Problem iii. The contact stresses assume the values:

$$\sigma_{yy}(x, 0) = \sigma_{xx}(x, 0) = -\frac{1}{\pi(1 - \nu^2)} \delta_1 \cosh^{-1}\left(\frac{c}{x}\right), \quad |x| < c. \tag{5.13}$$

In the case shown in Fig. 5.3b, the singularities of the type $(a^2 + x^2)^{-1/2}$ appear besides the singularity at the vertex.

PROBLEM vi. The contact problems with friction, or adhesion of the foundation. In the cases where the friction between the punch and the foundation has to be taken into account the boundary conditions undergo modification. For example in Problems i and ii, instead of the condition of zero shear stress $\sigma_{xy}(x, 0)$, we have

$$\sigma_{xy}(x, 0) = \begin{cases} -k\sigma_{yy}(x, 0), & x \in (-a, +a), \\ 0, & x \in (-\infty, -a)\cup(+a, +\infty), \end{cases} \tag{5.14}$$

where k is the friction coefficient. The remaining boundary conditions remain unchanged. The solution of the problem is not easy, the discussion and an approximate solution can be found, e.g. in Galin (1953). On the other hand, in the case of perfect adhesion of an undeformable punch, we have instead of zero shear stress $\sigma_{xy}(x, 0) = 0$:

$$\begin{aligned} u(x, 0) &= 0, & x \in (-a, +a), \\ \sigma_{xy}(x, 0) &= 0, & x \in (-\infty, -a)\cup(+a, +\infty). \end{aligned} \tag{5.15}$$

Also in this case, the solution is quite complicated, approximate solutions can be found in the monographs: Galin (1953), Muskhelishvili (1980). We find from the solution that the work performed by shear stress is equal to between ten and twenty percent of the work done by the contact forces.

PROBLEM vii. Punch moving with constant speed. In this case we take into account the inertia term on the right-hand side of Eq. (5.1). We introduce the speeds of the longitudinal (primary) wave c_1 and the shear wave c_2:

$$c_1 = \sqrt{\frac{\lambda + 2\mu}{\varrho}}, \qquad c_2 = \sqrt{\frac{\mu}{\varrho}},$$

where ϱ denotes the density of the continuum, $\lambda = \dfrac{2\mu\nu}{1 - 2\nu}$, and $\mu = \dfrac{E}{2(1+\nu)}$ are Lamé's constants. Not going into details of the solution (Galin, 1953), we write the formula for the contact stress, and the plane base punch, under force P, moving with constant velocity v_0 in the direction of the x-axis

$$\sigma_{yy}(x, 0) = -P\frac{\sin \pi\theta}{\pi}(a^2 - x^2)^{-1/2}\left(\frac{a+x}{a-x}\right)^{1/2-\theta}, \tag{5.16}$$

where

$$\theta = \frac{1}{\pi}\tan^{-1}\left\{-\frac{1}{2\varrho}m^2\left(1 - \frac{1-2\nu}{2-2\nu}m^2\right)\right\}\Big/\alpha,$$

where

$$\alpha = \left\{\left[1 + \left(\frac{3}{2} - 2\nu\right)m^2\right]\left[1 - \frac{1}{2}m^2\right]\sqrt{1 - \frac{1 - 2\nu}{2 - 2\nu}m^2} - \right.$$
$$\left. - \left(1 - \frac{1 - 2\nu}{2 - 2\nu}m^2\right)[1 + 2(1 - \nu)m^2]\sqrt{1 - m^2}\right\},$$

and $mc_2 = v_0$.

PROBLEM viii. Spatial problems. The simplest spatial problems have the property of axial symmetry. We shall present the solutions for an undeformable punch, indented into an elastic semi-space, of a circular cross-section plane base, and in the shape of a cone. The first of these problems corresponds to Problem i, while the second one to the problem considered in Problem v. Now P denotes a concentrated force, not a line force, with respect to the running length unit, as before.

The contact stresses for a plane base punch of a circular cross-section are equal to

$$\sigma_{zz}(r, 0) = -\frac{1}{2}\frac{P}{a}\frac{1}{\sqrt{a^2 - r^2}}, \qquad r \in \langle 0, a\rangle. \tag{5.17}$$
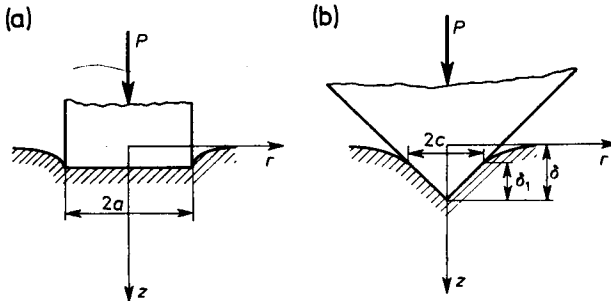
Fig. 5.4. Axially symmetrical punches

Also in this case of spatial problems, there exists the relationship between the applied force $P = 2\pi a^2 p$ and the indentation of the base of punch with respect to the undeformed state

$$(1 - \nu^2)P = 2Ea\delta. \tag{5.18}$$

The displacements of the bounding surface in the normal direction are given by the formula

$$w(r, 0) = \delta \begin{cases} 1, & r \in (0, a), \\ \dfrac{2}{\pi}\sin^{-1}\left(\dfrac{a}{r}\right), & r \in (a, \infty). \end{cases} \tag{5.19}$$

For a circular cone we obtain

$$w(r, 0) = \delta - \delta_1 \frac{r}{c}, \quad r \in \langle 0, c \rangle.$$

There is a logarithmic singularity in the value of contact stress at the vertex of the cone:

$$\sigma_{zz}(r, 0) = \frac{E}{2(1-\nu^2)} \frac{\delta_1}{c} \cosh^{-1}\left(\frac{c}{r}\right), \quad r \in (0, c). \tag{5.20}$$

The displacements in the direction of the z-axis, outside the contact, have the following form:

$$w(r, 0) = \delta_1 \left[\sin^{-1}\left(\frac{c}{r}\right) + (r^2 c^{-2} - 1)^{1/2} - r/c \right], \quad r \in (c, \infty). \tag{5.21}$$

We now have the relationship between the force and the indentation:

$$2(1-\nu^2)P = \pi c \delta_1 E. \tag{5.22}$$

PROBLEM ix. Torsion of a semi-space by a circular punch. This problem is called the Reissner–Sagocci problem. In this case the partial differential equation (5.1) reduces to the single scalar partial differential equation of the second order for circumferential displacement component u_θ:

$$\left(\frac{\partial^2}{\partial r^2} + \frac{1}{r} \frac{\partial}{\partial r} - \frac{1}{r^2} + \frac{\partial^2}{\partial z^2} \right) u_\theta = 0, \tag{5.23}$$

with the boundary condition in the form

$$\sigma_{rz}(r, 0) \equiv \tau_{rz}(r, 0) = 0, \quad r \in (a, \infty), \tag{5.24}$$

$$u_\theta(r, 0) = \alpha r, \quad r \in (0, a),$$

where α is the angle of torsion. The contact stresses are then given by the following formula:

$$\sigma_{rz}(r, 0) = -\frac{4\alpha \mu_r}{\pi \sqrt{a^2 - r^2}} = -\frac{3M_0}{4\pi a^3} \frac{r}{\sqrt{a^2 - r^2}}, \tag{5.25}$$

where M_0 is the torque. Displacements outside the contact region can be expressed by the formula:

$$u_\theta(r, 0) = \frac{2\alpha}{\pi} \left(r \sin^{-1}(a/r) - \frac{a}{r} \sqrt{r^2 - a^2} \right). \tag{5.26}$$

PROBLEM x. There are a whole variety of solutions for more complicated contact problems referring to the contact of punches of different cross-sections, and for problems of many punches. The other solutions concern the

contact problems for layers, and anisotropic or non-homogeneous bodies. Various effects can be included, for example the influence of creep, of thermal stresses. We do not discuss dynamical problems. The methods of complex variable are popular in solving two-dimensional problems. The three-dimensional problems are more difficult to solve.

PROBLEM xi. Contact problems with plastic zones. Here, we shall discuss the problems of indentation of a plane base punch in the case where the stresses exceed the yield limit in the entire region of contact. Two solutions are well known, namely Prandtl's and Hill's solutions. In both solutions, it is assumed that the contact stress under the punch is uniform. This solution cannot be satisfied when yield limit has been exceeded only on the part of the contact region. In Figs. 5.5a, b we have shown the slip lines in both cases. These
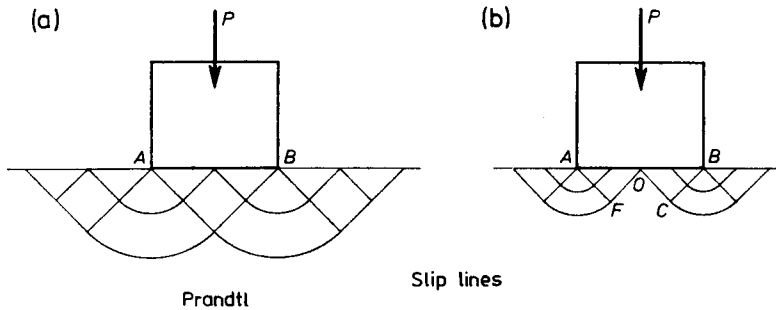
Fig. 5.5. Slip lines

solutions are not the only ones. Prager has noticed that one can construct solutions which are combinations of two, i.e. Prandtl's and Hill's, with any parameter characterizing the mutual superposition of both regions OBC and OAF.

5.3. Compression of Balls and Shafts

First, let us consider Boussinesq's problem (1878).

In fact, this problem had been solved by Kelvin already in 1848 (Huber, 1954) and it refers to a singular solution of the theory of elasticity where the force is applied perpendicularly to the bounding plane of a semi-space. The formulae are given in the coordinate system (R, ϑ, z) (Fig. 5.6)

$$\sigma_{RR} = \frac{1-2\nu}{R^3} P, \quad \sigma_{\vartheta\vartheta} = -\frac{1-2\nu}{2\pi R^3} P,$$

$$\sigma_{zz} = -\frac{3P}{2\pi R^2}\cos^3\vartheta, \quad \sigma_{Rz} = \tau_{Rz} = -\frac{3P}{2\pi R^2}\cos^2\vartheta\sin\vartheta.$$

(5.27)
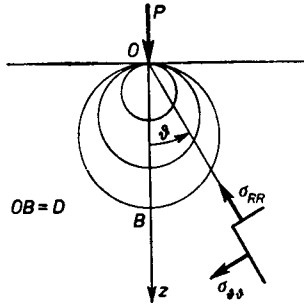
Fig. 5.6. Constant stresses surfaces

By means of these formulae we can express the stress in any plane perpendicular to the direction of the applied force P:

$$\sigma = \sqrt{\sigma_{zz}^2 + \sigma_{Rz}^2} = \frac{3P}{2\pi D^2}, \quad \text{where} \quad D = \overline{OB} = \frac{R}{\cos\vartheta}. \tag{5.28}$$

This means that the force transmits radially in such a way that the stress in a plane parallel to the bounding plane $z = 0$ is inversely proportional to the square of the distance from the point of the application of the force. Moreover, the stress in elementary planes parallel to the bounding plane is constant over the surface of each sphere as shown in Fig. 5.6.
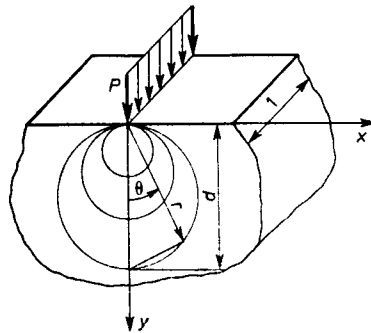
Fig. 5.7. Constant stress lines

In the two-dimensional case (see Fig. 5.7), we obtain in the cylindrical coordinate system

$$\sigma_{rr} = -\frac{2P}{\pi} \cdot \frac{\cos\theta}{r}. \tag{5.29}$$

The hoop and shear stress components $\sigma_{\theta\theta}$ and $\sigma_{r\theta}$ vanish identically. For a circle of diameter d we find that $r = d\cos\theta$. Consequently, for any circle

tangent to the bounding plane at the point of the application of the force
we obtain

$$\sigma_{rr} = -\frac{2P}{\pi d}.$$
(5.30)

From the two solutions, it is evident how the stresses in an elastic semi-space
diminish from the point or line of the force application. Usually, such prob-
lems are called the problems of the transmission of forces from the place
of loading. By means of Huber–Mises strength theory, we can also derive
the formulae for the reduced stress. The general formulae are quite compli-
cated; we shall write the results for the points on the bounding plane, and
on the z-axis, for the case where force acts as shown in Fig. 5.6. We have
for $z = 0$:

$$\sigma_{\text{red}} = \frac{\sqrt{3}P}{2\pi} \frac{1-2\nu}{x^2+y^2},$$

and for $x = y = 0$:

$$\sigma_{\text{red}} = \frac{3}{2} \frac{P}{\pi} z^{-2} \sqrt{1+(1/2-\nu)^2}.$$

Formulae (5.27), treated as Green's function, are very useful in calculating
stresses generated by a certain distribution of forces on the bounding plane.

The first problems of the compression of balls and shafts had already been
solved by Hertz in 1882 by means of the formulae for the potential of the
homogeneous ellipsoid, representing the simplest prototype of the solutions
of the theory of potential and the theory of integral equations. Hertz
who was a known experimenter guessed this solution in a genious way. He also
developed the theory of impact of elastic bodies, neglecting the inertia forces
of the impacting bodies, and determined the time of the impact duration.
The theory was supplemented by Dinnik who also confirmed Hertz's results
experimentally. Since then, many investigations have been conducted in this
field including the effects of shear forces, material anisotropy, etc.

In the problems of compression of elastic bodies, Hertz neglected the shear
stresses and assumed that the deformed surfaces of both bodies meet in the
region of contact. Next, he assumed that the region of contact of two elastic
bodies, of positive curvature of the bounding surfaces, is an ellipse whose
semi-axes must be determined. The numerical values of the semi-axes of the
contact ellipse depend on the force, on the initial curvature at the point of
contact, on the relative situation of the bodies, and on the constants of elas-
ticity. If only the value od force P changes, then the semi-axes of the ellipse

are proportional to $\sqrt[3]{P}$ while the decrease in the distance between the two bodies is proportional to $(P)^{3/2}$. The pressure over the surface of the contact increases from zero on the ellipse contour to its maximum value $p_0 = 3P/(2\pi ab)$ at the centre, where a and b denote the semi-axes of the ellipse.

In the case where the surface of contact is circular, we obtain the following formulae for the components of the stress tensor in the directions of the z-axis, perpendicular to the surface of contact, and in the radial and tangential, respectively, in the cylindrical coordinate system:

$$\sigma_{zz} = -p_0 \left(\frac{z}{\sqrt{t}}\right)^3 \frac{a^2 t}{t^2 + a^2 t^2},$$

$$\sigma_{rr} = p_0 \left\{ \frac{z}{\sqrt{t}} \left[-\frac{(1-\nu)t}{a^2+t} + (1+\nu)\frac{\sqrt{t}}{a} \tan^{-1}\frac{a}{\sqrt{t}} - 2 \right] + \right.$$

$$\left. + (1-2\nu)\frac{a^2}{3r^2}\left[1 - \left(\frac{z}{\sqrt{t}}\right)^3\right] + \left(\frac{z}{\sqrt{t}}\right)^3 \frac{a^2 t}{t^2 + a^2 z^2} \right\}, \tag{5.31}$$

$$\sigma_{\varphi\varphi} = -p_0 \left\{ (1-2\nu)\frac{a^2}{3r^2}\left[1 - \frac{z}{\sqrt{t}}\right]^3 + \right.$$

$$\left. + \frac{z}{\sqrt{t}}\left[2\nu + \frac{(1-\nu)t}{a^2+t} - (1+\nu)\frac{\sqrt{t}}{a}\tan^{-1}\left(\frac{a}{\sqrt{t}}\right)\right] \right\},$$

where

$$2t = \left[r^2 + z^2 - a^2 + \sqrt{(r^2+z^2-a^2)^2 + 4a^2 z^2}\right], \quad p_0 = \frac{3P}{2\pi a^2}.$$

For the strength computations we have to assume a strength theory. Belaev noticed that the place of the maximum strength effort in the case of compressed balls does not occur at the centre of the contact circle but at a certain depth, and calculated the reduced stresses using the hypothesis of maximum shear stress. Huber (1954) provides the results found by means of the Huber–Mises hypothesis. The maximum of the reduced stress occurs at the point the depth of which is $z = 0.481a$, where a is the radius of the contact circle, and is about 3 times the value of the reduced stress at the centre of the circle:

$$\sigma_{red} \approx (0.758 - 0.460\nu)p_0 \approx 0.62p_0 \quad \text{for } \nu = 0.3.$$

Below, we list the formulae for the particular cases:
   (i) Two parallel cylinders od diameters d_1 and d_2, respectively. By c we denote the width of the contact strip, q_0 is the maximum pressure in the contact region, w is the mutual displacement of the cylinders axes, E_1,

E_2, ν_1, ν_2 denote Young's moduli and Poisson's ratios of the two cylinders, respectively, and p is the loading with respect to unit length of the cylinders. We thus obtain

$$c = 1.6 \sqrt{p \frac{d_1 d_2}{d_1 + d_2} \left(\frac{1 - \nu_1^2}{E_1} + \frac{1 - \nu_2^2}{E_2} \right)},$$

$$q_0 = 0.798 \sqrt{\frac{p \dfrac{d_1 + d_2}{d_1 d_2}}{\dfrac{1 - \nu_1^2}{E_1} + \dfrac{1 - \nu_2^2}{E_2}}},$$

$$w = \frac{2}{E}(1 - \nu^2) \frac{p}{\pi} \left(\frac{2}{3} + \ln \frac{4 d_1 d_2}{c^2} \right) \quad \text{for} \quad E_1 = E_2 = E, \nu_1 = \nu_2 = \nu.$$

(ii) Two cylinders with perpendicular axes. We denote by a and b the semi-axes of the ellipse of contact, $p_0 = 3P/(2\pi ab)$, P is the compressive force, and α, β and γ are the coefficients below:

$$a = \alpha \sqrt[3]{\frac{P d_1 d_2}{d_1 + d_2} \left(\frac{1 - \nu_1^2}{E_1} + \frac{1 - \nu_2^2}{E_2} \right)}, \quad b = \beta a, \quad q_0 = \frac{3P}{2\pi ab},$$

$$w = \gamma \sqrt[3]{\frac{P^2}{\left(\dfrac{E_1}{1 - \nu_1^2} + \dfrac{E_2}{1 - \nu_2^2} \right)^2} \cdot \frac{d_1 + d_2}{d_1 d_2}},$$

$\dfrac{d_1}{d_2}$	1	1.5	2	3	4	6	10
α	0.908	1.045	1.158	1.350	1.505	1.767	2.175
β	1	0.765	0.632	0.482	0.400	0.308	0.221
γ	2.080	2.060	2.025	1.950	1.875	1.770	1.613

(iii) Two spheres of diameters D_1 and D_2 contacting externally; a is the contact radius, q_0 is the maximum stress in the surface of contact:

$$a = 0.721 \sqrt[3]{P \frac{D_1 D_2}{D_1 + D_2} \left(\frac{1 - \nu_1^2}{E_1} + \frac{1 - \nu_2^2}{E_2} \right)},$$

$$q_0 = 0.918 \sqrt[3]{\frac{P \left(\dfrac{D_1 + D_2}{D_1 D_2} \right)^2}{\left(\dfrac{1 - \nu_1^2}{E_1} + \dfrac{1 - \nu_2^2}{E_2} \right)^2}},$$

$$w = 1.04 \sqrt[3]{P^2 \frac{D_1 + D_2}{D_1 D_2} \left(\frac{1 - \nu_1^2}{E_1} + \frac{1 - \nu_2^2}{E_2} \right)^2}.$$

(iv) Sphere of diameter D_2 contacting internally with the sphere of diameter D_1, $D_1 > D_2$:

$$a = 0.721 \sqrt[3]{P \frac{D_1 D_2}{D_1 - D_2} \left(\frac{1 - \nu_1^2}{E_1} + \frac{1 - \nu_2^2}{E_2} \right)},$$

$$q_0 = 0.918 \sqrt[3]{P \left(\frac{D_1 - D_2}{D_1 D_2} \right)^2 \left[\frac{1 - \nu_1^2}{E_1} + \frac{1 - \nu_2^2}{E_2} \right]^2},$$

$$w = 1.55 \sqrt[3]{\frac{P^2}{E^2} \frac{D_1 - D_2}{D_1 D_2}} \qquad \text{for } E_1 = E_2 = E, \ \nu_1 = \nu_2 = \nu.$$

References to Part 5

Abramov, V. M., 1937, "The problem od contact of an elastic half-plane with an absolutely rigid foundation" (in Russian), *Doklady Akad. Nauk SSSR*, **17**, 4.

Advances in Research on the Strength and Fracture of Materials, Fracture 1977, Ed. D. M. R. Taplin, Vol. 1 — *An overview*, Fourth Intern. Conf. on Fracture, Waterloo, Pergamon Press, Russian translation in "Mekhanika" novoye w zarubiezhnoi nauke **17**, 1979, and 20, 1980.

Aleksandrov, V. M., 1983, "*O postanovke ploskikh kontaktnykh zadach teorii uprugosti pri iznose vzaimodeistvyushchikh tel*", (in Russian), *Dokl. Ak. Nauk SSSR*, **271**, 827–831.

Andreikov, A. E., 1979, *Fracture of Quasi-Brittle Solids with Cracks at a Complex State of Stress* (in Russian), Naukova Dumka, Kiev.

Arutunyan N. Kh., Mkhitaryan S. M., 1969, "Periodic contact problem for a half-plane with the elastic laps" (in Russian), *Prikl. Mat. i Mekh.* **33**.

Arutunyan N. Kh., Mkhitaryan S. M., 1971, "Some contact problems for a semi-plane with elastic stiffeners", in: *Trends in Elasticity and Thermoelasticity*, W. Nowacki, *Anniversary Volume*, Wolters-Noordhoff.

Atluri S. N. (Ed.), 1986, *Computational Methods in the Mechanics of Fracture*, North Holland.

Barber J. R., 1976, "Indentation of a semi-infinite elastic solid by a concave rigid punch", *Journal of Elasticity*, **6**.

Barenblatt G. I., 1959, "On equilibrium cracks occurring in brittle fracture" (in Russian), *Prikl. Mat. Mekh.*, No. 3, 4, and 5.

Brzoska Z., 1974, *Strength of Materials* (in Polish), PWN, Warszawa.

Cherepanov G. P., 1974, *Mechanics of Brittle Fracture* (in Russian), Izdat. Nauka, Moskva.

Dinnik A. N., 1909, *Impact and Compression of Elastic Solids* (in Russian), Izv. Kiev. Polit. Inst., Kiev.

Dugdale D. S., 1960, "Yielding of steel sheets containing slits", *J. Mech. Phys. Solids*, **2**.

Dundurs J., 1975, "Properties of elastic bodies in contact", In: *The mechanics of contact between deformable bodies*", Ed. A. D. Pater, J. J. Kalker, Delft University Press.

Dundurs J., Tsai K. C., Keer L. M., 1973, "Contact between elastic bodies with wavy surfaces", *Journal of Elasticity*.

Du Qinghua (Ed.), 1986, *Boundary Elements*, Proc. Int. Conf. Beining, China, Pergamon Press.

van Elst H. C., Bakker A. (Eds.), 1986, *Fracture Control of Engineering Structures*, Proc. of ECF6, Amsterdam, the Netherlands.

Erdogan F., Civelek M. B., 1974, "Contact problem for an elastic reinforcement bonded to an elastic plate", *J. Appl. Mechanics* **41**.

Felbeck D. K., Orowan E., 1955, *Welding Journal, Res. Suppl.*, **34**.

Forest P. G., 1962, *Fatigue of Metals*, Pergamon Press, Oxford.

Freund L. B., 1972, "Crack propagation in an elastic solid subjected to general loading. II. Non-uniform rate of extension", *J. Mech. Phys. Solids* **20**.

Frocht M. M., 1948–1957, *Photoelasticity*, Vol. I, II, John Wiley, New York.

Fujii T., Zako M., 1982, *Fracture Mechanics of Composite Materials* (in Russian), transl. from Japanese, Mir Publ., Moskva.

Galin L. A., 1953, *Contact Problems of the Theory of Elasticity* (in Russian), Gostekhizdat, Moskva; English transl. North Carolina State College, Raleigh, 1961, Ed. I. N. Sneddon.

Galin L. A., 1976, "Contact problems of the theory of elasticity in the presence of wear" (in Russian), *Prikl. Mat. i Mekh.*, **40**.

Galin L. A., Goryacheva I. G., 1977, "Osesimetrichnaya kontaktnaya zadacha teorii uprugosti pri nalichii iznosa" (in Russian), *Prikl. Mat. Mekh.*, 807–812.

Galin L. A., 1980, *Contact Problems of the Theory of Elasticity and Visco-Elasticity* (in Russian), Nauka, Moskva.

Gladwell G. L. M., 1980, *Contact Problems in the Classical Theory of Elasticity*, Sijthoff and Noordhoff.

Golub V. K., Mossakovskii V. I., 1960, "The bending of circular plate on an elastic half-plane in the presence of adhesion" (in Russian), *Izv. Ak. Nauk* SSSR **2**.

Griffith A. A., 1921, "The phenomena of rupture and flow in solids", *Phil. Trans. A.* **221**, 163.

Grigorovich V. M., 1973, "The contact of a spherical shell with a rigid punch in the presence of adhesion", *Prikl. Mekh.* **9**, 5.

Herrmann K. P. (Ed.), 1986, *Fracture of Non-Metallic Materials*, Proc. 5th Adv. Sem., J. R. C. Ispra, Martinus Nijhoff Publ.

Hertz H., 1881, "Über die Berührung fester elastischer Körper", *J. reine und angew. Math.* (Crelle), 92; Vol. 1, Leipzig, 1895.

Hetenyi M., 1946, *Beams on Elastic Foundation*, University of Michigan Press, Ann Arbor.

Hetenyi M., 1964, "Beams and plates on elastic foundations and related problems", *Appl. Mech. Rev.* **19**, 95–102.

Hirth J. P., Lothe J., 1967, *Theory of Dislocations*, McGraw-Hill.

Huber M. T., 1948, *Strength Criteria in Stereomechanics* (in Polish), Inst. Wyd. SIMP, Warszawa.

Huber M. T., 1954, *Theory of Elasticity* (in Polish), PWN, Warszawa.

Inglis C. E., 1913, "Stresses in a plate due to the presence of cracks and sharp corners", *Trans. Inst. Naval Arch., London*, **60**, 219.

Irwin G. R., 1958, Fracture, *Handbuch der Physik*, Vol. 6, Springer-Verlag.

Jakubowicz A., Orłoś Z., 1978, *Strength of Materials* (in Polish), WNT, Warszawa.

Kachanov L. M., 1974, *Foundations of Fracture Mechanics* (in Russian), Nauka, Moskva.

Keer L. M., Dundurs J., Tsai K. C., 1972, "Problems involving receding contact between a layer and a half space", *J. of Appl. Mech.* **39**, 1115.

Kilchevskii N. A., Kostyuk E. N., 1966, "20th century developments in the theory of contact interactions between solids" (in Russian), *Prikl. Mekh.* **2**, 3.

Kączkowski Z., 1968, *Plates Statics* (in Polish), Arkady, Warszawa.

Kirsch A., 1898, "Die Theorie d. Elastizität u.d., Bedürfnisse d. Festigkeitslehre", *Z. VDI*, **42**, 797.

Kocańda S., 1978, *Fatigue Failure of Metals*, Sijthoff and Nordhoof Int. Publ. Transl. from Polish edition, WNT, 1972.

Kolosov G. V., 1910, Dissertation, S. Petersburg, also: *Application of the Complex Variable in the Plane Problem of the Theory of Elasticity* (in Russian), G.T.G.I.   Moskva.

Kostrov B. V., 1975, *Mechanics of the Tectonic Earthquakes* (in Russian), Nauka, Moskva.

Krzyś W., Życzkowski M., 1962, *Elasticity and Plasticity, Selection of Problems and Examples* (in Polish), PWN, Warszawa.

Likhachev V. A., Khairov R. Yu., 1975, *Introduction to the Theory of Disclination* (in Russian), Leningrad Univ., Leningrad.

Lekhnitskii S. G., 1957, *Anisotropic Plates* (in Russian), Gosstekhizdat, Moskva.

Liebowitz H. (Ed.), 1968–1972, *Fracture, an Advanced Treatise*, in seven volumes, Academic Press.

Luxmoore A. R., Owen D. R. J., Kanninen M. F. (Eds.), 1987, *Numerical Methods in Fracture Mechanics*, Proceeding of the Third Int. Conf., Pineridge Press.

McClintock F. A., Argon A. S., 1966, *Mechanical Behaviour of Materials*, Addison-Wesley.

Morozov E. M., Nikishkov G. P., 1980, *Finite Element Method in Fracture Mechanics* (in Russian), Nauka, Moskva.

Muskhelishvili N. I., 1953, *Some basic problems of the mathematical theory of elasticity*, translation, Noordhoff Groningen. Russian second edition, Izd. Ak. Nauk SSSR, Moskva, 1949.

Neuber H., 1958, *Kerbspannungslehre, Grundlagen für genaue Festigkeitsberechnung mit Berücksichtigung von Konstruktionsform und Werkstoff*, Springer-Verlag, Berlin 1958; First edition 1937, Russian translation, Gostekhizdat, 1947.

Panasyuk V., 1968, *Limit Equilibrium of Brittle Solids with Cracks* (in Russian), Naukova Dumka, Kiev.

Panasyuk V. V., Savruk M. P., Datsyshyn A. P., 1976, *Stress Distribution around Cracks in Plates and Shells* (in Russian), Naukova Dumka, Kiev.

Popov G. Ya., 1982, *Contact Problems for Linearly Deformed Foundation* (in Russian), "Vyshcha Shkola".

Popov G. Ya., Rostovtsev N. A., 1967, *Contact (Mixed) Problems of the Theory of Elasticity* (in Russian), Trudy II sjezda po teoret. mekhanike, Vol. 3.

Ponomarev S. D. (Ed.), 1958, *Strength Computations in Machine Construction* (in Russian), vol. II, Mashgiz, Polish edition, PWN, Warszawa 1957.

Rice J. R., 1968, "A path independent integral and the approximate analysis of strain concentration by notches and cracks", *J. Appl. Mech.* **35**.

Rice J. R., 1980, *The Mechanics of Earthquake Rupture*, North Holland; in Russian: *Mekhanika, novoye w zarubezhnoi nauke*, Vol. 28, Mir, 1982.

Rvachev V. L., 1967, "Studies on the contact problems of the theory of elasticity in the Ukraine" (in Russian), *Prikl. Mekh.* **3**.

Rvachev V. L., Protsenko V. S., 1977, *Contact Problems of the Theory of Elasticity for Non-Classical Regions* (in Russian), Naukova Dumka, Kiev.

Rvachev V. L., Rvachev V. A., 1979, *Non-Classical Methods of the Theory of Approximation in the Boundary Value Problems* (in Russian), Naukova Dumka, Kiev.

Savin G. N., 1968, *Stress Distribution around Holes* (in Russian), Naukova Dumka, Kiev.

Savin G. N., Tulchyi V. I., 1971, *Plates Supported by Complex Rings and Elastic Laps* (in Russian), Naukova Dumka, Kiev.

Savin G. N., Tulchyi V. I., 1976, *Handbook on Stress Concentration* (in Ukrainian), Vyshcha Shkola, Kiev.

Schwalbe K. H. (Ed.), 1986, *The Crack Tip Opening Displacement in Elastic-Plastic Fracture Mechanics*, Proceedings, Springer-Verlag.

Serensen S. V., 1975, *Strength of Materials of Fatigue and Brittle Failure* (in Russian) Atomizdat, Moskva.

Series: Engineering Applications of Fracture Mechanics:

  Vol. 1, Ed. G. C. Sih and L. Faria: *Fracture Mechanics Methodology—Evaluation of Structural Components Integrity*;

  Vol. 2, by E. E. Gdoutos, Ed. G. C. Sih: *Problems of Mixed Mode Crack Propagation*, 1984;

  Vol. 3, Ed. A. Carpinteri and A. R. Ingraffea: *Fracture Mechanics of Concrete—Material Characterization and Testing*;

  Vol. 4, Ed. G. C. Sih and A. Ditomasso: *Fracture Mechanics of Concrete—Structural Application and Numerical Calculation*, 1984;

  Vol. 5, by A. Carpinteri, Ed. G. C. Sih: *Mechanical Damage and Crack Growth in Concrete—Plastic Collapse to Brittle Fracture*, 1986;

  Vol. 6, by J. W. Provan: *Probabilistic Fracture Mechanics and Reliability*, 1986, Martinus Nijhoff Publishers.

Shah S. P. (Ed.), 1985, *Applications of Fracture Mechanics to Cementitious Composites*, Proceedings of the NATO Adv. Res. Workshop, Martinus Nijhoff Publ.

Shaw M. C., 1973, *Fundamental Basis of the Hardness Test*, The Science of Hardness Testing and Its Research Applications, Amer. Soc. for Metals.

Shtayerman I. Ya., 1949, *Contact Problems of the Theory of Elasticity* (in Russian), Gostekhizdat, Moskva.

Shtayerman I. Ya., 1961, *Compression of Elastic Solids Contacting Along Straight Line Segment* (in Russian), Izd. Ak. Nauk SSSR.

Sih G. C., 1973, *Handbook of Stress Intensity Factors*, Inst. of Fracture and Solid Mechanics, Lehigh University.

Sih G. C. (Ed.), 1973, *Mechanics of Fracture*: Vol. 1—*Methods of Analysis and Solutions of Crack Problems*; Vol. 2—*Three-Dimensional Crack Problems*; Vol. 3—*Plates and Shells with Cracks*; Vol. 4—*Elastodynamic Crack Problems*; Vol. 5—*Stress Analysis of Notch Problems*, Noordhoff Int. Publ., 1973–1978.

Sih G. C., Michopoulos J. G., Chou S. C. (Eds.), 1986, *Hygrothermoelasticity*, Martinus Nijhoff Publ.

Sneddon I. W., 1962, *Crack Problems in the Mathematical Theory of Elasticity* (in Polish), PAN, Warszawa.

Sneddon I. N., Gladwell G. M. L., Coen S., 1975 "Bonded contact of an infinite plate and an elastic foundation", *Letters in appl. and engng. sciences*, 3.

Sneddon I. N., Lowengrub M., 1969, *Crack Problems in the Classical Theory of Elasticity*, John Wiley and Sons, Inc.

Tada H., Paris P. C., Irwin G. R., 1973, *The stress Analysis of Cracks*, Handbook, Del Research Corporation, Hellertown.

Tamuzh V. P., Kuksenko V. S., 1978, *Micromechanics of Fracture of Polymer Materials* (in Russian), Zanatne, Riga.

Technological Mechanics, 1978, Vol. IV. *Theory of Elasticity*, Vol. VIII, *Theory of Plates and Shells* (in Polish), PWN, Warszawa.

Timoshenko S., 1953, *History of Strength of Materials*, McGraw-Hill; in Polish: Arkady, Warszawa, 1966.

Tsai S. W., 1971, "A general theory of strength for anisotropic materials", *J. Composite Materials* **5**, 58–80.

Uflyand Ya. S., 1963, *Integral Transforms in the Problems of the Theory of Elasticity* (in Russian), Izd. Ak. Nauk SSSR.

Updike D. P., Kalnins A., 1970, "Axisymmetric behavior of an elastic spherical shell compressed between rigid plates", *J. Appl. Mech.* **37**.

Vainberg D. V., Vainberg E. D., 1959, *Plates, Discs, Wall-Beams* (in Russian), Gos. Izd. Lit. po Stroit. i Archit. USSR, Kiev.

Vainberg D. V., 1969, *Stress Concentration in Plates around Holes and Spalling* (in Russian), Tekhnika, Kiev.

Van-Fo-Fy G. A. *et al.* (Ed.), Frantsevitch I. N., Karpinos D. M., 1970, *Composite Materials of Fibrous Structure* (in Russian), Naukova Dumka, Kiev.

de Wit R., 1977, "Continuum theory of disclinations", Russian edition in *Mekhanika, Novoye za rubezhom*, Vol. 9, Mir.

Willis J. R., 1966, "Hertzian contact of anisotropic bodies", *J. Mech. Phys. of Solids* **14**.

Wilshire B., Owen D. R. J. (Eds.), 1981, *Creep and Fracture of Engineering Materials and Structures*, Proc. of the First Int. Conf.; Proc. of the Second Int. Conf., 1984, Pineridge Press.

Wnuk M. P., 1977, *Foundations of Fracture Mechanics* (in Polish), Akademia Górniczo-Hutnicza, Lecture 585, Kraków.

Yoffe E. H., 1951, "The moving Griffith crack", *Phil. Mag.* **42**, 739.

Introduction

Axially symmetrical elements and the structures they make, are frequently and keenly used in mechanical engineering, the main determinants here being manufacturing considerations, lightness, and character of the working processes involved. Such structures are fairly lucid and feature relatively simple distributions of loading and internal forces and also states of strain, all described by relationships easily lending themselves to analysis.

An element or a structure is said to be *axially symmetrical* (*circularly symmetrical*) *completely* or *exactly* if it is geometrically, elastically axially symmetrical and if the loadings are also axially symmetrical. Both the internal forces and the strains then have also axially symmetrical distributions (except special cases, e.g. loss of stability, Fleishman, 1962; Timoshenko and Goodier, 1962; Timoshenko and Woinowsky-Krieger, 1959).

Classified as axially symmetrical structural, elements are in the first place thick-walled cylinders (pipes), and also plates and disks as well as shells, whose cross-sections, i.e., sections normal to the axis of circular symmetry, are circles or circular rings. The present part of the book is devoted to such elements and to structures comprising these elements which satify the condition of complete axial symmetry.

The temperature field is treated in our considerations as a certain type of loading, called *thermal loading*.

Most machine structures involving elements featuring axial symmetry are chiefly of carbon or alloy steels, less often of light alloys. These materials, except for low-carbon structural steels, are described by offset yield strength R_e specified by standards. Low carbon steels are described by the physical yield point. The quantity R_e, determined experimentally—denoted by σ_{pl} in theory—plays an important role in structural calculation methods. In the case of a structure loaded below the yield point, therefore in the range of linearly elastic and small strains, common methods of stress and strain analysis are used for all materials.

In most cases, the loadings of axially symmetrical elements are simple, owing to which the determination of the states of stress and strain using the theory of elasticity does not present any major difficulty. The strength calcu-

lations used in practice for elements and structures are sufficiently accurate. There is a justifiable view that both the designer and the tester of a machine should concentrate primarily on problems relating to the determination of optimum operating conditions of the machine, on its rational forming, especially at places with distinct discontinuities of geometrical nature, and on the choice of proper materials, and eventually, they should take care that the terms adopted in the design and calculating stage be satisfied in practice.

Any opening, if placed in the wall of a pipe, shell, plate or disk, gives in effect the loss of complete axial symmetry, it also induces a stress concentration of local nature, which is frequently a determinant of safe operation of the structure involved. The designer of a structure to be endowed with axial symmetry deals in most cases with linearly elastic strains. Other cases, e.g., with non-linear elasticity, plastic and considerable elastic strains or creep are often due to high temperatures and very considerable mechanical loadings. These problems are out of the scope of the present part of the book, just as are problems relating to stability or large displacements, or to conl centrated forces introduced, for example, at the junctions of separable shells, because the complete axial symmetry condition is not met here. These are problems considered in the theory of non-linear elasticity or in the theory of stress concentrations, which come under other fields of applied mechanics.

The present trend in machine design is to arrive at optimum structures, for example, in terms of lightness, steady work safety or service life. Furthermore, ways and means are sought of raising the strength factor by endowing the componental structural elements with a suitable shape, which in the case of complete axial symmetry and with easy availability of digital computers presents no difficulty.

A completely axially symmetrical integrated elastic structure subjected to combined loadings can be represented as a sum of simple structural elements loaded in a simple way. If acting on an element are simultaneously a mechanical, static loading, intertial loading (e.g. in rotary motion) and a thermal loading, then the states of stress and strain existing in it can be considered as the resultants of the componental states corresponding to each loading separately. Such a procedure lengthens the calculation process, but simplifies the analysis and makes it more lucid. Unlimited linear elasticity of material is allowed in theoretical considerations, but on condition that the resultant state of strain must satisfy the design terms specified for the structure, and that the yield point has a definite value. An axially symmetrical structure, like most other structures, designed as optimal remains such only for a specified loading.

1. Axially Symmetrical Thick-Walled Elements

An axially symmetrical element is *thick-walled* if the inside-outside diameter ratio in the annular cross-section has a small value in relation to one. This definition applies both to thick-walled cylinders (pipes, shafts, pressure vessels) and to hollow spheres and hemispheres, constituting component parts of high-pressure vessels. High pressures and temperatures are the main factors enforcing a considerable thickness of walls, and the methods of elasticity theory describing the states of stress therein differ significantly from the methods for similar elements but having thin or very thin walls.

Thick-walled elements are used chiefly in chemical plants (high-pressure liquid tanks, high-pressure dispensers, combustion-chamber bodies), in mechanical engineering (e.g. hydraulic-press columns, liners in high-pressure servo motors and shock absorbers, transmission shafts, high-power coupling), in electrical engineering (e.g. turbine and generator rotors, bodies, and shafts, pressure conduits, thermal energy generators, nuclear reactor bodies), in building facilities (e.g. hoist bodies) and in armaments industry (barrels, recoil buffers), etc.

Usually, the loadings of axially symmetrical thick-walled elements are simple or almost simple, and they are likewise axially symmetrical; the stress and strain distributions described based on linear theory of elasticity are then expressed by relationships in closed form. Analogous stress distributions at junctions of thick-walled elements, e.g. two thick-walled conduits joined through a hemisphere or cone, or in some other way, can be determined either by approximative procedure, using the finite element method assisted by a digital computer, or by experimental techniques.

The problem of determining the stresses and strains in the wall of a thick-walled element with a long rectilinear axis, i.e., in the wall of a thick-walled cylinder (pipe), (length 1 markedly greater than the outside radius) subjected to internal and external pressure, is called the Lamé problem. It is discussed in general and specialized literature concerned with both theory of elasticity and thick-walled structures (Brzoska, 1972; Jakubowicz and Orłoś. 1968;

Krzyś and Życzkowski, 1962; Kurowski and Niezgodziński, 1970; Lipka, 1967; Timoshenko and Goodier, 1962; Walczak, 1971). The scope of the problem can be broadened introducing rotary motion about the z-axis and temperature fields (Pavlov, 1961; Timoshenko and Goodier, 1962).

1.1. The State of Stresses and Strain in a Thick-Walled Cylinder under Pressure, Heated and Rotating

A thick-walled cylinder subjected to internal pressure p_1 and external pressure p_2 and heated, rotates about the axis of circular symmetry with constant angular velocity Ω (Fig. 1.1a). We proceed from the following assumptions:
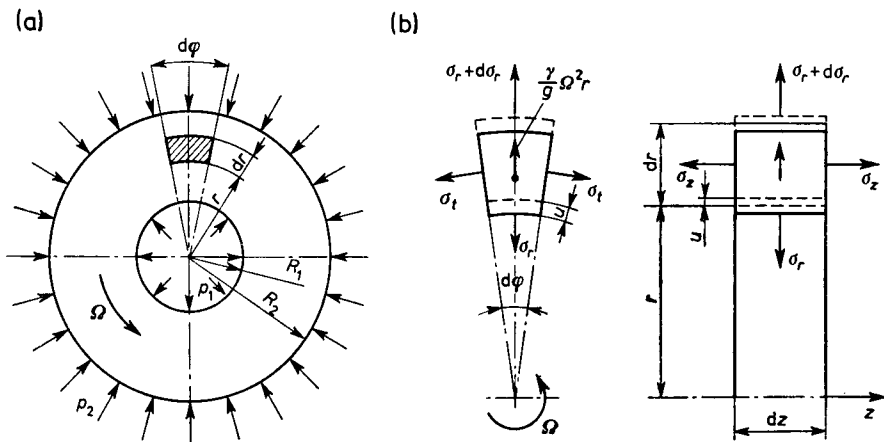
Fig. 1.1. Thick-walled cylinder: (a) loading by pressures p_1 and p_2; (b) wall element

— the material is isotropic and homogeneous and has no structural defects. Young's modulus E, Poisson's ratio ν, yield strength R_e and coefficient of thermal expansion α are all constant and independent of the heating temperature,
— Hooke's law is satisfied at any point of the wall; this means that the material is linearly elastic and that plastic strains are non-existent.
— the cylinder is long enough for any influence of its ends on the state of stress at sufficiently remote places to be treated as negligible,
— the shapes of the cross-sections over the entire length are not subject to change and remain plane,
— the initial state of stress, i.e., that before loading, is zero in value,
— the pressures on both surfaces are constant and of time independent. They may be identical or different:

— the temperature distribution is axially symmetrical, and the temperature on a given radius r and along the generatrix is constant, i.e., it is a function of the radius only,

— the elastic strains are so small that they produce no changes in loading.

Sufficiently slow changes in pressures, revolutions and temperatures are allowed without the axial symmetry being disturbed, which means that the loadings are static or quasi-static. The latter does not affect appreciably the accuracy of calculations (Alpert, 1965; Berenov, 1959; Birger *et al.*, 1959; Boyaroshinov, 1962).

Since the thick-walled cylinder is in the state of complete axial symmetry, the stress and strain distributions induced in it are also axially symmetrical; an arbitrary plane passed through the z-axis is a plane of symmetry and the shear stresses in its cross-sections equal zero. An infinitesimal element, cut out of the wall by two planes normal to the z-axis, dz distant from each other, by two planes inclined to each other at angle $d\varphi$ and intersecting along the z-axis and by two circular surfaces with a common z-axis and with radii r and $r+dr$, respectively, (Fig. 1.1b) is subjected only to normal stresses, radial σ_r, $\sigma_r+d\sigma_r$, circumferential σ_t, and longitudinal σ_z applied to the respective walls, and to a force of inertia of intensity Ω, where ϱ is the material density of the element. The forces acting on the element have to satisfy the equilibrium conditions. There remains however, only one equilibrium condition written for the sum of projections of all the forces on the plane of symmetry of the element; it leads to the differential equation

$$\frac{d\sigma_r}{dr} + \frac{\sigma_r - \sigma_t}{r} + \varrho\Omega^2 r = 0 \qquad (1.1)$$

known as the equation of internal equilibrium. It is not sufficient to determine both stress components. The determination of these stresses is therefore a statically indeterminate problem, and to solve it, it is necessary to use the strain-displacement relations and the relationships between the stress components and the unit elongations of the element considered.

The dimensions will change under the load, and the wall element placed originally at distance r from the z-axis will shift along the radius by a value u, and its side of length dr will experience elongation du. The unit radial elongation—in keeping with the definition—is then expressed as

$$\varepsilon_r = \frac{du}{dr} \qquad (1.2)$$

and the unit circumferential elongation measured on radius $r+u$ equals

$$\varepsilon_t = \frac{u}{r}. \qquad (1.3)$$

Differentiating (1.3) with respect to r and substituting the result into (1.2), we arrive at the relationship

$$\frac{\mathrm{d}(r\varepsilon_t)}{\mathrm{d}r} - \varepsilon_r = 0$$

called the *compatibility equation* of strain in the case of axial symmetry.

For a three-axial state of stress described by principal stress components σ_r, σ_t, σ_z, there exist three relationships

$$\varepsilon_r = \frac{1}{E}[\sigma_r - \nu(\sigma_t + \sigma_z)] + \alpha T, \tag{1.4}$$

$$\varepsilon_t = \frac{1}{E}[\sigma_t - \nu(\sigma_z + \sigma_r)] + \alpha T, \tag{1.5}$$

$$\varepsilon_z = \frac{1}{E}[\sigma_z - \nu(\sigma_r + \sigma_t)] + \alpha T, \tag{1.6}$$

which follow from Hooke's law of thermoelastic state of a body. In these relationships, α is the thermal coefficient of linear elongation of the material and T is the temperature difference between the initial state and the heated state. The former is described by temperature T_0 which is usually taken to be zero. In our further considerations, T stands for temperature increment (positive or negative) reckoned from a constant initial temperature. Obviously, $T = T(r)$.

The stresses determined from (1.4)–(1.6), with (1.2) and (1.3) considered, are expressed in the form

$$\sigma_r = \frac{E}{(1+\nu)(1-2\nu)}\left[(1-\nu)\frac{\mathrm{d}u}{\mathrm{d}r} + \nu\left(\frac{u}{r} + \varepsilon_z\right) - (1+\nu)\alpha T\right], \tag{1.7}$$

$$\sigma_t = \frac{E}{(1+\nu)(1-2\nu)}\left[(1-\nu)\frac{u}{r} + \nu\left(\frac{\mathrm{d}u}{\mathrm{d}r} + \varepsilon_z\right) - (1+\nu)\alpha T\right], \tag{1.8}$$

$$\sigma_z = \frac{E}{(1+\nu)(1-2\nu)}\left[(1-\nu)\varepsilon_z + \nu\left(\frac{u}{r} + \frac{\mathrm{d}u}{\mathrm{d}r}\right) - (1+\nu)\alpha T\right]. \tag{1.9}$$

Putting the relationships (1.7), (1.8) into (1.1), we express the equation of internal equilibrium by a single function, namely displacement $u(r)$ and express it in the form

$$\frac{\mathrm{d}^2 u}{\mathrm{d}r^2} + \frac{1}{r}\frac{\mathrm{d}u}{\mathrm{d}r} - \frac{u}{r^2} + Ar - B\frac{\mathrm{d}T}{\mathrm{d}r} = 0, \tag{1.10}$$

where

$$A = \frac{(1+\nu)(1-2\nu)}{1-\nu}\frac{\varrho}{E}\Omega^2, \quad B = \frac{\alpha(1+\nu)}{1-\nu} \quad \text{with} \quad \varepsilon_z = \text{const.}$$

This is a second-order linear differential equations whose solution in the form of the integral

$$u(r) = C_1 r + \frac{C_2}{r} - \frac{A}{8} r^3 + \frac{B}{r} \int\limits_{R_1}^{r} rT(r)\mathrm{d}r \qquad (1.11)$$

has constants of integration C_1 and C_2. The above consideration, specifically Eq. (1.11), shows that the examined states of stress and strain are three-dimensional in the general case of loading, and the values of the components are the sum of the respective components deriving from individual loadings. Stress component σ_z cannot be determined directly from Eqs. (1.4)–(1.9) and (1.11). Both constants, C_1 and C_2, are determined from the boundary conditions specified for a thick-walled cylinder in accordance with the functions it must perform in the structure. These conditions, mostly expressed by stresses, apply to both the outer and inner surface and to the end faces of the tkick-walled cylinder. The functions $u(r)$ and $\sigma_z(r)$ thus defined describe uniquely both the state of stress and strain (Brzoska, 1972; Jakubowicz and Orłoś, 1968; Krzyś and Życzkowski, 1962; Kurowski and Niezgodziński, 1970; Lipka, 1967).

As indicated above, the boundary conditions apply to both surfaces with radii R_1 and R_2 respectively and to the end faces of the cylinder, for $z = 0$ and $z = l$. The most common cases found in practice are as follows:

I. Pressures p_1 and p_2 are acting, then
   for $r = R_1$, we must have $\sigma_s = -p_1$,
   for $r = R_2$, we must have $\sigma_r = -p_2$,
   and both C_1 and C_2 differ from zero.
II. If $p_1 = 0$ and $p_2 = 0$, then
   for $r = R_1$ and $r = R_2$, we have $\sigma_r = 0$,
   and C_1 and C_2 differ from zero.
III. If $R_1 = 0$, i.e., a solid cylinder and if $p_2 = 0$, then
   for $r = 0$ we have $u = 0$ and for $r = R_2$, $\sigma_r = 0$.
   In this case, which is easily proved, using (1.11), $C_1 \neq 0$ and $C_2 = 0$
IV. If the condition that the radial displacement should not exceed the value δ, has been imposed on the outer surface, and $p_1 = 0$, then
   for $r = R_2$ we must have $u = \delta$ and
   for $r = R_1$ w must have $\sigma_r = 0$.
   Both constants of integration assume values that differ from zero.
V. If the increments of the radii are allowed to equal δ_1 and σ_2, respectively, then for
   $r = R_1$, we have $u = \delta_1$,

$r = R_2$, we have $u = \delta_2$

and both C_1 and C_2 are different from zero.

The conditions IV and V can also be used to determine unknown pressures p_1 and p_2 or else to determine, for example, the allowable angular velocity of a cylinder (a thick-walled shaft) or the allowable temperature. Obviously, the boundary conditions listed do not exhaust all possible cases encountered in practice.

Separate attention should be given to the conditions imposed on the ends of a thick-walled cylinder. We usually deal with three cases: both ends are free; both restrained so that $\varepsilon_z = 0$; both loaded by force N along the z-axis. These cases are discussed in greater detail in our further considerations (Huber, 1954, 1958; Ponomarev et al., 1958).

The assumptions brought into theory, to be called as very harsh requirements, have made it possible in fact to arrive ultimately at relatively simple considerations, in closed form. It appears therefore justifiable to ask whether these assumptions can actually be met, while the machine is run in exploitation, since it is precisely this on which the conformity of results derived from theoretical calculations with those based on experimental studies depends. Practical experience answers this question in the affirmative—in steady states, loadings can be kept under control by suitable design solutions and by checks on operational parameters. Numerous tests confirm the correctness of the above indications.

Generally speaking, stress components σ_r, σ_t, σ_z vary along radius r and their values depend chiefly on the loads applied. If the material of which a thick-walled cylinder has been made exhibits elastic-plastic properties and is homogeneous and isotropic, then the effort existing in it may be expressed by the distortional strain energy hypothesis (Huber, 1954, 1958) calculating the reduced (equivalent) stress for a three-axial state of stress as

$$\sigma_{\text{red H}} = \sqrt{\sigma_r^2 + \sigma_c^2 + \sigma_z^2 - \sigma_r \sigma_t - \sigma_t \sigma_z - \sigma_z \sigma_r}\Big|_{\text{max}}, \tag{1.12}$$

and for a biaxial state of stress, when, e.g., $\sigma_z = 0$, as

$$\sigma_{\text{red H}} = \sqrt{\sigma_r^2 + \sigma_t^2 - \sigma_r \sigma_t}\Big|_{\text{max}} \tag{1.13}$$

or by using the maximum shear stress hypothesis (τ_{max}, Tresca) expressed by maximal difference of principal stresses. If for example, $\sigma_t > \sigma_z > \sigma_r$, then

$$\sigma_{\text{red T}} = (\sigma_t - \sigma_r)\big|_{\text{max}}. \tag{1.14}$$

Both hypotheses are used in practice, they also enable a thick-walled element with a predetermined safety factor to be designed (Brzoska, 1972; Jakubowicz and Orłoś, 1968; Krzyś and Życzkowski, 1962; Kurowski and

Niezgodziński, 1970). Thus, generally speaking, the reduced stress also varies along radius r. The state of a thick-walled element is considered safe when the reduced maximum stress is not in excess of the allowable (safe) stress value k_r, determined with respect to the value R_e—determined from strength tests for a given material—with a safety factor $n_e > 1$. To find σ_{red}, Eq. (1.12), or possibly (1.13), is more commonly used as it gives lesser differences between reduced stress values calculated theoretically and determined experimentally, e.g., by means of strain-gauge measurements (Lipka *et al.*, 1977).

1.2. Loading of Thick-Walled Cylinders

The function $u(r)$ (1.11) bringing together the effects of three typical loadings, namely pressures, body forces and thermal loadings is relatively simple, but after the constants C_1 and C_2 have been determined it becomes more complex and when put into the relationships specifying the stresses, it makes these relationships difficult for analysis of the states of stress. Although the stress components and σ_{red} are expressed in closed forms, the equations are multi-term, complicated and inoperative in practice.

Bearing in mind the valid principle of summation of the effects of individual component loadings, solutions are sought for simple thick-walled cylinders, loaded by simple force systems. In this way we arrive at much simpler relationships and formulae, more convenient for purposes of design and calculation. This procedure is justifiable on practical grounds, since it is most uncommon for principal loadings to occur in real structures all at once.

Of special importance for analysis and optimization of structures with the use of a digital computer are relations (1.4)–(1.11).

1.2.1. Cylinders under pressures p_1 and p_2

Boundary conditions as in Fig. 1a, just as in case I (Section 1.1). Assuming at first $\sigma_z = 0$, meaning that a plane state of stress with components σ_r, σ_t prevails, the function $u(r)$ (1.11) is expressed as

$$u = C_1 r + \frac{C_2}{r}$$

and the stress components are determined from (1.7) and (1.8):

$$\sigma_r = \frac{E}{1-\nu^2}\left[(1+\nu)C_1 - (1-\nu)\frac{C_2}{r^2}\right],$$

$$\sigma_t = \frac{E}{1-\nu^2}\left[(1+\nu)C_1 + (1-\nu)\frac{C_2}{r^2}\right].$$

Adding the above equations by sides, we obtain the sum of radial and circumferential stresses

$$\sigma_r + \sigma_t = \frac{2E}{1-\nu} C_1, \tag{1.15}$$

which is constant at any point of the wall, meaning that it is independent of radius r. From relationship (1.9) it follows directly that

$$\varepsilon_z = -\frac{\nu}{E}(\sigma_r + \sigma_t) \tag{1.16}$$

and that it is constant at every point of the cross-section. Hence, the cross-sections remain plane after loading by p_1, p_2. Therefore, the assumption that every thick-walled cylinder has plane cross-sections, is valid and proved. The stresses σ_r, σ_t acting guarantee strain continuity in the plane of cross-section and in the direction of the cylinder axis.

Using the expressions for σ_r, σ_t and proceeding from the boundary conditions, we arrive at two conditional equations containing unknown constants C_1, C_2. Solving these equations we determine the two constants, which put into the relations for u, σ_r, σ_t, lead to the final formulae for radial displacement

$$u(r) = \frac{1-\nu^2}{E(R_2^2 - R_1^2)} \left[\frac{p_1 R_1^2 - p_2 R_2^2}{1+\nu} r + \frac{(p_1 - p_2)R_1^2 R_2^2}{1-\nu} \cdot \frac{1}{r} \right] \tag{1.17}$$

and for stress components

$$\sigma_r = \frac{p_1 R_1^2 - p_2 R_2^2}{R_2^2 - R_1^2} - \frac{p_1 - p_2}{R_2^2 - R_1^2} \cdot \frac{R_1^2 R_2^2}{r^2}, \tag{1.18}$$

$$\sigma_t = \frac{p_1 R_1^2 - p_2 R_2^2}{R_2^2 - R_1^2} + \frac{p_1 - p_2}{R_2^2 - R_1^2} \cdot \frac{R_1^2 R_2^2}{r^2}. \tag{1.19}$$

Obviously, displacements u_1 and u_2 on the two edges are determinable from (1.17) for radius value $r = R_1$ or $r = R_2$ (Brzoska, 1972; Jakubowicz and Orłoś, 1968; Krzyś and Życzkowski, 1962; Lipka, 1967; Timoshenko and Goodier, 1962; Vainberg and Vainberg, 1959; Walczak, 1971).

In the case common in practice where pressures $p_1 = p_2 = p$ are acting,

$$\sigma_r = \sigma_t = -p$$

and they are identical in the whole of the cross-section.

1.2.2. Thick-walled hollow cylinder under internal pressure p_1 inside

A case frequently encountered in engineering reduces to a special case where $p_1 \neq 0$ and $p_2 = 0$. The stress and displacement distributions are determined from general relationships and from boundary conditions, or else from Eqs.

(1.17)–(1.19), using appropriate values for p_1 with $p_2 = 0$. The latter procedure being much simpler is used below. It follows from the above relationships that

$$\sigma_r = \frac{p_1 R_1^2}{R_2^2 - R_1^2}\left(1 - \frac{R_2^2}{r^2}\right), \tag{1.20}$$

$$\sigma_t = \frac{p_1 R_1^2}{R_2^2 - R_1^2}\left(1 + \frac{R_2^2}{r^2}\right). \tag{1.21}$$

In layers on the edges with radii R_1 and R_2, the circumferential stresses are

$$\sigma_{tR_1} = p_1 \frac{R_1^2 + R_2^2}{R_2^2 - R_1^2}, \tag{1.22}$$

$$\sigma_{tR_2} = 2p_1 \frac{R_1^2}{R_2^2 - R_1^2}. \tag{1.23}$$

The radial stresses are compressive and the circumefrential tensile, and the maximum reduced stress occurs in the extreme layer of the hole, reaching the value

$$\sigma_{\text{red H}} = p_1 \frac{R_2^2}{R_2^2 - R_1^2}\sqrt{3 + \left(\frac{R_1}{R_2}\right)^4}. \tag{1.24}$$
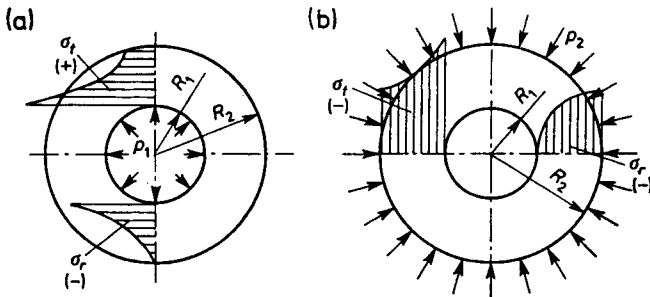
Fig. 1.2. Thick-walled cylinder: (a) pressure p_1 acting; (b) pressure p_2 acting, σ_r, σ_t stresses along wall thickness

The stress distributions are shown in Fig. 1.2a. If in (1.24) the condition is taken that the reduced stress does not exceed the allowable stress k_r then the outside radius R_2 satisfying this condition for given R_1, p_1 is specified by

$$R_2 \geqslant R_1\sqrt{\frac{1+\beta}{1-3\beta^2}} \quad \left(\beta = \frac{p_1}{k_r} < \frac{\sqrt{3}}{3}\right). \tag{1.25}$$

The respective increments of the radius of the hole R_1 and of the outer radius R_2 calculated from (1.17) for R_1 are

$$u_{R_1} = p_1 \frac{R_1}{E} \left(\frac{R_2^2 + R_1^2}{R_2^2 - R_1^2} + \nu \right) \tag{1.26}$$

and for R_2

$$u_{R_2} = 2p_1 \frac{R_1^2 R_2}{E(R_2^2 - R_1^2)} . \tag{1.27}$$

It should be noted that if the wall thickness $h = R_2 - R_1$ is very great compared to R_1 $(R_2 \gg R_1)$, then stresses σ_r, σ_t, σ_{red} diminish as R_2/R_1 increases and if this quotient tends to ∞, they do not tend to zero at places for which r is finite. Taking $R_2 - R_1 \approx R_2$ and assuming that for $r \ll R_2$ we have $1 \pm \dfrac{R_2}{r^2} \approx \pm \dfrac{R_2^2}{r^2}$; we then obtain the approximate relationships

$$\sigma_r \approx -p_1 \frac{R_1^2}{r^2} , \qquad \sigma_t \approx p_1 \frac{R_1^2}{r^2} \tag{1.28}$$

and on the edge of the hole, $\sigma_t(R_1) \approx p_1$. This means that in a very thick wall, both stress components, σ_r, σ_t, have practically the same absolute values. At a fairly distant point of the wall, for which say, $r = 5R_1$, both components reach values equalling 4% the maximum stress value, i.e., p_1. A practical conclusion is to be reached from above considerations, namely if such inaccuracies in calculations are admissible, then every thick-walled cylinder which satisfies, say, $R_2 > 5R_1$, can be treated as one having a wall almost infinitely thick. An elastic space with a small hole subjected to pressure satisfies this condition. The maximum reduced stress exists on the fringe of the hole.

$$\sigma_{red H} \approx \sqrt{3} p_1 . \tag{1.29}$$

Similarly, when wall thickness $h = R_2 - R_1$ remains small compared to R_1 (i.e., $h \ll R_1$), the mean value of circumferential stress calculated from the equilibrium condition written for half a slice of the cylinder cut out an transverse direction and intersected by a plane along the z-axis is

$$\sigma_{ts} = \frac{R_1}{h} p_1 . \tag{1.30}$$

The difference of the circumferential stress values on both edges of the cross-section after (1.22) and (1.23)

$$\sigma_{tR_1} - \sigma_{tR_2} \approx p_1 \tag{1.31}$$

is constant, and both σ_{tR_1} and σ_{tR_2} are much greater than p_1. The expression obtained from two-sided division of (1.31) by (1.30)

$$\frac{\sigma_{tR_1} - \sigma_{tR_2}}{\sigma_{ts}} \approx \frac{h}{R_1}$$

shows that the smaller the wall thickness h is compared to R_1, the smaller the difference between σ_{tR_1} and σ_{tR_2} will be and also the smaller will be the error involved here due to replacing σ_t by mean value σ_{ts}. For example, if $h = 0.05 R_1$, then $(\sigma_{tR_1} - \sigma_{tR_2}) \approx 0.05 \sigma_{ts}$, results in 5%. An inaccuracy of that order is allowable in many calculations.

1.2.3. Thick-walled cylinder under pressure p_2

If $p_1 = 0$ and $p_2 \neq 0$, then at any point of the cylinder's cross-section

$$\sigma_r = -p_2 \frac{R_2^2}{R_2^2 - R_1^2} \left(1 - \frac{R_1^2}{r^2} \right), \tag{1.32}$$

$$\sigma_t = -p_2 \frac{R_2^2}{R_2^2 - R_1^2} \left(1 + \frac{R_1^2}{r^2} \right), \tag{1.33}$$

and the displacement is

$$u(r) = -p_2 \frac{R_2 r}{E(R_2^2 - R_1^2)} \left[1 - \nu + (1 + \nu) \frac{R_1^2}{r^2} \right]. \tag{1.34}$$

The stress distributions are shown in Fig. 1.2b.

The circumferential stresses on the inner and outer edge are respectively

$$\sigma_{tR_1} = -2p_2 \frac{R_2^2}{R_2^2 - R_1^2}, \qquad \sigma_{tR_2} = -p_2 \frac{R_2^2 + R_1^2}{R_2^2 - R_1^2} \tag{1.35}$$

and the displacements are

$$u_{R_1} = -2p_2 \frac{R_1 R_2^2}{E(R_2^2 - R_1^2)},$$

$$u_{R_2} = -p_2 \frac{R_2^2}{E(R_2^2 - R_1^2)} \left[1 - \nu + (1 + \nu) \frac{R_1^2}{R_2^2} \right]. \tag{1.36}$$

It follows from these relationships that both stress components are compressive, and the circumferential stress attains a maximum value on the inner edge, where $\sigma_{\text{red HR}_1} = \sigma_{tR_1}$. If $R_1 \ll R_2$, then

$$\sigma_{tR_1} \approx -2p_2, \qquad \sigma_{tR_2} \approx -p_2. \tag{1.37}$$

If $R_1 = 0$, $p_2 \neq 0$, meaning that a hollow cylinder has turned into a solid one, then the stresses

$$\sigma_r = \sigma_t = -p_2$$

are constant throughout the cross-section, they are equal in value to the pressure acting, and they are compressive. The displacement on radius R_2 is

$$u_{R_z} = -\frac{1-\nu}{E} p_2 R_2. \tag{1.38}$$

1.3. Thick-Walled Cylinder with Heads

This is an important case from an engineering point of view. We deal here with a long thick-walled cylinder closed at both ends by axially symmetrical heads of sufficient strength, and of arbitrary shape, in principle, subjected to pressure p_1. This is essentially an axially symmetrical thick-walled structure, as exemplified by pressure vessels or machine bodies. Next to normal stresses σ_r, σ_t, a third component of the state of stress is involved in such cylinders, namely principal stress σ_z labelled longitudinal (Kammash *et al.*, 1960; Nemec, 1964). Referring to our earlier remark, the state of stress at the connecting place of the cylinder with the cover will not be considered because it constitutes a separate problem of the elasticity theory. Unit elongation ε_z in cross-sections sufficiently distant from the connecting places of the heads is constant throughout the cross-section, which has previously been proved. Since $(\sigma_r + + \sigma_t) = \text{const}$, therefore σ_z also remains constant at any point of the cross-section. This assumption in the case of combined loading is only approximate, but it is sufficiently accurate for practical purposes and is commonly used (Brzoska, 1972; Huber, 1954, 1958). The equilibrium condition written for cross-sectional forces specifies the longitudinal stress value

$$\sigma_z = p_1 \frac{R_1^2}{R_2^2 - R_1^2}. \tag{1.39}$$

The maximum reduced stress occurs at inner radius R_1 and reaches a value, for example, in terms of the distortional strain energy hypothesis,

$$\sigma_{\text{red HR}_1} = \sqrt{3} p_1 \frac{R_2^2}{R_2^2 - R_1^2}. \tag{1.40}$$

Reduced stress on the outer surface is appreciably smaller. By the maximum shear stress hypothesis, it is

$$\sigma_{\text{red TR}_1} = 2 p_1 \frac{R_2^2}{R_2^2 - R_1^2}. \tag{1.41}$$

Comparing the last two equations, it is seen that the proposed structure, using (1.41) with the assumed coefficient n_b, weighs more than does the analogous structure derived from (1.40). Radius R_1 in this case has increment

$$u_{R_1} = p_1 \frac{R_1}{E} \left[\frac{(1-\nu) R_1^2 + R_2^2}{R_2^2 - R_1^2} + \nu \right]. \tag{1.42}$$

1.4. Two- and Multilayer Thick-Walled Cylinder

In certain cases, specifically when due to very high pressure p_1, the outside radius of the cylinder R_2 is considerable compared to R_1, an excessive weight increase is involved. This difficulty can be overcome by the use of elements consisting of two or more layers. Although such a structure is much lighter, it is at the same time more costly to manufacture; it calls for very careful calculations of the states of stress and not only for normal operating conditions but also for the assembly stages, when heated or cooled, etc. The design calculations are also more complicated. It has to be remembered that such two- or multilayer structures even when they do no work, i.e., when they experience no loading, are constantly under initial stress. Generally speaking, the material of individual layers may be the same or different, which is dictated, for example, by requirements of lightness, temperature or inside pressure in the hole of the extreme inner layer and by strength considerations. Outlined below are two designs, one of a two-layer structure and the other of a three-layer structure (Fig. 1.3). Others are calculated in a similar manner.
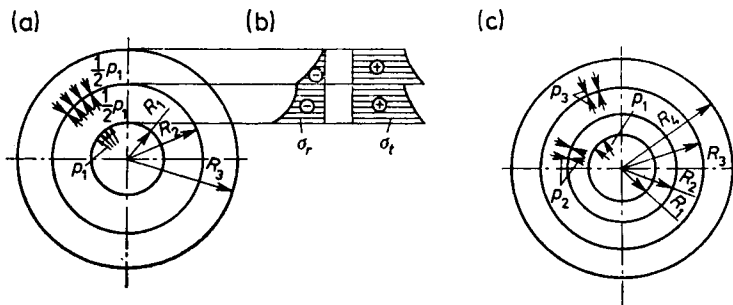
Fig. 1.3. Multilayer cylinder: (a) two-layer; (b) stresses σ_r, σ_t; (c) three-layer

Additional assumptions are usually made, relating chiefly to the mode of mating of individual layers, or else relating to the states of stress that occur in the assembly stage and during operation. For example:

(1) a state of stress is assumed on the inner wall of the inner layer, in which $\sigma_{\mathrm{red}\,R_1} \leqslant R_e$ has been reached (but not exceed) under pressure p_1,

(2) mutual pressure on the inner wall of the outer layer is assumed, say $1/2\,p_1$—which is completely arbitrary—at which also a state of stress $\sigma_{\mathrm{red}\,R_2} \leqslant R_e$ occurs. The material of both elements is identical and the structure has no heads. Considering the conditions and using the equations previously derived, we arrive at relationships expressing the cricumferential and radial stresses for the inner layer and radius R_1

$$\sigma_{tR_1} = p_1 \frac{R_1^2}{R_2^2 - R_1^2}, \tag{1.43}$$

$$\sigma_{rR_1} = -p_1 \tag{1.43a}$$

and

$$\sigma_{\mathrm{red}\,HR_1} = p_1 \sqrt{1 + \frac{R_1^2 R_2^2}{(R_2^2 - R_1^2)^2}} \leqslant R_e, \tag{1.44}$$

in which R_2 has to satisfy the condition by which the reduced stresses are required to reach the yield point. R_2 for the inner layer is determined from (1.44).

Similarly, we calculate the outside radius of the outer layer, namely the strength condition formulated for this layer reduces to

$$\frac{1}{2} p_1 \frac{1}{R_3^2 - R_2^2} \sqrt{R_2^4 + 3R_3^4} = R_e,$$

which determines the unknown R_3 and the condition

$$2\frac{R_e}{p_1} > \sqrt{3}$$

must be satisfied. The difference of the radii of contact surfaces of the two layers before assembly is

$$\Delta R = u_w + u_z,$$

where u_w and u_z are increments (elongations) of the outside radius of the inner layer and the inside radius of the outer layer. Shown in Fig. 1.3b are the states of stress along the wall thickness of the two layers. When pressure p_1 is absent, pressures other than $1/2\,p_1$ occur at the place of contact. These pressures ar ecalculated in a similar manner (Brzoska, 1972; Krzyś and Życzkowski, 1962; Lipka, 1967). Similarly, we calculate thick-walled multilayer (with more than two layers) cylinders. The choice of mutual pressures on the contact surfaces of respective layers is arbitrary in principle, but where lightness of the structure is an important design factor, it is advisable to allow states of stress coming close to the yield point either in all layers, though not everywhere but at particular points with the highest stress intensities, or in some selected layers (Brzoska, 1972; Krzyś and Życzkowski, 1962; Lipka, 1967).

Outlined below is the procedure to be followed in the design of a three-layer cylinder.

Pressures p_2 and p_3 are present between the contact surfaces (Fig. 1.3b),

induced by pressure p_1 in the hole of the layer with radius R_1. For preassumed reduced stresses we determine R_2 of the inner layer under p_1 and p_2 pressure conditions and then R_3 of the middle layer under p_2 and p_3 and lastly R_4 of the outer (extreme) layer subjected to only p_3. Use can be made here of the respective relationships for stresses and strains derived in Section 1.2. On technological grounds, it is necessary to calculate the indispensible differences of the radii, assuring that the assumed pressures between the layers will be attained and to check the states of stress in the layers for successive stages of the mounting of the individual componential layers in the state when $p_1 = 0$. The problem of an optimum—in terms of lightness of structure consisting of three or more layers can be solved in a relatively simple manner with a digital computer. Detailed calculations of multilayer thick-walled pipes, on which various surface loadings are acting, will be found in Krzyś and Życzkowski (1962). Using normal fits for connections of the layers, we check the pressures between the layers for upper and lower deviations of tolerance, avoiding in this way an undesirable state, e.g. the plastic state, or exceedingly small mutual pressures and insufficient strengthening of the cylinder. A considerably reduced weight of pressure vessels of circular cross-section is obtainable by the use of expanded multilayer structures. Their theory and technology differ from those used for the solutions considered above. Detailed considerations on the subject will be found in Krzyś et al. (1976), and Życzkowski (1964).

It is assumed in these considerations that all layers are of identical length. The changes in pressures and stresses at both ends after the layers have been laid on each other are not considered, being treated as negligibly small. If the particular layers joined by means of elastic contraction are of different length (e.g. a sleeve-shaft connection), the pressures between the contact surfaces along the generatrices distribute non-uniformly and increase near the edges of shorter layers (sleeves) to reach the highest values. When the sleeve length is small compared to the hole diameter, the highest real pressure is significantly greater than the analytical values. In the case described, we deal with the pressure concentration effect. This concentration can be reduced by using, for example, suitable shapes of the edges of the hole. A more detailed discussion of this question will be found in special contributions, e.g. Birger (1956, 1961), Birger et al. (1959), and Ponomarev et al. (1958). It is not considered in this part of the book.

Note that multilayer pressure cylinders, on account of the states of stress existing in them, are frequently described as prestressed or elastically strengthened structures.

1.5. Thick-Walled Cylinder in Rotary Motion

A long thick-walled element, solid or hollow (e.g. turbine rotor or propeller shaft) rotates at a constant angular velocity about the longitudinal z-axis. In cross-sections perpendicular to the z-axis, there also exist longitudinal stresses σ_z which sometimes can reach considerable values (Lipka, 1967; Ponomarev et al., 1958). Where temperature is not subject to change, expressions containing $T(r)$ disappear in relationships (1.4)–(1.11). Since the cross-sections remain plane, i.e., ε_z is constant or equals zero, these relationships become greatly simplified. Characteristically, the equation of internal equilibrium does not contain stress component σ_z whose value is independent of coordinate z but changes only along radius r. Both constants of integration for Eq. (1.11) without the last expression are determined from the conditions written for both surfaces of the cylinder, inner and outer, where radial stresses have to be equal to zero. The displacement function $u(r)$ with the integration constants determined after putting into (1.7)–(1.9) leads to the following relationships for stress components:

$$\sigma_r = \frac{3-2\nu}{8(1-\nu)}\, \varrho\Omega^2 R_2^2 \left(1 + \frac{R_1^2}{R_2^2} - \frac{R_1^2}{r^2} - \frac{r^2}{R_2^2}\right), \tag{1.45}$$

$$\sigma_t = \frac{3-2\nu}{8(1-\nu)}\, \varrho\Omega^2 R_2^2 \left(1 + \frac{R_1^2}{R_2^2} + \frac{R_1^2}{r^2} - \frac{1+2\nu}{3-2\nu}\cdot\frac{r^2}{R_2^2}\right), \tag{1.46}$$

$$\sigma_z = \varepsilon_z E + \frac{\nu(3-2\nu)}{4(1-\nu)}\, \varrho\Omega^2 R_2^2 \left(1 + \frac{R_1^2}{R_2^2} - \frac{2}{3-2\nu}\cdot\frac{r^2}{R_2^2}\right). \tag{1.47}$$

If at the ends of the cylinder and in its arbitrary cross-sction $\varepsilon_z = 0$, then

$$\sigma_z = \frac{\nu(3-2\nu)}{4(1-\nu)}\, \varrho\Omega^2 R_2^2 \left(1 + \frac{R_1^2}{R_2^2} - \frac{2}{3-2\nu}\cdot\frac{r^2}{R_2^2}\right) \tag{1.48}$$

varies along radius and is acting as tension. In this case, the longitudinal force

$$N = 2\pi \int_{R_1}^{R_2} r\sigma_z\, dr \tag{1.49}$$

differs from zero.

But if $N = 0$, we must have

$$\int_{R_1}^{R_2} r\sigma_z\, dr = 0 \tag{1.50}$$

and since the longitudinal stresses are expressed in accordance with relationship (1.6) as

$$\sigma_z = \varepsilon_z E + \nu(\sigma_r + \sigma_t);$$

hence also the following holds

$$\int_{R_1}^{R_2} r[\varepsilon_z E + \nu(\sigma_r + \sigma_t)] \, dr = 0. \tag{1.51}$$

In view of $\varepsilon_z = $ const, by integrating this relation and putting it again into relationship (1.6), we arrive at the expression for σ_z in its final form. It must be recalled that all the relationships for stress components hold for a solid cylinder ($R_1 = 0$).

1. Thus, for a hollow cylinder with both ends clamped, σ_r, σ_t are given by relationships (1.45), (1.46), (1.48), and in the case of free ends we have

$$\sigma_z = \frac{\nu}{4(1-\nu)} \varrho \Omega^2 R_2^2 \left(1 + \frac{R_1^2}{R_2^2} - 2 \frac{r^2}{R_2^2}\right) \tag{1.52}$$

and a change in sign.

2. Correspondingly, for a solid cylinder the following holds:

$$\sigma_r = \frac{3-2\nu}{8(1-\nu)} \varrho \Omega^2 R_2^2 \left(1 - \frac{r^2}{R_2^2}\right),$$

$$\sigma_t = \frac{3-2\nu}{8(1-\nu)} \varrho \Omega^2 R_2^2 \left(1 - \frac{1+2\nu}{3-2\nu} \cdot \frac{r^2}{R_2^2}\right), \tag{1.53}$$

with clamped ends:

$$\sigma_z = \frac{3-2\nu}{4(1-\nu)} \varrho \Omega^2 R_2^2 \left(1 - \frac{r^2}{R_2^2}\right) \tag{1.54}$$

and with free ends:

$$\sigma_z = \frac{\nu}{4(1-\nu)} \varrho \Omega^2 R_2^2 \left(1 - 2 \frac{r^2}{R_2^2}\right). \tag{1.55}$$

Stresses σ_z induced by rotary motion at low revolutions are not very great, but reach appreciable values when Ω is great and radius R_2 is considerable. The other stresses, σ_r, σ_t, are also great. Jointly with shear stresses, which is the case, for example, in drive shafts, they can produce a state of stress that determines strength.

1.6. Stresses in a Heated Thick-Walled Cylinder

In many cases, thermal stresses by themselves attain values so high that they cause considerable elastic strains, even plastic as well, and they are liable to lead to failure. This is very important, particularly where a brittle material is involved.

A decisive influence on the magnitude of thermal stress and its distribution has the character of the temperature field. The simplest way, in which this influence can be studied is to ignore all other loadings that may be involved (Jaworski and Raczyński, 1976; Krzyś and Życzkowski, 1962; Lipka, 1967; Ponomarev et al., 1958; Rogers and Lee, 1964; Skalski, 1970). The assumptions that E, ν, α are temperature independent is usually found true for steel in a temperature range up to 250°C. It is self-evident that expressions containing Ω disappear in equations and relationships describing states of stress and strain. Thus, function (1.11) loses the third expression, and the constants of integration are related to $T(r)$. They are determined from the conditions for both surfaces of the cylinder, the inner and the outer. In the absence of pressures, σ_r is of zero value on both surfaces.

If no external longitudinal force is acting on the ends $(N = 0)$, condition (1.50) must be satisfied. Where both ends are not free to shift freely against each other, elementary elongation $\varepsilon_z = 0$ as an additional condition, as in Section 1.5, σ_z can be determined in its relationships to the remaining stresses.

In the case of a heated solid shaft, constant C_2 becomes equal to zero.

Even if more detailed data concerning the form of function $T(r)$ are unavailable, we can utilize integral (1.11) converting relations (1.7)–(1.9) to a form easier to use. If both surfaces are free and not loaded, then

$$\sigma_r = \frac{E\alpha}{1-\nu} \cdot \frac{1}{r^2} \left[\frac{r^2 - R_1^2}{R_2^2 - R_1^2} \int_{R_1}^{R_2} rT(r)\,dr - \int_{R_1}^{r} rT(r)\,dr \right], \tag{1.56}$$

$$\sigma_t = \frac{E\alpha}{1-\nu} \cdot \frac{1}{r^2} \left[\frac{r^2 + R_1^2}{R_2^2 - R_1^2} \int_{R_1}^{R_2} rT(r)\,dr - r^2 T(r) + \int_{R_1}^{r} rT(r)\,dr \right], \tag{1.57}$$

$$\sigma_z = \frac{\nu\alpha E}{1-\nu} \left[\frac{1-\nu}{\nu} \varepsilon_z - \frac{1}{\nu} T(r) + \frac{2}{R_2^2 - R_1^2} \int_{R_1}^{R_2} rT(r)\,dr \right]. \tag{1.58}$$

If $N = 0$, then the solution of Eq. (1.50) with respect to unknown ε_z leads to the relationship

$$\sigma_z = \frac{E\alpha}{1-\nu} \left[\frac{2}{R_2^2 - R_1^2} \int_{R_1}^{R_2} rT(r)\,dr - T(r) \right]. \tag{1.59}$$

It has to be remembered that the above relationships allow all stress and strain components to be determined for a heat flow constant steady in time. The function of temperature distribution $T(r)$ along radius r can be arbitrary in principle. In practice, the states of temperature are also determined theoretical, using equations of heat conduction theory, or experimentally by temperature measurements on models or on real objects (Kobza and Lipiński, 1973; Pyzik et al., 1975).

Taking the heat flux passing between the walls to be steady and axially symmetrical at temperature T_1 of the inner surface and at temperature equaling zero on the outer surface, then in keeping with the theory of heat conduction, the temperature at any point of the cross-sction (Huber, 1954, 1958; Ponomarev et al., 1958) is given by the relation

$$T(r) = T_1 \frac{\ln \dfrac{r}{R_2}}{\ln \dfrac{R_1}{R_2}}. \tag{1.60}$$

Such a temperature field induces thermal stresses:

$$\sigma_r = \frac{E\alpha T_1}{2(1-\nu)(\ln R_1 - \ln R_2)} \left[\frac{R_1^2}{R_2^2 - R_1^2} \left(\frac{R_2^2}{r^2} - 1 \right) \ln \frac{R_1}{R_2} - \ln \frac{r}{R_2} \right], \tag{1.61}$$

$$\sigma_t = -\frac{E\alpha T_1}{2(1-\nu)(\ln R_1 - \ln R_2)} \left[\frac{R_1^2}{R_2^2 - R_1^2} \left(\frac{R_2^2}{r^2} + 1 \right) \ln \frac{R_1}{R_2} + \ln \frac{r}{R_2} + 1 \right], \tag{1.62}$$

$$\sigma_z = -\frac{E\alpha T_1}{2(1-\nu)(\ln R_1 - \ln R_2)} \left[\frac{2R_1^2}{R_2^2 - R_1^2} \ln \frac{R_1}{R_2} + 2\ln \frac{r}{R_2} + 1 \right]. \tag{1.63}$$

These stresses in the inner surface layer $(r = R_1)$ attain the values $\sigma_r = 0$, $\sigma_z = \sigma_t$ and

$$\sigma_{tR_1} = -\frac{E\alpha T_1}{2(1-\nu)(\ln R_1 - \ln R_2)} \left(\frac{2R_2^2}{R_2^2 - R_1^2} \ln \frac{R_1}{R_2} + 1 \right) \tag{1.64}$$

and on the outer surface (i.e., $r = R_2$), $\sigma_r = 0$, $\sigma_z = \sigma_t$ and

$$\sigma_{tR_2} = \frac{E\alpha T_1}{2(1-\nu)(\ln R_1 - \ln R_2)} \left(\frac{2R_1^2}{R_2^2 - R_1^2} \ln \frac{R_1}{R_2} + 1 \right). \tag{1.65}$$

The circumferential and longitudinal stresses have similar distributions over wall thickness and attain zero values—each in a different place (Fig. 1.4a, b). If the cylinder is sufficiently thin, i.e., R_2/R_1 tends to one, then
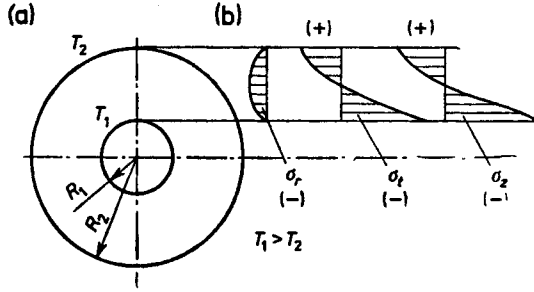
Fig. 1.4. Distribution of thermal stresses σ_r, σ_t, σ_z

$$\sigma_t \approx \frac{E\alpha T_1}{1-\nu} \left(\frac{2r}{R_2+R_1} - 1 \right),$$ (1.66)

$$\sigma_z = \sigma_t, \qquad \sigma_r \approx 0,$$

which is evidence of a linear thermal stress distribution along wall thickness. Compressive stress exists in the extreme inner layer

$$\sigma_{tR_1} = -\frac{E\alpha T_1}{2(1-\nu)}$$ (1.67)

and tensile stress of the same absolute value, in the outer layer.

For a cylinder heated to temperature T, identical at all points, Eq. (1.10) contains only the first three expressions, whereas in Eq. (1.11), only the expressions containing constants C_1 and C_2 and the definite integral remain.

If the walls are not loaded and remain free, then we get from simple calculations that $\sigma_r = 0$, $\sigma_t = 0$ in every cross-section. When no longitudinal force is acting, it follows from the equilibrium condition written for the z-axis that $\sigma_z = 0$ and $\varepsilon_z = \alpha T$ with radial displacement $u = \alpha Tr$. The conslusion that thermal stresses are non-existent in a uniformly heated cylinder is of major practical importance and it is utilized in calculations if the temperature on the outer surface differs from zero.

1.7. Thick-Walled Sphere under Pressure and Temperature

A thick-walled sphere with outer and inner radius R_2 and R_1, respectively, is subjected to pressure p_1 on the inner surface and to temperature $T(r)$ varying along the wall thickness. A differential volume element (Fig. 1.5), in which two walls are parts of concentric spheres with radii r and $(r+\mathrm{d}r)$ and the remaining ones are parts of planes making an apex at the intersection, which is at the same time the centre of the sphere, is in a three-axial state of stress
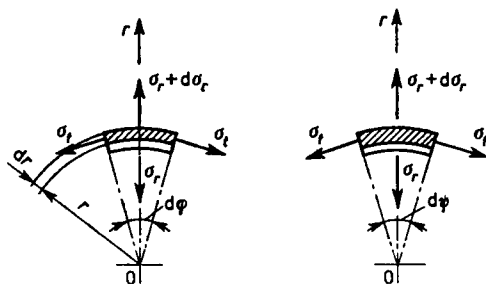
Fig. 1.5. Element of a thick-walled sphere

given by radial and circumferential stress components σ_r and σ_t, respectively, this being associated with symmetry.

The equilibrium condition written for the sum of projections of all forces on normal r to the element reduces to the differential equation

$$r \frac{d\sigma_r}{dr} + 2(\sigma_r - \sigma_t) = 0 \tag{1.68}$$

containing two unknowns σ_r and σ_t. In this case, the relationships between unit elongations—radial ε_r and circumferential ε_t—and stresses reduce to

$$\varepsilon_r = \frac{1}{E} (\sigma_r - 2\nu\sigma_t) + \alpha T, \tag{1.69}$$

$$\varepsilon_t = \frac{1}{E} [(1-\nu)\sigma_t - \nu\sigma_r] + \alpha T, \tag{1.70}$$

whereas relationships (1.2), (1.3) between ε_r, ε_t and radial displacement u remain unchanged. The stress components determined from (1.69), (1.70) are expressed by

$$\sigma_r = \frac{E}{(1+\nu)(1-2\nu)} \left[(1-\nu) \frac{du}{dr} + 2\nu \frac{u}{r} - (1+\nu)\alpha T \right], \tag{1.71}$$

$$\sigma_t = \frac{E}{(1+\nu)(1-2\nu)} \left[\frac{u}{r} + \nu \frac{du}{dr} - (1+\nu)\alpha T \right]. \tag{1.72}$$

Substituting the last two relationships into the internal equilibrium equation (1.68), we reduce the latter to the form

$$\frac{d^2u}{dr^2} + \frac{2}{r} \frac{du}{dr} - 2 \frac{u}{r} - \frac{1+\nu}{1-\nu} \alpha \frac{dT}{dr} = 0 \tag{1.73}$$

with a solution as the integral

$$u = u_1 + u_2$$

containing two functions, of which the first

$$u_1 = C_1 r + \frac{C_2}{r^2} \tag{1.74}$$

is the solution of Eq. (1.73) for $T = 0$, and u_2 depends on function $T(r)$ describing the distribution of temperature over wall thickness. Before finding u_2, we determine $T(r)$, using, for example, the theory of heat conduction. Function $u(r)$ can also be obtained by numerical methods. The problem becomes greatly simplified if $T(r) = 0$, since then only (1.74) with two constants, C_1 and C_2, determined as usual from the boundary conditions, remains to be considered. In the case $\sigma_r = -p_1$ on the surface with $r = R_1$ and $\sigma_r = 0$ for $r = R_2$, important in engineering, the stresses

$$\sigma_r = p_1 \frac{R_1^3}{R_2^3 - R_1^3} \left(1 - \frac{R_2^3}{r^3} \right),$$

$$\sigma_t = p_1 \frac{R_1^3}{R_2^3 - R_1^3} \left(1 + \frac{R_2^3}{2r^3} \right) \tag{1.75}$$

and the maximum circumferential stress

$$\sigma_{t\,max} = p_1 \frac{2R_1^3 + R_2^3}{2(R_2^3 - R_1^3)} \tag{1.76}$$

exists in the extreme inner layer $(r = R_1)$.

The reduced stress is also highest at this point and in the event of allowing the elastic state, it becomes the dimensioning condition for a thick-walled sphere (Bezukhov, 1968).

1.8. Combined Axially Symmetrical Problems of Thick-Walled Cylinders

Classified as combined problems in the theory of axially symmetrical thick-walled cylinders include all cases involving the character of loadings and strains and the physico-mechanical properties of materials, whose mathematical descriptions cannot be expressed by equations of (1.10) type and where we deal with more than one equation. Discussed in brief below are problems of this kind, most commonly encountered in modern engineering.

1.8.1. Thick-walled cylinder subjected to loadings variable along the axis of circular symmetry

Pressures p_1, p_2 and temperature alike vary along the z-axis but satisfy the condition of circular symmetry. Generally speaking, besides normal radial circumferential stresses σ_r, σ_t, there are also normal longitudinal stresses σ_z, and shear stresses τ_{zr} which depend on radius r and coordinate z.

Owing to the symmetry of the element cut out of the wall (Fig. 1.6) in the manner described in Section 1.1, no other shear stresses exist (Bezukhov, 1968; Huber, 1958; Ponomarev et al., 1958).
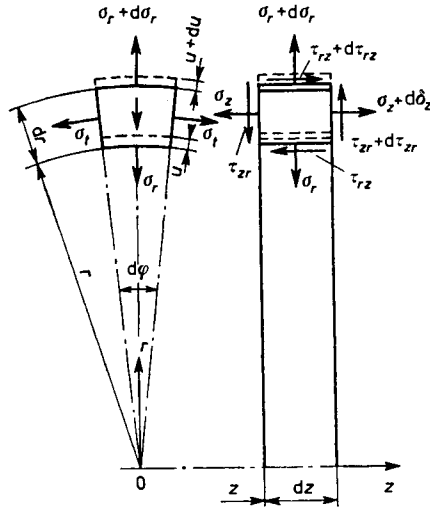
Fig. 1.6. Element of a thick-walled cylinder under p_1, p_2, varying along z-axis

The resultant displacement at any point of the wall has two components: radial u and longitudinal w, both being functions of coordinates r and z. The unit radial elongation is expressed as

$$\varepsilon_r = \frac{\partial u}{\partial r}, \tag{1.77}$$

the circumferential as

$$\varepsilon_t = \frac{u}{r}, \tag{1.78}$$

and the longitudinal as

$$\varepsilon_z = \frac{\partial w}{\partial z}. \tag{1.79}$$

Since shear stresses are involved here, angular strain

$$\gamma_{zr} = \frac{\partial u}{\partial z} + \frac{\partial w}{\partial r} \tag{1.80}$$

will appear. Corresponding to these strains are relationships (1.4)–(1.6) of Hooke's law, added to which is also the relationship

$$\gamma_{zr} = \frac{\tau_{zr}}{G} \tag{1.81}$$

in which the shear modulus $G = E/2(1+\nu)$. The equilibrium conditions described for projections of all forces acting in the direction of the radius and parallel to the z-axis on the differential element of the wall reduce to two differential equations

$$\frac{\partial(r\sigma_r)}{\partial r} - \sigma_t + \frac{\partial \tau_{zr}}{\partial z} = 0, \tag{1.82}$$

$$r \frac{\partial \sigma_z}{\partial z} + \frac{\partial(r\tau_{zr})}{\partial r} = 0. \tag{1.83}$$

The state of stress, as in Section 1.1, is described by relationships (1.7)–(1.9) together with (1.81), which taking into account (1.77)–(1.81) are expressed in the form

$$\sigma_r = \frac{E}{(1+\nu)(1-2\nu)} \left[(1-\nu)\frac{\partial u}{\partial r} + \nu\left(\frac{u}{r} + \frac{\partial w}{\partial z}\right) - (1+\nu)\alpha T \right], \tag{1.84}$$

$$\sigma_t = \frac{E}{(1+\nu)(1-2\nu)} \left[(1-\nu)\frac{u}{r} + \nu\left(\frac{\partial u}{\partial r} + \frac{\partial w}{\partial z}\right) - (1+\nu)\alpha T \right], \tag{1.85}$$

$$\sigma_z = \frac{E}{(1+\nu)(1-2\nu)} \left[(1-\nu)\frac{\partial w}{\partial z} + \nu\left(\frac{u}{r} + \frac{\partial u}{\partial r}\right) - (1+\nu)\alpha T \right], \tag{1.86}$$

$$\tau_{zr} = \frac{E}{2(1+\nu)} \left(\frac{\partial u}{\partial z} + \frac{\partial w}{\partial r} \right). \tag{1.87}$$

If the cylinder were in rotary motion, expression Ar would appear additionally in the equation of internal equilibrium (1.82); the other equations and relationships would remain unchanged. If (1.84)–(1.87) are put into differential equations (1.82) and (1.83), the latter will then determine two functions u and w. The constants of integration of these functions are determined as in the previously described cases, i.e., from the boundary conditions (e.g. for $r = R_1$ we have $\sigma_r = -p_1$, $\tau_{rz} = 0$ and for $r = R_2$: $\sigma_r = -p_2$, $\tau_{rz} = 0$). In addition, the boundary conditions at the pipe ends, specified as stresses or displacements, must be satisfied.

The solution of the set of equations (1.82), (1.83) for some cases of loading can be represented by Bessel's functions. The solving method whereby loadings are represented by series is also applicable to the case where loadings

are acting one a short sector along the generatrix. Detailed calculations of the components of the state of stress and strain are usually highly time-consuming but much time will be saved using a digitial computer.

1.8.2. Other cases of thick-walled cylinders with axial symmetry

The calculations grow considerably more complicated, if loadings p_1, p_2 and loadings due to T vary discontinuously along the z-axis. The states of stress and strain are described by a set of simultaneous differential equations. The calculations become less accurate, especially for sites featuring a strong discontinuity of loadings. Good results, with only small error, are obtainable with the use of the finite element method and digital computers. Cases of large displacements u and w are also classed as non-linear problems since non-linear expressions appear in relationships and equations. We deal with such cases specifically where Young's modulus E is small and the loadings are considerable. The situation is similar when the elastic state exhibits non-linear behaviour. The use of the approximate theory described above would involve a considerable error. The degree of inaccuracy depends on the degree of elastic non-linearity (weak or strong non-linearity); in the event of strong non-linearity, linearization is inadmissible and it is necessary then to use the general theory of non-linear elasticity. Here, too, wide possibilities are open for the use of the finite element method and computer techniques.

A separate group of non-linear problems includes cases where E, ν, α, R_e are variables—functions of temperature and position (r, z). In these cases, Young's modulus, number ν and coefficient α are, like temperature, functions of coordinates r and z in relationships (1.7)–(1.9), whereas in equations of internal equilibrium we have functions of material characteristics and their derivatives. Specifically, this is the case where temperatures change from low to very high values. Calculation leading to results are approximate as a rule and obtainable using a digital computer.

Descriptions of the states of strain become more complicated due to the appearance of plastic strain and creep, Jindra (1955), Krzyś et al. (1976), Życzkowski (1964),

The connecting places of thick-walled elements—a thick-walled cylinder with a hemisphere, cone or thick plate or cylinders varying in thickness—cannot be calculated with the aid of the theory presented, since these are parts of a structure with a disturbed state of stress. Good results are obtainable with the use of the finite element method and digital computers.

2. Circular Plates

We understand a *circular plate* to mean a plane element of circular shape, solid or with a concentric hole, whose thickness h (Fig. 2.1a) is small compared to radius R of the outer contour, and where the directions of external loadings,
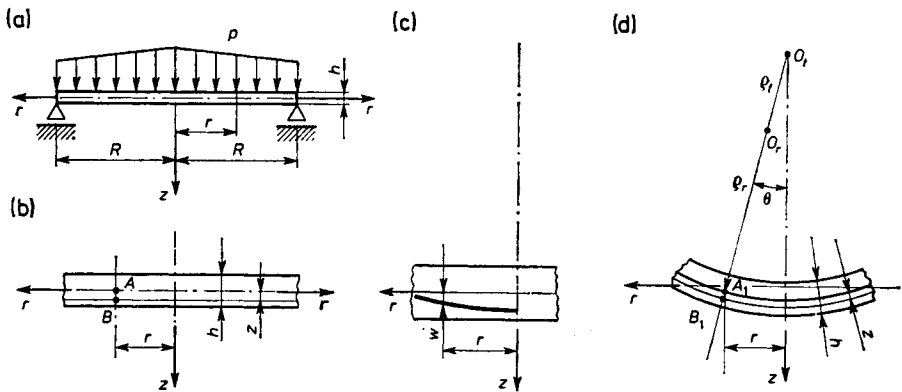
Fig. 2.1. Circular plate: (a) axially symmetrical loadings; (b) coordinates of points A and B; (c) deflection of mid-layer; (d) geometry of deformed layers

e.g. pressure p, are normal to the middle layer. The middle layer is the plane dividing the thickness in half. A plate of a homogeneous material having identical elastic properties in all directions and at every point is defined as isotropic.

Of major importance are solid plates and plates with a concentric hole, in other words, annular plates, under circularly symmetrical load. Our further considerations are concerned with elements of this kind; they have an extensive literature, e.g. Birger (1961), Brzoska (1972), Fleishman (1962), Kats (1966), Kalmanok (1959), Kączkowski (1968, 1971), Krzyś and Życz-kowski (1962), Lipka (1967), Mierzejewski (1976), Nowacki (1970), Thrun (1956), Timoshenko and Goodier (1951).

Plates as a structural element occur most commonly in combination with other elements, e.g. with shells or thick-walled pipes.

We encounter them in the design of:
— working machines (e.g. in propulsion systems in the form of body walls, disk springs or tank heads, or in rotors),
— heat engines (elements of internal combustion engines, body and heat-engine parts, balance pistons etc.),
— power systems (e.g. in heat compensation units, in pipeline joints, etc.),
— in chemical plants (tank heads, plate-shell support structures, surface girders, etc).

The above specification does not exhaust by any means the broad possibilities of applications of circular plates by virtue of their simple shape, easy construction and lucidity in analysis of internal forces.

The most frequent forms of loading in plates are pressures, transverse forces and bending moments applied on the edges or at other places of the plane of the plate in a manner assuring complete circular (axial) symmetry.

2.1. The State of Stress in Circularly Symmetrical Plates

Usually, a plate is regarded as thin, if $h < \frac{1}{5}R$, and so are deflections if they are not in excess of $\frac{1}{5}h$. These assumptions lead to the hypothesis of linear strain distribution in layers of a deflected plate (Vainberg and Vainberg, 1959; Volmir, 1956).

The relationships and equations of the theory of circular plates are derived on the following assuptions:
— the loadings are applied to the plane of the mid-layer and are circularly symmetrical,
— the plate is thin, therefore its thickness is much smaller than the outer radius, and it is constant all over the plate,
— the mid-layer deflections are small in relation to its thickness,
— only elastic strains exist in the plate material; Hooke's law remains valid et each point.
— the layers parallel to the mid-layer are not interacting,
— the plate material is isotropic and homogeneous, whereas E, ν, α are constant, independent of the heated plate temperature,
— if the plate is heated, the temperature field satisfies the axial symmetry condition.

These assumptions are regarded as classical in the theory of plates.

A three-dimensional state of stress exists basically in a plate, but the stress component normal to the mid-layer is not very great compared to the

other stress components, and based on the fifth assumption, it can be neglected.

As indicated in Fig. 2.1b, r is the radius of an arbitrary cylindrical section with the z-axis being simultaneously the axis of circular (axial) symmetry. Surface loading p of the plate is a function of radius r only.

In Fig. 2.1c, the mid-layer deflects under the load, and point A moves to a position corresponding to A_1 (Fig. 2.1d). The deflection is circularly symmetrical. A curvature of radius ϱ_r exists at point A_1 of the mid-layer in the cross-section along radius r, and a curvature of radius ϱ_t exists in the plane perpendicular to the cross-section along radius r and passing through the same point A_1. Point B lying in a plane z distant from the central plane will shift as the result of the deflection to position B_1. It is easily demonstrated that the radial and circumferential components of strain at this point are

$$\varepsilon_r = \frac{z}{\varrho_r}, \qquad \varepsilon_t = \frac{z}{\varrho_t}.$$

The noted radii of curvatures of the deflected mid-layer are expressed by the following geometrical relationships

$$\frac{1}{\varrho_r} = -\frac{d^2 w}{dr^2}, \qquad \frac{1}{\varrho_t} = -\frac{1}{r}\sin\theta.$$

Considering that small deflectins are assumed one can accept that for the angle of deflection $\sin\theta \approx \tan\theta \approx \theta$; hence, the strain components take the form

$$\varepsilon_r = -\frac{d^2 w}{dr^2} z, \tag{2.1}$$

$$\varepsilon_t = -\frac{1}{r}\frac{dw}{dr} z. \tag{2.2}$$

Dividing the above two equations by z and recalling the previously derived relationships, we find the derivative of ε_t with respect to r. We thus obtain the equation

$$r\frac{d}{dr}\left(\frac{1}{\varrho_t}\right) = \frac{1}{\varrho_r} - \frac{1}{\varrho_t} \tag{2.3}$$

or

$$\frac{1}{\varrho_r} = \frac{d}{dr}\left(\frac{r}{\varrho_t}\right) \tag{2.4}$$

termed the *compatibility condition*.

The principal components of the state of stress occur at point B_1, namely radial σ_r and circumferential σ_t. These components are related to the components of the state of strain by equations of Hooke's law for plane stress with thermal strain not being considered,

$$\varepsilon_r = \frac{1}{E}(\sigma_r - \nu\sigma_t), \qquad \varepsilon_t = \frac{1}{E}(\sigma_t - \nu\sigma_r).$$

Using the above relationships, we can express the stresses in the form

$$\sigma_r = -\frac{E}{1-\nu^2}\left(\frac{d^2w}{dr^2} + \frac{\nu}{r}\frac{dw}{dr}\right)z, \tag{2.5}$$

$$\sigma_t = -\frac{E}{1-\nu^2}\left(\frac{1}{r}\frac{dw}{dr} + \nu\frac{d^2w}{dr^2}\right)z, \tag{2.6}$$

where ν is Poisson's ratio and E is Young's modulus of plate material.

It is easily seem that the two stress components are linear functions of variable z. Their actions in cross-sections result in bending moments which referred to unit length of cross-sections of the plate amount to

$$m_r = \int_{h/2}^{h/2} \sigma_r z\, dz = -D\left(\frac{d^2w}{dr^2} + \frac{\nu}{r}\frac{dw}{dr}\right),$$

$$m_t = \int_{h/2}^{h/2} \sigma_t z\, dz = -D\left(\frac{1}{r}\frac{dw}{dr} + \frac{d^2w}{dr^2}\right), \tag{2.7}$$

and contain in principle only a single unknown, namely deflection w. The first bending moment is called *radial* and the second, *circumferential*. Representing the mid-layer curvatures in compatibility condition (2.3) by bending moments (Krzyś and Życzkowski, 1962), we arrive at the relationship

$$m_r - \nu m_t = \frac{d}{dr}[r(m_t - \nu m_r)]. \tag{2.8}$$

Quantity $D = EH^3/12(1-\nu^2)$ is called the *bending rigidity* of the plate. Knowing the magnitudes of moments m_r and m_t and of shearing force q, we can easily determine normal stresses and shear stresses in any layer parallel to the mid-layer from simple relationships like in theory of beams

$$\sigma_r = \frac{12m_r}{h^3}z, \qquad \sigma_t = \frac{12m_t}{h^3}z, \qquad \tau_{zr} = -\frac{6q}{h}\left(\frac{z^2}{h^2} - \frac{1}{4}\right), \tag{2.9}$$

and the maximum bending stresses, i.e., stresses in the extreme layers of the plate

$$\sigma_r = \pm\frac{6m_r}{h^2}, \qquad \sigma_t = \pm\frac{6m_t}{h^2}. \tag{2.10}$$

The σ_r, σ_t distributions and the shear stress τ_{zr} distribution are shown in Fig. 2.2a.

Evaluating the effort, for example, by using the hypothesis of distortional strain energy (1.12) by calculating the reduced stress values for the outer layer, where the stress is maximum, we obtain

$$\sigma_{\text{red H}} = \frac{6}{h^2} \sqrt{m_r^2 + m_t^2 - m_r m_t}\Big|_{\text{max}}, \tag{2.11}$$

and it should satisfy the plate strength condition, i.e., $\sigma_{\text{red H}}|_{\text{max}} \leqslant k_r$; k_r, as in Section 1.1, is the admissible tensile stress of plate material. The situation is similar for the extreme layer using hypothesis (τ_{max})

$$\sigma_{\text{red T}} = \frac{6}{h^2} |m_t - m_r|_{\text{max}}. \tag{2.12}$$

2.2. The Differential Equation for Mid-Layer of Circularly Symmetrical Plate. Boundary Conditions

To examine the internal equilibrium, we cut out of a circular plate a differential element (Fig. 2.2b), with two coaxial cylindrical surfaces having radii r and $r+dr$, respectively, and with two planes intersecting along the z-axis
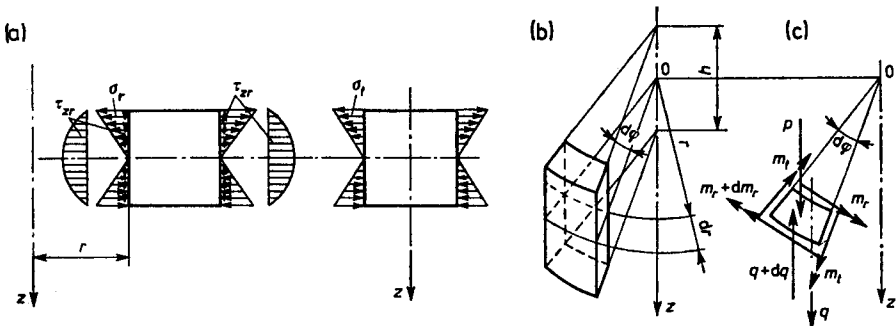
Fig. 2.2. Stress distribution in circular plate: (a) in cross-sections; (b) plate element; (c) cross-sectional forces and moments

and inclined to each other at angle $d\varphi$. Acting on the lateral surfaces of the symmetrical element thus separated out are cross-sectional moments m_t, m_r and $m_r + dm_r$, a surface force of intensity $p(r)$ brought down to the mid-layer (Fig. 2.2c), and shear forces q and $q + dq$, all referred to unit length of cross-sections. The equilibrium condition written for the bending moments reduces to the differential equation

$$r\frac{dm_r}{dr}+m_r-m_t+qr = 0 \tag{2.13}$$

in which two bending moments and a shear force are unknown. The equilibrium condition for projections of all the forces on the z-axis yields the next differential equation in the form

$$r\frac{dq}{dr}+q-pr = 0. \tag{2.14}$$

Combining the expressions for m_r and m_t with the first equation of equilibrium, we obtain the differential equation

$$r\frac{d^3w}{dr^3}+\frac{d^2w}{dr^2}-\frac{1}{r}\frac{dw}{dr} = \frac{r}{D}q \tag{2.15}$$

or in another form

$$\frac{d}{dr}\left(\frac{1}{\varrho_r}+\frac{1}{\varrho_t}\right) = -\frac{q}{D}$$

containing only two unknowns, q and w. This equation after differentiating with respect to variable r and after combining with the second equation of equilibrium reduces to

$$\frac{d^4w}{dr^4}+\frac{2}{r}\frac{d^3w}{dr^3}-\frac{1}{r^2}\frac{d^2w}{dr^2}+\frac{1}{r^3}\frac{dw}{dr} = \frac{p}{D}. \tag{2.16}$$

This is a fourth-order linear differential equation, its integral consisting of two functions

$$w = w_1+w_2,$$

where the first has the form

$$w_1 = C_1\ln r+C_2 r^2\ln r+C_3+C_4 r^2 \tag{2.17}$$

and the second

$$w_2 = w_2(r,p)$$

depends on the type of loading, it means on $p(r)$ of the plate.

If $p(r)$ is constant throughout the plate, i.e., $p = $ const, then

$$w_2 = \frac{pr^4}{64D}. \tag{2.18}$$

The quantities C_1, C_2, C_3, C_4 occurring in function w_1 are constants of integration determined from the boundary conditions of the plate. As we can see, by knowing function $w(r)$ we can calculate any static or geometrical

quantity of the deformed plate. We distinguish the following circularly symmetrical modes of support of edges in circular plates:

Simply supported (Fig. 2.3a). With this support, only free rotation of the plate edge about the support line can take place. Hence, the conclusion that radial moment m_r and deflection $w(r)$ equal to zero on this edge;
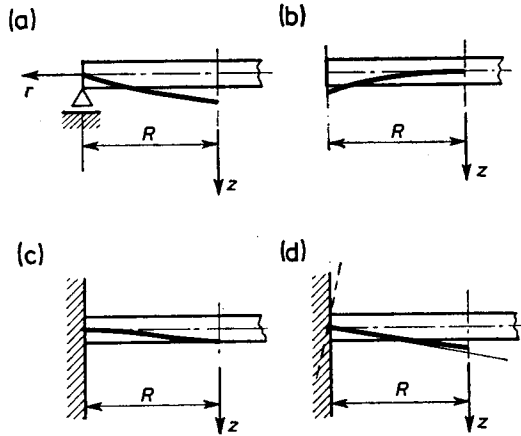
Fig. 2.3. Edges of circular plates: (a) simply supported (b) free; (c) rigidly clamped; (d) elastically clamped

Free edge (Fig. 2.3b), on which bending moment m_r and shearing force q equal zero;

Perfect rigid clamping (Fig. 2.3c). In this case, deflection $w(R)$ and slope $\dfrac{dw}{dr}(R)$ at the clamping site equal zero;

Elastic clamping (Fig. 2.3d). Here, deflection vanishes at the clamped boundary, and $\dfrac{dw}{dr}(R)$ and m_r differ from zero.

They depend on the elastic behaviour of the element clamping the plate on the edge. In addition, there are still other modes of support, e.g. and arbitrary but circularly symmetrical support inside the region of the plate.

Note that the principle of superposition is applicable in the theory of plates which satisfies the assumptions introduced at the beginning.

2.3. Particular Case of Circularly Symmetrical Plates

Considering the role played by circularly symmetrical plates in the design of many machines and appliances, and also their frequent uses, we present below solving methods and calculation results in the form equations for cases

of loadings and supports of plates important from an engineering point of view. The solutions for other, more complicated cases of supports and load-ings will be found in numerous publications, e.g., Biezeno and Grammel (1939), Brzoska (1972), Girkmann (1956), Krzyś et al. (1976), Lipka (1967), Ponomarev et al. (1958), Timoshenko and Woinowsky-Krieger (1959), Vainberg and Vainberg (1959), Volmir (1956).

1. A plate simply supported on the edge under constant pressure p. In this case, the boundary conditions and the conditions for the centre of plate are as follows: for $r = R$, we have $w = 0$, $m_r = 0$ and for $r = 0$, $dw/dr = 0$, $w = $ finite. The last two conditions are satisfied only if constants C_1 and C_2 equal zero. The first two conditions amount to a set of two equations with respect to constants C_3 and C_4, which are unknown. Putting them into function $w(r)$ we arrive at the equation of mid-surface of the deflected place

$$w(r) = \frac{pR^4}{64D} \left(1 - \frac{r^2}{R^2}\right)\left(\frac{5+v}{1+v} - \frac{r^2}{R^2}\right).$$

(2.19)

The deflection in the centre of the plate ($r = 0$)

$$w_0 = \frac{5+v}{1+v} \frac{pR^4}{64D}.$$

(2.20)

In cross–sections in the centre of the plate, m_r and m_t (for $r = 0$) are identical

$$m_{r0} = m_{t0} = \frac{3+v}{16} pR^2,$$

(2.21)

and on the edge of the plate (for $r = R$)

$$m_{tR} = \frac{1-v}{8} pR^2,$$

(2.22)

the shearing force is

$$q = \frac{pr}{2}.$$

(2.23)

The slope at support site is

$$\theta_R = -\frac{1}{8(1+v)D} pR^3.$$

(2.24)

2. A plate simply supported loaded on the edge by radial bending mo-ments m_0. The two conditions for the centre of the plate and the third for its edge are identical as before, but regarding the fourth one, for $r = R$,

we should have $m_r = m_0$; here, too, constants C_1, C_2 equal zero, and the equation of mid-surface has the form

$$w = C_3 + C_4 r^2.$$

From the conditional equations with respect to C_3 and C_4, we obtain the equation of mid-surface deflection

$$w = \frac{m_0 R^2}{2D(1+\nu)} \left(1 - \frac{r^2}{R^2} \right) \tag{2.25}$$

and the formula for deflection in the centre of the plate

$$w_0 = \frac{m_0 R^2}{2D(1+\nu)}. \tag{2.26}$$

Equation (2.25) is the equation of spherical-cap surface. It is easily proved that at any point of the plate, bending moments $m_r = m_t = m_0$ and shearing force $q = 0$.

The slope on the edge of the plate is

$$\theta_R = -\frac{m_0 R}{(1+\nu)D}. \tag{2.27}$$

3. A plate clamped of the edge and loaded by constant pressure p. The solution for the plate can be obtained in two ways, either by superposition of the two previous cases with an additional condition for the angle at the clamped edge or by means of the boundary conditions and by determining the constants of integration, C_1, C_2, C_3, C_4. Obviously, the first two constants equal zero.

The former technique, being simpler and more lucid, is described below. The plate can be treated as having a simple support on the edge and as being loaded by pressure p and moments m_0 so matched as to get the angle on the edge, which comes from the action of both loadings (p, m_0), equalling zero. Consequently, in accordance with the previous cases, we should have $\theta_R = 0$, which means that

$$\frac{1}{8(1+\nu)} \cdot \frac{pR^3}{D} - \frac{1}{1+\nu} \cdot \frac{m_0 R}{D} = 0;$$

hence, the radial moment satisfying this condition

$$m_0 = \frac{pR^2}{8}. \tag{2.28}$$

Proceeding in a similar manner, we obtain the equation of mid-surface

$$w(r) = \frac{pR^4}{64D}\left(1 - \frac{r^2}{R^2}\right).$$ (2.29)

The remaining static quantities are

$$m_r = \frac{pR^2}{16}\left[1 + \nu - (3 + \nu)\frac{r^2}{R^2}\right], \quad m_t = \frac{pR^2}{16}\left[1 + \nu - (1 + 3\nu)\frac{r^2}{R^2}\right]$$ (2.30)

in the centre

$$m_{r0} = \frac{1 + \nu}{16}pR^2, \quad m_{t0} = m_{r0}$$ (2.31)

and

$$q = \frac{1}{2}pr.$$ (2.32)

The descriptions of other cases of plates and the relationships for moments, deflections and slopes will be found, for example, in the considerations given below, where the solutions used are derived from e.g. Birger (1956), Lipka and Butt-Hussaim (1963), Ponomarev *et al.* (1958), Vainberg and Vainberg (1959). These literature items were utilized in our further considerations assuming $\nu = 0.3$, which corresponds roughly to such materials as steel and light alloys.
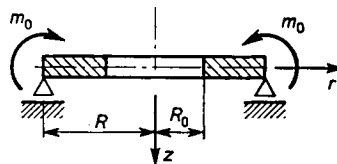
Fig. 2.4. Circular plate with a hole, loaded by means m_0 on the outer edge

4. A plate, as shown in Fig. 2.4, with a circular hole of radius R_0 and a rim of radius R, simply supported at the outer edge, with the inner free. The outer edge has been loaded by radial moment m_0. Boundary conditions: for $r = R_0$, we should have $m_r = 0$, $q = 0$, and when $r = R$, then $m_r = m_0$, $w = 0$. Let $x = r/R$, $x_0 = R_0/R$, then the equation of mid-surface of the plate takes the form

$$w = C_1 \ln x + C_2 x^2 \ln x + C_3 + C_4 x^2$$ (2.33)

being much more convenient than the previous one. The boundary condi-
tions reduce to a set of four equations with all integration constants differing
from zero. We obtain the following equation for the mid-surface:

$$w = \frac{m_0 R^2}{2(1+\nu)D} \cdot \frac{1}{1-x_0^2}\left(1-x^2-2\frac{1+\nu}{1-\nu}x_0^2\ln x\right)$$ (2.34)

and slope

$$\theta = -\frac{m_0 R}{(1+\nu)D} \cdot \frac{1}{1-x_0^2}\left(x+\frac{1+\nu}{1-\nu}\frac{x_0^2}{x^2}\right)$$ (2.35)

as a function of relative radius x.

Cross-sectional bending moments and shearing force are

$$m_r = \frac{m_0}{1-x_0^2}\left(1-\frac{x_0^2}{x^2}\right),$$ (2.36)

$$m_t = \frac{m_0}{1-x_0^2}\left(1+\frac{x_0^2}{x^2}\right), \quad q = 0,$$ (2.37)

and on the inner and outer edges

$$m_{tR_0} = \frac{2m_0}{1-x_0^2}, \quad m_{tR_0} = m_0\frac{1+x_0^2}{1-x_0^2}.$$ (2.38)

For the edge of radius R_0 we can write

$$\theta_{R_0} = -\frac{m_0 R}{D}A_1, \quad w_{R_0} = \frac{m_0 R^2}{D}A_2$$ (2.39)

and for the outer edge $(r = R)$

$$\theta_R = -\frac{m_0 R}{D}A_3,$$ (2.40)

where A_1, A_2, A_3 are constant coefficients. The values of these coefficients
calculated for various x_0 are listed in Table 2.1 in Lipka (1967).

5. A plate simply supported loaded by force P concentrated in the centre.
In this case, the shearing force in cross-section of radius r is:

$$q = \frac{P}{2\pi r},$$ (2.41)

whereas (2.15) reduces to the differential equation

$$\frac{d^3w}{dr^3}+\frac{1}{r}\frac{d^2w}{dr^2}-\frac{1}{r^2}\frac{dw}{dr} = \frac{P}{2\pi rD}$$ (2.42)

whose integral takes the form

$$
w = \frac{P}{8\pi D} r^2 \left(\ln \frac{r}{R} - 1 \right) - \frac{C_1}{4} r^2 - C_2 \ln \frac{r}{R} + C_3 . \tag{2.43}
$$

On the edge, i.e., for $r = R$, we have as before $w = 0$, $m_r = 0$, whereas in the centre ($r = 0$), deflection $w(0)$ is finite, and $dw/dr = 0$. Finally, after determining the constants of integration, the equation for the mid-surface and the equation for the slope at the edge takes the form

$$
w = \frac{PR^2}{8\pi D} \left[\frac{3+\nu}{2(1-\nu)} \left(1 - \frac{r^2}{R^2} \right) + \frac{r^2}{R^2} \ln \frac{r}{R} \right], \tag{2.44}
$$

$$
\theta_R = -\frac{1}{1+\nu} \frac{PR}{4\pi D} . \tag{2.45}
$$

The bending moments are

$$
m_r = -\frac{P}{4\pi}(1+\nu)\ln \frac{r}{R} , \qquad m_t = \frac{P}{4\pi} \left[1 - \nu - (1+\nu)\ln \frac{r}{R} \right].
$$

These relationships show that the absolute values of m_r and m_t tend to increase to infinity as r decreases to zero. This seeming inconsistency, at odds with observation, is due to the fact that shearing force q in the centre of the plate, determined from relationship (2.41), also tends to infinity, which is consistent with the adopted static representation of concentrated force P. But, in fact, this force is always continuously distributed on a certain area which though very small is finite, and in that case, quantities m_r, m_t in the centre of the plate are already finite. Such a case is discussed further. On the edge of the plate

$$
m_{tR} = \frac{1-\nu}{4\pi} P .
$$

Given below in brief are solutions for other common cases of plates loaded in various way. They contain formulated boundary conditions and ready relationships for deflections, slopes at the edges and bending moments.

6. A plate as in case 4, loaded by bending moments on the edge of the hole. Conditions at the hole are $m_r = m_0$, $q = 0$, and at the outer radius $w = 0$, $m_r = 0$. Deflection and slope on the inner edge are, respectively,

$$
w_{R_0} = \frac{m_0 R^2}{D} A_4 , \qquad \theta_{R_0} = -\frac{m_0 R}{D} A_5 , \tag{2.46}
$$

and on the outer edge

$$\theta_R = -\frac{m_0 R}{D} A_6. \tag{2.47}$$

Bending moments are

$$m_r = \frac{x_0^2}{1-x_0^2}\left(\frac{1}{x^2}-1\right)m_0, \qquad m_t = -\frac{x_0^2}{1-x_0^2}\left(1+\frac{1}{x^2}\right)m_0, \tag{2.48}$$

where $x = r/R$, $x_0 = R_0/R$. The values of A_4, A_5, A_6 are specified in Table 2.2 in Lipka (1967).

7. A plate simply supported at the outer edge, having a circular hole as shown in Fig. 2.4. Loading of intensity q_0 is uniformly distributed at the inner edge. The boundary conditions at the hole $m_r = 0$, $q = q_0$ and at the outer radius $w = 0$, $m_r = 0$.

In these relations we have

$$\beta = (1+\nu)\frac{x_0^2 \ln x_0}{1-x_0^2}.$$

At the inner edge we have

$$w_{R_0} = \frac{q_0 R^3}{D} A_7, \qquad \theta_{R_0} = \frac{q_0 R^2}{D} A_8, \tag{2.49}$$

and at the outer

$$\theta_R = \frac{q_0 R^2}{D} A_9. \tag{2.50}$$

Bending moments are

$$m_r = \frac{q_0 R_0}{2}\left[\beta\left(\frac{1}{x^2}-1\right)-(1+\nu)\ln x\right],$$

$$m_t = \frac{q_0 R_0}{2}\left[1-\nu-\beta\left(\frac{1}{x^2}+1\right)-(1+\nu)\ln x\right]. \tag{2.51}$$

The values of A_7, A_8, A_9 are specified in Table 2.3 in Lipka (1967).

8. A plate (Fig. 2.5a) simply supported at the edge loaded by constant pressure p present only on the area bounded by radii R_0 and R. The case is solved by replacing the plate with two plates as shown in Fig. 2.5c. The equations are for the mid-surfaces of the two plates: for the solid inner surface (2.33) and for the annular surface with the particular integral added (2.18). The constants occurring in these equations are determined from the
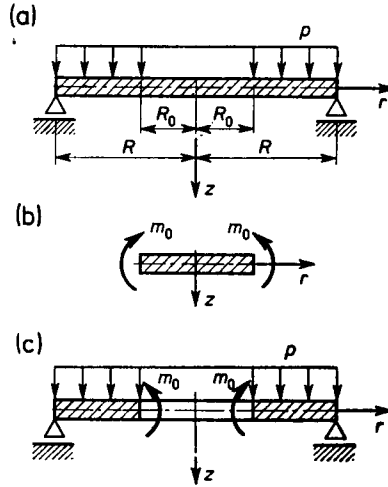
Fig. 2.5. Circular plate, solid: (a) loading by pressure p on ring surface; (b) central portion; (c) ring portion of plate

boundary conditions, the continuity conditions for the two componential plates and the condition for the centre of the plate. They are as follows:

$$\text{when } r = R, \quad \text{i.e. } x = 1, \text{ then } w_2 = 0, m_{r2} = 0, q_2 = \frac{pR}{2}(1 - x_0^2),$$

$$\text{when } r = R_0, \quad \text{i.e. } x = x_0, \text{ then } m_{r1} = m_{r2}, \frac{dw_1}{dr} = \frac{dw_2}{dr}, q_2 = 0,$$

$$\text{when } r = 0, \quad \text{i.e. } x = 0, \text{ then } \frac{dw_1}{dr} = 0, w_1 = \text{finite}.$$
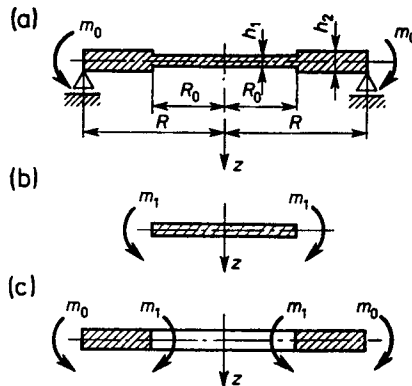
Fig. 2.6. Circular plate: (a) with slightly varying thickness; (b) central portion; (c) ring portion of plate

Having w_1 and w_2 thus determined, we can finally determine the bending moments and other quantities for both parts of the plate. This is, however, a labourious procedure.

9. A plate as shown in Fig. 2.6a simply supported at the outer radius and loaded by moments m_0. The central part of the plate is of thickness h_1 and outer part of thickness h_2. The problem is solved according to a procedure similar to that in the previous case. Two componential plates are considered (Fig. 2.6b, c). Acting on the outer part of the plate are only moments m_0 and unknown moment m_1, and on the edge of the outer plate, only m_1. The continuity condition for both plates $\dfrac{dw_1(x_0)}{dx} = \dfrac{dw_z(x_0)}{dx}$ on radius x_0 must be satisfied by moment m_1.

The slopes on the inner edge of the componential outer plate and on the edge of the central part are determined using the ready solutions of the previously discussed cases. It has to be remembered that the two parts have different plate rigidities

$$D_1 = \frac{Eh_1^3}{12(1-v^2)}, \qquad D_2 = \frac{Eh_2^3}{12(1-v^2)}.$$

It is easily seen that it was possible to omit in the solution not all the boundary and continuity conditions, thus greatly simplifying the calculations. All the static and geometrical quantities can be determined in a simple way using the relationships given for the particular cases of loading of the componential plates.

10. A solid plate simply supported at the edge and on the circumference of a circle of radius R_0 (Fig. 2.7). is loaded by constant pressure p. As in the former case, the plate is divided into two parts, annular and central (solid), both being identically supported, and the continuity conditions are then established, namely, equality of bending moments and slopes on the common
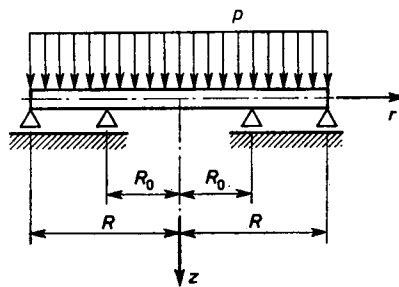
Fig. 2.7. Circular plate supported on two circles: loading p

edges, using the ready relationships derived for simpler plates. This is a simpler method, but the ultimate relationships are already very complex, thus greatly complicating the analysis of the calculation in general form. The simplest way to arrive at effective results for particular design solutions is to introduce definite values into the calculations, for R, R_0, p and $w(r)$. The calculation technique involving the boundary and continuity conditions for the two parts and the determination of constants $C_1, \ldots, C_4$ is far more labourious.
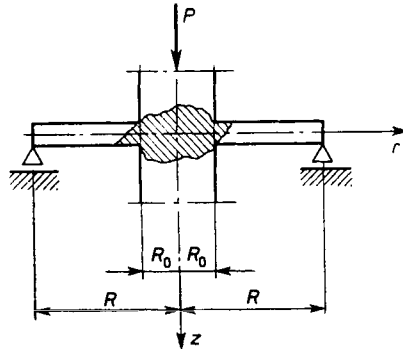
Fig. 2.8. Circular plate with a rigid mandrel

11. A plate, as shown in Fig. 2.8, simply supported at the outer edge, the inner one being rigidly joined to a mandrel of radius R_0 loaded by force P. Boundary conditions are: for $r = R$, we have $w = 0$, $m_r = 0$, for $r = R_0 - -\theta$, $q = q_0$ where $q_0 = P/2\pi R_0$. The technique for solving the equation by way of determining the constants of integration in function $w(r)$ is equally simple as the other technique which makes use of the solutions obtained for the fundamental cases of loading of the plotes.

2.4. Circular Ring Subjected to Bending by Moments Uniformly Distributed on the Circumference

A circular ring of rectangular cross-section, with the longer side differing not much from the shorter (Fig. 2.9a) is loaded by moments m_0 uniformly distributed on the circumference. The stresses and strains can be determined treating the ring as an annular, very narrow plate $(R - R_0)$, loaded on the outer radius by radial moments. This is, however, not an accurate method and for this reason a different procedure is called for. It is assumed that due to moments m_0 acting, the cross-section will not undergo deformation, but will only experience rotation by angle θ (Fig. 2.9b) about point A located in the mid-layer at distance R_1 from the z-axis. Point B of coordinates r and
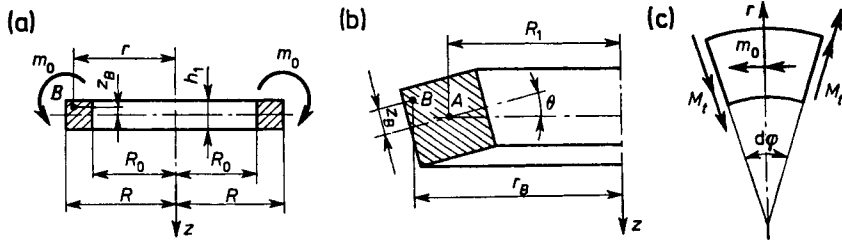
Fig. 2.9. Circular ring: (a) loading by moments m_0; (b) deformation; (c) ring element

z is in a new position at distance $r_B \approx r + \theta z_B$ from the z-axis. Unit circumferential elongation for this point is

$$\varepsilon_t = \frac{\theta z_B}{r}. \tag{2.52}$$

Assuming that compared to the circumferential stresses, the remaining stresses are not very great, we obtain the following approximate expression:

$$\sigma_t = \frac{E\theta z_B}{r} \tag{2.53}$$

for a uniaxial state of stress.

For the conditions of equilibrium of the cross-sectional forces to be satisfied, we must have the expression

$$\int_{-h_1/2}^{h_1/2} \int_{R_0}^{R} \sigma_t \, dz \, dr = 0$$

written for normal forces and the expression

$$M_t = \int_{-h_1/2}^{h_1/2} \int_{R_0}^{R} \sigma_t z_B \, dz \, dr$$

for moments. We put the first equation into (2.52) for stresses σ_t and we obtain ultimately the relationship for the circumferential moments

$$M_t = \theta \frac{E h_1^3}{12} \ln \frac{R}{R_0}.$$

From the equation of equilibrium

$$m_0 R_1 \, d\varphi - 2M_t \frac{d\varphi}{2} = 0$$

determined for an element (Fig. 2.9c) of the circular ring, it follows that $M_t = m_0 R_1$; hence the angle of rotation

$$\theta = \frac{12 m_0 R_1}{E h_1^3 \ln \dfrac{R}{R_0}}. \tag{2.54}$$

Extremal stresses occur at cross-sectional points with coordinates $r = R_0$, $z = \pm h_{1/2}$

$$\sigma_{t\min}^{\max} = \pm \frac{6 m_0 R_1}{R_0 h_1^2 \ln \dfrac{R}{R_0}}. \tag{2.55}$$

If the ring is thin, i.e., $\ln \dfrac{R}{R_0} \approx \dfrac{R}{R_0} - 1$, then

$$\sigma_{t\min}^{\max} = \pm \frac{6 m_0 R_1}{h_1^2 \delta}, \qquad \theta = \frac{12 m_0 R_1}{E h_1^2 \delta}, \tag{2.56}$$

where $R_1 = R_0 + \frac{1}{2}\delta$, $\delta = R - R_0$.

Such circular rings are encountered in the design of rib-reinforced plates (Huber, 1954; Krzyś and Życzkowski, 1962; Vodička, 1957; Ventzkovskii, 1958).

2.5. Circular Plates Reinforced by Circumferential Ribs

A plate has been reinforced on the edge by a ring-shaped rib of transverse dimensions h_1, δ (Fig. 2.10a). Plate thickness is h. The size of δ remains small compared to radius R, and the loading is, say, pressure $p = \mathrm{const}$ applied only to the central part. The edge is simply supported. To determine the internal forces acting in the plate itself, i.e., in the central part and in the
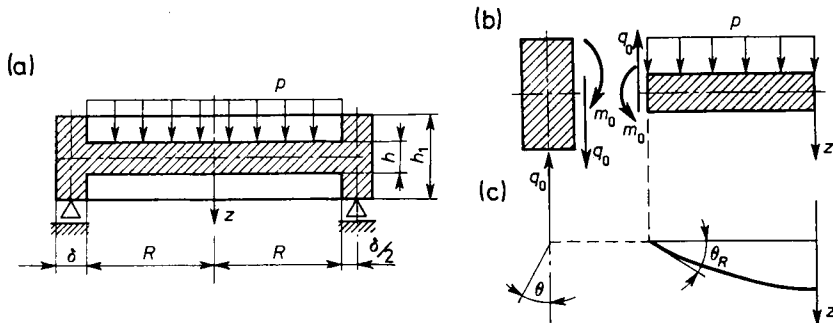
Fig. 2.10. Plate: (a) with outer perimeter in ring form; (b) component parts of plate

circular ring, the plate is divided into two parts (Fig. 2.10b), thus obtaining a ring loaded by moments m_0 and m_1 and a plate under pressure p, with moments m_0 and shearing forces q_0 acting on the edge of it. Moment m_0 is unknown, whereas

$$m_1 = q_0 \frac{\delta}{2},$$

where

$$q_0 = \frac{pR}{2}.$$

It is assumed that the design angle between the two elements is not subject to change, therefore the continuity condition can be written as $\theta_R = \theta$ (Fig. 2.10), where θ_R is the slope at the edge with radius R of the plate's central part. It is known from the theory of plates that for the central part

$$\theta_R = \frac{pR^3}{8(1+\nu)D} - \frac{m_0 R}{(1+\nu)D}$$

and for the ring

$$\theta = \frac{12(m_0 + m_1)}{Eh_1^3 \delta} \left(R + \frac{\delta}{2}\right)^2.$$

Comparing the right-hand sides of the two relations expressing angles θ and θ_R, we arrive at the equation

$$\frac{pR^3}{8(1+\nu)D} - \frac{m_0 R}{(1+\nu)D} = \frac{12(m_0 + m_1)}{Eh_1^3 \delta} \left(R + \frac{\delta}{2}\right)^2$$

from which it follows that the internal radial moment sought is

$$m_0 = \frac{pR}{2} \left[\frac{R^2}{4(1+\nu)D} - \frac{6(R+\frac{1}{2}\delta)^2}{Eh_1^3} \right] \frac{1}{\dfrac{R}{(1+\nu)D} + \dfrac{12(R+\frac{1}{2}\delta)^2}{Eh_1^3 \delta}}.$$
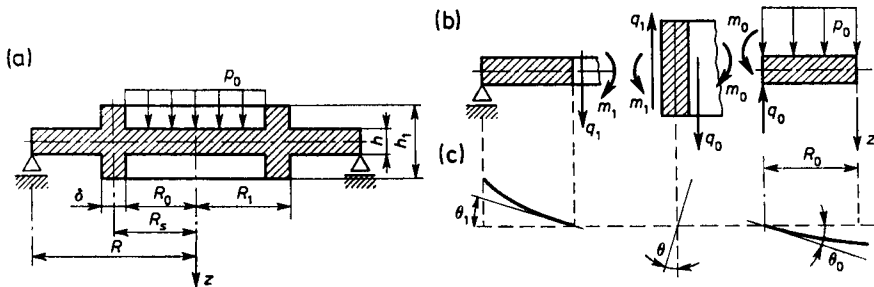
Fig. 2.11. Circular plate: (a) with ring-shaped rib; (b) component parts

An interesting structure is the circular plate in Fig. 2.11a, which has a ring-shaped rib. Let the external loading, which may be arbitrary, be pressure $p = $ const acting only on the central part of radius R_0. The plate is divided into three component parts (Fig. 2.11b): (1) central part of radius R_0, acting on which are pressure p, moments m_0, and transverse force q_0, applied on the edge; (2) external part in the form of an annular plate with a hole of radius R_1, supported on the outer perimeter, loaded by moments m_1 and transverse forces q_1; (3) a ring, acting on which are moments m_0, m_1 and transverse forces q_0, q_1. Assuming that δ is small compared to radius R_0, we can ignore the influence of moment $\frac{1}{2} q_0 \delta$ and also the difference between R_1 and R_0, thus greatly simplifying the calculations. We can then write $R_0 \approx R_1$ and $q_0 \approx q_1$; denoting by θ_0', θ_1', θ the slope on the outer edge of the central plate, the slope on the inner edge of the outer plate and the angle of rotation of the ring, we can formulate two conditions of equality of the angles for these component parts, namely $\theta_0' = \theta$ and $\theta_1' = \theta$-

It should be recalled that the value of θ_0 depends on pressure p and moments m_0, and θ_1' depends on moments m_1 and transverse forces q_1, whereas

$$\theta = \frac{12(m_0 - m_1) R_0^2}{E h_1^3} \tag{2.57}$$

which is consistent with the above considerations.

The further procedure to determine the values of moments m_0 and m_1 consists in solving a set of two equations derived from the above equilibrium conditions of angles. Usually, use is made of ready relationships for plates and rings, derived earlier in this section. The method of calculating plates ribbed with single circular rings can be extended to cases involving a greater number of co-axial rings-ribs, but then the calculations get more complicated, and they are moreover time consuming. Plates provided with tightly spaced co-axial reinforcing ribs of not very thick and high cross-sections can be solved based on the theory of elasticity, which introduces the concept of structural orthotropy of the elastic properties of material and which treats such plates as elements of equal thickness.

Numerous contributions on this subject will be found in the literature, e.g. Ambatsumian (1967), Gorskii (1961, 1962). Maslov (1965), Ventskovskii (1961). Much more difficult is the analysis of plates stiffened with radially or obliquely oriented ribs. These are in fact structures consisting of ribs of various shapes and circular plates (Leyko et al., 1972) of constant or variable thicknesses. Also for such structures, provided that they have a sufficient number of ribs of suitable shape, the theory of orthotropic plates proves useful in calculations. Obviously, the calculations are only approximate

with accuracy being difficult to estimate. It has to be remembered that at sites at which circumferential or radial ribs have been introduced—which incidentally, disturbs complete axial symmetry—there exist in reality internal force concentrations and resulting stress concentrations which are very difficult to assess. It should also be noted that plastic states in plates are seldom allowed in machine design, and the calculations, which are made on the assumptions of complete plasticization of cross-sections, are meant chiefly to determine the limit load (Gorski, 1961; Grigorev, 1952; Hopkins and Prager, 1954; Krontsenko, 1961; Ventskovskii, 1961; Tuliszka, 1960; Yusuff, 1961). However, this aspect is not considered in the present part of the book.

2.6. Circular Plates of Variable Thickness

Circular plates of variable thickness as structural elements find uses in mechanical engineering—chiefly in rotating machines and others. Their advantages are lightness, and better utilization of material, and sometimes a capacity for considerable elastic strains. The plate to be optimized generally has variable thickness (Conway, 1948, 1951; Gorskii, 1961; Hopkins and Prager, 1954; Kovalenko, 1959; König, 1971; Prasek, 1972).
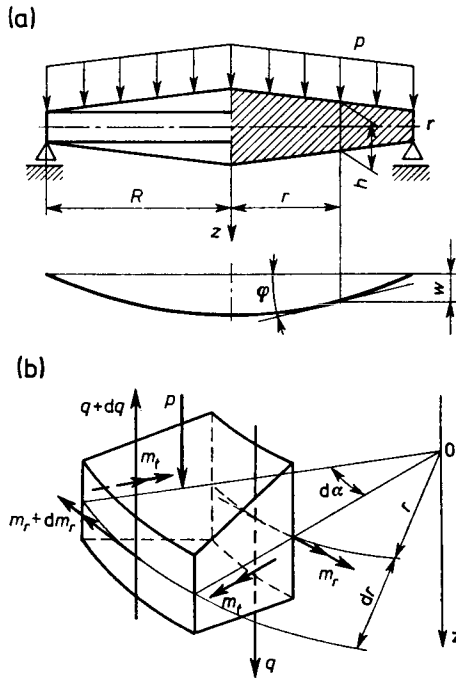
Fig. 2.12. Circular plate: (a) variable thickness; (b) plate element

If we consider a circular plate of variable thickness following the assumptions adopted under the theory of plates of constant thickness, we assume in addition that thickness h is an arbitrary function of radius r only, whereas the changes in thickness are continuous and the mid-plane is perpendicular to the z-axis and is the plane of symmetry (Birger, 1961; Grigorenko and Laivunik, 1965; Kats, 1966; Ponomarev et al., 1958).

If θ and $w(r)$ are the slope and the deflection of the mid-layer at distance r from the axis of symmetry (Fig. 2.12a), then strain in the layer z distant from the mid-layer is the same according the the theory of plates of constant thickness. Thus, considering small slopes, the relationships (2.1) and (2.2) remain valid and the stresses are expressed in the form

$$\sigma_r = -\frac{E}{1-\nu^2}\left(\frac{d\theta}{dr}+\frac{\nu}{r}\,\theta\right)z, \quad \sigma_t = -\frac{E}{1-\nu^2}\left(\frac{1}{r}\,\theta+\nu\,\frac{d\theta}{dr}\right). \tag{2.58}$$

Integrating expressions $\sigma_r z\,dz$, $\sigma_t z\,dz$ within the limits $(-h/2, h/2)$, we arrive at the relationships for the bending moments, radial and circumferential

$$m_r = -D\left(\frac{d\theta}{dr}+\frac{\nu}{r}\,\theta\right), \quad m_t = -D\left(\frac{1}{r}\,\theta+\nu\,\frac{d\theta}{dr}\right). \tag{2.59}$$

(a)

(b)

(c)
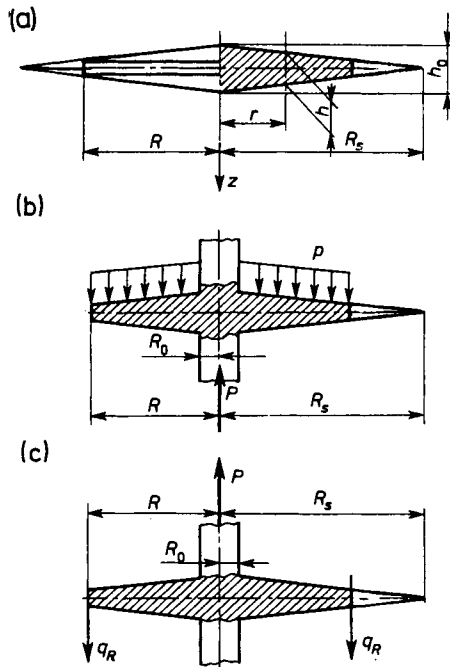
Fig. 2.13. Circular plate of linearly varying thickness: (a) solid (geometry); (b), (c) with a mandrel

The forces and moments acting on the plate element (Fig. 2.12b) must satisfy the conditions of equilibrium, which lead to the differential equations (2.13) and (2.14) already known. We put expressions (2.59) for m_r, m_t into the first equation, i.e., (1.23), bearing in mind that bending rigidity of the plate $D = \dfrac{Eh^3(r)}{12(1-v^2)}$ is a function of variable r. Finally, we arrive at the differential equation

$$\frac{d^2\theta}{dr^2} + \left(\frac{1}{r} + \frac{1}{D}\frac{dD}{dr}\right)\frac{d\theta}{dr} + \left(\frac{v}{D}\frac{dD}{dr} - \frac{1}{r}\right)\frac{\theta}{r} = \frac{q}{D} \tag{2.60}$$

expressing the relationship between slope θ and variable rigidity $D(r)$, on the one hand, and transverse force q of a plate of variable thickness $h(r)$, on the other. Detailed considerations concerning plates of linearly variable thickness are given, for example in Fleishman (1962), Gorskii (1961), Grigorenko and Laivunik (1965), Krontsenko (1961), Kovalenko (1959), Ponomarev et al. (1958), and Thrun (1956). According to Ponomarev et al. (1958), a plate of linearly variable thickness (Fig. 2.13a) satisfies the relation $h = h_0(1 - r/R_s)$, where h_0 is the thickness in the centre and R_s is the radius of the base of the cones. Putting $x = r/R_s$ changes the form of differential equation (2.60) reducing it to

$$x^2(1-x)^3 \frac{d^2\theta}{dx^2} + x(1-4x)(1-x)^2 \frac{d\theta}{dx} - (1-x)^2\theta = \frac{R_s^2 x^2}{D_0} q, \tag{2.61}$$

where

$$D_0 = \frac{Eh_0^3}{12(1-v^2)},$$

the integral of which consists of two functions

$$\theta = \theta_1 + \theta_2$$

the first being

$$\theta_1 = \frac{1+2x}{x} C_1 + \frac{3x-2x^2}{(1-x)^2} C_2 \tag{2.62}$$

and θ_2 depending on the type of loading.

Discussed below are two cases of loadings rather common in practice.

1. An annular plate (Fig. 2.13b) of outer radius R is joined to a rigid cylinder of diameter $2R_0$. The loading is pressure p, constant over the whole area of the plate. We have

$$q = \frac{pR_s}{2}\left(\frac{x_R}{x} - x\right),$$

where $x_R = R/R_s$ and $x = r/R_s$; the function θ_2 then takes the form:

$$\theta_2 = \frac{pR_s^3}{2D_0}\left[\frac{4x^3+15x^2-6x-6}{36x(1-x)^2} - \frac{x_R(2x^2+x-1)}{6x(1-x)^2} -\right.$$
$$\left. - \frac{(2x+1)(1-x_R^2)}{6x}\ln(1-x) - \frac{(3-2x)xx_R^2}{6(1-x)^2}\ln x\right]. \tag{2.63}$$

In the cases considered, for $r = R_0$, i.e., $x = x_0 = R_0/R_s$, we have $\theta = 0$, and when $x = x_R$, then $m_r = 0$. The function describing the deflection is obtained by integrating the equation relating w to slope θ. The third constant of integration, C_3, is calculated from the condition by which for $x = x_0$, $w = 0$.

2. A plate is loaded on the edge by uniformly distributed forces (Fig. 2.13c), the sum of which equals P, i.e., $q_R = p/2\pi R$, hence $q = p/2\pi R_s x$. If $\nu = 1/3$, which is the case for metals, the differential equation becomes much simpler:

$$x^2(1-x)^3\frac{d^2\theta}{dx^2} + x(1-4x)(1-x)^2\frac{d\theta}{dx} - (1-x)^2\theta = \frac{PR_sx}{2\pi D_0} \tag{2.64}$$

and its integral reduces to the function (Ponomarev et al., 1958)

$$\theta = \frac{2x+1}{x}C_1 + \frac{3x-2x^2}{(1-x)^2}C_2 +$$
$$+ \frac{PR_s}{2\pi D_0}\left[\frac{2x^2+x-1}{6x(1-x)^2} + \frac{2x-1}{6x}\ln(1-x) + \frac{3x-2x^2}{6(1-x)^2}\ln x\right]. \tag{2.65}$$

The cases presented show clearly that to determine $w(r)$ by integration of equations is laborious. It is much simpler to obtain an approximate solution which is sufficiently accurate for engineering purposes, replacing a plate of variable thickness by one of constant thickness over individual segments of radius R (Ponomarev et al., 1958).

In a similar way to that described above solutions can be obtained for ring-ribbed plates of variable thickness (Fleishman, 1962; Korotkin et al., 1955; Thrun, 1956).

Stress analysis in such plates turns out to be a much more involved problem, but the calculations can be significantly facilitated by the use of a digital computer. Shape optimization of plates, for example, in terms of lightness or equal strength, is another problem that can be solved with a digital computer.

2.7. Axially Symmetrical Heated Plates. Non-Linear Problems

We assume an axially symmetrical temperature increment, variable with thickness

$$T(r, z) = T(r) + z\beta(r)$$

and a temperature distribution, in which all the assumptions made in Section 2.1 are satisfied (Birger, 1956, 1961; Bezukhov, 1968; Hampe, 1963). Unit elongations of the layer with the coordinate z counted from the mid-layer of the plate are expressed as

$$\varepsilon_r = \frac{du}{dr} - \frac{d^2w}{dr^2}\,z, \tag{2.66}$$

$$\varepsilon_t = \frac{1}{r}\left(u - \frac{dw}{dr}\,z\right), \tag{2.67}$$

because displacements u and w are involved here. Stresses will exist in the circumferential and radial cross-sections, whose effects referred to unit length result in bending moments m_t and m_r and normal forces n_t and n_r.
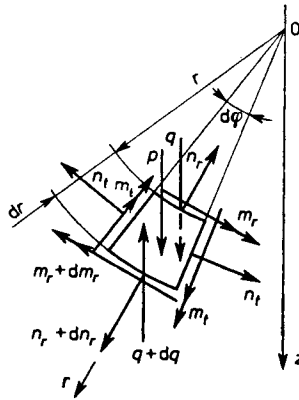
Fig. 2.14. Plate element. Internal forces at large deflections

In addition, shearing forces q may appear (Fig. 2.14). The conditions of equilibrium written for the moments and membrane forces take the form

$$r\frac{dm_r}{dr} + m_r - m_t = -qr, \tag{2.68}$$

$$r\frac{dn_r}{dr} + n_r - n_t = 0, \tag{2.69}$$

$$r\frac{dq}{dr} + q - pr = 0. \tag{2.70}$$

It follows from (2.68) and (2.70) that

$$\frac{d^2m_r}{dr} + \frac{2}{r}\frac{dm_r}{dr} - \frac{1}{r}\frac{dm_t}{dr} = -p. \tag{2.71}$$

Obviously, m_r and m_t are expressed by relationships (2.6), (2.7), and

$$n_r = \int_{-h/2}^{h/2} \sigma_r dz = \frac{Eh}{1-\nu} \left[\frac{du}{dr} + \nu \frac{u}{r} - \alpha T(r) \right], \tag{2.72}$$

$$n_t = \int_{-h/2}^{h/2} \sigma_t dz = \frac{Eh}{1-\nu} \left[\frac{u}{r} + \nu \frac{du}{dr} - \alpha T(r) \right]. \tag{2.73}$$

The state of stress will be given simultaneously by components resulting from bending and from normal forces.

As distinct from the case of unheated plates—where two equations of equilibrium are involved—heated plates are described by three differential equations, (2.68)–(2.70), the solutions of which are sought
— in approximate form, assuming a definite $T(r, tz)$;
— by introducing of stress function $F(r, z)$, which leads to a fourth-order equation with respect to w, the solution of which is usually approximate, as well.

The considerations grow more complicated if the plate has been heated to a temperature, at which Young's modulus E, Poisson's number ν and the coefficient of linear thermal expansion α are variable and depend on $T(r, z)$. In that case, the stresses are

$$\sigma_r = \frac{E(r,z)}{1-\nu^2(r, z)} \{ \varepsilon_r + \nu(r, z) \varepsilon_t - [1+\nu(r, z)] \alpha(r, z) T(r, z) \}, \tag{2.74}$$

$$\sigma_t = \frac{E(r, z)}{1-\nu^2(r, z)} \{ \varepsilon_t + \nu(r, z) \varepsilon_r - [1+\nu(r, z)] \alpha(r, z) T(r, z) \}. \tag{2.75}$$

If, moreover, unit elongations are sufficiently great for their more accurate determination to become necessary, then

$$\varepsilon_r = \frac{du}{dr} + \left[\frac{1}{2} \left(\frac{dw}{dr} \right)^2 + \frac{dw}{dr} \frac{dw_0}{dr} \right] - \frac{d^2 w}{dr^2} z, \tag{2.76}$$

$$\varepsilon_t = \frac{1}{r} \left(u - \frac{dw}{dr} z \right), \tag{2.77}$$

where w_0 is the initial deflection. The second expression contained in (2.76) introduces non-linearity into the equations. The equations of internal equilibrium, (2.68)–(2.70), remain unchanged, just as (2.71), but by eliminating from them successively the unknown quantities, we arrives at a set of two non-linear differential equations with variable coefficients. A simplification will also be achieved in this case, if we introduce stress function $F(r, z)$ and $\nu = $ constant.

2.8. The Case of a Plate Heated to a Moderate Temperature $T(r, z)$

If the heating temperature $T(r, z)$ of the plate is not very high, it can be as-
sumed that the physico-mechanical behaviour of the material does not change
and the unit elongations remain very small and are expressed by simple
linear relationships. When the temperature changes linearly across thickness
h of the plate, with $T = T(r)$, at mid-layer, then at distance z from the mid-
layer, $T(r, z) = \dfrac{T(r)}{h} z$, and in that case, bending moments are

$$m_r = -D\left[\frac{d^2w}{dr^2} + \frac{\nu}{r} \cdot \frac{dw}{dr} - (1+\nu)\alpha\,\frac{T(r)}{h}\right], \tag{2.78}$$

$$m_t = -D\left[\frac{1}{r} \cdot \frac{dw}{dr} + \nu\,\frac{d^2w}{dr^2} - (1+\nu)\alpha\,\frac{T(r)}{h}\right] \tag{2.79}$$

and shearing force is

$$q = -D\left[\frac{d}{dr}\left(\frac{d^2w}{dr^2} + \frac{1}{r} \cdot \frac{dw}{dr}\right) - (1+\nu)\alpha\,\frac{1}{h}\,\frac{dT(r)}{dr}\right]. \tag{2.80}$$

Proceeding as with unheated plates, we obtain the differential equation

$$\left(\frac{d^2}{dr^2} + \frac{1}{r}\,\frac{d}{dr}\right)\left(\frac{d^2w}{dr^2} + \frac{1}{r}\,\frac{dw}{dr}\right) = \alpha\,\frac{1+\nu}{h}\left[\frac{d^2T(r)}{dr^2} + \frac{1}{r}\,\frac{dT(r)}{dr}\right] \tag{2.81}$$

whose integral is determined by the classical method, and the integration
constants are determined, as previously, from the set of conditions written
for the edges of annular plate or for the edge and centre of a solid plate.

Interesting and rather common is the case of a heated plate where tem-
peratures T_1 and T_2 of the extreme surfaces of the plate are constant and so
is the difference between them $T = T_2 - T_1$. On the other hand, the tem-
perature at any point of a layer parallel to the mid-layer is identical, which
means that it depends only on distance z (Ilyushin and Ogibalov, 1960; Krzyś
and Życzkowski, 1962; Lipka, 1967). This temperature distribution exists by
and large under conditions of steady heat flow through the plate in a direction
normal to its surface. In many structures, specifically in liquid containers
and chemical reactors, we often come across thermally loaded plates. Due
to heating, an element of unit length in the cross-section along the plate
diameter undergoes deformation measured as thermal elongation αT_1 and
αT_2 of the extreme layers and the angle of inclination

$$\theta = \alpha\,\frac{T}{h}$$

of the element walls which are originally parallel. This goes to show that the mid-layer of the element assumes the shape of a spherical surface of radius ϱ_0, and as it follows from the diagram:

$$\frac{1}{\varrho_0} = \alpha \frac{T}{h}.$$

However, no thermal stresses occur in this plate (Krzyś and Życzkowski, 1962; Lipka, 1967).

If moments m_0 are acting on the edge of a free and unheated plate, then in keeping with the results obtained for mechanically loaded plates, the curvature of the mid-layer in the cross-section along the diameter

$$\frac{1}{\varrho} = \frac{m_0}{(1+\nu)D}$$

is constant. Therefore, in this case, the mid-surface also has the shape of a spherical cap. Assuming that the plate clamped perfectly rigid on the edge has been heated in the described manner and that it cannot freely be deformed, then radial moments m_0 will occur on the edge and the slope will vanish. The mid-layer will therefore be plane. Consequently, we can write the equation

$$\alpha \frac{T}{h} = \frac{m_0}{(1+\nu)D}$$

with respect to unknown moment m_0. Hence,

$$m_0 = (1+\nu)\frac{D\alpha T}{h}.$$

Maximum thermal stress (in extreme layers) is obviously correspondingly

$$\sigma_r = \pm \frac{6m_0}{h^2}, \qquad \sigma_t = \sigma_r$$

or   (2.82)

$$\sigma_r = \pm \frac{E\alpha T}{2(1-\nu)}.$$

Thickness h does not enter into this relationship, but the temperature difference does depend on h and the thicker the plate the greater it will be. It is easily seen that we have neglected in the considerations the influence of radial elongations of the mid-layer due to heating, which means that free thermal expansion in the direction of the radius exists on the edge of the plate. Restrained thermal elongation on the edges is a problem in the theory of disks.

Let a solid circular simply supported plate be unevenly heated so that the temperature distribution is expressed by the function

$$T = T_0 + b_1 z(1 + b_2 r),$$

where b_1 and b_2 are constant quantities (Krzyś and Życzkowski, 1962). The temperature difference of the extreme layers satisfies the condition of axial symmetry and changes linearly, increasing with radius r, owing to which mid-layer curvatures would be

$$\frac{1}{\varrho_{1r}} + \frac{1}{\varrho_{1t}} = \alpha b_1 (1 + b_2 r)$$

but the compatibility condition is not satisfied, which is easily proved. Consequently, additional bending moments will occur, causing change in the radii of curvatures respectively to condition (2.4). Introducing on an auxiliary basic fictitious cross-sectional moments and then using the relationships given in the theory of plates, from which the real curvatures are determined (a detailed description given in Krzyś and Życzkowski, 1962), we arrive finally at the differential equation

$$\frac{d}{dr}\left(\frac{1}{r}\frac{dw}{dr} + \frac{d^2w}{dr^2} \right) = -2\frac{d}{dr}[\alpha b_1(1 + b_2 r)] \tag{2.83}$$

whose integral is

$$w = \frac{C_1}{4}r^2 + C_2 \ln r + C_3 - 2\alpha b_1\left(\frac{1}{4} + \frac{b_2}{9}r\right)r^2. \tag{2.84}$$

As before, the constants of integration are determined from the conditions written for the centre of the plate edge. Considering these conditions, we arrive at the following deflection relationships for (assuming, for simplicity, a system resulting in $w(0) = 0$):

$$w = -\alpha b_1 \left[\frac{2}{9}b_2 r^3 + \frac{r^2}{2} - \frac{1-\nu}{6(1+\nu)}b_2 R r^2 \right] \tag{2.85}$$

and for bending moments

$$m_r = \frac{1-\nu}{3}Db_1 \alpha b_2 R\left(\frac{r}{R} - 1\right), \tag{2.86}$$

$$m_t = -\frac{1-\nu}{3}Db_1 \alpha b_2 R\left(\frac{r}{R} + 1\right), \tag{2.87}$$

which, as a result of the compatibility condition being satisfied by the curvatures—induced by free thermal strain of the plate—themselves fail to

satisfy this condition, being complementary fictitious cross-sectional bending moments.

The form of function $w(r)$ with the assumed thermal state depends chiefly on the boundary conditions. If for the sake of comparison, we assume that a similarly heated plate is rigidly clamped on the edge, then it is easily proved that

$$w = \frac{\alpha b_1 b_2}{3} r^3 \left(\frac{R}{r} - \frac{2}{3} \right) \tag{2.88}$$

and

$$m_r = D b_1 \alpha \left[\frac{1-\nu}{3} b_2 r - (1+\nu) \left(\frac{2}{3} b_2 R + 1 \right) \right], \tag{2.89}$$

$$m_t = D b_1 \alpha \left[\frac{\nu-1}{3} b_2 r - (1+\nu) \left(\frac{2}{3} b_2 R + 1 \right) \right]. \tag{2.90}$$

2.9. Thin Axially Symmetrical Circular Plates under Conditions of Large Deflections

By *thin plates* under conditions of large deflections we understand this to mean very thin plates, in which next to cross-sectional bending moments and shearing forces, there exist circumferential and radial tensions indiced by large deflections.

The influence of these tensions on the state of stress is considerable, and it cannot therefore the neglected.

Such plates are sometimes called *membranes*. They are frequently encountered in engineering, specifically in the structures of measuring instruments.

Retaining the assumptions introduced in Section 2.1 and accepting a state of loading without temperature changes—which is justifiable in most cases by very small temperature differences $(T_2 - T_1)$—we bring relationships (2.76) and (2.77) for the mid-layer to the form

$$\varepsilon_r = \frac{du}{dr} + \frac{1}{2} \left(\frac{dw}{dr} \right)^2, \tag{2.91}$$

$$\varepsilon_t = \frac{u}{r}. \tag{2.92}$$

From these relations, we derive the countability condition

$$\frac{d}{dr} (r \varepsilon_t) - \varepsilon_r = -\frac{1}{2} \left(\frac{dw}{dr} \right)^2. \tag{2.93}$$

The two curvatures of the mid-layer are expressed by relationships

$$\frac{1}{\varrho_r} = -\frac{d^2w}{dr^2}, \qquad \frac{1}{\varrho_t} = -\frac{1}{r}\frac{dw}{dr},$$

as proved in Section 2.1, and stresses σ_r and σ_t in this layer are expressed by the relationships

$$\sigma_r = \frac{E}{1-\nu^2}\left[\frac{du}{dr} + \frac{1}{2}\left(\frac{dw}{dr}\right)^2 + \nu\frac{u}{r}\right], \tag{2.94}$$

$$\sigma_t = \frac{E}{1-\nu^2}\left[\frac{u}{r} + \nu\frac{du}{dr} + \frac{1}{2}\nu\left(\frac{dw}{dr}\right)^2\right]. \tag{2.95}$$
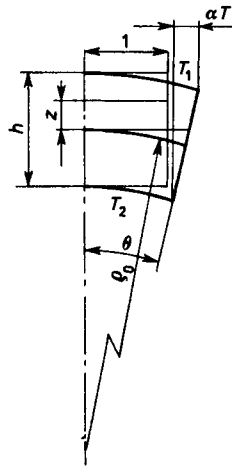
Fig. 2.15. Element of heated plate. Deformation

The internal and external forces acting on an element of the plate (Fig. 2.15) satisfy the equilibrium conditions

$$\frac{d}{dr}(r\sigma_r) - \sigma_t = 0, \tag{2.96}$$

$$r\frac{dm_r}{dr} + m_r - m_t = -qr, \tag{2.97}$$

$$\frac{1}{r}\int_0^r rp\,dr - \sigma_r h\theta = q, \tag{2.98}$$

the last condition relating to projections of all forces on the z-axis. The quantity θ is the slope at distance r. Let the expression containing the integral in

(2.98) equal $A(r)$. Relationships (2.94)–(2.98) reduce to the differential equation

$$D\frac{d}{dr}\left[\frac{1}{r}\frac{d}{dr}\left(r\frac{dw}{dr}\right)\right] = A(r) + \frac{h}{r}\,\sigma_r\,\frac{dw}{dr}. \tag{2.99}$$

If a stress function F exists that satisfies the conditions

$$\sigma_r = \frac{1}{r}\frac{dF}{dr}, \qquad \sigma_t = \frac{d^2F}{dr^2}, \tag{2.100}$$

then after substituting function F successively into (2.93)–(2.95), we arrive at the set of differential equations

$$D\frac{d}{dr}\left[\frac{1}{r}\frac{d}{dr}\left(r\frac{dw}{dr}\right)\right] = A(r) + \frac{h}{r}\frac{dF}{dr}\frac{dw}{dr}, \tag{2.101}$$

$$\frac{d}{dr}\left[\frac{1}{r}\frac{d}{dr}\left(r\frac{dF}{dr}\right)\right] = -\frac{F}{2r}\left(\frac{dw}{dr}\right)^2. \tag{2.102}$$

The integrals of these equations contain constants determined, as previously, from the boundary conditions. Two modes of clamping the plate edges are distinguished, namely simple support on the edge $(r = R)$

$$w(R) = 0, \qquad \left(\frac{d^2w}{dr^2} + \frac{\nu}{r}\frac{dw}{dr}\right)_{r=R} = 0,$$

clamped edge

$$w(R) = 0, \qquad \frac{dw(R)}{dr} = 0.$$

In both cases of a solid plate, we have for the centre

$$\frac{dw(0)}{dr} = 0.$$

If the clamping on the edge prevents radial displacement, then

$$u(R) = 0$$

should be satisfied. Only in few cases of $p(r)$ can be succeeded in determining $w(r)$, $u(r)$ and $F(r)$ in closed forms; in others, approximate solutions are obtainable (Ponomarev *et al.*, 1958).

2.10. Other Non-Linear Problems of Axially Symmetrical Plates

The problems discussed above do not exhaust all the aspects of plate analysis. The theory presented covers only plates and cases of loadings most common in the practice of engineering design and analysis and serving at

the same time as the basis and standards of procedure for solutions of other cases, including also those for which ready formulae are unavailable in the literature. This applies to an extent to linear problems, but above all to non-linear problems for which each case of a plate presents a separate problem for seeking solutions. Presented in brief below are some problems of this kind.

1. Thick plates. These cover all cases where the ratio $R/h < 5$. The state of stress is then described by four components, and under no circumstances can σ_z be omitted. Usually, great loadings and finite unit elongations are involved here, owing to which non-linear members occur in the expressions for strains. Considerations lead to a set of non-linear simultaneous differential equations (e.g. Kujawski, 1976) the solutions of which for particular loadings and boundary conditions are obtained by solving with the aid of a digital computer or using the finite element method assisted by a digital computer. Obviously, the considerations get more complicated if the plate is heated, and constants $E, \nu,$ α are temperature dependent (Kobza and Lipiński, 1973).

2. Plates of optimum shape under conditions of strong heating and large deflections. Additional conditions appear, e.g. lightness of plate, strength in the form $\sigma_{red} = k_r$ over all of its area. These are for the most part non-linear problems solved with the use of a computer (Jaworski and Raczyński, 1976; Thrun, 1956).

3. Heated plates under conditions of elastic-plastic strains. Large strains and new physical laws (such as the law of plasticity) appear (Bezukhov, 1968).

4. Orthotropic axially symmetrical plates. The orthotropy is related to the structure of the material or is due to the shape of the plate, by the introduction of closely spaced radial and circular ribs (of the ring type) (Birger, 1956, 1961). Two values of moduli E_r and E_t and $\nu_r,$ ν_t occur here. In the case of non-linearity of strains, the differential equations acquire a complex form, and the solutions are as a rule approximate and obtainable by numerical methods (Grigorenko and Laivunik, 1965; Maslov, 1965; Zhilin, 1970).

Problems of elastic stability, elastic-plastic states etc. have been omitted being non-linear, not satisfying the condition of complete axial symmetry, this being consistent with the subject matter covered by this part of the book. They represent a separate field of applied mechanics and also have ample literature (e.g. Biezeno and Grammel, 1939; Flügge, 1956; Korotkin *et al.*, 1955; Maslov, 1965; Ponomarev *et al.*, 1958; Timoshenko and Goodier, 1951, 1962; Timoshenko and Woinowsky-Krieger, 1959; Vainberg and Vainberg, 1959; Tuliszka, 1960; Yusuff, 1961).

3. Axially Symmetrical Disks

The disk is a three-dimensional flat structural element, in which two dimensions are significantly greater than the third defined as thickness h, with loadings acting in planes parallel to the central plane. This plane divides the thickness in half at each place of the disk.

A circular disk has an outline in the form of a circle and may have a co-axial circular hole. It is therefore geometrically an axially symmetrical element. If the material, loadings and states of stress and strain satisfy the condition of axial symmetry, then such a disk has complete axial symmetry.

Circular disks will be found in numerous industrial machines and plants
— in engineering and power industries (internal combustion and steam turbine disks, axial and centrifugal compressor disks, fan and blower disks, balance disks, disk-plates, and the like),
— in chemical industry (disks, disk-plates in gas pipings, separators, centrifuges, winders, fibre guides, compensators, and the like),
— in foodstuff and medical appliance industries (e.g. high-speed and ultra high-speed centrifuges, pressure-conduit joints, and the like).

Loading sources of disks can be classified by type into three groups, namely *surface loadings* (deriving often from the action of a flowing medium), *inertia loadings* and *thermal loadings*.

Loadings under the first group are chiefly forces induced by pressures of a flowing medium, e.g. on blades and on lateral and batting surfaces of a disk. Inertia loadings are induced by the body forces of a rotating disk and blades. Thermal loadings are generated by uneven heating along the radius or over the thickness. In the design of a disk, the main attention is paid to the profile-dimensioning principal loadings, whereas all others are considered only in approximate terms or are even neglected, regarded as insignificant, bearing in mind however that their effects have to be reduced to a minimum. Classified as disk-dimensioning loadings are: (1) body forces of the disk itself, (2) radial body forces induced, for example, by the action of the blade

rim and blades, (3) heating of the disk, constant over the thickness and variable along the radius (Lipka, 1961).

In practice, we deal with circular disks, either solid or with holes, of profiles of different shape, joined to shafts in various ways. Frequently, disks of variable thickness are produced according to certain predetermined curves, e.g. a curve corresponding to conditions of uniform strength or according to a hyperbola or an expotential curve.

Disks for machines of different type are all calculated by the same methods, and the existing significant differences relate only to the magnitude of the loadings and the service period of the machines (Alper, 1965; Budyka, 1962; Derski, 1958; Girkamann, 1956; Kozlov *et al.*, 1965; Kujawski, 1976; Lipka, 1961; Lokai, 1961; Malinin, 1962; Prasek, 1972; Sherbourne and Murthy, 1974).

Weighing least of all are disks of uniform strength. For technological reasons, a uniform strength profile is frequently replaced by sectors of straight lines resulting in the design of a disk that is easier to make, e.g. one composed of several cones or rectangles. Disks of uniform strength, provided that they remain unheated, retain their properties at relatively high rotational speeds, if the state of stress obeys Hooke's law.

A disk of uniform strength designed for a specified angular speed Ω and a specified state of temperature ceases to be such, if the rotational speed and the temperatures are changed (Lipka, 1961, 1967).

The change in temperature along the radius can be determined analytically or experimentally, but usually the state of temperature depends on the operating conditions of the disk (Lipka, 1961; Skubachevskii, 1955). In most cases, a parabolic temperature distribution along the radius is assumed

$$T = T_0 + (T_1 - T_0)\,\frac{r^2}{R^2},$$

where T_0 is the temperature in the centre of disk, T_1 is the temperature on the periphery, R is the outer radius of disk, and r is the current radius (Prokopovich *et al.*, 1967; Zhyrickii *et al.*, 1963). In the starting stage, a machine or a plant attains nominal parameters after a certain time but before they are reached it operates under conditions of intermediate parameters, the rotational speed and temperatures change in time. Calculations are then also for the intermediate parameters.

The influence of the degree of non-uniformity of heating on thermal stresses is considerable, and it depends on the character of the temperature changes. The higher the gradient dT/dt, the greater thermal stresses will be. Disks, even if heated to high temperatures but with a low temperature gradient, have relatively low thermal stresses. In the range of validity of Hooke's law

we can use the principle of superposition of mechanical and thermal loadings. The stresses and strain in a complex state of loading are the sum of stresses and strains from the individual component loadings. This greatly facilitates the calculations themselves. Stresses and strains in disks are determined assuming the existence of a plane state of stress (Laszlo, 1948; Malinin, 1961; Ryś and Życzkowski, 1971; Życzkowski, 1957; Tuliszka, 1960).

There are a number of methods for analysing the internal forces in disks, all based on common assumptions. They differ only in calculating efficiently and in the degree of inaccuracy. Mathematically exact solutions, in other words, the determination of the stresses and strains, are obtainable only in few cases; in all other cases, only approximate solutions can be obtained.

3.1. Heated Rotating Disk of Variable Thickness

The following assumptions are established:
— the disk satisfies the condition of complete axial symmetry,
— the central plane is the plane of symmetry; it is perpendicular to the x-axis of rotation,
— the material is homogeneous and isotropic,
— plane state of stress occurs at any point and Hooke's law is valid,
— the disk is heated so that on radius r, the temperature along thickness h is constant. The initial temperature is constant and can be taken to equal zero,
— modulus E, number ν and coefficient of linear thermal expansion are constant,
— rotations are constant, corresponding to which is $\Omega = \text{const.}$

A circular disk of arbitrarily varying thickness $h(r)$ is given rotating about the z-axis (Fig. 3.1a). Material density is ϱ. A volume element is cut out by
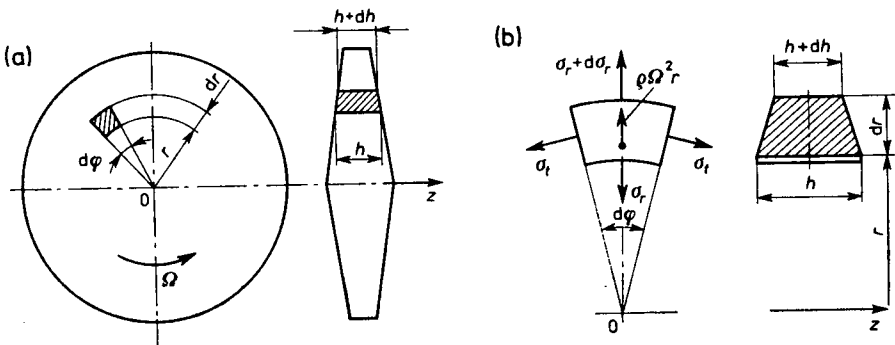
Fig. 3.1. Rotating circular disk: (a) of variable thickness; (b) disk element

two planes inclined to each other at angle $d\varphi$ and by two co-axial surfaces of radii r and $r+dr$, respectively. Acting on the walls of this element are radial stresses σ_r and circumferential stresses σ_t. A centrifugal force of intensity $\varrho\Omega^2 r$ is also acting. There exists therefore a plane state of stress, and the equations of equilibrium written for the element take the form

$$\frac{d(rh\sigma_r)}{dr} - \sigma_t h + \varrho\Omega^2 r^2 h = 0. \tag{3.1}$$

If u is the radial displacement of a point r of the disk then σ_r and σ_t are expressed by the relationships

$$\sigma_r = \frac{E}{1-\nu^2}\left[\frac{du}{dr} + \nu\frac{u}{r} - (1+\nu)\alpha T\right], \tag{3.2}$$

$$\sigma_t = \frac{E}{1-\nu^2}\left[\frac{u}{r} + \nu\frac{du}{dr} - (1+\nu)\alpha T\right] \tag{3.3}$$

in which the unit radial and circumferential elongations, ε_r and ε_t, respectively, are related to the stresses by equations of Hooke's law for a plane state of stress, and in which the relations (1.2) and (1.3) between the unit elongations and the displacement hold.

Substituting (3.2) and (3.3) into (3.1), we arrive at a single differential equation on its final form

$$\frac{d^2u}{dr^2} + \frac{1}{r}\left(1 + \frac{r}{h}\frac{dh}{dr}\right)\frac{du}{dr} - \left(1 - \nu\frac{r}{h}\frac{dh}{dr}\right)\frac{u}{r^2}$$

$$= -Ar + \alpha(1+\nu)\left(\frac{dT}{dr} + \frac{T}{h}\frac{dh}{dr}\right) \tag{3.4}$$

in which $A = \varrho\Omega^2\dfrac{1-\nu^2}{E}$ is a constant quantity. The integral of this equation has two constants whose values are determined as before from the boundary conditions. This equation, for arbitrary function $h(r)$, cannot be integrated in closed form.

3.2. Cases of Unheated Disks of Constant Thickness

Given below are solutions for cases of disks commonly used in machine design. If thickness h is constant along the radius, then differential equation (3.4) becomes greatly simplified, and relationships (3.2) and (3.3) remains unchanged. The final form of differential equation (3.4) reduces to

$$\frac{d^2u}{dr^2} + \frac{1}{r}\frac{du}{dr} - \frac{u}{r^2} = -Ar \tag{3.5}$$

and its integral

$$u = C_1 r + \frac{C_2}{r} - \frac{A}{8} r^3 \tag{3.6}$$

contains constants C_1, C_2, which can be determine without difficulty from the boundary conditions. Using these constants, we can express the stresses as follows:

$$\sigma_r = \frac{E}{1-\nu^2}\left[(1+\nu)C_1 - (1-\nu)C_2 \frac{1}{r^2}\right] - \frac{3+\nu}{8} \varrho\Omega^2 r^2,$$

$$\sigma_t = \frac{E}{1-\nu^2}\left[(1+\nu)C_1 + (1-\nu)C_2 \frac{1}{r^2}\right] - \frac{1+3\nu}{8} \varrho\Omega^2 r^2. \tag{3.7}$$

Adding and subtracting the last two expressions by sides, we obtain the relationship between the principal stresses

$$\sigma_t + \sigma_r = \frac{2E}{1-\nu} C_1 - \frac{1+\nu}{2} \varrho\Omega^2 r^2, \tag{3.8}$$

$$\sigma_t - \sigma_r = \frac{2E}{1+\nu} C_2 - \frac{1-\nu}{4} \varrho\Omega^2 r^2. \tag{3.9}$$

Only one constant occurs in each of them, either C_1 or C_2. This property is utilized in practical calculations.

Radial displacement of given point of the disk

$$u = \frac{r}{E}(\sigma_t - \nu\sigma_r) \tag{3.10}$$

which follows directly from Hooke's law. With stress components σ_r and σ_t determined, we can calculate directly displacement u. With the initial assumptions satisfied, Hooke's law in the first place, we are allowed to use the principle of superposition of mechanical loadings.

It will be useful for practical purposes to discuss in more detail some particular cases of loading of unheated disks of constant thickness (Biezeno and Grammel, 1939; Birger, 1956; Kobrin, 1963; Lipka, 1967; Lipka and Butt-Hussaim, 1963; Loffler, 1961; Skubachevskii, 1955; Vainberg and Vainberg, 1959).

3.2.1. A disk with a hole with tensions q_1 and q_2 acting on both edges

Boundary conditions are: if $r = R$, then $\sigma_r = q_1$ and for $r = R_2$ we have $\sigma_r = q_2$. Following the procedure already known to us, we arrive at the equations
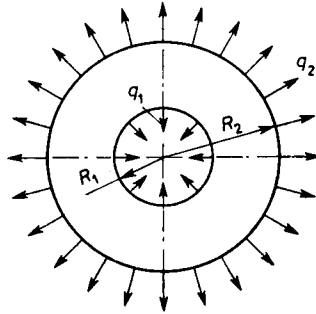
Fig, 3.2. Disk with a hole. Loadings by tensions on both edges

$$u = \frac{3+\nu}{8E}\,\varrho\Omega^2 R_2^3\left[(1-\nu)(1+x_1^2)x+(1+\nu)\frac{x_1^2}{x}-\frac{1-\nu^2}{3+\nu}\,x^3\right]+$$

$$+\frac{R_2}{(1-x_1^2)E}\left\{q_2\left[(1-\nu)x+\frac{1+\nu}{x}\,x_1^2\right]-q_1 x_1^2\left[(1-\nu)x+\frac{1+\nu}{x}\right]\right\},$$

$$\tag{3.11}$$

$$\sigma_r = \frac{3+\nu}{8}\,\varrho\Omega^2 R_2^2\left(1+x_1^2-x^2-\frac{x_1^2}{x^2}\right)+$$

$$+\frac{1}{1-x_1^2}\left[q_2\left(1-\frac{x_1^2}{x^2}\right)-q_1 x_1^2\left(\frac{1}{x^2}-1\right)\right],\tag{3.12}$$

$$\sigma_t = \frac{3+\nu}{8}\,\varrho\Omega^2 R_2^2\left(1+x_1^2+\frac{x_1^2}{x^2}-\frac{1+3\nu}{3+\nu}\,x^2\right)+$$

$$+\frac{1}{1-x_1^2}\left[q_2\left(1+\frac{x_1^2}{x^2}\right)-q_1 x_1^2\left(\frac{1}{x^2}+1\right)\right],\tag{3.13}$$

$$x_1 = \frac{R_1}{R_2},\quad x=\frac{r}{R_2}.$$

In this case, both principal stresses can simultaneously be tensile stresses. The state of stress depends not only on quantity Ω but also on q_1 and q_2.

If the hole is so small that $x_1 \approx 0$ and tensions on the edges are absent, then the circumferential stress on the edge of the hole is

$$\sigma_{t1} = \frac{3+\nu}{8}\,\varrho\Omega^2 R_2^2.\tag{3.14}$$

This value gives at the same time the maximum effort of the disk material. This brings forth an important conclusion, namely that where the hole in the disk is very small, the circumferential stresses and the effort on the edge of the hole are twice as great as in the centre of a solid disk.

When the hole is so large that, allowing for a minor inaccuracy, we can take $x_1 \approx 1$, then the disk turns into a thin ring. The radial stresses are so small that they can be neglected, whereas the circumferential stresses can be taken to be constant, equaling

$$\sigma_t = \varrho \Omega^2 R_2^2. \tag{3.15}$$

3.2.2. Two-stage disk

In rotor structures we encounter so-called *two-* or *multistage disks* consisting, in principle, of co-axial rings of various thicknesses, constant in sectors, continuously joined to each other. Actually, these are already axially symmetrical disk structures.
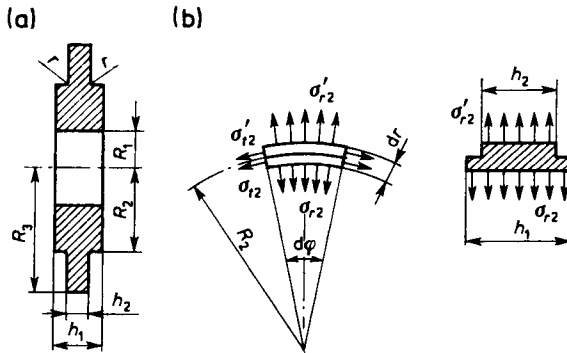
Fig. 3.3. Circular disk: (a) two-stage; (b) disk element at place of change of thickness

We shall consider a two-stage disk, being the simplest and at the same time most common type with radii R_1, R_2, R_3 (Fig. 3.3a). The disk is in rotary motion. The following additional assumptions are established:
— the differences in ring thicknesses h_1 and h_2 are not very great,
— at the point of change in thickness, the stress concentration is small enough to be neglected.

Multistage disks may weigh less compared to disks of constant thickness, while they do not differ much in strength. To determine the stresses, the stages are separated in the manner indicated in Fig. 3.3b. Stresses σ_{r2} and σ'_{r2} are acting at the connecting place. Each stage separately makes a circular ring loaded at one of the edges by unknown tensions in stress form over thicknesses h_1 and h_2. The relationships describing the radial displacements determined from (3.6) for the inner and outer ring

$$u_1 = C_1 r + \frac{C_2}{r} - \frac{A}{8} r^3, \qquad u_2 = C'_1 r + \frac{C'_2}{r} - \frac{A}{8} r^3 \tag{3.16}$$

contain four unknown constants of integration $C_1, \ldots, C_2'$, which will be determined from the boundary conditions and the continuity conditions for the two parts.

Boundary conditions are: on radii R_1 and R_3 we have $\sigma_r(R_1) = 0$ and $\sigma_r(R_3) = 0$. The additional indispensible conditions are established in the following manner. Where the two parts of the disk join each other, continuity of the material must be preserved, which is expressed by equality of the radial displacements at the site of transition from thickness h_1 to h_2, i..e.,

$$u_1(R_1) = u_2(R_1).\tag{3.17}$$

The element cut out of the disk as shown in Fig. 3.3b is under four different stresses. The equilibrium condition leads to the following relationship between radial stresses:

$$\sigma_{r2}' h_2 = \sigma_{r2} h_1.\tag{3.18}$$

The last two conditions, i.e., (3.17) and (3.18), are called *continuity conditions*. Thus, the boundary and continuity conditions, reduce to the following equations:

$$C_1 - C_2 \frac{1-\nu}{(1+\nu)R_1^2} = \frac{A}{8} R_1^2 \frac{3+\nu}{1-\nu},$$

$$C_1' - C_2' \frac{1-\nu}{(1+\nu)R_3^2} = \frac{A}{8} R_3^2 \frac{3+\nu}{1-\nu},$$

$$C_1 + \frac{C_2}{R_2^2} - C_1' - \frac{C_2'}{R_2^2} = 0,$$

$$C_1 - C_2 \frac{1-\nu}{(1+\nu)R_2^2} - C_2' \frac{h_2}{h_1} + C_2' \frac{(1-\nu)h_2}{(1+\nu)R_2^2 h_1}$$

$$= \frac{A}{8} R_2^2 \frac{3+\nu}{1+\nu}\left(1 - \frac{h_2}{h_1}\right).$$

The simplest way to determine these unknowns is to substitute particular values for the coefficients and free terms. In order to avoid considerable stress concentrations at sites of transition between the stages, suitable fillets with radii r should be introduced as shown in Fig. 3.3a.

Also classed as two-stage is a solid disk or disk with a hole having on the outline a rim in the shape of a thin ring, not very wide, making a single unit with the inner part. The calculation technique is similar to that described above.

3.2.3. Two-stage disk fitted in a shaft (Fig. 3.4a) *through an intermediary of elastic contraction forces*

This connection must therefore transmit the torque from, say, the forces acting on the blades (originating from flow). Usually, at the contact site
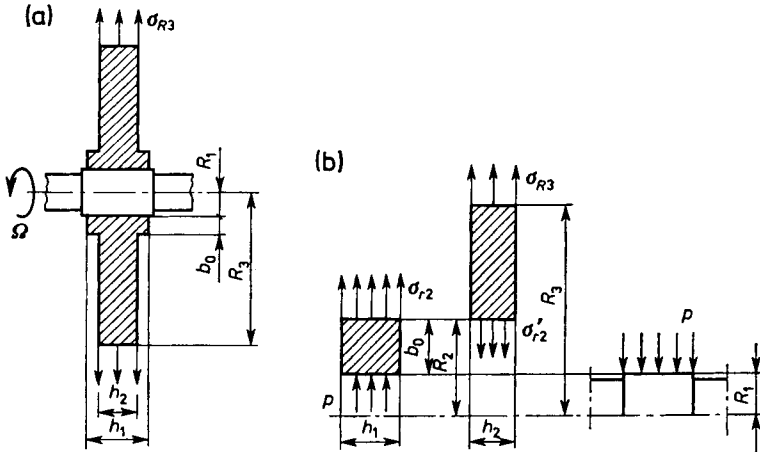
Fig. 3.4. Circular disk: (a) contraction fit on the shaft; (b) component parts

of the two elements—the disk and the shaft—a hub of suitable size is mounted so as to make a single unit with the disk proper. Such a hub prevents excessive mutual pressures on the contact surfaces, on the one hand, and reduced circumferential stresses and effort of the disk, on the other. This is a typical design of shaft-two-stage-disk rotor unit.

   If the size of b_0 is considerable compared to radius R, and thicknesses h_0 and h do not differ much, the problem amounts to solving a two-stage disk with a boundary condition at the contact site of the hub with the shaft, but if b_0 is small and the hub can be treated as a thin-walled ring, then the calculation is confined to the case of a disk with a hub.

   We shall consider the former case as it is more complicated and serves also as a model for the latter case. Let the connection between the shaft and the disk transmit torque M_0 through friction forces. The mutual pressure between the contact surfaces equals p, therefore with the coefficient of friction μ we have the relation

$$M_0 = 2\pi\mu p h_1 R_1.$$

Hence, the pressure required

$$p = \frac{M_0}{2\pi\mu h_1 R_1}$$

must be assured by a suitable difference between the shaft radius and the disk hole radius. Proceeding before, we obtain the three component parts of the rotor unit: an annular disk of thickness h_1 (first stage), a disk of thickness h_2 (second stage) and a shaft.

Existing at the first stage (Fig. 3.4b), are pressures p and tension σ_{r2} and at the second stage, tensions σ'_{r2}, and σ_{R3} in stress form over the respective thicknesses, the latter stresses deriving from the blades. Boundary conditions for the two stages are:

stage I—for $r = R_1$ we have $\sigma_r = -p$ and for $r = R_2$ $\sigma_r = \sigma_{r2}$,

stage II—for $r = R_2$ we have $\sigma'_r = \sigma'_{r2}$ and for $r = R_3$ $\sigma_r = \sigma_{R3}$.

The continuity conditions for the two disk elements are to ensure that $u_1 = u_2$ and $\sigma_{r2}h_1 = \sigma'_{r2}h_2$.

The radial displacements of the two stages at the connecting site are identical in accordance with (3.6), therefore

$$C_1 R_2 + \frac{C_2}{R_2} - \frac{A}{8} R_2^3 = C'_1 R_2 + \frac{C'_2}{R_2} - \frac{A}{8} R_2^3.$$

From the boundary and continuity conditions we now obtain a set of equations with respect to C_1, C_2, C'_1, C'_2 and σ_{rR} which after solving gives the complete solution of the disk.

If the shaft has a thickening for the hub to mount, then the elastic contraction of shaft radius R_1, neglecting small quantities, is

$$|u_w| = \frac{AR_1^3}{4(1+\nu)} - \frac{p}{E}(1-\nu)R_1 \tag{3.19}$$

and the radius of the hub hole will increase by the quantity

$$u_p = C_1 R_1 + \frac{C_2}{R_1} - \frac{A}{8} R_1^3. \tag{3.20}$$

Consequently, the least difference necessary between the radius of the hub hole and the radius of the shaft thickening is

$$\Delta R_p = u_p + |u_w|. \tag{3.21}$$

If the angular velocity of rotary motion Ω increases, the mutual pressure between the hub and the shaft will decrease and it may even decline to zero at a certain value of Ω_0. Pressures p will then disappear and together with the friction forces between the shaft and the hub as well. This takes place when

$$u_p(\Omega_0) = \Delta R_p - |u_w(\Omega_0)|. \tag{3.22}$$

In a similar manner we calculate the stresses existing after fitting the disk in the shaft, i.e., under conditions where $\Omega = 0$. These are routine calculations in the design of the shaft-disk contraction joint (Lipka, 1967).

3.3. Unheated Rotating Disk of Uniform Strength

It at any point the two principal stresses are identical, equalling, for example, stress σ which is constant throughout the disk, we deal then with a disk of uniform strength. It is easily seen that this type of disk has a profile of variable thickness h. The advantages of such disks compared to disks of constant thickness are better utilization of the material (since the effort at every point is identical) and low weight of the disk. They have, however, a lower bending rigidity, especially near the edge and they are much more costly to manufacture (Budyka, 1962; Lipka, 1967; Loffler, 1961; Ponomarev *et al.*, 1958; Sherbourne and Murthy, 1974).

The point of departure for calculations of unheated disks of equal strength is the differential equation of the theory of disks with variable thickness (3.1), in which we should have $\sigma_r = \sigma_t = \sigma$, where σ can be, for example, the allowable tensile stress of material k_r, or some other stress. The equilibrium equation then changes to the form

$$\frac{1}{h}\frac{dh}{dr} = -\frac{\varrho\Omega^2}{\sigma}r \tag{3.23}$$

and its integral is

$$h = Ce^{-\frac{\varrho\Omega^2}{2\sigma}r^2} \tag{3.24}$$

containing only one constant of integration C.

Considering that the profile is symmetrical to the central plane, curve $h(r)$ is at the same time the profile of a uniform-strength disk. Constant C is determined from the boundary condition or from the condition written for the centre of disk. If thickness h_1 on radius R of the rim is given, then for $r = R$ we have $h(R) = h_1$ and

$$h = h_1 e^{\frac{\varrho\Omega^2(R^2-r^2)}{2\sigma}}. \tag{3.25}$$

On the other hand, if thickness in the centre of disk h_0 is given, then for $r = 0$, $h(0) = h_0$; hence,

$$h = h_0 e^{-\frac{\varrho\Omega^2}{2\sigma}r^2}. \tag{3.26}$$

For the considered state of stress, displacement on an arbitrary radius in accordance with (3.10) is

$$u = (1-\nu)\frac{r\sigma}{E}. \tag{3.27}$$

In turn, we consider some cases of disks of uniform strength having practical importance.

3.3.1. Uniform-strength disk with blades (with a certain number of blades being mounted on its edge)

Ignoring the question of clamping of the blades around the rim, we assume that tensions q generated by their action are uniformly distributed over thickness h_1 and over the whole circumference. The condition that the radial stresses on the edge have to be equal to σ, determines the indispensable thickness of the disk

$$h_1 = \frac{q}{\sigma}$$

and its thickness in the centre

$$h_0 = \frac{q}{\sigma} e^{\frac{\varrho \Omega^2 R^2}{2\sigma}}. \tag{3.28}$$

If he blades are mounted in the disk through an intermediary of V-shaped or trapezoid keys, we should add to q also the tensions induced by these clamping elements.

3.3.2. Uniform-strength disk with a rim

The condition of uniform strength can also be satisfied for a disk having on the periphery a rim in the form of a ring provided with blades. In designs of rotors we usually find a rim of width b which is so small that they can be treated as thin-walled (Fig. 3.5a). Such an assumption lessens the accuracy of calculations only slightly, but it simplifies them. Let the blades and the
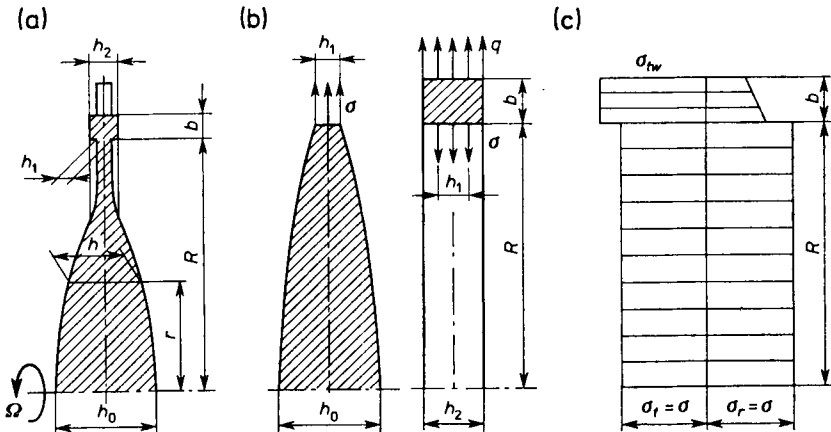
Fig. 3.5. Circular disk: (a) of variable thickness, with a rim and blades; (b) component parts; (c) stress distribution

elements joining the plates to the ring induce tension q. Separating the ring from the central portion (Fig. 3.5b), we obtain a disk of uniform strength loaded by radial tensions σ on the edge ot thickness h_1 and a ring, acting on which are radial loadings

$$q_w = q + \varrho\Omega^2 R_w bh_2 - \sigma h_1 \frac{R}{R_w},\qquad(3.29)$$

where $R_w = R + b/2$. Inside the disk there exists a biaxial state of stress, with both principal stresses equalling σ, as a result the increment of radius R of the part of the disk without a rim

$$u = \frac{\sigma R}{E}(1-\nu)\qquad(3.30)$$

and the increment of radius R of the rim ring

$$\Delta R = \frac{q_w R_w R}{Ebh_2}.\qquad(3.31)$$

Since the continuity condition between the rim and the central portion of the disk must be observed, $\Delta R = u$, from which it follows that:

$$\frac{RR_w}{Ebh_2}\left(q + \varrho\Omega^2 R_w bh_2 - \sigma h_1 \frac{R}{R_w}\right) = \frac{R}{E}(1-\nu).$$

Most frequently, in view of the assumed dimensions of b and h_2, all that remains to be done is to determine thickness h_1. We then have

$$h_1 = \frac{R_w}{\sigma R}(q + \varrho\Omega^2 R_w bh_2) - (1-\nu)\frac{bh_2}{R}.\qquad(3.32)$$

The influence of radial stresses in the rim ring can be regarded as negligible and omitted. Circumferential stresses acting in the rim

$$\sigma_{tw} = \frac{q_w R_w}{bh_2}\qquad(3.33)$$

are calculated only after the sizes of b, h_2, R_w have previously been chosen and h_1 calculated. We can also take h_1 and, say, h_2 is given, with quantities b and R to be determined. Knowing thickness h_1 the shape of the central disk is determined from the familiar relationship (3.25).

For a more accurate calculation, it is necessary to consider the radial stresses occurring in the rim itself. These stresses on the outside radius of the tim are q/h_2 and on radius R they equal roughly $\sigma\,h_1/h_2$; hence,

$$\Delta R = \frac{R}{E}\left(\sigma_{tw} - \nu\sigma\frac{h_1}{h_2}\right).$$

Using the continuity condition, we arrive at

$$h_1 = \frac{1}{\sigma R(1+\nu b/R)}[R_w(q+\varrho\Omega^2 R_w bh_2)-(1-\nu)\sigma bh_2]. \tag{3.34}$$

It is easily seen that when $\nu b/R \ll 1$, the last expression for h_1 is transformed as before. The state of stress in the disk and in the rim is given in Fig. 3.5c.

3.4. Unheated Disk of Trapezoid Profile

Disks of trapezoid profiles, next to disk of constant thickness, are keenly used because apart from their being easy to manufacture, their dimensions can be matched so as to obtain coefficients of utilization of material approximating coefficients specific to disks of uniform strength. Presented below in general outline is the theory of such disks (Birger, 1956; Birger *et al.*, 1959; Lipka, 1967).

If half the disk thickness on arbitrary radius r is taken to be h and half the thickness measured along the z-axis is h_0 (Fig. 3.6), then with $h = h_0(1-$
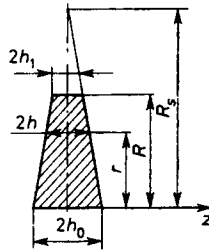
Fig. 3.6. Circular disk of trapezoid cross-section

$-r/R_s)$ satisfied, the disk is trapezoid-shaped, symmetrical, and frequently labelled conical. R_s is the radius of the bases of the two cones. Having thicknesses $2h_0$ and $2h_1$ given, it is easy to calculate radius $R_s = \dfrac{h_0}{h_0-h_1} R$, or for a disk with a hole, when half the thickness h_2 at the hole of radius R_0 and half the thickness h_1 on the outer perimeter are given,

$$R_s = \frac{h_2 R - h_1 R_0}{h_2 - h_1}.$$

Substituting the equation for the disk profile into the equation of internal equilibrium and eliminating unknowns σ_r, σ_t, by expressing them by displacement u, we obtain

$$\frac{d^2u}{dr^2} + \left(\frac{1}{r} - \frac{1}{R_s - r}\right)\frac{du}{dr} - \left(1 + \frac{rv}{R_s - r}\right)\frac{u}{r^2} + \varrho\Omega^2 r \frac{1 - v^2}{E} = 0. \qquad (3.35)$$

The solution of this equation contains hypergeometrical functions, on the basis of which we can write

$$\begin{aligned}
\sigma_r &= C_1 A + C_2 B + \varrho\Omega^2 R_s^2 F, \\
\sigma_t &= C_1 G + C_2 H + \varrho\Omega^2 R_s^2 K.
\end{aligned} \qquad (3.36)$$

In these relationships, C_1 and C_2 are the constants of integration, which are determined as always from the boundary conditions, with A, B, F, G, H, K being the functions of variable r. These functions have been calculated for different values of r and will be found in tabulated form in the literature concerned with the theory of disks (Kantorovich, 1952; Lipka, 1967; Malinin, 1962; Vainberg and Vainberg, 1959).

There are three possible cases to be considered:

— *Disks without a hole.* Since for r tending to zero, the functions B and H tend to infinity, whereas both stresses are finite and equal; hence constant $C_2 = 0$.

— *Disks with a sharp edge,* i.e., for $r/R_s = 1$, the disk thickness equals zero. In this case, quantities A and G tend to infinity. Since the two stress quantities are finite on the edge, constant $C_1 = 0$.

— *Disk without a hole and with a sharp edge.* In this case, for the very same reasons, we have both $C_1 = 0$ and $C_2 = 0$.

Radial displacements are most convenient to calculate from the familiar Eq. (3.10), although it is necessary here to calculate not only the constants but also the stress components.

All the cited relationships, values of functions — contained in tables— and conclusions remain valid when the disk is at rest ($\Omega = 0$), and only tensions or pressures are acting on its edges. Calculations for a trapezoid disk provided with a rim and hub are carried out in much the same way as for a disk of uniform strength with a rim.

3.5. Heated Disks of Constant Thickness

A disk of constant thickness h is given; it is at rest and is circularly symmetrically heated so that temperature increment T is only a function of radius r and is constant over thickness h. This increment is calculated as the difference between the initial temperature T_0 and heating temperature T_r constant throughout the disk; therefore, $T = T_r - T_0$, just as accordingly to the theory of heated thick-walled cylinders. The differential element isolated from the disk

is in equilibrium, which is given by Eq. (3.1) without the expression containing Ω.

The stress components are given by relationships (3.2) and (3.3), and the expressions containing dh/dr (this derivative equals zero) and $A = 0$ disappear. The integral of the equation thus simplified

$$u = C_1 r + \frac{C_2}{r} + \frac{1+\nu}{r} \int_{R_1}^{r} r T(r)\,dr \tag{3.37}$$

also contains two constants of integration, C_1 and C_2 with R being the radius of the disk hole. The constants of integration are determined from the boundary conditions of the problem, as with the theory of thick-walled cylinders. If the constants have been determined, then

$$\sigma_r = \frac{E}{1-\nu^2}\left[(1+\nu)C_1 - (1-\nu)\frac{1}{r^2}C_2\right] - \frac{E\alpha}{r^2}\int_{R_1}^{r} rT\,dr, \tag{3.38}$$

$$\sigma_t = \frac{E}{1-\nu^2}\left[(1+\nu)C_1 + (1-\nu)\frac{1}{r^2}C_2\right] - \frac{E\alpha}{r^2}\int_{R_1}^{r} rT\,dr - E\alpha T. \tag{3.39}$$

A more complex temperature distribution can be represented also as a sum of several simpler states, and the stresses are determined for each of them and then added up in accordance with the principle of superposition. But, it has to be remembered that the overall state of stress must satisfy Hooke's law.

We shall present further the solutions of selected, more important, cases of heated disks encountered in design practice. It should be noted that solutions obtained for cases of heated thickwalled cylinders in a plane state of stress are utilized in calculations for heated disks.

3.5.1. Solid free disk, temperature distribution according to quadratic parabola

In this case, the temperature along the radius changes in accordance with the law $T = T_R r^2/R^2$. Constants $C_2 = 0$ and $C_1 = \frac{1-\nu}{4}\alpha T_R$. Radial displacement is

$$u = \frac{1-\nu}{4}\alpha T_R\left(1 + \frac{1+\nu}{1-\nu}\cdot\frac{r^2}{R^2}\right)r$$

and stress components are

$$\sigma_r = \frac{E\alpha T_R}{4}\left(1 - \frac{r^2}{R^2}\right), \quad \sigma_t = \frac{E\alpha T_R}{4}\left(1 - 3\frac{r^2}{R^2}\right). \tag{3.40}$$

Stresses in the centre and on the outer edge of the disk are

$$\sigma_{r\,max} = \sigma_{t\,max} = \frac{E\alpha T_R}{4}, \qquad \sigma_{t\,min} = -\frac{E\alpha T_R}{2}.$$

3.5.2. Solid disks, uniformly heated with restrained rim

Notwithstanding the uniform heatings, a state of stress other than zero will occur in the disk. If the clamping of the rim is perfectly rigid, then after heating to temperature T_R (with $T_0 = 0$) we have $u = 0$ on the edge and in the centre of disk. Hence, $C_2 = 0$ and $C_1 = -\dfrac{1+\nu}{2}\alpha T_R$ and the stresses

$$\sigma_r = \sigma_t = -\frac{E\alpha T_R}{1-\nu} \tag{3.41}$$

are independent of radii r and R.

3.5.3. Disk with a hole, heated according to a quadratic parabola

The temperature distribution along the radius is $T = (T_R/R^2)r^2$. Radial displacement and stress components are

$$u = \frac{\alpha T_R}{4}\left\{(1+x_0^2)\left[(1-\nu)+(1+\nu)\frac{x_0^2}{x^2}\right]+(1+\nu)\frac{x^4-x_0^4}{x^2}\right\}r,$$

$$\sigma_r = \frac{E\alpha T_R}{4}\left[(1+x_0^2)\left(1-\frac{x_0^2}{x^2}\right)-\frac{x^4-x_0^4}{x^2}\right], \tag{3.42}$$

$$\sigma_t = \frac{E\alpha T_R}{4}\left[(1+x_0^2)\left(1+\frac{x_0^2}{x^2}\right)+\frac{x^4-x_0^4}{x^2}-4x^2\right],$$

and on the inner and outer edge

$$\sigma_{t\,max} = \frac{E\alpha T_R}{2}(1-x_0^2), \qquad \sigma_{t\,min} = -\frac{E\alpha T_R}{2}(1-x_0^2). \tag{3.43}$$

3.5.4. Two-stage disk heated according to the equation for a quadratic parabola (Fig. 3.7a)

The stresses and displacements are determined here as for mechanical loadings, thus the disk is divided into two parts (Fig. 3.7b): the central part is a solid disk, heated to temperature T_1 on radius R_1, with stresses σ_{R_1} acting on its rim of width h_1, the outer part is a disk with a hole, in which also stresses are acting but this time σ'_{R_1}. At the dividing place, i.e., on radius R_1, the stress conditions are

$$\sigma_{R_1} h_2 = \sigma'_{R_1} h_1, \qquad u_1(R_1) = u_2(R_1)$$
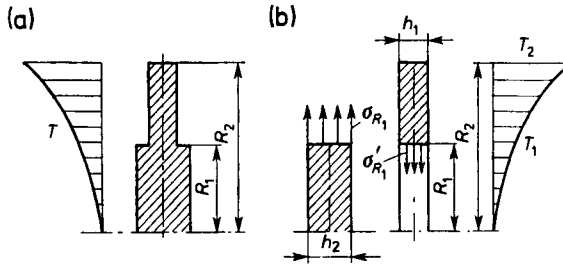
Fig. 3.7. Circular disk: (a) two-stage, heated; (b) component parts of disk

in which $u_1(R_1)$ and $u_2(R_1)$) are displacements at radius R_1. Using the prin-cinple of superposition and the results derived for individual disks, heated and unheated, but loaded on the boundaries, we obtain the equations giving the stresses in the central part, i.e., for $0 \leqslant r \leqslant R_1$

$$\sigma_r = \frac{E\alpha T_1}{4}\left(1 - \frac{r^2}{R_1^2}\right) + \frac{E\alpha T_2}{2}\;\frac{1}{(1-\nu)\dfrac{h_2}{h_1} + \dfrac{1+x_0^2}{1-x_0^2} + \nu}, \tag{3.44}$$

$$\sigma_t = \frac{E\alpha T_2}{2}\;\frac{1}{(1-\nu)\dfrac{h_2}{h_1} + \dfrac{1+x_0^2}{1-x_0^2} + \nu} + \frac{E\alpha T_1}{4}\left(1 - 3\frac{r^2}{R_1^2}\right), \tag{3.45}$$

and in the outer part, i.e., for $R_1 \leqslant r \leqslant R_2$

$$\sigma_r = \frac{E\alpha T_2}{4}\left[(1+x_0^2)\left(1 - \frac{x_0^2}{x^2}\right) - \frac{x^4 - x_0^4}{x^2}\right] + \sigma'_{R_1}\frac{x_0^2}{1-x_0^2}\left(\frac{1}{x^2} - 1\right), \tag{3.46}$$

$$\sigma_t = \frac{E\alpha T_2}{4}\left[(1+x_0^2)\left(1 + \frac{x_0^2}{x^2}\right) + \frac{x^4 - x_0^4}{x^2} - 4x^2\right] - \sigma'_{R_1}\frac{x_0^2}{1-x_0^2}\left(\frac{1}{x^2} + 1\right). \tag{3.47}$$

3.5.5. Unheated disk with strongly heated rim

We deal with such a case during a rapid start or a sudden stop of a rotating machine (Fig. 3.8); the effect is called *thermal shock*. Let the central part remain unheated ($T_0 = 0$), while the thin ring of the rim is strongly heated to temperature T_1. The stresses in the central part and in the rim ring are determined using the method cited for a heated two-stage disk. If σ_R is the stress on the circumference (of radius R) of the central part and σ_{tw} is the circumferential stress in the rim (constant in cross-section), then it follows from comparison of the displacements of the rim and the central disk of radius R that
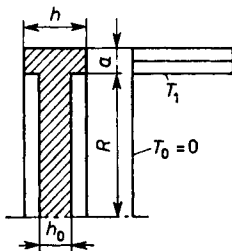
Fig. 3.8. Disk with strongly heated outer perimeter (rim)

$$\sigma_R = E\alpha T_1 \frac{1}{1-\nu+\left(\dfrac{R}{a}-\nu\right)\dfrac{h_0}{h}},$$

$$\sigma_{tw} = E\alpha T_1 \frac{1}{ah\left[1-\nu+\left(\dfrac{R}{a}-\nu\right)\dfrac{h_0}{h}\right]}.$$

(3.48)

Both stresses in the central part, circumferential and radial, equal σ_R and remain tensile, whereas the circumferential stresses in the rim are compressive. Detailed calculations show that the values of these stresses may reach the yield point even if the temperature difference is not too great (Lipka, 1967).

3.6. Disks of Variable Thickness According to the Equation of Hyperbola, Unevenly Heated and at Rest

We continue to follow the assumption adopted in Section 3.1. In view of $\Omega = 0$, the expression containing the quantity A on the right—hand side of Eq. (3.4) disappears. This equation in the case of disks of trapezoid or hyperbolic profile can be solved approximately, and the results are given in the literature in tabulated form or as ready formulae, e.g. Zhiritskii *et al.* (1963), with the principle of superposition remaining valid (Lipiński, 1972).

A disk of hyperbolic profile is given, and the assumptions are as above. The disk thickness varies in accordance with equation $h = m/r^n$, where m, $n > 0$ and the temperature distribution along the radius $T = T_1 r^2/R^2$. We put these two functions into the equation of equilibrium and obtain the differential equation

$$\frac{d^2u}{dr^2} + \frac{1-n}{r}\frac{du}{dr} - \frac{1+\nu n}{r^2}u = \alpha(1+\nu)(2-n)\frac{T_1}{R^2}r \qquad (3.49)$$

whose integral consists of two functions, $u = u_1 + u_2$. The first equals

$$u_1 = C_1 r^{k_1} + C_2 r^{k_2},$$

where

$$k_1 = \frac{n}{2} + \sqrt{\frac{n^2}{4} + 1 + \nu n}, \quad k_2 = \frac{n}{2} - \sqrt{\frac{n^2}{4} + 1 + \nu n},$$

and the second one may assume the form

$$u_2 = A + Br + Cr^2 + Dr^3.$$

This function is substituted into differential equation (3.49), thus allowing the unknown constants A, B, C, D to be determined, namely

$$A = 0, \quad B = 0, \quad C = 0, \quad D = \frac{(1+\nu)(2-n)}{8-(3+n)\nu} \alpha \frac{T_1}{R^2}.$$

The displacements are

$$u = C_1 r^{k_1} + C_2 r^{k_2} + \frac{(1+\nu)(2-n)}{8-(3+n)\nu} \alpha \frac{T_1}{R^2} r^3 \tag{3.50}$$

and the stresses are

$$\sigma_r = \frac{E}{1-\nu^2} \Bigg\{ (k_1 + \nu) r^{k_1-1} C_1 + (k_2 + \nu) r^{k_2-1} C_2 + $$

$$+ \left[\frac{(1+\nu)(2-n)}{8-(3+n)\nu} (3+\nu) - (1+\nu) \right] \alpha \frac{T_1}{R^2} r^2 \Bigg\}, \tag{3.51}$$

$$\sigma_t = \frac{E}{1-\nu^2} \Bigg\{ (1 + \nu k_1) r^{k_1-1} C_1 + (1 + \nu k_2) r^{k_2-1} C_2 + $$

$$+ \left[\frac{(1+\nu)(2-n)}{8-(3+m)\nu} (1+3\nu) - (1+\nu) \right] \alpha \frac{T_1}{R_2} r^2 \Bigg\}. \tag{3.52}$$

Both constants of integration, C_1 and C_2, are determined as always from the boundary conditions of the problem. In spite of the relatively simple temperature distribution, the relations (3.51) and (3.52) are not very simple.

3.7. The General Differential Equation for Rotating Disks of Arbitrarily Variable Thickness, Strongly Heated

In addition to the assumptions made in Section 3.1 we further assume that the characteristic material constants, such as Young's modulus E, Poisson's ratio ν and the coefficient of linear thermal expansion α are variable and temperature-dependent, and thereby they become functions of variable r.

The changes of ν are not very great and do not have a significant bearing on the accuracy of calculations. The equation of internal equilibrium (3.1) and relationships for stresses (3.38), (3.39) expressed in terms of $u(r)$ remain unchanged. Differentiating the expression for σ_r with respect to r and then introducing the derivative $d\sigma_r/dr$ and σ_r and σ_t, we arrive at the differential equation

$$\frac{du^2}{dr^2} + \frac{1}{r}\frac{du}{dr}\left[r\left(\frac{1}{h}\frac{dh}{dr} + \frac{1}{E}\frac{dE}{dr}\right)+1\right] -$$
$$-\frac{u}{r^2}\left[1-\nu r\left(\frac{1}{h}\frac{dh}{dr} + \frac{1}{E}\frac{dE}{dr}\right)\right]$$
$$= -Ar + (1+\nu)\alpha T\left[\frac{1}{h}\frac{dh}{dr} + \frac{1}{E}\frac{dE}{dr} + \frac{1}{\alpha T}\frac{d(\alpha T)}{dr}\right] \qquad (3.53)$$

determining displacements in a disk of arbitrary profile, rotating and heated, in its most general form. Very small quantities have been omitted in this equation. It has solutions in closed form only for some of the simplest cases of loading. Reduced stress at any point of the disk is determined mostly from (1.12) or (1.13), and it is necessary that $\sigma_{red} \leqslant k_r$, with the value of admissible tensile stress of material k_r depending on the degree of heating, i.e., on temperature $T(r)$ (Derski, 1958; Liszka and Życzkowski, 1976; Lokai, 1961; Szelągowski, 1958; Tuliszka, 1960; Zhiritskii et al., 1963). Particular calculations to solve Eq. (3.53) are made by approximate methods, including the finite element method with the aid of a digital computer. Having in hand full information about the properties of material, a disk of optimal shape can be designed. In practice, several solution methods are used. Some of them are discussed below.

3.7.1. Disk shape determination by Stechkin's method

Unlike other methods, this one enables the shape of a disk to be determined for predetermined strength requirements. It is, therefore, convenient in so far that repeated checking of the stresses for various successive versions of the disk shape can be avoided, which is impossible, for example, by the finite element method or with substitution by a multistage disk (Lipka, 1967).

Rotational speed of the rotor, temperature distribution along the radius $T(r)$ and outer radius of the disk are given. The initial quantities E, ν, α are taken to be constant, and the shape of the disk is to be determined for a pre-determined principal stress distribution along the radius. Let R, R_1, h_2 denote the outer radius, inner radius and width of the disk at the outer radius respectively (Fig. 3.9a). If radial tensions are acting on the circumference
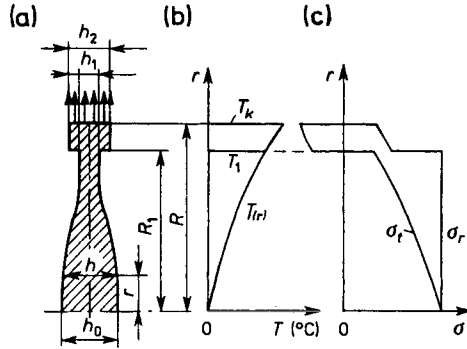
Fig. 3.9. Circular disk: (a)—of variable thickness, with a rim; (b) temperature distribution; (c) stress distribution σ_r, σ_t

of the disk, then with the predetermined, admissible stress σ_R, the width at the outer radius is given by ration $h_2 = q/\sigma_R$.

As shown in the diagram, T_k is the temperature on radius R, and the corresponding temperature in the centre of the disk is taken to equal zero. This assumption does not change in any way the situation even if the temperature in the centre of the disk were other than zero, since only temperature differences are involved in the calculations. Let the temperature along radius r change according to

$$T = T_k \left(\frac{r}{R}\right)^2 \quad \text{or} \quad T = T_1 \left(\frac{r}{R_1}\right)^2. \tag{3.54}$$

If radial stress σ_r is constant along the radius from zero to R_1 and equals k_r, then circumferential stress σ_t being related to σ_r by the familiar differential equation of compatibility of strains, is variable along the radius. Substituting $\dfrac{dT}{dr} = \dfrac{2r}{R_1^2} T_1$ and (3.2), (3.3) into this equation, we obtain

$$\frac{d\sigma_t}{dr} + (1+\nu)\frac{\sigma_t}{r} = (1+\nu)\frac{k_r}{r} - 2E\alpha T_1 \frac{r}{R_1^2}. \tag{3.55}$$

The integral of this equation is

$$\sigma_t = k_r - \frac{2E\alpha T_1}{3+\nu} \left(\frac{r}{R_1}\right)^2 + \frac{C}{r^{1+\nu}}.$$

Since the circumferential stresses in the centre of a solid disk are finite, the constant of integration is $C = 0$, and finally we have

$$\sigma_t = k_r - \frac{2E\alpha T_1}{(3+\nu)R_1^2} r^2. \tag{3.56}$$

It follows from the last relationship that in the centre of the disk, $\sigma_t = \sigma_r$ $= k_r$, whereas the circumferential stresses decrease as they approach the ring of the rim to assume on radius R_1 the value

$$\sigma_{tR_1} = k_r - \frac{2E\alpha T_1}{3+\nu}.$$

Taking the distribution of circumferential stress in the function of r

$$\sigma_t = k_r(1 - \beta x^2),$$

where $\beta = \dfrac{2E\alpha T_1}{(3+\nu)k_r}$, $x = \dfrac{r}{R_1}$, then, for example, in keeping with the distortional strain energy failure hypothesis, the reduced stresses equal

$$\sigma_{\text{red H}} = k_r \sqrt{1 - \beta x^2 + \beta^2 x^4}$$

and they are not larger than k_r in the range of temperature differences involved. It follows from the last relationship that the lowest value $\sigma_{\text{red H}}$ exists at a point with radius $r = R/\sqrt{2\beta}$ and equals $0.866\,k_r$, whereas radius R_1, i.e., directly under the ring of the rim, we have

$$\sigma_{\text{red H}} = k_r \sqrt{1 - \beta + \beta^2}.$$

Having expressed σ_t in the form of (3.56), we can proceed now to determine the profile of the disk. To this end, we substitute (3.56) into the equation of internal equilibrium and after ordering we bring it to the form

$$-k_r \frac{1}{h} \frac{dh}{dr} = \left(\varrho \Omega^2 R_1^2 + \frac{2E\alpha T_1}{3+\nu} \right) \frac{r}{R_1^2}.$$

The integral of the last equation

$$-k_r \ln h = \left(\varrho \Omega^2 R_1^2 + \frac{2E\alpha T_1}{3+\nu} \right) \frac{r^2}{2R_1^2} + C$$

is a relatively simple function, it contains only one constant C. Since for $r = 0$, we have h_0, therefore $C = -k_r \ln h_0$, and the equation for disk profile itself

$$k_r \ln \frac{h_0}{h} = \left(\varrho \Omega^2 R_1^2 + \frac{2E\alpha T_1}{3+\nu} \right) \frac{r^2}{2R_1^2}$$

contains all the design parameters used for initial data in the assumptions. When $r = R_1$, then h becomes equal to h_1 and the following relationship occurs between h_0 and h_1:

$$h_0 = h_1 e^{\left(\varrho \Omega^2 R_1^2 + 2E\alpha T_1 \frac{1}{3+\nu} \right) \frac{1}{2k_r}}. \tag{3.57}$$

It can be proved that

$$\ln \frac{h_0}{h} = \left(\frac{r}{R_1}\right)^2 \ln \frac{h_0}{h_1}. \tag{3.58}$$

Therefore, if h_1 is known, then by using Eqs. (3.57) and (3.58), we can determine directly h_0 and h at any point defined by radius r.

Consider the state of stress in the ring of the rim. The ring has a constant thickness and is unevenly heated. In terms of theory, heated rotating disks of constant thickness and with the assumed temperatures and the radial and circumferential stresses in the rim are determine from the equations

$$\sigma_r = \frac{E}{1-v} C_1 - \frac{E}{(1+v)r^2} C_2 - \frac{3+v}{8} \varrho \Omega^2 r^2 - \frac{E\alpha T_1}{r^2} \frac{r^4-R_1^4}{4R_1^2},$$

$$\sigma_t = \frac{E}{1-v} C_1 + \frac{E}{(1+v)r^2} C_2 - \frac{1+3v}{8} \varrho \Omega^2 r^2 - E\alpha T_1 + \frac{E\alpha T_1}{r^2} \frac{r^4-R_1^4}{4R_1^2}.$$

Radii R and R_1 as well as stresses σ_R on the edge of the rim ring are most frequently prescribed. Sometimes, instead of σ_R tensions q are given as

$$q = m_b \Omega^2 R_1 z \frac{1}{2\pi R},$$

where R_1 is the distance of the centre of mass of blade from the axis of rotation of disk, m_b is the weight of the blade (together with the root), and z is the number of blades. Next, we determine for the previously set thickness h_2 radial stresses σ_R on the edge of the rim ring.

If the ring is a disk with a hole, the boundary conditions and continuity conditions are then established, namely $h_1 k_r = \sigma_{R_1} h_2$, $u_t = u_w$ for $r = R_1$, and we arrive at equations whose solution gives the unknown constants C_1 and C_2 and thickness h_1 on radius R_1 of the disk. In this way, we finally determine the shape of the disk and the state of stress.

Where an unheated or uniformly heated disk is involved, all the above relationships take the form as for disk of uniform strength, kinetically loaded. The method described is relatively simple and quick.

3.7.2. Finite difference method

The equilibrium equations of the element and the relationships between radial displacement $u(r)$ and stresses σ_r and σ_t in the heated condition as

$$u = \frac{r}{E} (\sigma_r - v\sigma_t) + \alpha T r, \tag{3.59}$$

$$\frac{du}{dr} = \frac{1}{E}(\sigma_t - \nu\sigma_r) + \alpha Tr, \tag{3.60}$$

contain basically three unknowns, σ_r, σ_t and u. Considering the variability of E, ν and α, which are temperature-dependent along radius r, we differentiate Eq. (3.59) with respect to variable r and comparing the left-hand side of this equation to the left-hand side of (3.60), we obtain

$$\frac{r}{E}\left(\frac{d\sigma_t}{dr} - \nu\frac{d\sigma_r}{dr} - \sigma_r\frac{d\nu}{dr}\right) + \sigma_t\left(\frac{1}{E} + \frac{\nu}{E} - \frac{r}{E^2}\frac{dE}{dr}\right) -$$

$$- \sigma_r\left(\frac{\nu}{E} - \frac{1}{E} - \nu\frac{r}{E^2}\frac{dE}{dr}\right) - r\frac{d(\alpha T)}{dr} + \alpha T = 0. \tag{3.61}$$

Thus, two equations (3.1) and (3.61) contain only two unknowns σ_r and σ_t. We put $d\sigma_r/dr$ derived from the equation of internal equilibrium (3.1) into the last equation and in this way we obtain finally a set of two equations:

$$d\sigma_r = -\sigma_r\left(\frac{dh}{h} + \frac{dr}{r}\right) + \sigma_t\frac{dr}{r} - \varrho\Omega^2 r^2\frac{dr}{r},$$

$$d\sigma_t = \sigma_t\left(\frac{dE}{E} - \frac{dr}{r}\right) + \sigma_r\left(\frac{dr}{r} - \nu\frac{dh}{h} + d\nu - \nu\frac{dE}{E}\right) -$$

$$- \varrho\Omega^2 r^2\nu\frac{dr}{r} - Ed(\alpha T)$$

written with respect to stress differentials. Both equations are solved approximately, replacing differentials by finite differences (Lipka, 1967; Manson, 1947, 1949; Nillenson and Manson, 1948; Skubachevskii, 1955; Zhiritskii et al., 1963; Yella Reddy and Srinath, 1974), and the differential equations are transformed into difference equations

$$\sigma_{r_n} = \sigma_{t_{n-1}}\left(\frac{r_n}{r_{n-1}} - 1\right) + \sigma_{r_{n-1}}\left(3 - \frac{r_n}{r_{n-1}} - \frac{h_n}{h_{n-1}}\right) - \varrho\Omega^2 r_{n-1}^2\left(\frac{r_n}{r_{n-1}} - 1\right),$$

$$\sigma_{t_n} = \sigma_{t_{n-1}}\left(1 - \frac{r_n}{r_{n-1}} + \frac{E_n}{E_{n-1}}\right) + \tag{3.62}$$

$$+ \sigma_{r_{n-1}}\left[\frac{r_n}{r_{n-1}} - 1 - \nu_{n-1}\left(\frac{h_n}{h_{n-1}} + \frac{E_n}{E_{n-1}} - \frac{\nu_n}{\nu_{n-1}} - 1\right)\right] +$$

$$+ E_{n-1}[(\alpha T)_n - (\alpha T)_{n-1}] - \varrho\Omega^2 r_{n-1}^2\nu_{n-1}\left(\frac{r_n}{r_{n-1}} - 1\right).$$

We introduce for convenience the denotations

$$A_n = \frac{r_n}{r_{n-1}} - 1, \quad D_n = \frac{E_n}{E_{n-1}} - A_n, \quad B_n = 3 - \frac{r_n}{r_{n-1}} - \frac{h_n}{h_{n-1}},$$

$$H_n = A_n - \nu_{n-1}\left(\frac{h_n}{h_{n-1}} + \frac{E_n}{E_{n-1}} - \frac{\nu_n}{\nu_{n-1}} - 1\right), \quad C_n = \varrho\Omega^2 r_{n-1}^2 A_n,$$

$$K_n = E_{n-1}[(\alpha T)_n - (\alpha T)_{n-1}] + \nu_{n-1} C_n;$$

then

$$\sigma_{r_n} = A_n \sigma_{t_{n-1}} + B_n \sigma_{r_{n-1}} - C_n,$$

$$\sigma_{t_n} = D_n \sigma_{t_{n-1}} + H_n \sigma_{r_{n-1}} - K_n.$$

During calculations, the radius of the disk contour is divided into several segments which are numbered successively. Subscriptions n and $n-1$ serve to denote two consecutive cylindrical cross-sections corresponding to a single
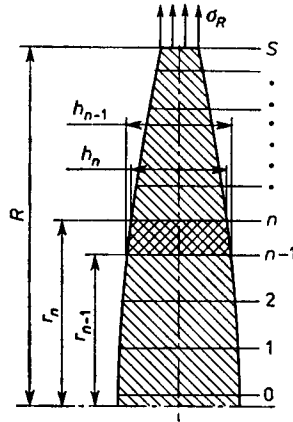
Fig. 3.10. Circular disk of variable thickness. Division of the radius into parts

arbitrary segment of the radius (Fig. 3.10) (Lipka, 1967; Manson, 1947; Skubachevskii, 1955). Three principal cases of disks are to be distinguished:

1. *Solid disk.* Equations (3.62) are singular for $r = 0$; hence the initial cross-section 0 is taken to be on a radius, for which $r_0/R = 0.05 - 0.1$. For this point, we know with fair accuracy that $\sigma_{r_0} = \sigma_{t_0} = \sigma_0$. Let

$$\sigma_{r_n} = \Phi_n \sigma_0 + \Psi_n, \quad \sigma_{t_n} = \varphi_n \sigma_0 + \psi_n. \tag{3.63}$$

The terms and coefficients in these expressions are then

$$\Phi_n = \Phi_{n-1} B_n + \varphi_{n-1} A_n, \quad \Psi_n = \Psi_{n-1} B_n + \psi_{n-1} A_n - C_n,$$

$$\varphi_n = \varphi_{n-1} D_n + \Phi_{n-1} H_n, \quad \psi_n = \psi_{n-1} D_n + \Psi_{n-1} H_n - K_n.$$

We can write for the initial cross-section that the stresses are

$$\sigma_0 = \Phi_0 \sigma_0 + \Psi_0,$$

$$\sigma_0 = \varphi_0 \sigma_0 + \psi_0$$

on account of the equality of circumferential and radial stresses in the centre of the disk. Hence, for a solid disk we have

$$\Phi_0 = 1, \quad \Psi_0 = 0, \quad \varphi_0 = 1, \quad \psi_0 = 0.$$

We start the calculations from the initial (zero) cross-section and end with extreme cross-section s, determining successively all values for Φ_n, Ψ_n, φ_n, ψ_n. Stresses σ_0 are determined as follows. There exist known stresses σ_R on the outer perimeter, induced, for example, by the action of the blades; therefore, we can write

$$\sigma_R = \Phi_s \sigma_0 + \psi_s;$$

hence

$$\sigma_0 = \frac{\sigma_R - \psi_s}{\Phi}.$$

Stresses in all cross-sections have thereby been calculated.

2. *Disk with a hole.* In this case, the initial cross-section is on a radius equalling the radius of the hole R_0. In an arbitrary cross-section the formulae (3.63) hold; in the initial cross-section, radial stresses $\sigma_{r0} = 0$, then

$$\Phi_0 \sigma_{t_0} + \Psi_0 = 0, \quad \varphi_0 \sigma_{t_0} + \psi_0 = \sigma_{t_0}$$

when we have

$$\Phi_0 = 0, \quad \Psi_0 = 0, \quad \varphi_0 = 1, \quad \psi_0 = 0;$$

hence

$$\sigma_R = \Phi_s \sigma_{t_0} + \Psi_s,$$

$$\sigma_{t_0} = \frac{\sigma_R - \Psi_s}{\Phi_s};$$

σ_R is the stress on the outer perimeter. All the other stresses are calculated in the same way.

3. *Disk with a hole into which a shaft has been force-fitted.* The initial cross-section is taken to be on radius R_0 of the hole. In an arbitrary cross-section the formulae (3.63) hold. With pressure of magnitude p present on the contact surfaces between the hole and shift, we can write

$$-p = \Phi_0 \sigma_{t_0} + \Psi_0, \quad \sigma_{t_0} = \varphi_0 \sigma_{r_0} + \psi_0$$

which is the case if $\Phi_0 = 0$, $\Psi_0 = -p$, $\varphi_0 = 1$, $\psi_0 = 0$. When the forced-in joint of the shaft with the disk is supposed to transmit a torque M_0 through friction forces, then the necessary pressure between the two contact surfaces under conditions of nominal power and revolutions should be

$$p = \frac{kM_0}{2\pi R_0^2 h_0 \mu},$$

where k is the safety factor or overload factor and R_0, h_0 are the radius of disk hole and thickness of disk at the hole, μ is the coefficient of friction. Usually, we take $k = 1.5-2.2$ and $\mu \approx 0.10$. The difference between the shaft radius and hole radius should be sufficiently great to guarantee that the yield point will not be exceeded, i.e., for example, $\sigma_{\text{red H}} < R_e$. The radius of the disk hole will obviously increase by the value

$$\Delta R_0 = R_0 \left[\frac{1}{E_0} (\sigma_{t_0} + \nu_0 p) + \alpha_0 T_0 \right]$$

and the shaft radius will correspondingly decrease by

$$\Delta R_w = R_0 \left[\frac{1}{E_w} (\sigma_{t R_0} + \nu_w p) + \alpha_w T_w) \right],$$

where E_w, ν_w, α_w are the elastic constants and coefficient of linear thermal expression of shaft material, respectively, T_0 and T_w are the temperature increments between standstill and operating conditions for radius R_0, and $\sigma_{t R_0}$ are the circumferential stresses of shaft on radius R_0. The accuracy of the calculations by this method depends on the number of segments. A large number of segments will make the calculations significantly more laborious. As practical experience bears out, a sufficient accuracy will usually be achieved at $s = 7$, and this number should be regarded as the minimum recommended. Any distances between cross-sections are allowed, but it is advisable to shorten them in the area of more marked changes of disk thickness and in the vicinity of the rim and the hub hole or near the centre of a solid disk. Generally, it is recommended that radius ratios $r_n/r_{n-1} = 1.07$ to 1.2 be abided by, and for subsequent ratio, less than 1.5. It is desirable for the thickness ratios to be kept within the limits $h_n/h_{n-1} = 0.75$ to 1.4.

If the number of segments is not very great and modulus E_{n-1} is subject to substantial changes induced by great temperature changes at successive radii r_{n-1} and r_n, the accuracy of calculations will be increased, if we use $(E_n + E_{n-1})/2$ in place of E_{n-1}. The method presented is sufficiently accurate for practical calculations, and the differences in stress values at extreme points (the hole perimeter or the centre of a solid disk) compared to exact solutions, for

$s = 8$ to 10, vary between 1.5% and 4% and they rapidly decrease as the number of divisions is increased, specifically in the area of the hub hole or the rim. With proficient computation techniques, the complete calculation of a disk takes a few hours, and the whole account is contained in a single table.

For elastic-plastic materials, a reliable criterion of service life and work safety is the magnitude of reduced (equivalent) stresses which at variable and high temperatures should not exceed, in principle, the yield point at any point of the disk.

3.7.3. A method of determining the profile of a disk with a predetermined admissible stress distribution. Disk profile optimization

By this method, all types of loading are allowed and so are all the properties of disk materials under high temperature conditions, though without creep and plastic strain (Lipka, 1961, 1967; Manson, 1947, 1949). Owing to a biaxial state of stress, reduced stresses given, for example, by

$$\sigma_{\text{red H}} = \sqrt{\sigma_r^2 + \sigma_t^2 - \sigma_r \sigma_t} \tag{3.64}$$

with the safety factor $n_b > 1$, by assumption, should not be in excess of admissible stress k_r in terms of failure of material at specified high temperatures. The admissible stress is then defined as $k_r = R_e/n_b$, where R_e is the yield-point stress. The equation of internal equilibrium for a disk element of variable thickness can be represented also in another form

$$\frac{\mathrm{d}h}{h} = \left(\frac{\sigma_t}{\sigma_r} - \varrho \frac{\Omega^2 r^2}{\sigma_r} - 1 \right) \frac{\mathrm{d}r}{r} - \frac{\mathrm{d}\sigma_r}{\sigma_r}.$$

It follows from relationships (3.59) and (3.60) that

$$\mathrm{d}\sigma_t - \mathrm{d}\sigma_r = \sigma_t \left[\frac{\mathrm{d}E}{E} - (1+\nu) \frac{\mathrm{d}r}{r} \right] +$$
$$+ \sigma_r \left[(1+\nu) \frac{\mathrm{d}r}{r} + \mathrm{d}\nu - \nu \frac{\mathrm{d}E}{E} \right] - E\mathrm{d}(\alpha T). \tag{3.65}$$

The last equation and the condition $\sigma_{\text{red H}} = k_r(r)$ do not contain unknown $h(r)$; the two can therefore make a single set of equations to be solved independent of the equation of internal equilibrium. As with the previously described finite difference method, here, differentials are replaced by finite increments, as a result of which Eq. (3.65) and strength condition (3.64) will be transformed as follows:

$$\bar{\sigma}_{t_n} - \nu_{n-1}\bar{\sigma}_{r_n} = H_n,$$ (3.66)

$$\sqrt{\bar{\sigma}_{t_n}^2 + \bar{\sigma}_{r_n}^2 - \bar{\sigma}_{t_n}\bar{\sigma}_{r_n}} = 1,$$ (3.67)

where

$$\bar{\sigma}_{t_n} = \frac{\sigma_{t_n}}{k_{r_n}}, \qquad \bar{\sigma}_{r_n} = \frac{\sigma_{r_n}}{k_{r_n}},$$

$$H_n = \frac{1}{k_{r_n}}(\sigma_{t_{n-1}} B_n + \sigma_{r_{n-1}} C_n - D_n).$$

Expression (3.66) is an equation for the straight line passing through points K and L, which are H_n and $-H_n/(n-1)$ distance from each other
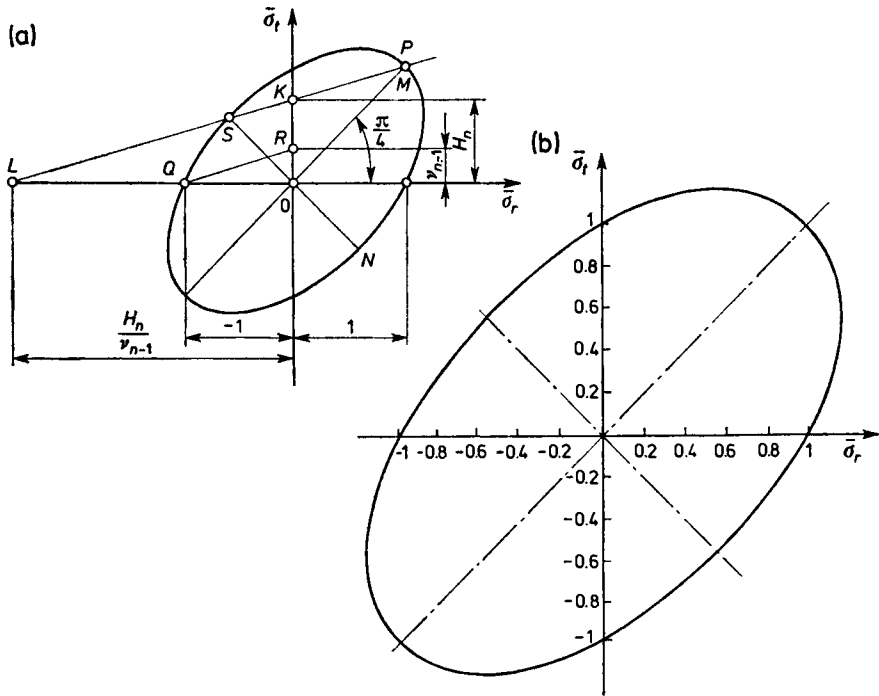
Fig. 3.11. Symmetry: (a) of stress ellipse; (b) stress ellipse (plot)

(Fig. 3.11), and the second equation represents an ellipse with its principal axis inclined at angle $\pi/4$ to axis $\bar{\sigma}_r$, with length of major axis $OM = 1.414$ and of minor axis $ON = 0.817$. Line KL intersects the ellipse at points P and S with the coordinates being the roots of the two equations, for the straight line and for of the ellipse. In the calculations, we should choose the pair of roots that appear to be physically feasible. These roots multiplied by k_{r_n}

determine uniquely stress components σ_{rn}, σ_{tn} at a given point of the disk. Dividing the equation of the straight line by H_n/v_{n-1} and denoting

$$y_n = v_{n-1}\frac{\overline{\sigma}_{tn}}{H_n}, \qquad x_n = \frac{\overline{\sigma}_{rn}}{H_n}v_{n-1},$$

we obtain the expression

$$y_n = (1+x_n)v_{n-1}$$

which is a new equation for the straight line parallel to KL and passing always through points $(-1, 0)$ and $(0, v_{n-1})$. This property can be exploited in graphical determination of the coordinates of the points of intersection of the straight line with the ellipse. Segment OL is usually so long that it stretches far beyond the diagram; in that case, it is enough to plot a straight line through points Q and R and next the line PK running parallel to it. For particular calculations of disks, we use the stress ellipse given in Fig. 3.11b. The equation of internal equilibrium reduces finally to the simple relationship

$$h_{n-1} = F_n h_n \tag{3.68}$$

as a result of converting to finite differences, and so we can calculate thickness h_n of the disk along radius r. In this relation, we have

$$F_n = \cfrac{1}{2 - \cfrac{\sigma_{rn}}{\sigma_{r_{n-1}}} - A_n\left(1 + \cfrac{\sigma_{tn}}{\sigma_{r_{n-1}}} - \cfrac{\varrho\Omega^2 r_{n-1}^2}{\sigma_{r_{n-1}}}\right)} . \tag{3.69}$$

For a solid disk in the centre, i.e., for $r = 0$, we have $\sigma_{r0} = \sigma_{t0} = k_{r0}$. Going successively from the centre to the outer perimeter, we determine the principal stress components from Eqs. (3.66), (3.67), using at the same time the plot of the stress ellipse for consecutive points of the disk radius. In this way, we reach the extreme edge with radius R, for which radial stress σ_R is derived from the calculations. This stress must be effected by tensions q_R deriving from, say, the blades. Hence, it follows that the necessary disk thickness on radius R amounts to

$$h_R = \frac{q_R}{\sigma_R}$$

and subsequently serves as the initial quantity for the thicknesses of the remaining parts of the disk subsequently determined. Therefore, Eq. (3.68) introduced earlier should be used.

Generally speaking, the method described may be regarded as a method of disk profile optimization; it is simple, convenient and as accurate as other methods, and quick in attaining the desired result.

General remarks

Usually, two or three methods are used simultaneously in the practical design of rotors. One serves as the primary calculation, the second or subsequent ones for checking the calculations. In this way, incidental errors are avoided and the accuracy is enhanced.

Using the finite difference method and Stechkin's method, we can determine the profile of a disk for particular data. The other methods described above serve in principle to check the magnitude of stresses in disks whose shapes have been designed earlier.

3.8. Torque-Induced Shear Stresses in Disks

The shaft-disk system usually transmits power N with rotational speed n in r.p.m., which corresponds to torque M_0. It is a system representing an axially symmetrical structure. Shear stresses exist in cylindrical cross-sections of the disk on radius r, their mean value being

$$\tau_{rz} = \frac{M_0}{2\pi r^2 h}. \tag{3.70}$$

Next to these stresses, stresses of the same kind but caused by inertia of the disk occur also during start or approaching a standstill. For example, during start there are angular acceleration $d\Omega/dt$ which also induce moment M_r in a cylindrical cross-section of radius r, equalling the moment deriving from inertia of part of the disk.

Maximum shear stresses exist on a circumference with a radius equalling the shaft radius R_0 and they are the sum of the stresses due to M_0 and $M_{r\,max}$.

Where high accuracy of calculations is required, also the moment of inertia of all blades with respect to the z-axis is considered. Strength (effort) calculations then take into account also maximum τ_{rz} (Lipka, 1967).

3.9. Heated Rotating Disks under Pressure

If pressure $p(r)$ is present on a surface so that it can be brought down to the mid-layer, then in principle such a carrying element works simultaneously as a rotating disk and as a plate. This is the case in rotor structures. Generally speaking, the wall may have thickness h either constant or varying along radius r, and there may be a rim on the outer perimeter to mount the blades.

Assuming that E, ν, α are temperature-independent and the deflections are finite, we can write for the mid-layer relationships (2.91) and (2.92),

and for the layer with the coordinate z—relationships (2.76) and (2.77). Simultaneously, ε_r and ε_t satisfy Eqs. (1.4), (1.5) with $\sigma_z = 0$. Thus, converting equations of internal equilibrium written for projections of forces along the z-axis and for moments of a disk-plate element acting on it in a deformed state, we obtain three differential equations

$$\frac{dn}{dr} + \frac{1}{r}(n-t) = -Arh(r),\tag{3.71}$$

$$\frac{dq}{dr} + \frac{q}{r} = p(r),\tag{3.72}$$

$$\frac{dm_r}{dr} + \frac{1}{r}(m_r - m_t) + q - n\frac{dw}{dr} = 0,\tag{3.73}$$

where cross-sectional forces n and t are expressed by the integrals for stresses σ_r and σ_t in the radial and circumferential cross-section of the disk-plate, q are the transverse (shearing) forces, m_r and m_t are the bending moments, and $A = \varrho\Omega^2$. By successive substitutions and by reduction of the number of unknowns, we arrive at equations written with respect to w and u and then at the stress and strain components sought (Birger, 1956, 1961; Birger et al., 1959; Bezukhov, 1968; Kovalenko, 1959; Malinin, 1959; Yella and Srinath, 1974).

3.10. Axially Symmetrical Orthotropic Disks

Axially symmetrical orthotropic disks are distinguished by different values of Young's moduli and Poisson's numbers in radial and circumferential directions. They change the form of Hooke's relationships.

Sometimes radially ribbed disks (centrifugal-action impellers) cross-type ribbed disks and even disks with circumferential ribs are reduced to being orthotropic. Such equivalent representations of real disks yield solutions, though only approximate, and theory and later calculations must satisfy additional conditions, for example, conditions of density or concentrations. There is relatively little literature available on the subject (Birger, 1961; Bezukhov, 1968; Kovalenko, 1959; Leyko et al., 1972; Misra, 1975).

4. Axially Symmetrical Shells

Shells are rated high among axially symmetrical carrying elements for their definite advantages, such as lightness, considerable stiffness, simple manufacturing technology and ease of application in many structures. Principal loadings occurring in shells are surface forces (pressure of gases or liquids), forces of thermal origin, and also body forces if the shell is in rotary motion. These loadings are axially symmetrical for the most part, which greatly simplifies theory and subsequent calculations.

The analysis of internal forces and strains in very thin axially symmetrical shells is relatively simple if stresses are assumed to be uniformly distributed over the wall thickness, with bending moments practically equalling zero. We deal then with membrane theory of shells. Furthermore, if shells vary slightly in thickness and there are no fastenings on the edges, whilst the loading itself is continuous and constant or only slightly variable, then the use of membrane theory for calculations also yields good results. In other cases, correct solutions are obtainable based on general bending theory of shells, since considerable local bending moments and transverse forces develop at sites of change in thickness in the area of the edges, at connecting sites of various elements, thus causing increased stresses.

It should be noted that the thinner the shell is compared to the dimensions in the direction perpendicular to the axis of circular symmetry, the smaller will be the error made when using the relationships of membrane theory for calculations. In this section, as in previous ones, stability problems of shells elements will not be considered.

4.1. General Equations of Equilibrium of Shell Element

Engineering theory of shells can be used in the considerations. It has ample literature, e.g. Bielak (1976), Bezukhov (1968), Chernina (1968), Chernykh (1964), Flügge (1956), Girkmann (1956), Hampe (1963), Hodge (1960), Kats (1966), Kan (1966), Kantorovich (1952), Korolev (1971), Kovalenko *et al.*

(1961), Novozhilov (1951), Collected Work (1971), Prokopovich *et al.* (1967), Tikhomirov (Ed.) (1967), Timoshenko and Goodier (1951), Timoshenko and Woinowsky-Krieger (1959), Volmir (1956), Volk (1965), Voloshin and Samsonov (1968).

The curved line of the shell, *KL*, rotating about *x*-axis produces an axially symmetrical surface of revolution (Fig. 4.1a). The plane band of width *h*
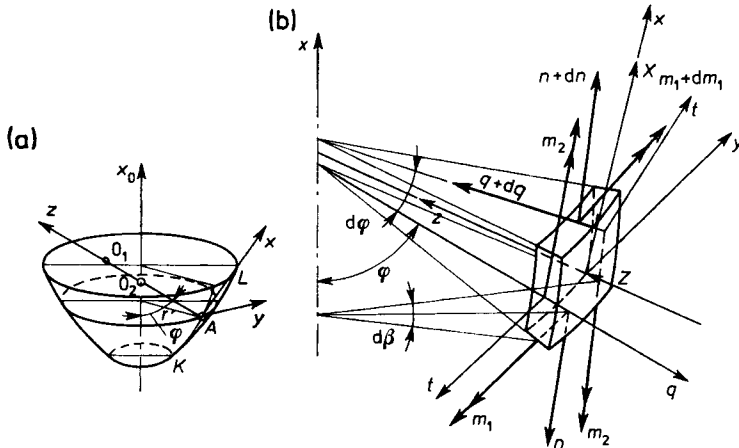
Fig. 4.1. Shell of revolution: (a) geometry; (b) shell element

containing this line as mid-line forms a shell as it revolves. The plane passing through axis of rotation x_0 cuts across the surface along the meridian. This is a meridional cross-section. Planes perpendicular to the axis or conical surfaces form latitudinal cross-sections. Two principal radii of curvature exist at given point *A* of the surface: R_1—meridional and R_2—in the plane perpendicular to the plane of the meridian. The centre of the curvature with radius R_1 lies at point O_1, and for R_2, at point O_2. Point O_2 is located on the axis of rotation and both points, O_1 and O_2, are on a single straight line perpendicular to the plane tangent to the surface at point *A*. Angle φ and radius R_2 give the position of the point on the meridian.

The relationship $r = R_2 \sin \varphi$ occurs between radii r and R_2, whereas the length of the arcs on the curve of the meridian and in the cross-section perpendicular to the meridian cross-section $dl_1 = R_1 d\varphi$, $dl_2 = R_2 \sin \varphi d\beta$ and the surface of element $dF = dl_1 dl_2 = R_1 R_2 \sin \varphi d\varphi d\beta$.

The following assumptions are established:
— the wall thickness is constant,
— the shell is completely axially symmetrical,
— a plane state of stress exists at any point of the wall, i.e., the stress compo-

nent normal to the surface is neglected, being very small compared to all other components,

— Hooke's law holds at every point of the shell,

— the initial state of stress is absent,

— the temperature satisfies the condition of axial symmetry and, generally speaking, is a function of r and x (x_0—axis of circular symmetry),

— the shell rotates at constant angular velocity Ω about the axis of circular symmetry,

— the strains and displacements experienced by points of the mid-layer of the shell are small,

— the material is homogeneous and isotropic, quantities E, ν, α constant.

These assumptions are common to shells in membrane state and general bending state irrespective of the shapes of the generatrices.

A shell of revolution of thickness h is given, sufficiently thin ($h \ll R_1, R_2$), whose central surface has been formed in the manner described above. An element is cut out of this shell as shown in Fig. 4.1b. Acting on the lateral walls are normal forces n, t, transverse force q, and bending moments m_1, m_2, as well as their increments referred to unit length of the cross-section. Denotations are: n—meridional forces, t—circumferential force, m_1, m_2—bending moments, meridional and circumferential. The external loading is continuous, axially symmetrical by assumption, and in its action on an infinitesimal element of the shell it amounts to component forces X and Z, their directions conforming to the directions of the x-axis and z-axis of the orthogonal coordinate system associated with point A. The equilibrium conditions of the element written for projections of the forces acting along the x- and z-axes and for the moments—after reducing and dividing both sides of the respective equations by $d\varphi$ and $d\beta$ are as follows:

$$\frac{d(nR_2 \sin\varphi)}{d\varphi} - tR_1 \cos\varphi - qR_2 \sin\varphi + XR_1 R_2 \sin\varphi = 0, \tag{4.1}$$

$$\frac{d(qR_2 \sin\varphi)}{d\varphi} + tR_1 \sin\varphi + nR_2 \sin\varphi + ZR_1 R_2 \sin\varphi = 0, \tag{4.2}$$

$$\frac{d(m_2 R_2 \sin\varphi)}{d\varphi} - m_1 R_1 \cos\varphi - qR_1 R_2 \sin\varphi = 0. \tag{4.3}$$

The normal stresses in the extreme layers along x and y, induced by the normal forces and bending moments acting, are

$$\sigma_1 = \frac{n}{h} \pm \frac{6m_1}{h^2} \quad \text{and} \quad \sigma_2 = \frac{t}{h} \pm \frac{6m_2}{h^2} \tag{4.4}$$

which is consistent with the assumption that the normal stresses from forces n are uniformly distributed in the cross-section. Mean shear stresses are

$$\tau_{zx} = \frac{q}{h}.$$

The above equations derived from the equilibrium conditions of the shell element are the basis of the bending theory of axially symmetrical shells.

4.2. Axially Symmetrical Shells in Membrane State

As indicated above, the influence of bending moments m_1 and m_2 on the overall state of stress and strain is slight in many cases and can be neglected. If this is the case, transverse force q becomes practically equal to zero, and the set of equations of equilibrium reduces two equations

$$\frac{d(nR_2\sin\varphi)}{d\varphi} - tR_1\cos\varphi + XR_1R_2\sin\varphi = 0, \tag{4.5}$$

$$tR_1 + nR_2 + ZR_1R_2 = 0$$

of a much simpler form. Multiplying both sides of the second equation by $\cos\varphi$ and adding by sides to the first one, we obtain a single differential equation,

$$\frac{d(nR_2\sin\varphi)}{d\varphi} + nR_2\cos\varphi + (X\sin\varphi + Z\cos\varphi)R_1R_2 = 0. \tag{4.6}$$

The differential increment of radius r equals

$$dr = d(R_2\sin\varphi) = R_2\cos\varphi\,d\varphi + \sin\varphi\,dR_2,$$

and that same increment is also

$$dr = dl_1\cos\varphi = R_1\cos\varphi\,d\varphi,$$

therefore

$$\frac{dR_2}{d\varphi} = (R_1 - R_2)\frac{\cos\varphi}{\sin\varphi},$$

Subsequently, we put this relationship into Eq. (4.6) and after integrating, we arrive at the first equilibrium equation of shell in the form

$$nR_2\sin^2\varphi + \int R_1R_2(Z\cos\varphi + X\sin\varphi)\sin\varphi\,d\varphi = C. \tag{4.7}$$

Constant C is determined as usually from the conditions written for the shell edges. Dividing both sides of Eq. (4.5b) by the product of radii R_1 and R_2, we arrive at the second equation of equilibrium

$$\frac{n}{R_1} + \frac{t}{R_2} = -Z. \tag{4.8}$$

The first equation specifies the equilibrium conditions of a part of the shell or of the whole shell, with the loadings on the edges considered, and the second equation is the equation of equilibrium for an element inside the shell. Both equations are sufficient to determine the internal forces at any place of a shell of revolution of arbitrary shape, axially symmetrically loaded, since they contain only two unknowns, n and t.

4.3. Particular Cases of Shells of Revolution in Membrane State

Considered below are some commonly used shells in membrane state of stress. Let pressure normal to the mid-surface of the shell be the loading (Flügge, 1956; Hampe, 1963; Lipka, 1967; Löffler, 1961; Ponomarev et al., 1958). In keeping with this assumption, the components of external loading are $Z = -p$, $X = 0$. If the shell is closed on one side, then the first equation of equilibrium changes to

$$nR_2 \sin^2\varphi - \int_0^\varphi R_1 R_2 p \sin\varphi \cos\varphi \, d\varphi = 0 \tag{4.9}$$

and in the case of pressure p being constant, the normal cross-sectional force is expressed as

$$n = \frac{p}{R_2 \sin^2\varphi} \int_0^\varphi r \, dr = \frac{pR_2}{2} \tag{4.10}$$

since

$$dr = R_1 \cos\varphi \, d\varphi, \quad r = R_2 \sin\varphi.$$

It follows from the equilibrium equation of the element that the magnitude of the circumferential force is

$$t = n\left(2 - \frac{R_2}{R_1}\right). \tag{4.11}$$

4.3.1. Conical shell (Fig. 4.2)

One radius, $R_1 = \infty$ and the other, $R_2 = r/\cos\varphi$; consequently,

$$\sigma_1 = \frac{pr}{2h\cos\varphi}, \qquad \sigma_2 = \frac{pr}{h\cos\varphi}. \tag{4.12}$$
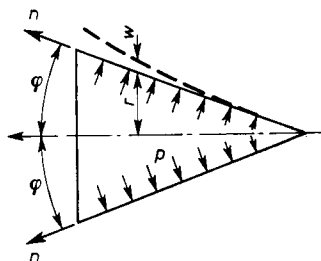
Fig. 4.2. Thin-walled conical shell

Unit elongations in the direction of the principal stresses equal

$$\varepsilon_1 = (1-2\nu)\frac{pr}{2hE\cos\varphi},$$

$$\varepsilon_2 = (2-\nu)\frac{pr}{2hE\cos\varphi}. \tag{4.13}$$

The increment of radius r of the shell is

$$w = (2-\nu)\frac{pr^2}{2hE\cos\varphi}. \tag{4.14}$$

4.3.2. Arbitrary shell of revolution rotating about its axis (e.g. Fig. 4.3)

An element of the shell of unit area, of thickness h, and of radial coordinate r is under centrifugal force

$$p_0 = \varrho\Omega^2 hr,$$
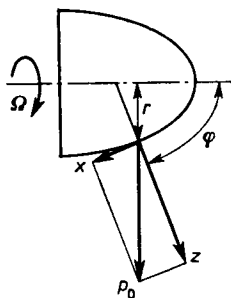
Fig. 4.3. Rotating thin-walled shell

whose components are

$$X = \varrho\Omega^2 hR_2 \sin\varphi\cos\varphi, \quad Z = \varrho\Omega^2 hR_2 \sin^2\varphi.$$

It follows from the equilibrium condition that at any point, $n = 0$; substituting this into the equilibrium equation of the element, we obtain the relationships for the circumferential force and stress

$$t = \sigma_2 h, \quad \sigma_2 = \varrho\Omega^2 r^2. \tag{4.15}$$

4.3.3. Toroidal shell (Fig. 4.4a)

Acting inside is pressure p. The radius of curvature R_1 is constant. For points of the shell in the 1st quadrant of the cross-section we have $0 \leqslant \varphi_1$
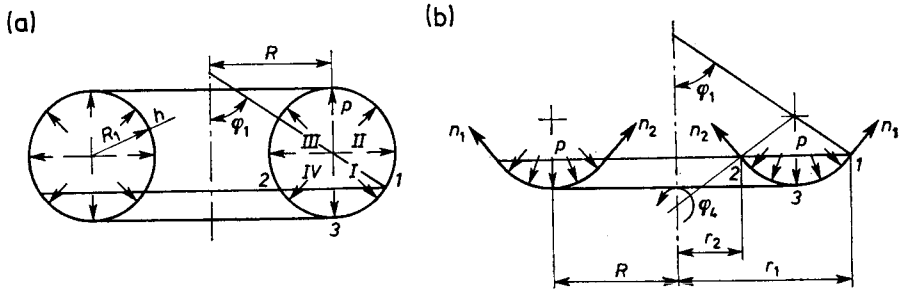
Fig. 4.4. Thin-walled shell: (a) toroidal; (b) part of the shell

$\leqslant \pi/2$, in the 2nd quadrant, $\pi/2 \leqslant \varphi_2 \leqslant \pi$, in the 3rd quadrant, $\pi \leqslant \varphi_3 \leqslant \frac{3}{2}\pi$ and in 4th quadrant, $\frac{3}{2}\pi \leqslant \varphi_4 \leqslant 2\pi$. Hence, it follows that radius R_2 becomes positive for the shell parts corresponding to the 1st and 2nd quadrants and negative for the remaining one, and it equals

$$R_2 = \frac{R}{\sin\varphi} + R_1 .$$

Cutting off a part of the shell having the length of the arc between points *1–3* and *2–3* (Fig. 4.4b), for radii r_1 and r_2, we can write the equations $r_1 = R + R_1 \sin\varphi_1$, $r_2 = R + R_1 \sin\varphi_4$, whereas the equations of equilibrium for the parts of the shell cut out

$$2\pi r_1 n_1 \sin\varphi_1 = \pi(r_1^2 - R^2)p,$$

$$2\pi r_2 t \sin\varphi_4 = \pi(R^2 - r_2^2)p$$

give after substituting the expressions for r_1 and r_2, the following relationship for the cross-sectional shell force:

$$n_1 = \frac{pR_1}{2} \frac{2 + \dfrac{R_1}{R}\sin\varphi_1}{1 + \dfrac{R_1}{R}\sin\varphi_1}. \tag{4.16}$$

We obtain the quantity t from the above equation putting angle φ_4 in place of φ_1. It follows from the equilibrium equation of the element that

$$t = \frac{pR_1}{2} \tag{4.17}$$

and it is independent of the coordinates of the position of the element on the shell. These relationships yield good results, if $R \geqslant 2R_1$. The displacements along the radius are calculated as before (Bulgakov, 1962).

4.4. Axially Symmetrical Shells in Bending State. Spherical and Conical Shells

The considerations below are based on the engineering theory of bending of shells of revolution, which differs from the preceding one in allowing for bending moments (Bielak, 1976; Berenov, 1959; Birger, 1956, 1961; Flügge, 1956; Hampe, 1963; Kats, 1956; Kan, 1966; Kantorovich, 1952; Kolkunov, 1963; Korotkin et al., 1955; Kuhn, 1956; Novozhilov, 1951; Collected Work, 1971; Prokopovich et al., 1967; Saranse et al., 1954; Timoshenko and Woinowsky-Krieger, 1959).

A shell element of length dl along the meridional cross-section (Fig. 4.5a) moves under the loadings to a new position, whereas segment AB corresponding to the layer z distance from the mid-layer experiences elongations
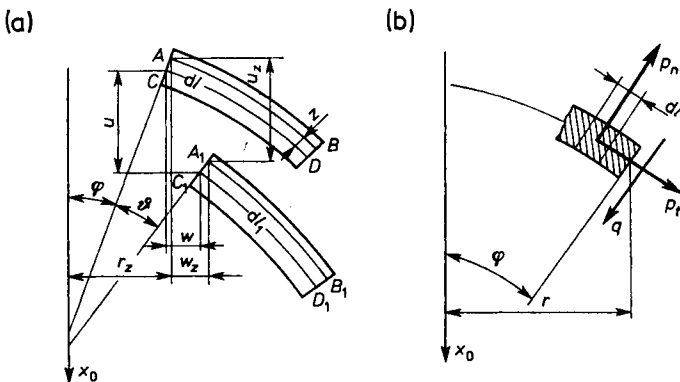
Fig. 4.5. Axially symmetrical shell: (a) displacement of shell element; (b) forces acting on element

and equals $A_1 B_1$. Let u_z and w_z be the displacements of point A in the axial and radial direction and let u and w be displacements of the same kind for point C lying in the mid-layer. Along with these displacements, rotation of the cross-section will take place by angle v. Denoting by ε_{1z}, ε_{2z} the elementary elongations in the meridional and circumferential direction of the layer with the coordinate z we can write

$$A_1 B_1 = (1 + \varepsilon_{1z}) AB, \quad dl_1 = (1 + \varepsilon_1) dl.$$

The displacements of points C and D are connected through the relations

$$w + dl(1 + \varepsilon_1) \cos(\varphi + \vartheta) = (w + dw) + dl \cos\varphi,$$

$$u + dl(1 + \varepsilon_1) \sin(\varphi + \vartheta) = (u + du) + dl \sin\varphi$$

which are derived from the geometry of strains and displacements of the shell element. Angle ϑ is small compared to φ; therefore, we can assume

$$\cos(\varphi + \vartheta) \approx \cos\varphi - \vartheta \sin\varphi,$$

$$\sin(\varphi + \vartheta) \approx \sin\varphi + \vartheta \cos\varphi.$$

Bearing in mind that $dl = R_1 d\varphi$, we arrive at the following differential equations:

$$\frac{1}{R_1} \frac{dw}{d\varphi} = \varepsilon_1 \cos\varphi - \vartheta \sin\varphi,$$

$$\frac{1}{R_1} \frac{du}{d\varphi} = \varepsilon_1 \sin\varphi + \vartheta \cos\varphi$$

$$(4.18)$$

with respect to displacement components u and w.

Similarly we obtain

$$\frac{1}{R_1 + z} \frac{dw_z}{d\varphi} = \varepsilon_{1z} \cos\varphi - \vartheta \sin\varphi, \tag{4.19}$$

$$\frac{1}{R_1 + z} \frac{du_z}{d\varphi} = \varepsilon_{1z} \sin\varphi - \vartheta \cos\varphi \tag{4.20}$$

for the layer parallel to the mid-layer. The following two relationships exist between displacements of points A and C

$$w_z = w + z\vartheta \cos\varphi, \quad u_z = u + z\vartheta \sin\varphi, \tag{4.21}$$

the first of which we put into Eq. (4.19) in place of w_z, obtaining

$$\frac{1}{R_1 + z} \frac{dw}{d\varphi} + \frac{z}{R_1 + z} \frac{d}{d\varphi}(\vartheta \cos\varphi) = \varepsilon_{1z} \cos\varphi - \vartheta \sin\varphi. \tag{4.21a}$$

Since according to (4.18)

$$\frac{dw}{d\varphi} = (\varepsilon_1 \cos\varphi - \vartheta \sin\varphi) R_1 ,$$

therefore, substituting it into (4.21a) and neglecting z with respect to R_1, we obtain

$$\varepsilon_{1z} = \varepsilon_1 + \frac{z}{R_1}\frac{d\vartheta}{d\varphi} .$$

Radius r_z experiences increment w_z; hence

$$\varepsilon_{2z} = \frac{w_z}{r_z} ,$$

but $r_z = (R_2 + z)\sin\varphi$, which leads to

$$\varepsilon_{2z} = \frac{w_z}{(R_2 + z)\sin\varphi} . \tag{4.22}$$

We have a similar relation for the mid-layer

$$\varepsilon_2 = \frac{w}{R_2 \sin\varphi} . \tag{4.23}$$

We put in place of w_z in Eq. (4.22) the first expression from (4.21), resulting in

$$\varepsilon_{2z} = \varepsilon_2 + z\frac{\vartheta}{R_2}\cot\varphi$$

and relationships (4.18), (4.19) and (4.23) reduce to the differential equation

$$\frac{d}{d\varphi}(R_2\,\varepsilon_2) - (R_1\,\varepsilon_1 - R_2\,\varepsilon_2)\cot\varphi + R_1\,\vartheta = 0. \tag{4.24}$$

A two-dimensional state of stress exists in the layer parallel to the mid-layer, for which the relations between stresses and elongations have the familiar form

$$\sigma_{1z} = \frac{E}{1-\nu^2}(\varepsilon_{1z} + \nu\varepsilon_{2z}), \qquad \sigma_{2z} = \frac{E}{1-\nu^2}(\varepsilon_{2z} + \nu\varepsilon_{1z}) .$$

Using the previously derived relations for elementary elongations ε_{1z}, ε_{2z}, we obtain the following relationships expressing the stress components:

$$\sigma_{1z} = \frac{E}{1-\nu^2}\left[\varepsilon_1 + \nu\varepsilon_2 + z\left(\frac{1}{R_1}\frac{d\vartheta}{d\varphi} + \frac{\nu\vartheta}{R_2}\cot\varphi\right)\right],$$

$$\sigma_{2z} = \frac{E}{1-\nu^2}\left[\varepsilon_2 + \nu\varepsilon_1 + z\left(\frac{\vartheta}{R_2}\cot\varphi + \frac{1}{R_1}\frac{d\vartheta}{d\varphi}\right)\right].$$

The resultants in cross-sections of the shell reduce to cross-sectional forces n and t and bending moments m_1 and m_2 acting along the meridian and the parallel

$$n = \int_{-h/2}^{h/2} \sigma_{1z} dz = \frac{Eh}{1-v^2}(\varepsilon_1 + v\varepsilon_2),$$

$$t = \int_{-h/2}^{h/2} \sigma_{2z} dz = \frac{Eh}{1-v^2}(\varepsilon_2 + v\varepsilon_1),$$

$$m_1 = -\int_{-h/2}^{h/2} z\sigma_{1z} dz = -D\left(\frac{1}{R_1}\frac{d\vartheta}{d\varphi} + v\frac{\vartheta}{R_2}\cot\varphi\right),$$

$$m_2 = -\int_{-h/2}^{h/2} z\sigma_{2z} dz = -D\left(\frac{\vartheta}{R_2}\cot\varphi + \frac{v}{R_1}\frac{d\vartheta}{d\varphi}\right),$$

whose values depend only on the components of the state of strain and on the displacements of the mid-layer. The quantity $D = \dfrac{Eh^3}{12(1-v^2)}$ is termed, as in the case of plates, the *bending rigidity* of shell.

It follows from the earlier considerations that elongations of the mid-layer can be represented as

$$\varepsilon_1 = \frac{1}{Eh}(n-vt), \qquad \varepsilon_2 = \frac{1}{Eh}(t-nv).$$

Putting those expressions into (4.24), we obtain the differential equation

$$\frac{d}{d\varphi}[R_2(n+vt)] - [n(R_1+vR_2) - t(R_2+vR_1)]\cot\varphi + EhR_1\vartheta = 0. \qquad (4.25)$$

Acting in the parallel cross-section are normal forces n and transverse forces q, in which they are interrelated through the equation of equilibrium written for the cut-off part (Fig. 4.5b), namely

$$2\pi r(n\sin\varphi + q\cos\varphi) = 2\pi\int (p_n\cos\varphi - p_t\sin\varphi)r\,dl + C$$

which contain the constant of integration C with a value corresponding to the external force parallel to the axis of the shell and distributed uniformly on any radius. Using the first equilibrium equation of the general theory of shells of revolution, we can write

$$R_2\sin\varphi(n\sin\varphi + q\cos\varphi) = C + \int R_1 R_2 \sin\varphi(p_n\cos\varphi - p_t\sin\varphi)d\varphi.$$

If the right-hand side is denoted by $F(\varphi)$, we then have

$$n = \frac{F(\varphi)}{R_2 \sin^2\varphi} - q\cot\varphi.$$

We put normal force n thus determined into the equilibrium equation of element

$$\frac{n}{R_1} + \frac{t}{R_2} + \frac{1}{R_1 R_2 \sin\varphi} \frac{d}{d\varphi}(qR_2 \sin\varphi) = p_n$$

and finally, we obtain

$$t = p_n R_2 - \frac{F(\varphi)}{R_1 \sin^2\varphi} - \frac{1}{R_1} \frac{d}{d\varphi}(qR_2).$$

Denoting for convenience $qR_2 = V$ and introducing this quantity, V together with the expressions for n and t into Eq. (4.25), we arrive at

$$EhR_1\vartheta = \frac{R_2}{R_1}\frac{d^2V}{d\varphi^2} + \left[\frac{R_2}{R_1}\cot\varphi + \frac{d}{d\varphi}\left(\frac{R_2}{R_1}\right)\right]\frac{dV}{d\varphi} - V\frac{R_1}{R_2}\cot^2\varphi -$$

$$- \nu V\left[\cot^2\varphi + h\frac{d}{d\varphi}\left(\frac{\cot\varphi}{h}\right)\right] + \frac{F(\varphi)}{\sin^2\varphi}\left[\left(\frac{R_1}{R_2} - \frac{R_2}{R_1}\right)\cot\varphi + \right.$$

$$\left. + h\frac{d}{d\varphi}\left(\frac{R_2}{R_1 h} + \frac{\nu}{h}\right)\right] - h\frac{d}{d\varphi}\left(\frac{R_2^2}{h}p_n\right) - (R_2 + \nu R_1)R_2 p_t, \quad (4.26)$$

this being the first equation of the theory of shells of revolution. Putting the expressions for bending moments m_1 and m_2 into the equilibrium equation of moments we get the second equation of theory of shells

$$\frac{R_2}{R_1}\frac{d^2\vartheta}{d\varphi^2} + \left[-\frac{R_2}{R_1}\cot\varphi + \frac{d}{d\varphi}\left(\frac{R_2}{R_1}\right)\right]\frac{d\vartheta}{d\varphi} - \frac{R_1}{R_2}\vartheta\cot^2\varphi - \vartheta\nu = \frac{R_1}{D}V. \quad (4.27)$$

Equations (4.26) and (4.27) make a set of two general differential equations of shells of revolution in bending state subject to axially symmetrical loadings.

4.5. Some Important Cases of Shells in Bending State

Spherical shells which are of special importance in engineering, are considered in detail in two cases: under a constants pressure and under centrifugal forces (Kantorovich, 1952; Lipka, 1967; Ponomarev et al., 1958).

4.5.1. Shell under constant pressure

$Z = -p$. In this case, both equations take a relatively simple form,

$$\frac{d^2V}{d\varphi^2} + \frac{dV}{d\varphi}\cot\varphi - (\cot^2\varphi - \nu)V = EhR\vartheta,$$

$$\frac{d^2\vartheta}{d\varphi^2} + \frac{d\vartheta}{d\varphi}\cot\varphi - (\cot^2\varphi + \nu)V = \frac{R}{D}V \qquad (4.28)$$

since $R_1 = R_2 = R$. This set of equations has a zero solution, and consequently, also transverse force $q = 0$. Hence, it follows that:

$$n = \frac{pR}{2}, \qquad t = \frac{pR}{2}$$

and

$$m_1 = m_2 = \frac{ph^2}{24},$$

whereas the displacement components are

$$u_1 = C_1 \sin\varphi, \qquad w_1 = C_1 \cos\varphi + \frac{1-\nu}{2hE}pR^2.$$

When $\varphi = \pi/2$, then $u_1 = C_1$ and

$$w_1 = w = \frac{1-\nu}{2hE}pR^2,$$

where w are displacements along the radius r.

4.5.2. Shell under centrifugal forces

The components are

$$X = \varrho h\Omega^2 R\sin\varphi\cos\varphi, \qquad Z = -\varrho h\Omega^2 R\sin^2\varphi.$$

The differential equations

$$\frac{d^2V}{d\varphi^2} + \frac{dV}{d\varphi}\cot\varphi - (\cot^2\varphi - \nu)V = hRE\vartheta + (3+\nu)\varrho h\Omega^2 R^3\sin\varphi\cos\varphi, \quad (4.29)$$

$$\frac{d^2\vartheta}{d\varphi^2} + \frac{d\vartheta}{d\varphi}\cot\varphi - (\cot^2\varphi + \nu)\vartheta = \frac{R}{D}V \qquad (4.30)$$

obtained from (4.26) and (4.27) can be solved assuming that the integrals are in the form

$$V = \frac{1}{2}A\sin 2\varphi, \qquad \vartheta = \frac{1}{2}B\sin 2\varphi$$

which leads to the following constants

$$A = \varrho h \Omega^2 \frac{(3+\nu)(5+\nu)DR^3}{(\nu^2-25)D - hER^2}, \quad B = \varrho h \Omega^2 \frac{(3+\nu)R^4}{(\nu^2-25)D - hER^2}$$

and to the relationships expressing the cross-sectional forces and moments

$$n = -\frac{A}{R}\cos^2\varphi, \quad t = -\frac{A}{R}\cos 2\varphi + \varrho \Omega^2 h R^2 \sin^2\varphi, \quad q = \frac{A}{2R}\sin 2\varphi,$$

$$m_1 = -\frac{BD}{R}(\cos 2\varphi + \nu \cos^2\varphi), \quad m_2 = -\frac{BD}{R}(\cos^2\varphi + \nu \cos 2\varphi).$$

The displacement components along the generatrix and normal to the surface are

$$u_1 = (A + \varrho \Omega^2 h R^3)\frac{1+\nu}{2hE}\sin 2\varphi,$$

$$w_1 = -(A + \varrho \Omega^2 h R^3)\frac{1+\nu}{hE}\cos^2\varphi - \frac{1}{hE}[A(\cos 2\varphi - \nu \cos^2\varphi) - \varrho \Omega^2 h R^3 \sin^2\varphi].$$

If $\varphi = \pi/2$, then $u_1 = 0$ and in that case

$$w_1 = w = \frac{1}{hE}(A + \varrho \Omega^2 h R^3).$$

Following a similar procedure to that previously described, we can solve the problem of determining internal forces and strains in conical and other types of shells. The above two cases, classed as very simple, illustrate adequately the difficulties encountered if the bending theory of shells is used.

Comparing the results obtained based on membrane and bending theory for shells identically loaded, we come to the practical conclusion, that in most cases, the differences are not very great and can be neglected without running into major error. However, they become quite considerable if the loadings are acting on the edges of shells.

4.6. Axially Symmetrical Shells Loaded on the Edges

As investigations bear out, the influence of loading uniformly distributed along an edge on stresses in the shell is considerable, especially in the area of the edge concerned. Assuming that the external, surface loadings equal zero, i.e., $Z = 0$, $X = 0$, and bearing in mind the principle of superposition, we can transform the differential equations of bending theory to

$$\frac{R_2}{R_1}\frac{d^2V}{d\varphi^2}+\left[\frac{d}{d\varphi}\left(\frac{R_2}{R_1}\right)+\frac{R_2}{R_1}\cot\varphi\right]\frac{dV}{d\varphi}-\left(\frac{R_1}{R_2}\cot^2\varphi-\nu\right)V = hER_1\vartheta,$$

$$\frac{R_2}{R_1}\frac{d^2\vartheta}{d\varphi^2}+\left[\frac{d}{d\varphi}\left(\frac{R_2}{R_1}\right)+\frac{R_2}{R_1}\cot\varphi\right]\frac{d\vartheta}{d\varphi}-\left(\frac{R_1}{R_2}\cot^2\varphi+\nu\right)\vartheta = -\frac{R_1}{D}V.$$

The set of these equations can be solved in closed form, but their integrals are rather complex and present much difficulty in practice. In keeping with de Saint Venant's principle, the effect of a load applied to the edge does not spread all over the shell but is confined to the close vicinity of the edge; thus, the internal forces decrease very rapidly with distance from the edge and even of a short distance they become so small that they can practically be neglected. Relying on this observation, low value terms can be omitted in the above equations. We start first with a spherical shell. The assumed equality of the radii, $R_1 = R_2 = R$, converts both differential equations to much simpler forms, and since the terms containing V, ϑ, $dV/d\varphi$ and $d\vartheta/d\varphi$ are small compared to the remaining ones and can be neglected without a significant error, we arrive at the simplified equations

$$\frac{d^2V}{d\varphi^2} - RhE\vartheta = 0, \qquad \frac{d^2\vartheta}{d\varphi^2} + \frac{R}{D}V = 0$$

which can easily be integrated. To this end, the first equation is differentiated twice and put into the second one. This operation leads to the following differential equation:

$$\frac{d^4V}{d\varphi^4} + 4k^4V = 0$$

containing parameter

$$k = \sqrt[4]{3(1-\nu^2)}\;\sqrt{\frac{R}{h}} \tag{4.31}$$

and unknown function V. Angle φ is an independent variable. For convenience, it is necessary to introduce a new variable, $\psi = \varphi_0 - \varphi$, as the angular distance of the cross-section from the edge, denoting by φ_0 the value of angle φ on the edge. In that case, differential equation (4.31) transforms into a new one

$$\frac{d^4V}{d\psi^4} + 4k^4V = 0 \tag{4.32}$$

whose integral

$$V = C_1 e^{k\psi}\cos(k\psi + \alpha_1) + C_2 e^{-k\psi}\cos(k\psi + \alpha_2)$$

contains four constants $C_1, \ldots, \alpha_2$. Considering that $\psi > 0$, and function V shows a strong downward trend with increasing distance from the edge, we can let constant $C_1 = 0$; then

$$V = Ce^{-k\psi}\cos(k\psi + \alpha) \tag{4.33}$$

contains only two constants. This integral constitutes a fair approximation, when the two edges of the shell are sufficiently far apart. We substitute function V as just determined into the equations for internal forces, so as to arrive after a number of operations at the relationships giving the bending forces and moments in a shell loaded only on the edge

$$n = -\frac{C}{R}e^{-k\psi}\cos(k\psi + \alpha)\cot\varphi,$$

$$t = -\sqrt{2}\,\frac{Ck}{R}\sin\left(k\psi + \alpha + \frac{\pi}{4}\right),$$

$$q = \frac{C}{R}e^{-k\psi}\cos(k\psi + \alpha),$$

$$m_1 = 2\sqrt{2}\,\frac{DCk^3}{hER^2}e^{-k\psi}\cos\left(k\psi + \alpha + \frac{\pi}{4}\right),$$

$$m_2 = \nu m_1 - D\frac{\vartheta\cot\varphi}{R}$$

and for displacements—angular, along the meridian and in the perpendicular direction to it

$$\vartheta = 2\frac{Ck^2}{hER}e^{-k\psi}\sin(k\psi + \alpha),$$

$$u_1 = C\sin\varphi + \frac{1+\nu}{hE}Rq,$$

$$w_1 = C\cos\varphi - \frac{R}{hE}(t - \nu n) + \frac{1+\nu}{hE}qR\cot\varphi.$$

There are four cases most commonly encountered in shell structures:

(1) perfect clamped edge: angle ϑ at the clamping site equals zero; hence, it follows that constant $\alpha = 0$,

(2) simply supported edge: here, $m_1 = 0$ on the edge, and this is the case where $\alpha = \pi/4$,

(3) free edge with only boundary forces acting; in that case, moment $m_1 = 0$, consequently, $\alpha = \pi/4$,

(4) free edge loaded by moments; transverse force $q = 0$, which is the case where $\alpha = \pi/2$.

The conclusions derived here are used for the analysis of internal forces in the vicinity of the edge of a spherical cap. Moments and forces radially oriented, uniformly distributed on the circumference, may be acting simultaneously on the free edge of a spherical cap. Bearing in mind the principle of superposition, we can consider both cases separately, which will lead to the relations obtained being more lucid and simpler.

4.6.1. The case of radial forces acting on the edge of spherical cap

Only forces of intensity p_0 are acting on the free edge of a spherical-cap segment (Fig. 4.6). They induce transverse forces on the edge to equal
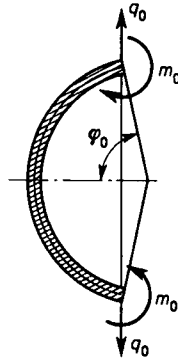
Fig. 4.6. Shell loaded on the edge by moments m_0 and radial forces q_0

$q_0 = p_0 \sin \varphi_0$. For the loaded edge, $\psi = 0$ and $\alpha = \pi/4$; therefore, we must have

$$q_0 = \frac{\sqrt{2}}{2} \frac{C}{R};$$

hence, $C = R\sqrt{2}p_0 \sin\varphi_0$. Constant C is put into the relationships giving the internal forces and displacements at any point of the shell. Next, after simplifying, we obtain

$$q = p_0 \sin\varphi_0 e^{-k\psi}(\cos k\psi - \sin k\psi), \quad n = -q \cot\varphi,$$

$$t = -2kp_0 \sin\varphi_0 e^{-k\psi}\cos k\psi,$$

$$m_1 = \frac{1}{k}p_0 R \sin\varphi_0 e^{-k\psi}\sin k\psi,$$

$$m_2 = \nu m_1 - \frac{D\vartheta}{R}\cot\varphi,$$

$$\vartheta = \frac{2k^2}{hE}p_0 \sin\varphi_0 e^{-k\psi}(\cos k\psi + \sin k\psi).$$

With the assumption $\psi = 0$, i.e., $\varphi = \varphi_0$, the respective quantities on the edge itself are expressed as

$$q_0 = p_0 \sin \varphi_0, \qquad n_0 = -p_0 \cos \varphi_0, \qquad t_0 = -2kp_0 \sin \varphi_0,$$

$$m_{10} = 0, \qquad m_{20} = -\frac{D\vartheta_0}{R} \cot \varphi_0, \qquad \vartheta_0 = \frac{2k}{hE} p_0 \sin \varphi_0.$$

The radial displacements along r are calculated from the simple geometrical relation

$$w = -u_1 \cos \varphi + w_1 \sin \varphi.$$

4.6.2. Moments m_0 acting on free edge of spherical-cap segment (Fig. 4.6)

In this case, transverse forces of the edge are $q = 0$ and constant $\alpha = \pi/2$. Substituting these values into the familiar equations, we obtain similar relations as before

$$n = -q \cot \varphi, \qquad t = \frac{2k^2}{R} m_0 e^{-k\psi}(\cos k\psi - \sin k\psi),$$

$$q = \frac{2k}{R} m_0 e^{-k\psi} \sin k\psi,$$

$$m_1 = m_0 e^{-k\psi}(\cos k\psi + \sin k\psi),$$

$$m_2 = \nu m_1 - \frac{D\vartheta}{R} \cot \varphi,$$

$$\vartheta = -\frac{4k^3}{hER} e^{-k\psi} \cos k\psi.$$

On the loaded edge, there exist

$$q_0 = 0, \qquad n_0 = 0, \qquad t_0 = \frac{2k^2}{R} m_0,$$

$$m_{10} = m_0, \qquad m_{20} = \nu m_0 - \frac{\vartheta_0}{R} D \cot \varphi_0,$$

$$\vartheta_0 = -\frac{4k^3}{hER} m_0, \qquad w_0 = -\frac{i2k^2}{hE} m_0 \sin \varphi_0.$$

Note that if in the vicinity of the edge of a shell with an arbitrary shape of the generatrix, the two radii of curvatures do not differ much from each other, we can use in calculations all the relationships derived above.

4.7. Axially Symmetrical Cylindrical Shells in Bending State

By a *cylindrical shell* we understand this to mean a carrying element formed by rotation of a rectangle about the axis running parallel to the longer side of the rectangle, whereby the ratio of the shorter to the longer side is a low number, much less than one. Shells of this type are commonly used in thin-walled structures (Chernina, 1968; Chernykh, 1964; Flügge, 1957; Girkman, 1956; Hampe, 1963; Ilyushin and Ogibalov, 1960; Kantorovich, 1952; Kobrin, 1963; Kolkunov, 1963; Korotkin *et al.*, 1955; Löffler, 1961; Prokopovich *et al.*, 1967; Timoshenko and Woinowsky-Krieger, 1959; Voloshin and Samsonov, 1968).
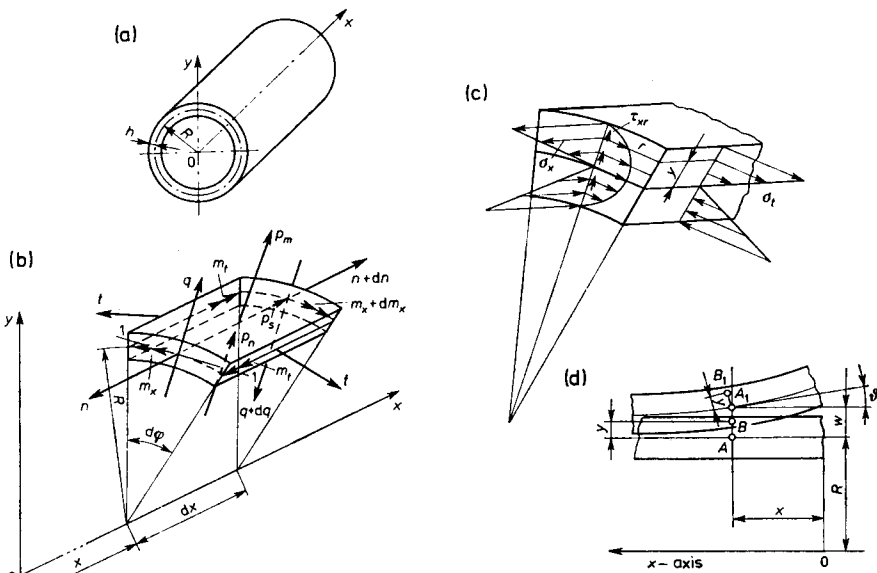
Fig. 4.7. Cylindrical shell in bending state: (a) geometry; (b) internal forces; (c) stress distribution; (d) deformation of mid-layer

We consider a thin cylindrical shell (Fig. 4.7a) using the assumptions adopted earlier within the theory of shells and establishing the following additional assumptions:

— the inertial loadings and the pressure are constant on the circumference; they are therefore axially symmetrical and may vary along the generatrix. We transfer these loadings down to the mid-layer which is a cylindrical surface of radius R,

— displacements are small compared to thickness h,

— the shell is heated, and the temperature varies over thickness h and along
  the x-axis, satisfying the condition of axial symmetry,
— the minor influence of axial forces on bending moments in the shell is
  neglected,
— E, ν, α are temperature-independent.

Radius R of the mid-layer remains considerable in relation to thickness
h. Since the shell is completely axially symmetrical, therefore, as in the struc-
tural elements previously discussed, internal forces appear in the shell. Let the
shell be under pressure p_n, the forces tangent to the central surface p_t and body
forces of variable intensity p_m acting along the x-axis; the latter forces, induced
by constant revolutions about the x-axis with angular velocity Ω, are applied
to the mid-layer. Acting on the walls of an element cut out of the shell (Fig.
4.7b), by means of two planes inclined to each other at angle $d\varphi$ which in-
tersect along the x-axis, and two planes normal to the x-axis of the cylinder
and dx apart, are cross-sectional forces, longitudinal n, circumferential t,
and transverse q and cross-sectional bending moments m_1 along the gener-
atrix and circumferential m_2, all referred to unit length of cross-section.
The cross-sectional forces and moments are the resultants for longitudinal
stresses σ_x, circumferential σ_t and shear stresses τ_{xr} (Fig. 4.7c). All relation-
ships for cross-sectional forces and strains can be obtained from the relations
derived earlier for shells of revolution of arbitrary shape, but for the sake
of clarity and noting the considerable role played by cylindrical shells in
engineering, it will be useful to discuss their theory separately.

For the shell element considered to be in equilibrium, the forces and mo-
ments acting on its walls have to satisfy the equilibrium conditions; therefore
they have to satisfy the conditions for the sum of projections of all the forces
on the x-axis, the sum of projections of all the forces on the y-axis and the
sum of moments expressed, say, with respect to straight line 1–1 normal
to the plane of symmetry and lying on the wall. In this way, we arrive at three
differential equations of internal equilibrium of the shell

$$\frac{dn}{dx} + p_t = 0, \tag{4.34}$$

$$\frac{dq}{dx} + \frac{t}{R} - (p_n + p_m) = 0, \tag{4.35}$$

$$\frac{dm_x}{dx} - q = 0. \tag{4.36}$$

It should be recalled that
$$p_m = \varrho \Omega^2 h R.$$

It follows from (4.34) that unit longitudinal force n is induced only by longitudinal surface loadings p_t or by forces applied at the ends, or in an arbitrary cross-section of the shell, since by integrating this equation we obtain $n = -\int p_t \, dx + C$, and the constant of integration C involved here depends on the value of loading of the shell on its edges or at any other point. Let $w(x)$ denote radial displacement of point A of the mid-layer (Fig. 4.7d), at distance x from the origin of the coordinates brought into the initial cross-section. In that case, derivative dw/dx, in view of the small deflections, is roughly equal to slope ϑ at point A_1. There exist in the shell layer at distance y from the mid-layer longitudinal and circumferential stresses, σ_x and σ_t, which according to Hooke's law for a biaxial state of stress induce unit longitudinal and circumferential elongations

$$\varepsilon_x = \frac{1}{E}(\sigma_x - \nu\sigma_t), \qquad \varepsilon_t = \frac{1}{E}(\sigma_t - \nu\sigma_x) \tag{4.37}$$

with heating not being considered $(T = 0)$; on the other hand, these elongations

$$\varepsilon_x = \varepsilon_0 + y\frac{d\vartheta}{dx}, \qquad \varepsilon_t = \frac{w}{R}, \tag{4.38}$$

which follow directly from the diagram, where ε_0 is the unit elongation of the mid-layer. Equations (4.37) and (4.38) reduce to

$$\sigma_x = \frac{E}{1-\nu^2}\left(\varepsilon_0 + \nu\frac{w}{R} + y\frac{d\vartheta}{dx}\right), \tag{4.39}$$

$$\sigma_t = \frac{E}{1-\nu^2}\left(\nu\varepsilon_0 + \frac{w}{R} + \nu y\frac{d\vartheta}{dx}\right). \tag{4.40}$$

The effects of these stresses result in cross-sectional longitudinal and circumferential forces

$$n = \int_{-h/2}^{h/2} \sigma_x \, dy, \qquad t = \int_{-h/2}^{h/2} \sigma_t \, dy,$$

and longitudinal and circumferential bending moments

$$m_x = \int_{-h/2}^{h/2} y\sigma_x \, dy, \qquad m_t = \int_{-h/2}^{h/2} y\sigma_t \, dy.$$

Substituting the expressions for stresses into these relationships we obtain

$$n = \frac{E}{1-\nu^2}\int_{-h/2}^{h/2}\left(\varepsilon_0 + \nu\frac{w}{R} + y\frac{d\vartheta}{dx}\right) dy,$$

$$t = \frac{E}{1-\nu^2} \int_{-h/2}^{h/2} \left(\nu \varepsilon_0 + \frac{w}{R} + \nu y \frac{d\vartheta}{dx} \right) dy,$$

$$m_x = \frac{E}{1-\nu^2} \int_{-h/2}^{h/2} \left(\varepsilon_0 + \nu \frac{w}{R} + y \frac{d\vartheta}{dx} \right) y \, dy,$$

$$m_t = \frac{E}{1-\nu^2} \int_{-h/2}^{h/2} \left(\nu \varepsilon_0 + \frac{w}{R} + \nu y \frac{d\vartheta}{dx} \right) y \, dy.$$

The quantities ε_0, $w(x)$ are independent of variable y, and

$$\int_{-h/2}^{h/2} dy = h, \qquad \int_{-h/2}^{h/2} y \, dy = 0, \qquad \int_{-h/2}^{h/2} y^2 dy = \frac{h^3}{12}.$$

Consequently, the equations of internal forces (cross-sectional) take the forms

$$n = \frac{Eh}{1-\nu^2} \left(\varepsilon_0 + \nu \frac{w}{R} \right), \tag{4.41}$$

$$t = \frac{Eh}{1-\nu^2} \left(\nu \varepsilon_0 + \frac{w}{R} \right), \tag{4.42}$$

$$m_x = \frac{d^2 w}{dx^2} D, \tag{4.43}$$

$$m_t = \nu \frac{d^2 w}{dx^2} D, \tag{4.44}$$

in which $D = \dfrac{Eh^3}{12(1-\nu^2)}$, as before. If we determine ε_0 from Eq. (4.41) and substitute it into (4.52), then

$$n - t + \frac{Eh}{R} w = 0.$$

The equations of equilibrium with relationship (4.43) substituted into them lead to the general differential equation written with respect to radial displacement

$$D \frac{d^4 w}{dx^4} + \frac{t}{R} = p_n + p_m \tag{4.45}$$

which after eliminating unknown t reduces to

$$\frac{d^4 w}{dx^4} + \frac{Ehw}{DR^2} = \frac{p_n + p_m}{D} - \nu \frac{n}{D}. \tag{4.46}$$

If we associate $4k^4 = \dfrac{Eh}{R^2 D}$ with the so-called *parameter k of shell*

$$k = \sqrt[4]{\frac{3(1-\nu^2)}{h^2 R^2}} \, ,$$

then Eq. (4.46) will take the simplest form

$$\frac{d^4 w}{dx^4} + 4k^4 w = \frac{p_n + p_m}{D} - \nu \frac{n}{D} \, . \tag{4.47}$$

Force n is usually known. If $p_t = 0$, then n is determined from the loadings at the ends of the shell, which are given in the problem. The integral of Eq. (4.47) consists of $w_1(x)$ as the integral of a homogeneous equation and $w_2(x)$ as the particular integral of a non-homogeneous equation, meaning that

$$w(x) = w_1(x) + w_2(x).$$

As we know, the former integral has the form

$$w_1(x) = e^{-kx}(C_1 \sin kx + C_2 \cos kx) + e^{kx}(C_3 \sin kx + C_4 \cos kx). \tag{4.48}$$

The latter depends on the mode of loading expressed by the function of loadings. Constants of integration $C_1, \ldots, C_4$ are determined, of course, from the boundary conditions of the shell. Knowing function $w(x)$, we determine directly the states of internal forces. The transverse force, determined from Eqs. (4.36) and (4.43), equals

$$q = D \frac{d^3 w}{dx^3} \, .$$

Normal longitudinal and circumferential stresses of extremal value (4.4) exist in extreme layers of the shell, and the maximum shear stress in the mid-layer equals

$$\tau_{xr\,\text{max}} = \frac{3}{2} \frac{q}{h} \, .$$

The maximum reduced stress in the extreme outer or inner layer at the dangerous point is usually given as

$$\sigma_{\text{red H}} = \sqrt{\sigma_x^2 + \sigma_t^2 - \sigma_x \sigma_t} \, \big|_{\text{max}} < R_e.$$

Three cases are to be distinguished here:

(1) $n = 0$, $p_n + p_m = p_0 = \text{const}$, then

$$w_2 = \frac{p_0 R^2}{Eh} \, .$$

(2) $\dfrac{p_n+p_m}{D}-\nu\dfrac{n}{RD}=p(x)$. Let this loading be representable as

$$p(x) = A_0+A_1x+A_2x^2+A_3x^3+A_4x^4,$$

and similarly, the displacements as

$$w_2(x) = a_0+a_1x+a_2x^2+a_3x^3+a_4x^4.$$

Both functions are put into differential equation (4.47), and in this way, we obtain a conditional equation which will be satisfied, if

$$a_0 = \frac{A_0}{4k^4}-\frac{3}{2}\frac{A_4}{k^8},\qquad a_1 = \frac{A_1}{4k^4},\qquad a_2 = \frac{A_2}{4k^4},$$

$$a_3 = \frac{A_3}{4k^4},\qquad a_4 = \frac{A_4}{4k^4}.$$

In principle, loading $p(x)$ may vary arbitrarily along the x-axis, but it must always be axially symmetrical. It can be represented by means of an algebraic polynomial of higher order or by a trigonometric series.

(3) $p_t = 0$, $p_0 =$ const but acting at the end of the cylinder are forces N applied axially. From the equation of equilibrium it follows that

$$2\pi R\int_{-h/2}^{h/2}\sigma_x dy = N.$$

However, since longitudinal stresses σ_x are expressed by (4.39), the condition written for the longitudinal force

$$2\pi R\frac{E}{1-\nu^2}\int_{-h/2}^{h/2}\left(\varepsilon_0+\nu\frac{w}{R}+y\frac{d^2w}{dx^2}\right)dy = N$$

is expressed by displacement w and strain ε_0. The integral of the last term in parentheses equals zero. Integrating, we arrive at a relationship, from which it follows that the strain in the mid-layer equals

$$\varepsilon_0 = \frac{1-\nu^2}{Eh}\frac{N}{2\pi R}-\nu\frac{w}{R}.$$

The last relationship put into (4.39), (4.40) enables the determination of both stresses, containing only a single unknown function $w(x)$. In this case of loading, Eq. (4.47) takes the form

$$\frac{d^4w}{dx^4}+4k^4w = \frac{p_0}{D}-\nu\frac{N}{2\pi R^2D}$$

and its integral is like in case (2), where $p(x) = A_0$, with constant A_0

$$= \frac{p_0}{D} - \nu \frac{N}{2R^2 D\pi}.$$

4.8. Types of Cylindrical Shells. Loading Cases

In practice, two types of cylindrical shells are differentiated—long and short. Specific to long shells is that the influence of the loadings of one edge on the state of stress of the other is slight and is neglected. In short shells, this influence is considerable and cannot be neglected. Expressions containing functions e^{-kx}, e^{kx}, $\sin kx$ and $\cos kx$ occur in integral $w(x)$. With increasing x, the first of these functions rapidly decreases and the second increases, the remaining two assume values between $(+1)$ and (-1). Assuming that the shell is very long and constants C_2, C_3, C_4 equal zero, with $C_1 \neq 0$, the function is

$$w(x) = C_1 e^{-kx} \sin kx,$$

where period 2π represents the distribution of displacements $w(x)$, hence also the distribution of internal forces in the wall along the x-axis—being in the nature of a rapidly decreasing wave whose length

$$L = \frac{2\pi}{k}.$$

If $kx_1 = \pi/2$, then $w(x_1) = C_1 e^{-\pi/2}$ and correspondingly for $kx_2 = \frac{3}{2}\pi$, we have $w(x_2) = -C_1 e^{-3\pi/2}$. The ratio

$$\frac{w(x_2)}{w(x_1)} = -e^{-\pi} \approx -\frac{1}{23 \cdot 1}$$

describes the rate of disappearance of the influence of the forces applied on the edge along the shell axis. If all four constants $C_1, \ldots, C_4$ differ from zero, then it is easily proved that C_3 and C_4 for a long shell are very small compared to C_1 and C_2. Consequently, for variable x near the edge ($x \approx 0$), products $C_3 e^{kx}$, $C_4 e^{kx}$ are small in relation to the others and can be neglected. In that case, for long shells,

$$w(x) = e^{-kx}(C_1 \sin kx + C_2 \cos kx). \tag{4.49}$$

The influence of the loadings of one edge on cross-sectional strains and forces along the generatrix and at the other edge, as indicated by $w(x_2)/w(x_1)$, quickly disappears, and the longer the shell, the lesser it is.

Allowing for an inaccuracy of the order of a few percent, we can take a shell to be long if its length l satisfies the condition $kl \geqslant \pi$, and to be short, when $kl < \pi$.

Taking $\nu = 0.3$ which is applicable to steel and light alloys, we obtain the condition defining a long shell

$$l \geqslant 2.4 \sqrt{Rh}$$

and the condition defining a short shell

$$l < 2.4 \sqrt{Rh}.$$

For short shells, the conditions written for both edges should be considered, and all four constants, $C_1, \ldots, C_4$, occur then in principle.

4.8.1. Particular cases of long cylindrical shells

Considered in detail below are two cases of loadings of long cylindrical shells, important from an engineering point of view.

I. The shell is loaded on the free edge by transverse forces q_0.

Boundary conditions are: for $x = 0$, we have $m_1 = 0$, $q = q_0$. Consequently, $C_1 = 0$, $C_2 = \dfrac{q_0}{2Dk^3}$; hence

$$w = \frac{q_0}{2Dk^3}e^{-kx}\cos kx, \qquad \frac{dw}{dx} = -\frac{q_0}{2Dk^2}e^{-kx}(\cos kx + \sin kx),$$

$$m_x = \frac{q_0}{k}e^{-kx}\sin kx, \qquad m_t = \nu\frac{q_0}{k}e^{-kx}\sin kx,$$

$$q = q_0 e^{-kx}(\cos kx - \sin kx), \qquad t = \frac{Ehq_0}{2RDk^3}e^{-kx}\cos kx.$$

At the end, i.e., for $x = 0$

$$w_0 = \frac{q_0}{2Dk^3}, \qquad \vartheta_0 = -\frac{q_0}{2Dk^2}, \qquad m_{t0} = 0, \qquad t_0 = \frac{Ehq_0}{2DRk^3}.$$

II. The shell is loaded on the free edge by moments m_0.

The boundary conditions are

$$D\frac{d^2 w}{dx^2}(0) = m_0 \quad \text{and} \quad D\frac{d^3 w}{dx^2}(0) = 0$$

and the equations with respect to constants are satisfied if

$$C_1 = -\frac{m_0}{2k^2 D}, \qquad C_2 = \frac{m_0}{2k}.$$

Therefore, the quantities sought equal

$$w = \frac{m_0}{2k^2 D}e^{-kx}(\cos kx - \sin kx), \qquad \vartheta = -\frac{m_0}{kD}e^{-kx}\cos kx,$$

$$m_x = m_0 e^{-kx}(\cos kx + \sin kx), \qquad m_t = \nu m_x,$$

$$q = -2km_0 e^{-kx}\sin kx, \qquad t = \frac{Ehm_0}{2k^2 DR} e^{-kx}(\cos kx - \sin kx).$$

If $x = 0$, then on the loaded edge

$$w_0 = \frac{m_0}{2k^2 D}, \qquad \vartheta_0 = -\frac{m_0}{kD}, \qquad m_{t0} = \nu m_0, \qquad q_0 = 0, \qquad t_0 = \frac{Ehm_0}{2k^2 DR}.$$

At distance $x = L$, moment m_x equals zero, if $L = 3\pi/4k$.

4.9. The Second Form of Function w(x) of Cylindrical Shells

Function (4.48) can be represented in the form

$$w(X) = B_1 X_1 + B_2 X_2 + B_3 X_3 + B_4 X_4, \tag{4.50}$$

where B_1, B_2, B_3, B_4 are constants also determined from the boundary conditions, and

$$X_1 = \text{ch}\,kx\cos kx, \qquad X_2 = \tfrac{1}{2}(\text{ch}\,kx\sin kx + \text{sh}\,kx\cos kx),$$
$$X_3 = \tfrac{1}{2}\text{sh}\,kx\sin kx, \qquad X_4 = \tfrac{1}{4}(\text{ch}\,kx\sin kx - \text{sh}\,kx\cos kx)$$

are functions of independent variable x. This form is convenient for short shells.

4.9.1. Particular cases of short cylindrical shells

Discussed below are solutions for two simple cases of loadings of short cylindrical shells, very common in practivce.

    I. A shell of length l is loaded on the left edge by moments m_0, both edges being free. Boundary conditions are: for $x = 0$, we have

$$D\frac{d^2 w}{dx^2} = m_0, \qquad \frac{d^3 w}{dx^3} = 0$$

and for $x = 1$,

$$\frac{d^2 w}{dx^2} = 0, \qquad \frac{d^3 w}{dx^3} = 0$$

which reduces the problem to determining the constants from the set of conditional equations, obtaining finally

$$w = \frac{m_0 l^2}{D}(\varphi_1 X_1 + \varphi_2 X_2 + \varphi_3 X),$$

$$\vartheta = \frac{m_0 l}{D}(-4\varphi_1 X_4 + \varphi_2 X_1 + \varphi_3 X_2)kl,$$

$$q = \frac{m_0}{l}(-\varphi_1 X_2 - \varphi_2 X_3 - \varphi_3 X_4)4k^3 l^3, \quad n = 0, \quad m_t = \nu m_x,$$

$$m_x = m_0(-4\varphi_1 X_3 - 4\varphi_2 X_4 + \varphi_3 X_1)k^2 l^2,$$

$$t = m_0 l^2 R(\varphi_1 X_1 + \varphi_2 X_2 + \varphi_3 X_3)4k^4.$$

On the left-hand edge, we have

$$w_0 = \frac{m_0 l^2}{D}\varphi_1, \quad \vartheta_0 = \frac{m_0 l}{D}\varphi_4,$$

on the right-hand edge

$$w_l = \frac{m_0 l^2}{D}\varphi_5, \quad \vartheta_l = \frac{m_0 l}{D}\varphi_6,$$

where

$$\varphi_1 = \left[\frac{X_1 X_3 - 4X_4^2}{4k^2 l^2(X_3^2 - X_2 X_4)}\right]_{x=l}, \quad \varphi_2 = \left[\frac{X_1 X_2 + 4X_3 X_4}{4k^2 l^2(X_2 X_4 - X_3^2)}\right]_{x=l},$$

$$\varphi_3 = \frac{1}{k^2 l^2}, \quad \varphi_4 = k l \varphi_2, \quad \varphi_5 = (\varphi_1 X_1 + \varphi_2 X_2 + \varphi_3 X_3)_{x=l},$$

$$\varphi_6 = k l(\varphi_2 X_1 - 4\varphi_1 X_4 + \varphi_3 X_2)_{x=l}.$$

II. A shell is loaded on one edge by transverse forces q_0. Both edges are free. Boundary conditions are: for $x = 0$, we have

$$\frac{d^2 w}{dx^2} = 0, \quad D\frac{d^3 w}{dx^3} = q_0,$$

for $x = l$,

$$\frac{d^2 w}{dx^2} = 0, \quad \frac{d^3 w}{dx^3} = 0;$$

they lead to a set of conditional equations for constants of integration and then to the relationships

$$w = \frac{q_0 l^3}{D}(\varphi_7 X_1 + \varphi_8 X_2 + \varphi_9 X_4),$$

$$\vartheta = \frac{q_0 l^2}{D}(\varphi_8 X_1 - 4\varphi_7 X_4 + \varphi_9 X_3)k l,$$

$$m_x = q_0 l(\varphi_9 X_2 - 4\varphi_7 X_3 - 4\varphi_8 X_4)k^2 l^2, \quad m_t = -\nu m_x,$$

$$q = q_0(\varphi_9 X_1 - 4\varphi_7 X_2 - 4\varphi_8 X_3)k^3 l^3, \quad n = 0,$$

$$t = q_0\frac{R}{l}(\varphi_7 X_1 + \varphi_8 X_2 + \varphi_9 X_4)4k^4 l^4;$$

for the left-hand edge

$$w_0 = \frac{q_0 l^3}{D} \varphi_7, \qquad \vartheta_0 = \frac{q_0 l^2}{D} \varphi_{10},$$

and for the right-hand edge

$$w_l = \frac{q_0 l^3}{D} \varphi_{11}, \qquad \vartheta_l = \frac{q_0 l^2}{D} \varphi_{12},$$

where

$$\varphi_7 = \left[\frac{X_2 X_3 - X_1 X_4}{4k^3 l^3 (X_3^2 - X_2 X_4)} \right]_{x=l}, \qquad \varphi_8 = \left[\frac{X_1 X_3 - X_2^2}{4k^3 l^3 (X_3^2 - X_2 X_4)} \right]_{x=l},$$

$$\varphi_9 = \frac{1}{k^3 l^3}, \qquad \varphi_{10} = kl\varphi_8, \qquad \varphi_{11} = (\varphi_7 X_1 + \varphi_8 X_2 + \varphi_9 X_4)_{x=l},$$

$$\varphi_{12} = kl(\varphi_8 X_1 - 4\varphi_7 X_4 + \varphi_9 X_2)_{x=l}.$$

The cases of combined loading of short shells are solved by two methods: (1) by making use of the integral of a differential equation in the form $w(x) = w_1(x) + w_2(x)$ and determining the constants of integration from the boundary conditions or (2) by making use of ready solutions of simple cases of loadings combined with the principle of superposition.

4.10. Cylindrical Shells Thermally Loaded

We assume, in addition, that the temperature distribution along x is axially symmetrical and can be arbitrary, and that the temperature varies linearly over wall thickness h, i.e.,

$$T(x) = T_x + \frac{T}{h} y, \qquad (4.51)$$

where T_x is the mean temperature over wall thickness h and T is the temperature difference between the outer and inner surfaces of the wall.

Temperatures T_x and T are functions of variable x (Lipka, 1967; Lipka and Butt-Hussaim, 1963₁, 1963₂; Ponomarev et al., 1958).

As indicated in the previous sections, unit elongations of a shell layer remain as

$$\varepsilon_x = \varepsilon_0 + y \frac{d^2 w}{dx^2}, \qquad \varepsilon_t = \frac{w}{R}.$$

Considering thermal elongation while assuming that the coefficient of linear thermal expansion α is constant, we obtain the relationships for the stress components

$$\sigma_x = \frac{E}{1-\nu^2}\left(\varepsilon_0 + y\frac{\mathrm{d}^2 w}{\mathrm{d}x^2} + \nu\frac{w}{R}\right) - \frac{E\alpha}{1-\nu}\left(T_x + \frac{T}{h}y\right),\tag{4.52}$$

$$\sigma_t = \frac{E}{1-\nu^2}\left(\nu\varepsilon_0 + \frac{w}{R} + \nu y\frac{\mathrm{d}^2 w}{\mathrm{d}x^2}\right) - \frac{E\alpha}{1-\nu}\left(T_x + \frac{T}{h}y\right).\tag{4.53}$$

If longitudinal force $N = 0$, then

$$2\pi R \int_{-h/2}^{h/2} \sigma_x \mathrm{d}y = 0$$

and by integrating, we obtain an equation which allows ε_0 to be determined as

$$\varepsilon_0 = (1+\nu)\alpha T_x - \nu\frac{w}{R}.\tag{4.54}$$

The relationships (4.52) and (4.53) reduce to the expression

$$\sigma_x = \frac{E}{1-\nu^2}y\frac{\mathrm{d}^2 w}{\mathrm{d}x^2} - \frac{E\alpha}{(1-\nu)h}yT,\tag{4.55}$$

$$\sigma_t = \frac{Ew}{R} + \frac{E\nu}{1-\nu^2}y\frac{\mathrm{d}^2 w}{\mathrm{d}x^2} - E\alpha T_x - \frac{E\alpha}{(1-\nu)h}yT.\tag{4.56}$$

The effects of these stresses, as for mechanical loadings, amount to cross-sectional bending moments

$$m_x = \int_{-h/2}^{h/2} y\sigma_x \mathrm{d}y = D\left[\frac{\mathrm{d}^2 w}{\mathrm{d}x^2} - \alpha(1+\nu)\frac{T}{h}\right],\tag{4.57}$$

$$m_t = \int_{-h/2}^{h/2} y\sigma_t \mathrm{d}y = D\left[\nu\frac{\mathrm{d}^2 w}{\mathrm{d}x^2} - \alpha(1+\nu)\frac{T}{h}\right]\tag{4.58}$$

and to circumferential force

$$t = Eh\left(\frac{w}{R} - \alpha T_x\right),\tag{4.59}$$

It follows from the equilibrium equations of the shell element that the transverse force equals

$$q = D\frac{\mathrm{d}^3 w}{\mathrm{d}x^3} - \frac{\alpha(1+\nu)}{h}\frac{\mathrm{d}T}{\mathrm{d}x}\tag{4.60}$$

and

$$\frac{\mathrm{d}^4 w}{\mathrm{d}x^4} + 4k^4 w = \frac{Eh\alpha}{DR}T_x + \frac{\alpha(1+\nu)}{h}\frac{\mathrm{d}^2 T}{\mathrm{d}x^2},\tag{4.61}$$

whose integral is the function

$$w(x) = e^{-kx}(C_1 \sin kx + C_2 \cos kx) + e^{kx}(C_3 \sin kx + C_4 \cos kx) + w_3 \qquad (4.62)$$

with parameter k as defined in (4.47).

Function w_3 depends, of course, on the form of T_x and T, and it has to be remembered that T at a given point of the shell is understood to be the temperature increase above the initial temperature T_0, which can be assumed, as before, to be equal to zero.

The following cases should be considered:

(1) if the right-hand side of Eq. (4.61) is represented, for example, in the form

$$B_0 + B_1 x + B_2 x^2 + B_3 x^3 + B_4 x^4,$$

then assuming that function w_3 can also be expressed by the algebraic polynomial

$$w_3 = b_0 + b_1 x + b_2 x^2 + b_3 x^3 + b_4 x^4,$$

we obtain a conditional equation which is satisfied only when

$$b_0 = \frac{B_0}{4k^4} - \frac{3}{2} \frac{B_4}{k^8} \qquad b_1 = \frac{B_1}{4k^4}, \qquad b_2 = \frac{B_2}{4k^4},$$

$$b_3 = \frac{B_3}{4k^4}, \qquad b_4 = \frac{B_4}{4k^4};$$

(2) when $T_x = T_1 = \text{const}$, i.e., the shell is uniformly heated all over then there exists only $B_0 = (Eh\alpha T_1)/DR$, the other constants, $B_1, \ldots, B_4$ and $b_1, \ldots, b_4$ equal zero, whereas $b_0 = R\alpha T_1$ and the integral (4.62) considered is represented as

$$w = e^{-kx}(C_1 \sin kx + C_2 \cos kx) +$$
$$+ e^{kx}(C_3 \sin kx + C_4 \cos kx) + R\alpha T_1. \qquad (4.63)$$

On the basis of the above considerations, the conclusion is reached that here, too, the principle of superposition remains fully valid.

4.10.1. Particular cases of heated shells, long and short

Also with thermal loadings acting, if only the shell is long, the function expressing radial displacements loses two constants, C_3 and C_4, since they are negligibly small, and reduces thereby to a simple form. Function w_3 is the integral of non-homogeneous equation (4.61), determined each time for a given state of temperature. We present below the calculation procedure for a heated shell of considerable length.

1. If a long shell is uniformly heated starting from $T_0 = 0$ to T_1, i.e., $T_x = T_1 = $ const, and if the clamping on the edge is rigid and is not subject to thermal strain with temperature changes, $T = 0$, then function $w_3 = R\alpha T_1$ is constant and

$$w(x) = e^{-kx}(C_1 \sin kx + C_2 \cos kx) + R\alpha T_1.$$

The boundary conditions which for $x = 0$ give $w = 0$, $dw/dx = 0$, reduce the problem to equations with respect to constants C_1 and C_2, with $C_1 = -R\alpha T_1$, $C_2 = C_1$. Thus, finally we have

$$w = R\alpha T_1[1 - e^{-kx}(\sin kx + \cos kx)], \qquad \vartheta = 2R\alpha T_1 k e^{-kx} \sin kx,$$
$$m_x = 2k^2 \alpha RT_1 D e^{-kx}(\cos kx - \sin kx), \qquad m_t = \nu m_x,$$
$$q = -4k^3 R\alpha T_1 D e^{-kx} \cos kx, \qquad t = -Eh\alpha T_1 e^{-kx}(\sin kx + \cos kx).$$

For the clamped edge (i.e., for $x = 0$), $m_{x0} = 2k^2 R\alpha T_1 D$, $q_0 = -4k^3 R\alpha T_1 D$, $t_0 = -Eh\alpha T_1$. At a considerable distance from the clamped edge, i.e., for high values of x, all the static quantities become practically equal to zero, and $w = R\alpha T_1$ assumes a constant value.

2. If thermally loaded cylindrical shells are not very long, in other words, if they satisfy the condition for short shells, then as for mechanical loadings, function $w(x)$ contains four constants of integration and takes the form

$$w(x) = B_1 X_1 + B_2 X_2 + B_3 X_3 + B_4 X_4 + w_3(x), \qquad (4.64)$$

and $w_3(x)$ is also the integral of non-homogeneous equation (4.61).

Serving as an example is a short shell simply supported on both edges, non-slidable in the normal direction to the x-axis, initial temperature $T_0 = 0°C$, mid-layer temperature $T_x = T_1 = $ const, and the temperature difference of the inner and outer surfaces $T = $ const. Forces in the axial direction are non-existent.

The equation for the central surface (4.64) is expressed in the form

$$w = B_1 X_1 + B_2 X_2 + B_3 X_3 + B_4 X_4 + R\alpha T_1$$

and has to satisfy the boundary conditions: $m_x = 0$ and $w = 0$, for $x = 0$ and $x = 1$. Finally, the expressions for the unknown constants are

$$B_1 = -R\alpha T_1, \qquad B_2 = \left(\frac{X_2 \varphi_1' + X_4 \varphi_2'}{4X_4^2 + X_2^2}\right)_{x=1}, \qquad B_3 = \frac{(1+\nu)\alpha T_1}{k^2 h},$$

$$B_4 = \left(\frac{4X_4 \varphi_1' - X_2 \varphi_2'}{4X_4^2 + X_2^2}\right)_{x=1},$$

$$\varphi_1' = (-B_1 X_1 - B_3 X_3 - R\alpha T_1)_{x=1},$$

$$\varphi_2' = \left(B_3 X_1 - 4B_1 X_3 - \alpha(1+\nu)\frac{T_1}{k^2 h}\right)_{x=1};$$

hence

$$\vartheta = k(-4B_1X_4 + B_2X_1 + B_3X_2 + B_4X_3),$$

$$m_x = Dk^2\left[-4B_1X_3 - 4B_2X_4 + B_3X_1 + B_4X_2 - \alpha(1+\nu)\frac{T_1}{k^2h}\right],$$

$$m_t = Dk^2\left[\nu(-4B_1X_3 - 4B_2X_4 + B_3X_1 + B_4X_2) - \alpha(1+\nu)\frac{T_1}{k^2h}\right],$$

$$q = Dk^3(-4B_1X_2 - 4B_2X_3 - 4B_3X_4 + B_4X_1),$$

$$t = \frac{Eh}{R}(B_1X_1 + B_2X_2 + B_3X_3 + B_4X_4).$$

There exist on both edges

$$\vartheta_0 = kB_2, \qquad q_0 = Dk^3B_4, \qquad t_0 = -E\alpha T_1.$$

4.11. Cylindrical Shells of Complete Axial Symmetry and Variable Wall Thickness

The theory of this type of shells has many in features common with theory of shells of constant wall thickness. Thus, cross-sectional forces n and t are expressed by relationships (4.41), (4.42), just as the relations between cross-sectional moments and shearing forces are expressed by (4.43), (4.44), which follow from the equations of equilibrium. Considering that wall thickness $h(x)$ varies along the x-axis, and ε_0 is very small, we obtain

$$\frac{d^2}{dx}\left(D\frac{d^2w}{dx^2}\right) + \frac{Eh}{R^2}w = p \tag{4.65}$$

with $p_t = 0$ and $p = p_n + p_m$, $D = \dfrac{Eh_{(x)}^3}{12(1-\nu^2)}$. If we cannot thickness $h = h_0$, say, at the place where $x = 0$, we can write then that

$$h = h_0 f(x) \quad \text{and} \quad D_0 = \frac{Eh_0^3}{12(1-\nu^2)} \quad \text{while} \quad D = D_0 f^3(x)$$

and Eq. (4.65) takes the form

$$\frac{d^2}{d\eta^2}\left[f^3(\eta)\frac{d^2w}{d\eta^2}\right] + 4k_0^4 f(\eta)w(\eta) = \frac{p(\eta)}{D_0}, \tag{4.66}$$

where $\eta = x/L$, L is the shell length and

$$k_0 = \sqrt{\frac{3(1-\nu^2)}{h_0^2 R^2}}. \tag{4.67}$$

Performing differentiations in (4.66), we obtain an expanded form of the equation

$$f^3(\eta)\frac{\mathrm{d}^4 w}{\mathrm{d}\eta^4} + \frac{2\mathrm{d}}{\mathrm{d}\eta}f^3(\eta)\frac{\mathrm{d}^3 w}{\mathrm{d}\eta^3} + \frac{\mathrm{d}^2}{\mathrm{d}\eta^2}f^3(\eta)\frac{\mathrm{d}^2 w}{\mathrm{d}\eta^2} + 4k_0^4 wf(\eta) = \frac{p(\eta)}{D_0}, \quad (4.68)$$

whose integral depends on $f(\eta)$ and $p(\eta)$ and contains four constants of integration (Hampe, 1963; Ponomarev *et al.*, 1958). This integral can be determined in closed form for only the few simplest functions $p(\eta)$ and $f(\eta)$, for example, when thickness h changes linearly. Cylindrical functions, as well as Hankel's functions, appear in the solutions.

Where a shell of varying thickness is heated axially-symmetrically, the relationships for unit elongations and stresses—as demonstrated in the theory of shells of constant thickness—contain expressions involving temperature together with coefficient α. The integral of an equation analogous to (4.68) grows more complex. Comments relating to solutions for unheated shells are also applicable to heated shells.

4.12. More General Problems of Cylindrical Shells of Complete Axial Symmetry

4.12.1. Strongly heated shells

There is a separate group of problems under the bending theory of shell of constant or varying thicknesses, but heated sufficiently high for considerable temperature dependence for E, α and ν though without creep. Functions $T(x)$, $E(x)$, $\alpha(x)$, $\nu(x)$ appear in Hooke's equations and in additional relationships, and the integrals of very complex final equations can be determined nearly always with the use of a digital computer and for particular engineering data. In these cases, especially when we seek optimum structural parameters or when strength is to be determined, it has to be remembered that σ_{red}, σ_{pl}, (R_e) are temperature-dependent.

4.12.2. Axially symmetrical orthotropic shells

This type of shells is distinguished by two different values of moduli E_x and E_t and numbers ν_x and ν_t, constant or variable in the function of independent variable x, if they are strongly heated. Orthotropy of these shells is provided by endowing them with a suitable structure: layered and oriented, or by out-fitting them with shell on longitudinal or circumferential ribs. We cite here just some monographs: Birger (1956, 1961), Bezukhov (1968) and specialized contributions dealing with problems relating to the theory of orthotropic shells and their behaviour under specified conditions.

4.12.3. Axially symmetrical cylindrical shells with large displacements

If the radial displacements of a shell are large, an additional expression, $\frac{1}{2}(dw^2/dx)$, will appear in the first relationship (4.38) and the second will remain unchanged. Hence, the relationships involving normal stress components undergo change. The equations of internal equilibrium remain unchanged, whereas the differential equation of shell deflection—corresponding to Eq. (4.46) written for small deflections—becomes non-linear. The integrals for this equation cannot be determined by classical methods. In the search for approximate solutions, good results can be obtained with the use of a digital computer e.g. in connection with the finite element method.

4.13. General Remarks on Shell Solving Methods

Simple cases of shell shapes and simple cases of shell loadings have known solutions, described by functions which can easily be calculated and are tabulated in practice. The situation is different when complex loadings and shells of variablet thickness are involved. The analytical solutions are then either highly time-consuming or are approximate with so high a degree of inaccuracy that seeking an exact solution leads nowhere. As with thick-walled elements (e.g. thick-walled cylinders) and with plates and disks, so is it with shells also; sufficiently accurate approximate solutions can be obtained, even in most complicated cases, by dividing the shell into parts and solving its individual segments (parts) using predetermined solutions of simple cases described by ready formulae.

Obviously, the complete solution must satisfy the conditions of continuity of segments and the boundary conditions. The error decreases as the number of segments is increased, but concomitantly the amount of work required for the calculations also increases. Very good results are obtained using a digital computer, e.g., in connection with the finite element method.

5. Analysis of Axially Symmetrical Structures

In speaking of axial symmetrical structures, we have in mind such a homogeneous or non-homogeneous structure, isotropic or anisotropic, which satisfies the conditions of complete axial symmetry and can be resolved into simple carrying elements which however still remain axially symmetrical, such as thick-walled cylinders, spheres, circular plates and disks, and cylindrical, toroidal and other shells. Generally speaking, the theory of these simple carrying elements is known and allows them to be reduced to simple fundamental cases having known solutions.

If individual simple structural elements are not mated and are not interacting, but are only subjected to simple loadings, they are calculated following the procedure described earlier, frequently making use of predetermined relationships and formulae derived therefrom. The situation is different if complex structures are involved, since at places of discontinuity of shape and loading, and even of properties of the materials, considerable local internal forces of interaction between individual elements of the structure develop, owing to which continuity of deformations is maintained. Simultaneously, these forces are a source of additional stresses, considerable in most cases. Thus, individual isolated elements of a complex structure, when not mated, exhibit sufficient strength or sufficient rigidity, but when mated, they often give a structure failing to satisfy the strength requirements or a structure featuring insufficient rigidity. This last statement also means inadmissibly high strains. Usually, cracks are formed at these places (brittle materials) or a fatigue process develops there (Krzyś and Latos, 1974; Kuhn, 1956; Leyko et al., 1972; Lipka, 1970; Lipka and Kubicki, 1968; Lipka and Sawicki, 1965; Łukasiewicz, 1960; Matryukova, 1959; Olesiak, 1958; Parszewski, 1956; Schnell, 1957; Zhilin, 1970).

One purpose of structural analysis among others is to uncover sites of discontinuity and to define and calculate the internal forces occurring therein, followed by an assessment of the influence of these forces on the overall and local carrying capacity of the structure.

Obviously, there exist in practice too many various machines satisfying the conditions of complete axial symmetry to be able to analyse all of them, to describe and solve, and then, for example, to make a complete list of them. It turns out, however, that they all have one thing in common, namely structure, and this makes it possible to work out a common procedure for them, which serves in fact for the basis of analysis, thanks to which peristent collection of a large number of solutions can be dispensed with.

In designing a structure, we deal nearly always with:

— determination of the principal dimensions of the component parts, e.g. wall thickness, being guided here by strength requirements under conditions of known loadings,

— determination of states of stress and strain for present dimensions and loadings.

Here, we actually check whether the structure satisfies the requirements imposed by service life terms.

Under both procedures we generally must determine the values of the internal forces, while the stress and strain values are the result of the forces already determined.

In every case, the loadings are regarded as external forces applied to the structure, and serve as the point of departure for analysis. All internal forces are functions of loadings.

Axially symmetrical structures are in fact statically indeterminate systems and the quantities sought are the unknowns, these being most frequently cross-sectional transverse and normal forces and bending moments. Two statically indeterminate forces occur almost always in the cross-section investigated, and they appear in conditions of structural continuity at junctions, being determined from these conditions.

In the case of a structure consisting of several simple shells, considerable cross-sectional forces usually develop at the connecting sites; they are induced by various free displacements on the edges of the component parts. These forces can sometimes be eliminated by choosing, for example, suitable wall thickness for the elements, so as to get identical circumferential elongations at the junctions of the component parts.

Given below are the analyses of the forces at junctions of elements in various structures, involving plates, disks and shells.

1. A thin-walled vessel (Fig. 5.1) containing a gas under pressure p consists of a cylindrical part and two hemispherical-cap-shaped heads. If wall thicknesses h_1 and h_2 are identical, then in terms of the membrane theory

of shells, the free radial displacements on the cylinder and head edges, w_1 and w_2, respectively (Fig. 5.1b)

$$w_1 = \frac{(2-\nu)pR}{2h_1 E}, \qquad w_2 = \frac{(1-\nu)pR}{2h_2 E}$$
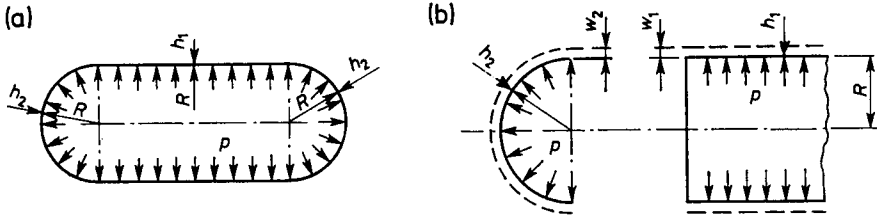
Fig. 5.1. Axially symmetrical thin-walled container: (a) geometry; (b) component parts

will not be equal and cross-sectional forces lowering the differences between the displacements will develop at the connecting site. To avoid the occurrence of these forces, it is enough that the condition $w_1 = w_2$ is satisfied which corresponds to

$$\frac{h_1}{h_2} = \frac{2-\nu}{1-\nu}.$$

In the case of steel and light alloys, we can take $\nu = 0.3$ and then $h_1/h_2 = 2.43$.

2. A similar behaviour will be exhibited by the thin-walled body of a liquid-mixing chamber operating under pressure p (Fig. 5.2a), consisting
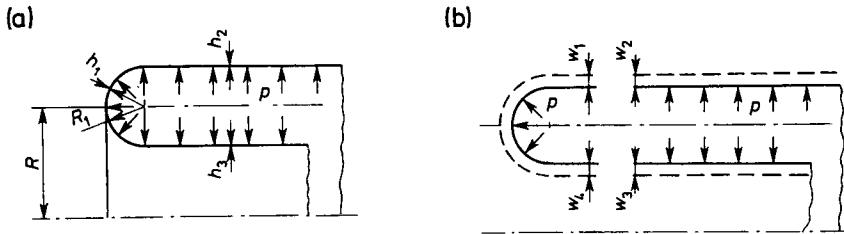
Fig. 5.2. This-walled body (a segment) of a mixing chamber: (a) loadings; (b) component parts

of two cylinders and a toroidal head, all working in a membrane state of stress. To avoid cross-sectional forces at the connecting sites (Fig. 5.2b), displacement equality conditions should be met

$$w_1 = w_2, \qquad w_3 = w_4$$

from which it follows that wall thicknesses h_1, h_2, h_3 will not be identical. Not in all structures can these conditions be met by optimal selection of wall thickness; specifically, they cannot be satisfied in structures operating in a bending state and also where next to various linear displacements on the edges, there are angular displacements. Not only are the wall thicknesses crucial here, but also the shapes of the component parts.

3. A shell consisting of a hemispherical cap and a long cylindrical part is in a bending state (Fig. 5.3a); it is loaded by pressure p. After detaching
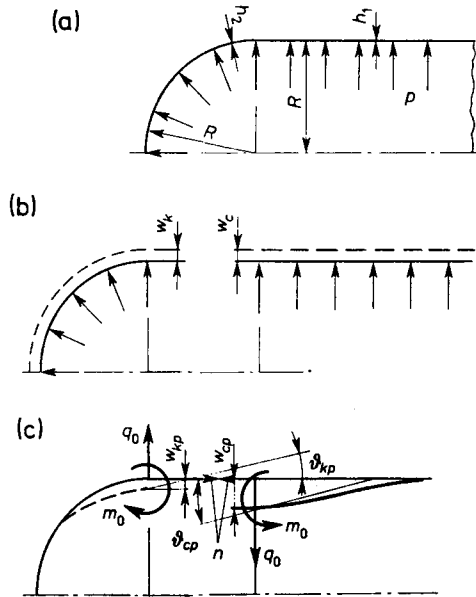
Fig. 5.3. Axially symmetrical thin-walled shell: (a) loadings; (b) component parts; (c) cross-sectional forces

the cylinder head, it will be seen that acting on the free edge are forces of intensity n, satisfying the equilibrium conditions $2\pi Rn - \pi R^2 p = 0$. Additional cross-sectional forces—bending moments m_0 and transverse forces q_0 are involved at the connecting of the two parts; they are caused by the incompatibility of the free radial and angular displacements (Fig. 5.3b, c), and they result in additional displacements denoted by subscript "a". Satisfying the displacement continuity conditions at the junctions of the two parts leads to

$$w_k + w_{kp} = w_c + w_{cp}, \qquad \vartheta_k + \vartheta_{kp} = \vartheta_c + \vartheta_{cp}. \tag{5.1}$$

Obviously, both ϑ_k and ϑ_c are induced by pressure p alone. They remain equal to zero, whereas

$$w_k = \frac{(1+\nu)pR^2}{2Eh_2}, \qquad\qquad w_c = \frac{(2-\nu)pR^2}{2Eh_1},$$

$$w_{kp} = \frac{2q_0 k_1 R}{Eh_2} - \frac{2m_0 k_1^2}{Eh^2}, \qquad w_{cp} = -\frac{q_0}{2k_2^3 D} - \frac{m_0}{2k_2^2 D},$$

$$\vartheta_{kp} = \frac{2q_0 k_1^2}{h_2 E} - \frac{4m_0 k_1^3}{h_2 ER}, \qquad \vartheta_{cp} = -\frac{q_0}{2k_2^2 D} - \frac{m_0}{k_2 D}.$$

Thus, the set of equations (5.1) solved with respect to unknown m_0 and q_0 ends the first and crucial stage of structural analysis. The remaining quantities, such as bending moments, transverse forces and stresses in the vicinity of the junstions can be determined without difficulty using the simple relationships given earlier in the section discussing individual simple cases of loadings of spherical caps and cylindrical shells. It is to be noted that the wall thicknesses of both shells can be selected so that m_0 and q_0 are as small as possible.

In the case of uneven but axially symmetrical heating of individual component parts of shells, the calculation technique remains exactly the same; only radial displacements induced by the temperature differences need additionally to be considered.

4. Consider a long cylindrical shell closed by an elastic plane bottom (Fig. 5.4a). The loading is a linearly variable pressure along the generatrix of the cylinder, but, it is not acting on the bottom. The corner is taken to be perfectly rigid. After detaching the bottom from the cylinder their mutual
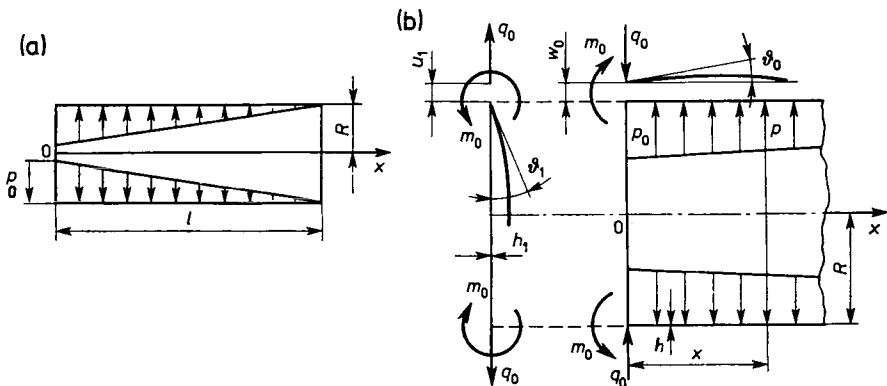
Fig. 5.4. Cylindrical shell, long type with bottom: (a) loadings by pressures varying along x-axis; (b) component parts

interaction manifests itself in the presence of moments m_0 and transverse forces q_0. Thus, the cylindrical shells is subjected to pressure $p = p_0(1-x/l)$, with moment m_0 and transverse force q_0 acting on its edge, and the bottom is a bircular, plate loaded on the edge by moments m_0 and simulateneously, it is a circular disk under radial tension q_0. Under these loadings, the shell experiences on its left-hand edge increment w_0 of the radius and slope ϑ_0 is formed (Fig. 5.4b). Slope ϑ_1 appears on the edge of the bottom as a plate and increment u_1 of the radius appears on the edge of the bottom as a disk. We can write that $u_1 = w_0$ and with the assumed rigidity of the corner, $\vartheta_1 = \vartheta_0$. These are equations of bottom-shell consistency. Based on the theory of circular disks and plates,

$$u_1 = \frac{(1-\nu)q_0 R}{Eh_1} \quad \text{and} \quad \vartheta_1 = \frac{m_0 R}{(1+\nu)D_1},$$

where $D_1 = \dfrac{Eh_1^3}{12(1-\nu^2)}$. Deflection $w(x)$ for a long shell

$$w = e^{-kx}(C_1 \sin kx + C_2 \cos kx) + w_2$$

and in keeping with theory $p = p_0 - p_0\dfrac{x}{l}$, $a_0 = \dfrac{p_0}{4k^4 D}$, $a_1 = -\dfrac{p_0}{4k^4 Dl}$

$$k = \sqrt[4]{\frac{3(1-\nu^2)}{R^2 h^2}}.$$

The relationships for displacement w_0 and slope ϑ_0 of the left-hand edge of a cylindrical shell are

$$w_0 = \frac{2k^2 R^2}{Eh}\left(m_0 - \frac{q_0}{k}\right), \quad \vartheta_0 = -\frac{m_0}{kD} + \frac{q_0}{2k^2 D} - \frac{p_0 R^2}{Ehl}.$$

Hence, the consistency equations in expanded form are

$$\frac{(1-\nu)q_0 R}{Eh_1} = \frac{2k^2 R^2}{Eh}\left(m_0 - \frac{q_0}{k}\right) + \frac{p_0 R^2}{Eh},$$

$$\frac{m_0 R}{(1+\nu)D_1} = -\frac{m_0}{kD} + \frac{q_0}{2k^2 D} - \frac{p_0 R^2}{Ehl},$$

from which we calculate unknown m_0 and q_0. Using equation for $w(x)$ and the relationships for plate and disk, we calculate the internal forces and stresses at an arbitrary point of the shell and bottom.

5. A long shell has been joined with a disk-plate and loaded by pressure p_0 (Fig. 5.5a). This structure consists of a shell, loaded on the edge by pressure p_0, transverse forces q_0 and moments m_0 and a plate with a hole, loaded
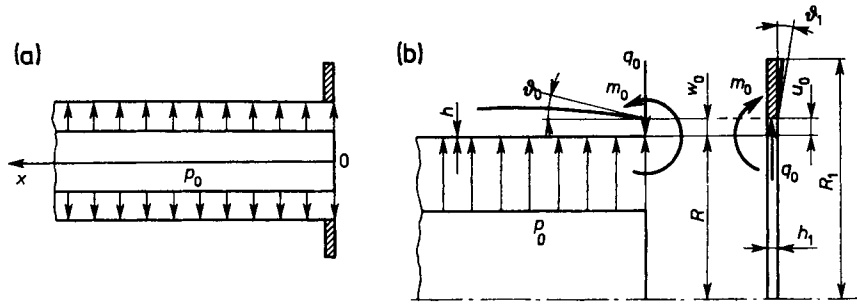
Fig. 5.5. Shell: (a) cylindrical with a flange; (b) component parts

on the inner edge by moments m_0 and radial pressure q_0 (Fig. 5.5b). Both m_0 and q_0 are unknown, assuming therefore that the loadings will not change the angle of the corner, we obtain the following conditions of consistency of the shell with the plate-disk (flange) written for radial displacements on the edge of the shell and the plate-disk and for the slopes of the central surfaces and the plate,

$$w_0 = u_0, \quad \vartheta_0 = \vartheta_1,$$

where

$$w_0 = w(p) - w(m_0) + w(q_0),$$

$$u_0 = u_0(q_0),$$

$$\vartheta_1 = \vartheta_1(m_0),$$

$$\vartheta_0 = \vartheta_0(q_0) - \vartheta_0(m_0).$$

The further procedure to determine q_0, m_0 is similar to that followed before.

6. A structure (Fig. 5.6a) consists of a long cylindrical shell, on which, when not loaded, rings have been mounted without clearance and without
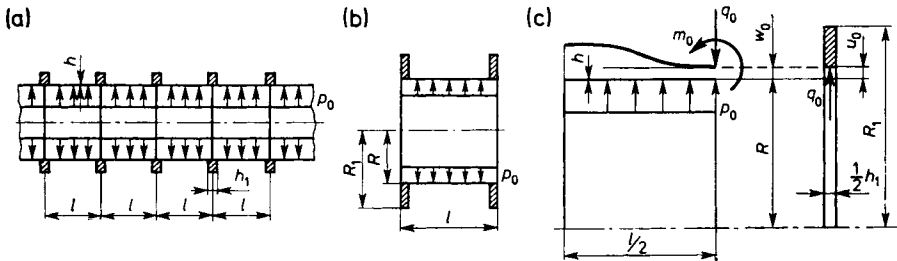
Fig. 5.6. Cylindrical shell with rings: (a) structure (diagram); (b) element of the structure; (c) component parts of element: deformation

negative allowance. Present inside is pressure p_0. Spacings l between the rings are identical and satisfy the condition

$$l < 2.4 \sqrt{Rh},$$

so that every segment of the shell (Fig. 5.6b) can be treated as short, loaded by pressure p and provided with elastic rings on the edges. Neglecting local concentrations, we can write the consistency conditions for the rings and the shell and the boundary conditions for the shell (Fig. 5.6c):

for $x = 0$ and $x = l$, we have $u_0 = w_0$ and $\vartheta_0 = 0$.

A ring of thickness $h_1/2$ is being stretched by pressure q_0 inducing increment of the radius u_0. Acting on the edge of the shell are moments m_0 and transverse forces q_0; therefore, for $x = 0$, there occurs $D \dfrac{d^2 w}{dx^2} = m_0$, $D \dfrac{d^3 w}{dx^3} = -q_0$. Since the system is symmetrical, at half-length l we have $\dfrac{dw}{dx} = 0$, $\dfrac{d^3 w}{dx^3} = 0$. These conditions reduce to the set of equations

$$m_0 = Dk^2 B_3,$$

$$-q_0 = Dk^3 B_4,$$

$$0 = (-4X_4 B_1 + X_1 B_2 + X_2 B_3 + X_3 B_4)_{x=l/2},$$

$$0 = (-4X_2 B_1 - 4X_3 B_2 - 4X_4 B_3 + X_1 B_4)_{x=l/2},$$

where

$$B_1 = \frac{1}{16} \left[\frac{B_4(4X_3^2 + X_1^2) - B_3 4(X_1 X_4 - X_2 X_3)}{X_1 X_2 + X_3 X_4} \right]_{x=l/2}, \qquad B_3 = \frac{m_0}{k^2 D},$$

$$B_2 = \left[\frac{B_4(X_1 X_4 - X_3 X_2) - B_3(X_2^2 + 4X_4^2)}{X_1 X_2 + X_3 X_4} \right]_{x=l/2}, \qquad B_4 = -\frac{q_0}{k^3 D}.$$

We can now determine the sought q_0 and m_0 from the consistency and boundary conditions; for these quantities we obtain the equations

$$\frac{2q_0 R_1 x_0^2}{Eh_1(1 - x_0^2)} \left[(1 - \nu)x_0 + \frac{1 + \nu}{x_0} \right] = B_1 + \frac{p_0 R^2}{Eh}, \qquad B_2 k = 0, \qquad x_0 = \frac{R}{R_1}.$$

These results can be obtained in a simpler way using predetermined solutions for simple cases of loadings.

7. A structure (e.g. a toothed wheel) in the form of a disk of constant thickness with a shell revolving with angular velocity Ω (Fig. 5.7a). After detaching the shell from the disk as shown in Fig. 5.7b, we replace the mutual
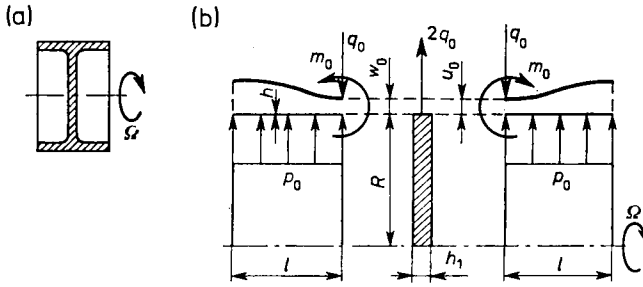
Fig. 5.7. Disk: (a) with a short shell on the outer perimeter; (b) component parts

interaction by moments m_0 and tensions $2q_0$. The system is symmetrical to the plane normal to the axis of rotation, halving the disk thickness. We have therefore a rotating disk, with radial tensions $2q_0$ acting on its edge and two identical short shells, each having one edge free and the other loaded by transverse forces q_0 and moments m_0, acting on which is radial tension $\sigma\Omega^2 Rh$ constant along the generatrix. The shell-disk consistency conditions, $u_0 = w_0$ and $\vartheta_0 = 0$, in which u_0 denotes radial displacement of the disk induced by body forces and tension $2q_0$ on the edge and w_0 is the increment of the shell radius on the edge, contributing to which are the body forces, moments m_0 and the edge forces q_0; ϑ_0 denotes the slope of the shell on the edge, equalling zero. All these quantities contain only two unkwons, m_0 and q_0. Evidently, the deformation of the shell (rim) may have an influence on the operation of the teeth of the wheel.

8. A long shell consists of two parts of different thickness, h_1 and h_2 (Fig. 5.8a). The shell is loaded only by pressure p. On separating the two parts as in Fig. 5.8b, q_0 and m_0 are acting on the edges. The consistency conditions for mid-layers are $w_{01} = w_{02}$ and $\vartheta_{01} = \vartheta_{02}$. It follows from these
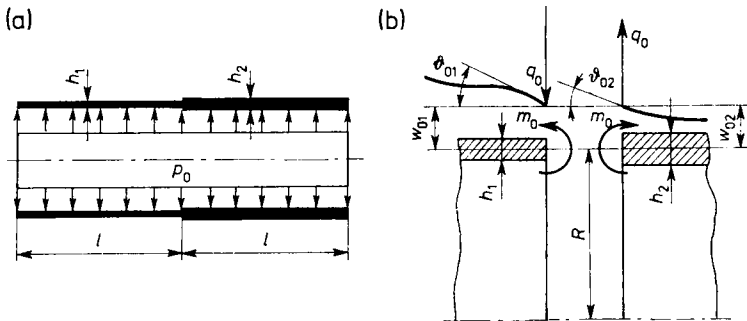
Fig. 5.8. Long shell: (a) wall thicknesses h_1 and h_2; (b) component parts

considerations that a change in thickness induces additional internal forces, and therefore, also stresses at the discontinuity site.

9. A long shell (Fig. 5.9) is heated (or cooled) to temperature $T_1 = \text{const}$ as from cross-section l–l along the right-hand side. The temperature of the
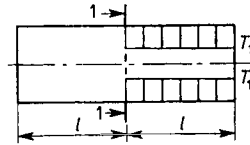
Fig. 5.9. Long shell heated over of part of its length

eft-hand side remains unchanged. A discontinuity of the thermal loading occurs in this case. We divide the shell into two parts as in Fig. 5.8b. Acting at the dividing place are moments m_0 and transverse forces q_0. It has to be remembered that for the left-hand side, we should take w_1 from (4.48) and $C_3 = C_4 = 0$, and for the right-hand side, w_2 from (4.63), with C_3', C_4' also equalling zero.

The consistency conditions for both parts are $w_1 = w_2$ and $\vartheta_1 = -\vartheta_2$.
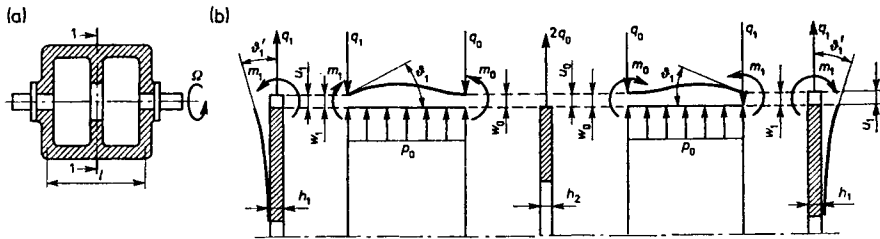
Fig. 5.10. Rotor: (a) diagram, (b) component parts: deformation

10. A rotor in the form of a shell with bottoms (Fig. 5.10a) is provided with a rib at half-length l to increase the rigidity of the structure. The shell thickness is constant and the bottom thicknesses are identical. The structure is symmetrical to cross-section l–l.

We obtain by decomposition (Fig. 5.10b)

(a) two shells symmetrical to each other, each being loaded along the generatrices by radial pressures, $p_0 = \text{const}$, and by moments m_0, m_1 and transverse forces q_0 and q_1, on the edges,

(b) two identical plates-disks loaded by centrifugel forces, and by moments m_1 and radial tension q_1, on the edge,

(c) a disk with a hole, loaded by centrifugal forces and by tensions $2q_0$, on the edge.

The static quantities m_0, m_1, q_0, q_1 are unknown. At the connecting sites of the bottoms and at the connecting site of the rib with the shells, the angles remain unchanged—in accordance with the design terms—whereas the shells and disks are subject to radial and angular displacements. Since the system is symmetrical, it is sufficient to consider only one half of it. We denote the radial displacements of the shell at the connecting site with the rib and with the bottom by w_0 and w_l, respectively, the slopes of the shell at same places by ϑ_0 and ϑ_l and lastly radial displacements on the outer perimeter of the bottom as a disk, the slope at the edge of the bottom as a plate and the radial displacements on the outer perimeter of the rib by u_1, ϑ_1', u_0, respectively. There are four equations following from the conditions of linkage of individual elements: $w_0 = u_0$, $w_1 = u_1$, $\vartheta_0 = 0$, $\vartheta_1 = \vartheta_1'$, from which we determine the sought unknowns m_0, m_1, q_0, q_1.

11. A non-symmetrical rotor (Fig. 5.11a) consists of
— a shell of length b (Fig. 5.11b), loaded by tensions $p_0 = \varrho\Omega^2 hR$, moments m_0, m_1 and transverse forces q_0, q_1 on the edges,
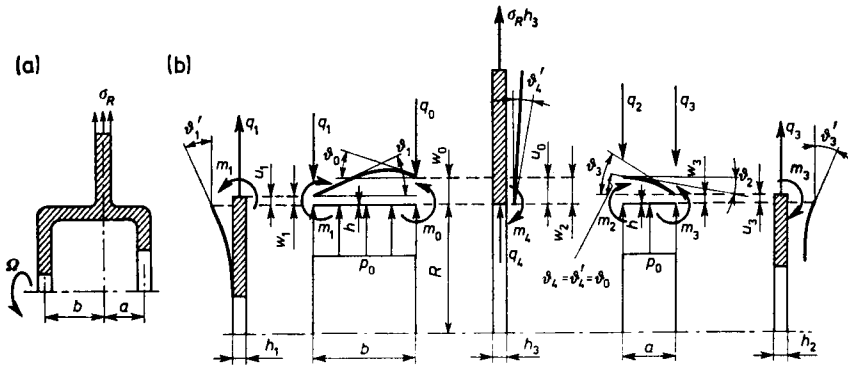
Fig. 5.11. Non-symmetrical rotor: (a) diagram; (b) component parts and deformation

— a shell of length a loaded by tensions p_0, moments m_2, m_3 and transverse forces q_2, q_3,
— two plates and two disks loaded by forces of inertia and radial tension q_3 and moment m_3 (right) and q_1, m_1 (left),
— a disk and a plate with a hole, loaded radially by force of inertia and radial loadings q_4 and $\sigma_R h_3$, and by moments m_4 on the edge of the hole. For the corner of the left bottom and the left shell

$$w_1 = u_1, \qquad \vartheta_1 = \vartheta_1',$$

for the corner of the right bottom and the right shell,

$$w_3 = u_3, \quad \vartheta_3 = \vartheta_3',$$

for both shells and the disk at the connecting site,

$$w_0 = u_0, \quad w_2 = u_0, \quad \vartheta_0 = \vartheta_2, \quad \vartheta_2 = \vartheta_4',$$

$$m_2 + m_4 = m_0, \quad q_0 + q_2 = q_4.$$
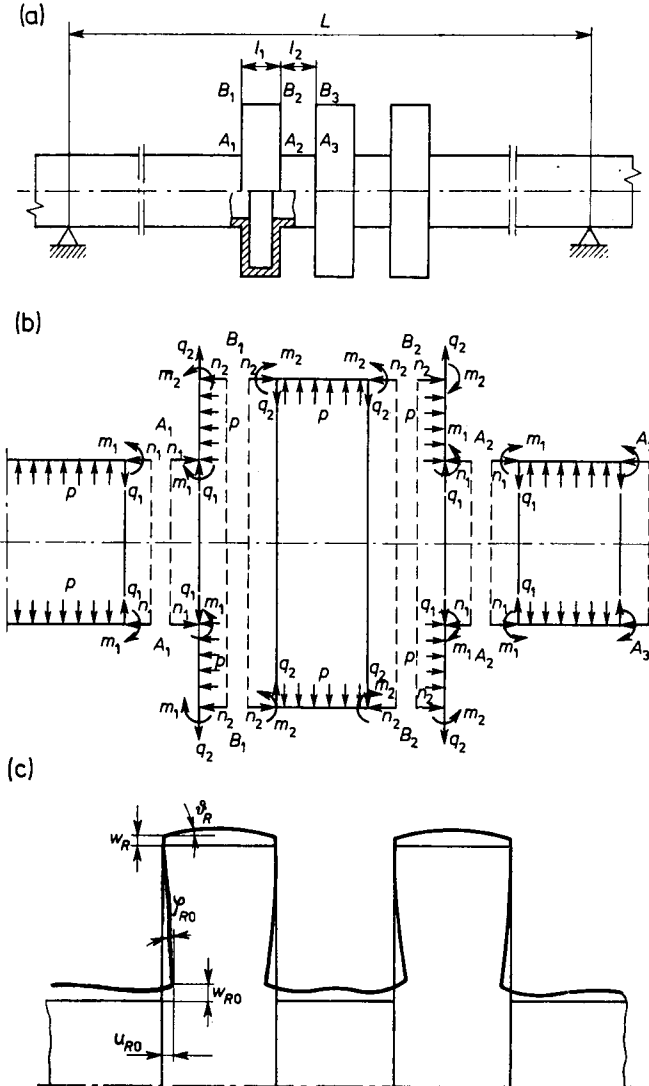
Fig. 5.12. Axial compensator: (a) diagram; (c) deformation geometry; (b) component parts and cross-sectional forces

12. An interesting case of a complex thin-walled structure operating by bending is represented by an axial compensator (Fig. 5.12a), subjected to inside pressure, an axial longitudinal force and temperature. It consists of several plates-disks, several short shells and two long cylindrical shells. Acting on these component parts, separated out as shown in Fig. 5.12b, are loadings and internal forces q_1, n_1, m_1, n_2, m_2, ...—if the indicated element of the compensator is completely symmetrical to the plane normal to the longitudinal axis (I–I) and halving $l_1' = l_1$. Shown in Fig. 5.12c is the predicted deformation mode, which assists in constructing equations of continuity and equations of consistency (Kemper and Duberg, 1947; Lipka and Majewski, 1976; Pacelt, 1970; Palatnikov, 1957; Schnell, 1955, 1957).

In special cases, where long or short shells are not made as cylindrical but as cones with very small angles (of the order of a few degrees), we can use all the relationships of the theory of cylindrical shells derived above, bearing in mind, however, that the differences of diameters of the extreme edges should not be very great. We then take for the calculations the mean radius from the two terminal radii. This is, however, an approximate method (Hodge, 1960; Lipka, 1967). This theory can also be used in the case of minor change in shell thickness h. The basic calculations are made for $h = $ constant, and the stresses are calculated for a current thickness at a given place. If the extreme differences $h_0 - h_1$ are small, the resulting inaccuracy will not be very great.

Occasionally, we encounter shells provided with grooves to mount guide-vanes of the casing (e.g. of a compressor). If the grooves are not deep, the theory of cylindrical shells of constant thickness yields good results, but the thickness must be calculated as equivalent thickness.

Generally speaking, if an error of less than 5% is admissible in calculations, then we can class as thin-walled all shells whose wall thicknesses are not in excess of 0.05 of the radius of curvature of the mid-layer.

Most widely used in mechanical engineering are thin-walled shells of sheet metal or rolled steel tubing. This comes from the fact that thin-walled elements are characterized by good strength properties. The replacement of plates or plate-lined beams by shells as carrying elements markedly reduces the weight of machines.

Shells have the most advantage under service conditions, where external bendings are not involved. The only internal forces then acting are longitudinal and tangential, if simultaneously a torque is involved. In these cases, cross-sectional forces n and t and shear stresses due to torsion are determinant of strength. However, if the edges of shells are loaded or joined to other

elements, additional internal forces and moments appear (a complex struc-
ture), which are almost always determinant of local and overall strength.
These phenomena can only be considered in terms of the general bending
theory of shells. Nor is the condition of complete axial symmetry satisfied.

What the design engineer should aim for, among other things, is to design
a carrying shell so as to get rid of bending in it or, should this prove imposs-
ible, to reduce bending to minimum. A structure like that will be distinguished
by low weight and considerable rigidity. It is to be noted that the strength
properties are most fully utilized when the external loadings are axially
symmetrical.

It has to be remembered that at the connecting sites of individual simple
elements making a complex structure there always exist stress concentrations,
varying in degree according to transition shapes, size of the radii of arcs,
and the like. Similarly, force and stress concentrations appear at the connect-
ing sites of elements, when bolted flanges are used. The latter fail to satisfy
the condition of complete axial symmetry and cannot be calculated by the
methods described in this part of the book. Relevant problems are con-
sidered in specialized contributions, with other methods being used. They
are considered in other parts of the present volume.

The reader has probably noticed that dealing here with problems relating
to axially symmetrical structures, we have not referred to stability, creep
and plasticity problems. We deliberately considered only linearly elastic
states. The other problems noted are given due consideration in separate
textbooks and monographs.

Comments on Some Works Concerning Part 6

Chapter VI of this book was completed in the years 1981–82, so the author
decided to include, in the form of a supplement, a short up-to-date presen-
tation of the state and trends of the knowledge progress in the years 1982–89
on problems of the theory and foundations for analysis of axially-symmetric-
structures and elements. In this area of the mechanics of linear and non-li-
near, isotropic and anisotropic—mainly with a distinctive orthotropy—elastic
systems there is published yearly, in the form of scientific papers, more than
500 works having the international character. Some of them, more general
and representative in the recent years, have been collected in the bibliographic
form together with their brief review.

The modern development trends of the theory of elastic axisymmetric structures and element (including their safety and optimization aspects with time effects included) are mainly stimulated by the acute needs of nuclear energy, building of highpower plants (thickwalled elements), chemical industry (thin-walled elements and with medium thicknesses), aerospace and cosmic techniques (thinwalled elements, laminates), shipbuilding (plates, shells). Simultaneously, there are developed and improved the approximated methods of analysis of the whole structures and their components with the leading, most popular finite element method (FEM). The finite element method is connected with the dynamic expansion of computerized computational techniques. It is a general numerical method and in the works of many authors it frequently deals simultaneously with plates and discs, plates and shells, interconnected thickwalled elements. In the field of plates and axisymmetric shells, a great attention has been paid to the formulation of more rigorous relations taking for instance into account the effects of tangential forces, large displacements or numerical methods for algebraic equations solving problems. The investigation of sets of insoparametric linear triangular or quadrangle finite elements (Blühmeier, 1983) by the assumed quadratic or biquadratic shape functions leads, for instance, to the possibility of taking into account of transverse shear effects in the stiffness matrix what permits also to calculate structures composed of elements with different wall thicknesses. The extension and introduction of the hybrid finite element methods (Dżygadło and Nowotarski, 1981; Dżygadło and Olejnik, 1981; Dżygadło and Manerowski, 1982; Dżygadło and Nowotarski, 1982, 1983; Nowotarski, 1984, 1986, 1987, 1988, 1989) and Love's stress functions made possible to find, in an approximate but more accurate way, solutions of two- or three-dimensional problems for plates, discs, shells and thickwalled cylinders at the different stages of their heating and plastic deformations. For plates, Pitkäranta (1986) obtained satisfactory approximate solutions applying simple finite elements. In geometrical and Lagrange description Pietraszkiewicz (1972, 1980, 1981), Schmidt (1980) derived non-linear equations of displacements and finite rotations describing shell bending. A solution for axisymmetric isotropic shells under bending was given by Xie Yu and Xie Zhicheng (1987), who applied the finite strains and large non-linear displacement shell theory. For displacements and generalized stresses, a basic set of equations of thin-walled cylindrical shells under constant symmetric or nonsymmetric forces and loading was formulated by Hampe and Burzel (1987); Kochno and Prokopov (1986) presented a detailed solution for axially-symmetric quasi-cylindrical shells with a slightly variable shell thicknes and a radius of

the midsurface; Krayterman and Sabnis (1985) investigated the effects of
loading path and large displacements on the solutions of plates and shells;
Nikolaev *et. al.* (1987) obtained with the use of the finite element method
the solutions for shells with various combinations of boundary conditions;
Nagórski and Trawiński (1980) and Wiśniakowski (1980) gave solutions for
iso- and ortho-tropic spherical shells. Błocki (1978) studied thickwalled shells
under surface and thermal loadings for particular boundary conditions (on
the base of three-dimensional elasticity theory). Investigations concerning
large deflections of thin plates in bending were carried out by Costa and
Brebbia (1984)—using computer, Johnson (1985)—series, Serebryakov (1986)
—the closed form of solutions obtained from the total potential energy
functional for deformed surface of membranes subjected to thermal and
surface loadings (very large displacements). In the distinction to the previous
cited works, Ren (1987) employed Fourier's series to the analysis of layered
othotropic cylindrical shells. Cheng (1985) analysed toroidal shells in the
applications to boilers, etc. Optimization problems of thin circular plates
were presented by Virak *et. al.* (1985) for thermally loaded membranes when
the heat was transferred only through planes (membranes) with isolated
boundaries. Solutions were obtained in the closed form. The optimization
condition was also formulated with the possibility of control by thermal
stresses.

References to Part 6

Alpert W. N., 1965, "Finite elastic-plastic deformations of non-uniformly heated rotating disc" (in Russian), *Prikl. Mekh.* **9**.

Ambarsoumian S. A., 1987, *Theory of Anisotropic Plates* (in Russian), Izd. Nauka, Moskva.

Anantra Ramu S., Janarchana Iyangar K., 1974, "Quasi-three-dimensional finite element method for plate bending", *Intern. Journ. of Mech. Sci.* **7**.

Biezeno K. B., Grammel R., 1939, *Technische Dynamik*, Springer, Berlin.

Berenov D. Y., 1959, *Strength Computations of Parts* (in Russian) Mashgiz, Moskva.

Bezukhov N. Y., 1968, *Fundamentals of the Theory of Elasticity, Plasticity and Creep* (in Russian), Moskva.

Bielak S., 1976, "Integral of a partial differential equation for solution of cylindrical shells" (in Polish), *Mech. Teor. i Stos.* **14, 2**.

Birger Y. A., 1956, *Some Mathematical Methods of Solution of Technical Problems* (in Russian), Oborongiz, Moskva.

Birger Y. A., 1961, *Round Plates and Shells of Revolution* (in Russian), Oborongiz, Moskva.

Birger Y. A., Shorr B. F., Shneyderovich R. M., 1959, *Strength Computations of Machine Parts* (in Russian), Mashgiz, Moskva.

Boyaroshinov S. V., 1962, "Approximate methods of computation of thick-walled solid cylinders subjected to axially symmetrical load" (in Russian), *Raschet na Prochnost'* **8**, Mashgiz, Moskva.

Brzoska Z., 1972, *Strength of Materials* (in Polish), PWN, Warszawa.

Budyka A., 1962, *Computation of Steam Turbine Disc* (in Russian), Mashgiz, Moskva.

Bulgakov V. N., 1962, *Statics of Toroidal Shells* (in Russian), Akad. Nauk USSR, Kiev.

Chernina V. S., 1968, *Statics of Thin-Walled Shells of Revolution* (in Russian), Izd. Nauka, Moskva.

Chernykh K. F., 1964, *Linear Theory of Shells*, Vol. II (in Russian), ILU, Leningrad.

Collective Work, 1971, *Theory of Plates and Shells* (in Russian), Akad. Nauk USSR, Moskva.

Conway H. D., 1948, "The bending of symmetrically loaded circular plates of variable thickness", *Journ. of Appl. Mech.* **1**.

Conway H. D., 1951, "Axially symmetrical plates with linearly varying thickness", *Journ. of Appl. Mech.* **12**.

Derski W., 1958, "State of stress in a thin circular disc induced by unsteady temperature field (in Polish), *Rozpr. Inż.* **49**.

Fleishman N. P., 1962, "Round and circular plates of minimum weight (in Russian), *Raschety na prochnost*, **8**, Mashgiz, Moskva.

Flügge W., 1957, *Statik und Dynamik der Schalen*, J. Springer, Berlin (Russian transl. 1961).

Girkmann K., 1956, *Flächentragwerke*, J. Springer, Wien.

Gorskii V. G., 1961, "Computation of round plates with variable thickness supported by circular elements" (in Russian), *Raschet na Prochnost'* 7, Mashgiz, Moskva.

Gorskii V. G., 1962, "Study on weight of round plates supported by rigid ribs (in Russian), *Raschet na prochnost'* 8, Mashgiz, Moskva.

Grigorenko Y. M., Laivunik Y. F., 1965, "Bending of a round plate with linearly variable thickness under anti-symmetrical load," (in Russian), *Prikl. Mekh. Akad. Nauk USSR*, 1, 7.

Grigoriev A. S., 1952, "On bending of round plate beyond the elasticity limit" (in Russian), *Prikl. Mat. i Mekh.*, 1.

Hampe E., 1963, *Statik rotationsymmetrischer Flächentragwerke*, Ed. 1, 2, 3, 4, VEB Verl. für Bauwesen, Berlin 1963, 1966.

Hodge P. H., 1960, "Plastic analysis of circular conical shells", *Journ. of Appl. Mechanics*, Ser. E, 4.

Hopkins H., Prager V., 1954, "Load carrying ability of round plates", *Journ. of Mech. and Physics of Solids*, 2 (Russian transl. in *Mekhanika* 3, 31, 1955).

Huber M. T., 1954, *Theory of Elasticity*, Part II (in Polish), PWN, Warszawa.

Huber M. T., 1958, *Engineering Stereomechanics*, Part II (in Polish), PWN, Warszawa.

Ilyushin A. A., Ogibalov P. M., 1960, *Elastic-Plastic Deformations of Solid Cylinders* (in Russian), IMU, Moskva.

Jakubowicz A., Orłoś Z., 1968, *Strength of Materials* (in Polish), WNT, Warszawa.

Jaworski A., Raczyński K., 1976, "Analysis of thermoelastic stresses and strains in bodies of revolution induced by an axial symmetrical temperature field with the use of finite elements method", *Arch. Bud. Masz.* 23, 4.

Jindra F., 1955, "Some applications of non-linear law of elasticity", *Ingenieur Archiv* 2 (*Mekhanika* 4, 1955).

Kachanov L. P., 1940, "Elastic-plastic equilibrium of a uniformly heated thin-walled cylinder (in Russian), *Zhurnal Tekh. Fiz.* 10.

Kalmanok A. S., 1959, *Computation of Plates* (in Russian), Moskva.

Kammash T. B., Murch S. A., Naghdi P. M., 1960, "The elastic-plastic cylinder subjected to radially distributed heat source, lateral pressure and axial force with application to nuclear reactor fuel elements", *Journ. of Mech. and Phys. of Solids* 1.

Kan S. N., 1966, *Structural Mechanics of Shells* (in Russian), Mashinostroene, Moskva.

Kantorovich B., 1952, *Principles of Computation of Chemical Plants and Apparatures* (in Russian), Mashgiz, Moskva.

Kączkowski Z., 1968, *Plates. Static Calculations* (in Polish), Arkady, Warszawa.

Kączkowski Z., 1971, "Theory of thick plates" (in Polish), *Arch. Mech. Stos.* 6 (23).

Kats A. M., 1956, *Theory of Elasticity* (in Russian), Gostekhizdat, Moskva.

Kempner J., Duberg J. E., 1947, "Charts for stress analysis of reinforced circular cylinders under lateral loads", *NACA—TN*, Nr 1310.

Kobrin M. M., 1963, *Strength of Rotating Discs* (in Russian), Sudpromgiz, Leningrad.

Kobza W., Lipiński J., 1973, "Finite element method of solving axial symmetrical heat conduction", *Arch. Bud. Masz.* 20, 4.

Kokai V. I., 1961, "Temperature field of discs and working blades of gas turbines at air cooling" (in Russian), *Aviatsionnaya Tekhnika* 1.

Kolkunov N. V., 1963, *Principles of Computation of Elastic* Shells (in Russian), Moskva.

Kopecki H., Walczak J., 1976, "The energy dissipation barrier as a criterion of creep failure of rotating discs" (in Polish), *Arch. Bud. Masz.* **23**, 4.

Kornyenko V. T., 1961, *A Complex State of Stress in Thin Round Plates of Constant and Variable Thickness under Non-Uniform Heating Conditions* (in Polish), *Raschet na prochnost'* 7, Mashgiz, Moskva.

Korolev V. I., 1971, *Elastic-Plastic Deformation of Shells* (in Polish), Mashinostroene, Moskva.

Korotkin J. I., Lokshin A. Z., Sivers N. L., 1955, *Bending and Stability of Plates and Round Cylindrical Shells* (in Russian), Sudpromgiz, Leningrad.

Kovalenko A. D., Grigorenko I. M., Lobkova N. A., 1961, *Computation of Conical Shells with Linearly Variable Thickness* (in Russian), Akad. Nauk USSR, Kiev.

Kovalenko A. D., 1959, *Round Plates with Variable Thickness*, GIML, Moskva.

Kozlov J. A., Bazhanov V. G., Leshchenko V. M., 1965, "Determination of the state of stress and strain in rotating discs beyond elasticity limit" (in Russian), *Prikl. Mekh.* **5**.

König J. A., 1971, "Optimal design of plates for cyclic loading" (in Polish), *Arch. Bud. Masz.*, **18**, 4.

Krzyś W., Latos W., 1974, "Fatigue shape optimization of a thin-walled pipe in the case of a complex load" (in Polish), *Arch. Bud. Masz.*, **21**, 4.

Krzyś W., Stodulski M., Trojnacki A., 1976, "Analysis of the process of experimental forming of an expanded multilayer vessel", *Arch. Bud. Masz.* **23**, 4.

Krzyś W., Życzkowski M., 1962, *Elasticity and Plasticity* (in Polish), PWN, Warszawa.

Kuhn P., 1956, *Stresses in Aircraft and Shell Structures*, McGraw-Hill, New York (Russian transl. 1961).

Kujawski J., 1976, "Thick circular disks in rotary symmetrical state of stress", *Arch. Bud. Masz.* **23**, 4.

Kurowski R., Niezgodziński M. E., 1970, *Strength of Materials* (in Polish), PWN, Warszawa.

Laszlo F., 1948, "Rotating disks in the region of permanent deformation", *NACA-TN*, 1192.

Leyko J., Królak M., Młotkowski A., 1972, "Approximate strength analysis of axial symmetrical circular plates of variable thickness, unilaterally ribbed and subjected to axial symmetrical loadings" (in Polish), *Arch. Bud. Masz.* **19**, 3.

Lipiński J., 1972, "The state of stress in a circular disk of hyperbolic cross-section induced by heat pulse" (in Polish), *Arch. Bud. Masz.* **19**, 1.

Lipka J., 1961, "The influence of physical properties of material on stresses in gas turbine disks" (in Polish), *Z. Nauk. Pol. Warsz., Mechanika*, 7.

Lipka J., 1961, "Shapes of rotating and heated disks with $\sigma_{red} = k_r(r, T)$ assumed" (in Polish), *Prace Instytutu Lotnictwa*, Warszawa.

Lipka J., 1967, *Strength of Rotating Machines* (in Polish), WNT, Warszawa.

Lipka J., 1970, "The state of stress in a piston under pressures, body forces and thermal loadings" (in Polish), *Prace Instytutu Lotnictwa* 4, WNT, Warszawa.

Lipka J., Butt-Hussaim A., 1963_1, "Auxiliary solutions for calculations of complex thin-walled structures" (in Polish), *Prace Instytutu Lotnictwa*, Warszawa.

Lipka J., Butt-Hussaim A., 1963_2, "Axial symmetrical thin-walled structures" (in Polish), *Prace Instytutu Lotnictwa*, Warszawa.

Lipka J., Kubicki B., 1968, "Thermal stresses in a cylinder sleeve" (in Polish), *Silniki Spalinowe* 4.

Lipka J., Majewski T., 1976, "Strength analysis of an axial compensator of thermal elonga-
tions", (in Polish), *Ciepłownictwo, Ogrzewnictwo, Wentylacja* 6 (81).

Lipka J., Orłoś Z., Szmelter J. *et al.*, 1977, *Experimental Strain and Stress Analysis* (in
Polish), PWN, Warszawa.

Lipka J., Sawicki A., 1965, "Internal forces and stresses in a cylinder sleeve" (in Polish),
Silniki Spalinowe Okrętowe i Kolejowe 1.

Liszka T., Życzkowski M., 1976, "Optimal forming of unevenly heated rotating disks
in terms of elastic carrying capacity and limit load" (in Polish), *Mech. Teor. i Stos.* 14,
2, 1976.

Loffler K., 1961, *Die Berechnung von rotierenden Scheiben und Schalen*, Berlin.

Łukasiewicz S., 1960, "Circular plates of uniform strength" (in Polish), *Arch. Bud. Maszyn* 1.

Malinin N. N., 1959, "Bending of turbine discs" (in Russian), *Raschet na prochnost'* 4,
Mashgiz, Moskva.

Malinin N. N., 1962, *Strength of Turbines* (in Russian), Mashgiz, Moskva.

Malinin N. N., 1968, *Applied Theory of Plasticity and Creep* (in Russian), Mashinostroienie,
Moskva.

Manson S. S., 1947, "The determination of elastic stresses in gas turbine disks", *NACA-TN*,
Nr 1279.

Manson S. S., 1949, "Direct method of design and stress analysis of rotating disks with
temperature gradient", *NACA-TN*, 1957.

Maslov N. M., 1965, "Bending of round orthotropic plates of a variable thickness" (in
Russian), *Prikl. Mat. and Mekh.*, 1, 2.

Matriukova A. S., 1959, "Bending of plane pistons" (in Russian), *Raschet na prochnost'*
4, Mashgiz, Moskva.

Mierzejewski W., 1976, "Nowacki's modified force method in plate dynamics with non-
dilatational strains and rotational inertia considered" (in Polish), *Mech. Teor. i Stos.*
14, 4.

Millenson M. B., Manson S. S., 1948, Determination of stresses in gas-turbine discs
subjected to plastic flow and creep", *NACA-TN*, 1636.

Misra J. C., 1975, "Thermal stresses in a rotating disc of anisotropic material", *Arch. Bud.
Masz.* 22, 2.

Nemec J., 1964, *Strength Calculations of Pressure Vessels* (in Russian), translation from
Czech, Mashinostroene, Moskva.

Novoshilov V. V., 1951, *Theory of Thin Shells* (in Russian), Sudpromgiz, Leningrad.

Nowacki W., 1970, *Theory of Elasticity* (in Polish), PWN, Warszawa.

Olesiak Z., 1958, "Application of trigonometric series to computation of closed cylindrical
shells" (in Polish), *Rozpr. Inż.*

Pacelt I., 1970, "Formation of the function of influence for a thin toroidal shell in the case
of an axially-symmetrical .load" (in Russian), *Mekh. Teor. i Stos.* 2.

Palatnikov E. A., 1957, *Calculation of Axial Compensators Introduced into Pipelines* (in
Russian), Oborongiz, Moskva.

Parszewski Z., 1956, "Equations of the engineers non-linear theory of thin shells", *Arch.
Mech. Stos.*, 8, 2.

Pavlov P. A., 1961, "Strength of flanged hollow shafts under simultaneous tension and
torsion" (in Russian), *Raschet na prochnost'* 7, Mashgiz, Moskva.

Ponomariev S. D., Biderman W. L., Likharev K. K., Makushin V. M., Malinin N. N.,

Feodsev V. T., 1958, *Strength Computations in Mechanical Engineering* (in Russian), Vol. 1, 2 and 3, Mashgiz, Moskva.

Prašek L., 1972, "Die Berechnung von Biegespannungen in den rotierenden Scheiben", *Arch. Bud. Masz.* **19**, 1.

Prokopovich I. E., Slesinger I. N., Shteinberg M. V., 1967, *Calculation of Cylindrical Shells* (in Russian), Kiev.

Pyzik J., Skalski K., Styczek A., 1975, "Numerical determination of the temperature field in a torus" (in Polish), *Arch. Bud. Masz.* **12**, 1.

Rogers T. G., Lee E. H., 1964, "Cylindrical problem of analysis of visco-elastic stresses" (in Russian), *Mekhanika* **6**.

Ryś J., Życzkowski M., 1971, "Calculation of disks with circular hole in the case of plastic hardening of material" (in Polish), *Arch. Bud. Masz.* **18**, 3.

Schnell W., 1955, "Krafteinleitung in versteifte Kreiszylinderschalen. Die orthotrope Schale", *Zeitschrift für Flugwissenschaften* **12**.

Schnell W., 1957, "Krafteinleitung in versteifte Kreiszylinderschalen. Die Schale mit endleich vielen Spanten", *Zeitschrift fur Flugwissenschaften* **1**.

Serensen S. V., Kagayev V. P., Kozlov L. A., Shneyderovich R. M., 1954, *Load Carrying Capacity and Calculation of Strength of Machine Elements* (in Russian), Mashgiz, Moskva.

Sherbourne A. N., Murthy D. N. S., 1974, "Stresses in disks with variable profile", *Internat. Journ. of Mech. Sci.* **7**.

Sismekov V. K., 1961, "On strange and density computations of flange joints" (in Russian), *Raschet na prochnost'* **7**, Mashgiz, Moskva.

Skalski K., 1970, "The state of stress in elastic and plastic regions of a thick-walled pipe subjected to a temperature field" (in Polish), *Arch. Bud. Masz.* **17**, 3.

Skubachevskii G. S., 1955, *Aircraft Gas-Turbine Engines*, Oborongiz, Moskva.

Szelągowski F., 1958, "A rotating disc with a rigid circular inclusion at the centre", *Arch Mech. Stos.* **10**, 2.

Thrun Z., 1956, "On thermal strains and stresses in thin rectangular and circular plates of variable thickness" (in Polish), *Rozpr. Inż.* **4**, 4.

Tikhomirov E. N. (ed.), 1967, *Strength and Stability of Elements of Thin-Walled Structures, Collected Papers in Mechanical Engineering* (in Russian), Moskva.

Timoshenko S., Goodier J. N., 1951, *Theory of Elasticity*, Mc Graw-Hill, New York–Toronto–London.

Timoshenko S., Goodier J. N., 1962, *Theory of Elasticity* (in Polish), Arkady, Warszawa.

Timoshenko S., Woinowsky—Krieger, 1959, *Theory of Plates and Shells*, Mc Graw-Hill, New York.

Tuliszka E., 1960, "Temperatures and thermal stresses in disk-type rotors of heat turbines under various operating conditions" (in Polish), *Arch. Bud. Masz.* **7**, 4.

Vodička V., 1957, "Bending of a toroid plate" (in Polish), *Rozpr. Inż.* **5**, 1.

Vainberg D. V., Vainberg E. D., 1959, *Plates, Discs, Column-Beams* (in Russian) GJULSA, Kiev.

Ventskovskii B. K., 1958, "Theory of bending of ring-plates subjected to a simultaneous action of transverse and radial forces" (in Russian), *Raschet na prochnost'*, **7**, Mashgiz, Moskva.

Ventskovskii B. K., 1961, "Load carrying capacity of round and circular plates reinforced

with annular ribs over circumference and in intermediate sections" (in Russian), *Raschet na prochnost'* 7, Mashgiz, Moskva.

Volk S. J., 1965, "Elastic conical shells loaded along generatrix and at boundary points of the structure" (in Russian), *Prikl. Mekh.* **11.**

Volmir A. S., 1956, *Flexible Plates and Shells* (in Russian), Gostekhizdat, Moskva.

Voloshin A. A., Samsonov Y. A., 1968, *Calculation and Design of Intersecting Vessel Shells* (in Russian), Mashinostroene, Leningrad.

Walczak J., 1971, *Strength of Materials and Foundations of Theory of Elasticity and Plasticity* (in Polish), PWN, Warszawa–Kraków.

Yella Reddy T., Srinath H., 1974, "Elastic stresses in a rotating anisotropic annular disk of variable thickness and variable density", *Internat. Journ. of Mech. Sci.* **2.**

Yusuff S., 1960, "Fracture phenomena in metal plates", *Stresa* (transl. in *Mekhanika* **5,** 1961).

Zhilin P. A., 1970, "Linear theory of ribbed shells" (in Russian), *Mekh. Teor. i Stos.* **34.**

Zhiritskii G. S., Lokai V. T., Maksutova M. K., Strunkin V. A., 1963, *Gas Turbines of Aircraft Engines* (in Russian), Oborongiz, Moskva.

Życzkowski M., 1956, "The limit load of a thick-walled tube in a general circularly symmetrical ease", *Arch. Mech. Stos.* **7,** 2.

Życzkowski M., 1957, "Limit load of non-homogeneous rotating circular disks" (in Polish), *Rozpr. Inż.* **5,** 1, Warszawa.

Życzkowski M., 1958, "Certain general equations for plane circularly-symmetrical plastic states", *Arch. Mech. Stos.* **10,** 4, Warszawa.

Życzkowski M., 1964, "Plastic strain and strength of expanded multilayer cylindrical pressure vessels" (in Polish), *Arch. Bud. Masz.* **11,** 1.

Additional References

Blühmeier J., 1983, *Ein Beitrag zur natürlichen Formulierung von Platten- und Schalenelementen beliebiger Dicke*, Diss. Dokt. Univ. Stuttgart, 1983.

Błocki J., 1978, "Thickwalled shells under surface and thermal loadings" (in Polish), *Mat. II Konf. "Konstrukcje powłokowe, teoria i zastosowanie"*, Gołuń.

Cheng Guodong, 1985, "Exact solutions of toroidal shells in pressure vessels and piping", *Int. J. Pressure Vessels a. Pip.* **19,** 2.

Costa J. A., Brebbia C. A., 1984, "Plate bending problems using B. E. N.", *Proc. 6th Int. Conf. Board Liner*, Southampton, N. Y. July 1984.

Dżygadło Z., Nowotarski J., 1981, "Finite elements strength analysis of rotatotaing shell-plate structures", *J. Tech. Phys.* **22,** 3.

Dżygadło Z., Olejnik A., 1981, "A numerical method of strength design of axially symmetric shell plate system", *J. Tech. Phys.* **22,** 1.

Dżygadło Z., Manerowski J., 1982, "Vibration and stability analysis of rotors on orthotropic supports", *J. Tech. Phys.* **23,** 3–4.

Dżygadło Z., Nowotarski J., 1982, "A hybrid finite element method for static analysis of axisymmetrical surface structures", *J. Tech. Phys.*, **23,** 2.

Dżygadło Z., Nowotarski J., 1983, "A. Comparative numerical analysis of axially symmetric shell-plate structures by the displacement and hybrid methods of finite elements", *J. Tech. Phys.* **24,** 1.

Hampe E., Burzel W., 1987, "Tragverhalten von zylidrischen Schalentragwerken unter nicht rotationssymetrischen Einwirkungen", *Beton- und Stahlbetonbau* **82**, 7.

Johnson Millard W., 1985, "On the foundations of the non-linear theory of the cylindrical deformation of thin elastic plates", *Int. Solids and Struct.*, **21**, 1.

Kokhno, G. F., Prokopov, V. K., 1986, "Axially symmetric bending of cylindrical shells with slightly variable thickness and variable radius" (in Russian), *Prikl. Mekh.* **22**, 11.

Krayterman B., Sabnis Grajanan, 1985, "Large deflected plates and shells with loading history", *J. Eng. Mech.* **111**, 5.

Nagórski R., Trawiński K., 1980, "Rotationally-symmetric bending of a low-rised orthotropic spherical shell" (in Polish), *Rozpr. Inż.* **26**, 2.

Nikolaev A. P., Bandurin N. G., Klochkov J. V., 1987, "On the calculations of branched axisymmetrical shells using the finite element method" (in Russian), *Probl. prochn.* **12**.

Nowotarski J., 1984, "Strength analysis of rotating axially symmetric structures by the method of one and two-dimensional finite elements", *J. Tech. Phys.* **25**, 1.

Nowotarski J., 1986, "Possible applications of Love's stress functions in the hydrid method of finite elements", *J. Techn. Phys.* **27**, 1–2.

Nowotarski J., 1987, "Statically compensated equilibrium model of the finite element method" (in Polish), *Bibl. WAT* **3**.

Nowotarski J., 1987, "Non-linear analysis of an axially symmetric stress field as a three-dimensional problem" *J. Tech. Phys.* **3**.

Nowotarski J., 1988, "Static analysis of aero-engine turbine disks with regard to plastic strains" (in Polish), *Biul. WAT* **3**.

Nowotarski J., 1989, "A discrete model for thermoelastic-plastic analysis of an axisymmetric body", *J. Tech. Phys.*

Pitkäranta J., 1986, "On simple finite element methods for Mindlin plates", *Comput. Mech.* '86. Tokyo, May 25–39. Vol. 1.

Pietraszkiewicz W., 1972, *Finite Rotations and Lagrangean Description in the Non-Linear Theory of Shell* (in Polish), PWN, Warszawa–Poznań.

Pietraszkiewicz W., 1980, *Finite Rotations in Shells*, North-Holland P. Co., Amsterdam.

Pietraszkiewicz W., 1981, "Three forms of geometrically non-linear bending shell equations", *Prace IMP* **81**.

Ren J. G., 1987, "Exact solutions for laminated cylindrical shells in cylindrical bending", *Compos. Sci. and Technol.* **29**, 3.

Schmidt R., Pietraszkiewicz W., 1981, "Variational principles in the geometrically non-linear theory of shells undergoing moderate rotations", *Ingenieur-Archiv.* **50**, 3.

Schmidt R., 1980, Systematische Herleitung von Variations-prinzipen für geometrisch nicht lineare Schalentheorien bei auftreten von Rotationen mittlerer Grössenordnung (Doktorarbeit), Ruhr-Universität, Bochum.

Serebryakov A. V., 1986, "Equilibrium equations of a flexible membrane" (in Russian), *Temp. Zad. Teor. Uprug.*, Saratov.

Virak V. M., Kolesov V. S., Jasinskii A. V., 1985, "Optimization of axisymmetric stresses in a prescribed cross-section of a thin circular membrane with the help of heat sources" (in Russian), *Prikl. Mekh.* **21**, 8.

Xie Yu, Xie Zhicheng, 1987, "The solution of axisymmetrical shells with finite deformation" *J. Tsin-ghu a Univ.* **27**, 5.

Wiśniakowski P., 1980, "A solution of the bending problem of a spherical shell rotationall-symmetric loaded" (in Polish), *Rozp. Inż.* **22**, 1.

Subject Index